GENERAL DYNAMICS
Convair Division and Space Systems Division

STRUCTURES ANALYSIS MANUAL

VOLUME 1 OF 2

Revision 2

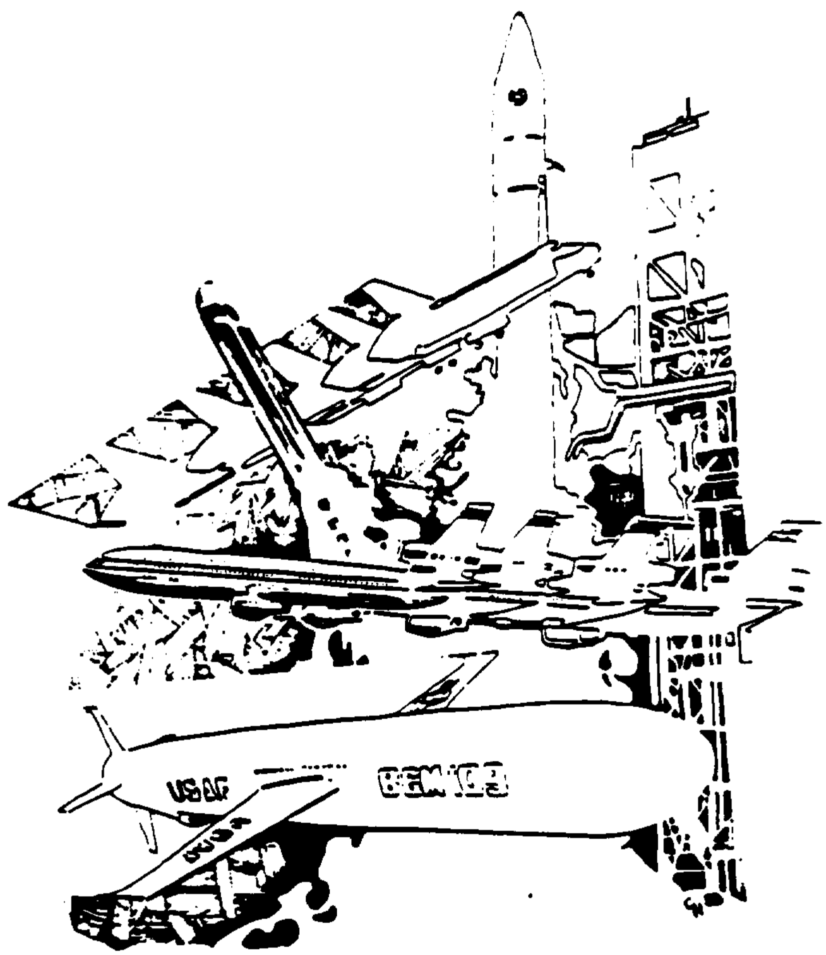

REVISION RECORD

CHAPTER - ISSUE	REVISION DESCRIPTION	DATE
All - 1	Original Issue	3/88
As noted -2	Deleted: Pages 14.9.2, 14.9.3, 14.9.4, 14.9.5, 20.0.1, [redacted] Added: [redacted] [redacted] Pages 4.8.21 4.8.22, 20.1.1 Revised: Pages [redacted] [redacted] 1.3.4 Vol. 1 & 2, 2.1.4, 2.7.1, 4.1.3, 4.9.1, 4.9.2, 4.9.3, 6.4.7, 6.4.15, 7.1.2, 7.1.3, 7.1.4, 7.1.5, 8.11.1, 8.11.3, 10.0.1, 10.1.1, 10.2.1, 10.5.2, 10.7.1, 10.8.2, 11.2.4, 14.1.4, 14.1.5, 14.1.24, 14.1.54, 14.9.1, 17.4.5, 17.5.27, 17.6.10, 17.6.17, 17.6.18, 17.6.19, 27.1.17 ALS GDFW	10/89

STRUCTURAL ANALYSIS MANUAL
GENERAL DYNAMICS/CONVAIR AND SPACE SYSTEMS DIVISION

PREFACE

This Structures Manual has been prepared by Convair and Space Systems Division Structures Analysis Groups as a reference source of data and procedures for use in the analysis and design of aerospace and ground handling structures. The manual has been compiled largely from material presented in the General Dynamics Fort Worth Structures Manual, Vol. 1. These data have been updated and expanded to cover current materials and construction methods.

In general, the source data reference numbers within the individual sections of the manual have been retained. This will enable the reader to easily locate any additional material that may be required from the original data source.

Comments and suggestions are welcome, and should be addressed to the Structural Analysis Group.

PREFACE - FORT WORTH DIVISION

The Fort Worth Division Structures Technology department endorses the Convair and Space System Division Structures Analysis Manual as a reference source of data and procedures for structural analysis at the Fort Worth Division. The data and procedures contained in Volumes I and II are recommended for use at the Fort Worth Division at the discretion of each structural analysis group Engineering Chief considering individual program guidelines. Use of all data and procedures including those contained herein and from other sources must be approved by the structural analysis group Engineering Chief and documented sufficiently to support customer approval.

A. L. Stratton
Engineering Manager for Structures Technology
General Dynamics/Fort Worth Division

STRUCTURAL ANALYSIS MANUAL
GENERAL DYNAMICS/CONVAIR AND SPACE SYSTEMS DIVISION

VOLUME 1
TABLE OF CONTENTS

	SECTION
PREFACE	1.0
TABLE OF CONTENTS	1.1
SYMBOLS AND ABBREVIATIONS	1.2
REFERENCES	1.3
SECTION PROPERTIES	2.0
GEOMETRICAL SHAPES	2.1
CIRCLES	2.2
90^o BENDS	2.3
ANGLES	2.4
CENTROID OF TRAPEZOID	2.5
SHEAR CENTER	2.6
MOMENT OF INERTIA SAMPLE CALCULATION	2.7
MATERIAL PROPERTY DEFINITIONS	3.0
STRESS-STRAIN CURVE DEFINITIONS	3.1
MATERIAL PROPERTIES: DUCTILE-BRITTLE BEHAVIOR	3.2
CREEP: STRAIN RATE AND IMPACT	3.3
"A" AND "B" MATERIAL PROPERTY VALUES	3.4
PLASTIC STRESS-STRAIN CURVES	3.5
SURFACE ROUGHNESS	3.6
NON-DIMENSIONAL STRESS-STRAIN CURVES	3.7
RAMBERG-OSGOOD CONSTANTS	3.8
BEAMS	4.0
BEAM TABLES	4.1
VARIABLE CROSS SECTION	4.2
CONTINUOUS BEAMS	4.3
MOMENT DISTRIBUTION METHOD	4.4
CURVED BEAMS	4.5
LATERAL STABILITY	4.6
SHEAR STRESSES	4.7
TENSION FIELD WEBS	4.8
CUT-OUTS	4.9
SLOTTED BEAM	4.10
ELASTIC FOUNDATION	4.11

VOLUME 1
TABLE OF CONTENTS (CONTINUED)

	SECTION
COLUMNS	5.0
THEORY	5.1
CONSTANT CROSS SECTION COLUMNS	5.2
VARIABLE CROSS SECTION COLUMNS	5.3
CRIPPLING OF SECTIONS	5.4
BEAM COLUMNS	5.5
CONTINUOUS BEAM COLUMNS	5.6
TORSIONAL INSTABILITY	5.7
COLUMN ALLOWABLES	5.8
PLATES	6.0
IN-PLANE STABILITY LOADING, RECTANGULAR	6.1
IN-PLANE STABILITY LOADING, PARALLELOGRAM	6.2
CURVED PLATES	6.3
NORMAL LOADING	6.4
MEMBRANES	6.5
STIFFENED PLATES	7.0
BUCKLING IN AXIAL COMPRESSION	7.1
ANALYTICAL METHODS	7.2
EFFECTIVE SKIN WIDTHS	7.2.4
ISOGRID STRUCTURES	7.3
SANDWICH CONSTRUCTION	8.0
GENERAL	8.1
MATERIALS	8.2
METHODS OF ANALYSIS	8.3
FACE WRINKLING	8.4
FACE DIMPLING	8.5
EDGEWISE COMPRESSION	8.6
EDGEWISE SHEAR	8.7
NORMAL LOADING	8.8
CYLINDER TORSION	8.9
CYLINDER AXIAL COMPRESSION	8.10
CYLINDER EXTERNALPRESSURE	8.11
BEAMS	8.12
ATTACHMENT DETAILS	8.13
ANALYSIS METHOD REFERENCES	8.14
PRESSURE VESSELS AND PIPES	9.0
STRESSES AND DEFLECTIONS	9.1
TANK GEOMETRY	9.2
PIPING SYSTEMS (ELBOWS, BELLOWS, DUCTS)	9.3
DISCONTINUITY ANALYSIS OF SHELLS	9.4

VOLUME 1
TABLE OF CONTENTS (CONTINUED)

	SECTION
CYLINDER AND SHELL STABILITY	10.0
UNPRESSURIZED	10.1
INTERNALLY PRESSURIZED	10.2
EXTERNALLY PRESSURIZED	10.3
TRUNCATED CONES	10.4
DOUBLY CURVED SHELLS	10.5
IMPERFECTIONS	10.6
POST-BUCKLING	10.7
LOCAL LOADING ON SHELLS	10.8
LANGLEY SOLUTION	10.9
TORSION	11.0
TORSION OF SOLID SECTIONS	11.1
TORSION OF THIN-WALLED CLOSED SECTIONS	11.2
TORSION OF THIN-WALLED OPEN SECTIONS	11.3
MULTI-CELL CLOSED BEAMS IN TORSION	11.4
PLASTIC TORSION	11.5
ALLOWABLE STRESSES	11.6
RESTRAINED TORSION	11.7
SPRINGS	12.0
COMPRESSION SPRINGS	12.1
EXTENSION SPRINGS	12.2
TORSION SPRINGS	12.3
CONSTANT FORCE SPRINGS	12.4
FLAT SPRINGS	12.5
CONED DISC (BELLEVILLE) SPRINGS	12.6
WORKING STRESSES	12.7

STRUCTURAL ANALYSIS MANUAL
GENERAL DYNAMICS/CONVAIR AND SPACE SYSTEMS DIVISION

VOLUME 2
TABLE OF CONTENTS

	SECTION
PREFACE	1.0
TABLE OF CONTENTS	1.1
SYMBOLS AND ABBREVIATIONS	1.2
REFERENCES	1.3
STRESS CONCENTRATION FACTORS	13.0
STATIC LOADING	13.1
REPEATED LOADING	13.2
GEOMETRIC EFFECTS	13.3
JOINTS AND FITTINGS	14.0
LUG ANALYSIS	14.1
MULTIPLE FASTENER PATTERNS	14.2
BEAM IN A SOCKET	14.3
INTERFERENCE FIT BUSHINGS	14.4
TENSION CLIPS AND TEES	14.5
BOLT STRENGTH	14.6
BATHTUB TYPE TENSION FITTINGS	14.7
WELD JOINTS	14.8
WELD-ON BRACKETS	14.9
BONDED JOINTS	14.10
JOINT FLEXIBILITY	14.11
PRELOADED BOLTS AND SCREWS	14.12
BOLT TORQUE EFFECTS	14.13
EFFICIENCY OF PLATES IN TENSION JOINTS	14.14
ACOUSTICS, VIBRATION, FLUTTER	15.0
LINEAR SYSTEMS	15.1
FORCED VIBRATION	15.2
METHODS OF CALCULATIONS	15.3
SONIC FATIGUE	15.4
FLUTTER	15.5
ACOUSTICS AND VIBRATION	15.6
EXPERIMENTAL STRESS ANALYSIS	16.0
STRAIN GAGES	16.1
PLASTIC ANALYSIS	17.0
BENDING STRENGTH IN PLASTIC RANGE	17.1
SIMPLE BENDING	17.2
COMPLEX BENDING	17.3
INTERACTION	17.4
PLASTIC BENDING MATERIAL PROPERTIES	17.5

VOLUME 2

TABLE OF CONTENTS (CONTINUED)

	SECTION
BENDING MODULUS SYMMETRICAL SECTIONS	17.6
MINIMUM PLASTIC BENDING CURVES	17.7
ELASTIC-PLASTIC THEORY	17.8
BENDING NEAR LIMIT LOAD	17.9
BENDING MODULUS FOR ROUND TUBES	17.10
SHEAR STRESS IN ROUND TUBES	17.11
RINGS, FRAMES AND ARCHES	18.0
RIGID RINGS	18.1
BENTS AND SEMI-CIRCULAR ARCHES	18.2
RIGID AND FLEXIBLE RINGS	18.3
REDUNDANT FRAMES	18.4
THERMAL EFFECTS	19.0
GENERAL	19.1
BEAMS AND COLUMNS	19.2
FLAT PLATES	19.3
BOX BEAMS	19.4
BOLTED JOINTS	19.5
THERMAL BUCKLING	19.6
THERMAL STRUCTURAL ANALYSIS WITH MSC NASTRAN	19.7
STATISTICAL ANALYSIS	20.0
INTRODUCTION	20.1
DEFINITIONS	20.2
DISCUSSION	20.3
SAMPLE PROBLEMS	20.4
TABLES OF STATISTICAL VALUES	20.5
MECHANISMS	21.0
BEARINGS	21.1
GEARS	21.2
ACTUATORS	21.3
COMPOSITE MATERIALS	22.0
FIBERGLASS LAMINATES, POLYESTER RESINS	22.1
FIBERGLASS LAMINATES, PHENOLIC OR EPOXY RESINS	22.2
KEVLAR EPOXY DESIGN ALLOWABLES	22.3
FRACTURE MECHANICS	23.0
GENERAL	23.1
STRESS INTENSITY FACTORS	23.2
FLAW GROWTH	23.3
APPLICATION OF TECHNOLOGY	23.4
DAMAGE TOLERANCE	23.5

VOLUME 2
TABLE OF CONTENTS (CONTINUED)

	SECTION
COMPUTERIZED METHODS	24.0
OPTIMIZATION DESIGN	25.0
MISCELLANEOUS TABLES AND CHARTS	26.0
TEMPERATURE CONVERSION	26.1
SI UNITS AND PREFIXES	26.1
METRIC CONVERSION FACTORS	26.2
HARDNESS CONVERSION	26.3
STANDARD ATMOSPHERE	26.4
TEMPERATURE VS. ALTITUDE	26.5
COEFFICIENTS OF STATIC AND SLIDING FRICTION	26.6
REPORT FORMAT	27.0
STRESS ANALYSIS REPORT STANDARDS	27.1

Data Source, Section 1.3 Reference 1

List of Standard Symbols and Abbreviations

A.... Ratio of stress amplitude and mean stress; area of cross section

a.... Length of panel edge: for compressive or bending loads, "a" is length not loaded; for shear loads, "a" is the longer edge of panel.

B.... Flexural rigidity of a beam

b.... Length of panel edge: for compressive or bending loads, "b" is the length of the loaded edge; for shear loads, "b" is the shorter edge of the panel. Width of sections; stiffener spacings.

C.... Circumference; damping coefficient; spring constant

C_{cr}.. Critical damping coefficient

c.... Fixity coefficient for columns; distance from neutral axis to extreme fiber

c_r... Rivet factor

D.... Diameter; bending stiffness; distribution factor; flexural rigidity parameter

d.... Depth, height, or thickness; distance between centroids of facings

E.... Modulus of elasticity in tension

e.... Elongation in percent; total deformation; eccentricity; the minimum distance from a hole center to the edge of a sheet

F.... Allowable stress; force

G.... Modulus of rigidity

g.... Acceleration due to gravity

H.... Extensional stiffness of sandwich

h.... Height or depth; distance between centroids of facings

I.... Moment of inertia

I_{xy}.. Product of inertia

J.... Polar moment of inertia

j.... Coefficient of critical shear for orthotropic sandwich panels

K.... A constant, generally empirical

k.... Stiffness factor; spring constant; radius of gyration

L.... Length, longitudinal grain direction; edgewise shear stiffness for sandwich

l.... (Not used, to avoid confusion with numeral 1)

M.... Bending moment or couple

m.... Mass; half width of corrugation; bending moment; number of half waves

N.... Load per inch of edge; sample size

n.... Load factor; number of half waves;

P.... Applied load or force (total, not unit load)

p.... Pressure

Q.... Static moment of a cross section

q.... Shear flow; dynamic pressure

R.... Stress ratio

r.... Radius

S.... Shear force; surface area

s.... Core cell size

T.... Applied torsional moment; torque; transverse grain direction; temperature

t.... Thickness; time

U.... Factor of utilization; gust velocity; transverse shear stiffness for sandwich; strain energy

V.... Shear force; velocity; volume; flexibility parameter for sandwich panels

W.... Total weight; length of cell wall in sandwich construction

w.... Distributed load

x.... Axis; distance along elastic curve of beam

y.... Axis; deflection; distance from neutral axis to given fiber

$\bar{y}$.... Distance to centroid of section

Z.... Section modulus

z.... Axis normal to surface of panel

α (Alpha)	Coefficient of thermal expansion; angle of attack; angle of diagonal tension; constant
β (Beta)	Stiffener angle; constant
γ (Gamma)	Unit shear strain
δ (Delta)	Deflection; relative retardation
ϵ (Epsilon)	Compression or expansion Strain; rotational restraint coefficient
η (Eta)	Plasticity coefficient
θ (Theta)	An angle with respect to a reference line
λ (Lambda)	One minus the product of two Poisson's ratios $(1 - \mu^2)$
Λ (Lambda)	Constant
μ (Mu)	Poisson's ratio
π (Pi)	A constant
ρ (Rho)	Density; radius of curvature
σ (Sigma)	Normal stress
τ (Tau)	Shear stress
ϕ (Phi)	Constant
ψ (Psi)	Angular displacement

Subscripts

1 ... Denotes facing of sandwich

2 ... Denotes facing of sandwich

a ... Allowable

b ... Bending

br .. Bearing

c ... Core, compression

cr .. Critical

E ... Elastic limit

e ... Endurance; eccentricity; Euler's equation

f ... Face

i ... Denotes final segment; intercellular

m ... Moment

n ... Normal; natural

o ... Denoting corrugation sheet

p ... Proportional limit; polar

r ... Effective; reduced

s ... Secant

si .. Denoting shear instability

t ... Tangent

u ... Ultimate

w ... Wrinkling

x ... Parallel to x axis

y ... Yield; parallel to y axis

z ... Parallel to z axis

Abbreviations

average	avg
British thermal unit	Btu
coefficient	coef
cosine	cos
cotangent	cot
cubic	cu
cubic foot	cu ft
cubic inch	cu in
decibel	db
degree	deg or °
degree Centigrade	C
degree Fahrenheit	F
diameter	diam
Division Standard Practice	D.S.P.
Engineering Department Instructions	E.D.I.
feet per minute	fpm
feet per second	fps
figure	fig
foot	ft
foot-pound	ft-lb
horsepower	hp
hour	hr
hyperbolic cosine	cosh
hyperbolic sin	sinh
hyperbolic tangent	tanh
inch	in
inch-pound	in-lb
inches per second	ips
inside diameter	ID
Inspection Minor Rework Order	IMRO
Inspection Rejection	IR
logarithm (common)	log
logarithm (natural)	$\log_e$ or ln
Material Review Board	MRB
maximum	max
minimum	min
minute	min
outside diameter	OD
pound	lb or #
pounds per cubic foot	lbs per cu ft
pounds per square foot	psf
pounds per square inch	psi
pounds per square inch absolute	psia
revolutions per minute	rpm
root mean square	rms
secant	sec
second	sec
sine	sin
standard	std
tangent	tan
temperature	temp
weight	wt

NOTE: With very few exceptions, the abbreviations and letter symbols conform with those approved by the American Standards Association, ANC #5, ANC #23 (Revised), and GD/FW Standard Practices.

Data Source, Section 1.3 Reference 1.

SECTION 1.3

REFERENCES:

IN ADDITION TO REFERENCES CONTAINED IN INDIVIDUAL SECTIONS OF THE REPORT, DATA SOURCES LISTED BELOW HAVE ALSO BEEN USED.

1. GD FORT WORTH STRUCTURES MANUAL VOL. 1 1963

2. CONVAIR/ASTRONAUTICS STRUCTURES MANUAL 4.15.60

3. BELL STRUCTURE DESIGN MANUAL

4. BOEING STRESS MANUAL APRIL 1970

5. NASA ASTRONAUTICS STRUCTURES MANUAL 7.1.69

6. LOCKHEED STRESS MEMO MANUAL 4.18.66

7. BRUHN, ANALYSIS & DESIGN OF FLIGHT VEHICLE STRUCTURES JAN. 1965

8. NACA TN 3784

9. NACA TN 3785

10. NASA CR-124075

11. NASA CR-1457

12. HEXEL TSB 123, DESIGN HANDBOOK FOR HONEYCOMB SANDWICH STRUCTURES OCT. 1967

13. ROARK, FORMULAS FOR STRESS AND STRAIN, 3RD ED. 1954

14. CONVAIR, ZP-7-022 TN, ANALYSIS OF MISSILE TANK GEOMETRIES, 2-14-56

15. NASA SP-8007

16. NASA SP-8019

17. NASA SP-8032

18. BRUSH AND ALMROTH, BUCKLING OF BARS, PLATES AND SHELLS.

19. GENERAL DYNAMICS/ASTRONAUTICS. GD/A-DDG 64-024A, POST-BUCKLING STRENGTH OF A PRESSURIZED CYLINDER 1964

20. GENERAL DYNAMICS CONVAIR, GDC-DDG-67-006. VOL VI

21. MIL-STD-29A, SPRINGS MECHANICAL; DRAWING REQUIREMENTS FOR 3.1.62

22. CONSOLIDATED VULTEE, ZS-202, FATIGUE DATA BOOK PART IV STRESS CONCENTRATIONS, 1.12.54

23. AFFDL-TR-69-42, STRESS ANALYSIS MANUAL, 4.30.69

24. MCDONNELL DOUGLAS DC-10 STRESS MANUAL, 4-1-68.

25. GENERAL DYNAMICS, GDSS-TC-87-010

26. LAUGHNER AND HARGAN, HANDBOOK OF FASTENING AND JOINING OF METAL PARTS.

27. AFFDL-TR-67-140, DESIGN CRITERIA FOR THE PREDICTION AND PREVENTION OF PANEL FLUTTER JAN. 1968

28. MIL-HDBK-5E, METALLIC MATERIALS AND ELEMENTS FOR AEROSPACE VEHICLE STRUCTURES. 9.15.76

29. PERRY, ADHESIVE BONDING OF REINFORCED PLASTICS, 1959

30. GENERAL DYNAMICS CONVAIR, GDC-BTD65-168, DESIGN ALLOWABLES FOR CENTAUR STRUCTURAL MATERIALS, 2/1/66.

31. GENERAL DYNAMICS ASTRONAUTICS, ZS-7-002, STRESS ANALYSIS REPORT STANDARDS, 8/14/63.

32. GENERAL DYNAMICS, CASD-SSO-76-021, ANALYSIS OF BLADE STIFFENED INTEGRALLY MACHINED PANELS, SPACE SHUTTLE ORBITER MID-FUSELAGE, 10/5/76.

33. GENERAL DYNAMICS CASD-SSO-76-007, ANALYSIS OF T-STIFFENED INTEGRALLY MACHINED PANELS, SPACE SHUTTLE ORBITER MID-FUSELAGE, 2/5/76.

34. GENERAL DYNAMICS CASD-SSO-76-016, "HONEYCOMB SANDWICH PANEL ANALYSIS METHOD, SPACE SHUTTLE ORBITER MID-FUSELAGE", W. S. BUSSEY JR., 22 JULY 1976.

35. E. F. BRUHN, J. I. ORLANDO, J. F. MEYERS, "ANALYSIS AND DESIGN OF MISSILE STRUCTURE", TRI-STATE OFFSET COMPANY, CINICINNATI, OHIO.

36. STRESS ANALYSIS MANUAL, AIR FORCE FLIGHT DYNAMICS LABORATORY, WRIGHT-PATTERSON AIR FORCE BASE, 1969.

37. GERALD, G. AND BECKER, H., HANDBOOK OF STRUCTURAL STABILITY, PART I- BUCKLING OF FLAT PLATES, NACA TN 3781, 1957.

38. BECKER, H., HANDBOOK OF STRUCTURAL STABILITY, PART II- BUCKLING OF COMPOSITE ELEMENTS, NACA TN 3782,1957.

39. SMITH, G. W., ANALYSIS OF MULTIPLE DISCONTINUITIES IN SHELLS, REPORT NO. AE61-0179, 1 MARCH 1961.

2

40. MIL-HDBK-17A MILITARY HANDBOOK, PLASTICS FOR AEROSPACE VEHICLES.

41. GDSS MEMO NUMBER 883-0-86-099, 30 OCTOBER 1986.

SECTION 2.0

SECTION PROPERTIES

METHODS FOR CALCULATING SECTION PROPERTIES AND THE SHEAR CENTER ARE PRESENTED, TOGETHER WITH DATA TABLES AND CURVES FOR THE MORE COMMONLY USED SHAPES.

		PAGE
2.1	GEOMETRICAL SHAPES	2.1.1
2.2	CIRCLES	2.2.1
2.3	90° BENDS	2.3.1
2.4	ANGLES	2.4.1
2.5	CENTROID OF TRAPEZOID	2.5.1
2.6	SHEAR CENTER	2.6.1
2.7	MOMENT OF INERTIA SAMPLE CALCULATION	2.7.1

Data Source, Section 1.3 Reference 1

2.0.0 SECTION PROPERTIES

2.1.0 Plane Sections

2.1.1 Areas, Centroids, Moments of Inertia, Products of Inertia, Radii of Gyration

Moment of Inertia

The moment of inertia, or the second moment of area, of an element of area, such as (dA) in Fig. 2.1.1-1, with respect to a given axis is defined as the product of the area of the element and the square of the distance from the axis to the element. For example,

$$dI_y = x^2 dA \quad . . . . \quad (1)$$

The sum of the moments of inertia of all the elements in the area is defined as the moment of inertia of the area; that is,

$$I_y = \int x^2 dA \quad . . . \quad (2)$$

and,

$$I_x = \int y^2 dA \quad . . . \quad (3)$$

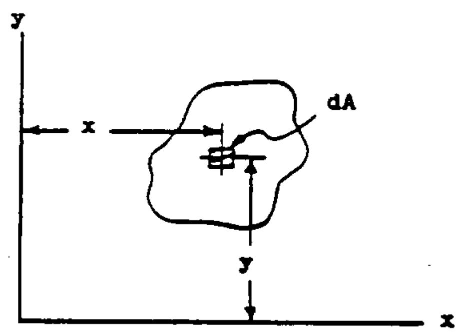

Fig. 2.1.1-1

where the subscripts (x) and (y) indicate the axis about which the moment of inertia is taken.

The moment of inertia of any area about any axis is equal to the moment of inertia of the area about an axis through the centroid of the area and parallel to the given axis plus the product of the area and the square of the distance between the two parallel axes; that is,

$$I_x = I_c + (\bar{y})^2 A \quad . . \quad (4)$$

as shown in Fig. 2.1.1-2 .

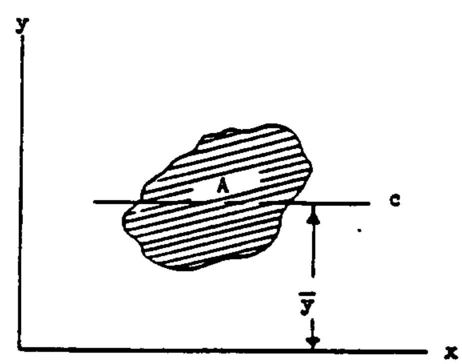

Fig. 2.1.1-2

Many plane areas can be divided into elementary shapes, such as rectangles, triangles, etc., for each of which an expression for I_o is known or can be obtained from tables. In such cases no integration is necessary to calculate the moment of inertia of the given area with respect to any axis.

The sum of the moments of inertia of the component parts of a composite section is equal to its moment of inertia. Voids are taken into account by subtracting the moment of inertia of the corresponding area.

Example. Using $I_o = bd^3/36$ for a triangle and $I_o = bd^3/12$ for a rectangle, calculate the moment of inertia of the area shown in Fig. 2.1.1-3 with respect to its horizontal centroidal axis.

Solution: The area will be divided into a triangle and a rectangle by the line (axis 1-1) shown. The distance from this line to the centroidal axis of the whole area is

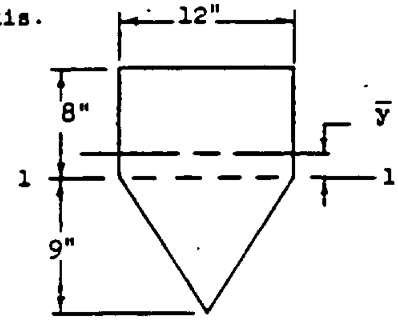

Fig. 2.1.1-3

$$\bar{y} = \frac{(8x12x8/2)-(12/2x9x9/3)}{(8x12) + (12/2x9)} = \frac{384-162}{96+54} = \frac{222}{150} = \underline{1.48 \text{ in.}}$$

The plus sign indicates that the centroid is above the axis, 1-1.

For the triangle, $I = \frac{1}{36} bd^3 = \frac{12x9x9x9}{36}$ . . . . . . = 243 in.^{4}

to "transfer" to the centroidal axis, add $Ad^2 = 54x4.48^2 = 1,086$

For the rectangle, $I = \frac{1}{12} bd^3 = \frac{12x8x8x8}{12}$ . . . . = 512

to "transfer" to the centroidal axis, add $Ad^2 = 96x2.52^2 =$ $\underline{609}$

Therefore, I_o for the whole area . . . . = 2,450 in.^{4}

Product of Inertia

The product of inertia of any elementary area, such as (dA) in Fig. 2.1.1-1, about any two mutually perpendicular axes is defined as the product of the area of the element and the distances to the axes; that is

$$dI_{xy} = xydA \quad . . . . \quad (5)$$

The product of inertia of the entire area is the sum of the products of inertia of all the elements. Thus,

$$I_{xy} = \int xy \, dA \quad . . . . . \quad (6)$$

When either or both the axes is an axis of symmetry, the product of inertia is zero.

The product of inertia may be transferred by the following equation:

$$I_{xy} = I_{x_o y_o} + A \bar{x} \bar{y} \qquad (7)$$

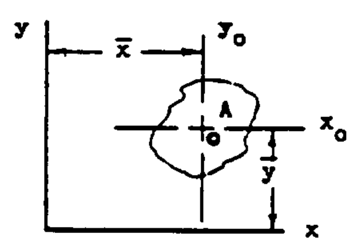

Fig. 2.1.1-4

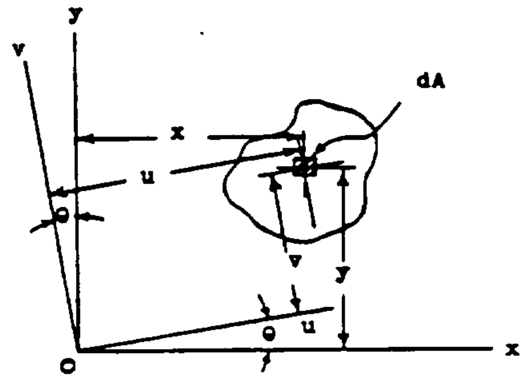

Fig. 2.1.1-5

Principal Moments of Inertia and the Location of the Principal Axes

The maximum and minimum moments of inertia of an area about an axis through a given point are called the principal moments of inertia and the axes are called the principal axes. Consider the axes in Fig. 2.1.1-5, where (x) and (y) are arbitrary axes through the point (o), and (v) and (u) are the principal axes through (o). Then,

$$I_u = I_x \cos^2 \theta - I_{xy} \sin 2\theta + I_y \sin^2 \theta \quad (8)$$

$$I_v = I_x \sin^2 \theta + I_y \cos^2 \theta + I_{xy} \sin 2\theta \quad (9)$$

$$I_{uv} = \frac{(I_x - I_y)}{2} \sin 2\theta + I_{xy} \cos 2\theta \quad (10)$$

The principal axes are at an angle (θ) with the arbitrary axis, and,

$$\tan 2\theta = \frac{2I_{xy}}{I_y - I_x} \quad (11)$$

The solution of (θ) from Equation (No. 11) yields two values 90° apart, one corresponding to the maximum moment of inertia and the other corresponding to the minimum moment of inertia. Substitution of these values of (θ) into Equations (No. 8) and (No. 9) gives the following equations for the principal moments of inertia:

$$I_u = \frac{I_x + I_y}{2} + \sqrt{I_{xy}^2 + \left(\frac{I_x - I_y}{2}\right)^2} \quad (12)$$

$$I_v = \frac{I_x + I_y}{2} - \sqrt{I_{xy}^2 + \left(\frac{I_x - I_y}{2}\right)^2} \quad (13)$$

It should be noted that the product of inertia of an area about the principal axes is zero; therefore, if an area has an axis of symmetry, such axis is one of the principal axes of inertia.

Radius of Gyration

The radius of gyration of an area about an inertia axis is defined as the distance from the inertia axis to that point at which the total given area would have to be concentrated to give the same moment of inertia. Thus,

$$k_x = \sqrt{\frac{I_x}{A}} \quad (14)$$

$$k_y = \sqrt{\frac{I_y}{A}} \quad (15)$$

2

TABLE 2.1.1.1

PROPERTIES FOR VARIOUS GEOMETRIC SHAPES

Form Of Section	Area (A)	Distance To Centroid	Moment And Product Of Inertia	Radius of Gyration
CIRCLE 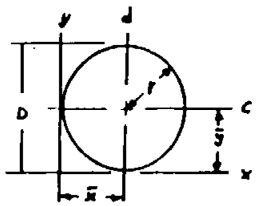	$A = \pi r^2 = \frac{\pi}{4} D^2$	$\bar{x} = \bar{y} = \frac{D}{2} = r$	$I_c = I_d = \frac{\pi}{64} D^4 = \frac{\pi}{4} r^4$ $I_x = I_y = \frac{5}{4} \pi r^4$ $I_{xy} = \pi r^4$	$k_c = k_d = \frac{D}{4} = \frac{r}{2}$ $k_x = k_y = 1.118 r$
SEMI-CIRCLE 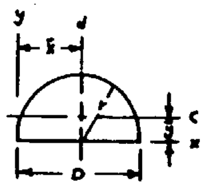	$A = \frac{\pi}{2} r^2$	$\bar{y} = \frac{4r}{3\pi}$ $\bar{x} = r$	$I_c = r^4 \left[\frac{\pi}{8} - \frac{8}{9\pi}\right]$ $I_d = .3927 r^4$ $I_x = .3927 r^4$ $I_{xy} = \frac{2r^4}{3}$	$k_c = .2643r$ $k_d = .50r$ $k_x = .50r$
QUARTER CIRCLE 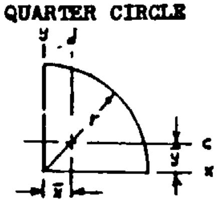	$A = .7854 r^2$	$\bar{x} = \bar{y} = .4244r$	$I_c = I_d = .0549 r^4$ $I_x = I_y = .1964 r^4$	
HOLLOW CIRCLE 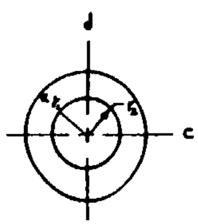	$A = \pi(r_1^2 - r_2^2)$		$I_c = I_d = \frac{\pi}{4}(r_1^4 - r_2^4)$ $I_{xy} = \pi r_1^2 (r_1^2 - r_2^2)$ Note: Use The Following Approximate Formula As $(r_1 - r_2) = t \to 0$ $I_c = \pi \left(\frac{r_1 - r_2}{2}\right)^3 t$ Error $<$ 1% For $\frac{D}{t} > 11$	$k_c = .354(r_1 + r_2)$ Error $<$ 1% For $\frac{D}{t} > 8$

TABLE 2.1.1.1a

PROPERTIES FOR VARIOUS GEOMETRIC SHAPES

Form Of Section	Area (A)	Distance To Centroid	Moment And Product Of Inertia	Radius of Gyration
SECTOR OF CIRCULAR SHELL 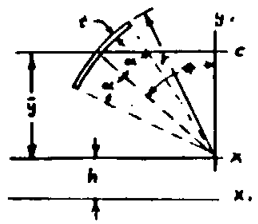	$A = 2rt\alpha$	$\bar{y} = \frac{r \sin\alpha \cos\theta}{\alpha}$	$I_c = r^3 t\left[\alpha + \frac{1}{2}\sin 2\alpha \cos 2\theta - \frac{2}{\alpha}\sin^2\alpha \cos^2\theta\right]$ $I_x = \frac{r^3 t}{2}(2\alpha + \sin 2\alpha \cos 2\theta)$ $I_{x_1} = rt\left[2\alpha(h^2 + \frac{r^2}{2}) + \frac{r^2}{2}\sin 2\alpha \cos 2\theta + 4hr \sin\alpha \cos\theta\right]$	
SEMI-CIRCULAR SHELL 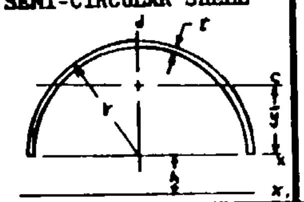	$A = \pi rt$	$\bar{y} = \frac{2r}{\pi}$	$I_c = \pi r^3 t(\frac{1}{2} - \frac{4}{\pi^2})$ $I_x = \frac{\pi r^3 t}{2}$ $I_{x_1} = rt(\frac{\pi r^2}{2} + 4hr + \pi h^2)$	
CIRCULAR SHELL 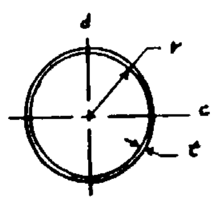	$A = 2\pi rt$		$I_c = \pi r^3 t$	$k = .707r$
HOLLOW SEMI-CIRCLE 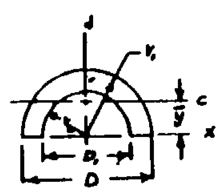	$A = \frac{\pi}{2}(r_1^2 - r_2^2)$	$\bar{y} = \frac{4(r_1^3 - r_2^3)}{3\pi(r_1^2 - r_2^2)}$	$I_c = \frac{\pi}{8}(r_1^4 - r_2^4) - \frac{8(r_1^3 - r_2^3)^2}{9\pi(r_1^2 - r_2^2)}$ $I_x = \frac{\pi}{8}(r_1^4 - r_2^4)$	$k_x = \sqrt{\frac{r_1^2 + r_2^2}{2}}$

TABLE 2.1.1.1b

PROPERTIES FOR VARIOUS GEOMETRIC SHAPES

Form Of Section	Area (A)	Distance To Centroid	Moment And Product Of Inertia	Radius Of Gyration
HOLLOW ELLIPSE 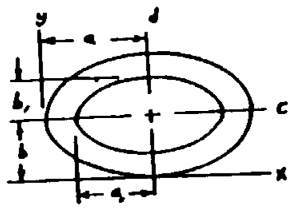	$A = \pi(ab - a_1 b_1)$		$I_c = \frac{\pi}{4}(ab^3 - a_1 b_1^3)$ $I_d = \frac{\pi}{4}(a^3 b - a_1^3 b_1)$ $I_{xy} = \pi ab(ab - a_1 b_1)$	$k_c = \frac{1}{2}\sqrt{\frac{ab^3 - a_1 b_1^3}{ab - a_1 b_1}}$ $k_d = \frac{1}{2}\sqrt{\frac{a^3 b - a_1^3 b_1}{ab - a_1 b_1}}$
HOLLOW-SEMI ELLIPSE 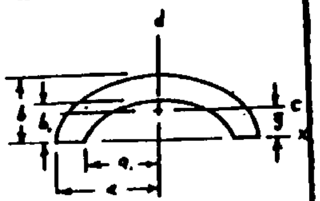	$A = \frac{\pi}{2}(ab - a_1 b_1)$	$\bar{y} = .424\left(\frac{ab^2 - a_1 b_1^2}{ab - a_1 b_1}\right)$	$I_c = \frac{\pi}{2}\left[\frac{ab^3 - a_1 b_1^3}{4} - \frac{.1798(ab^2 - a_1 b_1^2)^2}{ab - a_1 b_1}\right]$ $I_x = \frac{\pi}{8}(ab^3 - a_1 b_1^3)$	$k_c = \sqrt{\frac{I_c}{A}}$
UNEQUAL ANGLE 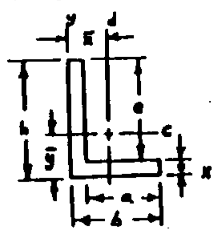	$A = t(b+e)$	$\bar{x} = \frac{t(2a+h)+a^2}{2(a+h)}$ $\bar{y} = \frac{t(b+2e)+e^2}{2(b+e)}$	$I_c = \frac{t(h-\bar{y})^3 + b\bar{y}^3 - a(\bar{y}-t)^3}{3}$ $I_d = \frac{t(b-\bar{x})^3 + h\bar{x}^3 - e(\bar{x}-t)^3}{3}$ $I_{cd} = \pm\frac{abeht}{4(b+e)}$	$k = \sqrt{\frac{I}{A}}$
CHANNEL 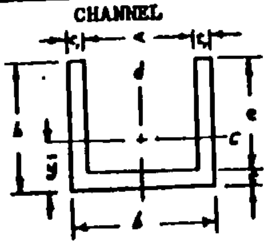	$A = 2ht_1 + at$	$\bar{y} = \frac{h^2 t_1 + \frac{1}{2}t^2 a}{2ht_1 + at}$	$I_c = \frac{2t_1 h^3 + at^3}{3} - \frac{(h^2 t_1 + \frac{1}{2}t^2 a)^2}{2ht_1 + at}$ $I_d = \frac{hb^3 - ea^3}{12}$	

TABLE 2.1.1.1c

PROPERTIES FOR VARIOUS GEOMETRIC SHAPES

Form Of Section	Area (A)	Distance To Centroid	Moment And Product Of Inertia	Radius Of Gyration
CIRCULAR SEGMENT 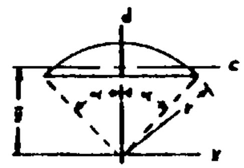	$A = r^2\left(\alpha - \frac{\sin 2\alpha}{2}\right)$	$\bar{y} = \frac{2r^3\sin^3\alpha}{3A}$	$I_c = \frac{Ar^2}{4}\left(1 + \frac{2\sin^3\alpha\cos\alpha}{\alpha - \sin\alpha\cos\alpha} - \frac{16r^4\sin^6\alpha}{9A^2}\right)$ $I_d = \frac{Ar^2}{4}\left[1 - \frac{2\sin^3\alpha\cos\alpha}{3(\alpha - \sin\alpha\cos\alpha)}\right]$	$k = \sqrt{\frac{I}{A}}$
CIRCULAR SECTOR 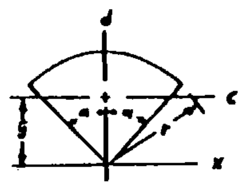	$A = r^2\alpha$	$\bar{y} = \frac{2r\sin\alpha}{3\alpha}$	$I_c = \frac{Ar^2}{4}\left(1 + \frac{\sin\alpha\cos\alpha}{\alpha} - \frac{16\sin^2\alpha}{9\alpha^2}\right)$ $I_d = \frac{Ar^2}{4}\left(1 - \frac{\sin\alpha\cos\alpha}{\alpha}\right)$	$k = \sqrt{\frac{I}{A}}$
HOLLOW CIRCULAR SECTOR 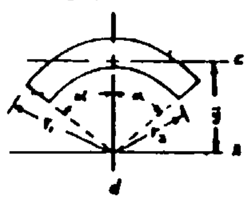	$A = \alpha(r_1^2 - r_2^2)$	$\bar{y} = \frac{2\sin\alpha(r_1^3 - r_2^3)}{3\alpha(r_1^2 - r_2^2)}$	$I_x = \frac{(r_1^4 - r_2^4)(2\alpha + \sin 2\alpha)}{8}$ Note: Use The Following Approx. Formula As $(r_1 - r_2) = t \to 0$ $\bar{y} = \frac{\sin\alpha}{\alpha}\left(\frac{r_1 + r_2}{2}\right)$ Error $<1\%$ For $\frac{D}{t} > 7$ $I_x = \left(\frac{r_1 + r_2}{2}\right)^3 \frac{t}{2}(2\alpha + \sin 2\alpha)$ Error $<1\%$ For $\frac{D}{t} > 11$	$k_x = \sqrt{\frac{(r_1^2 + r_2^2)(2\alpha + \sin 2\alpha)}{8\alpha}}$
CIRCULAR COMPLEMENT 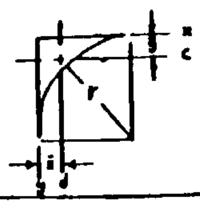	$A = 0.2146r^2$	$\bar{x} = \bar{y} = 0.2234r$	$I_c = I_d = 0.007545r^4$ $I_x = I_y = 0.0182r^4$	$k_c = k_d = 0.187r$ $k_x = k_y = 0.292r$

TABLE 2.1.1.1d

PROPERTIES FOR VARIOUS GEOMETRIC SHAPES

Form Of Section	Area (A)	Distance To Centroid	Moment And Product Of Inertia	Radius Of Gyration
ELLIPSE 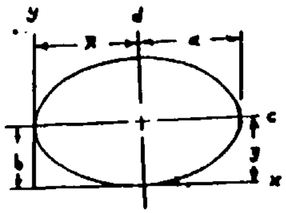	$A = \pi ab$	$\bar{x} = a$ $\bar{y} = b$	$I_c = 0.7854\ ab^3$ $I_d = 0.7854\ ba^3$ $I_{xy} = \pi a^2b^2$ $I_x = \frac{5}{4}\pi ab^3$	$k_c = \frac{b}{2}$ $k_d = \frac{a}{2}$ $k_x = 1.118b$
HALF ELLIPSE 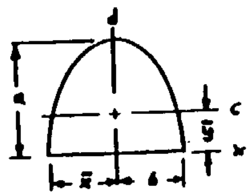	$A = 1.5708\ ab$	$\bar{x} = b$ $\bar{y} = 0.4244a$	$I_c = 0.1098\ a^3b$ $I_d = 0.3927\ ab^3$ $I_x = 0.3927\ a^3b$	
QUARTER ELLIPSE 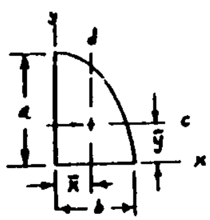	$A = 0.7854\ ab$	$\bar{y} = 0.4244a$ $\bar{x} = 0.4244b$	$I_c = 0.05488\ a^3b$ $I_d = 0.05488\ b^3a$ $I_x = 0.1963\ a^3b$	
ELLIPTIC COMPLEMENT 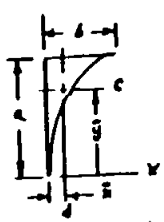	$A = 0.2146\ ab$	$\bar{y} = 0.7766a$ $\bar{x} = 0.7766b$	$I_c = 0.00754\ a^3b$ $I_d = 0.00754\ ab^3$	

TABLE 2.1.1.1e

PROPERTIES FOR VARIOUS GEOMETRIC SHAPES

Form of Section	Area (A)	Distance To Centroid	Moment And Product Of Inertia	Radius of Gyration
OBLIQUE FILLET 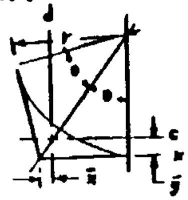	$A = (\tan\theta - \theta) r^2$	$\bar{y} = r\left[1 - \frac{\sin^2\theta\tan\theta}{3(\tan\theta-\theta)}\right]$ $\bar{x} = r\left[\tan\theta - \frac{\sin^2\theta\tan^2\theta}{3(\tan\theta-\theta)}\right]$	$I_c = r^4\left[\frac{\sin^5\theta}{3\cos\theta} + \frac{\sin\theta\cos\theta(1+2\sin^2\theta)-\theta}{4} - \frac{\sin^4\theta\tan^2\theta}{9(\tan\theta-\theta)}\right]$ $I_d = r^4\left[\frac{\tan^3\theta(1+\cos^2\theta)}{6} - \frac{3\theta-\sin\theta\cos\theta(3-2\sin^2\theta)}{12} - \frac{\sin^4\theta\tan^4\theta}{9(\tan\theta-\theta)}\right]$	
PARABOLA 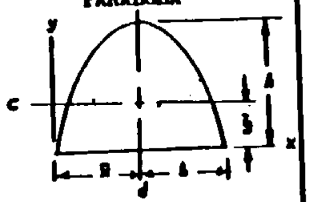	$A = \frac{4}{3} hb$	$\bar{x} = b$ $\bar{y} = 0.40h$	$I_c = 0.09143\ bh^3$ $I_d = 0.2667\ hb^3$ $I_x = 0.3048\ bh^3$	$k_c = 0.2619h$ $k_d = 0.4472b$
HALF PARABOLA 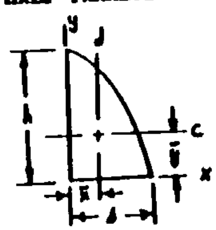	$A = \frac{2}{3} hb$	$\bar{y} = 0.40h$ $\bar{x} = 0.375b$	$I_c = 0.04571\ bh^3$ $I_d = 0.03958\ hb^3$ $I_x = 0.15238\ bh^3$	$k_c = 0.2619h$ $k_d = 0.2437b$
COMPLEMENT OF HALF PARABOLA 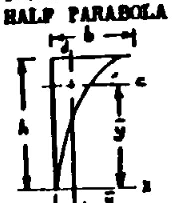	$A = \frac{1}{3} hb$	$\bar{y} = 0.70h$ $\bar{x} = 0.25b$	$I_c = 0.01762\ bh^3$ $I_d = 0.0125\ hb^3$	$k_c = .2299h$ $k_d = .1937b$

TABLE 2.1.1.1f

PROPERTIES OF VARIOUS GEOMETRIC SHAPES

Form Of Section	Area (A)	Distance To Centroid	Moment And Product Of Inertia	Radius Of Gyration
RECTANGLE 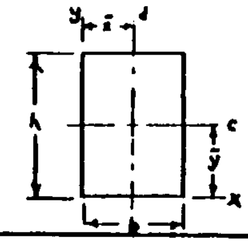	$A = bh$	$\bar{x} = \frac{b}{2}$ $\bar{y} = \frac{h}{2}$	$I_d = \frac{hb^3}{12}$ $I_x = \frac{bh^3}{3}$ $I_c = \frac{bh^3}{12}$ $I_{xy} = \frac{b^2h^2}{4}$	$k_d = 0.2887b$ $k_c = 0.2887h$ $k_x = 0.5773h$
RECTANGLE 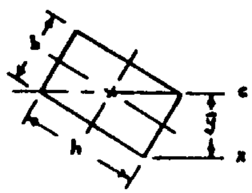	$A = bh$	$\bar{y} = \frac{bh}{\sqrt{b^2+h^2}}$	$I_c = \frac{b^3h^3}{6(b^2+h^2)}$	$k_c = \frac{bh}{\sqrt{6(b^2+h^2)}}$
RECTANGLE 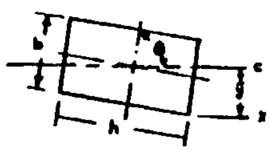	$A = bh$	$\bar{y} = \frac{b\sin\theta + h\cos\theta}{2}$	$I_c = \frac{bh(b^2\sin^2\theta + h^2\cos^2\theta)}{12}$	$k_c = \sqrt{\frac{b^2\sin^2\theta + h^2\cos^2\theta}{12}}$
HOLLOW RECTANGLE 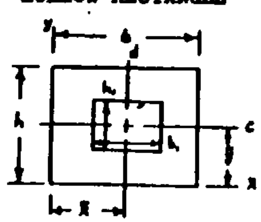	$A = bh - b_1h_1$	$\bar{x} = \frac{1}{2}b$ $\bar{y} = \frac{1}{2}h$	$I_c = \frac{bh^3 - b_1h_1^3}{12}$ $I_d = \frac{hb^3 - h_1b_1^3}{12}$ $I_x = \frac{bh^3}{3} - \frac{b_1h_1}{12}(3h^2 + h_1^2)$ $I_{xy} = \frac{bh(bh - b_1h_1)}{4}$	$k_c = \sqrt{\frac{bh^3 - b_1h_1^3}{12(bh - b_1h_1)}}$ $k_d = \sqrt{\frac{hb^3 - h_1b_1^3}{12(hb - h_1b_1)}}$

TABLE 2.1.1.1g
PROPERTIES OF VARIOUS GEOMETRIC SHAPES

Form Of Section	Area (A)	Distance To Centroid	Moment And Product Of Inertia	Radius Of Gyration
ISOSCELES TRIANGLE 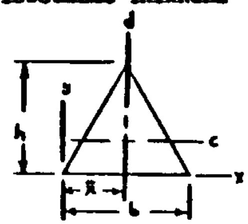	$A = \frac{1}{2}bh$	$\bar{x} = \frac{1}{2}b$ $\bar{y} = \frac{1}{3}h$	$I_c = \frac{bh^3}{36}$ $I_x = \frac{bh^3}{12}$ $I_d = \frac{b^3h}{48}$	$k_c = .236h$ $k_d = .204b$ $k_x = .408h$
OBLIQUE TRIANGLE 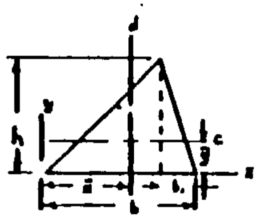	$A = \frac{1}{2}bh$	$\bar{x} = \frac{1}{3}(2b-b_1)$ $\bar{y} = \frac{1}{3}h$	$I_c = \frac{bh^3}{36}$ $I_d = \frac{bh}{36}(b^2-bb_1+b_1^2)$ $I_x = \frac{bh^3}{12}$	$k_c = .236h$ $k_x = .408h$
OBTUSE TRIANGLE 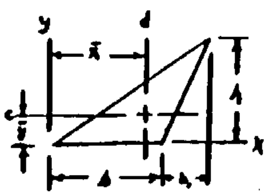	$A = \frac{1}{2}bh$	$\bar{x} = \frac{2b+b_1}{3}$ $\bar{y} = \frac{1}{3}h$	$I_c = \frac{bh^3}{36}$ $I_d = \frac{bh}{36}(b^2+bb_1+b_1^2)$ $I_x = \frac{bh^3}{12}$	$k_c = .236h$ $k_d = .236\sqrt{b^2+b_1^2+bb_1}$ $k_x = .408h$
ISOSCELES TRAPEZOID 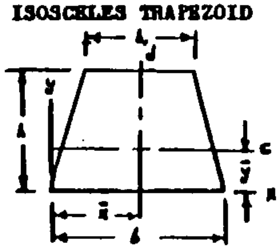	$A = \frac{1}{2}h(b+b_1)$	$\bar{x} = \frac{1}{2}b$ $\bar{y} = \frac{h(2b_1+b)}{3(b+b_1)}$	$I_c = \frac{h^3(b^2+4bb_1+b_1^2)}{36(b+b_1)}$ $I_x = \frac{h^3(b+3b_1)}{12}$ $I_d = \frac{h}{48}(b_1^3+b^3+b^2b_1+bb_1^2)$	$k = \sqrt{\frac{I}{A}}$

TABLE 2.1.1.1 h

PROPERTIES OF VARIOUS GEOMETRICAL SHAPES

Data Source, Section 1.3 Reference 3

DOUBLE WEDGE SECTION

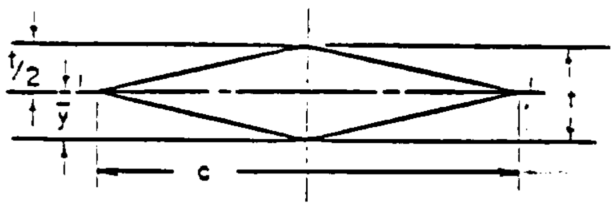

$$A = \frac{ct}{2}$$

$$\bar{y} = \frac{t}{2}$$

$$I_{1-1} = \frac{ct^3}{48} = .0208\, ct^3$$

$$\frac{I_{1-1}}{y} = \frac{ct^2}{24} = .0416\, ct^2$$

BI – CONVEX SECTION

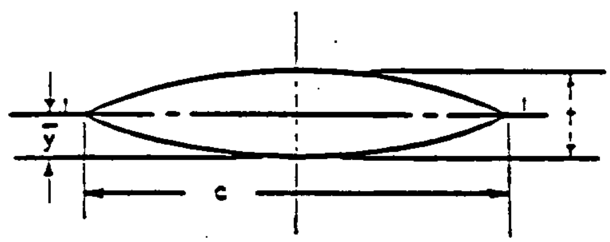

$$A = \frac{2}{3}\, ct$$

$$\bar{y} = \frac{t}{2}$$

$$I_{1-1} = \frac{4}{105}\, ct^3 = .0381\, ct^3$$

$$\frac{I_{1-1}}{y} = \frac{8ct^2}{105} = .0761\, ct^2$$

VALUES OF A AND I ARE BASED ON BI – PARABOLIC SECTION. ERROR IS NEGLIGIBLE WHEN $t/c < 0.10$.

SECTION PROPERTIES OF CIRCULAR SEGMENTS ABOUT y-y AXIS

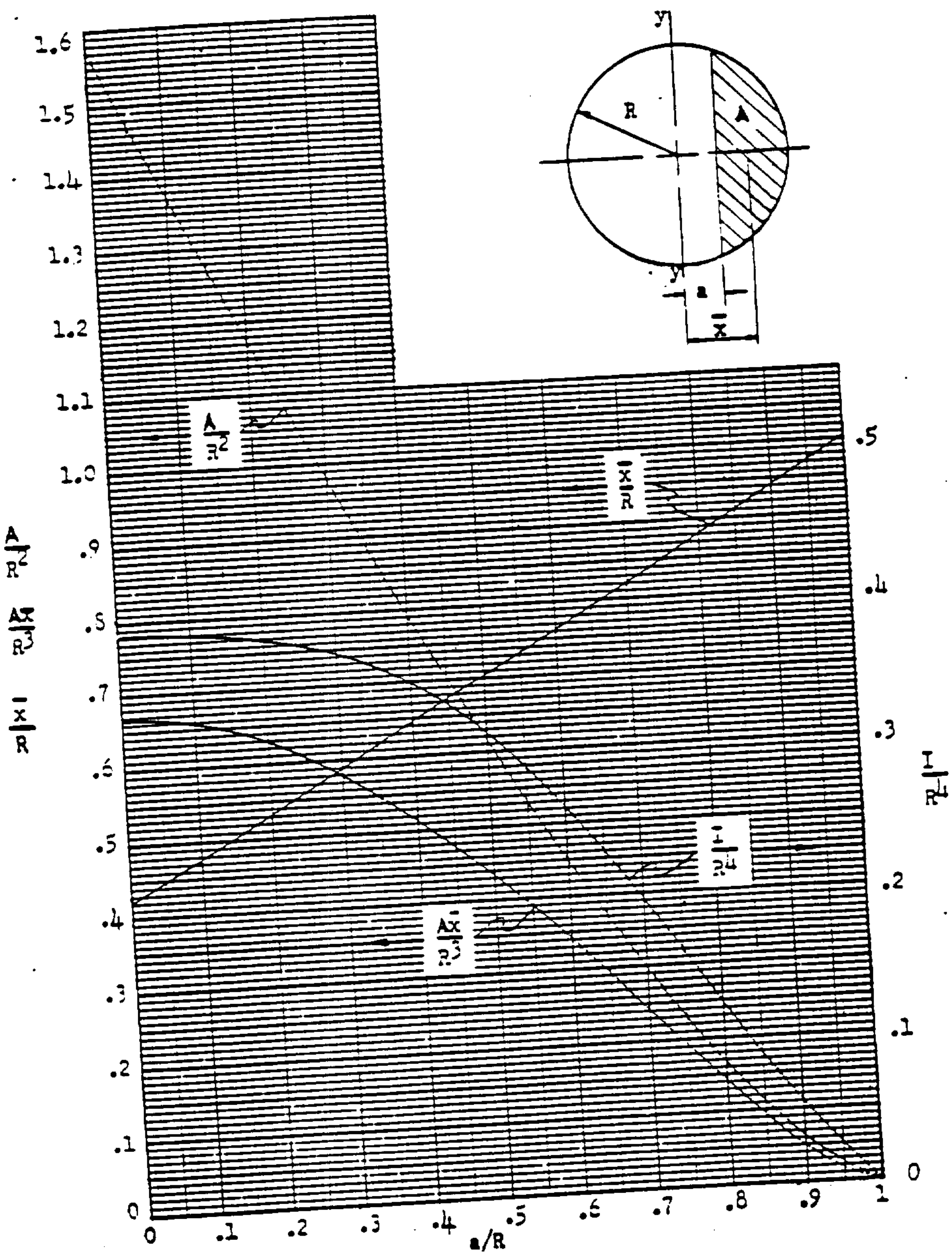

ECCENTRIC TUBULAR SECTIONS

$$\frac{I_{NA}}{I_{xx}} = 1 - 4\left(\frac{e}{t}\right)^2 \frac{1}{\left(\frac{1}{N}+1\right)^2\left(1+N^2\right)}$$

$$\frac{\bar{y}}{e} = \frac{1}{\left(\frac{1}{N}\right)^2 - 1}$$

$$t = \frac{D-d}{2} \qquad N = \frac{d}{D}$$

I_{xx} calculated for $e = 0$

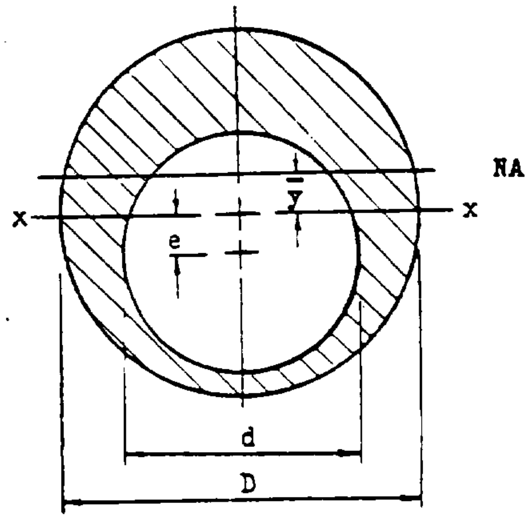

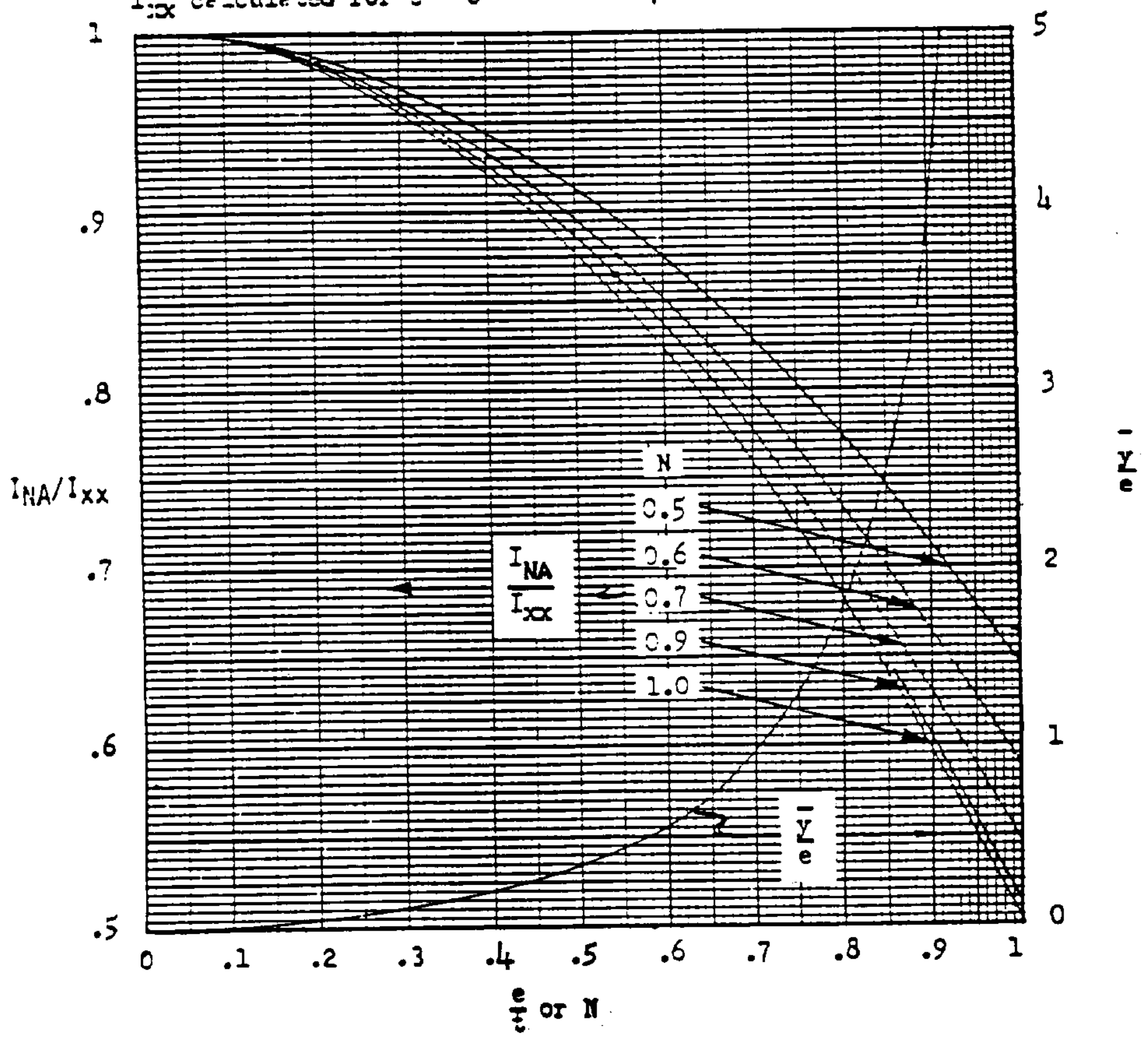

Data Source, Section 1.3 Reference 1

TABLE 2.1.1.5

PROPERTIES OF CIRCLES

DIAMETER (IN.)		AREA	MOMENT OF	CIRCUMFERENCE	RADIUS OF
FRACTION	DECIMAL	(SQ. INCHES)	INERTIA (I)	(INCHES)	GYRATION (k)
3/16	.1875	.02761	6.066×10^{-5}	.5891	.0469
13/64	.2031	.03241	8.358×10^{-5}	.6381	.0508
7/32	.2188	.03758	.0001125	.6872	.0547
15/64	.2344	.04314	.0001481	.7363	.0586
1/4	.2500	.04909	.0001918	.7854	.0625
9/32	.2813	.06213	.0003072	.8836	.0703
5/16	.3125	.07670	.0004682	.9818	.0781
11/32	.3438	.09281	.0006854	1.0799	.0860
3/8	.3750	.1105	.0009710	1.1781	.0938
13/32	.4063	.1296	.001337	1.2763	.1016
7/16	.4375	.1503	.001798	1.3744	.1094
15/32	.4688	.1726	.002370	1.4726	.1172
1/2	.5000	.1964	.003068	1.5708	.1250
17/32	.5313	.2217	.003910	1.6690	.1328
9/16	.5625	.2485	.004914	1.7671	.1406
19/32	.5938	.2769	.006101	1.8653	.1485
5/8	.6250	.3068	.007490	1.9635	.1563
21/32	.6563	.3382	.009104	2.0617	.1641
11/16	.6875	.3712	.01097	2.1598	.1719
23/32	.7188	.4057	.01310	2.2580	.1797
3/4	.7500	.4418	.01553	2.3562	.1875
25/32	.7813	.4794	.01829	2.4544	.1953
13/16	.8125	.5185	.02139	2.5525	.2031
27/32	.8438	.5591	.02488	2.6507	.2110
7/8	.8750	.6013	.02878	2.7489	.2188
29/32	.9063	.6450	.03311	2.8471	.2246
15/16	.9375	.6903	.03792	2.9452	.2344
31/32	.9688	.7371	.04323	3.0434	.2422
1	1.0000	.7854	.04908	3.1416	.2500
1 1/16	1.0625	.8866	.06256	3.3380	.2656
1 1/8	1.1250	.9940	.07863	3.5343	.2813
1 3/16	1.1875	1.1075	.09761	3.7307	.2969
1 1/4	1.2500	1.2272	.1198	3.9270	.3125
1 5/16	1.3125	1.3530	.1457	4.1234	.3281
1 3/8	1.3750	1.4849	.1755	4.3197	.3438
1 7/16	1.4375	1.6230	.2096	4.5161	.3594
1 1/2	1.5000	1.7671	.2485	4.7124	.3750
1 9/16	1.5625	1.9175	.2926	4.9088	.3906
1 5/8	1.6250	2.0739	.3423	5.1051	.4063
1 11/16	1.6875	2.2365	.3980	5.3015	.4219
1 3/4	1.7500	2.4053	.4603	5.4978	.4375
1 13/16	1.8125	2.5802	.5298	5.6942	.4531
1 7/8	1.8750	2.7612	.6067	5.8905	.4688
1 15/16	1.9375	2.9483	.6917	6.0869	.4844
2	2.0000	3.1416	.7854	6.2832	.5000

TABLE 2.1.1.5

PROPERTIES OF CIRCLES (Cont'd)

DIAMETER (IN.)		AREA	MOMENT OF	CIRCUMFERENCE	RADIUS OF
FRACTION	DECIMAL	(SQ. INCHES)	INERTIA (I)	(INCHES)	GYRATION (k)
2 1/16	2.0625	3.3410	.8883	6.4796	.5156
2 1/8	2.1250	3.5466	1.0009	6.6759	.5313
2 3/16	2.1875	3.7583	1.1240	6.8723	.5469
2 1/4	2.2500	3.9761	1.2580	7.0686	.5625
2 5/16	2.3125	4.2000	1.4038	7.2650	.5781
2 3/8	2.3750	4.4301	1.5618	7.4613	.5938
2 7/16	2.4375	4.6664	1.7328	7.6577	.6094
2 1/2	2.5000	4.9087	1.9175	7.8540	.6250
2 9/16	2.5625	5.1572	2.1165	8.0504	.6406
2 5/8	2.6250	5.4119	2.3307	8.2467	.6563
2 11/16	2.6875	5.6727	2.5607	8.4431	.6719
2 3/4	2.7500	5.9396	2.8074	8.6394	.6850
2 13/16	2.8125	6.2126	3.0714	8.8358	.7031
2 7/8	2.8750	6.4918	3.3537	9.0321	.7188
2 15/16	2.9375	6.7771	3.6549	9.2285	.7344
3	3.0000	7.0686	3.9761	9.4248	.7500
3 1/16	3.0625	7.3662	4.3179	9.6212	.7656
3 1/8	3.1250	7.6699	4.6813	9.8175	.7813
3 3/16	3.1875	7.9798	5.0673	10.0139	.7969
3 1/4	3.2500	8.2958	5.4765	10.2102	.8125
3 5/16	3.3125	8.6179	5.9101	10.4066	.8281
3 3/8	3.3750	8.9462	6.3689	10.6029	.8438
3 7/16	3.4375	9.2806	6.8540	10.7993	.8594
3 1/2	3.5000	9.6211	7.3662	10.9956	.8750
3 9/16	3.5625	9.9678	7.9066	11.1920	.8906
3 5/8	3.6250	10.321	8.4765	11.3883	.9063
3 11/16	3.6875	10.680	9.0764	11.5847	.9219
3 3/4	3.7500	11.045	9.7072	11.7810	.9375
3 13/16	3.8125	11.416	10.371	11.9774	.9531
3 7/8	3.8750	11.793	11.067	12.1737	.9688
3 15/16	3.9375	12.177	11.799	12.3701	.9844
4	4.0000	12.566	12.556	12.5664	1.0000
4 1/8	4.1250	13.364	14.214	12.9591	1.0313
4 1/4	4.2500	14.186	16.025	13.3518	1.0625
4 3/8	4.3750	15.033	17.992	13.7445	1.0938
4 1/2	4.5000	15.904	20.128	14.1372	1.1250
4 5/8	4.6250	16.800	22.550	14.5299	1.1563
4 3/4	4.7500	17.721	25.124	14.9226	1.1875
4 7/8	4.8750	18.666	27.738	15.3153	1.2188
5	5.0000	19.635	30.675	15.7080	1.2500
5 1/8	5.1250	20.629	33.852	16.1006	1.2813
5 1/4	5.2500	21.648	37.321	16.4933	1.3125
5 3/8	5.3750	22.691	40.980	16.8860	1.3438
5 1/2	5.5000	23.758	44.915	17.2787	1.3750

Data Source, Section 1.3 Reference 1

TABLE 2.1.1.6

AREA, CENTROID & MOMENT OF INERTIA OF 90° BENDS

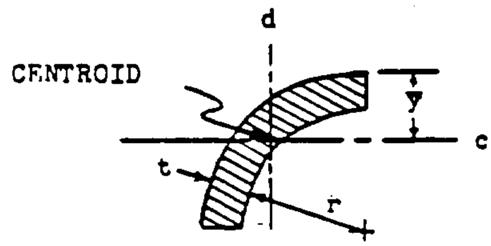

t	r	Area	ȳ	I_c
.012	.03	.00679	.01887	.0889x10^{-6}
	.06	.001244	.0299	.524 "
.016	.03	.000955	.0215	.1446 "
	.06	.001709	.0325	.773 "
.020	.03	.001257	.0240	.219 "
	.06	.00220	.0351	1.071 "
	.09	.00314	.0461	3.05 "
.025	.06	.00285	.0384	1.519 "
	.09	.00403	.0494	4.15 "
	.13	.00560	.0640	10.96 "
.032	.06	.00382	.0429	2.31 "
	.13	.00734	.0686	15.25 "
	.16	.00885	.0797	26.5 "
.040	.06	.00503	.0480	3.50 "
	.09	.00691	.0592	8.55 "
	.13	.00442	.0739	20.9 "
	.22	.01508	.1069	83.7 "
.050	.09	.00903	.0656	12.60 "
	.13	.01217	.0805	29.5 "
	.16	.01453	.0915	49.2 "
	.25	.0216	.1244	157.8 "
.063	.13	.01598	.0889	43.1 "
	.22	.0249	.1221	154.7 "
	.31	.0338	.1550	381 "
.071	.13	.01846	.0940	.532x10^{-4}
	.16	.0218	.1052	.853 "
	.25	.0318	.1383	2.55 "
	.38	.0463	.1859	7.71 "
.080	.13	.0214	.0998	.562 "
	.19	.0289	.1221	1.554 "
	.28	.0402	.1552	4.05 "
	.41	.0565	.203	11.05 "
.090	.13	.0247	.1061	.832 "
	.19	.0332	.1286	1.891 "
	.31	.0502	.1728	6.22 "
	.47	.0728	.231	18.62 "
.100	.16	.0330	.1238	1.566x10^{-4}
	.22	.0424	.1462	3.17 "
	.38	.0675	.205	12.22 "
	.56	.0958	.271	34.3 "
.125	.19	.0496	.1510	3.43 "
	.28	.0672	.1845	8.07 "
	.44	.0987	.243	24.5 "
	.69	.1478	.335	80.6 "
.160	.25	.0829	.1958	9.76 "
	.38	.1156	.244	24.9 "
	.56	.1609	.310	64.8 "
	.88	.241	.427	214 x 10^{-4}
.190	.31	.1209	.237	.00213
	.44	.1597	.286	.00466
	.75	.252	.400	.01757
	1.13	.366	.539	.0527
.250	.50	.245	.347	.00996
	.63	.296	.395	.01707
	1.00	.442	.531	.0545
	1.50	.638	.713	.1619
.313	.63	.387	.436	.0248
	.81	.475	.502	.0447
	1.25	.692	.664	.1335
	2.00	1.060	.738	.473
.375	.75	.552	.520	.0504
	1.00	.670	.613	.0991
	1.50	.994	.796	.276
	2.50	1.583	1.161	1.096
.500	1.00	.982	.694	.1593
	1.50	1.374	.878	.418
	2.00	1.767	1.062	.873
	3.25	2.75	1.518	3.23

Data Source, Section 1.3 Reference 1

TABLE 2.1.1.7

PROPERTIES OF ANGLES

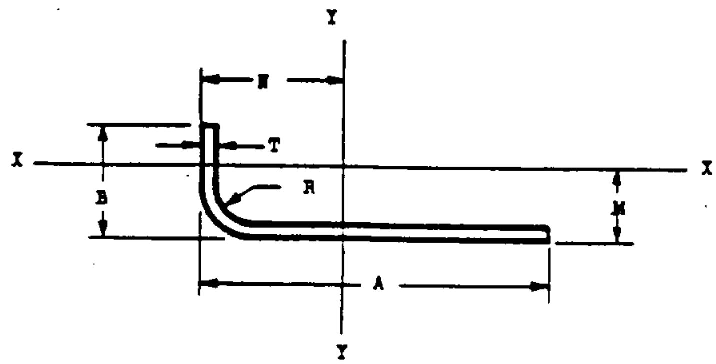

A	B	T	R	AREA	WT/FT	DEVEL WIDTH	M	N	M. INERTIA XX	M. INERTIA YY	RAD. GYR. XX	RAD. GYR. YY
9/16	1/4	.020	1/16	.015	.018	.76	.048	.211	.0001	.0005	.068	.183
		.032	3/32	.023	.028	.73	.054	.221	.0001	.0008	.066	.180
5/8	1/4	.020	1/16	.016	.020	.82	.045	.240	.0001	.0007	.066	.203
		.032	3/32	.025	.031	.76	.051	.250	.0001	.0010	.064	.200
11/16	1/4	.020	1/16	.018	.021	.89	.043	.269	.0001	.0009	.064	.223
		.032	3/32	.028	.033	.86	.049	.279	.0001	.0013	.062	.220
		.040	1/8	.033	.040	.84	.052	.266	.0001	.0016	.062	.216
3/4	5/16	.020	1/16	.020	.024	1.01	.056	.281	.0001	.0012	.064	.245
		.032	3/32	.031	.038	.98	.062	.209	.0002	.0018	.083	.242
		.040	1/8	.038	.046	.96	.066	.299	.0003	.0022	.082	.240
		.051	5/32	.048	.057	.93	.072	.309	.0003	.0027	.081	.237
7/8	5/16	.020	1/16	.023	.027	1.14	.051	.340	.0001	.0018	.081	.285
		.032	3/32	.035	.043	1.11	.056	.350	.0002	.0028	.080	.282
		.040	1/8	.043	.052	1.09	.061	.358	.0003	.0034	.078	.279
		.051	5/32	.054	.065	1.06	.066	.368	.0003	.0041	.077	.276
1	5/16	.020	1/16	.025	.030	1.26	.047	.399	.0002	.0026	.077	.324
		.032	3/32	.039	.047	1.23	.052	.409	.0002	.0041	.076	.321
		.040	1/8	.048	.057	1.21	.057	.418	.0003	.0049	.075	.316
		.051	5/32	.060	.072	1.18	.062	.426	.0003	.0060	.075	.314
1 1/8	5/16	.040	1/8	.053	.064	1.34	.053	.478	.0003	.0068	.073	.356
		.051	5/32	.067	.080	1.31	.050	.489	.0003	.0083	.072	.352
		.064	3/16	.082	.098	1.28	.065	.501	.0004	.0094	.071	.347
1 1/4	5/16	.040	1/8	.058	.070	1.46	.050	.539	.0003	.0091	.071	.394
		.051	5/32	.073	.088	1.43	.056	.550	.0004	.0111	.069	.390
		.064	3/16	.090	.109	1.40	.062	.562	.0004	.0133	.068	.384
		.072	7/32	.099	.119	1.38	.066	.572	.0005	.0144	.068	.380
1 3/8	5/16	.040	1/8	.063	.076	1.50	.048	.600	.0003	.0118	.069	.432
		.051	5/32	.079	.095	1.56	.053	.611	.0004	.0146	.067	.428
		.064	3/16	.098	.118	1.53	.060	.624	.0004	.0174	.066	.422
		.072	7/32	.108	.130	1.51	.054	.634	.0005	.0189	.066	.417
1 1/2	5/16	.040	1/8	.068	.032	1.71	.046	.661	.0003	.0151	.066	.470
		.051	5/32	.086	.103	1.66	.051	.672	.0004	.0186	.065	.465
		.064	3/16	.106	.127	1.65	.058	.685	.0004	.0223	.064	.459
		.072	7/32	.117	.141	1.63	.062	.696	.0005	.0242	.064	.454
1 3/4	3/8	.051	5/32	.102	.122	2.00	.057	.771	.0006	.0306	.079	.548
		.064	3/16	.126	.151	1.97	.063	.784	.0008	.0370	.079	.542
		.072	7/32	.140	.168	1.95	.068	.794	.0009	.0405	.078	.538
		.081	1/4	.155	.186	1.92	.073	.804	.0009	.0441	.078	.533
1 7/8	3/8	.051	5/32	.108	.130	2.12	.055	.833	.0007	.0381	.078	.586
		.064	3/16	.134	.161	2.09	.062	.845	.0008	.0450	.077	.579
		.072	7/32	.149	.179	2.07	.066	.856	.0009	.0493	.076	.575
		.081	1/4	.166	.199	2.05	.071	.866	.0009	.0528	.076	.570
2	1/2	.051	5/32	.121	.145	2.37	.074	.848	.0016	.0490	.114	.636
		.064	3/16	.150	.180	2.34	.080	.860	.0019	.0598	.112	.631
		.072	7/32	.167	.200	2.32	.064	.870	.0021	.0658	.112	.628
		.081	1/4	.186	.223	2.29	.089	.880	.0023	.0723	.111	.624
2 1/4	1/2	.064	3/16	.166	.199	2.59	.076	.982	.0019	.0830	.106	.706
		.072	7/32	.186	.222	2.57	.080	.992	.0021	.0915	.107	.705
		.081	1/4	.206	.247	2.54	.084	1.002	.0023	.1000	.106	.699
		.091	9/32	.229	.275	2.52	.089	1.013	.0026	.1105	.106	.694

TABLE 2.1.1.7

PROPERTIES OF ANGLES (Cont'd)

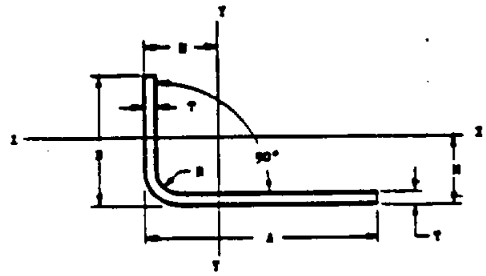

A	B	T	R	AREA	WT/FT	DEVEL. WIDTH	X	Y	M. INERTIA XX	M. INERTIA YY	RAD. GYR. XX	RAD. GYR. YY
9/16	7/16	.025	3/32	.023	.028	.91	.111	.176	.0006	.0008	.134	.182
		.032	3/32	.029	.035	.92	.113	.179	.0005	.0010	.133	.181
		.040	1/8	.036	.043	.90	.118	.186	.0006	.0012	.132	.180
5/8	1/2	.032	3/32	.034	.040	1.05	.125	.198	.0006	.0013	.133	.201
		.040	1/8	.041	.049	1.02	.131	.200	.0009	.0016	.132	.199
		.051	5/32	.051	.061	1.00	.131	.200	.0012	.0020	.132	.199
11/16	7/16	.032	3/32	.034	.040	1.05	.101	.232	.0006	.0017	.125	.229
		.040	1/8	.041	.049	1.02	.106	.238	.0007	.0020	.126	.221
		.051	5/32	.051	.061	1.00	.113	.244	.0008	.0025	.127	.220
	9/16	.032	3/32	.038	.045	1.17	.144	.209	.0011	.0018	.171	.222
		.040	1/8	.046	.055	1.15	.149	.215	.0014	.0022	.171	.222
		.051	5/32	.057	.068	1.12	.156	.222	.0017	.0027	.171	.219
3/4	1/2	.032	3/32	.037	.045	1.17	.117	.246	.0008	.0022	.148	.244
		.040	1/8	.046	.055	1.15	.122	.255	.0010	.0027	.148	.242
		.051	5/32	.057	.068	1.12	.128	.262	.0012	.0033	.147	.240
		.064	3/16	.070	.084	1.09	.135	.271	.0015	.0040	.145	.238
		.072	7/32	.077	.092	1.07	.141	.279	.0016	.0042	.143	.234
	5/8	.032	3/32	.041	.050	1.29	.160	.224	.0016	.0025	.198	.242
		.040	1/8	.051	.061	1.27	.165	.230	.0019	.0030	.193	.241
		.051	5/32	.063	.075	1.24	.172	.238	.0023	.0036	.191	.239
		.064	3/16	.076	.090	1.22	.179	.246	.0026	.0043	.188	.236
		.072	7/32	.084	.101	1.19	.186	.251	.0030	.0047	.187	.234
7/8	1/2	.040	1/8	.051	.061	1.27	.112	.308	.0011	.0041	.144	.284
		.051	5/32	.064	.076	1.25	.116	.316	.0013	.0050	.143	.282
		.064	3/16	.076	.090	1.22	.126	.326	.0015	.0061	.141	.279
		.072	7/32	.086	.103	1.19	.130	.334	.0017	.0065	.140	.276
		.081	1/4	.095	.114	1.17	.135	.342	.0018	.0071	.139	.276
		.091	9/32	.104	.125	1.15	.142	.351	.0020	.0077	.138	.271
	5/8	.040	1/8	.056	.067	1.40	.152	.283	.0020	.0045	.190	.285
		.051	5/32	.070	.084	1.37	.158	.289	.0024	.0056	.187	.282
		.064	3/16	.086	.103	1.34	.165	.300	.0029	.0066	.185	.279
		.072	7/32	.095	.114	1.32	.171	.306	.0032	.0072	.184	.276
		.081	1/4	.105	.126	1.29	.177	.313	.0035	.0079	.182	.274
		.091	9/32	.115	.138	1.27	.183	.322	.0038	.0085	.180	.272
	3/4	.040	1/8	.061	.073	1.52	.196	.261	.0035	.0046	.235	.281
		.051	5/32	.076	.091	1.50	.203	.268	.0041	.0058	.233	.278
		.064	3/16	.093	.113	1.47	.210	.276	.0050	.0072	.230	.275
		.072	7/32	.104	.125	1.44	.215	.283	.0054	.0079	.228	.275
		.081	1/4	.115	.138	1.42	.222	.290	.0058	.0086	.227	.273
		.091	9/32	.127	.152	1.40	.228	.297	.0063	.0093	.225	.271
1	1/2	.040	1/8	.056	.067	1.40	.103	.364	.0011	.0069	.140	.327
		.051	5/32	.070	.084	1.37	.109	.375	.0013	.0075	.130	.324
		.064	3/16	.086	.103	1.34	.116	.384	.0016	.0088	.137	.320
		.072	7/32	.095	.114	1.32	.121	.391	.0018	.0095	.136	.317
		.081	1/4	.105	.126	1.29	.126	.400	.0018	.0105	.135	.314
		.091	9/32	.115	.138	1.27	.132	.408	.0020	.0111	.133	.310
	5/8	.040	1/8	.061	.073	1.52	.131	.336	.0021	.0065	.185	.326
		.051	5/32	.076	.092	1.50	.137	.344	.0025	.0080	.181	.325
		.064	3/16	.093	.113	1.47	.154	.355	.0031	.0096	.181	.320
		.072	7/32	.104	.125	1.44	.159	.360	.0034	.0105	.180	.318
		.081	1/4	.115	.138	1.42	.165	.366	.0037	.0115	.178	.316
		.091	9/32	.127	.152	1.40	.171	.377	.0040	.0124	.176	.313
	3/4	.040	1/8	.066	.079	1.65	.183	.312	.0035	.0069	.230	.325
		.051	5/32	.082	.098	1.62	.188	.319	.0043	.0086	.228	.322
		.064	3/16	.102	.122	1.59	.195	.328	.0052	.0104	.226	.320
		.072	7/32	.113	.136	1.57	.201	.335	.0057	.0114	.225	.318
		.081	1/4	.125	.150	1.55	.207	.343	.0063	.0125	.224	.318
		.091	9/32	.138	.166	1.52	.216	.348	.0067	.0136	.221	.314
	7/8	.040	1/8	.071	.085	1.77	.227	.282	.0045	.0075	.251	.324
		.051	5/32	.089	.107	1.75	.231	.289	.0056	.0090	.272	.320
1	7/8	.064	3/16	.110	.132	1.72	.241	.307	.0080	.0111	.270	.318
		.072	7/32	.122	.146	1.69	.247	.313	.0088	.0122	.268	.316
		.081	1/4	.135	.162	1.67	.252	.320	.0097	.0134	.267	.314
		.091	9/32	.150	.179	1.64	.259	.327	.0106	.0146	.265	.312
1 1/8	5/8	.040	1/8	.066	.078	1.65	.132	.391	.0021	.0089	.181	.368
		.064	3/16	.102	.122	1.58	.143	.408	.0032	.0133	.176	.362
		.081	1/4	.125	.150	1.53	.151	.426	.0038	.0160	.172	.358
		.102	11/32	.152	.183	1.49	.160	.444	.0045	.0187	.170	.350
	3/4	.040	1/8	.071	.085	1.77	.171	.364	.0036	.0096	.225	.368
		.064	3/16	.110	.132	1.72	.184	.382	.0053	.0144	.222	.362
		.081	1/4	.135	.162	1.67	.193	.396	.0065	.0175	.219	.358
		.102	11/32	.165	.198	1.62	.208	.414	.0077	.0205	.219	.353
	7/8	.040	1/8	.076	.091	1.90	.211	.342	.0076	.0101	.249	.365
		.064	3/16	.118	.141	1.85	.226	.357	.0085	.0134	.260	.361
		.081	1/4	.145	.174	1.79	.238	.371	.0101	.0166	.263	.350
		.102	11/32	.178	.213	1.76	.251	.386	.0126	.0221	.260	.352
	1	.040	1/8	.081	.097	2.02	.250	.327	.0080	.0108	.314	.356
		.064	3/16	.127	.151	1.97	.272	.337	.0121	.0162	.310	.355
		.081	1/4	.156	.187	1.92	.263	.350	.0148	.0198	.307	.355
		.102	11/32	.190	.229	1.87	.297	.362	.0176	.0235	.304	.351
1 1/4	5/8	.040	1/8	.071	.085	1.77	.125	.448	.0020	.0135	.181	.408
		.064	3/16	.110	.132	1.72	.136	.465	.0029	.0179	.171	.408
		.081	1/4	.135	.162	1.67	.146	.480	.0039	.0214	.171	.398
		.102	11/32	.165	.198	1.62	.159	.501	.0048	.0252	.167	.391
	3/4	.040	1/8	.076	.091	1.90	.161	.419	.0039	.0127	.225	.409
		.064	3/16	.118	.141	1.85	.176	.438	.0058	.0195	.217	.405
		.081	1/4	.145	.174	1.79	.184	.450	.0067	.0235	.215	.408
		.102	11/32	.178	.213	1.76	.197	.468	.0079	.0277	.211	.395
	7/8	.040	1/8	.081	.097	2.02	.201	.395	.0059	.0155	.269	.408
		.064	3/16	.126	.151	1.97	.214	.411	.0086	.0205	.262	.405
		.072	7/32	.140	.168	1.94	.222	.420	.0093	.0232	.258	.407
		.081	1/4	.156	.187	1.92	.225	.424	.0105	.0269	.258	.402
		.102	11/32	.190	.229	1.87	.238	.441	.0125	.0297	.256	.395
	1	.040	1/8	.086	.103	2.15	.244	.373	.0085	.0161	.315	.406
		.064	3/16	.135	.161	2.09	.257	.388	.0126	.0216	.307	.402
		.081	1/4	.166	.199	2.04	.268	.401	.0155	.0263	.306	.398
		.102	11/32	.205	.246	1.99	.282	.417	.0183	.0315	.300	.392
	1 1/8	.040	1/8	.091	.109	2.27	.289	.353	.0116	.0167	.356	.402
		.064	3/16	.142	.170	2.22	.303	.368	.0173	.0226	.351	.399
		.081	1/4	.176	.211	2.17	.314	.380	.0211	.0276	.349	.396
		.102	11/32	.216	.259	2.12	.328	.395	.0257	.0331	.345	.392
1 3/8	3/4	.040	1/8	.081	.097	2.02	.152	.475	.0040	.0166	.221	.451
		.064	3/16	.126	.151	1.97	.160	.492	.0057	.0251	.211	.446
		.081	1/4	.156	.187	1.92	.175	.508	.0069	.0303	.211	.442
		.102	11/32	.190	.229	1.87	.187	.526	.0082	.0361	.208	.435
	7/8	.040	1/8	.086	.103	2.15	.191	.446	.0060	.0175	.265	.451
		.064	3/16	.134	.160	2.09	.205	.464	.0086	.0267	.257	.446
		.081	1/4	.166	.199	2.04	.215	.478	.0108	.0324	.279	.443
		.102	11/32	.203	.243	1.98	.227	.500	.0129	.0385	.253	.435
	1	.040	1/8	.091	.109	2.27	.239	.425	.0087	.0183	.309	.449
		.064	3/16	.142	.170	2.22	[illegible]	.439	.0130	.0261	.302	.443
		.081	1/4	.176	.211	2.17	[illegible]	.453	.0152	.0331	[illegible]	.437
		.102	11/32	.215	.258	2.10	.270	.473	.0182	[illegible]	[illegible]	.436
	1 1/8	.040	1/8	.096	.115	2.40	.275	.401	.0116	.0180	.351	.443
		.064	3/16	.150	.180	2.34	.288	.419	.0180	.0285	.347	.442
		.081	1/4	.185	.222	2.30	.298	.431	.0220	.0358	.344	.439
		.102	11/32	.227	.272	2.23	.316	.449	.0266	.0431	.341	.433
	1 1/4	.040	1/8	.101	.121	2.52	.320	.385	.0151	.0198	.385	.443
		.064	3/16	.158	.190	2.47	.334	.399	.0248	.0309	.391	.439
		.081	1/4	.195	.235	2.42	.343	.411	.0297	.0373	.389	.437

TABLE 2.1.1.7

PROPERTIES OF ANGLES (Cont'd)

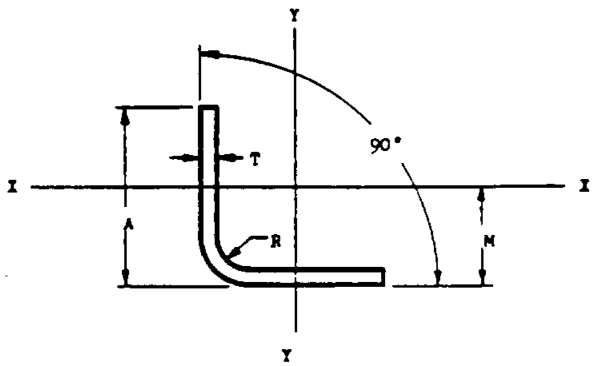

A	T	R	AREA	WT/FT	DEVEL. WIDTH	M	Ixx	RAD. GYR.
1/2	.020	3/32	.019	.022	.94	.139	.0005	.159
	.025	3/32	.023	.028	.93	.141	.0006	.158
	.032	3/32	.030	.035	.92	.144	.0007	.157
9/16	.025	3/32	.026	.032	1.06	.162	.0008	.173
	.032	3/32	.033	.040	1.05	.159	.0011	.177
	.040	1/8	.041	.049	1.02	.165	.0013	.176
5/8	.032	3/32	.037	.045	1.17	.175	.0015	.198
	.040	1/8	.046	.055	1.15	.181	.0018	.197
	.051	5/32	.057	.069	1.12	.188	.0022	.197
11/16	.032	3/32	.042	.050	1.30	.191	.0020	.218
	.040	1/8	.051	.061	1.27	.196	.0024	.216
	.051	5/32	.063	.076	1.24	.203	.0029	.216
3/4	.032	3/32	.045	.055	1.42	.207	.0026	.238
	.040	1/8	.056	.067	1.40	.212	.0031	.237
	.051	5/32	.070	.084	1.37	.218	.0039	.236
	.064	3/16	.086	.103	1.34	.227	.0047	.234
	.072	7/32	.095	.114	1.32	.233	.0051	.235
13/16	.040	1/8	.061	.073	1.52	.228	.0040	.257
	.051	5/32	.076	.092	1.49	.234	.0050	.256
	.064	3/16	.094	.113	1.47	.242	.0060	.254
	.072	7/32	.104	.125	1.44	.248	.0066	.252
	.081	1/4	.115	.138	1.42	.254	.0072	.250
7/8	.040	1/8	.066	.079	1.65	.242	.0051	.278
	.051	5/32	.083	.099	1.62	.249	.0063	.277
	.064	3/16	.102	.122	1.59	.257	.0076	.274
	.072	7/32	.113	.135	1.57	.264	.0084	.273
	.081	1/4	.125	.150	1.54	.270	.0091	.270
1	.040	1/8	.076	.091	1.90	.274	.0077	.318
	.051	5/32	.095	.115	1.87	.280	.0096	.317
	.064	3/16	.118	.141	1.84	.288	.0116	.314
	.072	7/32	.131	.157	1.82	.294	.0128	.313
	.081	1/4	.145	.175	1.80	.300	.0141	.312
	.091	9/32	.161	.193	1.77	.307	.0154	.310
1 1/8	.040	1/8	.086	.103	2.15	.305	.0109	.356
	.051	5/32	.108	.130	2.12	.311	.0138	.357
	.064	3/16	.134	.161	2.09	.319	.0169	.356
	.072	7/32	.149	.179	2.07	.325	.0185	.355
	.081	1/4	.166	.199	2.04	.331	.0221	.353
	.091	9/32	.184	.221	2.02	.337	.0226	.351
	.102	11/32	.203	.244	1.99	.346	.0247	.349
1 1/4	.040	1/8	.096	.115	2.40	.337	.0154	.400
	.051	5/32	.221	.145	2.37	.343	.0190	.397
1 1/4	.064	3/16	.150	.180	2.34	.350	.0234	.395
	.072	7/32	.167	.200	2.32	.356	.0258	.393
	.081	1/4	.186	.223	2.29	.362	.0285	.392
	.091	9/32	.206	.248	2.27	.368	.0317	.392
	.102	11/32	.229	.274	2.24	.376	.0346	.391
1 3/8	.040	1/8	.106	.127	2.65	.367	.0206	.441
	.051	5/32	.134	.160	2.62	.374	.0256	.438
	.064	3/16	.166	.199	2.59	.381	.0315	.435
	.072	7/32	.185	.222	2.57	.387	.0349	.435
	.081	1/4	.206	.247	2.55	.392	.0387	.433
	.091	9/32	.229	.275	2.52	.399	.0426	.431
	.102	11/32	.254	.305	2.49	.407	.0468	.429
1 1/2	.051	5/32	.146	.176	2.88	.405	.0334	.478
	.064	3/16	.182	.218	2.84	.413	.0411	.475
	.072	7/32	.203	.244	2.82	.418	.0459	.475
	.081	1/4	.226	.272	2.80	.423	.0509	.474
	.091	9/32	.252	.302	2.77	.430	.0563	.473
	.102	11/32	.280	.336	2.74	.438	.0615	.468
1 5/8	.051	5/32	.150	.191	3.12	.435	.0430	.519
	.064	3/16	.198	.236	3.10	.443	.0528	.517
	.072	7/32	.221	.265	3.07	.448	.0586	.515
	.081	1/4	.248	.297	3.06	.453	.0652	.514
	.091	9/32	.275	.330	3.02	.461	.0727	.513
	.102	11/32	.305	.366	2.99	.468	.0796	.511
1 3/4	.051	5/32	.172	.206	3.37	.467	.0537	.559
	.064	3/16	.214	.257	3.34	.475	.0666	.558
	.072	7/32	.239	.287	3.32	.479	.0739	.556
	.081	1/4	.267	.320	3.30	.483	.0823	.555
	.091	9/32	.297	.357	3.27	.493	.0911	.554
	.102	11/32	.341	.397	3.24	.500	.1008	.553
1 7/8	.051	5/32	.184	.221	3.62	.498	.0652	.594
	.064	3/16	.230	.276	3.50	.506	.0820	.597
	.072	7/32	.257	.308	3.57	.512	.0917	.597
	.081	1/4	.287	.347	3.55	.518	.1018	.596
	.091	9/32	.320	.384	3.52	.523	.1125	.596
	.102	11/32	.356	.427	3.49	.529	.1252	.593
2	.051	5/32	.197	.237	3.87	.529	.0809	.640
	.064	3/16	.246	.295	3.85	.537	.0998	.637
	.072	7/32	.275	.330	3.82	.543	.1114	.636
	.081	1/4	.307	.368	3.79	.548	.1241	.636
	.091	9/32	.342	.411	3.77	.555	.1382	.635
	.102	11/32	.382	.457	3.74	.562	.1527	.633

TABLE 2.1.1.8
PROPERTIES OF CHANNELS

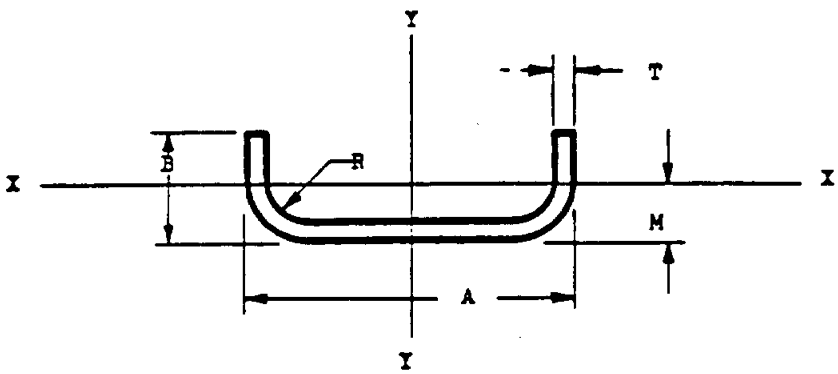

A	B	T	R	AREA	WT/FT	DEVEL. WIDTH	M	M. INERTIA XX	M. INERTIA YY	RAD. GYR. XX	RAD. GYR. YY
5/8	1/4	.032	3/32	.031	.037	.97	.074	.0002	.0016	.075	.226
		.040	1/8	.037	.044	.92	.080	.0002	.0016	.073	.218
3/4	1/4	.032	3/32	.035	.042	1.09	.068	.0002	.0025	.072	.267
		.040	1/8	.042	.050	1.05	.073	.0002	.0028	.071	.259
7/8	1/4	.032	3/32	.039	.047	1.22	.062	.0002	.0037	.070	.308
		.040	1/8	.047	.056	1.17	.068	.0002	.0042	.069	.299
	3/8	.032	3/32	.047	.056	1.47	.105	.0006	.0051	.115	.330
		.040	1/8	.057	.068	1.43	.111	.0007	.0059	.113	.323
1	1/4	.032	3/32	.043	.052	1.34	.058	.0002	.0052	.068	.347
		.040	1/8	.052	.062	1.30	.063	.0002	.0059	.067	.330
	3/8	.040	1/8	.062	.074	1.55	.103	.0008	.0082	.112	.385
		.051	5/32	.076	.091	1.49	.110	.0009	.0096	.110	.356
		.064	3/16	.092	.110	1.43	.118	.0011	.0110	.108	.346
1 1/8	1/4	.032	3/32	.047	.056	1.47	.054	.0002	.0071	.066	.386
		.040	1/8	.057	.068	1.42	.059	.0002	.0081	.066	.377
	1/2	.040	1/8	.077	.092	1.92	.141	.0018	.0140	.154	.427
		.051	5/32	.095	.114	1.87	.148	.0022	.0167	.152	.419
		.064	3/16	.116	.139	1.81	.157	.0026	.0194	.150	.410
1 1/4	3/8	.040	1/8	.072	.068	1.79	.092	.0008	.0144	.108	.447
		.051	5/32	.089	.107	1.75	.098	.0010	.0170	.106	.438
		.064	3/16	.108	.129	1.68	.106	.0012	.0196	.104	.427
1 3/8	3/8	.040	1/8	.077	.092	1.92	.087	.0009	.0182	.106	.487
		.051	5/32	.095	.114	1.87	.093	.0010	.0217	.104	.478
		.064	3/16	.116	.139	1.81	.100	.0012	.0252	.102	.467
1 1/2	1/2	.051	5/32	.114	.137	2.25	.128	.0025	.0339	.146	.544
		.064	3/16	.140	.168	2.18	.135	.0029	.0399	.145	.534
		.072	7/32	.154	.185	2.14	.141	.0032	.0427	.143	.527
1 3/4	1/2	.051	5/32	.125	.153	2.49	.118	.0026	.0496	.142	.625
		.064	3/16	.156	.187	2.43	.12[illegible]	.0031	.0589	.141	.615
		.072	7/32	.172	.206	2.39	.130	.0033	.0633	.140	.607
2	5/8	.051	5/32	.153	.183	2.99	.147	.0051	.0816	.183	.731
		.064	3/16	.188	.225	2.93	.154	.0061	.0978	.181	.721
		.081	1/4	.230	.275	2.84	.165	.0073	.1147	.179	.706
2 1/2	3/4	.064	3/16	.236	.283	3.68	.174	.0111	.1946	.217	.909
		.072	7/32	.262	.314	3.64	.178	.0122	.2128	.216	.901
		.091	9/32	.322	.386	3.54	.190	.0147	.2521	.214	.885
3	3/4	.064	3/16	.268	.321	4.18	.157	.0117	.3059	.209	1.069
		.091	9/32	.367	.441	4.04	.172	.0156	.4004	.206	1.044
		.102	11/32	.404	.484	3.96	.180	.0168	.4279	.204	1.030

Data Source, Section 1.3 Reference /

DISTANCES FROM SIDES OF A
TRAPEZOID TO ITS CENTROID

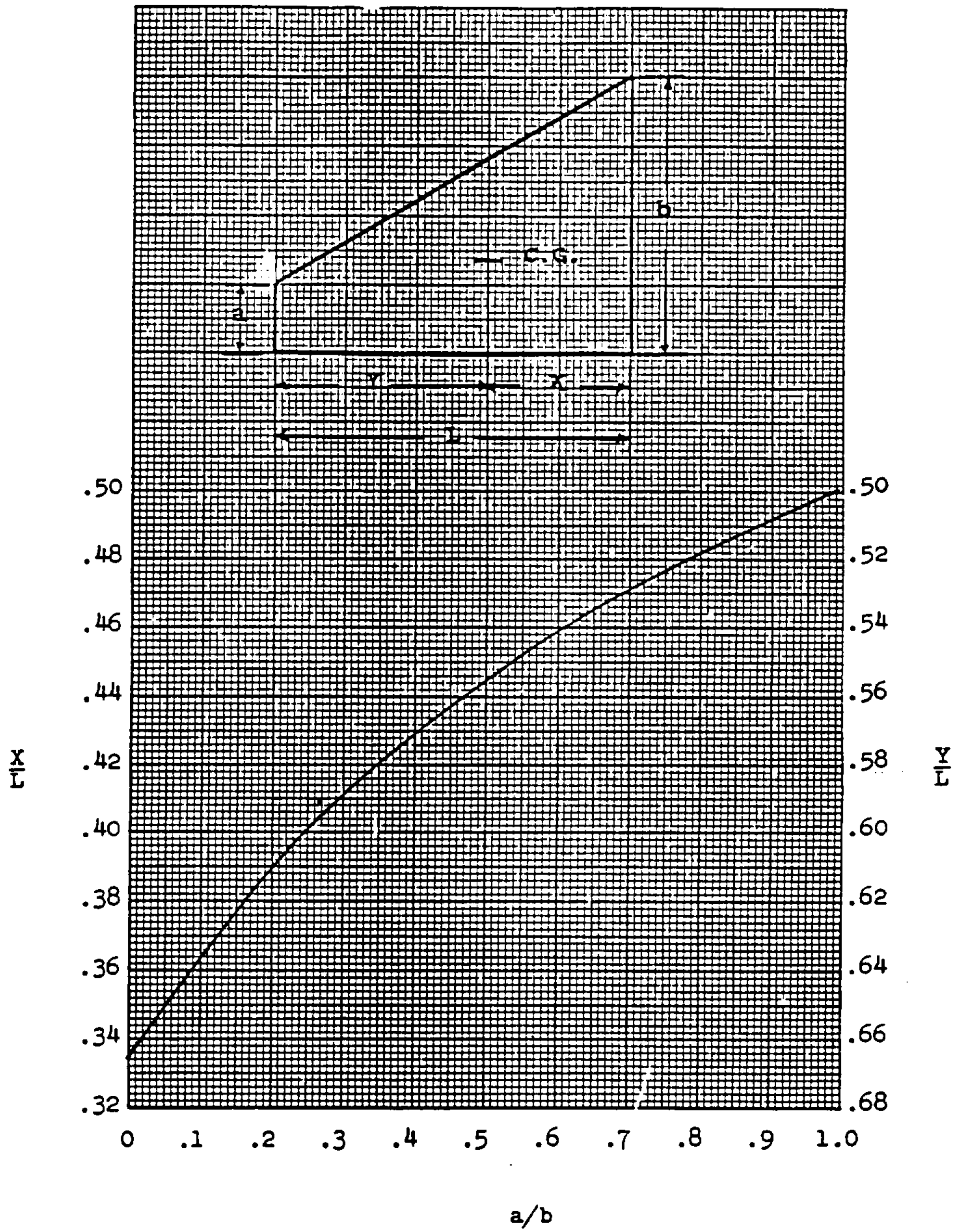

FIG. 2.1.1.9

Data Source, Section 1.3 Reference 1

2.1.2

Shear Center

The shear center is defined as the point on the cross-sectional plane of a beam through which the resultant of the transverse shear load must be applied in order that the stresses in the beam may be determined only from the theories of pure bending and transverse shear.

In the case of a beam of variable cross-section, the shear center can be determined for each section, but these points will not necessarily connect to form a straight line. For instance, a cantilever beam of non-uniformly varying cross-section may have a load so placed on the end that the end section will not rotate, but all other sections of the beam may rotate. Thus it may be seen that the shear center has real significance only in the case of prismatic beams, or beams with a uniform taper.

For any doubly symmetrical section or a section with point symmetry, the shear center coincides with the center of gravity.

For any singly symmetrical section, the shear center is somewhere on the axis of symmetry.

For any section made up of two intersecting plates, the shear center is at the point of intersection of the plates.

Example:

Consider a cantilever beam with an applied load at the free end. Assume a constant cross-section. The centroidal (x) axis is an axis of symmetry; therefore, the shear center will be located somewhere on this axis.

Calculate the moment of inertia about the centroidal (x) axis,

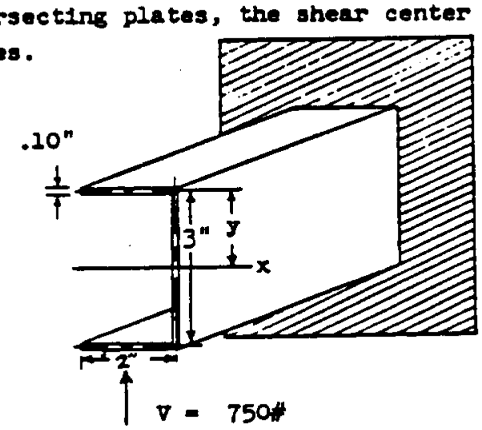

Fig. 2.1.2-1

$$I_x = 2\left[.10 \times 2 \times (1.5)^2\right] + \frac{.10 \times (3)^3}{12} = 1.125 \text{ in.}^4$$

NOTE: The moment of inertia of the horizontal webs about their centroids are negligible.

Calculate the bending stress.

The difference in the bending moment on two cross sections one inch apart is equal to the vertical load (V). The difference in the bending stress on the two cross sections is shown by the following formula:

$\frac{V\,Y}{I}$ (where (Y) is the vertical distance from the centroidal axis.)

Horizontal Webs:

$$\frac{V\,Y}{I} = \frac{750 \times 1.5}{1.125} = 1000 \text{ PSI}$$

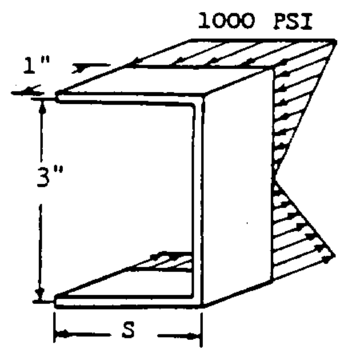

Vertical Web:

The bending stress will vary from zero at the centroidal axis to 1000 PSI as shown.

The shear load (q) in the horizontal webs at a distance (S) from the free edge must balance the bending stress of 1000 PSI acting over an area (.10 S) as follows:

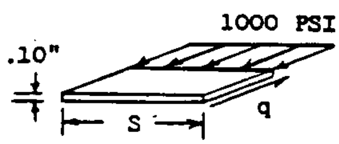

$q = 1000 \times (.10S)$

For a maximum (q)

$S = 2"$ (Therefore)

$q = 1000 \times .10 \times 2 = 200$ lbs.

The shear load (q) in the vertical web is 750 lbs. or the same as the applied load.

Calculate the distance to the shear center (Ref. e).

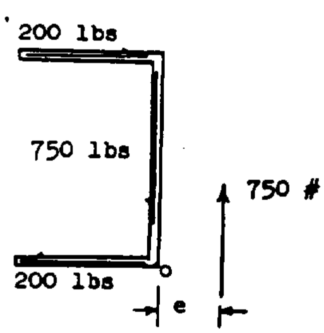

$$\sum M_o = 750 \times e = 200 \times 3$$

$$e = \frac{200 \times 3}{750} = .80"$$

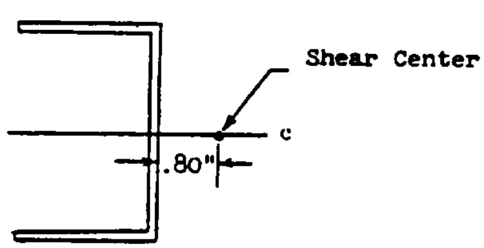

TABLE 2.1.2.1

FORM OF SECTION	LOCATION OF SHEAR CENTER, Q, FOR SECTIONS HAVING ONE AXIS OF SYMMETRY
1. Triangle 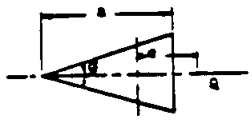	$e = 0.47\,a$ for narrow triangle ($\phi < 12^\circ$) approx.
2. Sector of thin circular tube 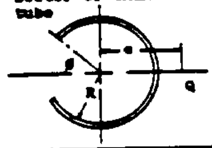	$e = \frac{2R}{(\pi-\phi)+\sin\phi\cos\phi}\left[(\pi-\phi)\cos\phi+\sin\phi\right]$
3. Semicircular area 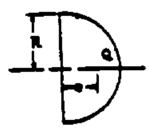	$e = \left(\frac{8}{15\pi}\,\frac{3+4\mu}{1+\mu}\right)R$ Q is to right of centroid
4. Angle 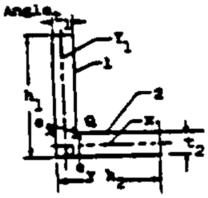	I_1 = moment of inertia of leg 1 about Y_1 (central axis) I_2 = moment of inertia of leg 2 about X_1 (central axis) $e_x = \frac{1}{2} h_2\left(\frac{I_1}{I_1+I_2}\right)$ $e_y = \frac{1}{2} h_1\left(\frac{I_1}{I_1+I_2}\right)$ If t_1 & t_2 are small, $e_x = e_y = 0$ (practically) and Q is at O
5. Channel 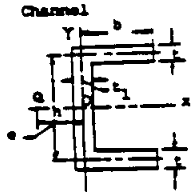	$e = h\left(\frac{H_{xy}}{I_x}\right)$ where H_{xy} = product of inertia of the half section (about x) with respect to axis X and Y ; and I_x = moment of inertia of whole section with respect to axis x. If $t = t_1$, $e = \frac{b^2h^2t}{4\,I_x}$, See Fig. 2.1.2.2
6. I with unequal flanges and thin webs 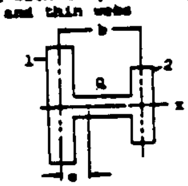	$e = b\left(\frac{I_2}{I_1+I_2}\right)$ where I_1 and I_2, respectively, denote moments of inertia about x-axis of flange 1 and flange 2
7. Tee Section 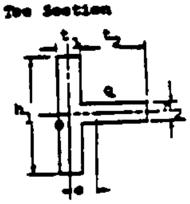	$e = \frac{1}{2}(t_1+t_2)\left[\frac{1}{1+\frac{h_1^3t_1}{h_2^3t_2}}\right]$ For a T - beam of ordinary proportions, Q may be assumed to be at O

TABLE 2.1.2.1

FORM OF SECTION	LOCATION OF SHEAR CENTER (Continued)

8. I with unequal legs

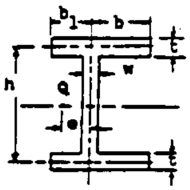

$$e = \frac{3\left[b^2 - b_1^2\right]}{(w/t)h + 6(b+b_1)} \quad ; \quad b_1 < b$$

9. Right angle with lips

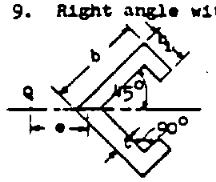

$$e = \frac{\left[b(b_1)^2\right] \quad (3b - 2b_1)}{\sqrt{2} \quad \left[2b^3 - (b - b_1)^3\right]}$$

10. Sector of arc

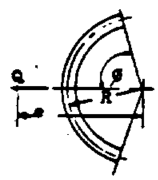

$$e = 4R\,\frac{\sin\phi - \phi\cos\phi}{2\phi - \sin 2\phi}$$

11. Lipped channel (t small)

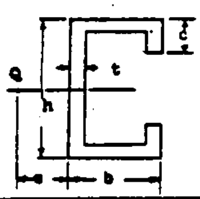

Values of e/h

c/h \ b/h	1.0	0.8	0.6	0.4	0.2
0	0.430	0.330	0.236	0.141	0.055
0.1	0.477	0.380	0.280	0.183	0.087
0.2	0.530	0.425	0.325	0.222	0.115
0.3	0.575	0.470	0.365	0.258	0.138
0.4	0.610	0.503	0.394	0.280	0.155
0.5	0.621	0.517	0.405	0.290	0.161

12. Hat section (t small)

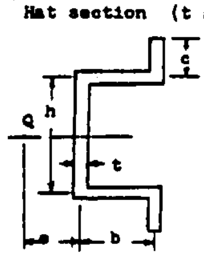

Values of e/h

c/h \ b/h	1.0	0.8	0.6	0.4	0.2
0	0.430	0.330	0.236	0.141	0.055
0.1	0.464	0.367	0.270	0.173	0.080
0.2	0.474	0.377	0.280	0.182	0.090
0.3	0.453	0.358	0.265	0.172	0.085
0.4	0.410	0.320	0.235	0.150	0.072
0.5	0.355	0.275	0.196	0.123	0.056
0.6	0.300	0.225	0.155	0.095	0.040

13. D-Section (A=enclosed area)

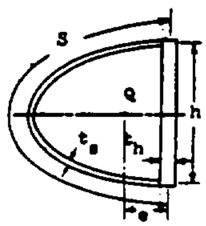

Values of e(h/A)

t_h/t_s \ S/h	1	1.5	2	3	4	5	6	7
0.5	-----	------	1.000	0.800	0.665	0.570	0.500	0.445
0.6	-----	------	0.910	0.712	0.588	0.498	0.434	0.386
0.7	-----	0.980	0.831	0.641	0.525	0.443	0.384	0.338
0.8	-----	0.910	0.770	0.590	0.475	0.400	0.345	0.305
0.9	-----	0.850	0.710	0.540	0.430	0.360	0.310	0.275
1.0	1.0	0.800	0.662	0.500	0.400	0.330	0.285	0.250
1.2	0.905	0.715	0.525	0.380	0.304	0.285	0.244	0.215
1.6	0.765	0.588	0.475	0.345	0.270	0.221	0.190	0.165
2.0	0.660	0.497	0.400	0.285	0.220	0.181	0.155	0.135
3.0	0.500	0.364	0.285	0.200	0.155	0.125	0.106	0.091

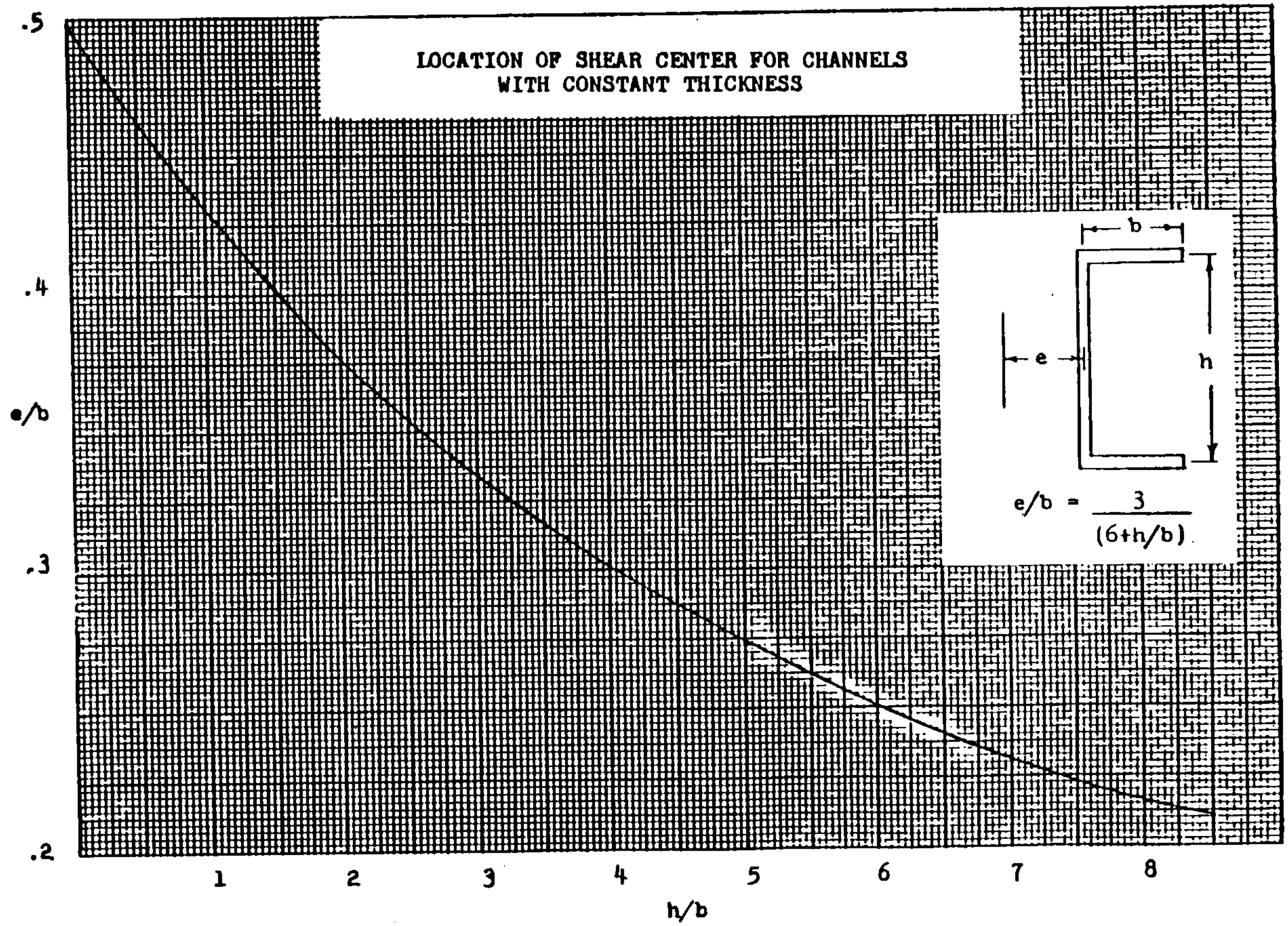
LOCATION OF SHEAR CENTER FOR CHANNELS
WITH CONSTANT THICKNESS
.5
.4
.3
.2
e/b
1
2
3
4
5
6
7
8
h/b
b
e
h
$e/b = \frac{3}{(6+h/b)}$

Fig. 2.1.2.2

MOMENT OF INERTIA SAMPLE CALCULATION. TABULAR METHOD.

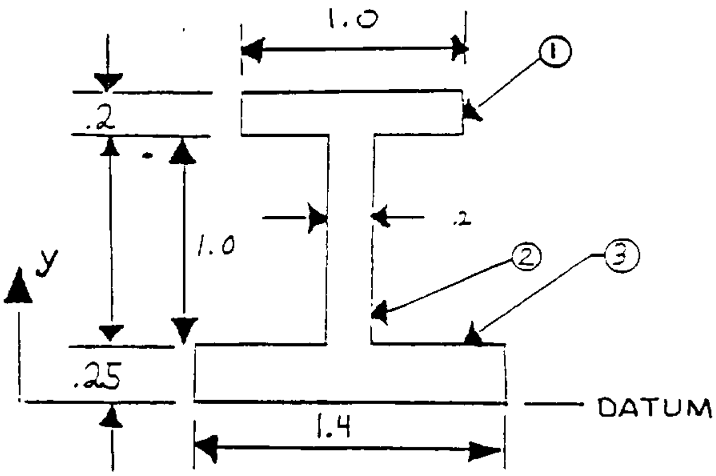

NOMENCLATURE:

b = WIDTH (IN.) d = DEPTH (IN.)

A = AREA (IN^2) = $b \times d$

y = ITEM CENTROID DISTANCE FROM DATUM (IN.)

I_{CG} = ITEM M OF I ABOUT ITS C.G (IN^4) = $bd^3/12$

I_{DATUM} = ITEM M OF I ABOUT DATUM (IN^4)

I_{NA} = TOTAL SECTION M OF I ABOUT N.A. (IN^4) 2

N.A. = NEUTRAL AXIS

$\bar{y}$ = DISTANCE OF N.A. FROM DATUM (IN.)

ITEM	b (IN)	d (IN)	A (IN^2)	y (IN)	Ay (IN^3)	Ay^2 (IN^4)	I_{CG} (IN^4)	I_{DATUM} (IN^4)
1	1.0	.2	.2	1.35	.27	.3645	.0007	.3652
2	.2	1.0	.2	.75	.15	.1125	.0167	.1292
3	1.4	.25	.35	.125	.0438	.0055	.0018	.0073
			Σ .75		.4638			.5017

$$\bar{y} = \Sigma Ay \div \Sigma A = .4638 \div .75 = .618 \text{ IN.}$$

$$I_{NA} = \Sigma I_{DATUM} - \Sigma A . \bar{y}^2 = .5017 - .75 \times .618^2$$

$$= .215 \text{ IN}^4$$

SECTION 3.0

MATERIAL PROPERTY DEFINITIONS

THIS SECTION PRESENTS A GENERAL REVIEW OF THE STRENGTH PROPERTIES OF MATERIALS REPRESENTED BY ENGINEERING STRESS-STRAIN CURVES. IT ALSO CONTAINS DEFINITIONS OF CRITICAL STRENGTH OF MATERIAL TERMS.

		PAGE
3.1	STRESS-STRAIN CURVE DEFINTIONS	3.1.1
3.2	MATERIAL PROPERTIES: DUCTILE-BRITTLE BEHAVIOR	3.2.1
3.3	CREEP, STRAIN RATE AND IMPACT	3.3.1
3.4	"A" AND "B" MATERIAL PROPERTY VALUES	3.4.1
3.5	PLASTIC STRESS-STRAIN CURVES	3.5.1
3.6	SURFACE ROUGHNESS	3.6.1
3.7	NON-DIMENSIONAL STRESS-STRAIN CURVES	3.7.1
3.8	RAMBERG-OSGOOD CONSTANTS	3.8.1

3.1 Data Source, Section 1.3 Reference 2

3.01 GENERAL

3.01.01 MATERIAL PROPERTIES REPRESENTED BY "ENGINEERING" STRESS-STRAIN CURVES

Numerous engineering properties of a material can be obtained from a stress-strain curve. Only the tension stress-strain test can be carried to ultimate even though F_{cu} is assumed equal to F_{tu} for most materials. Many materials have tension and compression stress-strain curves that nearly coincide while the curves of work hardened materials may be significantly different. A few materials exhibit a difinite yield point, however, most aircraft and missile materials do not. For these materials, the 0.2% offset method is used to define the yield point. An engineering stress-strain curve for a material exhibiting no definite yield point is illustrated in Figure 3.01.01. An engineering stress-strain curve is not a true curve in that the stress and strain are based on the original cross sectional area and the original gage length of the specimen. A true stress-strain curve would be based on the actual values at the given load; see Section 3.01.11. Following Figure 3.01.01, there are brief definitions of significant properties of the curve.

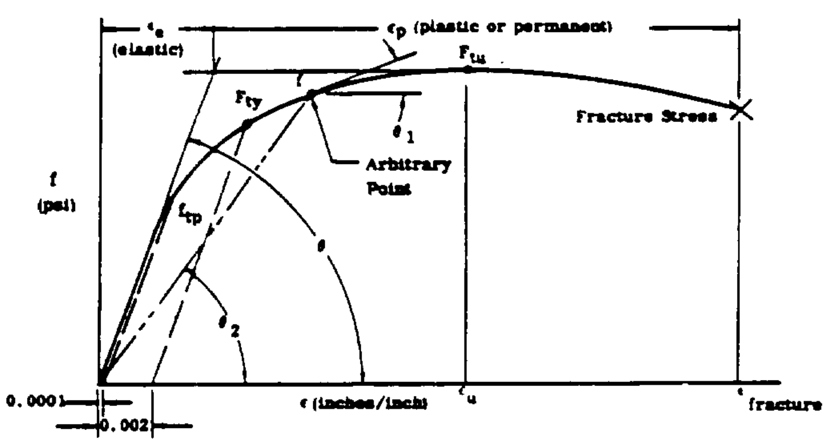

Engineering Stress-Strain Curve (Tension)

Figure 3.01.01

Definitions Pertaining to the Stress-Strain Curve:

$E = \frac{f_t}{\epsilon} = \tan\theta$ Modulus of elasticity in tension; average ratio of stress to strain for stress below the proportional limit.

$E_c = \frac{f_c}{\epsilon} = \tan\theta$ Modulus of elasticity in compression; average ratio of stress to strain for stress below the proportional limit.

$E_s = \frac{f}{\epsilon} = \tan\theta_2$ Secant modulus; ratio of stress to strain for stress above the proportional limit; reduces to E in the elastic range.

$E_t = \frac{df}{d\epsilon} = \tan\theta_1$ Tangent modulus; slope of stress-strain curve; reduces to E in the elastic range.

F_{tu} Ultimate tensile stress; the maximum stress reached in tensile tests of standard specimens.

F_{cu} Ultimate compressive stress; because the ultimate compressive stress is difficult to obtain, F_{tu} is usually used for F_{cu} when it is safe to do so.

F_{ty} Tensile yield stress; since many materials do not exhibit a definite yield point, the 0.2% offset method is used. This is done by constructing a line with slope E at a strain of .002 in./in.; the intersection with the stress-strain curve defines F_{ty}. See Figure 3.01.01.

F_{cy} Compressive yield stress.

F_{tp} — Proportional limit stress in tension; the stress at which the stress-strain curve ceases to be linear; usually an offset of 0.01% is used. This is done by constructing a line with slope E at a strain of .0001 in/in; the intersection with the stress-strain curve defines F_{tp}.

F_{cp} — Proportional limit stress in compression.

T — Modulus of Toughness; the area under the stress-strain curve. This property is sometimes used as a measure of the energy absorbing capacity either for materials that are not highly rate sensitive or for materials loaded under approximately the same rate and temperature conditions as those used to obtain the stress-strain curve. This property gives the amount of energy necessary to fracture a unit volume of uniformly stressed material.

ϵ_u — The strain corresponding to the ultimate tensile stress F_{tu}.

ϵ_e — Elastic strain; See Figure 3.01.01.

ϵ_p — Plastic Strain; See Figure 3.01.01; plastic strain is permanent while elastic strain is recoverable.

%Elongation — The total plastic elongation in the gage length of a tensile specimen after failure, expressed as a percentage of the original (unloaded) gage length; used as an indication of relative ductility.

Data Source, Section 1.3 Reference 2

3.01.02 MATERIAL PROPERTIES: TEMPERATURE

TEMPERATURE:

Reduced or elevated temperatures usually cause a significant change in the stress-strain curve. As a result, analysis involving the stress-strain curve cannot be treated by the use of factors for temperature effects. For example; plastic bending, plastic buckling, and plastic thermal stresses must be obtained by the use of the stress-strain curve at the specific temperature in question. See Sections 7.00, 8.00, 9.00, 17.01, and 19.00.

THERMAL EXPANSION:

α = Coefficient of linear thermal expansion (in/in °F).

THERMAL CONDUCTIVITY:

k = Thermal conductivity; the time rate of heat transfer by conduction through a material of unit thickness over a unit area, for a unit difference in temperature (BTU in/hr in^2 °F).

SPECIFIC HEAT CAPACITY:

c_p = Heat capacity per pound (BTU/lb °F).

3.2

3.01.03 MATERIAL PROPERTIES: DUCTILE - BRITTLE BEHAVIOR AND TOUGHNESS

The terms ductile, brittle, and toughness are currently used in a qualitative manner. The extreme case of brittleness is the complete absence of plastic strain; the stress-strain diagram consists of a single straight line to failure. Ductile materials, conversely, are characterized by large plastic deformation preceding fracture.

Data Source, Section 1.3 Reference - 2

Until recently, many investigators have used the terms ductility and toughness interchangeably when actually they are indices of two distinctly different material deformation characteristics. Ductility, as measured by elongation and reduction of area, is the ability of a material to deform plastically throughout the section under conditions of slowly applied loads and in the absence of notches or other stress concentrations. Toughness is the property of a material to absorb energy by plastic deformation before fracture, under conditions of rapid loading rates, stress concentrations, or both. Charpy or Izod impact tests, central or side notched tensile tests, various tear tests, bend tests, explosion bulge tests, drop weight tests, and a wide variety of crack propagation tests -- all impose various combinations of loading rate, triaxial stresses, and temperatures on materials. These tests attempt to simulate service conditions on actual structures containing stress conditions, such as notches, fatigue or machine cracks, rivet holes, inclusions, sharp re-entrant corners, etc. Variations in temperature, loading rate, and stress concentration geometry, in addition to changes in composition and microstructure, can effect the ductile-brittle behavior of a material.

Results of the tests described above can be validly used as a preliminary performance index for comparison of similar materials subjected to the same temperatures and utilized for identical structural configurations.

3.3

3.01.04 MATERIAL PROPERTIES: CREEP, STRAIN RATE AND IMPACT

CREEP:

Creep is defined as a continuous deformation which increases with time, and it usually occurs when an engineering material is subjected to stress either at high temperatures or over a long period of time or both. If a component is stressed for a long period of time, cumulative creep may cause it to rupture at

a stress level below that indicated by short-time tensile properties or to deform a prohibitive amount. The conditions a component is expected to experience during its working life determines whether creep should be an important design consideration.

Stress, temperature, time and deformation are all variables which effect creep behavior. Creep data is represented graphically by many different combinations of these variables and is available in various Air Force publications.

Reference 1 provides stress versus time, time to failure, creep and minimum creep rate curves for most aircraft structural materials. This data can be used to determine if creep is an important design consideration and if it is, to establish an allowable stress.

STRAIN RATE:

Maneuver, gust, flight and landing loads on aircraft and missile structures result in conditions ranging from those where strains are constant to those where strains are changing rapidly. The stress-strain curve, ultimate strength and ductility of some materials are affected by such changes in the rate of strain.

In general, strength properties at lower temperatures (up to about 800°F) increase only slightly or remain constant for small increases in strain rate. As a material approaches higher temperatures, however, the effects of strain rates become much more pronounced and the strength properties decrease greatly with a decrease in strain rate.

Strain rate has little or no effect upon modulus of elasticity values except at high temperatures where the apparent modulus decreases with a decrease in strain rate. This is apparently a result of a small amount of creep deformation which occurs during the elastic region of loading at slower strain rates.

The total elongation of a material has a tendency to decrease with increasing strain rate, particularly at high temperatures. This effect, however, is not entirely consistent and total elongation values may vary erratically with changes in temperature, strain rate and holding time.

Unless otherwise stated, strain rates for data in this manual can be assumed to have been between 0.001 and 0.01 inch per inch per minute up to yield and 0.10 to 0.20 inch per minute head travel after yield. Property variations in this range are normally considered too small to necessitate consideration in design.

A comparison of the effect of an increase in strain rate from 0.00005 to 1.0 inch per inch per second at elevated temperatures for several materials is illustrated in Figure 3.01.02.

IMPACT:

Impact stresses occur under dynamic loading conditions where the load velocity is in the region of several feet per second or greater. Many engineering metals (low and medium alloy steels, for example) undergo a marked change in deformation and fracture characteristics between static and impact loading conditions and with changes of temperature at which impact loads are applied.

Impact tests are generally performed at a series of temperatures in order to determine the "transition temperature" of a material, which is the temperature level or range at which a transition from ductile to brittle behavior is exhibited. This "transition temperature" determined by these methods for carbon steels is in excellent agreement with material behavior in design applications.

Two of the most common impact testing methods are the Charpy and Izod. Both of these use a pendulum to apply an impact load to a notched test specimen. The energy absorbed during fracture is then determined from the change in height of the pendulum before and after fracture. This type of data has been published for many materials.

Tension impact tests involving either circumferentially notched round specimens or side notched sheet specimens are also used to evaluate the impact resistance of metallic materials, but these tests have not been conducted as extensively as the Charpy V-notch impact test and much less data are available to permit comparisons to be made among different materials.

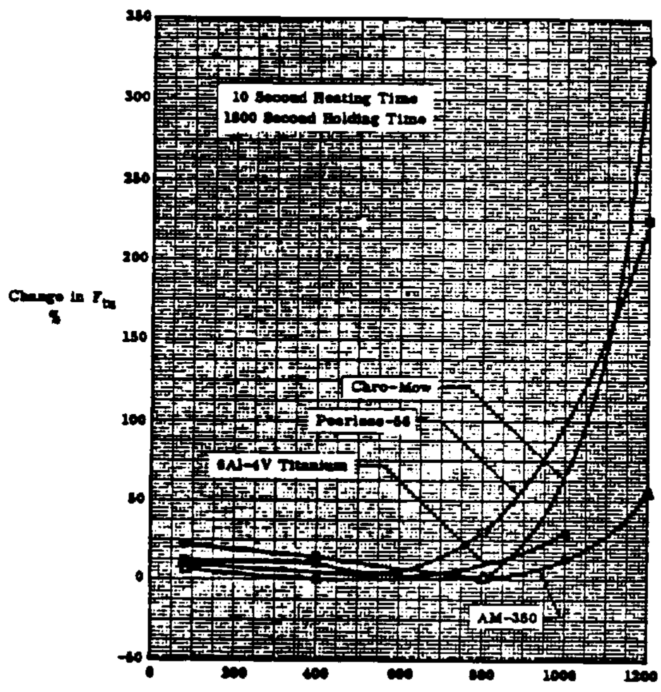

Effect of Temperature on the Percentage Change in Ultimate Tensile Strength Resulting from an Increase in Strain Rate From 0.00005 to 1.0 in/in/sec.

Figure 3.01.02

3.01.05 OTHER MATERIAL PROPERTIES

F_{su} Ultimate shear stress.

F_{sp} Proportional limit in shear; usually taken equal to 0.577 times the proportional limit in tension.

μ Poisson's Ratio; the ratio of transverse strain to axial strain in a tension or compression test. It usually varies from .25 to .33 for most structural materials and is reasonably constant in the elastic range. For materials stressed beyond the elastic limit, Poisson's Ratio is not a constant, but is a function of the axial strain. By the conservation of volume in ideally plastic action, Poisson's Ratio becomes equal to 1/2.

μ_p Plastic Poisson's ratio; this value is used for convenience only in the plastic range since Poisson's ratio was intended only for elastic action. It is known from experiments that the value of Poisson's ratio increases beyond the proportional limit and for most materials the average value becomes about 0.5 which is the same value found theoretically by the conservation of volume in ideally plastic action.

$\bar{\mu}$ Effective value of Poisson's ratio; an average value for the total strain which includes the elastic and plastic portions. See Section 3.01.10.

$G = \dfrac{E}{2(1+\mu)}$ Modulus of rigidity or shearing modulus of elasticity for pure shear in isotropic materials; this property is the ratio of the shear stress (f_s) to the shear strain (γ)* in the elastic range as shown in Figure 3.01.03.

* See Figure 10.10.01.

Data Source, Section 1.3 Reference 2

F_{bru} Bearing ultimate; the actual failing stress of a material in bearing; usually given for e/D ratios of 1.5 and 2.0, where e is the edge distance and D is the diameter of a pin.

F_{bry} Bearing yield; a load-deformation curve is plotted where deformation is the change in hole diameter. A 2% offset method is used on this curve to define F_{bry} similar to that used in defining F_{ty}.

FATIGUE See Section 18.00.

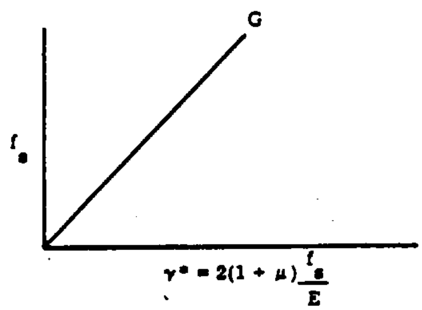

Shear Stress-Strain Curve
Figure 3.01.03

3.4
3.01.06 MATERIAL PROPERTY VALUES

Scatter of test results necessitates that design properties be defined in terms of probability-levels. The selection of such levels naturally depends on the particular design, its chances of failure, and the consequences of failure.

Two strength levels in common use are the "A" and "B" values specified in Reference 1. "A" values in Reference 1 represent "Minimum" strength properties guaranteed by material producers, and "B" values represent strengths which producers assure will be met or exceeded by 90% of the material supplied by them.

*See figure 10.10.01

It is often necessary to establish comparable design allowables for materials or structural elements not shown in Reference 1, in which case more specific definitions of the "A" and "B" values are required in terms of probabilities and confidence levels. The definitions adopted are as follows:

"A" values - that level which would be exceeded by at least 99% of the entire population* with 95% confidence**; i.e., the confidence** is 95% that at least 99% of the entire population* would exceed the "A" value. In the Structures Manual, "Minimum" values will correspond to "A" values, until such times as more statistically based data is available.

"B" values - that level which would be exceeded by at least 90% of the entire population* with 95% confidence**; i.e., the confidence** is 95% that at least 90% of the entire population* would exceed the "B" value. In the Structures Manual, "90% Probability" values will correspond to "B" values.

Application of "A" and "B" values:

"A" values - Single load path structures.

"B" values - Multiple load path structures.

3.01.07 STRESS-STRAIN CURVES

Stress-strain curves will not appear in Section 3.00 since the k = 1 plastic bending curves of Section 17.01 are stress-strain curves and may be referenced as such. Where tension and compression stress-strain curves nearly coincide, the lower curve has been used and where they differ significantly both tension and

* The entire population may be defined as the entire data from which the sample is drawn if all of it were available. For example, the testing of a group of specimens would be the sample and all material which would ever be accepted to the material specification would be the population.

** Generally, information concerning the entire population is not known. Through statistics, inferences may be made regarding the entire population through examination of a small part of that population. The confidence or confidence level is the degree of surety that the estimated value does describe the population.

compression plastic bending curves have been presented. When requiring a stress-strain curve to pass through a yield point different from that on the k = 1 curve, use the method described in Section 3.01.08.

3.01.08 CONSTRUCTION OF A STRESS-STRAIN CURVE THROUGH A GIVEN YIELD POINT USING A TYPICAL (DETERMINED BY TEST) STRESS-STRAIN CURVE

Providing the typical and constructed stress-strain curves have the same E, the following procedure can be used as a standard method:

1. Locate the given yield point, A, using the 0.2% offset method as shown in Figure 3.01.04.
2. Construct a line from the origin, 0, through point A and intersecting the typical curve at point B. Point A may be above or below the typical curve.
3. Locate any point on the typical curve such as point C and construct a line from the origin, 0, through point C.
4. Locate point D on line $\overline{0C}$ by the following ratio:

$$\overline{0D} = \frac{\overline{0A}}{\overline{0B}} \times \overline{0C}$$

5. Repeat step 4 until enough points are obtained so that a similar curve may be drawn through these points.

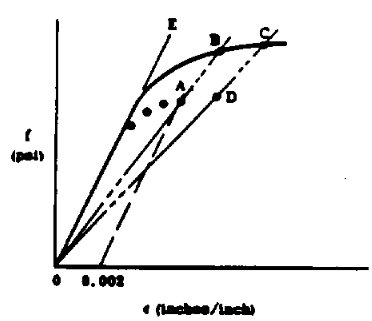

Figure 3.01.04

Data Source, Section 1.3 Reference 2

3.5

3.01.09 PLASTIC STRESS-STRAIN CURVE

The plastic stress-strain curve can be constructed from the engineering stress-strain curve. The procedure is to subtract the elastic strain, ϵ_{i_e}, of any point i on the curve of Figure 3.01.05(a), from the total strain, ϵ_i, to obtain the plastic strain, ϵ_{i_p}. By taking a sufficient number of such points, a plot of stress vs. plastic strain can be plotted as shown in Figure 3.01.05(b).

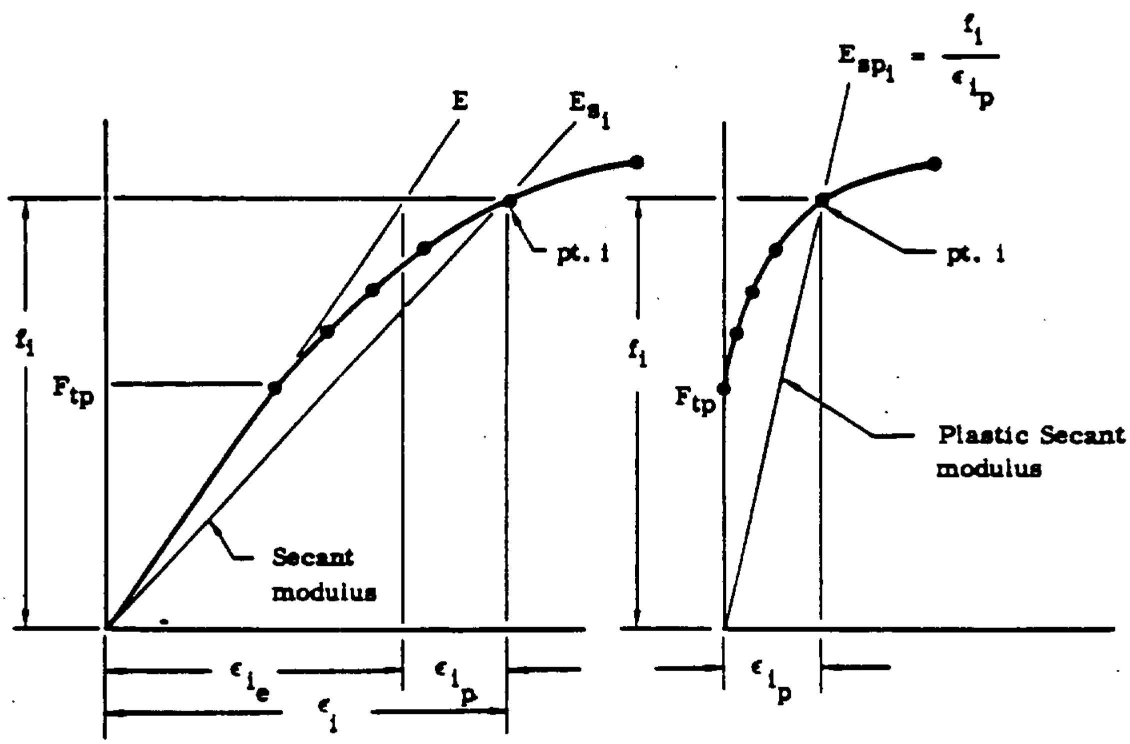

(a) Engineering stress-strain curve (b) Plastic stress-strain curve

Figure 3.01.05

3.01.10 EFFECTIVE POISSON'S RATIO; AN AVERAGE VALUE OF POISSON'S RATIO FOR THE TOTAL (ELASTIC AND PLASTIC) STRAIN

This average value of Poisson's ratio $\bar{\mu}$ may be expressed as follows:

$$\bar{\mu} = \frac{\mu \epsilon_e + \mu_p \epsilon_p}{\epsilon} \qquad (3.01.01)$$

or

$$\bar{\mu} = E_s \left(\frac{\mu}{E} + \frac{\mu_p}{E_{sp}} \right) \qquad (3.01.02)$$

where all the terms are defined in Section 3.01.01 and shown in Figure 3.01.05.

For most materials, $\mu = 0.3$ and $\mu_p = 0.5$, approximately, and $\bar{\mu}$ becomes

$$\bar{\mu} = \frac{0.3 \epsilon_e + 0.5 \epsilon_p}{\epsilon} \qquad (3.01.03)$$

or

$$\bar{\mu} = E_s \left(\frac{0.3}{E} + \frac{0.5}{E_{sp}} \right) \qquad (3.01.04)$$

3.01.11 MATERIAL PROPERTIES REPRESENTED BY TRUE STRESS-TRUE STRAIN CURVES IN THE PLASTIC RANGE

For uniaxial tension or compression, the conventional procedure is to define the material properties based on an "engineering" stress-strain curve; see Section 3.01.01. A more accurate measure of material properties in the plastic range would be based on the true stress-true strain curves. A true stress-true strain curve is based on the true values of stress and strain at each point on the curve as determined by the use of the actual rather than the original cross-sectional areas. A plastic true stress-true strain curve is shown with the corresponding plastic "engineering" stress-strain curve in Figure 3.01.06. See

Section 3.01.09 for the presentation of an "engineering" plastic stress-strain curve. A true plastic curve may be constructed similarly.

Fracture in a uniaxial tensile test actually occurs when the strain hardening ability of the material is no longer able to compensate for the reduction in area that occurs during plastic flow.

Ductility is usually based on the % elongation of a tensile test specimen at fracture while the true measure of ductility would actually be at the strain corresponding to the maximum load on the stress-strain curve. This is referred to as the "point of instability" since significant reduction of area or "necking" begins to occur here while the load is dropping off before the onset of fracture.

True toughness should be based on the area under the true stress-true strain curve up to the "point of instability" instead of the area up to fracture under the "engineering" stress-strain curve; see Section 3.01.03 on Toughness.

The reason that a sudden and violent rupture does not occur is that the straining ability of the test specimen exceeds the cross-head movement of the testing machine, thereby permitting the load to drop off. This is registered in the tensile test by a reduction of load beyond the point of maximum load where the coupon actually separates into two parts.

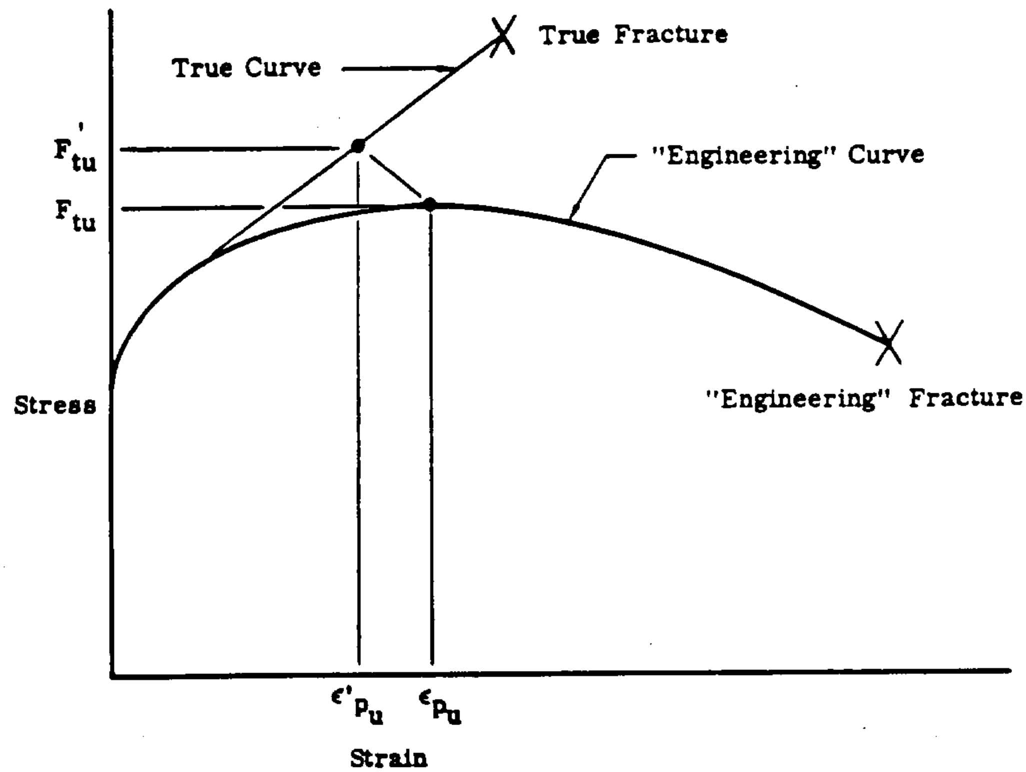

Plastic "Engineering" and True Stress-True Strain Curves

Figure 3.01.06

Definitions

f	"Engineering" stress
ϵ_p	"Engineering" plastic strain
f'	True stress
ϵ'	True strain
ϵ'_p	True plastic strain

ϵ_{p_u} "Engineering" plastic strain corresponding to F_{tu}, the engineering ultimate tensile stress.

ϵ'_{p_u} True plastic strain corresponding to F'_{tu}, the true ultimate tensile stress.

A_o Original cross-sectional area of the test specimen.

L_o Original gage length of the test specimen.

A Actual cross-sectional area of the test specimen at a prescribed load.

L Actual gage length of the test specimen at a prescribed load.

n Strain hardening exponent.

k Strength coefficient.

e Napierian base (2.718....).

Equations showing the relationship between the "engineering" and true curves are presented as follows:

$$\epsilon' = \int_{L_o}^{L} \frac{dL}{L} = \ln \frac{L}{L_o} \qquad (3.01.05)$$

Assuming the elastic strain to be negligible:

$$\epsilon'_p = \int_{L_o}^{L} \frac{dL}{L} = \ln \frac{L}{L_o} \qquad (3.01.06)$$

and

$$\frac{L}{L_o} = (e)^{\epsilon'_p} \qquad (3.01.07)$$

$$\epsilon_p = \frac{L - L_o}{L_o} = \frac{L}{L_o} - 1 \qquad (3.01.08)$$

and

$$\frac{L}{L_o} = \epsilon_p + 1 \qquad (3.01.09)$$

From Equations 3.01.06 and 3.01.08

$$\epsilon'_p = \ln(\epsilon_p + 1) \qquad (3.01.10)$$

Plastic deformations can be assumed to take place at constant volume.

$$A_o L_o = AL \qquad (3.01.11)$$

The load at any point in the tensile test is P and

$$f' = \frac{P}{A}$$

From Equation 3.01.11

$$f' = \left(\frac{P}{A_o}\right)\left(\frac{L}{L_o}\right) = f\left(\frac{L}{L_o}\right) \qquad (3.01.12)$$

Using Equation 3.01.09 and 3.01.12 all values of true stress including F'_{tu} become as follows:

$$f' = f(\epsilon_p + 1) \qquad (3.01.13)$$

$$F'_{tu} = F_{tu}(\epsilon_{p_u} + 1) \qquad (3.01.14)$$

It has been found that the plastic true stress-true strain relations may be expressed by:

$$f' = k(\epsilon'_p)^n \qquad (3.01.15)$$

$$F'_{tu} = k\,(\epsilon'_{p_u})^n \qquad (3.01.16)$$

or

$$\ln f' = n \ln \epsilon'_p + \ln k \qquad (3.01.17)$$

$$\ln F'_{tu} = n \ln \epsilon'_{p_u} + \ln k \qquad (3.01.18)$$

By considering the differential of load dP equal to zero at the point of instability or maximum load, the values for n and k become as follows:

$$n = \epsilon'_{p_u} = \ln(\epsilon_{p_u} + 1) \qquad (3.01.19)$$

$$k = F'_{tu}\left(\frac{1}{n}\right)^n = F_{tu}\,(\epsilon_{p_u} + 1)\left(\frac{1}{n}\right)^n \qquad (3.01.20)$$

In plotting Equation 3.01.17 on rectangular coordinates, n, the strain hardening exponent, becomes equal to the slope of the curve as shown in Figure 3.01.07.

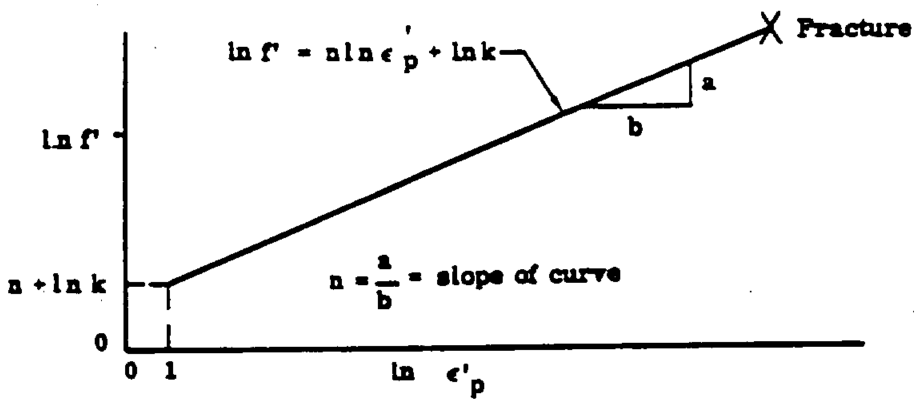

Plastic Logarithmic True Stress-Strain Curve

Figure 3.01.07

Data Source, Section 1.3 Reference 2

In conclusion, n may be determined in either of two ways:

a. By Equation 3.01.19 if a plastic "engineering" stress-strain curve is available.

b. By the slope of the logarithmic true stress-true strain curve as shown in Figure 3.01.07, if available.

3.6

3.01.12 SURFACE ROUGHNESS

In Section 1-25 of the Drafting Room Manual, surface roughness requirements and specifications are given.

The surfaces of machined parts exhibit notches and grooves of varying size depending on the cutting speed, cutting tool, and the machine. The surface roughness number is a physical value representing the maximum permissible RMS (Root Mean Square) average deviation from the mean surface line both above and below the mean surface in millionths of an inch.

Fatigue failure can occur due to stress concentrations at these grooves and notches. Therefore, Table 3.01.01 is provided as a general guide to indicate the maximum surface roughness values for moderately and highly stressed parts. Maximum surface roughness values for functional requirements will not be the responsibility of the Structures Engineer.

Table 3.01.01

Maximum Surface Roughness Values

MATERIAL	Room Temperature and Elevated Temperatures		Room Temperature to -100°F		-100°F to -420°F *	
	Moderately Stressed	Highly Stressed	Moderately Stressed	Highly Stressed	Moderately Stressed	Highly Stressed
AISI 301, 302, etc. All Strengths	250	125	250	125	250	125
AM 350, 355 All Strengths	250	125	250	125	250	125
17-4PH, 17-7PH	125	63	63	63	63	63
19-9 DL, DX	250	125	250	125	250	125
Inconel X	250	125	125	63	125	63
K-Monel	250	125	125	63	125	63
A-286	250	125	125	63	125	63
Pure Titanium	250	125	125	63	63	63
Titanium Alloy	125	63	63	63	63	63
4130, 4140 N HT to 180	250	125	125	63	63	63
4340 HT 150 to 180	250	125	125	63	63	63
4340 HT 180 to 260	125	63	63	63	63	63
Aluminum Alloys	250	125	250	125	250	125
Magnesium	250	125	250	125	250	125

* Do not use this table for selection of materials at low temperature environment; consult the Structures Development Group.

Data Source, Section 1.3 Reference 2

3.7

3.01.13 NON-DIMENSIONAL STRESS-STRAIN CURVES

Stress-strain curves are of fundamental importance in the computation of plastic bending and buckling stresses.

Ramberg and Osgood* have proposed a three parameter representation of stress-strain relations in the yield region.

$$\frac{E\epsilon}{F_{0.7}} = \frac{f}{F_{0.7}} + \left(\frac{f}{F_{0.7}}\right)^n \quad (3.01.21)$$

$F_{0.7}$ - Secant yield stress (corresponding to the intersection of the stress-strain curve and a straight line through the origin, having a slope of 0.7 E). Fig. 3.01.08

$F_{0.85}$ - Corresponds to the intersection of the stress-strain curve and a straight line through the origin, having a slope of 0.85 E: Fig. 3.01.08

$$n = 1 + \log_e (17/7)/\log_e (F_{0.7}/F_{0.85}) \quad (3.01.22)$$

(See Figure 3.01.09 for plot of equation.)

The quantities $E\epsilon/F_{0.7}$ are non-dimensional and may be used in determining the non-dimensional curves of Figure 3.01.10. E, n, and $F_{0.7}$ must then be known to use these curves.

* From Reference 3.

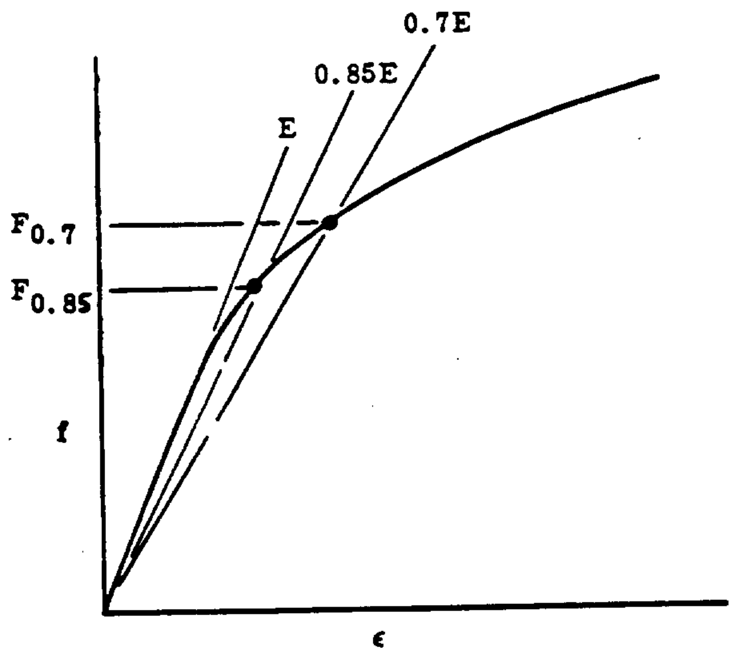

NON-DIMENSIONAL STRESS - STRAIN CURVES

Figure 3.01.08

PLOT OF EQUATION 3.01.22

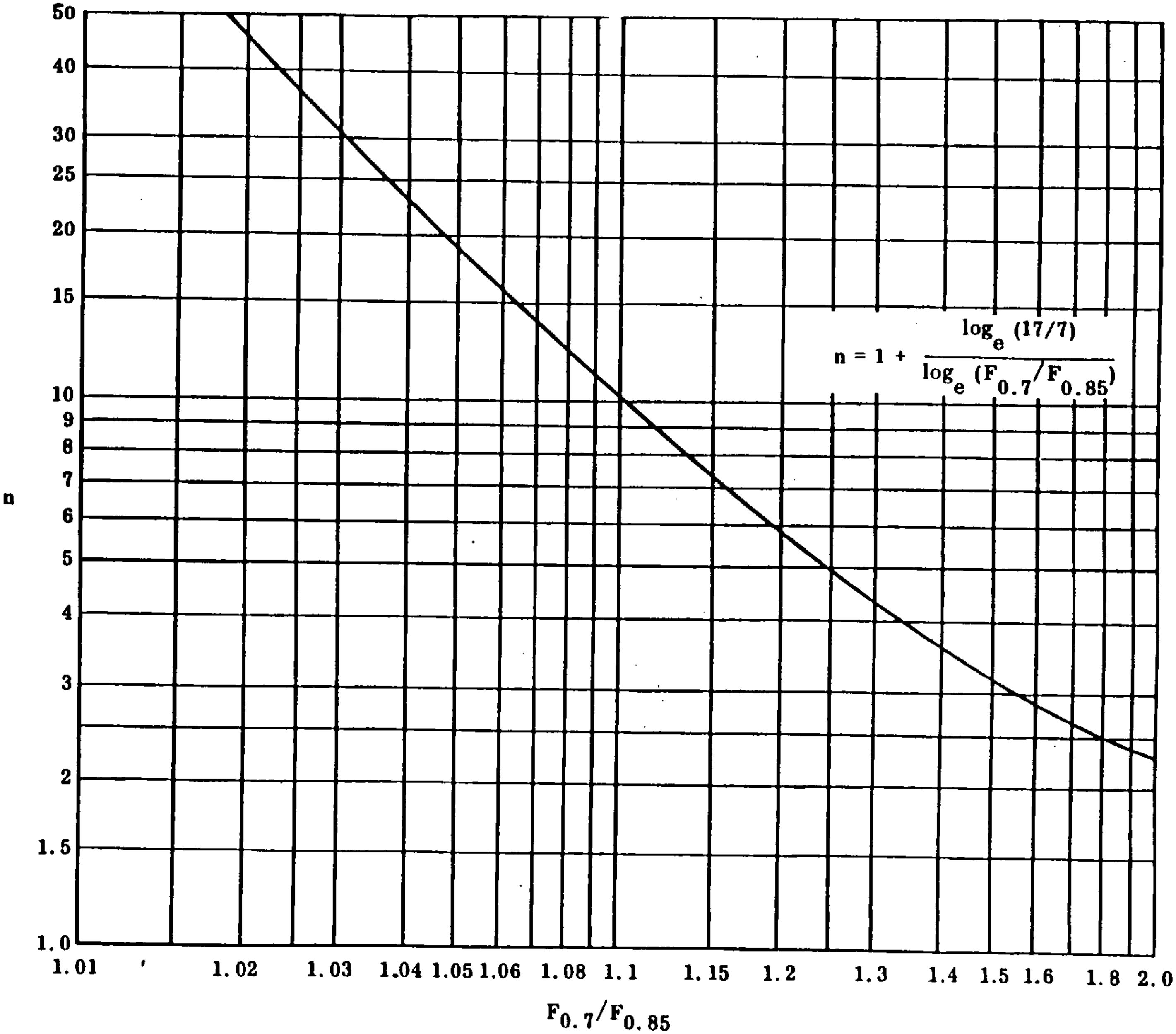

Figure 3.01.09

PLOT OF EQUATION 3.01.21

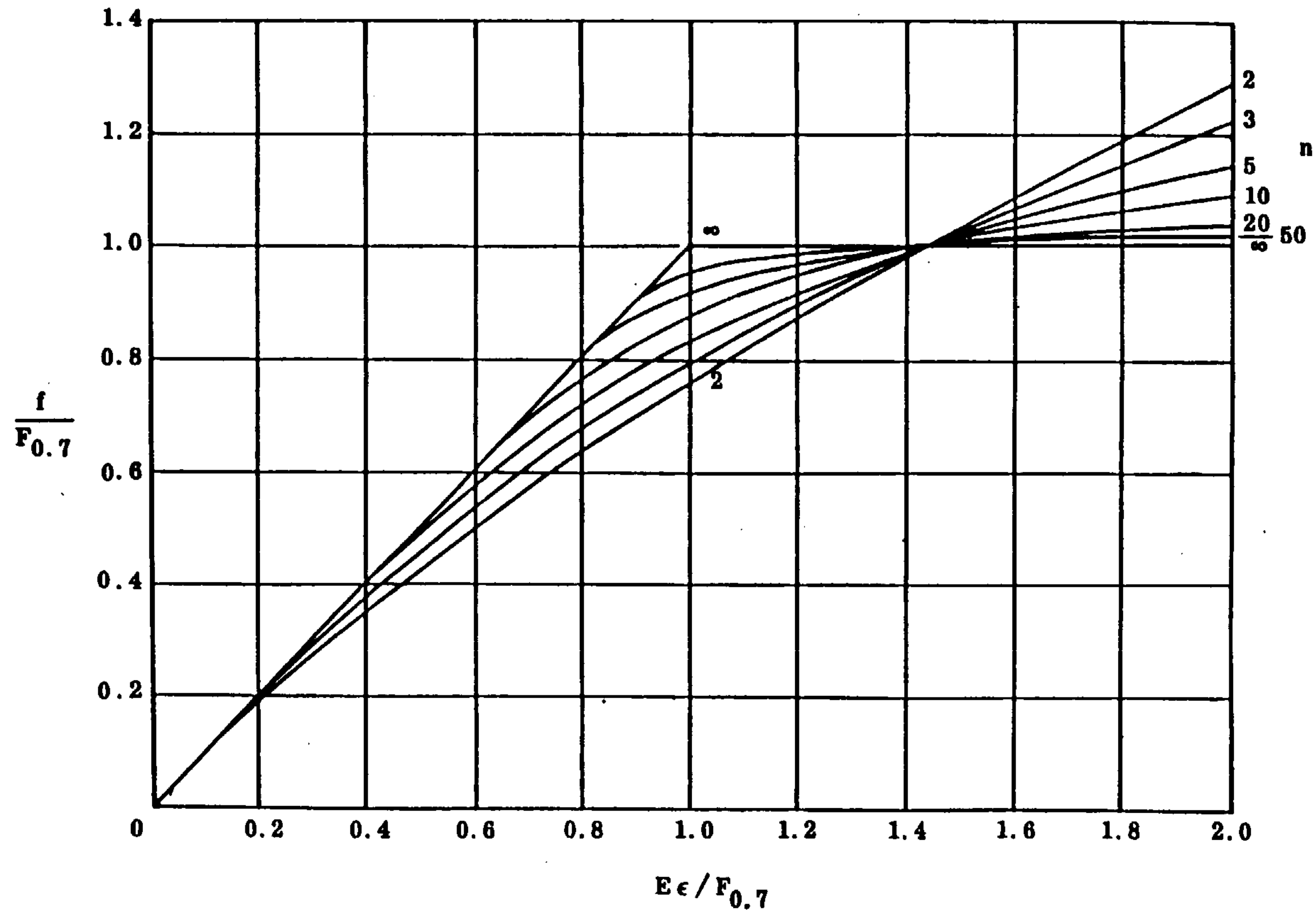

Figure 3.01.10

Data Source, Section 1.3 Reference 2

3.02 MATERIAL PROPERTIES AT ROOM AND ELEVATED TEMPERATURES

3.8

3.02.01 TABULATED MINIMUM MATERIAL PROPERTY VALUES INCLUDING THE RAMBERG-OSGOOD CONSTANTS

This section presents the required material properties for the determination of Ramberg-Osgood constants (Reference Section 3.01.13). Values of $F_{0.7}$ and $F_{0.85}$ were obtained from minimum engineering stress-strain curves and the parameter n from Figure 3.01.09

Material property values should be obtained from Reference 18 ⚠ or other official source. Where these values correspond directly to the values called out in Table 3.02.02, the Ramberg-Osgood constants are applicable as shown.

Table 3.02.01

PAGE

Stainless Steels 3.8.2

Low Carbon and Alloy Steels 3.8.5

Heat Resistant Alloys 3.8.6

Aluminum Alloys 3.8.6

Magnesium Alloys 3.8.9

Titanium Alloys 3.8.10

⚠ Data Source, Section 1.3

Table 3.02.02

MATERIAL	Temp Exp, Hr	Temp °F	e, %	F_{tu}, ksi	F_{cy}, ksi	E_c 10^6 psi	$F_{0.7}$ ksi	$F_{0.85}$ ksi	n
STAINLESS STEEL									
AISI 301 1/4 Hard Sheet Transverse Compression	1/2	RT	25	125	80	27.0	73	63	6.9
	1/2	400							
	1/2	600							
	1/2	1000							
Longitudinal Compression	1/2	RT	25	125	43	26.0	26.2	23	5.2
	1/2	400							
	1/2	600							
	1/2	1000							
AISI 301 1/2 Hard Sheet Transverse Compression	1/2	RT	15	150	118	27.0	116.5	105	9.2
	1/2	400		118	108.5	23.2	108.5	97	8.6
	1/2	600		110	107.5	20.9	108.5	96.5	8.2
	1/2	1000		86	86	16.2	94.5	83.5	8.0
Longitudinal Compression	1/2	RT	15	150	58	26.0	48	37	4.4
	1/2	400		118	53.3	22.4	45.5	36	4.7
	1/2	600		110	52.8	20.1	44	31	3.5
	1/2	1000		86	45.2	15.6	40	30.5	4.3
AISI 301 3/4 Hard Sheet Transverse Compression	1/2	RT	12	175	160	27.0	163.5	151.5	13.2
	1/2	400		148	148	24.1	153	142.5	13.2
	1/2	600		138	138	22.4	152	140	11.2
	1/2	1000		112	112	18.9	127	121	19.2
Longitudinal Compression	1/2	RT	12	175	76	26.0	70	61.5	7.6
	1/2	400		148	71	23.3	65	56	6.8
	1/2	600		138	70.3	21.6	65.5	56.5	6.8
	1/2	1000		112	59.3	18.2	55	46	5.9

MATERIAL	Temp Exp, Hr	Temp °F	e, %	F_{tu}, ksi	F_{cy}, ksi	E_c 10^6 psi	$F_{0.7}$ ksi	$F_{0.85}$ ksi	n
AISI 301 3/4 Hard Sheet (CV Special), Longitudinal Compression	1/2	RT	12	175	68	26.0	57	44	4.4
	1/2	400		148	63.6	23.3	54	44	5.3
	1/2	600		138	63.0	21.6	54	45	5.8
	1/2	1000		112	53.0	18.2	46	38	5.7
AISI 301 Full Hard Sheet Transverse Compression	1/2	RT	8	185	179	27.0	183	172	16
	1/2	400		168	168	25.1	174	164	16
	1/2	600		159	159	23.8	172	162	16
	1/2	1000		131	130	21.6	141.5	135.5	21.5
Longitudinal Compression	1/2	RT	8	185	85	26.0	77.5	63	5.2
	1/2	400		168	80.8	24.2	74	59.5	5
	1/2	600		159	79.9	22.9	74	58	4.6
	1/2	1000		131	66.3	20.8	58	42.5	3.9
AISI 301 Extra Hard Sheet Longitudinal Compression	1/2	RT	2	200					
	1/2	400							
	1/2	600							
	1/2	800							
AISI 321 Annealed Sheet	1/2	RT	40	75					
	1/2	400							
	1/2	800							
	1/2	1200							
17-4 PH Bar & Forgings	1/2	RT	6	180	165	27.5	166	160	24
	1/2	400		162	135	25.3	137	129	16
	1/2	700		146	105.5	23.1	106	97	11
	1/2	1000		88	62.6	21.2	60	52	7.1

MATERIAL	Temp Exp, Hr	Temp °F	e, %	F_{tu}, ksi	F_{cy}, ksi	E_c 10^6 psi	$F_{0.7}$ ksi	$F_{0.85}$ ksi	n
17-7 PH (TH1050) Sheet, Strip & Plate, t = .010 to .125 in.	1/2	RT		180	162	29.0	166	145	7.4
	1/2	400		169	144	27.8	146	126	6.8
	1/2	700		144	118	24.9	117	104	8.4
	1/2	1000		88	61.5	20.3	56	47	6
17-7 PH (RH950) Sheet, Strip & Plate, t = .010 to .125 in.	1/2	RT		210	205	29.0	208	196	16.4
	1/2	400							
	1/2	600							
	1/2	800							
19-9DL (AMS 5526) & 19-9DX (AMS 5538), Sheet, Strip & Plate	1/2	RT	30	95	45	29.0	36.5	32	7.6
	1/2	400		84	39.6				
	1/2	700		79	35.1				
	1/2	1000		65	31.9				
19-9DL (AMS 5527) & 19-9DX (AMS 5539) Sheet, Strip & Plate	1/2	RT	12	125	90	29.0	85	74	7.2
	1/2	400		110	79.2				
	1/2	700		103	70.2				
	1/2	1000		86	63.9				
PH15-7Mo (TH1050) Sheet & Strip, t = .020 to .187 in.	1/2	RT	5	190	170	28.0	171	164	22.5
	1/2	300							
	1/2	600							
	1/2	800							
	1/2	1000							
PH15-7Mo (RH 950) Sheet & Strip, t = .020 to .187 in.	1/2	RT	4	225	200	28.0	218	189	7.3
	1/2	300							
	1/2	600							
	1/2	800							
	1/2	1000							

MATERIAL	Temp Exp, Hr	Temp °F	e, %	F_{tu}, ksi	F_{cy}, ksi	E_c 10^6 psi	$F_{0.7}$ ksi	$F_{0.85}$ ksi	n
AM 355 Sheet, Heat Treated	1/2	RT							
	1/2	400							
	1/2	600							
	1/2	800							
LOW CARBON & ALLOY STEELS									
AISI 1023 & 1025 Tube, Sheet & Bar, Cold Finished		RT	22	55	36	29.0	32.7	31.5	24
AISI 4130 Normalized, t > .188 in.	1/2	RT	23	90	70	29.0	61.5	53	6.8
	1/2	500		81	61.5	27.3	55	48	7.3
	1/2	800		68	46.2	23.8	40	32.5	5.2
	1/2	1000		46	30.8	20.6	28	22	4.7
AISI 4130, 4140, 4340 Heat Treated	1/2	RT	23	125	113	29.0	111	102	10.9
	1/2	500		113	98.3	27.3	96	88	10.9
	1/2	850		88	68.9	23.2	66.5	61.5	12
	1/2	1000		64	49.7	20.6	45.5	41	9.2
AISI 4130, 4140, 4340 Heat Treated	1/2	RT	18.5	150	145	29.0	145	140	25
	1/2	500		135	126	27.3	126	122	29
	1/2	850		105	88.5	23.2	88	83.5	18.5
	1/2	1000		76	63.8	20.6	62	57	10.9
AISI 4130, 4140, 4340 Heat Treated	1/2	RT	15	180	179	29.0	179	176	50
	1/2	500		162	156	27.3	156	153	46
	1/2	850		126	109.3	23.2	109.4	105	22
	1/2	1000		92	77	20.6	75	68	9.8
AISI 4130, 4140, 4340 Heat Treated	1/2	RT	13.5	200	198	29.0	198	196	90
	1/2	500		180	170	27.3	172.5	169	46
	1/2	850		140	121	23.2	121.5	117	25
	1/2	1000		104	87.1	20.6	87	83	19

MATERIAL	Temp Exp, Hr	Temp °F	e, %	F_{tu}, ksi	F_{cy}, ksi	E_c 10^6 psi	$F_{0.7}$ ksi	$F_{0.85}$ ksi	n
HEAT RESISTANT ALLOYS									
A-286 (AMS 5725A) Sheet, Plate & Strip	1/2	RT	15	140	95	29.0	93	87	14
	1/2	600		129	88.4	24.4	87	81	13.5
	1/2	1000		115	81.7	19.8	81	75	12.5
	1/2	1400		52	50.3	14.2	50	47	15.3
K-MONEL Sheet, Age Hardened	1/2	RT	15	125	90	26.0	88	82	13.5
	1/2	400							
	1/2	600							
	1/2	800							
	1/2	1000							
MONEL Sheet, Cold Rolled & Annealed	1/2	RT	35	70	28	26.0	20	17	6.4
	1/2	400							
	1/2	600							
	1/2	800							
	1/2	1000							
INCONEL-X	1/2	RT	20	155	105	31.0	104	100	23.5
	1/2	400		152	95.6	28.9	94	89	17
	1/2	800		141	90.2	26.4	88.6	84	18.5
	1/2	1200		104	83	23.2	82	78.6	21
ALUMINUM ALLOYS									
2014-T6 Extrusions $t \leq 0.499$ in.	2	RT	7	60	53	10.7	53	50.3	18.5
	2	300		51	42.5	10.2	41.5	40	24
	2	450		28	21	9.2	20.5	19.5	25
	2	600		10	8.0	7.4	5.5	4.5	5.4
	1/2	300		51	43.5	10.2	44.0	42.5	25
	1/2	450		31	26	9.2	26	25.2	29

MATERIAL	Temp Exp, Hr	Temp °F	e, %	F_{tu}, ksi	F_{cy}, ksi	E_c 10^6 psi	$F_{0.7}$ ksi	$F_{0.85}$ ksi	n
2014-T6 Forgings	2	RT	7	62	52	10.7	52.3	50	20
t ≤ 4 in.	2	300		53	41	10.2	40.5	38.5	19
	2	450		29	22	9.2	21.5	20	12.6
	2	600		10	7.5	7.4	4.5	3.0	3.2
	1/2	300		53	43	10.2	42.5	40	15.8
	1/2	450		32	25.5	9.2	25.0	23.5	15.6
2024-T3 Sheet & Plate,	2	RT	12	65	40	10.7	39	36	11.5
Heat Treated, t ≤ .250 in.	2	300			37	10.3	35.7	33.5	15
	2	500			26	8.4	24.8	22.8	10.9
	2	700			7.5	6.4	6.2	5.5	8.2
2024-T4 Sheet & Plate,	2	RT	12	65	38	10.7	36.7	34.5	15.6
Heat Treated, t ≤ 0.50 in.	2	300			34	10.3	32.5	30.5	14.6
	2	500			24	8.4	23	21	10.2
	2	700			7	6.4	60	5.7	18.5
2024-T3 Clad Sheet & Plate,	2	RT	12	60	37	10.7	35.7	33	12
Heat Treated, t = .020 to .062 in.	2	300			34	10.3	33	30.3	11
	2	500			24.5	8.4	22.7	20	7.9
	2	700			6.5	6.4	5.8	5.5	18.5
2024-T6 Clad Sheet & Plate,	2	RT	8	62	49	10.7	49	45	11
Heat Treated, t ≥ 0.063 in.	2	300			45	10.3	44.3	40.7	11
	2	500			22	8.4	31.5	28	8.3
	2	700			6	6.4	7.0	6.0	6.6
2024-T6 Clad Sheet & Plate,	2	RT	8	60	47	10.7	47	43	10.6
Heat Treated; t < 0.063 in.	2	300			43.2	10.3	42.3	38.7	10.8
	2	500			21	8.4	29.5	26	7.8
	2	700			6	6.4	5.0	4.0	4.9

MATERIAL	Temp Exp. Hr	Temp °F	e, %	F_{tu}, ksi	F_{cy}, ksi	E_c 10^6 psi	$F_{0.7}$ ksi	$F_{0.85}$ ksi	n
2024-T81 Clad Sheet, Heat Treated,	2	RT	5	62	55	10.7	56	51.6	11.2
t < 0.064 in.	2	300			50.5	10.3	51.2	46.5	10
	2								
	2								
6061-T6 Sheet, Heat Treated & Aged,	1/2	RT	10	42	35	10.1	35	34	31
t < 0.25 in.	1/2	300			29.5	9.5	29	28	26
	1/2	450			20.5	8.5	19.3	17.7	10.9
	1/2	600			7.5	7.0	6.6	6.2	15.2
7075-T6 Bare Sheet & Plate,	2	RT	7	76	67	10.5	70	63	9.2
t ≤ 0.50 in.	2	300			54	9.4	55.8	52.5	15.6
	2	425			25.5	8.1	25.4	23.5	12.1
	2	600			8	5.3	7.2	5.2	3.7
	1/2	425			30	8.1	34.5	32.5	16
7075-T6 Extrusions,	2	RT	7	75	70	10.5	72	68	16.6
t ≤ 0.25 in.	2	300			54	9.4	58.5	54.5	13.4
	2	450			22.5	7.8	21.3	18.5	7.2
	2	600			8	5.3	6.5	4.3	3.2
	1/2	450			25	7.8	29	26	8.8
7075-T6 Die Forgings,	2	RT	7	71	58	10.5	58.5	55.1	15.2
t ≤ 2 in.	2	300			47.6	9.4	47.8	45	15.6
	2	450			18.5	7.8	17.3	16	12
	2	600			7.0	5.3	5.0	3.7	3.9
	1/2	450			23	7.8	24	22	10.9
7075-T6 Hand Forgings,	2	RT	4	72	63	10.5	63.8	61.5	25
Area ≤ 16 sq in.	2	300			51.6	9.4	52.2	50	21.5
	2	450			20.2	7.8	20.3	19	13.7
	2	600			7.6	5.3	6.0	5.0	5.8
	1/2	450			24	7.8	26.5	25.3	19.5

MATERIAL	Temp Exp, Hr	Temp °F	e, %	F_{tu}, ksi	F_{cy}, ksi	E_c 10^6 psi	$F_{0.7}$ ksi	$F_{0.85}$ ksi	n
7075-T6 Clad Sheet & Plate, $t \leq 0.50$ in.	2	RT	8	70	64	10.5	64.5	61.6	19.5
	2	300			50	9.4	54	51.7	20
	2	450			20.5	7.8	19.7	17.5	4.6
	2	600			7.7	5.3	7.7	5.5	3.6
	1/2	450			23	7.8	27.2	25.3	12.4
7079-T6 Hand Forgings, $t \leq 6.0$ in.	1/2	RT	4	67	59	10.5	59.5	57.5	26
	1/2	300			47	9.4	46.5	45	29
	1/2	450			21	7.8	20	18.5	12
	1/2	600			7.0	5.3	5.5	3.5	3.0
MAGNESIUM ALLOYS									
AZ61A Extrusions, $t \leq 0.249$ in.		RT	8	38	14	6.3	12.9	12.3	19
HK31A-0 Sheet $t = 0.016$ to 0.250 in.	1/2	RT	12	30	12	6.5	10	8.4	6
	1/2	300		20	11.1	6.16	8.9	6.9	4.5
	1/2	500		15	9.3	4.94	7.5	5.6	4.2
	1/2	600		10	4.9	3.77	3.3	1.6	2.2
HK31A-H24 Sheet, $t < 0.250$ in.	1/2	RT	4	34	19	6.5	17.3	14.6	6.2
	1/2	300		22	17.7	6.2	15.6	12.6	5.1
	1/2	500		17	14.8	4.9	13.1	10.5	4.9
	1/2	600		11	7.8	3.8	6.7	5.2	4.5

MATERIAL	Temp Exp, Hr	Temp °F	e, %	F_{tu}, ksi	F_{cy}, ksi	E_c 10^6 psi	$F_{0.7}$ ksi	$F_{0.85}$ ksi	n
TITANIUM ALLOYS									
Ti-8Mn Annealed Sheet, Plate & Strip	1000	RT	10	120	110	15.5	119.5	102	13.7
	1000	400		100	72.6				
	1000	600		91	66				
	1000	800		75	53.9				
	1000	1000		38	24.2				
Ti-6Al-4V Annealed Bar & Sheet, t ≤ .187 in.	1/2	RT	10	130	126	16.0	127	124.5	43
	1/2	400		105	96	14.1	97	93	22
	1/2	600		99	84.5	13.0	85.5	82	22
	1/2	800		87	79.4	11.8	80.5	77	21.5
	1/2	1000		70	60.6	7.7	61	59.5	36

SECTION 4.0

BEAMS

ANALYTICAL METHODS FOR STRAIGHT, CURVED AND BUILT-UP BEAMS ARE PRESENTED. ADDITIONAL TABLES FOR BEAM ANALYSIS ARE GIVEN IN " FORMULAS FOR STRESS AND STRAIN " R.J. ROARK.

3RD EDITION, SEE CHAPTER 8

		PAGE
4.1	BEAM TABLES	4.1.1
4.2	VARIABLE CROSS SECTION	4.2.1
4.3	CONTINUOUS BEAMS	4.3.1
4.4	MOMENT DISTRIBUTION METHOD	4.4.1
4.5	CURVED BEAMS	4.5.1
4.6	LATERAL STABILITY	4.6.1
4.7	SHEAR STRESSES	4.7.1
4.8	TENSION FIELD WEBS	4.8.1
4.9	CUT-OUTS	4.9.1
4.10	SLOTTED BEAM	4.10.1
4.11	ELASTIC FOUNDATION	4.11.1

Data Source, Section 1.3 Reference 1

BEAMS

4.1.0 Simple Beams

4.1.1 Shear, Moment, and Deflection

The general equations for a beam in pure bending are given in Table 4.1.1-1. These equations are given in terms of deflection, bending moment, and applied loads in columns 1, 2, and 3, respectively.

Table 4.1.1-1

TITLE	(1)	(2)	(3)
Deflection	$\Delta = y$	$\Delta = \iint \frac{M}{EI}\, dxdx$	
Slope	$\theta = dy/dx$	$\theta = \int \frac{M}{EI}\, dx$	
Bending Moment	$M = EI\, d^2y/dx^2$	M	$M_x = M_o + V_o x$ - Moments of any loads on the segment
Shear	$V = EI\, d^3y/dx^3$	$V = dM/dx$	$V_x = V_o$ + algebraic sum of the ext. loads on the segment
Load	$w = EI\, d^4y/dx^4$	$w = dV/dx = d^2M/dx^2$	w

With reference to Fig. 4.1.1-2, the sign convention is:

a) $\underline{x}$ is positive to the right.
b) $\underline{y}$ is positive upward.
c) $\underline{M}$ is positive when the compressed fibers are on the top.
d) $\underline{w}$ is positive in the direction of positive $\underline{y}$.
e) $\underline{V}$ is positive when the part of the beam to the left of the section tends to move upward under the action of the resultant of the vertical forces.

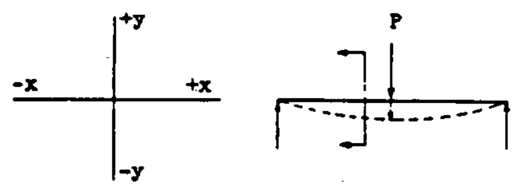

Fig. 4.1.1-2

The limiting assumptions are:

a) The material follows Hooke's law.
b) Plane cross sections remain plane.
c) Shear deflections are neglected.
d) The deflections are small.

In short beams, the deflection due to vertical shear sometimes is appreciable and may need to be considered. If deflections due to shear are considered, the differential equations of the deflection curve of the beam is

$$y = \iint \frac{M dx\, dx}{EI} + \int \frac{KV\, dx}{AG} \quad . \quad (1)$$

where (K) is the ratio of the maximum shearing stress on the cross-section to the average shearing stress. The value of (K) is given by the equation

$$K = \frac{A}{Ib} \int_0^a b' y dy \quad . \; . \; . \; . \quad (2)$$

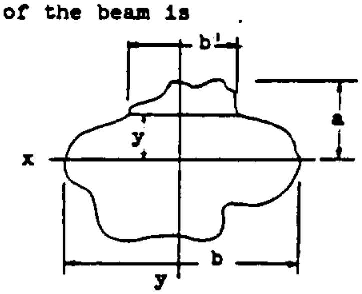

Fig. 4.1.1-3

Where (I) is the moment of inertia of the cross section with respect to the centroidal axis and (a), (b), (b'), and (y) are the dimensions shown in Fig. 4.1.1-3.

TABLE 4.1.1.1

BEAMS - SIMPLE SUPPORT AT EACH END			
TYPE OF LOADING	REACTIONS	BENDING MOMENTS	DEFLECTIONS
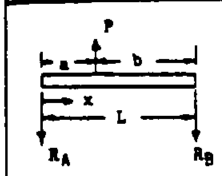	$R_A = +\frac{Pb}{L}$ $R_B = +\frac{Pa}{L}$	$M_x = -\frac{Pbx}{L}$; $x<a$ $M_x = -\frac{Pa}{L}(x-a)$; $x>a$ $M_{max} = -\frac{Pba}{L}$; at $x = a$	$y = \frac{Pbx}{6EIL}(L^2-b^2-x^2)$; $x<a$ $y = \frac{Pa(L-x)}{6EIL}(2Lx-a^2-x^2)$; $x>a$ $y_{max} = \frac{Pab}{27EIL}(a+2b)\sqrt{3a(a+2b)}$; at $x = \sqrt{\frac{1}{3}a(a+2b)}$ with $a>b$
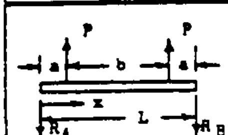	$R_A = +P$ $R_B = +P$	$M_x = -P_x$; $x<a$ $M_x = -P_a$; $a<x<(L-a)$ $M_{max} = -P_a$; From $x = a$ To $x = a+b$	$y = \frac{Px}{6EI}(3La-3a^2-x^2)$; $x<a$ $y = \frac{Pa}{6EI}(3Lx-3x^2-a^2)$; $a<x<(a+b)$ $y_{max} = \frac{Pa}{24EI}(3L^2-4a^2)$; at $x = \frac{L}{2}$
	$R_A = +\frac{W}{2}$ $R_B = +\frac{W}{2}$	$M_x = -\frac{Wx}{2L}(L-x)$ $M_{max} = -\frac{WL}{8}$, at $x = \frac{L}{2}$	$y = \frac{Wx}{24EIL}(L^3-2Lx^2+x^3)$ $y_{max} = \frac{5WL^3}{384EI}$, at $x = \frac{L}{2}$
	$R_A = +\frac{W}{2}$ $R_B = +\frac{W}{2}$	$M_x = -Wx\left(\frac{1}{2} - \frac{2}{3}\frac{x^2}{L^2}\right)$; $x<\frac{L}{2}$ $M_{max} = -\frac{WL}{6}$, at $x = \frac{L}{2}$	$y = \frac{Wx}{6EIL^2}\left(\frac{L^2x^2}{2} - \frac{x^4}{5} - \frac{5L^4}{16}\right)$; $x<\frac{L}{2}$ $y_{max} = \frac{WL^3}{60EI}$, at $x = \frac{L}{2}$
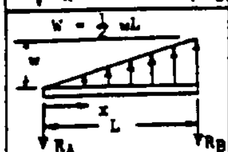	$R_A = +\frac{1}{3}W$ $R_B = +\frac{2}{3}W$	$M_x = -\frac{Wx}{3}\left(1-\frac{x^2}{L^2}\right)$ $M_{max} = -0.128WL$; at $x = 0.5774L$	$y = \frac{Wx}{180EIL^2}(3x^4-10L^2x^2+7L^4)$ $y_{max} = 0.01304\frac{WL^3}{EI}$; at $x = 0.519L$
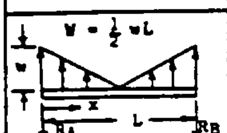	$R_A = +\frac{W}{2}$ $R_B = +\frac{W}{2}$	$M_x = -Wx\left(\frac{1}{2} - \frac{x}{L} + \frac{2x^2}{3L^2}\right)$; $x<\frac{L}{2}$ $M_{max} = -\frac{WL}{12}$, at $x = \frac{L}{2}$	$y = \frac{W}{12EI}\left(x^3 - \frac{x^4}{L} + \frac{2x^5}{5L^2} - \frac{3L^2}{8}x\right)$; $x<\frac{L}{2}$ $y_{max} = \frac{3}{320}\frac{WL^3}{EI}$, at $x = \frac{L}{2}$
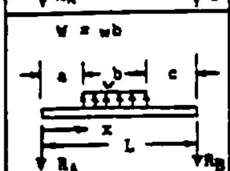	$R_A = +\frac{W(2c+b)}{2L}$ $R_B = +\frac{W(2a+b)}{2L}$	$M_x = -\frac{W(2c+b)x}{2L}$; $x<a$ $M_x = -\frac{W(2c+b)x}{2L} + \frac{W(x-a)^2}{2b}$ $a<x<(a+b)$ is maximum when $x = \frac{b}{2L}(2c+b)+a$	
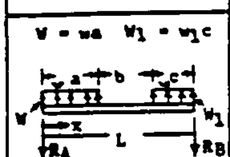	$R_A = +\frac{W(2L-a)+W_1c}{2L}$ $R_B = +\frac{W_1(2L-c)+Wa}{2L}$	$M_x = -\left(R_Ax - \frac{Wx^2}{2a}\right)$; $x<a$ $M_x = -\left[R_Ax - \frac{W}{2}(2x-a)\right]$; $a<x<(a+b)$ For $R_A<W$ $M_{max} = -\frac{aR_A^2}{2W}$; at $x = \frac{aR_A}{W}$	
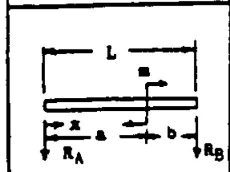	$R_A = +\frac{m}{L}$ $R_B = -\frac{m}{L}$	$M_x = -\frac{mx}{L}$; $x<a$ $M_x = -\frac{mx}{L} + m$; $x>a$ $M_{max} = -\frac{ma}{L}$; $a>b$	$y = \frac{mx}{6EIL}(L^2-3b^2-x^2)$; $x<a$ $y = \frac{m(L-x)}{6EIL}(x^2+3a^2-2Lx)$; $x>a$ For $a>b$ $y_{max} = \frac{mx^3}{3EIL}$; at $x = \sqrt{\frac{L^2}{3}-b^2}$

TABLE 4.1.1.2

CANTILEVER BEAMS				
TYPE OF LOADING	REACTIONS	BENDING MOMENTS	DEFLECTIONS	
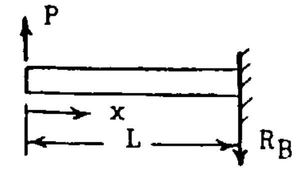	$R_B = +P$	$M_x = +Px$ $M_{max} = +PL$	$y = \frac{P}{6EI}(2L^3-3L^2x+x^3)$ $y_{max} = \frac{PL^3}{3EI};\ x = 0$	
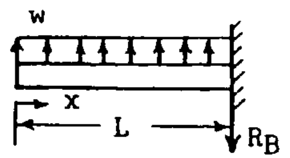	$R_B = +wL$	$M_x = +\frac{wx^2}{2}$ $M_{max} = +\frac{wL^2}{2}$	$y = \frac{w}{24EI}(3L^4-4L^3x+x^4)$ $y_{max} = \frac{wL^4}{8EI};\ x = 0$	
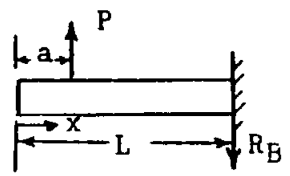	$R_B = +P$	$M_x = +P(x-a)$ $M_{max} = +P(L-a)$	$y = \frac{P(L-a)^2}{6EI}(2L-3x+a)\quad ;\ x<a$ $y = \frac{P(L-x)^2}{6EI}(2L-3a+x)\quad ;\ x>a$ y_{max} at $x = a = 0$	2
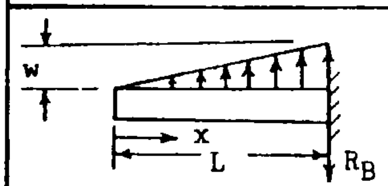	$R_B = +\frac{wL}{2}$	$M_x = +\frac{wx^3}{6L}$ $M_{max} = +\frac{wL^3}{6L}$	$y = \frac{w}{120EIL}(x^5-5L^4x+4L^5)$ $y_{max} = \frac{wL^4}{30EI};\ x = 0$	
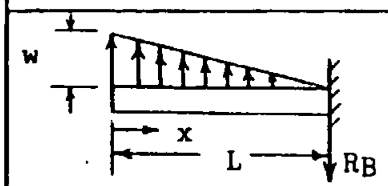	$R_B = +\frac{wL}{2}$	$M_x = \frac{wx^2}{6L}(3L-x)$ $M_{max} = \frac{wL^2}{3}$	$y_{max} = \frac{11wL^4}{120EI};\ x = 0$	2
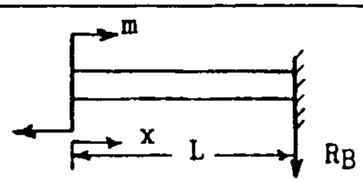	$R_B = 0$	$M_x = m$	$y = \frac{m}{2EI}(L^2-2Lx+x^2)$ $y_{max} = \frac{mL^2}{2EI};\ x = 0$	

TABLE 4.1.1.3

BEAMS RESTRAINED AT ONE END, SIMPLE SUPPORT AT OTHER			
TYPE OF LOADING	REACTIONS	BENDING MOMENTS	DEFLECTIONS
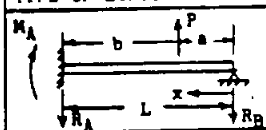	$R_A = +P + R_B$ $R_B = +\frac{P}{2}\left(\frac{3b^2L-b^3}{L^3}\right)$	$M_x = -R_B x;\ x < a$ $M_A = \frac{P}{2}\left(\frac{b^3+2bL^2-3b^2L}{L^2}\right)$ $M_x = -R_B x + P(x-L+b);\ x > a$	For $x < a$ $y = \frac{1}{6EI}\left[R_B(x^3-3L^2x)+3Pb^2x)\right]$
	$R_A = +\frac{11}{16}P$ $R_B = +\frac{5}{16}P$	$M_A = +\frac{3}{16}PL$ $M_x = -P\left(\frac{L}{2} - \frac{11}{16}x\right);\ x > \frac{L}{2}$ $M_x = -\frac{5}{16}Px$	$y = \frac{P}{EI}(5x^3-3L^2x);\ x < \frac{L}{2}$ $y = \frac{P}{EI}\left[5x^3-16(x-\frac{L}{2})^3-3L^2x\right];$ $x > \frac{L}{2}$ $y_{max} = -0.00932\frac{PL^3}{EI};\ x = .447L$
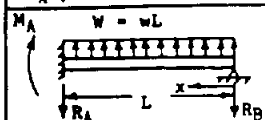	$R_A = +\frac{5}{8}W$ $R_B = +\frac{3}{8}W$	$M_A = \frac{WL}{8}$ $M_x = -W\left(\frac{3}{8}x-\frac{x^2}{2L}\right)$	$y = -\frac{W}{48EIL}(3Lx^3-2x^4-L^3x)$
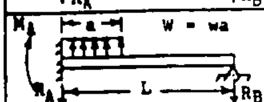	$R_A = +\frac{wa^2}{8L^3}\left[a^2-4aL+\frac{8L^3}{a}\right]$ $R_B = \left[+\frac{wa^3}{8L^3}(4L-a)\right]$	$M_A = \frac{wa^2(2L-a)^2}{8L^2}$	
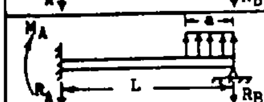	$R_A = +\frac{wa^2}{8L^3}\left[6L^2-a^2\right]$ $R_B = +\frac{wa^2}{8L^3}\left[a^2+\frac{8L^3}{a}-6L^2\right]$	$M_A = \frac{wa^2(2L^2-a^2)}{8L^2}$	
	$R_A = +\frac{m}{2L^4}(2b^3-3a^2b$ $-a^3+2L^3)$ $R_B = \frac{m}{2L^4}(2b^3-3a^2b-a^3+2L^3)$	$M_A = m\frac{(2b^3-3a^2b-a^3)}{2L^3}$	
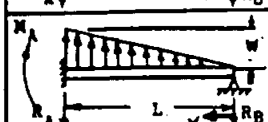	$R_A = +\frac{6wL}{15}$ w #/in $R_B = +\frac{wL}{10}$	$M_A = \frac{wL^2}{15}$	$y = \frac{W}{60EIL}(2Lx^3-L^3x-\frac{x^5}{L})$
	$R_A = +\frac{27}{120}wL$ $R_B = +\frac{33}{120}wL$	$M_A = \frac{7}{120}wL^2$	
	$R_A = +\frac{wa^2}{120L^3}\left(3a^2-15aL\right.$ $\left.+\frac{60L^3}{a}\right)$ $R_B = +\frac{wa^2}{120L^3}\left(15aL-3a^2\right)$	$M_A = \frac{wa^2(3a^2-15aL+20L^2)}{120L^2}$	
	$R_A = +\frac{wa^2}{40L^3}\left(15aL-4a^2-\frac{20L^3}{a}\right)$ $R_B = +\frac{wa^2}{40L^3}\left(15aL-4a^2\right)$	$M_A = \frac{wa^2(40L^2-45aL+12a^2)}{120L^2}$	
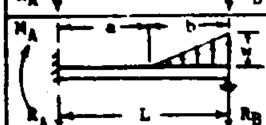	$R_A = +\frac{wb^2}{40L^3}\left(b^2-10L^2\right)$ $R_B = +\frac{wb^2}{40L^3}\left(b^2-10L^2\right)-\frac{wb}{2}$	$M_A = \frac{wb^2(10L^2-3b^2)}{120L^2}$	
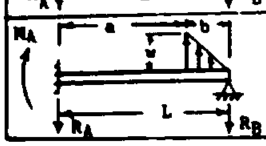	$R_A = +\left(\frac{M}{L} + \frac{3b^2}{3L}\right)$ $R_B = +\left[\left(L-\frac{2}{3}b\right)\frac{bw}{2L}-\frac{M}{L}\right]$	$M_A = \frac{w(2L^5-15a^2L^2+25a^3L^2-15a^4L+3a^5)}{30bL^2}$	

TABLE 4.1.1.4

RESTRAINED BEAMS			
TYPE OF LOADING	SUPPORT REACTIONS	BENDING MOMENTS	DEFLECTIONS
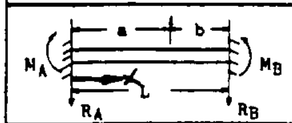	$R_A = +\frac{Pb^2(3a+b)}{L^3}$ $R_B = +\frac{Pa^2(3b+a)}{L^3}$	$M_A = \frac{Pab^2}{L^2}$ $M_B = \frac{Pa^2b}{L^2}$ $M_{max} = -R_A a + M_A$	$y = \frac{Pb^2x^2}{6EIL^3}(3aL-3ax-bx)$ $x < a$ $y_{max} = \frac{2Pa^3b^2}{3EI(3a+b)^2}$ $x = \frac{2aL}{3a+b};\ a > b$
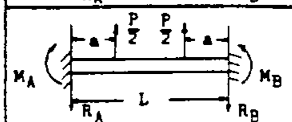	$R_A = R_B = +\frac{P}{2}$	$M_A = M_B = \frac{Pa(L-a)}{2L}$	$y_{max} = \frac{Pa^2}{48EI}(4a-3L)$
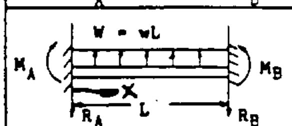	$R_A = R_B = +\frac{W}{2}$	$M_A = M_B = -\frac{WL}{12}$ $M_x = \frac{W}{2L}(-\frac{L^2}{6}+Lx-x^2)$ $M_{max} = -\frac{WL}{24};\ x = \frac{L}{2}$	$y = \frac{Wx^2}{24EIL}(L^2-2Lx+x^2)$ $y_{max} = \frac{WL^3}{384EI};\ x = \frac{L}{2}$
	$R_A = R_B = +\frac{W}{2}$	$M_A = M_B = \frac{5WL}{48}$ $M_x = -\left[M_A + \frac{Wx}{2} - \frac{2Wx^3}{3L^2}\right]$ $M_{max} = -\frac{WL}{16};\ x = \frac{L}{2}$	$y_{max} = \frac{7WL^3}{1920}\ \frac{1}{EI}$
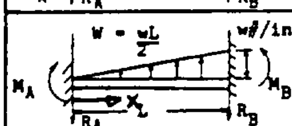	$R_A = +\frac{3W}{10}$ $R_B = +\frac{7W}{10}$	$M_A = \frac{WL}{15}$ $M_x = -W(\frac{3x}{10}-\frac{L}{15}-\frac{x^3}{3L^2})$ $M_{max} = -.043WL;\ x = .548L$	$y_{max} = \frac{WL^3}{384}\frac{1}{EI}$
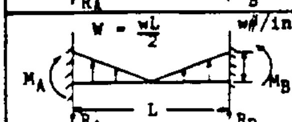	$R_A = R_B = +\frac{W}{2}$	$M_A = M_B = \frac{WL}{16}$ $M_{max} = \frac{WL}{48};\ x = \frac{L}{2}$	
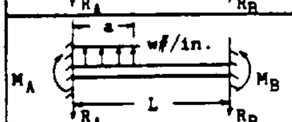	$R_A = +wa - R_B$ $R_B = +\frac{wa^3}{L^2}(1-\frac{a}{2L})$	$M_A = \frac{wa^2}{12L^2}(6L^2-8aL+3a^2)$ $M_B = \frac{wa^2}{12L^2}(4aL-3a^2)$	
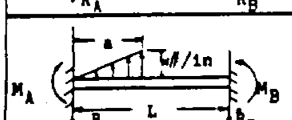	$R_A = -\frac{(M_A-M_B)}{L}+\frac{Wa}{2L}(L-\frac{2a}{3})$ $R_B = -\frac{(M_B-M_A)}{L}+\frac{wa^2}{3L}$	$M_A = \frac{wa^2}{30L^2}(10L^2-15aL+6a^2)$ $M_B = \frac{wa^3}{20L^2}(5L-4a)$	
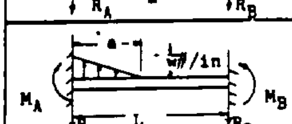	$R_A = -(\frac{M_A-M_B}{L})+\frac{wa}{2L}(L-\frac{a}{3})$ $R_B = -(\frac{M_B-M_A}{L})+\frac{wa^2}{L}$	$M_A = \frac{wa^2}{60L^2}(10L^2-10aL+3a^2)$ $M_B = \frac{wa^2}{60L^2}(5L-3a)$	
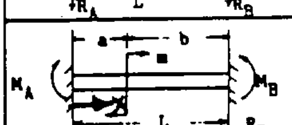	$R_A = +6\frac{m}{L^3}ab$ $R_B = -6\frac{m}{L^3}ab$	$M_A = \frac{mb}{L}(\frac{3a}{L}-1)$ $M_B = -\frac{ma}{L}(\frac{3b}{L}-1)$	
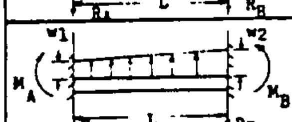	$R_A = +\frac{L}{20}(7w_1+3w_2)$ $R_B = +\frac{L}{20}(3w_1+7w_2)$	$M_A = \frac{L^2}{60}(3w_1+2w_2)$ $M_B = \frac{L^2}{60}(2w_1+3w_2)$	
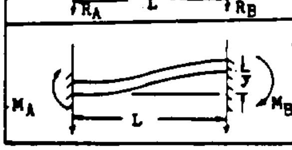		$M_A = \frac{6EIy}{L^2}$ $M_B = -\frac{6EIy}{L^2}$	

4.1.2

Stress Analysis

The maximum bending stress in a beam is:

$$\sigma = \frac{Mc}{I} \quad \ldots\ldots\ldots\ldots\ldots\ldots \quad (1)$$

This equation is true only when:

a) plane cross sections remain plane

b) the material follows Hooke's law

If the calculated maximum stress does exceed the proportional limit, a suitable reduced modulus must be used.

The maximum shearing stress in a beam in combined bending and shear is

$$\tau = \frac{V}{A} K \quad \ldots\ldots\ldots\ldots\ldots\ldots \quad (2)$$

where (K) is the ratio of maximum shearing stress and average shearing stress as calculated in section 4.1.1. The maximum shearing stress is often expressed as:

$$\tau = \frac{VQ}{It}$$

where $Q = \int_{y_1}^{c} y \, dA$ (First moment of area)

Variable Cross Section

The following formulas and figures present a method of analyzing beams with uniformly tapering cross sections. Beams are often tapered so that the bending stresses will remain constant. Figure 4.1.3-1 shows a tapered cantilever beam consisting of two concentrated flange areas joined by a vertical web which resists no bending. The vertical components of the loads in the flanges, $P\tan\alpha_1$, and $P\tan\alpha_2$, resist some of the external force V. Letting V_f equal the force resisted by the flanges and V_w the force resisted by the webs, then

$$V = V_f + V_w \quad \dots\dots\dots\dots \quad (1)$$

$$V_f = P(\tan\alpha_1 + \tan\alpha_2) \quad \dots\dots\dots\dots \quad (2)$$

From Fig. 4.1.3-1, $\tan\alpha_1 = \frac{h_1}{c}$, $\tan\alpha_2 = \frac{h_2}{c}$, and $\tan\alpha_1 + \tan\alpha_2 = \frac{h_1 + h_2}{c} = \frac{h}{c}$. From this $V_f = P\frac{h}{c}$, and since $P = V\frac{b}{h}$, then

$$V_f = V\frac{b}{c} \quad \dots\dots\dots\dots \quad (3)$$

The load in the web is $V\frac{a}{c}$, so by writing a, b, and c in terms of h_o and h, we have

$$V_w = V\frac{h_o}{h} \quad \dots\dots\dots\dots \quad (4)$$

$$V_f = V\frac{h-h_o}{h} \quad \dots\dots\dots\dots \quad (5)$$

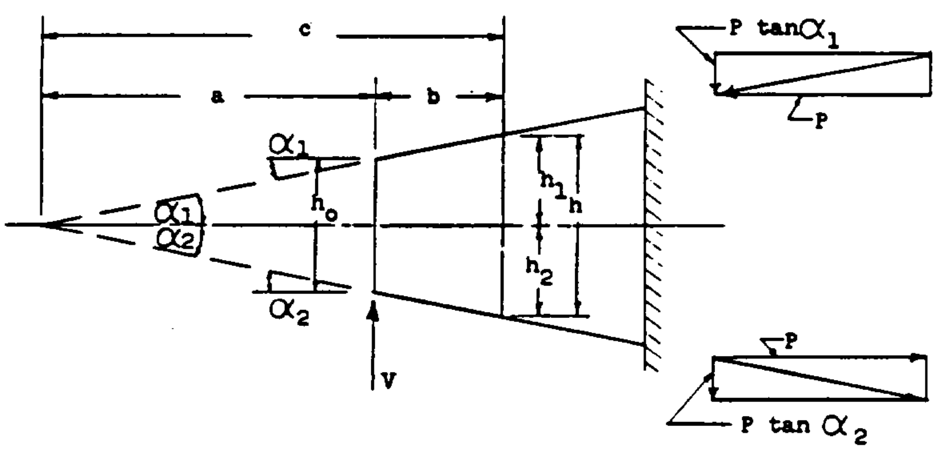

Fig. 4.1.3-1

The reactions and moments for tapered beams with different end conditions and various types of loadings can be found in Figures 4.1.3.1, 4.1.3.2, etc. Each figure is used independently for beams whose moments of inertia vary in proportion to h^2 or h^3 as shown on each graph. The letter w represents the maximum loading in lbs. per inch and L is the length of the beam.

TAPERED BEAM COEFFICIENTS

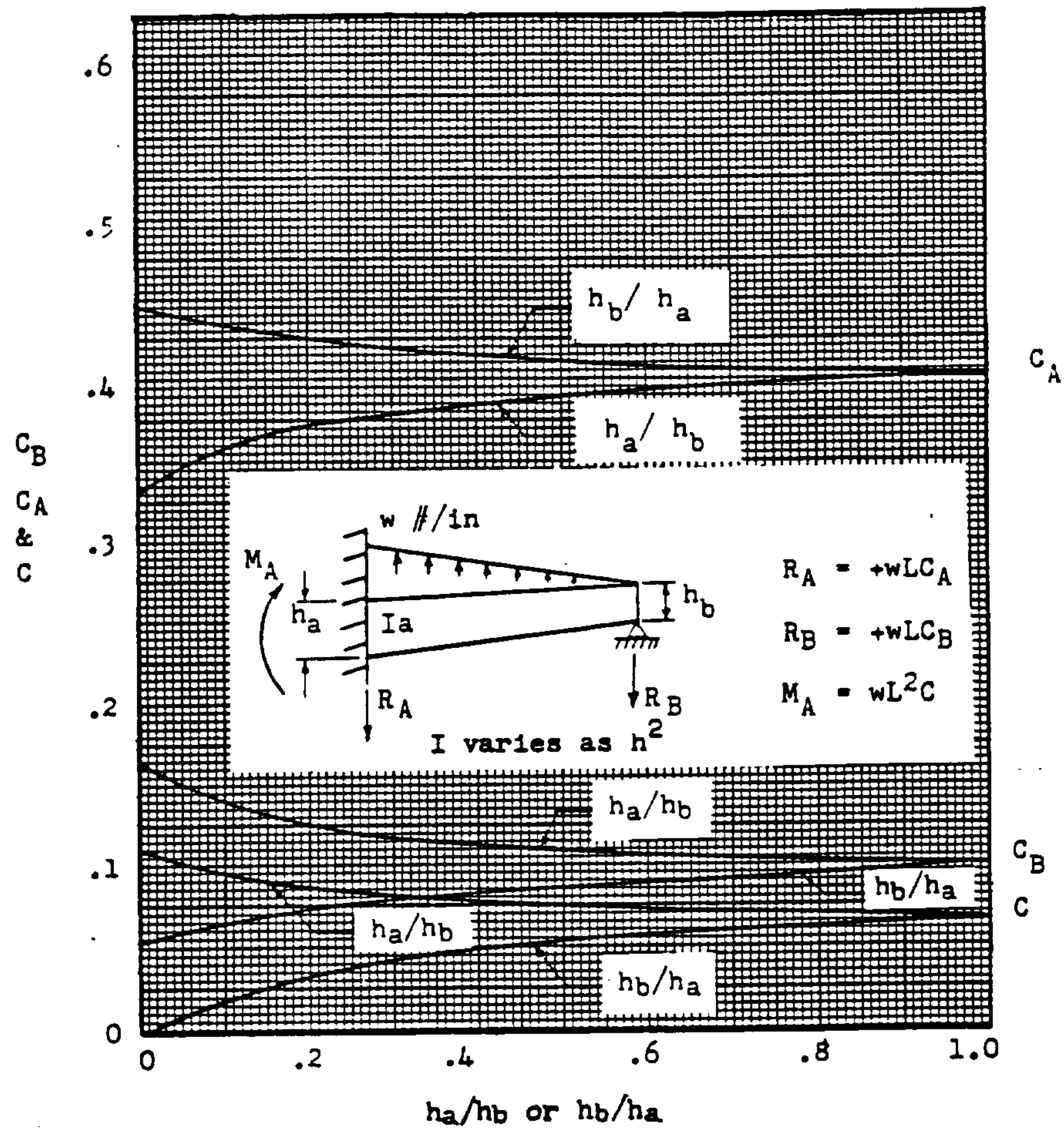

Fig. 4.1.3.1

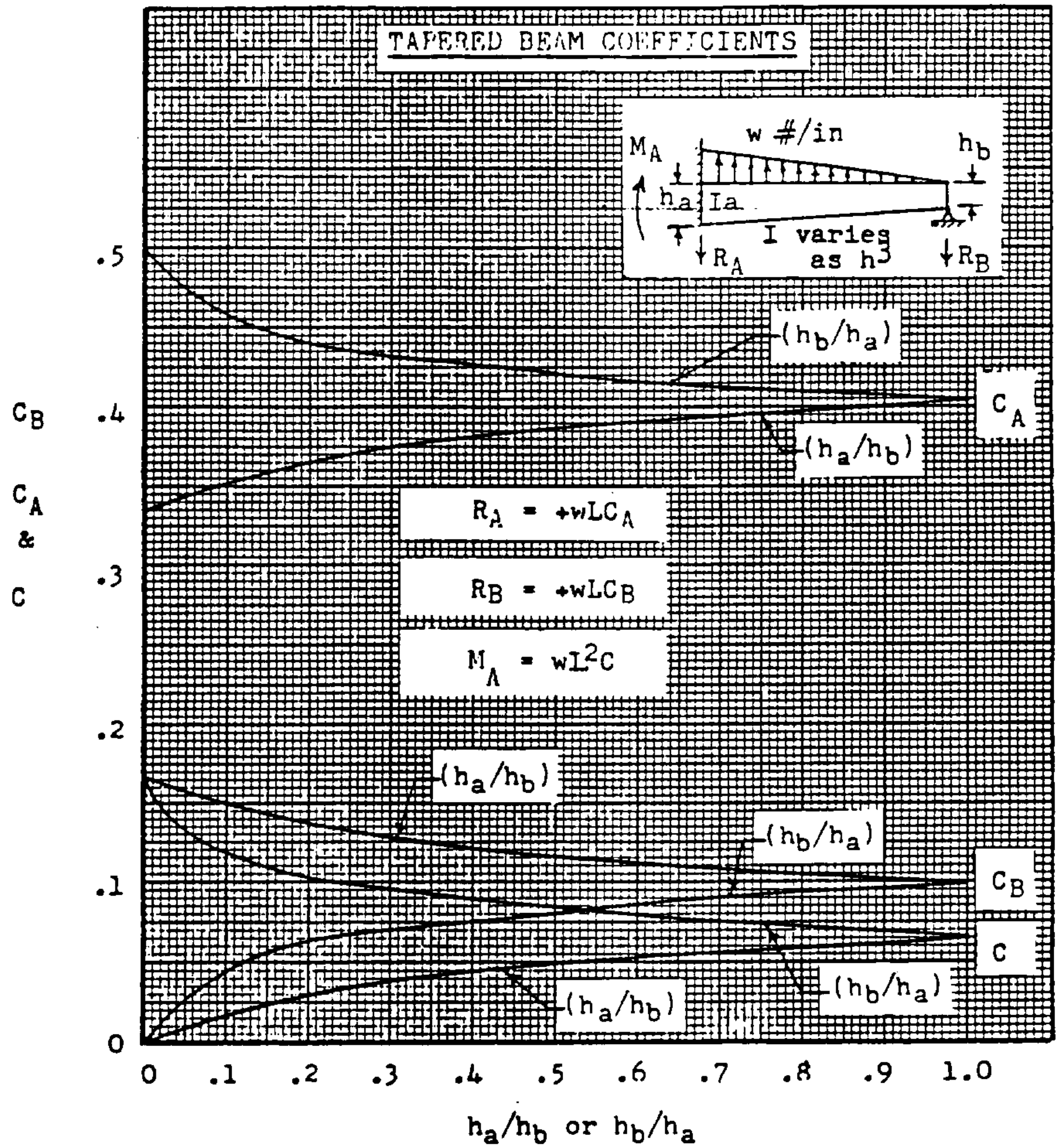
TAPERED BEAM COEFFICIENTS
w #/in
M_A
h_b
h_a
Ia
I varies as h^3
R_A
R_B
(h_b/h_a)
C_A
(h_a/h_b)
R_A = +wLC_A
R_B = +wLC_B
M_A = wL^2C
(h_a/h_b)
(h_b/h_a)
C_B
C
(h_b/h_a)
(h_a/h_b)
C_B
C_A
&
C
0
.1
.2
.3
.4
.5
.6
.7
.8
.9
1.0
h_a/h_b or h_b/h_a

Fig. 4.1.3.2

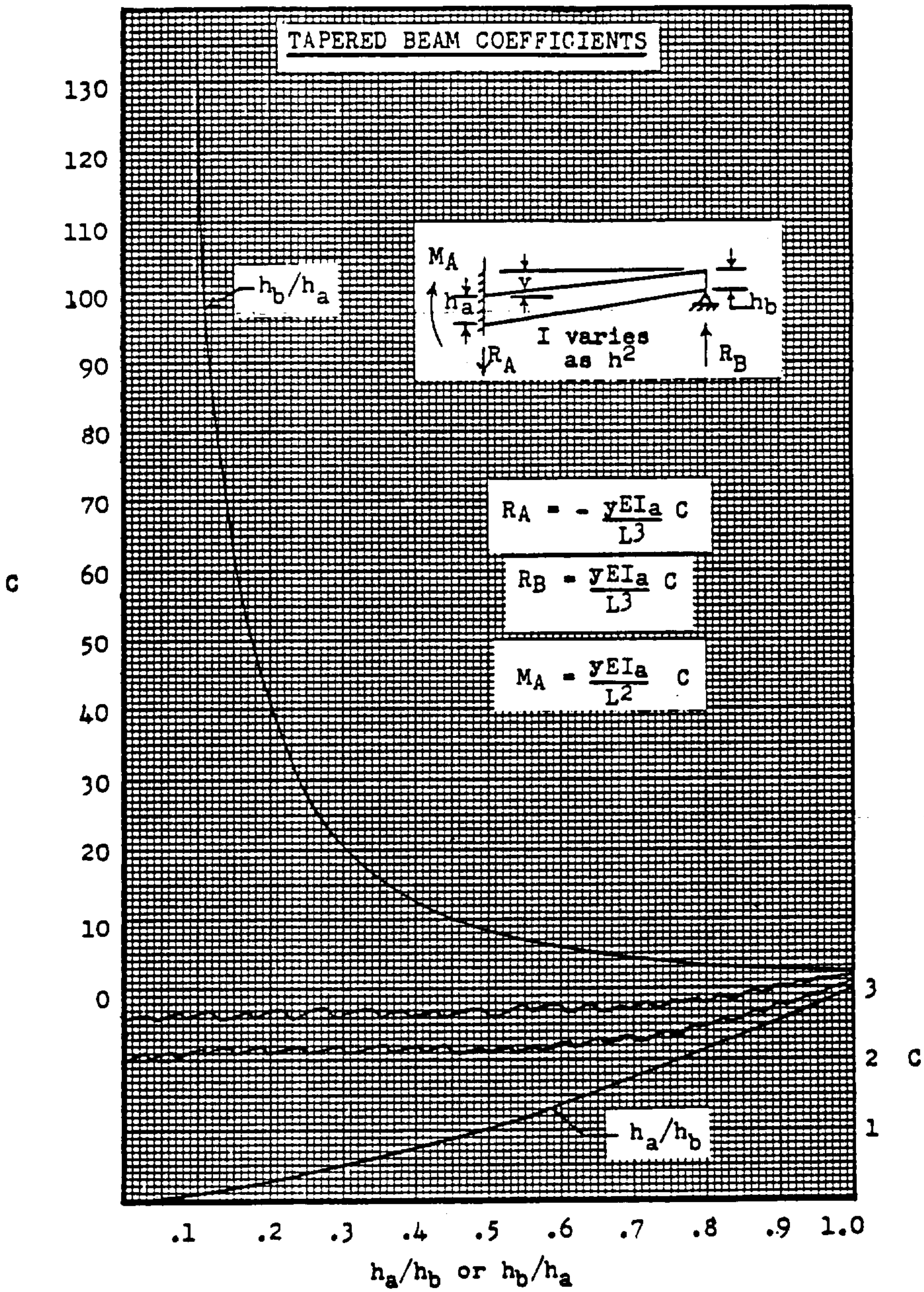
TAPERED BEAM COEFFICIENTS
130
120
110
100
90
80
70
60
50
40
30
20
10
0
C
h_b/h_a
M_A
h_a
y
h_b
I varies as h^2
R_A
R_B
$R_A = -\frac{yEI_a}{L^3} C$
$R_B = \frac{yEI_a}{L^3} C$
$M_A = \frac{yEI_a}{L^2} C$
h_a/h_b
3
2
1
C
.1 .2 .3 .4 .5 .6 .7 .8 .9 1.0
h_a/h_b or h_b/h_a

Fig. 4.1.3.3

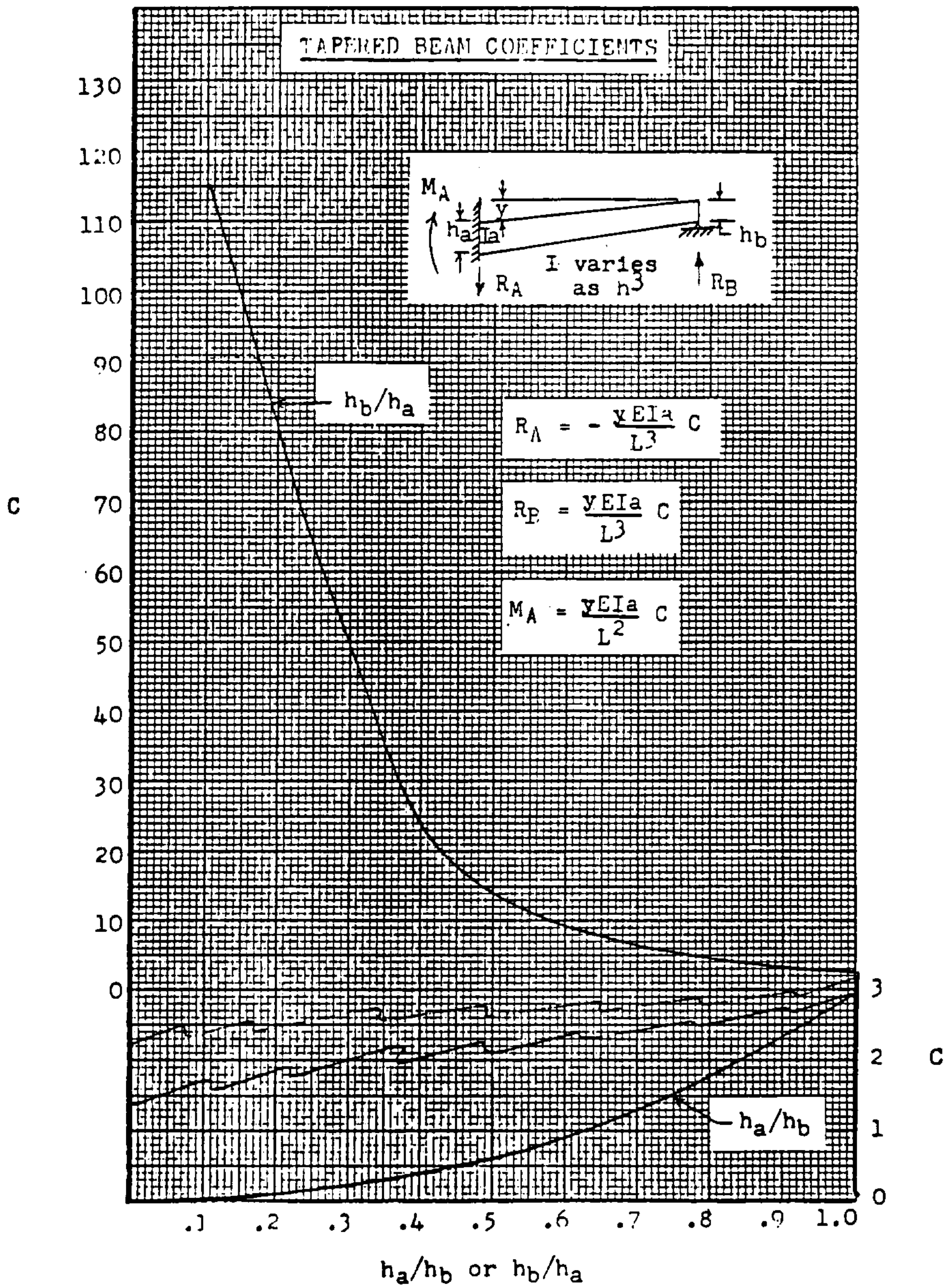
TAPERED BEAM COEFFICIENTS
M_A
y
h_a
I_a
h_b
I varies as h^3
R_A
R_B
h_b/h_a
$R_A = -\frac{yEIa}{L^3}C$
$R_B = \frac{yEIa}{L^3}C$
$M_A = \frac{yEIa}{L^2}C$
h_a/h_b
C
130
120
110
100
90
80
70
60
50
40
30
20
10
0
3
2
1
0
.1
.2
.3
.4
.5
.6
.7
.8
.9
1.0
h_a/h_b or h_b/h_a

Fig. 4.1.3.4

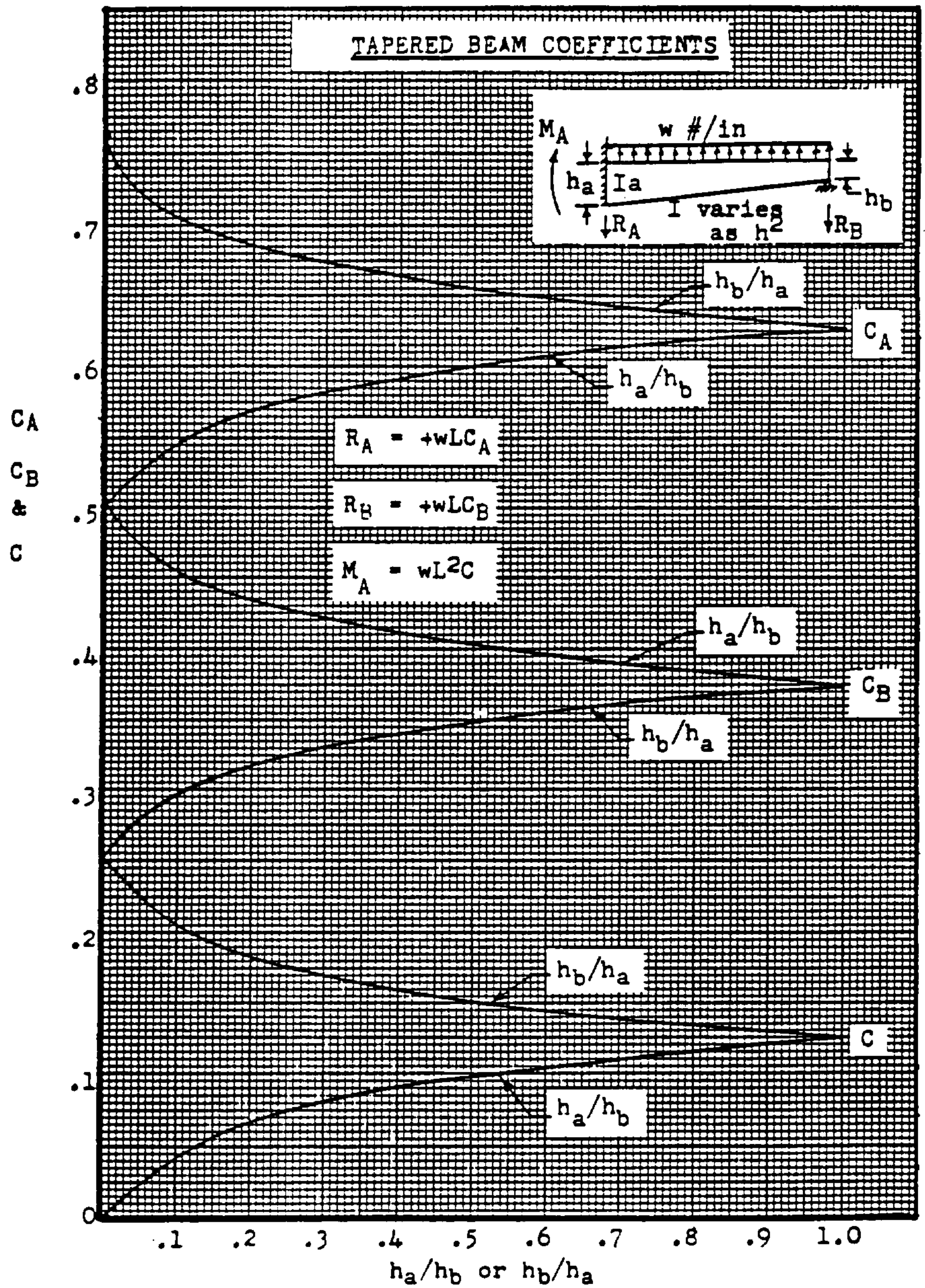
TAPERED BEAM COEFFICIENTS
M_A
w #/in
h_a
Ia
h_b
I varies as h^2
R_A
R_B
h_b/h_a
C_A
h_a/h_b
$R_A = +wLC_A$
$R_B = +wLC_B$
$M_A = wL^2C$
h_a/h_b
C_B
h_b/h_a
h_b/h_a
C
h_a/h_b
C_A C_B & C
.8
.7
.6
.5
.4
.3
.2
.1
0
.1 .2 .3 .4 .5 .6 .7 .8 .9 1.0
h_a/h_b or h_b/h_a

Fig. 4.1.3.5

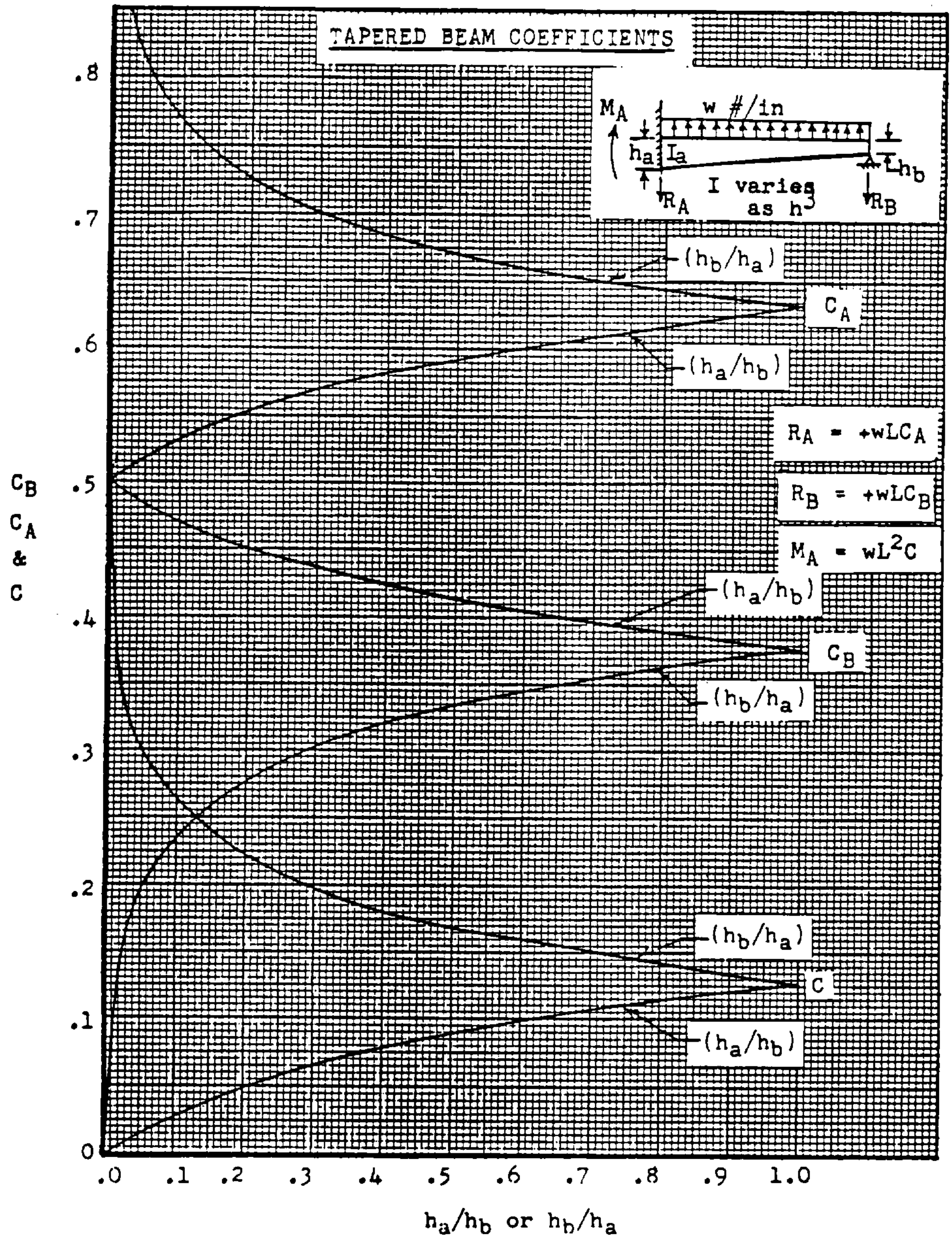
TAPERED BEAM COEFFICIENTS
M_A
w #/in
h_a
I_a
h_b
I varies as h^3
R_A
R_B
(h_b/h_a)
C_A
(h_a/h_b)
$R_A = +wLC_A$
$R_B = +wLC_B$
$M_A = wL^2C$
(h_a/h_b)
C_B
(h_b/h_a)
(h_b/h_a)
C
(h_a/h_b)
C_B C_A & C
.8
.7
.6
.5
.4
.3
.2
.1
0
.0 .1 .2 .3 .4 .5 .6 .7 .8 .9 1.0
h_a/h_b or h_b/h_a

Fig. 4.1.3.6

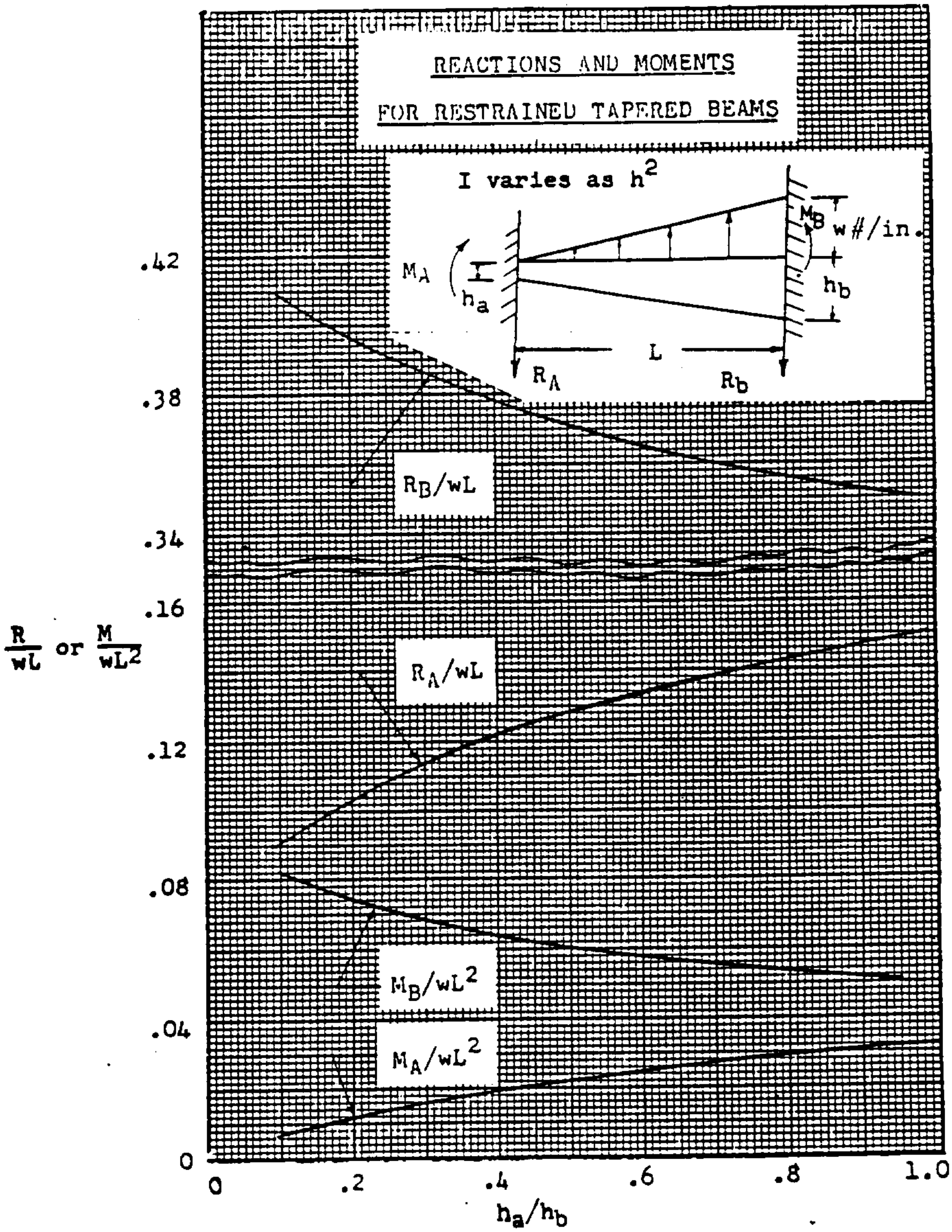
REACTIONS AND MOMENTS
FOR RESTRAINED TAPERED BEAMS
I varies as h^2
M_A
h_a
M_B
w#/in.
h_b
L
R_A
R_b
R_B/wL
R_A/wL
M_B/wL^2
M_A/wL^2
$\frac{R}{wL}$ or $\frac{M}{wL^2}$
.42
.38
.34
.16
.12
.08
.04
0
0
.2
.4
.6
.8
1.0
h_a/h_b

Fig. 4.1.3.7

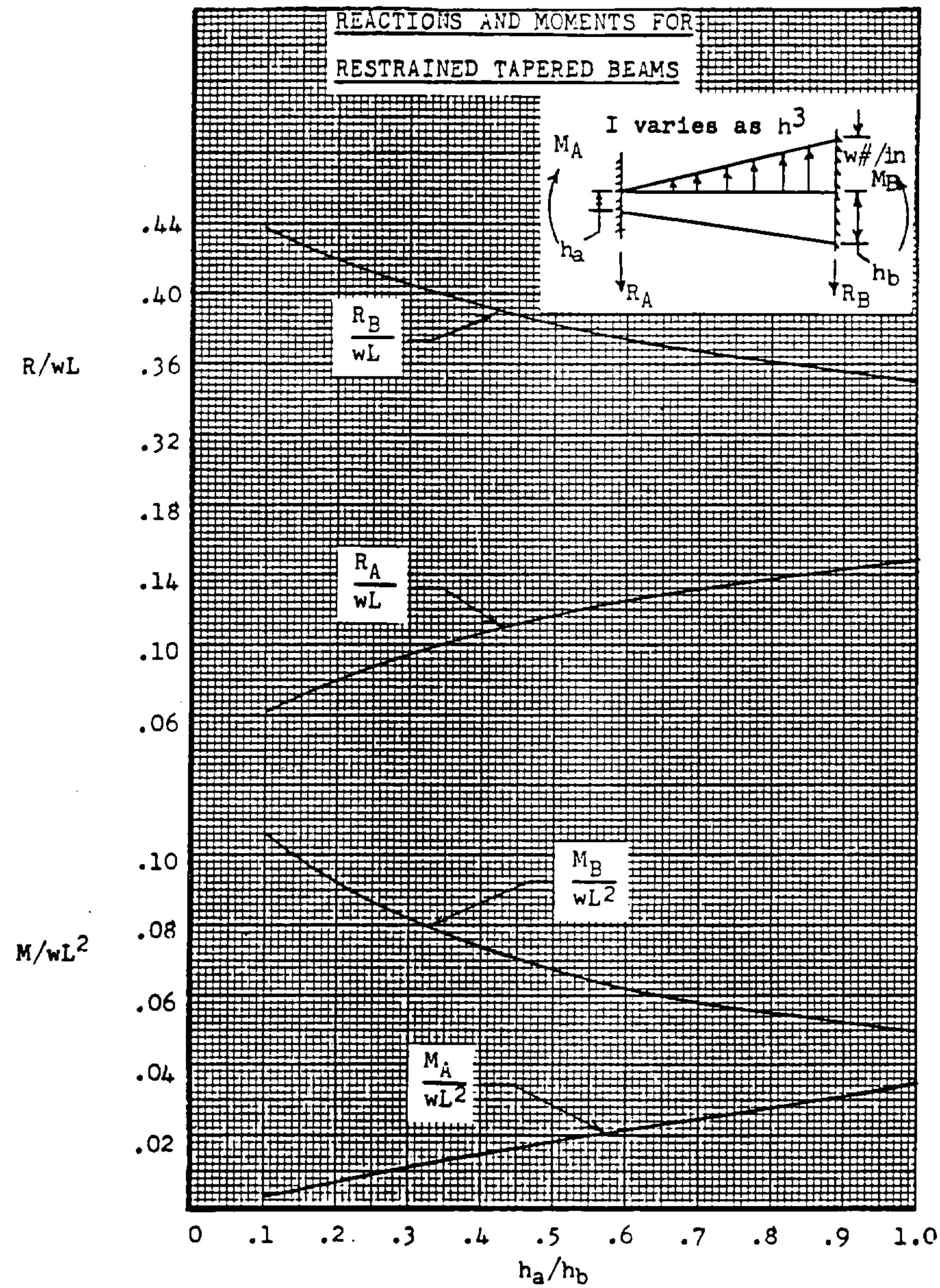
REACTIONS AND MOMENTS FOR
RESTRAINED TAPERED BEAMS
I varies as h^3
M_A
w#/in
M_B
h_a
h_b
R_A
R_B
$\frac{R_B}{wL}$
$\frac{R_A}{wL}$
$\frac{M_B}{wL^2}$
$\frac{M_A}{wL^2}$
R/wL
.44
.40
.36
.32
.18
.14
.10
.06
M/wL^2
.10
.08
.06
.04
.02
0
.1
.2
.3
.4
.5
.6
.7
.8
.9
1.0
h_a/h_b

Fig. 4.1.3.8

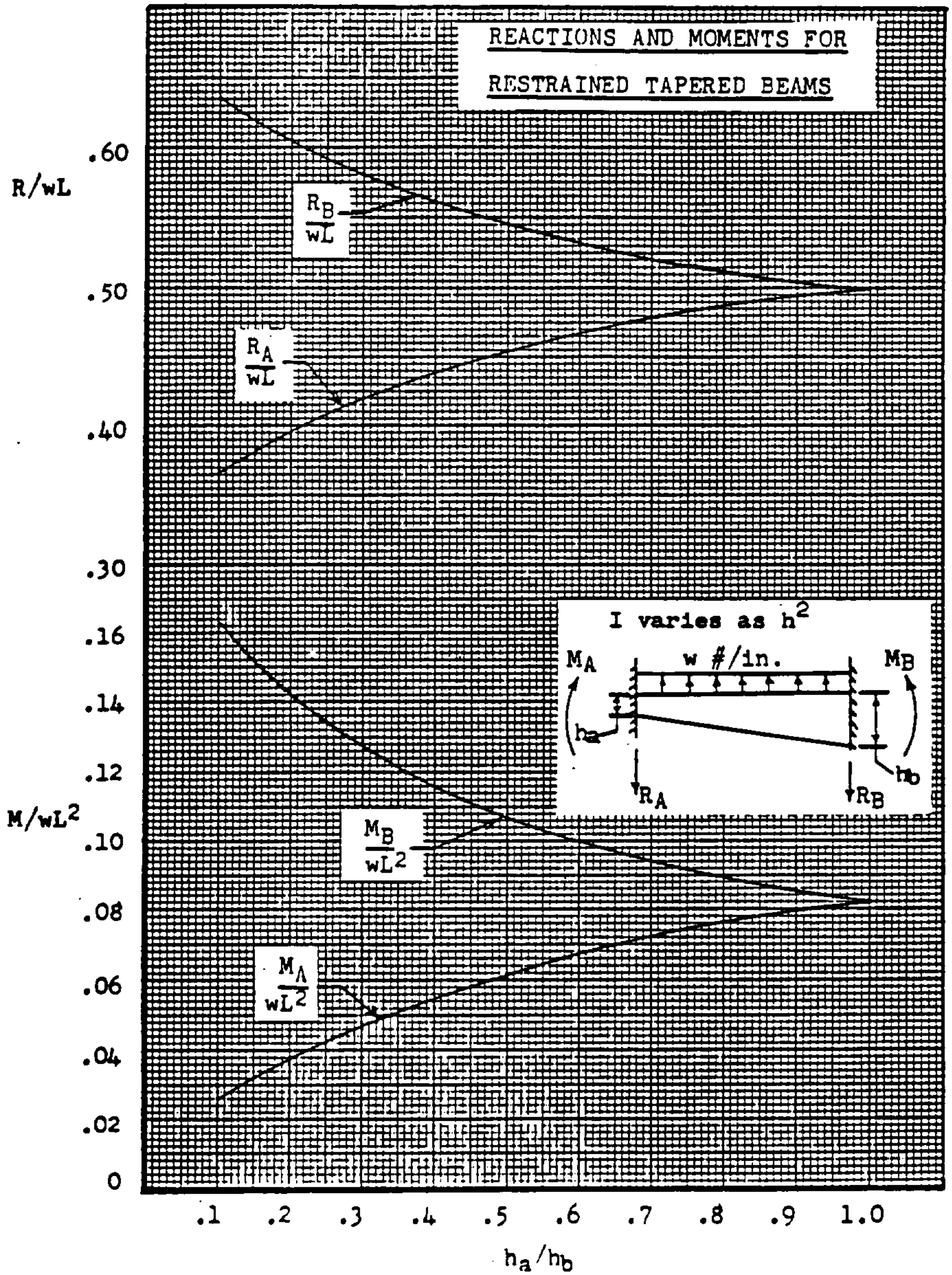
REACTIONS AND MOMENTS FOR
RESTRAINED TAPERED BEAMS
R/wL
.60
.50
.40
.30
.16
.14
.12
.10
.08
.06
.04
.02
0
M/wL2
RB/wL
RA/wL
MB/wL2
MA/wL2
I varies as h2
w #/in.
MA
MB
ha
hb
RA
RB
.1 .2 .3 .4 .5 .6 .7 .8 .9 1.0
ha/hb

Fig. 4.1.3.9

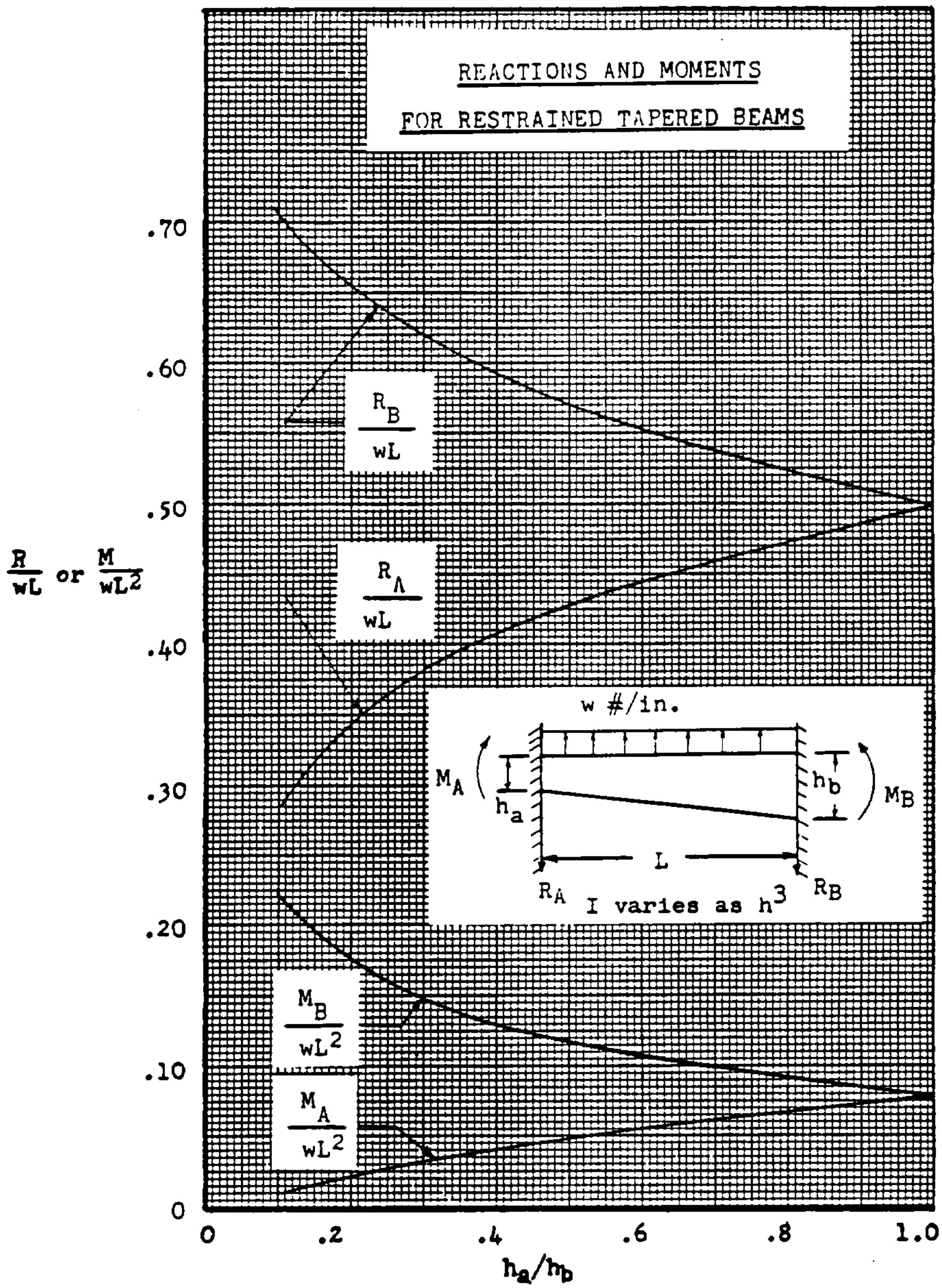
REACTIONS AND MOMENTS
FOR RESTRAINED TAPERED BEAMS
.70
.60
.50
.40
.30
.20
.10
0
R/wL or M/wL²
R_B/wL
R_A/wL
M_B/wL²
M_A/wL²
w #/in.
M_A
M_B
h_a
h_b
L
R_A
R_B
I varies as h³
0
.2
.4
.6
.8
1.0
h_a/h_b

Fig. 4.1.3.10

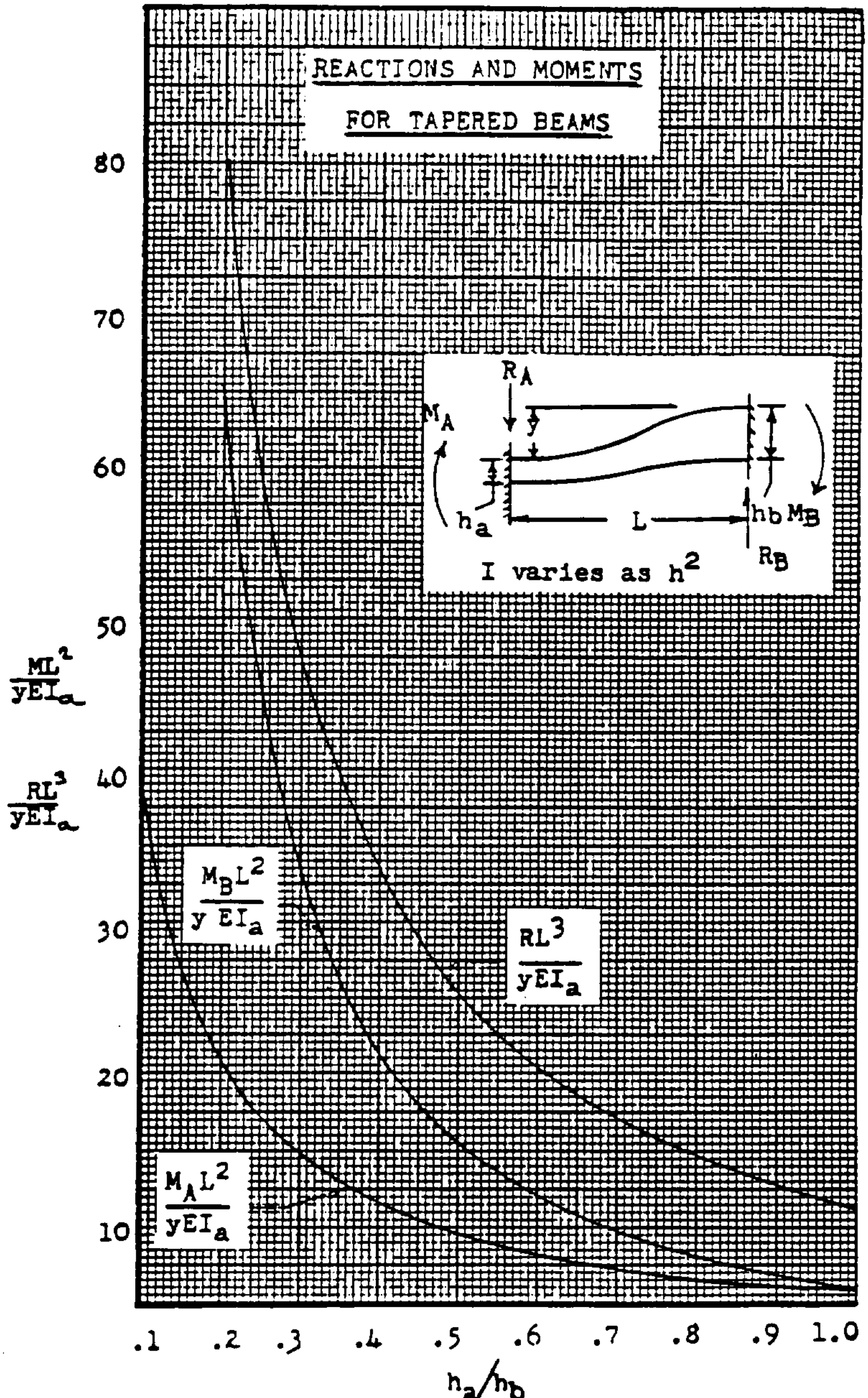
REACTIONS AND MOMENTS
FOR TAPERED BEAMS
80
70
60
50
40
30
20
10
$\frac{ML^2}{yEI_a}$
$\frac{RL^3}{yEI_a}$
R_A
M_A
y
h_a
L
hb
M_B
R_B
I varies as h^2
$\frac{M_B L^2}{y\,EI_a}$
$\frac{RL^3}{yEI_a}$
$\frac{M_A L^2}{yEI_a}$
.1
.2
.3
.4
.5
.6
.7
.8
.9
1.0
h_a/h_b

Fig. 4.1.3.11

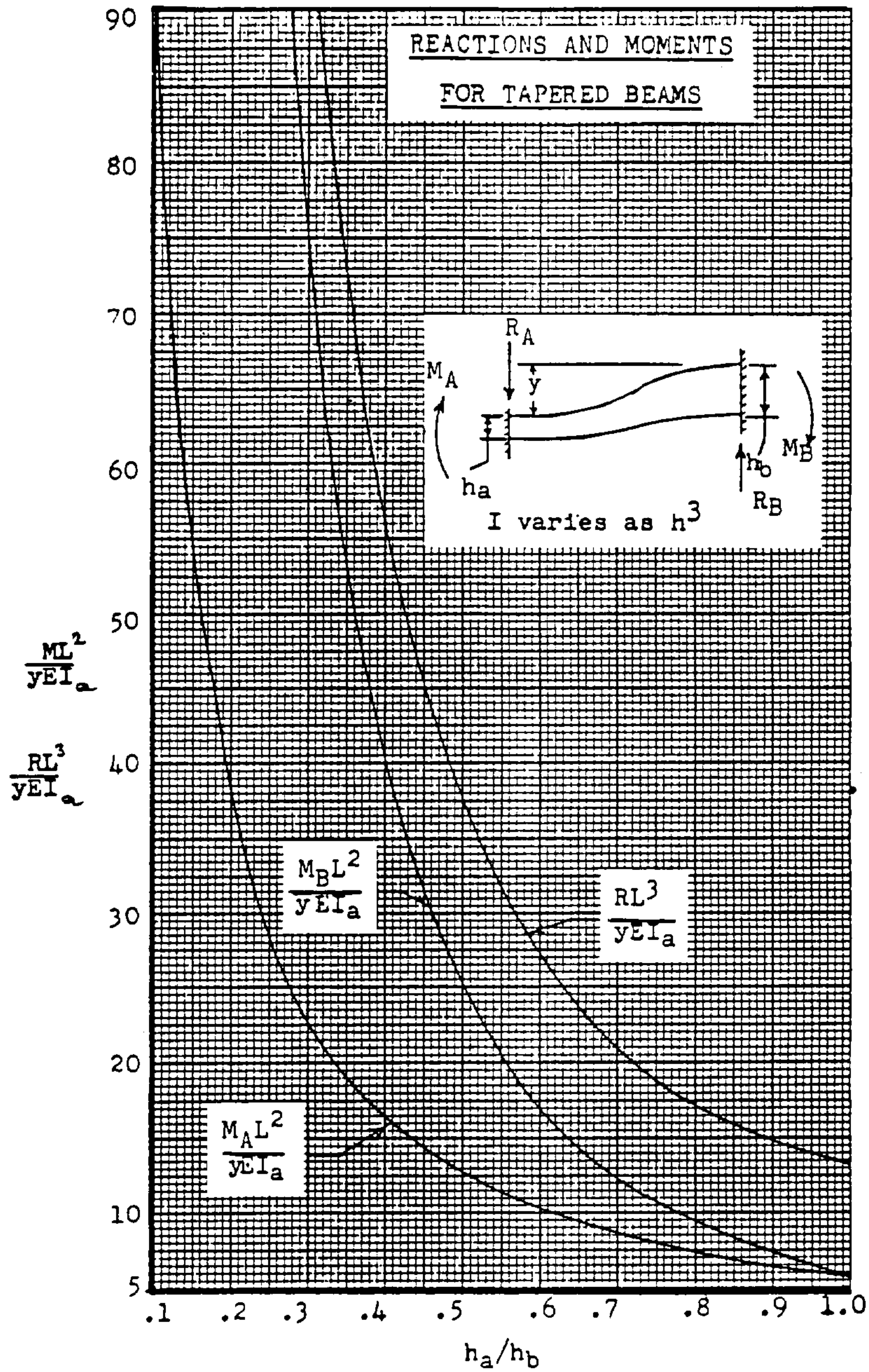
REACTIONS AND MOMENTS
FOR TAPERED BEAMS
R_A
M_A
y
h_a
h_b
M_B
R_B
I varies as h^3
90
80
70
60
50
40
30
20
10
5
$\frac{ML^2}{yEI_a}$
$\frac{RL^3}{yEI_a}$
$\frac{M_B L^2}{yEI_a}$
$\frac{RL^3}{yEI_a}$
$\frac{M_A L^2}{yEI_a}$
.1
.2
.3
.4
.5
.6
.7
.8
.9
1.0
h_a/h_b

Fig. 4.1.3.12

Data Source, Section 1.3 Reference |

4.2.0 CONTINUOUS BEAMS

4.2.1 Castigliano's Theorem

Castigliano's Theorem is useful in the solution of problems involving continuous beams with only one or two redundant supports. The theorem can be written in integral form as

$$\delta = \frac{1}{E\,I}\int_0^L M\,\frac{\partial M}{\partial P}\,ds \quad (1)$$

and

$$\theta = \frac{1}{EI}\int_0^L M\,\frac{\partial M}{\partial M_a}\,ds \quad (2)$$

where (δ) is the deflection under the load (P) and (θ) is the slope at the point of application of the moment (M_a).

The reaction of a redundant support can be solved for by setting (δ) equal to zero and solving for (P). The moment at a fixed end can be solved for by setting (θ) equal to zero and solving for (M_a).

4.2.2 Three Moment Equation

The three moment equation is useful in the solution of problems involving continuous beams with relatively few redundant supports. The equation is

$$\frac{M_A L_1}{I_1} + \frac{2M_B L_1}{I_1} + \frac{2M_B L_2}{I_2} + \frac{M_C L_2}{I_2} = K_1 + K_2 + \frac{6E}{L_1}(y_A - y_B) + \frac{6E}{L_2}(y_C - y_B) \quad (1)$$

where (K_1) and (K_2) are functions of loadings on span (1) and span (2), respectively.

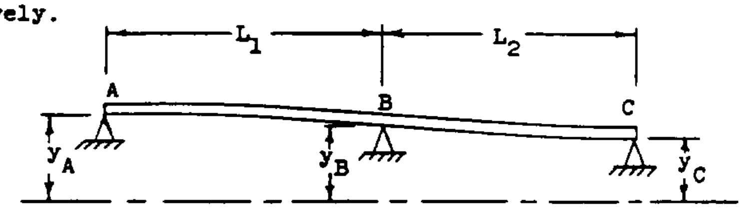

Fig. 4.2.2-1

One equation must be written for each intermediate support. The system of simultaneous equations is then solved for the moments at the intermediate supports.

Values of (K_1) and (K_2) for various types of loading are tabulated in Table 4.2.2.1.

TABLE 4.2.2.1

TYPE OF LOADING	LEFT BAY - K_1	RIGHT BAY - K_2
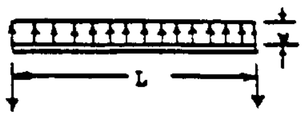	$+\frac{w_1L_1^3}{4I_1}$	$+\frac{w_2L_2^3}{4I_2}$
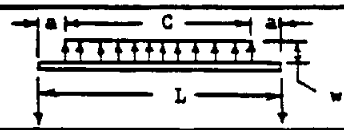	$+\frac{w_1C_1(3L_1^2-C_1^2)}{8I_1}$	$+\frac{w_2C_2(3L_2^2-C_2^2)}{8I_2}$
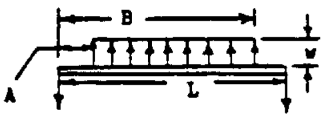	$K_1 = +\frac{w_1\left[B_1^2(2L_1^2-B_1^2)-A_1^2(2L_1^2-A_1^2)\right]}{4I_1L_1}$ $K_2 = +\frac{w_2\left[B_2^2(2L_2-B_2)^2-A_2^2(2L_2-A_2)^2\right]}{4I_2L_2}$	
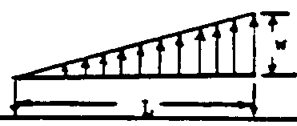	$+\frac{2w_1L_1^3}{15I_1}$	$+\frac{7w_2L_2^3}{60I_2}$
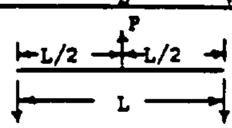	$+\frac{3L_1^2P_1}{8I}$	$+\frac{3L_2^2P_2}{8I}$
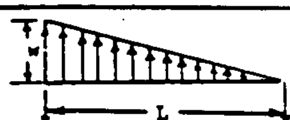	$+\frac{7w_1L_1^3}{60I_1}$	$+\frac{2w_2L_2^3}{15I_2}$
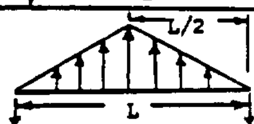	$+\frac{5w_1L_1^3}{32I_1}$	$+\frac{5w_2L_2^3}{32I_2}$
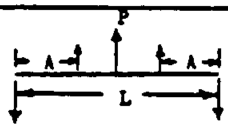	$+\frac{3P_1A_1(L_1-A_1)}{I}$	$+\frac{3P_2A_2(L_2-A_2)}{I}$
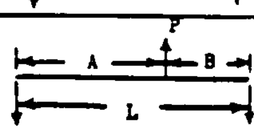	$+\frac{P_1A_1(L_1^2-A_1^2)}{I_1L_1}$	$+\frac{P_2B_2(L_2^2-B_2^2)}{I_2L_2}$
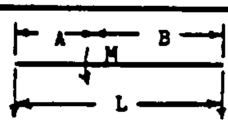	$+\frac{M_1}{I_1}(L_1-\frac{3A_1^2}{L_1})$	$+\frac{M_2}{I_2}\left(\frac{3B_2^2}{L_2}-L_2\right)$
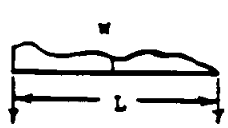	$+\frac{L_1^2}{I_1}\int\left[\frac{A_1}{L_1}-\left(\frac{A_1}{L_1}\right)^3\right]w_1dA_1$ $+\frac{L_2^2}{I_2}\int\left[\frac{L_2-A_2}{L_2}-\left(\frac{L_2-A_2}{L_2}\right)^3\right]w_2dA_2$	

4.2.3
Moment Distribution Method

The following method is suggested for the solution of problems involving continuous beams with many redundant supports. This discussion will be limited to members with uniform cross sections within each span. Information on beams with varying sections can be found in paragraph 4.2.4.

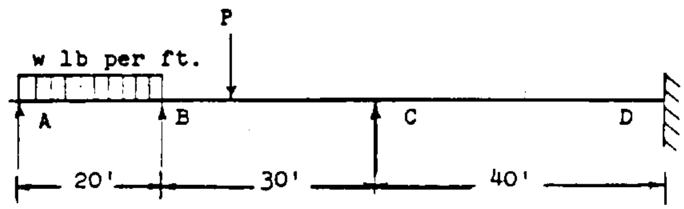

Fig. 4.2.3-1. Continuous Beam With Uniform and Concentrated Load

The signs of the fixed-end moments need careful attention. Fig. 4.2.3-2 illustrates the signs for the conditions of loading shown in Fig. 4.2.3-1. The sign of an end moment is positive if that moment tends to rotate the adjacent joint in a clockwise direction. The sign is negative if it tends to rotate the adjacent joint counterclockwise.

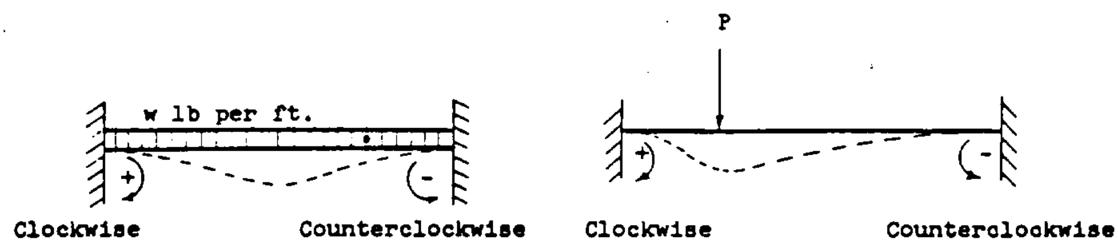

Fig. 4.2.3-2. Signs of Fixed-End Moments

The structure is first considered as a series of single span fixed-end beams. The moment restraints at the supports are successively removed one by one, and the bending moments are corrected by successive approximations until the conditions for the actual structure are obtained. Numerical values are used in the successive approximations as shown in Fig. 4.2.3.1. It is not necessary to set up algebraic equations for the redundants.

Stiffness Factor

An external moment applied at any joint is distributed among the members meeting at that joint in proportion to the stiffness factor, k , of each member. The formula for the stiffness factor

$$k = \frac{EI}{L} \text{ (Note this is "Relative" stiffness factor only)} \qquad (1)$$

will reduce to $\frac{I}{L}$ when all members are of the same material. If EI is constant for all spans, k will reduce to $\frac{1}{L}$.

Carry Over Factor

For a beam of uniform section, the balancing moment which enters the nearer end of a member produces a fixed-end moment at the opposite end equal to one-half of its value and of like sign. This value, one half, is called the carry over factor.

Distribution Factor

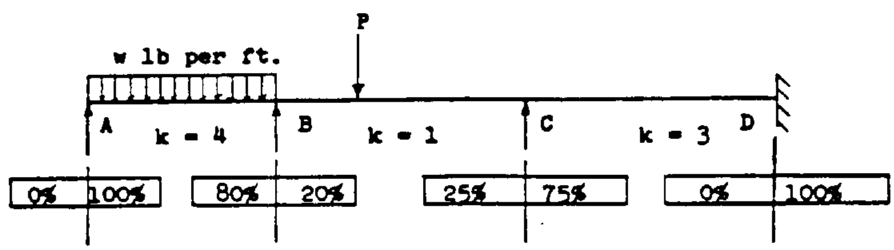

Fig. 4.2.3-3

If a moment is applied at a joint where two or more members are rigidly connected, the distribution factor for each member is the proportional part of the applied load that is resisted by that member. The distribution factor for any member,

$$D = \frac{k}{\sum k} \quad \ldots\ldots\ldots\ldots\ldots\ldots\ldots\ldots \quad (2)$$

where $\sum k$ is the sum of the k values for all the members of that joint.
Ref. Fig. 4.2.3-3, span BA ; $D = \frac{4}{4+1} = .80$

For span BC; $D = \frac{1}{4+1} = .20$

The sum of the D values for any joint must equal unity.

Note that when the end member on a continuous beam is fixed, it will not redistribute the moments distributed to it but will retain them at that joint as shown in Fig. 4.2.3.1. If the end member is simply supported, it will redistribute all its moment.

Balancing Process

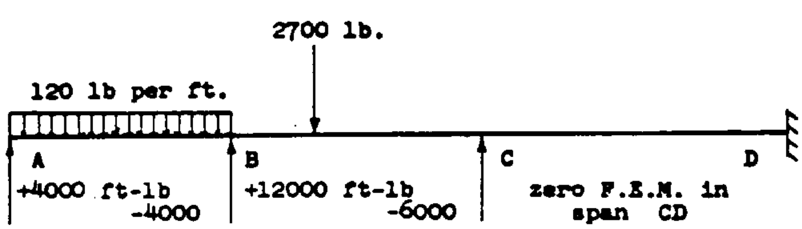

Fig. 4.2.3-4

It can be seen in Fig. 4.2.3-4 that the locked joints, "B" and "C", of the beam are not in static equilibrium unless they are held in place by an outside restraining moment. Joint B has a counterclockwise or negative moment of 4000 ft-lb. on the left and a clockwise or positive moment of 12,000 ft-lb. on the right. The joint is unbalanced by (12,000 - 4,000) or + 8,000 ft.-lb.

Procedure

(1) Compute the fixed-end moments for each loaded span and record them with correct signs at their proper locations on a diagram of the structure as shown in Fig. 4.2.3.1. Several cases of fixed-end moments are shown in Fig. 4.2.3.2.

(2) Calculate the stiffness factor using formula (1).

(3) Compute the distribution factors at the joints from the k-values of the members using formula (2). Record these factors inside a box at each joint. These distribution factors may be expressed as percentages if preferred, Ref. Fig. 4.2.3.1.

(4) Select any joint which has a large unbalanced moment and compute the balancing moments by multiplying the unbalanced moment of that joint by the distribution factors for the respective members. Record each balancing moment underneath the corresponding fixed-end moment as shown in Fig. 4.2.3.1. Balancing moments are of opposite sign to the unbalanced joint moment. Draw a horizontal line under each balancing moment to show that the moments above this line are balanced and need not be rebalanced later.

(5) Record the carry-over moment at the opposite end of the member as shown in Fig. 4.2.3.1. Place the carry-over moment in a column underneath the fixed-end moment or the balancing moment existing there. Each carry-over moment is of the same sign but one-half the value of the balancing moment that produced it. Carry-over moments must be considered as additional fixed-end moments at the joints where they are recorded.

(6) Successively balance each other joint of the structure, taking care to record balancing moments and carry-over moments with proper signs. Note that the carry-over moments unbalance previously balanced joints and that such joints must be rebalanced. Only those moments recorded after the last balance of a joint (below the last horizontal line) are considered during the process of rebalancing that joint.

(7) The process of balancing joints is carried on in any desired sequence of joints until the carry-over moments become negligibly small, which shows that the joints are all balanced. This result will be reached after each joint has been balanced about three times.

(8) Add columns of moments at each joint; the algebraic sum of the final moments around any joint in equilibrium should be zero.

MOMENT DISTRIBUTION SAMPLE CALCULATION

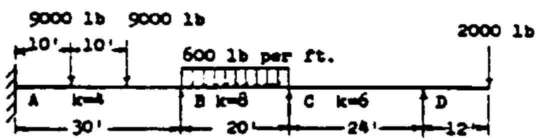

A	B	B	C	C	D	D	
.0	.33	.67	.57	.43	1.00	0	Distribution Factors
+60	-60	+20	-20	0	0	+24	Fixed-End Moments ÷ 1000
+ 6 ←	+13	+27 →	+13	-12 ←	-24		1st Balance at B & D
		+ 5 ←	+11	+ 8 →	+ 4		1st Balance at C
- 1 ←	- 2	- 3 →	- 1	- 2 ←	- 4		2nd Balance at B & D
		+ 1 ←	+ 2	+ 1 →	+ 1		2nd Balance at C
		- 1			- 1		3rd Balance at B & D
+65	-49	+49	+ 5	- 5	-24	+24	ΣM for Total Moment

(a) Analysis of a Continuous Beam With a Cantilever End

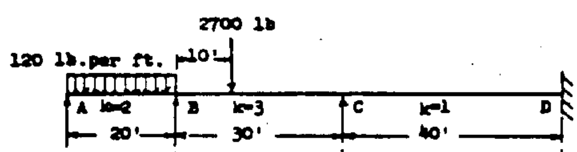

A	A	B	B	C	C	D	
0%	100%	40%	60%	75%	25%	0%	Distribution Factors
	+40	-40	+120	-60	0	0	Fixed-End Moments ÷ 100
	-16 ←	-32	-48 →	-24			1st Balance at B
			+31 ←	+63	+21 →	+10	1st Balance at C
	-24 →	-12					1st Balance at A
	-4 ←	-8	-11 →	-5			2nd Balance at B
	+4 →	+2					2nd Balance at A
			+2 ←	+4	+1 →	0	2nd Balance at C
	-1 ←	-2	-2 →	-1			3rd Balance at B
	+1			+1	0		3rd Balance at A & C
	0	-92	+92	-22	+22	+10	ΣM for Total Moment

(b) Analysis of A Continuous Beam

Fig. 4.2.3.1 Analysis by Moment Distribution

Fig. 4.2.3.2

FIXED-END MOMENTS FOR MEMBERS OF CONSTANT CROSS SECTION

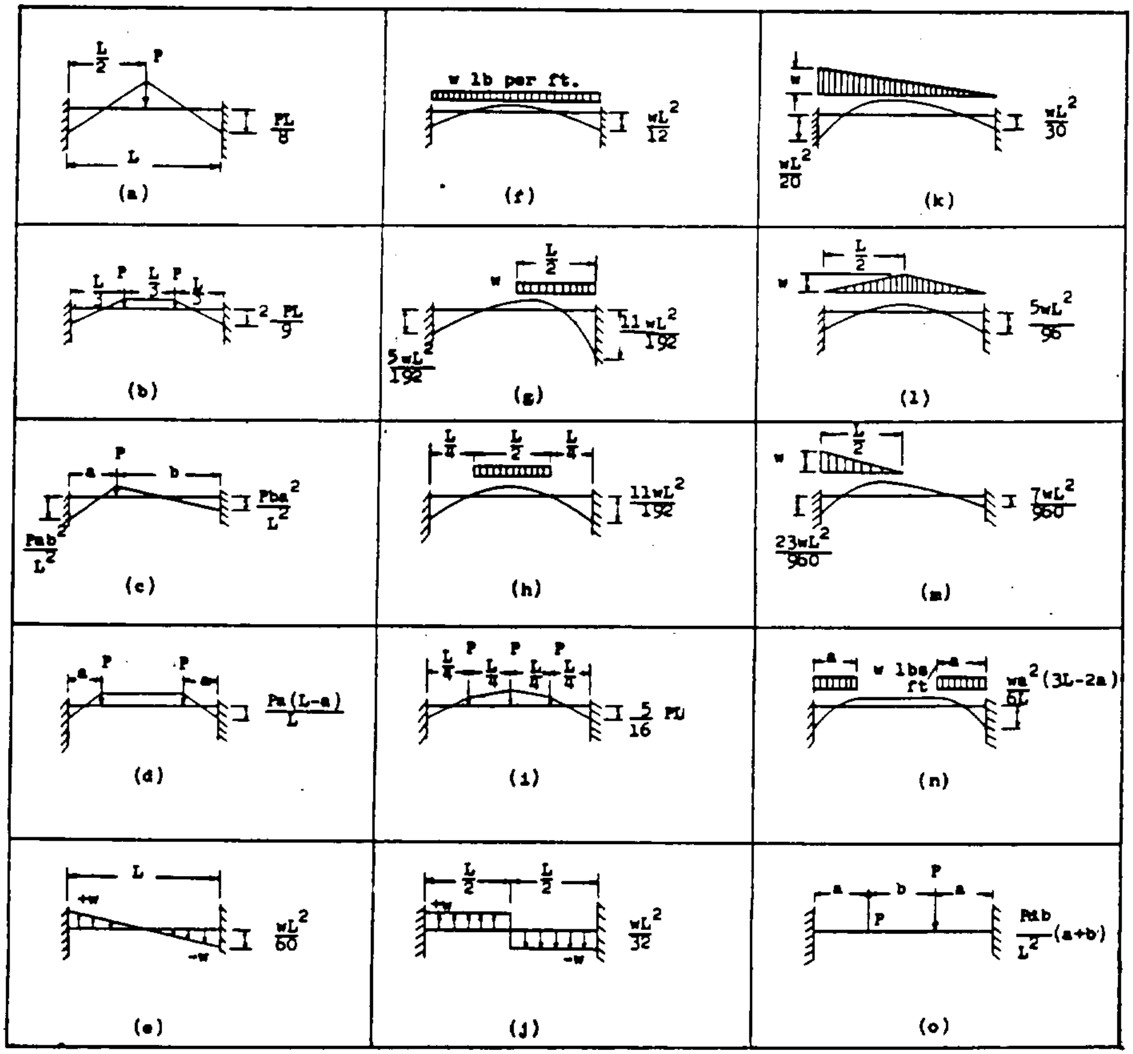

4.3.0 CURVED BEAMS

4.3.1 Curved Beam

When a curved beam is bent in the plane of initial curvature, plane sections remain plane, but because of the different lengths of the fibers on the inner and outer sides of the beam, the distribution of stress and strain is not linear; the neutral axis therefore does not pass through the centroid of the section and equation (4.1.2-1) does not apply. The maximum stresses in curved beams in bending are determined by the equations

$$\sigma_o = K_o \frac{M}{I} c_o \quad \text{. . . . . (stress in outer fibers)} \quad (1)$$

and

$$\sigma_i = K_i \frac{M}{I} c_i \quad \text{. . . . . (stress in inner fibers)} \quad (2)$$

where (c_o) and (c_i) are the distances from the centroidal axis to the outer and inner edges, respectively.

Values of (K_o) and (K_i) for several cross-sections are given in Tables 4.3.1.1 and 4.3.1.2. .

TABLE 4.3.1.1

SECTION	R/c	FACTOR K	
		INSIDE FIBER-K_i	OUTSIDE FIBER-K_o
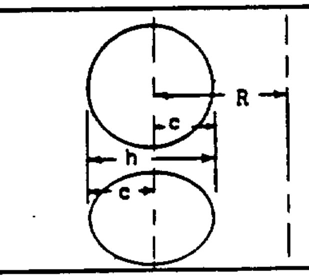	1.2	3.41	0.54
	1.4	2.40	0.60
	1.6	1.96	0.65
	1.8	1.75	0.68
	2.0	1.62	0.71
	3.0	1.33	0.79
	4.0	1.23	0.84
	6.0	1.14	0.89
	8.0	1.10	0.91
	10.0	1.08	0.93
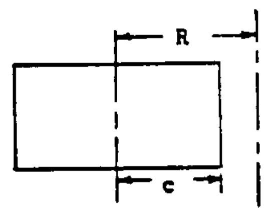	1.2	2.89	0.57
	1.4	2.13	0.63
	1.6	1.79	0.67
	1.8	1.63	0.70
	2.0	1.52	0.73
	3.0	1.30	0.81
	4.0	1.20	0.85
	6.0	1.12	0.90
	8.0	1.09	0.92
	10.0	1.07	0.94
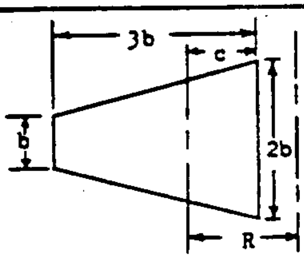	1.2	3.09	0.56
	1.4	2.25	0.62
	1.6	1.91	0.66
	1.8	1.73	0.70
	2.0	1.61	0.73
	3.0	1.37	0.81
	4.0	1.26	0.86
	6.0	1.17	0.91
	8.0	1.13	0.94
	10.0	1.11	0.95
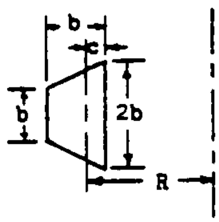	1.2	3.01	0.54
	1.4	2.18	0.60
	1.6	1.87	0.65
	1.8	1.69	0.68
	2.0	1.58	0.71
	3.0	1.33	0.80
	4.0	1.23	0.84
	6.0	1.13	0.88
	8.0	1.10	0.91
	10.0	1.08	0.93
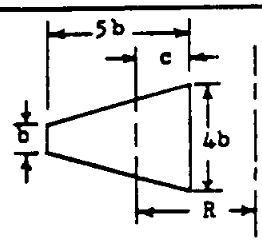	1.2	3.14	0.52
	1.4	2.29	0.54
	1.6	1.93	0.62
	1.8	1.74	0.65
	2.0	1.61	0.68
	3.0	1.34	0.76
	4.0	1.24	0.82
	6.0	1.15	0.87
	8.0	1.12	0.91
	10.0	1.10	0.93
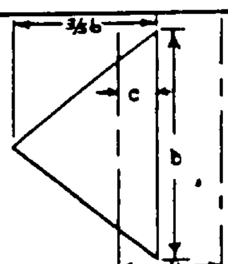	1.2	3.26	0.44
	1.4	2.39	0.50
	1.6	1.99	0.54
	1.8	1.78	0.57
	2.0	1.66	0.60
	3.0	1.37	0.70
	4.0	1.27	0.75
	6.0	1.16	0.82
	8.0	1.12	0.86
	10.0	1.09	0.88

K FACTOR FOR CURVED BEAMS

TABLE 4.3.1.2

SECTION	R/c	FACTOR K: INSIDE FIBER-K_i	FACTOR K: OUTSIDE FIBER-K_o
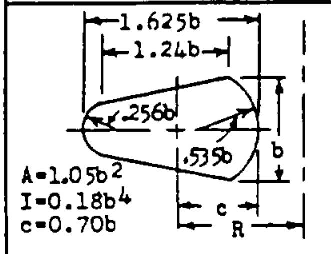	1.2	3.65	0.53
	1.4	2.50	0.59
	1.6	2.08	0.63
	1.8	1.85	0.66
	2.0	1.69	0.69
	2.5	1.49	0.74
	3.0	1.38	0.78
	4.0	1.27	0.83
	6.0	1.19	0.90
	8.0	1.14	0.93
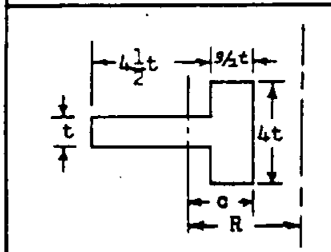	1.2	3.63	0.58
	1.4	2.54	0.63
	1.6	2.14	0.67
	1.8	1.89	0.70
	2.0	1.73	0.72
	3.0	1.41	0.79
	4.0	1.29	0.83
	6.0	1.18	0.88
	8.0	1.13	0.91
	10.0	1.10	0.92
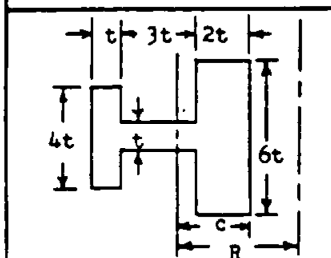	1.2	3.55	0.67
	1.4	2.48	0.72
	1.6	2.07	0.76
	1.8	1.83	0.78
	2.0	1.69	0.80
	3.0	1.38	0.86
	4.0	1.26	0.89
	6.0	1.15	0.92
	8.0	1.10	0.94
	10.0	1.08	0.95
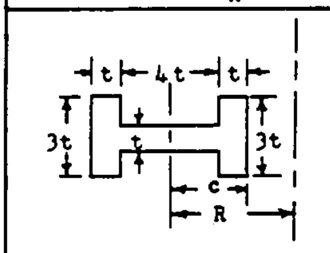	1.2	2.52	0.67
	1.4	1.90	0.71
	1.6	1.63	0.75
	1.8	1.50	0.77
	2.0	1.41	0.79
	3.0	1.23	0.86
	4.0	1.16	0.89
	6.0	1.10	0.92
	8.0	1.07	0.94
	10.0	1.05	0.95
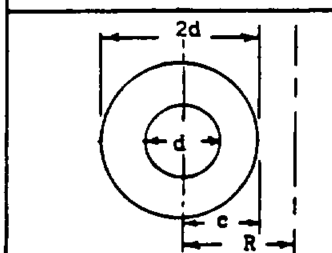	1.2	3.28	0.58
	1.4	2.31	0.64
	1.6	1.89	0.68
	1.8	1.70	0.71
	2.0	1.57	0.73
	3.0	1.31	0.81
	4.0	1.21	0.85
	6.0	1.13	0.90
	8.0	1.10	0.92
	10.0	1.07	0.93
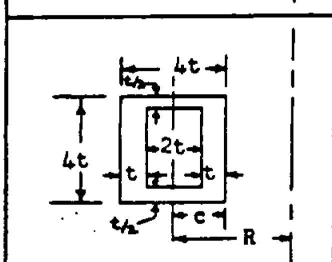	1.2	2.63	0.68
	1.4	1.97	0.73
	1.6	1.66	0.76
	1.8	1.51	0.78
	2.0	1.43	0.80
	3.0	1.23	0.86
	4.0	1.15	0.89
	6.0	1.09	0.92
	8.0	1.07	0.94
	10.0	1.06	0.95

K FACTOR FOR CURVED BEAMS

Data Source, Section 1.3 Reference 1

4.4.0

Lateral Stability

Rectangular bars are occasionally used in the form of beams with the long dimension of the rectangle in the plane of the loads. When the depth of such a beam is great compared with the width, the beam may become unstable in a lateral direction with a consequent sidewise buckling.

The expression for the critical stress in a deep rectangular beam is

$$\sigma_{cr} = K' E \frac{b^2}{Ld} \quad \ldots\ldots\ldots\ldots\ldots\ldots \quad (1)$$

where (σ_{cr}) is the maximum compressive stress in the beam and (K^1) is a constant depending on the conditions of loading and lateral support. Values of (K') for a variety of conditions are given in Table 4.4.0.1.

TABLE 4.4.01
CONSTANTS FOR DETERMINING THE LATERAL
STABILITY OF SOLID DEEP RECTANGULAR BEAMS

CASE	SIDE VIEW	TOP VIEW	K'
1	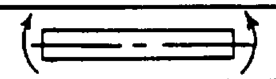		1.86
2	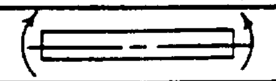		3.71
3	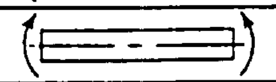	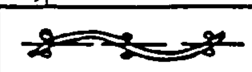	3.71
4	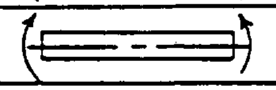		5.45
5	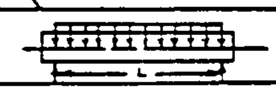		2.09
6			3.61
7		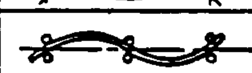	4.87
8	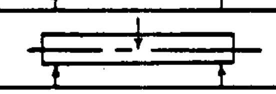		2.50
9	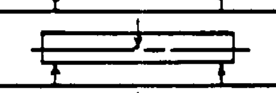		3.82
10	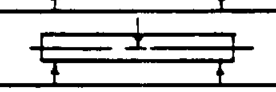	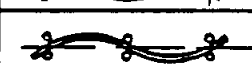	6.57
11	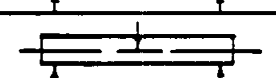	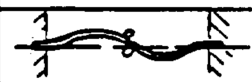	7.74
12	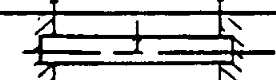		3.13
13	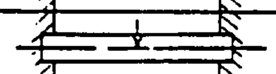		3.48
14	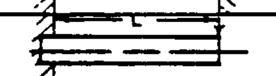		2.37
15			2.37
16			3.80
17			3.80

$F_{cr} = K'E\,\frac{b^2}{Ld}$ Where:
b = Width of Beam, d = Depth of Beam, L = Length of Beam

4.6.0 Shear Stresses

4.6.1 Shear Stresses in Ordinary Beams

The shear force (V) parallel to a beam cross section produces a shear stress (τ) of varying intensity over the cross section of the beam. The shearing stresses on any two perpendicular planes are equal; therefore, the shearing stress on any horizontal plane through the beam must be equal to the shearing stress on the vertical cross section at the point of intersection of the planes. The shear stresses in a beam of constant cross section are not affected by the magnitude of the bending moment but the difference between the bending moment of two cross sections of a beam must be considered.

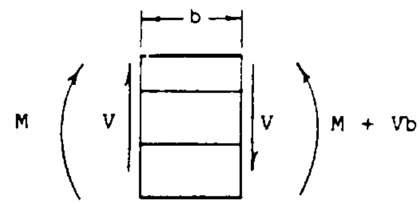

Fig. 4.6.1-1

Consider a portion of an "I" beam between two vertical cross sections a distance (b) apart and in equilibrium under the forces shown. The bending moment on the cross section to the right is equal to the sum of the bending moment (M) and the couple (Vb). The bending stresses on the two cross sections at a distance (y) from the neutral axis will be shown as follows:

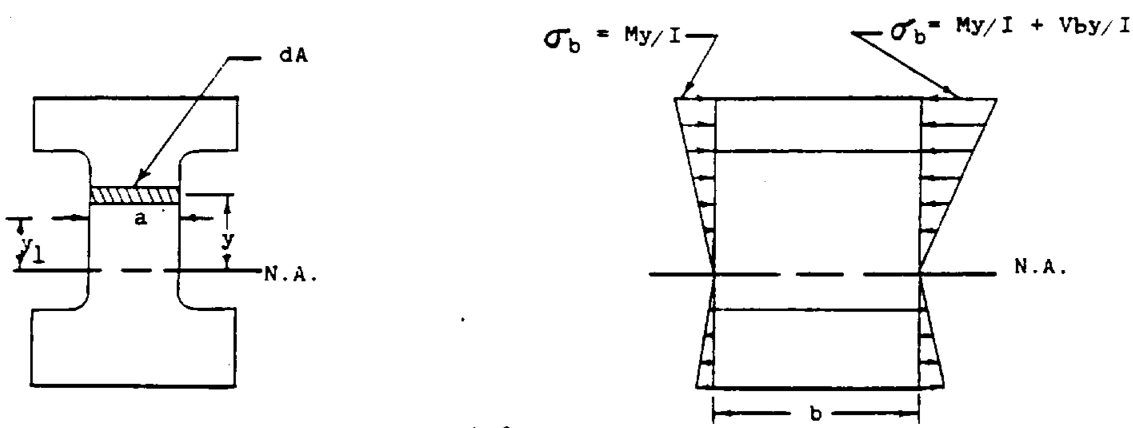

Fig. 4.6.1-2

In order to obtain the shear stress at a distance (y_1) above the neutral axis, the portion of the beam above (y_1) will be considered a free body as shown in (Fig. 4.6.1-3). The resultant force on the cross section to the right is greater than the resultant force on the cross section to the left. In order for the horizontal forces to be in equilibrium, the force produced by the shear stress (τ_s) must be equal to the difference in the two bending stresses (σ_b). Since only the difference in

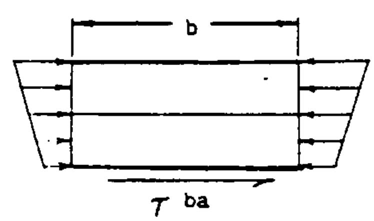

Fig. 4.6.1-3

the forces is considered, the loading condition shown in (Fig. 4.6.1-4) can be used in computing the shear stress (τ_s).

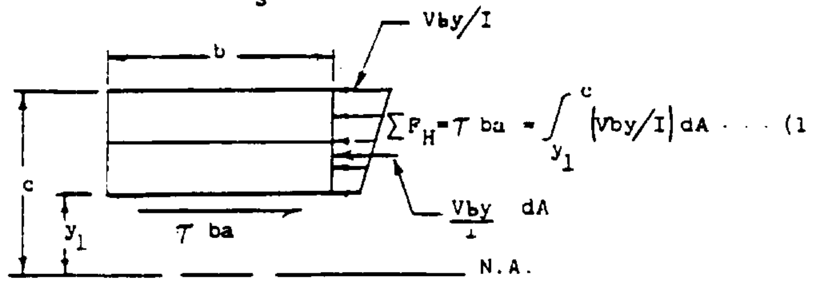

Fig. 4.6.1-4

Equation (1) represents the total horizontal force on the cross section of the element shown in (Fig. 4.6.1-4). Equation (1) can be simplified as follows:

$$\tau = \frac{V}{Ia} \int_{y_1}^{c} y\,dA \quad . . . . \quad (2)$$

Equation (2) was derived on the assumption that the beam cross section was symmetrical about either the horizontal or vertical axis through the centroid. The assumption that stress is proportional to strain was also used; therefore, the equation does not apply if the bending stresses exceed the elastic limit. The beam cross section is assumed to be the same at all points along the span (no taper).

4.6.2
Shear Flows in Thin Webs

The shear stresses at the free surface of a member are parallel to the surface; therefore there can be no abrupt change in stress distribution and it will be sufficiently accurate to assume that the shear stresses in thin webs are parallel to the surfaces for the entire thickness of the web.

Consider the curved web shown in Fig. 4.6.2-1. The shear stresses are shown in the direction of the web at all points. The shear flow (q), which is the product of the shear stress (τ) and the web thickness (t), is usually more convenient to use than the shear stress. The shear flow can be determined before the web thickness is determined, but the shear stress depends on the web thickness. Sometimes it is necessary to obtain the resultant force on a curved web in which the shear flow (q) is constant for the length of the web. Consider an element of the web as shown in (Fig. 4.6.2-2)

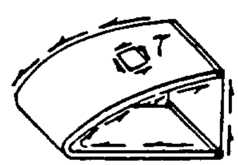

Fig. 4.6.2-1

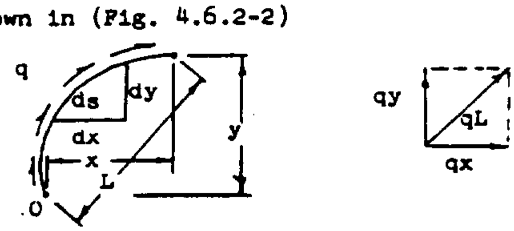

Fig. 4.6.2-2

The element has a length (ds), and the horizontal and vertical components of this length are (dx) and (dy). The force on the element of length is (qds), and the components of the force are (qdx) horizontally and (qdy) vertically. The total horizontal force is as follows:

$$F_x = \int_o^x qdx = qx \quad . \quad . \quad . \quad . \quad . \quad . \quad . \quad . \quad (1)$$

The total vertical force is as follows:

$$F_y = \int_o^y qdy = qy \quad . \quad . \quad . \quad . \quad . \quad . \quad . \quad . \quad (2)$$

The resultant force is (qL) and is parallel to the length (L). Equations (1) and (2) are independent of the shape of the web, but depend only on the components of the distance between the ends of the web. The moment of the force (qdS) about any point (o) as shown in (Fig. 4.6.2-3) is the product of the force and the moment arm (r).

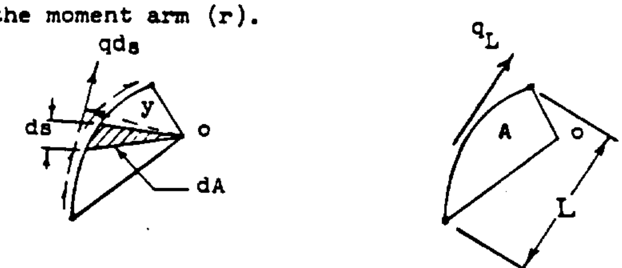

Fig. 4.6.2-3

The area (dA) of the triangle is (r ds/2). The moment of the shear flows along the entire length of the web can be obtained as follows:

$$M = \int qrds = \int 2qdA = 2q\int dA = 2Aq \quad . \quad . \quad . \quad . \quad . \quad (3)$$

where (A) is the area enclosed by the web and by the lines joining the ends of the web with point (o).

4.6.3
Shear Flow Distribution in Symmetrical Box Beams

The shear flows in box beams with several stringers may be obtained from the summation of spanwise loads on various stringers. The shear flows may all be expressed in terms of one unknown shear flow (q_o). If two cross sections one inch apart are considered as shown in Fig. 4.6.3-1, the difference in axial load (ΔP) on the stringers between the two cross sections is found by multiplying the difference in the bending stresses on the two sections by the stringer areas. The shear flow (q_o) can be obtained by equating the moments of the shear flows to the external torsional moment about a spanwise axis. For the beam shown in (Fig. 4.6.3-1) all the shear flows (q_1, q_2, ..., q_n) can be

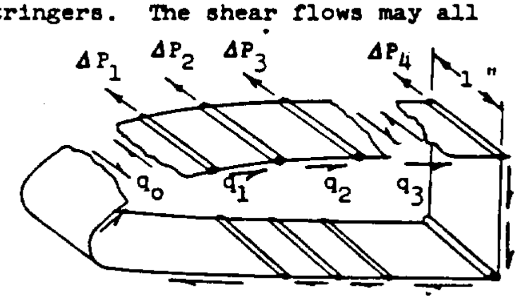

Fig. 4.6.3-1

expressed in terms of the shear flow (q_o) by considering the spanwise equilibrium of the stringers between the web (o) and the web under consideration.

$$q_1 = q_o + \Delta P_1$$

$$q_2 = q_o + \Delta P_1 + \Delta P_2$$

$$q_n = q_o + \sum_o^n \Delta P_n$$

where ($\sum_o^n \Delta P_n$) represents the summation of loads (ΔP) between web (o) and any web (n). The negative sign must be used if the values of (ΔP) are positive when they indicate tension increments. The flange elements are numbered in a clockwise order around the box, and the shear flows are positive when in a clockwise direction around the box. After expressing all the shear flows in terms of the unknown shear flow (q_o), the value of (q_o) can be obtained from torsional moments.

4.6.4
Shear Flows Distribution in Unsymmetrical Box Beams

In the analysis of beams with unsymmetrical cross section, it is necessary to obtain the bending stresses by obtaining section properties about the principal axes and superimposing the stresses from bending about each of the principal axes or by making use of the following formula.

$$\sigma_b = \frac{M_x I_{xy} - M_y I_x}{I_x I_y - I_{xy}^2}(x) + \frac{M_y I_{xy} - M_x I_y}{I_x I_y - I_{xy}^2}(y) \quad \ldots\ldots\ldots \quad (1)$$

where (x) and (y) are the coordinates of the various elements of area.

In analyzing an unsymmetrical beam for shearing stresses, it is necessary either to consider separately the shears along each of the two principal axes or to derive an equation for shearing stress from the general bending equation (1). If two cross sections of a beam a distance (a) apart are considered, the change in bending moment about any axis is equal to the product of the shear perpendicular to that axis and the distance (a). The change in bending stress ($\Delta\sigma_b$) between the two cross sections is obtained by substituting the terms ($M_x = V_y a$) and ($M_y = V_x a$) in formula (1):

$$\frac{\Delta\sigma_b}{a} = \frac{V_y I_{xy} - V_x I_x}{I_x I_y - I_{xy}^2}(x) + \frac{V_x I_{xy} - V_y I_y}{I_x I_y - I_{xy}^2}(y) \quad \ldots\ldots\ldots \quad (2)$$

The change (ΔP) in the axial load on any flange area between two cross sections a unit distance apart is obtained by multiplying the flange area by the change in bending stress (Δ_b/a). The shear flows can now be obtained from the axial load (ΔP) by the method in Section 4.6.3. The shear flows around the box beam change at each flange area by an amount shown by Formula (3).

$$\Delta q = \Delta P = \left[\frac{V_y I_{xy} - V_x I_x}{I_x I_y - I_{xy}^2}(x) + \frac{V_x I_{xy} - V_y I_y}{I_x I_y - I_{xy}^2}(y)\right] A_f \quad \ldots \quad (3)$$

4.6.5

Shear Flow in Tapered Webs

The distribution of the shear flow in a tapered web will now be considered since a large proportion of the shear webs in an airplane structure are tapered rather than rectangular; consider the beam shown in (Fig. 4.6.5-1).

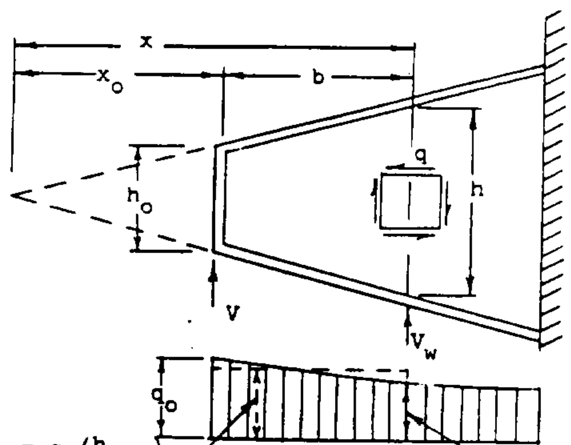

Fig. 4.6.5-1

The shear load (V_w) registered by the web at any place along the span is shown by similar triangles to be:

$$V_w = V\frac{h_o}{h} = V\frac{x_o}{x} \quad . \; . \; . \; . \; . \; . \; . \; . \; . \; . \; . \; . \; . \qquad (1)$$

The shear flow (q) may also be expressed in terms of the shear flow (q_o) at the free end as follows:

$$q = \frac{V_w}{h} = V\frac{h_o}{h^2} = q_o\left(\frac{h_o}{h}\right)^2 = q_o\left(\frac{x_o}{x}\right)^2 \; . \; . \; . \; . \qquad (2)$$

Sometimes it is necessary to find the average shear flow in a tapered web. The average shear flow between the free end and the point (x) of the beam as shown in (Fig. 4.6.5-1) can be obtained from the spanwise equilibrium of the flange (Fig. 4.6.5-2). The horizontal component of the flange load is found by dividing the bending

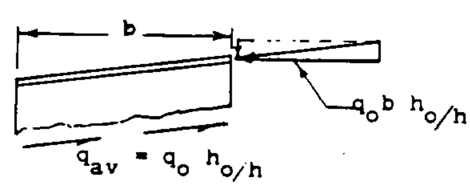

Fig. 4.6.5-2

moment ($q_o$hob) by the beam depth (h). The average shear flow in this length (q_{av}) is therefore obtained by dividing this force by the horizontal length (b).

$$q_{av} = q_o\frac{h_o}{h} = q_o\frac{x_o}{x} \; . \; . \; . \; . \; . \; . \; . \; . \; . \; . \qquad (3)$$

It has been assumed that the stresses existing on all four boundaries of the tapered plate were pure shearing stresses. It has been shown previously that pure shearing stresses may exist on only two planes, which must be at right angles to each other. The corners of a tapered web do not form right angles, therefore it is necessary for some normal stresses to act at the boundary of the web. In order to estimate the magnitude of these normal stress, consider the tapered web shown in (Fig. 4.6.5-3).

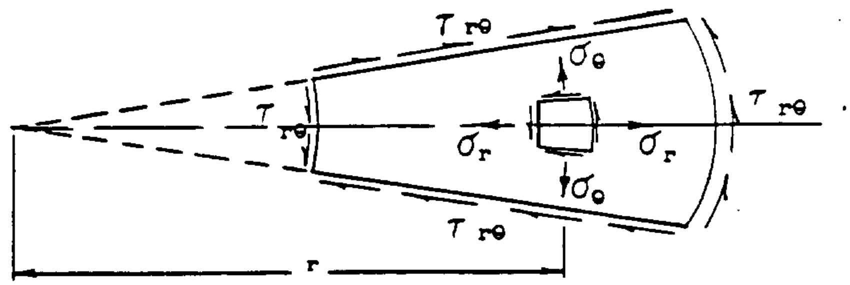

Fig. 4.6.5-3

It can be shown that a sector such as the one shown in (Fig. 4.6.5-3) may have pure shearing stress on all the boundaries. Under these conditions, any element such as the one shown will have no normal stress (σ_r) in the radial direction and no normal stress (σ_θ) in the tangential direction. By comparing the sector of (Fig. 4.6.5-3) with the tapered web of (Fig. 4.6.5-1) it is seen that the assumption of pure shear on the top and bottom boundaries was correct, however, the left and right boundaries must also resist some normal stress. The magnitude of these normal stresses may be determined for the Mohr circle in Fig. 4.6.5-4.

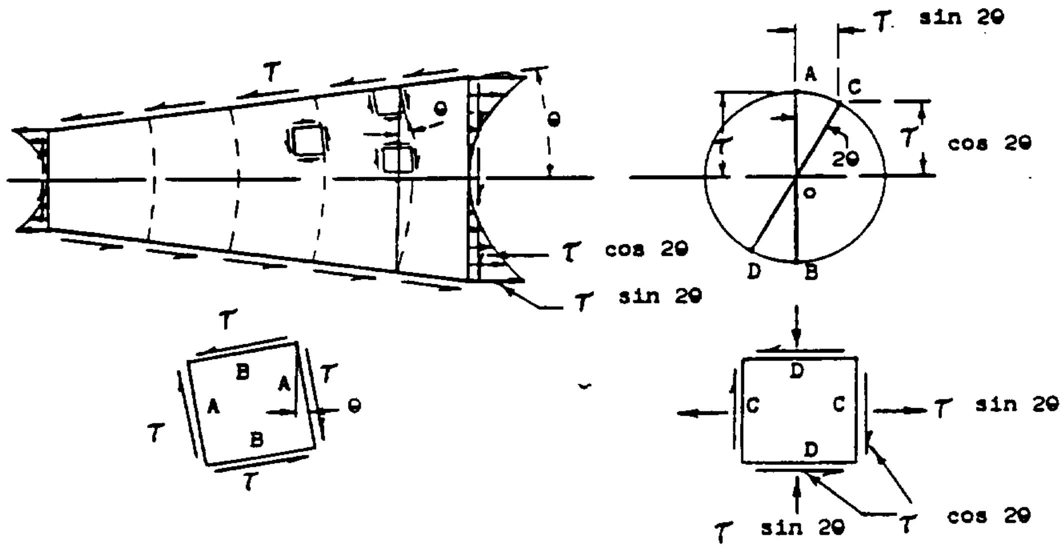

Fig. 4.6.5-4

The element under pure shearing stresses has faces (A) and (B) which are inclined at an angle (θ) with the vertical and horizontal. The Mohr circle for the pure shear condition will have a center at the origin and a radius (τ). Point (A) will be at the top of the circle, and Point (C), representing stresses on the vertical plane, will be clockwise at an angle (2θ) from Point (A). The coordinates of Point (C) represent a tensile stress of ($\tau \cos 2\theta$) on the vertical plane. For small values of (θ) the normal stresses are obviously negligible.

Incomplete Tension Field Webs

4.7.1 Stiffened

If the external shear load applied to a beam with a thin flat sheet as a web is less than the buckling load for the web, the web is in a state of pure shear at the neutral axis as indicated in Fig. 4.7.1-1. If the stresses due to bending are negligible over the depth of the web, this shear stress arrangement can be assumed constant over the full depth of the web.

If the web is so thin that it is incapable of carrying a compressive load, it will buckle into a pure tension field pattern as indicated in Fig. 4.7.1-2.

In an actual incomplete tension field beam, the state of stress in the web is intermediate between pure shear and pure diagonal tension. The engineering theory presented in NACA TN 2661 considers that this intermediate state of incomplete diagonal tension may be based on the assumption that the total shear force in the web can be divided into two parts, a part (S_s) carried by pure shear and a part (S_{dt}) carried by pure diagonal tension.

Thus, under this assumption one can write,

$$S = S_s + S_{dt} \quad \dots\dots\dots \quad (1)$$

which can be written in the form

$$S_{dt} = KS \quad \dots\dots\dots \quad (2)$$

$$S_s = (1-K)S \quad \dots\dots\dots \quad (3)$$

where (K) is the "diagonal tension factor" which expresses the degree to which the diagonal tension is developed by a given load. Thus the case of pure shear is described by K = 0 and the case of pure diagonal tension by K = 1.

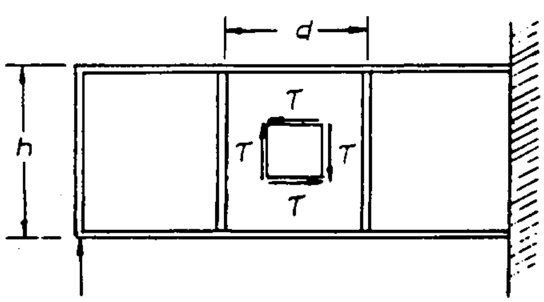

NONBUCKLED "SHEAR RESISTANT WEB"

Fig. 4.7.1-1

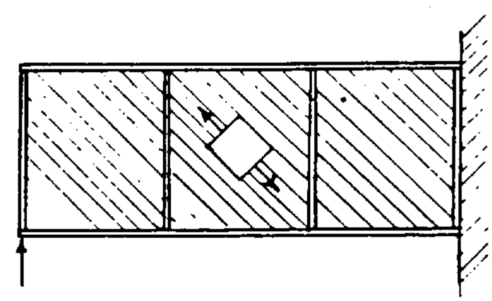

PURE DIAGONAL-TENSION WEB

Fig. 4.7.1-2

4.7.2

Critical Shear Stress

In the elastic range, the stress which will cause the web to buckle is given by

$$\tau_{cr} = K_{ss}\, E\, \left(\frac{t}{d_c}\right)^2 \left[R_h + \frac{1}{2}(R_d - R_h)\left(\frac{d_c}{h_c}\right)^3\right] \quad \ldots\ldots \quad (1)$$

for $d_c < h_c$

or

$$\tau_{cr} = K_{ss}\, E\, \left(\frac{t}{h_c}\right)^2 \left[R_d + \frac{1}{2}(R_h - R_d)\left(\frac{h_c}{d_c}\right)^3\right] \quad \ldots\ldots \quad (2)$$

for $h_c < d_c$

where (K_{ss}) is the theoretical buckling coefficient for a plate with simply supported edges having width (d_c) and length (h_c) (see Fig. 4.7.2.1), and (d_c) and (h_c) are "clear dimensions" (see Fig. 4.7.2.1.). If ($d_c > h_c$), the abscissa of Fig. 4.7.2.1 should be read as (dc/hc). The parameters (R_d) and (R_h) are restraint coefficients from Fig. 4.7.2.2. (Subscript h refers to edges along uprights; subscript d to edges along flanges).

If (τ_{cr}) exceeds the proportional limit, a suitable reduced modulus should be used (see Fig. 4.7.2.3 for 24S-T3 and 75S-T6 alloys).

If (τ_{cr}) calculated by these equations is less than (τ_{cr}) calculated with the presence of up-rights disregarded, use the latter value.

The following symbols are to be used with Figure 4.7.2.1

t_u = Thickness of upright

t_F = Thickness of flange

t = Thickness of web

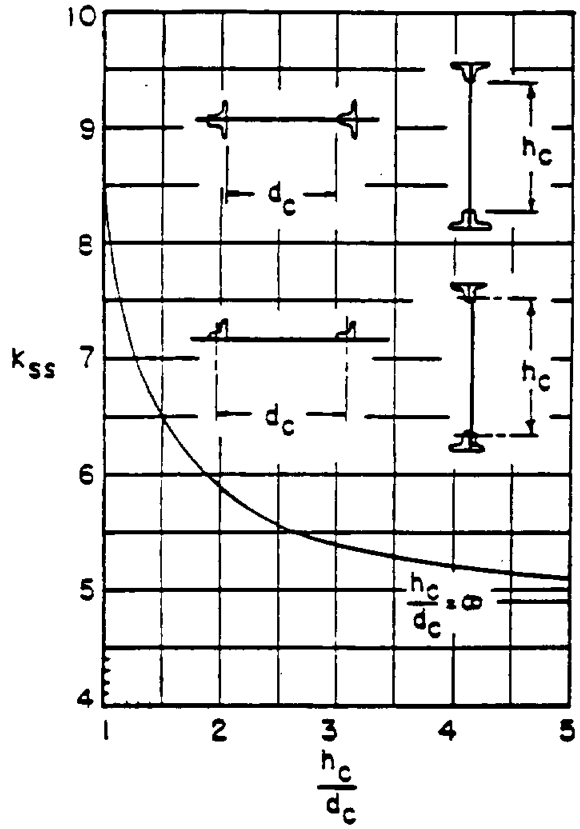

Theoretical coefficients for plates with simply supported edges.

Fig. 4.7. 2.1

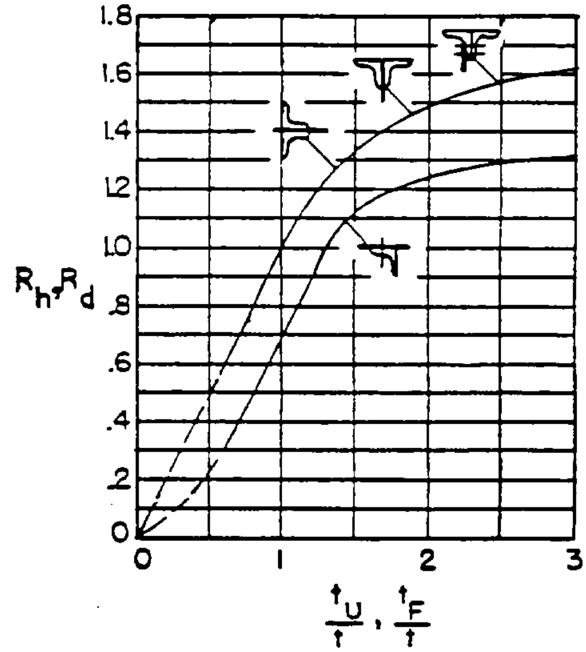

Empirical restraint coefficients.

Fig. 4.7 2.2

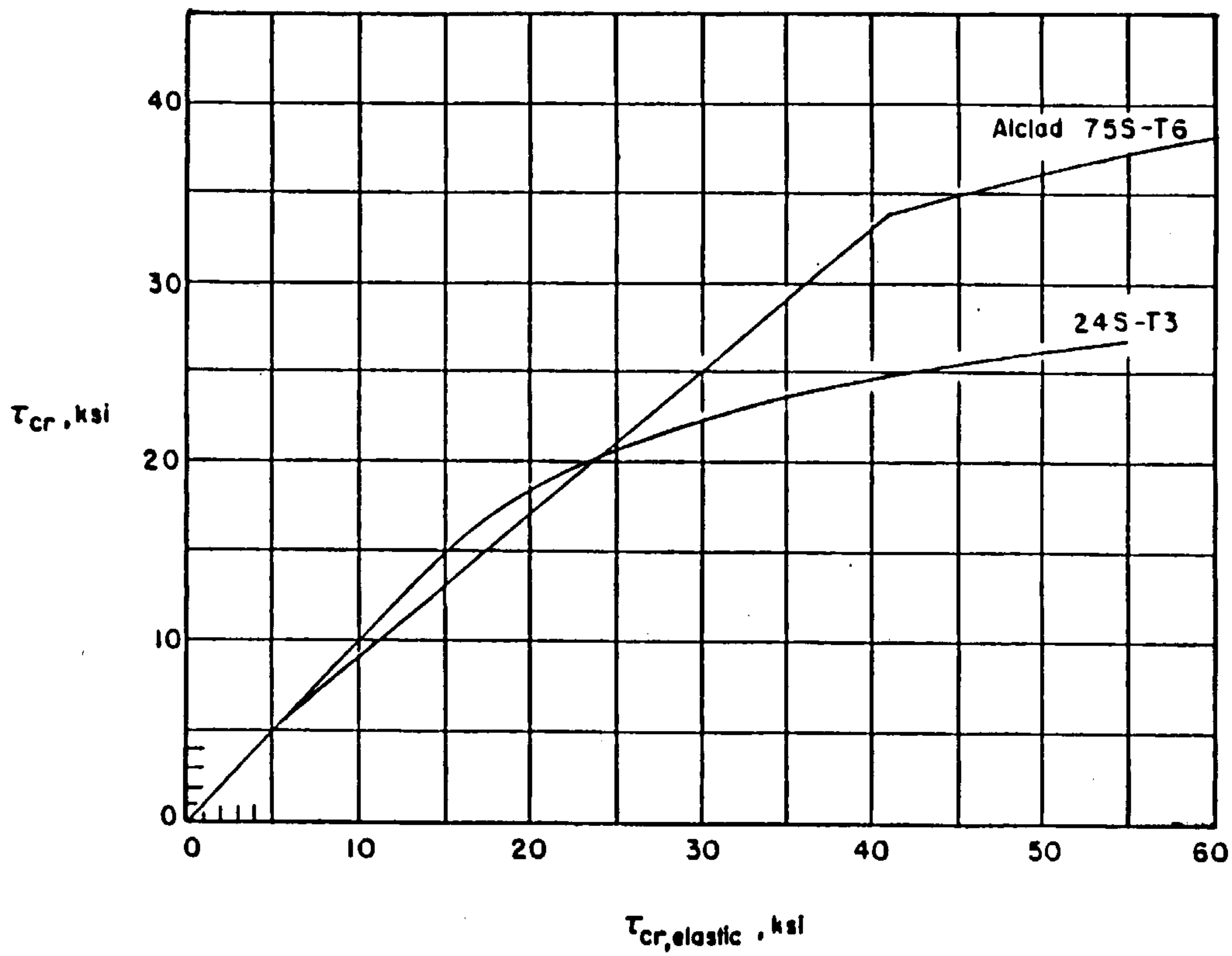

Plasticity correction.

Fig. 4.7.2.3

Nominal Web Shear Stress

When the depth of the flanges is small compared with the depth of the beam and the flanges are angle sections, the nominal web shear stress is given by

$$\tau = \frac{S_w}{h_e t} \quad \text{(1)}$$

where (S_w) is the web shear force (external shear minus vertical component of flange forces), (h_e) is the depth of the beam measured between the centroids of the flanges, and (t) is the thickness of the web.

In beams with other cross-sections, the nominal web shear stress is given by

$$\tau = \frac{S_w Q_F}{I_t}\left(1 + \frac{2Q_w}{3Q_F}\right) \quad \text{(2)}$$

where (Q_f) is the first moment of the flange area about the neutral axis and (Q_w) is the first moment of the web area above the neutral axis. Before values of (Q_w) and (I) are calculated for use with this formula, the web thickness must be multiplied by the estimated diagonal-tension factor (K).

4.7.4 Diagonal-Tension Factor

The diagonal tension factor (K) is given graphically in Fig. 4.7.4.1. For flat plates ($R = \infty$) therefore the ratio (td/Rh or $th/Rd = 0$) as shown in Fig. 4.7.4.1. When ($\tau/\tau_{cr} < 2$), (K) is given by the formula

$$K = .434\left(k + \frac{k^3}{3}\right) \quad \text{(1)}$$

where

$$k = \frac{\tau - \tau_{cr}}{\tau + \tau_{cr}} \quad \text{(2)}$$

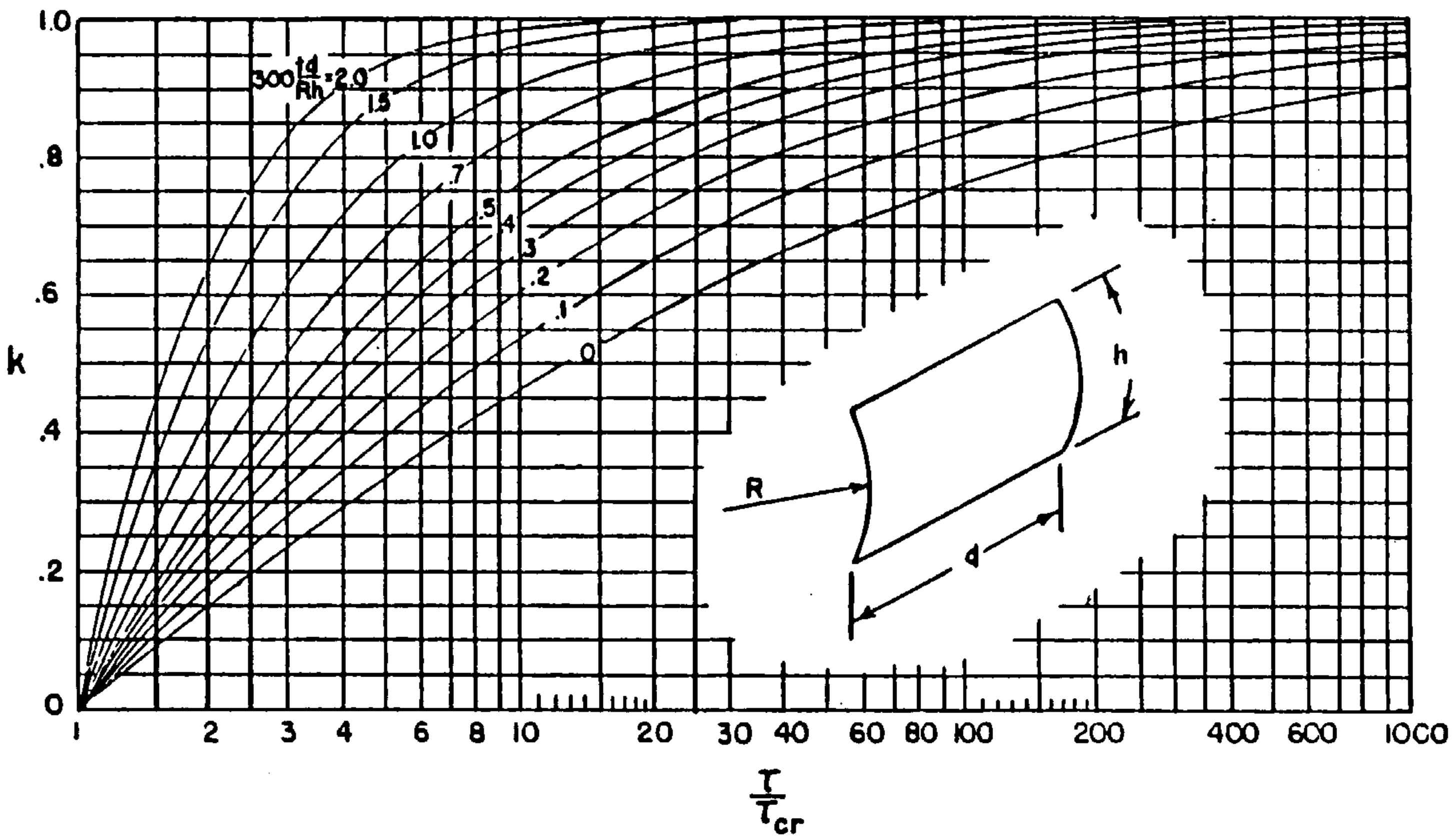

Diagonal-tension factor k. (If $h>d$, replace $\frac{td}{Rh}$ by $\frac{th}{Rd}$; if $\frac{d}{h}$ $\left(\text{or } \frac{h}{d}\right) > 2$, use 2.)

Fig. 4.7.4.1

4.7.5
Effective Area of Upright

The effective area of the uprights is

$$A_{ue} = A_u \quad \ldots \ldots \quad (1)$$

for double (symmetrical) uprights or

$$A_{ue} = \frac{A_u}{1 + (e/R)^2} \quad \ldots \ldots \quad (2)$$

for single uprights, where (A_u) is the actual area of the upright, (e) is the distance from the median plane of the web to the centroid of the cross-section, and (R) is the radius of gyration of the cross-section with respect to its centroidal axis parallel to the web.

When the outstanding leg of an upright is very wide, (A_{ue}) is equal to the area of the attached leg plus ($12\ t_u^2$).

4.7.6
Stresses in Uprights

The stress (σ_u) is the average taken along the length of the upright. For a double upright, (σ_u) is uniform over the cross section; for a single upright, (σ) is the stress in the median plane of the web along the upright-to-web rivet line.

If the flanges are heavy enough to make the flange strain (ϵ_F) small in comparison to the web strain (ϵ), the ratio (σ_u/τ) is given graphically in Fig. 4.7.6.1.

If the flanges are light, (σ_u) can be solved for by use of the following equations.

$$\sigma_u = -\frac{K\tau \tan \alpha}{\frac{A_{ue}}{dt} + .5(1-K)} \quad \ldots \ldots \quad (1)$$

$$\sigma_F = -\frac{K\tau \cot \alpha}{\frac{2A_F}{ht} + .5(1-K)} \quad \ldots \ldots \quad (2)$$

$$\tan^2\alpha = \frac{\epsilon - \epsilon_F}{\epsilon - \epsilon_u} \quad \ldots \ldots \quad (3)$$

$$\epsilon = \frac{\tau}{E}\left[\frac{2K}{\sin 2\alpha} + (1-K)(1+\mu)\sin 2\alpha\right] \quad \ldots \ldots \quad (4)$$

$$\epsilon_F = \frac{\sigma_F}{E} \quad \ldots \ldots \quad (5)$$

$$\epsilon_u = \frac{\sigma_u}{E} \quad \ldots \ldots \quad (6)$$

where (α) is the angle of diagonal tension in degrees. These equations must be solved by successive approximations. A value of (α) is assumed and equations (1), (2), and (4) are evaluated. From the resulting stresses, the strains are computed and inserted into equation (3). If the angle computed from equation (3) does not agree with the assumed angle, a new computation cycle is made with a changed value of (α).

The maximum value of (σ_u) occurs at the middle of the upright. The ratio ($\sigma_{u\,max}/\sigma_u$) is given graphically in Fig. 4.7.6.2.

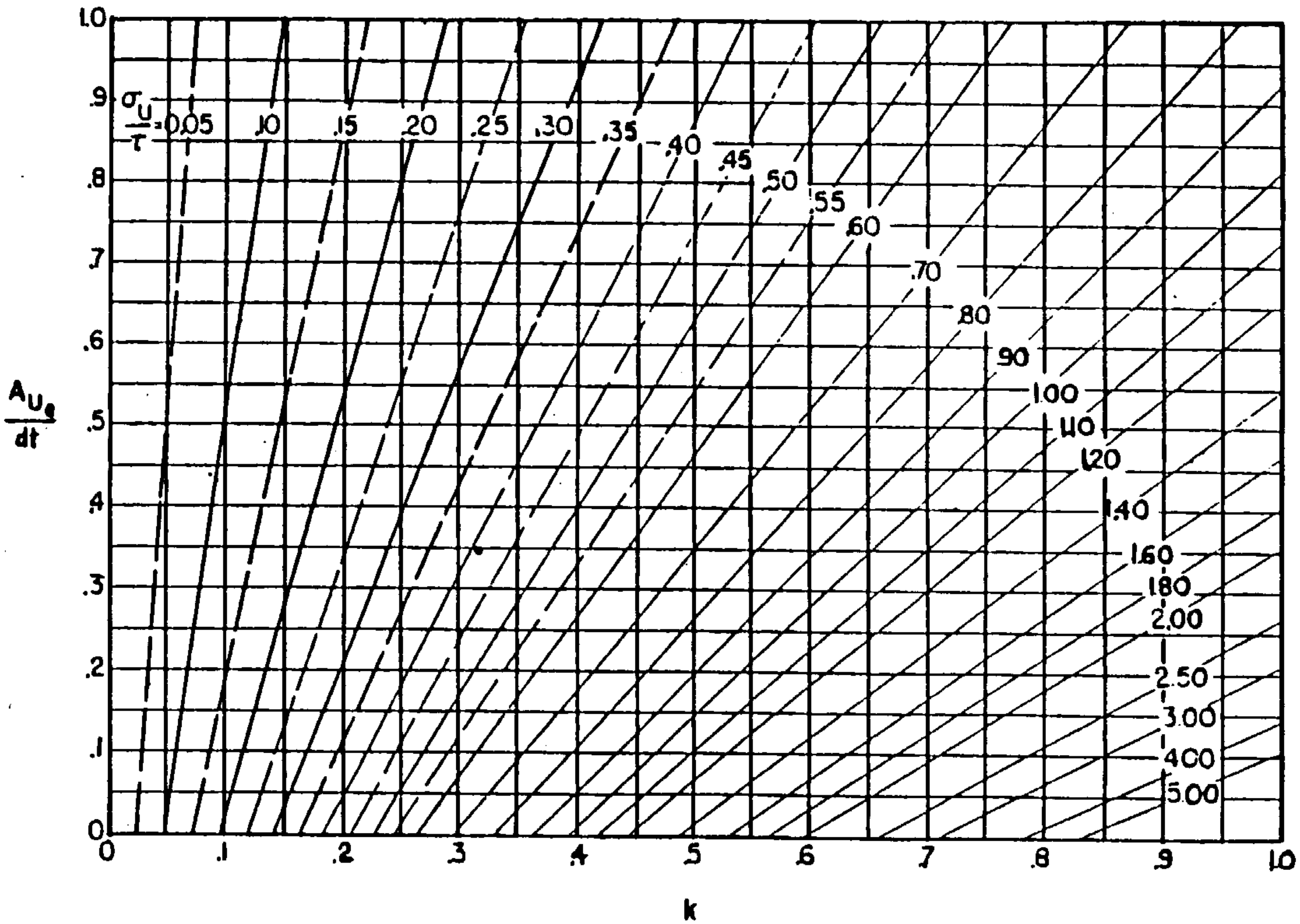

Diagonal-tension analysis chart.

Fig. 4.7.6.1

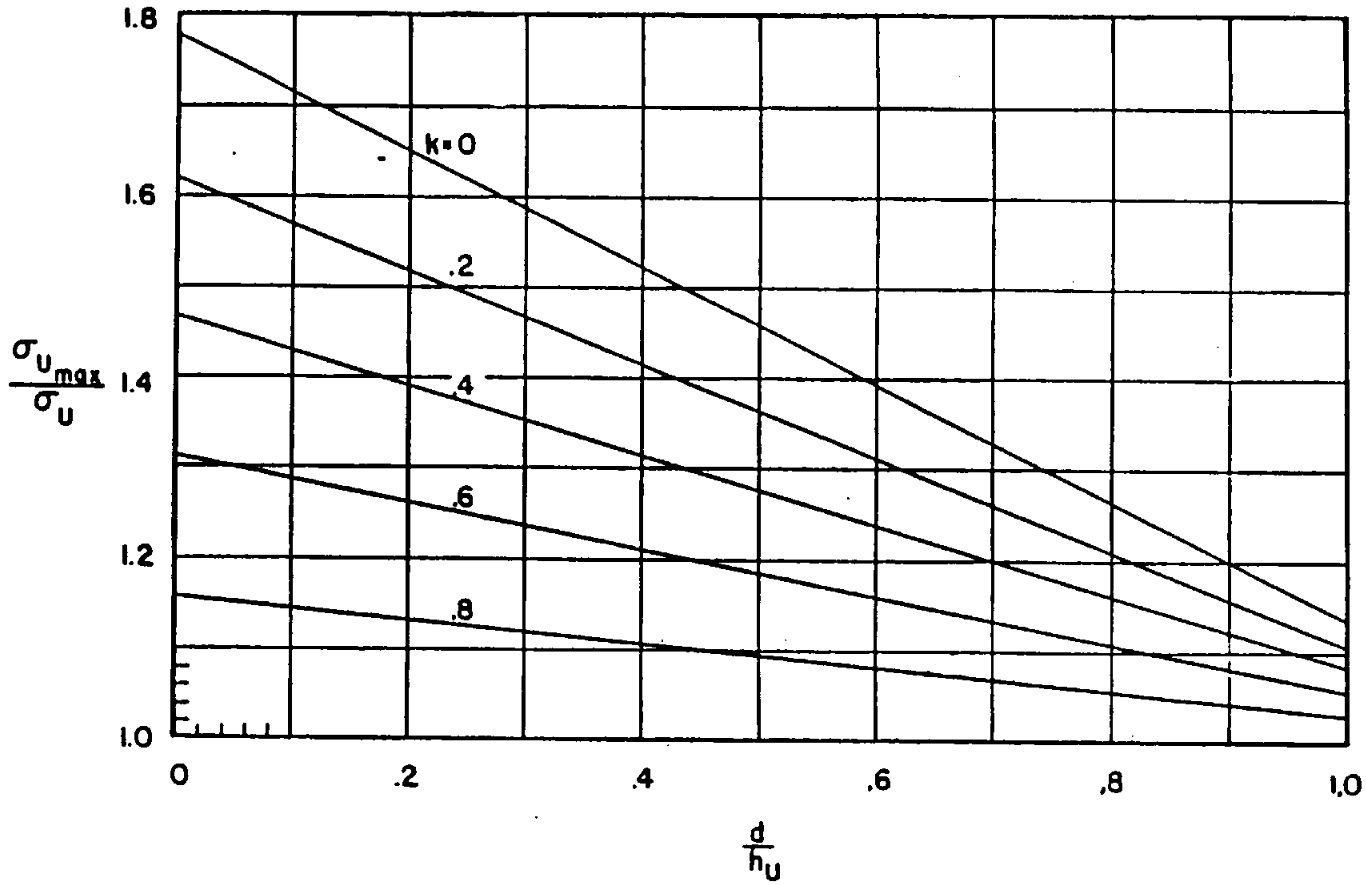

Ratio of maximum stress to average stress in web stiffener

Note for use on curved webs:
For rings, read abscissa as $\frac{d}{h}$, for stringers, read abscissa as $\frac{h}{d}$.

Fig. 4.7.6.2

4.7.7

Angle of Diagonal Tension

. Having determined (K) and (σ_u/τ), the angle (α) between the direction of the diagonal tension and the axis of the beam can be determined by use of Fig. 4.7.7-1.

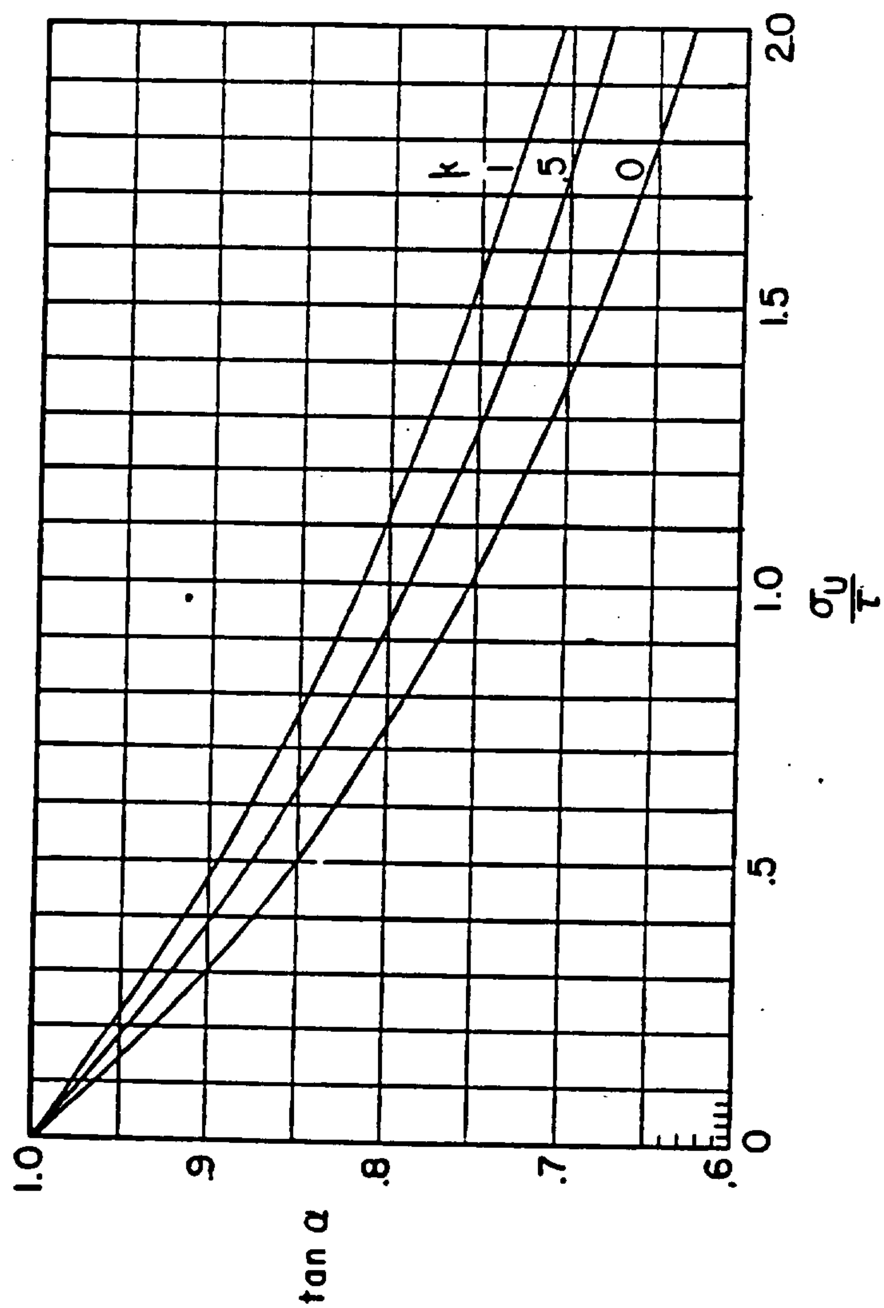

Incomplete Diagonal Tension

Fig. 4.7.7-1

4.7.8 Column Failure

Column failures due to instability, without previous bowing are possible only in double uprights. When column buckling begins, the uprights will force the web out of its original plane causing the web to develop tensile forces normal to the plane of the web which tend to force the uprights back. This bracing action is taken into account by use of a reduced "effective" column length (L_e) of the upright, which is given by the empirical formula,

$$L_e = \frac{h_u}{\left[1+K^2\left(3-2\frac{d}{h_u}\right)\right]^{1/2}} \qquad (d < 1.5h) \quad . \; . \; . \; . \; . \qquad (1)$$

$$L_e = h_u \qquad (d > 1.5h) \quad . \; . \; . \; . \qquad (2)$$

where (h_u) is the length of the upright, measured between centroids of upright-to-flange rivet patterns. The stress (σ_u) at which column failure takes place can be solved for by use of the standard column equations with the actual height of the column replaced by (L_e).

To avoid column failure or excessive deformation of a single upright, the stress (σ_u) should not exceed the column yield stress, and the average stress over the cross section of the upright

$$\sigma_{u_{avg}} = \frac{\sigma_u A_{ue}}{A_u} \quad . \; . \; . \; . \; . \; . \; . \; . \; . \; . \; . \; . \; . \; . \; . \; . \; . \; . \; . \qquad (3)$$

should not exceed the allowable stress for a column with the slenderness ratio ($h_u/2R$).

4.7.9 Forced Crippling Failure

The shear buckles in the web can force buckling of the upright in a leg attached to the web, particularly if the upright leg is thinner than the web. These buckles provide a lever arm to the compressive force acting in the leg which produces a severe stress condition. The buckles in the attached leg will in turn induce buckling of the outstanding legs.

To avoid forced crippling failure of double uprights, the maximum upright stress ($\sigma_{u_{max}}$) should not exceed the allowable value (σ_o) defined by the empirical formulas

$$\sigma_o = 21\, K^{2/3} \left({}^{t}u/t\right)^{1/3} \text{ ksi} \quad \text{(24S-T3 alloy)} \; . \; . \; . \; . \qquad (1)$$

$$\sigma_o = 26\, K^{2/3} \left({}^{t}u/t\right)^{1/3} \text{ ksi} \quad \text{(75S-T6 alloy)} \; . \; . \; . \; . \qquad (2)$$

Nomographs for these formulas are given in Figs. 4.7.9.1 and 4.7. 9.2.

To avoid forced crippling failure of single uprights, the maximum upright stress ($\sigma_{u_{max}}$) should not exceed the allowable value (σ_o) defined by the empirical formulas

$$\sigma_o = 26\, K^{2/3} \left({}^{t}u/t\right)^{1/3} \text{ ksi} \quad \text{(24S-T3 alloy)} \; . \; . \; . \; . \qquad (3)$$

$$\sigma_o = 32.5\ K^{2/3}\ ({}^{t}u/t)^{1/3}\ \text{ksi} \quad \text{(75S-T6 alloy)} \quad \ldots\ldots \quad (4)$$

Nomographs of these formulas are given in Figs. 4.7.9.1 and 4.7.9.2.

If (σ_o) exceeds the proportional limit, it should be multiplied by a plasticity correction factor (n), which can be taken as

$$n = \frac{E_{sec}}{E} \quad \ldots\ldots \quad (5)$$

with the moduli determined from the compressive stress-strain curve of the upright material.

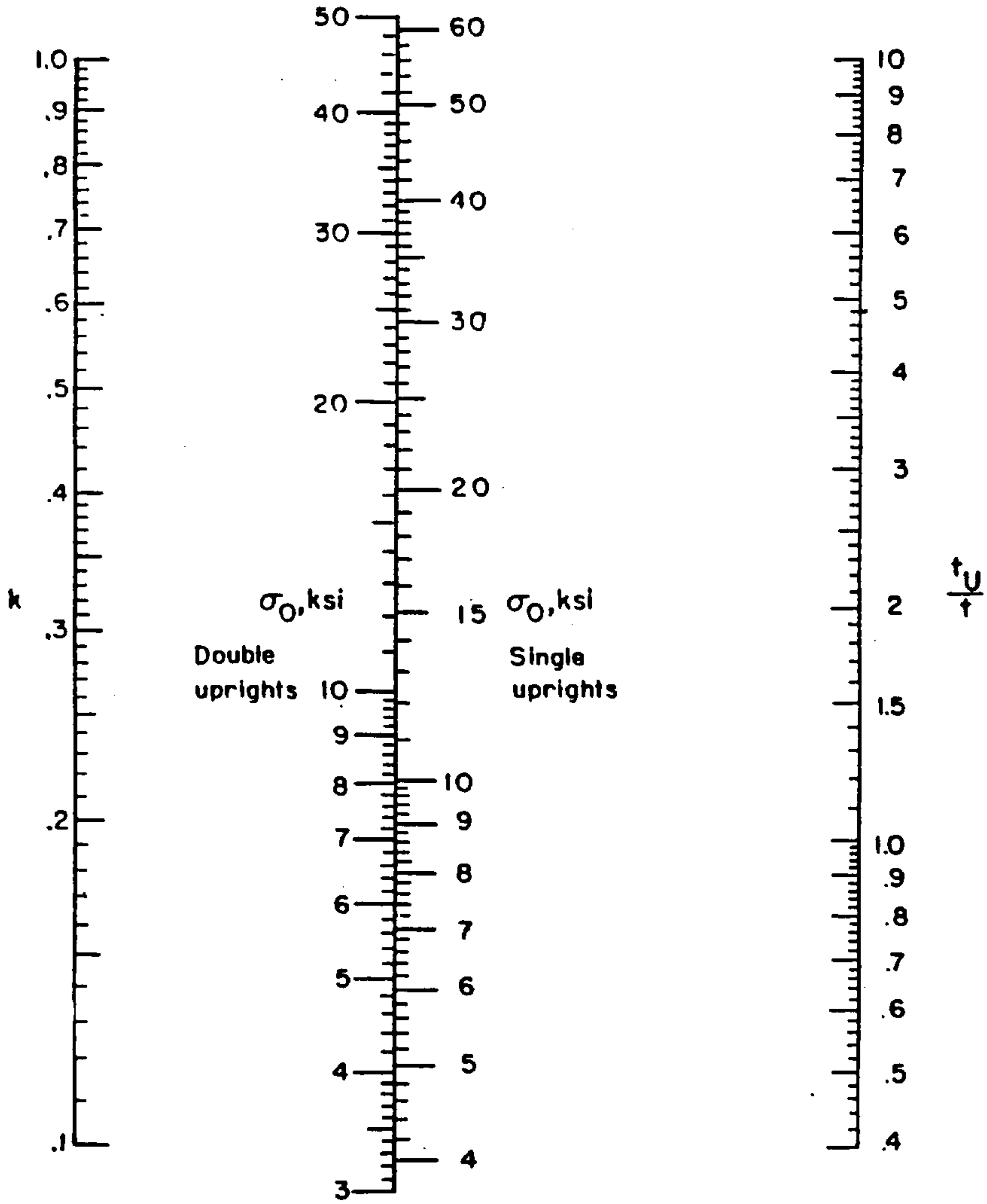

24S-T3 aluminum alloy.

Nomogram for allowable upright stress

Fig. 4.7.9.1

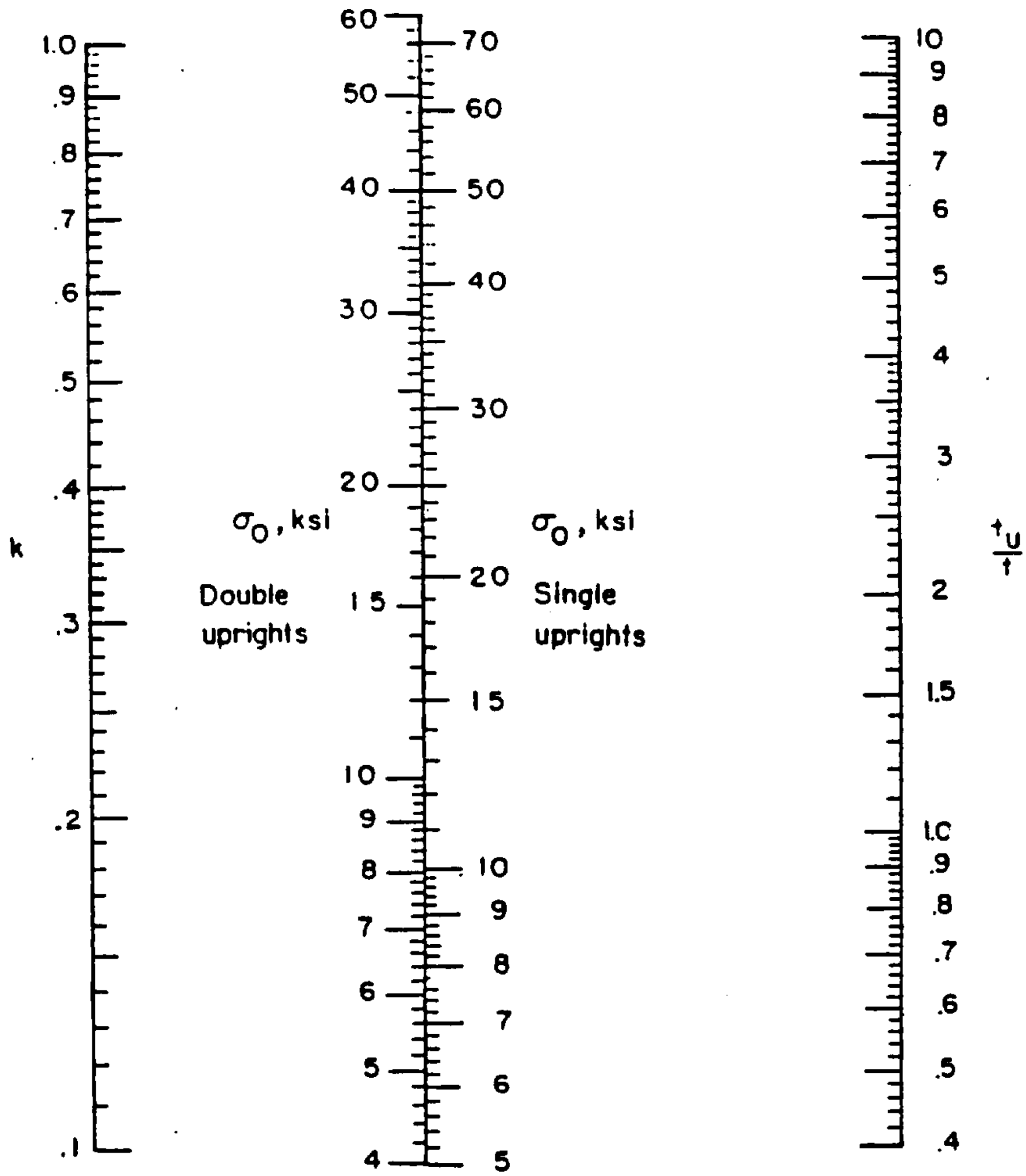

75S-T6 aluminum alloy.

Nomogram for allowable upright stress

Fig. 4.7.9.2

4.7.10

Maximum Web Stress

The maximum (nominal) web stress within a bay is given by the formula

$$\tau_{max} = \tau(1+K^2C_1)(1+KC_2) \quad (1)$$

The factors (C_1) and (C_2) are given graphically in Fig. 4.7.10-1 and 4.7.10-2, respectively. The angle (α) is given graphically in Fig. 4.7.7-1 The flange flexibility factor, (wd) is equal to :

$$wd = .7\, d\left[\sqrt[4]{\frac{t}{(I_c+I_t)h_e}}\right]$$

where (d) is the spacing of uprights, (t) is the thickness of the web, (h_e) is the depth of the beam measured between centroids of flanges, and (I_c) and (I_t) are moments of inertia of compression and tension flanges, respectively.

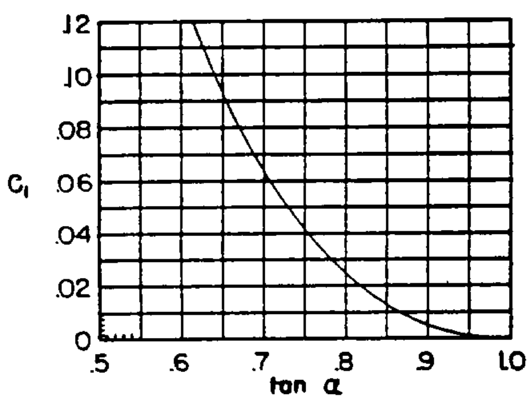

ANGLE FACTOR C_1

Fig. 4.7.10-1

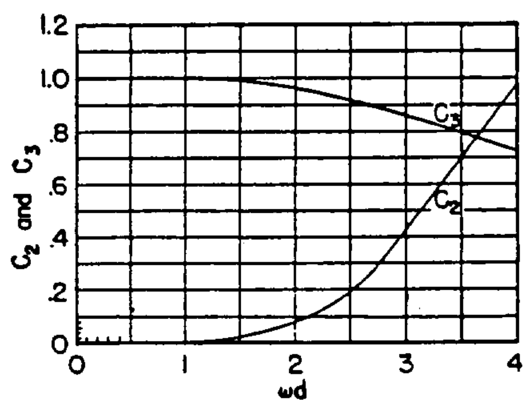

STRESS CONCENTRATION FACTORS, C_2 & C_3

Fig. 4.7.10-2

Allowable Web Stresses

Fig. 4.7.15.1 and 4.7.15.2 give "basic allowable" values (denoted by τ^*_{all}) for (τ_{max}) that are used as follows for different types of construction:

(a) Bolts just snug, heavy washers under bolt heads, or web plate sandwiched between flange angles: Use basic allowables,

(b) Bolts just snug, bolt heads bearing directly on sheet: Reduce basic allowables 10 percent.

(c) Rivets assumed to be tight: Increase basic allowables 10 percent.

(d) Rivets assumed to be loosened in service: Use basic allowables.

These allowables are not valid for rivets of any countersunk type.

When single uprights are used, the simplest construction results if the web is riveted to the outside of the flange angle. Preliminary results indicate that such an unsymmetrical arrangement of the web results in lower web failing stresses if the web is thick. With webs having ($h/t = 60$) and offset by 2.4 times their thickness from the center line of the flanges, the web failing stress is reduced by about 10 percent. For webs with ($h/t = 120$) or more, no detrimental effect has been noted.

At points where local loads are introduced into the web, the allowable web stress cannot be estimated with any degree of accuracy. The only safe procedure is to reinforce the web with doubler plates in adjacent bays.

The above criteria is valid only if the standard allowable bearing stresses (on sheet or rivets) are not exceeded.

4.7.12
Web to Flange Rivets

The rivet load per inch of beam is given by

$$R'' = \frac{S_w}{h_r}(1 + .414\ K) \quad \text{. . . . .} \quad (1)$$

where (h_r) is the depth of the beam measured between centroids of rivet patterns, top and bottom flanges.

4.7.13
Upright to Flange Rivets

The end rivets must carry the load existing in the upright into the flange. If the gusset effect (decrease in upright load towards the end of the upright) is neglected, these loads are

$$P_u = \sigma_u A_u \quad \text{. . . . .} \quad (1)$$

for double uprights, and

$$P_u = \sigma_u A_{ue} \quad \text{. . . . .} \quad (2)$$

for single uprights.

4.7.14
Upright to Web Rivets

The upright to web rivets for double uprights must be checked for two possibilities of failure, one due to shear caused by column bending, and one due to tension in the rivets caused by the tendency of the web folds to force the two components of the upright apart.

To avoid shear failure, the total rivet shear strength for an upright of 24S-T3 alloy should be

$$R_R = \frac{100\ Qh_u}{bL_e} \quad \ldots \quad (1)$$

where (Q) is the first moment of the cross-sectional area of one upright with respect to an axis in the median plane of the web, (b) is the width of the outstanding leg of the upright, and (h_u/L_e) is the ratio given by formula 4.7.8-1 or 4.7.8-2. For uprights of other materials, it is suggested that the right-hand side of Equation (1) be multiplied by the factor: Compressive yield stress of material divided by compressive yield stress of 24S-T3 alloy.

If the actual rivet strength (R) is less than the required strength (R_R), the allowable stress for column failure must be multiplied by the reduction factor given in Fig. 4.7.15.3.

To avoid tension failures, the tensile strength of the rivets per inch run must be greater than ($.15\ t\,\sigma_{ult}$) where (σ_{ult}) and (t) are the tensile strength and thickness of the web, respectively.

For single uprights, the tensile strength of the rivets per inch run must be greater than ($.22\ t\,\sigma_{ult}$) to keep the folds of the web from lifting off the uprights.

The tensile strength of a rivet is defined as the tensile load that causes any type of failure.

The pitch of the rivets on single uprights should be small enough to prevent inter-rivet buckling of the web or the upright at a compressive stress equal to ($\sigma_{u_{max}}$). The pitch should also be less than (d/4) in order to justify the assumption of edge support used in the determination of (τ_{cr}).

4.7.15 Secondary Stresses in Flanges

The compressive stress in a flange caused by the diagonal tension is given by

$$\sigma = -\frac{KS_w \operatorname{Cot}\alpha}{2\ A_F} \quad \ldots \quad (1)$$

The primary maximum bending moment in the flange (over an upright) is given by

$$M_{Max} = KC_3\,\frac{S_w d^2 \tan\alpha}{12\ h} \quad \ldots \quad (2)$$

where (C_3) is given graphically in Fig. 4.7.10-2. Because these moments are highly localized, the block compressive strength is probably acceptable as the allowable value. The calculated moments are believed to be conservative and are often completely neglected in practice.

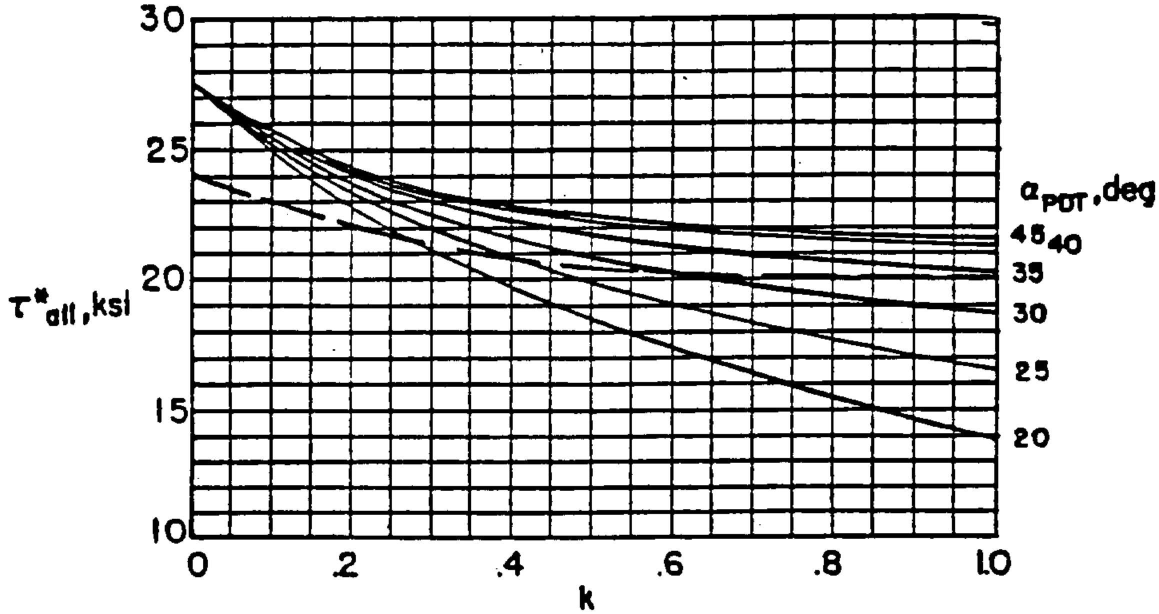

24S-T3 aluminum alloy. σ_{ult} = 62 ksi.
Dashed line is allowable yield stress.

Fig. 4.7.15.1

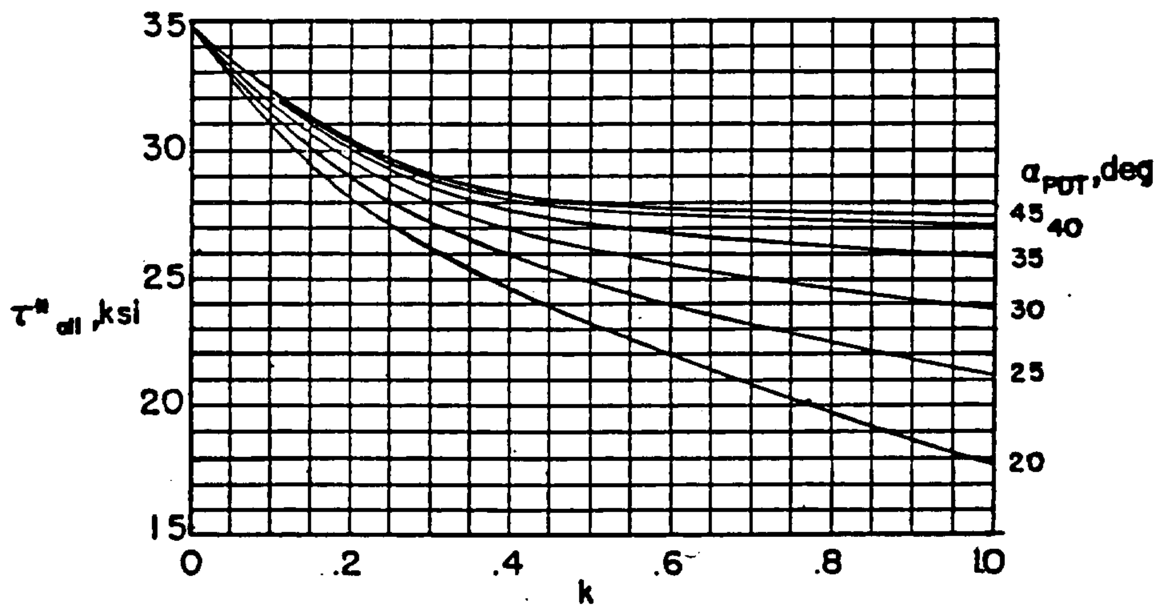

Alclad 75S-T6 aluminum alloy. σ_{ult} = 72 ksi.

Basic allowable values of τ_{max}

Fig. 4.7.15.2

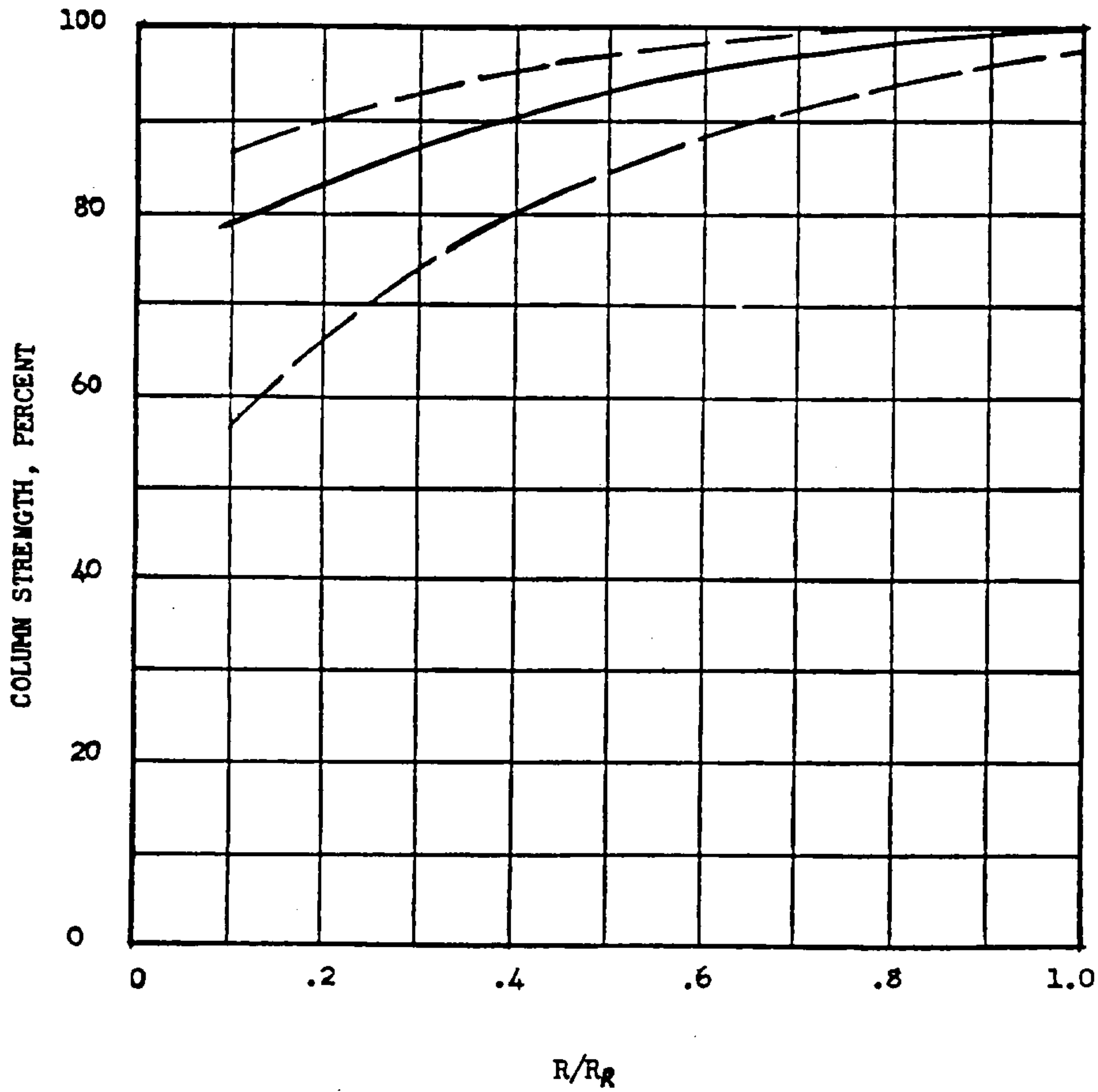

STRENGTH OF RIVETED COLUMNS

Fig. 4.7.15.3

REFERENCES

BEAMS

4.1.0 Peery, D. J., Ph.D., Aircraft Structures, McGraw-Hill, 1950

4.2.0 Grinter, T. E., Ph.D., C.E., Theory of Modern Steel Structures, The Macmillan Company, 1956.

Peery, D. J., Ph.D., Aircraft Structures, McGraw-Hill, 1950

Bruhn, E. F., Analysis and Design of Aircraft Structures, Tri-State Offset Company, 1958.

4.3.0 N.A.C.A. 929

4.6.0 Peery, D. J., Ph.D., Aircraft Structures, McGraw-Hill, 1950

4.7.0 N.A.C.A. TN 2661
N.A.C.A. TN 2662

Data Source, Section 1.3 Reference 7

Stiffener Size to Use with Non-Buckling Web.

A web stiffener is used to decrease the size of web panel; thus when buckling of the web starts, the stiffener tends to keep buckles from extending across the stiffener or causes the sheet to buckle in two panels instead of one. Mr. H. Wagner in a paper presented before a meeting of the A.S.M.E. in 1930 offered the following expression as the required moment of inertia of a stiffener to be used with a shear resistant web.

$$I_V = \frac{2.29d}{t}\left(\frac{V\ h_W}{33\ E}\right)^{4/3} \quad \text{-----------} \quad (C10.8)$$

where

I_V = moment of inertia of stiffener

d = center line distance between stiffeners

h_W = depth of web plate

V = vertical shear at section

t = web thickness

E = modulus of elasticity

A more recent criteria for stiffener stiffness (I_V) for both flat and curved webs is given by the curve in Fig. C10.9. When the stiffener is used purely as such and not as a means to transfer a concentrated external load to the beam web, the question arises as to what is the minimum number of fasteners required in attaching the stiffener to the web. For non-buckling webs, two criteria are suggested:-

(1) The stiffener should be attached to the flange at each end.

(2) The rivet pitch (spacing) should be at the most equal to 1/4 times the stiffener spacing, or 1/4 the web height if this is smaller, in order to justify the assumption of simple support at the edges of the web panel. Normal practice uses more rivets.

Data Source, Section 1.3 Reference 7

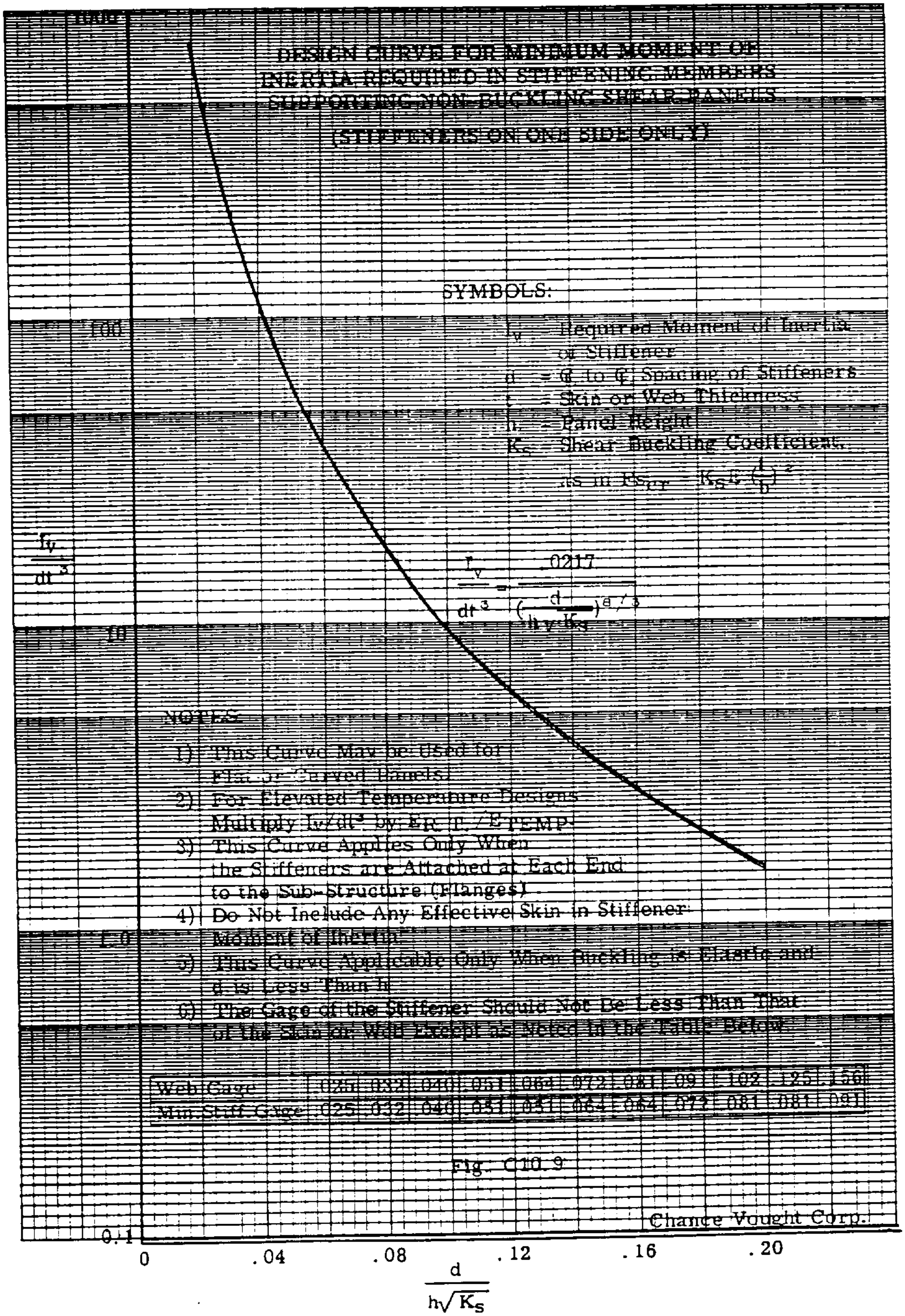

Web Gage	.025	.032	.040	.051	.064	.072	.081	.091	.102	.125	.156
Min. Stiff. Gage	.025	.032	.040	.051	.051	.064	.064	.072	.081	.081	.091

Fig. C10.9

Data Source, Section 1.3 Reference 3

10.2 SHEAR WEB REINFORCEMENT FOR ROUND HOLES

10.2.1 Doubler Reinforcement

The thickness of the reinforcing doubler may be obtained through the use of the equations below. The figure below defines the variables used in the equations.

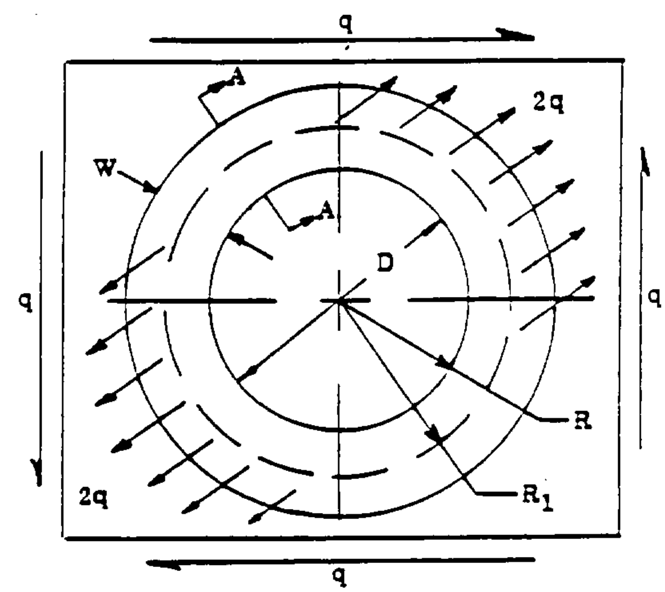

FIGURE 10.12 - SHEAR WEB REINFORCEMENT

$R_1 = R + \frac{W}{2}$

$D = 2R$

q = Web shear flow

F_{tu} = Ultimate tensile strength

f_b = Bending stress

f_t = Tensile stress

W = Doubler width

t_d = Doubler thickness

t_{web} = Web thickness

t_{ring} = "Smeared" flanged doubler thickness or unflanged doubler thickness 2

The stresses at section A-A are:

$$f_b = \frac{\text{Moment}}{\text{Section Modulus}} = \frac{2q(.25R)(R_1)}{t_d\left(\frac{W^2}{6}\right)}$$ 2

$$f_t = \frac{2qR}{Wt_d} = \frac{Dq}{Wt_d}$$

The stress interaction, assumed at failure, is:

$$F_{tu} = f_b + f_t = \frac{.75qD(D + W)}{t_d W^2} + \frac{qD}{Wt_d}$$

Therefore,

$$t_d = \frac{.75q\left(\frac{D}{W}\right)^2 + 1.75q\left(\frac{D}{W}\right)}{F_{tu}}$$

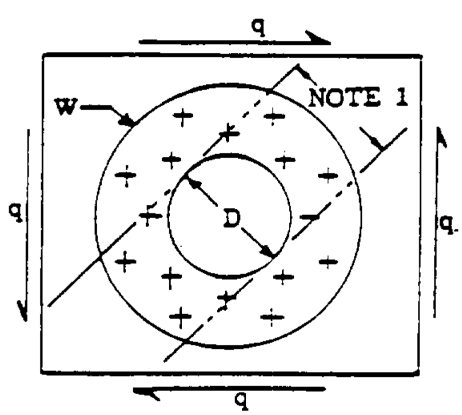

FIGURE 10.13 - RIVET PATTERN LOAD

For flanged doublers the total thickness, $t_{web} + t_d$, may be obtained from Figure 10.14. 2

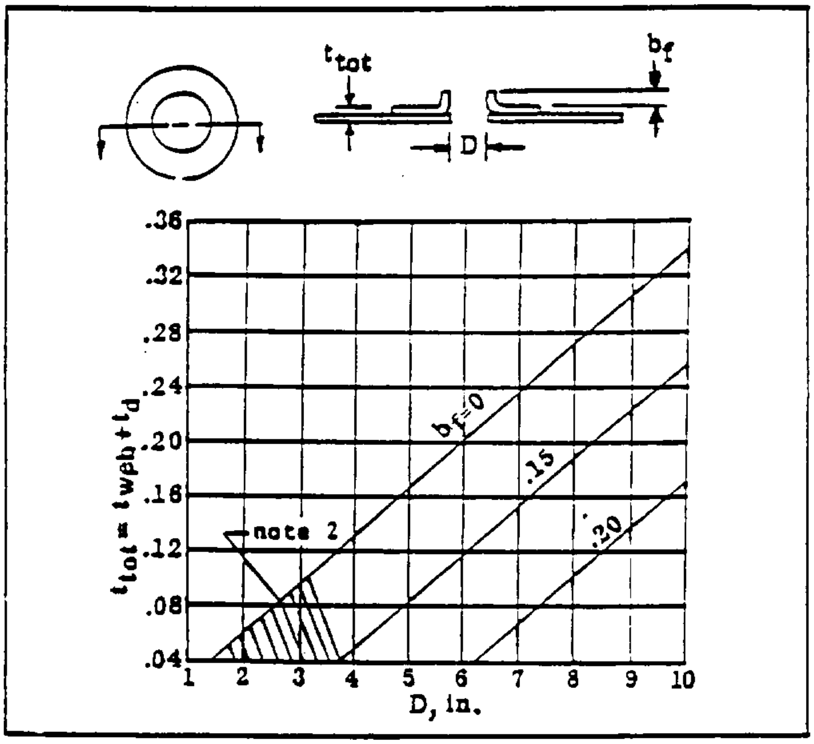

FIGURE 10.14 - TOTAL THICKNESS FOR FLANGED DOUBLERS

Note 1: The rivet pattern is to be uniform, and develop a running load strength per inch (between the tangent lines) of

$$2q \left| \frac{t_{ring}}{t_d + 0.8\ t_{web}} \right|$$

Note 2: In this region, increase t_{tot} to correspond to $b_f = 0$ for the same D and omit the flange.

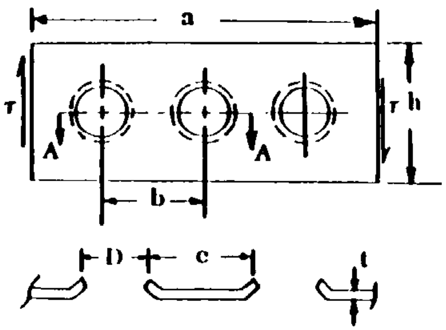

NOTE: The limits of the curve for τ_{all}:

$50 < h/t < 300$
$.15 < D/h < .75$
$60 < c/t < 300$

For $c/t < 60$, use correction factor, K, at right

$\tau_{cor} = K\,\tau_{all}$

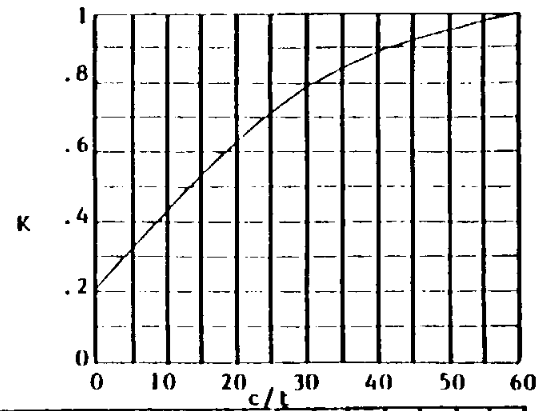

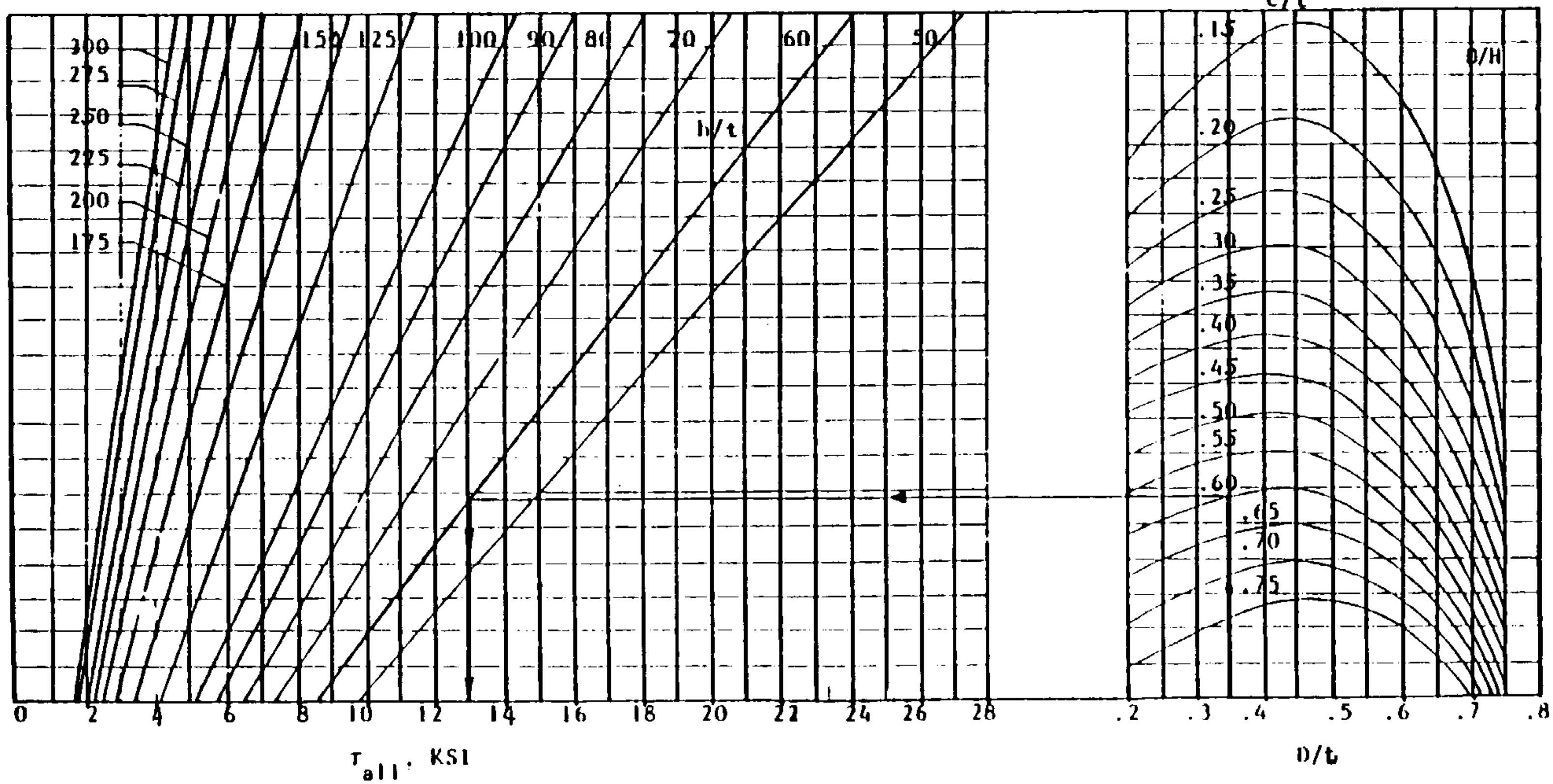

FIGURE 10.15 - ALLOWABLE SHEAR STRESS FOR 2024 WEBS WITH CIRCULAR HOLES HAVING 45° FLANGES

10.2.2 45° Flange Reinforcement

Allowables for panels loaded by pure shear (no addition bending forces) are given in Figure 10.15. Limited available data indicates that beaded lightening panels are more efficient than flanged panels. (Reference NACA RB No. 4B23, "Tests of Beams with Large Circular Lightening Holes".)

10.3 SHEAR WEBS WITH BEADS

Beaded panels are one type of non-buckling shear webs. Stiffeners must be added at load points to prevent premature collapse. Since the collapsing stress is only slightly higher than the buckling stress, the buckling stress is considered the ultimate allowable. The critical shear stress τ_{cr} for a beaded web can be expressed as:

$$\tau_{cr} = K_s K_1 E\left(\frac{t}{h}\right)^2\left(\frac{\pi^2}{12(1-\mu^2)}\right)$$

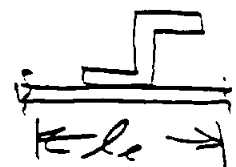

where

K_s = Simply supported flat sheet, shear buckling constant based on a/b from Figure 10.18.

K_1 = Beaded-web shear buckling coefficient obtained from Figure 10.17.

Figure 10.17 is based on test results obtained from 2024-T4 clad panels with a bead spacing of 2 to 5 inches, panel heights of 7 to 12 inches, and gages of 0.032 to 0.064 inches. It is suggested that above the proportional limit τ_{cr} be reduced by the factor G_t/G.

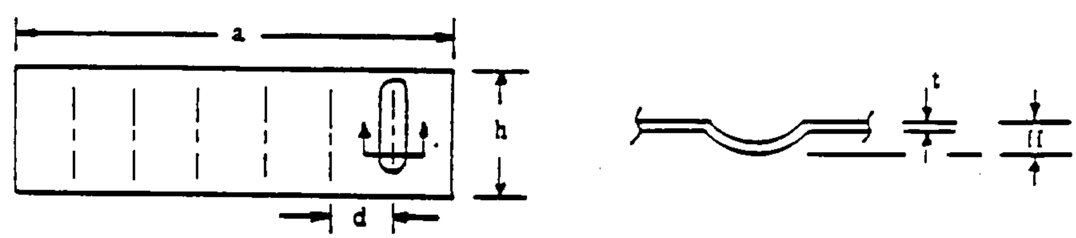

FIGURE 10.16 - GEOMETRY OF BEADED WEBS

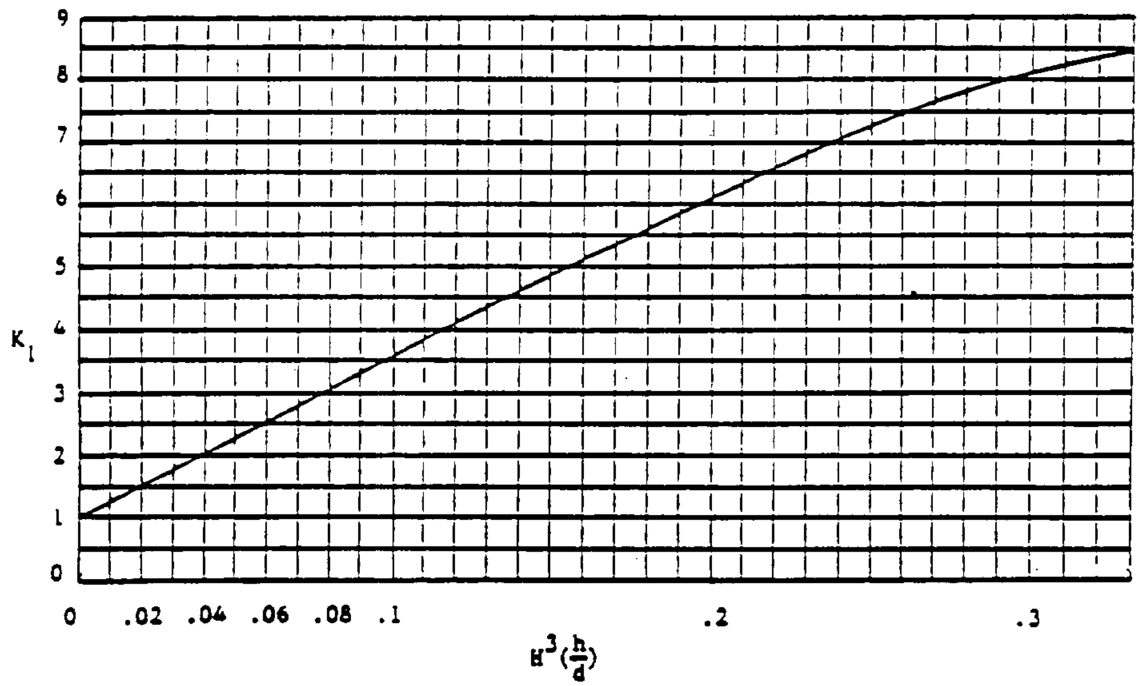

FIGURE 10.17 - BEADED WEB SHEAR BUCKLING CONSTANT

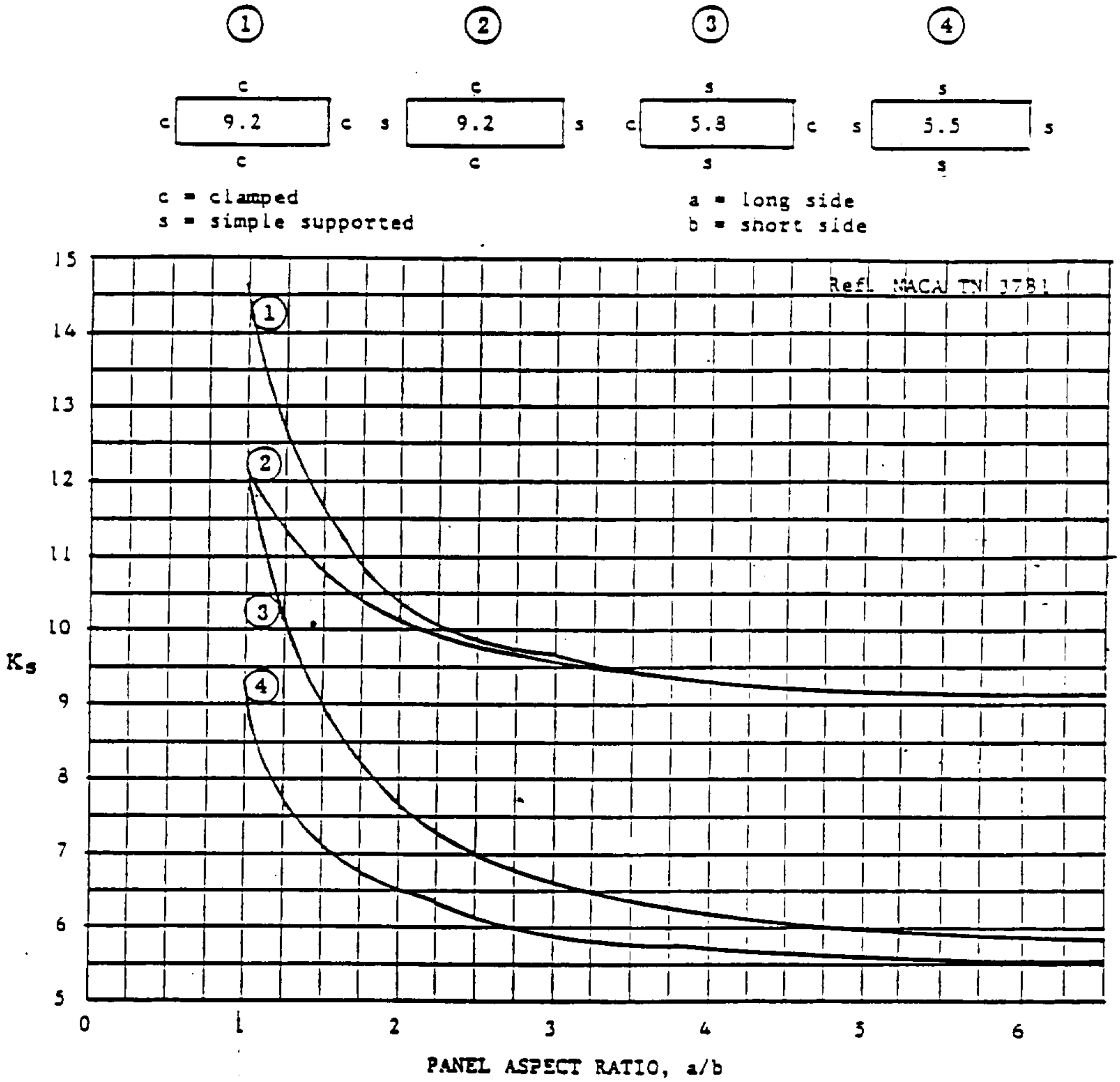

FIGURE 10.18 - SHEAR BUCKLING COEFFICIENT, K_s

Slotted Beam.—If the web of a beam is pierced by a hole or slot (Fig. 20), the stresses in the extreme fibers a and b at any section B are given by

$$s_a = \frac{M_A}{I/c} + \frac{V_A x[I_1/(I_1 + I_2)]}{(I/c)_1} \text{ (compression)}$$

$$s_b = \frac{M_A}{I/c} + \frac{V_A x[I_2/(I_1 + I_2)]}{(I/c)_2} \text{ (tension)}$$

Here M_A is the bending moment at A (mid-length of the slot), V_A is the vertical shear at A; I/c is the section modulus of the net beam section at B; I_1 and I_2 are the moments of inertia, and $(I/c)_1$ and $(I/c)_2$ the section moduli of the cross sections of parts 1 and 2 about their own central axes. M and V are positive or negative according to the usual convention, and x is positive when measured to the right.

The above formulas are derived by replacing all forces acting on the beam to the left of A by an equivalent couple M_A and shear V_A acting at A. The couple produces a bending stress given by the first term of the formula. The shear divides between parts 1 and 2 in proportion to their respective I's and produces in each part an additional bending stress given by the second term of the formula. The stress at any other point in the cross section can be found by similarly adding the stresses due to M_A and those due to this secondary bending caused by the shear. At the ends of the slot there is a stress concentration at the corners which is not here taken into account.

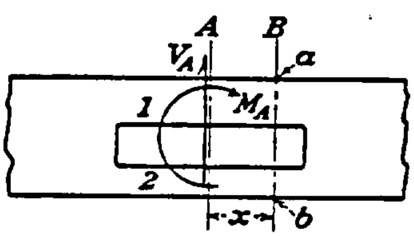

FIG. 20.

The above analysis applies also to a beam with multiple slots of equal length; all that is necessary is to modify the term in brackets so that the numerator is the I of the part in question and the denominator is the sum of the I's of all the parts 1, 2, 3, etc. The formulas can also be used for a rigid frame consisting of beams of equal length joined at their ends by rigid members; thus in Fig. 20 parts 1 and 2 might equally well be two separate beams joined at their ends by rigid crosspieces.

Data Source, Section 1.3 Reference 4

34.4 BEAMS ON ELASTIC FOUNDATIONS

Many airframe beams having partial support from transverse skin or web structure are analogous to a beam on an elastic support. The bending of frames attached to light skins can be analyzed in this fashion, and so can reinforcing rings around openings, which are subject to transverse bending.

The general case for a beam on an elastic foundation is shown in Fig. 34.4-1. It is assumed that the magnitude of the reaction offered by the foundation to the deflection of the beam is a variable quantity proportional to the deflection. Thus, the reaction per unit length of the beam is Ky, where y is deflection and K is a constant called the modulus of the foundation. K is, in effect, a "spring constant," i.e. if 1,000 lb distributed over 1 in. of length causes a deflection of 1 in., then K = 1,000 psi.

BEAM ON ELASTIC FOUNDATION

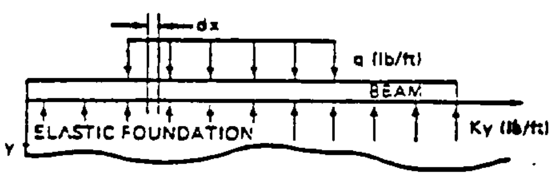

FIGURE 34.4-1

It is important to note that the elastic foundation is effective in both tension and compression, as though springs were attached to the beam. Also, the theory breaks down if either the beam or the foundation reaches a plastic condition.

The stiffness of the beam should be considerably larger than that of the foundation; otherwise factors such as contact stresses may decide the design and method of analysis.

The forces acting on the beam of Fig. 34.4-1 constitute a parallel system of forces to which two equations of equilibrium apply: $\Sigma F = 0$ and $\Sigma M = 0$. These two equations are not sufficient to determine the distribution of the reaction, and hence the problem is a statically indeterminate one. Therefore, as is usual in statically indeterminate beam problems, the equation of the elastic curve assumed by the beam is used for obtaining the necessary additional equations.

The equation of the elastic curve in familiar form is:

$$EI\frac{d^2y}{dx^2} = -M \quad \text{(where positive directions are as shown in Fig. 34.4-1)} \qquad (34\text{-}1)$$

From which

$$EI\frac{d^4y}{dx^4} = -Ky \quad \text{for the unloaded portion of the beam} \qquad (34\text{-}2)$$

or

$$EI\frac{d^4y}{dx^4} = q - Ky \quad \text{for the loaded portion of the beam} \qquad (34\text{-}3)$$

The solution of Eq. (34-2) is:

$$y = e^{\beta x}(A\cos\beta x + B\sin\beta x) + e^{-\beta x}(C\cos\beta x + D\sin\beta x) \qquad (34\text{-}4)$$

where A, B, C, and D are constants of integration determined by the boundary conditions of the problem and

$$\beta = \sqrt[4]{K/4EI} \qquad (34\text{-}5)$$

The solution of Eq. (34-4) for specific problems is facilitated by Figs. 34.4-2 and -3, which give values for the various functions of βx. Figure 34.4-4 gives solutions for certain beams on elastic foundations. See Refs. 4, 10, and 20 for a complete theoretical background.

169

SOME SOLUTIONS FOR BEAMS ON ELASTIC FOUNDATIONS

GEOMETRY	DEFLECTION y	MOMENT M	SHEAR Q
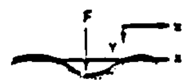 INFINITE BEAM, CONCENTRATED LOAD	$\frac{F\phi_1}{8\beta^3 EI}$	$\frac{F\phi_2}{4\beta}$	$-\frac{F\phi_3}{2}$
 INFINITE BEAM, APPLIED MOMENT	$\frac{M_o\phi_4}{4\beta^2 EI}$	$\frac{M_o\phi_3}{2}$	$-\frac{M_o\beta\phi_1}{2}$
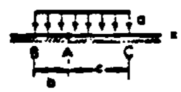 INFINITE BEAM, DISTRIBUTED LOAD	$y_A = \frac{q}{8\beta^4 EI}(2 - \phi_{3b} - \phi_{3c})$	$M_A = \frac{q}{4\beta^2}(\phi_{4b} + \phi_{4c})$	$Q_A = \frac{q}{4\beta}(\phi_{2b} - \phi_{2c})$
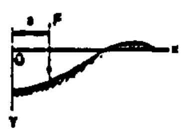 SEMI-INFINITE BEAM, CONCENTRATED LOAD	$\frac{F}{8\beta^3 EI}\left[(\phi_{2a} + 2\phi_{3a})\phi_{1x} - 2(\phi_{2a} + \phi_{3a})\phi_{4x} + \phi_{1(a-x)}\right]$ ▷1	$\frac{F}{4\beta}\left[\phi_{2x}(\phi_{2a} + 2\phi_{3a}) - 2\phi_{3x}(\phi_{2a} + \phi_{4a}) + \phi_{2(a-x)}\right]$	$-\frac{F}{2}\left[\phi_{3x}(\phi_{2a} + 2\phi_{3a}) - \phi_{1x}(\phi_{2a} + \phi_{3a}) \pm \phi_{3(a-x)}\right]$
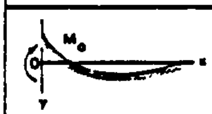 SEMI-INFINITE BEAM, APPLIED MOMENT	$-\frac{M_o\phi_2}{2\beta^2 EI}$	$M_o\phi_1$	$2M_o\beta\phi_4$

▷1 ϕ_{2a}, FOR EXAMPLE, IN CURVE 2, FIG. 34.4-2, $x = a$

Ref. 4

FIGURE 34.4-4

FUNCTIONS OF βx FOR COMPUTING STRESSES

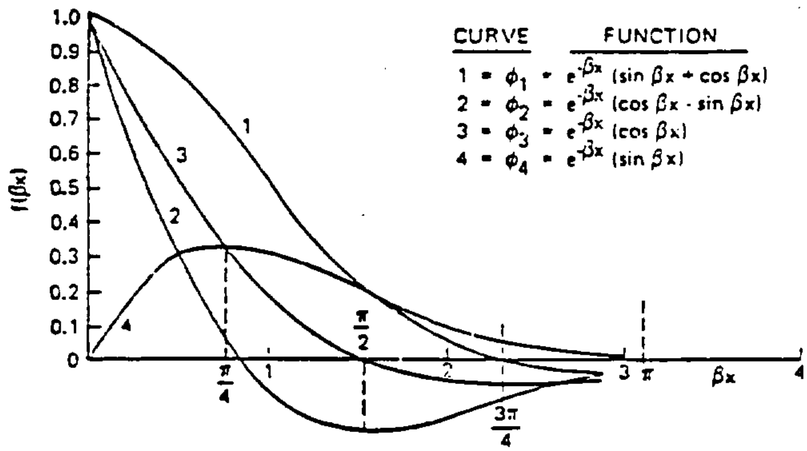

FIGURE 34.4-2

FUNCTIONS OF ϕ

βx	ϕ_1	ϕ_2	ϕ_3	ϕ_4	βx	ϕ_1	ϕ_2	ϕ_3	ϕ_4
0	1.0000	1.0000	1.0000	0	3.5	-0.0389	-0.0177	-0.0283	-0.0106
0.1	0.9907	0.8100	0.9003	0.0903	3.6	-0.0366	-0.0124	-0.0245	-0.0121
0.2	0.9651	0.6398	0.8024	0.1627	3.7	-0.0341	-0.0079	-0.0210	-0.0131
0.3	0.9267	0.4888	0.7077	0.2189	3.8	-0.0314	-0.0040	-0.0177	-0.0137
0.4	0.8784	0.3564	0.6174	0.2610	3.9	-0.0286	-0.0009	-0.0147	-0.0140
					4.0	-0.0258	0.0019	-0.0120	-0.0139
0.5	0.8231	0.2415	0.5323	0.2908	4.1	-0.0231	0.0040	-0.0095	-0.0136
0.6	0.7628	0.1431	0.4530	0.3099	4.2	-0.0204	0.0057	-0.0074	-0.0131
0.7	0.6997	0.0599	0.3798	0.3199	4.3	-0.0179	0.0070	-0.0054	-0.0125
0.8	0.6354	-0.0093	0.3131	0.3223	4.4	-0.0155	0.0079	-0.0038	-0.0117
0.9	0.5712	-0.0657	0.2527	0.3185					
					4.5	-0.0132	0.0085	-0.0023	-0.0108
1.0	0.5083	-0.1108	0.1988	0.3096	4.6	-0.0111	0.0089	-0.0011	-0.0100
1.1	0.4476	-0.1457	0.1510	0.2967	4.7	-0.0092	0.0090	0.0001	-0.0091
1.2	0.3899	-0.1716	0.1091	0.2807	4.8	-0.0075	0.0089	0.0007	-0.0082
1.3	0.3355	-0.1897	0.0729	0.2626	4.9	-0.0059	0.0087	0.0014	-0.0073
1.4	0.2845	-0.2011	0.0419	0.2430					
					5.0	-0.0046	0.0084	0.0019	-0.0065
1.5	0.2384	-0.2068	0.0158	0.2226	5.1	-0.0033	0.0080	0.0023	-0.0057
1.6	0.1959	-0.2077	-0.0059	0.2018	5.2	-0.0023	0.0075	0.0026	-0.0049
1.7	0.1576	-0.2047	-0.0235	0.1812	5.3	-0.0014	0.0069	0.0028	-0.0042
1.8	0.1234	-0.1985	-0.0376	0.1610	5.4	-0.0006	0.0064	0.0029	-0.0035
1.9	0.0932	-0.1899	-0.0484	0.1415					
					5.5	0.0000	0.0058	0.0029	-0.0029
2.0	0.0667	-0.1794	-0.0563	0.1230	5.6	0.0005	0.0052	0.0029	-0.0023
2.1	0.0439	-0.1675	-0.0618	0.1057	5.7	0.0010	0.0046	0.0028	-0.0018
2.2	0.0244	-0.1548	-0.0652	0.0895	5.8	0.0013	0.0041	0.0027	-0.0014
2.3	0.0080	-0.1416	-0.0668	0.0748	5.9	0.0015	0.0036	0.0026	-0.0010
2.4	-0.0056	-0.1282	-0.0669	0.0613					
					6.0	0.0017	0.0031	0.0024	-0.0007
2.5	-0.0166	-0.1149	-0.0658	0.0492	6.1	0.0018	0.0026	0.0022	-0.0004
2.6	-0.0254	-0.1019	-0.0636	0.0383	6.2	0.0019	0.0022	0.0020	-0.0002
2.7	-0.0320	-0.0895	-0.0608	0.0287	6.3	0.0019	0.0018	0.0018	0.0001
2.8	-0.0369	-0.0777	-0.0573	0.0204	6.4	0.0018	0.0015	0.0017	0.0003
2.9	-0.0403	-0.0666	-0.0534	0.0132					
					6.5	0.0015	0.0012	0.0015	0.0004
3.0	-0.0423	-0.0563	-0.0493	0.0071	6.6	0.0017	0.0009	0.0013	0.0005
3.1	-0.0431	-0.0469	-0.0450	0.0019	6.7	0.0016	0.0006	0.0011	0.0006
3.2	-0.0431	-0.0383	-0.0407	-0.0024	6.8	0.0015	0.0004	0.0010	0.0005
3.3	-0.0422	-0.0306	-0.0364	-0.0058	6.9	0.0014	0.0002	0.0008	0.0006
3.4	-0.0408	-0.0237	-0.0323	-0.0085	7.0	0.0013	0.0001	0.0007	0.0006

FIGURE 34.4-3

171

SECTION 4.10

BEAMS ON ELASTIC FOUNDATION

REFERENCES:

BOEING STRESS MANUAL

4. J. H. FAUPEL, ENGINEERING DESIGN, WILEY AND SONS, NEW YORK 1964

10. F. B. SEELY AND J. O. SMITH, ADVANCED MECHANICS OF MATERIALS, 2ND ED., WILEY AND SONS, NEW YORK 1957

20. S. TIMOSHENKO, STRENGTH OF MATERIALS, PART II - AVANCED THEORY AND PROBLEMS, 3RD ED. VAN NOSTRAND, NEW YORK, FEB. 1959.

HETENYI, M., BEAMS ON ELASTIC FOUNDATION, THE UNIVERSITY OF MICHIGAN PRESS, ANN ARBOR MICHIGAN 1958.

SECTION 5.0

COLUMNS

COLUMN THEORY, CHARTS AND TABLES FOR COLUMNS AND BEAM COLUMNS ARE PRESENTED.

		PAGES
5.1	THEORY	5.1.1
5.2	CONSTANT CROSS SECTION COLUMNS	5.2.1
5.3	VARIABLE CROSS SECTION COLUMNS	5.3.1
5.4	CRIPPLING OF SECTIONS	5.4.1
5.5	BEAM COLUMNS	5.5.1
5.6	CONTINUOUS BEAM COLUMS	5.6.14
5.7	TORSIONAL INSTABILITY	5.7.1
5.8	COLUMN ALLOWABLES	5.8.1

Data Source, Section 1.3 Reference 1

5.0.0
COLUMNS
5.1.0
Theory
5.1.1
Definition

A column is a structural member, either straight or having a small initial curvature, whose cross-sectional dimensions are short with respect to its length, and that is subjected to an axial compressive force only. Hence, columns are under a uniaxial stress.

5.1.2
Failure

A column is considered to have failed when it stops fulfilling the function for which it was designed. Contrary to most structural members, failure of a column does not necessarily imply yielding of the material nor any permanent damage in the member.

Column failure is more related to the stability of the member than it is to the stress or the cross-sectional area of the column; however, the geometry of the member is of primary importance in predicting the type of failure of the member. The geometrical characteristics of a column are summarized in a parameter known as the "slenderness ratio," which is the ratio between the length of the column (L), and the minimum radius of gyration (k) of its cross section, where

$$k = \sqrt{\frac{I_{min}}{A}} \quad \dots\dots\dots\dots\dots \quad (1)$$

I_{min} = Minimum moment of inertia of the section

A = Cross-sectional area.

In general, by determining the slenderness ratio of a column, it is possible to predict the type of failure that the column will experience.

The four modes of failure are represented graphically in Fig. 5.1.2-1 as a function of the slenderness ratio.

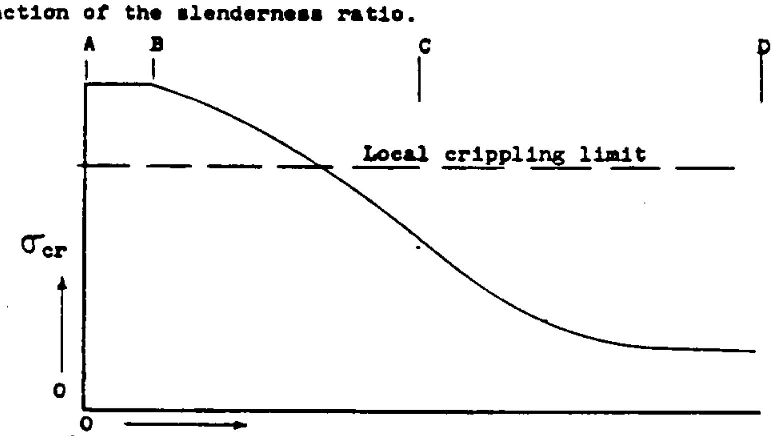

Slenderness Ratio (L/k)

Fig. 5.1.2-1

Zone:

(AB) Block Compression (P/A)

(BC) Primary or general failure in the short column range.
(Use the tangent modulus in Euler's equation.)

(CD) Primary or general failure in the long column range.
(Use Euler's equation.)

--- Secondary or local failure (Use method in Sect. 5.4.0).

Block Compression

A short compression member for which L/k is so small as to make the effect of lateral deflection negligible is called a "compression block." The maximum axial load which a compression block can carry is determined solely by the strength of the material. The member is considered to have failed when its average stress reaches the compression yield strength of the material. Point "B" is usually located at an L/k value from 20 to 30 depending upon the material properties of the column.

Short Columns (Inelastic Buckling)

A column with an L/k value so small that the average stress on the cross section reaches the elastic limit before the critical stress is reached is called a short column. After small lateral deflections occur, the column will reach the conditions of instability associated with total collapse. In other words, inelastic strain occurs and is followed by instability and collapse after some increase in load. The dividing point between long and short columns is marked by the critical slenderness ratio (Point "C", Fig. 5.1.2-1). This point can be located by plotting the elastic limit on the curve in Fig. 5.1.2-1. The critical slenderness ratio is usually located at an L/k value between 50 and 160 depending upon the material properties of the column. The critical buckling load of a short column can be calculated by substituting "E_t" for "E" in Euler's equation.

Note: For most materials the elastic limit is considerably lower than the yield strength.

Long Column (Elastic Buckling)

A slender column will fail by buckling before the stress exceeds the elastic limit of the material. This type of column fails through lack of stiffness instead of a lack of strength. It should be noted that if a column is perfectly straight, the load truly axial, and the material perfectly homogeneous, the column will remain straight under any value of the load. If the column is slightly deflected laterally, the critical buckling load is that load which will hold the column in the slightly bent position. The significant characteristic of buckling is that the elastic deflections and stresses are not proportional to the loads as buckling takes place. The slenderness ratio for long columns will be greater than the critical slenderness ratio (Point "C", Fig. 5.1.2.-1). The critical buckling load can be obtained by the use of Euler's formula.

Local Crippling or Secondary Failure

This type of failure is defined as any type of failure in which the cross sections are distorted in their own planes, but not translated or rotated. This type of failure is limited to thin walled sections. Since the buckling phenomena seem to be identical, "Local Failure," and "Crippling" will be used as synonymous terms.

Note: The position of the dashed line, Local Crippling Limit, in Fig. 5.1.2.-1 depends upon the geometrical characteristics of the column being analyzed.

Data Source, Section 1.3 Reference 1

5.2.0

Constant Cross-Section Columns

Long Columns

The critical, or buckling, load (P_{cr}) of a constant cross-section column can be shown in terms of the well-known Euler's equation as follows:

$$P_{cr} = \frac{\pi^2 E\, I}{L^2} \quad \ldots\ldots\ldots\ldots\ldots \quad (1)$$

where (E) is the Modulus of Elasticity of the material, (L) is the length of the column, and (I) is the moment of inertia of the column cross-section.

It is often more convenient to work with a buckling stress, ($\sigma_{cr} = P_{cr}/A$). This may be obtained by introducing the radius of gyration of the cross-sectional area ($k = \sqrt{I/A}$) in equation (1).

$$\sigma_{cr} = \frac{\pi^2 E}{(L/k)^2} \quad \text{(Elastic buckling)} \quad (2)$$

Short Columns

In the derivation of equation (2), it was assumed that the stress-strain curve for the material was a straight line, and, hence, that the stiffness (E) (Modulus of Elasticity) of the material remained constant as the load (P) increased to the value (P_E). This condition limits the applicability of Euler's equation to elastic buckling, and to a column having a slenderness ratio (L/k) above a certain limiting value, depending on the properties of the materials. When (L/k) has a value such that the stress (P_E/A) is equal to the elastic limit, any increase in (P_E) will cause a rapid decrease in the stiffness from the value of (E) to E_t (which is the slope to the stress-strain diagram at the inelastic stress caused by increasing P_E slightly). This decrease in stiffness permits the column to bend and to quickly acquire a large deflection with a small increase in load. This failure is called inelastic buckling and is represented by the following equation:

$$\sigma_{cr} = \frac{\pi^2 E_T}{(L/k)^2} \quad \text{(Inelastic buckling)} \quad (3)$$

where (E_T) is obtained from the stress strain curve of the material.

The solution of the tangent-modulus equation (3) for a column of a given material and dimensions involves a trial-and-error process, for the reason that the value (E_T) is not constant. Therefore, values of the tangent modulus (E_T) must be known for every value of the stress above the elastic limit. Corresponding values of (σ) and (E_T) are found from an ordinary stress-strain curve and are usually given in the form of a curve.

End Fixity

In the foregoing equations it has been assumed that the column is hinged at both ends so that it can rotate freely. Such a condition occasionally exists in an aircraft structure where a member is connected by a single bolt at each end. In most cases, however, compression members are connected in such a way that they are restrained against rotation at the ends. If a compressive member is rigidly fixed against rotation at both

ends, the deflection curve for elastic buckling will have the shape shown in Fig. 5.2.0-1-(b). At the quarter points of the fixed column there will be points of reverse curvature, or points of contraflexure. At points of contraflexure there is no curvature and hence no bending moment. The

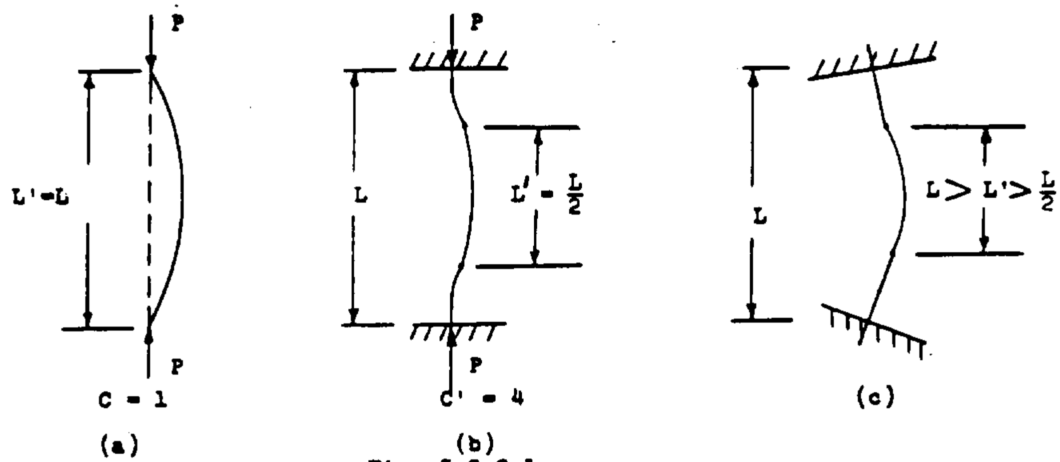

Fig. 5.2.0-1

portion of the column between points of contraflexure may therefore be treated as a pined-end column. The length (L') between the points of contraflexure is used in place of (L) in the previous column equations, (2) and (3), and the slenderness ratio is defined as (L'/k). An end-fixity term (C) is often used and is defined in the following equations:

$$\sigma_{cr} = \frac{\pi^2 E}{(L'/k)^2} = \frac{C\pi^2 E}{(L/k)^2} \quad \ldots\ldots\ldots\ldots (4)$$

$$\text{or} \quad L' = L/\sqrt{C} \quad \ldots\ldots\ldots\ldots\ldots (5)$$

For the fixed end condition of Fig. 5.2.0-1-(b), (L' = L/2), and (C = 4), the fixed-ended column will therefore resist four times the load of a similar pin-ended column if both are in the long-column range. This same relation does not hold in the short-column range, because the value of (E_T) in equation (3) is smaller for the smaller values of (L'). This fact is obvious because it can be seen that a reduction of (L'/k) has a much smaller effect on (σ_{cr}) in the short column range than it has in the long -column range.

Moct practical columns have end conditions somewhere between hinged and fixed ends, as shown in Fig. 5.2.0-1-(c). The ends are rigidly attached to a structure which deflects and permits the ends to rotate slightly. The true end-fixity conditions can seldom be determined exactly, and conservative assumptions must be made. Fortunately, short columns are usually used and the effect of end fixity on the allowable compressive stress is much smaller than it would be for long columns. Some common end-fixity conditions are given in Figs. 5.2.0.1 through 5.2.0.4.

LONG COLUMNS END FIXITY

Type of Fixity	C	$1/\sqrt{c}$	Type of Fixity	C
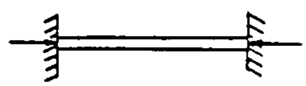	4	.50	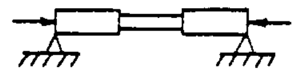	1.00
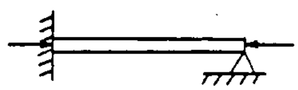	2.05	.70	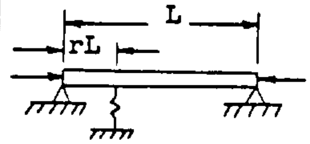	Fig. 5.2.0.3
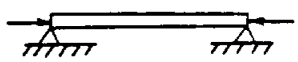	1.00	1.00	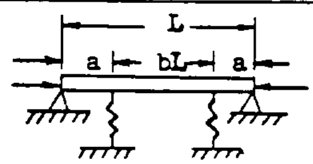	Fig. 5.2.0.4
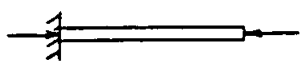	.25	2.00	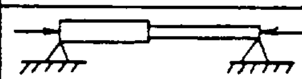 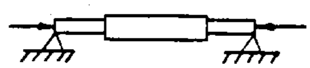	Sect. 5.3.0 Sect. 5.3.0
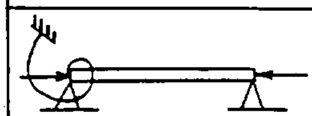	Fig. 5.2.0.2		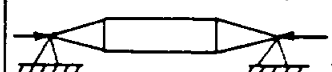	Sect. 5.3.0
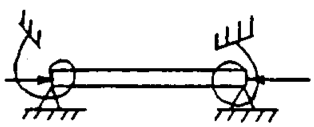 Equal End Restraint	Fig. 5.2.0.2			

L_2/L_1	.25	.50	1.0	4.0	(C_2=1.00
C_1	.059	.095	.138	.21	Applies to L_2)

Fig. 5.2.0.1

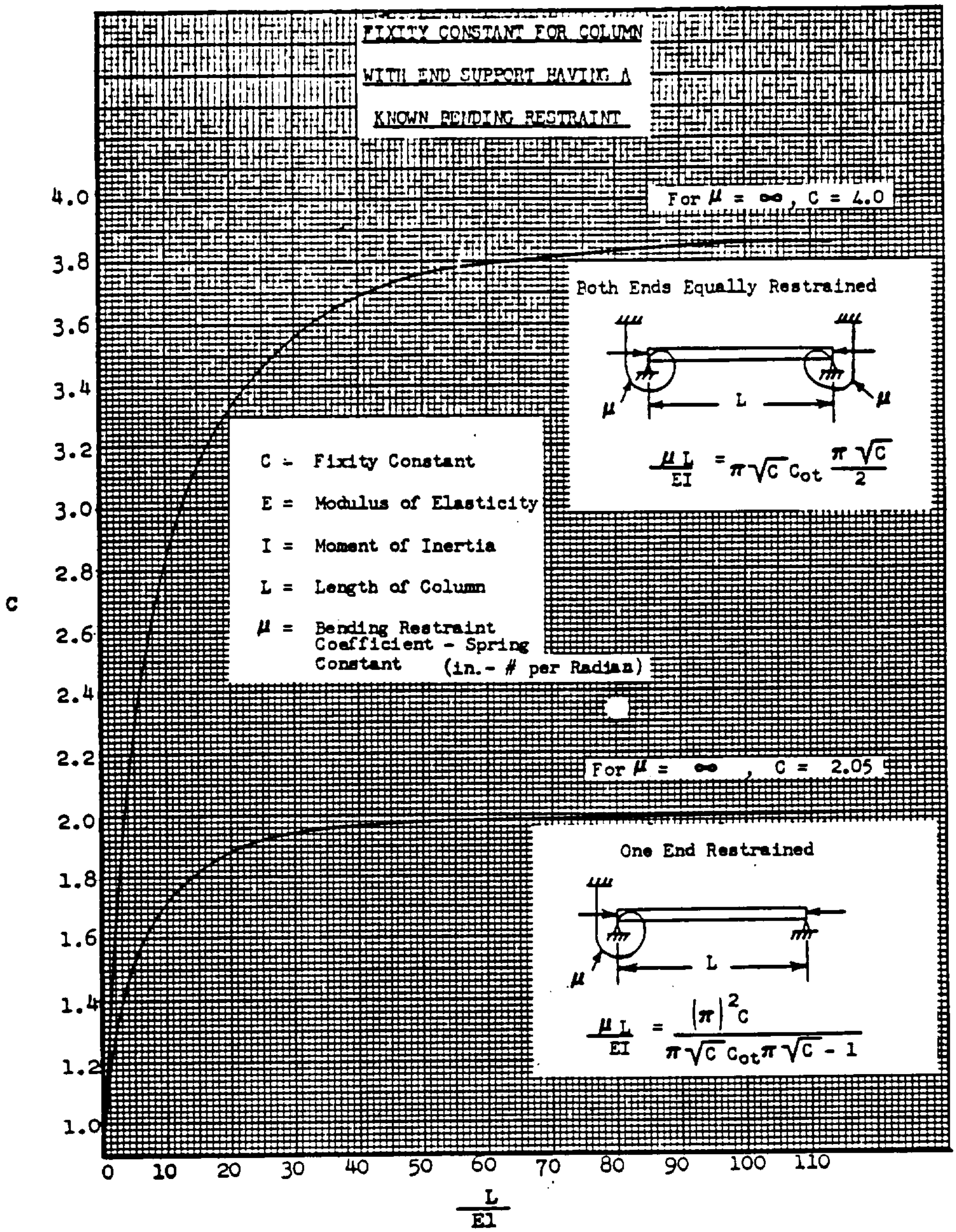
FIXITY CONSTANT FOR COLUMN
WITH END SUPPORT HAVING A
KNOWN BENDING RESTRAINT
For μ = ∞, C = 4.0
Both Ends Equally Restrained
L
μ
$\frac{\mu L}{EI} = \pi\sqrt{C}\,\mathrm{Cot}\,\frac{\pi\sqrt{C}}{2}$
C - Fixity Constant
E = Modulus of Elasticity
I = Moment of Inertia
L = Length of Column
μ = Bending Restraint Coefficient - Spring Constant (in.- # per Radian)
For μ = ∞, C = 2.05
One End Restrained
L
μ
$\frac{\mu L}{EI} = \frac{(\pi)^2 C}{\pi\sqrt{C}\,\mathrm{Cot}\,\pi\sqrt{C} - 1}$
C
4.0
3.8
3.6
3.4
3.2
3.0
2.8
2.6
2.4
2.2
2.0
1.8
1.6
1.4
1.2
1.0
0
10
20
30
40
50
60
70
80
90
100
110
$\frac{L}{EI}$

Fig. 5.2.0.2

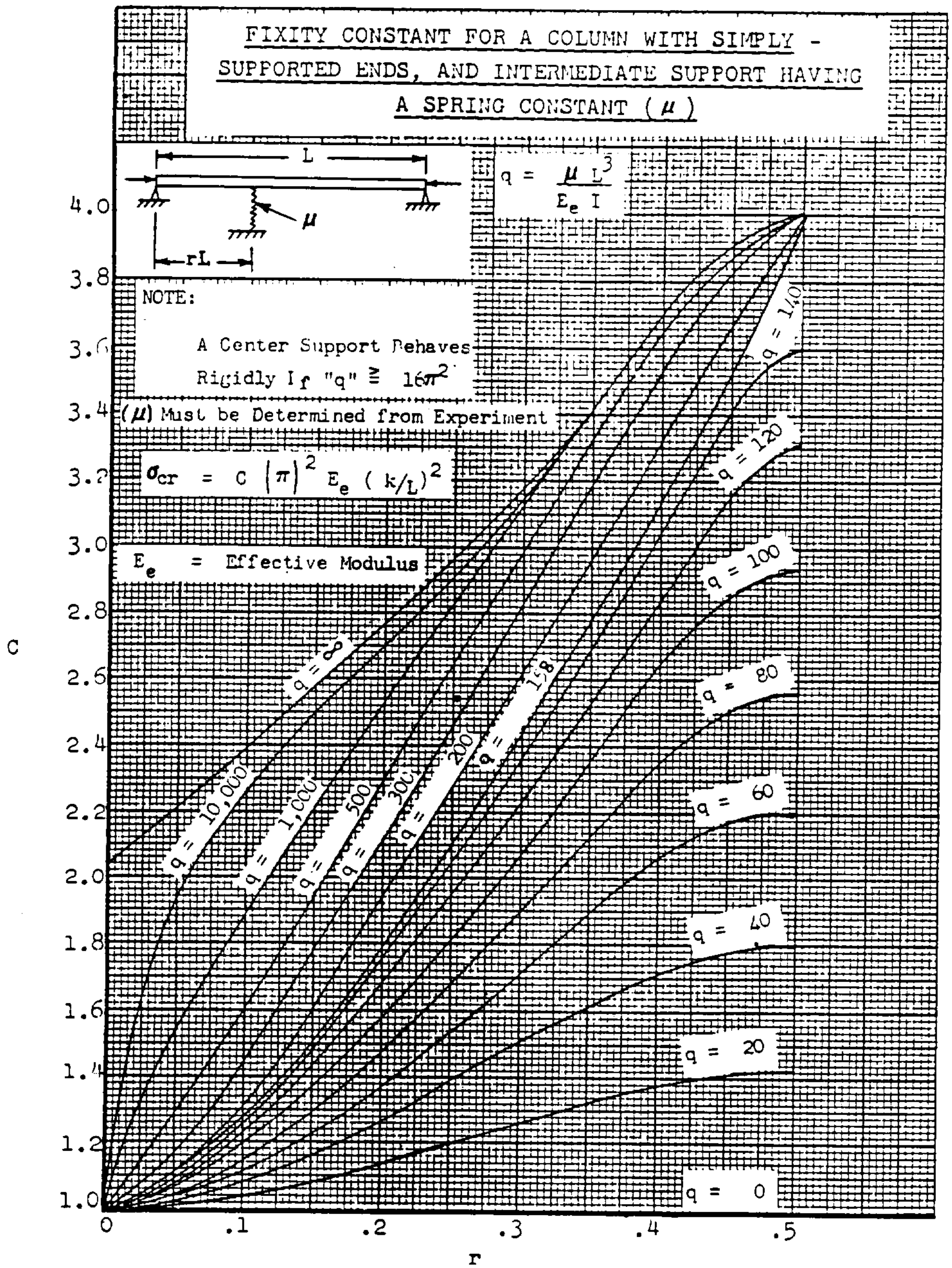
FIXITY CONSTANT FOR A COLUMN WITH SIMPLY - SUPPORTED ENDS, AND INTERMEDIATE SUPPORT HAVING A SPRING CONSTANT (μ)
L
μ
rL
q = μ L^3 / E_e I
NOTE:
A Center Support Behaves Rigidly If "q" ≧ 16π^2
(μ) Must be Determined from Experiment
σcr = C (π)^2 E_e (k/L)^2
E_e = Effective Modulus
q = ∞
q = 10,000
q = 1,000
q = 500
q = 300
q = 200
q = 158
q = 140
q = 120
q = 100
q = 80
q = 60
q = 40
q = 20
q = 0
C
4.0
3.8
3.6
3.4
3.2
3.0
2.8
2.6
2.4
2.2
2.0
1.8
1.6
1.4
1.2
1.0
0
.1
.2
.3
.4
.5
r

Fig. 5.2.0.3

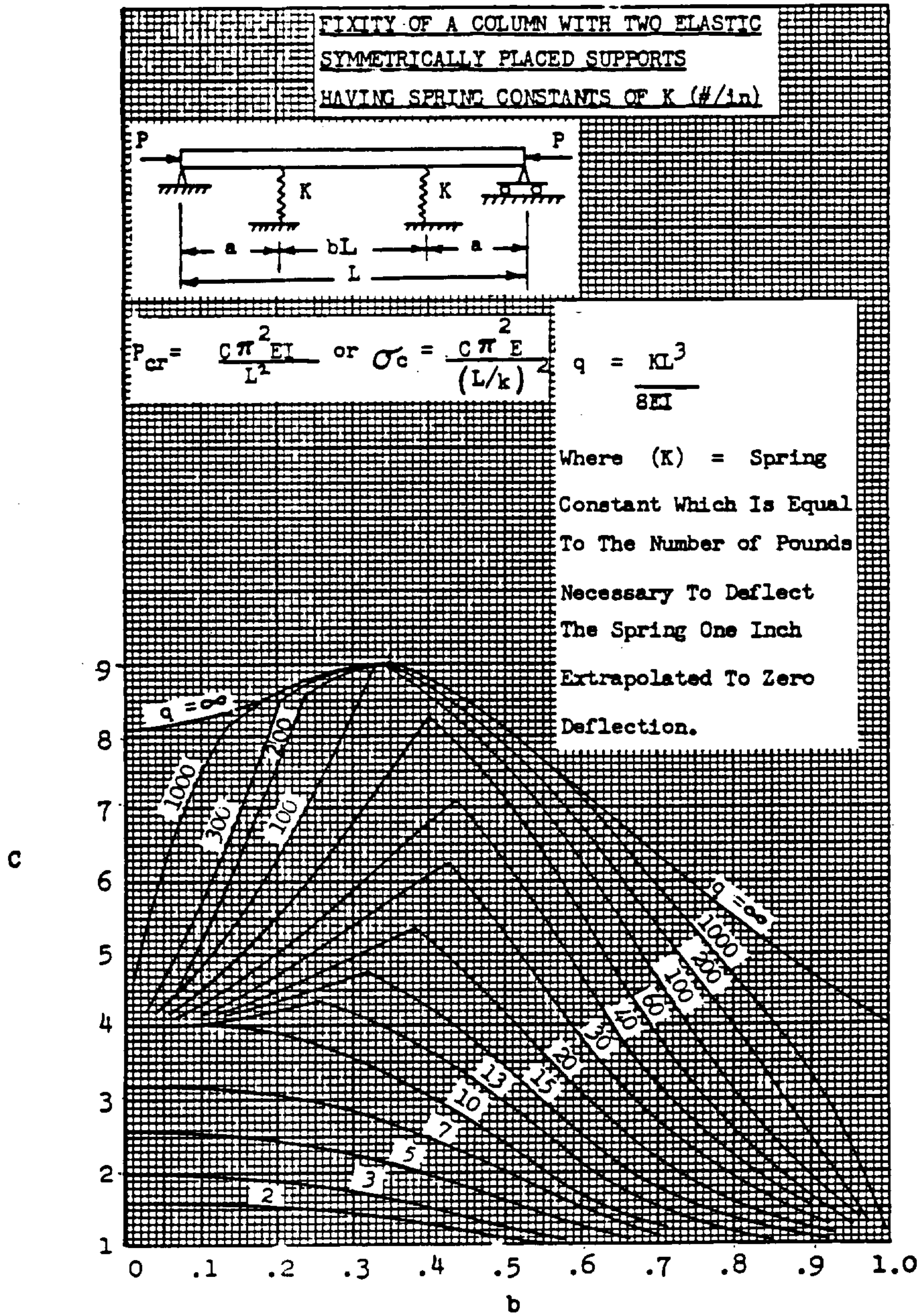
FIXITY OF A COLUMN WITH TWO ELASTIC
SYMMETRICALLY PLACED SUPPORTS
HAVING SPRING CONSTANTS OF K (#/in)
P
P
K
K
a
bL
a
L
$P_{cr} = \frac{C\pi^2 EI}{L^2}$ or $\sigma_c = \frac{C\pi^2 E}{(L/k)^2}$
$q = \frac{KL^3}{8EI}$
Where (K) = Spring Constant Which Is Equal To The Number of Pounds Necessary To Deflect The Spring One Inch Extrapolated To Zero Deflection.
q = ∞
1000
300
200
100
q = ∞
1000
200
100
60
40
30
20
15
13
10
7
5
3
2
C
9
8
7
6
5
4
3
2
1
0
.1
.2
.3
.4
.5
.6
.7
.8
.9
1.0
b

Fig. 5.2.0.4

Data Source, Section 1.3 Reference 1

5.3.0

Variable Cross-Section Columns

The condition under which the conventional modified Euler critical column load formula

$$P_{cr} = \frac{C\pi^2 EI}{L^2} \quad \ldots\ldots\ldots\ldots\ldots \quad (1)$$

is valid, is for a straight column with constant area and bending rigidity along its length loaded in edge compression. The determination of the Euler load becomes more difficult when the bending rigidity varies along the length of the column. This section gives appropriate column buckling coefficient curves and formulas for computing the Euler loads for varying cross-section columns.

Stepped and Uniformly Tapered Columns

The general equation for the critical buckling load of variable cross-section columns is

$$P_{cr} = \frac{mEI}{L^2} \quad \ldots\ldots\ldots\ldots\ldots \quad (2)$$

where (m), the column buckling coefficient, is a function of the column geometry, bending rigidity, and end restraint.

Values of (m) for the stepped columns shown in Table 5.3.0 are given in Figures 5.3.0.1 through 5.3.0.5. The values of (m) for tapered columns are shown in Figures 5.3.0.6 thru 5.5.0.19. (Note small "ℓ" from Fig. 5.3.0 through Fig. 5.3.0.19 will be used as large "L" in the given equations.)

The following two examples are typical for calculating the critical buckling loads for a stepped column and a tapered column.

Example No. 1:

Given:

$E_1 = 10.3 \times 10^6$ (75ST6 Aluminum)

$I_1 = .282$ in.^{4}

$E_2 = 29 \times 10^6$ (4130-150 HT Steel)

$I_2 = 2.60$ in.^{4}

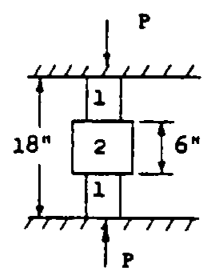

(1) Stepped Column

Find Critical Buckling Load (P_{cr})

From Fig. 5.3.0.4 :

$a/L = 6/18 = 1/3$

$$\frac{E_1I_1}{E_2E_2} = \frac{10.3 \times 2.82 \times 10^6}{29 \times 2.6 \times 10^6} = .0385$$

$m = 3.6$

$$P_{cr} = \frac{mE_2I_2}{L^2} = \frac{3.6 \times 29 \times 10^6}{(18)^2} = 840{,}000 \text{ lbs.}$$

Example No. 2:

Given:

$E_1 = 29 \times 10^6$ (4130-150 HT Steel)

$I_1 = .01067$ in.^{4}

$E_2 = 29 \times 10^6$ (4130-150 HT Steel)

$I_2 = .0853$ in.^{4}

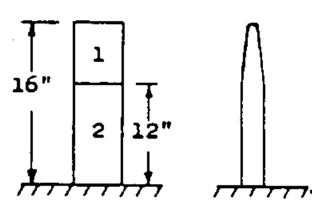

(2) Tapered Column

Consider A Transverse Axis Of Symmetry

From Fig. 5.3.0.12

$$a/L = 12/16 = .75 \qquad \frac{E_1 I_1}{E_2 I_2} = \frac{.01067}{.0853} = .126$$

$$m = 9.65$$

$$P_{cr} = \frac{m E_2 I_2}{4L^2} = \frac{9.65 \times 29 \times 10^6 \times .0853}{4(16)^2} = 23{,}300 \text{ lbs.}$$

Note: The accuracy of equation (2) is decreased for columns whose critical stresses are in the plastic range.

TABLE 5.3.0 CATALOGUE OF CASES OF COLUMNS OF VARIABLE CROSS-SECTION

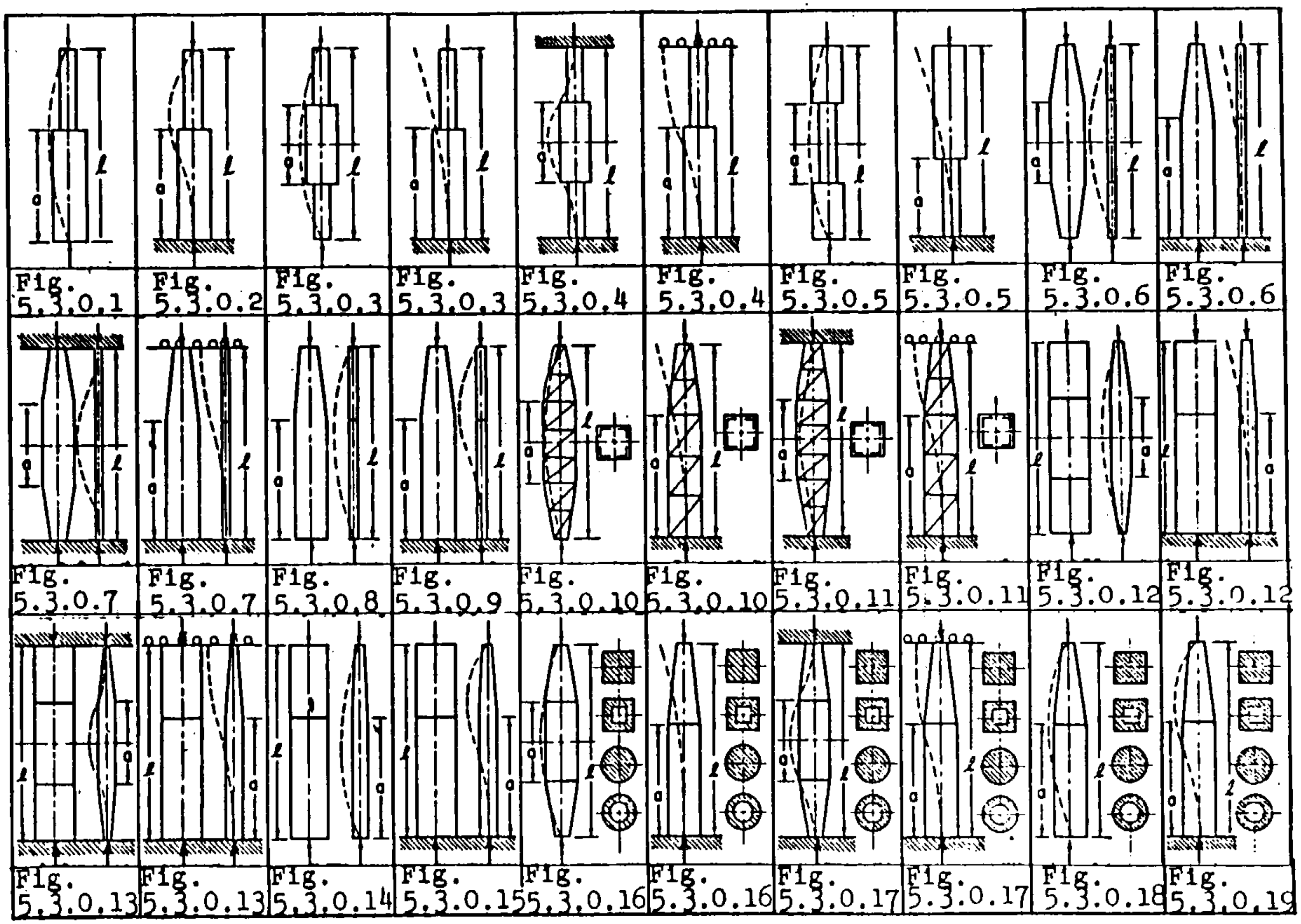

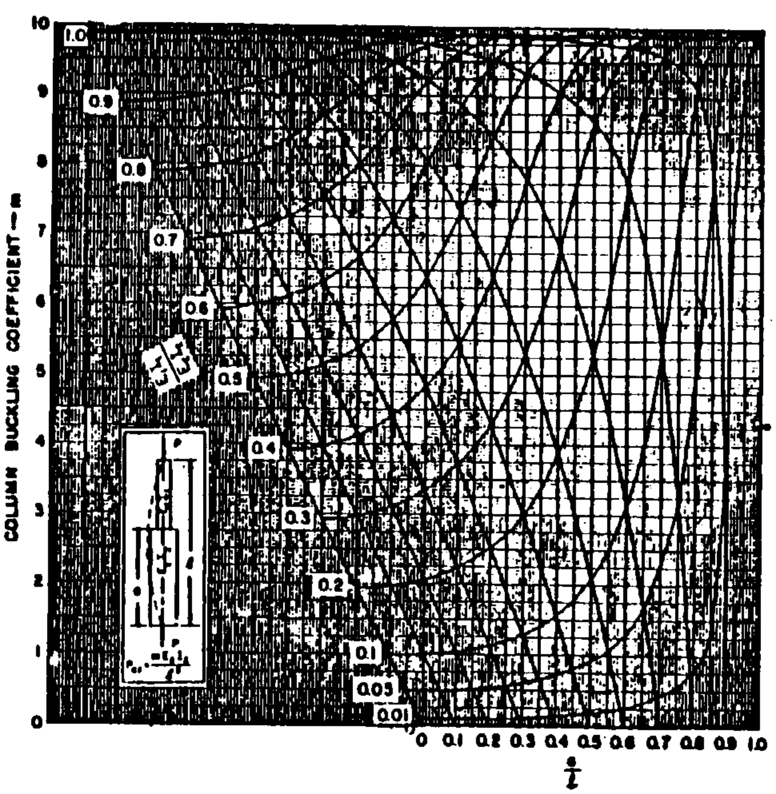

3tepped Column With Both Ends Pinned And No Transverse Axis Of Symmetry

Fig. 5.3.0.1

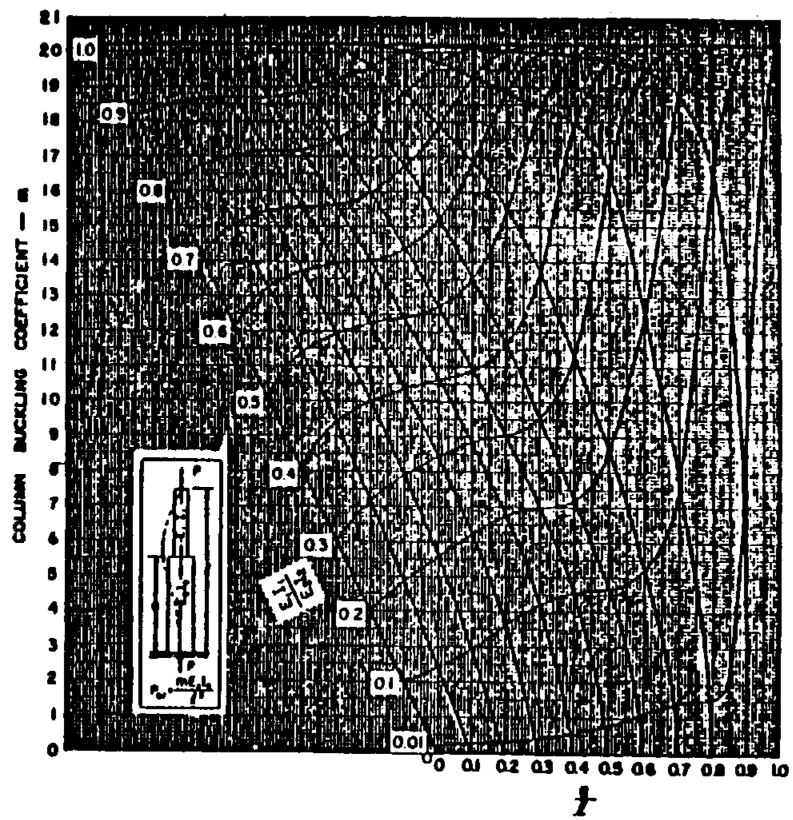

Stepped Column With One End Pinned And The Other Fixed And No Transverse Axis Of Symmetry

Fig. 5.3.0.2

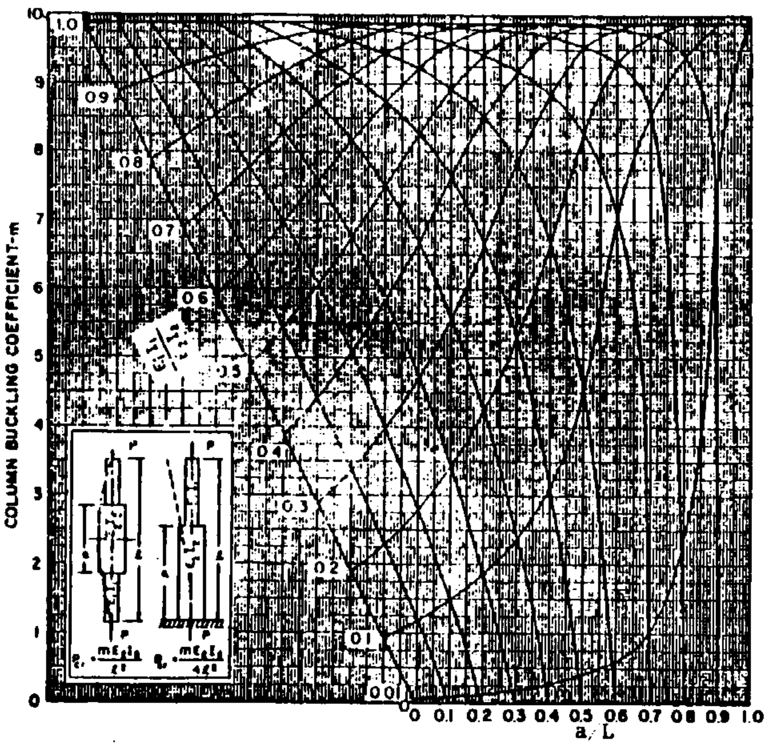

Stepped Column With Smaller Moment Of
Inertia At Ends, Both Ends Pinned, And A
Transverse Axis Of Symmetry

Fig. 5.3.0.3

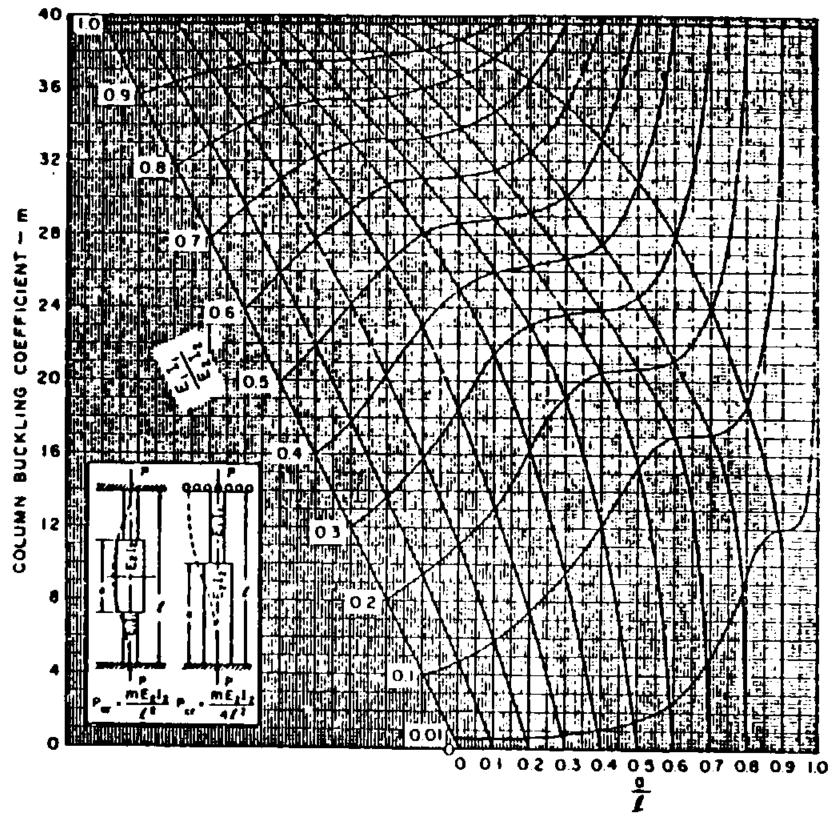

Stepped Column With Smaller Moment Of
Inertia At Ends, Both Ends Fixed, And
A Transverse Axis Of Symmetry

Fig. 5.3.0.4

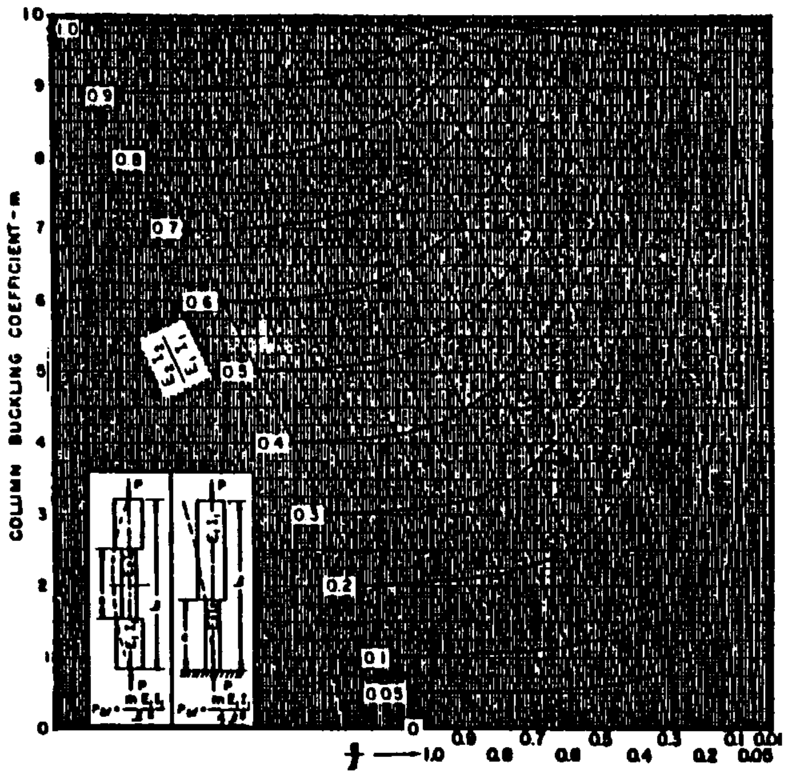

Stepped Column With Larger Moment Of
Inertia At Ends, Both Ends Pinned, And
A Transverse Axis Of Symmetry

Fig. 5.3.0.5

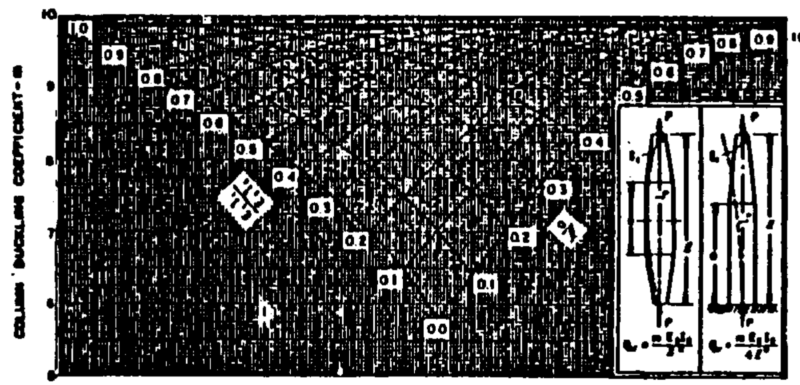

Moments Of Inertia For Ends Varying As The
First Power (N=1) With Both Ends Pinned And
A Transverse Axis Of Symmetry

Fig. 5.3.0.6

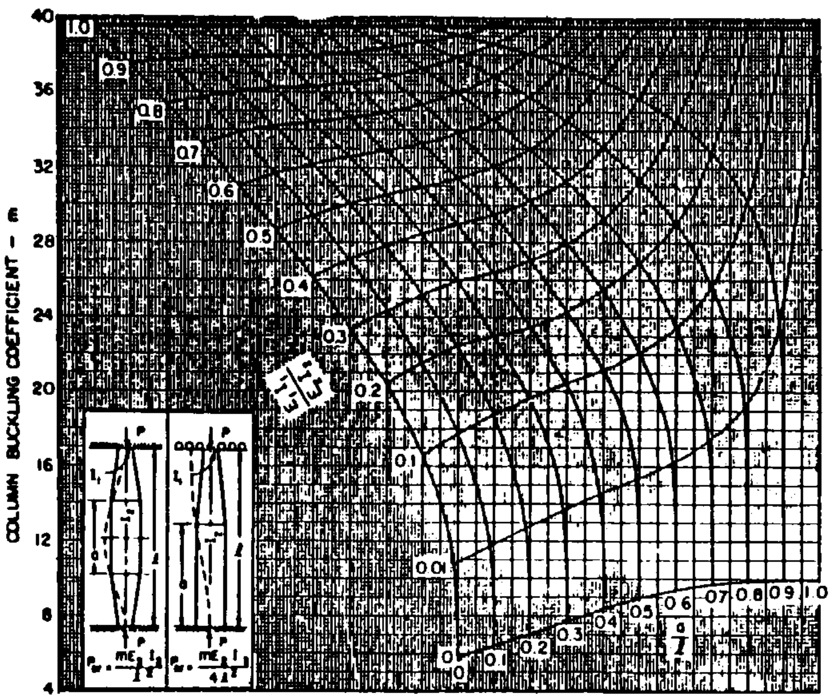

Moments Of Inertia For Ends Varying As
The First Power (N=1) With Both Ends
Fixed And A Transverse Axis Of Symmetry

Fig. 5.3.0.7

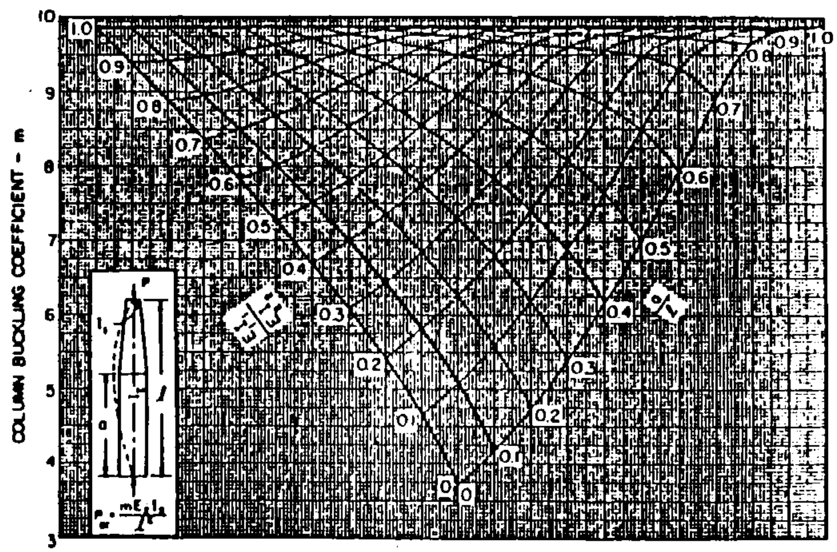

Moment Of Inertia For End Varying As
The First Power (N=1) With Both Ends Pinned
And No Transverse Axis Of Symmetry

Fig. 5.3.0.8

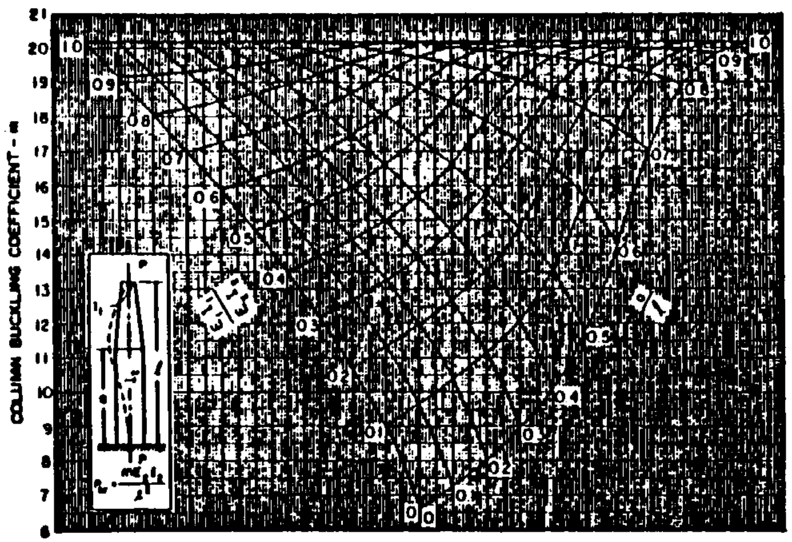

Moment Of Inertia For One End Varying As
The First Power (N=1) With One End Pinned And
The Other Fixed And No Transverse Axis Of Symmetry

Fig. 5.3.0.9

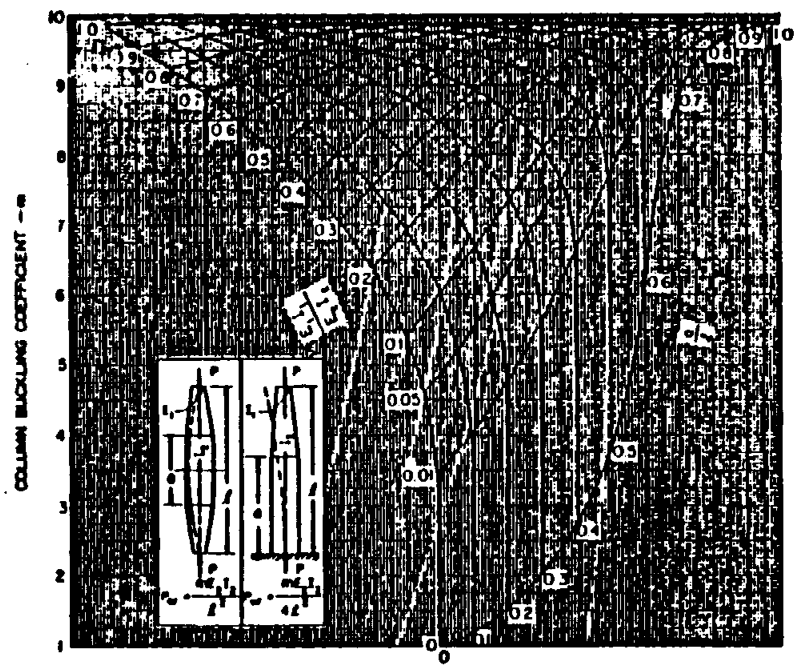

Moment Of Inektia For Ends Varying As
The Second Power (N=2) With Both Ends Pinned
And A Transverse Axis Of Symmetry

Fig. 5.3.0.10

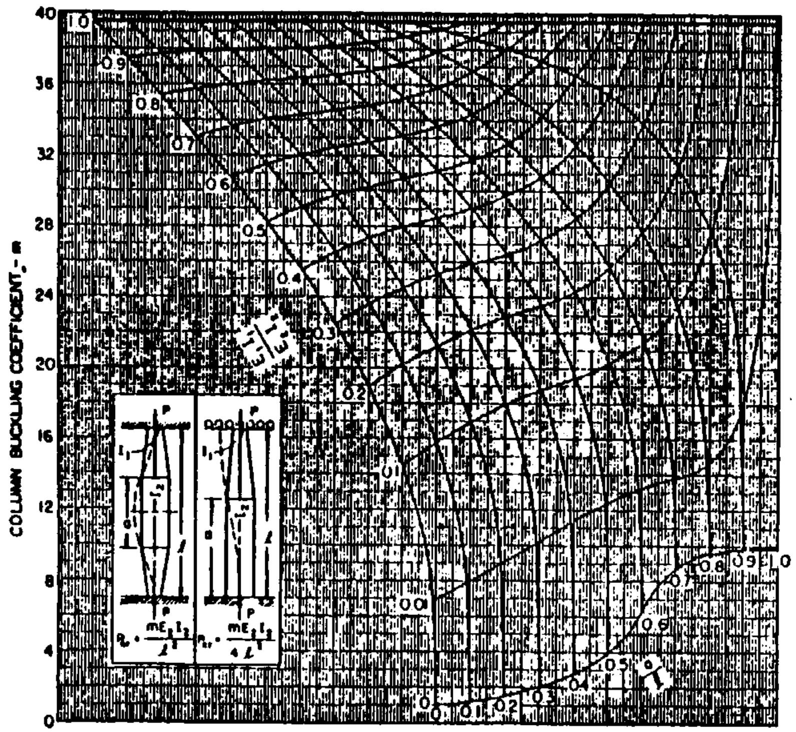

Moments Of Inertia For Ends Varying As
The Second Power (N=2) With Both Ends Fixed
And A Transverse Axis Of Symmetry

Fig. 5.3.0.11

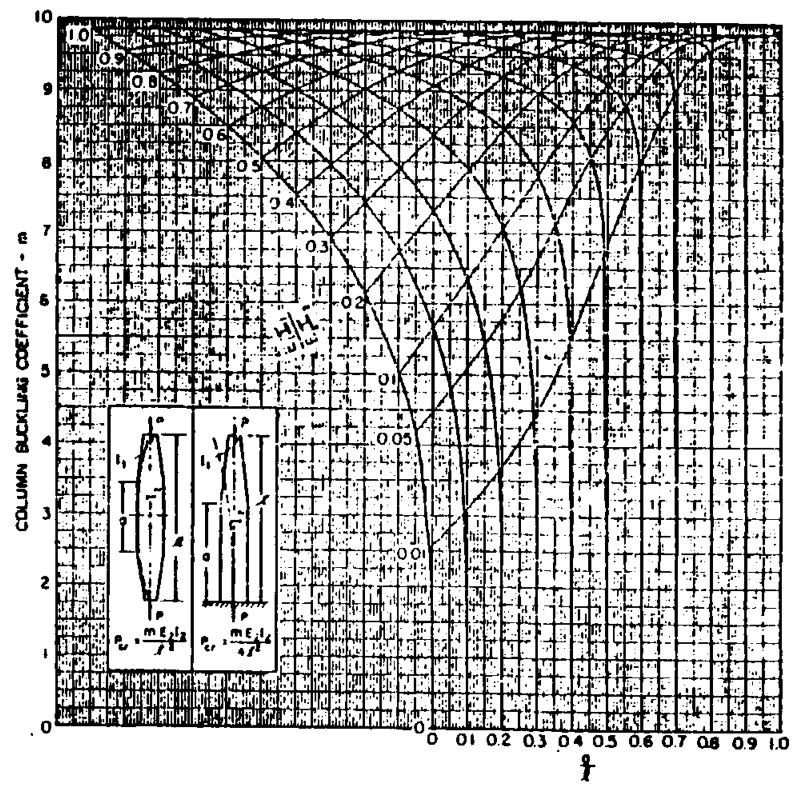

Moment Of Inertia For Ends Varying As The
Third Power (N=3) With Both Ends Pinned And
A Transverse Axis Of Symmetry

Fig. 5.3.0.12

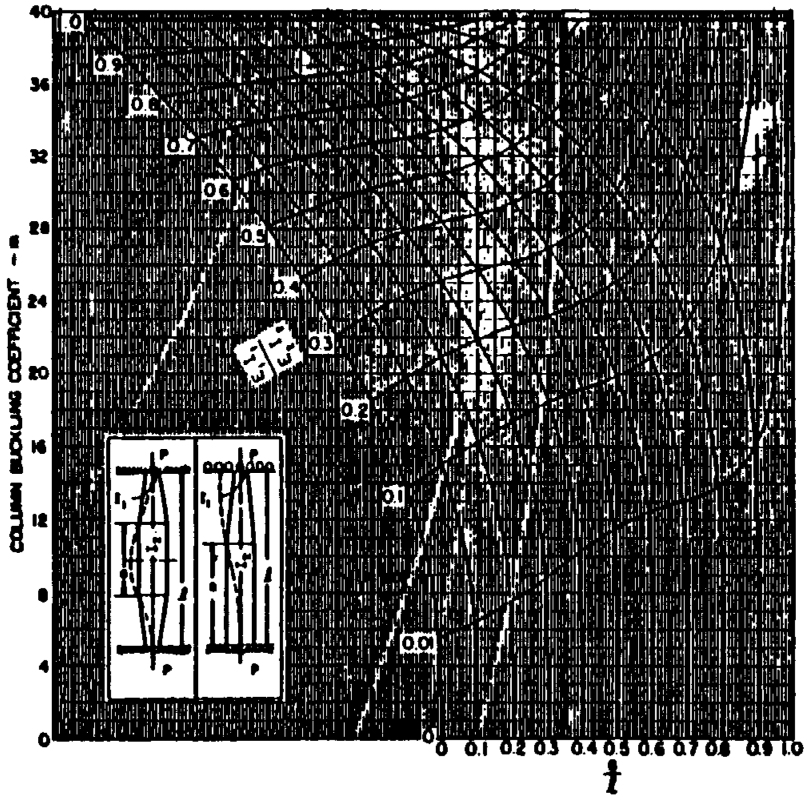

Moments Of Inertia For Ends Varying As The Third Power (N=3) With Both Ends Fixed And A Transverse Axis Of Symmetry

Fig. 5.3.0.13

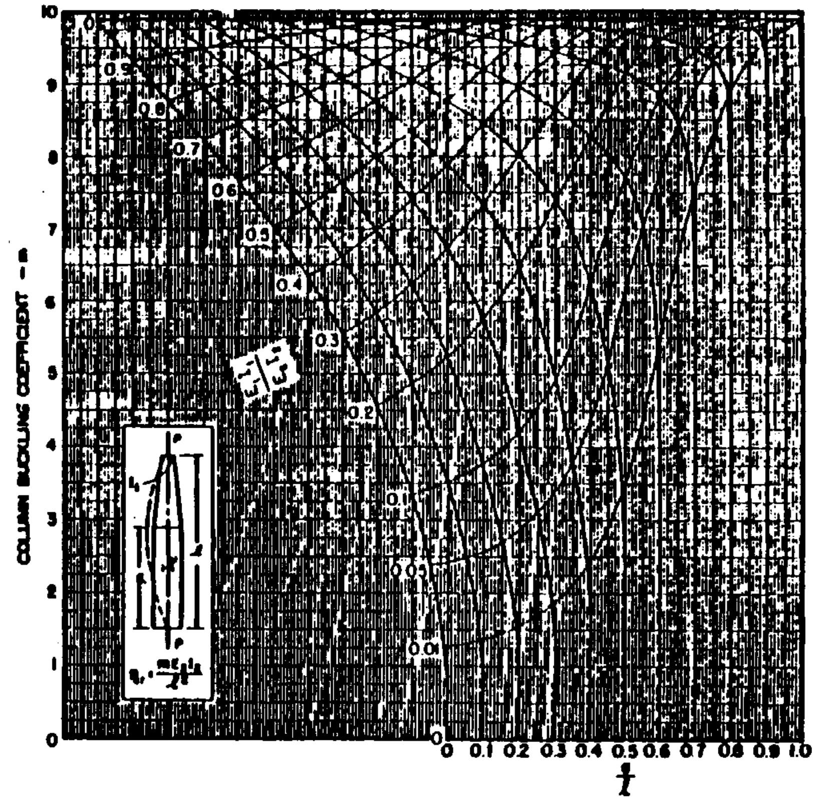

Moment Of Inertia For One End Varying As The Third Power (N=3) With Both Ends Pinned And No Transverse Axis Of Symmetry.

Fig. 5.3.0.14

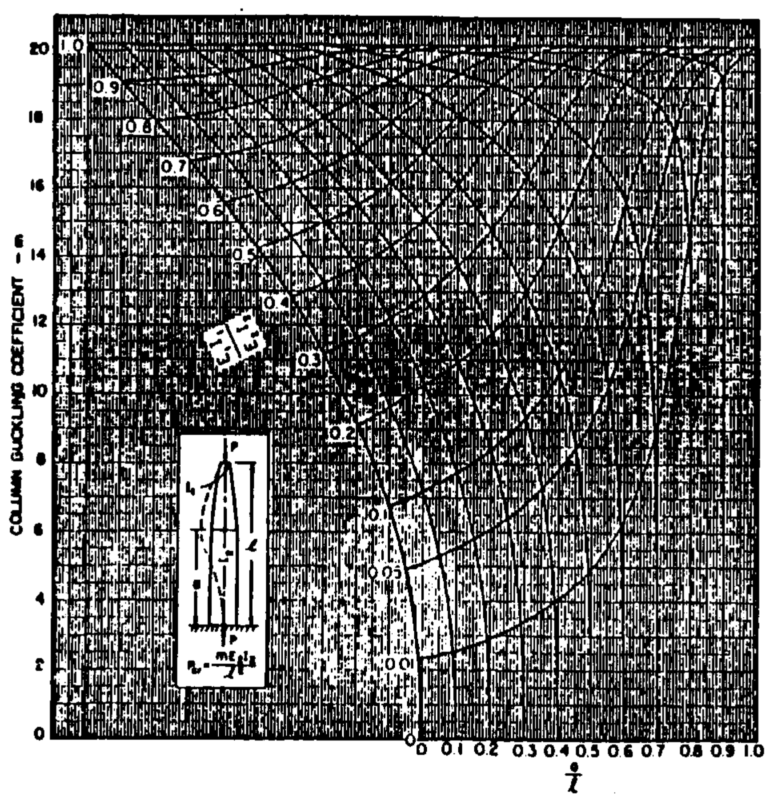

Moments Of Inertia For One End Varying As The Third Power (N=3) With One End Pinned And The Other Fixed, And No Transverse Axis Of Symmetry

Fig. 5.3.0.15

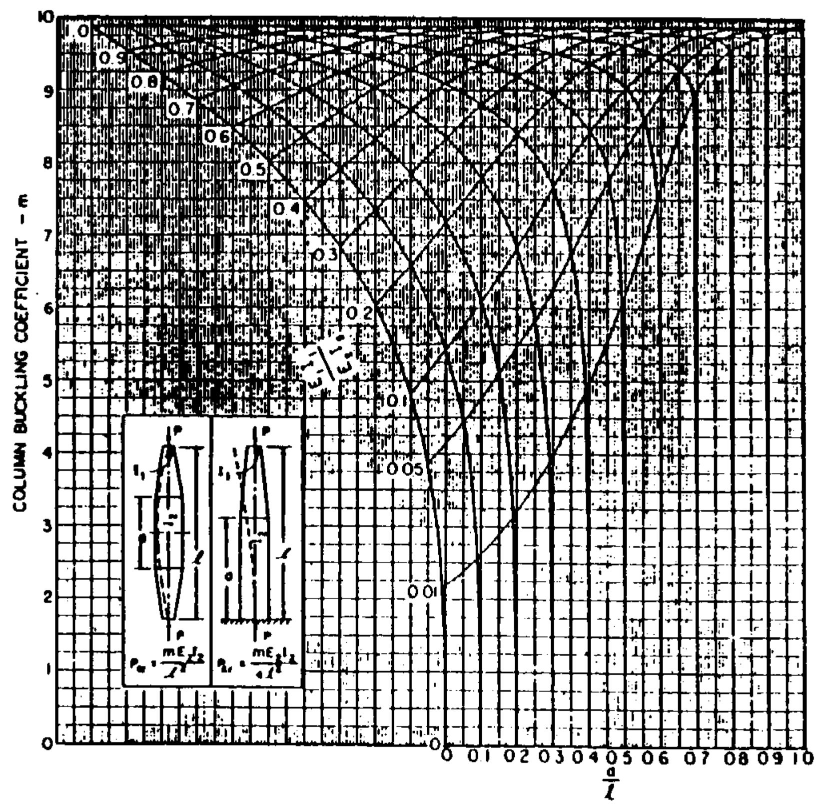

Moment Of Inertia For Ends Varying As The Fourth Power (N=4) With Both Ends Pinned And A Transverse Axis Of Symmetry

Fig. 5.3.0.16

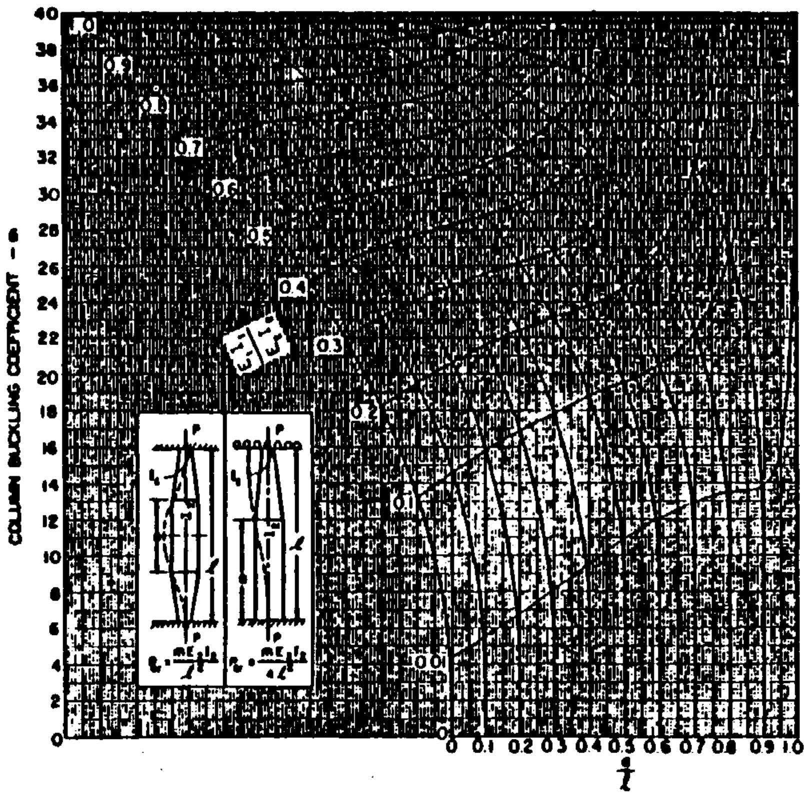

Moment Of Inertia For Ends Varying As The Fourth Power (N=4) With Both Ends Fixed And A Transverse Axis Of Symmetry

Fig. 5.3.0.17

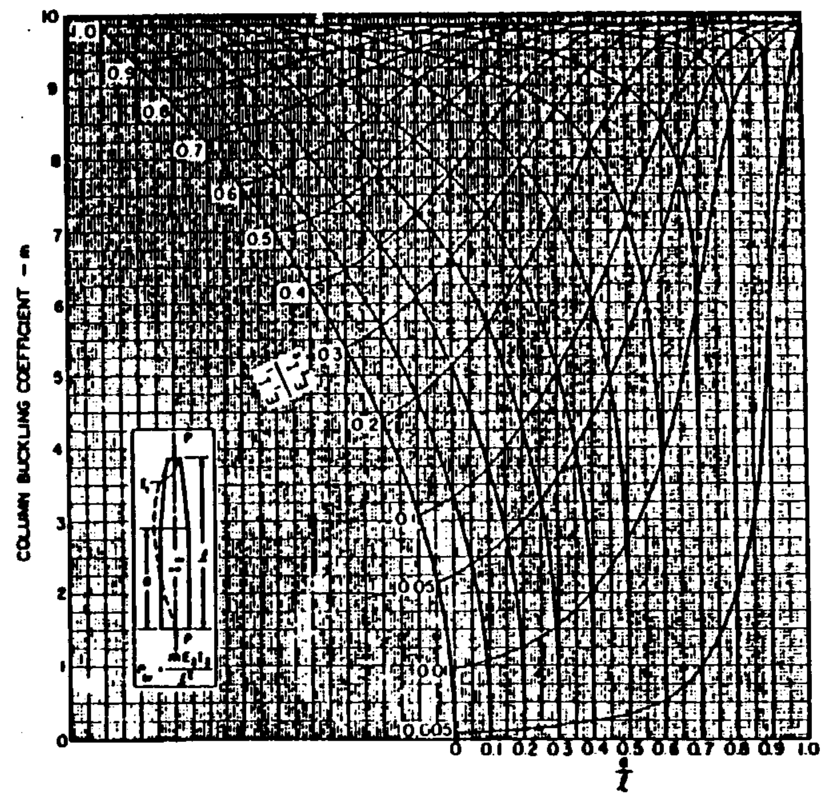

Moment Of Inertia For One End Varying As The Fourth Power (N-4) With Both Ends Fixed And A Transverse Axis Of Symmetry

Fig. 5.3.0.18

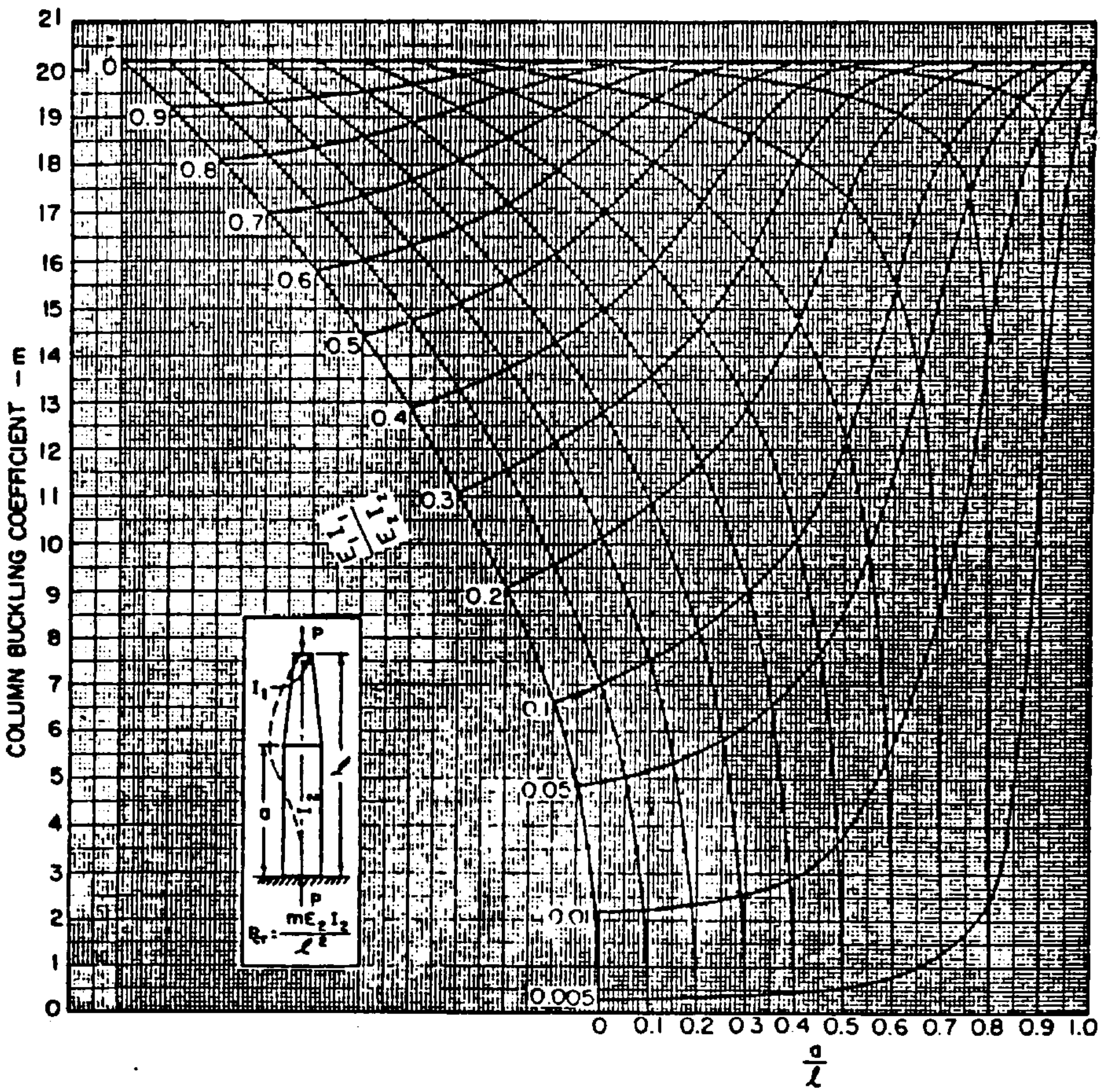

Moment Of Inertia For One End Varying As The Fourth Power (N=4) With One End Pinned And The Other Fixed And No Transverse Axis Of Symmetry

Fig. 5.3.0.19

5.4.0 Crippling of Sections

This type of failure is limited to thin walled sections. These thin walled sections can be classed as stable or unstable.

Unstable sections are those in which collapse would occur simultaneously with the buckling of any one of its components. Probably the best example of this type of section is an angle.

Stable sections are those which can carry additional load after one or more of its components have buckled. One of the best examples of this type of section is a channel. The channel will probably be able to carry some additional load after one of its flanges has buckled.

Two methods are given here to calculate crippling loads. One method will be used for formed sections whereas the other will be used for extruded sections.

5.4.1 Formed Sections

Any formed section in general can be assumed as made out of several angles. These angles are formed by dividing the cross-sectional area midway between bends as shown in Fig. 5.4.1-1. The angles will consist of unequal legs designated as (a) and (b). The angles can have either of three boundary conditions: both edges free, one edge free, or no edges free.

By calculating the ratio $\left(\frac{a+b}{2t}\right)$ and using the curves of Fig. 5.4.1.1, the following expression can be obtained.

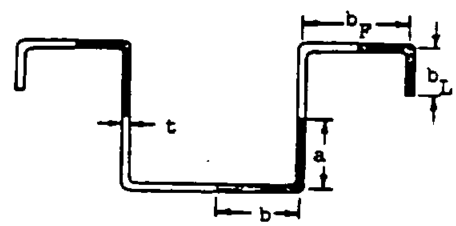

Fig. 5.4.1-1

$$\sigma_{cc}/\sqrt{\sigma_{cy} E}$$

where σ_{cc} = Crippling stress

σ_{cy} = Compressive yield stress

E = Modulus of elasticity of the material

The crippling stress (σ_{cc}) for each angle or element can now be obtained by multiplying the number read from Fig. 5.4.1.1 by $(\sqrt{\sigma_{cy} E})$

For sections consisting of several angles such as the hat in Fig. 5.4.1-1, a weighted average should be used to obtain (σ_{cc}). This can be shown by the following expression.

$$\sigma_{cc} = \frac{\sum(\text{Crippling Loads Of Angles})}{\sum(\text{Area Of Angles})}$$

This method of obtaining the crippling stress of formed sections is in good agreement with test results provided the size of the lip is long enough to stablize the section. The following procedure should be used to determine the effectiveness of the lip.

The lip's size or length (b_L) necessary to give due restraint to the flange, depends on the length of the flange (b_F) and on the thickness (t) of the section. When the length of the lip (b_L) is too small, its function as a stabilizing agent is practically non-existent.

Using the data obtained from a series of tests, Fig. 5.4.1.2 was plotted having as coordinates the ratios (b_F/b_L) and (b_L/t). For points falling under the lowest curve, the section should be evaluated assuming the lip as one leg of an unequal angle as shown in Fig. 5.4.1-1; for points falling above the highest curve, the lip should be neglected but considering the end having the lip as fixed; for points falling between the two lines, an average of the crippling loads given by the two methods should be used.

Three numerical examples will be given. The sections will be considered as formed sections of 7178-T6 aluminum alloy.

Example No. 1

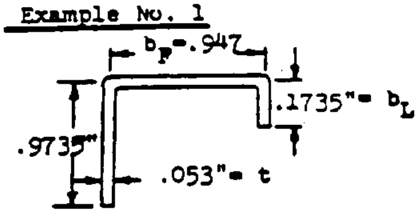

Determine Coordinates for use in Fig. 5.4.1.2

$$b_F/b_L = .947''/.1735'' = 5.46$$

$$b_L/t = .1735/.053 = 3.30$$

A point having these two coordinates will fall above the upper or highest curve of Fig. 5.4.1.2; hence, the lip should be neglected and this edge considered fixed.

One edge free

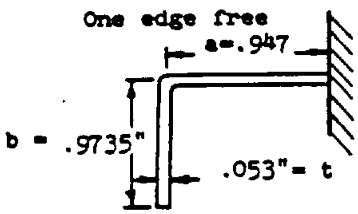

Determine Abscissa for use in Fig. 5.4.1.1

$$\frac{a+b}{2\,t} = \frac{.947'' + .9735''}{2(.053'')} = 18.11$$

From Fig. 5.4.1.1,

$$\sigma_{cc}/\sqrt{\sigma_{cy}\,E} = .039$$

$$\sigma_{cc} = \sqrt{\sigma_{cy}\,E}\,(.039) = \sqrt{78{,}000(10.5\times10^6)}\,(039) = 35{,}100 \text{ psi}$$

Example No. 2

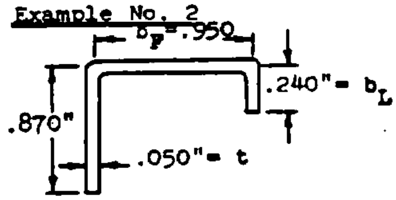

$$b_F/b_L = .950''/.240'' = 3.96$$

$$b_L/t = .240''/.050'' = 4.80$$

A point having these two coordinates will fall under the lower curve of Fig. 5.4.1.2 hence, the lip will be considered.

(1) one edge free

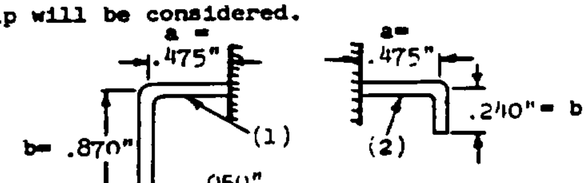

(2) One edge free

For angle (1)

$$\frac{a+b}{2t} = 1.345/.1 = 13.45$$

From Fig. 5.4.1.1

$$\sigma_{cc}/\sqrt{\sigma_{cy}\,E} = .0486$$

For angle (2) $\frac{a+b}{2t} = .715/.1 = 7.15$

From Fig. 5.4.1.1 $\sigma_{cc}/\sqrt{\sigma_{cy}\,E} = .065$

The weighted average will be: $\sigma_{cc} = \frac{\sum(\text{Crippling loads of angles})}{\sum(\text{Area of angles})}$

$$\sigma_{cc} = \sqrt{\sigma_{cy}\,E}\left[\frac{(.0486)(1.345) + (.065)(.715)}{1.345 + .715}\right] = 48,900$$

Example No. 3

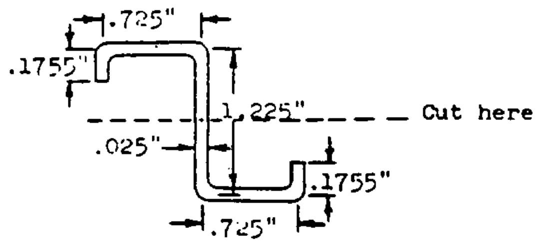

Cut the section midway between bends as shown.

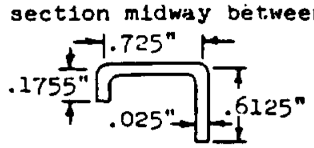

$b_F/b_L = .725''/.175'' = 4.14$

$b_L/t = .175''/.025'' = 7.02$

A point having these two coordinates will fall between the upper and lower curves of Fig. 5.4.1.2 hence, the average of the two methods used in example No. 1 and No. 2 should be used.

Case 1 Neglecting the lip:

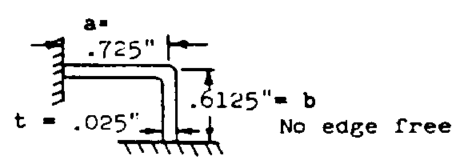

$\frac{a+b}{2t} = 1.3375/.05 = 26.75$

From Fig. 5.4.1.1,

$\sigma_{cc}/\sqrt{\sigma_{cy}\,E} = .0312$

Case 2 Considering the lip:

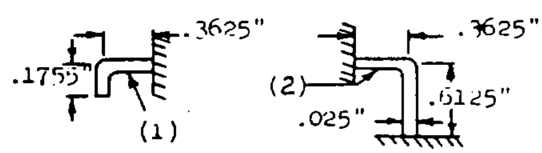

(1) One edge free

(2) No edge free

For angle (1) $\frac{a+b}{2t} = .538/.05 = 10.76$

From Fig. 5.4.1.1 $\sigma_{cc}/\sqrt{\sigma_{cy}\,E} = .0575$

For angle (2) $\frac{a+b}{2t} = .975/.05 = 19.5$

From Fig. 5.4.1.1 $\sigma_{cc}/\sqrt{\sigma_{cy}\,E} = .0395$

The weighted average will be:

$$\sigma_{cc} = \frac{\sum(\text{Crippling loads of angles})}{\sum(\text{Area of angles})}$$

$$\sigma_{cc} = \frac{(.538)(.0575) + (.0395)(.975)}{.538 + .975} = .0459$$

The average of the two cases will now be obtained.

$$\sigma_{cc}/\sqrt{\sigma_{cy}\,E} = \frac{.0312 + .0459}{2} = .03855$$

$$\sigma_{cc} = (.03855)(9.01)\,10^5 = 34{,}800 \text{ psi}$$

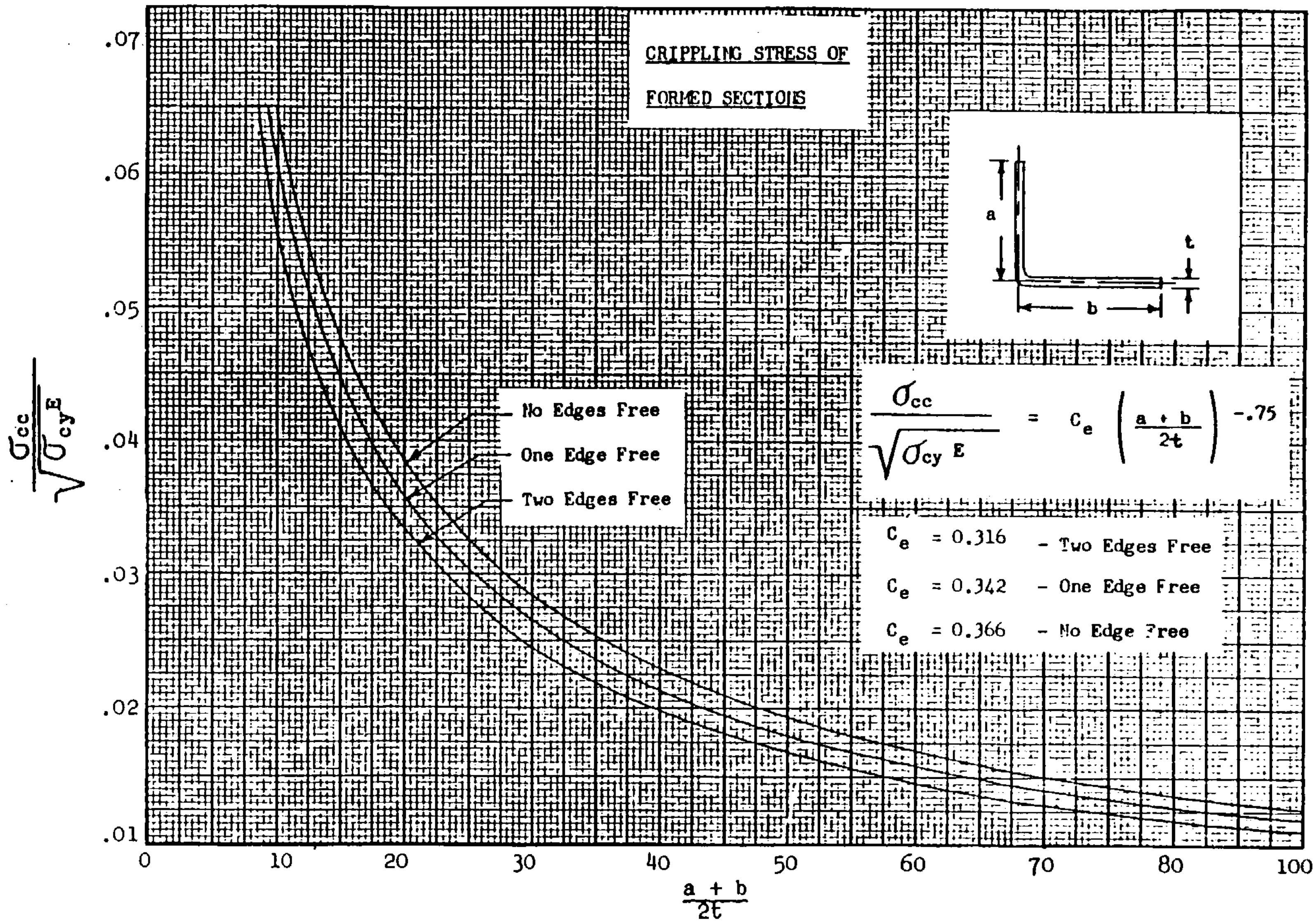
CRIPPLING STRESS OF
FORMED SECTIONS
a
b
t
No Edges Free
One Edge Free
Two Edges Free
$\frac{\sigma_{cc}}{\sqrt{\sigma_{cy} E}} = C_e \left(\frac{a+b}{2t}\right)^{-.75}$
C_e = 0.316 - Two Edges Free
C_e = 0.342 - One Edge Free
C_e = 0.366 - No Edge Free
.07
.06
.05
.04
.03
.02
.01
$\frac{\sigma_{cc}}{\sqrt{\sigma_{cy} E}}$
0
10
20
30
40
50
60
70
80
100
$\frac{a+b}{2t}$

Fig. 5.4.1.1

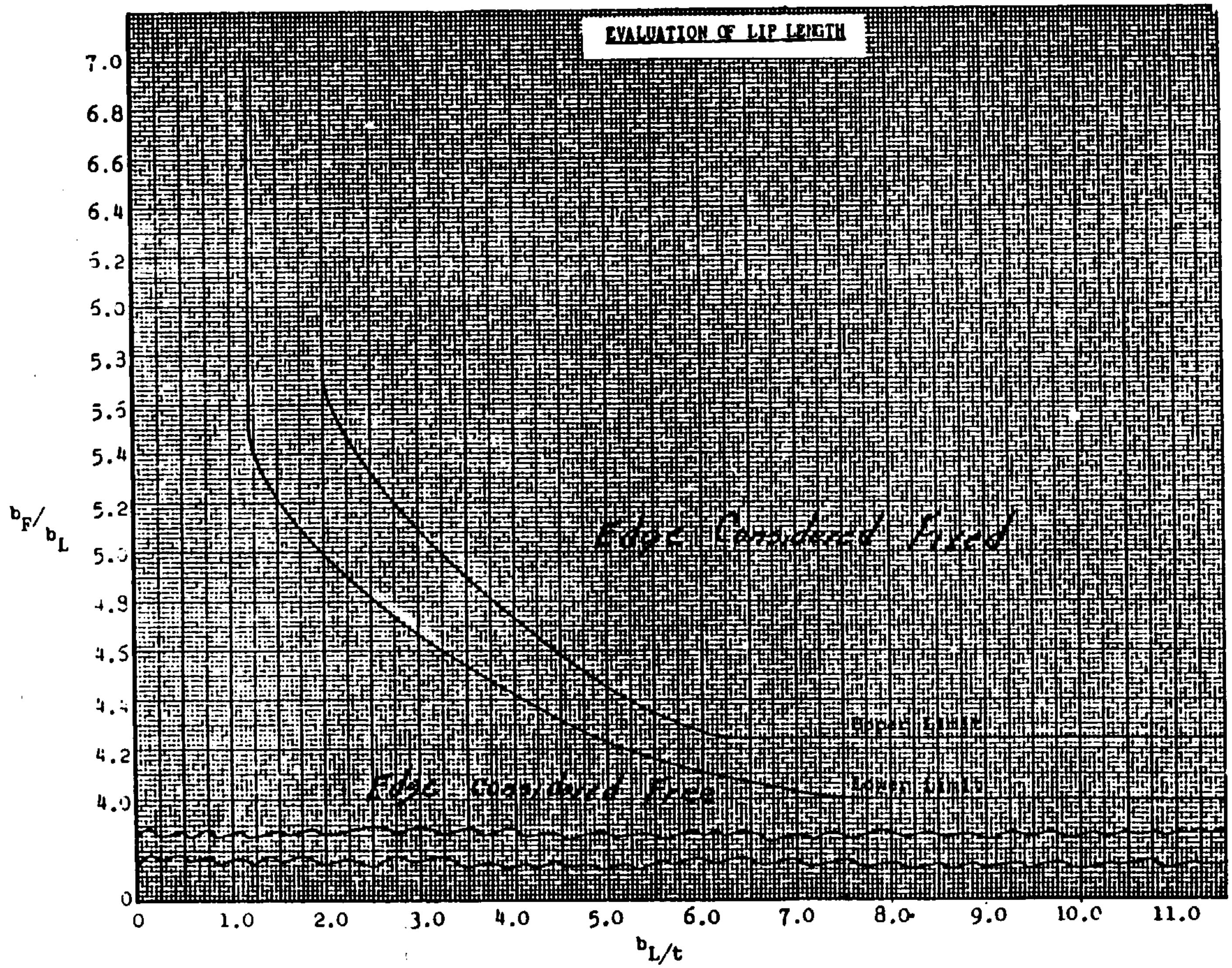
EVALUATION OF LIP LENGTH
7.0
6.8
6.6
6.4
5.4
5.2
4.2
4.0
0
b_F/b_L
Edge Considered Fixed
Upper Limit
Lower Limit
Edge Considered Free
0
1.0
2.0
3.0
4.0
5.0
6.0
7.0
8.0
9.0
10.0
11.0
b_L/t

Fig. 5.4.1.2

5.4.2
Extruded or Built-up Sections

The relationship between allowable compression stress and section properties is given in Figure 5.4.2.1. The dimensionless parameter $\frac{\sigma_{max.}}{\sqrt{E_c \sigma_{cy}}}$ has a rational derivation, however the curve relating it to the term $\frac{b}{t\sqrt{K}}$ is empirical. This curve includes the results from tests of most of the commonly used aircraft materials. In calculating the material parameter, $\sqrt{E_c \sigma_{cy}}$, minimum guaranteed (ANC-5 "A") values should be used. Room temperature material parameters for some of the more common materials are given in Table 5.4.2.6. In determining the material parameter for clad materials, the secondary modulus of elasticity must be used. The allowable compression stress at elevated temperatures can be determined by utilizing the elevated temperature values for "E_c" and σ_{cy} in calculating the material parameter. The allowable compression stress, $\sigma_{max.}$, should never be greater than 1.14 σ_{cy}.

It may be necessary to use a modification of "E" for materials having a very low ratio of compressive yield to modulus, σ_{cy}/E, such as aluminum at 600°F, etc.

The term "crippling stress" means the stress at which local instability occurs as evidenced by distortion of a cross section in its own plane.

The allowable compression stress is the maximum stress which can be safely applied to a column without producing complete failure of the column. In stable sections the allowable compression stress may be somewhat higher than the critical crippling stress. Unstable sections collapse and fail at stresses little or no higher than the crippling stress.

Unstable Sections

An example of an unstable section is an angle lacking intermediate supports. For angles of this type, the abscissa in Figure 5.4.2.1, $\frac{b}{t\sqrt{K}}$, can be determined by taking $1/\sqrt{K}$ as 1.56 and using an average b/t for the two legs.

In computing the allowable compression strength of lipped angles, the method given in Section 5.4.1 should be used. The crippling stress, σ_{cc}, obtained from Section 5.4.1 will be the allowable compression stress.

Stable Sections

Stable sections are defined as sections which do not fail immediately upon the occurrence of crippling. Channels, zees, I's, H's, and all closed sections are in this category. Back-to-back angles, various built up combinations, and tees are usually considered stable when functioning as a compression flange of a conventionally proportioned plate girder type beam, the web stiffners of which are riveted to the flanges and thus act as stabilizing members for the compression flange. Allowable compression stresses applicable to stable sections are to be obtained from Figure 5.4.2.1.

For channel, zee, I (or H) sections and rectangular tubes in compression, values of $1/\sqrt{K}$ can be obtained from Figures 5.4.2.2 through 5.4.2.4. The values of "b" and "t" are as indicated on the sketches. The same values of $(1/\sqrt{K})$ may be used to determine conservative values of allowable bending modulus.

Plain and lipped angles used as compression flanges of plate girder beams (fuselage and hull framed sections, for instance) are treated as shown in Table 5.4.2.5, Cases 1 and 2.

Case 3a shows an example in which a skin riveted to a flange may benefit the allowable compression stress by increasing the effective thickness of the flange to the extent of one-half the skin thickness (but not more than one-half the flange thickness). The effective (b/t) is not to be reduced below 10 by using the skin to increase the effective "t". This increase in thickness should not be assumed unless the skin-to-flange riveting is adequate to prevent buckling of the skin at the calculated allowable compression stress of the composite section. In Case 3b the allowable compression stress is not assumed to be benefited by the skin. To the contrary, the allowable stress may be reduced due to deformation of the flange by shear buckles in the skin. In the event that the skin shear stresses are high, attention should be given to this possibility and to means of combating it, such as increasing the buckling stress by reducing the dimension to the adjacent stringer, etc. Case 3a usually does not suffer from this trouble because the corner of the angle breaks up the skin buckles.

In Case 4 the thickness of an angle is increased by one-half the thickness of the thinner nested angle. The additional angle should not be considered to reduce the b/t to less than 8.

In general, only one element should be considered to reinforce a particular flange. Thus, in Case 4, no added thickness is assumed to result from the presence of the skin. Exception may be taken to this rule in cases where the composite member is unusually well supported by adjoining structure.

Many variations of Case 4 are possible, such as a lipped basic angle with a plain reinforcing angle and vice versa, a reinforcing angle longer or shorter than the basic angle on either or both legs, etc. A weighted average value of b should be used (measuring b from the inside face of the inside angle, as shown in Case 4) except that where the basic angle and the reinforcing angle differ by not more than one gauge, a straight average may be used for simplicity. Where either the basic angle or the reinforcing angle is lipped ($1/\sqrt{K}$) may be assumed 1.0 unless the lipped flange is lighter than the plain flange by more than one gauge, in which case use 1.25.

See Case 6 for back-to-back angles.

Note: The above rules concerning effective t apply only to the determination of the allowable compression stresses. In calculating actual stresses due to applied loads, the area to be used should include all elements plus the effective width of skin at full thickness.

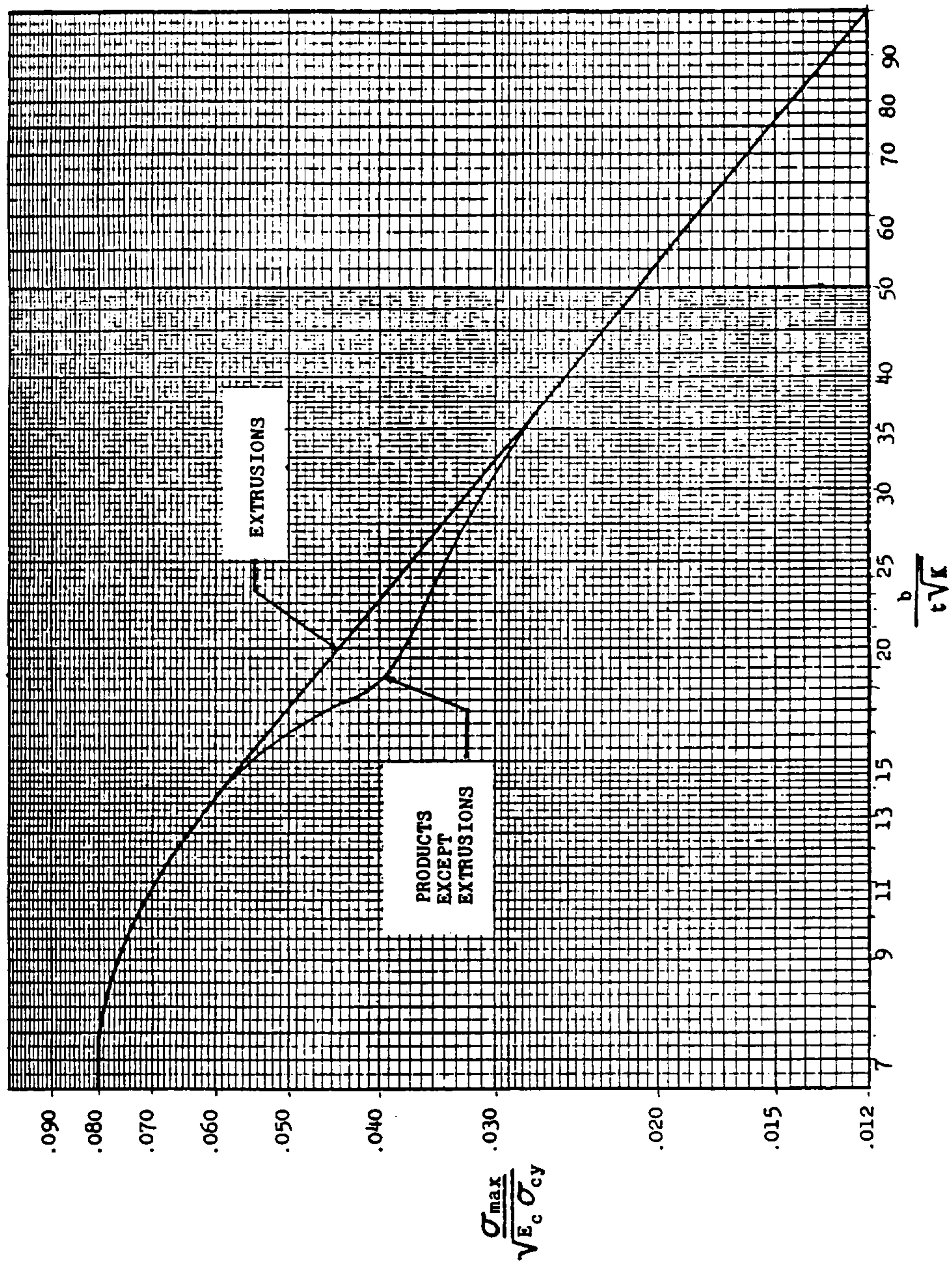
EXTRUSIONS
PRODUCTS
EXCEPT
EXTRUSIONS
$\frac{b}{t\sqrt{K}}$
7
9
11
13
15
20
25
30
35
40
50
60
70
80
90
$\frac{\sigma_{max}}{\sqrt{E_c \sigma_{cy}}}$
.090
.080
.070
.060
.050
.040
.030
.020
.015
.012

Fig. 5.4.2.1

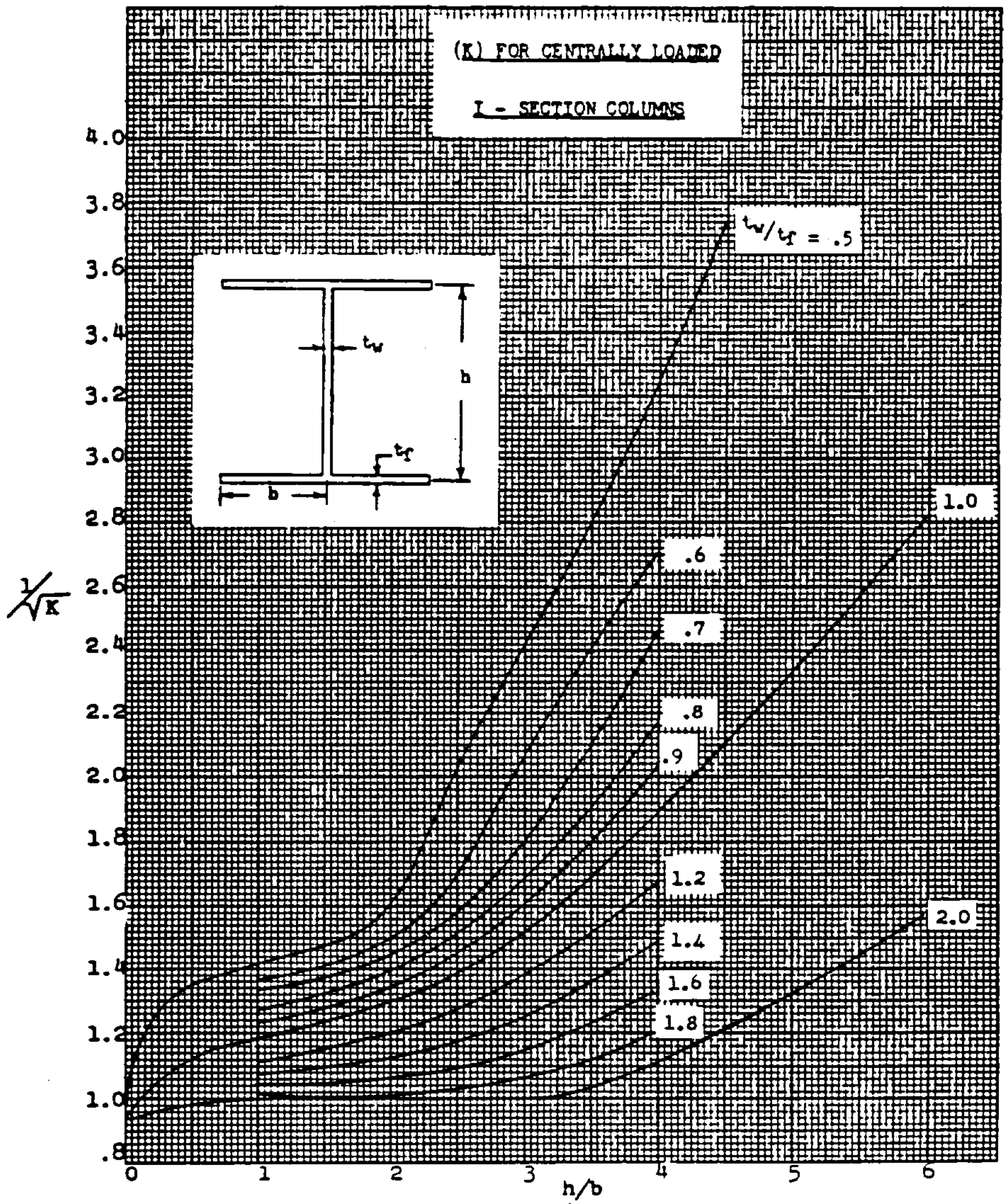
(K) FOR CENTRALLY LOADED
I - SECTION COLUMNS
t_w/t_f = .5
.6
.7
.8
.9
1.0
1.2
1.4
1.6
1.8
2.0
t_w
t_f
h
b
$1/\sqrt{K}$
h/b
4.0
3.8
3.6
3.4
3.2
3.0
2.8
2.6
2.4
2.2
2.0
1.8
1.6
1.4
1.2
1.0
.8
0
1
2
3
4
5
6

Fig. 5.4.2.2

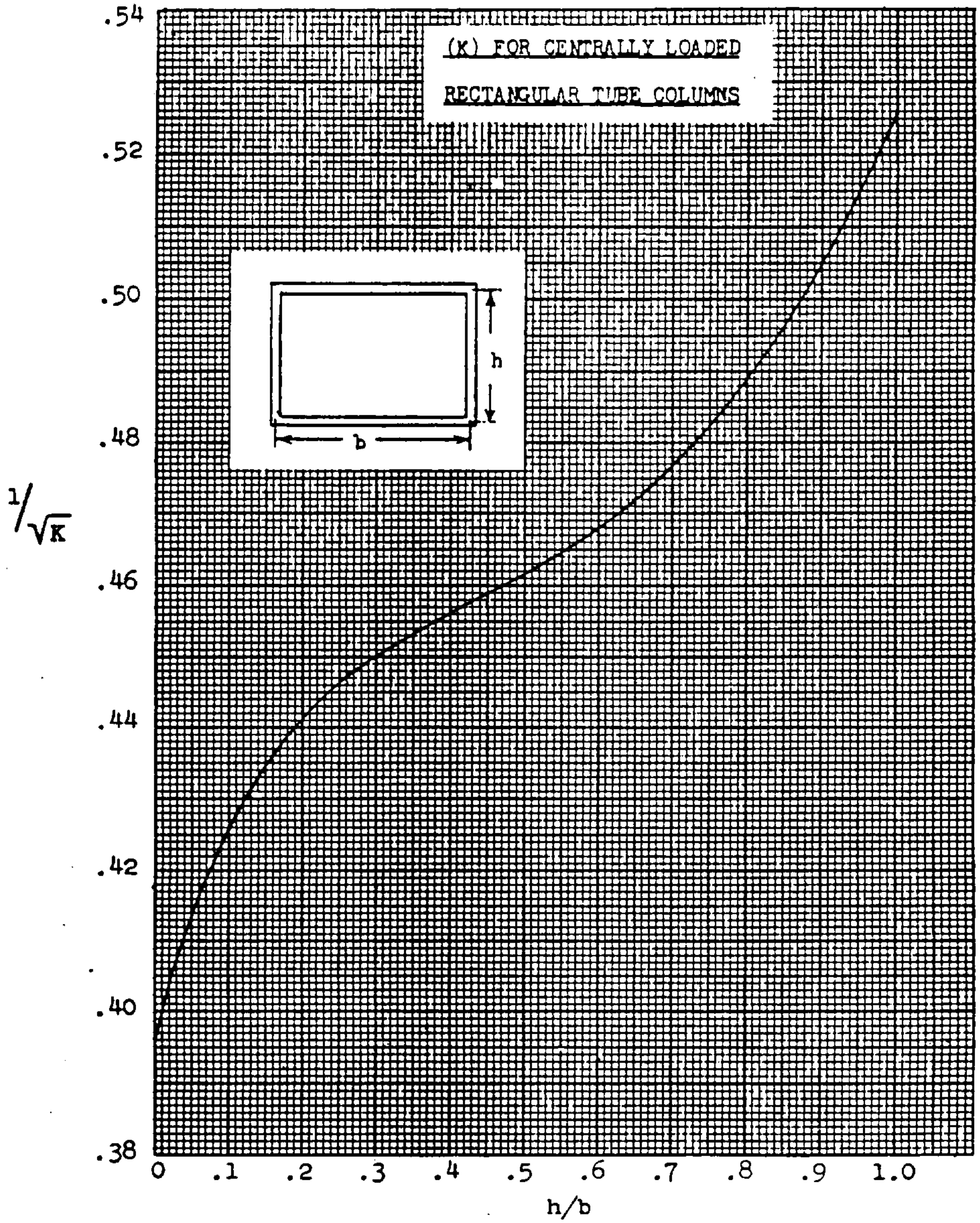
(K) FOR CENTRALLY LOADED
RECTANGULAR TUBE COLUMNS
h
b
.54
.52
.50
.48
.46
.44
.42
.40
.38
$1/\sqrt{K}$
0
.1
.2
.3
.4
.5
.6
.7
.8
.9
1.0
h/b

Fig. 5.4.2.3

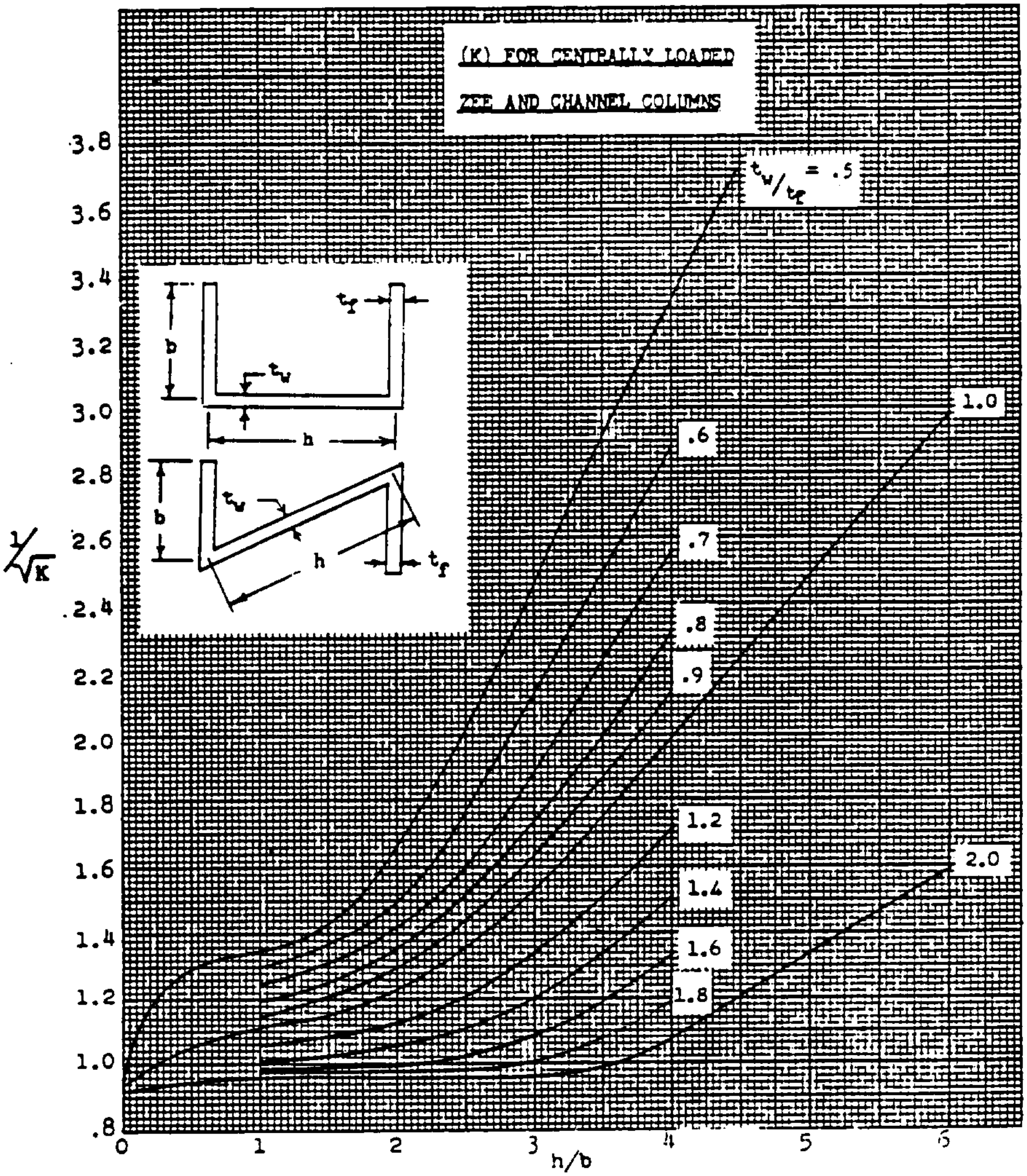
(K) FOR CENTRALLY LOADED
ZEE AND CHANNEL COLUMNS
t_w/t_f = .5
.6
.7
.8
.9
1.0
1.2
1.4
1.6
1.8
2.0
b
h
t_w
t_f
$1/\sqrt{K}$
h/b
.8
1.0
1.2
1.4
1.6
1.8
2.0
2.2
2.4
2.6
2.8
3.0
3.2
3.4
3.6
3.8
0
1
2
3
4
5
6

Fig. 5.4.2.4

TABLE 5.4.2.5

Different Types of Compressive Flanges

CASE 1.

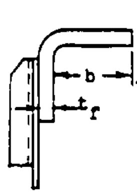

outstanding leg: $1/\sqrt{K} = 1.25$

web leg : $1/\sqrt{K} = 1.00$

$t_{eff} = t_f$

CASE 2.

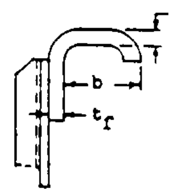

both legs $1/\sqrt{K} = 1.00$

$t_{eff} = t_f$

CASE 3a.

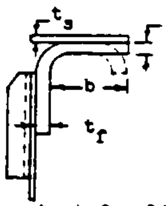

skin leg:
$1/\sqrt{K}=1.25$(plain flange)
$1/\sqrt{K}=1.00$(clipped ")
$t_{eff} = t_f + 1/2\ t_s$

web leg:
$1/\sqrt{K} = 1.00$
$t_{eff} = t_f$

(See text for limit on effective b/t)

CASE 3b.

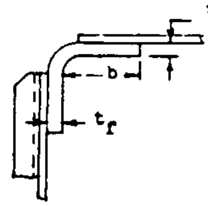

skin leg: $1/\sqrt{K} = 1.25$
$t_{eff} = t_f$

web leg: $1/\sqrt{K} = 1.00$
$t_{eff} = t_f$

CASE 4.

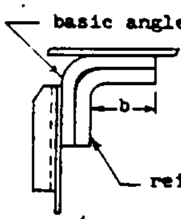

skin leg: $1/\sqrt{K} = 1.25$
$t_{eff} = t_{f(thicker)} + 1/2\ t_{f(thinner)}$

web leg: $1/\sqrt{K} = 1.00$

(see text for limit on effective b/t)

CASE 5.

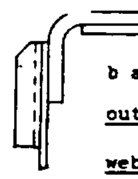

b and t same as basic angle

outstanding leg: $1/\sqrt{K} = 1.25$

web leg: $1/\sqrt{K} = 1.00$

CASE 6.

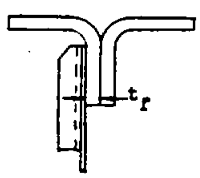

skin leg - see CASE 1.

web leg:
$1/\sqrt{K} = 1.00$
$t_{eff} = t_{f(thicker)} + 1/2\ t_{f(thinner)}$

CASE 7.

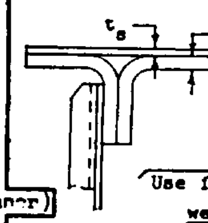

skin leg-see CASE 1 - $1/\sqrt{K}$
$t_{eff} = t_f + 1/2\ t_s$
Use for reinforcing strip only

web leg - see CASE 6.

CASE 8.

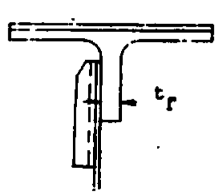

skin leg - see CASE 7.

web leg - see CASE 6.

$t_{eff} = t_f$

TABLE 5.4.2.6
ROOM TEMPERATURE MATERIAL PARAMETERS

MATERIAL	FORM	COND.	THICK-NESS	GRAIN DIRECTION	$\sqrt{E_c \sigma_{cy}}$ (KSI)
2024 AL.	Clad Sheet	T3	$\leq .062$	L	599
			$\geq .062$	L	624
		T80	$\leq .062$	L & T	676
			$\geq .062$	L & T	709
		T81	$\leq .062$	L & T	730
			$\geq .062$	L & T	765
		T84	$\leq .062$	L	777
			$\geq .062$	L	815
		T86	$\leq .062$	L & T	784
			$\geq .062$	L & T	820
	Bare Sheet	T3	$\leq .250$	L	655
			$\leq .250$	T	695
	Bar & Rod	T4	≤ 3.00	L	655
			≤ 3.00	T	630
	Ext.	T4	$\leq .250$	L & T	639
7075 AL.	Clad Sheet	T6	$\leq .039$	L	777
			.040-.250	L	788
	Bare Sheet	T6	$\leq .039$	L	840
			.040-.250	L	845
	Bar & Rod	T6	≤ 3.00	L	832
			≤ 3.00	T	794
	Ext.	T6	$\leq .250$	L & T	859
18-8 Stainless Steel	Sheet	Annealed		L & T	995
	Cold Rolled Sheet	1/4 Hard		L	1421*
		1/2 Hard		L	1605*
		3/4 Hard		L	1700*
		Full Hard		L	1827*
Alloy Steels		125 HT			1815
		150 HT			2050
		180 HT			2280
		200 HT			2395
		260 HT			2653
17-7 PH S.S.	Sheet	TH1050			2192
17-4 PH S.S.	Bar&Rod	H900			2139
C110M Ti	Sheet	$\sigma_{cy} = 110$			1305
C130 AM Ti	Bar&Rod	$\sigma_{cy} = 130$			1420

* Values adjusted to account for the fact that this material is highly anisotropic.

Data Source, Section 1.3 Reference 1

5.5.0
Beam Columns

A beam column is a structural member, either straight or having a small initial curvature, whose cross sectional dimensions are small with respect to its length and that is subjected to both axial and transverse loads. The axial loads can be either tensile or compressive.

5.5.1
Beam Columns Subjected to Axial Compressive Loads

Beam columns under axial compressive loads are far more critical than beam columns under axial tension loads. Axial compressive loads increase the bending moment and add the possibility of instability or buckling types of failure. This type of beam column is subjected to the limitations of both beams and columns. The critical column load should be determined considering only the axial load (5.1.0 and 5.2.0). The critical load is not the maximum load that the beam column can carry, but rather the load under which the member would be unstable even if there were no side load. The critical load is independent of the magnitude or distribution of the transverse load. The following equations should be used to calculate the effects of the combined loads on a single span beam column:

Bending Moment $= M = C_1 \sin\frac{x}{j} + C_2 \cos\frac{x}{j} + f(w)$ (1)

Shear $= V = \frac{C_1}{j}\cos\frac{x}{j} - \frac{C_2}{j}\sin\frac{x}{j} + f'(w)$ (2)

$f'(w) = 1^{st}$ derivative of $f(w)$

Deflection $= \delta = \frac{M_o - M}{P}$ (3)

Slope $= \theta = \frac{V_o - V}{P}$ (4)

$j = \sqrt{EI/P}$ (5)

Where (M_o) and (V_o) are the primary bending moment and shear, respectively, i.e. the bending moment and shear that would be produced by the transverse loads and end moments acting without the axial loads. The particular expressions for (C_1), (C_2), and $f(w)$ depend on the character of the transverse load. Table 5.5.1.1 contains (C_1), (C_2), and $f(w)$ for some of the more common types of transverse loads. The moment (M) is positive when producing compression in the upper fibers and (W) or (w) is positive when upward. The load (P) and the distance (x) are as shown on the sketches in Table 5.5.1.1.

Limitations

1. The results obtained from these equations become inaccurate as the ratio M/M_o approaches or becomes less than 1.1.
2. It is recommended that at least four significant figures be used in all computations.

The following example will illustrate the procedure to be used.

Example: (Beam Column with axial compressive load)

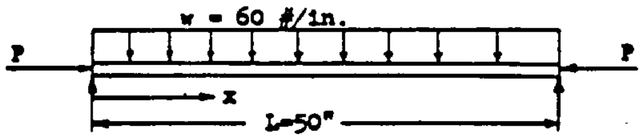

$P = 100{,}000\#$
$w = 60\ \#/in.$
$E = 10x10^6$ psi
$I = 6.75\ in.^4$
$A = 9.00\ in.^2$

Find: (M) and (δ) at (x = 20")

$$M = C_1 \sin \frac{x}{j} + C_2 \cos \frac{x}{j} + f(w) \qquad \text{equation (1)}$$

where:

$$j = \sqrt{\frac{EI}{P}} = \sqrt{\frac{(10x10^6)(6.75)}{10^5}} = 25.98 \qquad \text{equation (5)}$$

and from Table 5.5.1.1

$$C_1 = \frac{wj^2(\cos L/j - 1)}{\sin L/j} = \frac{-60(675)(\cos 1.92 - 1)}{\sin 1.92} = 56{,}961.21$$

$$C_2 = -wj^2 = -\left[-60(675)\right] = +40{,}500$$

$$f(w) = wj^2 = -40{,}500$$

Then from eq. (1):

$$M = (56{,}961.21)(\sin .77) + (40{,}500)(\cos .77) - 40{,}500$$

$$M = 28{,}942.97 \text{ in-lbs.}$$

<u>Consider transverse load only:</u>

$$M_o = \frac{wLx}{2} \frac{wx^2}{2} = \frac{wx}{2}(L-x) \qquad \text{(Ref. Table 4.1.1.1)}$$

$$M_o = \frac{(60)(20)}{2}\left[50-20\right] = (600)(30) = 18{,}000 \text{ in-lbs.}$$

From eq. (3):

$$\delta = \frac{M_o - M}{P} = \frac{18{,}000 - 28{,}942.97}{10^5}$$

$$\delta = -.1094 \text{ inches}$$

<u>Modified Principle of Superposition</u>

The method of superposition can be applied provided each of the superimposed bending moments is the effect of the combined action of one or more of the transverse loads and the entire axial load. In this connection an end moment is to be considered as a transverse load. In order to obtain the proper formula for the bending moment on a beam-column subjected to two or more transverse loads, all that is necessary is to add the values from Table 5.5.1.1 for each of the transverse loads to obtain C_1, C_2, and $f(w)$ to be used in equations (1), (2), (3), and (4).

TABLE 5.5.1.1

BEAM COLUMNS WITH AXIAL COMPRESSION LOAD

LOADING	C_1	C_2	$f(w)$	MAX. MOMENT
Unequal End Moments 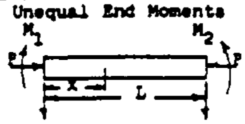	$\frac{M_2 - M_1 \text{ Cos } L/j}{\text{Sin } L/j}$	M_1	0	$M_{max} = \frac{M_1}{\text{Cos } x/j}$ where $\text{Tan } \frac{x}{j} = \left[\frac{M_2 - M_1 \text{Cos} L/j}{M_1 \text{ Sin} L/j}\right]$
Equal End Moments 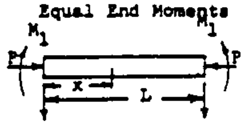	$M_1 \text{ Tan } L/2j$	M_1	0	$M_{max} = \frac{M_1}{\text{Cos } L/2j}$ At Midspan
Uniform Load 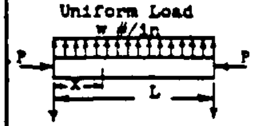	$\frac{w j^2 (\text{Cos } L/j - 1)}{\text{Sin } L/j}$	$-w j^2$	$w j^2$	$M_{max} = w j^2 (1 - \text{Sec} L/2j)$ At Midspan
Uniform Load Plus End Moments 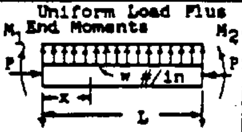	$\frac{D_2 - D_1 \text{ Cos } L/j}{\text{Sin } L/j}$ See Note 4	D_1 See Note 4	$w j^2$	$M_{max} = \frac{D_1}{\text{Cos } x/j} + w j^2$ where $\text{Tan } x/j = \frac{D_2 - D_1 \text{Cos} L/j}{D_1 \text{Sin } L/j}$
Concentrated Load 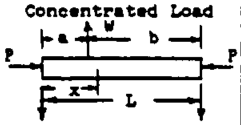	$x < a$: $\frac{-Wj \text{ Sin } b/j}{\text{Sin } L/j}$ $x > a$: $\frac{Wj \text{ Sin } a/j}{\text{Tan } L/j}$	0 $-Wj \text{ Sin } a/j$	0 0	$M_{max} = \frac{C_1^2 + C_2^2}{C_2} \text{ Cos } x/j$ where $\text{Tan } x/j = \frac{C_1}{C_2}$
Uniformly Increasing Load 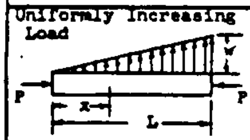	$-\frac{w j^2}{\text{Sin } L/j}$	0	$\frac{w j^2 x}{L}$	Occurs at $\text{Cos } x/j = j/L \text{Sin} L/j$ Solve for x/j and x, Substitute in Eq(1)
Uniformly Decreasing Load 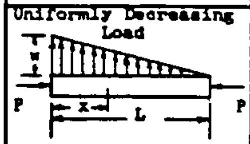	$\frac{w j^2}{\text{Tan } L/j}$	$-w j^2$	$w j^2 (1 - x/L)$	Occurs at $\text{Cos } \frac{L-x}{j} = j/L \text{Sin} L/j$ Solve for x/j and x, Substitute in Eq(1)
Symmetrical Triangle Load 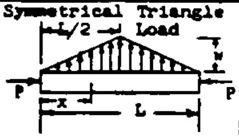	$x < L/2$: $-\frac{2 w j^3}{L \text{ Cos } L/2j}$ $x > L/2$: $\frac{2w j^3 \text{ Cos } L/j}{L \text{ Cos } L/2j}$	0 $-\frac{4w j^3}{L} \text{ Sin } L/2j$	$\left[\frac{2w j^2 x}{L}\right]$ $\left[2w j^2 (1 - x/L)\right]$	$M_{max} = -\frac{2wj^3}{L}\text{Tan} L/2j + wj^2$ at Midspan

TABLE 5.5.1.1 (Cont'd)

BEAM COLUMNS WITH AXIAL COMPRESSION LOAD

LOADING	C_1	C_2	f (w)	MAX. MOMENT
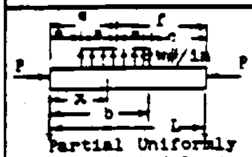 Partial Uniformly Distributed Load	x < a: $-\frac{2wj^2 \sin e/j \sin f/j}{\sin L/j}$ a < x < b: $\frac{2wj^2 \sin e/j \sin e/f}{\tan L/j} - wj^2 \sin b/j$ b < x < L: $\frac{2wj^2 \sin e/j \sin e/f}{\tan L/j}$	0 $-wj^2 \cos a/j$ $-2wj^2 \sin e/j \sin e/j$	0 wj^2 0	See Note (6)
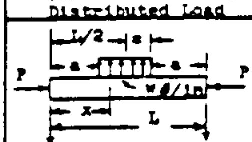 Symmetrical Partially Uniform Distrib. Load	x < a: $-wj^2 \sin e/j \sec L/2j$ a < x < L-a: $-wj^2 \tan L/2j \cos a/j$ L-a < x < L: $wj^2 \sin e/j \sec L/2j \cos L/j$	0 $-wj^2 \cos a/j$ $-2wj^2 \sin e/j \sin L/2j$	0 wj^2 0	$wj^2\left[1-\frac{\cos a/j}{\cos L/2j}\right]$ At Midspan
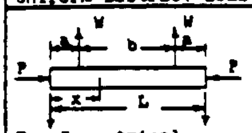 Two Symmetrical Concentrated Loads	x < a: $-Wj\frac{\cos b/2j}{\cos L/2j}$ a < x < L-a: $-Wj \sin a/j \tan L/2j$ L-a < x < L: $Wj\frac{\cos L/j \cos b/2j}{\cos L/2j}$	0 $-Wj \sin a/j$ $-Wj\frac{\sin L/j \cos b/2j}{\cos L/2j}$	0 0 0	$-Wj\frac{\sin a/j}{\cos L/2j}$ At Midspan
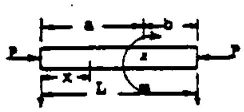 Concentrated Moment	x < a: $-\frac{m \cos b/j}{\sin L/j}$ x > a: $-\frac{m \cos a/j}{\tan L/j}$	0 $m \cos a/j$	0 0	See Note (6)
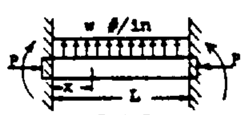 Fixed End Beam - Uniform Load	$-\frac{wjL}{2}$	$-\frac{wLj}{2 \tan L/2j}$	wj^2	At x = 0: $M = wj^2\left[1-\frac{L/2j}{\tan L/2j}\right]$ At x = L/2: $M = -wj^2\left[\frac{L/2j}{\sin L/2j} - 1\right]$
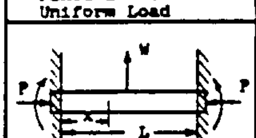 Fixed End Beam-Concentrated Load at Center	x < L/2: $-1/2\ Wj$ x > L/2: $1/2Wj\left[2\cos L/2j - 1\right]$	$1/2Wj\left[\frac{1-\cos L/2j}{\sin L/2j}\right]$ $1/2Wj\left[\frac{\cos L/j - \cos L/2j}{\sin L/2j}\right]$	0 0	M_{max} = ? $1/2Wj\left[\frac{1-\cos L/2j}{\sin L/2j}\right]$ At x = 0 $(M_x = L/2) = -M_{max}$
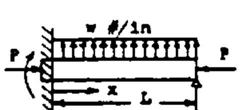 Fixed Simple Beam Uniform Load	x < L/2: $-\frac{\tan L/2j - L/2j}{\tan L/j - L/j}\ wLj$ x > L/2: $-\frac{1-\cos L/j}{\sin L/j}\ wj^2$	$\left[\frac{\tan L/2j - L/2j}{\tan L/j - L/j}\right] \times$ $\left[\tan L/j (wLj)\right] - wj^2$	$+wj^2$	$M_{max} =$ $wLj\left[\frac{\tan L/2j - L/2j}{\tan L/j - L/j}\right]$ $\times \left[\tan L/j\right]$ At x = 0
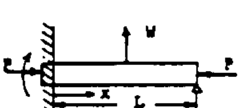 Fixed Simple Beam Concentrated Load	x < L/2: $-\frac{Wj}{2}\left[\frac{j \tan L/j \sec L/2j - L}{j \tan L/j - L}\right]$ x > L/2: $Wj/2\left[\frac{L + 2j \sin L/2j - 2L \cos L/2j}{j \tan L/j - L}\right]$	$\frac{WL}{2}\left[\frac{j \tan L/j(\sec L/2j - 1)}{j \tan L/j - L}\right]$ $\frac{Wj}{2}\left[\frac{L \tan L/j(\sec L/2j - 1)}{j \tan L/j - L} - 2 \sin L/2j\right]$	0 0	$M_{max} =$ $\frac{WL}{2}\left[\frac{j \tan L/j(\sec L/2j - 1)}{j \tan L/j - L}\right]$ At x = 0

TABLE 5.5.1.1 (Cont'd)

BEAM COLUMNS WITH AXIAL COMPRESSION LOADS

LOADING	C_1	C_2	MAX. MOMENT
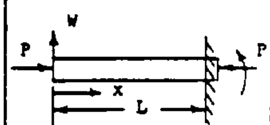 Cantilever-Concentrated End Load			$M_{max} = Wj \tan L/j$ At $x = L$
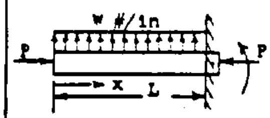 Cantilever-Uniform Load			$M_{max} = wj\left[j(1 - \sec L/j) + L \tan L/j\right]$ At $x = L$
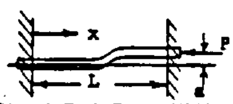 Fixed End Beam With Lateral Displacement			$M_{max} = \dfrac{a\ P \tan L/2j}{2\left[\tan L/2j - L/2j\right]}$ At $x = 0$ And $-M_{max}$ At $x = L$

NOTES:

(1) W or w is positive when upward

(2) M is positive when producing compression in upper fibers

(3) $j = \sqrt{\frac{EI}{P}}$ with a dimension of length.

(4) $D_1 = M_1 - wj^2$; $D_2 = M_2 - wj^2$

(5) All angles for trigonometric functions are in radians.

(6) When the formula for the maximum moment is not provided in the table, methods of differential calculus may be employed, if applicable, to find the location of maximum moment; or moments at several points in a span may be computed and a smooth curve then drawn through the plotted results. The same principle applies in the case of a complicated combination of loadings.

(7) All points where concentrated loads or moments are acting should also be checked for maximum possible bending moments.

(8) Before the total stress can reach the yield point a compression beam column may fail due to buckling. This instability failure is independent of lateral loads and the maximum P that the structure can sustain may be computed pertaining to the boundary condition without regard to lateral loads. A check using ultimate loads should always be made to insure that P is not beyond the critical value.

(9) It is recommended that all calculations should be carried to at least four significant figures.

5.5.2

Beam Columns Subjected to Axial Tension Loads

Since axial tension loads usually tend to decrease the bending moment at any section, beam columns may be designed neglecting the axial loads. If the axial loads are neglected, conservative results will be obtained.

More precise results can be obtained with the equations given below:

Bending Moment $= M = C_1 \sinh \frac{x}{j} + C_2 \cosh \frac{x}{j} + f(w)$ . . . . (6)

Shear $= V = \frac{C_1}{j} \cosh \frac{x}{j} + \frac{C_2}{j} \sinh \frac{x}{j} + f'(w)$ . . . . . . (7)

Deflection $= \delta = \frac{M-M_o}{P}$ . . . . (8)

Slope $= \theta = \frac{V-V_o}{P}$ . . . . (9)

$j = \sqrt{EI/P}$ . . . . (5)

where (M_o) and (V_o) are primary bending moment and shear, respectively. The particular expressions for (C_1), (C_2), and $f(w)$ depend on the character of the transverse load. Table 5.5.2.1 contains (C_1), (C_2), and $f(w)$ for some of the more common types of loading. The load (P) and the distance (x) are as shown on the sketches in Table 5.5.2.1. The moment (M) is positive when producing compression in the upper fibers and (W) or (w) is positive when upward.

Limitations

1. The results obtained from these equations become inaccurate as the ratio M/M_o approaches or becomes more than 0.90 ($M/M_o > .90$).
2. It is recommended that at least four significant figures be used in all calculations.

The following example will illustrate the procedure to be used for a beam column subjected to an axial tension load.

Example:

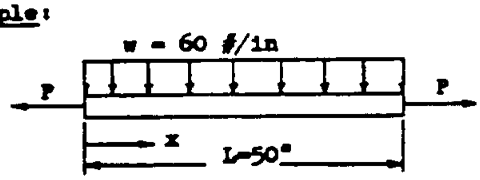

P = 100,000#
w = 60 #/in.
$E = 10 \times 10^6$ psi
$I = 6.75$ in.^{4}
$A = 9.00$ in.^{2}

Find: (M) and (S) at (X = 20")

$$M = C_1 \sinh \frac{X}{j} + C_2 \cosh \frac{X}{j} + f(w) \qquad \text{equation (6)}$$

where:

$$j = \sqrt{\frac{EI}{P}} = \sqrt{\frac{(10\text{x}10^6)6.75}{10^5}} = 25.98 \qquad \text{equation (5)}$$

and from Table 5.5.2.1

$$C_1 = \frac{w\,j^2(1-\cosh L/j)}{\sinh L/j} = \frac{-60(676)(1-\cosh 1.92)}{\sinh 1.92} = 30{,}147.44$$

$$C_2 = w\,j^2 = -60(676) = -40{,}500$$

$$f(w) = -wj = -\left[-60(676)\right] = +40{,}500$$

Then Eq. (6) :

$$M = (30{,}147.44)(\sinh .77) - (40{,}500)(\cosh .77) + 40{,}500$$

$$M = 12{,}964.78 \text{ in-lbs.}$$

From previous example (Axial Compression):

$$M_e = 18{,}000 \text{ in-lbs.}$$

From Eq. (8)

$$\delta = \frac{M-M_o}{P} = \frac{12{,}964.78-18{,}000}{10^5} = -.0595 \text{ inches}$$

Modified Principle of Superposition

The method of superposition can be applied to beam columns in axial tension in the same manner as when the axial load is compression.

TABLE 5.5.2.1

BEAM COLUMNS WITH AXIAL TENSION LOAD

LOADING	C_1	C_2	f (w)	MAX. MOMENT
Unequal End Moments 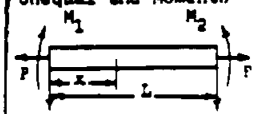	$\frac{M_2 - M_1 \text{ Cosh } L/j}{\text{Sinh } L/j}$	M_1	0	$M_{max} = \frac{M_1}{\text{Cosh } x/j}$ where $\text{Tanh} x/j = \frac{M_2 - M_1 \text{ Cosh} \frac{L}{j}}{-M_1 \text{ Sinh } L/j}$
Equal End Moments 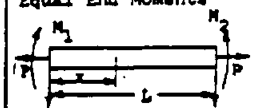	$- M_1 \text{ Tanh } L/2j$	M_1	0	$M_{max} = \frac{M_1}{\text{Cosh } L/2j}$
Uniform Load w #/in 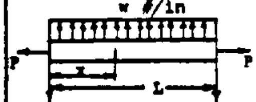	$\frac{wj^2 (1 - \text{Cosh } L/j)}{\text{Sinh } L/j}$	wj^2	$-wj^2$	$M_{max} = j^2(\text{Sech} \frac{L}{2j} - 1)$
Uniform Load Plus End Moments w #/in 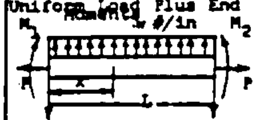	$\frac{D_2 - D_1 \text{ Cosh } L/j}{\text{Sinh } L/j}$ See Note 4	D_1 See Note 4	$-wj^2$	$M_{max} = \frac{D_1}{\text{Cosh} x/j} - wj^2$ where $\text{Tanh} x/j = -\frac{D_2 - D_1 \text{ Cosh} \frac{L}{j}}{D_1 \text{ Sinh } L/j}$ See Note 4
Concentrated Load 	$x < a$: $\frac{-Wj \text{ Sinh } b/j}{\text{Sinh } L/j}$ $x > a$: $\frac{Wj \text{ Sinh } a/j}{\text{Tanh } L/j}$	0 $-Wj \text{ Sinh } a/j$	0 0	$M_{max} = \frac{C_2^2 - C_1^2}{C_2} \text{ Cosh } x/j$ where $\text{Tanh } x/j = -\frac{C_1}{C_2}$
Uniform Increasing Load 	$\frac{wj^2}{\text{Sinh } L/j}$	0	$-\frac{wj^2 x}{L}$	Occurs at: $\text{Cosh} x/j = j/L \text{ Sinh} L/j$ Solve for x/j and x. Substitute into Eq'n (1)
Uniform Decreasing Load 	$-\frac{wj^2}{\text{Tanh } L/j}$	wj^2	$-wj^2(1-\frac{x}{L})$	Occurs at: $\text{Cos} \frac{L-x}{j} = \frac{j}{L} \text{ Sinh} L/j$ Solve for x/j and x and substitute into Eq'n (1)
Symmetrical Triangle Load 	$x < L/2$: $\frac{2wj^3}{L \text{ Cosh } L/2j}$ $x > L/2$: $\frac{-2wj^3 \text{ Cosh } L/j}{L \text{ Cosh } L/2j}$	0 $\frac{4wj^3}{L} \text{ Sinh } L/2j$	$-\frac{2wj^2 x}{L}$ $-2wj^2(1-\frac{x}{L})$	$M_{max} = \frac{2wj^3}{L} \text{Tanh} \frac{L}{2j} - wj^2$

TABLE 5.5.2.1 (Cont d)

BEAM COLUMNS WITH AXIAL TENSION LOAD

LOADING	C_1	C_2	$f(x)$	MAX. MOMENT
Partial Uniformly Distributed Load 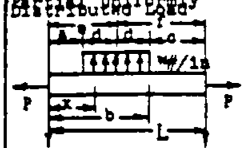	$x < a$: $-\frac{2wj^2 \sinh d/2j \sinh f/j}{\sinh L/j}$ $a < x < b$: $\frac{2wj^2 \sinh d/2j \sinh e/j}{\tanh L/j}$ $b < x < L$: $\frac{2wj^2 \sinh d/2j \sinh e/f}{\tanh L/j}$	0 $-wj^2 \sinh b/j$ $wj^2 \cosh a/j$ $-2wj^2 \sinh d/j \sinh e/f$	0 $-wj^2$ 0	See Note (6)
Symmetrical Partial Uniform Distributed Load 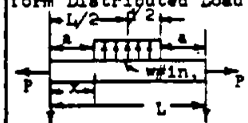	$x < a$: $-\frac{wj^2 \sinh d/2j}{\cosh L/2j}$ $a < x < L-a$: $-wj^2 \cosh a/j \tanh L/2j$ $L-a < x < L$: $\frac{wj^2 \sinh d/2j \cosh L/j}{\cosh L/2j}$	0 $-wj^2 \cosh a/j$ $-2wj^2 \sinh d/2j \sinh L/2j$	0 $-wj^2$ 0	$wj^2 \left[\frac{\cosh a/j}{\cosh L/2j} - 1\right]$ At Midspan
Two Symmetrical Concentrated Loads 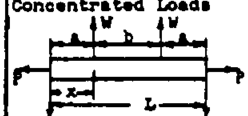	$x < a$: $-\frac{Wj \cosh b/2j}{\cosh L/2j}$ $a < x < L-a$: $Wj \sinh a/j \tanh L/2j$ $L-a < x < L$: $\frac{Wj \cosh L/j \cosh b/2j}{\cosh L/2j}$	0 $-Wj \sinh a/j$ $-\frac{Wj \sinh L/j \cosh b/2j}{\cos L/2j}$	0 0 0	$-Wj \frac{\sinh a/j}{\cosh L/2j}$ At Midspan
Concentrated Moment 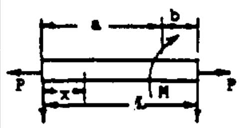	$x < a$: $-\frac{m \cosh b/j}{\sinh L/j}$ $x > a$: $-\frac{m \cosh a/j}{\tanh L/j}$	0 $M \cosh a/j$	0 0	See Note (6)
Fixed End Beam - Uniform Load 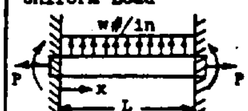	$-\frac{wLj}{2}$	$\frac{wLj}{2 \tanh L/2j}$	$-wj^2$	At $x = 0$ $M_{max} = wj^2 \left[\frac{L/2j}{\tanh L/2j} - 1\right]$
Fixed End Beam-Concentrated Load at Center 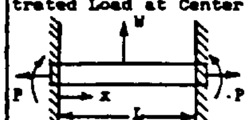	$x < L/2$: $-Wj/2$ $x > L/2$: $\frac{Wj}{2}\left[2 \cosh L/2j - 1\right]$	$\frac{Wj}{2}\left[\frac{\cosh L/2j - 1}{\sinh L/2j}\right]$ $\frac{Wj}{2}\left[\frac{\cos L/2j - \cosh L/j}{\sinh L/2j}\right]$	0 0	$M_{max} = \frac{Wj}{2}\left[\frac{1 - \cosh L/2j}{\sinh L/2j}\right]$ At $x = L/2$
Cantilever-Concentrated End Load 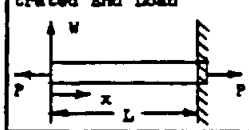				$M_{max} = Wj \tanh L/j$ At $x = L$
Cantilever-Uniform Load 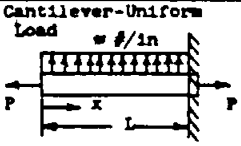				$M_{max} = wj\left[L \tanh L/j - j(1 - \sec L/j)\right]$ At $x = L$

TABLE 5.5.2.1 (Cont'd)

BEAM COLUMNS WITH AXIAL TENSION LOADS

LOADING	C_1	C_2	$f(w)$	MAX. MOMENT
Fixed End Beam-Lateral Displacement 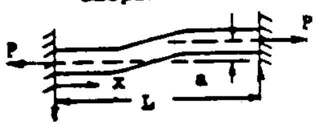				$\frac{a\ P \text{ Tanh } L/2j}{2\left[L/2j - \text{Tanh } L/2j\right]}$ At $x = 0$ And $-M_{max}$ At $x = L$

NOTES:

(1) W or w is positive when upward.

(2) M is positive when producing compression in the upper fibers.

(3) $j = \sqrt{\frac{E\ I}{P}}$ with a dimension of length.

(4) $D_1 = M_1 + wj^2$; $D_2 = M_2 + wj^2$

(5) All angles for hyperbolic functions are in radians.

(6) When formula for maximum moment is not provided in the Table, methods of differential calculus may be employed, if applicable, to find the location of maximum moment; or moments at several points in the span may be computed and a smooth curve drawn thru plotted results. The same principle applies in the case of a complicated combination of loadings.

(7) Values given in Table 5.5.2.1 were obtained from Table 5.5.1.1 by the following substitutions: Sin L/j = i Sinh L/j ; Cos L/j = Cosh L/j ; Sin x/j = i Sinh x/j ; Cos x/j = Cosh L/j and $j = ij$ where $i = \sqrt{-1}$.

(8) All points where concentrated loads or moments are acting should also be checked for possible bending moments.

(9) Axial tension helps to stabilize the structure. Usually, instability failures need not be considered unless the beam is very thin for which bending buckling should be checked.

(10) It is recommended that all calculations should be carried to at least four significant figures.

24

REFERENCES

COLUMNS

Timoshenko, Strength of Materials, Vol. 1 & 2, D. Van Nostrand Co., Inc., 1955; Perry, D. J., Aircraft Structures, McGraw-Hill, 1950; Shanley, F. R., Strength of Materials, McGraw-Hill, 1957

Peery, D. J., Aircraft Structures, McGraw-Hill, 1950

Bell Aircraft Corp., Structures Manual, 1954

R. A. Needham, Thesis, The Ultimate Strength of Aluminum Alloy Formed Shapes in Compression, 1953; R. A. Needham, Thesis, Compression Crippling of Reinforced Sheet, 1953; Convair, Fort Worth Test Data.

Niles, A. S. and Newell, J. S., Airplane Structures, Vol. 1, Fourth Ed., Wiley & Sons, Inc., 1954.

Data Source, Section 1.3 Reference 2

BEAM COLUMNS

Single Span Beam Columns:

Bending Moment $M = C_1 \sin \frac{x}{j} + C_2 \cos \frac{x}{j} + f(w)$

Shear $S = \frac{C_1}{j} \cos \frac{x}{j} - \frac{C_2}{j} \sin \frac{x}{j} + \frac{\partial f(w)}{\partial x}$

Deflection $y = \frac{M_o - M}{P}$

Slope $i = \frac{S_o - S}{P}$

where $j = \sqrt{\frac{EI}{P}}$

C_1 and C_2 are constants given in Tables 4.21 and 4.22. $f(w)$ is a function of loading given in Tables 4.21 and 4.22. M_o and S_o are primary bending moments and shears.

Limitation: In highly stressed beams changes of E due to plasticity will affect the accuracy of the above formulae. This is particularly true when the beam column approaches instability and M, S, y and i increase very rapidly with P.

Superposition: The principle of superposition does not hold for loadings involving different axial loads. However, the effects of transverse loadings may be superimposed as follows:

When an axial load P combined with a transverse loading A produces moments, sheafs, etc. M_A, S_A, y_A, i_A
and the identical axial load P combined with a transverse loading B produces moments, shears, etc. M_B, S_B, y_B, i_B
then the same axial load P combined with loadings A and B acting simultaneously will produce moments, shears, etc.
$M = M_A + M_B$, $S = S_A + S_B$, $y = y_A + y_B$,
$i = i_A + i_B$

TABLE 4.21

TERMS FOR BEAM-COLUMN FORMULAS

AXIAL COMPRESSION

Ref. Airplane Structures Vol. #2, Niles & Newell, 2nd Edition.

LOADING		C_1	C_2	$f(w)$
END MOMENTS	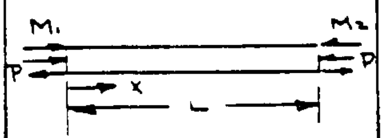	$\frac{M_2 - M_1 \cos\frac{L}{j}}{\sin\frac{L}{j}}$	M_1	0
EQUAL END MOMENTS	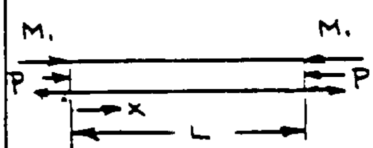	$M_1 \tan\frac{L}{2j}$	M_1	0
UNIFORM	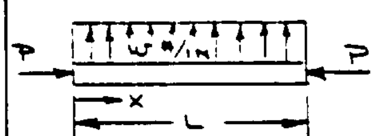	$\frac{wj^2(\cos\frac{L}{j} - 1)}{\sin\frac{L}{j}}$	$-wj^2$	wj^2
UNIFORM PLUS END MOMENTS	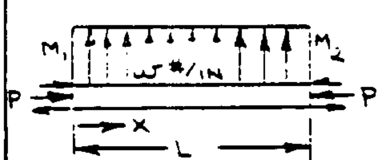	$\frac{D_2 - D_1 \cos\frac{L}{j}}{\sin\frac{L}{j}}$ $D_1 = M_1 - wj^2$ $D_2 = M_2 - wj^2$	D_1	wj^2
CONCENTRATED LOAD	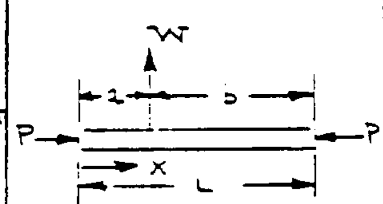	$x<a,\ -\frac{Wj\sin\frac{b}{j}}{\sin\frac{L}{j}}$ $x>a,\ +\frac{Wj\sin\frac{a}{j}}{\tan\frac{L}{j}}$	0 $-Wj\sin\frac{a}{j}$	0 0

TABLE 4.22

TABLE FOR BEAM-COLUMN FORMULAS

AXIAL COMPRESSION

Ref. Airplane Structures Vol. #2, Niles & Newell, 2nd Edition.

LOADING		C_1	C_2	$f(w)$
CONCENTRATED LOAD AT $X = \frac{L}{2}$	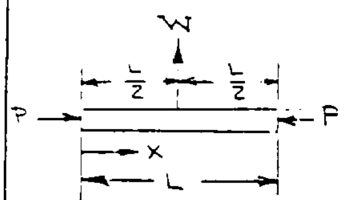	$X < \frac{L}{2}$; $-\frac{Wj}{2}\sec\frac{L}{2j}$ $X > \frac{L}{2}$; $\frac{Wj}{2}\cos\frac{L}{j}\sec\frac{L}{2j}$	0 $-Wj\sin\frac{L}{2j}$	0 0
UNIFORMLY VARYING INCREASING TO RIGHT	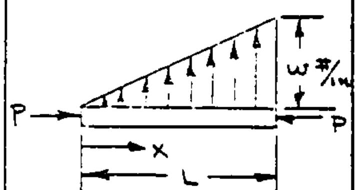	$-\frac{wj^2}{\sin\frac{L}{j}}$	0	$\frac{wj^2 x}{L}$
UNIFORMLY VARYING DECREASING TO RIGHT	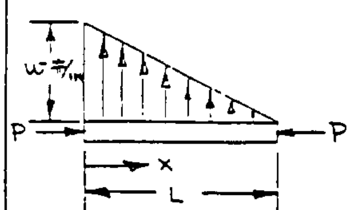	$\frac{wj^2}{\tan\frac{L}{j}}$	$-wj^2$	$wj^2(1-\frac{x}{L})$
SYMMETRICAL TRIANGLE	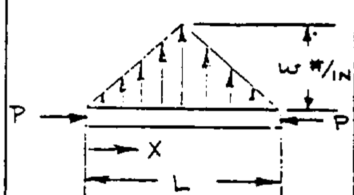	$X < \frac{L}{2}$; $-\frac{2wj^3}{L\cos\frac{L}{2j}}$ $X > \frac{L}{2}$; $\frac{2wj^3\cos\frac{L}{j}}{L\cos\frac{L}{2j}}$	0 $-\frac{4wj^3}{L}\sin\frac{L}{2j}$	$\frac{2wj^2 x}{L}$ $2wj^2(1-\frac{x}{L})$
PARTIAL UNIFORMLY DISTRIBUTED	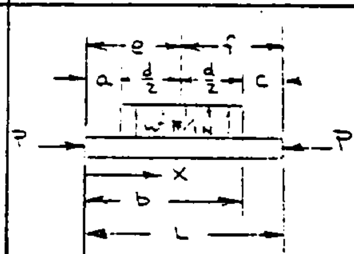	$x < a$ $-2wj^2\sin\frac{d}{2j}\sin\frac{f}{j} / \sin\frac{L}{j}$ $a < x < b$ $\frac{2wj^2\sin\frac{d}{2j}\sin\frac{e}{j}}{\tan\frac{L}{j}} - wj^2\sin\frac{a}{j}$ $b < x < L$ $\frac{2wj^2\sin\frac{d}{2j}\sin\frac{e}{j}}{\tan L/j}$	0 $-wj^2\cos\frac{a}{j}$ $-2wj\sin\frac{d}{2j}\sin\frac{e}{j}$	0 wj^2 0

TABLE 4.23

TERMS FOR BEAM-COLUMN FORMULAS

AXIAL COMPRESSION

Ref. Airplane Structures Vol. 2, Niles & Newell, 2nd Edition.

LOADING		C_1	C_2	$f(x)$
SYMMETRICAL PARTIAL UNIFORMLY DISTRIBUTED	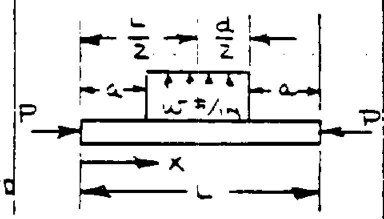	$x < a$		
		$-wj^2 \sin\frac{d}{2j} \sec\frac{L}{2j}$	0	0
		$a < x < L-a$		
		$-wj^2 \tan\frac{L}{2j} \cos\frac{a}{j}$	$-wj^2 \cos\frac{a}{j}$	wj^2
		$L-a < x < L$		
		$wj^2 \sin\frac{d}{2j} \sec\frac{L}{2j} \cos\frac{L}{j}$	$-2wj^2 \sin\frac{d}{2j} \sin\frac{L}{2j}$	0
TWO SYMMETRICAL CONCENTRATED LOADS	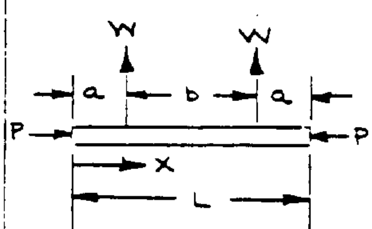	$x < a$		
		$-Wj \frac{\cos\frac{b}{2j}}{\cos\frac{L}{2j}}$	0	0
		$a < x < L-a$		
		$-Wj \sin\frac{a}{j} \tan\frac{L}{2j}$	$-Wj \sin\frac{a}{j}$	0
		$L-a < x < L$		
		$Wj \frac{\cos\frac{L}{j} \cos\frac{b}{2j}}{\cos L/2j}$	$Wj \frac{\sin\frac{L}{j} \cos\frac{b}{2j}}{\cos\frac{L}{2j}}$	0
CLOCKWISE COUPLE	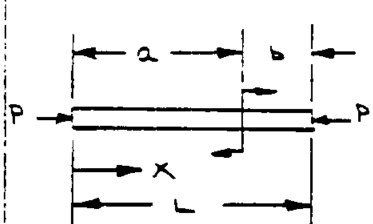	$x < a$		
		$-\frac{m \cos\frac{b}{j}}{\sin\frac{L}{j}}$	0	0
		$x > a$		
		$-\frac{m \cos\frac{a}{j}}{\tan\frac{L}{j}}$	$m \cos\frac{a}{j}$	0

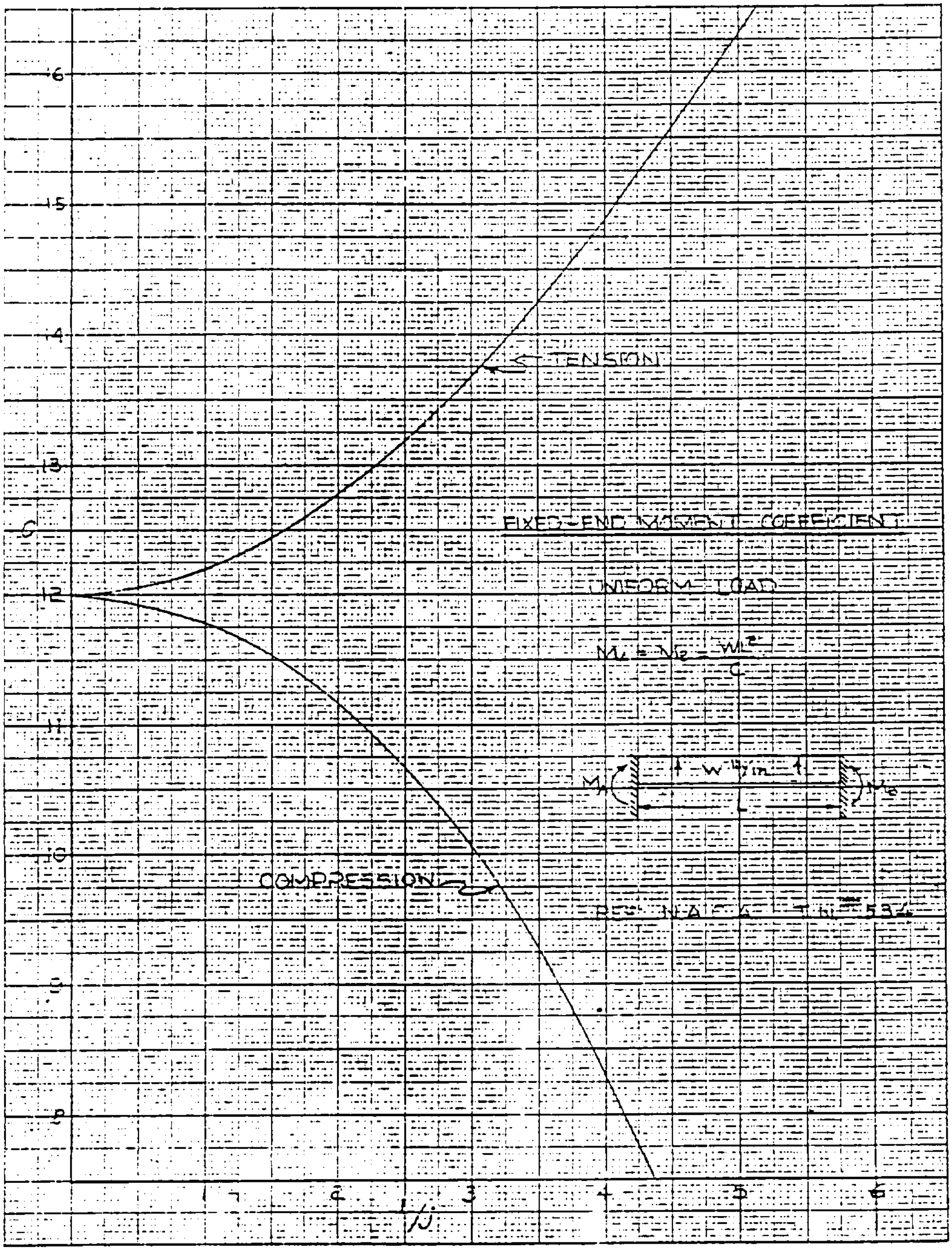
TENSION
COMPRESSION
FIXED-END MOMENT COEFFICIENT
UNIFORM LOAD
C
12
1
2
3
4
5
6

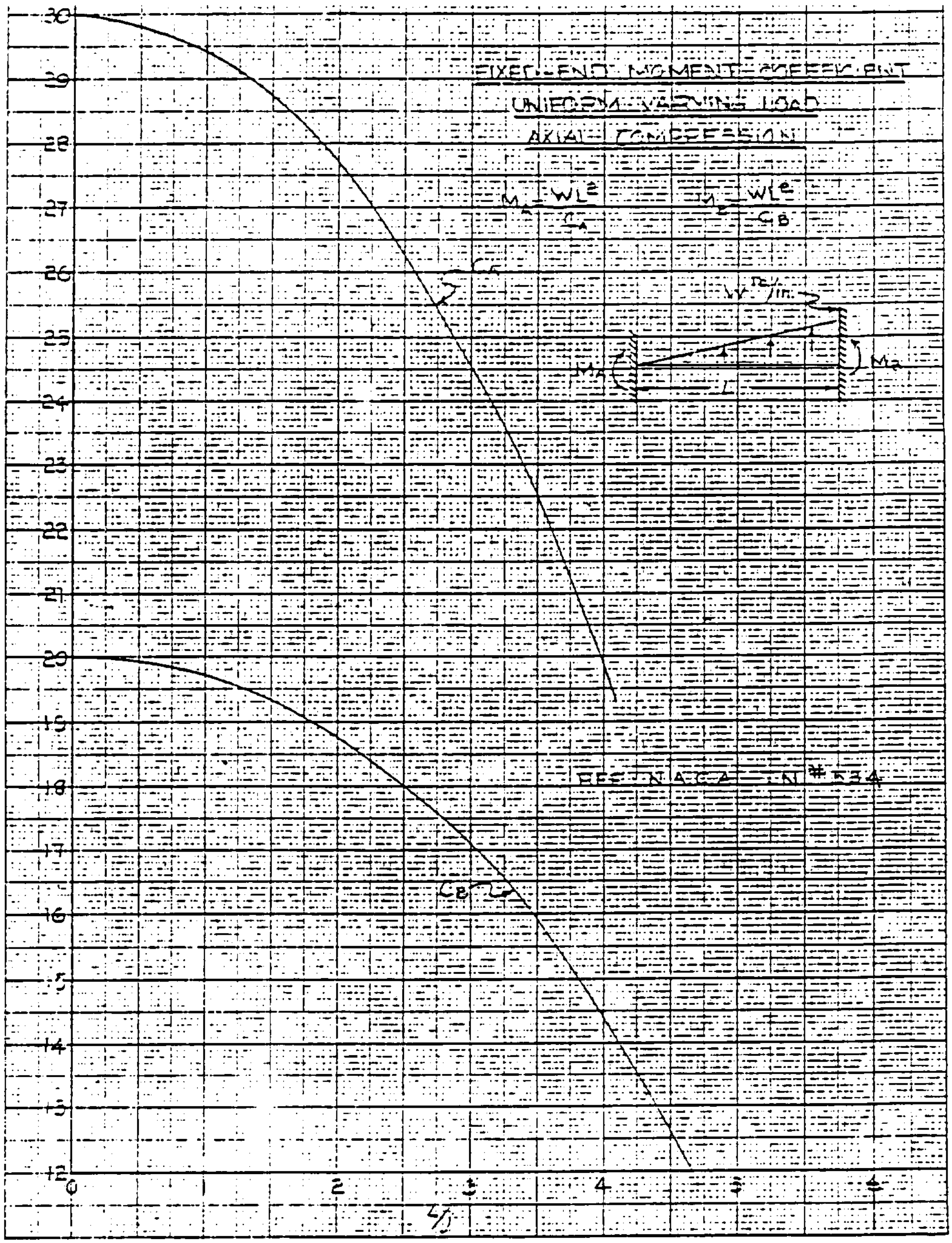
FIXED-END MOMENT COEFFICIENT
UNIFORMLY VARYING LOAD
AXIAL COMPRESSION
$M_A = \frac{WL^2}{C_A}$
$M_B = \frac{WL^2}{C_B}$
C_A
C_B
M_A
M_B
L
REF. N.A.C.A. TN #534
30
29
28
27
26
25
24
23
22
21
20
19
18
17
16
15
14
13
12
0
1
2
3
4
5
6

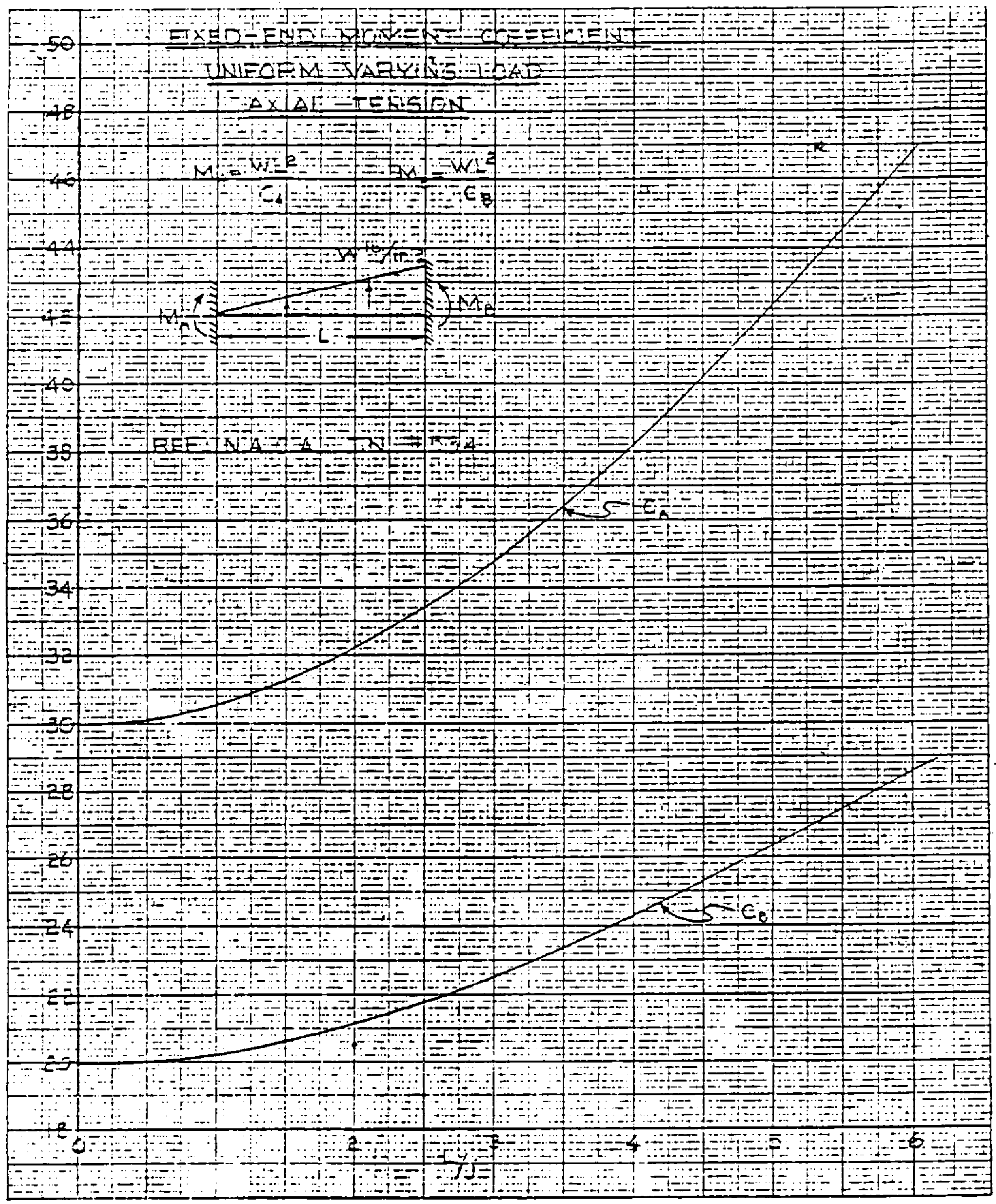
FIXED-END MOMENT COEFFICIENT
UNIFORM VARYING LOAD
AXIAL TENSION
M_A = WL²/C_A
M_B = WL²/C_B
W lb/in
M_A
M_B
L
REF. NACA TN 534
C_A
C_B
50
48
46
44
42
40
38
36
34
32
30
28
26
24
22
20
18
0
2
3
4
5
6
L/J

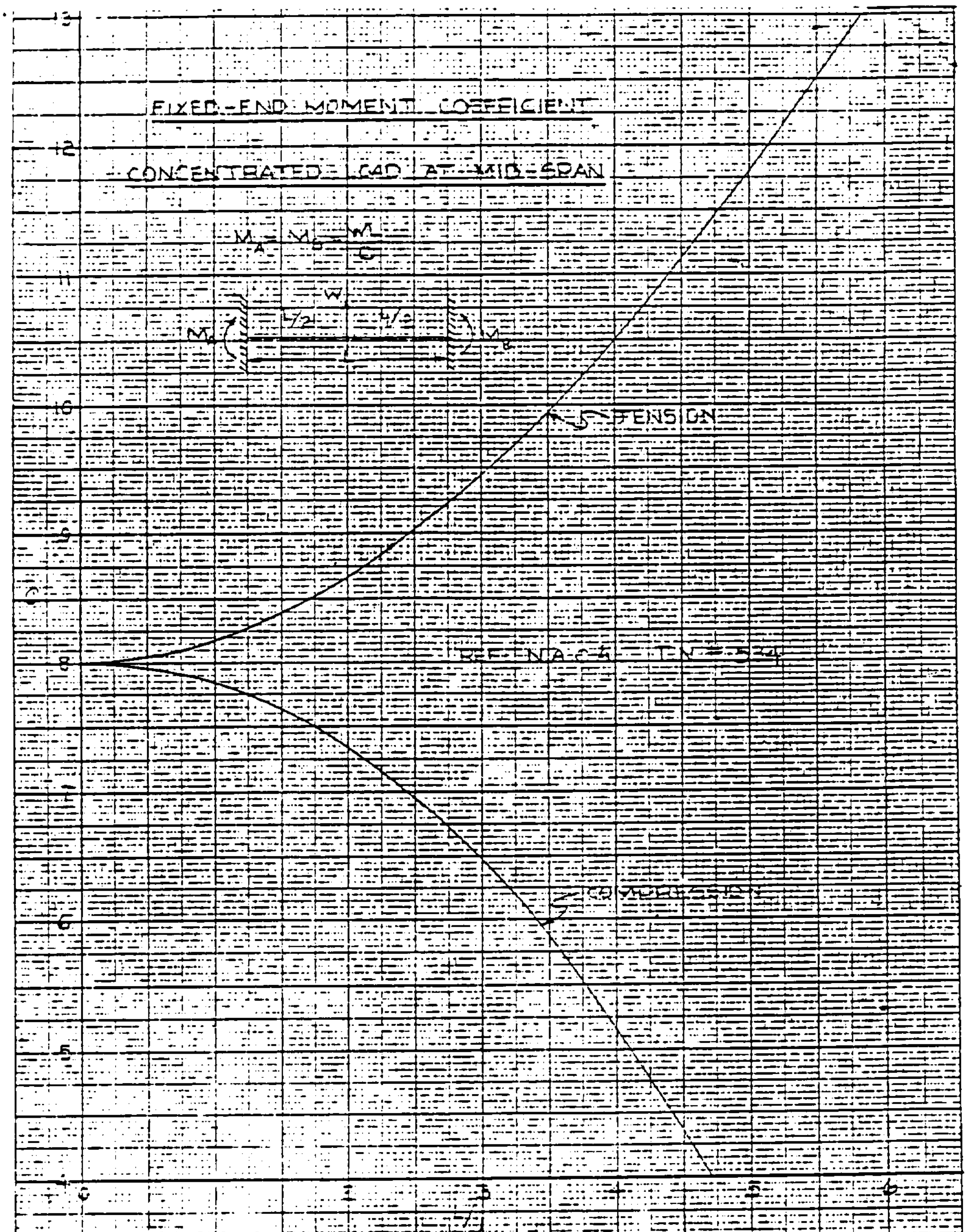
FIXED-END MOMENT COEFFICIENT
CONCENTRATED LOAD AT MID-SPAN
TENSION
13
12
11
10
9
8
6
5
4
0
1
3
4
5
6

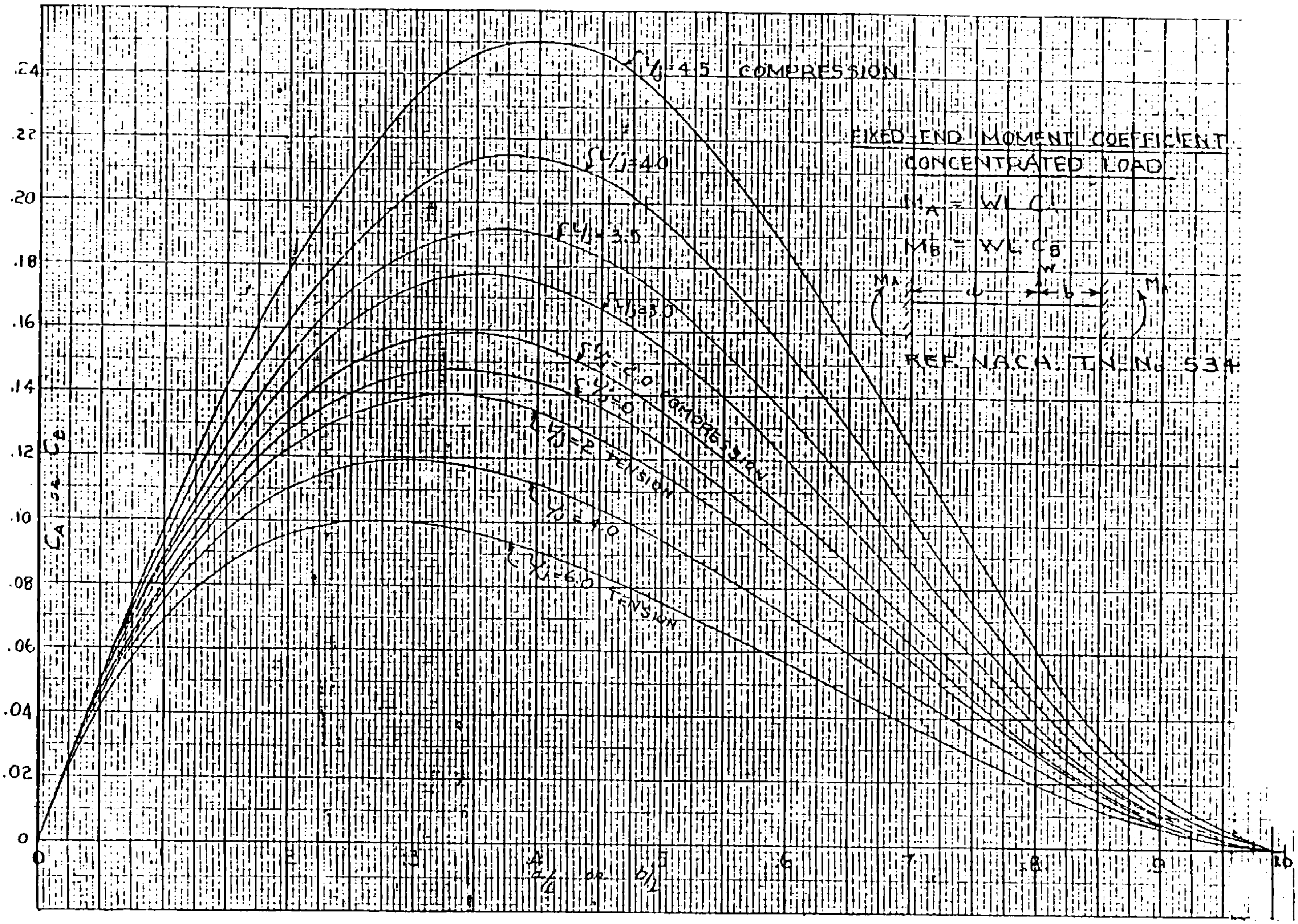
FIXED END MOMENT COEFFICIENT
CONCENTRATED LOAD
MA = WL CA
MB = WL CB
REF. N.A.C.A. T.N. No. 534
L/j = 4.5 COMPRESSION
L/j = 4.0
L/j = 3.5
L/j = 3.0
L/j = 2.0
L/j = 2.0 COMPRESSION
L/j = 2 TENSION
L/j = 4.0
L/j = 6.0 TENSION
CA or CB
a/L or b/L
.24
.22
.20
.18
.16
.14
.12
.10
.08
.06
.04
.02
0
.1
.2
.3
.4
.5
.6
.7
.8
.9
1.0

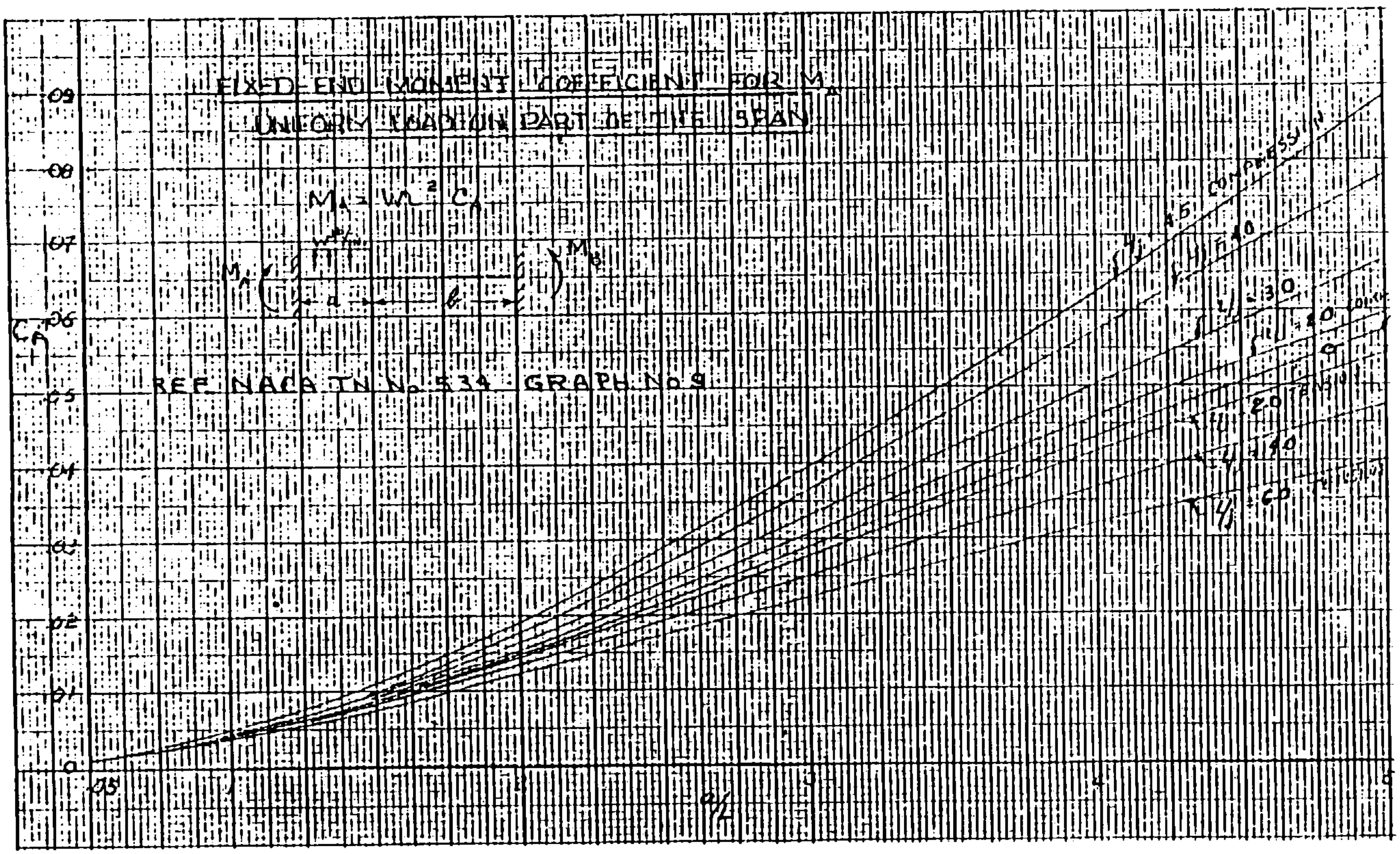
FIXED END MOMENT COEFFICIENT FOR M_A
UNIFORM LOAD ON PART OF THE SPAN
$M_A = wL^2 C_A$
REF. NACA TN No. 534 GRAPH No. 9
C_A
a/L
COMPRESSION
TENSION

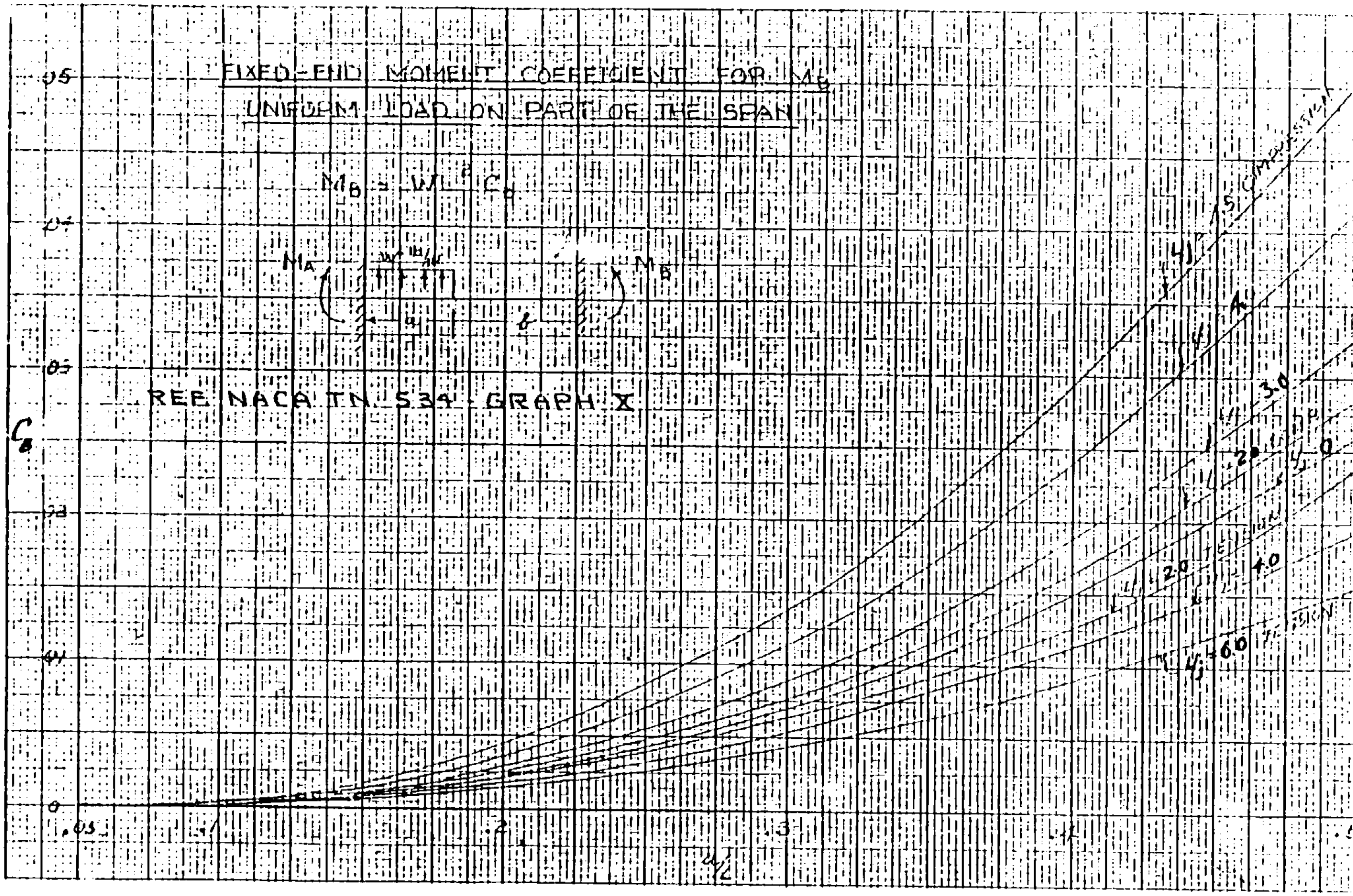
FIXED-END MOMENT COEFFICIENT FOR M_B
UNIFORM LOAD ON PART OF THE SPAN
$M_B = WL^2 C_d$
M_A
M_B
a
b
REF. NACA T.N. 534 GRAPH X
C_d
.05
.04
.03
.02
.01
0
.05
.1
.2
.3
.4
.5
a/L
COMPRESSION
TENSION
3.0
2.0
1.0
4.0
6.0

Continuous Beam Columns

Three-Moment Equation

$$\frac{M_A L_1 \alpha_1}{I_1} + \frac{2M_B L_1 \beta_1}{I_1} + \frac{2M_B L_2 \beta_2}{I_2} + \frac{M_C L_2 \alpha_2}{I_2} =$$

$$K_1 + K_2 + \frac{6E(y_A - y_B)}{L_1} + \frac{6E(y_C - y_B)}{L_2}$$

where $j = \sqrt{\frac{EI}{P}}$

Where K_1 and K_2 are functions of loading on Bay 1 and Bay 2, respectively. Values for α, β and are tabulated on pages 5.6.15 To 5.6.22. K_1 and K_2 are tabulated below:

(Ref. Airplane Structures by Niles & Newell Vol. #II, 2nd Edition)

Loading		Terms for Three-moment Equation	
		Left Bay K_1	Right Bay K_2
End Moments	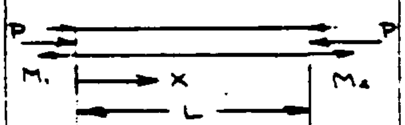	0	0
Equal End Moments	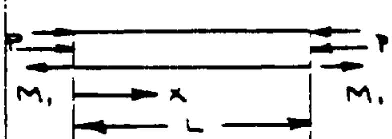	0	0
Uniform	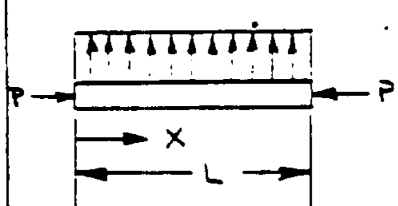	$\frac{w_1 L_1^3 \gamma_1}{4I_1}$	$\frac{w_2 L_2^3 \gamma_2}{4I_2}$

BEAM COLUMN COEFFICIENTS

LOADING		TERMS FOR THREE-MOMENT EQUATION LEFT BAY K_1	TERMS FOR THREE-MOMENT EQUATION RIGHT BAY K_2
UNIFORM PLUS END MOMENTS	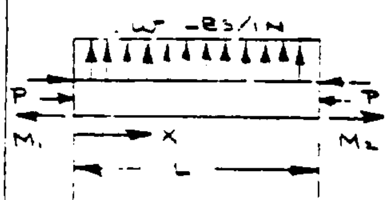	$\frac{w_1 L_1^3 \gamma_1}{4 I_1}$	$\frac{w_2 L_2^3 \gamma_2}{4 I_2}$
CONCENTRATED LOAD	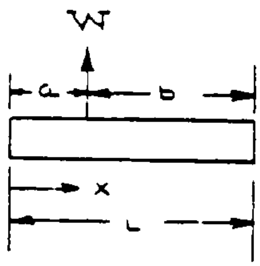	$\frac{6 W_1 j_1^2}{I_1}\left[\frac{\sin\frac{a_1}{j_1}}{\sin\frac{L_1}{j_1}} - \frac{a_1}{L_1}\right]$	$\frac{6 W_2 j_2^2}{I_2}\left[\frac{\sin\frac{b_2}{j_2}}{\sin\frac{L_2}{j_2}} - \frac{b_2}{L_2}\right]$
CONCENTRATED LOAD AT $x = \frac{L}{2}$	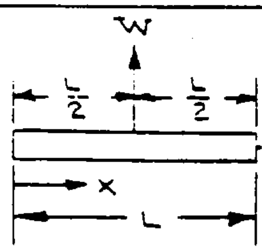	$\frac{3 W_1 j_1^2}{I_1}\left[\sec\frac{L_1}{2 j_1} - 1\right]$	$\frac{3 W_2 j_2^2}{I_2}\left[\sec\frac{L_2}{2 j_2} - 1\right]$
UNIFORMLY VARYING INCREASING TO RIGHT	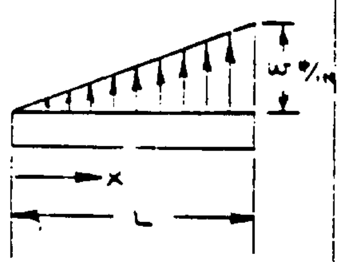	$\frac{2 w_1 L_1 j_1^2 (\beta_1 - 1)}{I_1}$	$\frac{w_2 L_2 j_2^2 (\alpha_2 - 1)}{I_2}$
UNIFORMLY VARYING DECREASING TO RIGHT	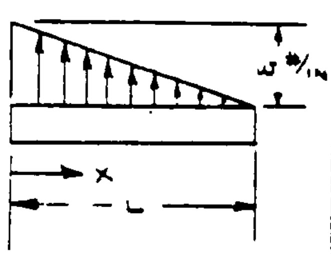	$\frac{w_1 L_1 j_1^2 (\alpha_1 - 1)}{I_1}$	$\frac{2 w_2 L_2 j_2^2 (\beta - 1)}{I_2}$

735

BEAM COLUMN COEFFICIENTS

LOADING		TERMS FOR THREE-MOMENT EQUATION	
		LEFT BAY K_1	RIGHT BAY K_2
SYMMETRICAL TRIANGLE	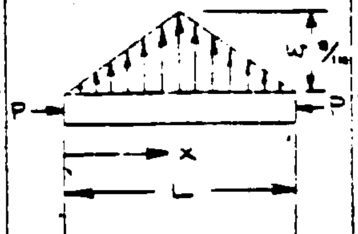	$\frac{12 w_1 j_1^2}{I_1}\left[\frac{4 j_1^2}{L_1}\left(\sec\frac{L_1}{2j_1}-1\right)-\frac{L_1}{8}\right]$	$\frac{12 w_2 j_2^2}{I_2}\left[\frac{4 j_2^2}{L_2}\left(\sec\frac{L_2}{2j_2}-1\right)-\frac{L_2}{8}\right]$
PARTIAL UNIFORMLY DISTRIBUTED	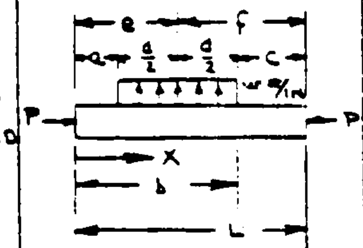	$\frac{12 w_1 j_1^2}{I_1}\left[\frac{j_1 \sin\frac{f_1}{j_1}\sin\frac{d_1}{2j_1}}{\sin\frac{L_1}{j_1}}-\frac{d_1 e_1}{2L_1}\right]$	$\frac{12 w_2 j_2}{I_2}\left[\frac{j_2 \sin\frac{f_2}{j_2}\sin\frac{d_2}{2j_2}}{\sin\frac{L_2}{j_2}}-\frac{d_2 f_2}{2L_2}\right]$
SYMMETRICAL PARTIAL UNIFORMLY DISTRIBUTED	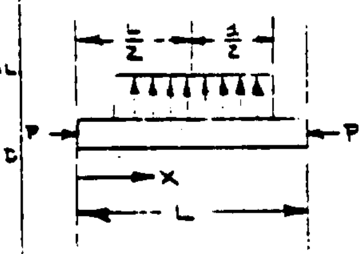	$\frac{3 w_1 j_1^2}{I_1}\left[\frac{2 j_1 \sin\frac{d_1}{2j_1}}{\cos\frac{L_1}{2j_1}}-d_1\right]$	$\frac{3 w_2 j_2^2}{I_2}\left[\frac{2 j_2 \sin\frac{d_2}{2j_2}}{\cos\frac{L_2}{2j_2}}-d_2\right]$
TWO SYMMETRICAL CONCENTRATED LOADS	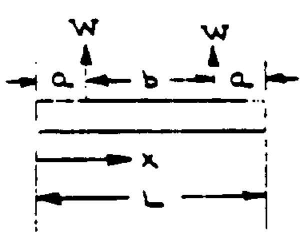	$\frac{6 W_1 j_1^2}{I_1}\left[\frac{\cos\frac{b_1}{2j_1}}{\cos\frac{L_1}{2j_1}}-1\right]$	$\frac{6 W_2 j_2^2}{I_2}\left[\frac{\cos\frac{b_2}{2j_2}}{\cos\frac{L_2}{2j_2}}-1\right]$
CLOCKWISE COUPLE	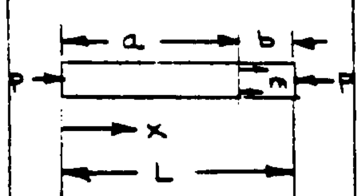	$\frac{6 m_1 j_1}{I_1}\left[\frac{j_1}{L_1}-\frac{\cos\frac{a_1}{j_1}}{\sin\frac{L_1}{j_1}}\right]$	$\frac{6 m_2 j_2}{I_2}\left[\frac{\cos\frac{b_2}{j_2}}{\sin\frac{L_2}{j_2}}-\frac{j_2}{L_2}\right]$

FUNCTIONS FOR THREE-MOMENT EQUATIONS WITH AXIAL COMPRESSION.

REF. "AIRPLANE STRUCTURES" BY NILES & NEWALL. VOL. II 2ND. EDITION

$$\alpha = \frac{6\left(L/j \operatorname{cosec} L/j - 1\right)}{(L/j)^2}$$

$$\beta = \frac{3\left(1 - L/j \cot L/j\right)}{(L/j)^2} \qquad j = \sqrt{\frac{EI}{P}}$$

$$\gamma = \frac{3\left(\tan L/2j - L/2j\right)}{(L/2j)^3}$$

GENERAL RELATIONSHIP: $\alpha + 2\beta - 3 = \gamma\,(L/2j)^2$

L/j	α	$\Delta\alpha$	β	$\Delta\beta$	γ	$\Delta\gamma$	L/j
0	1.0000		1.0000		1.0000		0
		0.0008		0.0007		0.0010	
0.10	1.0008		1.0007		1.0010		0.10
		0.0039		0.0020		0.0030	
0.20	1.0047		1.0027		1.0040		0.20
		0.0059		0.0034		0.0051	
0.30	1.0106		1.0061		1.0091		0.30
		0.0083		0.0047		0.0072	
0.40	1.0189		1.0108		1.0163		0.40
		0.0110		0.0063		0.0094	
0.50	1.0299		1.0171		1.0257		0.50
		0.0132		0.0078		0.0117	
0.60	1.0437		1.0249		1.0374		0.60
		0.0166		0.0094		0.0142	
0.70	1.0603		1.0343		1.0515		0.70
		0.0198		0.0111		0.0168	
0.80	1.0801		1.0454		1.0684		0.80
		0.0232		0.0131		0.0198	
0.90	1.1033		1.0585		1.0882		0.90
		0.0271		0.0152		0.0231	
1.00	1.1304		1.0737		1.1113		1.00
		0.0151		0.0085		0.0128	
1.05	1.1455		1.0822		1.1241		1.05
		0.0162		0.0090		0.0138	
1.10	1.1617		1.0912		1.1379		1.10
		0.0175		0.0097		0.0148	
1.15	1.1792		1.1009		1.1527		1.15
		0.0187		0.0105		0.0159	
1.20	1.1979		1.1114		1.1686		1.20
		0.0201		0.0111		0.0170	
1.25	1.2180		1.1225		1.1856		1.25
		0.0216		0.0120		0.0183	
1.30	1.2396		1.1345		1.2039		1.30
		0.0232		0.0128		0.0196	
1.35	1.2628		1.1473		1.2235		1.35
		0.0250		0.0137		0.0210	

FUNCTIONS FOR THREE-MOMENT EQUATIONS WITH AXIAL COMPRESSION (Contd.)

L/j	α	$\Delta\alpha$	β	$\Delta\beta$	γ	$\Delta\gamma$	L/j
1.40	1.2878		1.1610		1.2445		1.40
		0.0268		0.0147		0.0226	
1.45	1.3146		1.1757		1.2671		1.45
		0.0288		0.0158		0.0243	
1.50	1.3434		1.1915		1.2914		1.50
		0.0310		0.0169		0.0260	
1.55	1.3744		1.2084		1.3174		1.55
		0.0334		0.0182		0.0281	
1.60	1.4078		1.2266		1.3455		1.60
		0.0361		0.0196		0.0303	
1.65	1.4439		1.2462		1.3758		1.65
		0.0391		0.0211		0.0327	
1.70	1.4830		1.2673		1.4085		1.70
		0.0422		0.0228		0.0353	
1.75	1.5252		1.2901		1.4438		1.75
		0.0458		0.0246		0.0383	
1.80	1.5710		1.3147		1.4821		1.80
		0.0498		0.0267		0.0416	
1.85	1.6208		1.3414		1.5237		1.85
		0.0542		0.0290		0.0452	
1.90	1.6750		1.3704		1.5689		1.90
		0.0593		0.0316		0.0493	
1.95	1.7343		1.4020		1.6192		1.95
		0.0650		0.0345		0.0540	
2.00	1.7993		1.4365		1.6722		2.00
		0.0137		0.0073		0.0114	
2.01	1.8130		1.4438		1.6836		2.01
		0.0140		0.0074		0.0117	
2.02	1.8270		1.4512		1.6953		2.02
		0.0143		0.0075		0.0118	
2.03	1.8413		1.4587		1.7071		2.03
		0.0145		0.0077		0.0121	
2.04	1.8558		1.4664		1.7192		2.04
		0.0148		0.0078		0.0122	
2.05	1.8706		1.4742		1.7314		2.05
		0.0152		0.0080		0.0126	
2.06	1.8858		1.4822		1.7440		2.06
		0.0154		0.0082		0.0128	
2.07	1.9012		1.4904		1.7568		2.07
		0.0156		0.0083		0.0130	
2.08	1.9168		1.4987		1.7698		2.08
		0.0161		0.0084		0.0134	
2.09	1.9329		1.5071		1.7832		2.09
		0.0164		0.0087		0.0135	
2.10	1.9493		1.5158		1.7967		2.10
		0.0168		0.0088		0.0139	
2.11	1.9661		1.5246		1.8106		2.11
		0.0170		0.0090		0.0141	

FUNCTIONS FOR THREE-MOMENT EQUATIONS WITH AXIAL COMPRESSION (Contd.)

L/j	α	$\Delta\alpha$	β	$\Delta\beta$	γ	$\Delta\gamma$	L/j
2.12	1.9831		1.5336		1.8247		2.12
		0.0174		0.0091		0.0145	
2.13	2.0005		1.5427		1.8392		2.13
		0.0179		0.0094		0.0147	
2.14	2.0184		1.5521		1.8539		2.14
		0.0182		0.0095		0.0150	
2.15	2.0366		1.5616		1.8689		2.15
		0.0186		0.0097		0.0154	
2.16	2.0552		1.5713		1.8843		2.16
		0.0189		0.0100		0.0157	
2.17	2.0741		1.5813		1.9000		2.17
		0.0194		0.0101		0.0160	
2.18	2.0935		1.5914		1.9160		2.18
		0.0198		0.0104		0.0163	
2.19	2.1133		1.6018		1.9323		2.19
		0.0203		0.0106		0.0168	
2.20	2.1336		1.6124		1.9491		2.20
		0.0207		0.0109		0.0172	
2.21	2.1543		1.6233		1.9663		2.21
		0.0211		0.0110		0.0174	
2.22	2.1754		1.6343		1.9837		2.22
		0.0218		0.0114		0.0179	
2.23	2.1972		1.6457		2.0016		2.23
		0.0222		0.0115		0.0183	
2.24	2.2194		1.6572		2.0199		2.24
		0.0228		0.0118		0.0187	
2.25	2.2422		1.6690		2.0386		2.25
		0.0232		0.0122		0.0192	
2.26	2.2654		1.6812		2.0578		2.26
		0.0237		0.0124		0.0197	
2.27	2.2891		1.6936		2.0775		2.27
		0.0244		0.0126		0.0201	
2.28	2.3135		1.7062		2.0976		2.28
		0.0249		0.0130		0.0205	
2.29	2.3384		1.7192		2.1181		2.29
		0.0256		0.0133		0.0211	
2.30	2.3640		1.7325		2.1392		2.30
		0.0262		0.0136		0.0216	
2.31	2.3902		1.7461		2.1608		2.31
		0.0269		0.0140		0.0222	
2.32	2.4171		1.7601		2.1830		2.32
		0.0277		0.0143		0.0227	
2.33	2.4448		1.7744		2.2057		2.33
		0.0283		0.0147		0.0233	
2.34	2.4731		1.7891		2.2290		2.34
		0.0291		0.0150		0.0239	
2.35	2.5022		1.8041		2.2529		2.35
		0.0298		0.0154		0.0245	
2.36	2.5320		1.8195		2.2774		2.36
		0.0305		0.0159		0.0251	

FUNCTIONS FOR THREE-MOMENT EQUATIONS WITH AXIAL COMPRESSION (Contd.)

L/j	α	$\Delta\alpha$	β	$\Delta\beta$	γ	$\Delta\gamma$	L/j
2.37	2.5625		1.8354		2.3025		2.37
		0.0314		0.0162		0.0259	
2.38	2.5939		1.8516		2.3284		2.38
		0.0323		0.0167		0.0266	
2.39	2.6262		1.8683		2.3550		2.39
		0.0334		0.0171		0.0272	
2.40	2.6596		1.8854		2.3822		2.40
		0.0339		0.0177		0.0281	
2.41	2.6935		1.9031		2.4103		2.41
		0.0352		0.0181		0.0288	
2.42	2.7287		1.9212		2.4391		2.42
		0.0362		0.0186		0.0296	
2.43	2.7649		1.9398		2.4687		2.43
		0.0372		0.0191		0.0306	
2.44	2.8021		1.9589		2.4993		2.44
		0.0382		0.0197		0.0313	
2.45	2.8403		1.9786		2.5306		2.45
		0.0395		0.0203		0.0324	
2.46	2.8798		1.9989		2.5630		2.46
		0.0406		0.0209		0.0334	
2.47	2.9204		2.0198		2.5964		2.47
		0.0420		0.0215		0.0343	
2.48	2.9624		2.0413		2.6307		2.48
		0.0432		0.0222		0.0355	
2.49	3.0056		2.0635		2.6662		2.49
		0.0446		0.0229		0.0365	
2.50	3.0502		2.0864		2.7027		2.50
		0.0461		0.0236		0.0378	
2.51	3.0963		2.1100		2.7405		2.51
		0.0475		0.0243		0.0389	
2.52	3.1438		2.1343		2.7794		2.52
		0.0493		0.0252		0.0403	
2.53	3.1931		2.1595		2.8197		2.53
		0.0506		0.0260		0.0415	
2.54	3.2437		2.1855		2.8612		2.54
		0.0526		0.0269		0.0431	
2.55	3.2963		2.2124		2.9043		2.55
		0.0545		0.0278		0.0445	
2.56	3.3508		2.2402		2.9488		2.56
		0.0564		0.0288		0.0461	
2.57	3.4072		2.2690		2.9949		2.57
		0.0585		0.0298		0.0478	
2.58	3.4657		2.2988		3.0427		2.58
		0.0605		0.0309		0.0495	
2.59	3.5262		2.3297		3.0922		2.59
		0.0628		0.0321		0.0513	
2.60	3.5890		2.3618		3.1435		2.60
		0.0652		0.0332		0.0533	
2.61	3.6542		2.3950		3.1968		2.61
		0.0678		0.0345		0.0554	

FUNCTIONS FOR THREE-MOMENT EQUATIONS WITH AXIAL COMPRESSION (Contd.)

L/j	α	$\Delta\alpha$	β	$\Delta\beta$	γ	$\Delta\gamma$	L/j
2.62	3.7220	0.0705	2.4295	0.0359	3.2522	0.0575	2.62
2.63	3.7925	0.0734	2.4654	0.0373	3.3097	0.0599	2.63
2.64	3.8659	0.0762	2.5027	0.0388	3.3696	0.0623	2.64
2.65	3.9421	0.0797	2.5415	0.0404	3.4319	0.0650	2.65
2.66	4.0218	0.0829	2.5819	0.0422	3.4969	0.0677	2.66
2.67	4.1047	0.0867	2.6241	0.0439	3.5646	0.0707	2.67
2.68	4.1914	0.0906	2.6680	0.0460	3.6353	0.0739	2.68
2.69	4.2820	0.0946	2.7140	0.0479	3.7092	0.0771	2.69
2.70	4.3766	0.0991	2.7619	0.0502	3.7863	0.0808	2.70
2.71	4.4757	0.1038	2.8121	0.0527	3.8671	0.0846	2.71
2.72	4.5795	0.1090	2.8648	0.0551	3.9517	0.0888	2.72
2.73	4.6885	0.1144	2.9199	0.0579	4.0405	0.0932	2.73
2.74	4.8029	0.1204	2.9778	0.0608	4.1337	0.0980	2.74
2.75	4.9233	0.1266	3.0386	0.0641	4.2317	0.1032	2.75
2.76	5.0499	0.1336	3.1027	0.0675	4.3349	0.1087	2.76
2.77	5.1835	0.1410	3.1702	0.0712	4.4436	0.1148	2.77
2.78	5.3245	0.1491	3.2414	0.0752	4.5564	0.1213	2.78
2.79	5.4736	0.1579	3.3166	0.0797	4.6797	0.1285	2.79
2.80	5.6315	0.1675	3.3963	0.0844	4.8082	0.1362	2.80
2.81	5.7990	0.1780	3.4807	0.0897	4.9444	0.1448	2.81
2.82	5.9770	0.1894	3.5704	0.0955	5.0892	0.1540	2.82
2.83	6.1664	0.2021	3.6659	0.1017	5.2432	0.1643	2.83
2.84	6.3685	0.2160	3.7676	0.1088	5.4075	0.1757	2.84
2.85	6.5845	0.2315	3.8764	0.1164	5.5832	0.1881	2.85
2.86	6.8160	0.2486	3.9928	0.1251	5.7713	0.2020	2.86

FUNCTIONS FOR THREE-MOMENT EQUATIONS WITH AXIAL COMPRESSION (Contd.)

L/j	α	$\Delta\alpha$	β	$\Delta\beta$	γ	$\Delta\gamma$	L/j
2.87	7.0646		4.1179		5.9733		2.87
		0.2676		0.1346		0.2174	
2.88	7.3322		4.2525		6.1907		2.88
		0.2890		0.1452		0.2348	
2.89	7.6212		4.3977		6.4255		2.89
		0.3131		0.1573		0.2543	
2.90	7.9343		4.5550		6.6798		2.90
		0.3402		0.1709		0.2763	
2.91	8.2745		4.7259		6.9561		2.91
		0.3710		0.1862		0.3012	
2.92	8.6455		4.9121		7.2573		2.92
		0.4061		0.2039		0.3298	
2.93	9.0516		5.1160		7.5871		2.93
		0.4466		0.2241		0.3625	
2.94	9.4982		5.3401		7.9496		2.94
		0.4933		0.2474		0.4004	
2.95	9.9915		5.5875		8.3500		2.95
		0.5478		0.2747		0.4446	
2.96	10.5393		5.8622		8.7946		2.96
		0.6117		0.3066		0.4964	
2.97	11.1510		6.1688		9.2910		2.97
		0.6876		0.3446		0.5579	
2.98	11.8386		6.5134		9.8489		2.98
		0.7785		0.3901		0.6315	
2.99	12.6171		6.9035		10.4804		2.99
		0.8886		0.4451		0.7209	
3.00	13.5057		7.3486		11.2013		3.00
		1.0238		0.5127		0.8304	
3.01	14.5295		7.8613		12.0317		3.01
		1.1924		0.5970		0.9671	
3.02	15.7219		8.4583		12.9988		3.02
		1.4063		0.7040		1.1405	
3.03	17.1282		9.1623		14.1393		3.03
		1.6834		0.8426		1.3651	
3.04	18.8116		10.0049		15.5044		3.04
		2.0513		1.0265		1.6633	
3.05	20.8629		11.0314		17.1677		3.05
		2.5547		1.2782		2.0711	
3.06	23.4176		12.3096		19.2388		3.06
		3.2684		1.6350		2.6498	
3.07	26.6860		13.9446		21.8886		3.07
		4.3300		2.1659		3.5103	
3.08	31.0160		16.1105		25.3989		3.08
		6.0084		3.0051		4.8712	
3.09	37.0244		19.1156		30.2701		3.09
		8.8990		4.4503		7.2138	
3.10	45.9234		23.5659		37.4839		3.10
		14.5332		7.2675		11.7808	
3.11	60.4566		30.8334		49.2647		3.11
		27.9956		13.9987		22.6930	

FUNCTIONS FOR THREE-MOMENT EQUATIONS WITH AXIAL COMPRESSION (Contd.)

L/j	α	Δα	β	Δβ	γ	Δγ	L/j
3.12	88.4522		44.8321		71.9577		3.12
		76.2965		38.1491		61.8440	
3.13	164.7487		82.9812		133.8017		3.13
		1034.4142		517.2088		838.4545	
3.14	1199.1629		600.1900		972.2562		3.14
		∞		∞		∞	
3.15	-227.1668		-112.9747		-183.8716		3.15
		123.4092		61.7055		100.0325	
3.16	-103.7576		-51.2692		-83.8391		3.16
		36.5228		18.2624		29.6049	
3.17	-67.2348		-33.0068		-54.2342		3.17
		17.5035		8.7527		14.1884	
3.18	-49.7313		-24.2541		-40.0458		3.18
		10.2713		5.1365		8.3263	
3.19	-39.4600		-19.1176		-31.7195		3.19
		6.7537		3.3778		5.4750	
3.20	-32.7063		-15.7398		-26.2445		3.20
		4.7787		2.3903		3.8742	
3.21	-27.9276		-13.3495		-22.3703		3.21
		3.5593		1.7807		2.8858	
3.22	-24.3683		-11.5688		-19.4845		3.22
		2.7541		1.3779		2.2330	
3.23	-21.6142		-10.1909		-17.2515		3.23
		2.1940		1.0980		1.7790	
3.24	-19.4202		- 9.0929		-15.4725		3.24
		1.7890		0.8954		1.4507	
3.25	-17.6312		- 8.1975		-14.0218		3.25
		1.4865		0.7443		1.2057	
3.26	-16.1447		- 7.4532		-12.8161		3.26
		1.2548		0.6284		1.0178	
3.27	-14.8899		- 6.8248		-11.7983		3.27
		1.0733		0.5376		0.8707	
3.28	-13.8166		- 6.2872		-10.9276		3.28
		0.9285		0.4652		0.7533	
3.29	-12.8881		- 5.8220		-10.1743		3.29
		0.8111		0.4066		0.6581	
3.30	-12.0770		- 5.4154		- 9.5162		3.30
		4.6522		2.3367		3.7784	
3.40	- 7.4248		- 3.0787		- 5.7378		3.40
		2.0479		1.0354		1.6681	
3.50	- 5.3769		- 2.0433		- 4.0697		3.50
		1.1477		0.5861		0.9389	
3.60	- 4.2292		- 1.4572		- 3.1308		3.60
		0.7302		0.3785		0.6016	
3.70	- 3.4990		- 1.0787		- 2.5292		3.70
		0.5029		0.2659		0.4179	
3.80	- 2.9961		- 0.8128		- 2.1113		3.80
		0.3647		0.1981		0.3070	
3.90	- 2.6314		- 0.6147		- 1.8043		3.90
		0.2744		0.1544		0.2349	

FUNCTIONS FOR THREE-MOMENT EQUATIONS WITH AXIAL COMPRESSION (Contd.)

L/J	α	$\Delta\alpha$	β	$\Delta\beta$	γ	$\Delta\gamma$	L/J
4.00	-2.3570		-0.4603		-1.5694		4.00
		0.2116		0.1248		0.1854	
4.10	-2.1454		-0.3355		-1.3840		4.10
		0.1662		0.1038		0.1498	
4.20	-1.9792		-0.2317		-1.2342		4.20
		0.1317		0.0887		0.1237	
4.30	-1.8475		-0.1430		-1.1105		4.30
		0.1046		0.0778		0.1036	
4.40	-1.7429		-0.0652		-1.0069		4.40
		0.0826		0.0696		0.0881	
4.50	-1.6603		+0.0044		-0.9188		4.50
		0.0641		0.0638		0.0757	
4.60	-1.5962		0.0682		-0.8431		4.60
		0.0810		0.1169		0.1235	
4.80	-1.5152		0.1851		-0.7196		4.80
		0.0238		0.1124		0.0962	
5.00	-1.4914		0.2975		-0.6234		5.00
		0.0568		0.1520		0.0938	
5.25	-1.5482		0.4495		-0.5296		5.25
		0.1964		0.1975		0.0733	
5.5	-1.7446		0.6470		-0.4563		5.5
		0.4898		0.3277		0.0589	
5.75	-2.2344		0.9747		-0.3974		5.75
		1.5111		0.8268		0.0482	
6.0	-3.7455		1.8015		-0.3492		6.0
		25.3412		12.7331		0.0404	
6.25	-29.0867		14.5346		-0.3088		6.25
		∞		∞		0.0048	
2π	$\pm\infty$		$\pm\infty$		-0.3040		2π
		∞		∞		0.0295	
6.5	4.1490		-2.0242		-0.2745		6.5

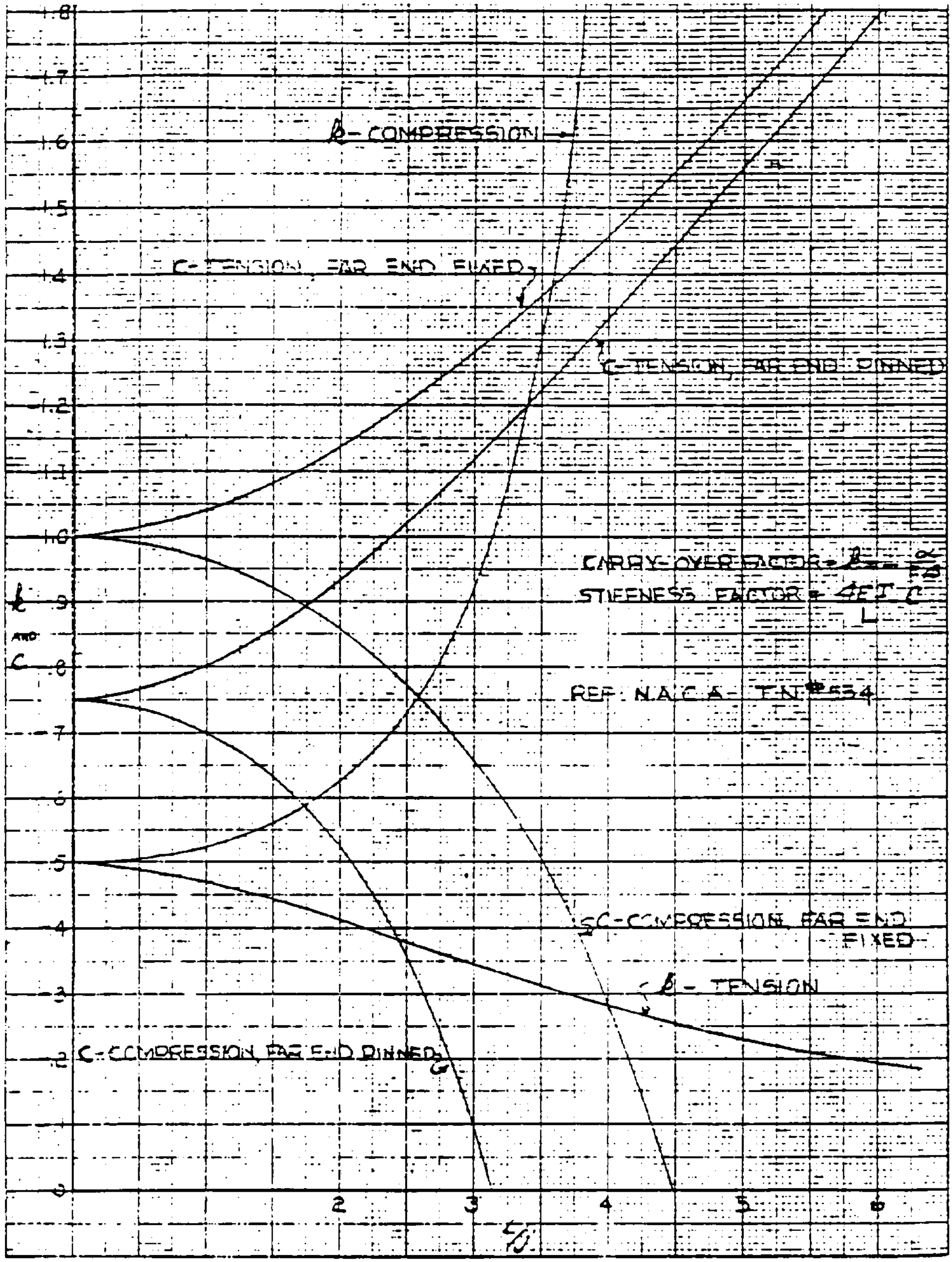
k - COMPRESSION
C - TENSION, FAR END FIXED
C - TENSION, FAR END PINNED
CARRY-OVER FACTOR = k
STIFFNESS FACTOR = 4EI C / L
REF. N.A.C.A. - T.N. #534
C - COMPRESSION, FAR END FIXED
k - TENSION
C - COMPRESSION, FAR END PINNED
k AND C
.1
.2
.3
.4
.5
.6
.7
.8
.9
1.0
1.1
1.2
1.3
1.4
1.5
1.6
1.7
1.8
0
2
3
4
5
6

245

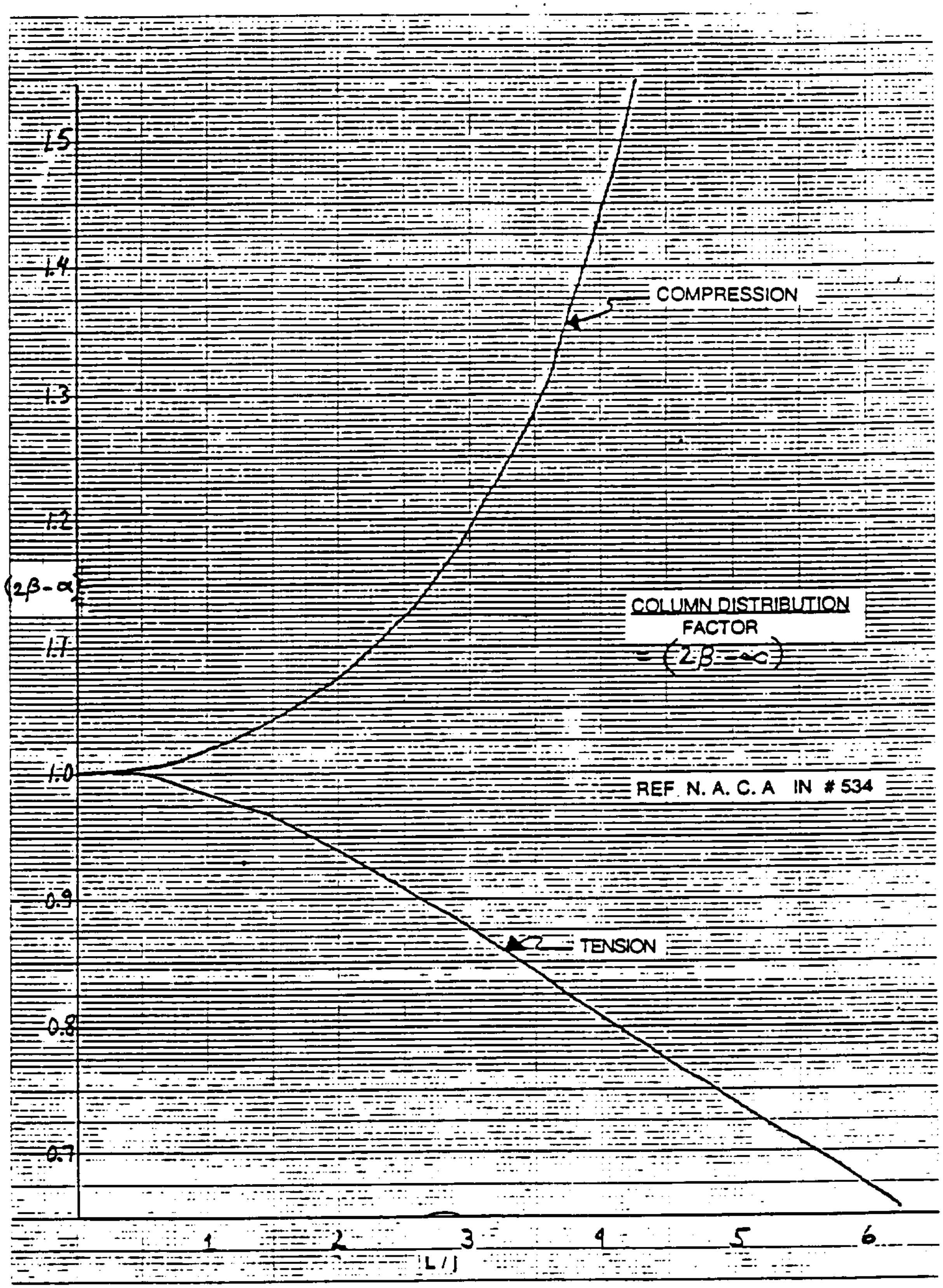
1.5
1.4
1.3
1.2
(2β-α)
1.1
1.0
0.9
0.8
0.7
COMPRESSION
TENSION
COLUMN DISTRIBUTION
FACTOR
= (2β-α)
REF. N. A. C. A IN # 534
1
2
3
4
5
6
L/j

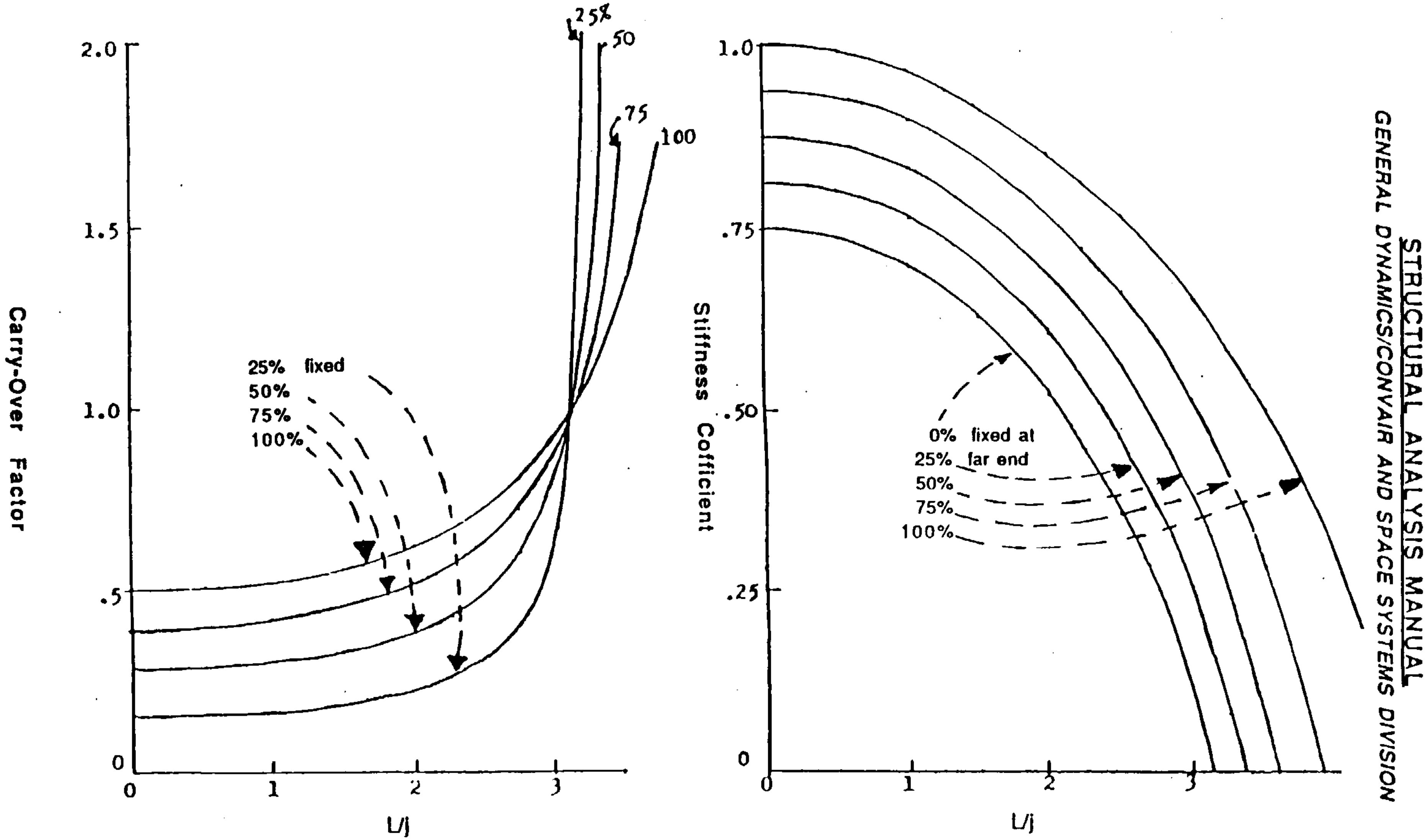

STIFFNESS COEFFICIENTS AND CARRY-OVER FACTORS FOR MEMBERS UNDER AXIAL LOAD WITH VARIOUS AMOUNTS OF FIXITY AT FAR END

11.3 Torsional Instability of Columns

The previous sections have assumed that the column was torsionally stable: i.e., the column would either fail by bending in a plane of symmetry of the cross section, by crippling or by a combination of crippling and bending. There are cases when a column will fail either by twisting or by a combination of bending and twisting. These torsional buckling failures occur when the torsional rigidity of the section is very low. Thin walled open sections, for instance, can buckle by twisting at loads well below the Euler load. Often in thin open sections the centroid and shear center do not coincide, therefore, torsion and flexure interact.

In this section, it will be assumed that the plane cross sections of the column warp, but their geometric shape does not change during buckling; that is, the theories consider primary failure of columns and not secondary failures, characterized by distortion of the cross sections. There is coupling of primary and secondary failures but no method has been developed to handle them so secondary failures will be ignored.

11.3.1 Centrally Loaded Columns

Centrally loaded columns can buckle in one of three possible modes: (1) they can bend in the plane of one of the principal axes; (2) they can twist about the shear center axis; or (3) they can bend and twist simultaneously. Bending in the plane of one of the principal axes has been discussed previously. The latter two modes will be discussed here.

11.3.1.1 Two Axes of Symmetry

When the cross section has two axes of symmetry or is point symmetric, the shear center and centroid coincide. In this case, the purely torsional buckling load about the shear center is given by

$$P_\phi = 1/r_o^2 \left\{ GJ + E\Gamma \pi^2/l^2 \right\} \qquad (11.27)$$

where:

- r_o = polar radius of gyration of the section about its shear center
- G = shear modulus of elasticity
- J = torsion constant (Section 8.0)
- E = modulus of elasticity
- Γ = warping constant of the section (Section 8.0)
- l = effective length of the member

For a cross section with two axes of symmetry there are three critical values of the axial load. They are the flexural buckling loads about the principal

axes, P_x and P_y and the purely torsional buckling load, P_ϕ. One of these loads will be minimum and will determine the mode of failure. In this case there is no interaction and the column fails either in pure bending or in pure twisting. Shapes in this category include I-sections, Z-sections and cruciforms.

11.3.1.2 General Cross Section

In general a thin walled open section buckling occurs by a combination of torsion and bending. Purely flexural or purely torsional failure cannot occur. Consider a general section with the x and y axes the principal centroidal axes of the cross section and x_o and y_o the coordinates of the shear center. The cross section will undergo translation and rotation during buckling. The translation is defined by the deflections of the shear center u and v in the x and y directions. During translation of the cross section, point O moves to O' and point C to C' where O is the shear center and C is the centroid. The cross section rotates an angle ϕ about the shear center. Equilibrium of a longitudinal element yields three simultaneous equations, the solution of which results in the following cubic equation for calculating the critical value of buckling load.

$$r_o^2(P_{cr}-P_y)(P_{cr}-P_x)(P_{cr}-P_\phi) - P_{cr}^2 y_o^2(P_{cr}-P_x) - P_{cr}^2 x_o^2(P_{cr}-P_y) = 0 \qquad (11.28)$$

where

$$P_x = \pi^2 EI_x/L^2 \qquad (11.29)$$

$$P_y = \pi^2 EI_y/L^2 \qquad (11.30)$$

$$P_\phi = 1/r_o^2(GJ + E\Gamma\,\pi^2/L^2) \qquad (11.31)$$

Solution of the cubic equation, 11.28, gives three values of the critical load, P_{cr}, of which the smallest will be used. The lowest value of P_{cr} will always be less than P_x, P_y, or P_ϕ. By use of the effective length, L, various end conditions can be considered.

11.3.1.3 Cross Sections With One Axis of Symmetry

A number of singly symmetric sections are shown in Figure 11.76. If the x-axis is considered to be the axis of symmetry, the $y_o = 0$ and the equation for a general section reduces to

$$(P_{cr} - P_y)\{r_o^2(P_{cr} - P_x)(P_{cr} - P_\phi) - P_{cr}^2 x_o^2\} = 0 \qquad (11.32)$$

There are again three solutions, one of which is $P_{cr} = P_y$ and represents purely flexural buckling about the y-axis. The other two are the roots of the quadratic term inside the brackets equated to zero and give two torsional-flexural buckling loads. The lowest torsional-flexural load will always be below P_x and P_ϕ. It may, however, be above or below P_y. Therefore, a singly symmetrical section (such as an angle, channel or hat) can buckle in either of two modes, by bending or in torsional-flexural buckling. Which of these two actually occurs depends on the dimensions and shape of the gi section.

Failure of singly symmetrical sections can occur either in pure bending or in simultaneous bending and twisting. The evaluation of the torsional-flexural buckling load can never be as simple as the determination of the Euler load, therefore, steps have been taken to categorize modes of failure. Certain combinations of dimensions will prohibit torsional-flexural failures.

For sections symmetrical about the x-axis, the critical buckling load is given by equation 11.32. The load at which the member actually buckles is either P_y or the smaller root of the quadratic equation.

The buckling domain can be visualized as being composed of three regions. These are shown in Figure 11.77 for a section whose shape is defined by the ratio, b/a. Region 1 contains all sections for which $I_y > I_x$. In this region only torsional-flexural buckling can occur. Sections for which $I_x > I_y$ falls into Region 2 or 3. In Region 2, the mode of buckling depends on the parameter tL/a^2. The $(tL/a^2)_{min}$ curve represents the boundary between the two possible modes of failure. It is a plot of the value of tL/a^2 at which the buckling mode changes from purely flexural to torsional-flexural. The boundary between Regions 2 and 3 is located at the intersection of the $(tL/a^2)_{min}$ curve with the b/a axis. Sections in Region 3 will always fail in the flexural mode regardless of the value of tL/a^2.

Figure 11.78 defines these curves for angles, channels, and hat sections. In this figure, members that plot below and to the right of the curve fail in the torsional-flexural mode, whereas those to the left and above fail in the pure bending mode. The curves in Figure 11.78 also give the location of the boundaries between the various buckling domains. Each of the curves approaches a vertical asymptote, indicated as a dashed line in the figure. The asymptote, which is the boundary between Regions 1 and 2, is located at b/a corresponding to sections for which $I_x = I_y$. Sections with b/a larger than the transition value at the asymptote will always fail in torsional-flexural buckling, regardless of their other dimensions. If b/a is smaller than the value for the asymptote, then the section fails in Region 2 and failure can be either by pure flexural buckling or in the torsional-flexural mode. In this region, the parameter, tL/a^2, will determine which of the two possible modes of failure is critical. In the case of the plain and lipped channel section, there is a lower boundary Region 2. This transition occurs where the $(tL/a^2)_{lim}$ curve intersects the b/a axis. Sections for which b/a is less than the value at this intersection are located in Region 3. These sections will always fail in the flexural mode, regardless of the value of tL/a^2. For the lipped angle and hat sections the $(tL/a^2)_{lim}$ curve does not intersect the b/a axis. Region 3, where only flexural buckling occurs, does not exist for these sections.

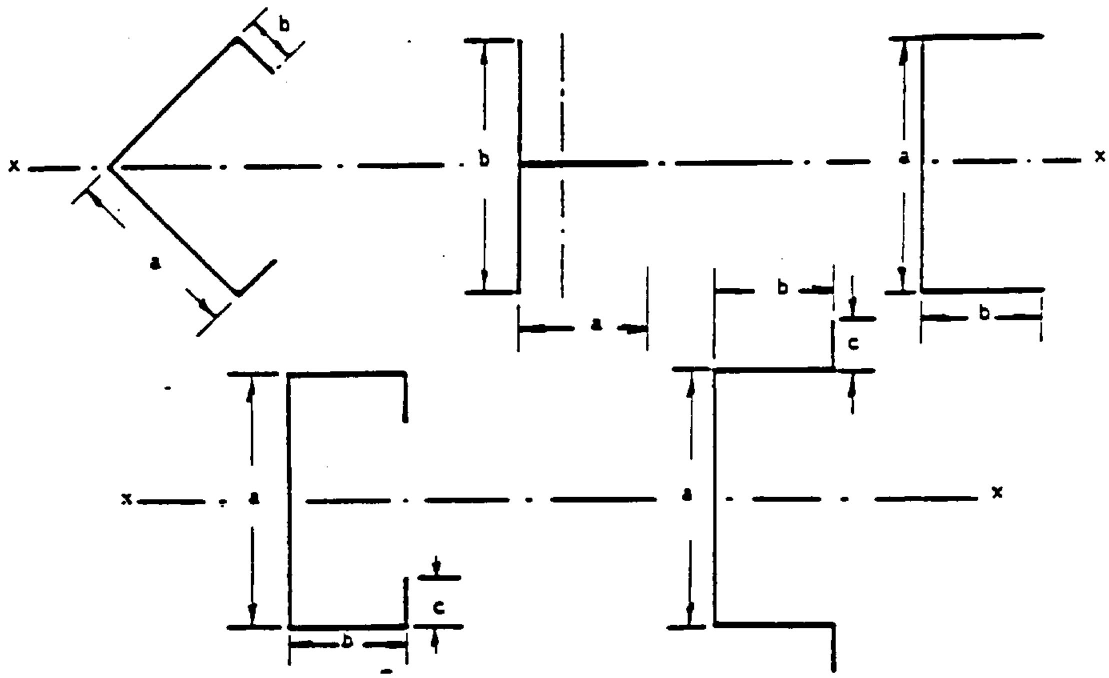

FIGURE 11.76 - SINGLY SYMMETRICAL SECTIONS

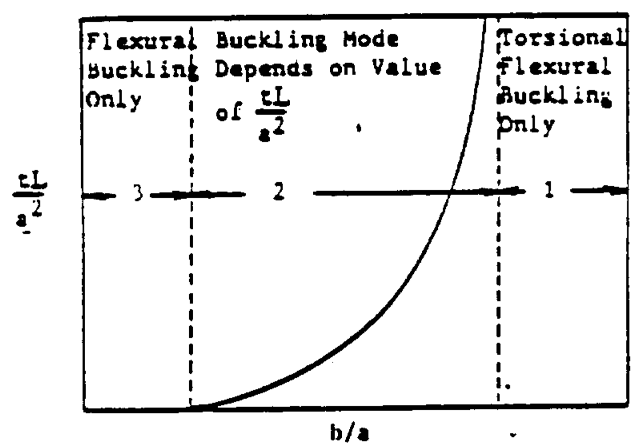

FIGURE 11.77 BUCKLING REGIONS

The critical buckling load for singly symmetrical sections (x-axis is the axis of symmetry) that buckle in the torsional-flexural mode is given by the lowest root of

$$r_o^2(P_{cr}-P_x)(P_{cr}-P_\phi) - P_{cr}^2 x_o^2 = 0. \tag{11.33}$$

Dividing this equation by $P_x P_\phi r_o^2$, and rearranging results in the following interaction equation:

$$\frac{P}{P_\phi} + \frac{P}{P_x} - K\frac{P^2}{P_x P_\phi} = 1 \tag{11.34}$$

in which

$$K = 1 - \left(\frac{x_o}{r_o}\right)^2 \tag{11.35}$$

is a shape factor that depends on geometrical properties of the cross section.

Figure 11.79 is a plot of equation 11.34. This plot provides a simple method for checking the safety of a column against failure by torsional-flexural buckling.

To determine if a given member can safely carry a certain load, P, it is only necessary to compute P_x and P_ϕ for the section in question and then, knowing K, use the correct curve to check whether the point determined by the arguments P/P_x and P/P_ϕ falls below (safe) or above (unsafe) the pertinent curve. If it is desired to determine the critical load of a member instead of ascertaining whether it can safely carry a given load, use

$$P_{cr} = \frac{1}{2K}\left\{(P_\phi + P_x) - \sqrt{(P_\phi + P_x)^2 - 4KP_\phi P_x}\right\} \tag{11.36}$$

which is another form of equation 11.34.

The interaction equation 11.34 indicates that P_{cr} depends on three factors: the loads, P_x and P_ϕ, and the shape factor, K. P_x and P_ϕ are the two factors which interact, while K determines the extent to which they interact. The reason bending and twisting interact is that the shear center and the centroid do not coincide. A decrease in x_o, the distance between these points, therefore causes a decrease in the interaction.

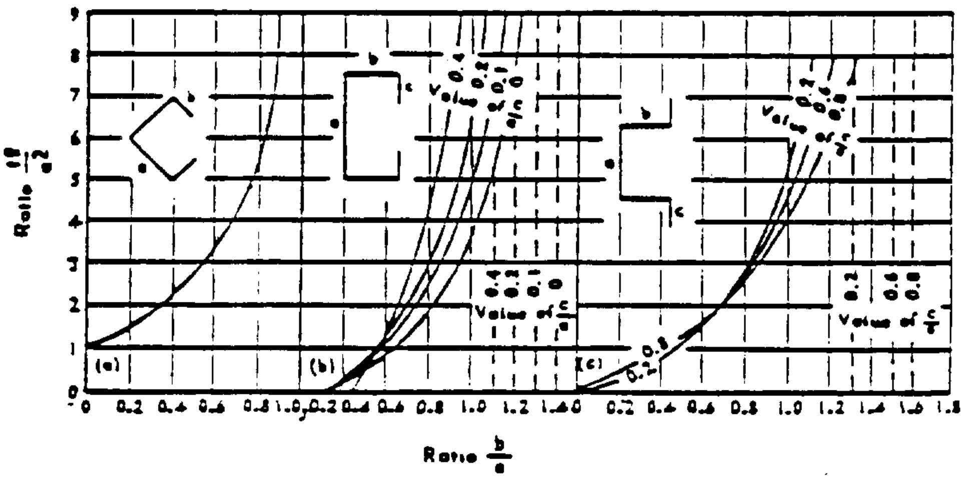

FIGURE 11.78 - BUCKLING MODE OF SINGLY SYMMETRICAL SECTIONS

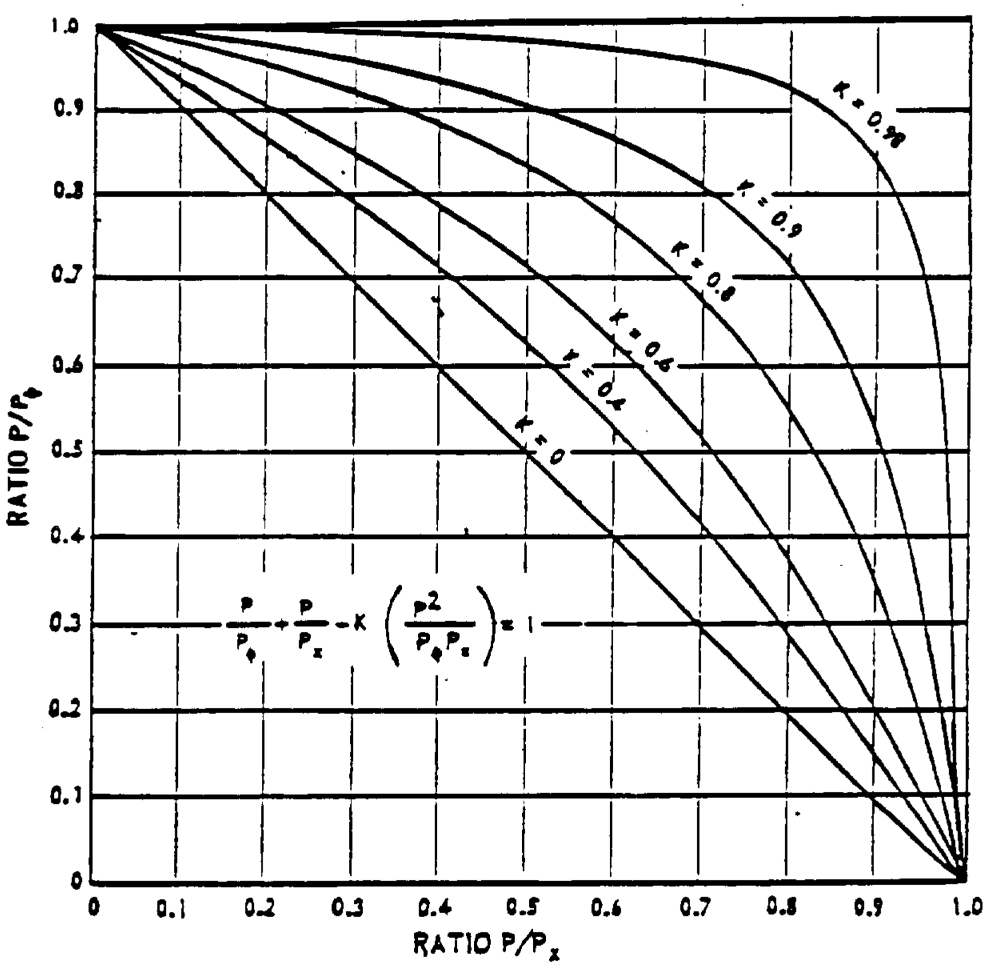

FIGURE 11.79 - INTERACTION CURVES

To evaluate the torsional-flexural buckling load by means of the interaction equation, it is necessary to know P_ϕ and K. A convenient method for determining these two parameters is therefore an assential part of the procedure.

For any given section, K is a function of certain parameters that define the shape of the section. Starting with equation 11.35 and substituting for x_o and r_o, K can be reduced to an expression in terms of one or more of these parameters. If the thickness of the member is uniform, the parameters will be of the form b/a, in which a and b are the widths of two of the flat components of the section. In the case of a tee section, for example, equation 11.35 can be reduced to:

$$K = 1 - \frac{4}{\{1 + b/a\}\{(b/a)^3 + 1\}} \qquad (11.37)$$

in which b/a is the ratio of the flange to the leg width (Fig. 11.76).

In general, the number of elements of which a section is composed and the number of width ratios required to define its shape will determine the complexity of the relation for K. Because all equal-legged angles without lips have the same shape, K is a constant for this section. For channels and lipped angles, K is a function of a single variable, b/a, while lipped channels and hat sections require two parameters, b/a and c/a, to define K (Fig. 11.76).

Curves for determination of K have been obtained for angles, channels, and hat sections. These curves are shown in Figures 11.80 and 11.81. A single curve covers all equal-legged lipped angle sections. The value of K for all plain equal-legged angles, K = 0.625, is given by the point b/a = 0 on this curve (Fig. 11.80). For hats and channels (Fig. 11.81), a series of curves is given.

The evaluation of P_ϕ follows the same scheme as that used to determine K. Starting with the equation for P_ϕ, given in equation 11.27, and substituting for r_o, J, and Γ yields:

$$P_\phi = EA\{C_1(t/a)^2 + C_2(a/l)^2\} \qquad (11.38)$$

a general relation for P_ϕ, in which, E = Young's modulus, A = cross-sectional area; t = the thickness of the section; L = effective length of the member; a = the width of one of the elements of the section; and C_1 and C_2 = functions of b/a and c/a, in which b and c are the widths of the remaining elements.

Equation 11.35 indicates the important parameters in torsional buckling and their effect on the buckling load. Similar to Euler buckling, P_ϕ varies directly with E and A. The term inside the bracket consists of two parts, the St. Venant torsional resistance and the warping resistance. In the first of these, the parameter, t/a, indicates the decrease in torsional resistance with decreasing relative wall thickness; whereas, in the second the parameter a/L shows the decrease in warping resistance with increasing slenderness.

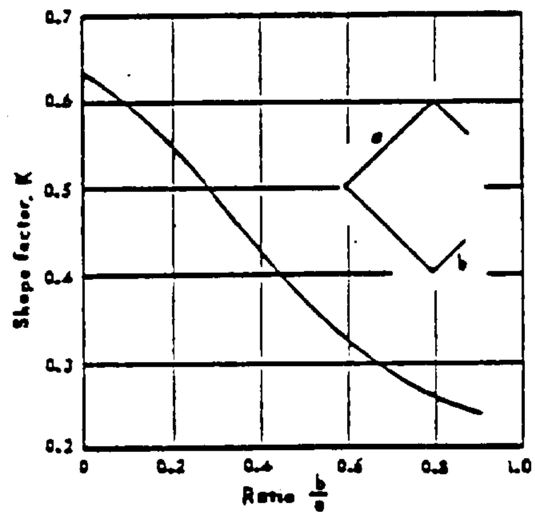

FIGURE 11.80 - SHAPE FACTOR FOR ANGLES.

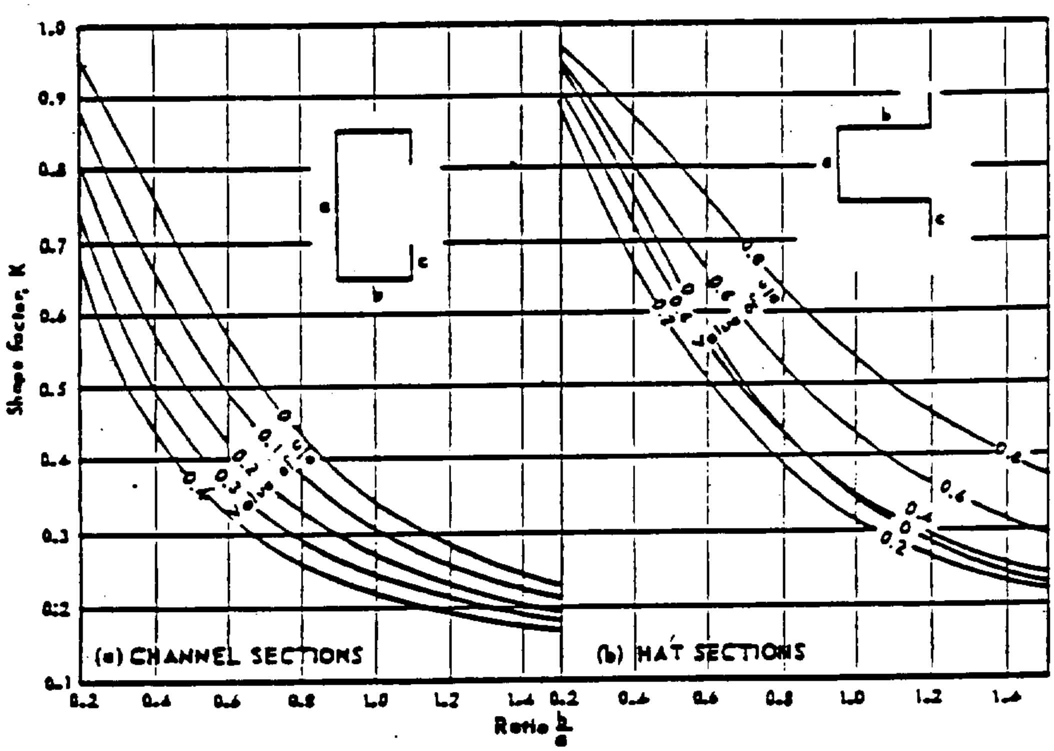

FIGURE 11.81 - SHAPE FACTORS FOR COMPLEX SECTIONS

The coefficients, C_1 and C_2, in the St. Venant and warping terms are functions of b/a and c/a, respectively. These terms therefore indicate the effect that the shape of the section has on P_ϕ.

Sections composed of thin rectangular elements whose middle lines intersect at a common point have negligible warping stiffness; i.e., $\Gamma = 0$. Because C_2 is proportional to Γ, the torsional buckling load of these sections reduces to:

$$P_\phi = EAC_1(t/a)^2 \tag{11.39}$$

For the plain equal-legged angle, which falls into this category, P_ϕ can be further reduced to:

$$P_\phi = AG(t/a)^2 \tag{11.40}$$

in which G is the shear modulus of elasticity, and a is the length of one of the legs.

In general, however, C_1 and C_2 must be evaluated. Curves for these values are given in Figures 11.82, 11.83, and 11.84 for angles, hats, and channels.

For other cross sections values of the warping constant, Γ, and location of shear center are given in Figure 11.85.

11.3.2 Eccentrically Loaded Columns

The previous section described the buckling of columns with centrally applied loads, i.e., at the centroid of the section. If the load, P, is applied eccentrically as shown in Figure 11.86 the general cubic equation for calculating P_{cr} is:

$$A_3 P_{cr}^3 + A_2 P_{cr}^2 + A_1 P_{cr} + A_o = 0 \tag{11.41}$$

Where

$$A_3 = A/I_o \{ e_x \beta_2 + e_y \beta_1 - (e_y - y_o)^2 - (e_x - x_o)^2 \} + 1$$

$$A_2 = A/I_o \{ P_x(y_o - e_y)^2 + P_y(x_o - e_x)^2 - e_x \beta_2 (P_x + P_y) - e_y \beta_1 (P_x + P_y) \} - (P_x + P_y + P_\phi)$$

$$A_1 = A/I_o \{ P_x P_y e_x \beta_2 + P_x P_y e_y \beta_1 \} + (P_x P_y + P_y P_\phi + P_x P_\phi)$$

$$A_o = -P_x P_y P_\phi \qquad I_o = I_x + I_y + A(X_o^2 + Y_o^2)$$

$$P_x = EI_x \pi^2/L^2 \qquad \beta_1 = 1/I_x\left(\int_A Y^3 dA + \int_A X^2 Y dA\right) - 2Y_o$$

$$P_y = EI_y \pi^2/L^2 \qquad \beta_2 = 1/I_y\left(\int_A X^3 dA + \int_A XY^2 dA\right) - 2X_o$$

$$P_\phi = A/I_o(GJ + E\Gamma \pi^2/L^2)$$

In the general case, buckling occurs by combined bending and torsion. In each case the three roots of the cubic can be evaluated for the lowest value.

If P acts along the shear center axis:

$$e_x = X_o$$

$$e_y = Y_o$$

and the buckling loads become independent of each other, the critical load will be the lowest of the two Euler loads, P_x, P_y and the load corresponding to purely torsional buckling which is:

$$P_\phi = (I_o/A)\ P/e_y\ \beta_1 + \bar{e}_x\ \beta_2 + I_o/A \tag{11.42}$$

When the column has one plane of symmetry and the load acts in the plane of symmetry $e_x = 0$ and buckling in this plane takes place independently and the critical load is the same as the Euler load. However, lateral buckling and torsional buckling are coupled and the critical loads are obtained from the following quadratic equation:

$$(P_y - P)\left\{(I_o/A)\ P_\phi - P(e_y\ \beta_1 + I_o/A)\right\} - P^2(Y_o - e_y)^2 = 0 \tag{11.43}$$

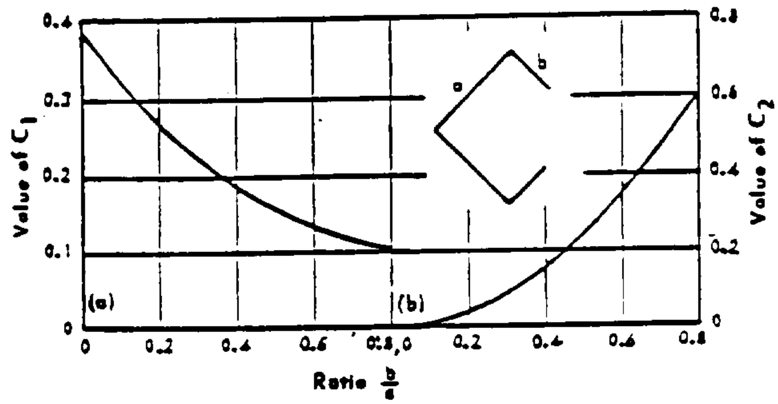

FIGURE 11.82 - TORSIONAL BUCKLING COEFFICIENTS C_1 AND C_2 FOR ANGLES

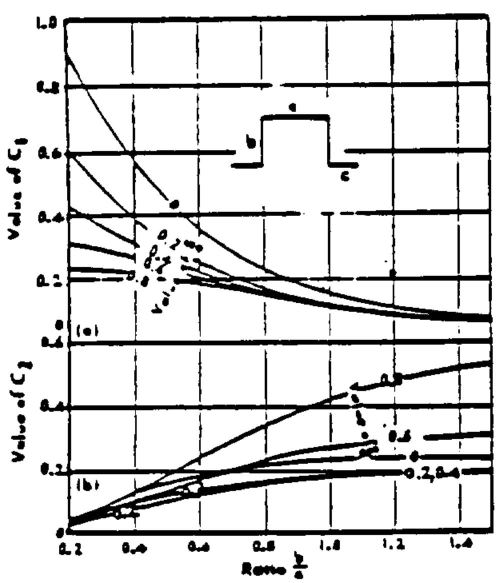

FIGURE 11.83 - TORSIONAL BUCKLING COEFFICIENTS C_1 AND C_2 FOR HAT SECTIONS.

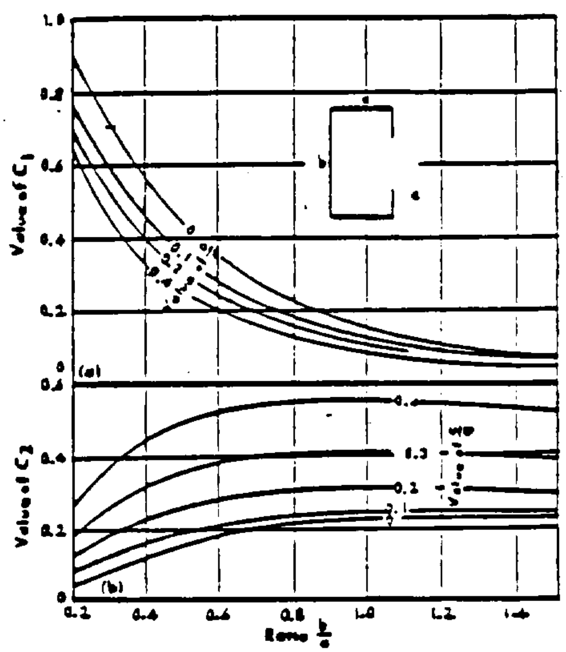

FIGURE 11.84 - TORSIONAL BUCKLING COEFFICIENTS C_1 AND C_2 FOR CHANNEL SECTIONS.

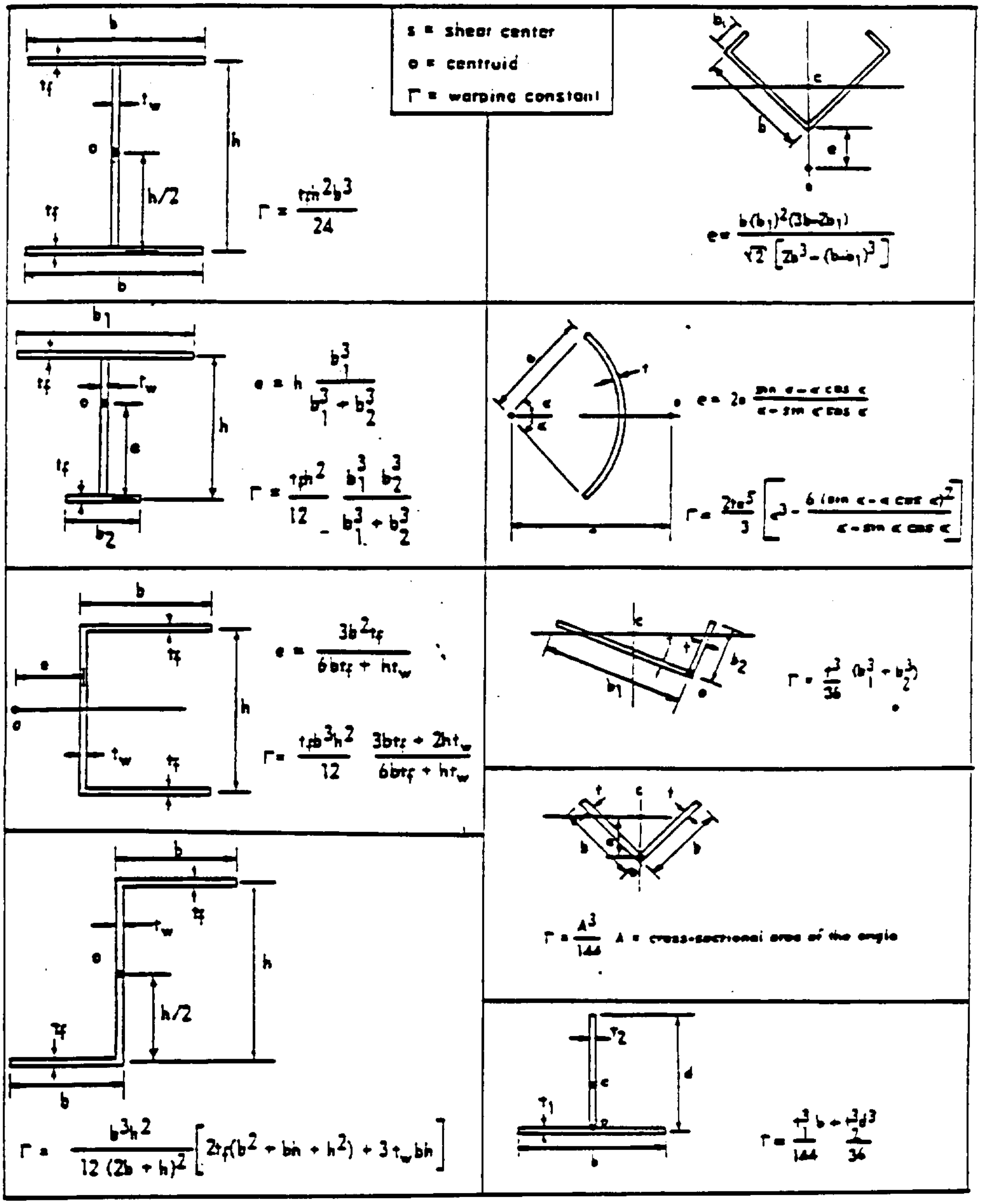

FIGURE 11.35 - SHEAR CENTER LOCATIONS AND WARPING CONSTANTS

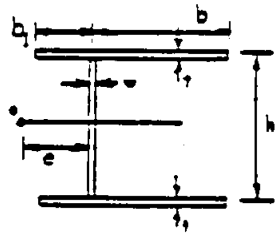

$$e = \frac{3(b^2 - b_1^2)}{(w/t)h + 6(b + b_1)} \quad ; \; b_1 < b$$

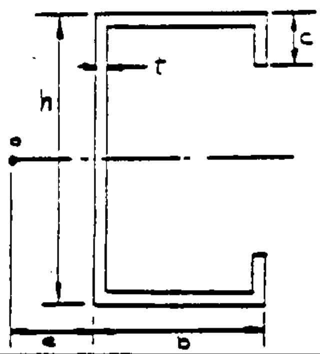

Values of e/h						
c/h \ b/h	1.0	0.8	0.6	0.4	0.2	
0	.430	.330	.236	.141	.055	
0.1	.477	.380	.280	.183	.087	
0.2	.530	.425	.325	.222	.115	
0.3	.575	.470	.365	.258	.138	
0.4	.610	.503	.394	.280	.155	
0.5	.621	.517	.405	.290	.161	

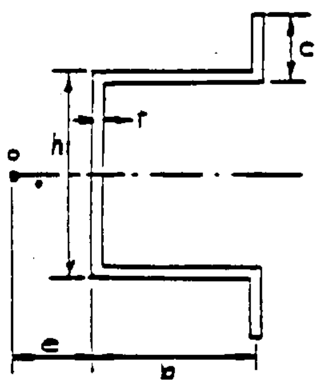

Values of e/h						
c/h \ b/h	1.0	0.8	0.6	0.4	0.2	
0	.430	.330	.236	.141	.055	
0.1	.464	.367	.270	.173	.080	
0.2	.474	.377	.280	.182	.090	
0.3	.453	.358	.265	.172	.085	
0.4	.410	.320	.235	.150	.072	
0.5	.355	.275	.196	.123	.056	
0.6	.300	.225	.155	.095	.040	

Figure 11.85 (Cont'd) - Shear Center Locations and Warping Constants.

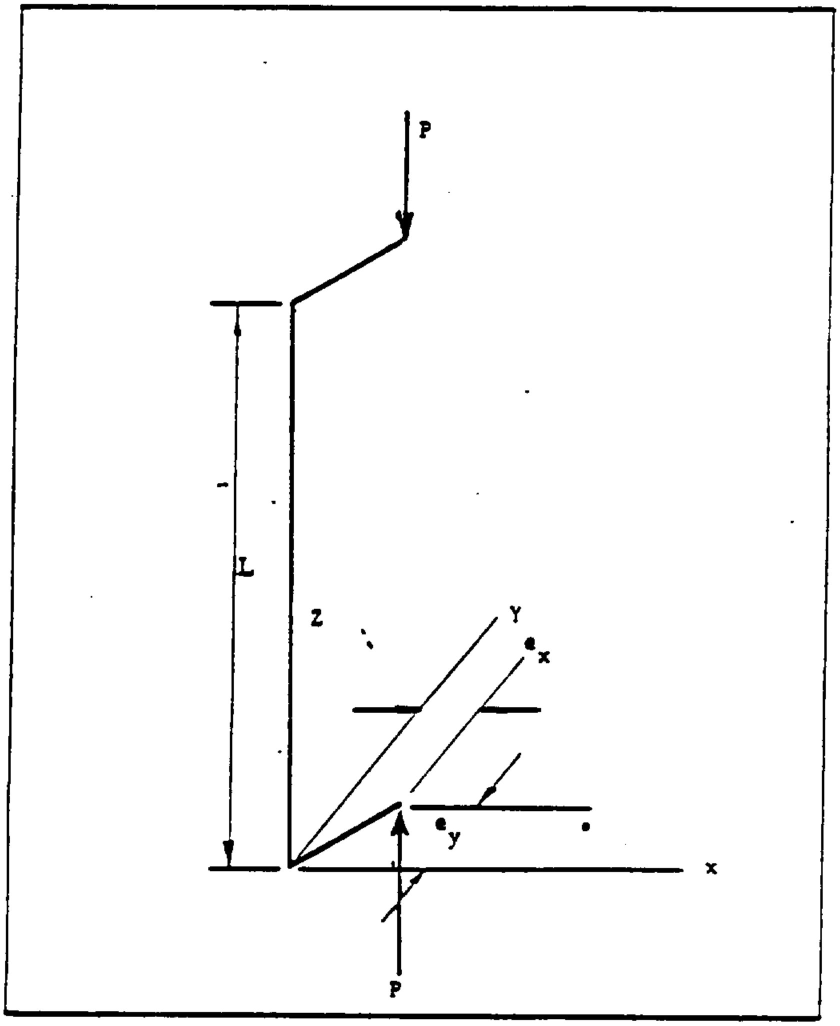

FIGURE 11.36 - ECCENTRICALLY APPLIED LOAD

Reference 11.3.2

Data Source, Section 1.3 Reference 6

SUBJECT: Column Allowables

The column allowables given in Figures 1 through 49 are based on the tangent modulus theory and predict primary failure through lateral bending.

The column allowables are based on minimum guaranteed properties, Basis A, or probability properties, Basis B, if the latter are available. The pertinent basis is indicated in the figures.

INDEX

	Figure
Aluminum Alloys	
2014 Extrusion	6
2024 Bare Sheet and Plate	1
Bare Plate	2
Clad Sheet	3
Clad Sheet and Plate	4
Extrusion	5
7075 Bare Sheet and Plate	2
Clad Sheet	3
Extrusion	6
Die Forging	8
7178 Bare Sheet and Plate, Clad Sheet and Plate, and Extrusions	9
356 Casting	7
Alloy Steel	
Heat-treated F_{tu} = 180 - 260 ksi	10
Heat-treated F_{tu} = 90 - 150 ksi	11
Stainless Steel	
18-8 Cold Rolled - With Grain	12
Cold Rolled & Heat Treated - With Grain	13
Cold Rolled - Cross Grain	14
Cold Rolled & Heat Treated - Cross Grain	15
AM 350 Sheet	16
PH 13-8Mo Plate and Bar	19
PH 14-8Mo Sheet	19
PH 15-7Mo Sheet and Plate	18
17-7 PH Bar	16
17-7 PH Sheet and Plate	17

Figure

Magnesium Alloys
AZ63A-T6 Casting 24
ZK60A-T5 Extrusion 24
AZ31B-H24 Sheet 20
HM21A-T8 Sheet 21
HM31A-F Extrusion, Area < 1.000 in.^{2} 22
HM31A-F Extrusion, Area: 1.000 - 3.999 in.^{2} 23

Titanium Alloys
Commercially Pure Sheet 25
8Mn Annealed Sheet 25
4Al-3Mo-1V Solution Treated and Aged Sheet and Plate t ≤ .250 26
5Al-2.5Sn Annealed Sheet, Plate, Bar and Forging 27
6Al-4V Annealed Extrusion 28
Annealed Sheet t ≤ .250 29
Solution Treated and Aged Sheet t ≤ .187 30
Annealed Bar t ≤ 3.0 31
Solution Treated and Aged Bar t ≤ 1.0 32
Solution Treated and Aged Bar 1.01 ≤ t ≤ 2.0 33
Solution Treated and Aged Bar 2.01 ≤ t ≤ 3.0 34
Solution Treated and Aged Extrusion t ≤ .500 38
Solution Treated and Aged Extrusion .501 ≤ t ≤ .750 39
Solution Treated and Aged Extrusion .751 ≤ t ≤ 1.000 40
Solution Treated and Aged Extrusion 1.001 ≤ t ≤ 2.000 41
Solution Treated and Aged Extrusion t > 2.000 42
6Al-6V-2Sn Solution Treated and Aged Bar 1.01 ≤ t ≤ 2.0 35
Solution Treated and Aged Bar 2.01 ≤ t ≤ 3.0 36
Solution Treated and Aged Bar 3.01 ≤ t ≤ 4.0 37
8Al-1Mo-1V Single Annealed Sheet and Plate t ≤ .500 43
Single Annealed Plate .501 ≤ t ≤ 1.000 44
Single Annealed Plate 1.001 ≤ t ≤ 2.500 45
Duplex Annealed Sheet and Plate t ≤ 1.000 46
Duplex Annealed Plate 1.001 ≤ t ≤ 2.000 47
13V-11Cr-3Al Solution Treated and Aged Sheet and Plate t ≤ .250 48
Annealed Sheet and Plate t ≤ .250 49

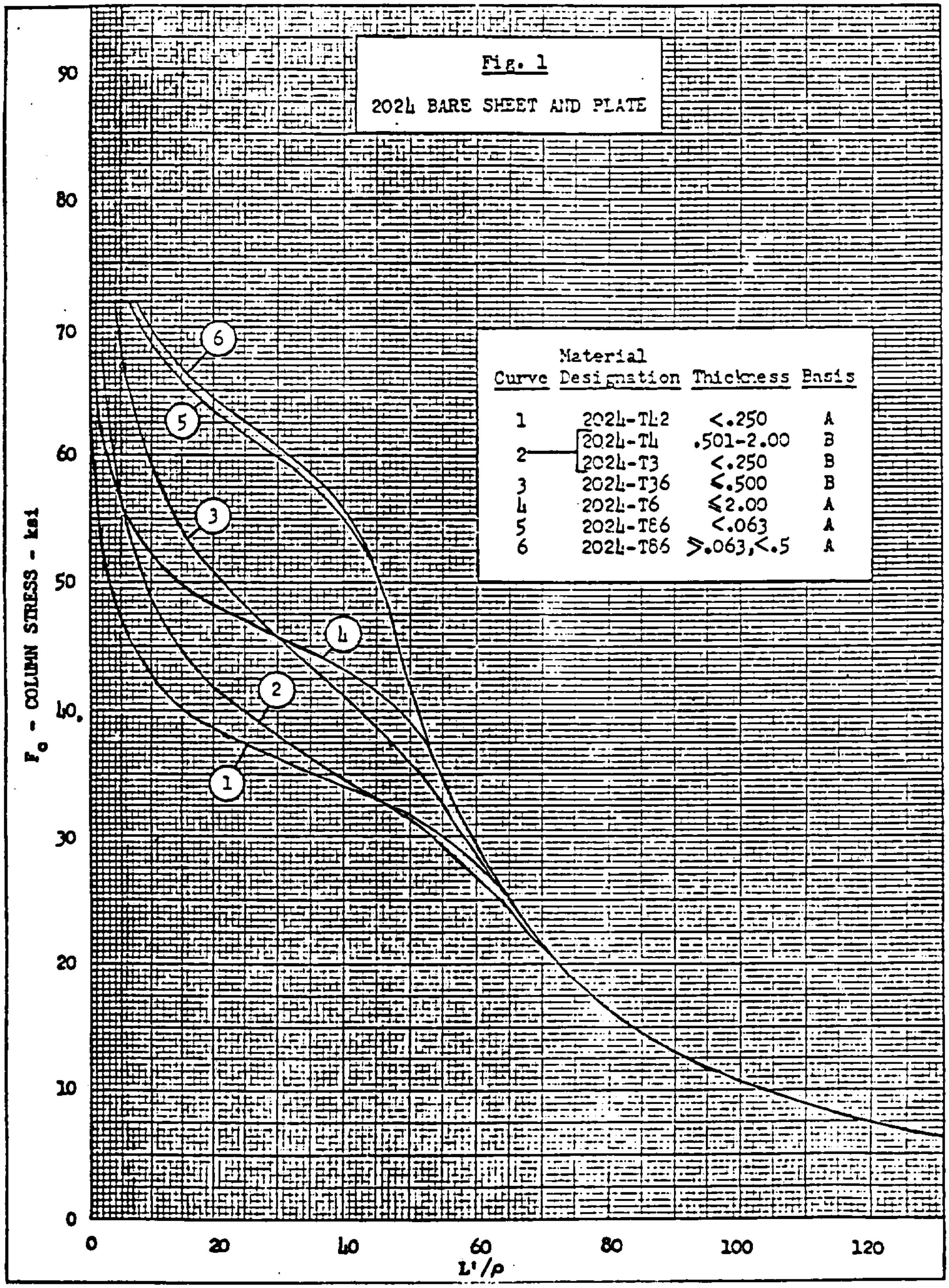

Fig. 1

2024 BARE SHEET AND PLATE

265

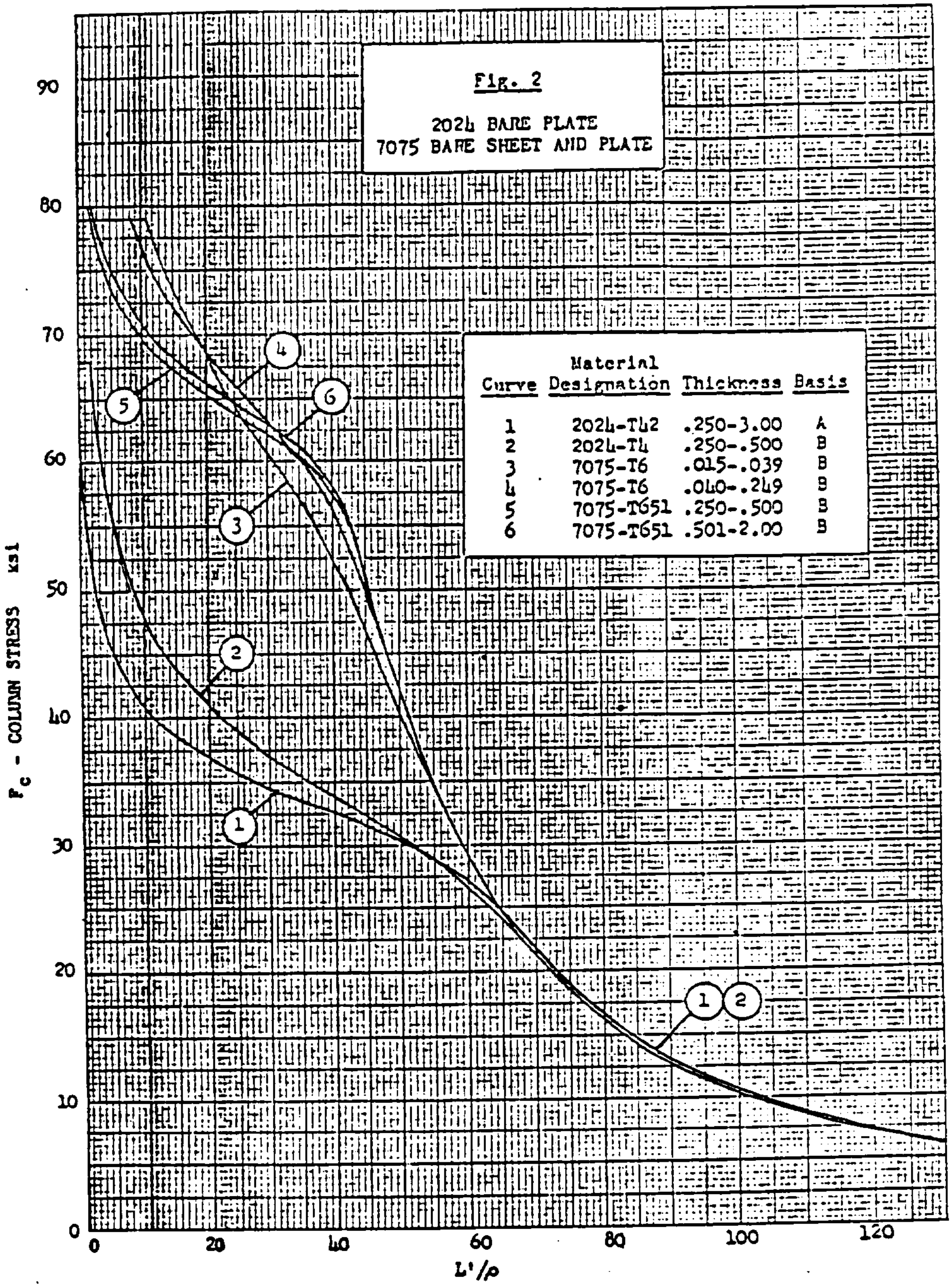
Fig. 2
2024 BARE PLATE
7075 BARE SHEET AND PLATE
Material
Curve Designation Thickness Basis
1 2024-T42 .250-3.00 A
2 2024-T4 .250-.500 B
3 7075-T6 .015-.039 B
4 7075-T6 .040-.249 B
5 7075-T651 .250-.500 B
6 7075-T651 .501-2.00 B
F_c - COLUMN STRESS ksi
L'/ρ
0
10
20
30
40
50
60
70
80
90
0
20
40
60
80
100
120

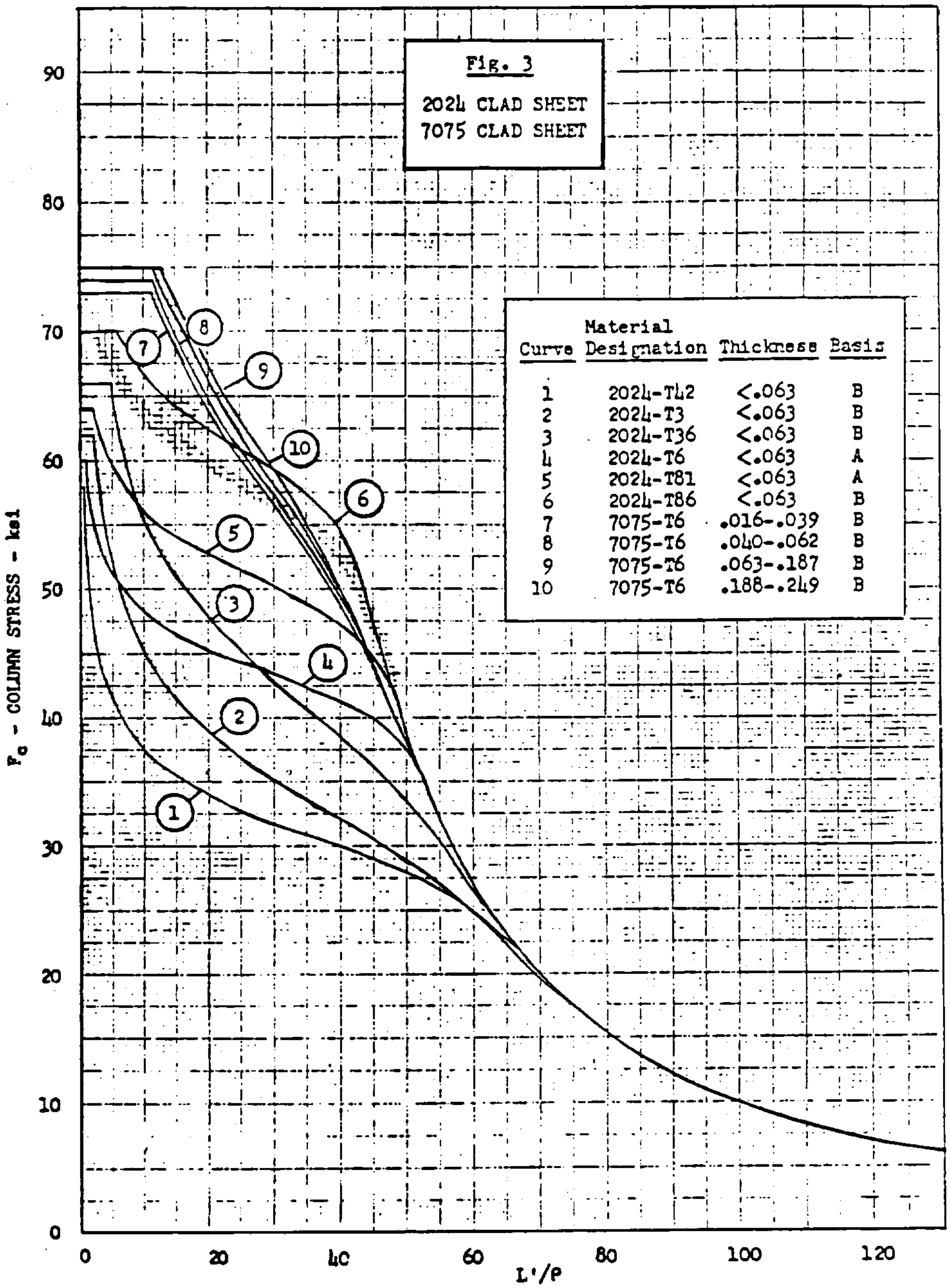
Fig. 3
2024 CLAD SHEET
7075 CLAD SHEET
Curve | Material Designation | Thickness | Basis
1 | 2024-T42 | <.063 | B
2 | 2024-T3 | <.063 | B
3 | 2024-T36 | <.063 | B
4 | 2024-T6 | <.063 | A
5 | 2024-T81 | <.063 | A
6 | 2024-T86 | <.063 | B
7 | 7075-T6 | .016-.039 | B
8 | 7075-T6 | .040-.062 | B
9 | 7075-T6 | .063-.187 | B
10 | 7075-T6 | .188-.249 | B
F_c - COLUMN STRESS - ksi
L'/ρ
0
10
20
30
40
50
60
70
80
90
100
120

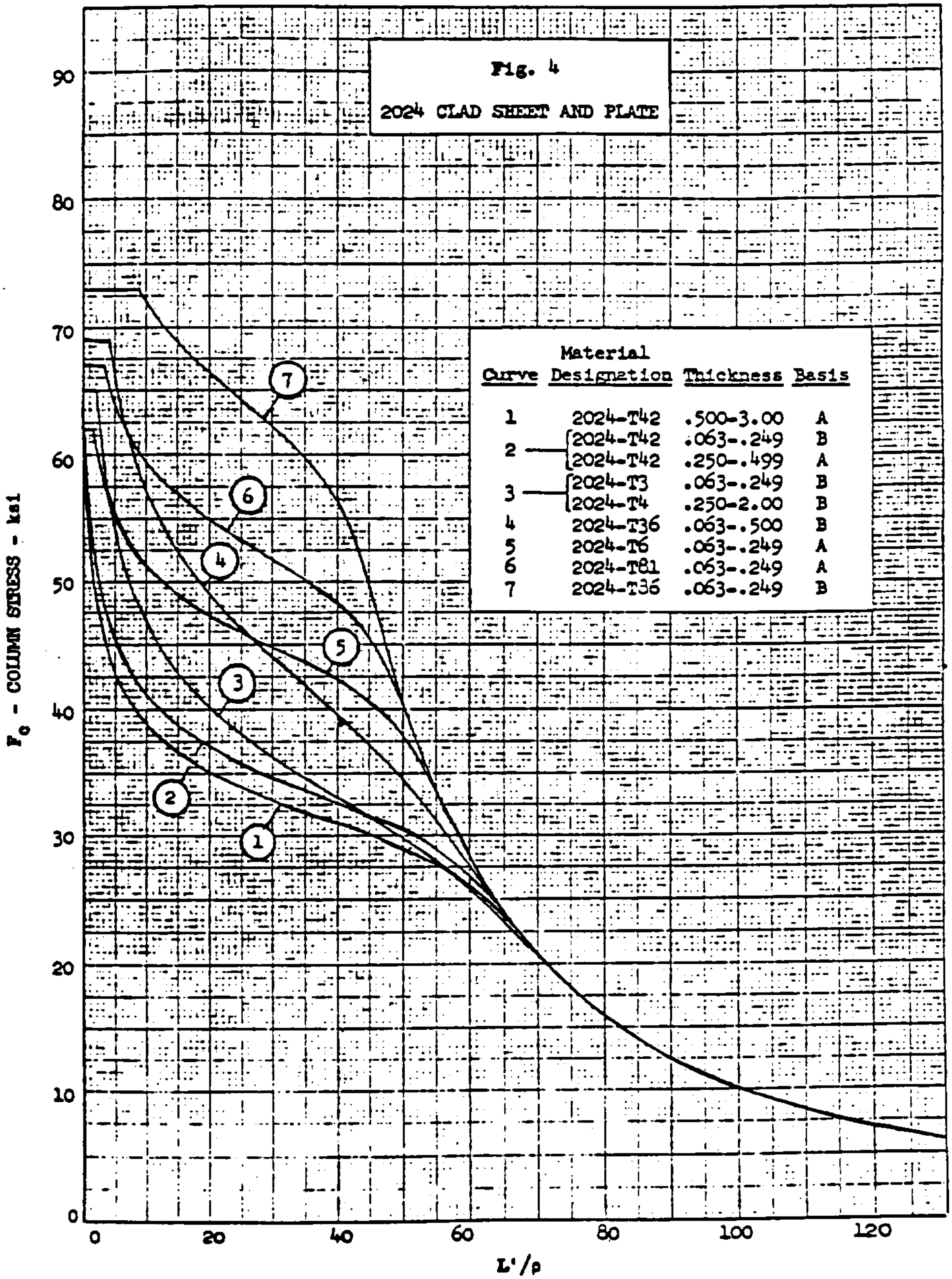

Curve	Material Designation	Thickness	Basis
1	2024-T42	.500-3.00	A
2	2024-T42	.063-.249	B
	2024-T42	.250-.499	A
3	2024-T3	.063-.249	B
	2024-T4	.250-2.00	B
4	2024-T36	.063-.500	B
5	2024-T6	.063-.249	A
6	2024-T81	.063-.249	A
7	2024-T36	.063-.249	B

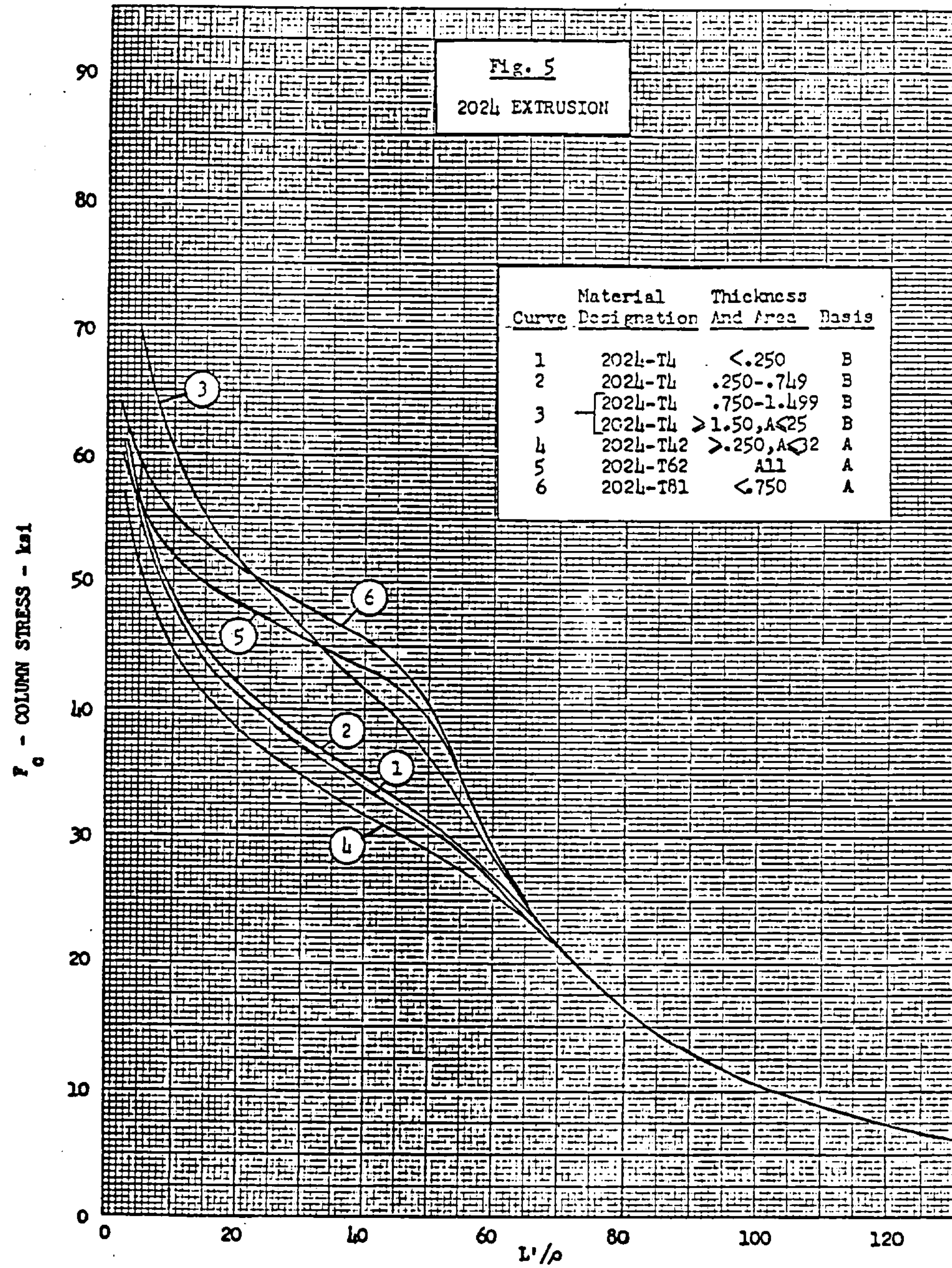
Fig. 5
2024 EXTRUSION
Curve | Material Designation | Thickness And Area | Basis
1 | 2024-T4 | <.250 | B
2 | 2024-T4 | .250-.749 | B
3 | 2024-T4 | .750-1.499 | B
3 | 2024-T4 | ≥1.50,A≤25 | B
4 | 2024-T42 | >.250,A≤32 | A
5 | 2024-T62 | All | A
6 | 2024-T81 | <.750 | A
1
2
3
4
5
6
F_c - COLUMN STRESS - ksi
0
10
20
30
40
50
60
70
80
90
0
20
40
60
80
100
120
L'/ρ

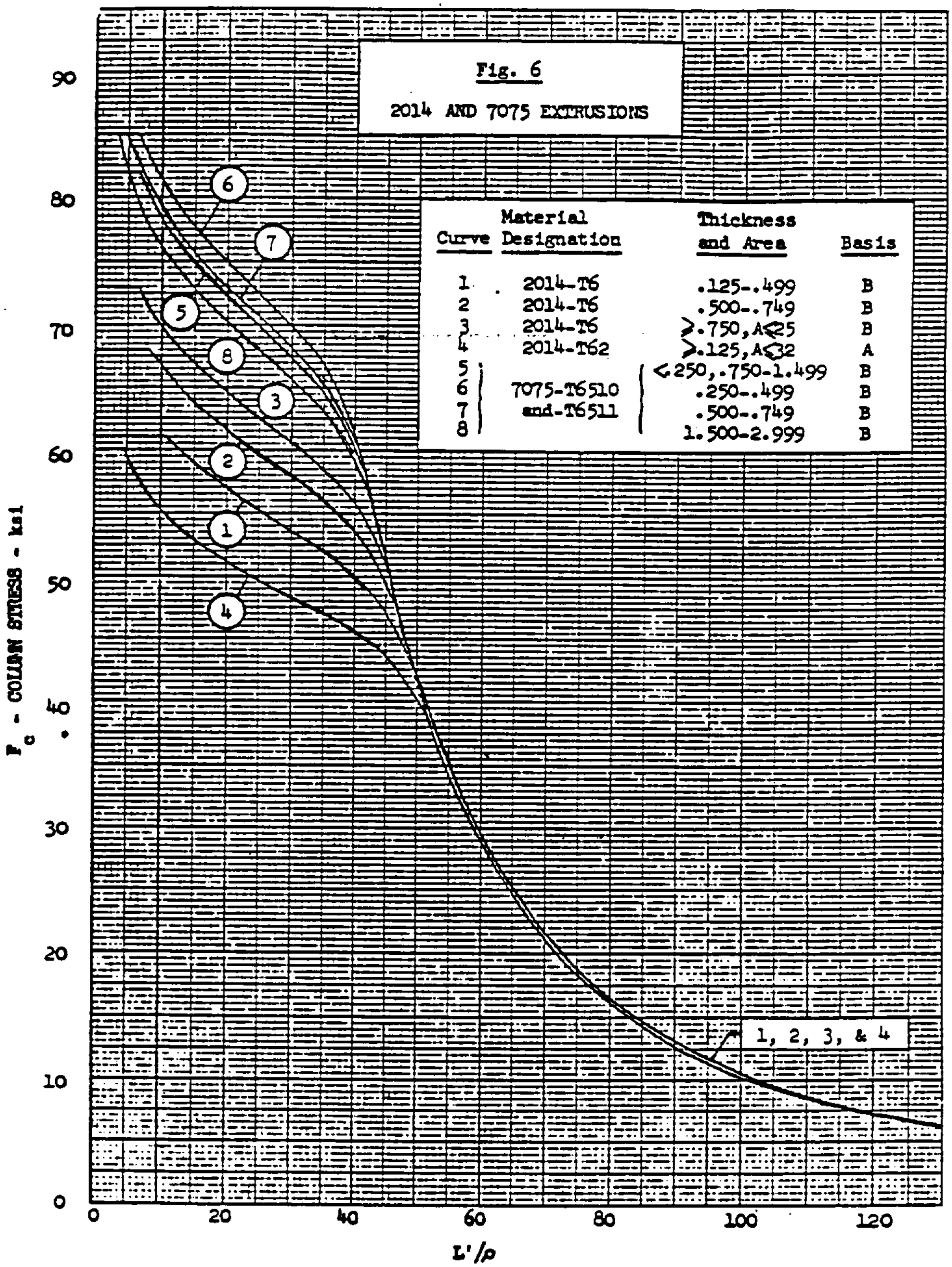
Fig. 6
2014 AND 7075 EXTRUSIONS
Curve | Material Designation | Thickness and Area | Basis
1 | 2014-T6 | .125-.499 | B
2 | 2014-T6 | .500-.749 | B
3 | 2014-T6 | ≥.750, A≤25 | B
4 | 2014-T62 | ≥.125, A≤32 | A
5 | 7075-T6510 and-T6511 | <.250, .750-1.499 | B
6 | | .250-.499 | B
7 | | .500-.749 | B
8 | | 1.500-2.999 | B
1, 2, 3, & 4
F_c - COLUMN STRESS - ksi
L'/ρ
0
10
20
30
40
50
60
70
80
90
100
120

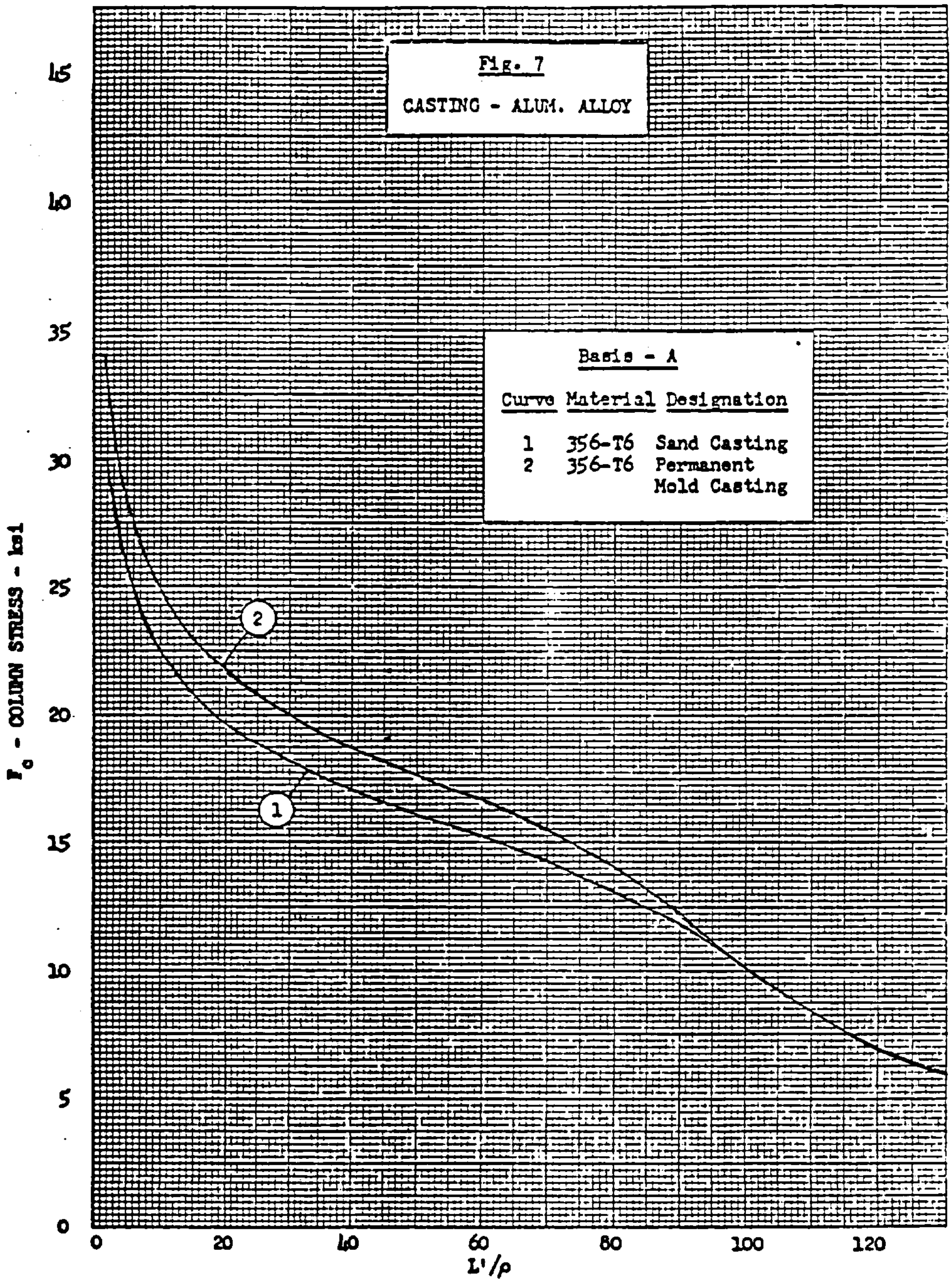
Fig. 7
CASTING - ALUM. ALLOY
Basis - A
Curve Material Designation
1 356-T6 Sand Casting
2 356-T6 Permanent Mold Casting
F_c - COLUMN STRESS - ksi
L'/ρ
0
5
10
15
20
25
30
35
40
45
0
20
40
60
80
100
120
1
2

271

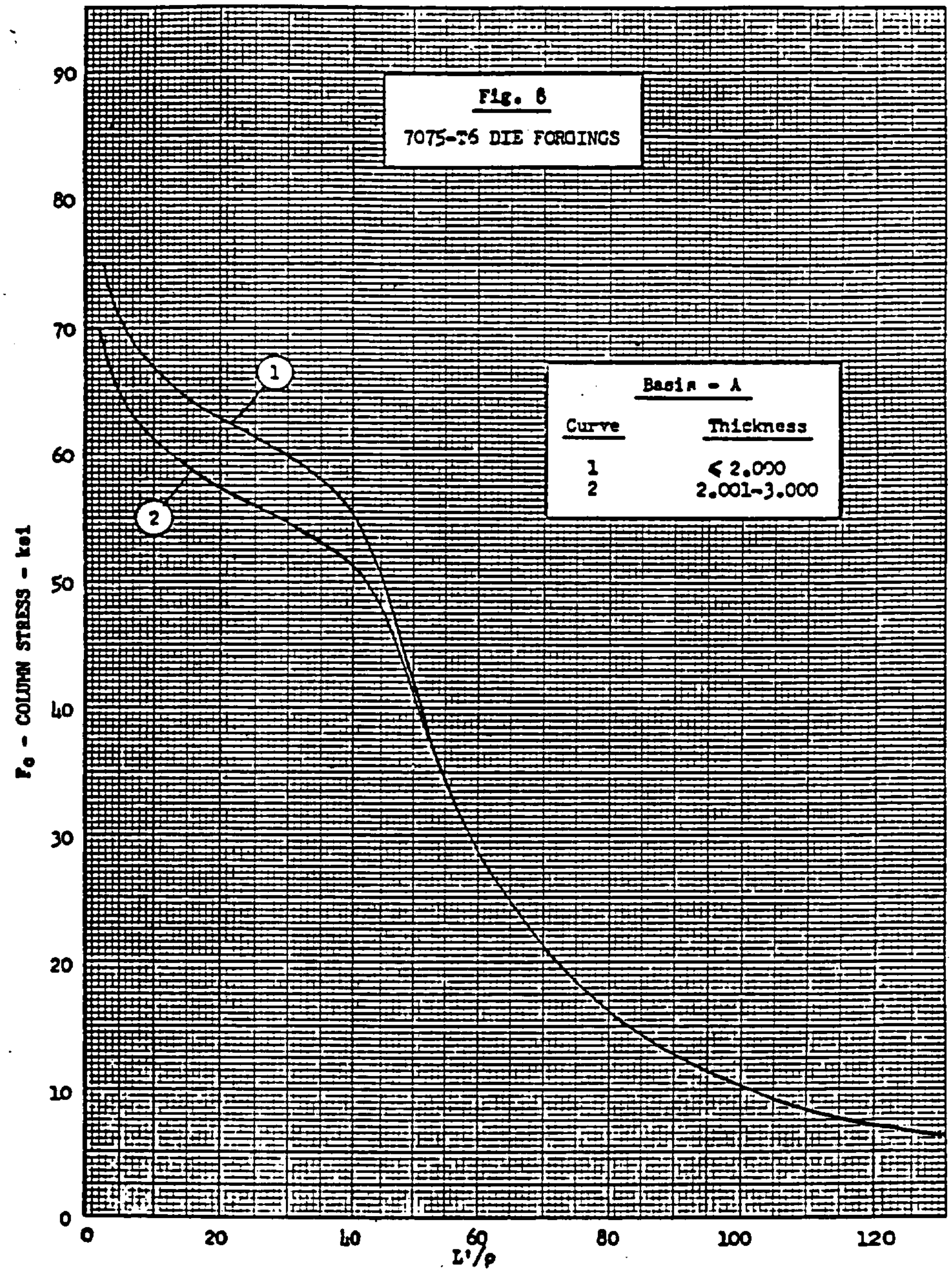
Fig. 8
7075-T6 DIE FORGINGS
Basis - A
Curve
Thickness
1
≤ 2.000
2
2.001-3.000
1
2
F_c - COLUMN STRESS - ksi
90
80
70
60
50
40
30
20
10
0
0
20
40
60
80
100
120
L'/ρ

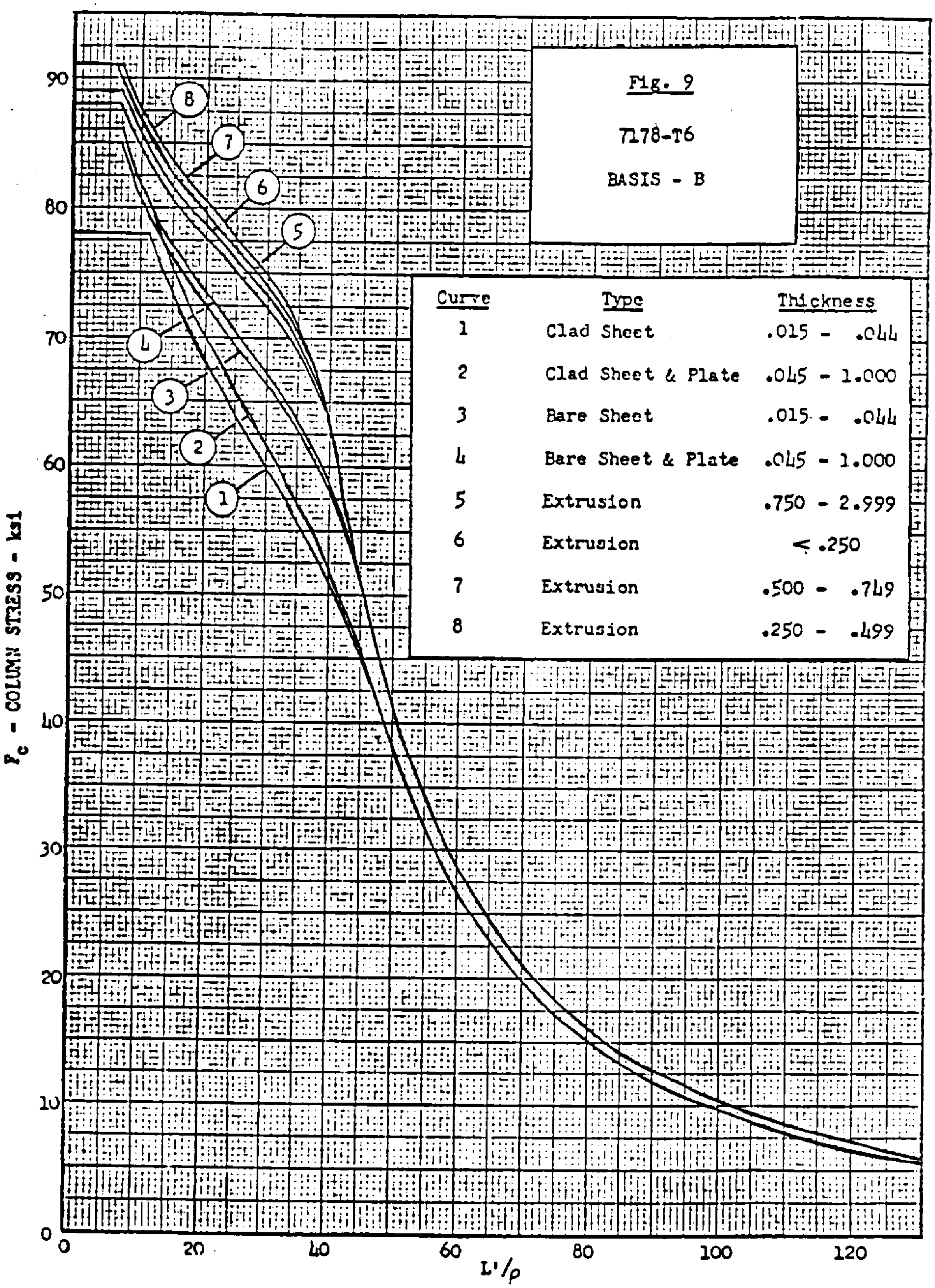
Fig. 9
7178-T6
BASIS - B
Curve Type Thickness
1 Clad Sheet .015 - .044
2 Clad Sheet & Plate .045 - 1.000
3 Bare Sheet .015 - .044
4 Bare Sheet & Plate .045 - 1.000
5 Extrusion .750 - 2.999
6 Extrusion < .250
7 Extrusion .500 - .749
8 Extrusion .250 - .499
Fc - COLUMN STRESS - ksi
L'/ρ
0
20
40
60
80
100
120
10
30
50
70
90

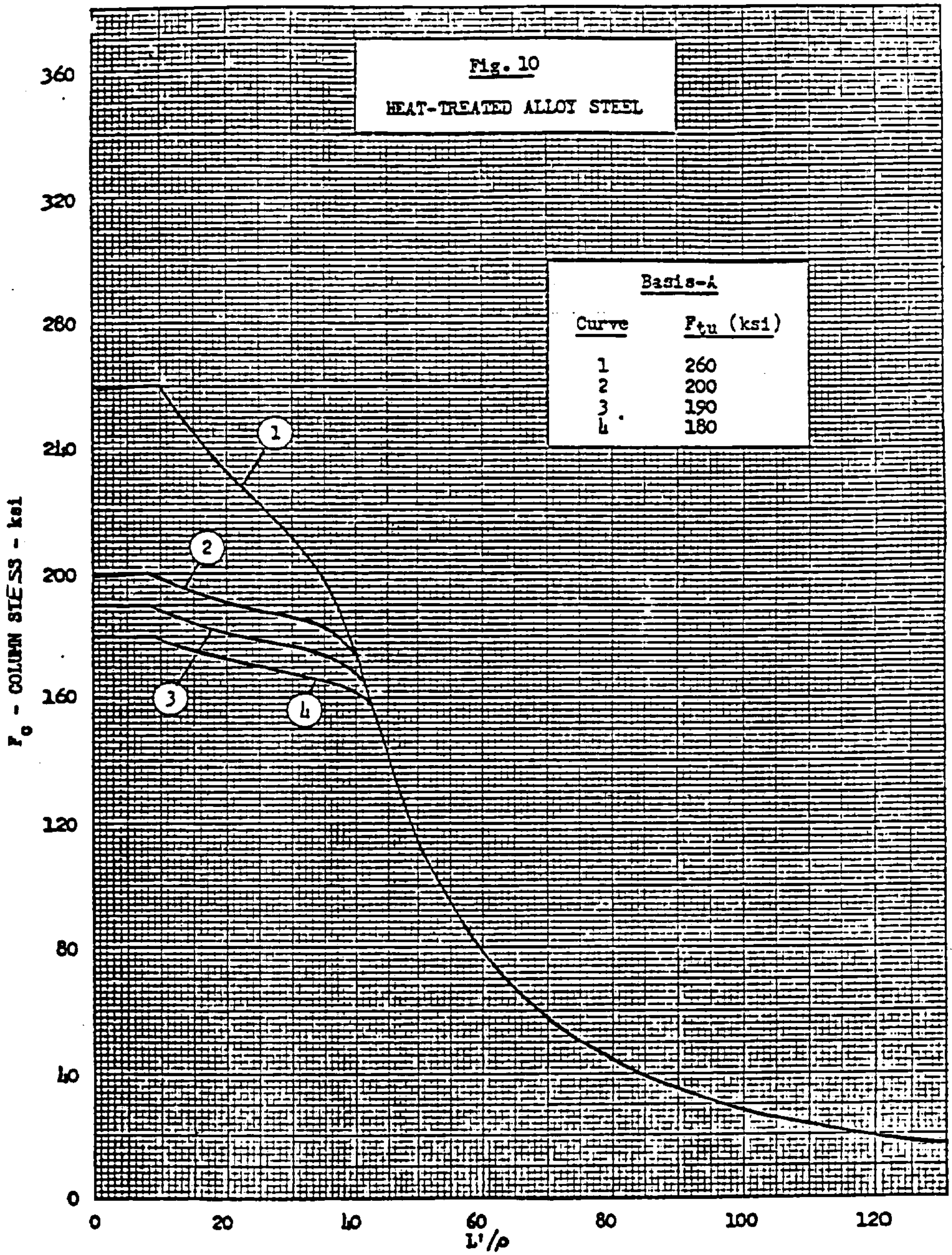
Fig. 10
HEAT-TREATED ALLOY STEEL
Basis-A
Curve
F_{tu} (ksi)
1
260
2
200
3
190
4
180
F_c - COLUMN STRESS - ksi
360
320
280
240
200
160
120
80
40
0
20
40
60
80
100
120
L'/ρ
1
2
3
4

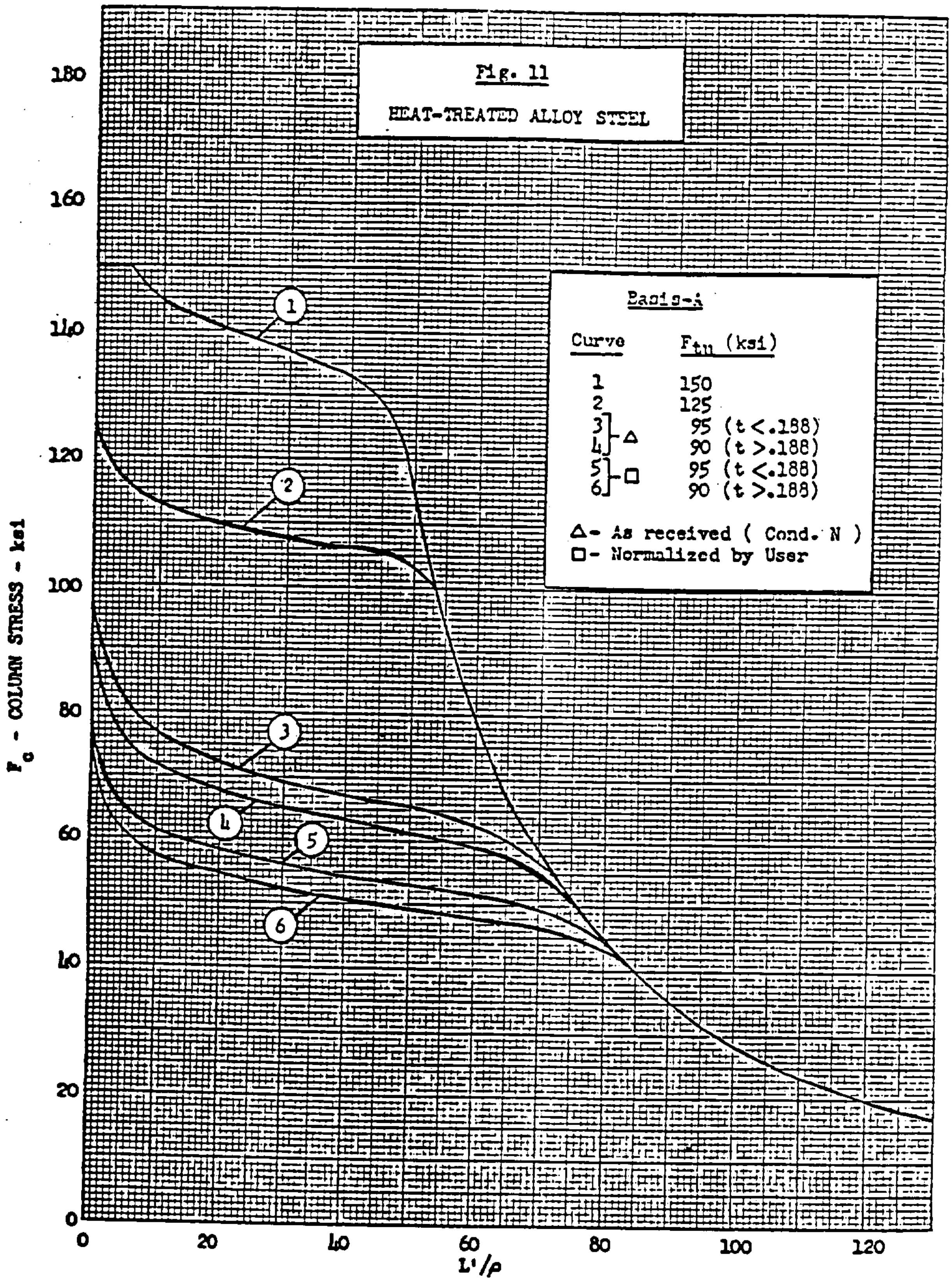
Fig. 11
HEAT-TREATED ALLOY STEEL
Basis-A
Curve
F_{tu} (ksi)
1 150
2 125
3 95 (t <.188)
4 90 (t >.188)
5 95 (t <.188)
6 90 (t >.188)
Δ- As received (Cond. N)
□- Normalized by User
F_c - COLUMN STRESS - ksi
L'/ρ
0
20
40
60
80
100
120
140
160
180
1
2
3
4
5
6

275

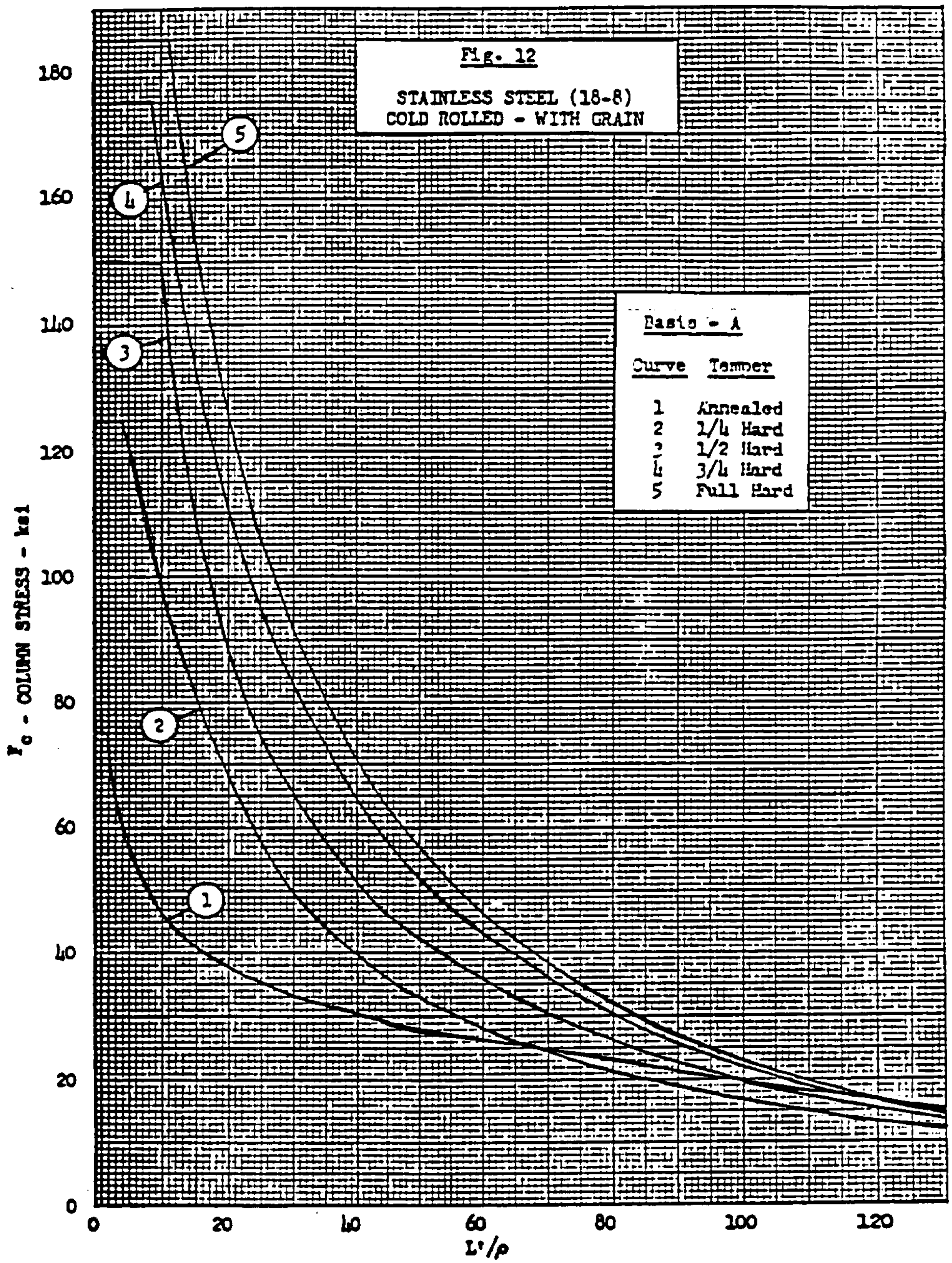
Fig. 12
STAINLESS STEEL (18-8)
COLD ROLLED - WITH GRAIN
Basis - A
Curve Temper
1 Annealed
2 1/4 Hard
3 1/2 Hard
4 3/4 Hard
5 Full Hard
F_c - COLUMN STRESS - ksi
L'/ρ
0
20
40
60
80
100
120
140
160
180
1
2
3
4
5

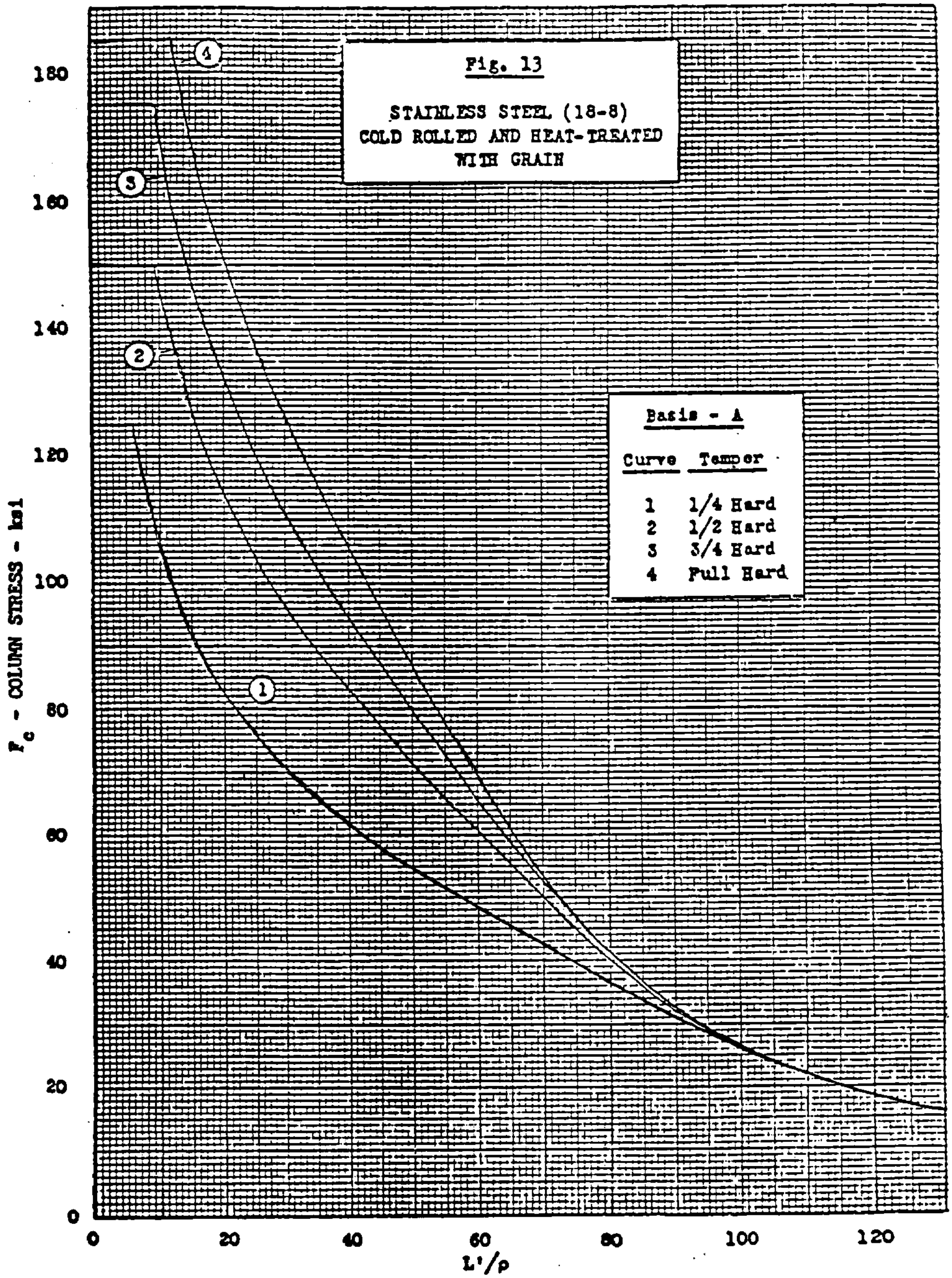
Fig. 13
STAINLESS STEEL (18-8)
COLD ROLLED AND HEAT-TREATED
WITH GRAIN
Basis - A
Curve Temper
1 1/4 Hard
2 1/2 Hard
3 3/4 Hard
4 Full Hard
1
2
3
4
F_c - COLUMN STRESS - ksi
0
20
40
60
80
100
120
140
160
180
L'/ρ
0
20
40
60
80
100
120

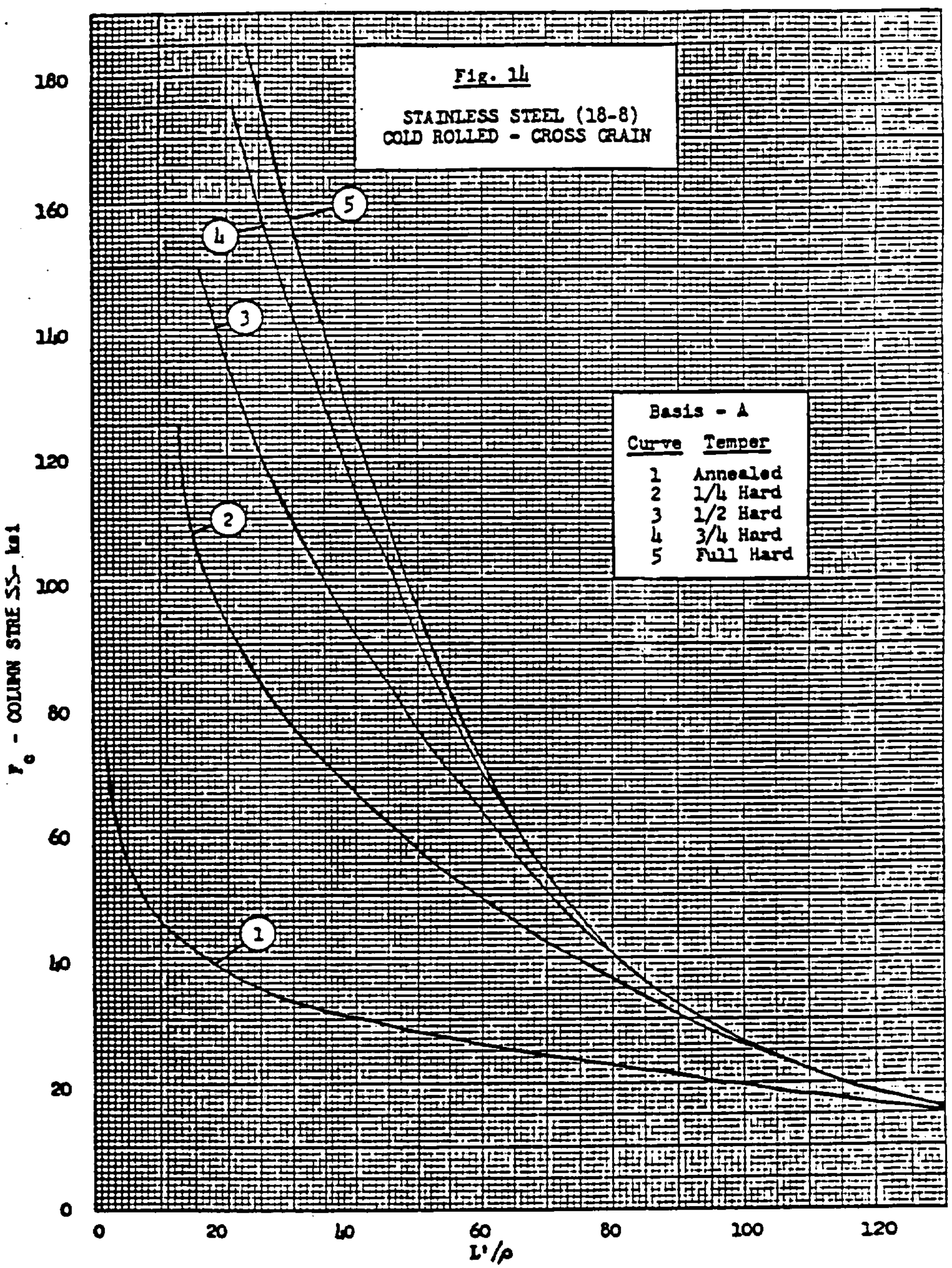
Fig. 14
STAINLESS STEEL (18-8)
COLD ROLLED - CROSS GRAIN
Basis - A
Curve Temper
1 Annealed
2 1/4 Hard
3 1/2 Hard
4 3/4 Hard
5 Full Hard
F_c - COLUMN STRESS - ksi
L'/ρ
0
20
40
60
80
100
120
140
160
180

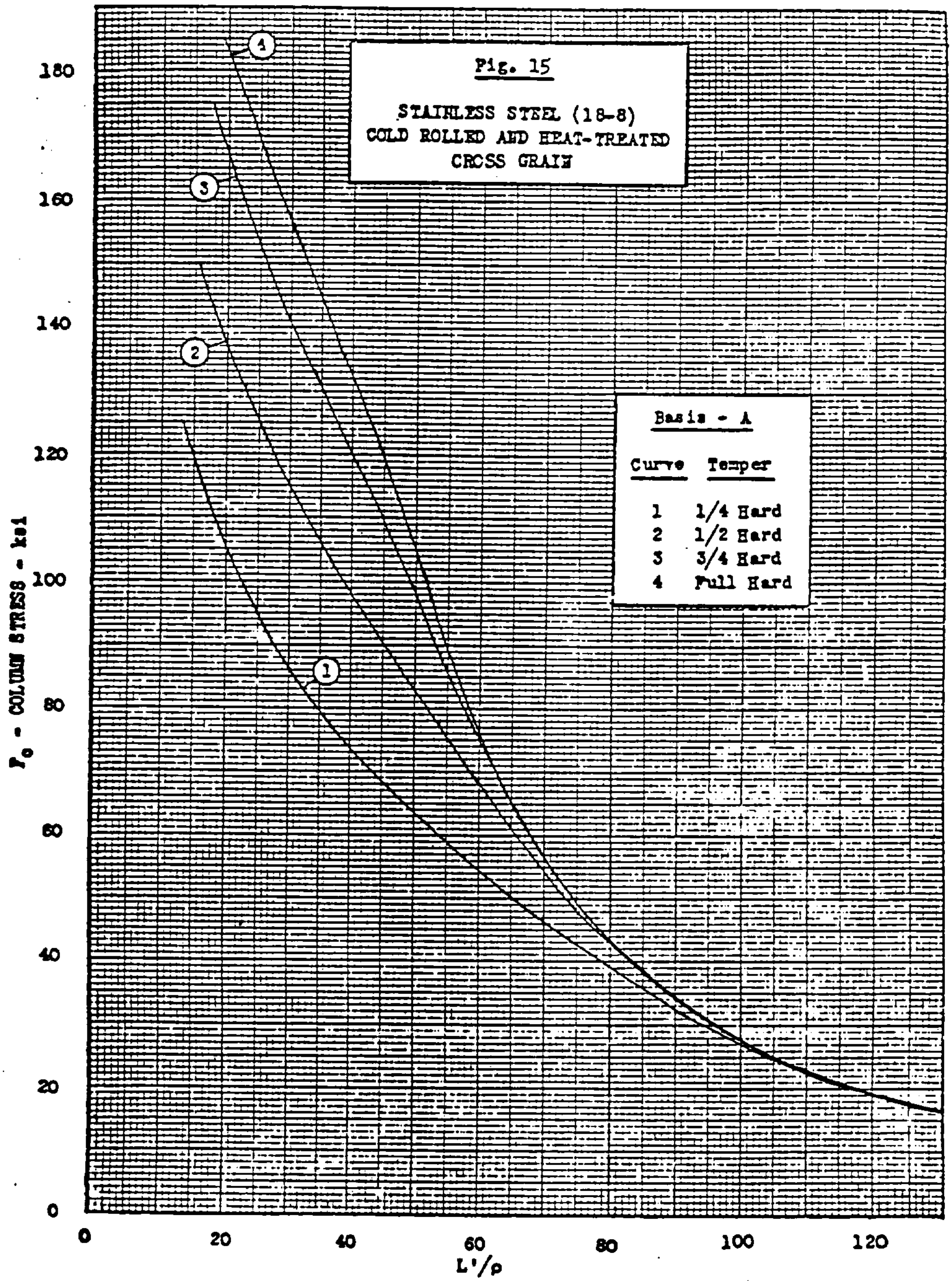
Fig. 15
STAINLESS STEEL (18-8)
COLD ROLLED AND HEAT-TREATED
CROSS GRAIN
Basis - A
Curve Temper
1 1/4 Hard
2 1/2 Hard
3 3/4 Hard
4 Full Hard
1
2
3
4
F_c - COLUMN STRESS - ksi
0
20
40
60
80
100
120
140
160
180
0
20
40
60
80
100
120
L'/ρ

774

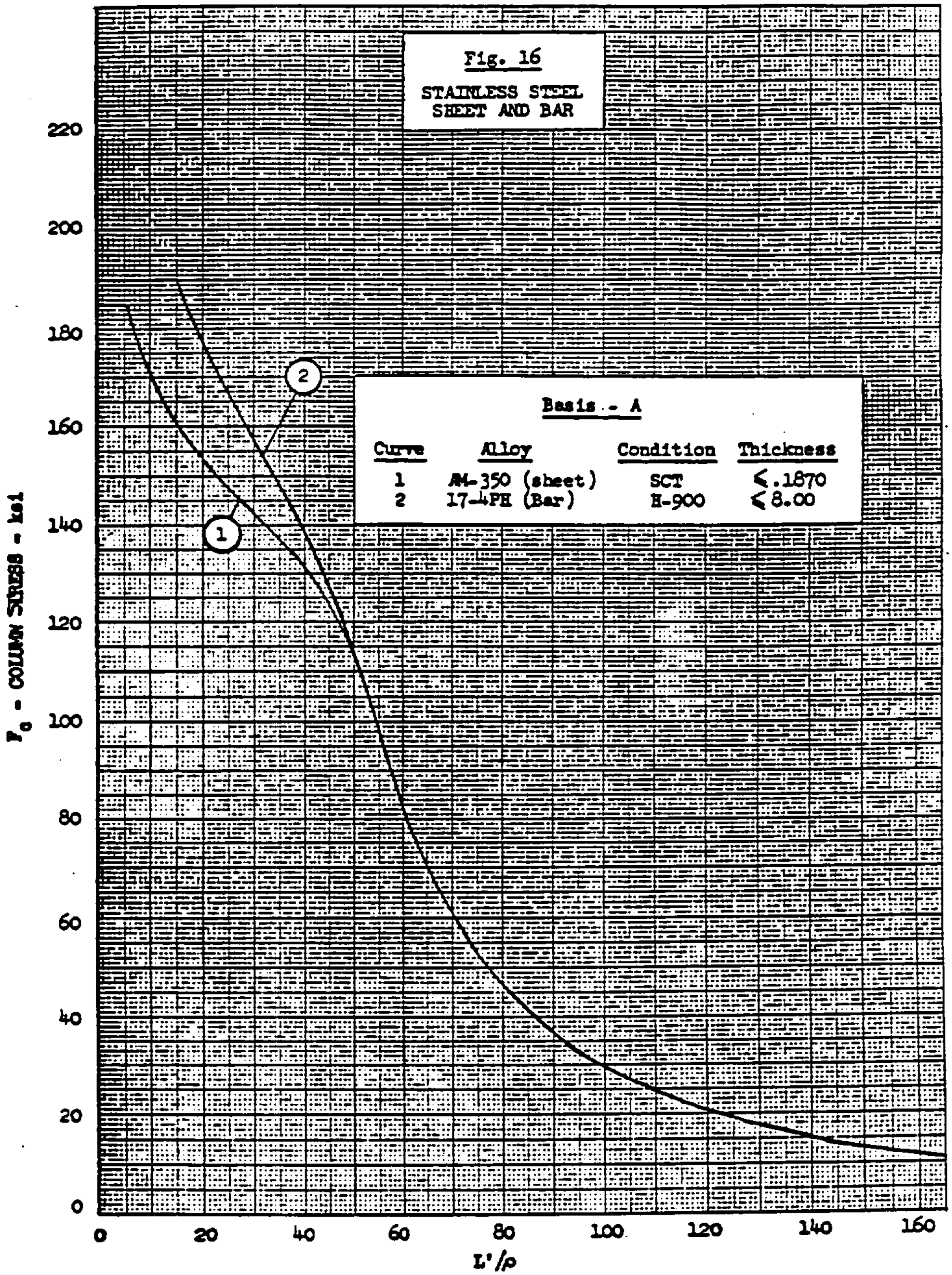
Fig. 16
STAINLESS STEEL
SHEET AND BAR
Basis - A
Curve | Alloy | Condition | Thickness
1 | AM-350 (sheet) | SCT | ≤ .1870
2 | 17-4PH (Bar) | H-900 | ≤ 8.00
1
2
F_c - COLUMN STRESS - ksi
0
20
40
60
80
100
120
140
160
180
200
220
L'/ρ
0
20
40
60
80
100
120
140
160

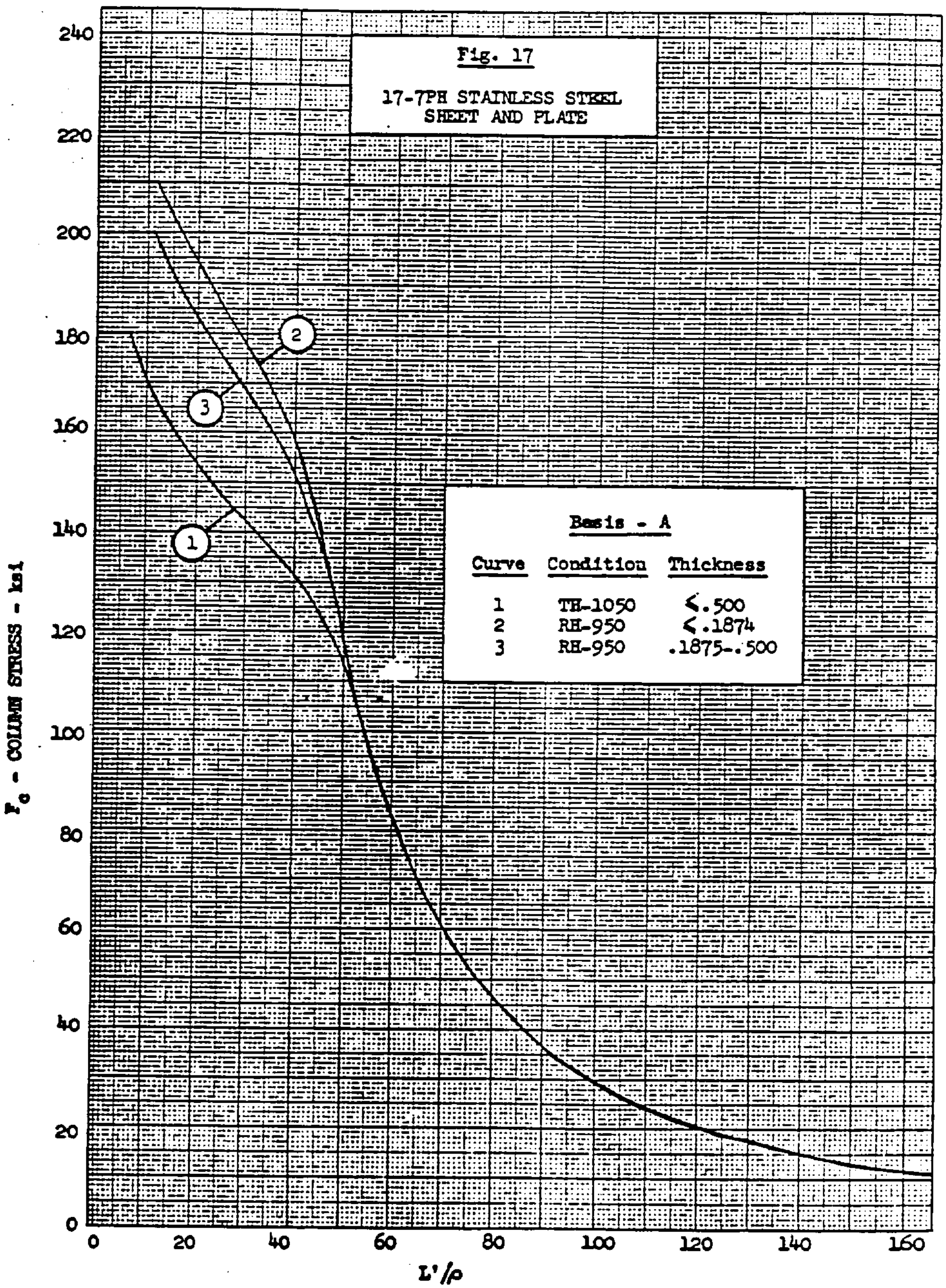
Fig. 17
17-7PH STAINLESS STEEL
SHEET AND PLATE
Basis - A
Curve Condition Thickness
1 TH-1050 ≤.500
2 RH-950 ≤.1874
3 RH-950 .1875-.500
F_c - COLUMN STRESS - ksi
L'/ρ
0
20
40
60
80
100
120
140
160
180
200
220
240
1
2
3

28

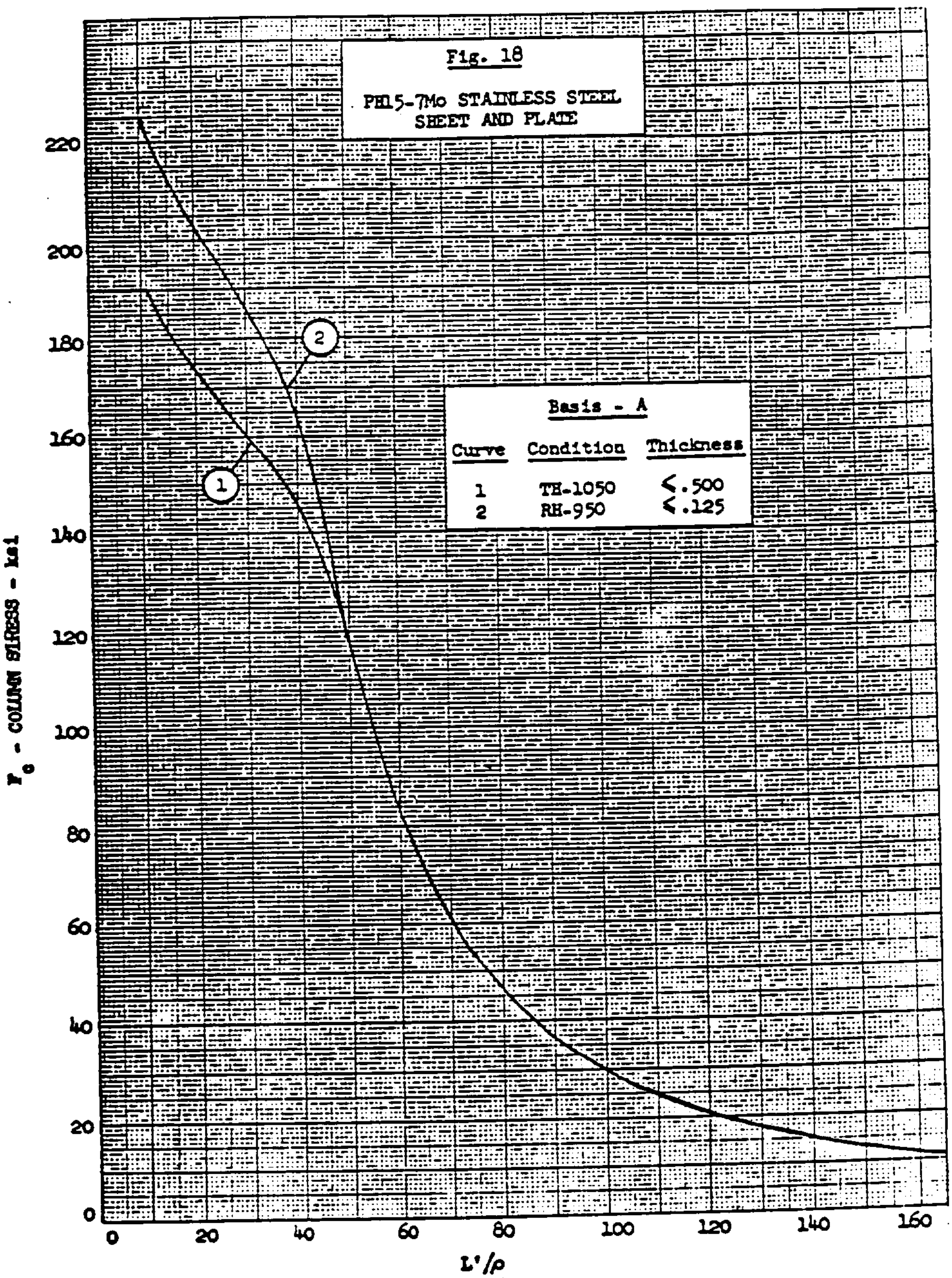
Fig. 18
PH15-7Mo STAINLESS STEEL
SHEET AND PLATE
Basis - A
Curve Condition Thickness
1 TH-1050 ≤ .500
2 RH-950 ≤ .125
1
2
F_c - COLUMN STRESS - ksi
0
20
40
60
80
100
120
140
160
180
200
220
0
20
40
60
80
100
120
140
160
L'/ρ

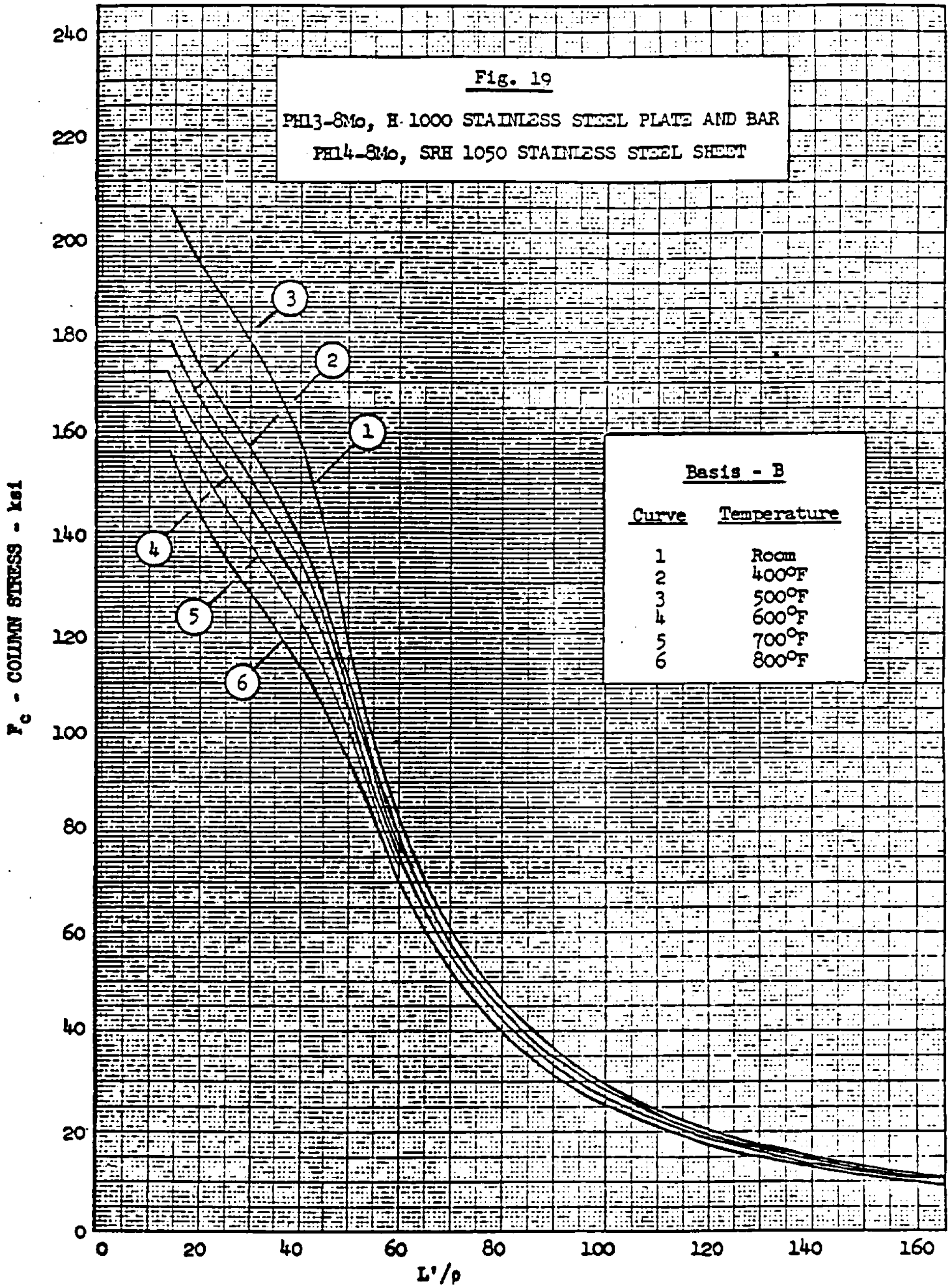
Fig. 19
PH13-8Mo, H 1000 STAINLESS STEEL PLATE AND BAR
PH14-8Mo, SRH 1050 STAINLESS STEEL SHEET
Basis - B
Curve
Temperature
1
Room
2
400°F
3
500°F
4
600°F
5
700°F
6
800°F
1
2
3
4
5
6
F_c - COLUMN STRESS - ksi
L'/ρ
0
20
40
60
80
100
120
140
160
180
200
220
240

283

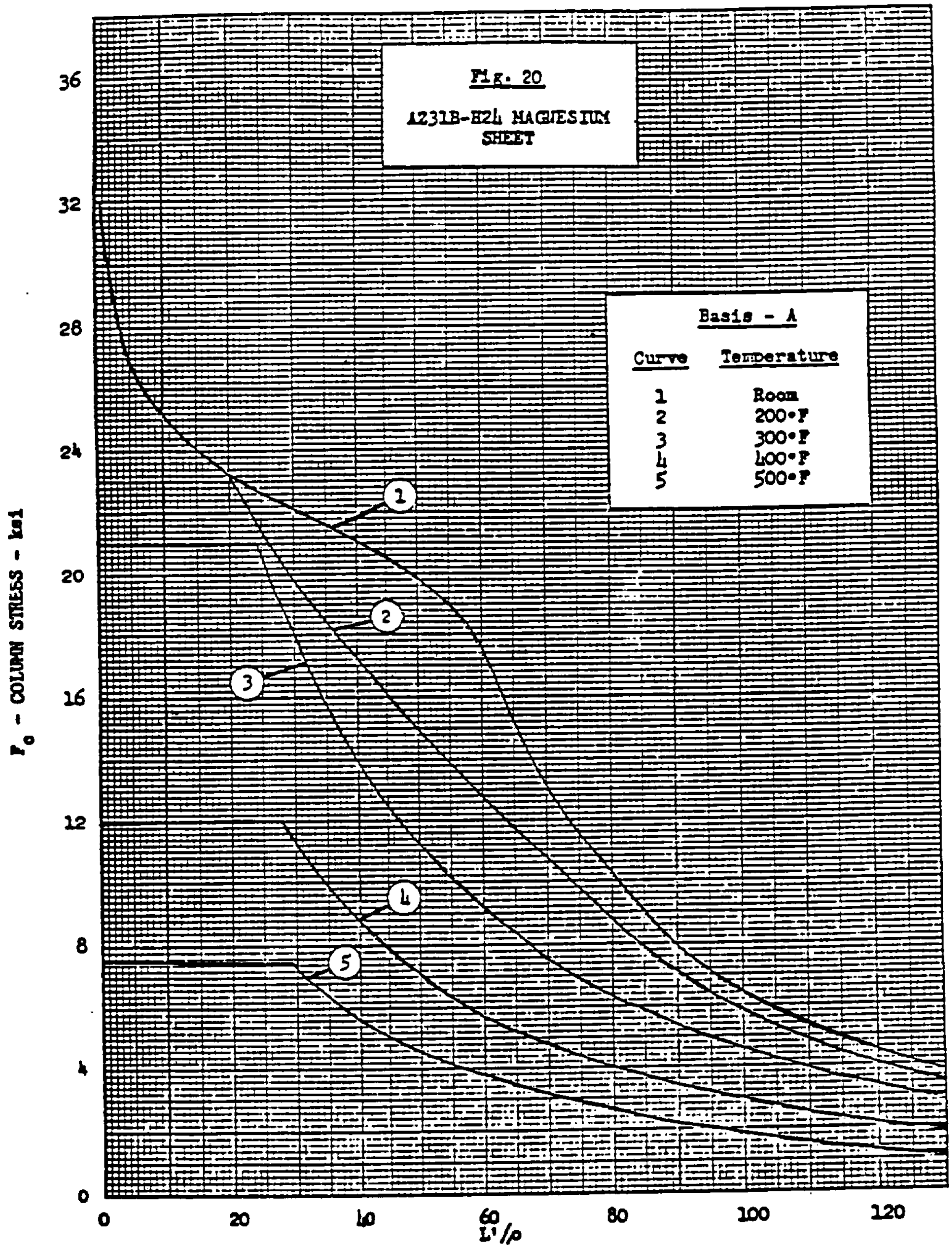
Fig. 20
AZ31B-H24 MAGNESIUM SHEET
Basis - A
Curve Temperature
1 Room
2 200°F
3 300°F
4 400°F
5 500°F
F_c - COLUMN STRESS - ksi
L'/ρ
0
4
8
12
16
20
24
28
32
36
20
40
60
80
100
120
1
2
3
4
5

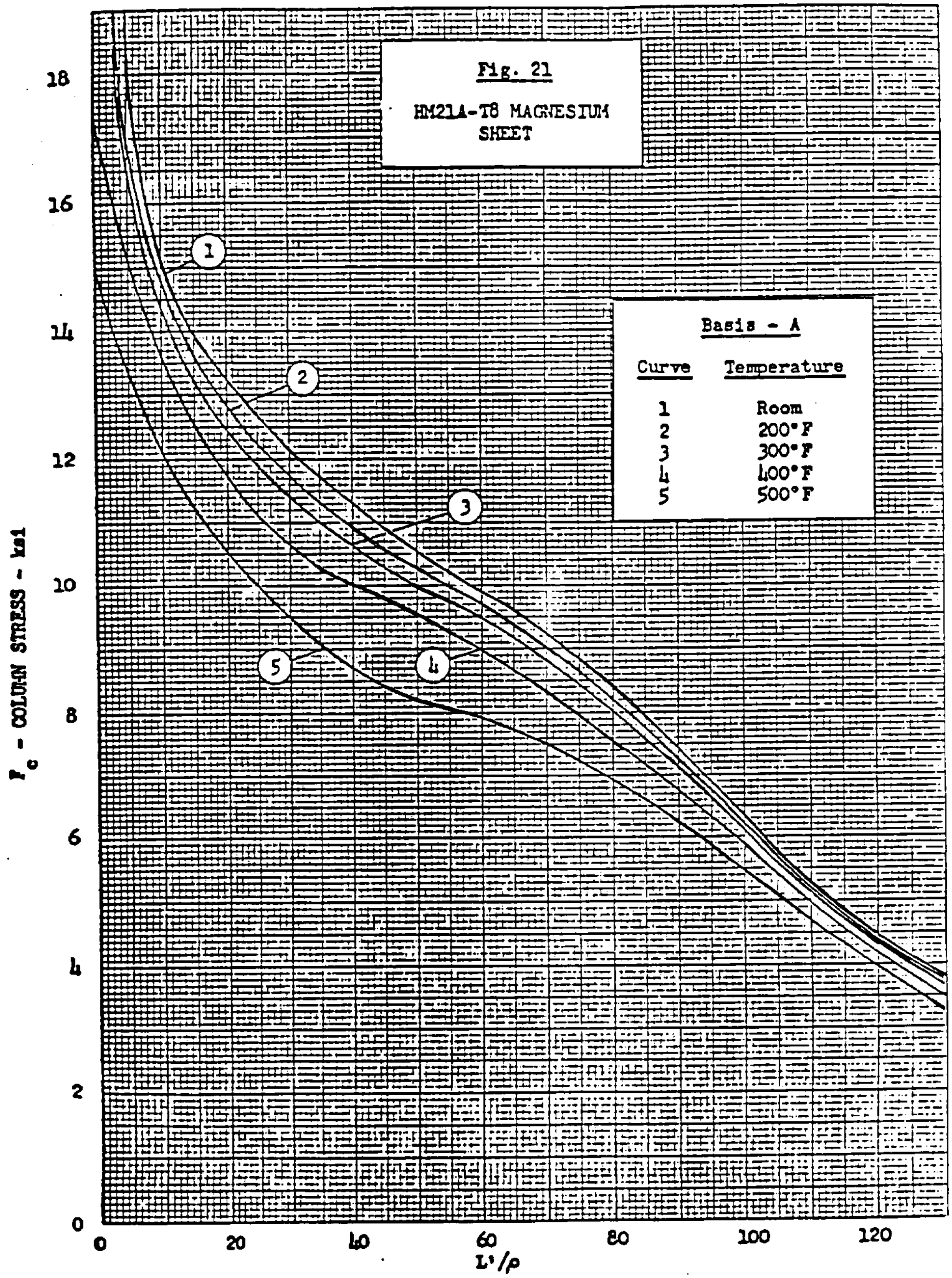
Fig. 21
HM21A-T8 MAGNESIUM SHEET
Basis - A
Curve Temperature
1 Room
2 200°F
3 300°F
4 400°F
5 500°F
F_c - COLUMN STRESS - ksi
L'/ρ
0
2
4
6
8
10
12
14
16
18
20
40
60
80
100
120
1
2
3
4
5

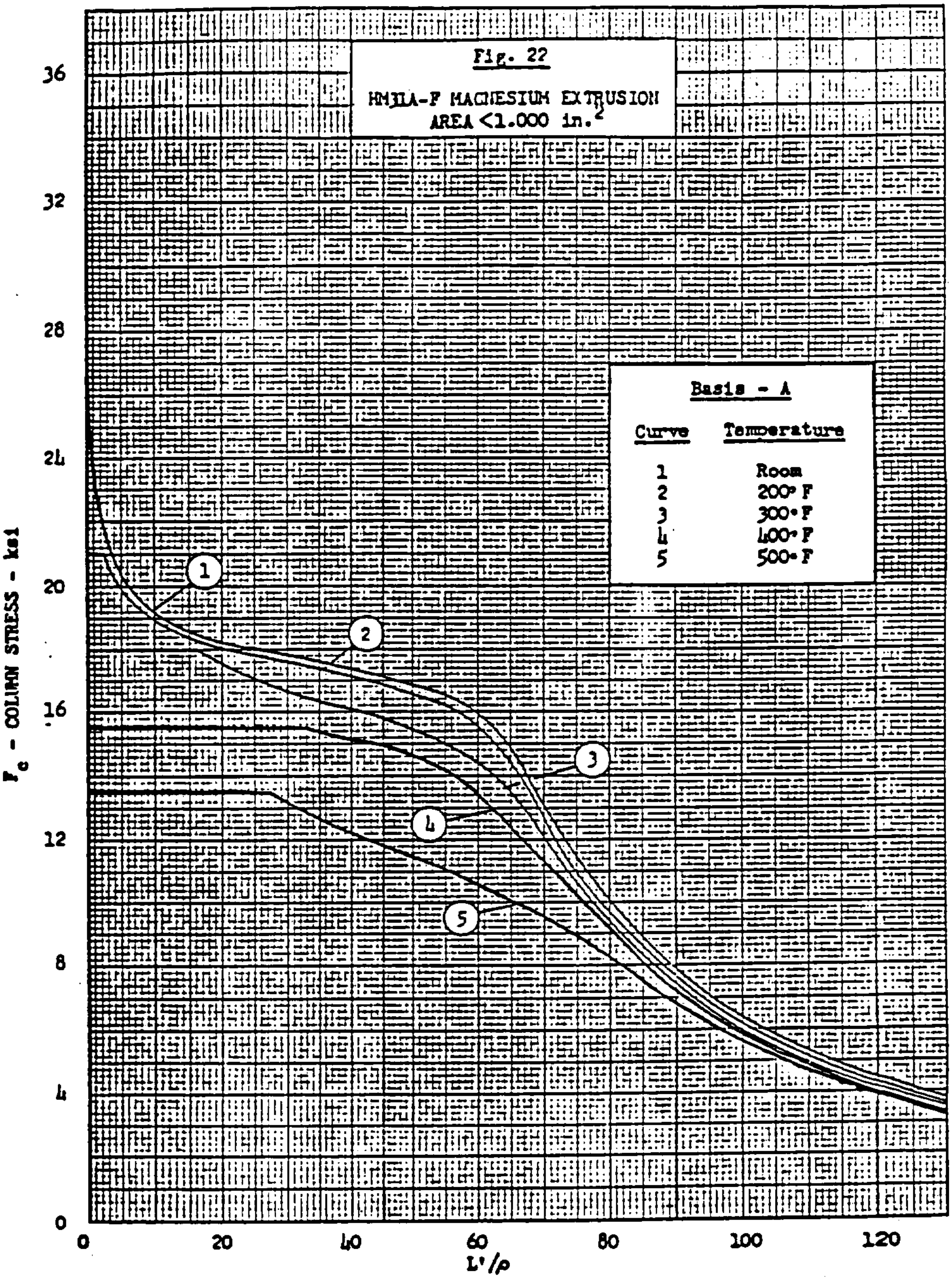
Fig. 22
HM31A-F MAGNESIUM EXTRUSION
AREA <1.000 in.²
Basis - A
Curve | Temperature
1 | Room
2 | 200° F
3 | 300° F
4 | 400° F
5 | 500° F
1
2
3
4
5
F_c - COLUMN STRESS - ksi
0
4
8
12
16
20
24
28
32
36
0
20
40
60
80
100
120
L'/ρ

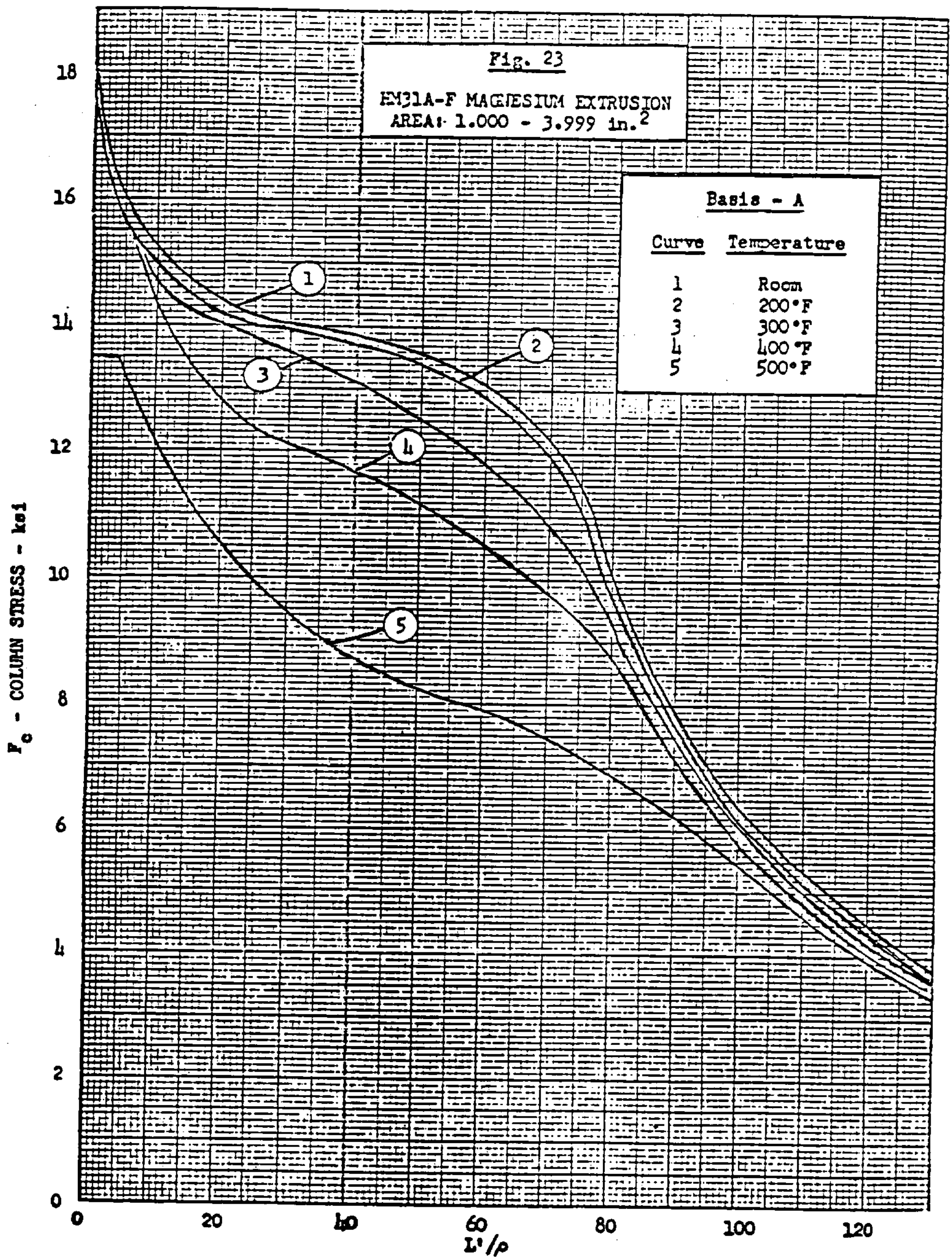
Fig. 23
EM31A-F MAGNESIUM EXTRUSION
AREA: 1.000 - 3.999 in.^{2}
Basis - A
Curve Temperature
1 Room
2 200°F
3 300°F
4 400°F
5 500°F
F_c - COLUMN STRESS - ksi
L'/ρ
0
2
4
6
8
10
12
14
16
18
20
40
60
80
100
120

287

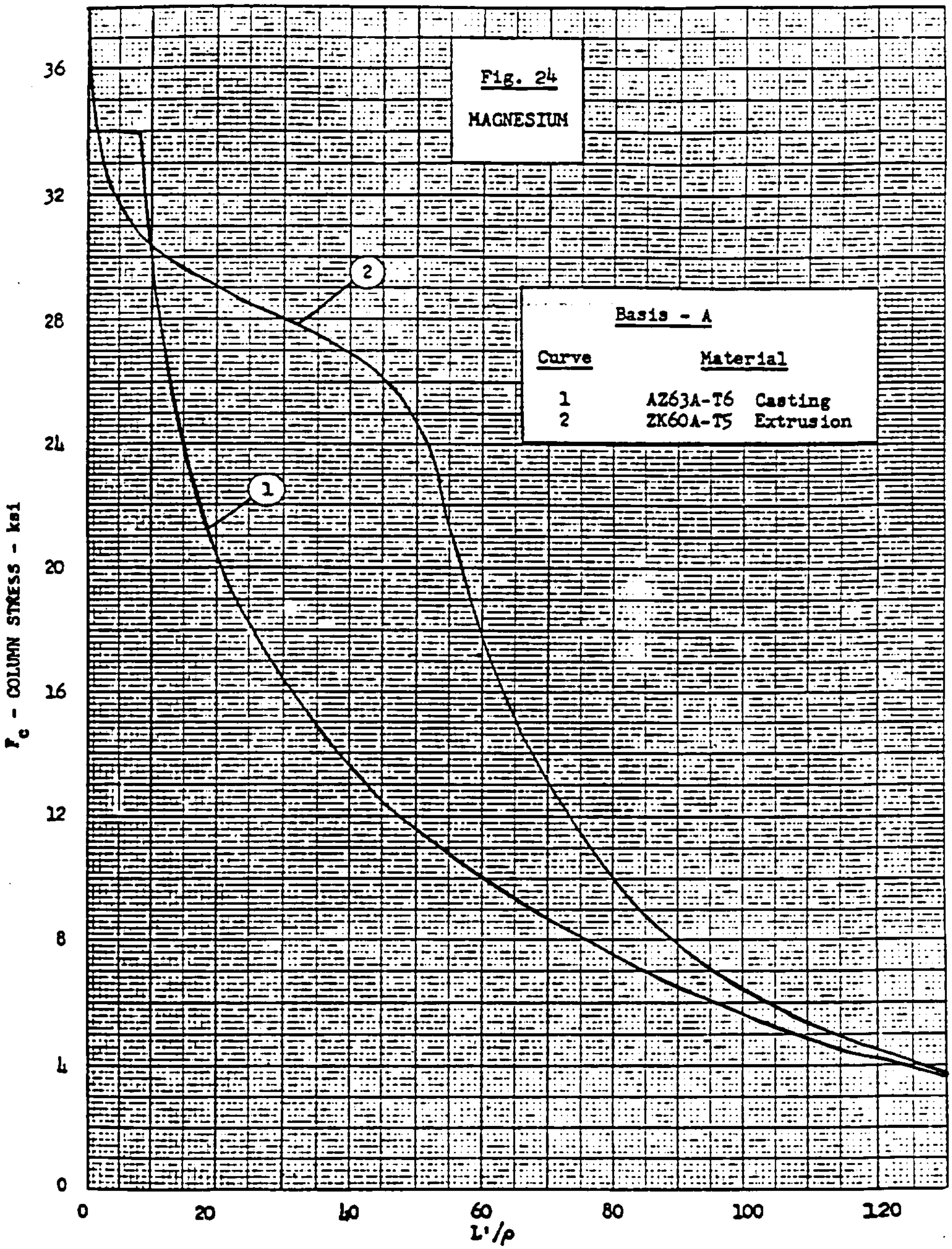
Fig. 24
MAGNESIUM
Basis - A
Curve Material
1 AZ63A-T6 Casting
2 ZK60A-T5 Extrusion
F_c - COLUMN STRESS - ksi
0
4
8
12
16
20
24
28
32
36
0
20
40
60
80
100
120
L'/ρ
1
2

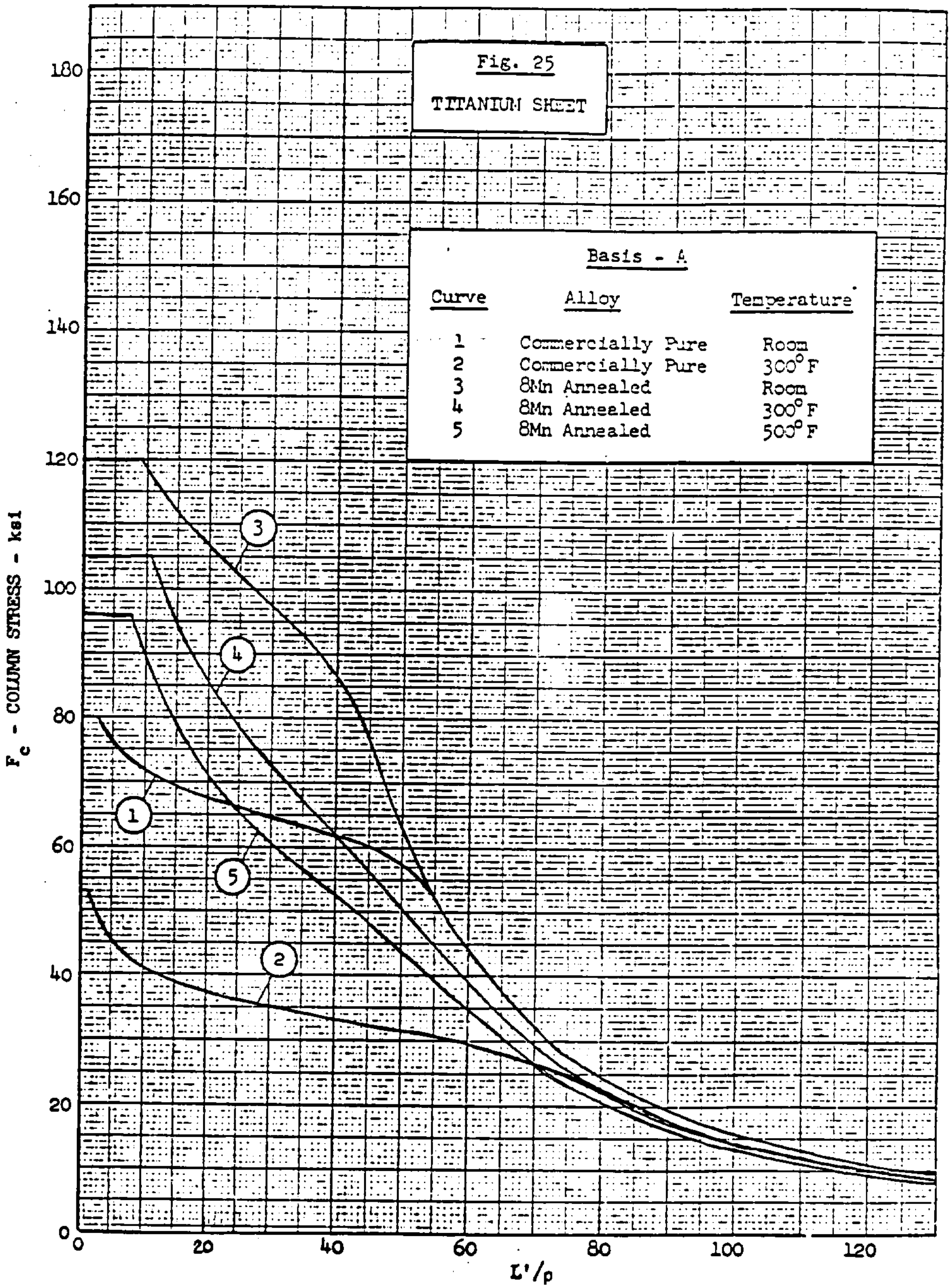
Fig. 25
TITANIUM SHEET
Basis - A
Curve Alloy Temperature
1 Commercially Pure Room
2 Commercially Pure 300° F
3 8Mn Annealed Room
4 8Mn Annealed 300° F
5 8Mn Annealed 500° F
F_c - COLUMN STRESS - ksi
0
20
40
60
80
100
120
140
160
180
0
20
40
60
80
100
120
L'/ρ
1
2
3
4
5

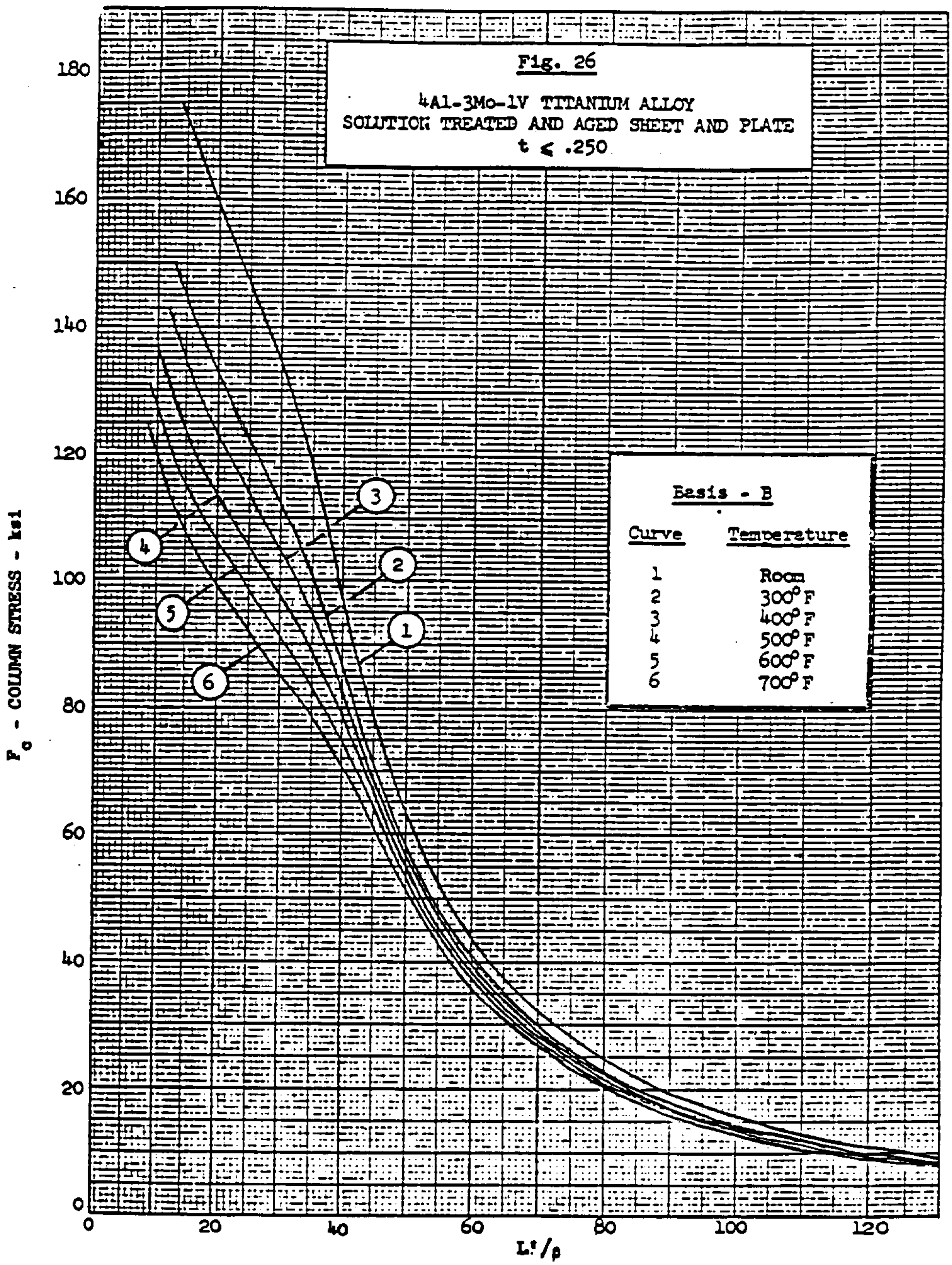
Fig. 26
4Al-3Mo-1V TITANIUM ALLOY
SOLUTION TREATED AND AGED SHEET AND PLATE
t ≤ .250
Basis - B
Curve Temperature
1 Room
2 300° F
3 400° F
4 500° F
5 600° F
6 700° F
Fc - COLUMN STRESS - ksi
L'/ρ
0 20 40 60 80 100 120
20 40 60 80 100 120 140 160 180
1 2 3 4 5 6

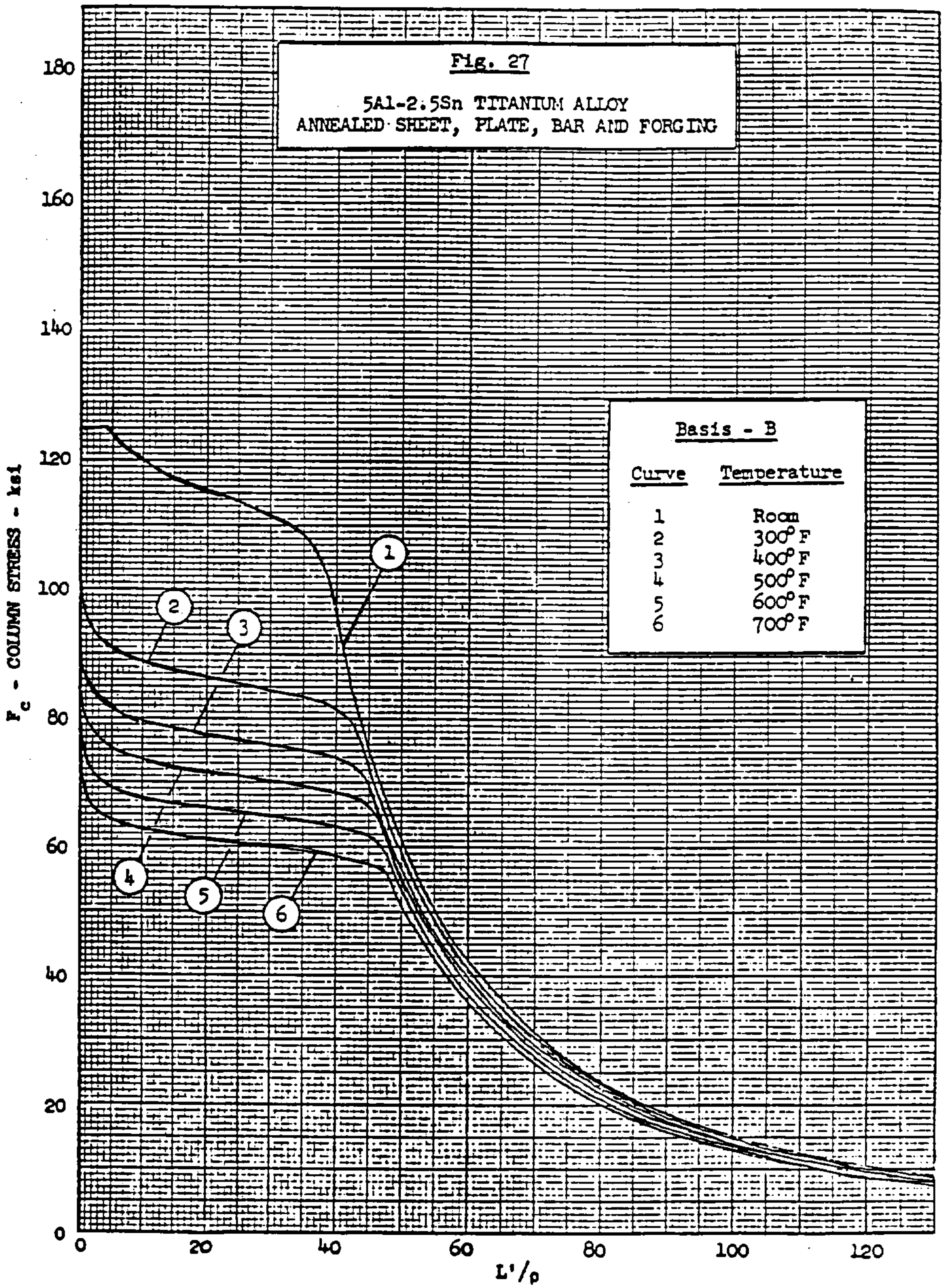
Fig. 27
5Al-2.5Sn TITANIUM ALLOY
ANNEALED SHEET, PLATE, BAR AND FORGING
Basis - B
Curve
Temperature
1 Room
2 300°F
3 400°F
4 500°F
5 600°F
6 700°F
1
2
3
4
5
6
F_c - COLUMN STRESS - ksi
0
20
40
60
80
100
120
140
160
180
0
20
40
60
80
100
120
L'/ρ

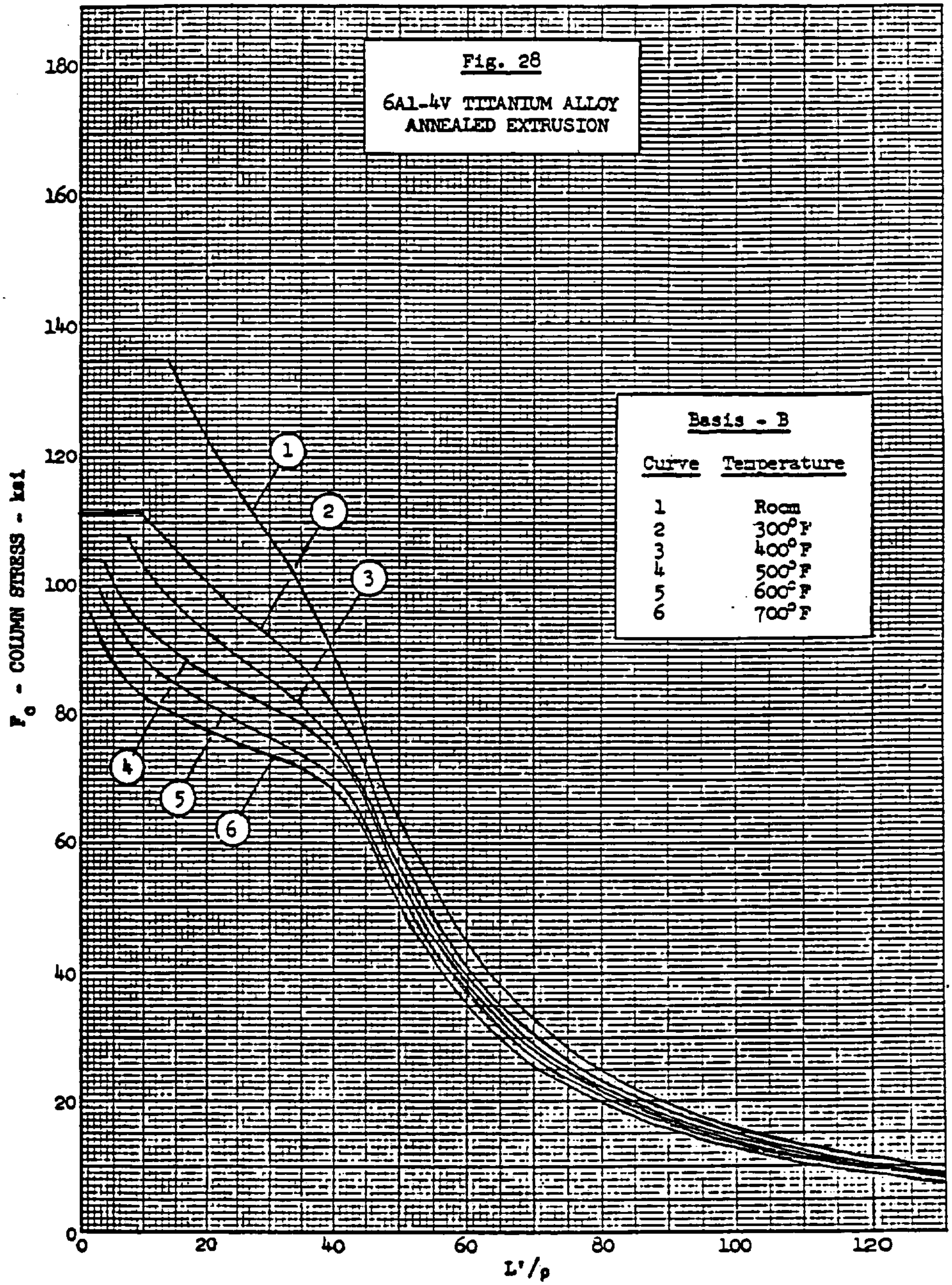
Fig. 28
6Al-4V TITANIUM ALLOY
ANNEALED EXTRUSION
Basis - B
Curve Temperature
1 Room
2 300°F
3 400°F
4 500°F
5 600°F
6 700°F
1
2
3
4
5
6
F_c - COLUMN STRESS - ksi
0
20
40
60
80
100
120
140
160
180
L'/ρ
0
20
40
60
80
100
120

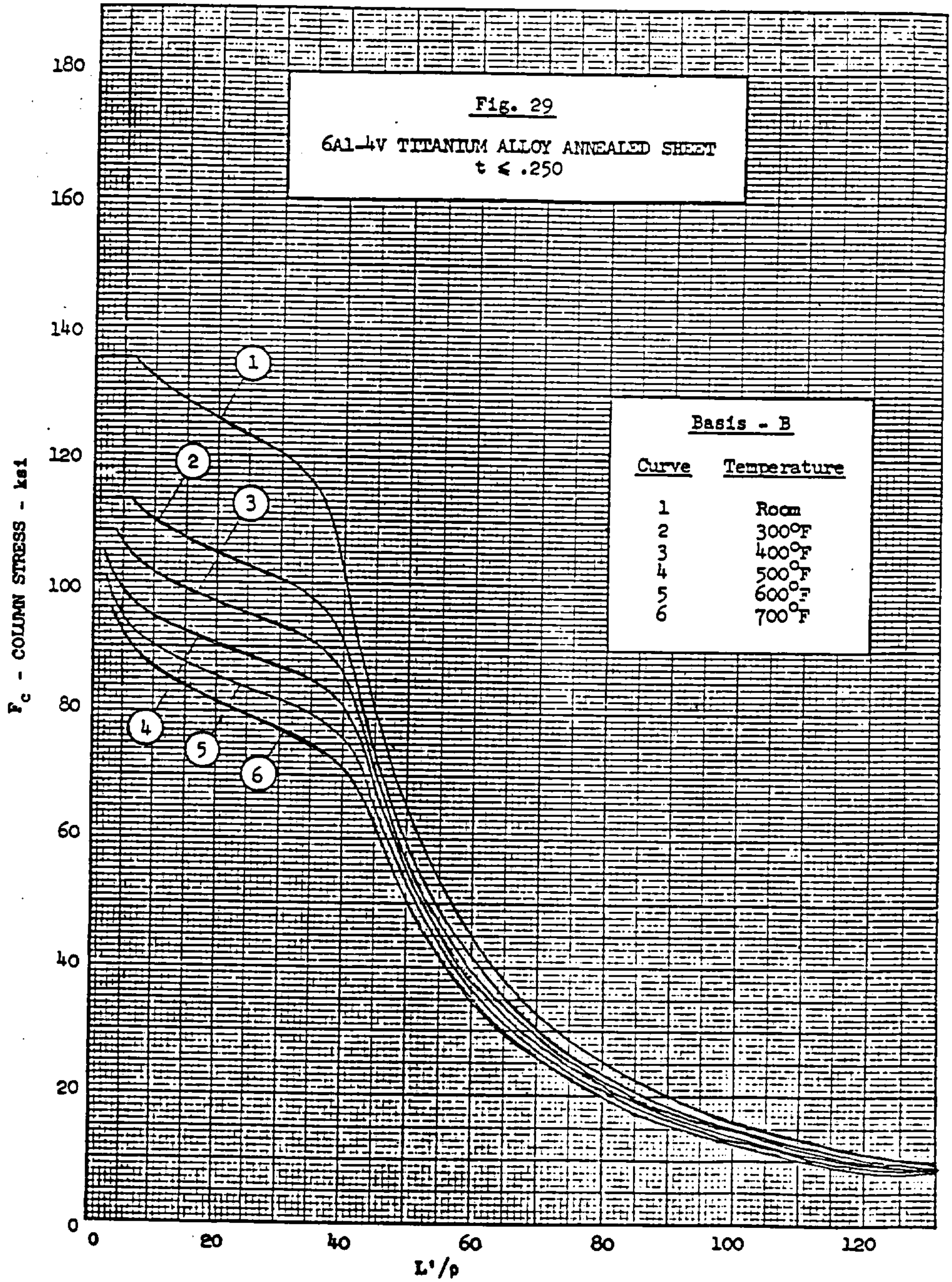
Fig. 29
6Al-4V TITANIUM ALLOY ANNEALED SHEET
t ≤ .250
Basis - B
Curve
Temperature
1 Room
2 300°F
3 400°F
4 500°F
5 600°F
6 700°F
F_c - COLUMN STRESS - ksi
L'/ρ
0
20
40
60
80
100
120
140
160
180

293

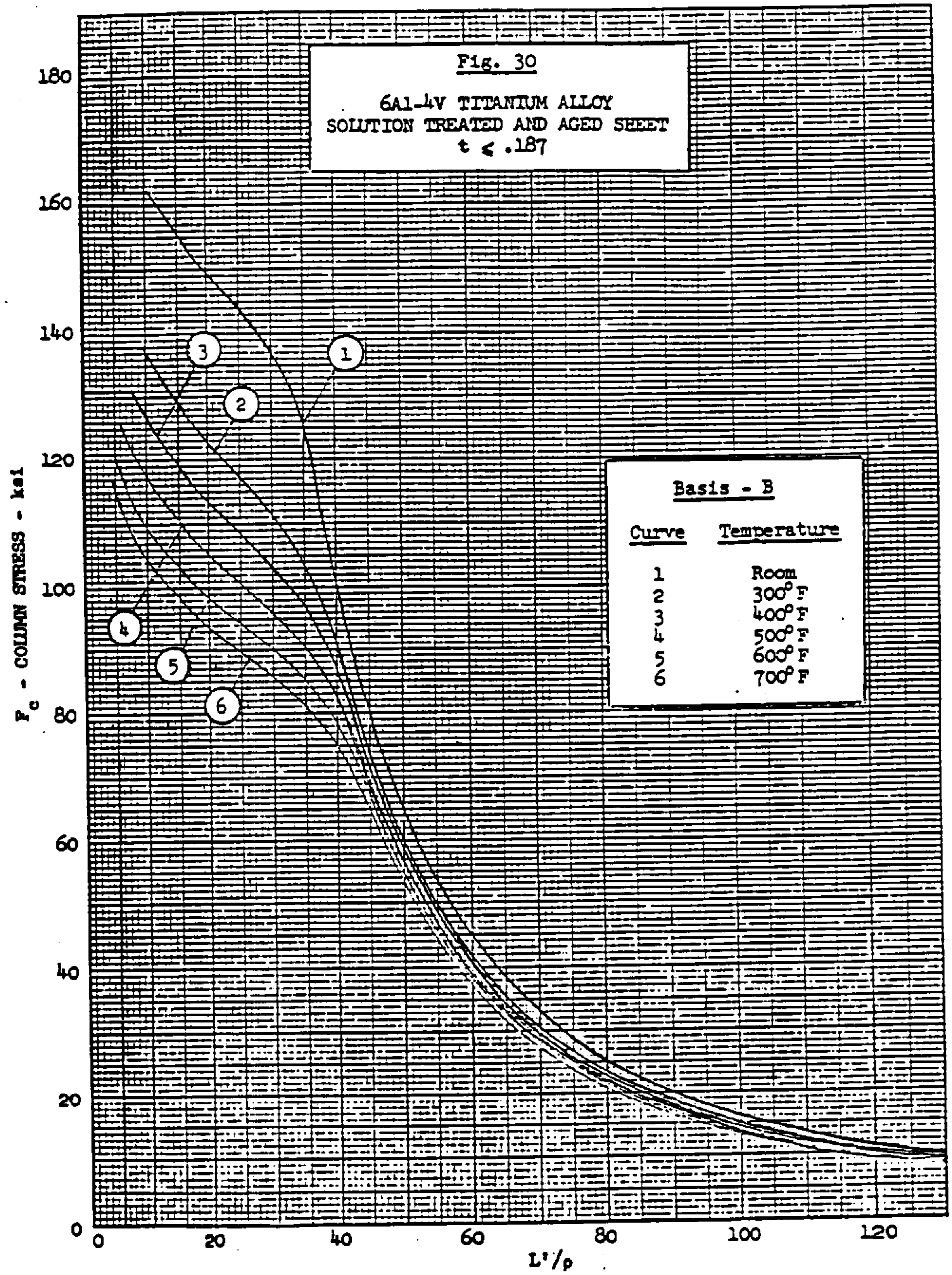
Fig. 30
6Al-4V TITANIUM ALLOY
SOLUTION TREATED AND AGED SHEET
t ≤ .187
Basis - B
Curve Temperature
1 Room
2 300° F
3 400° F
4 500° F
5 600° F
6 700° F
F_c - COLUMN STRESS - ksi
180
160
140
120
100
80
60
40
20
0
0
20
40
60
80
100
120
L'/ρ

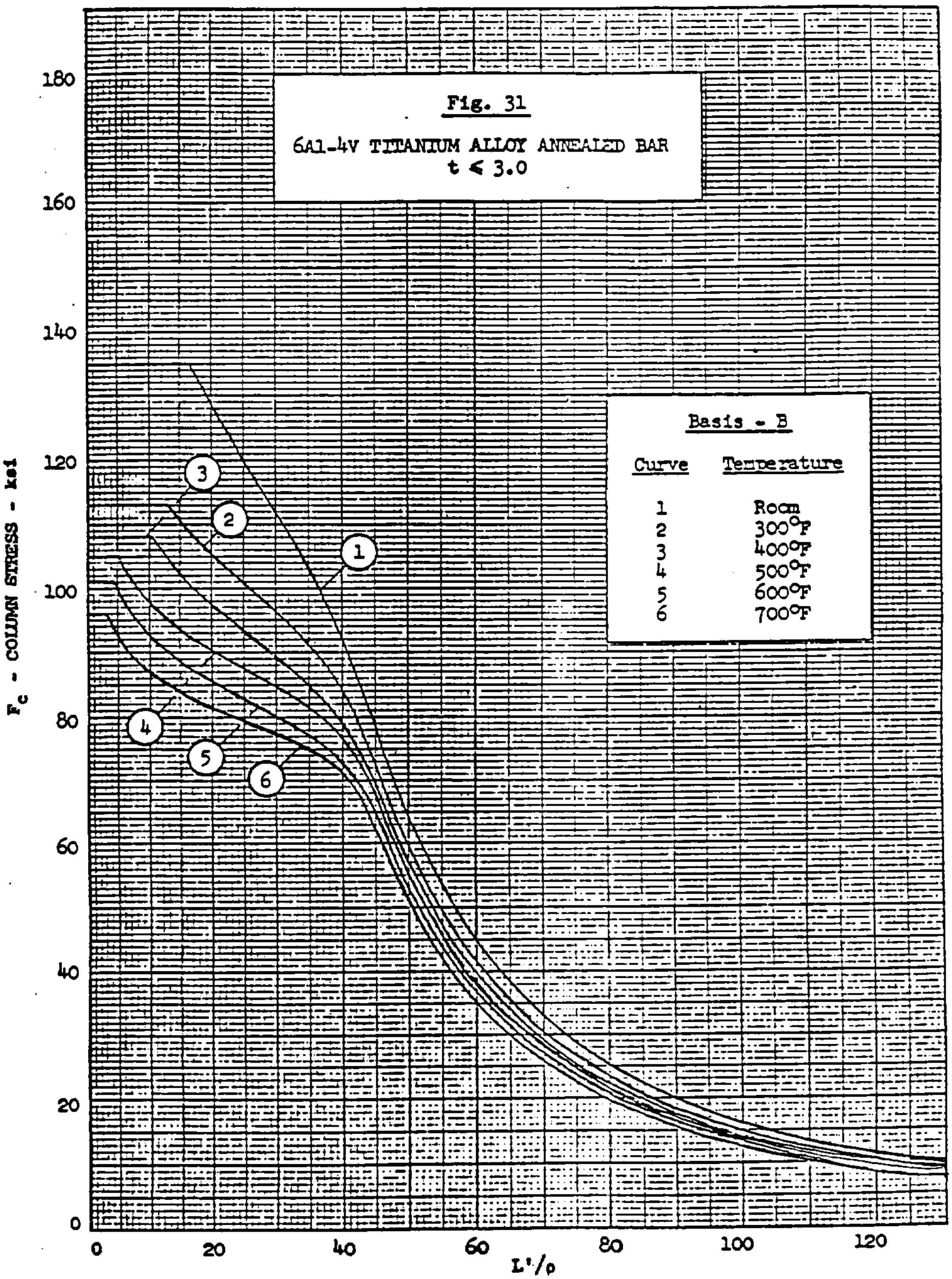
Fig. 31
6Al-4V TITANIUM ALLOY ANNEALED BAR
t ≤ 3.0
Basis - B
Curve Temperature
1 Room
2 300°F
3 400°F
4 500°F
5 600°F
6 700°F
F_c - COLUMN STRESS - ksi
L'/ρ
0
20
40
60
80
100
120
140
160
180

295

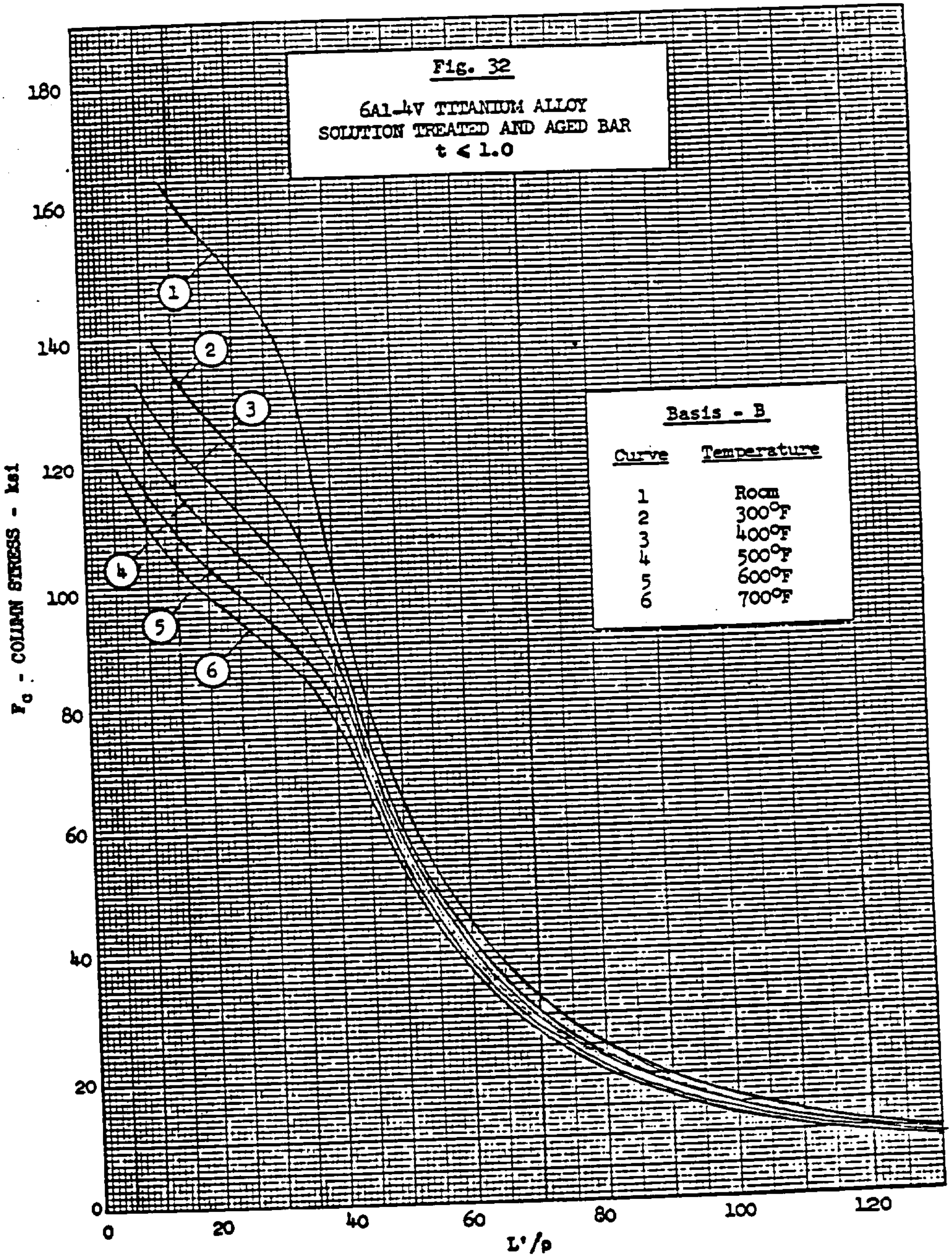
Fig. 32
6Al-4V TITANIUM ALLOY
SOLUTION TREATED AND AGED BAR
t < 1.0
Basis - B
Curve Temperature
1 Room
2 300°F
3 400°F
4 500°F
5 600°F
6 700°F
F_c - COLUMN STRESS - ksi
L'/ρ
0
20
40
60
80
100
120
140
160
180

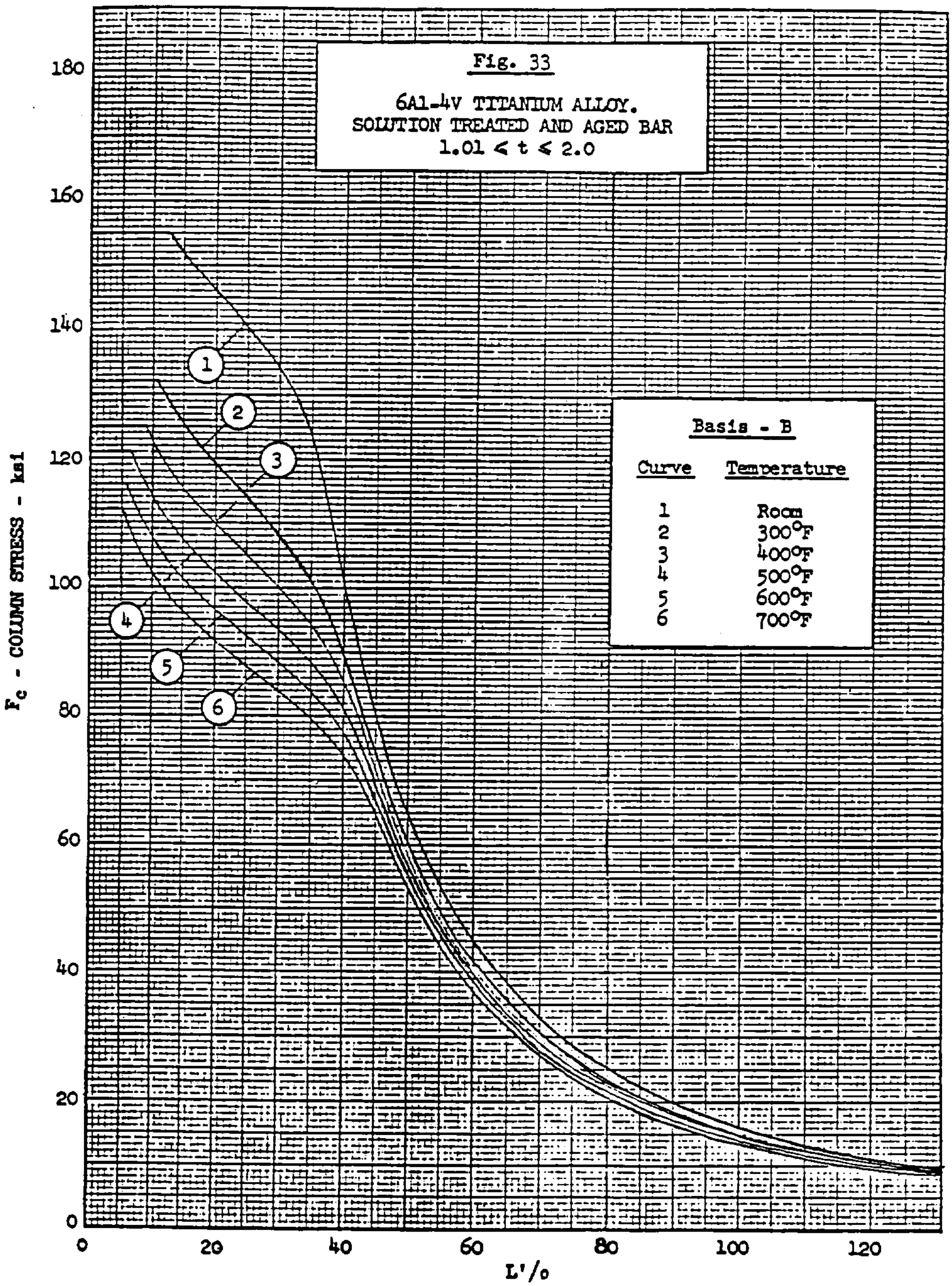
Fig. 33
6Al-4V TITANIUM ALLOY.
SOLUTION TREATED AND AGED BAR
1.01 < t ≤ 2.0
Basis - B
Curve Temperature
1 Room
2 300°F
3 400°F
4 500°F
5 600°F
6 700°F
F_c - COLUMN STRESS - ksi
0
20
40
60
80
100
120
140
160
180
L'/ρ
0
20
40
60
80
100
120
1
2
3
4
5
6

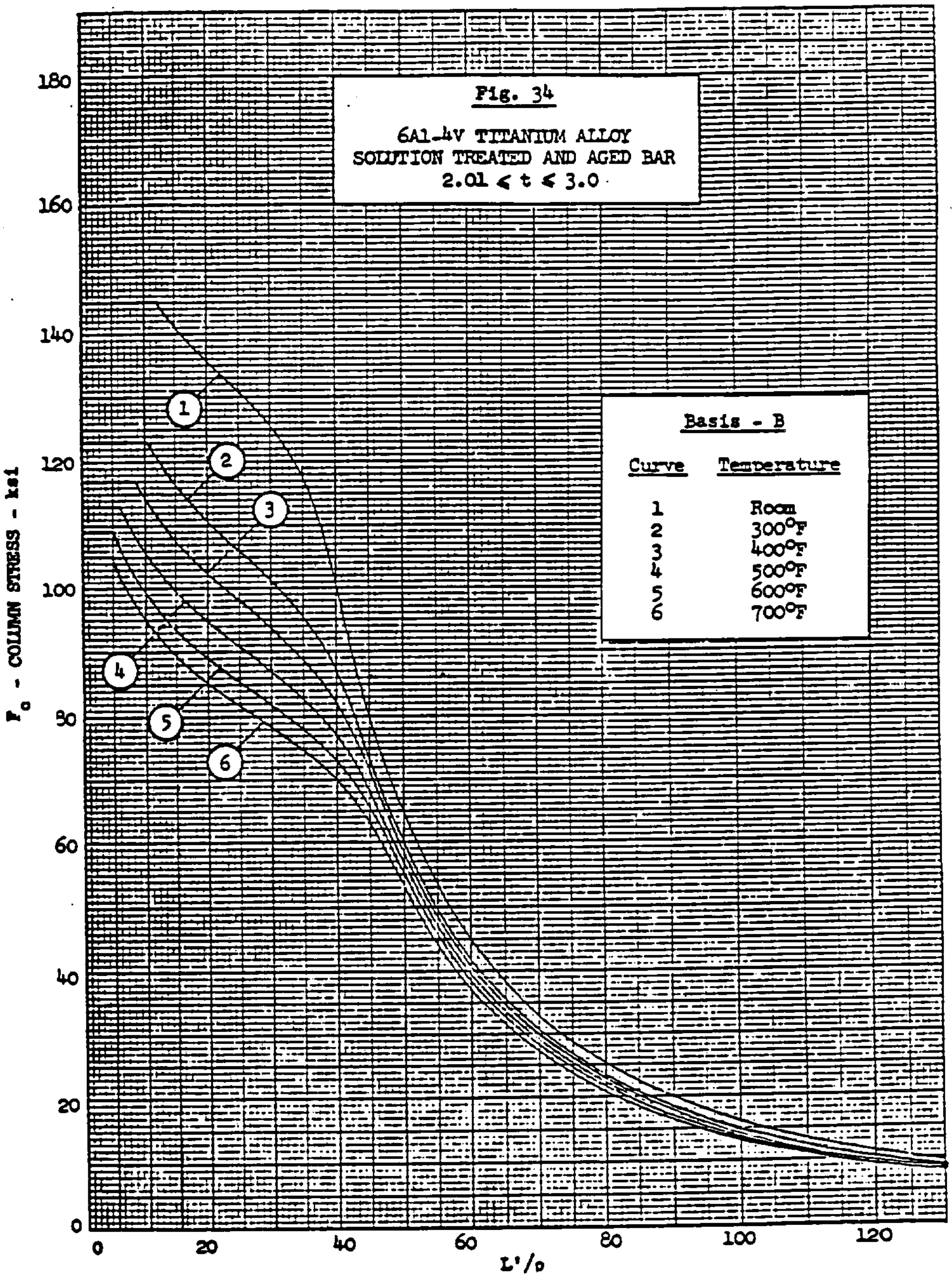
Fig. 34
6Al-4V TITANIUM ALLOY
SOLUTION TREATED AND AGED BAR
2.01 ≤ t ≤ 3.0
Basis - B
Curve Temperature
1 Room
2 300°F
3 400°F
4 500°F
5 600°F
6 700°F
F_c - COLUMN STRESS - ksi
L'/ρ
0
20
40
60
80
100
120
140
160
180

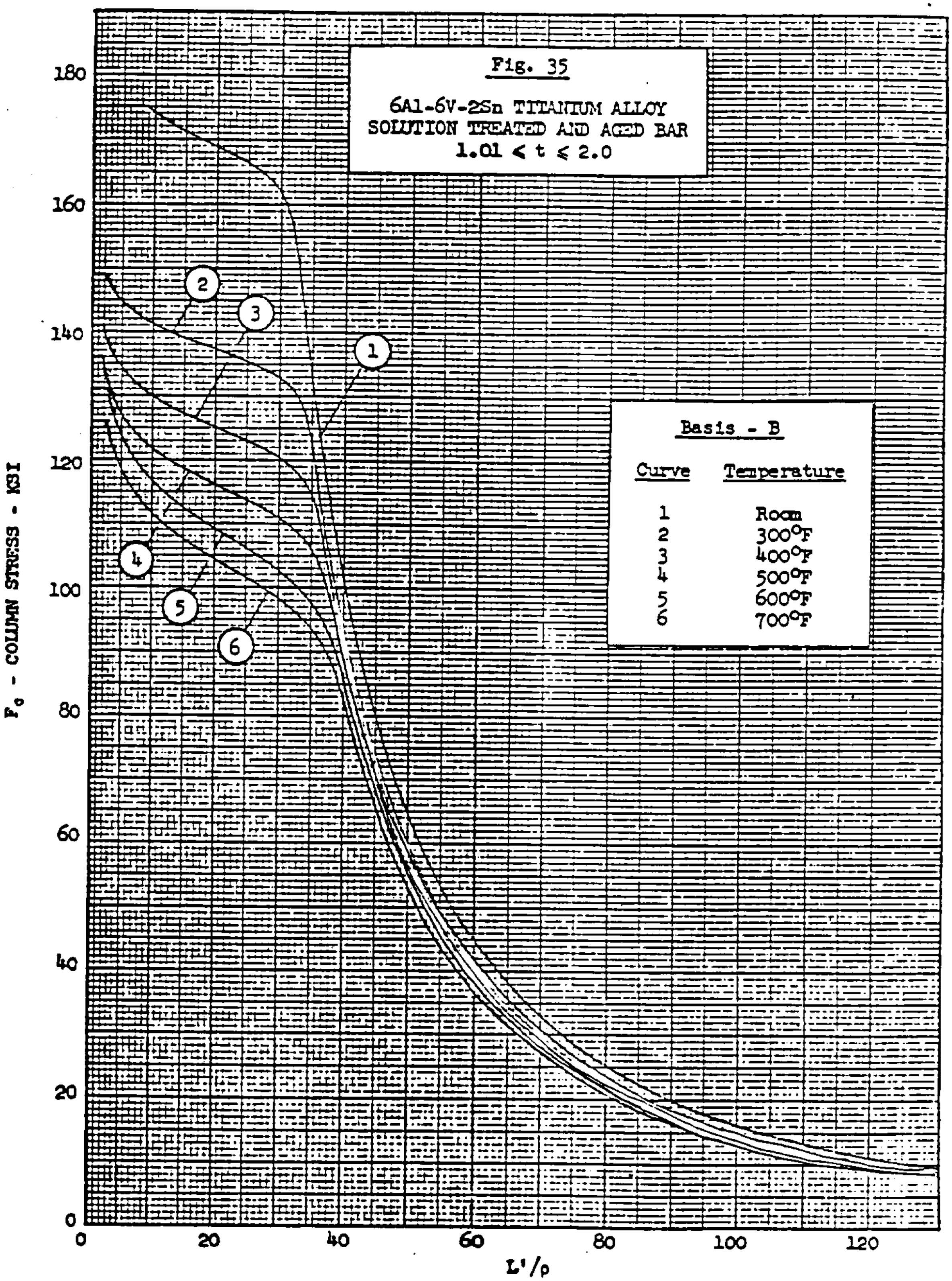
Fig. 35
6Al-6V-2Sn TITANIUM ALLOY
SOLUTION TREATED AND AGED BAR
1.01 < t ≤ 2.0
Basis - B
Curve Temperature
1 Room
2 300°F
3 400°F
4 500°F
5 600°F
6 700°F
Fc - COLUMN STRESS - KSI
L'/ρ
0
20
40
60
80
100
120
140
160
180

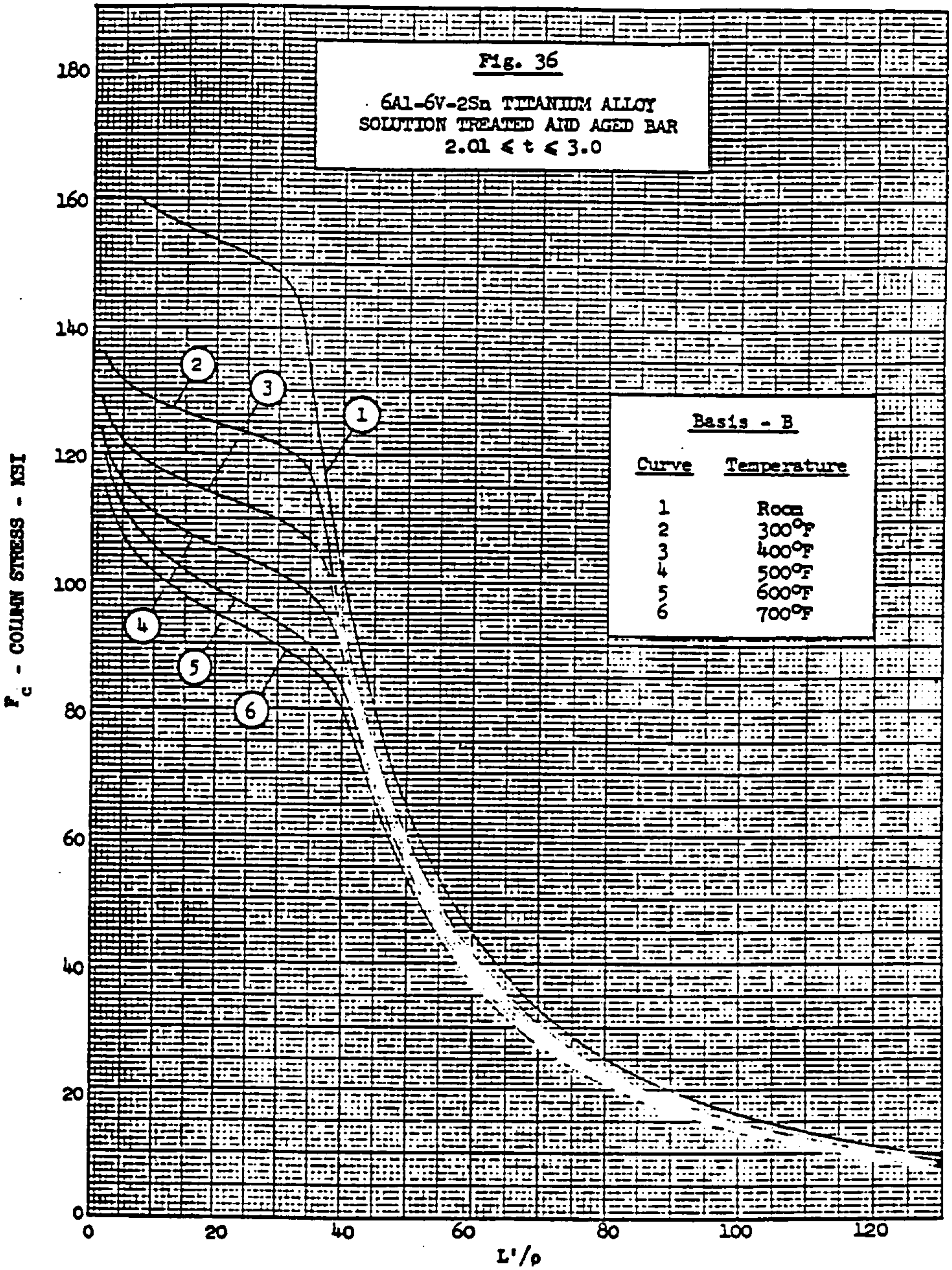
Fig. 36
6Al-6V-2Sn TITANIUM ALLOY
SOLUTION TREATED AND AGED BAR
2.01 ≤ t ≤ 3.0
Basis - B
Curve Temperature
1 Room
2 300°F
3 400°F
4 500°F
5 600°F
6 700°F
F_c - COLUMN STRESS - KSI
L'/ρ
0
20
40
60
80
100
120
140
160
180

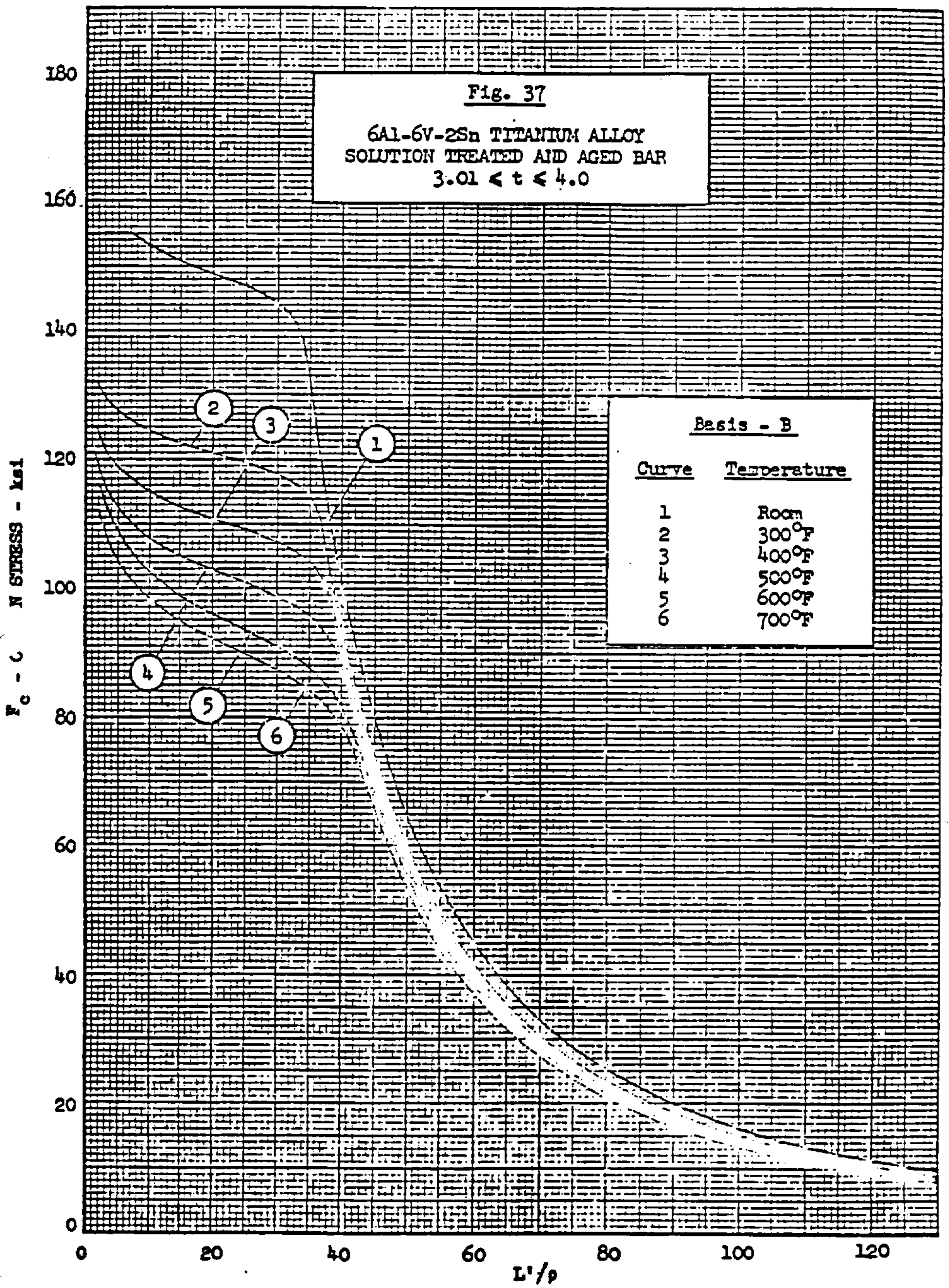
Fig. 37
6Al-6V-2Sn TITANIUM ALLOY
SOLUTION TREATED AND AGED BAR
3.01 ≤ t ≤ 4.0
Basis - B
Curve Temperature
1 Room
2 300°F
3 400°F
4 500°F
5 600°F
6 700°F
F_c - C N STRESS - ksi
0
20
40
60
80
100
120
140
160
180
0
20
40
60
80
100
120
L'/ρ
1
2
3
4
5
6

307

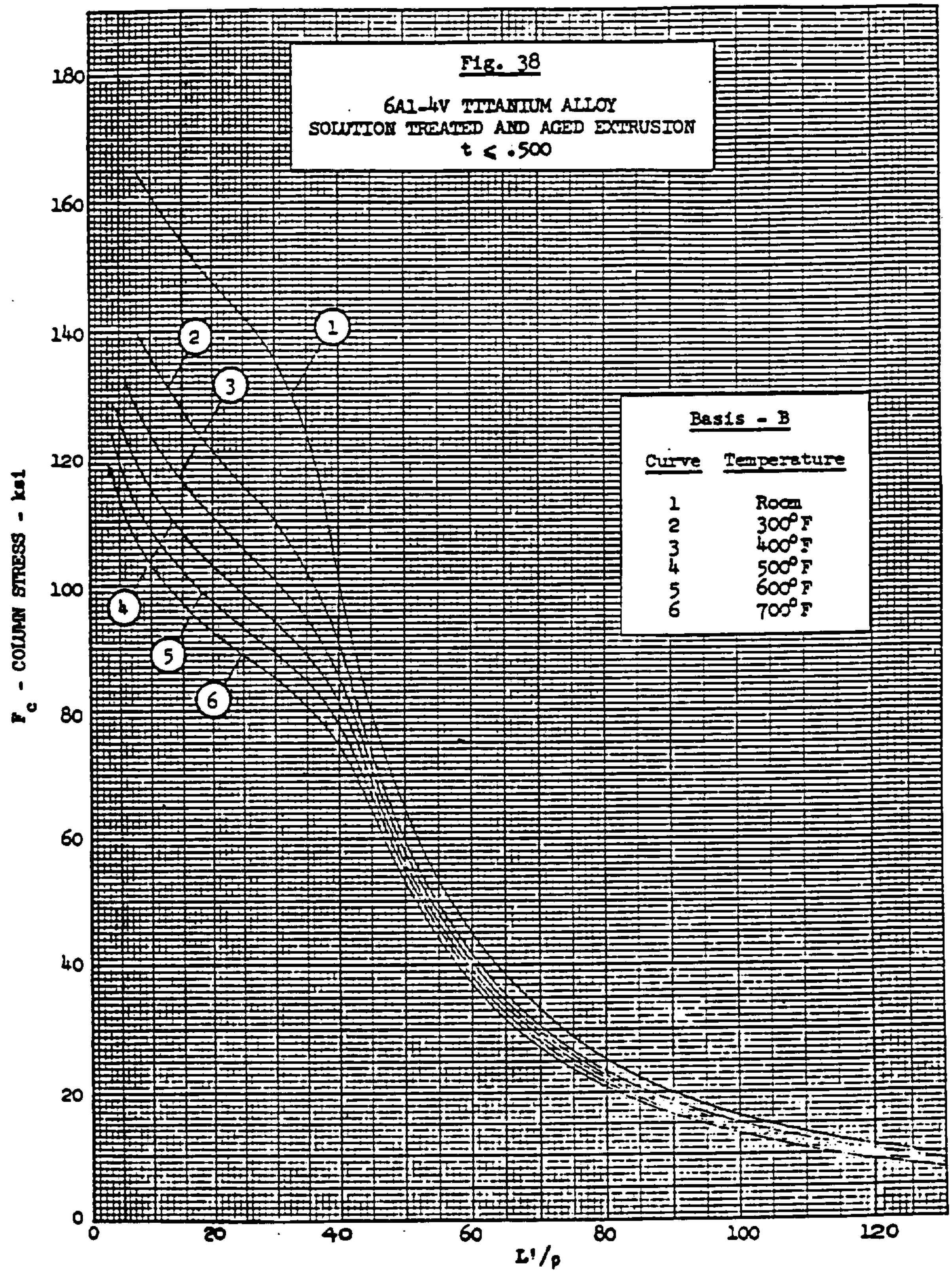
Fig. 38
6Al-4V TITANIUM ALLOY
SOLUTION TREATED AND AGED EXTRUSION
t ≤ .500
Basis - B
Curve Temperature
1 Room
2 300°F
3 400°F
4 500°F
5 600°F
6 700°F
1
2
3
4
5
6
F_c - COLUMN STRESS - ksi
0
20
40
60
80
100
120
140
160
180
L'/ρ

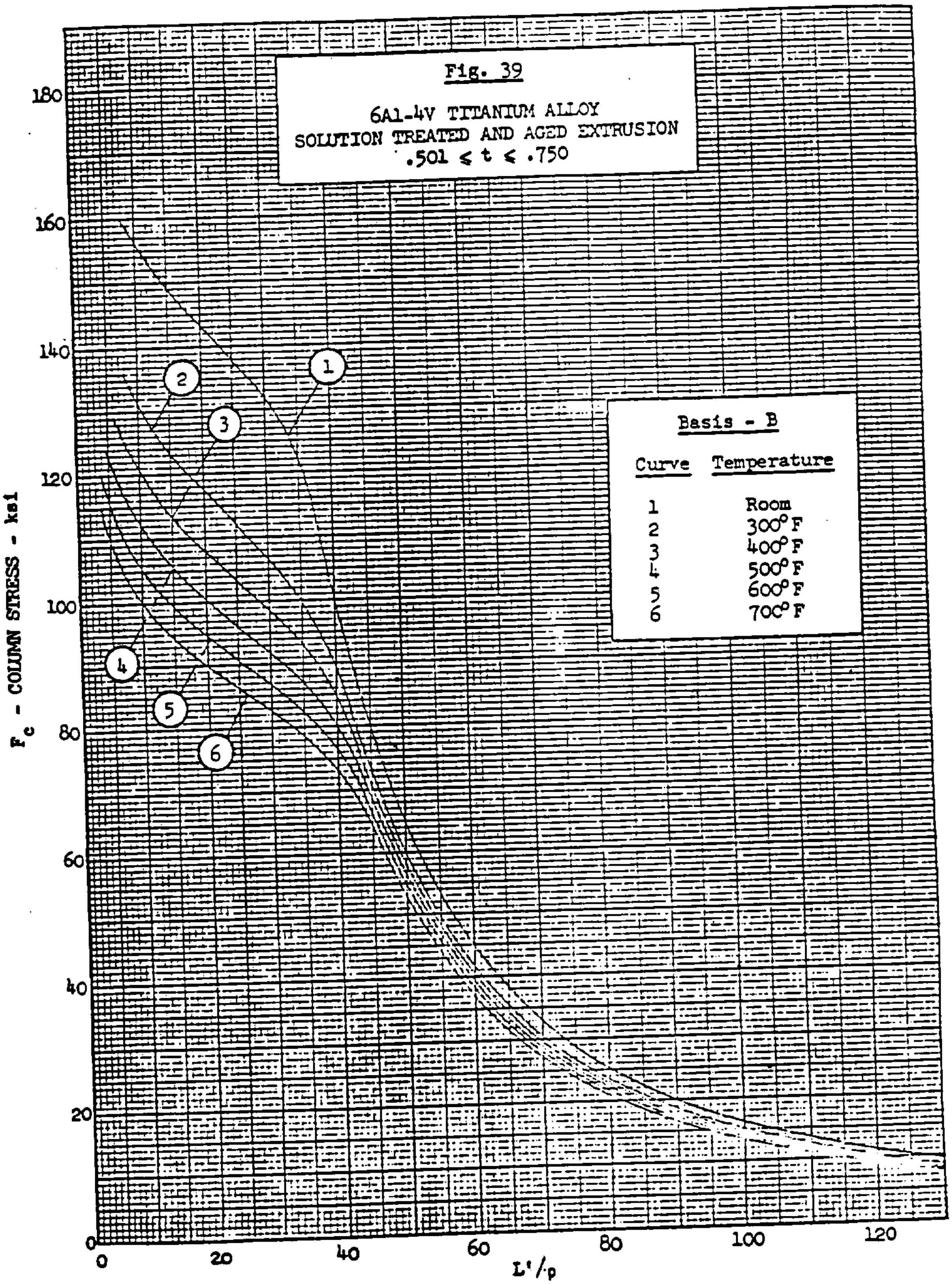
Fig. 39
6Al-4V TITANIUM ALLOY
SOLUTION TREATED AND AGED EXTRUSION
.501 ≤ t ≤ .750
Basis - B
Curve Temperature
1 Room
2 300°F
3 400°F
4 500°F
5 600°F
6 700°F
F_c - COLUMN STRESS - ksi
L'/ρ
0
20
40
60
80
100
120
140
160
180

303

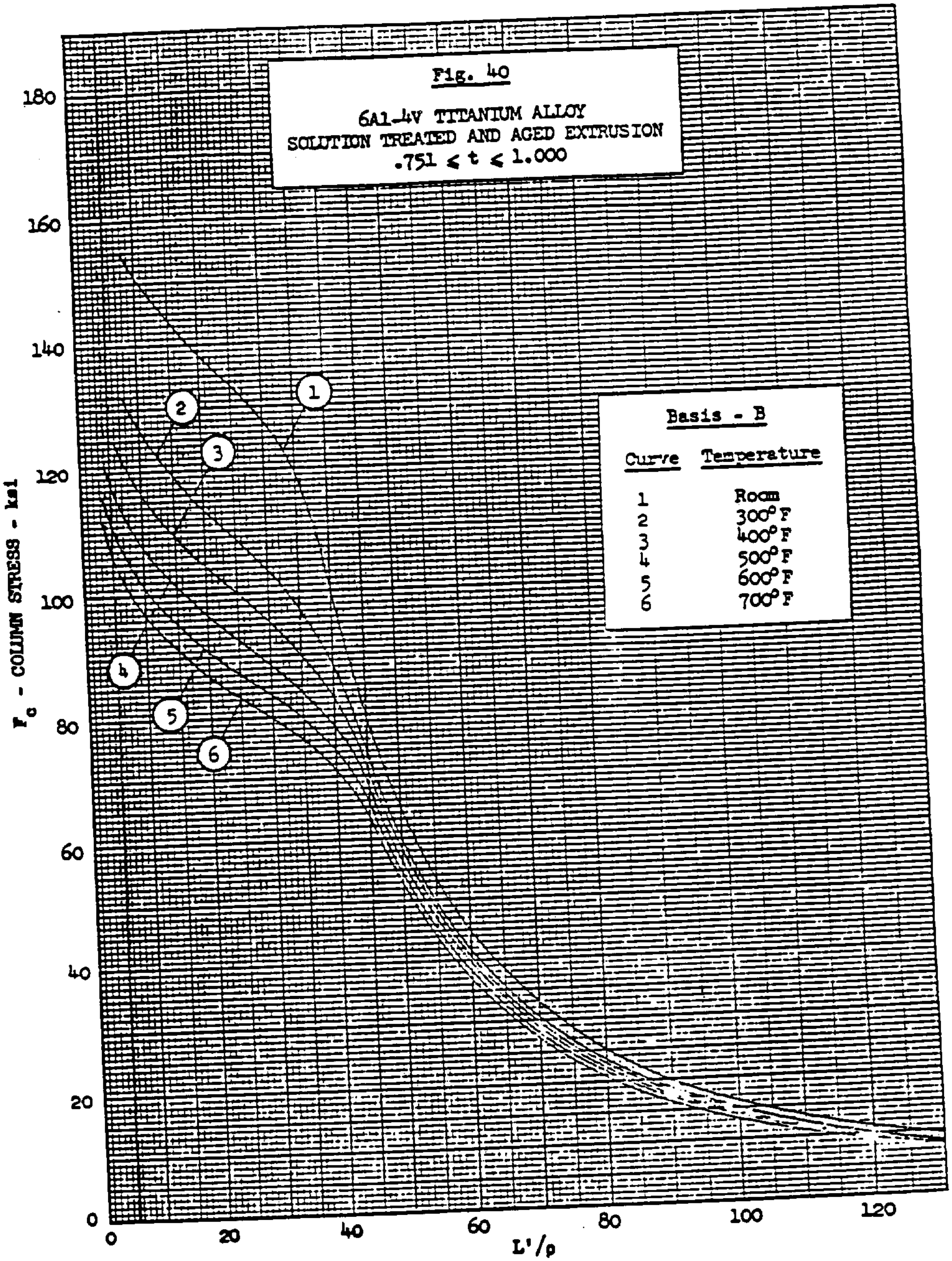
Fig. 40
6Al-4V TITANIUM ALLOY
SOLUTION TREATED AND AGED EXTRUSION
.751 ≤ t ≤ 1.000
Basis - B
Curve Temperature
1 Room
2 300° F
3 400° F
4 500° F
5 600° F
6 700° F
Fc - COLUMN STRESS - ksi
L'/ρ
0
20
40
60
80
100
120
140
160
180

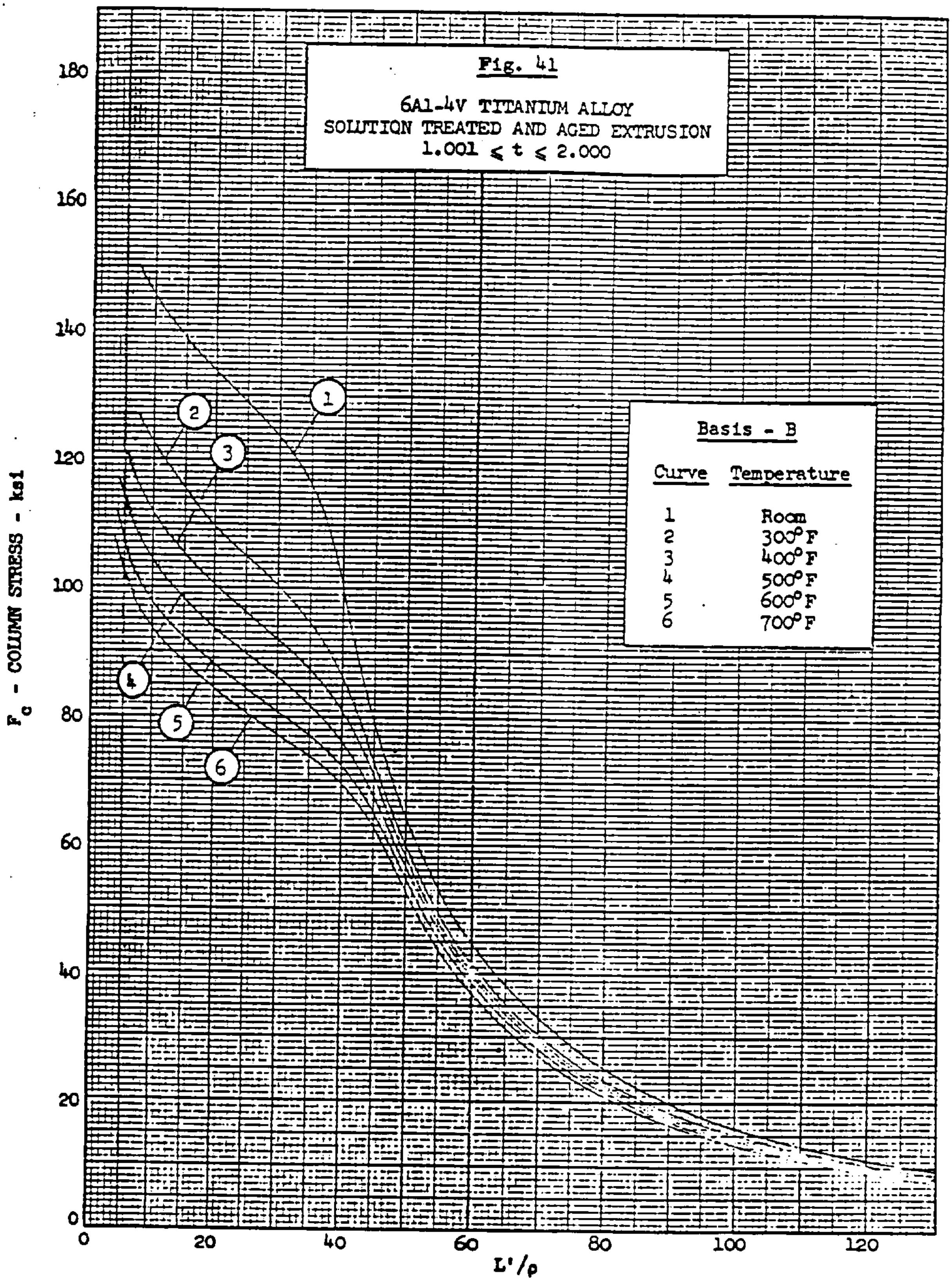
Fig. 41
6Al-4V TITANIUM ALLOY
SOLUTION TREATED AND AGED EXTRUSION
1.001 ≤ t ≤ 2.000
Basis - B
Curve Temperature
1 Room
2 300°F
3 400°F
4 500°F
5 600°F
6 700°F
F_c - COLUMN STRESS - ksi
L'/ρ
0
20
40
60
80
100
120
140
160
180

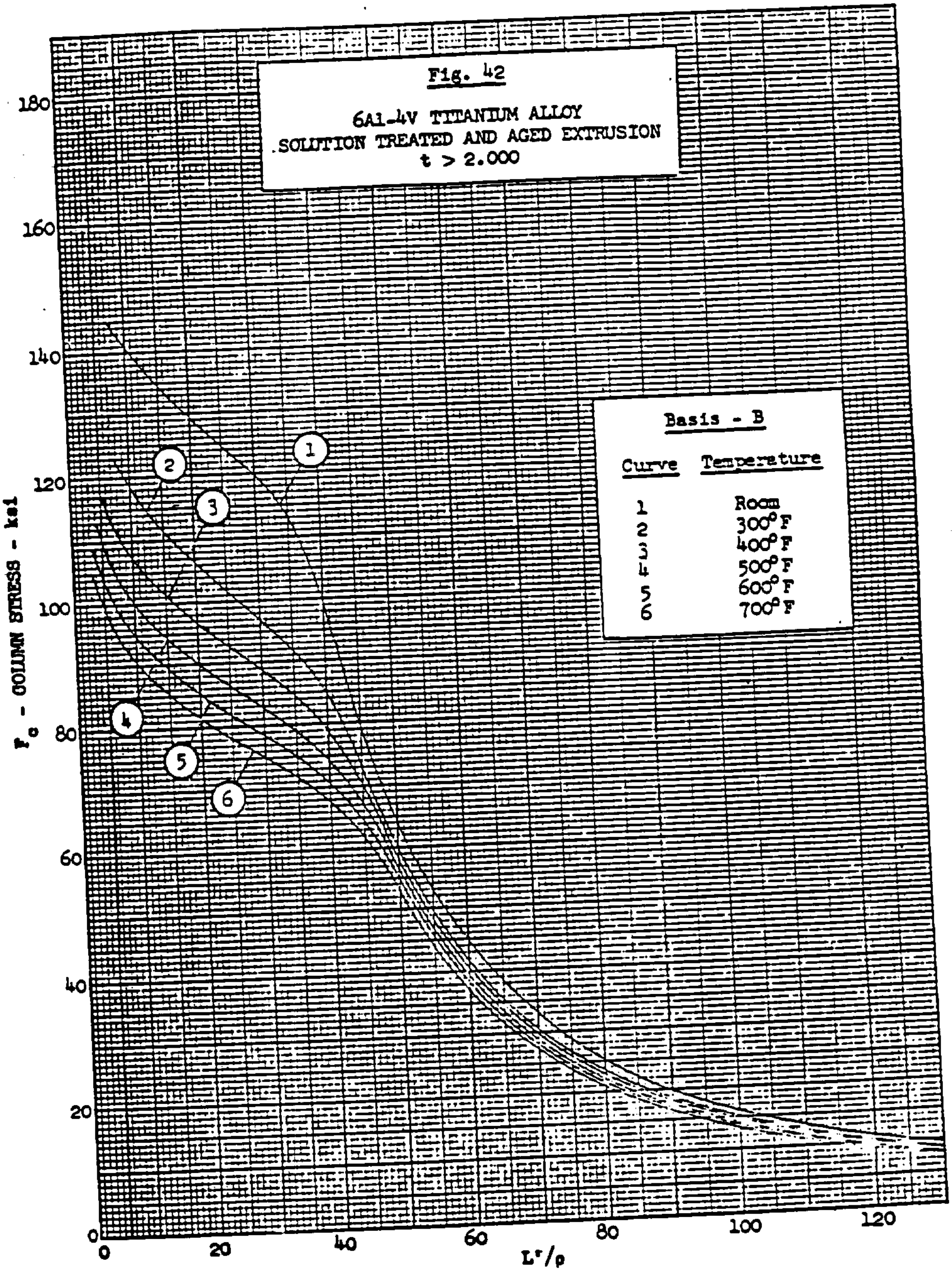
Fig. 42
6Al-4V TITANIUM ALLOY
SOLUTION TREATED AND AGED EXTRUSION
t > 2.000
Basis - B
Curve Temperature
1 Room
2 300°F
3 400°F
4 500°F
5 600°F
6 700°F
F_c - COLUMN STRESS - ksi
L'/ρ
0
20
40
60
80
100
120
140
160
180
1
2
3
4
5
6

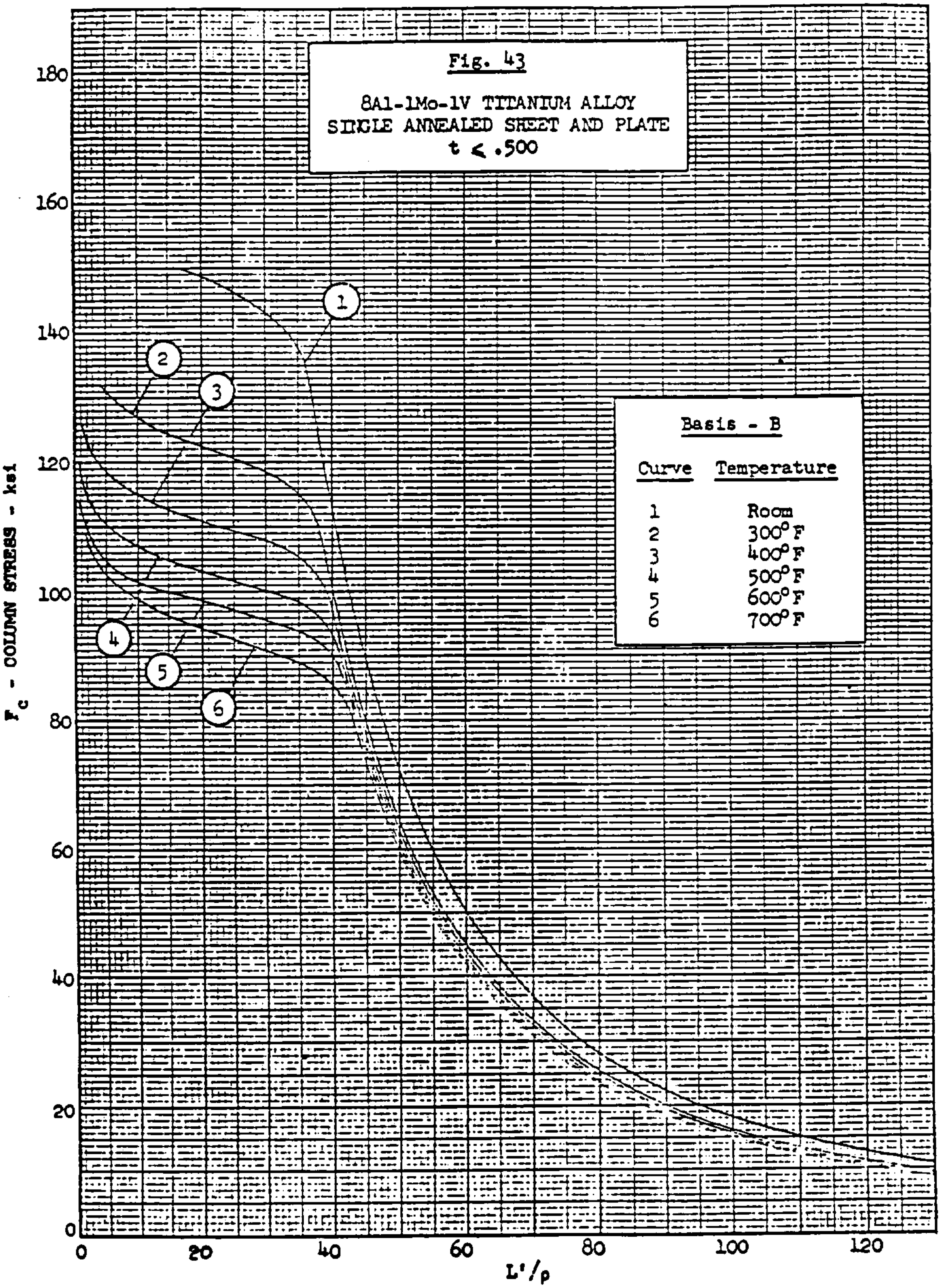
Fig. 43
8Al-1Mo-1V TITANIUM ALLOY
SINGLE ANNEALED SHEET AND PLATE
t ≤ .500
Basis - B
Curve Temperature
1 Room
2 300° F
3 400° F
4 500° F
5 600° F
6 700° F
F_c - COLUMN STRESS - ksi
L'/ρ
0
20
40
60
80
100
120
140
160
180
1
2
3
4
5
6

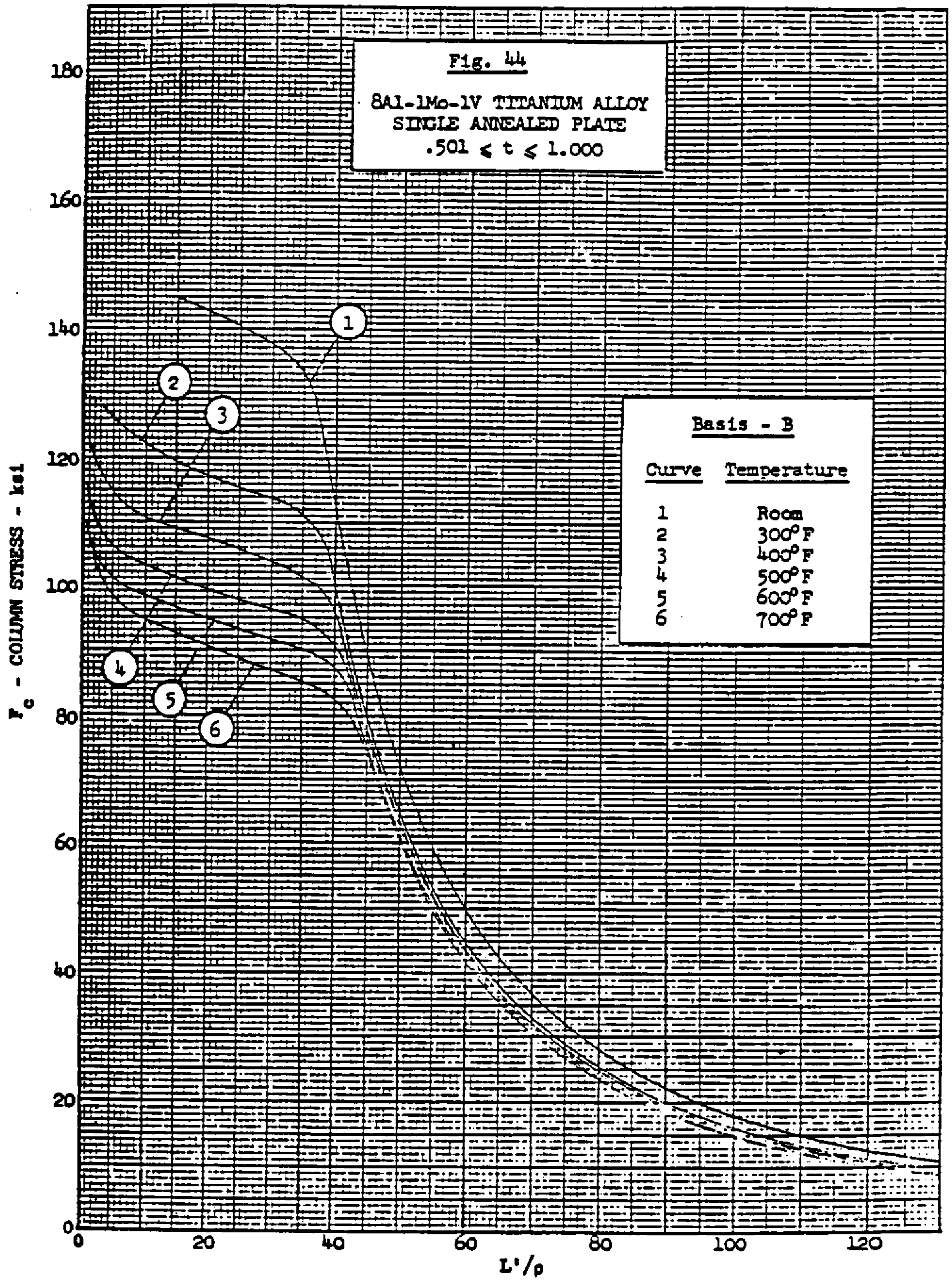
Fig. 44
8Al-1Mo-1V TITANIUM ALLOY
SINGLE ANNEALED PLATE
.501 ≤ t ≤ 1.000
Basis - B
Curve Temperature
1 Room
2 300°F
3 400°F
4 500°F
5 600°F
6 700°F
Fc - COLUMN STRESS - ksi
L'/ρ
0
20
40
60
80
100
120
140
160
180
1
2
3
4
5
6

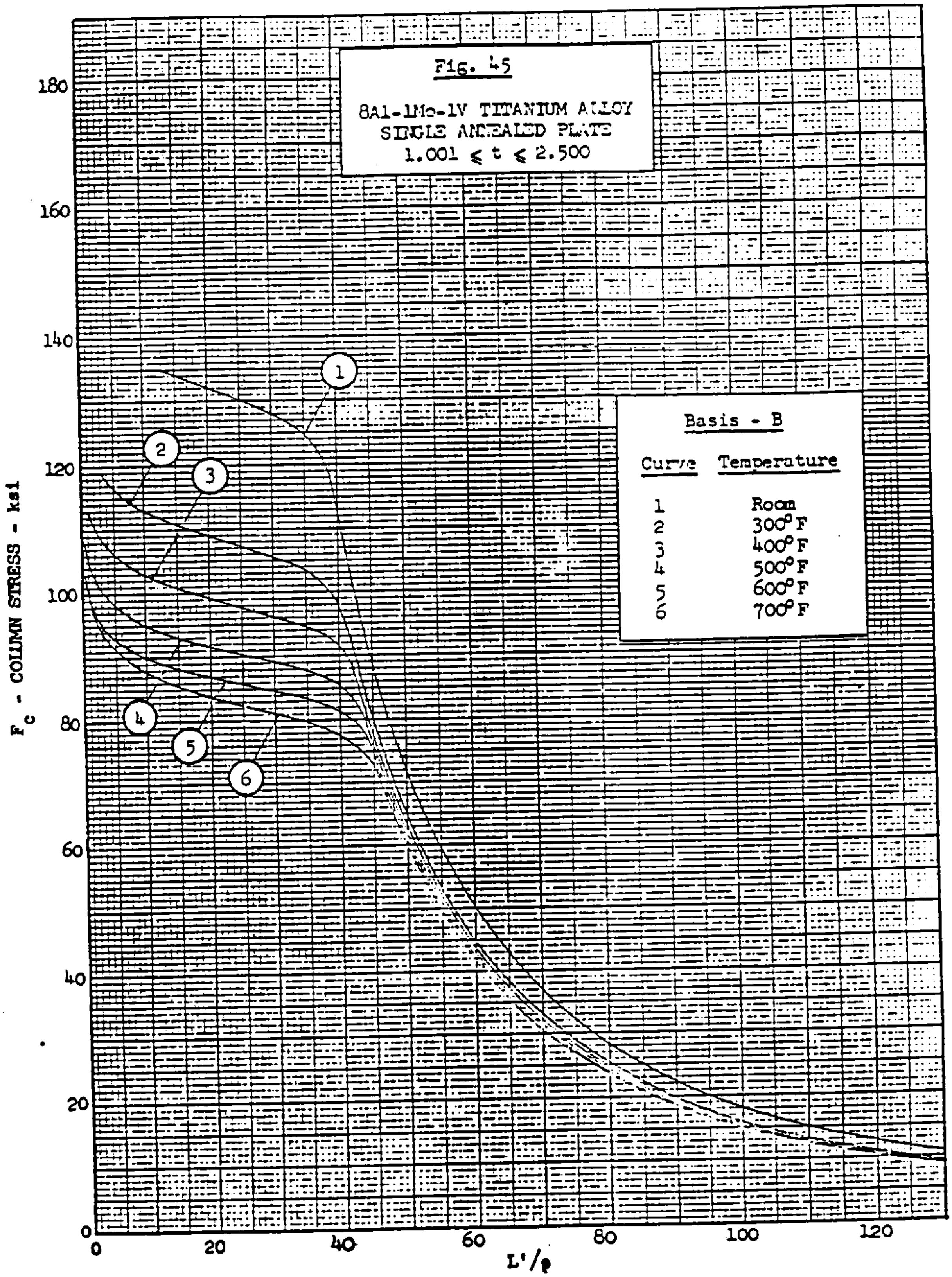
Fig. 45
8Al-1Mo-1V TITANIUM ALLOY
SINGLE ANNEALED PLATE
1.001 ≤ t ≤ 2.500
Basis - B
Curve Temperature
1 Room
2 300°F
3 400°F
4 500°F
5 600°F
6 700°F
F_c - COLUMN STRESS - ksi
L'/ρ
0
20
40
60
80
100
120
140
160
180

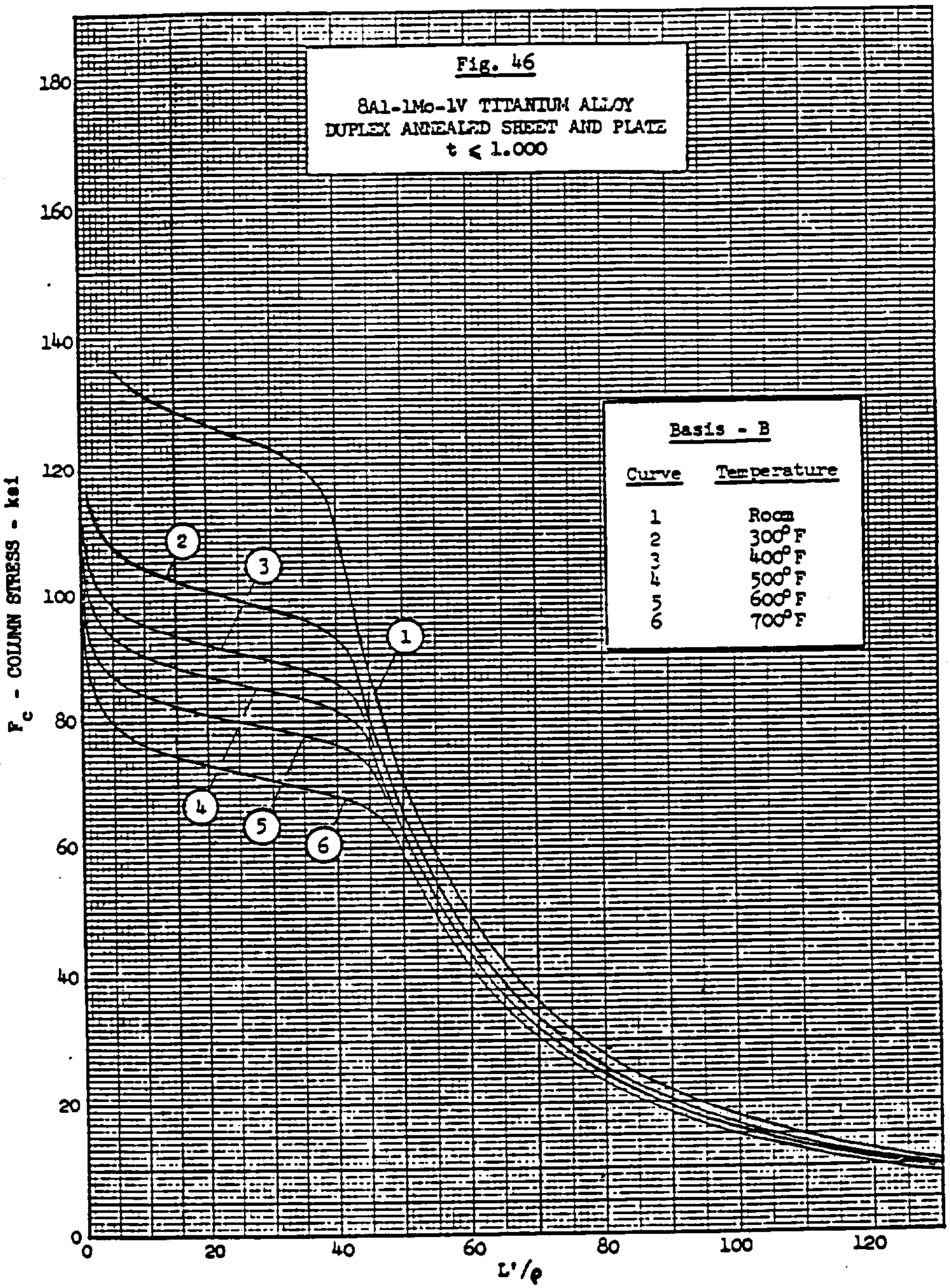
Fig. 46
8Al-1Mo-1V TITANIUM ALLOY
DUPLEX ANNEALED SHEET AND PLATE
t ≤ 1.000
Basis - B
Curve Temperature
1 Room
2 300° F
3 400° F
4 500° F
5 600° F
6 700° F
F_c - COLUMN STRESS - ksi
L'/ρ
0
20
40
60
80
100
120
140
160
180

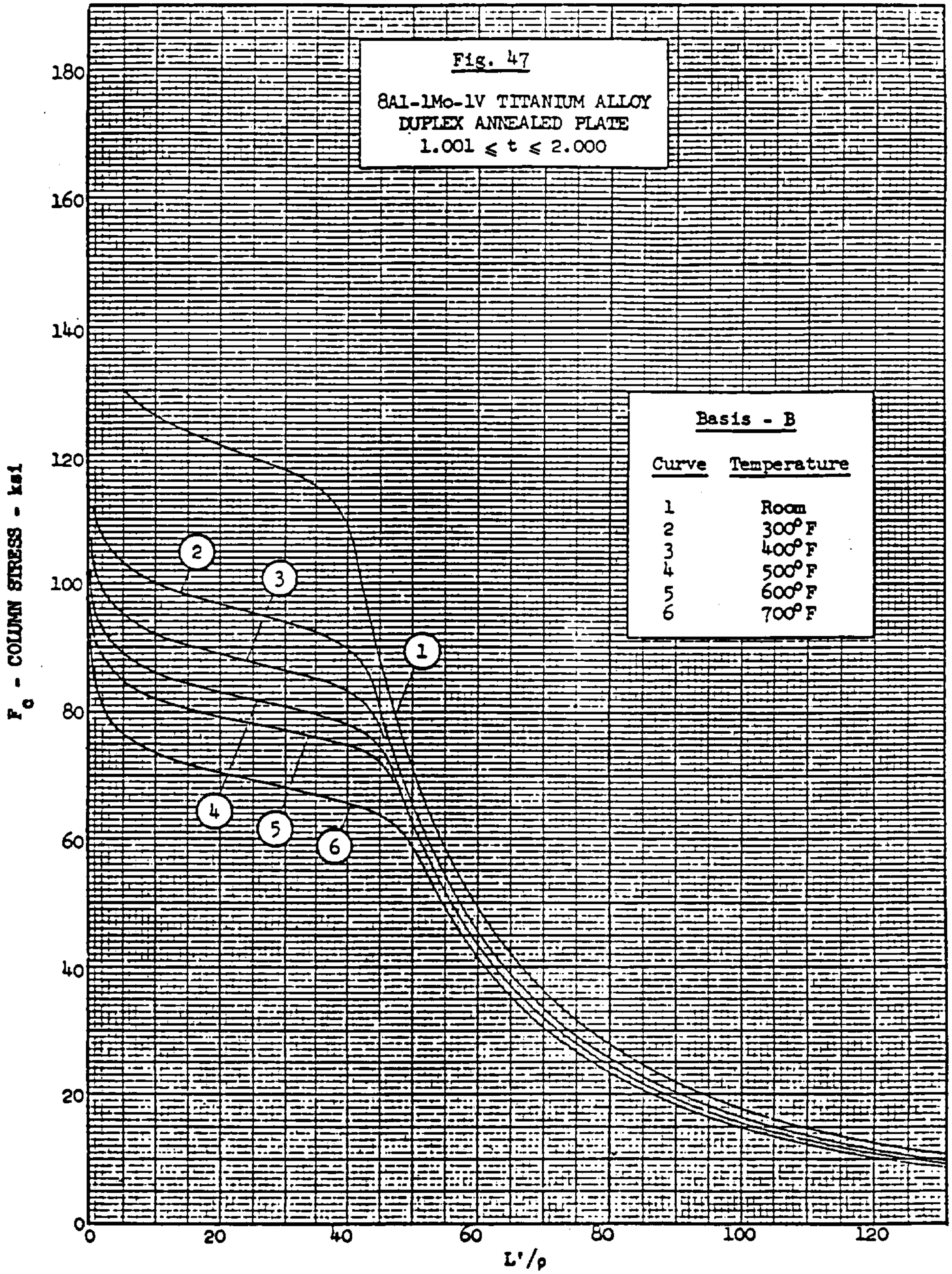
Fig. 47
8Al-1Mo-1V TITANIUM ALLOY
DUPLEX ANNEALED PLATE
1.001 ≤ t ≤ 2.000
Basis - B
Curve Temperature
1 Room
2 300° F
3 400° F
4 500° F
5 600° F
6 700° F
F_c - COLUMN STRESS - ksi
L'/ρ
0
20
40
60
80
100
120
140
160
180
1
2
3
4
5
6

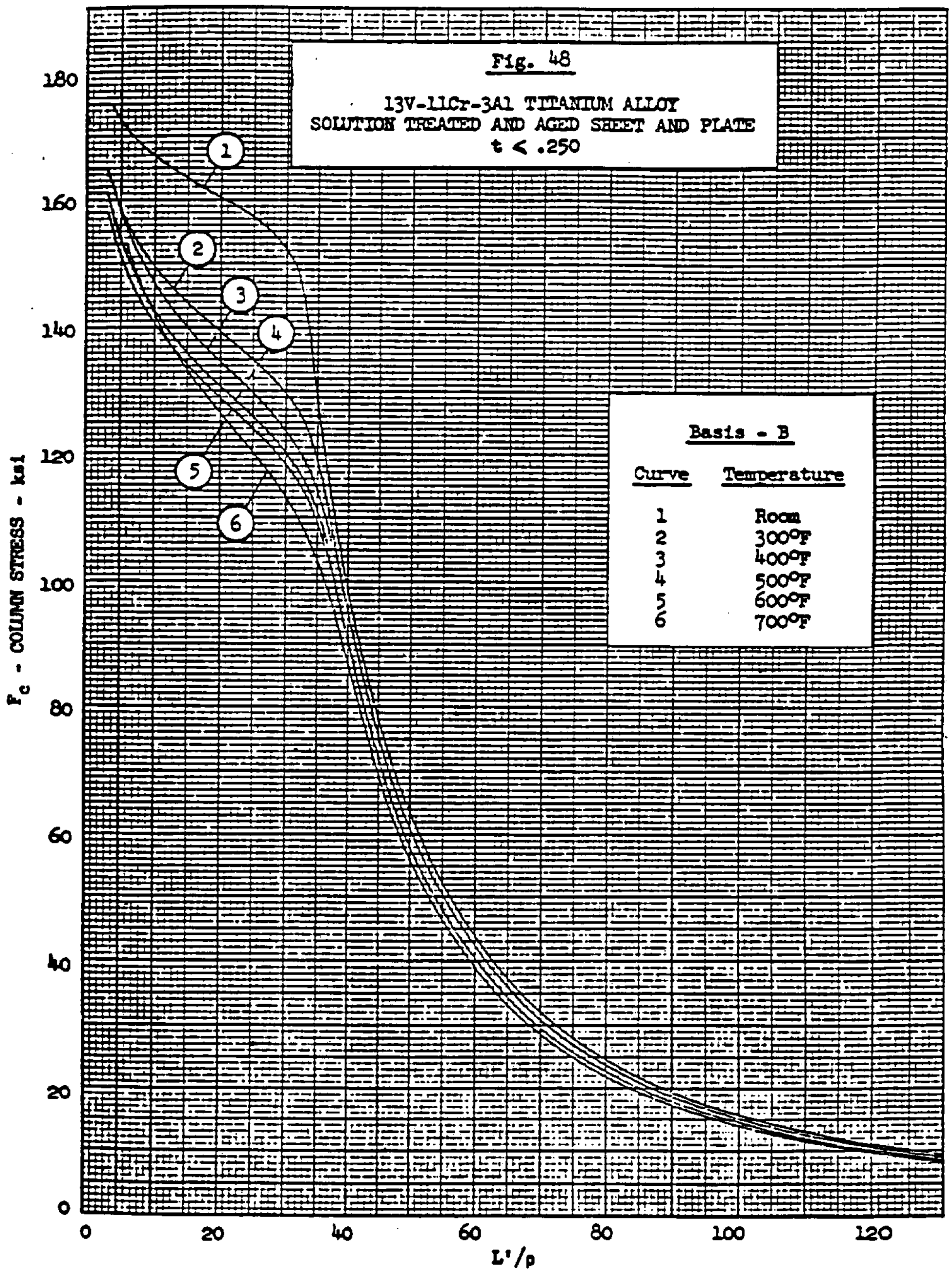
Fig. 48
13V-11Cr-3Al TITANIUM ALLOY
SOLUTION TREATED AND AGED SHEET AND PLATE
t < .250
Basis - B
Curve Temperature
1 Room
2 300°F
3 400°F
4 500°F
5 600°F
6 700°F
F_c - COLUMN STRESS - ksi
L'/ρ
0
20
40
60
80
100
120
140
160
180
1
2
3
4
5
6

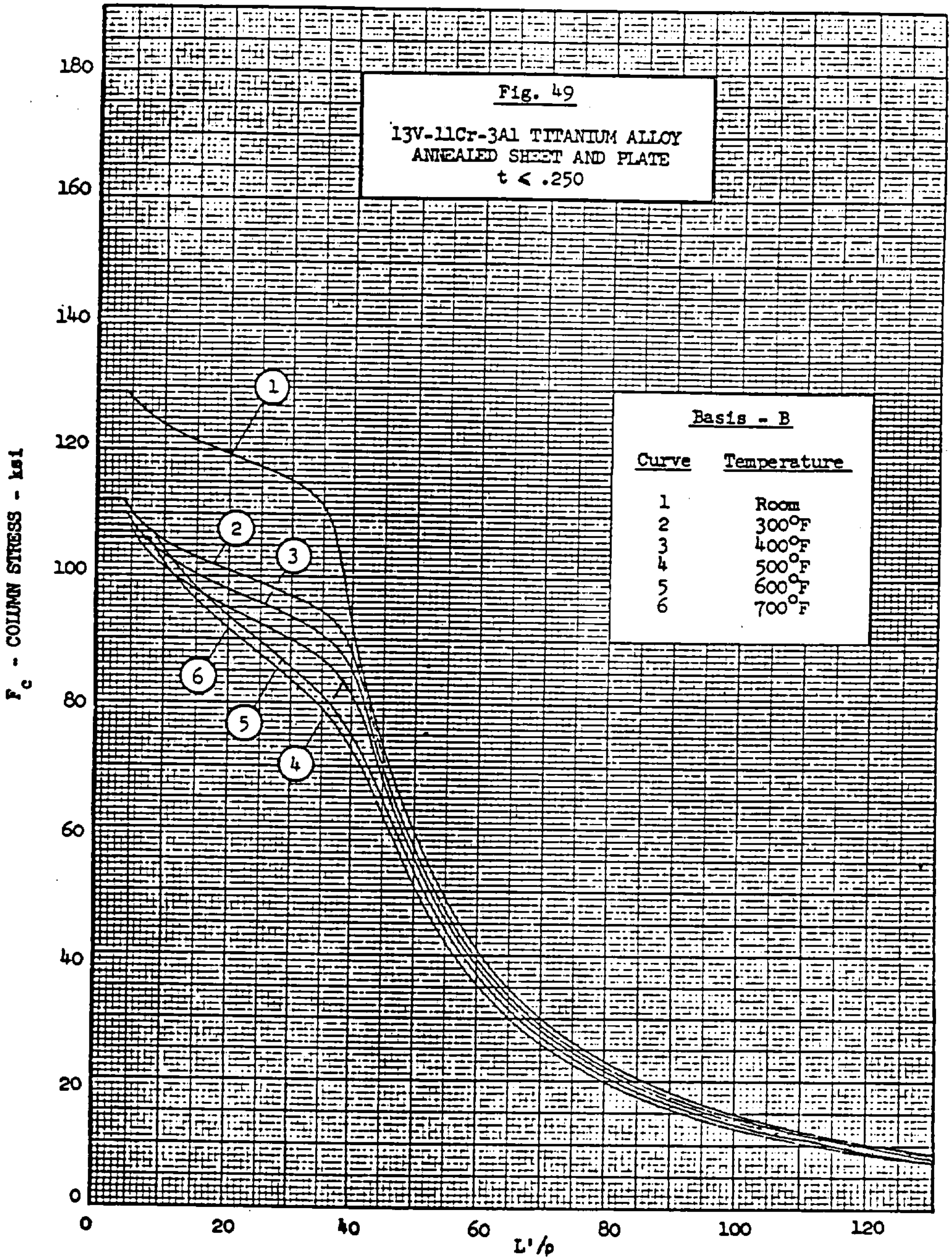
Fig. 49
13V-11Cr-3Al TITANIUM ALLOY
ANNEALED SHEET AND PLATE
t < .250
Basis - B
Curve Temperature
1 Room
2 300°F
3 400°F
4 500°F
5 600°F
6 700°F
1
2
3
4
5
6
F_c - COLUMN STRESS - ksi
L'/ρ
0
20
40
60
80
100
120
140
160
180

SECTION 6.0

PLATES

DATA IS PRESENTED IN GRAPHICAL AND TABULAR FORM FOR PLATES WITH IN-PLANE OR NORMAL APPLIED LOADING.

		PAGE
6.1	IN-PLANE LOADING STABILITY RECTANGULAR	6.1.1
6.2	IN-PLANE LOADING STABILITY PARALLELOGRAM	6.2.1
6.3	CURVED PLATES	6.3.1
6.4	NORMAL LOADING	6.4.1
6.5	MEMBRANES	6.5.1

6.0.0 PLATES

A plate is a member whose thickness is small compared to the other dimensions. A plate differs from a beam in that a plate bends in all planes normal to the plate whereas a beam may be assumed to bend in only one plane.

6.1.0 General

6.1.1 Classification of Plates

Plates are generally divided into four groups:

(1) Thick Plates are plates in which the shearing stresses are important, corresponding to short, deep beams.

(2) Thin Plates (Small deflection) are plates in which bending is the main action resisting normal loads. The deflection should be less than about 1/2 the thickness.

(3) Very Thin Plates (Large deflection)

The useful resistance of these plates to normal loads depends in part on the direct tension accompanying the stretching of the middle plane. The deflection will be larger than about 1/2 the thickness.

(4) Membranes

The resistance of these plates to normal loads depends exclusively on the stretching of the middle plane. The effects of bending can be neglected in this type of plate, and it may be assumed that tension is the main action on which useful resistance depends.

6.1.2 Plasticity Coefficient "η"

Efficiently designed plates often buckle at a stress above the proportional limit. In order to handle problems in the plastic range, a reduction factor is introduced into the conventional formulas for elastic buckling. This reduction factor is referred to as the plasticity coefficient, η. The equation used to obtain "η" is shown below

$$\eta = \frac{E_t}{E} \quad \ldots\ldots\ldots\ldots\ldots\ldots \quad (1)$$

If the critical stress is below the proportional limit, the plasticity coefficient, η, is equal to "one" since $E_t = E$. Above this point the tangent modulus, E_t, must be used to obtain the plasticity coefficient. Since "E_t" is a function of stress, an estimate of the actual stress must be made in order to obtain an initial value of "E_t." Using this value of "E_t" the critical stress can be calculated.

1. If the computed stress is greater than the estimated stress, the actual stress will be greater than the estimated stress and less than the computed stress.

2. If the computed stress is less than the estimated stress, the actual stress will be less than the estimated stress but greater than the computed stress.

This procedure should be repeated until the assumed stress and computed stress converge.

6.1.3
Edge Restraint - (Fixity)

The degree of edge support provided to the plate element at its edges by the adjoining structural elements has a marked effect on the buckling and bending stresses. The degree of edge restraint may be approximated from the following idealized edge conditions.

(a) Elastically Restrained Edges: This is an edge about which the plate is elastically restrained from rotating freely. The deflection in the transverse direction along the edge is zero. The degree of restraint is defined by the rotational restraint coefficient, ϵ, which is proportional to the ratio of the stiffness of the restraining medium to that of the plate.

(b) Fixed or Built-In Edge ($\epsilon = \infty$): This is an edge about which the plate cannot rotate. The deflection in the transverse direction along the edge is zero. The tangent plane to the deflected surface along this edge coincides with the initial position of the plate.

(c) Simply Supported Edges ($\epsilon = 0$): This is an edge condition where the plate is free to rotate about the centerline of the edge (no restraining bending moments about the edge). The deflection in the transverse direction along the edge is zero.

(d) Free Edge ($\epsilon = 0$): This is an edge that is entirely free to rotate and to deflect transversely.

In general, torsionally weak edge members such as open sections used in a compression panel will act almost as simple supports, while torsionally stiff edge members such as closed sections and heavy flanges will provide almost clamped edges.

In order to identify the edge conditions, the following notations have been employed on the various charts, etc.:

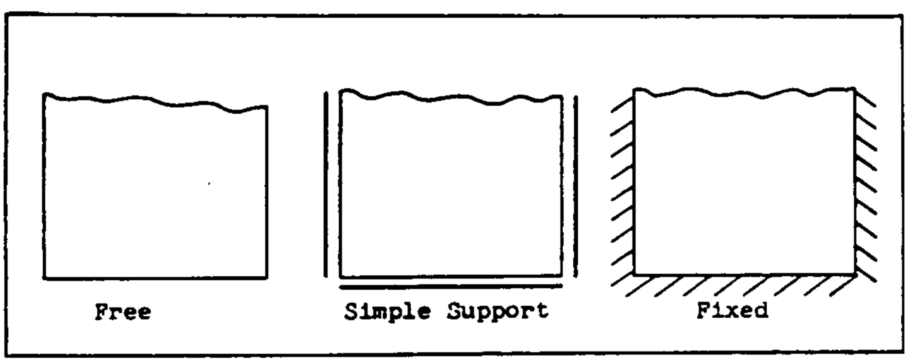

Fig. 6.1.3-1

6.1.4
Assumptions

Throughout this section it is assumed that the bodies undergoing the action of external forces are perfectly elastic within the elastic limit of the material. The matter of this body is assumed to be homogeneous and continuously distributed over its volume so that the smallest element cut from the body possesses the same specific physical properties as the body. It is further assumed that the body is isotropic, i.e., that the elastic properties are the same in all directions. Basic assumptions are listed below:

(a) Perfectly Elastic
(b) Homogeneous
(c) Continuous
(d) Isotropic
(e) Constant Thickness

6.1.5
Stress Ratios, Interaction Curves, and Margins of Safety

In the analysis of plates subjected to combined loading, it is general engineering practice to make use of the stress-ratio method because of its simplicity and nondimensional character.

Stress Ratios

Stress ratios express the relationship between the applied or allowable stress and the critical buckling or failing stress if the load were acting alone. Stress ratios are the ordinate and abscissa of the interaction curves. The interaction equations are expressed in terms of stress ratios. There are two basic types of stress ratios:

Applied Stress Ratios (R)

$$R = \frac{\sigma}{\sigma_{cr}} \frac{\text{Applied Stress}}{\text{(Critical Buckling or Failing Stress for Load Acting Alone)}} \quad \ldots\ldots \quad (1)$$

Allowable Stress Ratios (R_a)

$$R_a = \frac{\sigma_a}{\sigma_{cr}} \frac{\text{(Allowable Buckling or Failing Stress in Combined Loading)}}{\text{(Critical Buckling or Failing Stress for Load Acting Alone)}} \quad \ldots\ldots \quad (2)$$

When the applied stress ratio, R, is more than the allowable stress ratio, R_a, the plate will buckle.

Interaction Curves

The effect of one type of loading (R_1) on another simultaneous type of loading (R_2) is represented by an interaction equation or curve. This method provides a means of predicting structural failure under combined loading. The interaction curve is obtained empirically from test data or from a plot of the interaction equation. The generalized interaction equation is:

$$R_{a_1}^x + R_{a_2}^y + R_{a_3}^z = 1.0 \quad \ldots\ldots\ldots\ldots \quad (3)$$

Where R_{a_1}, R_{a_2}, R_{a_3} = allowable stress ratios.

The exponents, x, y, and z, are constants which depend on the type of loadings acting in combination. The numerical subscripts attached to the stress ratios indicate the type of loading such as compression, tension, shear, bending and pressure.

In many cases, the exponents, x, y, and z, are whole numbers, and the interaction relationship can be determined analytically with ease. These exponents may be determined analytically or empirically from test data. If these exponents are not whole numbers, it is much easier to use the interaction curves.

Margin of Safety

The margin of safety is an indication of the degree of utilization of a structure and is given by the formula:

$$M.S. = \frac{\text{Allowable Stress}}{\text{Applied Load}} - 1 \qquad (4)$$

To determine the margin of safety from the interaction curves, the following procedures should be used:

Procedure for Two Loads Acting

(1) Determine the critical buckling stress for each load as if it were acting alone. Use the associated buckling curve from articles 6.2.0, 6.3.0, 6.4.0, and 6.5.0. (One load acting - Shear, Compression, Tension, or Bending.)

(2) Calculate the applied stress ratios R_1, and R_2 using equation (1), the applied stresses, and the critical buckling stresses obtained from step (1).

(3) Locate on the proper interaction chart the point corresponding to the stress ratios calculated. Point "A" on Fig. 6.1.5-1 represents this point. If point "A" falls on the outside of the curve, the plate will buckle and a negative margin of safety will be obtained.

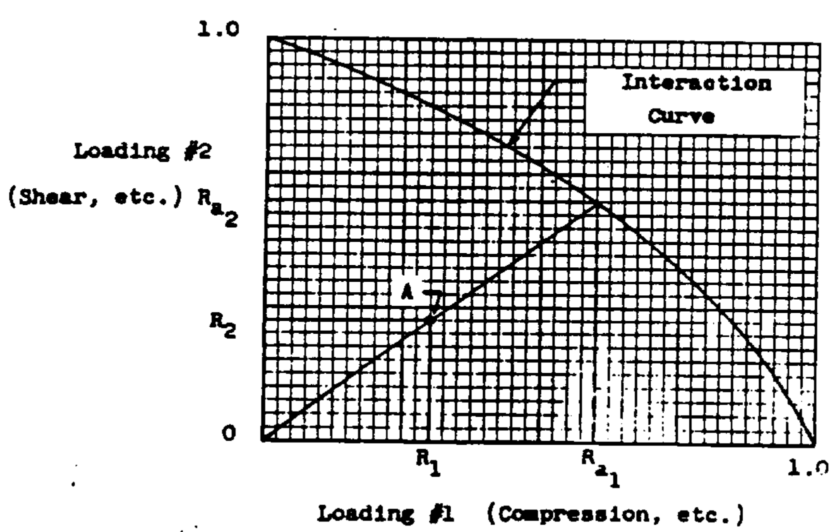

Fig. 6.1.5-1

(4) Draw a straight line from the origin through this point and at the intersection of this straight line with the interaction curve read the corresponding allowable stress ratios R_{a_1} and R_{a_2}.

(5) The margin of safety is then calculated by using the stress ratios obtained from steps (2) and (4) and equation (4).

$$M.S. = \frac{R_{a_1}}{R_1} - 1 = \frac{R_{a_2}}{R_2} - 1 \quad \ldots\ldots\ldots \quad (5)$$

Procedure for Three Loads Acting

(1) Perform operations (1) and (2) from the procedure above. These calculations must be made for all three loadings.

(2) Using the loading conditions and the aspect ratio, a/b, select the proper family of curves.

(3) Locate on the chart selected from step (2) the point corresponding to the stress ratios R_1 and R_2. Point "A" on Fig. 6.1.5-2 represents this point. The stress ratios R_1 and R_2 are the coordinates of the interaction curve and R_3 is a parameter (see Fig. 6.1.5-2).

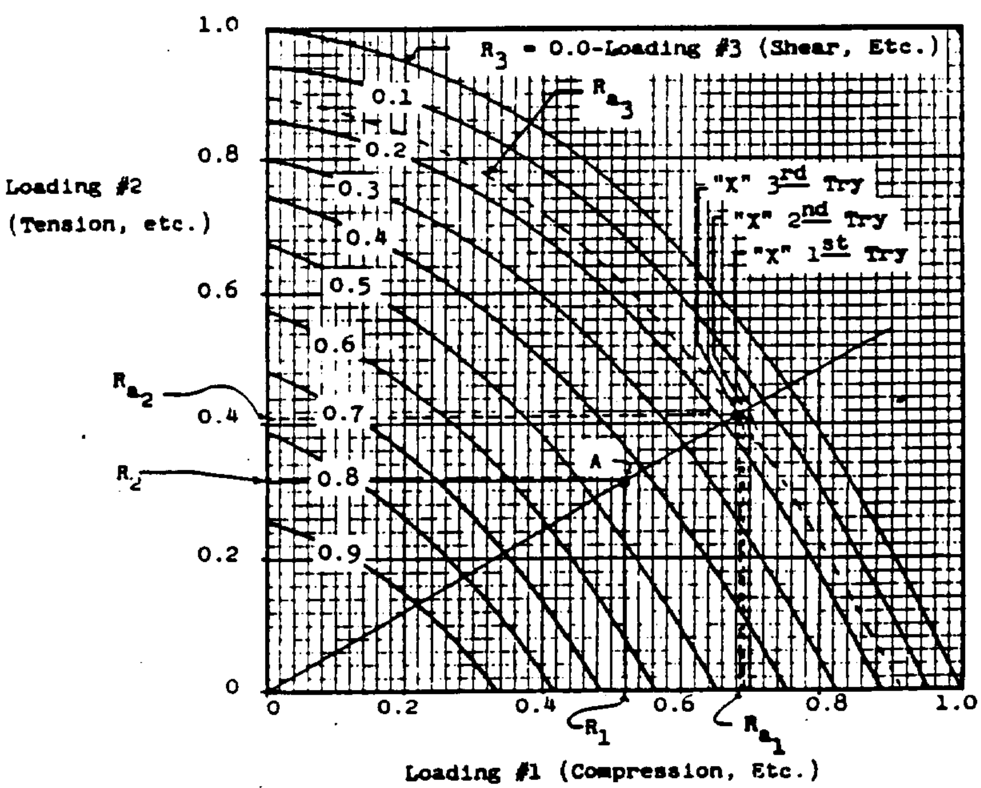

Fig. 6.1.5-2

(4) Draw a straight line through this point, point "A", Fig. 6.1.5-2, and the origin.

(5) Extend this line to locate an arbitrary point "x" which satisfies the following relationship:

$$\frac{R_1}{R_{a_1}} = \frac{R_3}{R_{a_3}} \quad \ldots\ldots\ldots\ldots\ldots\ldots \quad (6)$$

or

$$R_{a_3} = \frac{R_3}{R_1} R_{a_1} \quad \ldots\ldots\ldots\ldots\ldots\ldots \quad (7)$$

Where R_1 and R_3, the applied stress ratios, are obtained from step (1) above.

This is best accomplished by trial and error and is illustrated below:

<u>Example Problem</u>

Given: A plate with applied stress ratios $R_1 = .520$, $R_2 = .315$, $R_3 = .125$ and $a/b = 1$. Assume the Interaction Curves on Fig. 6.1.5-2 correspond to the fixity and loading of this panel.

Find: Find the allowable stress ratio "R_{a_1}"

Solution:

Establish point "A" on Fig. 6.1.5-2 corresponding to $R_1 = .520$ and $R_2 = .315$.

Using equation (7), $R_{a_3} = \frac{.125}{.520} R_{a_1} = .240 R_{a_1}$ . . . (8)

<u>1st Try</u>: Let $R_{a_1} = .6$ (Trial and error procedure)

then $R_{a_3} = .240\ (.6) = .144$ . . . . (9)

Using this initial value of R_{a_3} establish an arbitrary location of point "x" on the line extended from the origin through point "A." From this point on Fig. 6.1.5-2, the initial value of "R_{a_1}" is found to be .700. Therefore, the actual value of R_{a_1} must be between .60 and .700. Repeat this procedure until the values of R_{a_1} converge.

<u>2nd Try</u>: Let $R_{a_1} = .650$ then $R_{a_3} = .156$ from eq. (8) and

$R_{a_1} = .690$ from Fig. 6.1.5-2.

3rd Try: Let R_{a_1} = .670 then R_{a_3} = .161 from eq. (8)

and R_{a_1} = .685 from Fig. 6.1.5-2.

Use R_{a_1} = .677

(6) Calculate the margin of safety by using the allowable stress ratios obtained from (5) above and equation (4).

$$M.S. = \frac{R_{a_1}}{R_1} - 1 = \frac{R_{a_2}}{R_2} - 1 = \frac{R_{a_3}}{R_3} - 1 \quad \ldots\ldots \quad (10)$$

Example

From the example in (5), R_{a_1} = .677 and R_1 = .520

$$M.S. = \frac{R_{a_1}}{R_1} - 1 = \frac{.677}{.520} - 1 \quad \ldots\ldots \quad +.300$$

Note: This method is based on the assumption that all loadings are applied proportionately. This coincides closely with the loading in actual airplanes.

6.2.0 Buckling of Flat Rectangular Plates

The critical buckling stress in plates and shells is given by the equation:

$$\sigma_{cr} = \frac{k\pi^2 E\eta}{12(1-\mu^2)}\left(\frac{t}{b}\right)^2 \quad \ldots\ldots \quad (1)$$

Where "k" is the nondimensional buckling coefficient for the configuration under consideration, and "b" is the loaded edge unless otherwise noted. The incorporation of the plasticity coefficient, η, makes the above equation applicable in both the elastic and plastic range. In the elastic range "η" is equal to one (1) and in the plastic range "η" is less than one. The value of "η" can be determined by use of the method outline in article 6.1.2. The material constants "E" and "μ" are for a given material at a given temperature.

The following table gives values of $\pi^2/12(1-\mu^2)$ for various values of Poisson's ratio.

TABLE 6.2.0-1

μ	$\frac{\pi^2}{12(1-\mu^2)}$	μ	$\frac{\pi^2}{12(1-\mu^2)}$	μ	$\frac{\pi^2}{12(1-\mu^2)}$
.20	.857	.30	.904	.40	.979
.21	.860	.31	.910	.41	.989
.22	.864	.32	.916	.42	.998
.23	.887	.33	.923	.43	1.009
.24	.873	.34	.930	.44	1.020
.25	.877	.35	.937	.45	1.031
.26	.882	.36	.945		
.27	.887	.37	.953		
.28	.892	.38	.961		
.29	.898	.39	.970		

6.2.1

Uniaxial Compression

The equation and curves in Figures 6.2.1.1 through 6.2.1.5 can be used to determine the critical buckling strength of rectangular flat plates subjected to uniaxial compression.

Loading diagrams and fixity notations have been placed on each of the various figures to indicate the proper use of each curve.

Procedure

1. Calculate the a/b ratio from the dimensions of the plate.
2. Select the curve for the fixity which most closely represents the problem, and determine "k" using the ratio of a/b obtained above.
3. Using this value of "k" and the associated equation from the same figure, solve for the critical buckling stress, σ_{cr}.

NOTE: In Fig. 6.2.1.5, care should be taken to use the "k" values obtained from the k_c' curve with the equation containing k_c' , etc.

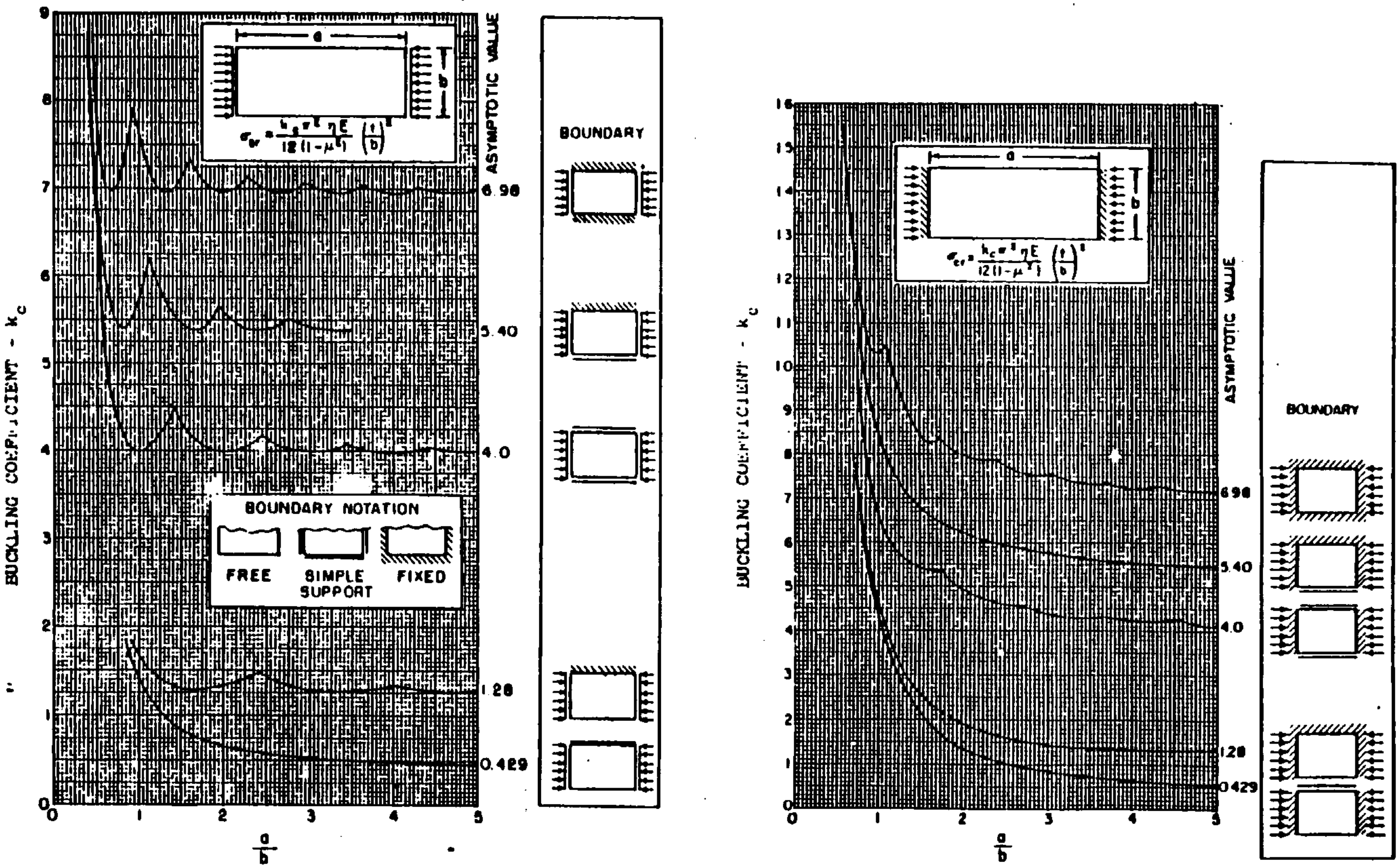

(a) Loaded Edges Simply Supported

(b) Loaded Edges Clamped

Fig. 6.2.1.1

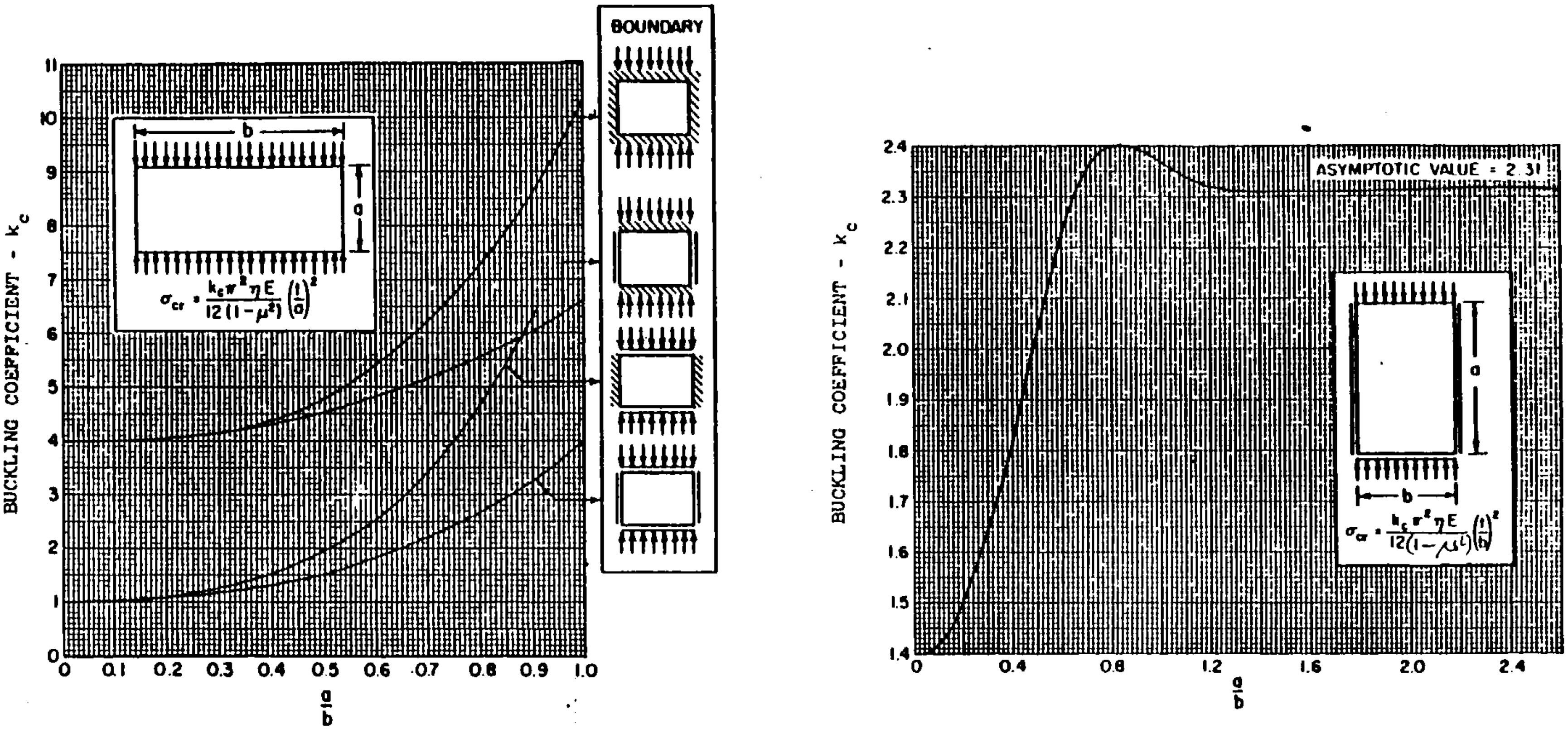

(a) Wide Plates

(b) One Loaded Edge Free, and One Loaded Edge Simply Supported

Fig. 6.2.1.2

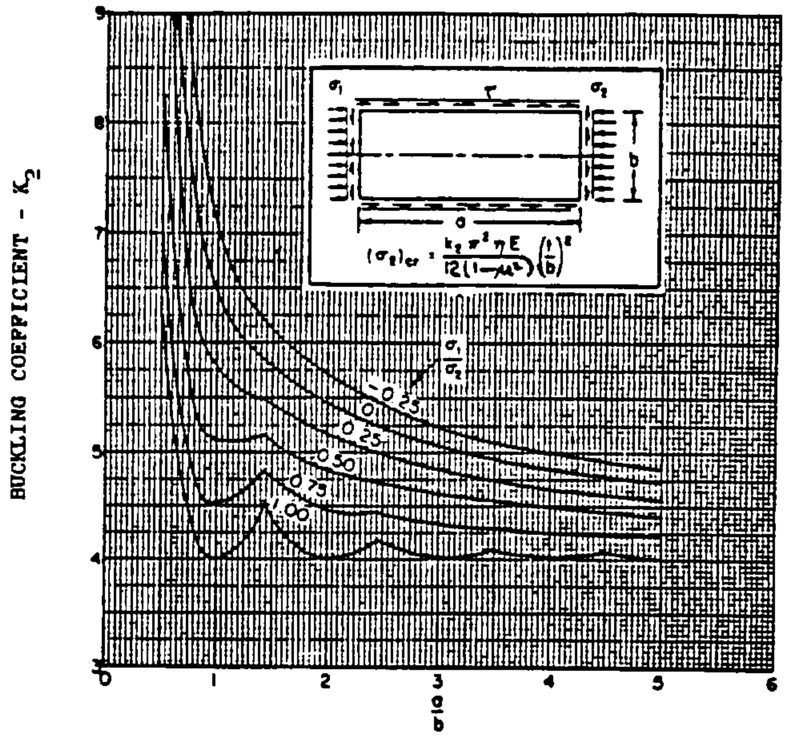

(a) Long Simply Supported Plate With Varying Compressive Load

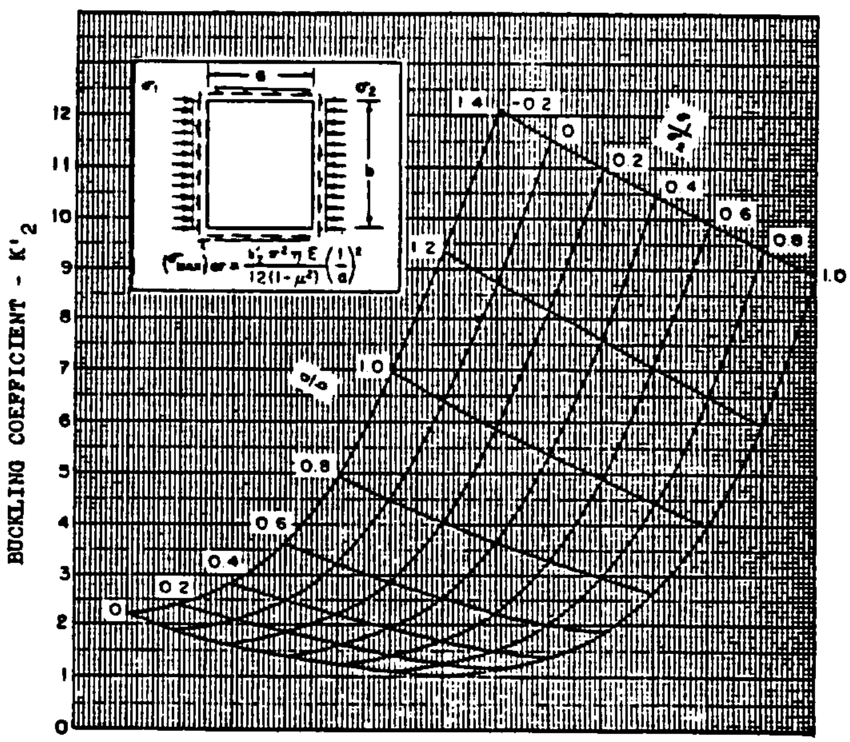

(b) Short Simply Supported Plate With Varying Compressive Load

Fig. 6.2.1.3

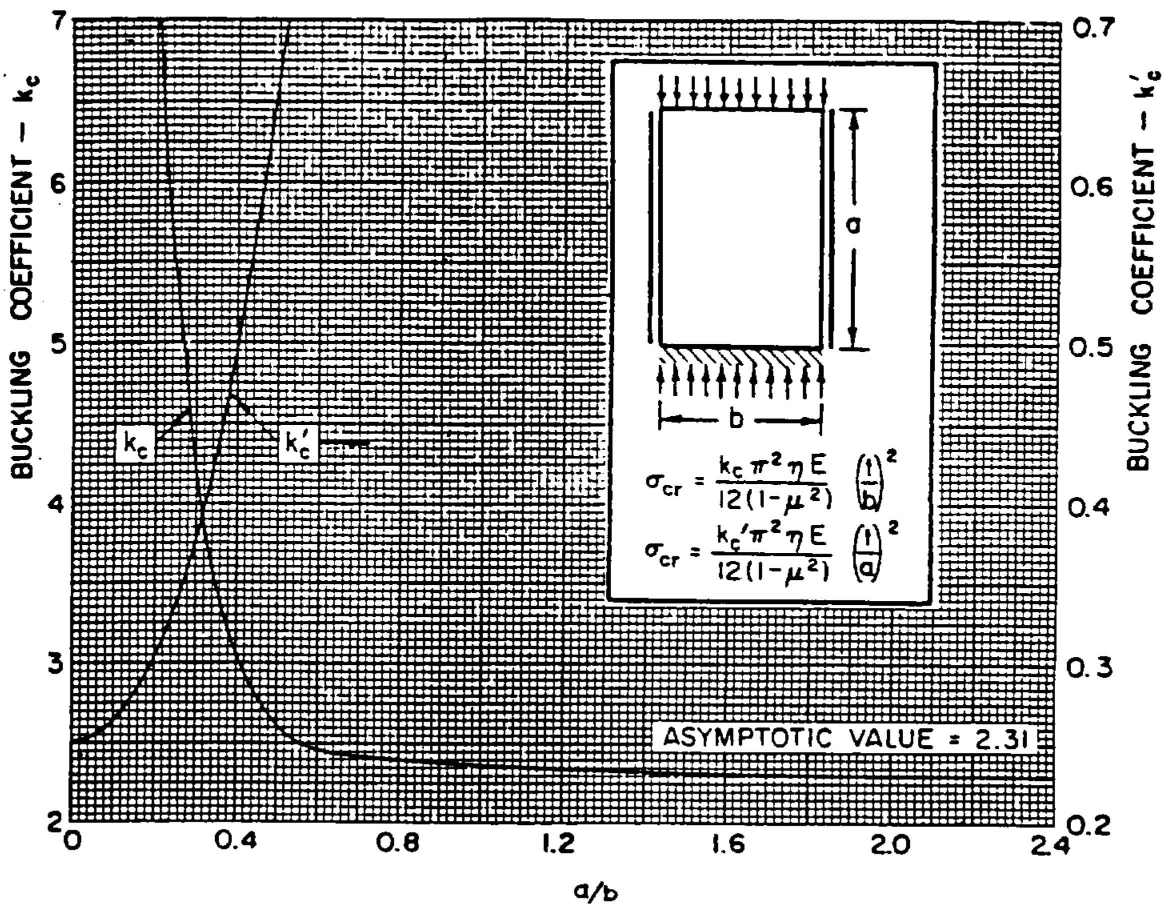

Fig. 6.2.1.4. One Loaded Edge Free and One Loaded Edge Fixed

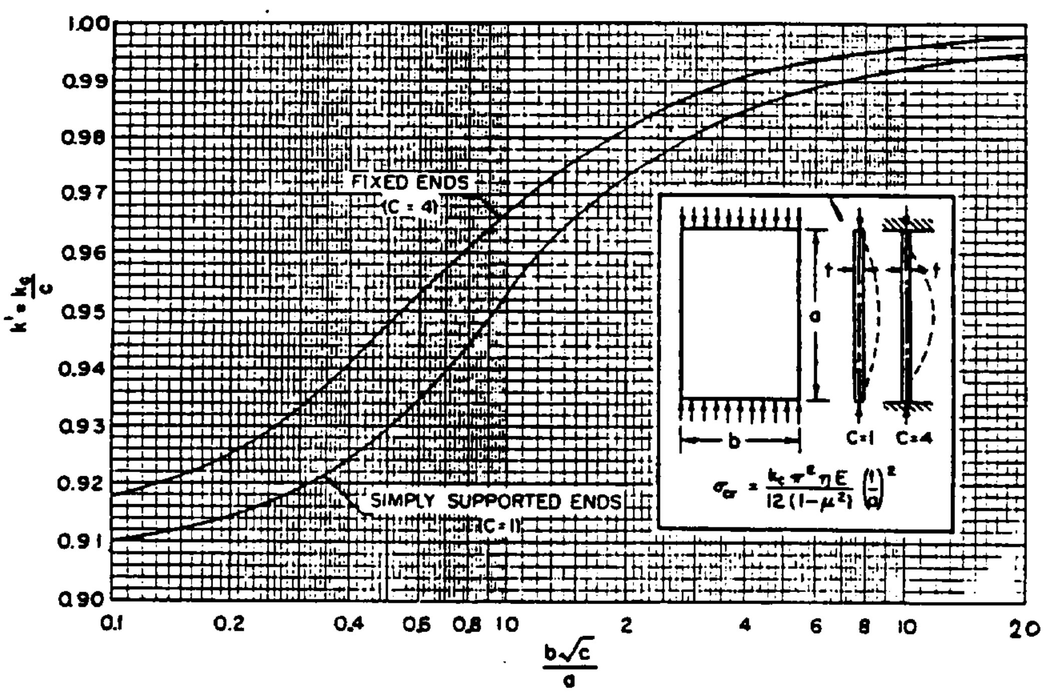

Fig. 6.2.1.5 Buckling Coefficients for Plate Columns

6.2.3

Shear

The buckling stress coefficients for rectangular flat plates under shear are presented in Figure 6.2.3-1. The term "b" is always the shorter dimension of the rectangular plate.

Procedure

1. Calculate the ratio b/a from the dimension of the panel.
2. Select the curve whose fixity most closely represents the problem, and determine "k_s" (Fig. 6.2.3-1).
3. Using this value of "k_s" and the equation from Fig. 6.2.3-1, solve for the critical buckling stress, τ_{cr}
4. If "τ_{cr}" is above the proportional limit, use the method of article 6.1.2.

Assume $\tau_{CR} = .55\,\sigma_T$ in using Tangent Modulus Curves

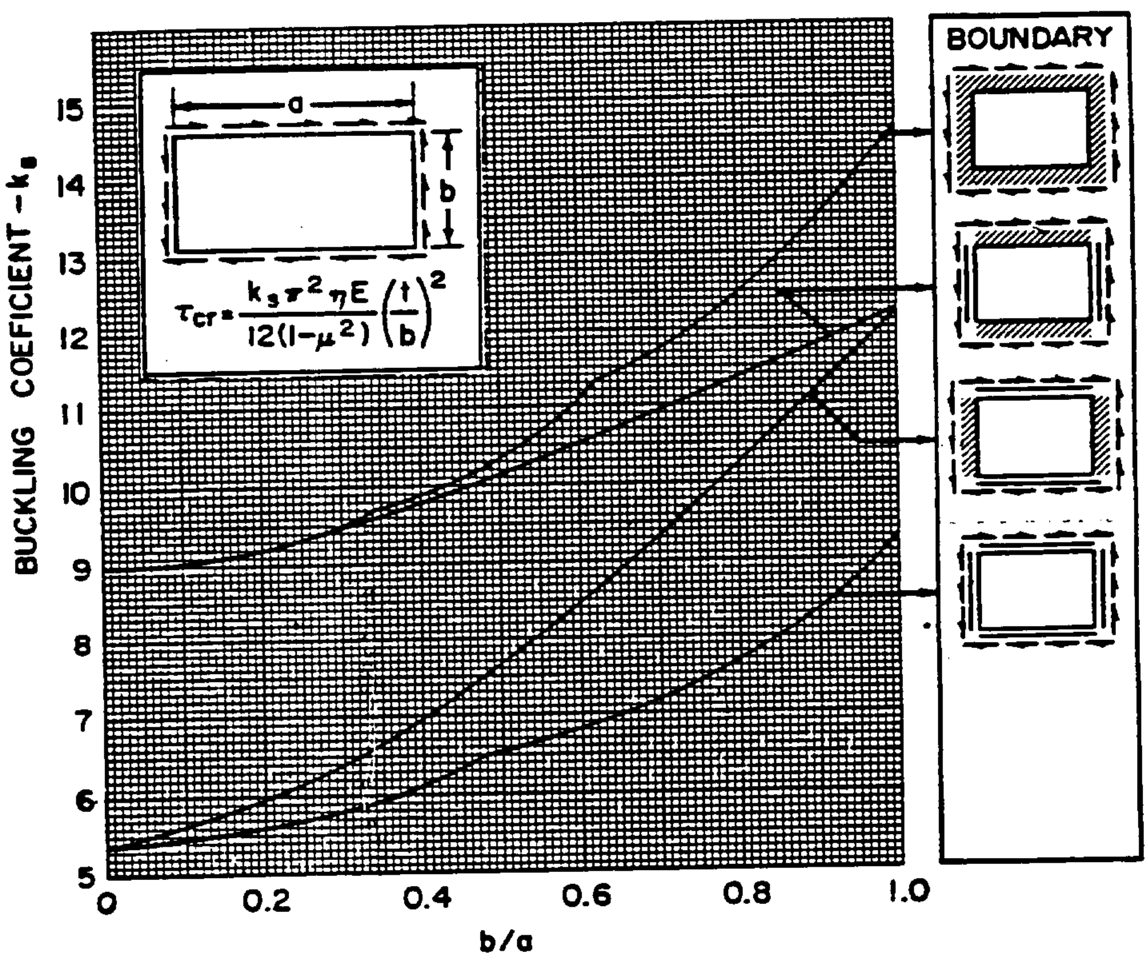

Flat Plates in Shear

Fig. 6.2.3-1

6.2.4
Combined Shear and Uniaxial Compression or Tension

Interaction curves for simply supported rectangular flat plates under combined shear and uniaxial compression or tension are presented in Fig. 6.2.4.1(a). If the aspect ratio, a/b, is less than one, the plate is under a longitudinal direct stress and the curve for a/b = 1.0 should be used. If a/b approaches zero, the curve for a/b = 1.0 is valid for all edge restraints, $0 < \epsilon < \infty$.

Interaction curves for infinitely long rectangular flat plates with varying edge restraints are presented in Fig. 6.2.4.1(b). The parameter "ϵ" is defined as the coefficient of edge restraint (see Section 6.1.3), and is equal to

$$\epsilon = \frac{Sb}{D} \quad \ldots\ldots\ldots\ldots \quad (1)$$

where

$$D = \frac{EI}{(1-\mu^2)} = \frac{Et^3}{12(1-\mu^2)} \quad \ldots\ldots\ldots \quad (2)$$

S = Rotational stiffness per inch of edge

NOTE: When $\epsilon = 0$, the edges are simply supported.
When $\epsilon = \infty$, the edges are fixed.
When $0 < \epsilon < \infty$, the edges are elastically restrained.

Procedure

Use the procedure presented in article 6.1.5 (Two Loads Acting).

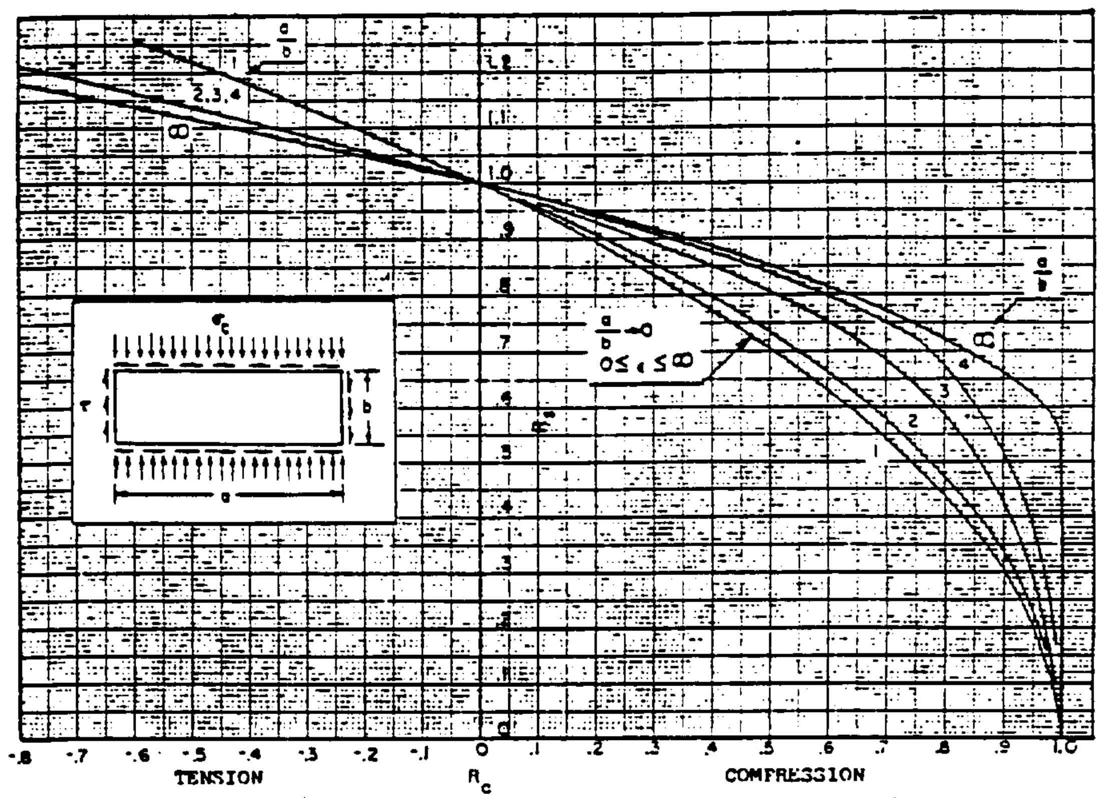

(a) Interaction Curves for Plates of Finite Length

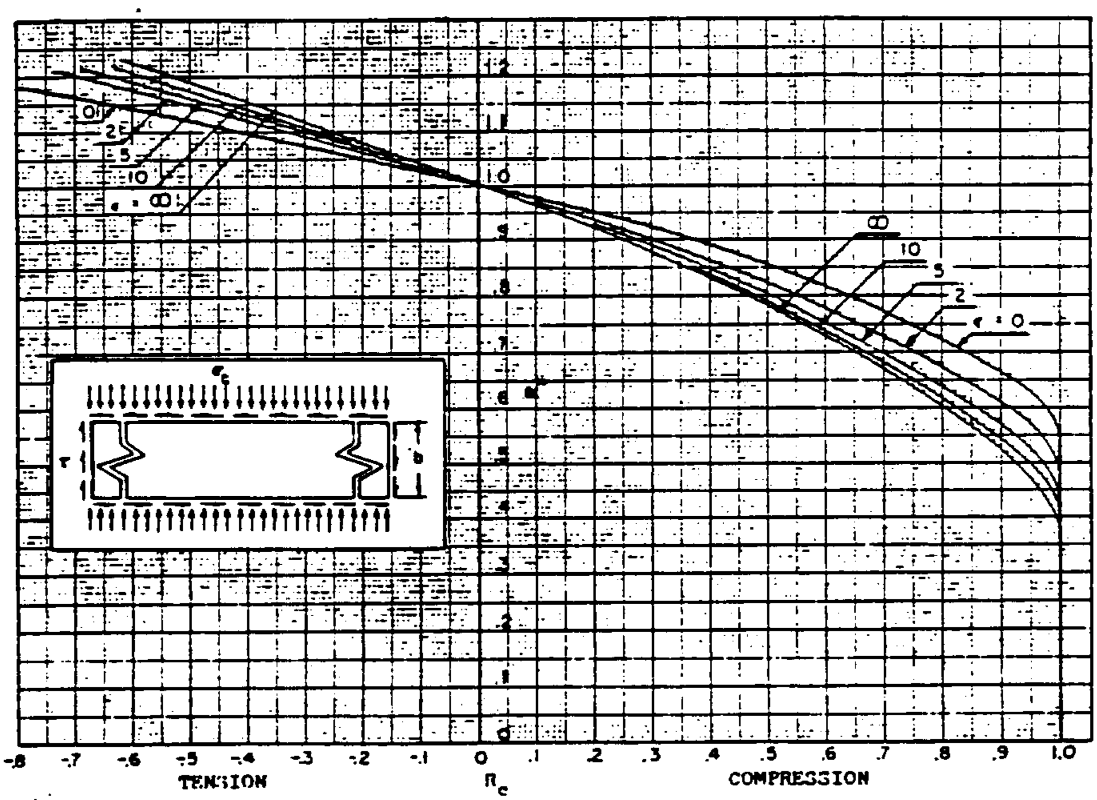

(b) Interaction Curves for Infinitely Long Plates

Fig. 6.2.4.1

6.2.5

Biaxial Compression or Compression and Tension

Interaction curves for simply supported and rigidly supported rectangular flat plates under combined compression and compression or tension are presented in Fig. 6.2.5.1. When "σ_x" is tension and $b < a$, use the value of $\beta = b/a$ and reverse the co-ordinate axis by taking "R_x" as ordinate and "R_y" as abscissa.

Procedure

Use the procedure presented in article 6.1.5 (Two Loads Acting).

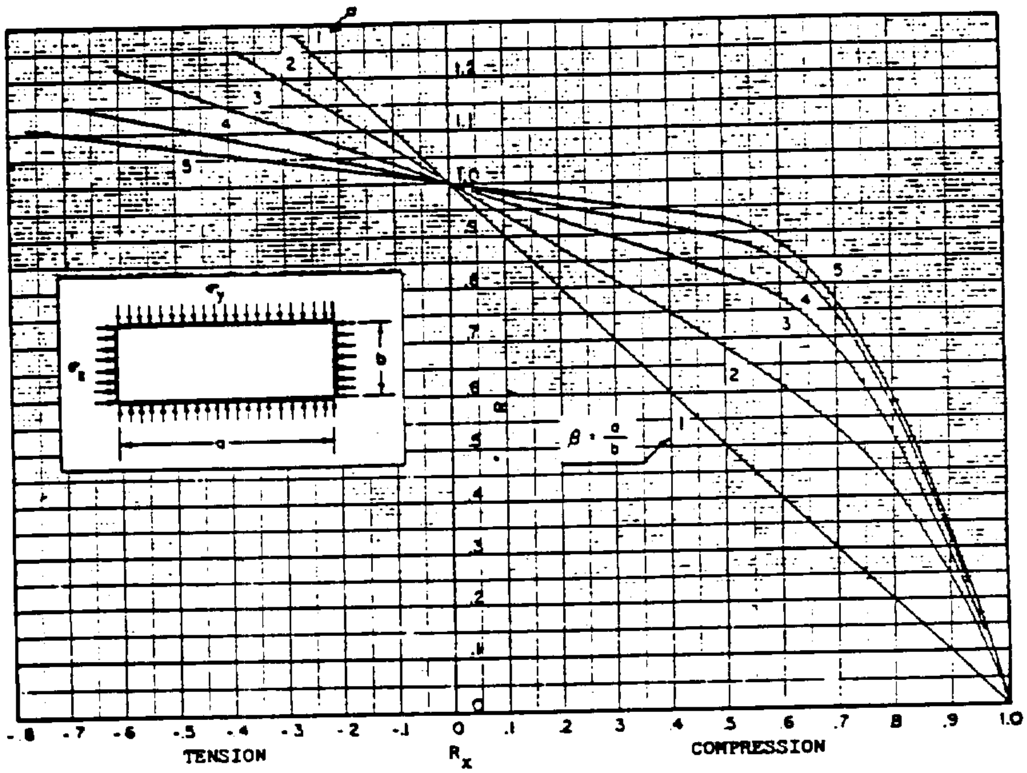

(a) Interaction Curves for Simply Supported Flat Plates

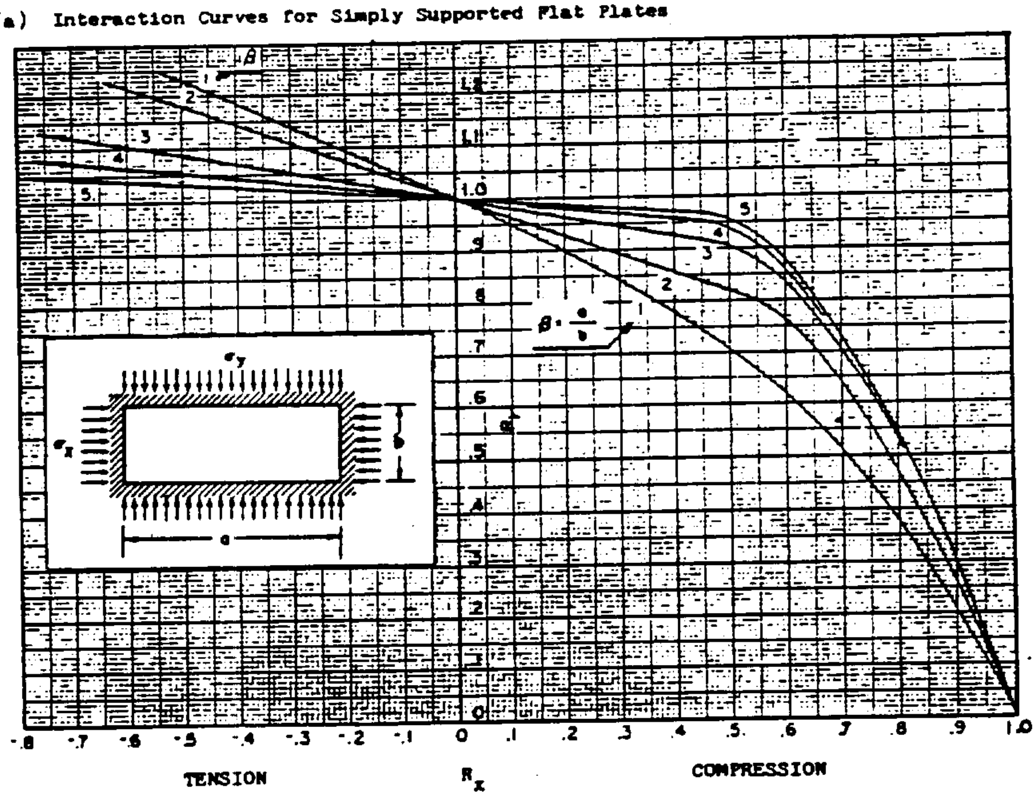

(b) Interaction Curves for Flat Plates With Clamped Edges

Fig. 6.2.5.1

6.2.6

Biaxial Compression and Shear

Interaction curves for simply supported flat rectangular plates under biaxial compression and shear are presented in Fig. 6.2.6.1 through Fig. 6.2.6.3. These interaction curves were obtained from theoretical considerations. In general, there are two possible buckling modes, symmetrical and antisymmetrical. The interaction curves correspond to that mode which gives the lower combination of stress ratios.

Procedure

Use the procedure presented in article 6.1.5 (Three Loads Acting).

It should be noted that for the case of $R_S = 0$, the result is identical with section 6.2.5, biaxial compression. If R_x or R_y are equal to zero, the results are identical with section 6.2.4, combined shear and axial load.

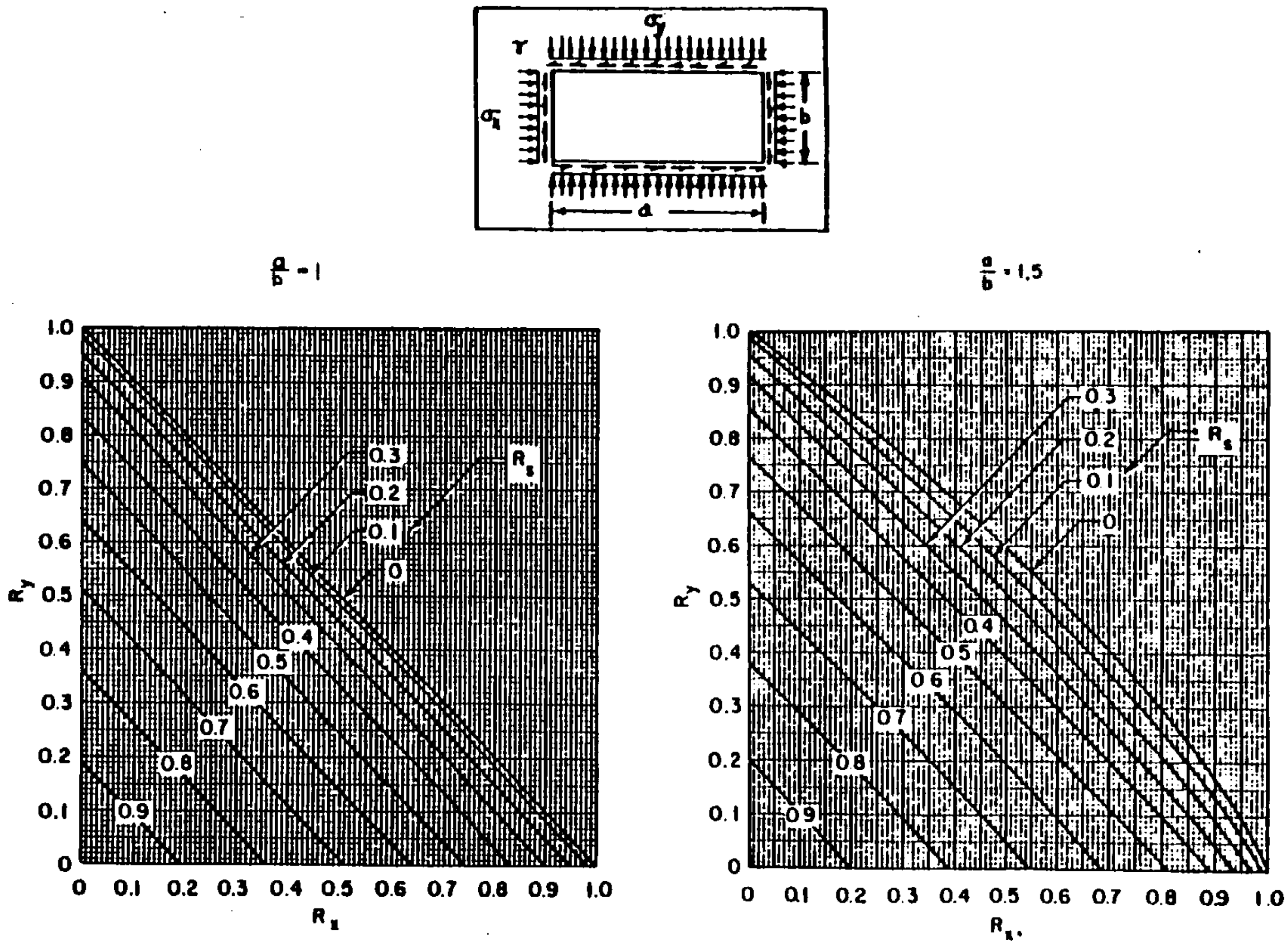

(a) (b)

Interaction Curves for Simply Supported Flat Plates Under
Biaxial Compression With Shear

Fig. 6.2.6.1

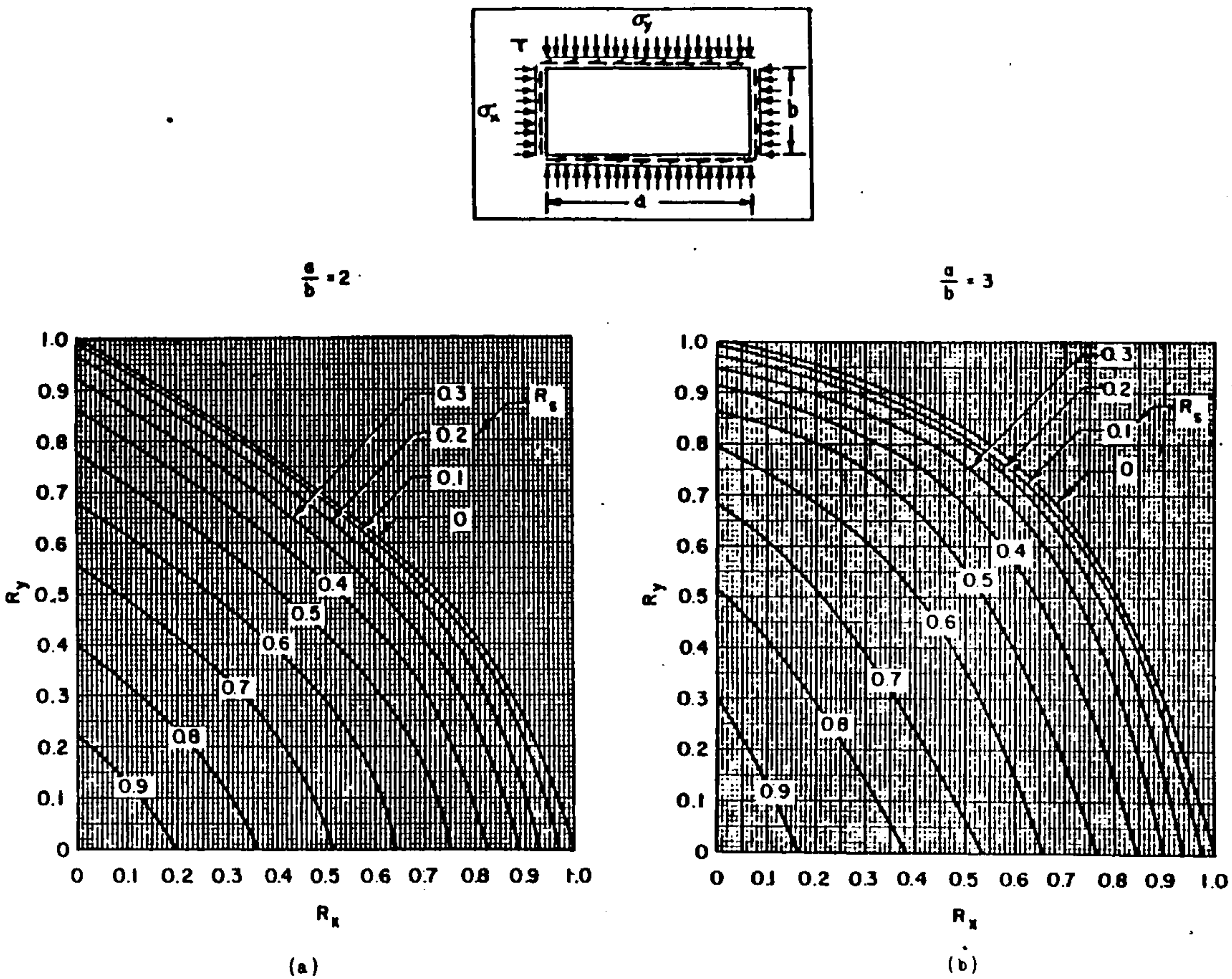

Interaction Curves for Simply Supported Flat Plates Under
Biaxial Compression With Shear

Fig. 6.2.6.2

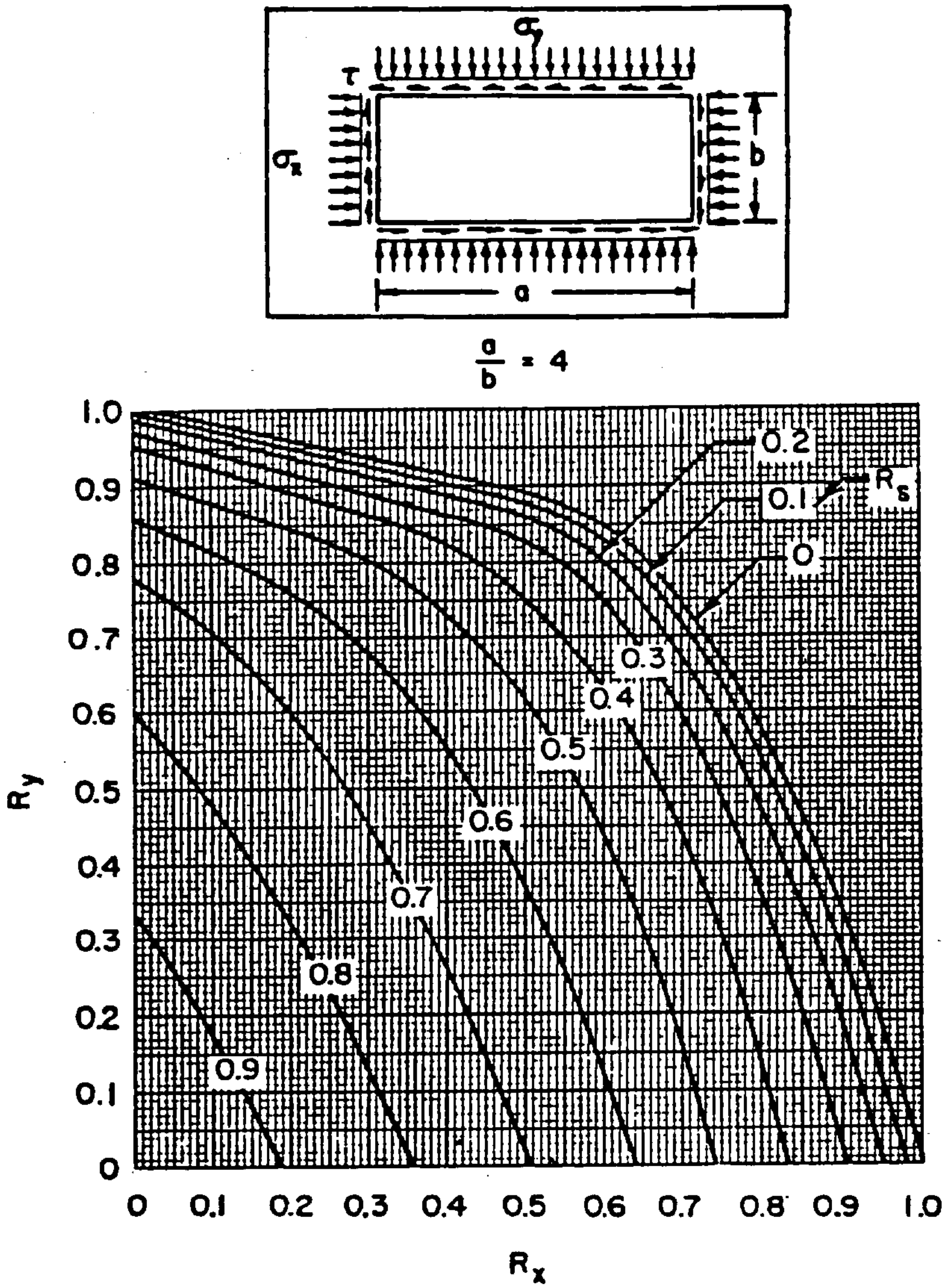

Interaction Curves for Simply Supported Flat Plates Under Biaxial Compression With Shear

Fig. 6.2.6.3

6.2.7

Bending

The buckling coefficients for rectangular flat plates under bending are presented in Fig. 6.2.7.1 through Fig. 6.2.7.3. The critical stress for flat plates in bending in the plane of the plate can be obtained from

$$(\sigma_b)_{cr} = \frac{k_b \pi^2 \eta E}{12(1-\mu^2)} \left(\frac{t}{b}\right)^2 \quad . \; . \; . \; . \; . \; . \; . \; . \quad (1)$$

where "k_b" is the buckling coefficient.

The plate stress distribution is shown below:

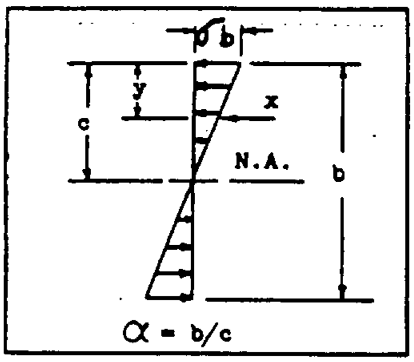

Fig. 6.2.7-1

$\sigma_x = \sigma_b \left[1 - \alpha\left(\frac{y}{b}\right)\right]$ (Stress distribution at loaded edge)

a/b = aspect ratio

α = b/c

c = the distance from the neutral axis (N.A.) to the outer compressive fiber.

σ_b = Max. compressive stress at the edge of the plate.

When $\alpha = 2$, the plate is under pure bending.
When $\alpha = 0$, the plate is under pure compression.
When $0 < \alpha < 2$, the plate is under combined bending and compression.

Procedure to Determine $(\sigma_b)_{cr}$

1. Calculate the a/b ratio from the dimensions of the plate.
2. Select the curve for the fixity which most closely represents the problem, and determine "k_b" using the "a/b" ratio obtained above.
3. Using this value of "k_b" and equation (1), solve for the critical buckling stress, $(\sigma_b)_{cr}$.

NOTE: The fixed edges in Fig. 6.2.7.2 and 6.2.7.3 are not restrained in the plane of the plate.

380

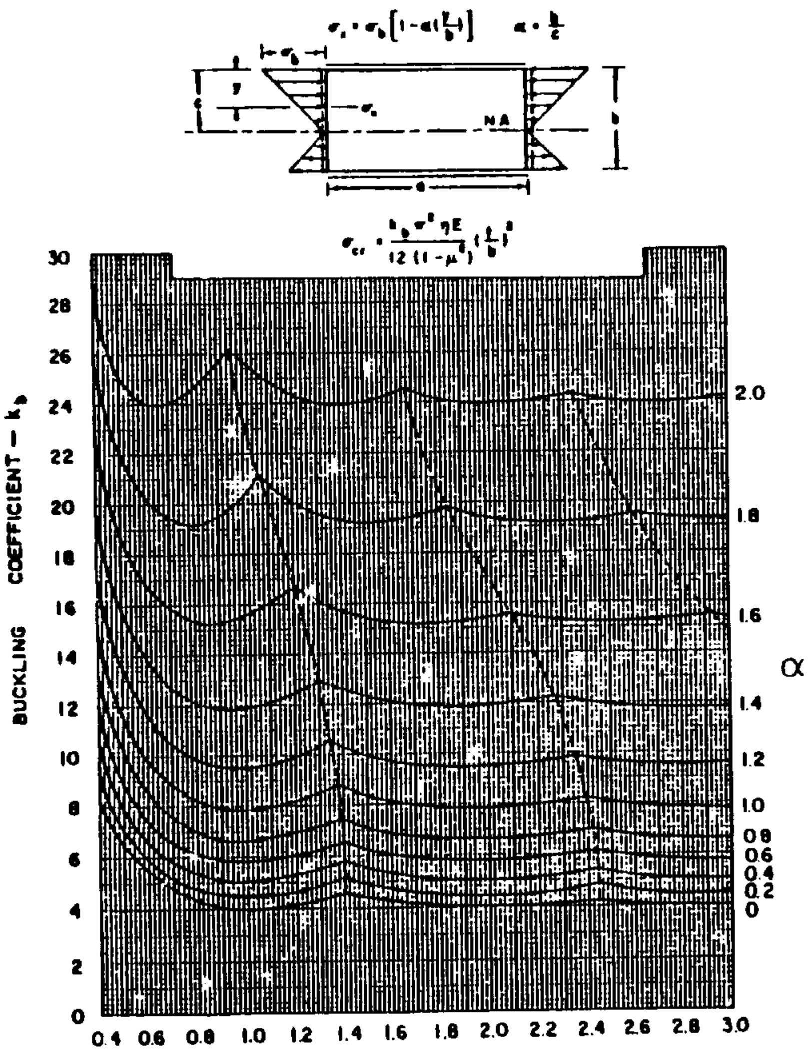

(a) Bending in Plane of Plate for $a/b \leq 3.0$

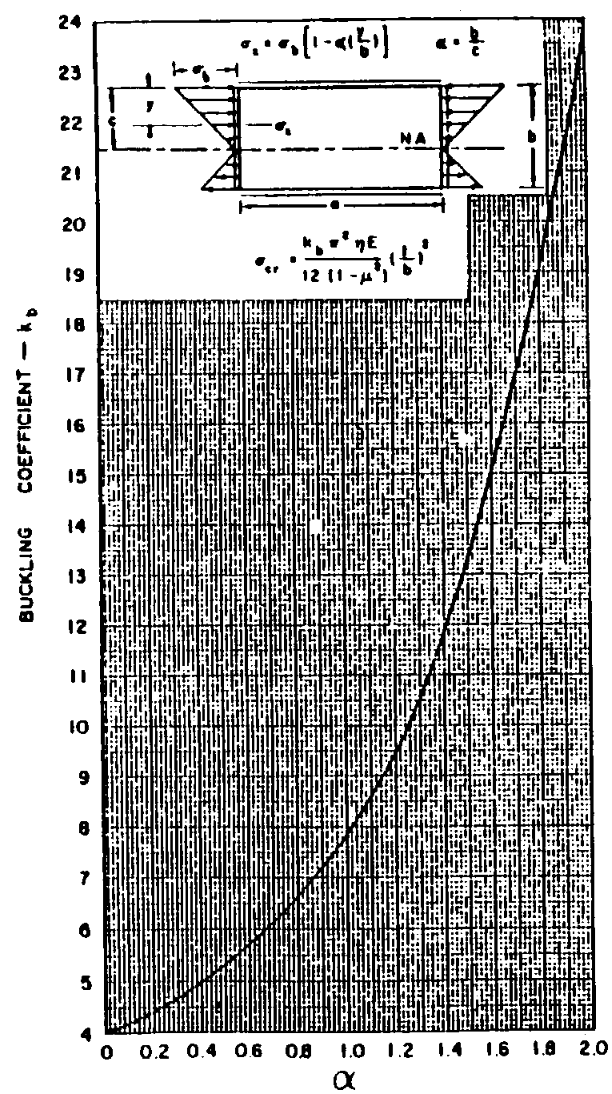

(b) Bending in Plane of Plate for $a/b \geq 4.0$

Fig. 6.2.7.1

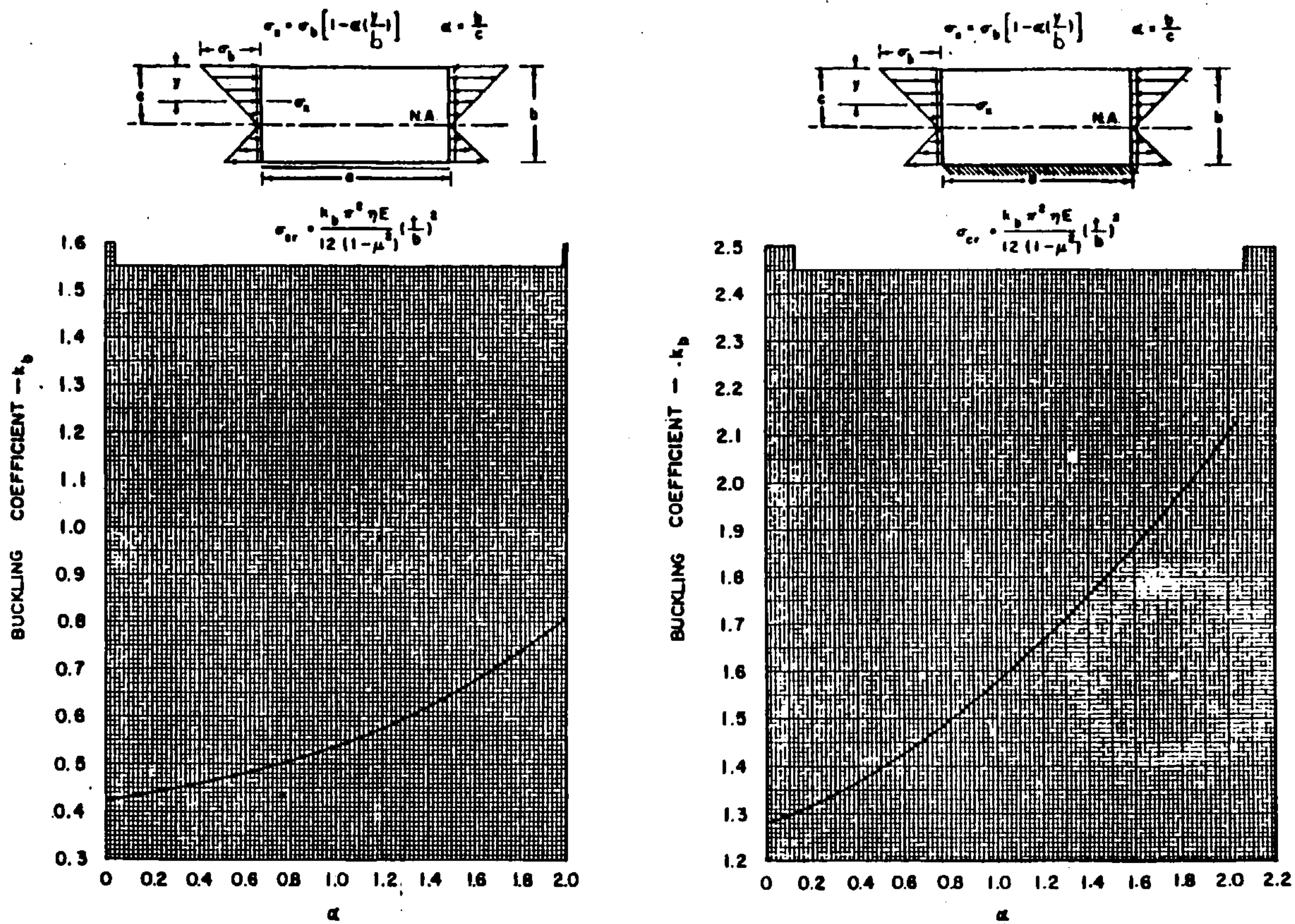

(a) Compression Edges Free and $a/b \geq 4.0$

(b) Compression Edges Free and $a/b \geq 2$

Fig. 6.2.7.3

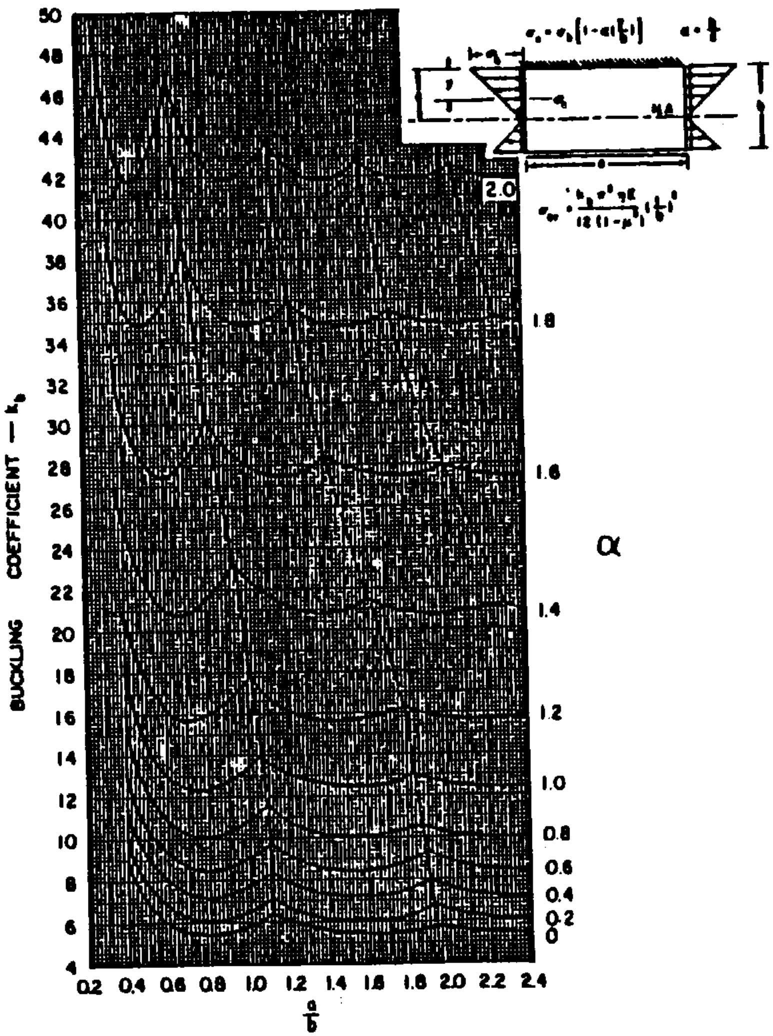

(a) Compression Edge Fixed and a/b $\leq$ 2.4

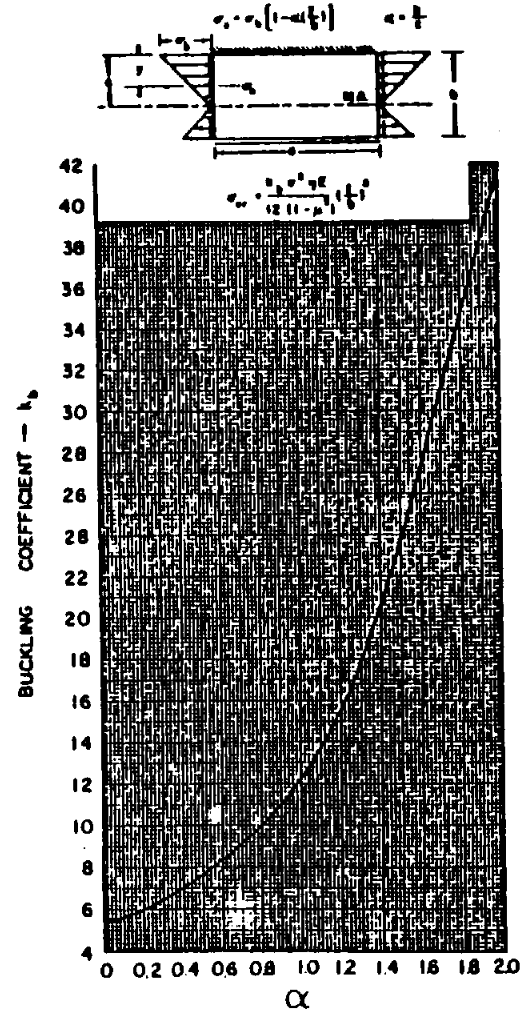

(b) Compression Edge Fixed and a/b $\geq$ 2.4

Fig. 6.2.7.2

6.2.8

Combined Bending and Shear

The interaction curve for simply supported flat rectangular plates under combined bending and shear is given in Fig. 6.2.8-1. This curve is applicable for any plate aspect ratio, and is a plot of the equation

$$R_b^2 + R_x^2 = 1 \quad . \; . \; . \; . \; . \; . \; . \; . \; . \; . \qquad (1)$$

Procedure

Use the procedure presented in article 6.1.5 (Two Loads Acting).

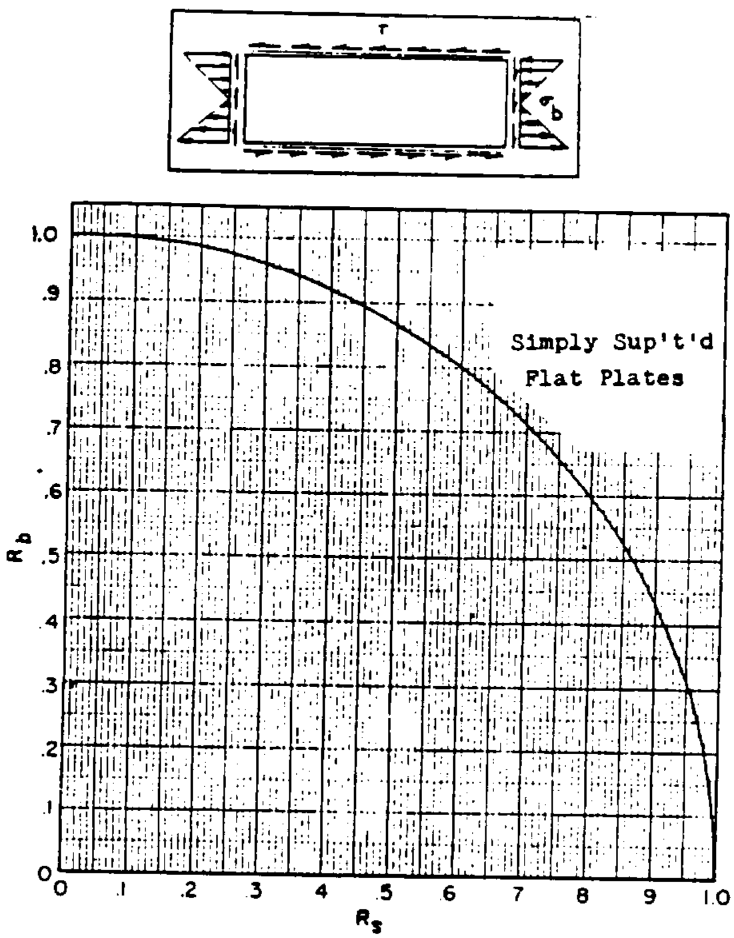

Combined Bending and Shear

Fig. 6.2.8-1

6.2.9 Combined Bending, Shear, and Transverse Compression

The interaction curves for infinitely long flat plates subjected to combined bending shear, and transverse compression are presented in Fig. 6.2.9.1. The curves in Fig. 6.2.9.1(a) are for simply supported edges. The curves in Fig. 6.2.9.1(b) are for plates whose tension edge is simply supported and whose compression edge is fixed.

The flat portion of the interaction curve corresponding to $R_c = 1.0$ (Fig. 6.2.9.1(a)) indicates that appreciable bending and shear stress can be applied to the plate without reducing the critical transverse compressive stress. In the region $R_c = 1.0$, the plate buckles essentially as a Euler column.

Procedure

Use the procedure presented in article 6.1.5 (Three Loads Acting).

NOTE: The fixed edges in Fig. 6.2.9.1(b) are not restrained in the plane of the plate.

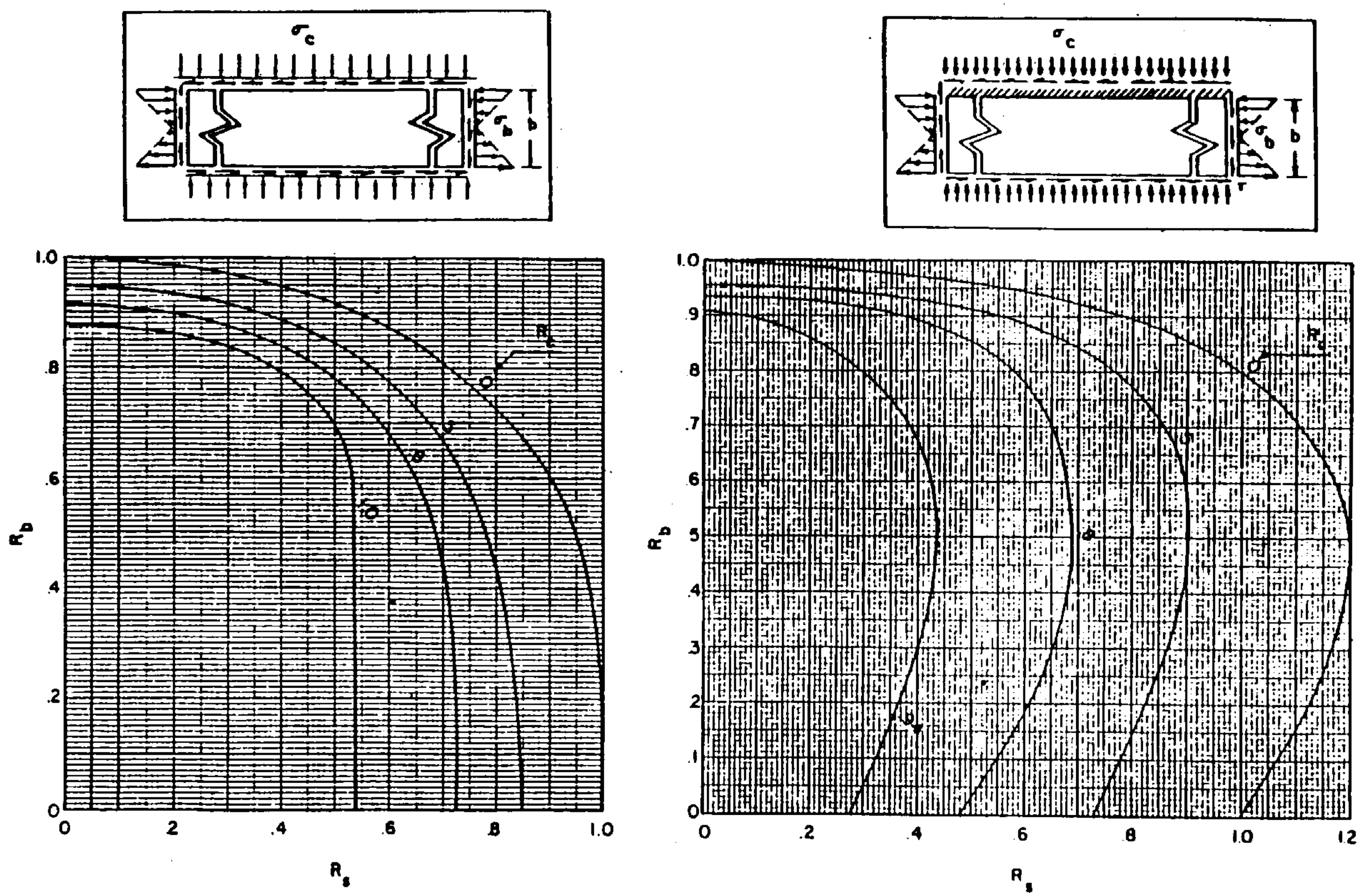

(a) Simply Supported Flat Plate

(b) Compression Edge Clamped

Infinitely Long Flat Plates Under Combined
Bending, Shear, and Transverse Compression

Fig. 6.2.9.1

6.2.10
Combined Bending and Biaxial Compression

Interaction curves for simply supported flat rectangular plates under combined and biaxial compression are presented in Fig. 6.2.10.1 through Fig. 6.2.10.4 for various aspect ratios from 0.8 to ∞ .

When $R_x = 0$, curves can be drawn for the various aspect ratios that will represent the interaction curves for a rectangular flat plate under critical combinations of longitudinal bending and transverse compression. This is accomplished in Fig. 6.2.11.1.

Procedure

Use the procedure presented in article 6.1.5 (Three Loads Acting).

6.2.11
Combined Bending and Transverse Compression

Interaction curves for simply supported flat rectangular plates under combined longitudinal bending and transverse compression are presented in Fig. 6.2.11.1.

Procedure

Use the procedure presented in article 6.1.5 (Two Loads Acting).

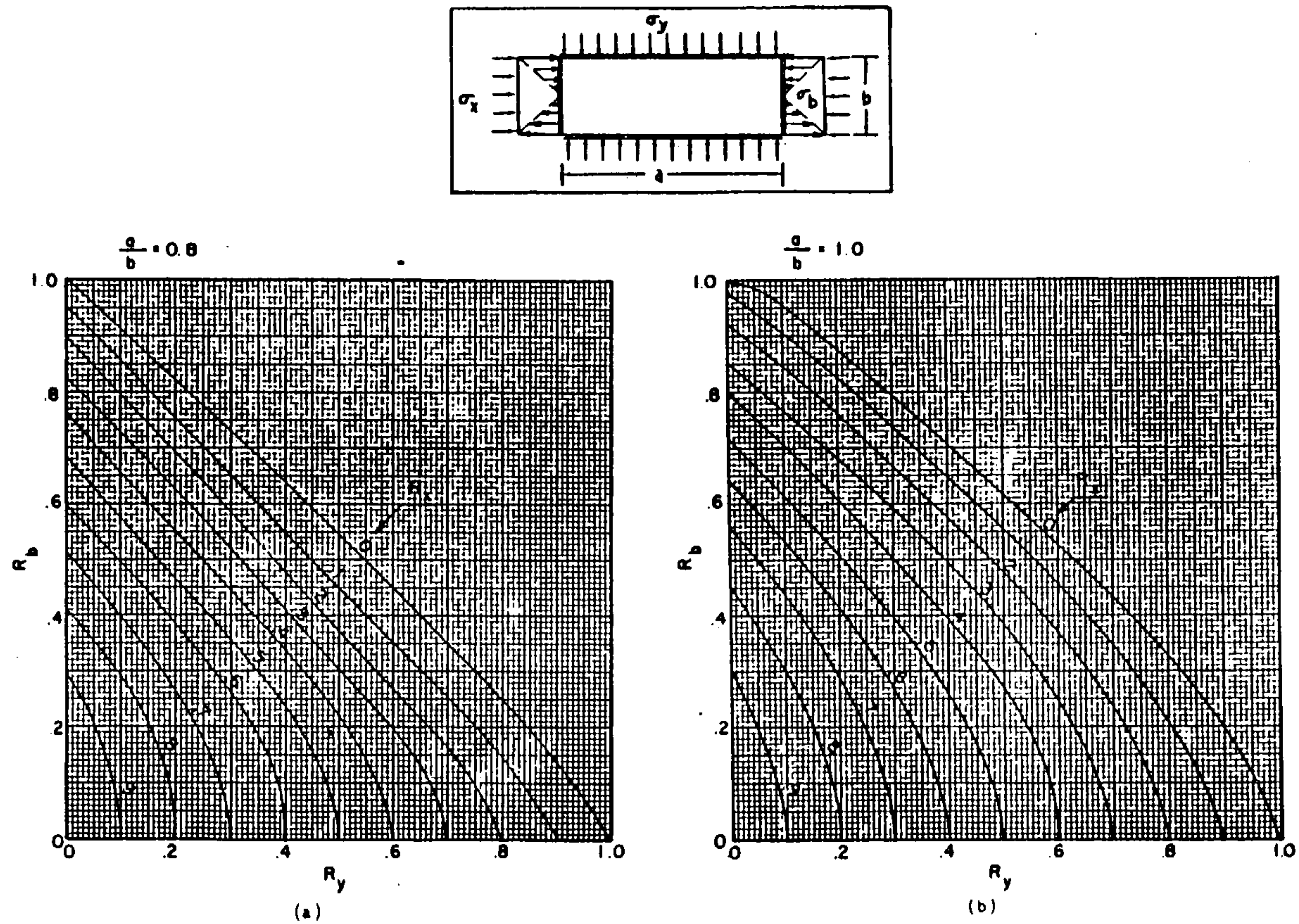

Interaction Curves for Simply Supported Flat Plates Under Combined Bending, and Biaxial Compression

Fig. 6.2.10.1

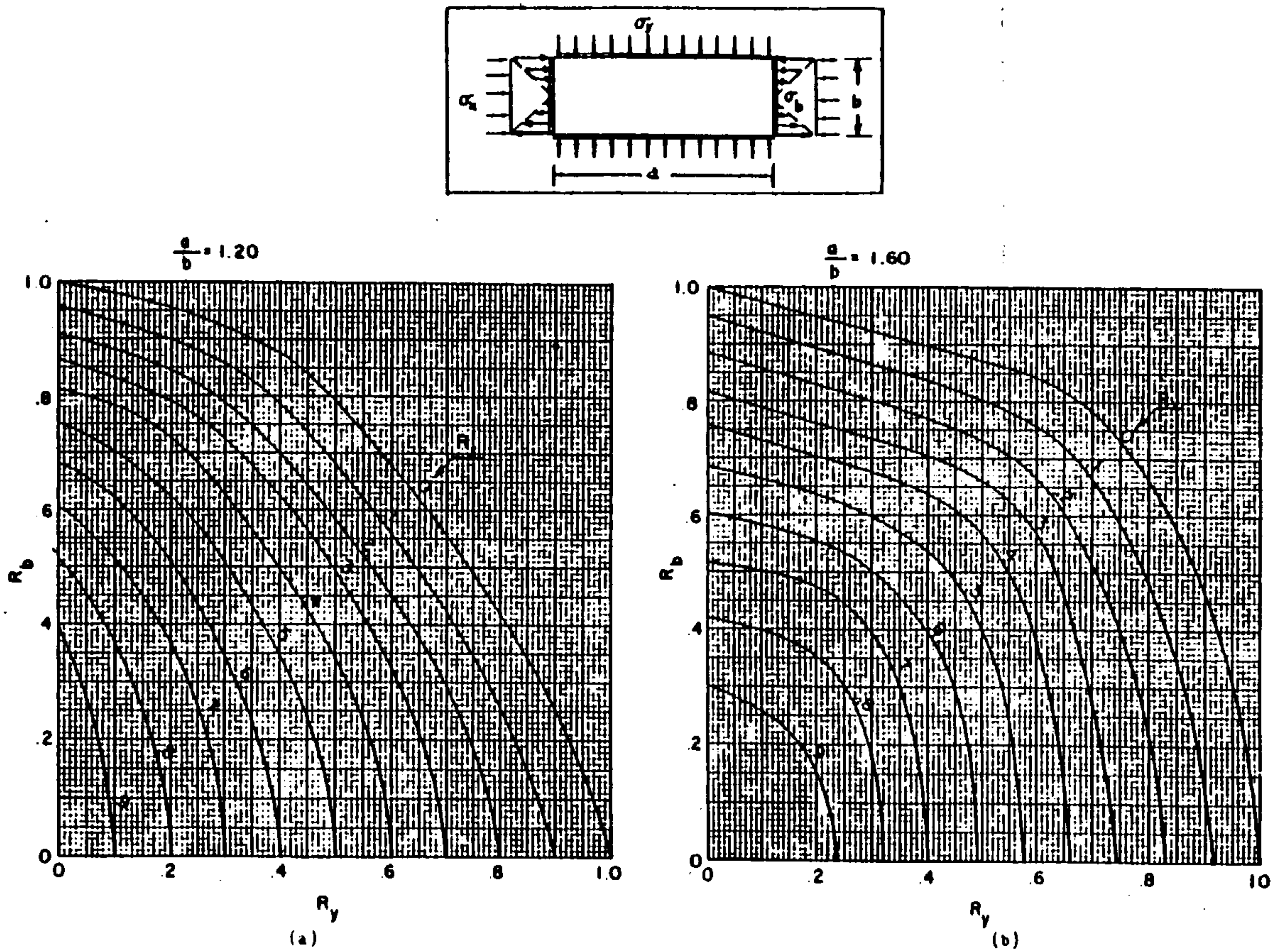

Interaction Curves for Simply Supported Flat Plates Under Combined Bending and Biaxial Compression

Fig. 6.2.10.2

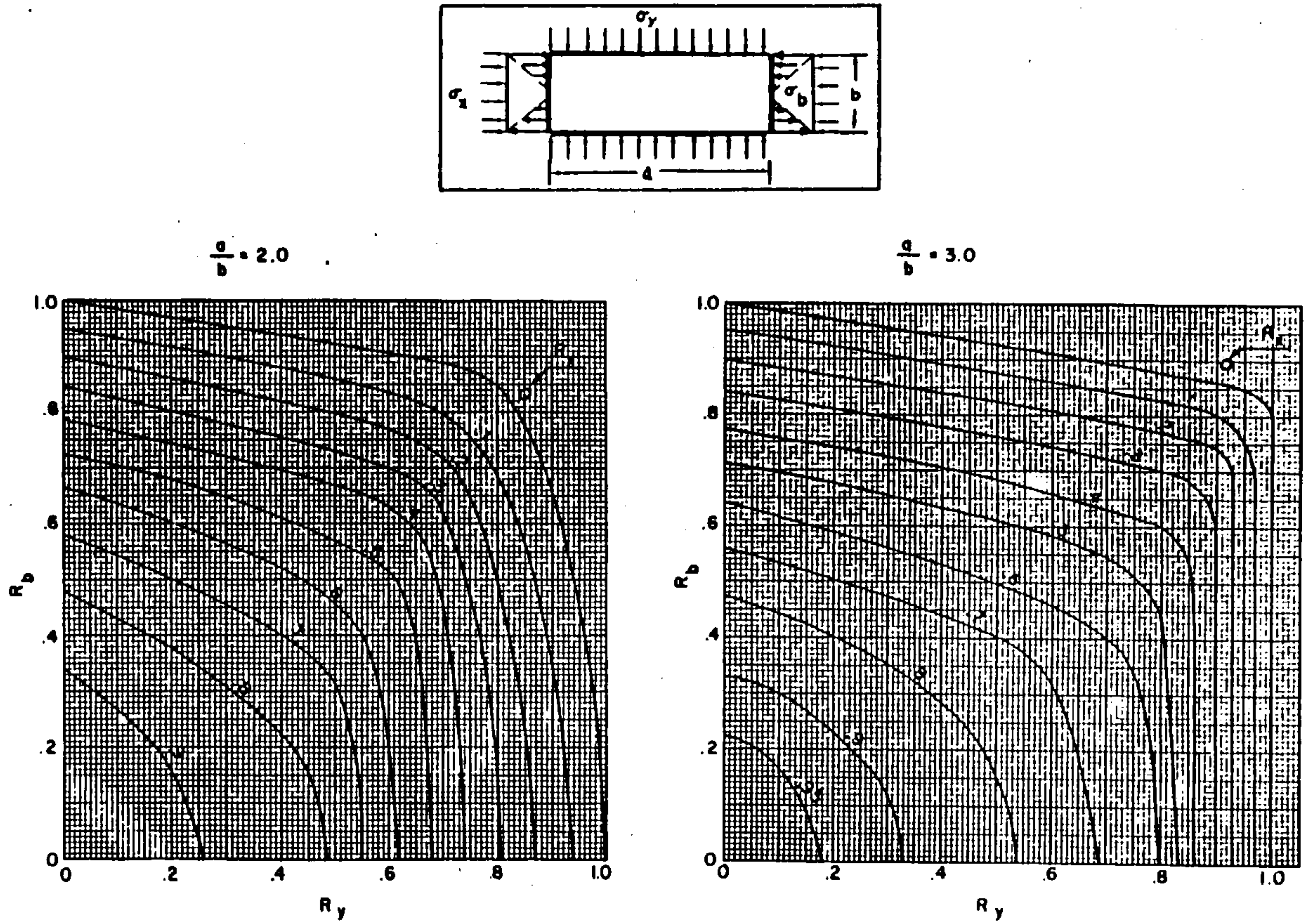

(a)

Interaction Curves for Simply Supported Flat Plates Under Combined Bending and Biaxial Compression

Fig. 6.2.10.3

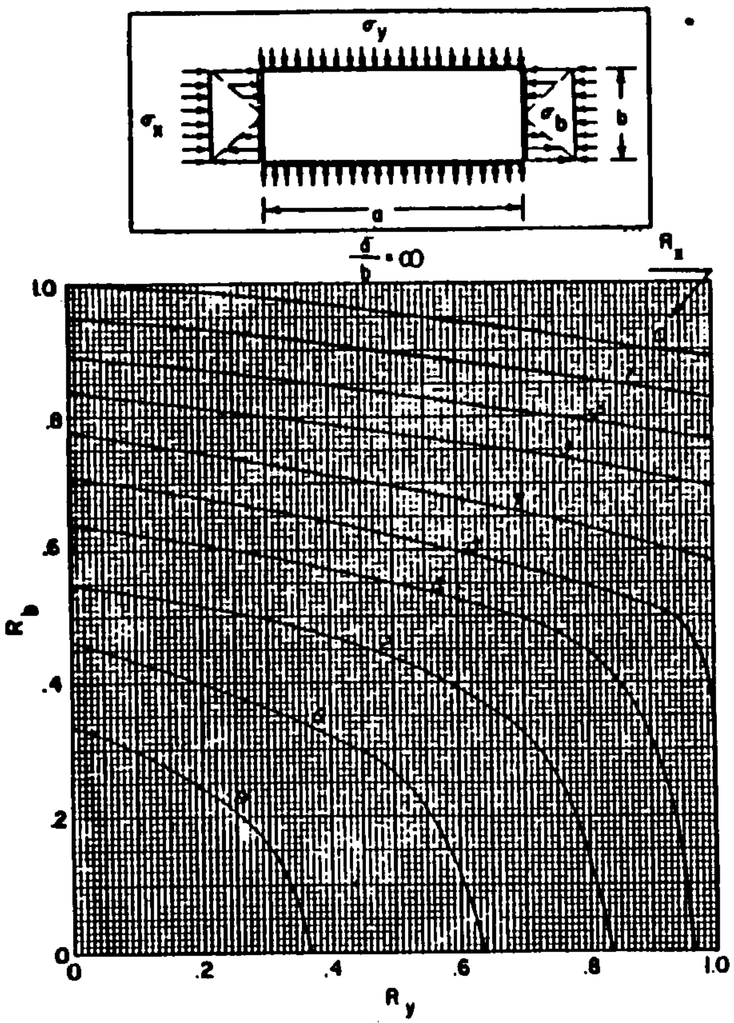

Fig. 6.2.10.4. Interaction Curves for Combined Bending and Biaxial Compression of Simply Supported Flat Plates

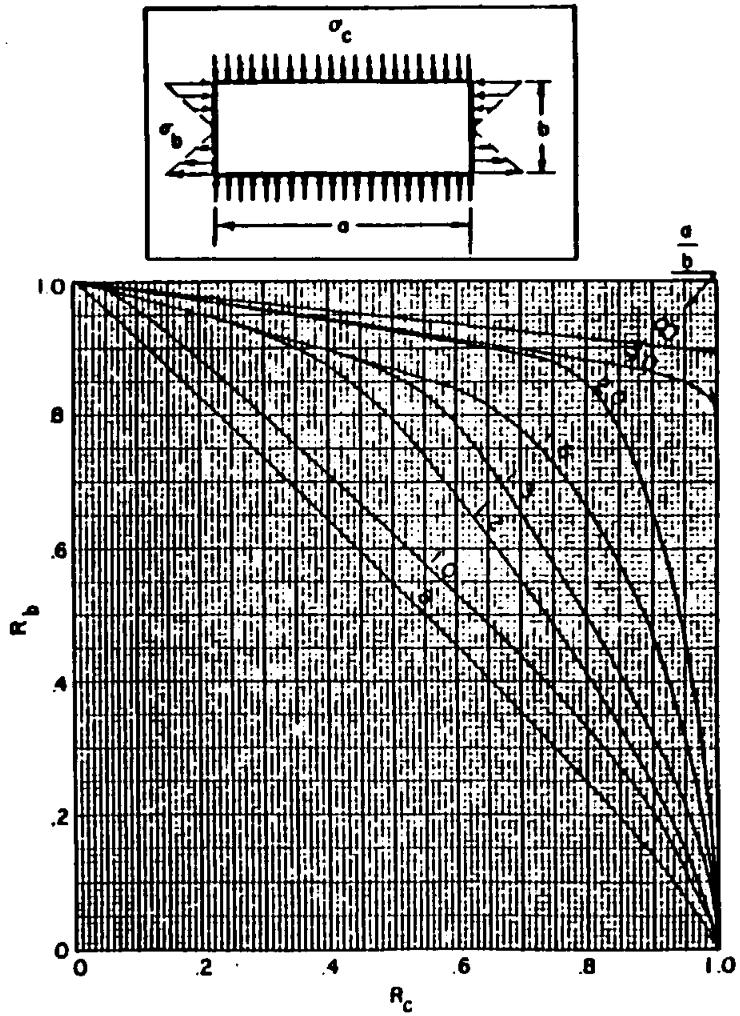

Fig. 6.2.11.1. Interaction Curve for Combined Bending and Transverse Compression of Simply Supported Flat Plates

6.2.12

Combined Bending, Shear, and Compression or Tension

The interaction curves for simply supported flat plates under combined longitudinal bending, shear, and compression or tension are presented in Fig. 6.2.12.1. These curves are plotted from the following interaction equation

$$R_s^2 + R_b^2 + R_c = 1 \quad . \; . \; . \; . \; . \; . \; . \; . \quad (1)$$

Procedure

Use the procedure presented in article 6.1.5 (Three Loads Acting).

The margin of safety should be calculated from the following equation

$$M.S. = \frac{2}{R_c + \sqrt{R_c^2 + 4(R_s^2 + R_b^2)}} - 1 \quad . \; . \; . \; . \quad (2)$$

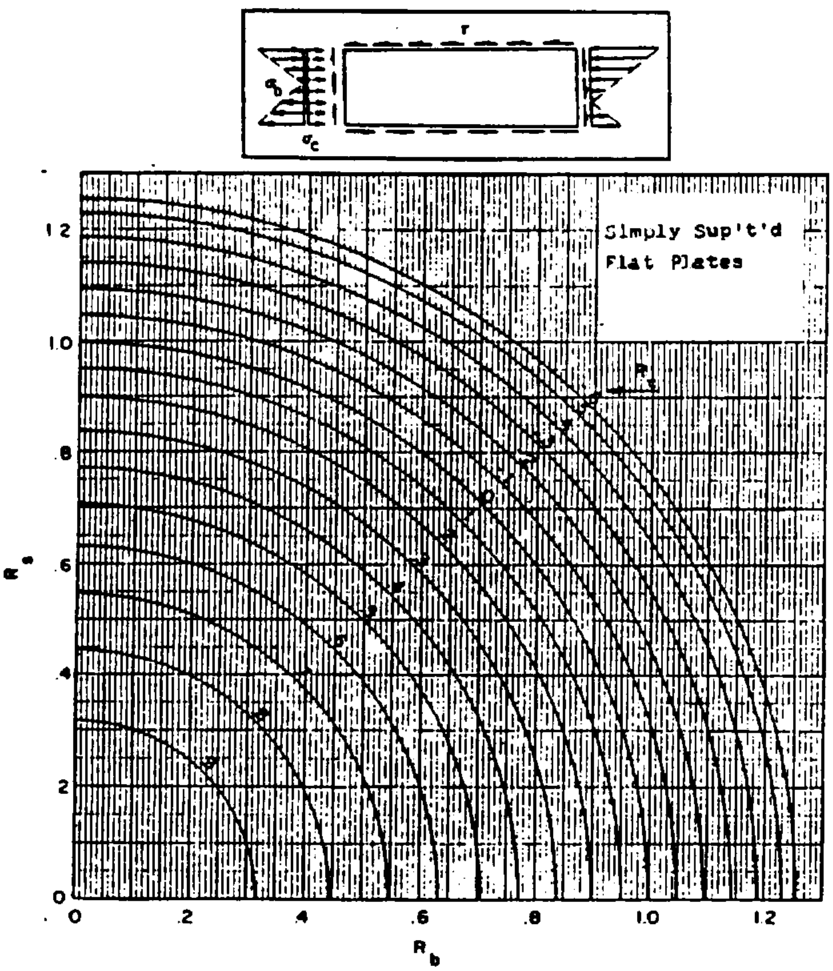

Combined Bending, Shear, and Compression or Tension

Fig. 6.2.12-1

6.3.0 Buckling of Parallelogram Shaped Plates

6.3.1 Flat Parallelogram Shaped Plates

This section contains the buckling coefficients for a few of the commonly used parallelogram shaped plates (Skewed Plates). This type of plate often occurs in swept-wing plan forms and offers some advantages over rectangular plates.

A. One Load Acting - Simply Supported

Buckling coefficients for simply supported parallelogram shaped panels are presented in Fig. 6.3.1.1. The data for these curves are based on the assumption that the supporting members are rigid enough to prevent deflection of the edges normal to the plane of the sheet but offer no restraint to rotation. The curves show that the stability of a flat continuous sheet is definitely increased if the sheet is divided by supporting members into skewed panels.

Procedure

1. Calculate the a/b ratio from the plate dimensions and the sketches on the appropriate figure.
2. Select the curve for the skew angle involved, and determine the buckling coefficient, k_x or k_y.
3. Solve for the critical buckling stress, σ_{cr}, using the buckling coefficient obtained above and the following equation

$$\sigma_{cr} = \frac{k \pi^2 \eta E}{12(1-\mu^2)} \left(\frac{t}{b}\right)^2 \quad \ldots\ldots\ldots \quad (1)$$

4. If the critical buckling stress is above the proportional limit, use the method of article 6.1.2.

B. One Load Acting - Clamped Edges

Fig. 6.3.1.2(a) gives the buckling coefficients for skewed plates with clamped edges under uniform compressive loading acting parallel to a set of sides, for various aspect ratios and skew angles "Ø."

Procedure

Use the procedure presented above for simply supported edges.

C. Two Loads Acting - Simply Supported

The interaction curves for simply supported skewed panels under combined compression in the "x" and "y" directions are presented in Fig. 6.3.1.2(b). This interaction curve is for an array of equal-sided panels with various skew angles. This implies that "b" must equal to the quantity (a cosØ).

Procedure

Use the procedure presented in article 6.1.5 (Two Loads Acting).

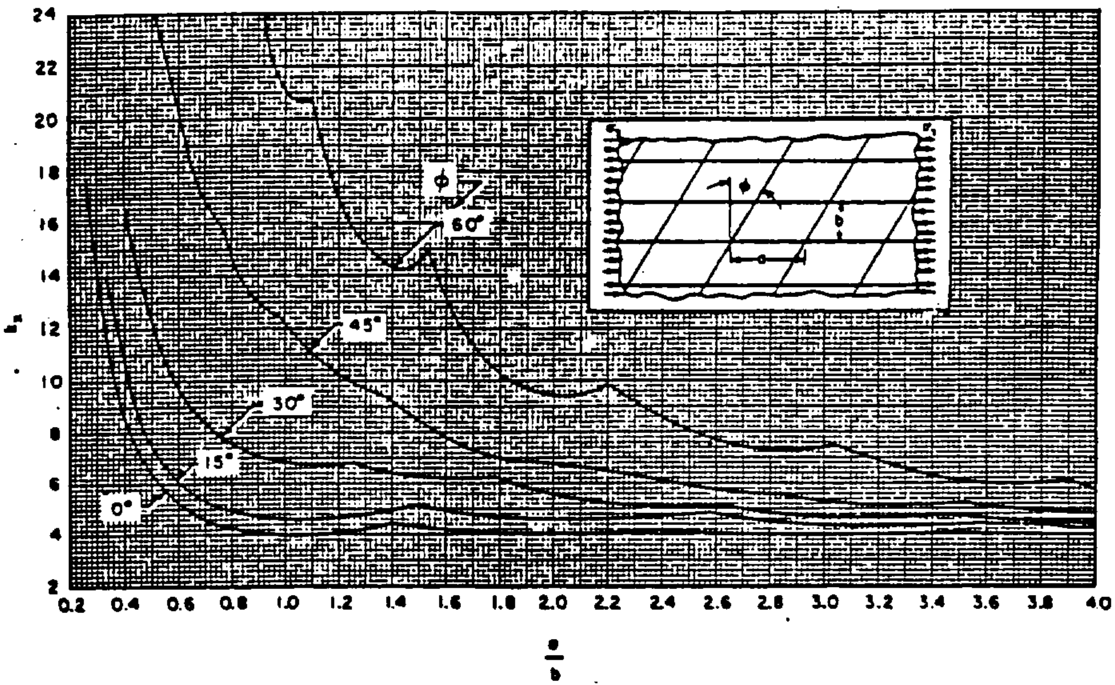

(a) Load Parallel to a Set of Sides

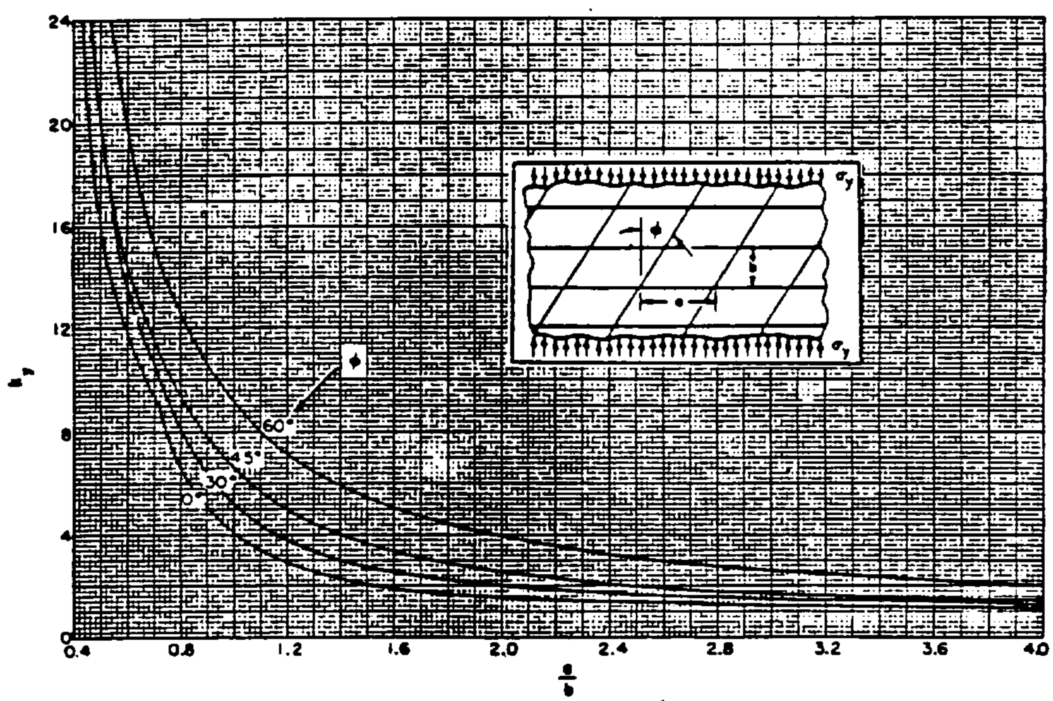

(b) Load Perpendicular to a Set of Sides

Buckling Coefficients for Simply Supported
Parallelograms Shaped Panels

Fig. 6.3.1.1

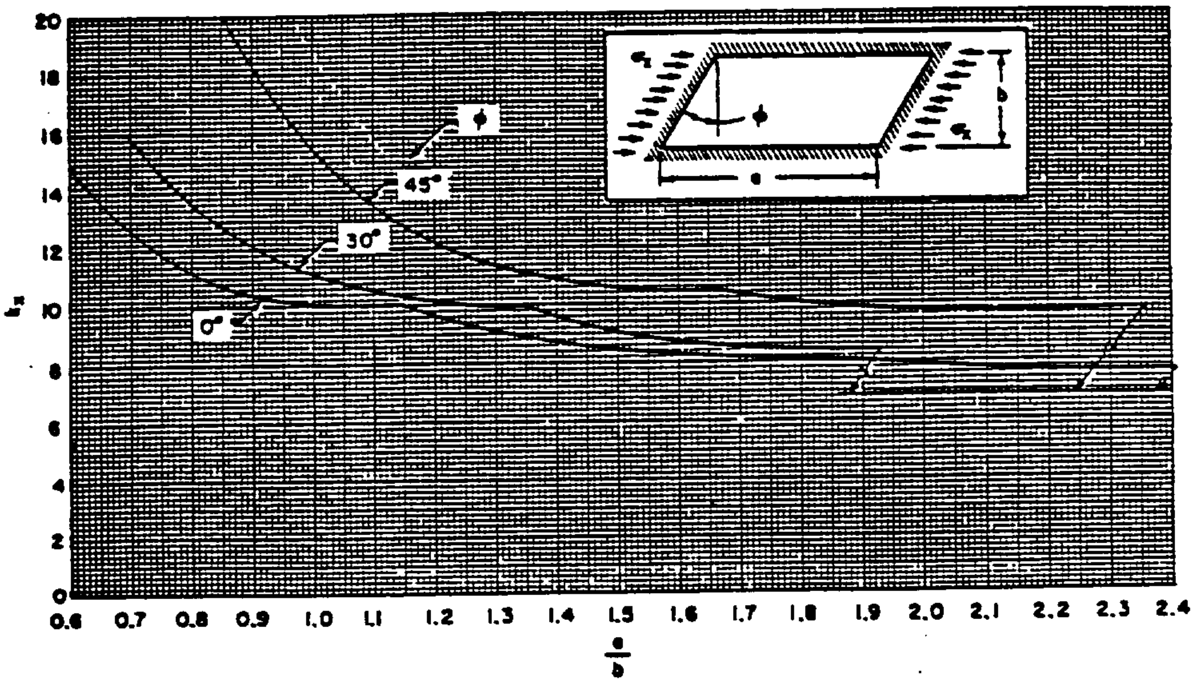

(a) Buckling Coefficients for Parallelogram Shaped Panels With Clamped Edges Load Acting Parallel to a Set of Sides

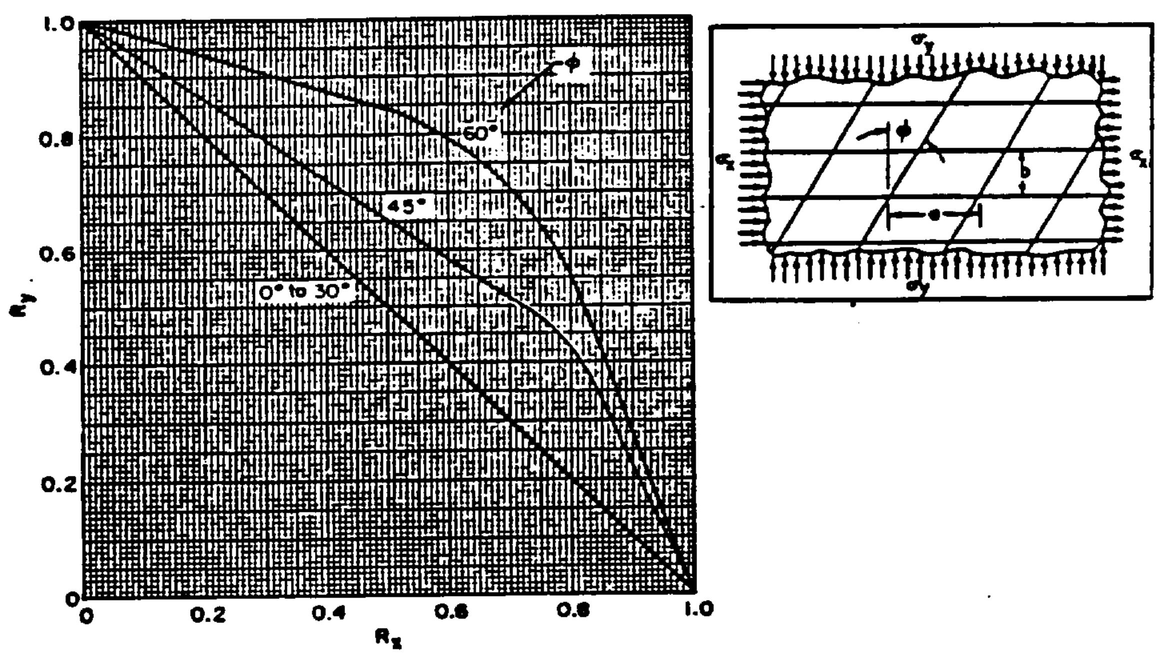

(b) Interaction Curve for Simply Supported Equal-Sided Parallelogram Shaped Panels Under Uniform Biaxial Compression.

Fig. 6.3.1.2

6.0.0	PLATES
6.1.0	Timoshenko, S., Theory of Elastic Stability, McGraw-Hill, New York, 1936
6.2.1	Perry, D. J., Aircraft Structures, McGraw-Hill, New York, 1949 Gerard, G. and Becker, H., N.A.C.A. TN-3781, Buckling of Flat Plates, 1957
6.2.3	Gerard, G. and Becker, H., N.A.C.A. TN-3781, Buckling of Flat Plates, 1957 Timoshenko, S., and Goodier, J. N., Theory of Elasticity, McGraw-Hill, New York, Sec. Ed. 1951.
6.2.4	Batdorf, S. and Houbolt, J., N.A.C.A. TN-847, Critical Combination of Shear and Transverse Direct Stress for an Infinitely Long Flat Plate With Edges Elastically Restrained Against Rotation, 1946. Batdorf, S. and Stein, M., N.A.C.A. TN-1223, Critical Combination of Shear and Direct Stress for Simply Supported Rectangular Flat Plates, 1947. Peters, R. W., N.A.C.A. TN-1750, Buckling Tests of Flat Rectangular Plates Under Combined Shear and Longitudinal Compression, 1948. Stowell, E. Z., Plastic Buckling of a Long Flat Plate Under Combined Shear and Longitudinal Compression, 1949.
6.2.5	Libove, C. and Stein, M., N.A.C.A. ARR L6A05, Charts for Critical Combinations of Longitudinal and Transverse Direct Stress for Flat Rectangular Plates, 1946.
6.2.6	Johnson, J. H., Critical Buckling Stress of Simply Supported Flat Rectangular Plates Under Combined Longitudinal Compression, Transverse Compression, and Shear, Journal of the Aeronautical Sciences, Vol. 21, No. 6, 1954.
6.2.7	Timoshenko, S., Theory of Elastic Stability, McGraw-Hill, 1936 Bleich, F., Buckling Strength of Metal Structures, McGraw-Hill, 1952.
6.2.8	Schuette, E. and McCullock, N., N.A.C.A. TN-1323, Charts for the Minimum Weight Design of Multiweb Wings in Bending, 1947.
6.2.9	Johnson, A.E. and Buchert, K. P., N.A.C.A. TN-2536, Critical Combination of Bending, Shear, and Transverse Compressive Stresses for Buckling of Infinitely Long Flat Plates, 1951
6.2.10 6.2.11	Crossman, N., Elastic Stability of Simply Supported Flat Rectangular Plates Under Critical Combinations of Transverse Compression and Longitudinal Bending, Journal of the Aero. Sciences, Vol. 16, 1949
6.2.12	Stowell, E. and Swartz, E., N.A.C.A. ARR3K13, Critical Stress for an Infinitely Long Flat Plate With Elastically Restrained Edges Under Combined Shear and Direct Stress, 1943
6.3.0	Anderson, R. A., N.A.C.A. TN-2392, Charts Giving Critical Compressive Stress of Continuous Flat Sheet Divided into Parallelogram - Shaped Panels, 1951 Wittrick, W. H., Buckling of Oblique Plates With Clamped Edges Under Uniform Compression, The Aero-Quarterly, Vol. IV, Part II, 1953.
General	Bell Aircraft Corporation, Structures Manual (Krivetsky, Alexander).

Data Source, Section 1.3 Reference 5

2.2 CURVED PLATES.

Design information is presented in this section for the prediction of buckling in plates of single curvature which are both stiffened and unstiffened.

2.2.1 UNSTIFFENED CURVED PLATES.

2.2.1.1 Compression Buckling.

The behavior of curved plates uniformly compressed along their curved edges is similar in many respects to that of a circular cylinder under axial compression (e.g., both buckle at stresses considerably below the predictions of small deflection theory, and it is necessary to resort to semi-empirical methods to show agreement with the available test results).

It is recommended that the methods for predicting buckling of axially compressed monocoque cylinders (Section 10.1) be used to predict buckling of curved plates.

2.2.1.2 Shear Buckling.

Critical shear buckling stresses for curved plates are calculated by the following formula:

$$F_{s_{cr}} \doteq \frac{k_s \eta \pi^2 E}{12(1-\nu_e^2)} \left(\frac{t}{b}\right)^2 \qquad (39)$$

where k is determined from Fig. C2-68, and $\eta = \sqrt{E_T/E}$.

2.2.2 STIFFENED CURVED PLATES IN COMPRESSION.

Information is presented in the following paragraphs for stiffened plates of single curvature in compression where the stiffening members are either axial or circumferential. In these considerations, both the local and general modes of instability must be considered.

2.2.2.1 Curved Plates With Axial Stiffeners.

A method for predicting buckling of simply supported curved plates with a single central axial stiffener has been developed in Reference 29. This method is similar to that presented in Paragraph 2.1.2.1 for stiffened flat plates in compression, in that the same basic equation is used in conjunction with specified buckling coefficients. However, in the present case, the buckling coefficients for the local and the general modes of instability are shown on the same chart. Figures C2-69a through C2-69d present these coefficients, which may be used with the following equation to predict buckling when $Z_b \leq 0.25$:

$$F_{c_{cr}} = \frac{k_c \pi^2 E}{12(1 - \nu_e^2)} \left(\frac{t}{b}\right)^2 \tag{40}$$

This equation may also be written as

$$F_{c_{cr}} = \frac{k_c \pi^2 E}{12\sqrt{1 - \nu_e^2}\; Z_b \left(\frac{R}{t}\right)} \tag{41}$$

where Z_b is the plate curvature parameter, $\frac{b^2}{Rt}\sqrt{1-\nu_e^2}$; R is the plate radius of curvature; and b is the half-width of the loaded (curved) edge of plate.

Figures C2-69a through C2-69d yield buckling coefficients as a function of Z_b, A/bt, and EI_s/bD for values of the ratio a/b equal to 4/3, 2, 3, and 4, respectively, where terms are defined as follows:

I_s bending moment of inertia of the stiffener cross section taken about the stiffener centroidal axis

D flexural stiffness of the plate per inch of width, $Et^3/12(1-\nu_e^2)$

a length of plate

The sloping portions of the curves to the left in each of the charts of Figs. C2-69a through C2-69d represent designs wherein the general mode of instability is critical. Local instability is represented by the horizontal lines to the right in each chart. The intersection of these curves represents efficient design, since less moment-of-inertia in the stiffener induces general instability and a lowering of the buckling stress, while more moment-of-inertia in the stiffener has no effect on the buckling stress of the stiffened plate.

Although not specifically shown in Fig. C2-69a through C2-69d, the increase in the curved-plate buckling stress, due to the addition of a central axial stiffener, is negligible when $Z_b > 2.5$. Thus, plates with a

large degree of curvature are not benefited by stiffening with a central axial member. In this case, buckling stress should be determined by the techniques in Section C3. 1. 1.

Also, the methods cited above should not be applied with two or more axial stiffeners, since the stiffener geometrical requirements needed to satisfy the general mode of instability are sensitive to the number of stiffeners when the number is small. With multiple stiffeners, the methods described for orthotropic cylinders in Section C3. 1. 2 should be used.

2\. 2. 2. 2 Curved Plates With Circumferential Stiffeners.

Curved plates stiffened with a single central circumferential stiffener have been considered by Batdorf and Schildcrout [30]. They determined analytically that the addition of a single central circumferential stiffener increases the buckling stress of a curved plate but only within a rather restricted range of plate geometries. This range is a function of both the ratio a/b (where a is the half-length of the plate, b is the width of the curved, loaded edge) and the geometric parameter Z_b. For the buckling stress of the curved plate to increase with the addition of a single central circumferential stiffener, a/b must be 0.6 or less. The parameter Z_b imposes further restrictions as a function of a/b which are shown in Fig. C2-70. For a given value of a/b, Z_b for the design must be equal to or smaller than that value read from the chart. If Z_b for the design is larger than the value read from the chart, no gain in the buckling stress results from the addition of the stiffener to the curved plate.

Small deflection theory was used in Reference 30 to predict the buckling stress of curved plates with circumferential stiffeners. Consequently, the results are presented in terms of a gain factor which indicates the gain in buckling stress for a stiffened curved plate over an unstiffened curved plate, where the gain is based on theoretical predictions of the buckling stress for both configurations. The information presented here, therefore, may be applied by multiplying the gain factor by the buckling stress for an unstiffened curved plate of the same overall dimensions by methods given in Paragraph 2.2.1.1.

Maximum gain factors are presented as a function of a/b and Z_b in Fig. C2-71. The term "maximum" implies that the stiffener has sufficient bending rigidity to enforce a buckle node at the stiffener line.

The required stiffener bending rigidity needed to enforce a buckle node at the stiffener line is defined in Fig. C2-72 when the figure is entered with a maximum gain factor obtained from Fig. C2-71.

Figure C2-72 may also be used to determine gain factors when an existing stiffener has either more or less bending rigidity than that required to enforce a node along the stiffener line. In this case, the same geometrical limitations stipulated in Fig. C2-70 apply and must be observed. (Note that the gain factors obtained here may not be maximum; therefore, the ordinate of Fig. C2-72 is labeled to take this possibility into account.)

After first referring to Fig. C2-70 to ascertain whether or not a gain is indeed possible, find the gain factor (from Fig. C2-72) based on the properties of the existing stiffener. Now plot this gain factor on Fig. C2-71. If the point is below and to the left of the a/b curve to which it relates, then the gain factor is less than the maximum permissible and the bending rigidity of the stiffener is less than the minimum required. In this case, general instability of the curved plate represents the critical mode, and buckling may be predicted using the gain factor obtained from Fig. C2-70. When the point is above and to the right of the a/b curve in Fig. C2-71 to which it relates, the contrary is true, and local instability of the curved plate represents the critical mode. In this case, buckling may be predicted using the maximum gain factor obtained from the a/b, Z_b intersection in Fig. C2-71.

The methods of this section should not be applied to curved plates with two or more circumferential stiffeners. The general instability stresses predicted by the design charts are sensitive to the number of stiffeners when their total number is small. In this case, recourse should be had to Section C3. 1. 2.

2. 2. 3 STIFFENED CURVED PLATES IN SHEAR.

Methods are presented in the following paragraphs for predicting the buckling stress of plates of single curvature in shear having a single stiffener in either the axial or circumferential direction. The methods account for both the local and general modes of instability, and charts are

given that present the buckling coefficient k_s versus EI/bD, where at low values of EI/bD the general mode of instability is critical. As EI/bD increases, the local mode of instability becomes critical and is signified by a constant value of k_s. Thus, to enforce a node at the stiffener, the design must have an EI/bD which falls on the horizontal portion of the design curve. Note that the EI/bD value representing the extreme left point of the horizontal line yields the most efficient design; local and general instability are both critical here.

2.2.3.1 Curved Plates With Axial Stiffeners.

The buckling stress for curved plates with a single, central stiffener may be determined from the equation:

$$F_{c_{cr}} = \eta \frac{k_s \pi^2 E}{12(1 - \nu_e^2)} \left(\frac{t}{b}\right)^2 \qquad (42)$$

where k_s is taken from Fig. C2-73, b is the overall dimension of the curved plate, and t is the thickness of the curved plate. Figure C2-73(a) applies when axial length is greater than circumferential width, and Fig. C2-73(b) applies when axial length is less than circumferential width. Note that in both cases, b is denoted the short overall dimension of the plate. Curves are presented as a function of the aspect ratio of the plate, a/b, as well as of the plate curvature parameter, Z_b. Note also that the data of Fig. C2-73 are based on small deflection theory and agree satisfactorily

with experimental results except in the case of cylinders for which a 16 percent reduction is recommended.

The preceding method should not be extended to apply to curved plates with multiple axial stiffeners. The bending rigidity required of each stiffener to support general instability is sensitive to the total number of stiffeners when this number is small.

2.2.3.2 Curved Plates With Circumferential Stiffeners.

The buckling stress for curved plates stiffened circumferentially with a single central stiffener may be determined from equation (42) with the buckling coefficients, k_s, taken from Fig. C2-74. As in Fig. C2-73 for a cylinder, a 16 percent reduction of the horizontal portions of the curves (the portion signifying local instability) is recommended.

The data above should not be applied to curved plates with multiple circumferential stiffeners for the reasons noted previously in Paragraph 2.2.3.1.

2.2.4 CURVED PLATES UNDER COMBINED LOADING.

Interaction relations for longitudinal compression combined with normal pressure, shear combined with normal pressure, and longitudinal compression combined with shear are presented in the following paragraphs for unstiffened, curved plates. Interaction relations for stiffened, curved plates are presently unavailable; however, techniques discussed in Section C3.1.2 may be used. The normal pressure in the first two cases is

applied to the concave face of the curved plate. The interaction relations apply only to elastic stress conditions, since verification of their application to plastic stress conditions is lacking at present.

2.2.4.1 Longitudinal Compression Plus Normal Pressure.

The interaction equation for longitudinal compression plus normal pressure applied to the concave face of an unstiffened curved plate is

$$R_c^2 - R_p = 1 \tag{43}$$

where $R_c = F_c/F_{c_{cr}}$ and $R_p = p/p_{cr}$, where the following definitions apply:

F_c applied longitudinal compression stress

$F_{c_{cr}}$ buckling stress of the curved plate where subjected to simple axial compression, determined by the methods of Section 2.2.1.1

p absolute value of the applied normal pressure

p_{cr} absolute value of the external pressure which would buckle the cylinder of which the plate is a section, determined by the methods of Section C3.1.1.5

Note that absolute values of the quantities p and p_{cr} are substituted into the interaction equation since their difference in sign is already accounted for in the equation. It can be seen that normal pressure applied to the concave face of the unstiffened, curved plate increases the axial compression load which may be carried by the plate prior to buckling.

2.2.4.2 Shear Plus Normal Pressure.

When an unstiffened curved plate is subjected to shear combined with normal pressure acting on the concave face of the plate, the following interaction equation applies:

$$R_s^2 - R_p = 1 \qquad (44)$$

where $R = F_s/F_{s_{cr}}$ (F_s is applied shear stress and $F_{s_{cr}}$ is buckling stress of the curved plate when subjected to simple in-plane shear, determined by the methods of Section 2.2.1.2), and R_p is as previously defined.

2.2.4.3 Longitudinal Compression Plus Shear.

The interaction equation for an unstiffened curved plate subjected to longitudinal compression and shear is

$$R_c + R_s^2 = 1 \qquad (45)$$

where R_c and R_s are as defined in previous paragraphs. This relationship represents approximately an average curve through the available experimental results while the lower bound of the test results may be represented by a linear relation between R_c and R_s.

$$F_{s_{cr}} = \frac{k_s \pi^2 E}{12(1-\nu_e^2)} (t/b)^2 \qquad Z_b = b^2/rt \ (1-\nu_e^2)^{1/2}$$

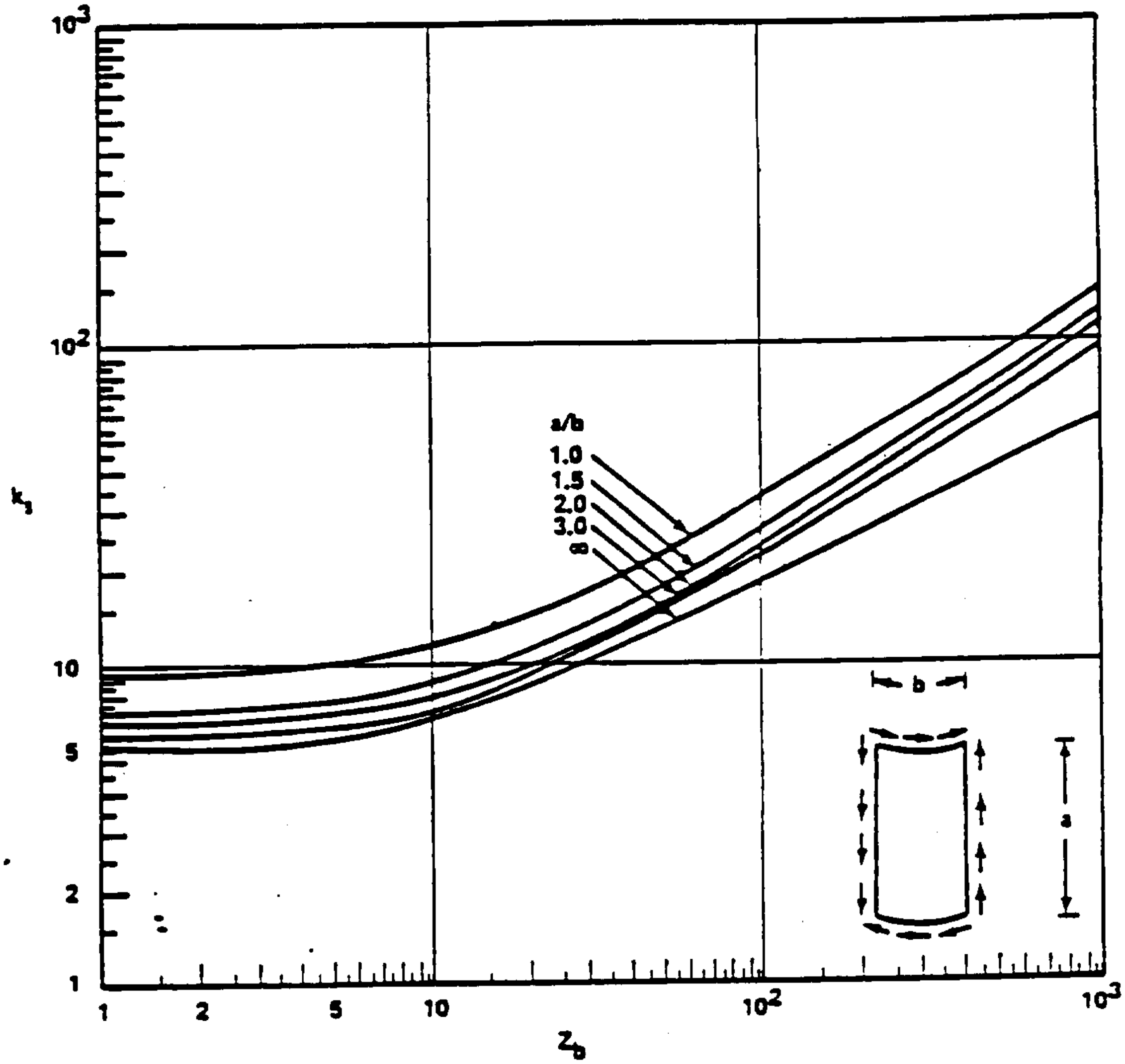

(a) LONG SIMPLY SUPPORTED PLATES

FIGURE C2-68. SHEAR BUCKLING COEFFICIENTS FOR VARIOUS CURVED PLATES

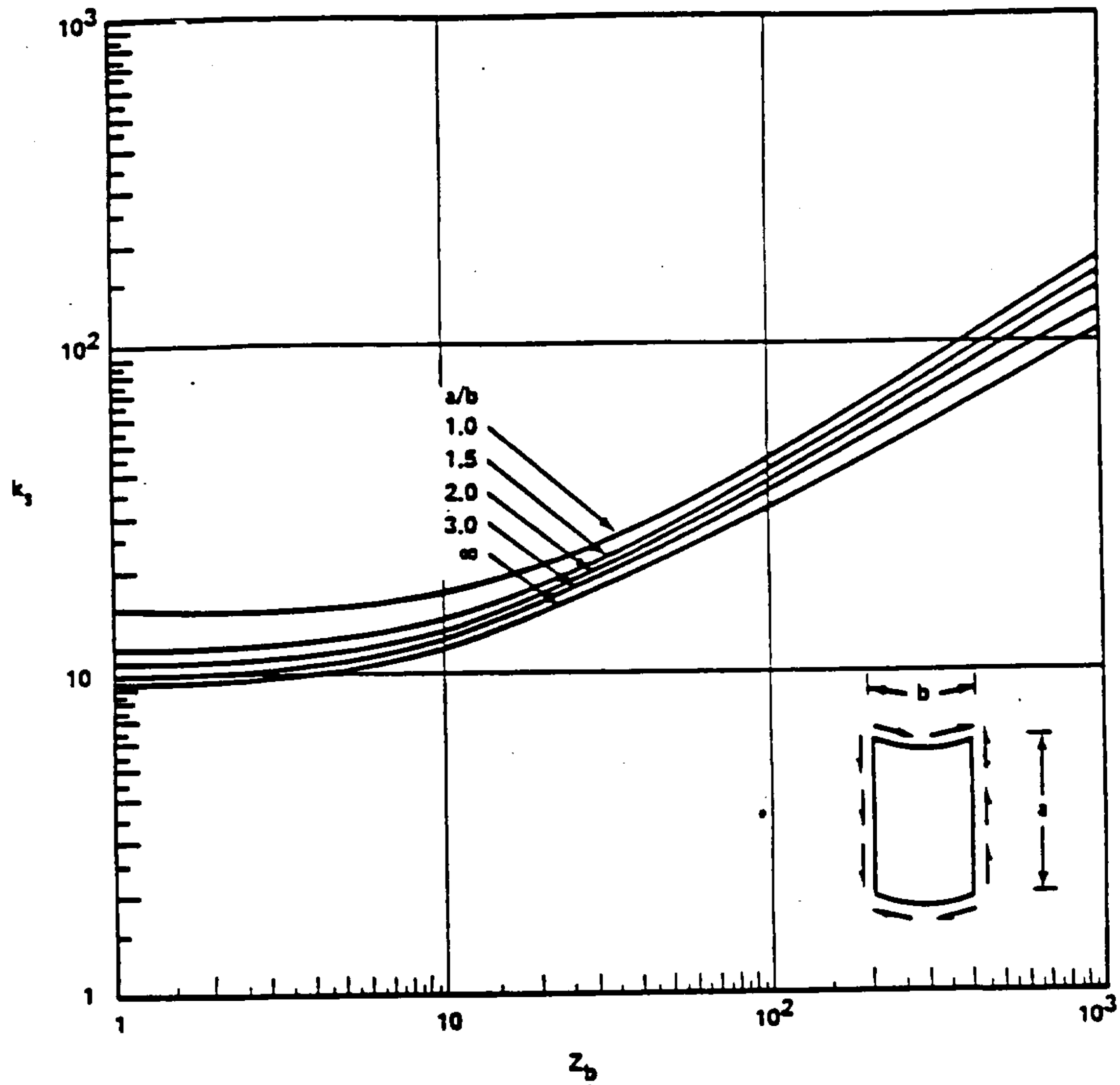

(b) LONG CLAMPED PLATES

FIGURE C2-68. (Continued)

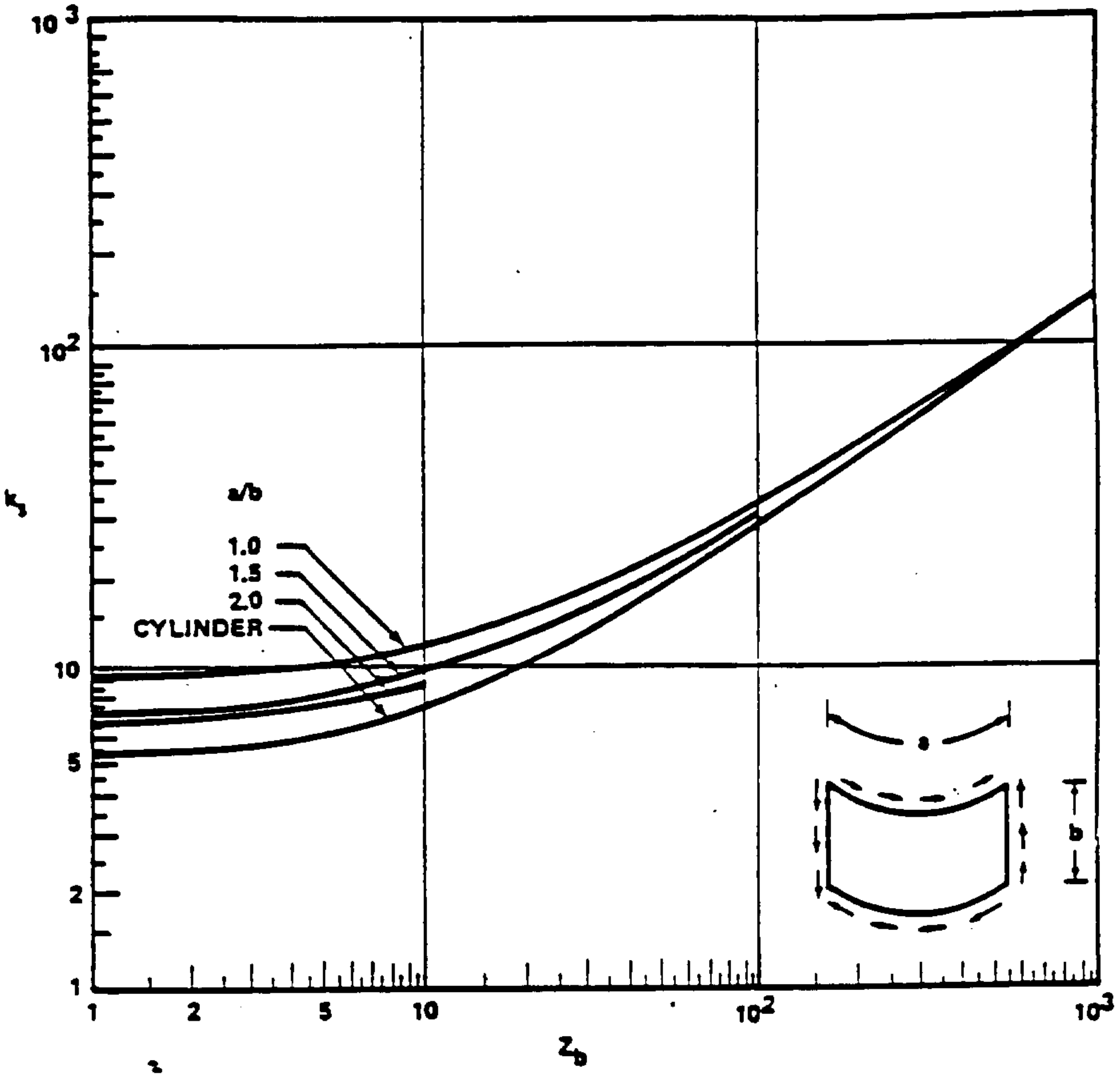

(c) WIDE, SIMPLY SUPPORTED PLATES

FIGURE C2-68. (Continued)

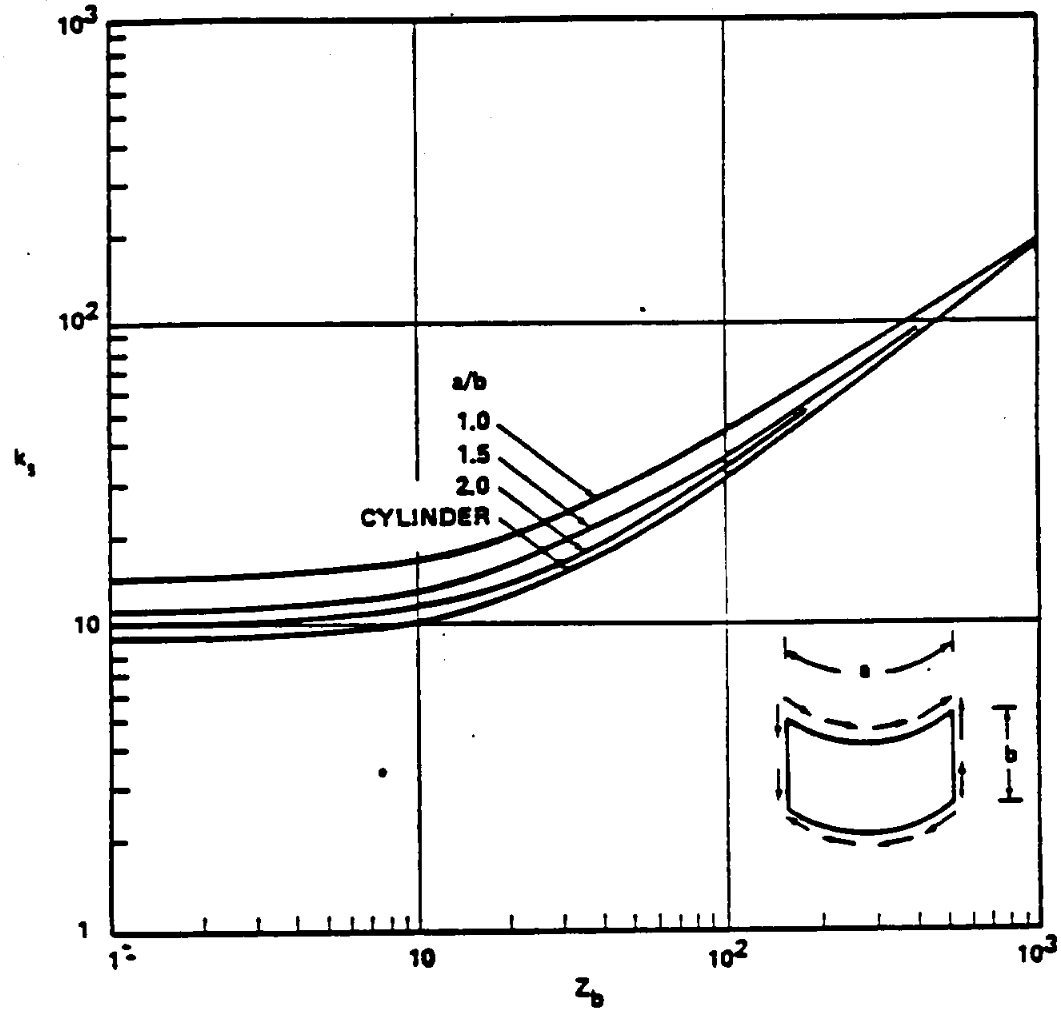

(d) WIDE CLAMPED PLATES

FIGURE C2-68. (Concluded)

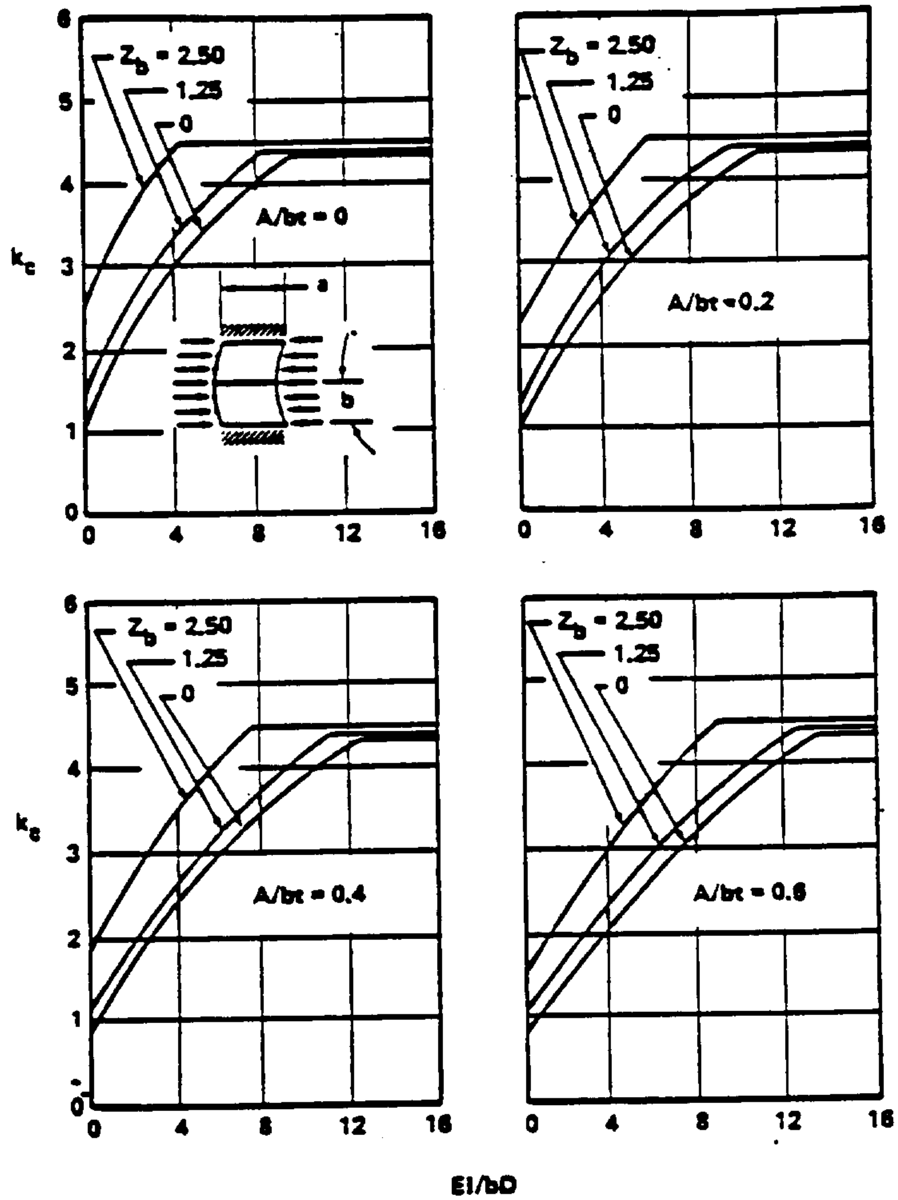

(a) a/b = 4/3

FIGURE C2-69. COMPRESSIVE-BUCKLING COEFFICIENTS FOR SIMPLY SUPPORTED CURVED PLATES WITH CENTER AXIAL STIFFENER

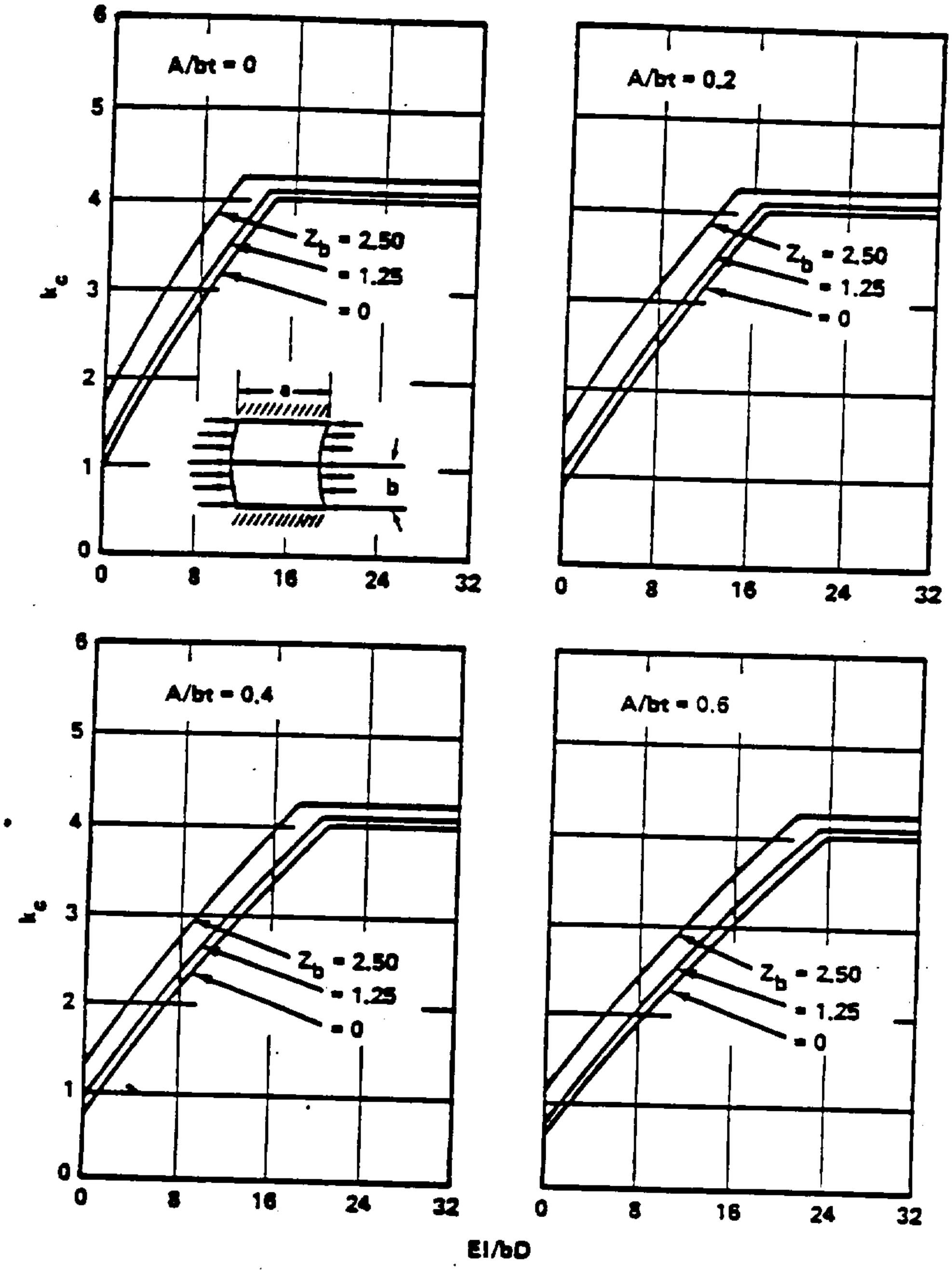

(b) a/b = 2

FIGURED C2-69. (Continued)

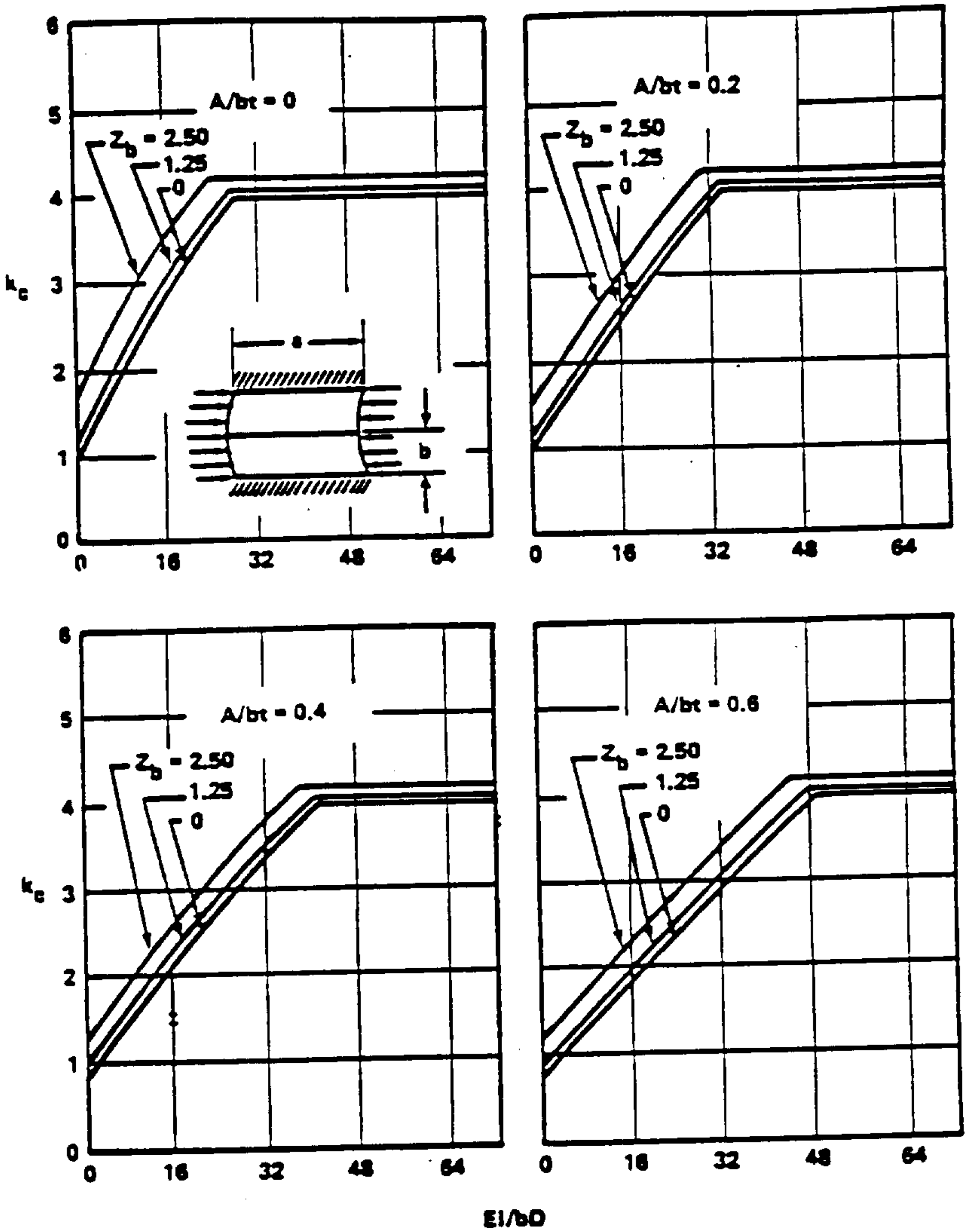

(c) a/b = 3

FIGURE C2-69. (Continued)

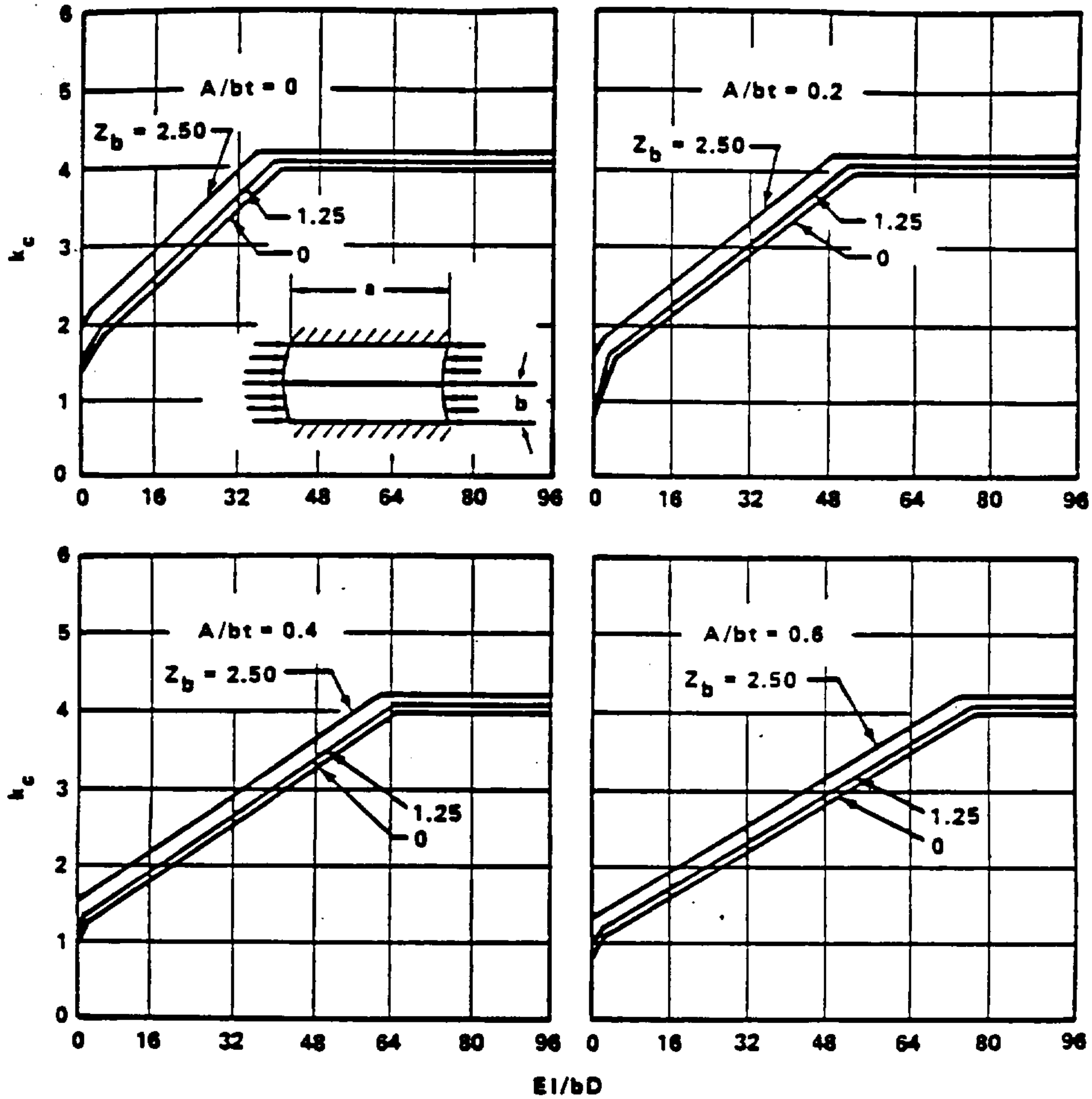

(d) a/b = 4

FIGURE C2-69. (Concluded)

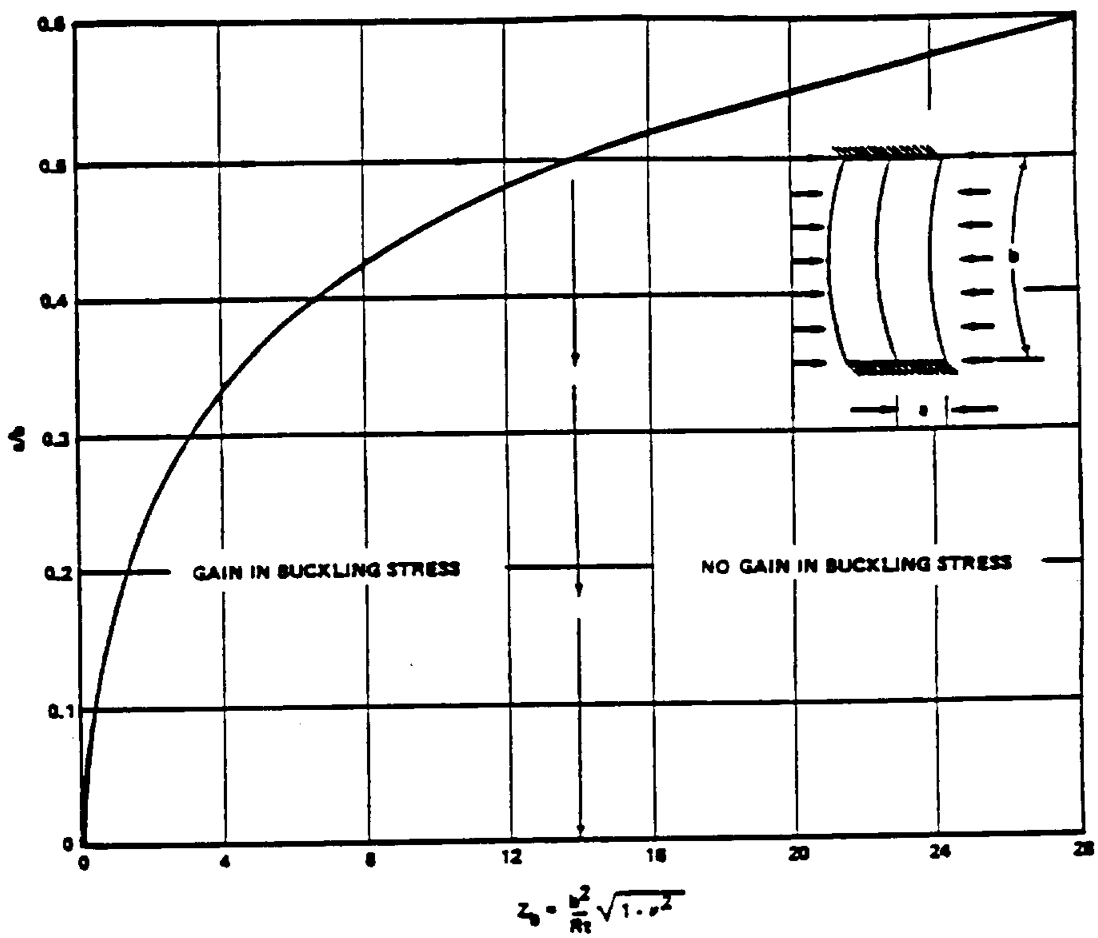

FIGURE C2-70. DEFINITION OF a/b VS Z_b RELATIONSHIP FOR GAIN IN BUCKLING STRESS OF AXIALLY COMPRESSED CURVED PLATES DUE TO ADDITION OF SINGLE CENTRAL CIRCUMFERENTIAL STIFFENER

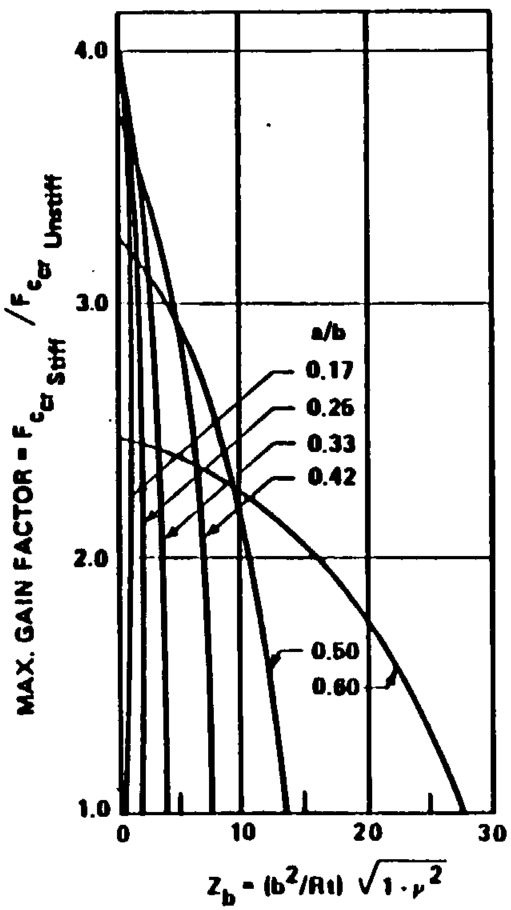

FIGURE C2-71. MAXIMUM GAIN FACTORS FOR SIMPLY SUPPORTED CURVED PLATES WITH A SINGLE, CENTRAL, CIRCUMFERENTIAL STIFFENER

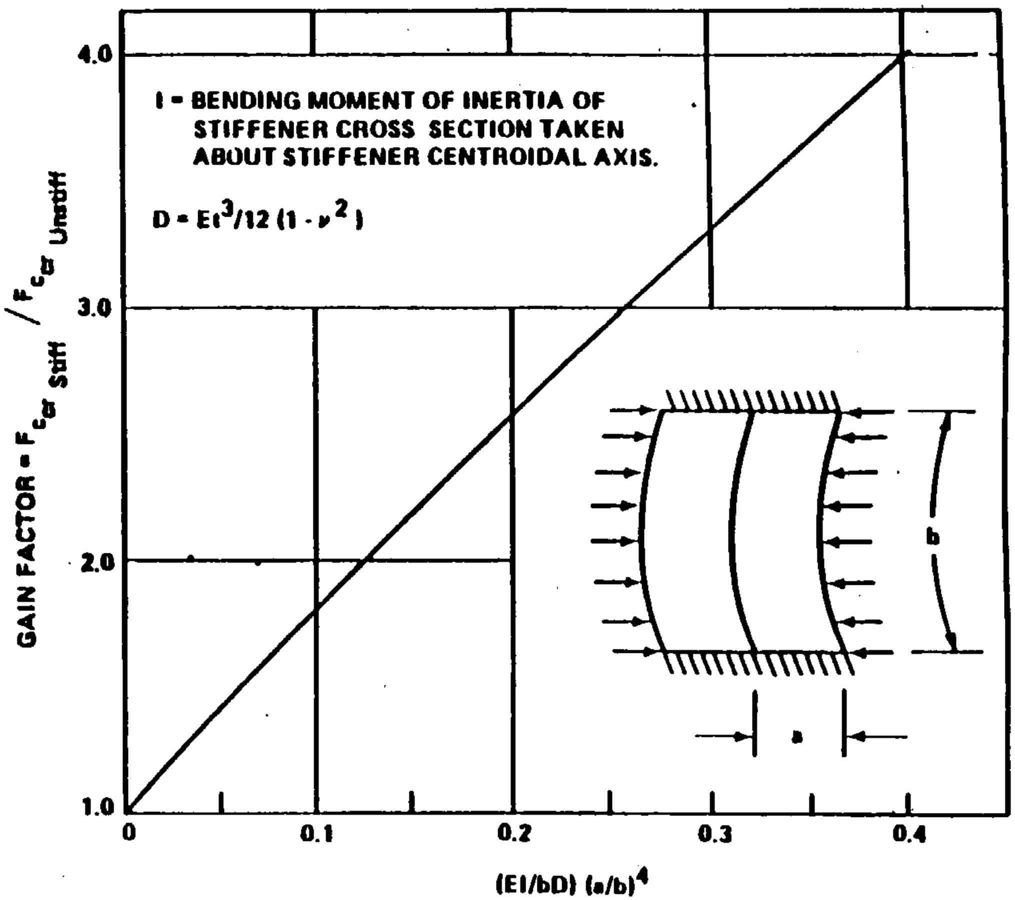

FIGURE C2-72. STIFFNESS REQUIREMENTS AS A FUNCTION OF GAIN FACTOR FOR SIMPLY SUPPORTED CURVED PLATES WITH A SINGLE CENTRAL CIRCUMFERENTIAL STIFFENER

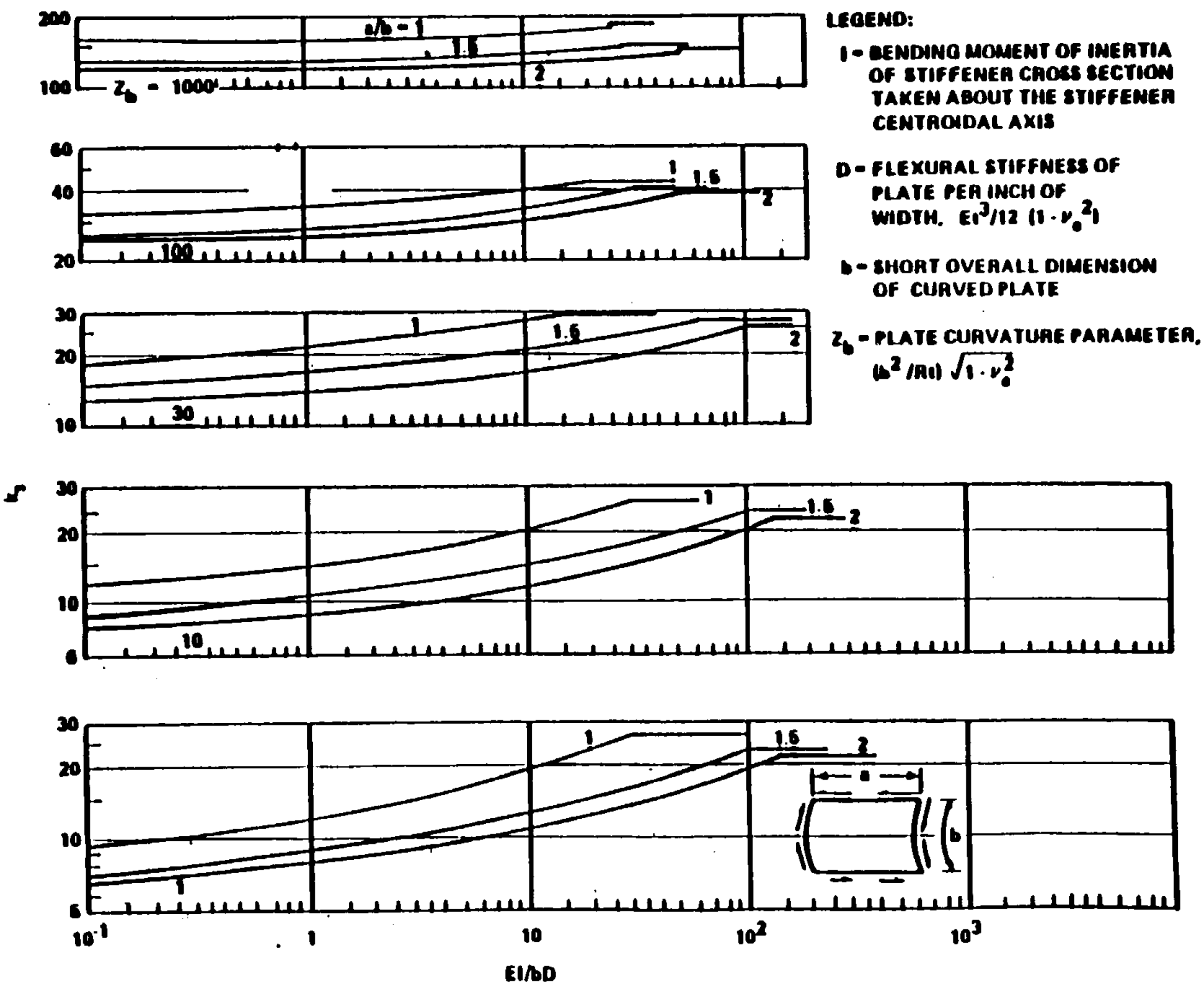

FIGURE C2-73a. SHEAR BUCKLING COEFFICIENTS FOR SIMPLY SUPPORTED CURVED PLATES WITH CENTER AXIAL STIFFENER, AXIAL LENGTH GREATER THAN CIRCUMFERENTIAL WIDTH

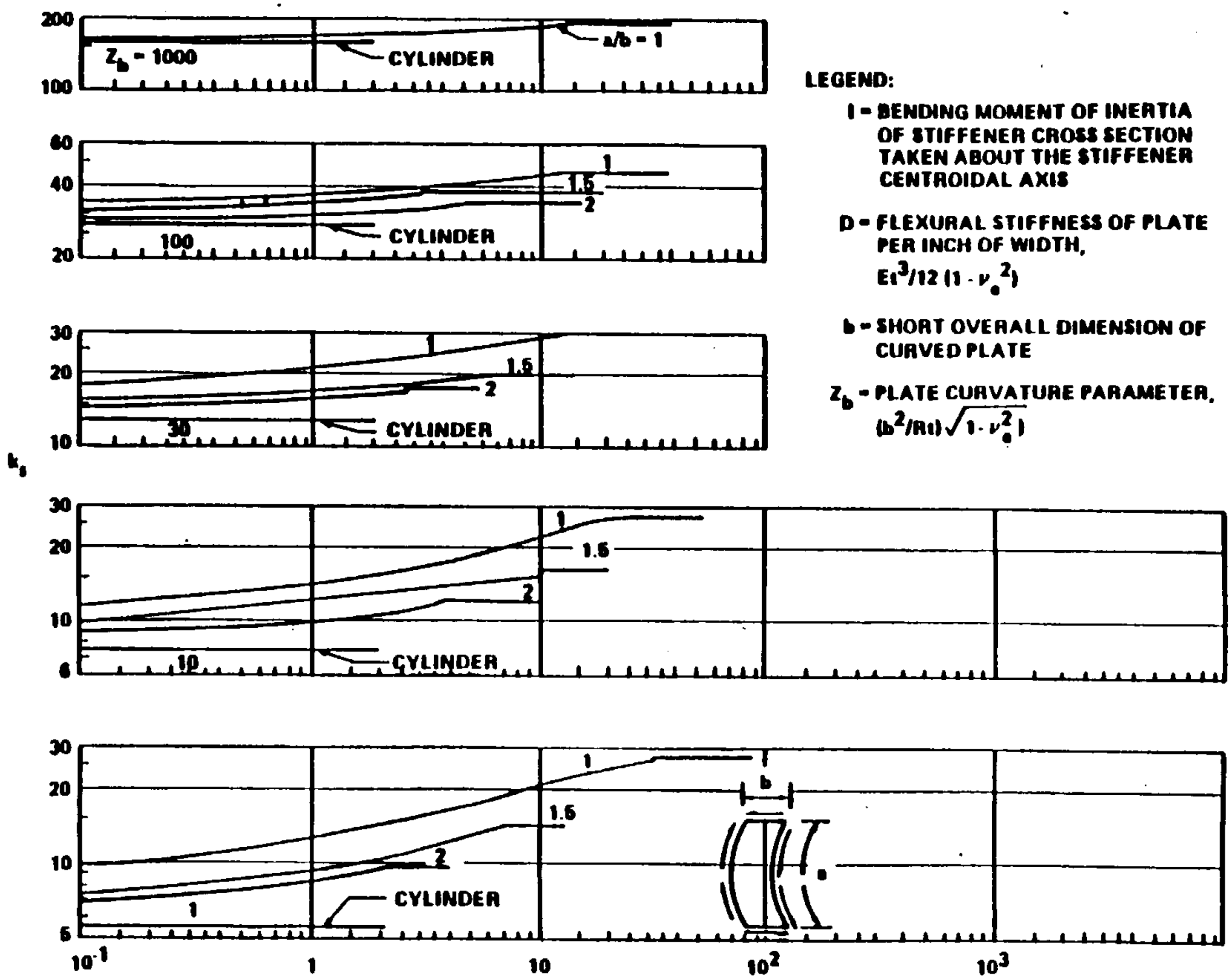

FIGURE C2-73b. SHEAR BUCKLING COEFFICIENTS FOR SIMPLY SUPPORTED CURVED PLATES WITH CENTER AXIAL STIFFENER, AXIAL LENGTH LESS THAN CIRCUMFERENTIAL WIDTH

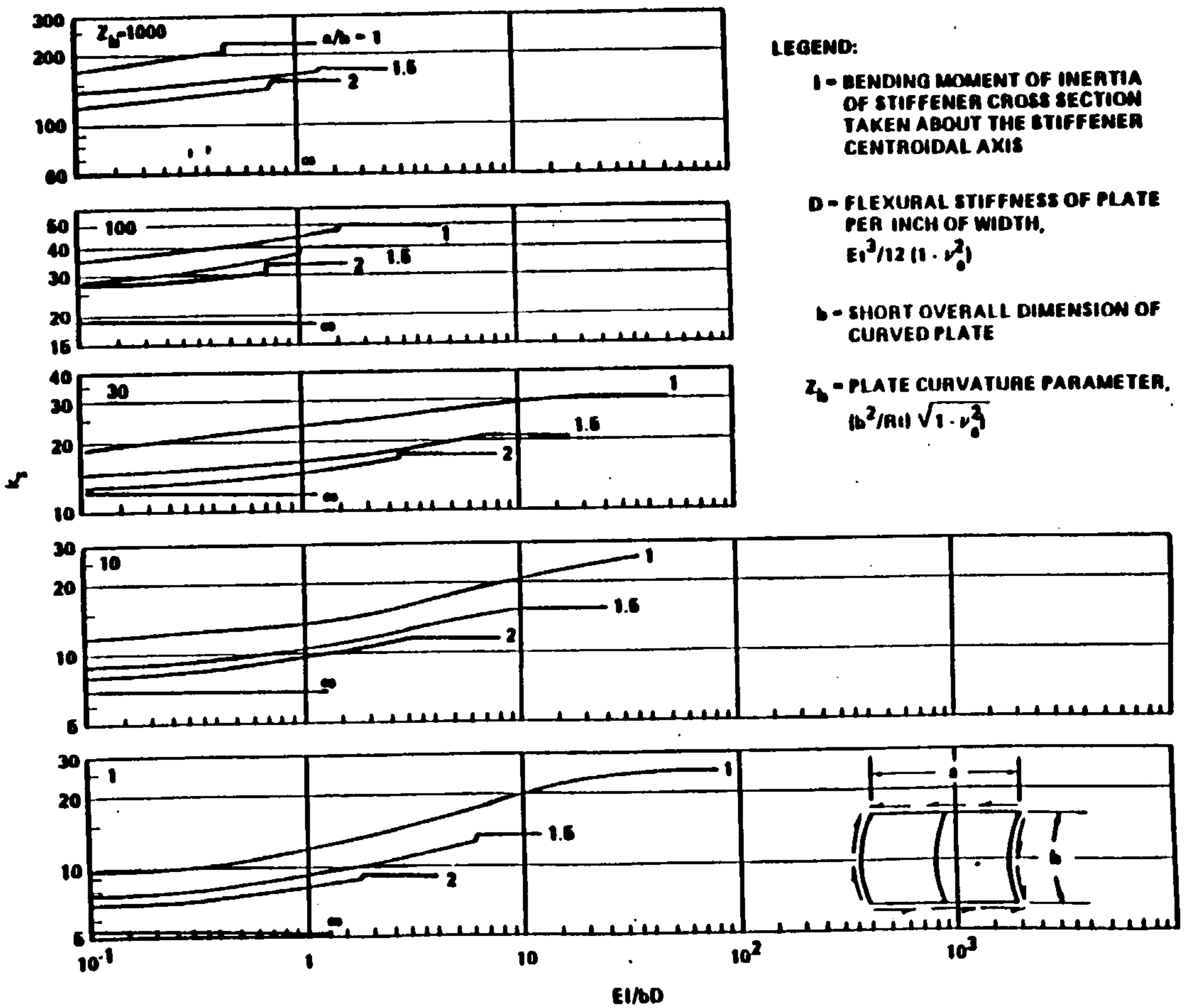

FIGURE C2-74a. SHEAR BUCKLING COEFFICIENTS FOR SIMPLY SUPPORTED CURVED PLATES WITH CENTER CIRCUMFERENTIAL STIFFENER, AXIAL LENGTH GREATER THAN CIRCUMFERENTIAL WIDTH

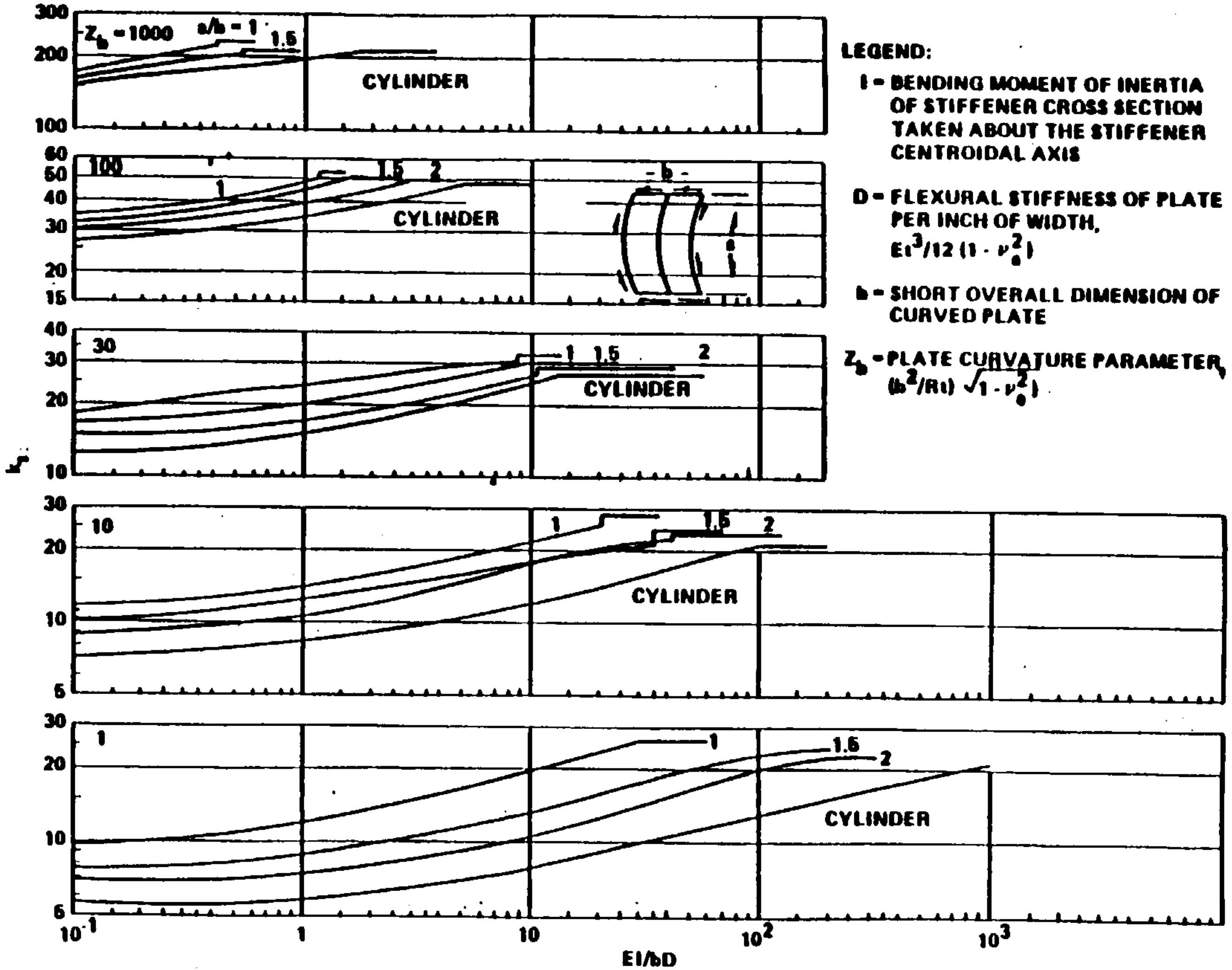

FIGURE C2-74b. SHEAR BUCKLING COEFFICIENTS FOR SIMPLY SUPPORTED CURVED PLATES WITH CENTER CIRCUMFERENTIAL STIFFENER, AXIAL LENGTH LESS THAN CIRCUMFERENTIAL WIDTH

B9 PLATES

B9.1 INTRODUCTION

Plate analysis is important in aerospace applications for both lateral applied loads and also for sheet buckling problems. The plate can be considered as a two-dimensional counterpart of the beam except that the plate bends in all planes normal to the plate, whereas the beam bends in one plane only.

Because of the varied behavior of plates, they have been classified into four types, as follows:

Thick Plates — Thick plate theory considers the stress analysis of plates as a three-dimensional elasticity problem. The analysis becomes, consequently, quite involved and the problem is completely solved only for a few particular cases. In thick plates, shearing stresses become important, similar to short, deep beams.

Medium-Thick Plates — In medium-thick plates, the lateral load is supported entirely by bending stresses. Also, the deflections, w, of the plate are small compared to its thickness, t, ($w < t/3$). Theory is developed by making the following assumptions:

1. There is no in-plane deformation in the middle plane of the plate.
2. Points of the plate lying initially on a normal-to-the-middle plane of the plate remain on the normal-to-the-middle surface of the plate after bending.
3. The normal stresses in the direction transverse to the plate can be disregarded.

Thin Plates — The thin plate supports the applied load by both bending and direct tension accompanying the stretching of the middle plane. The deflections of the plate are not small compared to the thickness ($1/3t < w < 10t$) and bending of the plate is accompanied by strain in the middle surface. These supplementary tensile stresses act in opposition to the given lateral load and the given load is now transmitted partly by the flexural rigidity and partly by a membrane action of the plate. Thus, nonlinear equations can be obtained and the solution of the problem becomes much more complicated. In the case of large deflections, one must distinguish between immovable edges and edges free to move in the plane of the plate, which may have a considerable bearing upon the magnitude of deflections and stresses in the plate.

Membranes — For membranes, the resistance to lateral load depends exclusively on the stretching of the middle plane and, hence, bending action is not present. Very large deflections would occur in a membrane ($w > 10t$).

In the literature on plates, the greatest amount of information is available on medium-thick plates. Many solutions have been obtained for plates of various shapes with different loading and boundary conditions [1, 2]. However, in the aerospace industry, thin plates are the type most frequently encountered. Some approximate methods of analysis are available for thin plates for common shapes and loads.

Figure B9-1 shows the differential element of an initially flat plate acted upon by bending moments (per unit length) M_x, and M_y about axes parallel to the y and x directions, respectively. Sets of twisting couples $M_{xy} (= -M_{yx})$ also act on the element.

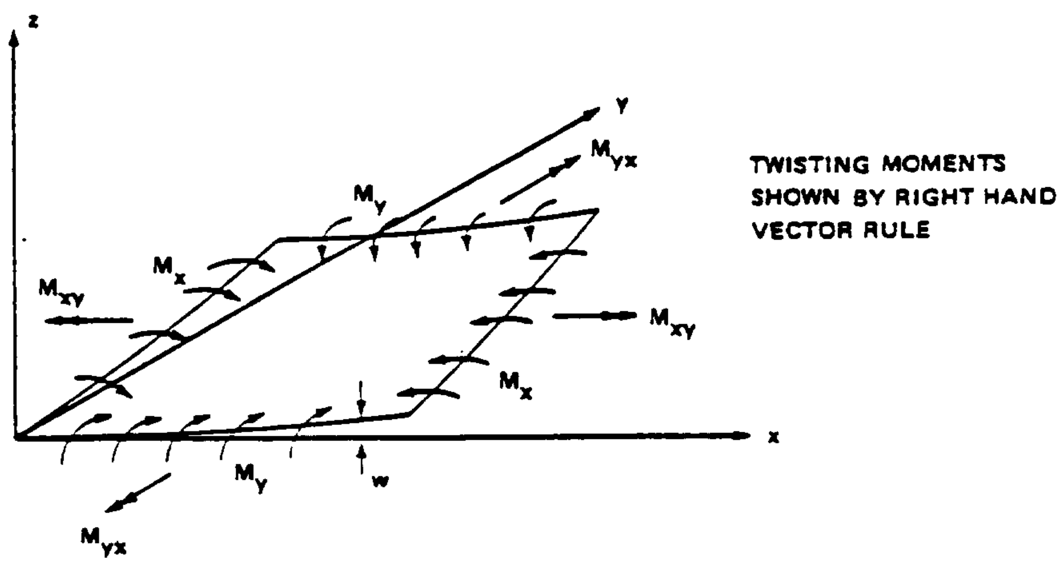

FIGURE B9-1. DIFFERENTIAL PLATE ELEMENT

Figure B9-2 shows the same plate elements as the one in Fig. B9-1, but with the addition of internal shear forces Q_x and Q_y (corresponding to the "v" of beam theory) and a distributed transverse pressure load q(psi). With the presence of these shears, the bending and twisting moments now vary along the plate as indicated in Fig. B9-2a.

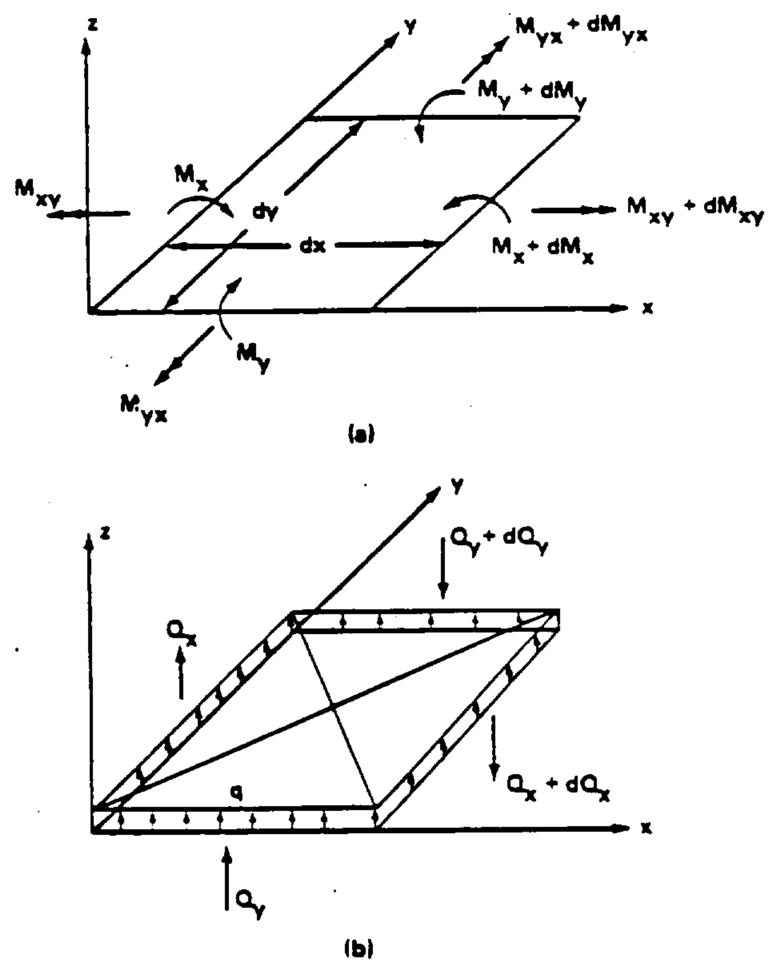

FIGURE B9-2. DIFFERENTIAL PLATE ELEMENT WITH LATERAL LOAD

Table B9-1. Tabulation of Plate Equations

Class	Item	Plate Theory	Beam Theory
Geometry	Coordinates	$x \quad y$	x
	Deflections	w	y
	Distortions	$\frac{\partial^2 w}{\partial x^2}, \frac{\partial^2 w}{\partial y^2}, \frac{\partial^2 w}{\partial x \partial y}$	$\frac{d^2 v}{dx^2}$
Structural Characteristic	Bending Stiffness	$D = \frac{Et^3}{12(1-\mu^2)}$	EI
Loadings	Couples	M_x, M_y, M_{xy}	M
	Shears	Q_x, Q_y	V
	Lateral	q	q or w
Hooke's Law	Moment	$M_x = D\left(\frac{\partial^2 w}{\partial x^2} + \mu \frac{\partial^2 w}{\partial y^2}\right)$	
	Distortion	$M_y = D\left(\frac{\partial^2 w}{\partial y^2} + \mu \frac{\partial^2 w}{\partial x^2}\right)$	$M = EI\frac{d^2 v}{dx^2}$
	Relation	$M_{xy} = D(1-\mu)\frac{\partial^2 w}{\partial x \partial y}$	
Equilibrium	Moments	$Q_x = \frac{\partial M_x}{\partial x} + \frac{\partial M_{xy}}{\partial y}$ $Q_y = \frac{\partial M_y}{\partial y} + \frac{\partial M_{xy}}{\partial x}$	$V = \frac{dM}{dx}$
	Forces	$q = \frac{\partial Q_x}{\partial x} + \frac{\partial Q_y}{\partial y}$	$q = \frac{dV}{dx}$

Data Source, Section 1.3 Reference 5

B9.3 MEDIUM-THICK PLATES (SMALL DEFLECTION THEORY)

This section includes solutions for stress and deflections for plates of various shapes for different loading and boundary conditions. All solutions in this section are based on small deflection theory.

B9.3.1 Circular Plates

For a circular plate it is naturally convenient to express the governing differential equations in polar coordinate form. The deflection surface of a laterally loaded plate in polar coordinate form is

$$\left(\frac{\partial^2}{\partial r^2} + \frac{1}{r}\frac{\partial}{\partial r} + \frac{1}{r^2}\frac{\partial^2}{\partial \theta^2}\right)\left(\frac{\partial^2 w}{\partial r^2} + \frac{1}{r}\frac{\partial w}{\partial r} + \frac{1}{r^2}\frac{\partial^2 w}{\partial \theta^2}\right) = \frac{q}{D} \quad . \tag{23}$$

If the load is symmetrically distributed with respect to the center of the plate, w is independent of θ and the equation becomes

$$\frac{1}{r}\frac{d}{dr}\left\{r\frac{d}{dr}\left[\frac{1}{r}\frac{d}{dr}\left(r\frac{dw}{dr}\right)\right]\right\} = \frac{q}{D} \tag{24}$$

The bending and twisting moments are

$$M_r = D\left[\frac{\partial^2 w}{\partial r^2} + \mu\left(\frac{1}{r}\frac{\partial w}{\partial r} + \frac{1}{r^2}\frac{\partial^2 w}{\partial \theta^2}\right)\right] \tag{25}$$

$$M_t = D\left(\frac{1}{r}\frac{\partial w}{\partial r} + \frac{1}{r^2}\frac{\partial^2 w}{\partial \theta^2} + \mu\frac{\partial^2 w}{\partial r^2}\right) \tag{26}$$

$$M_{rt} = (1-\mu)D\left(\frac{1}{r}\frac{\partial^2 w}{\partial r \partial \theta} - \frac{1}{r^2}\frac{\partial w}{\partial \theta}\right) \tag{27}$$

B9.3.1.1 Solid, Uniform-Thickness Plates

Solutions for solid circular plates have been tabulated for many loadings and boundary conditions. The results are presented in Table B9-3.

Table B9-3. Solutions for Circular Solid Plates

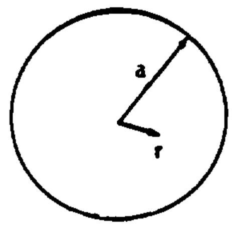

NOTE:
LOG = LOG_e = NATURAL LOG.
SEE TABLE B9-1 FOR NOMENCLATURE

Case	Formulas For Deflection And Moments
Supported Edges, Uniform Load 	$w = \frac{qa^2}{16D(1+\mu)}(a^2-r^2)$ $\qquad w_{max} = \frac{(5+\mu)}{64(1+\mu)} \frac{qa^4}{D}$ $M_r = \frac{q}{16}(3+\mu)(a^2-r^2)$ $\qquad (M_r)_{max} = (M_t)_{max} = \frac{3+\mu}{16} qa^2$ $M_t = \frac{q}{16}[a^2(3+\mu) - r^2(1+3\mu)]$ At Edge $\theta = \frac{Pa}{8\pi(1+\mu)} \times \frac{1}{D}$ 2
Clamped Edges, Uniform Load 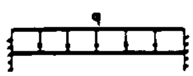	$w = \frac{q}{64D}(a^2-r^2)$ $\qquad w_{max} = \frac{qa^4}{64D}$ $M_r = \frac{q}{16}[a^2(1+\mu) - r^2(3+\mu)]$ $(M_r)_{max}$ at $r=a$ $= \frac{-qa^2}{8}$ $M_t = \frac{q}{16}[a^2(1+\mu) - r^2(1+3\mu)]$ $(M_r)_{r=0} = \frac{qa^2}{16}(1+\mu)$
Supported Edges, Uniform Load Over Concentric Circular Area of Radius, c 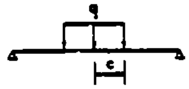 $P = \pi c^2 q$	$w = \frac{P}{16\pi D}\left\{\frac{3+\mu}{1+\mu}(a^2-r^2) + 2r^2 \log\frac{r}{a} + c^2\left[\log\frac{r}{a} - \frac{1-\mu}{2(1+\mu)} \frac{a^2-r^2}{a^2}\right]\right\}$ $w_{r=0} = \frac{P}{16\pi D}\left[\frac{3+\mu}{1+\mu} a^2 + c^2 \log\frac{c}{a} - \frac{7+3\mu}{4(1+\mu)} c^2\right]$ At Center $M_{max} = \frac{P}{4\pi}\left[(1+\mu) \log\frac{a}{c} + 1 - \frac{(1-\mu)c^2}{4a^2}\right]$ At Edge $\theta = \frac{Pa}{4\pi(1+\mu)} \times \frac{1}{D}$ 2

Table B9-3. (Continued)

Case	Formulas For Deflection And Moments
Simply Supported, Uniform Load On Concentric Circular Ring Of Radius, b P = 2π bq 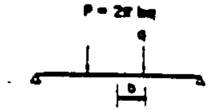	$(w)_{r=b} = \frac{P}{8\pi D}\left[(a^2-b^2)\left(1 + \frac{1}{2}\frac{1-\mu}{1+\mu}\frac{a^2-b^2}{a^2}\right) + 2b^2\log\frac{b}{a}\right]$ $\max(w)_{r=0} = \frac{P}{8\pi D}\left[b^2\log\frac{b}{a} + (a^2-b^2)\frac{(3+\mu)}{2(1+\mu)}\right]$ $M_{r=b} = \frac{(1+\mu)P(a^2-b^2)}{8\pi a^2} - \frac{(1+\mu)P\log\frac{b}{a}}{4\pi}$
Fixed Edges, Uniform Load On Concentric Circular Ring Of Radius, b P = 2π bq 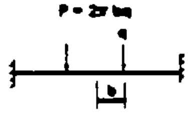	$(w)_{r=b} = \frac{P}{8\pi D}\left(\frac{a^4-b^4}{2a^2} + 2b^2\log\frac{b}{a}\right)$ $\max(w)_{r=0} = \frac{P}{8\pi D}\left[b^2\log\frac{b}{a} + \frac{(a^2-b^2)}{2}\right]$ $M_{r=a} = \frac{P}{4\pi}\frac{a^2-b^2}{a^2}$
Simply Supported, Concentrated Load At Center 	$w = \frac{P}{16\pi D}\left[\frac{3+\mu}{1+\mu}(a^2-r^2) + 2r^2\log\frac{r}{a}\right]$ $w_{max} = \frac{(3+\mu)}{16\pi(1+\mu)}\frac{Pa^2}{D}$ $M_r = \frac{P}{4\pi}(1+\mu)\log\frac{a}{r}$ $M_t = \frac{P}{4\pi}\left[(1+\mu)\log\frac{a}{r} + 1 - \mu\right]$
Fixed Edges, Concentrated Load At Center 	$w = \frac{Pr^2}{8\pi D}\log\frac{r}{a} + \frac{P}{16\pi D}(a^2-r^2)$ $w_{max} = \frac{3}{48\pi}\frac{Pa^2}{D}$ $M_r = \frac{P}{4\pi}\left[(1+\mu)\log\frac{a}{r} - 1\right]$ $M_t = \frac{P}{4\pi}\left[(1+\mu)\log\frac{a}{r} - \mu\right]$
Clamped Edges, Uniform Load Over Concentric Circular Area Of Radius, c 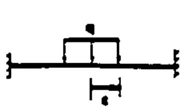 P = π c²q	$w_{max}(r=0) = \frac{P}{64\pi D}\left(4a^2 - 4c^2\log\frac{a}{c} - 3c^2\right)$ At r=a $M_r = \frac{P}{4\pi}\left(1 - \frac{c^2}{2a^2}\right)$ $\quad M_t = \mu M_r$ At r=0 $M_r = M_t = \frac{P(1+\mu)}{4\pi}\left(\log\frac{a}{c} + \frac{c^2}{4a^2}\right)$

Table B9-3. (Continued)

Case	Formulas For Deflection And Moments
Supported By Uniform Pressure Over Entire Lower Surface, Uniform Load Over Concentric Circular Area Of Radius, c $P = \pi c^2 q$ 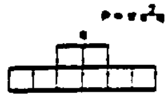	At r=0 $w = \frac{P}{64\pi D}\left[4c^2 \log\frac{a}{c} + 2c^2\left(\frac{3+\mu}{1+\mu}\right) - \frac{c^4}{a^2} - a^2\left(\frac{7+3\mu}{1+\mu}\right) + \frac{(a^2-c^2)c^2}{a^2}\right]$ $M_r = M_t = \frac{P}{4\pi}\left[(1+\mu)\log\frac{a}{c} + \frac{1}{4}(1-\mu)\left(1-\frac{c^2}{a^2}\right)\right]$ If c→0 $w = \frac{Pa^2}{64\pi D}\,\frac{(7+3\mu)\mu}{(1+\mu)}$
No Support, Uniform Edge Moment 	$w = \frac{M(a^2-r^2)}{2D(1+\mu)}$ $\qquad w_{r=0} = \frac{Ma^2}{2D(1+\mu)}$ Edge Rotation $\phi = \frac{Ma}{D(1+\mu)}$
Edges Supported, Central Couple (Trunnion Loading) 	At r=c $M = \frac{9m}{2\pi c}\left[1 + (1+\mu)\log\frac{2(a-c)}{Ka}\right]$ where $K = \frac{0.49\,a^2}{(c+0.7a)^2}$
Edges Clamped, Central Couple (Trunnion Loading) 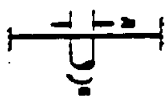	At r=c $M = \frac{9m}{2\pi c}\left[1 + (1+\mu)\log\frac{2(0.45\,a-c)}{0.45\,km}\right]$ where $k = \frac{0.1\,a^2}{(c+0.28\,a)^2}$
Edges Supported, Uniform Load Over Small Eccentric Circular Area Of Radius, r_o 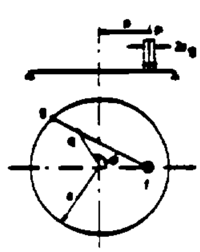 LOAD AT f	At Point of Load: $M_r = M_t = \frac{P}{4\pi}\left\{1 + (1+\mu)\log\frac{a-p}{r_o} - (1-\mu)\left[\frac{r_o^2}{4(a-p)^2}\right]\right\}$ At Point q: $w = K_0(r^3-b_0ar^2+c_0a^3) + K_1(r^4-b_1ar^3+c_1a^3r)\cos\phi$ $+ K_2(r^4-b_2ar^3+c_2a^2r^2)\cos\phi$ where $K_0 = \frac{2(1+\mu)P(p^3-b_0ap^2+c_0a^3)}{9(5+\mu)K\pi a^3}$, $\quad K = \frac{Et^3}{12(1-\mu^2)}$ $K_1 = \frac{2(3+\mu)P(p^4-b_1ap^3+c_1a^3p)}{3(9+\mu)K\pi a^4}$, $\quad b_0 = \frac{3(2+\mu)}{2(1+\mu)}$ $K_2 = \frac{(4+\mu)^2P(p^4-b_2ap^3+c_2a^2p^2)}{(9+\mu)(5+\mu)K\pi a^4}$, $\quad b_1 = \frac{3(4+\mu)}{2(3+\mu)}$ $b_2 = \frac{2(5+\mu)}{4+\mu}$, $\quad c_0 = \frac{4+\mu}{2(1+\mu)}$, $\quad c_1 = \frac{6+\mu}{2(3+\mu)}$, $\quad c_2 = \frac{6+\mu}{4+\mu}$

Table B9-3. (Concluded)

Case	Formulas For Deflection and Moments
Edges Fixed, Uniform Load Over Small Eccentric Circular Area of Radius, r_0 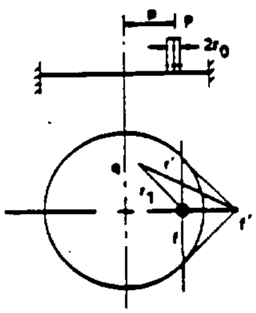	At Point of Load: $M_r = \frac{P}{4\pi}\left[(1+\mu)\log\frac{a-p}{r_0} + (1+\mu)\frac{r_0^2}{4(a-p)^2}\right]$ = max M when $r_0<0.6(a-p)$ $w = \frac{3P(1-\mu^2)(a^2-p^2)^2}{4\pi E t^3 a^2}$ At Point q: $w = \frac{3P(1-\mu^2)}{2\pi E t^3}\left[\frac{1}{2}\left(\frac{p^2 r'^2}{a^2} - r_1^2\right) - r_1^2\log\frac{p r'}{a r_1}\right]$ At Edge: $M_r = \frac{P}{4\pi}\left[1 - \frac{r_0^2}{2(a-p)^2}\right]$ = max M when $r_0 > 0.6(a-p)$
Supported At Several Points Along The Boundary 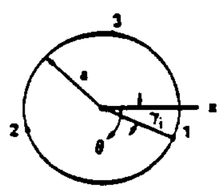	Supported At Two Points: $(\gamma_1 = 0,\ \gamma_2 = \pi)$ Load P at Center: $w_{r=0} = 0.116\frac{Pa^2}{D}$ $w_{r=a,\ \theta=\pi/2} = 0.118\frac{Pa^2}{D}$ Uniformly Loaded Plate: $w_{r=0} = 0.269\frac{qa^4}{D}$ $w_{r=a,\ \theta=\pi/2} = 0.371\frac{qa^4}{D}$ Supported At Three Points 120 Deg Apart: Load P at Center $w_{r=0} = 0.0670\frac{Pa^2}{D}$ Uniformly Loaded $w_{r=0} = 0.1137\frac{qa^4}{D}$
Edge Supported, Linearly Distributed Load Symmetrical About Diameter 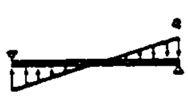	max $M_r = \frac{qa^2(5+\mu)}{72\sqrt{3}}$ at $r = 0.577a$ max $M_t = \frac{qa^2(5+\mu)(1+3\mu)}{72(3+\mu)}$ at $r = 0.675a$ max edge reaction per linear inch $= \frac{1}{4}qa$ max $w = 0.042\frac{qa^4}{Et^3}$ at $r = 0.503a$ $(\mu = 0.3)$

B9.3.1.2 Annular, Uniform-Thickness Plates

Solutions for annular circular plates with a central hole are tabulated in Table B9-4.

B9.3.1.3 Solid, Nonuniform-Thickness Plates

For the plates treated here, the thickness is a function of the radial distance, and the acting load is symmetrical with respect to the center of the plate.

I. Linearly Varying Thickness:

The plate of this type is shown in Fig. B9-6.

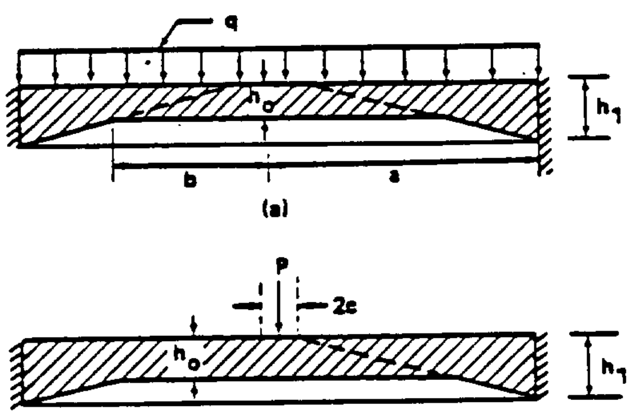

FIGURE B9-6. CIRCULAR PLATE WITH LINEARLY VARYING THICKNESS

Tables B9-5 and B9-6 give the deflection w_{max} and values of bending moments of the plate in two cases of loading. To calculate the bending moment at the center in the case of a central load P, one may assume a uniform distribution of that load over a small circular area of a radius c. The moment $M_r = M_t$ at $r = 0$ can be expressed in the form

$$M_{max} = \frac{P(1+\mu)}{4\pi}\left(\log\frac{a}{c} + \frac{c^2}{4a^2}\right) + \gamma_1 P \qquad (28)$$

Table B9-4. Solutions For Annular, Uniform-Thickness Plates

NOTE:
LOG = LOG_e = NATURAL LOG.
SEE TABLE B9-1 FOR NOMENCLATURE

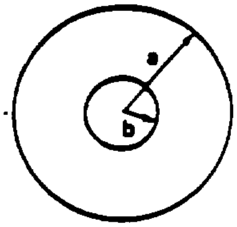

Case	Formulas For Deflection And Moments
Outer Edge Supported, Uniform Load Over Entire Actual Surface 	At Inner Edge: $\max M = M_t = \frac{q}{8(a^2-b^2)}\left[a^4(3+\mu) + b^4(1-\mu) - 4a^2b^2 - 4(1+\mu)a^2b^2 \log \frac{a}{b}\right]$ When b Is Very Small $\max M = M_t = \frac{qa^2}{8}(3+\mu)$ $\max w = \frac{q}{8D}\left[\frac{a^4(5+\mu)}{8(1+\mu)} + \frac{b^4(7+3\mu)}{8(1+\mu)} - \frac{a^2b^2(3+\mu)}{2(1+\mu)} + \frac{a^2b^2(3+\mu)}{2(1-\mu)} \log \frac{a}{b} - \frac{2a^2b^4(1+\mu)}{(a^2-b^2)(1-\mu)}\left(\log \frac{a}{b}\right)^2\right]$
Outer Edge Clamped, Uniform Load Over Entire Actual Surface 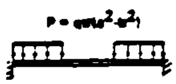	At Outer Edge: $\max M_r = \frac{q}{8}\left[a^2 - 2b^2 + \frac{b^4(1-\mu) - 4b^4(1+\mu)\log \frac{a}{b} + a^2b^2(1+\mu)}{a^2(1-\mu) + b^2(1+\mu)}\right]$ $\max w = \frac{q}{64D}\left\{a^4 + 5b^4 - 6a^2b^2 + 8b^4 \log \frac{a}{b} - \frac{[8b^6(1+\mu) - 4a^2b^2(3+\mu) - 4a^2b^2(1+\mu)] \log \frac{a}{b} - 16a^2b^4(1+\mu)\left(\log \frac{a}{b}\right)^2}{a^2(1-\mu) + b^2(1+\mu)} - \frac{4a^2b^4 - 2a^4b^2(1+\mu) - 2b^4(1-\mu)}{a^2(1-\mu) + b^2(1+\mu)}\right\}$
Outer Edge Supported, Uniform Load Along Inner Edge 	At Inner Edge: $\max M = M_t = \frac{P}{4\pi}\left[\frac{2a^2(1+\mu)}{a^2-b^2} \log \frac{a}{b} + (1-\mu)\right]$ $\max w = \frac{P}{16\pi D}\left[\frac{(a^2-b^2)(3+\mu)}{(1+\mu)} - \frac{4a^2b^2(1+\mu)}{(1-\mu)(a^2-b^2)}\left(\log \frac{a}{b}\right)^2\right]$

Table B9-4. (Continued)

Case	Formulas For Deflection And Moments
Outer Edge Clamped, Uniform Load Along Inner Edge 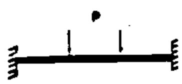	At Outer Edge: $$\max M_r = \frac{P}{4\pi}\left[1 - \frac{2b^2 - 2b^2(1+\mu)\log\frac{a}{b}}{a^2(1-\mu) + b^2(1+\mu)}\right] = \max M \text{ when } \frac{a}{b} < 2.4$$ At Inner Edge: $$\max M_t = \frac{P\mu}{4\pi}\left[1 + \frac{a^2(1-\mu) - b^2(1+\mu) - 2(1-\mu^2)a^2\log\frac{a}{b}}{\mu a^2(1-\mu) + b^2(1+\mu)}\right]$$ $$= \max M \text{ when } \frac{a}{b} > 2.4$$ $$\max w = \frac{P}{16\pi D}\left[a^2 - b^2 + \frac{2b^2(a^2-b^2) - 8a^2b^2\log\frac{a}{b} + 4a^2b^2(1+\mu)\left(\log\frac{a}{b}\right)^2}{a^2(1-\mu) + b^2(1+\mu)}\right]$$
Supported Along Concentric Circle Near Outer Edge, Uniform Load Along Concentric Circle Near Inner Edge 	At Inner Edge: $$\max M = M_t = \frac{P}{4\pi}\left[\frac{2a^2(1+\mu)}{a^2-b^2}\log\frac{c}{d} + (1-\mu)\frac{c^2-d^2}{a^2-b^2}\right]$$
Inner Edge Supported, Uniform Load Over Entire Actual Surface $P = q\pi(a^2-b^2)$ 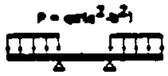	At Inner Edge: $$\max M = M_t = \frac{q}{8(a^2-b^2)}\left[4a^4(1+\mu)\log\frac{a}{b} + 4a^2b^2 + b^4(1-\mu) - a^4(1+3\mu)\right]$$ At Outer Edge: $$\max w = \frac{q}{64D}\left[a^4(7+3\mu) + b^4(5+\mu) - a^2b^2(12+4\mu) - \frac{4a^2b^2(3+\mu)(1+\mu)}{(1-\mu)}\log\frac{a}{b} + \frac{16a^4b^2(1+\mu)^2}{(a^2-b^2)(1-\mu)}\left(\log\frac{a}{b}\right)^2\right]$$
Outer Edge Fixed And Supported, Inner Edge Fixed, Uniform Load Over Entire Actual Surface $P = q\pi(a^2-b^2)$ 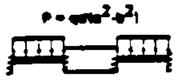	At Outer Edge: $$\max M_r = \frac{q}{8}\left[(a^2-3b^2) + \frac{4b^4}{a^2-b^2}\left(\log\frac{a}{b}\right)^2\right]$$ At Inner Edge: $$M_r = \frac{q}{8}\left[(a^2+b^2) - \frac{4a^2b^2}{(a^2-b^2)}\left(\log\frac{a}{b}\right)\right]$$ $$\max w = \frac{q}{64D}\left[a^4 + 3b^4 - 4a^2b^2 - 4a^2b^2\log\frac{a}{b} + \frac{16a^2b^2}{a^2-b^2}\left(\log\frac{a}{b}\right)^2\right]$$

Table B9-4. (Continued)

<table>
<tr><th>Case</th><th>Formulas For Deflection And Moments</th></tr>
<tr><td>Outer Edge Fixed And Supported, Inner Edge Fixed, Uniform Load Along Inner Edge
</td><td>At Outer Edge:
$$M_r = \frac{P}{4\pi}\left[1 - \frac{2b^2}{a^2 - b^2}\left(\log \frac{a}{b}\right)\right]$$
At Inner Edge:
$$\max M_r = \frac{P}{4\pi}\left[1 - \frac{2a^2}{a^2 - b^2}\left(\log \frac{a}{b}\right)\right]$$
$$\max w = \frac{P}{16\pi D}\left[a^2 - b^2 - \frac{4a^2b^2}{a^2 - b^2}\left(\log \frac{a}{b}\right)^2\right]$$</td></tr>
<tr><td>Inner Edge Fixed And Supported, Uniform Load Over Entire Actual Surface
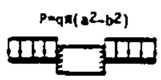</td><td>At Inner Edge:
$$\max M_r = \frac{q}{8}\left[\frac{4a^4(1+\mu)\log \frac{a}{b} - a^4(1+3\mu) + b^4(1-\mu) + 4a^2b^2\mu}{a^2(1+\mu) + b^2(1-\mu)}\right]$$
At Outer Edge:
$$\max w = \frac{q}{64D}\left\{\frac{a^6(7+3\mu) + b^6(1-\mu) - a^4b^2(1+7\mu) - a^2b^4(7-5\mu)}{a^2(1+\mu) + b^2(1-\mu)}\right.$$
$$\left.\frac{4a^4b^2[a^2(5-\mu) + b^2(1+\mu)]\log \frac{a}{b} + 16a^4b^2(1+\mu)\left(\log \frac{a}{b}\right)^2}{a^2(1+\mu) + b^2(1-\mu)}\right\}$$</td></tr>
<tr><td>Inner Edge Fixed And Supported, Uniform Load Along Outer Edge
</td><td>At Inner Edge:
$$\max M_r = \frac{P}{4\pi}\left[\frac{2a^2(1+\mu)\log \frac{a}{b} + a^2(1-\mu) - b^2(1-\mu)}{a^2(1+\mu) + b^2(1-\mu)}\right]$$
At Outer Edge:
$$\max w = \frac{P}{16\pi D}\left[\frac{a^4(3+\mu) - b^4(1-\mu) - 2a^2b^2(1+\mu) - 8a^2b^2\log \frac{a}{b}}{a^2(1+\mu) + b^2(1-\mu)}\right.$$
$$\left.- \frac{4a^2b^2(1+\mu)\left(\log \frac{a}{b}\right)^2}{a^2(1+\mu) + b^2(1-\mu)}\right]$$</td></tr>
<tr><td>Outer Edge Fixed, Uniform Moment Along Inner Edge
</td><td>At Inner Edge:
$$\max w = \frac{M}{2D}\left[\frac{a^2b^2 - b^4 - 2a^2b^2\log \frac{a}{b}}{a^2(1-\mu) + b^2(1-\mu)}\right]$$
At Outer Edge:
$$\max M_r = M\left[\frac{2b^2}{(1+\mu)b^2 + (1-\mu)a^2}\right]$$</td></tr>
<tr><td>Inner Edge Fixed, Uniform Moment Along Outer Edge
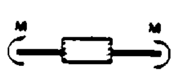</td><td>At Inner Edge:
$$\max M_r = M\left[\frac{2a^2}{(1+\mu)a^2 + (1-\mu)b^2}\right]$$
At Outer Edge:
$$\max w = \frac{M}{2D}\left[\frac{a^4 - a^2b^2 - 2a^2b^2\log \frac{a}{b}}{a^2(1+\mu) + b^2(1-\mu)}\right]$$</td></tr>
</table>

Table B9-4. (Continued)

Case	Formulas For Deflection and Moments
Outer Edge Supported, Unequal Uniform Moments Along Edges 	$M_r = \frac{1}{a^2 - b^2}\left[a^2M_a - b^2M_b - \frac{a^2b^2}{r^2}(M_a - M_b)\right]$ $w = \frac{1}{D(a^2 - b^2)}\left\{\frac{a^2 - r^2}{2}\left(\frac{a^2M_a - b^2M_b}{1+\mu}\right) + \log\frac{a}{r}\left[\frac{a^2b^2(M_a - M_b)}{(1-\mu)}\right]\right\}$
Outer Edge Supported, Inner Edge Fixed, Uniform Load Over Entire Actual Surface $P = q\pi(a^2 - b^2)$ 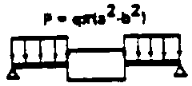	At Inner Edge: $\max M_r = \frac{q}{8}\left[\frac{4a^2b^2(1+\mu)\log\frac{a}{b} - a^4(3+\mu) + a^2b^2(5+\mu)}{a^2(1+\mu) + b^2(1-\mu)} - b^2\right]$ $\max w = \frac{q}{64D}\left\{a^4 - 3b^4 + 2a^2b^2 - 8a^2b^2\log\frac{a}{b}\right.$ $- \frac{16(1+\mu)a^2b^2\log^2\frac{a}{b} + [4(7+3\mu)a^2b^4 - 4(5+3\mu)]\log\frac{a}{b}}{a^2(1+\mu) + b^2(1-\mu)}$ $\left.- \frac{4(4+\mu)a^4b^2 - 2(3-\mu)a^6 - 2(5+\mu)a^2b^4}{a^2(1+\mu) - b^2(1-\mu)}\right\}$
Both Edges Fixed, Balanced Loading (Piston) $P = q\pi(a^2 - b^2)$ 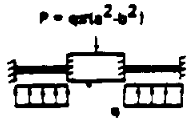	At Inner Edge: $\max M_r = \frac{q}{8}\left(\frac{4a^4}{a^2 - b^2}\log\frac{a}{b} - 3a^2 + b^2\right)$ $\max w = \frac{q}{64D}\left[3a^4 - 4a^2b^2 + b^4 + 4a^2b^2\log\frac{a}{b} - \frac{16a^4b^2}{a^2 - b^2}\left(\log\frac{a}{b}\right)^2\right]$
Outer Edge Supported, Inner Edge Free, Uniform Load On Concentric Circular Ring of Radius, r_0 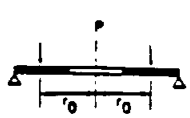	At Inner Edge: $\max M_t = -\frac{P}{4\pi}\left[\frac{1}{2}(1-\mu) + (1+\mu)\log\frac{a}{r_0} - (1-\mu)\frac{r_0^2}{2a^2}\right] - \frac{c(a^2 + b^2)}{(a^2 - b^2)}$ $\max w = -\frac{P}{8\pi D}\left[\frac{(a^2 - b^2)(3+\mu)}{2(1+\mu)} - (b^2 + r_0^2)\log\frac{a}{b} - \frac{r_0^2(a^2 - b^2)(1-\mu)}{2a^2(1+\mu)}\right]$ $- \frac{c}{2D}\left[\frac{b^2}{(1+\mu)} + \frac{2a^2b^2}{(a^2 - b^2)(1-\mu)}\log\frac{a}{b}\right]$ where $c = \frac{P}{8\pi}\left[(1-\mu) + 2(1+\mu)\log\frac{a}{r_0} - (1-\mu)\frac{r_0^2}{a^2}\right]$

2

Table B9-4. (Concluded)

<table>
<tr><th>Case</th><th>Formulas For Deflection and Moments</th></tr>
<tr><td>Outer Edge Fixed, Inner Edge Free, Uniform Load Of Concentric Circular Ring Of Radius, r_0
</td><td>At Inner Edge:
$$\max M_t = \frac{P}{8\pi}\left[(1+\mu)\left(2\log\frac{a}{r_0} + \frac{r_0^2}{a^2} - 1\right)\right] - c\left[\frac{a^2(1-\mu) - b^2(1+\mu)}{a^2(1-\mu) + b^2(1-\mu)}\right]$$
At Outer Edge:
$$M_r = \frac{P}{8\pi}\left(1 - \frac{r_0^2}{a^2}\right) + c\left[\frac{2b^2}{a^2(1-\mu) + b^2(1+\mu)}\right]$$
$$\max w = \frac{P}{8\pi D}\left[\frac{(a^2 + r_0^2)(a^2 - b^2)}{2a^2} - (b^2 + r_0^2)\log\frac{a}{b}\right] - \frac{c}{2D}\left[\frac{b^4 + 2a^2b^2\log\frac{a}{b} - a^2b^2}{b^2(1+\mu) + a^2(1-\mu)}\right]$$
where
$$c = \frac{P}{8\pi}\left[(1+\mu)\left(2\log\frac{a}{r_0} + \frac{r_0^2}{a^2} - 1\right)\right]$$</td></tr>
<tr><td>Central Couple Balanced By Linearly Distributed Pressure
</td><td>At Inner Edge:
$\max M_r = \beta\frac{M}{6a}$ where
<table><tr><td>$\frac{a}{b}$</td><td>1.25</td><td>1.50</td><td>2</td><td>3</td><td>4</td><td>5</td></tr><tr><td>β</td><td>0.1625</td><td>0.456</td><td>1.106</td><td>2.25</td><td>3.385</td><td>4.470</td></tr></table>(μ = 0.3)</td></tr>
<tr><td>Concentrated Load Applied At Outer Edge
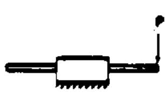</td><td>At Inner Edge:
$\max M_r = \beta\frac{P}{6}$ where
<table><tr><td>$\frac{a}{b}$</td><td>1.25</td><td>1.50</td><td>2</td><td>3</td><td>4</td><td>5</td></tr><tr><td>β</td><td>3.7</td><td>4.25</td><td>5.2</td><td>6.7</td><td>7.9</td><td>9.8</td></tr></table>for μ = 0.3</td></tr>
</table>

Table B9-5. Deflections and Bending Moments of Clamped Circular Plates Loaded Uniformly (Fig. B9-6a) ($\mu = 0.25$)

$\frac{b}{a}$	$w_{max} = \alpha \frac{qa^4}{Eh_0^3}$	$M_r = \beta qa^2$			$M_t = \beta_1 qa^2$		
		r=0	r=b	r=a	r=0	r=b	r=a
	α	β	β	β	β_1	β_1	β_1
0.2	0.008	0.0122	0.0040	-0.161	0.0122	0.0078	-0.040
0.4	0.042	0.0332	0.0007	-0.156	0.0332	0.0157	-0.039
0.6	0.094	0.0543	-0.0188	-0.149	0.0543	0.0149	-0.037
0.8	0.148	0.0709	-0.0591	-0.140	0.0709	0.0009	-0.035
1.0	0.176	0.0781	-0.125	-0.125	0.0781	-0.031	-0.031

Table B9-6. Deflections and Bending Moments of Clamped Circular Plates Under a Central Load (Fig. B9-6b) ($\mu = 0.25$)

$\frac{b}{a}$	$w_{max} = \alpha \frac{Pa^2}{Eh_0^3}$	$M_r = M_t$	$M_r = \beta P$		$M_t = \beta_1 P$	
		r = 0	r = b	r = a	r = b	r = a
	α	γ_1	β	β	β_1	β_1
0.2	0.031	-0.114	-0.034	-0.129	-0.028	-0.032
0.4	0.093	-0.051	-0.040	-0.112	-0.034	-0.028
0.6	0.155	-0.021	-0.050	-0.096	-0.044	-0.024
0.8	0.203	-0.005	-0.063	-0.084	-0.057	-0.021
1.0	0.224	0	-0.080	-0.080	-0.020	-0.020

The last term is due to the nonuniformity of the thickness of the plate and the coefficient γ_1 is given in Table B9-6.

Symmetrical deformation of plates such as those shown in Fig. B9-7 have been investigated and some results are given in Tables B9-7, B9-8, and B9-9.

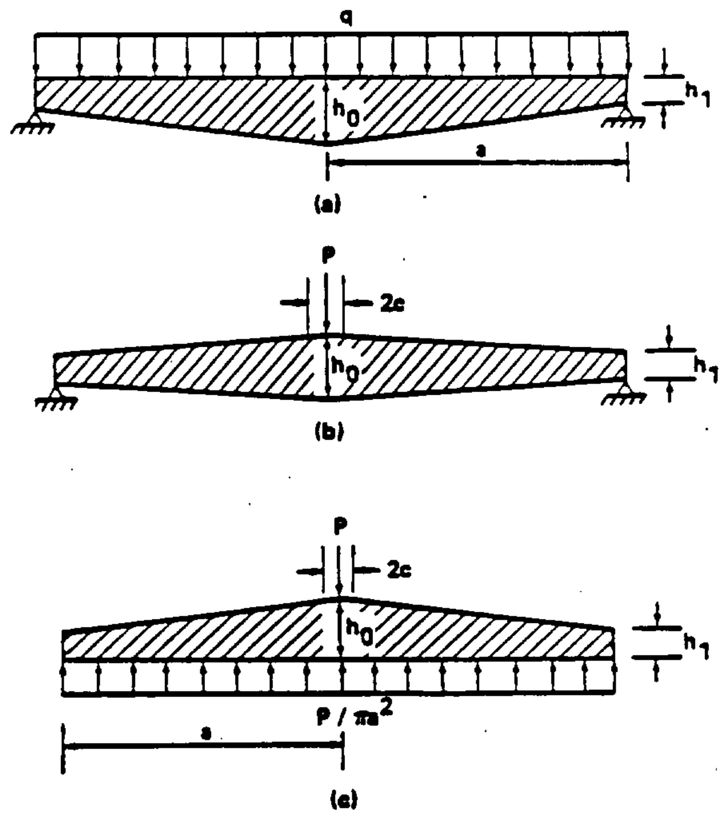

FIGURE B9-7. TAPERED CIRCULAR PLATE

For bending moments under central load P (Fig. B9-7b) the following equation is true (γ_2 is given in Table B9-8):

$$M_{max} = \frac{P}{4\pi}\left[(1+\mu)\log\frac{a}{c} + 1 - \frac{(1-\mu)c^2}{4a^2}\right] + \gamma_2 P \quad . \qquad (29)$$

Table B9-7. Deflections and Bending Moments of Simply Supported Plates Under Uniform Load (Fig. B9-7a) ($\mu = 0.25$)

$\frac{h_0}{h_1}$	$w_{max} = \alpha \frac{qa^4}{Eh_0^3}$	$M_r = \beta qa^2$		$M_t = \beta_1 qa^2$		
		$r = 0$	$r = \frac{a}{2}$	$r = 0$	$r = \frac{a}{2}$	$r = a$
	α	β	β	β_1	β_1	β_1
1.00	0.738	0.203	0.152	0.203	0.176	0.094
1.50	1.26	0.257	0.176	0.257	0.173	0.054
2.33	2.04	0.304	0.195	0.304	0.167	0.029

Table B9-8. Deflections and Bending Moments of Simply Supported Circular Plates Under Central Load (Fig. B9-7b) ($\mu = 0.25$)

$\frac{h_0}{h_1}$	$w_{max} = \alpha \frac{Pa^2}{Eh_0^3}$	$M_r = M_t$	$M_r = \beta P$	$M_t = \beta_1 P$	
		$r = 0$	$r = \frac{a}{2}$	$r = \frac{a}{2}$	$r = a$
	α	γ_2	β	β_1	β_1
1.00	0.582	0	0.069	0.129	0.060
1.50	0.93	0.029	0.088	0.123	0.033
2.33	1.39	0.059	0.102	0.116	0.016

Table B9-9. Bending Moments of a Circular Plate With Central Load And Uniformly Distributed Reacting Pressure (Fig. B9-7c) ($\mu = 0.25$)

$\frac{h_0}{h_1}$	$M_r = M_t$	$M_r = \beta P$	$M_t = \beta_1 P$	
	$r = 0$	$r = \frac{a}{2}$	$r = \frac{a}{2}$	$r = a$
	γ_2	β	β_1	β_1
1.00	-0.065	0.021	0.073	0.030
1.50	-0.053	0.032	0.068	0.016
2.33	-0.038	0.040	0.063	0.007

Of practical interest is a combination of loadings shown in Figs. B9-7a and b. For this case the γ_2 to be used in equation (29) is given in Table B9-9.

II. Nonlinear Varying Thickness:

In many cases the variation of the plate thickness can be represented with sufficient accuracy by the equation

$$y = e^{-\beta x^2/6} \tag{30}$$

in which β is a constant that must be chosen in each particular case so that it approximates as closely as possible the actual proportions of the plate. The variation of thickness along a diameter of a plate corresponding to various values of the constant β is shown in Fig. B9-8.

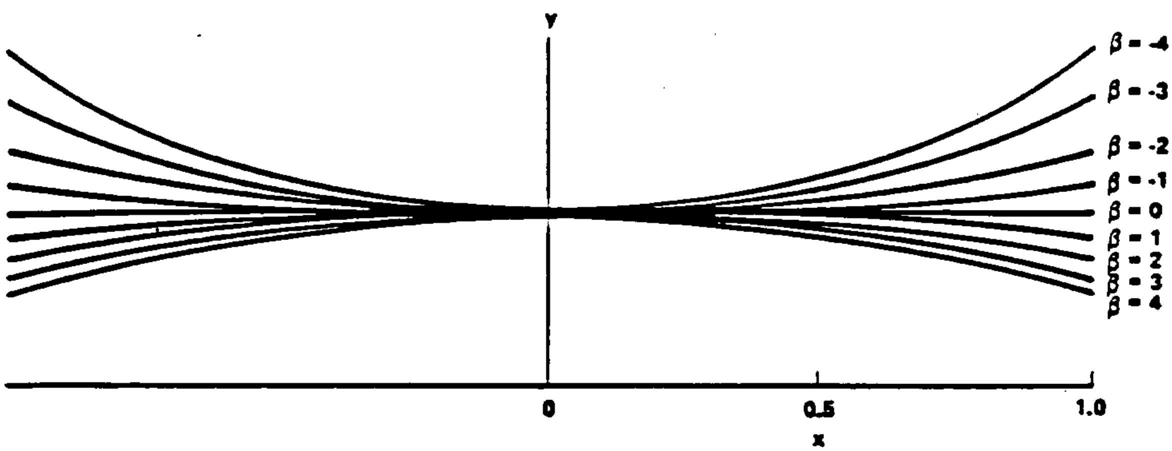

FIGURE B9-8. VARIATION OF PLATE THICKNESS FOR CIRCULAR PLATES

Solutions for this type of variation for uniformly loaded plates with both clamped edges and simply supported edges are given in Reference 1, pages 301-302.

B9.3.1.4 Annular Plates with Linearly Varying Thickness

Consider the case of a circular plate with a concentric hole and a thickness varying as shown in Fig. B9-9.

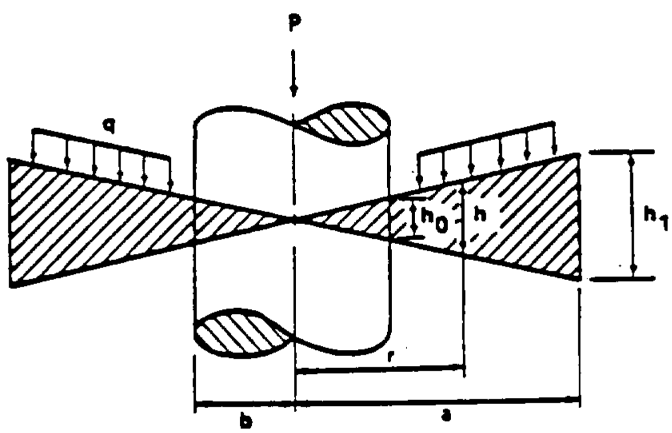

FIGURE B9-9. ANNULAR PLATE WITH LINEARLY VARYING THICKNESS

The plate carries a uniformly distributed surface load q and a line load $p = P/2\pi b$ uniformly distributed along the edge of the hole.

Table B9-10 gives values of coefficients k and k_1, to be used in the following expressions for the numerically largest stress and the largest deflection of the plate:

$$(\sigma_r)_{max} = k\frac{qa^2}{h_1^2} \qquad \text{or} \qquad (\sigma_r)_{max} = k\frac{P}{h_1^2}$$

$$w_{max} = k_1\frac{qa^4}{Eh_1^3} \qquad \text{or} \qquad w_{max} = k_1\frac{Pa^2}{Eh_1^3} \qquad (31)$$

Table B9-10. Values of Coefficients in Equations (31) for Various Values of the Ratio $\frac{a}{b}$ (Fig. B9-9) $(\mu = \frac{1}{3})$

Case	Coef-ficient	$\frac{a}{b}$ = 1.25	1.5	2	3	4	5	Boundary Conditions
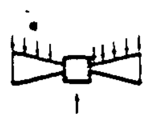	k	0.249	0.638	3.96	13.64	26.0	40.6	$P = \pi q(a^2 - b^2)$ $\phi_b = 0$
	k_1	0.00372	0.0453	0.401	2.12	4.25	6.28	$M_a = 0$
	k	0.149	0.991	2.23	5.57	7.78	9.16	$P = 0$ $\phi_b = 0$
	k_1	0.00651	0.0564	0.412	1.673	2.79	3.57	$M_a = 0$
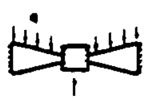	k	0.1275	0.315	2.05	7.97	17.35	30.0	$P = \pi q(a^2 - b^2)$ $\phi_b = 0$
	k_1	0.00105	0.0115	0.0934	0.537	1.261	2.16	$\phi_a = 0$
	k	0.159	0.396	1.091	3.31	6.55	10.78	$q = 0$ $\phi_b = 0$
	k_1	0.00174	0.0112	0.0606	0.261	0.546	0.876	$\phi_a = 0$
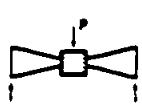	k	0.353	0.933	2.63	6.88	11.47	16.51	$q = 0$ $\phi_b = 0$
	k_1	0.00816	0.0583	0.345	1.358	2.39	3.27	$M_a = 0$
	k	0.0785	0.208	0.52	1.27	1.94	2.52	$P = 0$ $\phi_b = 0$
	k_1	0.00092	0.008	0.0496	0.193	0.346	0.482	$\phi_a = 0$

401

B9.3.1.5 Sector of a Circular Plate

The general solution developed for circular plates can also be adapted for a plate in the form of a sector (Fig. B9-10), the straight edges of which are simply supported. For a uniformly loaded plate simply supported along the straight and circular edges the expressions for the deflections and bending moments at a given point can be represented in each particular case by the following formulas:

$$w = \alpha \frac{qa^4}{D}, \quad M_r = \beta\, qa^2, \quad M_t = \beta_1\, qa^2, \tag{32}$$

in which α, β, and β_1 are numerical factors. Several values of these factors for points taken on the axis of symmetry of a sector are given in Table B9-11.

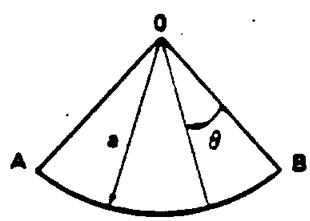

FIGURE B9-10. SECTOR OF A CIRCULAR PLATE

The coefficients for the case of a sector clamped along the circular boundary and simply supported along the straight edges are given in Table B9-12. It can be seen that in this case the maximum bending stress occurs at the midpoint of the unsupported circular edge. The following equation is used for the case when $\pi/k = \pi/2$

$$w_{max} = 0.0633 \frac{qa^4}{D}$$

The bending moment at the same point is

$$M_t = 0.1331\, qa^2$$

Table B9-11. Values of the Factors α, β, and B_1 for Various Angles $\frac{\pi}{k}$ of a Sector Simply Supported at the Boundary ($\mu = 0.3$)

$\frac{\pi}{k}$	$\frac{r}{a} = \frac{1}{4}$			$\frac{r}{a} = \frac{1}{2}$			$\frac{r}{a} = \frac{3}{4}$			$\frac{r}{a} = 1$		
	α	β	β_1	α	β	β_1	α	β	β_1	α	β	β_1
$\frac{\pi}{4}$	0.00006	-0.0015	0.0093	0.00033	0.0069	0.0183	0.00049	0.0161	0.0169	0	0	0.0025
$\frac{\pi}{3}$	0.00019	-0.0025	0.0177	0.00080	0.0149	0.0255	0.00092	0.0243	0.0213	0	0	0.0044
$\frac{\pi}{2}$	0.00092	0.0036	0.0319	0.00225	0.0353	0.0352	0.00203	0.0381	0.0286	0	0	0.0088
π	0.00589	0.0692	0.0357	0.00811	0.0868	0.0515	0.00560	0.0617	0.0468	0	0	0.0221

Table B9-12. Values of the Coefficients α and β for Various Angles $\frac{\pi}{k}$ of a Sector Clamped Along the Circular Boundary and Simply Supported Along the Straight Edges ($\mu = 0.3$)

$\frac{\pi}{k}$	$\frac{r}{a} = \frac{1}{4}$		$\frac{r}{a} = \frac{1}{2}$		$\frac{r}{a} = \frac{3}{4}$		$\frac{r}{a} = 1$	
	α	β	α	β	α	β	α	β
$\frac{\pi}{4}$	0.00005	-0.0008	0.00026	0.0087	0.00028	0.0107	0	-0.025
$\frac{\pi}{3}$	0.00017	-0.0006	0.00057	0.0143	0.00047	0.0123	0	-0.034
$\frac{\pi}{2}$	0.00063	0.0068	0.00132	0.0272	0.00082	0.0113	0	-0.0488
π	0.00293	0.0472	0.00337	0.0446	0.00153	0.0016	0	-0.0756

In the general case of a plate having the form of a circular sector with radial edges clamped or free, one must apply approximate methods. Another problem which allows an exact solution is that of bending of a plate clamped along two circular arcs. Data regarding the clamped semicircular plate are given in Table B9-13.

Table B9-13. Values of the Factors α, β, and β_1 for a Semicircular Plate Clamped Along the Boundary ($\mu = 0.3$)

Load Distribution	$\frac{r}{a} = 0$ β	$\frac{r}{a} = 0.483$ β_{max}	$\frac{r}{a} = 0.486$ α_{max}	$\frac{r}{a} = 0.525$ β_{1max}	$\frac{r}{a} = 1$ β
Uniform Load q	-0.0731	0.0355	0.00202	0.0194	-0.0584
Hydrostatic Load $q\frac{v}{a}$	-0.0276	—	—	—	-0.0355

I. <u>Annular Sectored Plate:</u>

For a semicircular annular sectored plate with outer edge supported and the other edges free, with uniform load over the entire actual surface as shown in Fig. B9-11, the equations for maximum moment and deflection are:

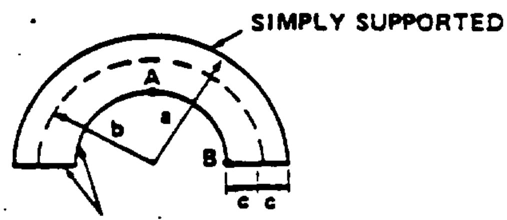

FIGURE B9-11. ANNULAR SECTORED PLATE

At A

$$M_t = qcb\left(\frac{b}{c} - \frac{1}{3}\right)\left[c_1\left(1 - \gamma_1^2\frac{c}{b}\right) + c_2\left(1 - \gamma_2^2\frac{c}{b}\right) + \frac{c}{b}\right]K \quad ,$$

At B

$$w = \frac{24qc^2b^2}{Et^3}\left(\frac{b}{c} - \frac{1}{3}\right)\left[c_1 \cosh \frac{\gamma_1 \pi}{2} + c_2 \cosh \gamma_2 \frac{\pi}{2} + \frac{c}{b}\right] ,$$

where

$$c_1 = \frac{1}{\left(\frac{b}{c} - \gamma_1^2\right)(\lambda - 1) \cosh \gamma_1 \frac{\pi}{2}} , \quad c_2 = \frac{1}{\left(\frac{b}{c} - \gamma_2^2\right)\left(\frac{1}{\lambda} - 1\right) \cosh \gamma_2 \frac{\pi}{2}} ,$$

$$\gamma_1 = \frac{\gamma}{\sqrt{2}} \sqrt{1 + \sqrt{1 - \frac{4b^2}{c^2\gamma^4}}} , \quad \gamma_2 = \frac{\gamma}{\sqrt{2}} \sqrt{1 - \sqrt{1 - \frac{4b^2}{c^2\gamma^4}}} ,$$

$$\gamma = \sqrt{\frac{2b}{c} + 4\left(1 - \frac{0.625t}{2c}\right)\frac{G}{E}\left(1 + \frac{b}{c}\right)^2} ,$$

$$\lambda = \frac{\gamma_1\left(\frac{b}{c} - \gamma_1^2 + \lambda_1\right)\left(\frac{b}{c} - \gamma_2^2\right) \tanh \gamma_1 \frac{\pi}{2}}{\gamma_2\left(\frac{b}{c} - \gamma_2^2 + \lambda_1\right)\left(\frac{b}{c} - \gamma_1^2\right) \tanh \gamma_2 \frac{\pi}{2}} ,$$

$$\lambda_1 = 4\left(1 - \frac{0.625t}{2c}\right)\frac{G}{E}\left(1 + \frac{b}{c}\right)^2 .$$

K is a function of $\frac{b-c}{b+c}$ and has the following values:

$\frac{b-c}{b+c} =$	0.05	0.10	0.2	0.3	0.4	0.5	0.6	0.7	0.8	0.9	1.0
K =	2.33	2.20	1.95	1.75	1.58	1.44	1.32	1.22	1.13	1.06	1.0

B9.3.2 Rectangular Plates

Solutions for many rectangular plate problems with various loadings and boundary conditions are given in Tables B9-14 through 18. For loads and boundary conditions not covered here, solutions can be found by applying the various theoretical, approximate, or complete solutions discussed in

Table B9-14. Solutions for Rectangular Plates

$b/a = \alpha$

NOTE: LOG = LOG$_e$ = NATURAL LOG
SEE TABLE B9-1 FOR NOMENCLATURE

*All Edges Supported. Uniform Load Over Entire Surface

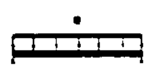

At Center:

$$M_a = (0.0375 + 0.0637\alpha^2 - 0.0633\alpha^4)qb^2$$

$$M_b = \frac{0.125qb^2}{(1 + 1.61\alpha^4)} = \max M$$

$$\max w = \frac{0.1422}{(1 + 2.21\alpha^4)} \frac{qb^4}{Et^3}$$

All Edges Supported. Uniform Load Over Small Concentric Circular Area Of Radius, r_o

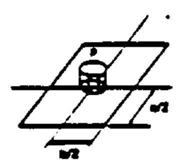

At Center:

$$M_b = \frac{P}{4\pi}\left[(1 + \mu)\log\frac{b}{2r_o} + (1 + k)\right]$$

where

$$k = \frac{0.914}{1 + 1.6\alpha^2} - 0.6$$

$$\max w = \frac{0.203Pb^2}{12D(1 + 0.462\alpha^4)}$$

All Edges Supported. Uniform Load Over Central Rectangular Area Shown Shaded

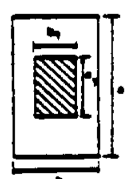

At Center: $\max \sigma = \sigma_b = \beta \frac{P}{t^2}$ where β is found in the following ($\mu = 0.3$):

b_1/b \ a_1/b (a = b)	0	0.2	0.4	0.6	0.8	1.0
0		1.82	1.38	1.12	0.93	0.76
0.2	1.82	1.28	1.08	0.90	0.76	0.63
0.4	1.39	1.07	0.84	0.72	0.62	0.52
0.6	1.12	0.90	0.72	0.60	0.52	0.43
0.8	0.92	0.76	0.62	0.51	0.42	0.36
1.0	0.76	0.63	0.52	0.42	0.35	0.30

b_1/b \ a_1/b (a = 1.4b)	0	0.2	0.4	0.8	1.2	1.4
0		2.0	1.55	1.12	0.84	0.73
0.2	1.78	1.43	1.23	0.95	0.74	0.64
0.4	1.39	1.13	1.00	0.80	0.62	0.55
0.6	1.10	0.91	0.82	0.68	0.53	0.47
0.8	0.90	0.76	0.68	0.57	0.45	0.40
1.0	0.73	0.62	0.57	0.47	0.38	0.33

b_1/b \ a_1/b (a = 2b)	0	0.4	0.8	1.2	1.6	2.0
0		1.64	1.20	0.97	0.78	0.64
0.2	1.73	1.31	1.03	0.84	0.68	0.57
0.4	1.32	1.08	0.88	0.74	0.60	0.50
0.6	1.04	0.90	0.76	0.64	0.54	0.44
0.8	0.87	0.78	0.63	0.54	0.44	0.38
1.0	0.71	0.61	0.53	0.45	0.38	0.30

Table B9-14. (Continued)

All Edges Supported, Distributed Load Varying Linearly Along Length

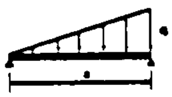

$\max \sigma = \beta \frac{qb^2}{t^2}$, $\max w = \delta \frac{qb^4}{Et^3}$ where β and δ are found in the following:

$\frac{a}{b}$	1	1.5	2.0	2.5	3.0	3.5	4.0
β	0.16	0.26	0.34	0.38	0.43	0.47	0.49
δ	0.022	0.043	0.060	0.070	0.078	0.086	0.091

All Edges Supported, Distributed Load Varying Linearly Along Breadth

$\max \sigma = \beta \frac{qb^2}{t^2}$, $\max w = \delta \frac{qb^4}{Et^3}$ where β and δ are found as follows:

$\frac{a}{b}$	1	1.5	2.0	2.5	3.0	3.5	4.0
β	0.16	0.26	0.32	0.35	0.37	0.38	0.38
δ	0.022	0.042	0.056	0.063	0.067	0.069	0.070

All Edges Fixed, Uniform Load Over Entire Surface

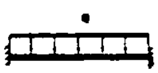

At Centers of Long Edges:

$$M_b = \frac{qb^2}{12(1+0.623\alpha^6)} = \max M$$

At Centers of Short Edges:

$$M_a = \frac{qb^2}{24}$$

At Center

$$M_b = \frac{qb^2}{8(3+4\alpha^4)} , \quad M_a = 0.009qb^2(1+2\alpha^2-\alpha^4)$$

$$\max w = \frac{0.0284}{(1+1.056\alpha^5)}\frac{qb^4}{Et^3} ,$$ formulas for M_b, $\mu = 0.3$; others $\mu = 0$

One Long Edge Fixed, Other Free, Short Edges Supported, Uniform Load Over Entire Surface

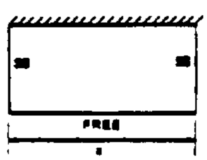

At Center of Fixed Edge:

$$\max M = M_b = \frac{qb^2}{2(1+3.2\alpha^3)}$$

At Center of Free Edge:

$$M_a = \frac{6qa^2}{\left(1+\frac{0.285}{\alpha^4}\right)} , \quad \max w = \frac{1.37qb^4}{Et^3(1+10\alpha^3)}$$

($\mu = 0.3$)

One Long Edge Clamped, Other Three Edges Supported, Uniform Load Over Entire Surface

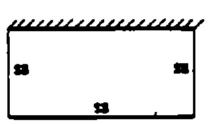

Max Stress $\sigma = \beta \frac{qb^2}{t^2}$, $\max w = \frac{\alpha qb^4}{Et^3}$

where β and α may be found from the following:

$\frac{a}{b}$	1.0	1.5	2.0	2.5	3.0	3.5	4.0
β	0.50	0.67	0.73	0.74	0.74	0.75	0.75
α	0.03	0.046	0.054	0.056	0.057	0.058	0.058

($\mu = 0.3$)

Table B9-14. (Continued)

One Short Edge Clamped, Other Three Edges Supported, Uniform Load Over Entire Surface

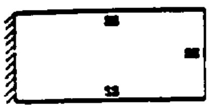

Max Stress $\sigma = \beta \frac{qb^2}{t^2}$, $\max w = \frac{\alpha q b^4}{E t^3}$

where β and α may be found from the following:

$\frac{a}{b}$	1.0	1.5	2.0	2.5	3.0	3.5	4.0
β	0.50	0.67	0.73	0.74	0.75	0.75	0.75
α	0.03	0.071	0.101	0.122	0.132	0.137	0.139

(μ = 0.3)

One Short Edge Free, Other Three Edges Supported, Uniform Load Over Entire Surface

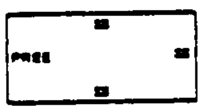

$\max \sigma = \frac{\beta q b^2}{t^2}$, $\max w = \frac{\alpha q b^4}{E t^3}$

where β and α are found from the following:

$\frac{a}{b}$	1.0	1.5	2.0	4.0
β	0.67	0.77	0.79	0.80
α	0.14	0.16	0.165	0.167

(μ = 0.3)

One Short Edge Free, Other Three Edges Supported, Distributed Load Varying Linearly Along Length

$\max \sigma = \frac{\beta q b^2}{t^2}$, $\max w = \frac{\alpha q b^4}{E t^3}$

where β and α are found from the following:

$\frac{a}{b}$	1.0	1.5	2.0	2.5	3.0	3.5	4.0
β	0.2	0.28	0.32	0.35	0.36	0.37	0.37
α	0.04	0.05	0.058	0.064	0.067	0.069	0.070

(μ = 0.3)

One Long Edge Free, Other Three Edges Supported, Uniform Load Over Entire Surface

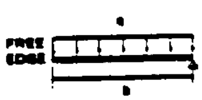

$\max \sigma = \frac{\beta q b^2}{t^2}$, $\max w = \frac{\alpha q b^4}{E t^3}$

where β and α are found from the following:

$\frac{a}{b}$	1.0	1.5	2.0
β	0.67	0.45	0.36
α	0.14	0.106	0.080

(μ = 0.3)

One Long Edge Free, Other Three Edges Supported, Distributed Load Varying Linearly Along Length

$\max \sigma = \frac{\beta q b^2}{t^2}$, $\max w = \frac{\alpha q b^4}{E t^3}$

where β and α are found from the following:

$\frac{a}{b}$	1.0	1.5	2.0
β	0.2	0.16	0.11
α	0.04	0.033	0.026

(μ = 0.3)

Table B9-14. (Continued)

All Edges Fixed, Uniform Load Over Small Concentric Circular Area Of Radius, r_0

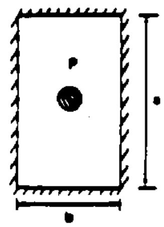

At Center:

$$M_b = \frac{P}{4\pi}\left[(1+\mu)\log\frac{b}{2r_0} + 5(1-\alpha)\right] = \max M \quad , \quad w = \beta\frac{Pb^2}{12}$$

where β has values as follows:

$\frac{a}{b}$	4	2	1
β	0.072	0.0816	0.0624

Long Edges Fixed, Short Edges Supported, Uniform Load Over Entire Surface

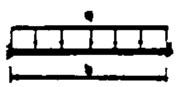

At Centers of Long Edges:

$$\max M = M_b = \frac{qb^2}{12(1+0.2\alpha^4)}$$

At Center:

$$M_b = \frac{qb^2}{24(1+0.8\alpha^4)} \quad , \quad M_a = \frac{qb^2(1+0.3\alpha^2)}{80}$$

$(\mu = 0)$

Short Edges Fixed, Long Edges Supported, Uniform Load Over Entire Surface

At Centers of Short Edges:

$$\max M = M_a = \frac{qb^2}{8(1+0.8\alpha^4)}$$

At Center:

$$M_b = \frac{qb^2}{8(1+0.8\alpha^2+6\alpha^4)} \quad , \quad M_a = \frac{0.015qb^2(1+3\alpha^2)}{(1+\alpha^4)}$$

$(\mu = 0)$

All Edges Supported, Distributed Load in Form of Triangular Prism

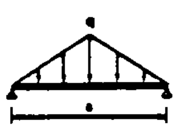

$$\max M = \beta qb^2 \quad , \quad \max w = \frac{\alpha qb^4}{D}$$

β and α found from the following:

$\frac{a}{b}$	1.0	1.5	2.0	3.0	∞
β	0.034	0.0548	0.0707	0.0922	0.1250
α	0.00263	0.00308	0.00686	0.00868	0.01302

$(\mu = 0.3)$

409

Table B9-14. (Continued)

All Edges Supported, Uniformly Distributed Edge Moment

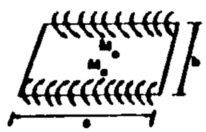

At Center:

$$M_a = \beta M_o \quad , \quad M_b = \beta_1 M_o \quad , \quad w = \frac{\alpha M_o b^2}{D}$$

β, β_1, and α are found from the following:

$\frac{b}{a}$	α	β	β_1
0	0.1250	0.300	1.000
0.5	0.0964	0.387	0.770
0.75	0.0620	0.424	0.476
1.00	0.0368	0.394	0.256
1.50	0.0280	0.264	0.048
2.00	0.0174	0.153	-0.010

One Edge Fixed, Opposite Edge Free, Other Edges Supported, Concentrated Load On Center Of Free Edge

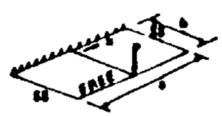

On Free Edge: $w = \frac{\alpha P b^2}{D}$ where

x	0	$\frac{b}{4}$	$\frac{b}{2}$	b	2b
α	0.168	0.150	0.121	0.068	0.016

At Center of Fixed Edge: $M = \beta P$ where

$\frac{b}{a}$	4	2	1.5	1	$\frac{2}{3}$	0.5	0.25
β	-0.000030	-0.0117	-0.0456	-0.163	-0.366	-0.436	-0.507

Table B9-15. Coefficients For Maximum Moments For Various Loads, Plate With Three Sides Fixed, One Free (μ = 0.2)

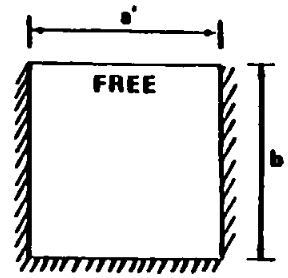

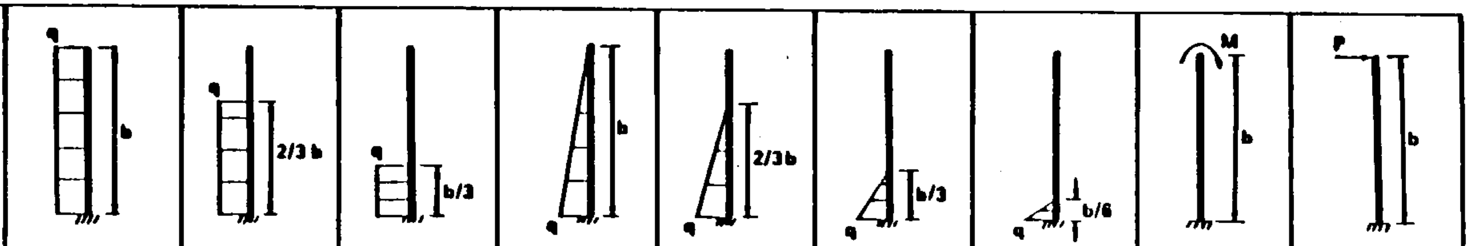

Load / a/b	q, b	q, 2/3 b	q, b/3	q, b	q, 2/3b	q, b/3	q, b/6	M, b	P, b
1/4	0.0052 qb^2	0.0051 qb^2	0.0044 qb^2	0.0038 qb^2	0.0032 qb^2	0.0017 qb^2	0.0004 qb^2	1.000 M	0.0471 Pb
1/2	0.0209 qb^2	0.0184 qb^2	0.0105 qb^2	0.0114 qb^2	0.0084 qb^2	0.0040 qb^2	0.0009 qb^2	1.000 M	0.1522 Pb
3/4	0.0476 qb^2	0.0330 qb^2	0.0140 qb^2	0.0208 qb^2	0.0131 qb^2	0.0051 qb^2	0.0013 qb^2	1.1461 M	0.2723 Pb
1	0.0852 qb^2	0.0433 qb^2	0.0131 qb^2	0.0277 qb^2	0.0165 qb^2	0.0050 qb^2	0.0012 qb^2	1.3643 M	0.3938 Pb
3/2	0.1788 qb^2	0.0617 qb^2	0.0140 qb^2	0.0433 qb^2	0.0190 qb^2	0.0042 qb^2	0.0010 qb^2	1.6292 M	0.6266 Pb
2	0.2613 qb^2	0.0757 qb^2	0.0136 qb^2	0.0644 qb^2	0.0208 qb^2	0.0039 qb^2	0.0008 qb^2	1.7779 M	0.8094 Pb
3	0.3304 qb^2	0.1036 qb^2	0.0146 qb^2	0.0857 qb^2	0.0270 qb^2	0.0038 qb^2	0.0006 qb^2	1.7980 M	0.9388 Pb

Table B9-16. Coefficients For Maximum Moments For Various Loads, Plate With Three Sides Fixed, One Hinged (μ = 0.2)

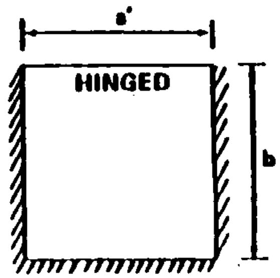

Load / a/b	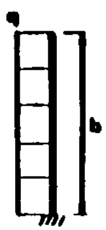	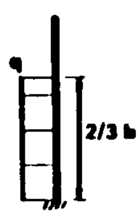		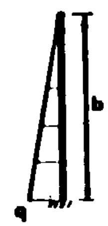	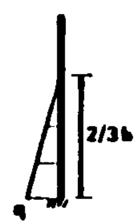	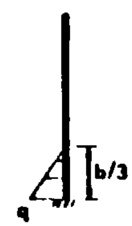	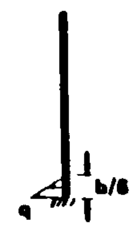	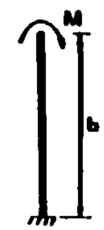
	q, b	q, 2/3 b	q, b/3	q, b	q, 2/3b	q, b/3	q, b/6	M, b
1/4	0.0052 qb^2	0.0051 qb^2	0.0044 qb^2	0.0038 qb^2	0.0032 qb^2	0.0017 qb^2	0.0014 qb^2	1.00 M
1/2	0.0201 qb^2	0.0185 qb^2	0.0105 qb^2	0.0114 qb^2	0.0084 qb^2	0.0040 qb^2	0.0025 qb^2	1.00 M
3/4	0.0403 qb^2	0.0329 qb^2	0.0132 qb^2	0.0207 qb^2	0.0131 qb^2	0.0051 qb^2	0.0027 qb^2	1.00 M
1	0.0572 qb^2	0.0425 qb^2	0.0131 qb^2	0.0269 qb^2	0.0163 qb^2	0.0050 qb^2	0.0032 qb^2	1.00 M
3/2	0.0695 qb^2	0.0472 qb^2	0.0132 qb^2	0.0302 qb^2	0.0176 qb^2	0.0041 qb^2	0.0036 qb^2	1.00 M
2	0.0664 qb^2	0.0451 qb^2	0.0120 qb^2	0.0289 qb^2	0.0161 qb^2	0.0035 qb^2	0.0038 qb^2	1.00 M
3	-0.0704 qb^2	-0.0477 qb^2	-0.0111 qb^2	-0.0297 qb^2	-0.0154 qb^2	-0.0029 qb^2	0.0039 qb^2	1.00 M

Table B9-17. Coefficients For Maximum Moments For Various Loads, Plate Fixed Along One Edge, Free On Opposite Edge And Hinged On Other Two Edges (μ = 0.2)

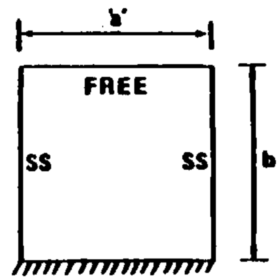

Load / a/b	q, b	q, 2/3 b	q, b/3	q, b	q, 2/3 b	q, b/3	q, b/6	M, b	P, b
1/4	-0.0080 qb^2	0.0073 qb^2	0.0066 qb^2	0.0061 qb^2	0.0055 qb^2	0.0038 qb^2	0.0020 qb^2	1.0 M	-0.0534 Pb
1/2	-0.0317 qb^2	0.0269 qb^2	0.0177 qb^2	0.0199 qb^2	0.0156 qb^2	0.0080 qb^2	0.0030 qb^2	1.0 M	-0.1300 Pb
3/4	-0.0644 qb^2	0.0497 qb^2	0.0250 qb^2	0.0353 qb^2	0.0243 qb^2	0.0101 qb^2	0.0032 qb^2	1.0 M	-0.2007 Pb
1	0.1108 qb^2	0.0757 qb^2	0.0317 qb^2	0.0535 qb^2	0.0333 qb^2	0.0122 qb^2	0.0036 qb^2	1.0 M	-0.2590 Pb
3/2	0.2136 qb^2	0.1216 qb^2	0.0406 qb^2	0.0871 qb^2	0.0471 qb^2	0.0147 qb^2	0.0040 qb^2	1.0 M	-0.3114 Pb
2	0.3007 qb^2	0.1552 qb^2	0.0461 qb^2	0.1128 qb^2	0.0565 qb^2	0.0161 qb^2	0.0043 qb^2	1.0 M	0.4831 Pb
3	0.4084 qb^2	0.1929 qb^2	0.0516 qb^2	0.1426 qb^2	0.0666 qb^2	0.0175 qb^2	0.0046 qb^2	1.0 M	0.7513 Pb

Table B9-18. Coefficients For Maximum Moments For Various Loads, Plate Fixed On Two Adjacent Sides, Free On Other Sides (μ = 0.2)

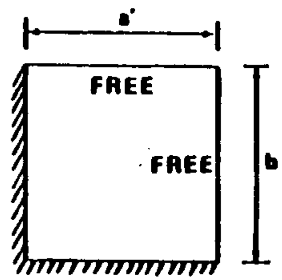

Load / a/b	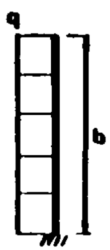	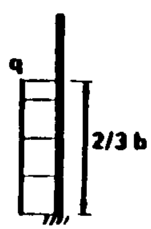		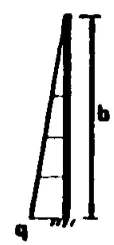	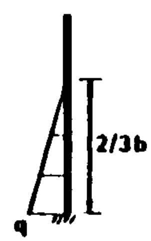	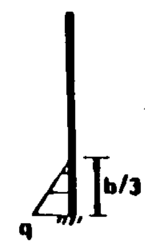	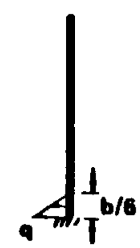
	q, b	q, 2/3 b	q, b/3	q, b	q, 2/3b	q, b/3	q, b/6
1/8	0.0083 qb^2	0.0083 qb^2	0.0057 qb^2	0.0072 qb^2	0.0066 qb^2	0.0041 qb^2	0.0027 qb^2
1/4	0.0313 qb^2	0.0289 qb^2	0.0165 qb^2	0.0221 qb^2	0.0181 qb^2	0.0087 qb^2	0.0036 qb^2
3/8	0.0664 qb^2	0.0495 qb^2	0.0238 qb^2	0.0354 qb^2	0.0257 qb^2	0.0118 qb^2	0.0038 qb^2
1/2	0.1074 qb^2	0.0775 qb^2	0.0310 qb^2	0.0546 qb^2	0.0358 qb^2	0.0140 qb^2	0.0043 qb^2
3/4	0.2076 qb^2	0.1262 qb^2	0.0402 qb^2	0.0896 qb^2	0.0507 qb^2	0.0167 qb^2	0.0048 qb^2
1	0.2949 qb^2	0.1605 qb^2	0.0456 qb^2	0.1157 qb^2	0.0603 qb^2	0.0181 qb^2	0.0050 qb^2

B9.3.3 Elliptical Plates

For plates whose boundary is the shape of an ellipse, solutions have been found for some common loadings. Table B9-19 presents the available solutions for elliptical plates. For additional information as to method of solution to the plate differential equations see Reference 1.

B9.3.4 Triangular Plates

Solutions for several loadings on triangular shaped plates are presented in Table B9-20.

B9.3.5 Skew Plates

Solutions have been obtained for skew plates in References 1 and 5. The significant results from these references are presented in Table B9-21.

Table B9-19. Solutions For Elliptical, Solid Plates

NOTE:

LOG = LOG$_e$ = NATURAL LOG.

SEE TABLE B9-1 FOR NOMENCLATURE

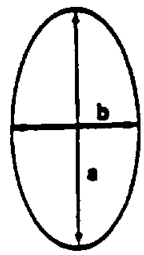

b/a = α

Edge Supported, Uniform Load Over Entire Surface	At Center: max stress $= \sigma_b = \dfrac{-0.3125(2-\alpha)qb^2}{t^2}$ max w $= \dfrac{(0.146 - 0.1\alpha)qb^4}{Et^3}$ (for $\mu = \frac{1}{3}$)
Edge Supported, Uniform Load Over Small Concentric Circular Area of Radius, r_0	At Center: max M $= M_b = \dfrac{P}{4\pi}\left[(1+\mu)\log\dfrac{b}{2r_0} + 6.57\mu - 2.57\alpha\mu\right]$ max w $= \dfrac{Pb^2}{Et^3}(0.19 - 0.045\alpha)$ $(\mu = \frac{1}{4})$
Edge Fixed, Uniform Load Over Entire Surface	At Edge: $M_a = \dfrac{qb^2\alpha^2}{4(3+2\alpha^2+3\alpha^4)}$, $M_b = \dfrac{qb^2}{4(3+2\alpha^2+3\alpha^4)}$ At Center: $M_a = \dfrac{qb^2(\alpha^2+\mu)}{8(3+2\alpha^2+3\alpha^4)}$, $M_b = \dfrac{qb^2(1+\alpha^2\mu)}{8(3+2\alpha^2+3\alpha^4)}$ max w $= \dfrac{qb^4}{64D(6+4\alpha^2+6\alpha^4)}$
Edge Fixed, Uniform Load Over Small Concentric Circular Area of Radius, r_0	At Center: $M_b = \dfrac{P(1+\mu)}{4\pi}\left(\log\dfrac{b}{r_0} - 0.317\alpha - 0.376\right)$ max w $= \dfrac{Pb^2(0.0815 - 0.026\alpha)}{Et^3}$ $(\mu = 0.25)$

Table B9-20. Solutions For Triangular Plates

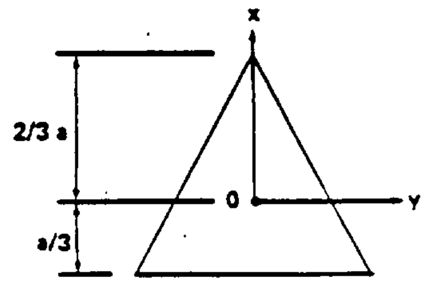

<table>
<tr>
<td>Equilateral Triangle, Edges Supported, Distributed Load Over Entire Surface</td>
<td>

$\max \sigma_x = 0.1488 \frac{qa^2}{t^2}$ at $y = 0$, $x = -0.062a$ $(\mu = 0.3)$

$\max \sigma_y = 0.1554 \frac{qa^2}{t^2}$ at $y = 0$, $x = 0.129a$ $(\mu = 0.3)$

$\max w = \frac{qa^4}{342D}$ at point 0

</td>
</tr>
<tr>
<td>Edges Supported, Load P Concentrated At 0 On Small Circular Area Of Radius, r_0</td>
<td>

$$\max \sigma_y = \frac{3(1+\mu)P}{2\pi t^2}\left[\log \frac{0.378a}{\sqrt{1.6r_0^2 + t^2} - 0.675t} - 0.379 + \frac{(1-\mu)}{2(1+\mu)}\right]$$

$\max w = 0.06852 \frac{Pa^2(1-\mu^2)}{Et^3}$ at point 0

</td>
</tr>
<tr>
<td>Right-Angle Isosceles Triangle, Edges Supported, Distributed Load Over Entire Surface

</td>
<td>

$\max \sigma_x = 0.131 \frac{qa^2}{t^2}$, $\max \sigma_y = 0.1125 \frac{qa^2}{t^2}$

$\max w = 0.0095 \frac{qa^4}{Et^3}$ $(\mu = 0.3)$

</td>
</tr>
<tr>
<td>Equilateral Triangle With Two Or Three Edges Clamped, Uniform Or Hydrostatic Load

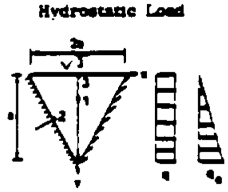

</td>
<td>

$M = \beta qa^2$ or $M = \beta_1 q_0 a^2$ where

<table>
<tr><th rowspan="2">Load Distribution</th><th colspan="4">Edge y = 0 Supported</th><th colspan="4">Edge y = 0 Clamped</th></tr>
<tr><th>M_{x_1}</th><th>M_{y_1}</th><th>M_{n_2}</th><th>M_{y_3}</th><th>M_{x_1}</th><th>M_{y_1}</th><th>M_{n_2}</th><th>M_{y_3}</th></tr>
<tr><td>Uniform β</td><td>0.0126</td><td>0.0147</td><td>-0.0285</td><td>0</td><td>0.0113</td><td>0.0110</td><td>-0.0238</td><td>-0.0238</td></tr>
<tr><td>Hydrostatic β_1</td><td>0.0053</td><td>0.0035</td><td>-0.0100</td><td>0</td><td>0.0051</td><td>0.0034</td><td>-0.0091</td><td>-0.0060</td></tr>
</table>

$(\mu = 0.2)$

</td>
</tr>
</table>

117

Table B9-21. Solutions for Skew Plates

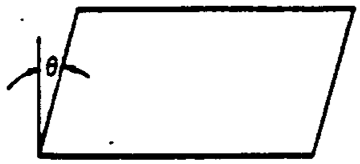

All Edges Supported, Distributed Load Over Entire Surface

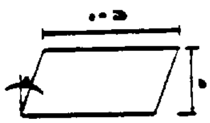

$$\max \sigma = \sigma_b = \frac{\beta q b^2}{t^2} \qquad \text{where } \beta \text{ is}$$

θ	0 deg	30 deg	45 deg	60 deg	75 deg
β	0.501	0.50	0.45	0.40	0.18

($\mu = 0.2$)

Edges b Supported, Edges a Free, Uniform Distributed Load Over Entire Surface

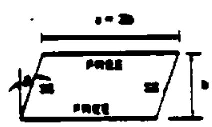

$$\max \sigma = \sigma_b = \frac{\beta q b^2}{t^2} \qquad \text{where } \beta \text{ is}$$

θ	0 deg	30 deg	45 deg	60 deg
β	0.762	0.615	0.437	0.250

All Edges Clamped, Uniform Distributed Load Over Entire Surface

At Center: $M = \beta q a^2 \qquad w = \frac{\beta_1 q a^4}{D}$

where β and β_1 are

Skew Angle θ (deg)	$\frac{a}{b} = 1$		$\frac{a}{b} = 1.25$		$\frac{a}{b} = 1.5$		$\frac{a}{b} = 2.0$	
	β	β_1	β	β_1	β	β_1	β	β_1
15	0.024	0.001123	0.019	0.00066	0.015	0.00038	0.0097	0.00014
30	0.020	0.00077	0.018	0.00045	0.0125	0.00026	0.0075	0.00009
45	0.015	0.00038	0.011	0.00022	0.014	0.00012	0.006	0.00004
60	0.0085	0.00011	0.0062	0.00006	0.0048	0.00003	0.0025	0.00001
75	0.0025	0.000009	0.0027	0.000006	0.00125	0.000002	0.00125	

Along Fixed Edge:

The coefficient β_2 for maximum bending moment along the edge at a distance fa from the acute corner is

($M = \beta_2 q a^2$ for $\frac{a}{b} = 1$)

Skew Angle (deg)	β_2	f
15	-0.0475	0.6
30	-0.0400	0.69
45	-0.0299	0.80

REFERENCES

1. Timoshenko, S. and Woinowsky-Krieger, S.: Theory of Plates and Shells. McGraw-Hill, New York, 1959.

2. Den Hartog, J. P.: Advanced Strength of Materials. McGraw-Hill, New York, 1952.

3. Bruhn, E. F.: Analysis and Design of Flight Vehicle Structures. Tri-State Offset Company, Cincinnati, Ohio, 1965.

4. Heuhert, M. and Sommer, A.: Rectangular Shell Plating Under Uniformly Distributed Hydrostatic Pressure. NACA TM 965.

5. Iyengar, K. T. and Srinivasan, R. S.: Clamped Skew Plate Under Uniform Normal Loading. Journal of the Royal Aeronautical Society, February 1967.

6. Dow, N. F. and Hubka, R. F.: Formulas for the Elastic Constants of Plates with Integral Waffle-Like Stiffening. NACA Report 1195, 1954.

7. MIL-HDBK-23, Structural Sandwich Composites. Department of Defense, Washington, D. C., July 1968.

8. Kan, Han-Pin and Huang, Ju-Chin: Large Deflection of Rectangular Sandwich Plates. Tennessee Technological University, Cookeville, Tennessee, February 1967.

9. Smith, C. V.: Large Deflections of Circular Sandwich Plates. Georgia Institute of Technology, Atlanta, Georgia, October 1967.

BIBLIOGRAPHY

Roark, R. J.: Formulas for Stress and Strain. McGraw-Hill, New York, Third Edition, 1954.

419

Data Source, Section 1.3 Reference 3

7.11 Introduction to Membranes

A membrane may be defined as a plate that is so thin that it may be consiered to have no bending rigidity. The only stresses present are in the plane of the surface and are uniform throughout the thickness of the membrane. This section consists of methods of analysis of circular membranes, long rectangular membranes ($a/b > 5$), and short rectangular membranes ($a/b < 5$).

7.12 Nomenclature for Membranes

a	= length dimension of membrane
b	= width dimension of membrane
D	= diameter
E	= modulus of elasticity
f	= calculated stress
f_{max}	= calculated maximum stress
$n_1 - n_7$	= coefficients given in Figure 7.40
p	= pressure
R	= outside radius of circular membrane
r	= cylindrical coordinate
t	= thickness of membrane
x, y	= rectangular coordinates
δ	= deflection
δ_c	= center deflection of circular membrane
μ	= Poisson's ratio

7.13 Circular Membranes

Figure 7.35 shows two views of a circular membrane with the edge clamped under a uniform pressure, p.

The maximum deflection of this membrane is at the center and is given by

$$\delta_c = 0.662\, R \sqrt[3]{\frac{p\, R}{Et}} \qquad (7\text{-}32)$$

The deflection of the membrane at a distance, r, from the center is

$$\delta = \delta_c \left[1 - .09 \left(\frac{r}{R} \right)^2 - 0.1 \left(\frac{r}{R} \right)^5 \right] \qquad (7\text{-}33)$$

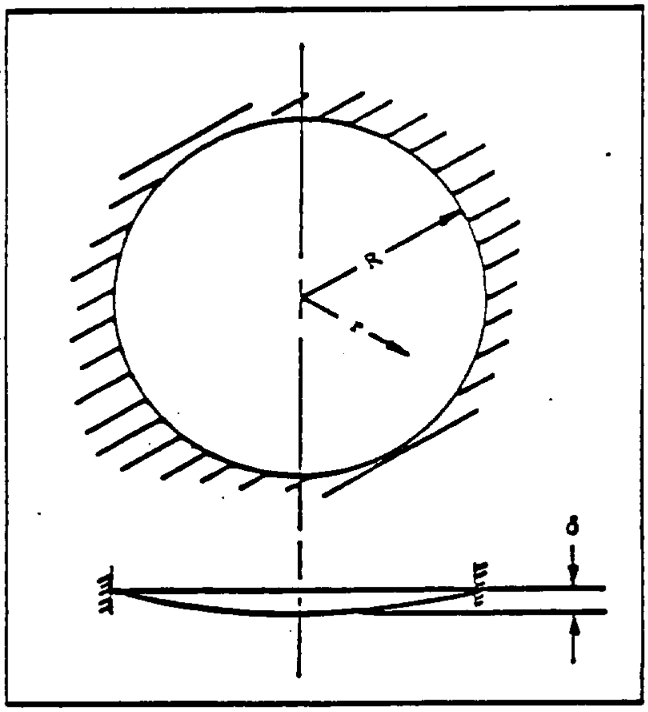

FIGURE 7.35. CIRCULAR MEMBRANE WITH CLAMPED EDGE

The stress at the center of this membrane is

$$f = 0.423 \sqrt[3]{\frac{Ep^2R^2}{t^2}} \qquad (7\text{-}34)$$

while that at the edge is

$$f = 0.328 \sqrt[3]{\frac{Ep^2R^2}{t^2}} \qquad (7\text{-}35)$$

7.14 Long Rectangular Membranes

Figure 7.36 shows a long rectangular membrane ($a/b > 5$) clamped along the two long sides.

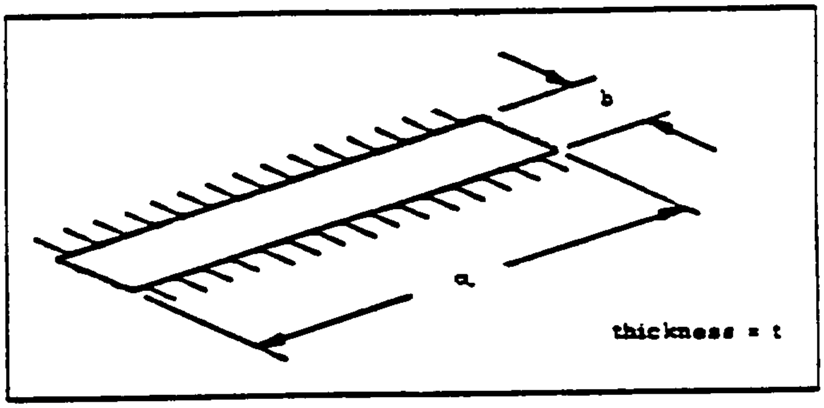

FIGURE 7.36. LONG RECTANGULAR MEMBRANE CLAMPED ON TWO LONG SIDES

The deflection and stress at the center of a long membrane clamped on all four sides are approximately the same as those in a long membrane clamped along the two long sides. The maximum stress and center deflection of the membrane in Figure 7.36 under uniform pressure p are given by Equations (7-36) and (7-37).

$$f_{max} = \left[\frac{p^2Eb^2}{24(1-\mu^2)t^2}\right]^{1/3} \qquad (7\text{-}36)$$

$$\frac{\delta}{b} = \frac{1}{8}\left[\frac{24(1-\mu^2)pb}{Et}\right]^{1/3} \qquad (7\text{-}37)$$

These equations are presented graphically in Figures 7.37 and 7.38 for $\mu = 0.3$.

A long rectangular plate may be considered to be a membrane if $P/E(b/t)^4$ is greater than 100.

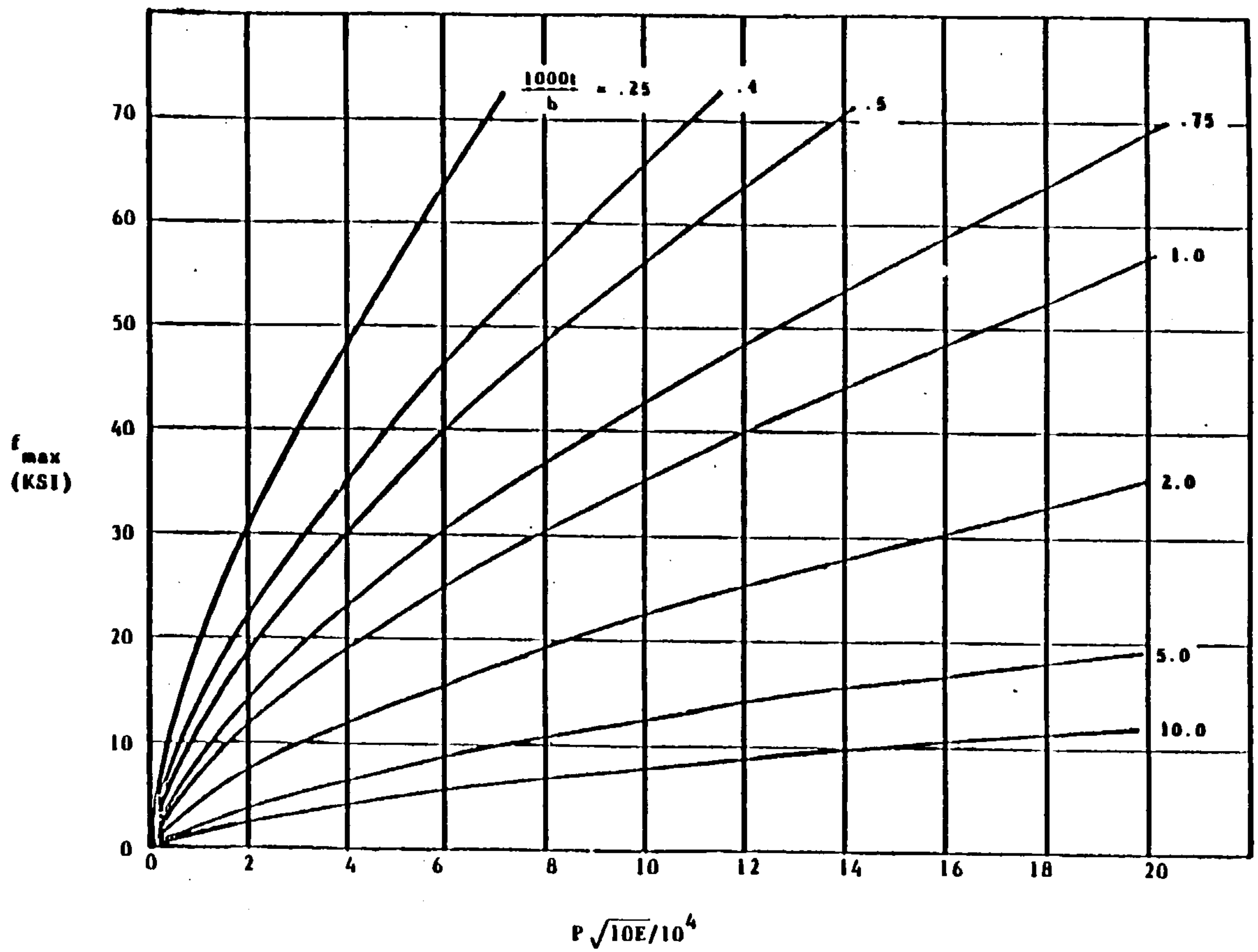

FIGURE 7.37 MAXIMUM STRESS IN LONG RECTANGULAR MEMBRANES ($a/b > 5$) HELD ALONG LONG SIDES ($\mu = 0.3$)

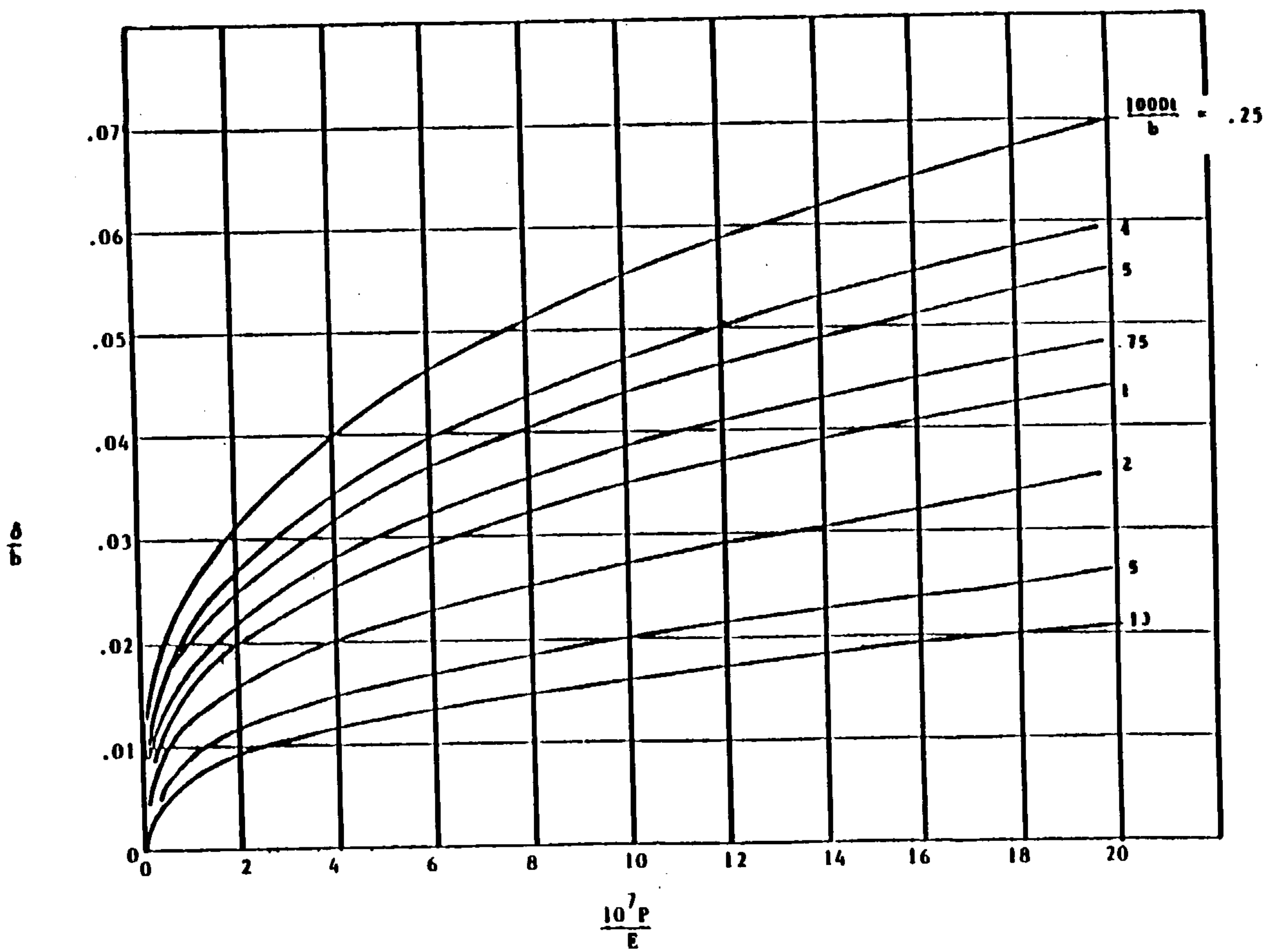

FIGURE 7.38 CENTER DEFLECTION OF LONG RECTANGULAR MEMBRANES (a/b > 5) HELD ALONG LONG SIDES (μ = 0.3)

7.15 Short Rectangular Membranes

Figure 7.39 shows a short rectangular membrane ($a/b < 5$) clamped on four sides under a uniform pressure p.

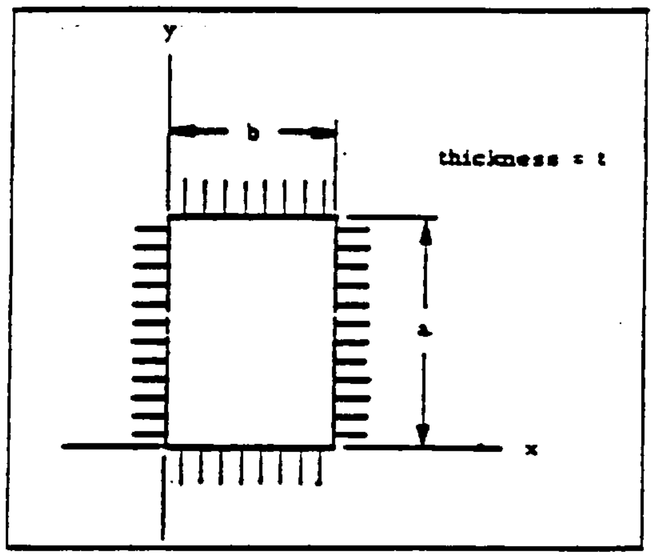

FIGURE 7.39. SHORT RECTANGULAR MEMBRANE CLAMPED ON FOUR SIDES

The deflection at the center of such a membrane is

$$\delta = n_1 \, a \sqrt[3]{\frac{pa}{Et}} \qquad (7\text{-}38)$$

where n_1 is given in Figure 7.40.

The stresses at various locations on short rectangular membranes are given by the following equations for which the values of the coefficients n_2 through n_7 are given in Figure 7.40.

Center of plate ($x = b/2$, $y = a/2$)

$$f_x = n_2 \sqrt[3]{p^2 E \left(\frac{a}{t}\right)^2} \qquad (7\text{-}39)$$

$$f_y = n_3 \sqrt[3]{p^2 E \left(\frac{a}{t}\right)^2} \qquad (7\text{-}40)$$

-125

Center of short side ($x = b/2$, $y = 0$)

$$f_x = n_4 \sqrt[3]{p^2 E \left(\frac{a}{t}\right)^2} \qquad (7\text{-}41)$$

$$f_y = n_5 \sqrt[3]{p^2 E \left(\frac{a}{t}\right)^2} \qquad (7\text{-}42)$$

Center of long side ($x = 0$, $y = a/2$)

$$f_x = n_6 \sqrt[3]{p^2 E \left(\frac{a}{t}\right)^2} \qquad (7\text{-}43)$$

$$f_y = n_7 \sqrt[3]{p^2 E \left(\frac{a}{t}\right)^2} \qquad (7\text{-}44)$$

It should be noted that the <u>maximum</u> membrane stress occurs at the center of the long side of the plate.

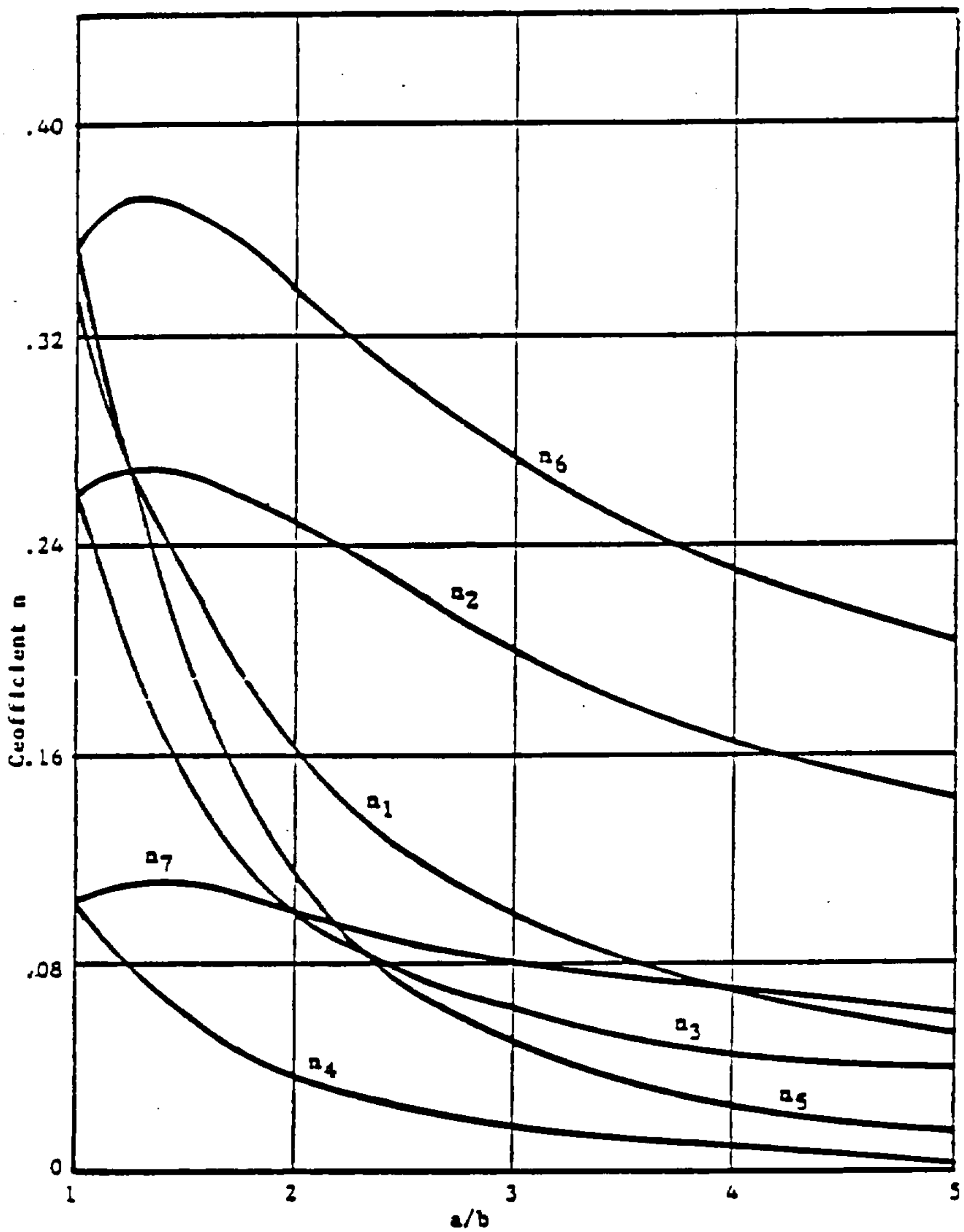

FIGURE 7.40 COEFFICIENTS FOR EQUATIONS (7-38) THROUGH (7-44)

SECTION 7.0

STIFFENED PLATES

DATA IS PRESENTED FOR BUCKLING OF PLATES WITH VARIOUS STIFFENER CONFIGURATIONS.

		PAGE
7.1	BUCKLING IN AXIAL COMPRESSION	7.1.1
7.2	ANALYTICAL METHODS	7.2.1
	EFFECTIVE SKIN WIDTHS	7.2.4
7.3	ISOGRID STRUCTURES	7.3.1

Data Source, Section 1.3 Reference 3

7.3.2 Buckling of Stiffened Flat Plates in Axial Compression

The treatment of stiffened flat plates is the same as that of unstiffened plates except that the buckling coefficient, k, is now also a function of the stiffener geometry. Equation (7-1) is the basic analysis tool for the critical buckling stress.

As the stiffener design is a part of the total design, Figures 7-11 and 7-12 present buckling coefficients for various types of stiffeners. The applicable critical buckling equation is indicated on each figure.

A plasticity reduction factor η applicable to channel and Z- section stiffeners is given by Equation (7-8)

$$\eta = .95 \left(\frac{E_s}{E}\right)\left(\frac{1-\nu_e^2}{1-\nu^2}\right) \tag{7-8}$$

For other structural elements such as hat and rectangular sections, no specific plasticity correction factor has been established.

Values for the buckling coefficient, k_c, for axially stiffened, infinitely wide plates are given in Figure 7-13.

Figure 7-14 presents curves for finding a value for k for plates with transverse stiffeners. It is noted that in these plots, the torsional rigidity, GJ, of the stiffener itself is used, whereas in most data for longitudinal stiffeners, no torsional properties of the stiffeners are included.

In this brief section on buckling, an attempt has been made to present data that is most often used for routine analysis. Should the user require a more comprehensive treatment of buckling,* References 36, 37 and 38 are excellent sources of additional data.

* Data Source, Section 1.3 Reference 3

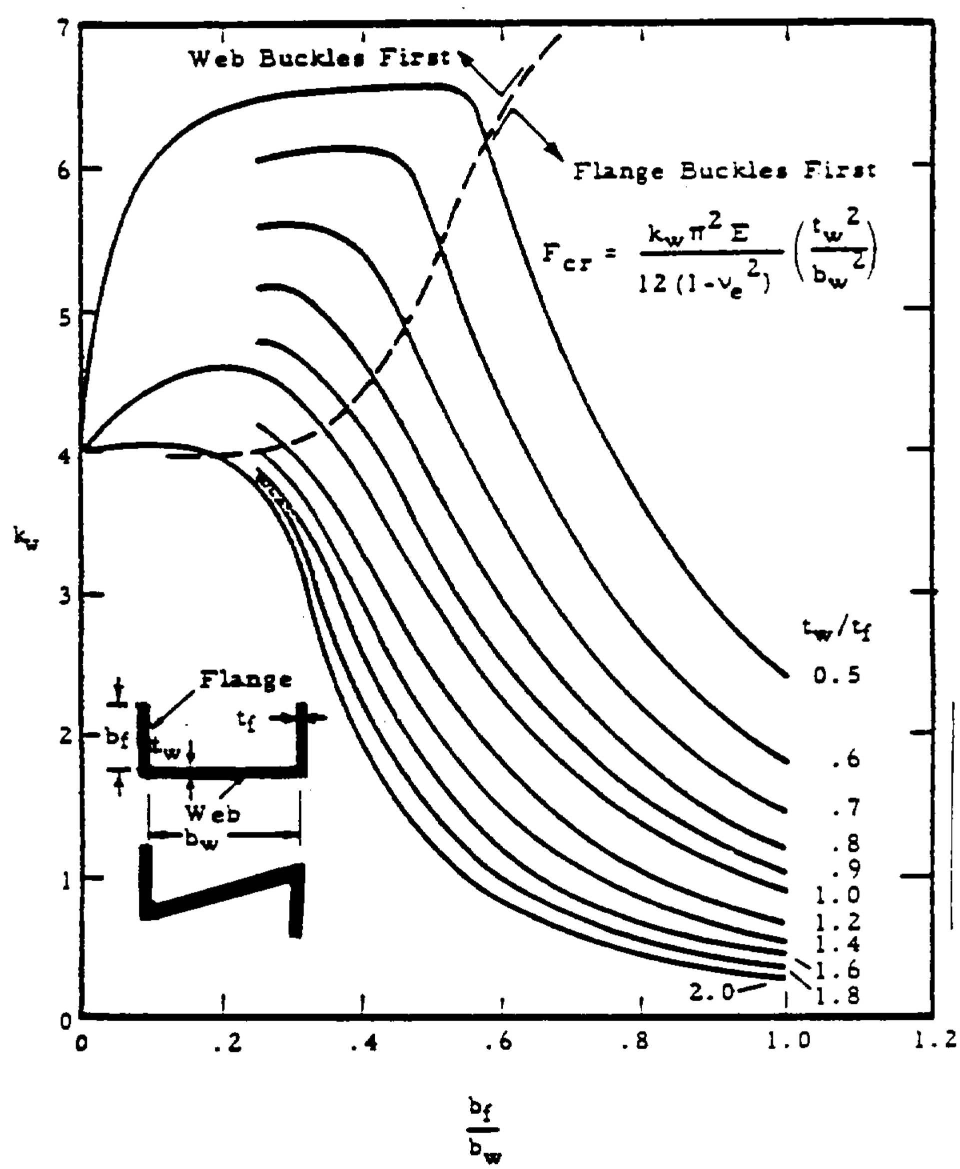

(a) Channel and Z Section Stiffeners

FIGURE 7.11 BUCKLING COEFFICIENTS FOR STIFFENERS

2

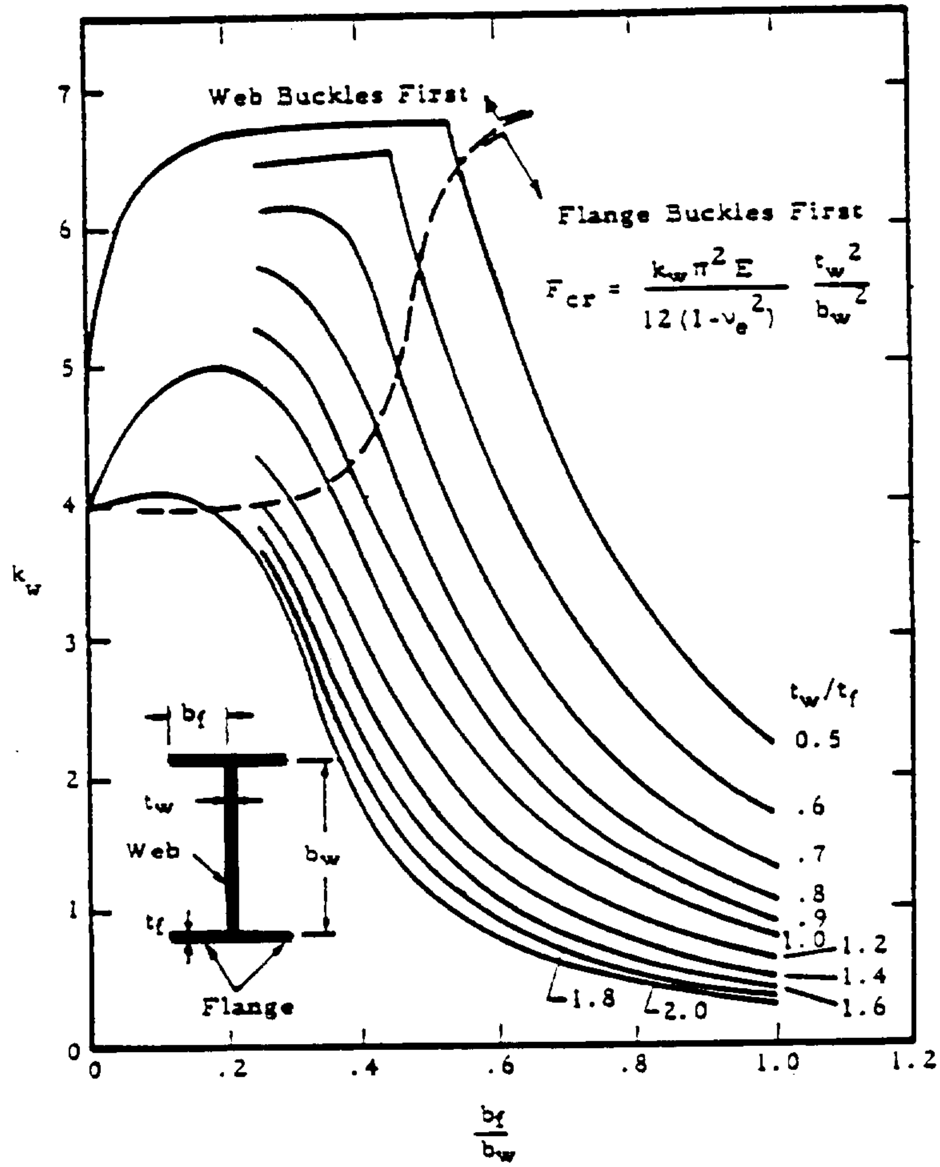

(b) H Section Stiffeners

FIGURE 7.11 (CONT'D) BUCKLING COEFFICIENTS FOR STIFFENERS

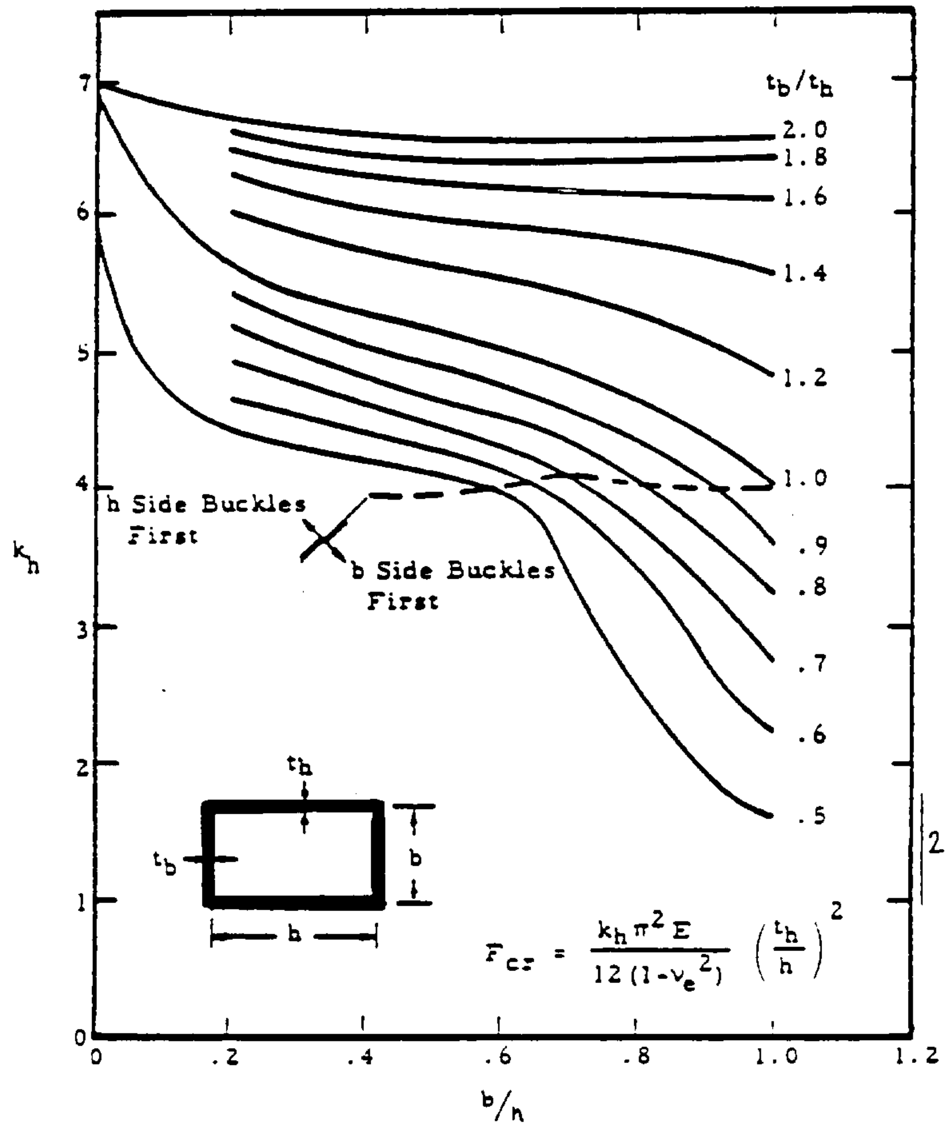

(c) Rectangular Tube Section Stiffeners

FIGURE 7.11 (CONT'D) BUCKLING COEFFICIENTS FOR STIFFENERS

2

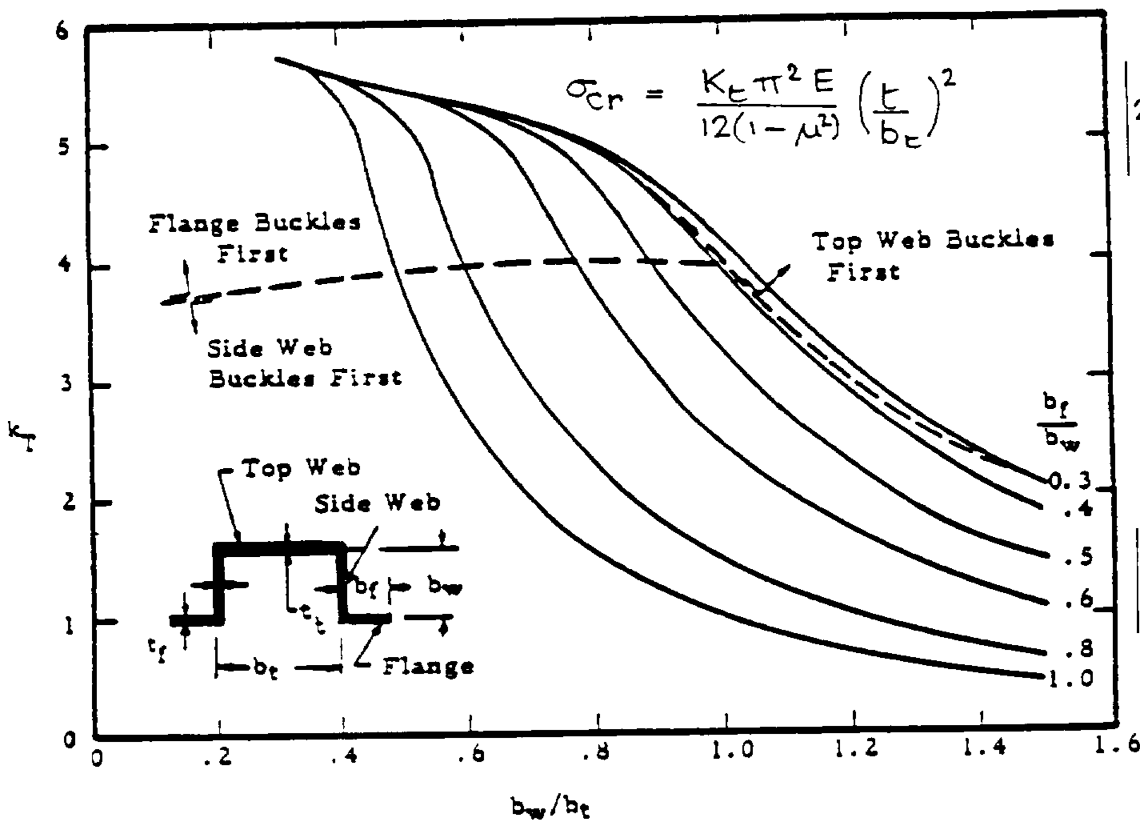

FIGURE 7.12 BUCKLING STRESS FOR HAT SECTION STIFFENERS ($t = t_f = t_w = t_t$)

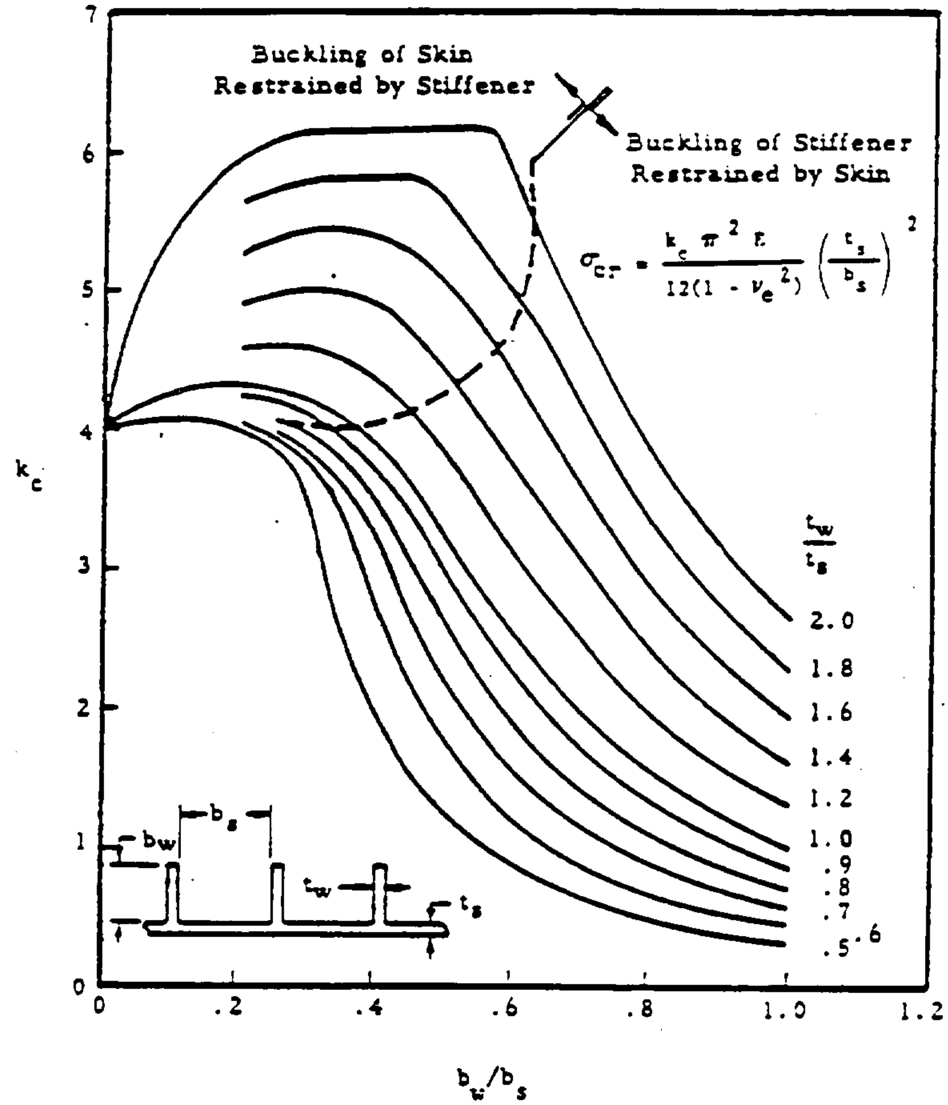

a) Web Stiffeners. $0.5 < t_w/t_s < 2.0$

FIGURE 7.13 COMPRESSIVE LOCAL BUCKLING COEFFICIENTS FOR INFINITELY WIDE IDEALIZED STIFFENED FLAT PLATES

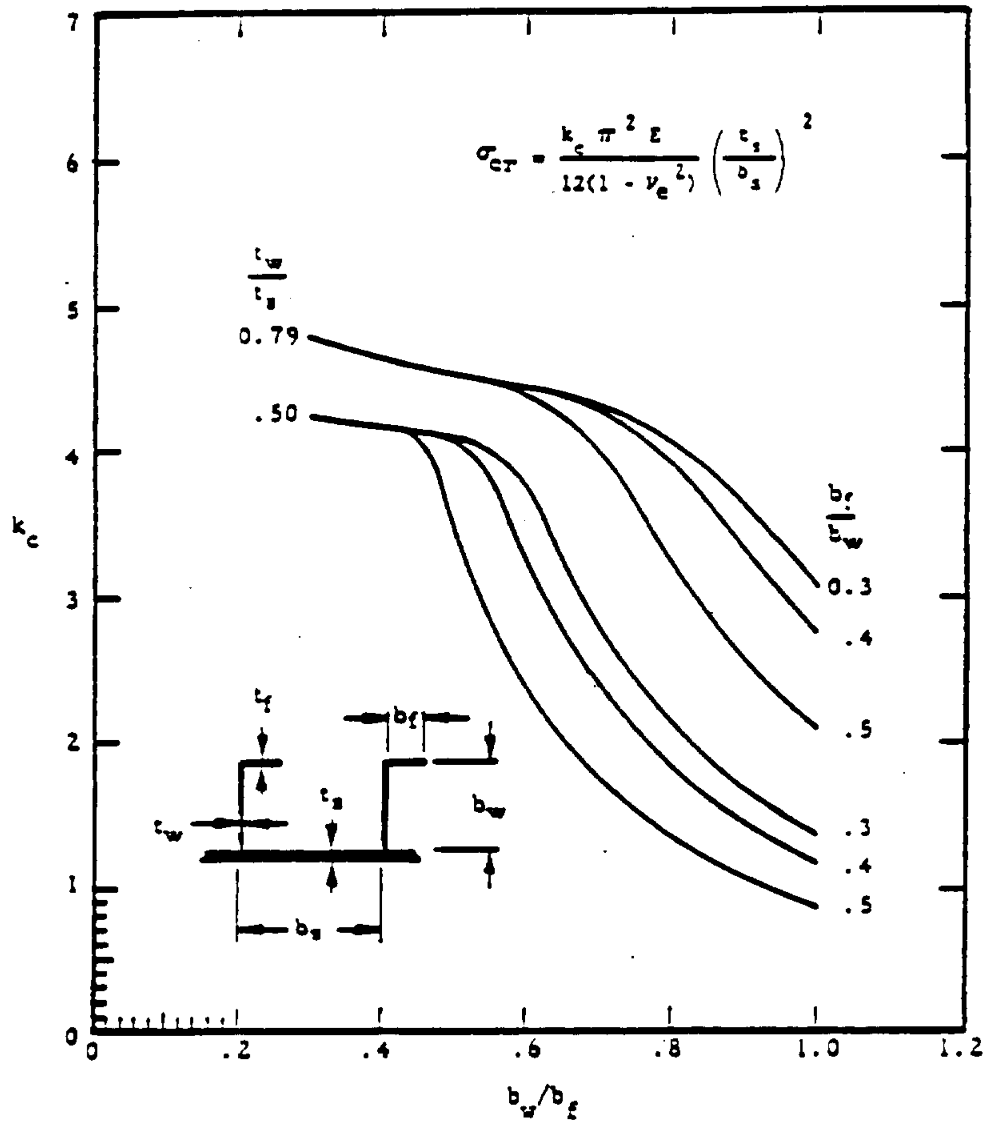

b) Z-Section Stiffeners. t_w/t_s = 0.50 and 0.79

FIGURE 7.13 (CONT'D) COMPRESSIVE LOCAL BUCKLING COEFFICIENTS FOR INFINITELY WIDE IDEALIZED STIFFENED FLAT PLATES

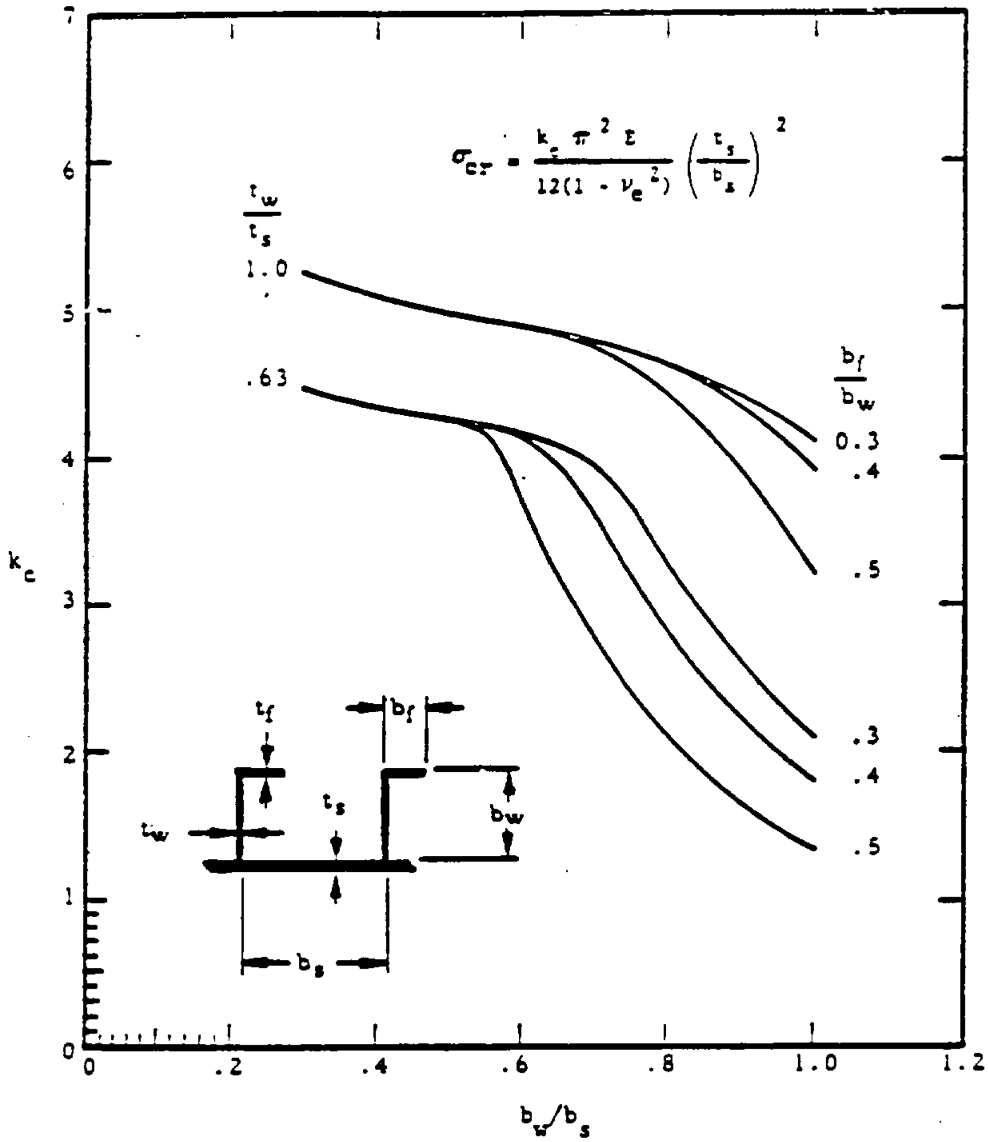

c) Z-Section Stiffeners. t_w/t_s = 0.63 and 1.0

FIGURE 7.13 (CONT'D) COMPRESSIVE LOCAL BUCKLING COEFFICIENTS FOR INFINITELY WIDE IDEALIZED STIFFENED FLAT PLATES

437

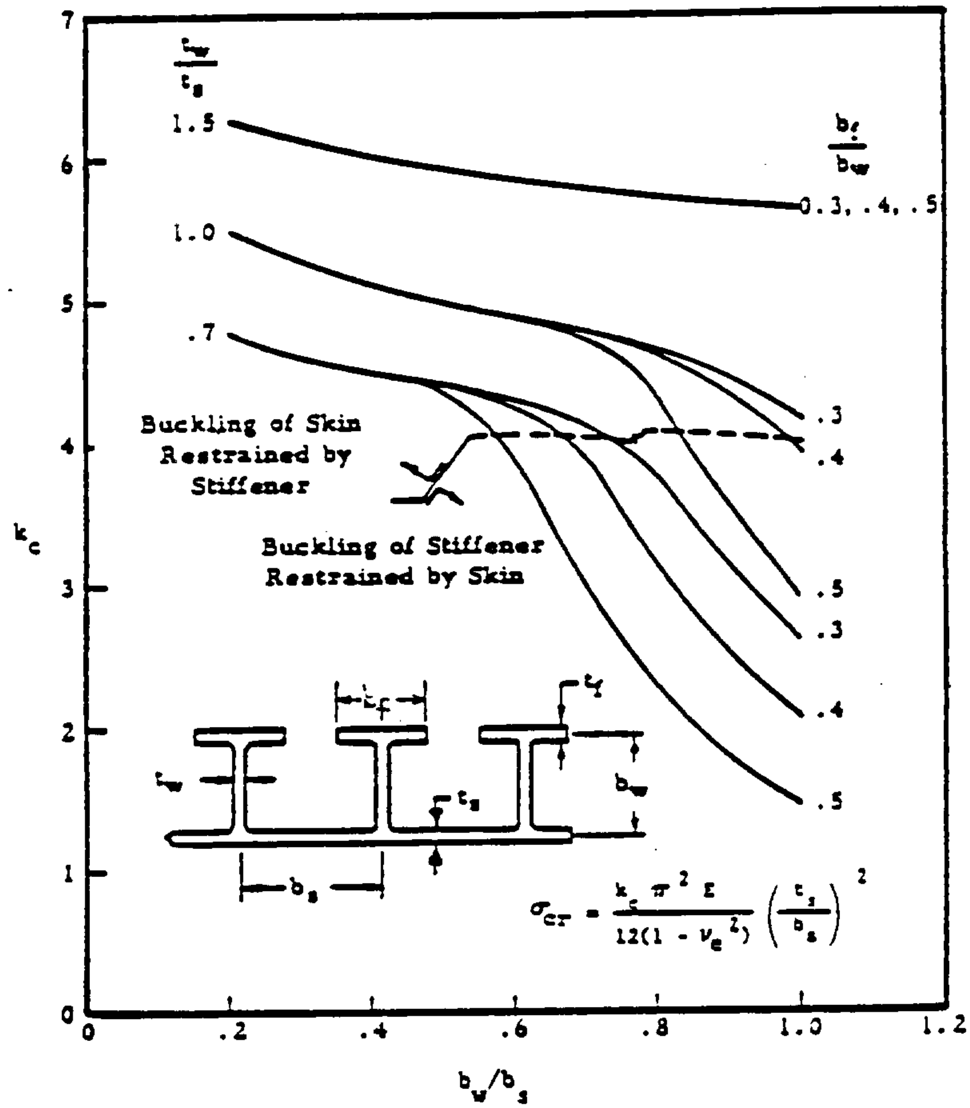

d) T-Section Stiffeners. $\frac{t_w}{t_f} = 1.0$; $\frac{b_f}{t_f} > 10$; $\frac{b_w}{b_s} > 0.25$

FIGURE 7.13 (CONT'D) COMPRESSIVE LOCAL BUCKLING COEFFICIENTS FOR INFINITELY WIDE IDEALIZED STIFFENED FLAT PLATES

FOR $\frac{t_w}{t_f} = 0.7$, SEE NACA TN. 3782

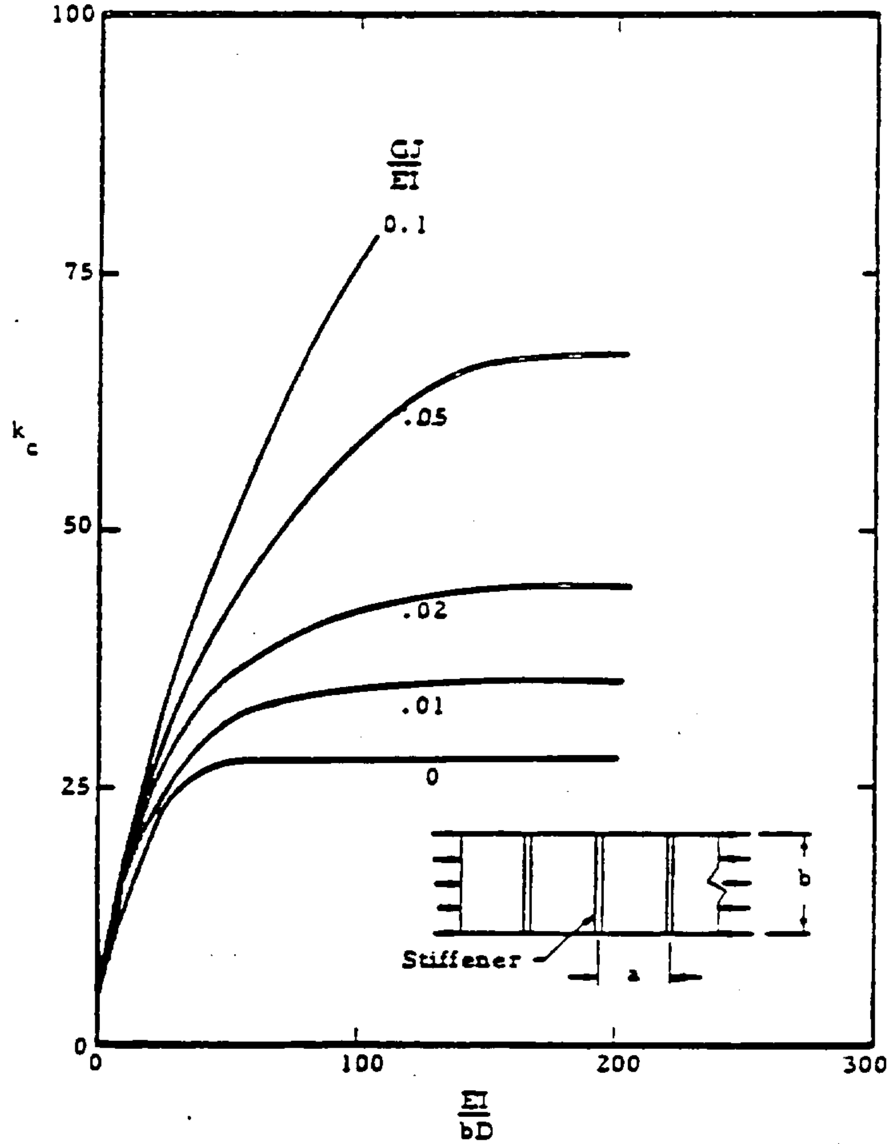

(a) a/b = 0.20

FIGURE 7.14 LONGITUDINAL COMPRESSIVE BUCKLING COEFFICIENTS FOR SIMPLY SUPPORTED PLATES WITH TRANSVERSE STIFFENERS

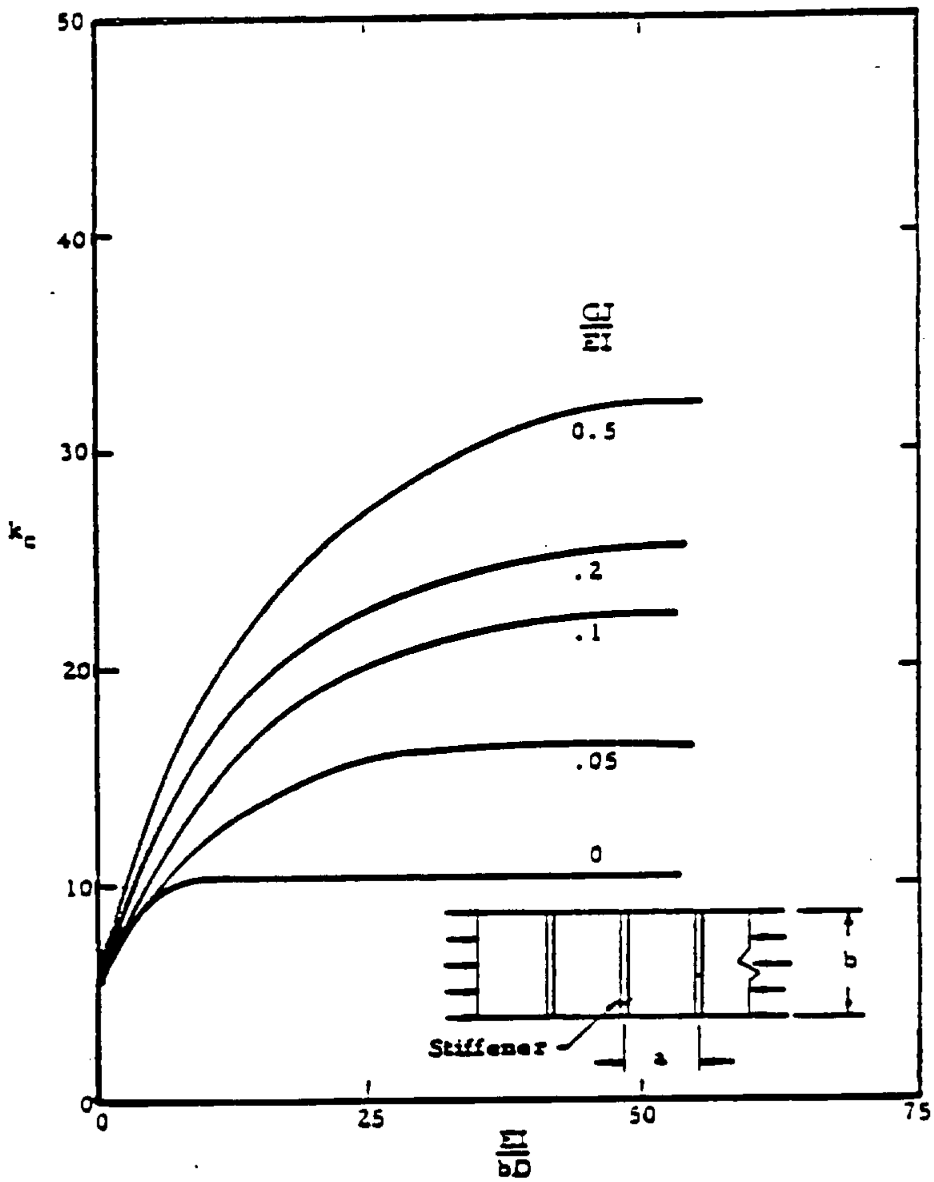

(b) a/b = 0.35

FIGURE 7.14 (CONT'D) LONGITUDINAL COMPRESSIVE BUCKLING COEFFICIENTS FOR SIMPLY SUPPORTED PLATES WITH TRANSVERSE STIFFENERS

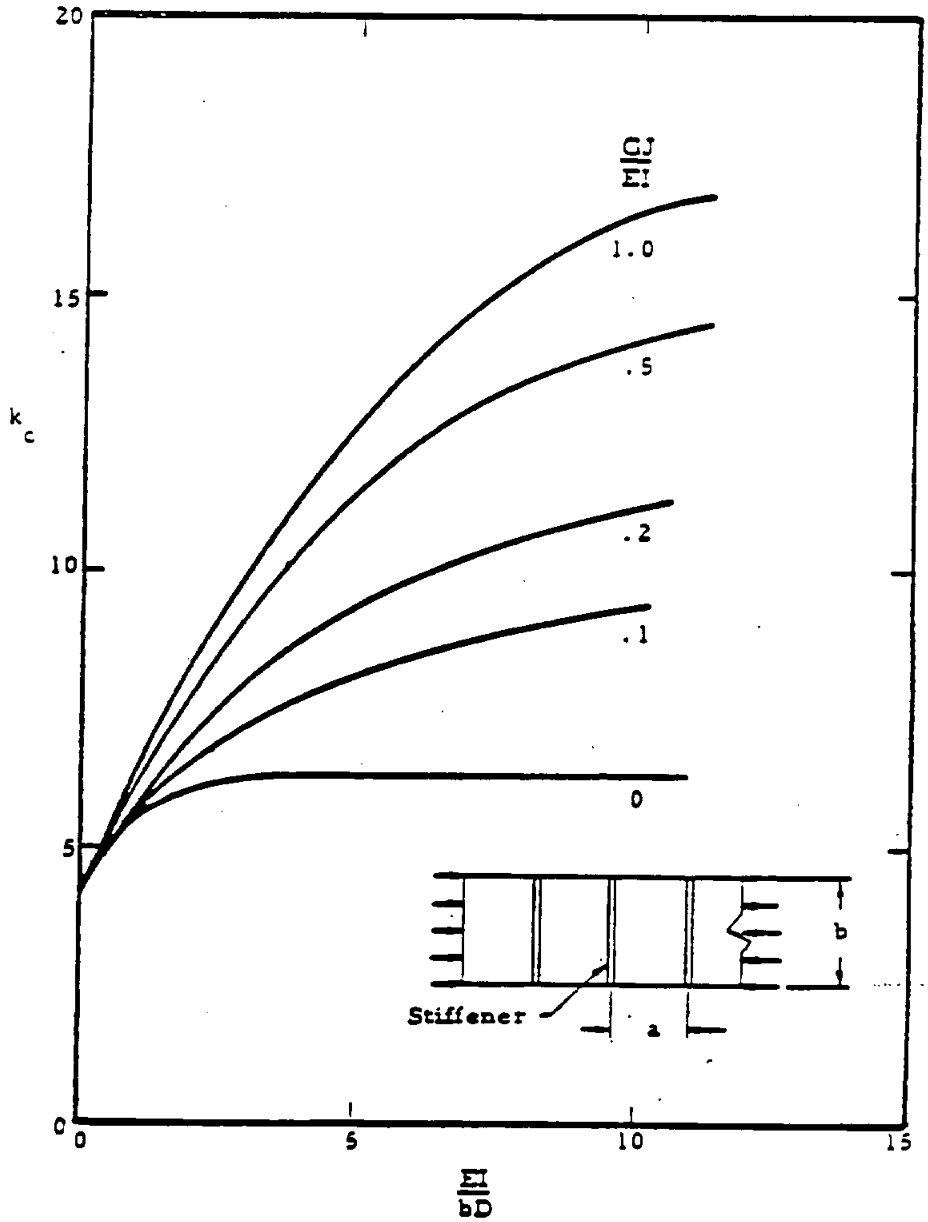

(c) a/b = 0.50

FIGURE 7.14 (CONT'D) LONGITUDINAL COMPRESSIVE BUCKLING COEFFICIENTS FOR SIMPLY SUPPORTED PLATES WITH TRANSVERSE STIFFENERS

7.3.3 Crippling Failure of Flat Stiffened Plates in Compression

For stiffened plates having slenderness ratios $L'/\rho \leq 20$, considered to be short plates, the failure mode is crippling rather than buckling when loaded in compression. The crippling strength of individual stiffening elements is considered in Section 5.0 The crippling strength of panels stiffened by angle-type elements is given by Equation (7-9).

t_w = STIFF. THICKNESS
t_s = SKIN THICKNESS.

$$\frac{\overline{F}_f}{F_{cy}} = \beta_g \left[\frac{g t_w t_s}{A} \left(\frac{\overline{\eta} \; E}{F_{cy}} \right)^{\frac{1}{2}} \right]^{0.85} \qquad (7-9)$$

For more complex stiffeners such as Y sections, the relation of Equation (7-10) is used to find a weighted value of t_w.

$$\overline{t_w} = \frac{\Sigma \; a_i \, t_i}{\Sigma \; a_i} \qquad (7-10)$$

where a_i and t_i are the length and thickness of the cross-sectional elements of the stiffener. Figure 7-15 shows the method of determining the value of g used in Equation (7-9) based on the number of cuts and flanges of the stiffened panels. Figure 7-16 gives the coefficient β_g for various stiffening elements.

If the skin material is different from the stiffener material, a weighted value of F_{cy} given by Equation (7-11) should be used. Here $\overline{t}$ is the effective thickness of the stiffened panel.

$$\overline{F}_{cy} = \frac{F_{cy_s} + F_{cy_w} \left[(\overline{t}/t_s) - 1 \right]}{(\overline{t}/t_s)} \qquad (7-11)$$

The above relations assume the stiffener-skin unit to be formed monolithically; that is, the stiffener is an integral part of the skin. For riveted construction, the failure between the rivets must be considered. The interrivet buckling stress is determined as to plate buckling stress, and is given by Equation (7-12).

$$F_i = \left(\frac{c \, \pi^2 \, \eta \, \overline{\eta} \, E}{12(1-\nu^2)} \right) \left(\frac{t_s}{p} \right)^2 \qquad (7-12)$$

Values of c, the edge fixity, are given in Table 7-2.

After the interrivet buckling occurs, the resultant failure stress of the panel is given by Equation (7-13).

$$\overline{F}_{f_T} = \frac{F_i \; (2b_{e_i} \; t_s) + \overline{F}_{f_{st}} \; A_{st}}{(2b_{e_i} \; t_s) + A_{st}} \qquad (7-13)$$

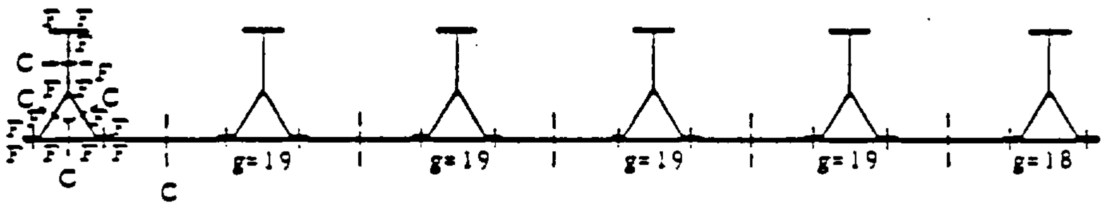

5 cuts
14 flanges
19 = g

Average g = 18.85

(a) Y-stiffened panel

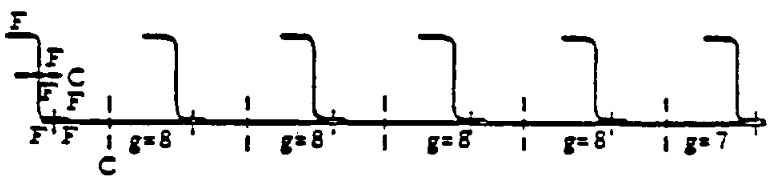

2 cuts
6 flanges
8 = g

Average g = 7.83

(b) Z-stiffened panel

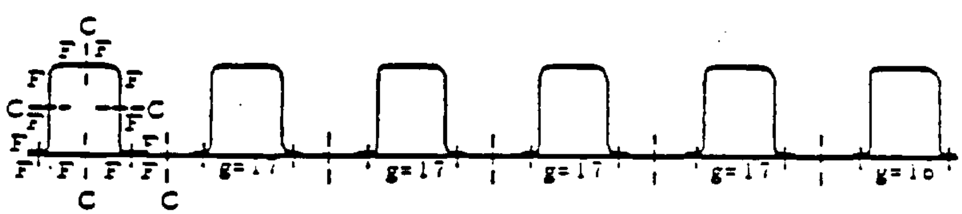

Average g = 16.83

5 cuts
12 flanges
17 = g

(c) Hat-stiffened panel

FIGURE 7.15 METHOD OF CUTTING STIFFENED PANELS TO DETERMINE g

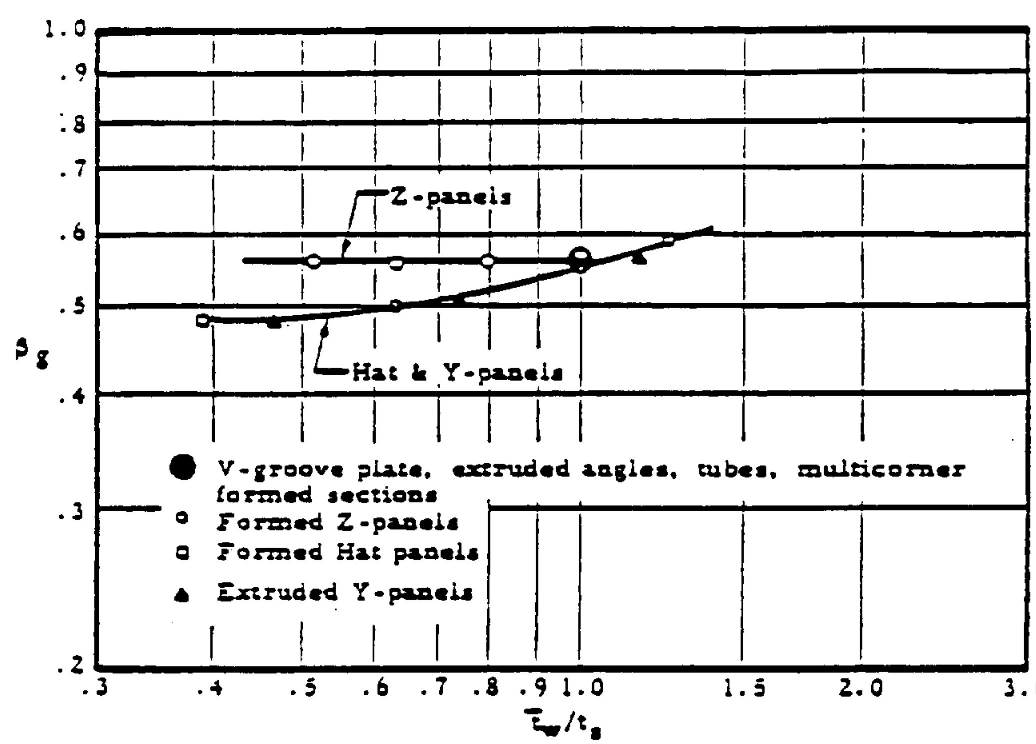

FIGURE 7.15 CRIPPLING COEFFICIENTS FOR ANGLE-TYPE ELEMENTS

INTER RIVET BUCKLING END FIXITY

Fastener Type	(Fixity-Coefficient) c
Flathead rivet	4
Spotwelds	3.5
Brazier-head rivet	3
Countersunk rivet	1

TABLE 7.2 END FIXITY COEFFICIENTS FOR ANGLE-TYPE ELEMENTS

Stringer Stability	Panel Strength
$\bar{F}_{f_{st}} \geq \bar{F}_w$ - stable	$\bar{F}_{fr} = \bar{F}_w$
$\bar{F}_{f_{st}} < \bar{F}_w$ - unstable	$\bar{F}_{fr} = \dfrac{\bar{F}_w b_s t_s + \bar{F}_{f_{st}} A_{st}}{b_s t_s + A_{st}}$

TABLE 7.3 RIVETED PANEL STRENGTH DETERMINATION

Here the value b_{ei} is the effective width of skin corresponding to the interrivet buckling stress F_i . The failure stress of short riveted panels by wrinkling can be determined. The following quantities are used:

- $\overline{F}_{fst}$ crippling strength of stringer alone (see Section 11, Column Analysis)
- $\overline{F}_w$ wrinkling strength of the skin
- $\overline{F}_f$ crippling strength of a similar monolithic panel
- $\overline{F}_{fr}$ strength of the riveted panel

The wrinkling strength of the skin can be determined from Equation (7-14) and Figure 7-17. Here f is the effective rivet offset distance given in Figure 7-18. This was obtained for aluminum rivets having a diameter greater than 90% of the skin thickness.

$$F_w = \left(\frac{k_w \pi^2 \eta \overline{\eta} E}{12(1-\nu^2)}\right)\left(\frac{t_s}{b_s}\right)^2 \qquad (7\text{-}14)$$

Now, based on the stringer stability, the strength of the panel can be calculated. Table 7-3 shows the various possibilities and solutions.

It is noted that in no case should $\overline{F}_{fr} > \overline{F}_f$. Thus, the lower of these two values should be used.

The use of the coefficient k_w is based upon aluminum alloy data for other materials. The procedure is to use Equation (7-15) for the panel crippling strength.

$$\frac{F_{fr}}{F_{cy}} = 17.9 \left(\frac{t_w}{f}\right)^{4/3}\left(\frac{t_w}{b_w}\right)^{1/6}\left[\frac{t_s}{b_s}\left(\frac{\eta E}{F_{cy}}\right)\right]^{1/2} \qquad (7\text{-}15)$$

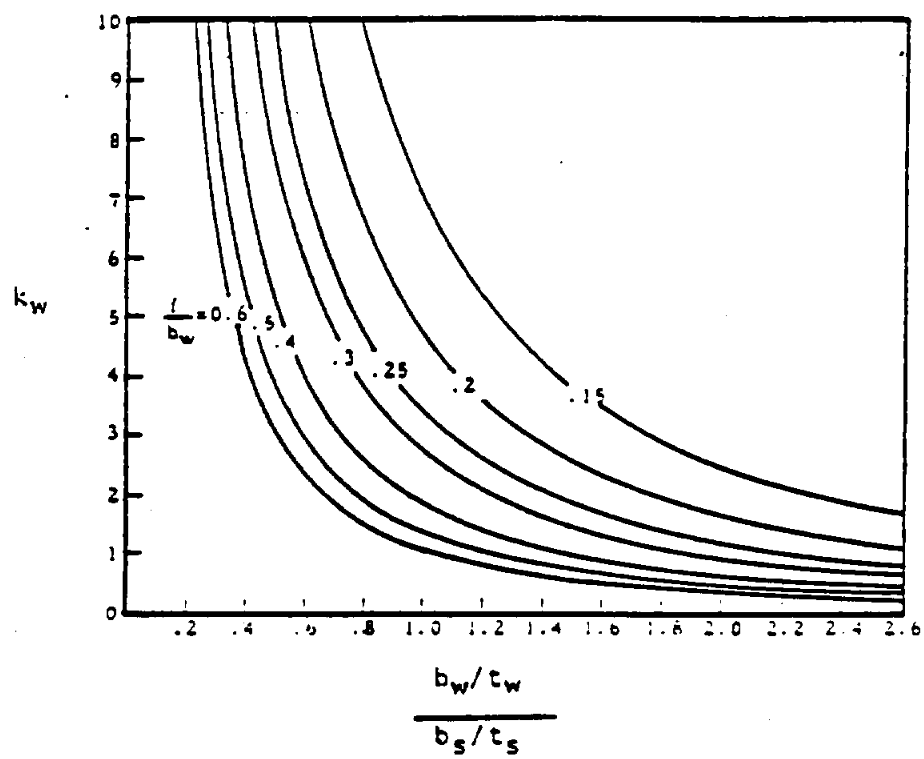

FIGURE 7.17 EXPERIMENTALLY DETERMINED COEFFICIENTS FOR FAILURE IN WRINKLING MODE

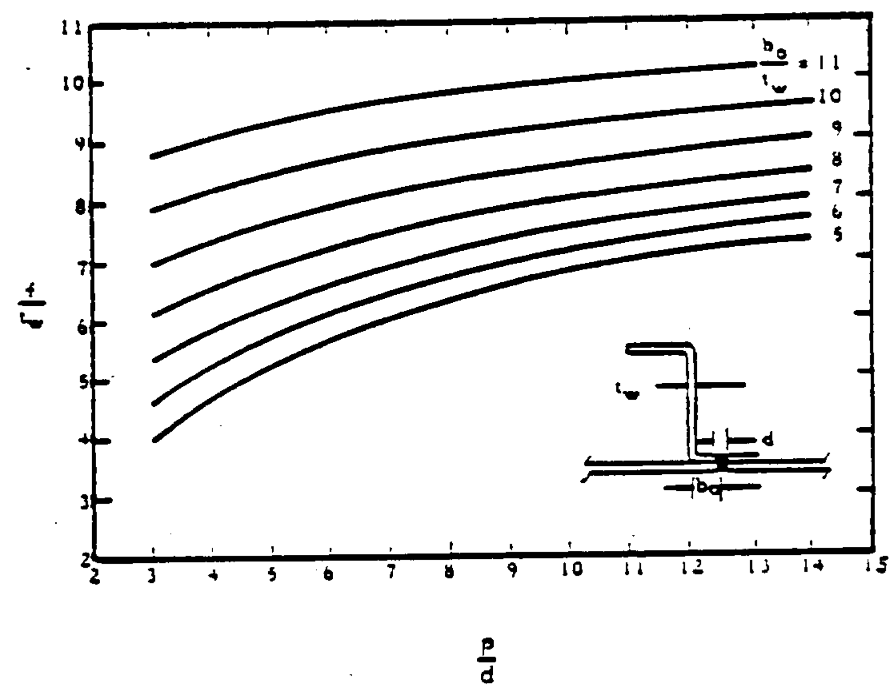

FIGURE 7.18 EXPERIMENTALLY DETERMINED VALUES OF EFFECTIVE RIVET OFFSET (P = Rivet Spacing)

SECTION 7.2

STIFFENED PLATES-ANALYTICAL METHODS

THE " GERARD METHOD " (REFERENCE NACA TN 3784 " HANDBOOK OF STRUCTURAL STABILITY PART IV - FAILURE OF PLATES AND COMPOSITE ELEMENTS " AND NACA TN 3785 " HANDBOOK OF STRUCTURAL STABILITY PART V - COMPRESSIVE STRENGTH OF FLAT STIFFENED PANELS ") FOR PLATE STRINGER ANALYSIS HAS BEEN USED EXTENSIVELY AT GD/CONVAIR FOR INTEGRALLY STIFFENED PANELS (E. G. C-5A EMPENNAGE AND ORBITER MID - FUSELAGE), AND HAS BEEN FOUND TO GIVE EXCELLENT CORRELATION WITH PANEL TEST RESULTS. THIS METHOD IS PRESENTED IN SECTION C7.18 THRU C7.26 OF " ANALYSIS AND DESIGN OF FLIGHT VEHICLE STRUCTURES " BY E. F. BRUHN, AND EXPANDED UPON IN SPACE SHUTTLE ORBITER MID-FUSELAGE REPORTS NUMBER CASD-SSO-76-007, AND CASD-SSO-76-021 BY W.S. BUSSEY JR. (A SYNOPSIS OF THE CONTENTS OF THESE TWO REPORTS IS INCLUDED IN THIS SECTION OF THE MANUAL). WHEN USING THIS METHOD, STRESS RATIOS ARE USED TO ACCOUNT FOR BEAM COLUMN AND COMBINED LOAD EFFECTS. THE METHOD FOR DETERMINING EFFECTIVE SKIN WIDTH IS SHOWN ON PAGE 7.24 THIS METHOD IS APPROPRIATE FOR PLATE STRINGERS UTILIZING DIFFERENT SKIN AND STRINGER MATERIALS AND WHEN SUBJECTED TO THERMAL EFFECTS.

SYNOPSIS

ANALYSIS OF T-STIFFENED INTEGRALLY MACHINED PANELS

Strength analysis methods are presented for T-stiffened integrally machined panels subjected to various combinations of in-plane and lateral pressure loading. The most common design loading for this type of panel is uniaxial compression in the direction of the stringers with possibly the simultaneous application of in-plane shear and/or lateral pressure. Usually, the in-plane compression normal to the stringers is small or nonexistent and is generally ignored in the panel stability analysis. However, it is conceivable that situations may arise where the in-plane transverse compression load becomes significant and, therefore, may affect the overall panel strength and deflection behavior. This situation was encountered in the design of the Space Shuttle's mid-fuselage skin panels. The transverse compression was caused primarily by panel thermal gradients, differential temperatures between the frames and skin panels, and overall fuselage shell distortion due to thermal effects. Of course, transverse in-plane compression loads due to mechanical effects (aircraft inertia or dynamic loads) also contributed to the total panel loading.

Convair conducted biaxial compression tests on T-stiffened panels which were representative of typical side and bottom surface panels on the Space Shuttle mid-fuselage. Generally, these tests revealed that even if the transverse in-plane compression load is large enough to cause buckling, the longitudinal (stringer direction) compression strength is only moderately affected.

In the Space Shuttle mid-fuselage structure, the transverse compression imposed on the skin panels was frequently large enough to cause: (a) buckling with consequent out-of-plane deflection of the skin and stringers or (b) skin buckling between stringers. In the former mode, each buckle half-wave length encompasses one or more stringers. This is characterized by the stringers in adjacent half-waves deflecting in opposite directions, this process continuing in an alternate wave pattern across the width of panel. In the latter mode, the skin buckles locally between stringers, the stringers having sufficient flexural stiffness to force longitudinal nodes along their axes; hence, the stringers remain straight.

It was necessary in the Space Shuttle design to be able to evaluate the effects of in-plane transverse compression on both the ultimate panel strength and the buckled or deflected shapes that occur. The deflected panel definition was important because the thermal protection system tiles must withstand the skin surface movement without cracking or breaking off.

The analytical approach presented below is a composite of several well known and accepted theoretical and semi-empirical techniques. The methods selected produce analytical results which appear to be in good agreement with panel tests conducted at Convair in conjunction with the Space Shuttle program and the Lockheed C-5A Transport airplane. Certain empirical adjustments or factors have been incorporated in some instances. Also, other innovations are employed in order to account for the post-buckling characteristics of a panel subjected to biaxial compression loading.

The overall problem of analyzing a panel subjected to biaxial compression, shear and lateral pressure with possible joint or mid-bay initial eccentricities becomes formidable. However, the analytical procedure can be formulated so that the computations are performed by means of a digital computer. Iteration techniques may be employed for plasticity corrections. Optimum cross sections for given applied load combinations may also be achieved by computer utilization.

Data Source, Section 1.3 Reference 33

SYNOPSIS

Integrally machined blade stiffened panels are frequently used because of their relative structural efficiency in carrying complex loading. Since the blades are normally machined by means of end-mill type cutters, it is possible to achieve almost any reasonable stiffener grid size. Thus, the minimum stiffener spacing is not limited due to manufacturing considerations as it is with some other types of integrally machined panel designs.

Methods are presented here for the strength analysis of blade stiffened integrally machined panels subjected to normal pressure and in-plane biaxial compression and shear loading. These methods are applicable to both panels stiffened uniaxially by blades as well as to panels stiffened by blades in an orthogonal "waffle" grid pattern.

The original analysis methods given in the October 15, 1976, release of this report were predicated on the panel cross sections remaining stable until overall failure occurs. Since the associated computer program, BIMØP, was intended for "optimum sizing" usage, this restriction was considered satisfactory. Subsequently, however, it became necessary to analyze existing panel configurations for revised complex loading. In order to avoid any over-conservatism which might result by disallowing local skin buckling in the analysis, it became necessary to account for the post-buckled panel strength. This has been accomplished by the analytical methods presented in the February 1, 1980, revision to the report. A new version of the computer optimization program has been developed and identified as BIMØP2. An analysis program, BIMAP2, has also been developed.

BIMØP2 provides the capability of suppressing, limiting or unlimiting local skin buckling due to complex in-plane loading. Also included in both BIMØP2 and BIMAP2 is a torsional instability analysis which accounts for skin buckling and biaxial compression effects. Further, provisions for initial out-of-plane eccentricities and edge loading eccentricities have been added, as well as the capability of computing the panel edge pad thicknesses required.

Data Source, Section 1.3 Reference 34

10.8 EFFECTIVE SKIN WIDTH

The effective skin width is used to calculate the amount of skin that contributes to the stiffness of the attached flange. Figure 10.46 shows several types of skin-flange attachments and the corresponding effective skin widths. The skin width equations are based on the buckling compressive stress equation for sheet panels:

$$F_{cr} = \frac{k_c \, \pi^2 E}{12(1 - \mu^2)} \left(\frac{t}{b}\right)^2$$, where b is the stiffener spacing.

If the stiffener provides a boundary restraint equal to a simple support, then $k_c = 4.0$.

Assuming $\mu = .3$,

$$F_{cr} = 3.6\ E\left(\frac{t}{b}\right)^2.$$

When F_{cr} is equal or less than the yield stress of the material, the ultimate strength of a simply supported sheet is independent of the width of the sheet. The term b may then be replaced with an effective width term, w.

$$F_c = 3.6\ E\left(\frac{t}{w}\right)^2$$

Solving for w

$$w = 1.9\ t\left(\frac{E}{F_c}\right)^{.5} = 1.9t\sqrt{\frac{E}{F_{cc}}} \qquad 10.4$$

The constant 1.9 in the preceeding equation is valid for heavy stiffeners. For relatively light stiffeners a constant of 1.7 is suggested. The radius of gyration of the stiffener should include the effective skin area.

For skin-stiffener attachments that develop a fixed or clamped condition -

$$w = 2.52\ t(E/F_c)^{.5} \qquad 10.5$$

Note A - (Fig. 10.46-b) Staggered Rivet Rows
In calculating the crippling stress of the stiffener, use a stiffener flange thickness of three-fourths the sum of the flange thickness plus the sheet thickness.

Note B - (Fig. 10.46-c) $t_s \le t_f < 2t_s$
Find the crippling stress for the tee section, assuming the vertical member of the tee has both ends simply supported. For t (equ. 10.4) use

$$(t_s + t_f)/2.$$

$t_f \ge 2t_s$ - Find the crippling stress for the I section. The column properties should include the I section plus effective skin.

Note C - (Fig. 10.46-d) For a sheet with one edge free, the buckling coefficient is 0.43. The effective width w, is:

$$w_1 = 0.62\ t(E/F_{cy})^{.5}$$

$t_f \geq 2t_s$ - Find the crippling stress for the I section. The column properties should include the I section plus effective skin.

Note C - (Fig. 10.46-d) For a sheet with one edge free, the buckling coefficient is 0.43. The effective width w_1 is:

$$w_1 = 0.62\ t(E/F_{cy})^{.5}$$

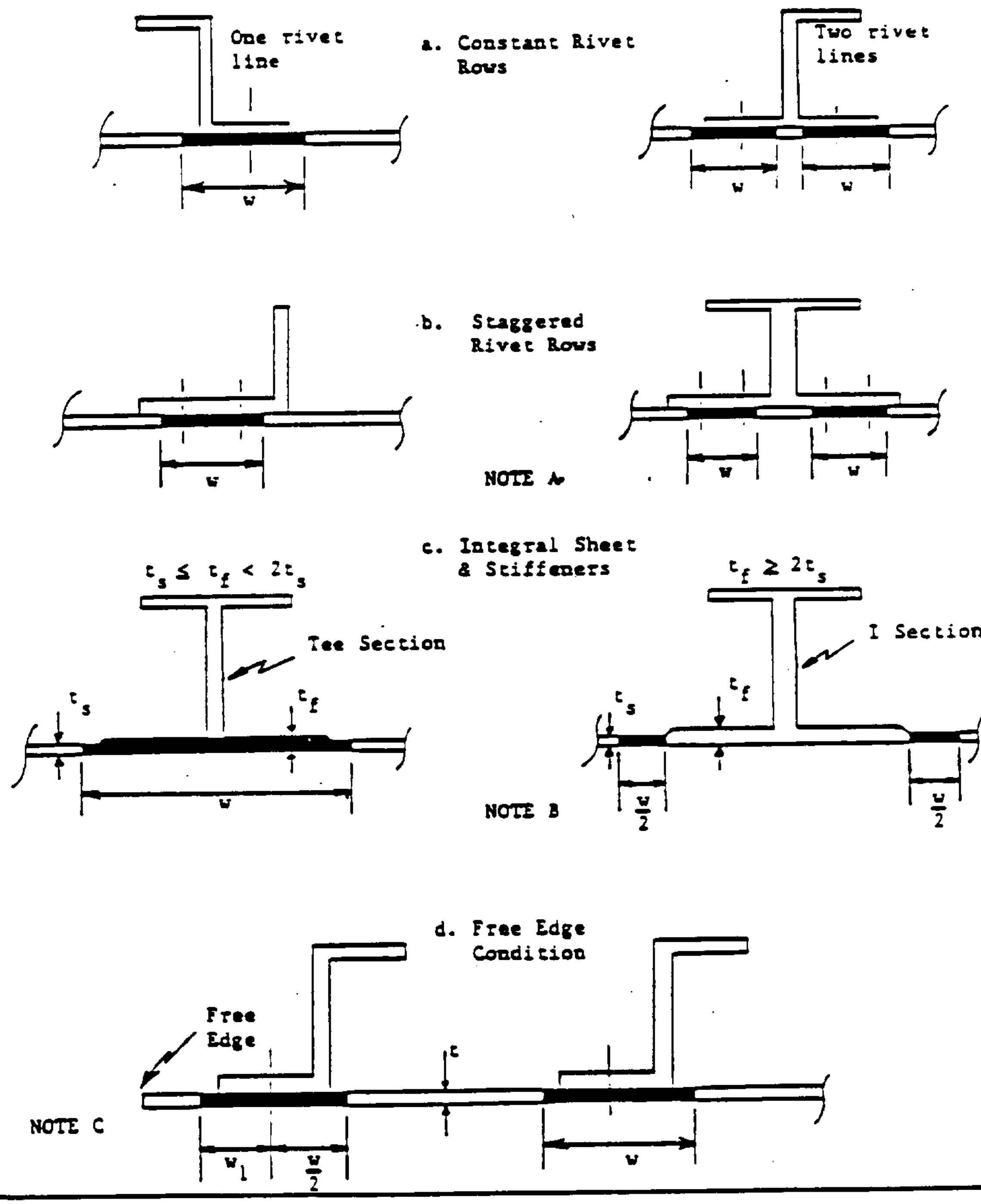

FIGURE 10.46 - EFFECTIVE SKIN WIDTHS

Data Source, Section 1.3 Reference 10

SECTION 7.3

ISOGRID STRUCTURE

REFERENCE:

NASA CR-124075 " ISOGRID DESIGN HANDBOOK " MCDONNELL DOUGLAS ASTRONAUTICS COMPANY. FEB. 1973

SECTION 8.0

SANDWICH CONSTRUCTION

ANALYSIS OF HONEYCOMB CORE SANDWICH CONSTRUCTION IS PRESENTED IN THIS SECTION.

		PAGE
8.1	GENERAL	8.1.1
8.2	MATERIALS	8.2.1
8.3	METHODS OF ANALYSIS	8.3.1
8.4	FACE WRINKLING	8.4.1
8.5	FACE DIMPLING	8.5.1
8.6	EDGEWISE COMPRESSION	8.6.1
8.7	EDGEWISE SHEAR	8.7.1
8.8	NORMAL LOADING	8.8.1
8.9	CYLINDER TORSION	8.9.1
8.10	CYCLINDER AXIAL COMPRESSION	8.10.1
8.11	CYLINDER EXTERNAL PRESSURE	8.11.1
8.12	BEAMS	8.12.1
8.13	ATTACHMENT DETAILS	8.13.1
8.14	ANALYSIS METHOD REFERENCES	8.14.1

457

Data Source, Section 1.3 Reference 3

SECTION 13

SANDWICH ANALYSIS

13.0 GENERAL

Structural sandwich is a layered composite, formed by bonding two thin facings to a thick core. It is a type of stressed-skin construction in which the facings resist nearly all of the applied edgewise (in-plane) loads and flatwise bending moments. The thin spaced facings provide nearly all of the bending rigidity to the construction. The core spaces the facings and transmits shear between them so that they are effective about a common neutral axis. The core also provides most of the shear rigidity of the sandwich construction. By proper choice of materials for facings and core, constructions with high ratios of stiffness to weight can be achieved.

A basic design concept is to space strong, thin facings far enough apart to achieve a high ratio of stiffness to weight; the lightweight core that does this also provides the required resistance to shear and is strong enough to stabilize the facings to their desired configuration through a bonding media such as an adhesive layer, braze or weld. The sandwich is analogous to an I-beam in which the flanges carry direct compression and tension loads, as do the sandwich facings, and the web carries shear loads, as does the sandwich core.

In order that sandwich cores be lightweight, they are usually made of low density material, some type of cellular construction (honeycomb-like core formed of thin sheet material) or of corrugated sheet material. As a consequence of employing a lightweight core, design methods account for core shear deformation because of the low effective shear modulus of the core. The main difference in design procedures for sandwich structural elements as compared to design procedures for homogeneous material is the inclusion of the effects of core shear properties on deflection, buckling and stress for the sandwich.

Because thin facings can be used to carry loads in a sandwich, prevention of local failure under edgewise direct or flatwise bending loads is necessary just as prevention of local crippling of stringers is necessary in the design of sheet stringer construction. Modes of failure that may occur in sandwich under edge load are shown in Figure 13.1.

Shear crimping failure, as shown in Figure 13.1, appears to be a local mode of failure, but is actually a form of general overall buckling in which the wavelength of the buckles is very small because of low core shear modulus. The crimping of the sandwich occurs suddenly and usually causes the core to fail in shear at the crimp; it may also cause shear failure in the bond between the facing and core.

Crimping may also occur in cases where the overall buckle begins to appear and then the crimp occurs suddenly because of severe local shear stresses at the ends of the overall buckle. As soon as the crimp appears, the overall buckle may disappear. Therefore, although examination of the failed sandwich indicates crimping or shear instability, failure may have begun by overall buckling that finally caused crimping.

If the core is of cellular (honeycomb) or corrugated material, it is possible for the facings to buckle or dimple into the spaces between core walls or corrugations

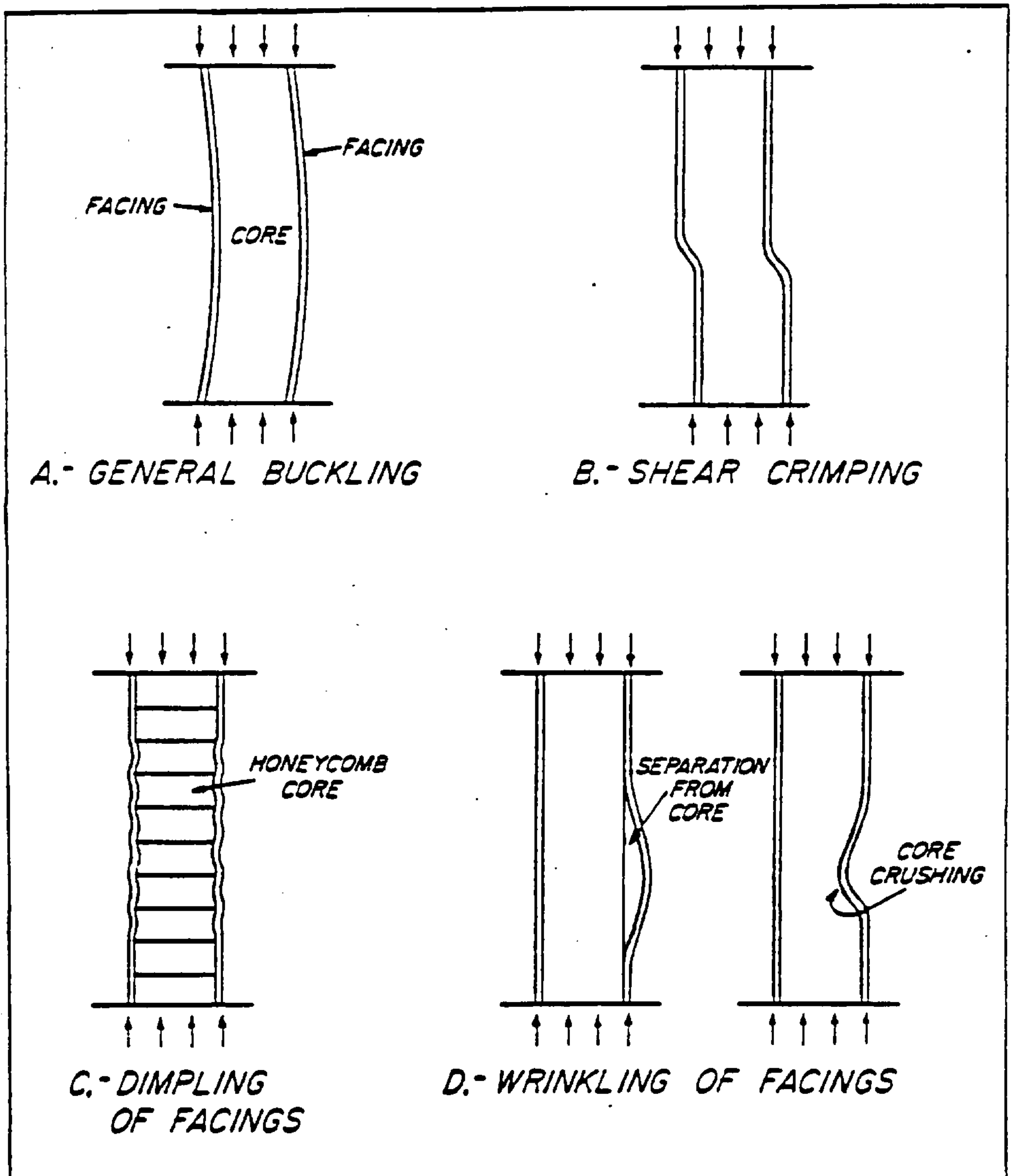

FIGURE 13.1 - POSSIBLE MODES OF FAILURE OF SANDWICH UNDER EDGEWISE COMPRESSION

459

as shown in Figure 13.1. Dimpling may be severe enough so that permanent dimples remain after removal of load and the amplitude of the dimples may be large enough to cause the dimples to grow across the cell walls and result in a wrinkling of the facings.

Wrinkling, as shown in Figure 13.1, may occur if a sandwich facing subjected to edgewise compression buckles as a plate on an elastic foundation. The facing may buckle inward or outward depending on the flatwise compressive strength of the core relative to the flatwise tensile strength of the bond between the facing and core. If the bond between facing and core is strong, facings can wrinkle and cause tension failure in the core. Thus, the wrinkling load depends upon the elasticity and strength of the foundation system; namely, the core and the bond between facing and core. Since the facing is never perfectly flat, the wrinkling load will also depend upon the initial eccentricity of the facing or original waviness.

The local modes of failure may occur in sandwich panels under edgewise loads or normal loads. In addition to overall buckling and local modes of failure, sandwich is designed so that facings do not fail in tension, compression, shear or combined stresses due to edgewise loads or normal loads and cores and bonds do not fail in shear, flatwise tension or flatwise compression due to normal loads.

The basic design principles can be summarized into four conditions as follows:

(1) Sandwich facings shall be at least thick enough to withstand chosen design stresses under design loads.

(2) The core shall be thick enough and have sufficient shear rigidity and strength so that overall sandwich buckling, excessive deflection and shear failure will not occur under design loads.

(3) The core shall have high enough modulus of elasticity and the sandwich shall have great enough flatwise tensile and compressive strength so that wrinkling of either facing will not occur under design loads.

(4) If the core is cellular (honeycomb) or of corrugated material and dimpling of the faces is not permissible, the cell size or corrugation spacing shall be small enough so that dimpling of either facing into the core spaces will not occur under design loads.

The facing to core bond shall have sufficient flatwise tensile and shear strength to develop the core strength in the expected environment. The environment includes effects of temperature, water or moisture, corrosive atmosphere and fluids, fatigue, creep and any other condition that affects material properties.

13.1 Materials

13.1.1 Facing Materials

The facings of a sandwich part serve many purposes, depending upon the application, but in all cases they carry the major applied loads. The stiffness, stability, configuration and, to a large extent, the strength of the part are determined by the characteristics of the facings as stabilized by the core. To perform these functions the facings must be adequately bonded to a core of acceptable quality. Facings sometimes have additional functions, such as providing a profile of proper

aerodynamic smoothness, a tough nonskid surface, or a tough wear-resistant floor covering. To better fulfill these special functions, one facing of a sandwich is sometimes made thicker or of slightly different construction than the other.

Any thin sheet material can serve as a sandwich facing. A few of the materials usually used are shown in Table 13.1.

13.1.2 Core Materials

To permit an airframe sandwich construction to perform satisfactorily, the core of the sandwich must have certain mechanical properties, thermal characteristics and dielectric properties under conditions of use and still conform to weight limitations. Cores of densities ranging from 1.6 to 23 pounds per cubic foot have found use in airframe sandwich, but the usual density ranges from 3 to 10 pounds per cubic foot.

A wide variety of core materials can be constructed of thin sheet materials or ribbons formed to honeycomb-like configurations. By varying the sheet material, sheet thickness, cell size and cell shape cores of a wide range in density and properties can be produced. Most honeycomb cores can be formed to moderate amounts of single curvature, but some can easily be formed to fairly severe single curvature and to moderate compound curvature.

Honeycomb core cell size is determined by the diameter of a circle which can be inscribed in a cell. Two types of honeycomb core showing the cell size "s" are shown in Figure 13.2. Honeycomb core cell sizes used in airframes vary from about 1/16 to 7/16 inch, usually in multiples of 1/16 inch. Not all sheet materials are formed to all of these cell sizes because some sheet materials are so thick and stiff that they cannot be formed to core of cells less than 3/16 inch in size. For special use, such as an insert, honeycomb cores can be densified locally by under-expanding, crushing the core locally or by inserting a higher density core locally. Cores for airframe sandwich construction are presently being made of thin sheets of aluminum alloys, resin-treated glass fabric, resin-treated asbestos, resin-treated paper, stainless steel alloys, titanium alloys and refractory metals.

Honeycomb cores fabricated from nonmetallic materials have better thermal insulating characteristics than metallic honeycomb cores, even though both allow transmission of heat by radiation in the open cells. In considering thermal effects on sandwich structure, it should be understood that the sandwich can act as a reflective thermal insulator. The effective thermal conductivity of a honeycomb core depends upon conduction of the material of which the core is made, radiation between facings and connection within the core cell and can be computed approximately as

$$K_e = K_o A_c + \frac{4\sigma t_c (1 - A_c) T_m^3}{\frac{1}{\epsilon_1} + \frac{1}{\epsilon_2} - 2 + \frac{2}{1 + F_{12}}} + t_c (1 - A_c)\eta \qquad 13.1$$

where
K_e = effective conductivity
K_o = conductivity of core ribbon material
A_c = core solidity = W_c/W_o
W_c = core density
W_o = core ribbon material density
σ = Stefan-Boltzmann constant

441

FACING	YIELD STRENGTH $F_f \sim psi$	MODULUS OF ELASTICITY $E_f \sim psi$	$\lambda_f = 1 - \mu^2$	WEIGHT PER MIL THICKNESS LBS/FT^2
ALUMINUM:				
1100-H14	17,000	10×10^6	.89	.014
2024-T4	47,000	10×10^6	.89	.014
3003-H16	25,000	10×10^6	.89	.014
5052-H38	37,000	10×10^6	.89	.014
6061-T4	21,000	10×10^6	.89	.014
7075-T6	73,000	10×10^6	.89	.014
MILD CARBON STEEL	50,000	30×10^6	.91	.040
STAINLESS STEEL:				
316	60,000	30×10^6	.94	.040
17-7	200,000	30×10^6	.94	.040
TITANIUM:				
Ann.Ti-75A	80,000	15×10^6	.94	.0235
H.T. 6Al-4V	143,000	16.8×10^6	.94	.0230
FIBERGLASS PRE-PREG:				
EPOXY F155	63,000	3.5×10^6	.98	.0095
EPOXY F161	62,000	3.5×10^6	.98	.0088
PHENOLIC F120	48,000	3.5×10^6	.98	.0094
POLYESTER F141	48,000	3.5×10^6	.98	.010
PLYWOOD:				
DOUGLAS FIR	2,650	1.8×10^6	.99	.003
HARDBOARD	300	0.4×10^6	.99	.004

TABLE 13.1 - TYPICAL SANDWICH FACING MATERIALS

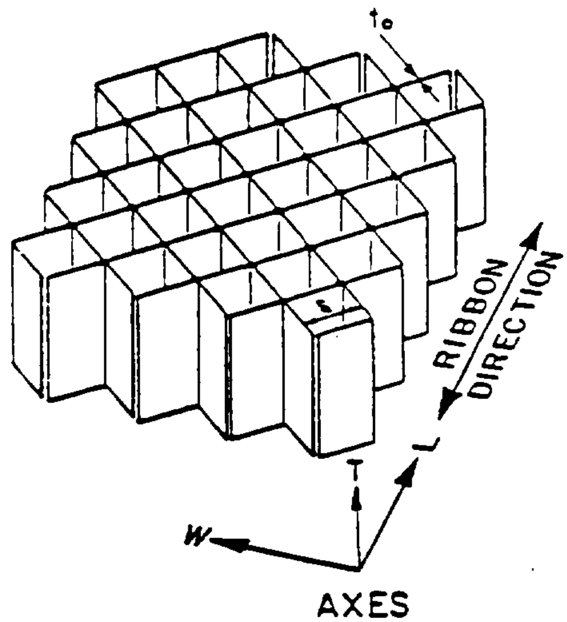

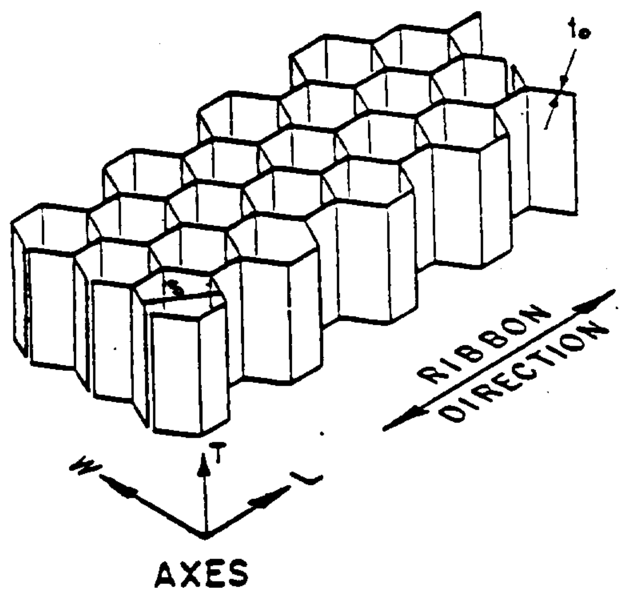

FIGURE 13.2 - HONEYCOMB CORE NOTATION

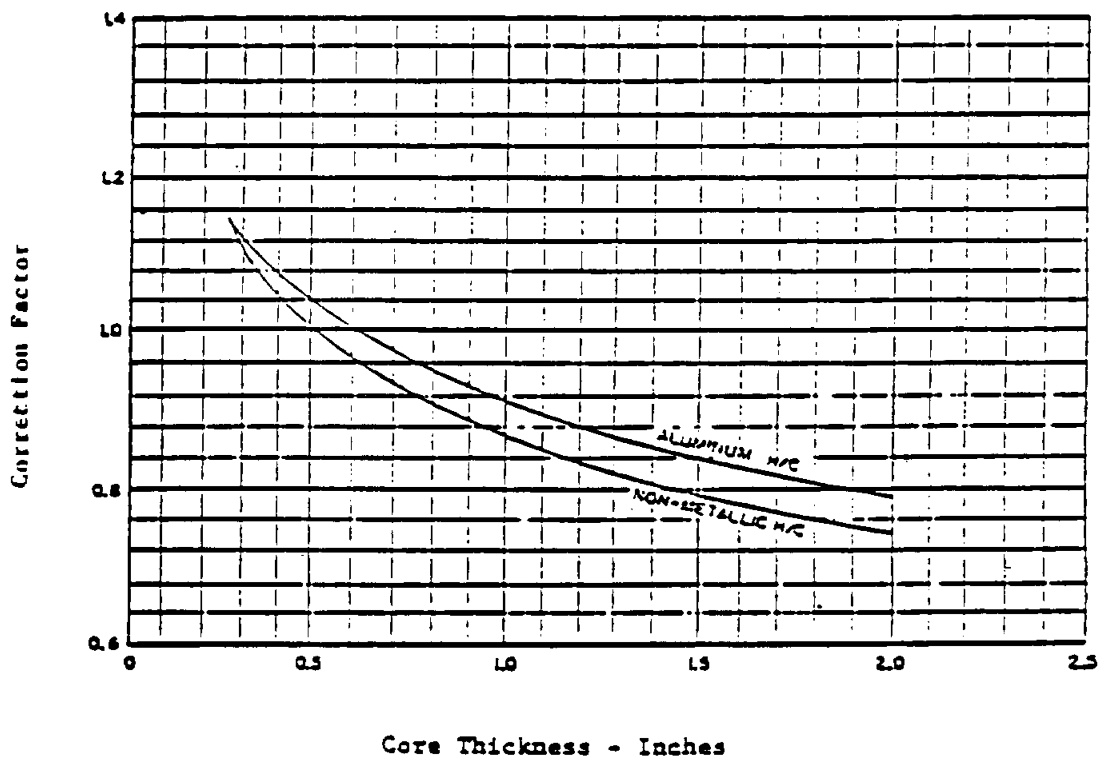

FIGURE 13.2a - SHEAR STRENGTH CORRECTION FACTORS

t_c = core thickness
T_m = mean absolute temperature of the two facings
ϵ_1 = emissivity of inside of facing 1
ϵ_2 = emissivity of inside of facing 2
F_{12} = geometric view factor between facings
η = connective heat transfer coefficient inside core cell

Sheets of corrugated metal foil are usually assembled with the corrugations parallel to form honeycomb cores. The foil may be perforated for use in core where solvents or gasses must be vented. Perforated foil in sandwich panels that are not sealed or are poorly sealed will allow penetration of moisture, etc., which may cause severe deterioration of the core. If the sheets are assembled with the corrugations in adjacent sheets perpendicular to each other, a well vented crossbanded core is produced. Crossbanded cores may be cut so that the corrugation flutes are at an angle of 45° to the sandwich facings, giving the core a trussed appearance.

Crossbanded cores are not as strong in compressions in the T direction or in shear in the TL or TW planes as honeycomb cores of the same density. Honeycomb cores, however, have negligible compressive strength in the W and L directions and shear strength in the WL plane, whereas crossbanded cores have considerable strength in these directions. Crossbanded core is not readily formed to curved surfaces because of its relatively high stiffness in all directions.

Many core materials and core configurations are available, but the aluminum honeycomb with a hexagonal cell is the most commonly used. Table 13.2 shows the mechanical and physical properties for many of the available core materials.

Figure 13.2a shows correction factors for core shear strength at various core thicknesses.

13.1.3 Adhesives

In the fabrication of sandwich, adhesives are used for bonding faces to core and bonding facings and fittings, reinforcing plates, edge strips and other inserts. The adhesives used are resin formulations especially developed to give high strength bonds over a wide range of exposure and stressing conditions. Adhesives can be used to bond many types of metal in highly stressed applications. They can also be formulated to have resistance to moderately elevated temperatures.

The intrinsic elastic properties and strength of adhesives have not been evaluated to any large extent. Instead, adhesive bonded lap joints are used to evaluate the strength of an adhesive. The standard test is .063 aluminum sheets bonded with an overlap of 1/2 inch. The lap joint strength is the load required to shear the bond divided by the bonded area. Table 13.3 shows typical lap joint strengths of several adhesives.

Lap joint strength is not considered of prime use for determining adequacy of adhesives for bonding sandwich facings to honeycomb cores. The need of an adhesive to form strong fillets at the ends of the core cells to produce satisfactory sandwich has prompted the evaluation of peel strength and sandwich flatwise tensile strength.

445

5052 ALLOY HEXAGONAL ALUMINUM HONEYCOMB
AEROSPACE GRADE

HONEYCOMB DESIGNATION Cell-Material-Gage	Nominal Density pcf	COMPRESSIVE Bare Strength psi		Stabilized Strength psi		Stabilized Modulus ksi	Crush Strength psi	PLATE SHEAR "L" Direction Strength psi		"L" Direction Modulus ksi	"W" Direction Strength psi		"W" Direction Modulus ksi
		typ	min	typ	min	typical	typ	typ	min	typical	typ	min	typ
1/8-5052-.0007	3.1	270	200	290	215	75	130	210	155	45.0	130	90	22.0
1/8-5052-.001	4.5	520	375	545	405	150	260	340	285	70.0	220	168	31.0
1/8-5052-.0015	6.1	870	650	910	680	240	450	505	455	98.0	320	272	41.0
1/8-5052-.002	8.1	1400	1000	1470	1100	350	750	725	670	135.	455	400	54.0
5/32-5052 - .0007	2.6	200	150	215	160	55	90	165	120	37.0	100	70	19.0
5/32-5052 - .001	3.8	395	285	410	300	110	185	270	215	56.0	175	125	26.4
5/32-5052 - .0015	5.3	690	490	720	535	195	340	420	370	84.0	270	215	36.0
5/32-5052 - .002	6.9	1080	770	1130	800	285	575	590	540	114.	375	328	46.4
5/32-5052 - .0025	8.4	1530	1070	1600	1180	370	800	760	690	140.	475	420	56.0
3/16-5052 - .0007	2.0	130	90	135	100	34	60	120	80	27.0	70	46	14.3
3/16-5052 - .001	3.1	270	200	290	215	75	130	210	155	45.0	130	90	22.0
3/16-5052 - .0015	4.4	500	360	525	385	145	250	330	280	68.0	215	160	30.0
3/16-5052 - .002	5.7	770	560	810	600	220	390	460	410	90.0	300	244	38.5
3/16-5052 - .0025	6.9	1080	770	1130	800	285	575	590	540	114.	375	328	46.4
3/16-5052 - .003	8.1	1400	1000	1470	1100	350	750	725	670	135	455	400	54.0
1/4-5052-.0007	1.6	85	60	95	70	20	40	85	60	21.0	50	32	11.0
1/4-5052-.001	2.3	165	120	175	130	45	75	140	100	32.0	85	57	16.2
1/4-5052-.0015	3.4	320	240	340	250	90	150	235	180	50.0	150	105	24.0
1/4-5052-.002	4.3	480	350	505	370	140	230	320	265	66.0	210	155	29.8
1/4-5052-.0025	5.2	670	500	690	510	190	335	410	360	82.0	265	200	35.4
1/4-5052-.003	6.0	850	630	880	660	235	430	495	445	96.0	315	265	40.5
1/4-5052-.004	7.9	1360	970	1420	1050	340	725	700	650	130.	440	390	52.8
3/8-5052 - .0007	1.0	30	20	45	20	10	25	45	32	12.0	30	20	7.0
3/8-5052 -.001	1.6	85	60	95	70	20	40	85	60	21.0	50	32	11.0
3/8-5052 - .0015	2.3	165	120	175	130	45	75	140	100	32.0	85	57	16.2
3/8-5052 -.002	3.0	260	190	270	200	70	120	200	145	43.0	125	85	21.2
3/8-5052 - .0025	3.7	370	270	390	285	105	180	260	200	55.0	170	115	26.0
3/8-5052 -.003	4.2	460	335	485	355	135	220	310	255	65.0	200	150	29.0
3/8-5052 -.004	5.4	720	500	745	535	200	360	430	380	86.0	280	228	36.8
3/8-5052 -.005	6.5	970	700	1020	750	265	505	545	500	105.	350	300	43.5

TABLE 13.2 - PROPERTIES OF TYPICAL SANDWICH CORES

5056 HEXAGONAL ALUMINUM HONEYCOMB
AEROSPACE GRADE

HONEYCOMB DESIGNATION Cell-Material-Gage	Nominal Density pcf	COMPRESSIVE					Crush Strength psi	PLATE SHEAR					
		Bare		Stabilized				"L" Direction			"W" Direction		
		Strength psi		Strength psi		Modulus ksi		Strength psi		Modulus	Strength psi		Modulus ksi
		typ	min	typ	min	typ	typ	typ	min	typ	typ	min	typ
1/8-5056-.0007	3.1	340	250	360	260	97	170	250	200	45.0	155	110	20.0
1/8-5056-.001	4.5	630	475	670	500	185	320	425	350	70.0	255	205	38.0
1/8-5056-.0015	6.1	1000	760	1100	825	295	535	640	525	102.	370	305	38.0
1/8-5056-.002	8.1	1520	1200	1700	1300	435	810	900	740	143.	520	440	51.0
5/32-5056-.0007	2.6	255	180	260	185	70	120	200	152	36.0	120	80	17.0
5/32-5056-.001	3.8	475	360	500	375	140	235	335	272	57.0	205	155	24.0
5/32-5056-.0015	5.3	820	615	865	650	240	420	530	435	85.0	310	250	33.0
5/32-5056-.002	6.9	1220	920	1340	1000	350	650	760	610	118	430	360	43.0
3/16-5056-.0007	2.0	155	110	160	120	45	75	140	105	27.0	85	50	13.0
3/16-5056-.001	3.1	340	250	360	260	97	170	255	200	45.0	155	110	20.0
3/16-5056-.0015	4.4	600	460	650	490	180	310	410	340	68.0	245	198	27.5
3/16-5056-.002	5.7	910	685	980	735	270	480	585	480	94.0	340	280	36.0
1/4-5056-.0007	1.6	100	75	110	80	30	50	90	78	20.0	60	38	12.0
1/4-5056-.001	2.3	205	145	210	155	58	100	170	130	32.0	105	62	15.0
1/4-5056-.0015	3.4	395	300	420	315	115	200	290	230	50.0	175	130	22.0
1/4-5056-.002	4.3	580	440	620	465	172	300	400	325	67.0	240	190	27.0
1/4-5056-.0025	5.2	790	600	820	645	230	410	500	425	84.0	300	245	32.0
3/8-5056-.0007	1.0	35	25	50	35	15	35	60	45	15.0	35	25	9.0
3/8-5056-.001	1.6	100	75	110	80	30	50	90	78	20.0	60	38	12.0
3/8-5056-.0015	2.3	205	155	210	155	58	100	170	130	32.0	105	62	15.0
3/8-5056-.002	3.0	320	240	340	260	92	160	245	190	43.0	145	100	19.0
2024 HEXAGONAL ALUMINUM HONEYCOMB													
		typ	min	typ	min	typ	typ	typ	min	typ	typ	min	typ
1/8-2024-.0015	5.2	700	525	780	620	200	425	500	400	82.0	315	250	33.0
1/8-2024-.002	6.7	1100	825	1225	980	300	640	760	600	118	470	375	45.0
1/8-2024-.0025	8.0	1480	1100	1650	1320	380	840	960	770	148	590	470	54.0
1/8-2024-.003	9.5	1970	1475	2300	1725	480	1120	1150	950	170	630	585	64.0
3/16-2024-.0015	3.5	330	250	370	290	86	200	290	230	55.0	180	143	23.0
1/4-2024-.0015	2.8	220	165	250	165	40	110	200	140	42.0	120	88	19.0

TABLE 13.2 (CONTINUED) - PROPERTIES OF TYPICAL SANDWICH CORES

5052 ALUMINUM FLEX-CORE - AEROSPACE GRADE

HONEYCOMB DESIGNATION Material-Cell-Gage Count	Nominal Density pcf	COMPRESSIVE Bare Strength psi		COMPRESSIVE Stabilized Strength psi		COMPRESSIVE Stabilized Modulus psi	Crush Strength pcf	PLATE SHEAR "L" Direction Strength psi		PLATE SHEAR "L" Direction	PLATE SHEAR "W" Direction Strength psi		PLATE SHEAR "W" Direction Modulus psi
		typ	min	typ	min	typ	typ	typ	min	typ	typ	min	typ
5052/F40-.0013	2.1	180	126	225	157	65	80	90	63	18	50	37	10
5052/F40-.0019	3.1	340	238	400	280	125	165	180	126	32	100	75	13
5052/F40-.0025	4.1	540	378	600	420	185	250	260	182	45	150	115	17
5052/F40-.0037	5.7	900	630	1000	700	290	380	400	280	68	230	170	23
5052/F80-.0013	4.3	575	-	650	-	195	-	280	-	45	160	-	18
5052/F80-.0019	6.0	1000	-	1050	-	310	-	440	-	72	240	-	24
5052/F80-.0025	8.0	1570	-	1600	-	400	-	620	-	98	345	-	31
		typ	min	typ	min	typ	typ	typ	min	typ	typ	min	typ
5056/F40-.0014	2.1	215	-	260	-	65	-	105	-	18	55	-	10
5056/F40-.0020	3.1	405	-	470	-	125	-	215	-	32	120	-	13
5056/F40-.0026	4.1	645	-	690	-	185	-	310	-	45	175	-	17
5056/F80-.0014	4.3	680	-	740	-	195	-	335	-	47	185	-	18
5056/F80-.0020	6.0	1150	-	1300	-	310	-	520	-	73	285	-	24
5056/F80-.0026	8.0	1730	-	1800	-	410	-	740	-	100	410	-	32
		typical		typical		typ	typ	typical		typ	typical		typ
ACG 1/4-.003	5.2	595		610		148	245	345		63	215		31
ACG 3/8-.003	3.6	325		340		92	175	210		40	130		20
ACG 3/4-.003	1.8	95		110		24	50	95		16	55		8

TABLE 13.2 (CONTINUED) - PROPERTIES OF TYPICAL SANDWICH CORES

HRP GLASS REINFORCED PHENOLIC HONEYCOMB

HONEYCOMB DESIGNATION Mat'l-Cell-Density	COMPRESSIVE					PLATE SHEAR					
	Bare		Stabilized			"L" Direction			"W" Direction		
	Strength		Strength		Modulus ksi	Strength psi		Modulus ksi	Strength psi		Modulus ksi
Hexagonal	typ	min	typ	min	typ	typ	min	typ	typ	min	typ
HRP-3/16-4.0	500	350	600	480	57	260	210	11.5	140	110	5.0
HRP-3/16-5.5	800	600	940	750	95	425	370	19.5	220	190	8.5
HRP-3/16-7.0	1150	900	1230	-	136	500	-	28.0	290	-	12.5
HRP-3/16-8.0	1400	1100	1600	1280	164	660	600	34.0	400	370	15.0
HRP-3/16-12.0	2280	1600	2300	-	260	940	-	55.0	570	-	25.0
HRP-1/4-3.5	350	260	500	400	46	230	170	9.0	120	100	3.5
HRP-1/4-4.5	630	450	700	560	70	300	250	14.0	170	140	6.0
HRP-1/4-5.0	700	510	820	660	84	340	-	17.0	200	-	7.5
HRP-1/4-6.5	1025	850	1180	900	120	450	-	25.0	260	-	11.0
HRP-3/8-2.2	150	105	200	145	13	105	75	5.0	60	45	2.0
HRP-3/8-3.2	320	245	440	350	38	200	160	8.0	105	85	3.0
HRP-3/8-4.5	610	450	690	530	65	300	260	14.0	170	150	6.0
HRP-3/8-6.0	900	750	1000	750	100	400	340	22.5	260	210	10.0
HRP-3/8-8.0	1060	920	1200	-	150	520	-	31.0	320	-	13.0
OX-CORE											
HRP/OX-1/4-4.5	520	350	625	-	43	210	-	8.0	250	-	15.2
HRP/OX-1/4-5.5	810	600	950	-	65	270	-	10.5	330	-	18.0
HRP/OX-1/4-7.0	1150	-	1230	-	84	395	-	14.0	450	-	20.0
HRP/OX-3/8-3.2	340	260	425	-	32	140	-	4.5	150	-	9.0
HRP/OX-3/8-5.5	700	580	820	-	60	240	-	10.0	300	-	17.0
FLEX-CORE											
HRP/F35-2.5	180	-	240	-	.25	125	-	12.5	70	-	7.0
HRP/F35-3.5	320	-	400	300	37	200	140	15.0	105	75	10.0
HRP/F35-4.5	440	-	600	-	49	280	-	22.0	140	-	12.0
HRP/F50-3.5	300	-	425	300	37	195	140	20.0	100	75	10.0
HRP/F50-4.5	400	-	600	500	49	265	200	25.0	140	100	13.0
HRP/F50-5.5	600	-	880	-	61	390	-	31.5	205	-	16.0

TABLE 13.2 (CONTINUED) - PROPERTIES OF TYPICAL SANDWICH CORES

469

NP GLASS REINFORCED POLYESTER HONEYCOMB

HONEYCOMB DESIGNATION Mat'l-Cell-Fabric-Density	COMPRESSIVE Bare Strength psi		COMPRESSIVE Stabilized Strength psi		COMPRESSIVE Stabilized Modulus ksi	PLATE SHEAR "L" Direction Strength psi		PLATE SHEAR "L" Direction Modulus ksi	PLATE SHEAR "W" Direction Strength psi		PLATE SHEAR "W" Direction Modulus ksi
Hexagonal	typ	min	typ	min	typ	typ	min	typ	typ	min	typ
NP 3/16-4.5	520	470	670	470	80	280	195	13.5	130	90	5.2
NP 3/16-6.0	880	615	1050	735	116	330	230	15.0	155	110	5.8
NP 3/16-9.0	1700	1200	1800	1260	180	460	320	20.0	230	160	7.5
NP 1/4-4.0	420	295	560	390	68	260	180	13.0	120	85	5.0
NP 1/4-6.0	880	615	1050	736	116	330	230	15.0	155	110	5.8
NP 1/4-8.0	1400	980	1540	1080	160	410	290	18.0	205	145	7.0
NP 3/8-2.5	200	140	280	195	34	170	120	10.0	100	70	4.0
NP 3/8-4.5	520	365	670	470	80	280	195	13.5	13.5	90	5.2
OX-CORE											
NP/OX 1/4-4.0	350	-	-	-	-	160	-	5.0	190	-	12.0
NP/OX 1/4-6.0	700	-	-	-	-	275	-	7.5	375	-	19.5
NP/OX 3/8-4.5	420	-	-	-	-	190	-	5.5	285	-	15.0

HRH-327 GLASS REINFORCED POLYIMIDE HONEYCOMB

HONEYCOMB DESIGNATION Mat'l-Cell-Density	COMPRESSIVE Stabilized Strength psi		COMPRESSIVE Stabilized Modulus ksi	PLATE SHEAR "L" Direction Strength psi		PLATE SHEAR "L" Direction Modulus ksi	PLATE SHEAR "W" Direction Strength psi		PLATE SHEAR "W" Direction Modulus ksi
	typ	min	typ	typ	min	typ	typ	min	typ
HRH 327-3/16-4.0	440	-	50	280	-	29	130	-	10
HRH 327-3/16-4.5	520	400	58	320	220	33	150	110	11
HRH 327-3/16-5.0	600	-	68	370	-	37	180	-	25.5
HRH 327-3/16-6.0	780	625	87	460	345	45	230	170	15
HRH 327-3/16-8.0	1300	1000	126	650	500	62	410	330	22
HRH 327-1/4-4.0	440	-	50	280	-	29	130	-	10
HRH 327-1/4-5.0	600	-	68	370	-	37	180	-	12.5
HRH 327-3/8-4.0	440	325	50	280	195	29	150	100	12
HRH 327-3/8-5.5	680	540	78	420	300	41	210	160	13.5
HRH 327-3/8-7.0	1000	-	106	550	-	53	310		18.5

TABLE 13.2 (CONTINUED) - PROPERTIES OF TYPICAL SANDWICH CORES

ADHESIVE TYPE	AVERAGE ALUMINUM TO ALUMINUM LAP SHEAR BOND STRENGTH AT ROOM TEMPERATURE - (PSI)
(A) NITRILE PHENOLIC	3500
(B) VINYL PHENOLIC	4200
(C) EPOXY PHENOLIC	3400
(D) UNMODIFIED EPOXY	3100
(E) MODIFIED EPOXY - 250 CURE	4500
(F) MODIFIED EPOXY - 350 CURE	3300
(G) EPOXY POLYAMIDE	5500
(H) POLYAMIDE	3300

STRUCTURAL ADHESIVES
USEFUL TEMPERATURE RANGE, STRENGTH PROPERTIES
192 HR. EXPOSURE

ADHESIVE TYPE	USEFUL TEMP. RANGE (°F)	TYPICAL VALUES LAP SHEAR (PSI)	PEEL STRENGTH
(A) NITRILE PHENOLIC	-67 350	3500-4300 300-1700	GOOD TO EXCELLENT
(B) VINYL PHENOLIC	-67 225	2000-3000 100-1800	FAIR TO GOOD
(C) EPOXY PHENOLIC	-70 500	1300-5000 200-1900	POOR TO MEDIUM
(D) UNMODIFIED EPOXY	-67 300	1300-3000 800-3000	POOR TO MEDIUM
(E) MODIFIED EPOXY-250 CURE	-250 180	1500-2500 1000-1900	GOOD
(F) MODIFIED EPOXY-350 CURE	-67 250	3000-3500 1500-2500	GOOD
(G) EPOXY POLYAMIDE	-300 250	4000-5000 2800-3300	GOOD
(H) POLYAMIDE	UP TO 600	3300	POOR

TABLE 13.3 - ADHESIVE PROPERTIES

Peel strength is determined as the torque necessary to peel a facing from a sandwich core. Table 13.4 shows values of peel strength and fillet strength for several adhesives.

Adhesives are available in the form of liquid, paste, powders and supported or unsupported films and can be applied by spray, roller, spatula or hand lay-up. The form of the adhesive (liquid, paste or film) is chosen to suit the lay-up operation and glue line thickness requirement.

Structural adhesives have good shear and tensile strength, but resistance to peel stresses is relatively poor. Bonded joints should be designed to take advantage of the high shear and tensile strengths of the adhesive and avoid peel stresses in the bond where possible.

ADHESIVE	FILLET STRENGTH			PEEL STRENGTH		
	$73^{\circ}F$ lb/in	$180^{\circ}F$ lb/in	$-67^{\circ}F$ lb/in	$73^{\circ}F$ in-lb/in	$180^{\circ}F$ in-lb/in	$-67^{\circ}F$ in-lb/in
NITRILE ELASTOMER-PHENOLIC PLUS MODIFIED EPOXY FILM	73	51	84	66	32	21
POLYVINYL-PHENOLIC	42	35	49	25	22	14
EPOXY-POLYAMIDE	71	39	66	18	24	15
MODIFIED EPOXY-350°F CURE	62-86	27-65	61-87	16-97	13-82	12-49
MODIFIED EPOXY-250°F CURE	46-76	34-38	47-91	15-40	18-23	19-26
NITRILE EPOXIDE	61	33	89	27	18	28

TABLE 13.4 - STRENGTH OF ADHESIVES IN SANDWICH WITH HONEYCOMB CORE

Data Source, Section 1.3 Reference 3

13.2 Methods of Analysis

The analysis procedures described in this section apply to sandwich structures having isotropic facings and either orthotropic or isotropic cores. The isotropic materials are those having essentially constant properties in all directions. The orthotropic materials are those whose strength properties are not constant in all directions, such as honeycomb cores.

The assumption is made that adhesive failure does not occur, a reasonable assumption if proper care is taken in the selection of the adhesive system. This requires that the adhesive shear and flatwise tensile strength be greater than the respective core strength.

If the sandwich has thin facings on a core of negligible bending stiffness, as is usually the case, and after assuming $\lambda_1 = \lambda_2 = \lambda$, the bending stiffness is given by the formula:

$$D = \frac{E_1' t_1 E_2' t_2 h^2}{(E_1' t_1 + E_2' t_2)\lambda} \qquad \text{(for unequal facings)}$$

$$D = \frac{E' t h^2}{2\lambda} \qquad \text{(for equal facings)}$$

Figure 13.3 shows the notation used for the analysis of sandwich panels in this section.

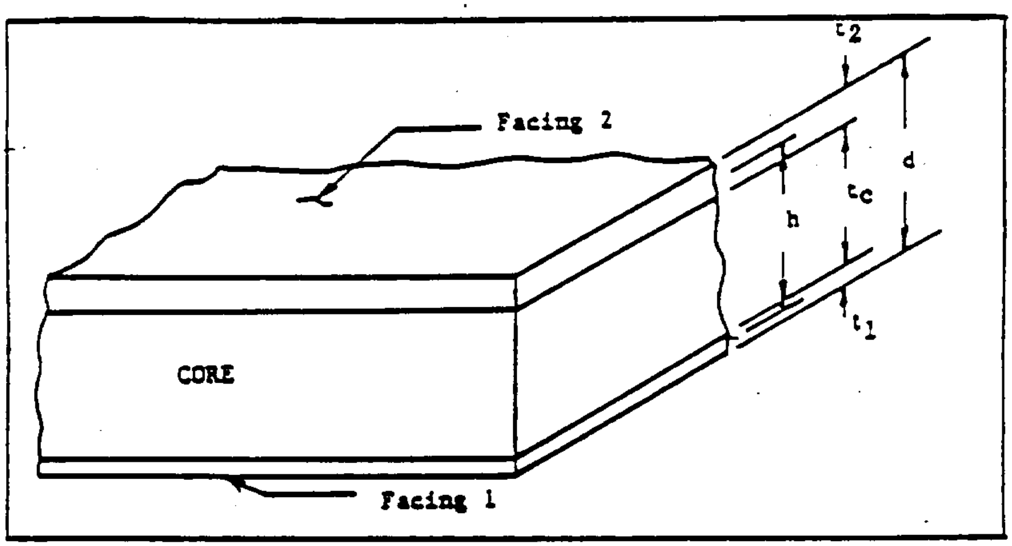

FIGURE 13.3 NOTATION FOR SANDWICH COMPOSITE

The notation used throughout this section is shown below:

1 - subscript denoting facing 1
2 - subscript denoting facing 2

Data Source, Section 1.3 Reference 3

- a, b - length of panel edge; subscripts denoting parallel to a or b
- c - subscript denoting core or compression
- cr - subscript denoting critical
- D - bending stiffness
- d - total sandwich depth or thickness
- E - modulus of elasticity
- E' - effective modulus
- F - allowable stress
- f - applied stress
- G - modulus of rigidity
- h - distance between facings centroids
- J - polar moment of inertia
- K - a constant
- L - length
- M - bending moment
- N - load per unit length of edge
- P - load
- p - distributed load
- r - radius; subscript denoting reduced
- R - ratio
- S - shear load normal to surface of panel
- s - core cell size; subscript denoting shear
- T - torque
- t - thickness; facing without subscript
- U - transverse shear stiffness - - - - - - - $U = G_c h^2/t_c$
- V - parameter relating shear and bending stiffness
- W - weight
- w - density
- x - axis
- y - axis perpendicular to x axis
- z - axis normal to surface of sandwich
- α - $\sqrt{E'_a/E'_b}$
- β - $\alpha\mu_{ab} + 2\gamma$
- γ - shear strain; elastic property parameter $= \lambda G'_{ba}/\sqrt{E'_a E'_b}$
- δ - deflection
- ϵ - strain
- λ - $(1 - \mu^2)$
- μ - Poisson's ratio

13.2.1 Wrinkling of Facings Under Edgewise Load

Wrinkling of sandwich facings, as shown in Figure 13.4, may occur if a sandwich facing buckles as a plate on an elastic foundation. It may buckle into the core or

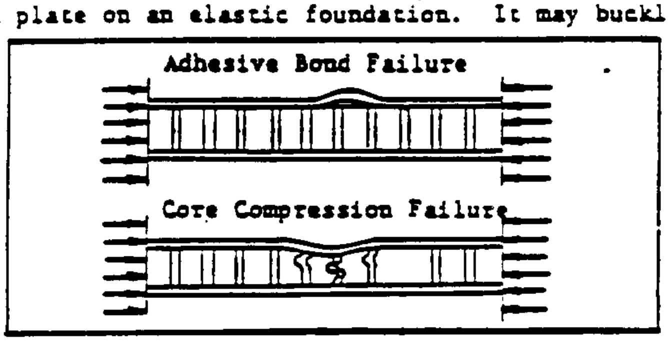

FIGURE 13.4 FACE WRINKLING

away from the core depending on the relative strengths of core in compression and adhesive in flatwise tension.

The facings of a sandwich shall not wrinkle under design load. The wrinkling stress formulas are given for two types of sandwich; sandwich with continuous cores and sandwich with honeycomb cores for which elastic-moduli in the plane of the core are very small compared with the elastic modulus in a direction normal to the core plane.

13.2.1.1 Continuous Core

(1) Determine the parameter q:

$$q = \frac{t_c}{t} G_c \left(\frac{\lambda}{E_f E_c G_c} \right)^{1/3} \qquad 13.2$$

where E_c = core flatwise modulus of elasticity
G_c = core modulus of rigidity

(2) Determine parameter K:

$$K = \frac{E_c \eta}{F_c t_c} \qquad 13.3$$

where η = total amplitude of initial facing waviness usually between .0005 - .005 inch
Fc = flatwise strength of core or bond, whichever is less

(3) Enter Figure 13.5 with q and K and determine value of parameter Q.

(4) Find the stress F_{cr} at which face wrinkling occurs:

$$F_{cr} = Q \left(\frac{E_f E_c G_c}{\lambda} \right)^{1/3} \qquad 13.4$$

(5) Computed compressive stress (f_f) must not exceed F_{cr}.

13.2.1.2 Honeycomb Core

(1) Enter Figure 13.6 with values of η/t and F /E to obtain K.

(2) Enter Figure 13.7 with value for K and $(E_c t/E_f t_c)^{1/2}$ to obtain F_{cr}/E_f.

(3) Solve for F_{cr}.

(4) Computed compressive stress (f_f) must not exceed F_{cr}.

13.2.2 Dimpling of Facings Under Edgewise Load

If the core of a sandwich construction is of cellular (honeycomb) material, it is possible for the facings to buckle or dimple into the spaces between core walls as shown in Figure 13.8. Dimpling of the facings may not lead to failure unless the amplitude of the dimples becomes large and causes the dimples or buckles to grow across core cell walls and result in wrinkling of the faces. Dimpling that does not

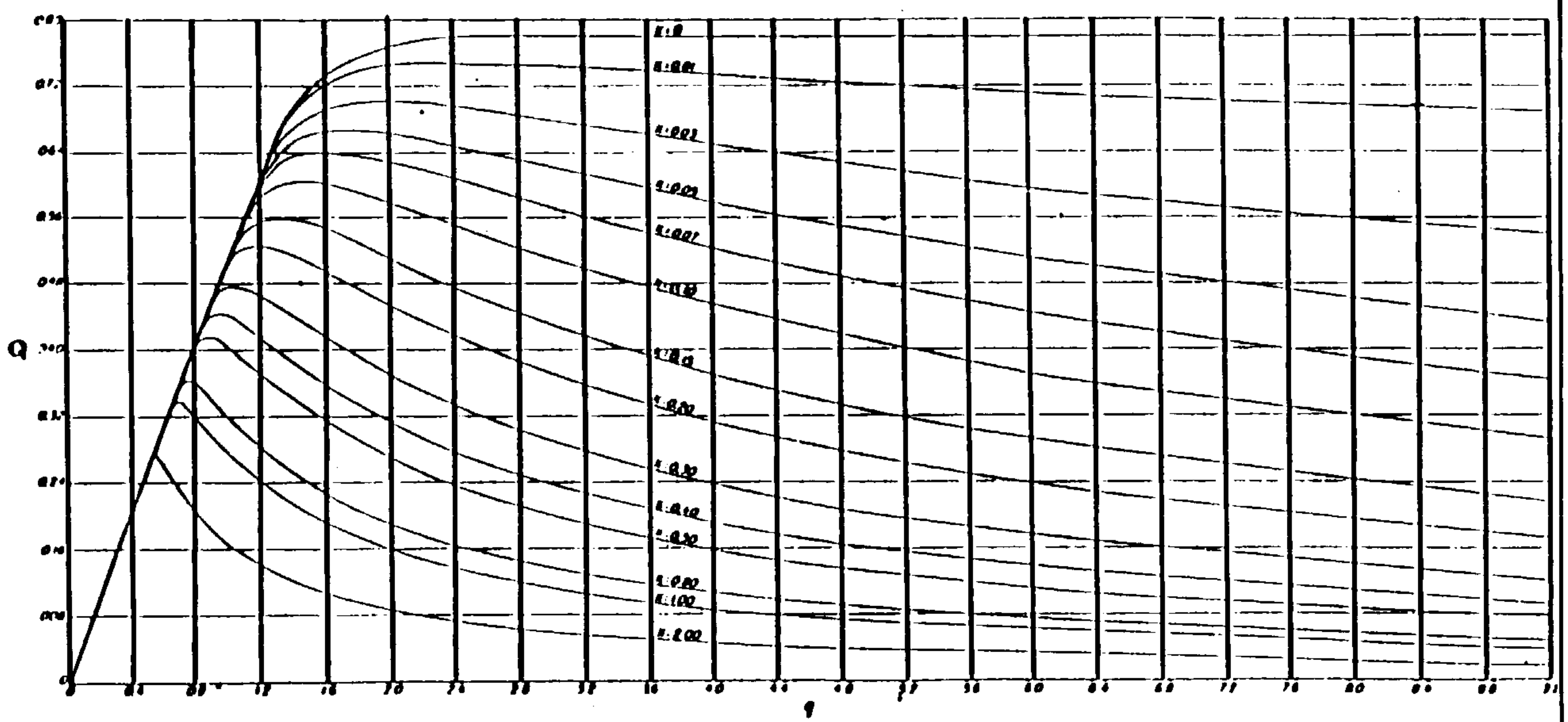

FIGURE 13.5 - PARAMETERS FOR DETERMINING WRINKLING OF FACINGS OF SANDWICH WITH CONTINUOUS CORES

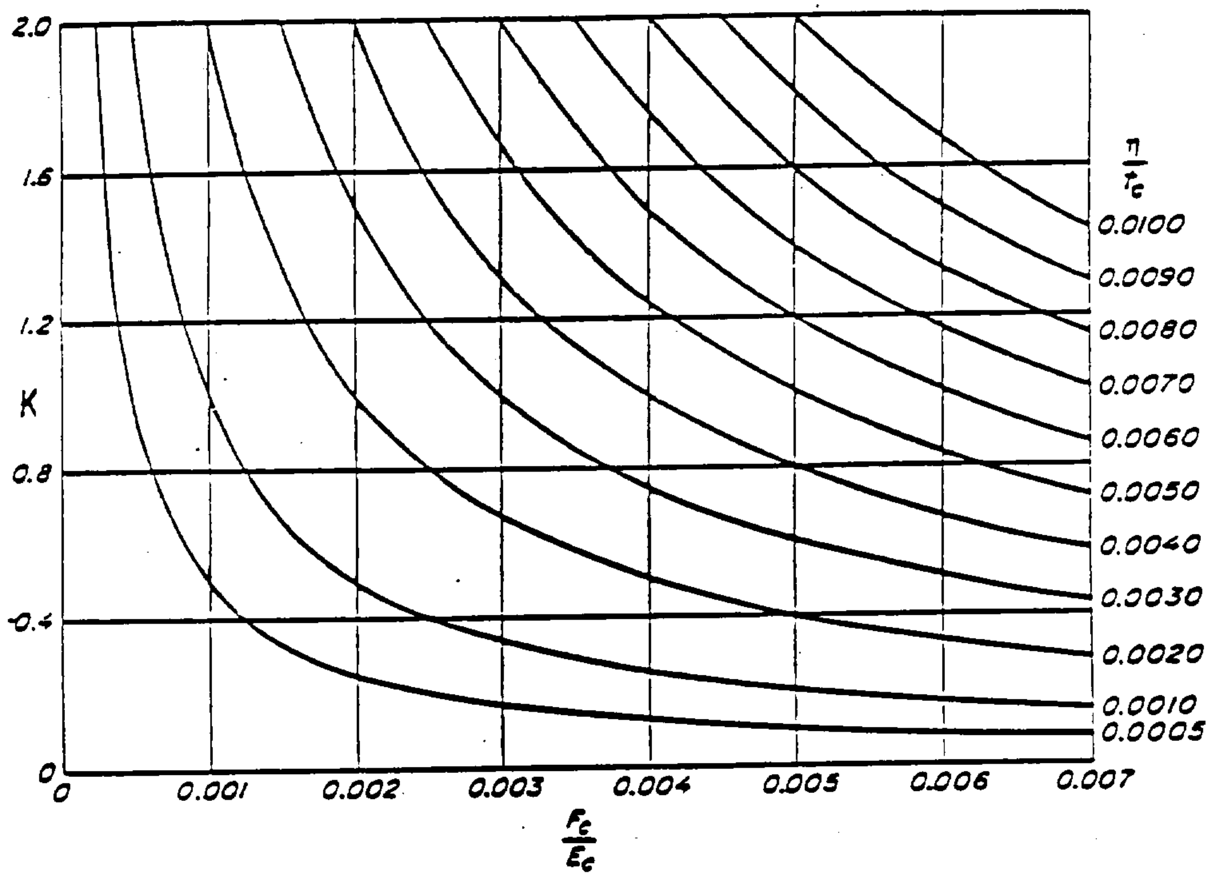

FIGURE 13.6 - RELATIONSHIP OF K TO CORE PROPERTIES (F_c/E_c) AND FACING WAVINESS (δ/tc)

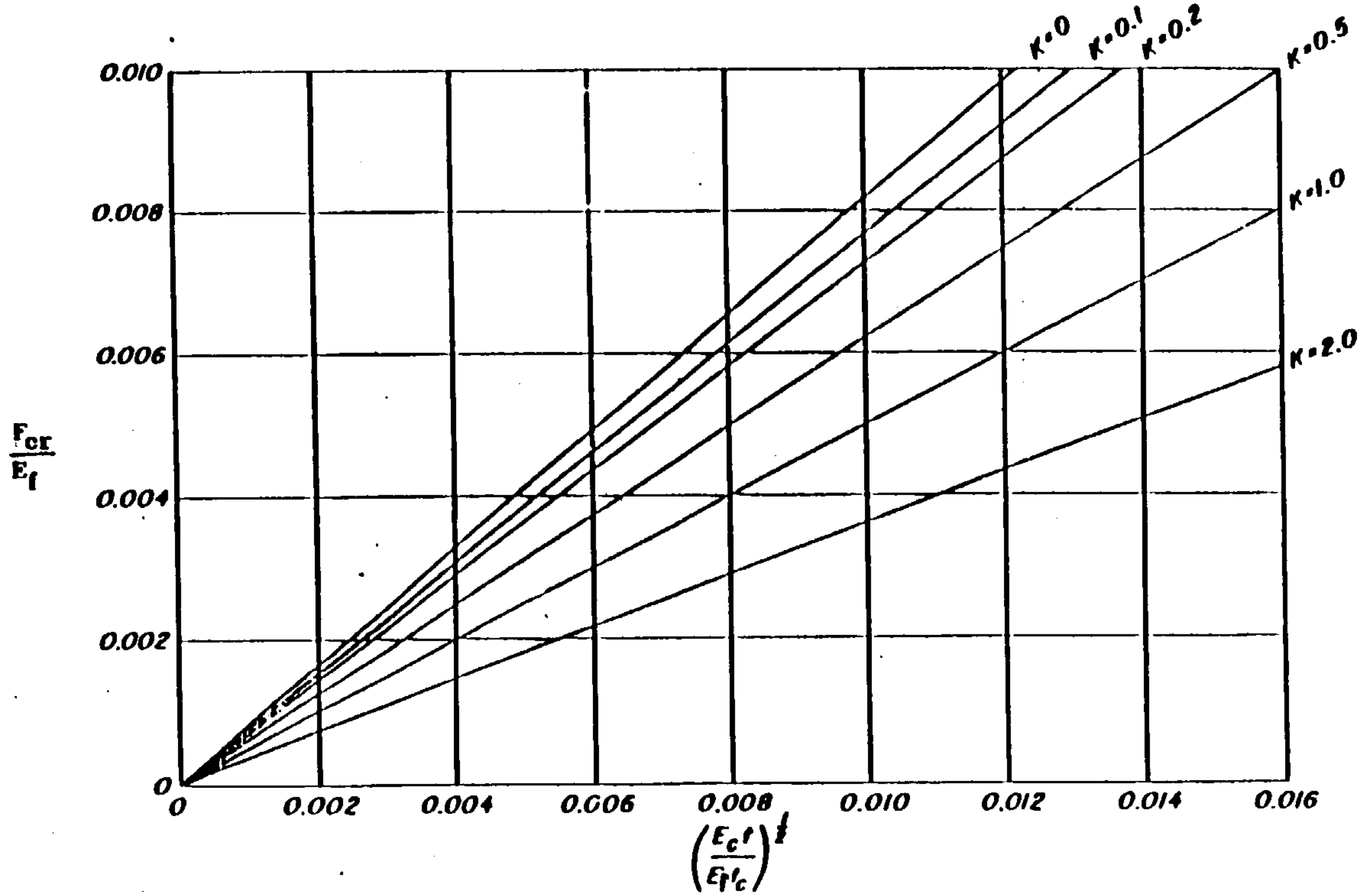

FIGURE 13.7 - GRAPH FOR THE WRINKLING STRESS OF FACINGS OF SANDWICH WITH HONEYCOMB CORES

Data Source, Section 1.3 Reference 3.

cause total structural failure may, of course, be severe enough so that permanent dimples remain after removal of load.

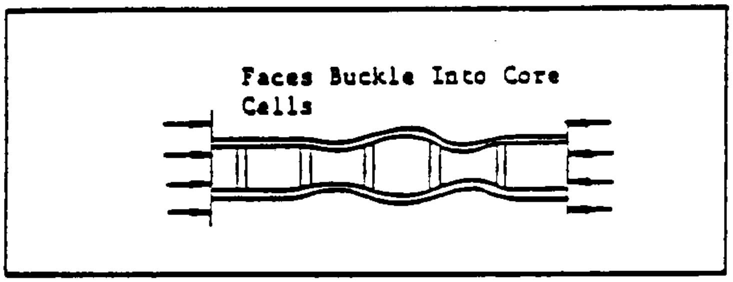

FIGURE 13.8 INTRACELL BUCKLING (FACE DIMPLING)

If dimpling of the facings is not permissible, the core cell size shall be small enough so that dimpling will not occur under design loads. It is assumed that failure in the facing-to-core bond cannot occur prior to dimpling.

Figure 13.9 can be used to determine the critical facing stress (stress at which dimpling will occur). The curves in Figure 13.9 represent a plot of equation 13.5 which can be used instead of Figure 13.9.

$$\frac{F_{cr}}{E_f} = \frac{2}{\lambda}\left(\frac{t}{s}\right)^2 \qquad 13.5$$

13.2.3 Flat Rectangular Panels with Edgewise Compression

The method presented here is used in design of a flat, rectangular sandwich panel subjected to edge compression. The panel is simply supported at the four edges and the load is applied equally and uniformly to the facings at two opposite edges as shown in Figure 13.10.

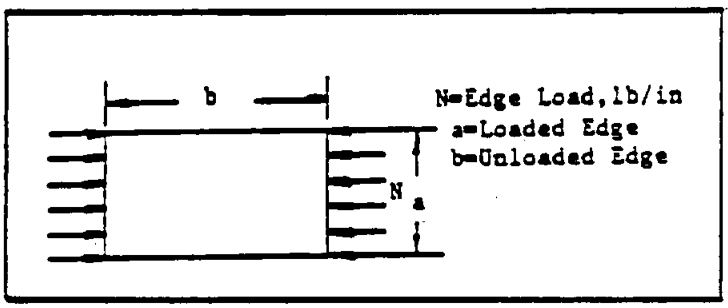

FIGURE 13.10 COMPRESSION PANELS

Overall buckling of the sandwich or dimpling or wrinkling of the facings cannot occur without possible total collapse of the panel. Detailed procedures follow giving theoretical formulas and graphs for determining dimensions of the facings and core, as well as necessary core properties. Facing modulus of elasticity, E, and stress values, F, shall be compression values at the conditions of use; that is, if

479

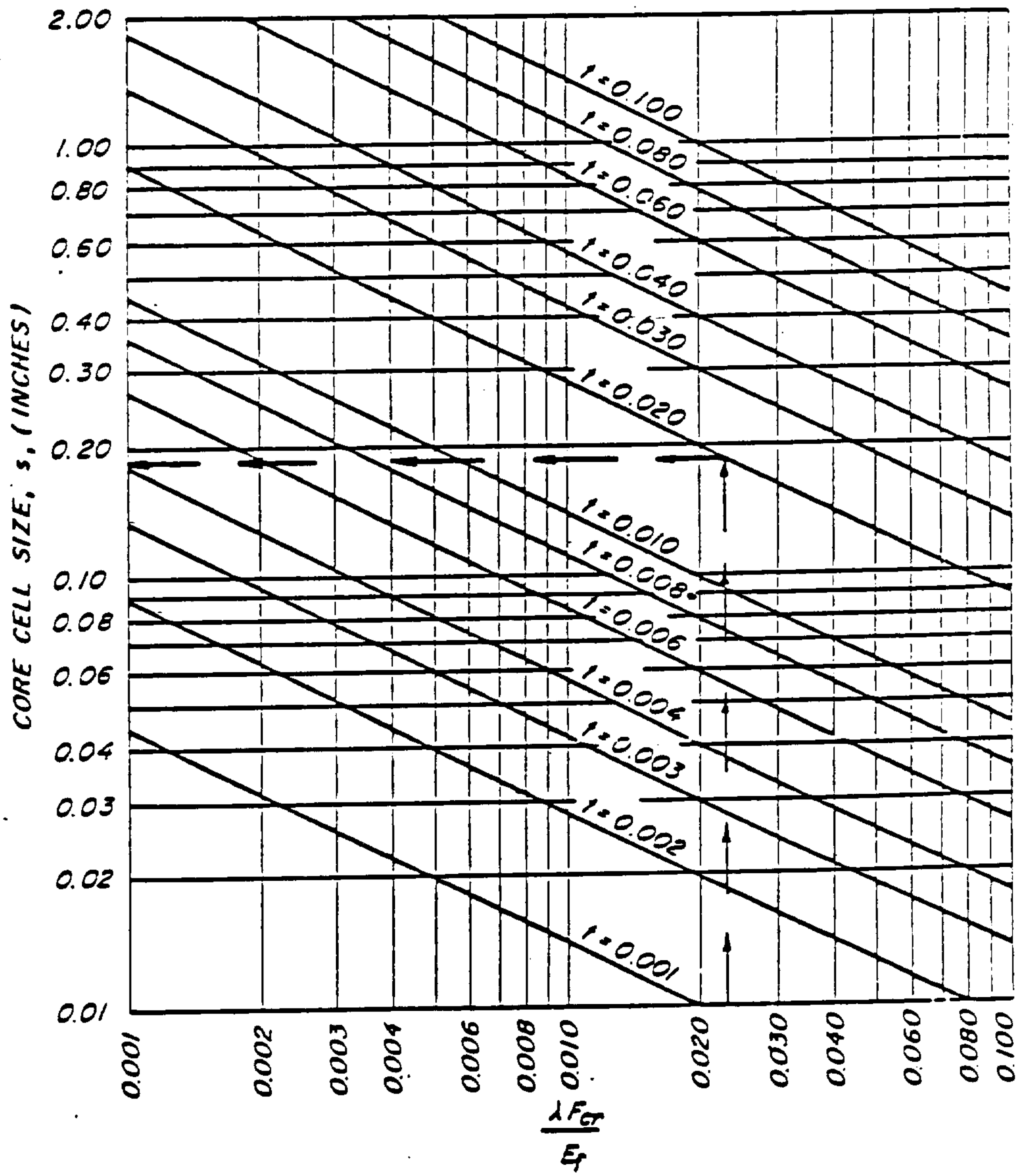

FIGURE 13.9 - CHART FOR DETERMINING CELLULAR CORE CELL SIZE SUCH THAT DIMPLING (INTRACELL BUCKLING) OF SANDWICH FACING WILL NOT OCCUR

application is at elevated temperature, then facing properties at elevated temperature shall be used in design. The facing modulus of elasticity is the effective value at the facing stress. If this stress is beyond the proportional limit value, an appropriate tangent, reduced or modified compression modulus shall be used.

(1) Choose an allowable design compressive stress (F_f) and determine the required facing thickness from

$$t_1 F_{f1} + t_2 F_{f2} = N; \text{ unequal faces} \qquad 13.6$$

$$t = N/2F_f; \text{ equal faces} \qquad 13.7$$

When the elastic modulus of one face is different from the elastic modulus of the other face, equation 13.6 must be satisfied, but also the stresses F_{f1} and F_{f2} must be chosen so that

$$\frac{F_{f1}}{E_1} = \frac{F_{f2}}{E_2} \qquad 13.8$$

The lower of the ratios in equation 13.8 must be used for design, otherwise the face with the lower ratio will be overstressed.

(2) The critical facing stress (F_{cr}) at which buckling of the panel will occur is

$$F_{cr} = \pi^2 K \frac{E_{f1} t_1 E_{f2} t_2}{(E_{f1} t_1 + E_{f2} t_2)^2} \left(\frac{h}{a}\right)^2 \left(\frac{E_f}{\lambda}\right) \qquad 13.9$$

where E_f and λ are values for the facing with least F_f/E_f ratio as determined from equation 13.8.

If the facings are of equal thickness and of the same material, equation 13.9 becomes

$$F_{cr} = \frac{\pi^2 K}{4} \left(\frac{h}{a}\right)^2 \left(\frac{E_f}{\lambda}\right) \qquad 13.10$$

In equations 13.9 and 13.10

$$K = K_M + K_F \qquad 13.11$$

K is determined first by going through the following steps 3 to 8.

(3) Determine the value of parameters:

$$a/b \text{ or } b/a, \text{ whichever is } < 1 \qquad 13.12$$

$$\frac{E_{f2}t_2}{E_{f1}t_1} \qquad 13.13$$

$$\frac{F_f \lambda}{E_f} \qquad 13.14$$

(4) Enter the appropriate figure (13.11, 13.12, 13.13 or 13.14) with equation 13.12 at V = .01 (Choosing a low finite value of V to start with since V = 0 gives h as a minimum and G_c as infinite). Project laterally to parameter 13.13 then vertically down to parameter 13.14 and horizontally to h/a. Evaluate h.

(5) Determine core thickness from

$$t_c = h - \frac{t_1 + t_2}{2} \text{ ; for unequal faces} \qquad 13.15$$

$$t_c = h - t\text{; for equal faces} \qquad 13.16$$

(6) Determine constant K' in the equation $V = K'/G_c$ from

$$K' = \frac{\pi^2 t_c E_{f1} t_1 E_{f2} t_2}{\lambda a^2 (E_{f1} t_1 + E_{f2} t_2)} \text{ ; for unequal faces} \qquad 13.17$$

$$K' = \frac{\pi^2 t_c E_f t}{2\lambda a^2} \text{ ; for equal faces} \qquad 13.18$$

(7) Determine tentative core modulus of rigidity (G_c) from $G_c = K'/V$ for V = .01. If this value of G_c is not within the range available in the desired core material and type, enter Figure 13.15. Project diagonally along the line $V = K'/G_c$ until a practical value is reached. For the new value of V, repeat steps (4), (5) and (6).

(8) From the appropriate Figure (13.16 through 13.27) find the value of K_M. From Figure 13.28 obtain the value of K_{MO}. Find K_F

$$K_F = \frac{(E_{f1} t_1^3 + E_{f2} t_2^3)(E_{f1} t_1 + E_{f2} t_2)}{12 E_{f1} t_1 E_{f2} t_2 h^2} K_{MO} \qquad 13.19$$

$$K_F = \frac{t^2 K_{MO}}{3h^2} \text{ ; for equal faces} \qquad 13.20$$

For values of b/a greater than those in Figure 13.28 assume $K_F = 0$.

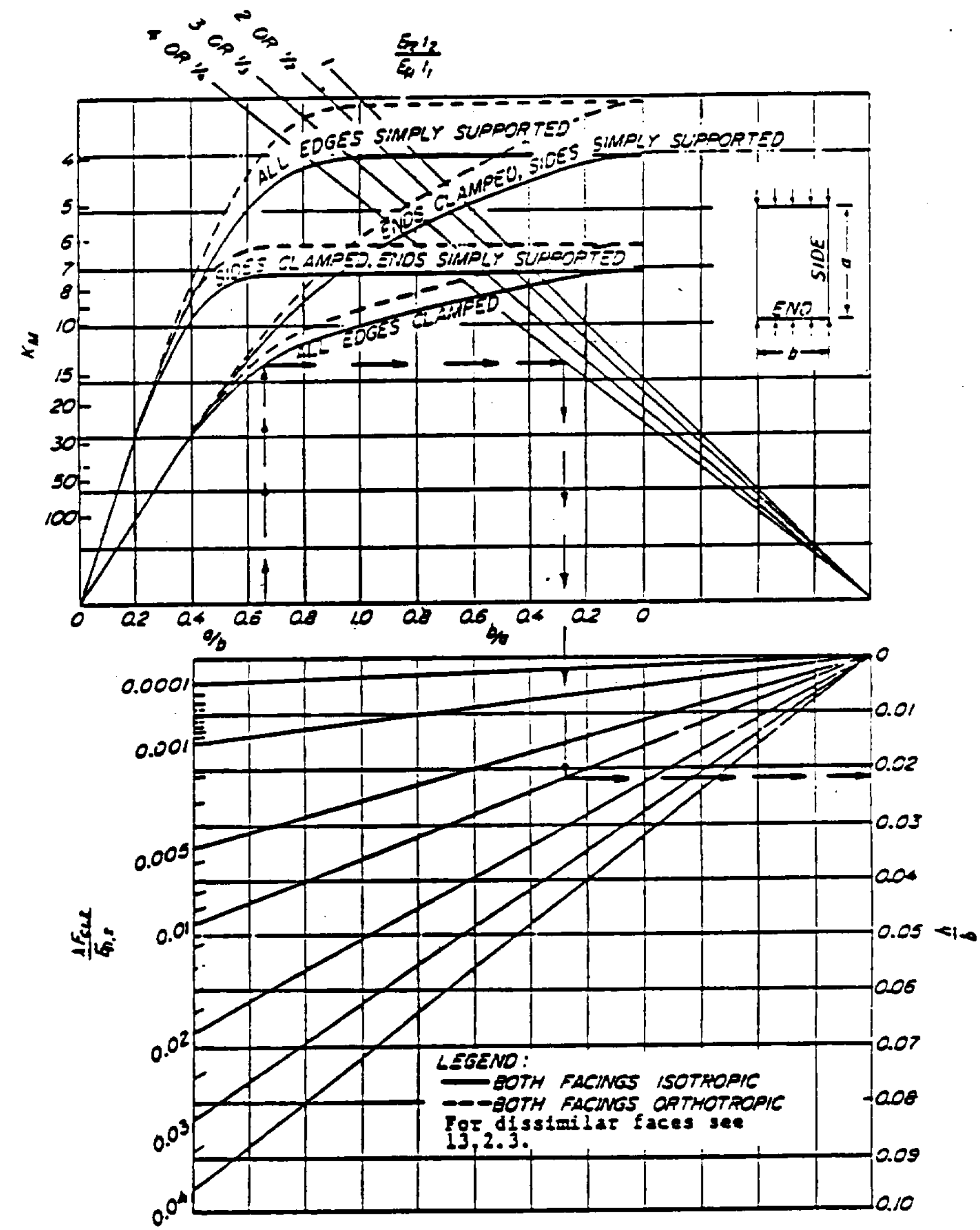

FIGURE 13.11 - CHART FOR DETERMINING h/b RATIO (V=0) SUCH THAT A SANDWICH PANEL WILL NOT BUCKLE UNDER EDGEWISE COMPRESSION LOAD

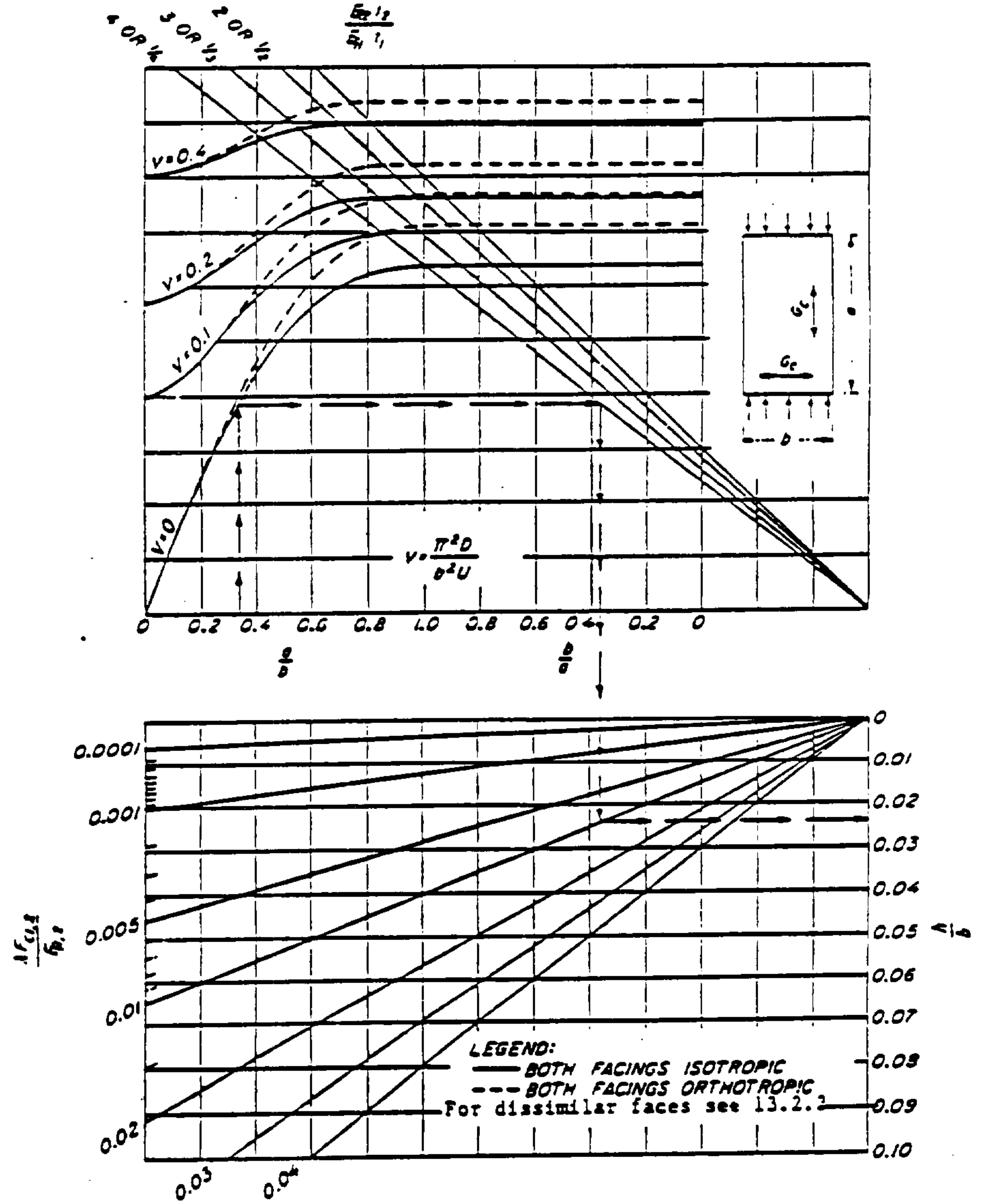

FIGURE 13.12 - CHART FOR DETERMINING h/b RATIO SUCH THAT A SIMPLY SUPPORTED SANDWICH PANEL WITH ISOTROPIC ($G_{cb} = G_{ca}$) WILL NOT BUCKLE UNDER EDGEWISE COMPRESSION LOAD

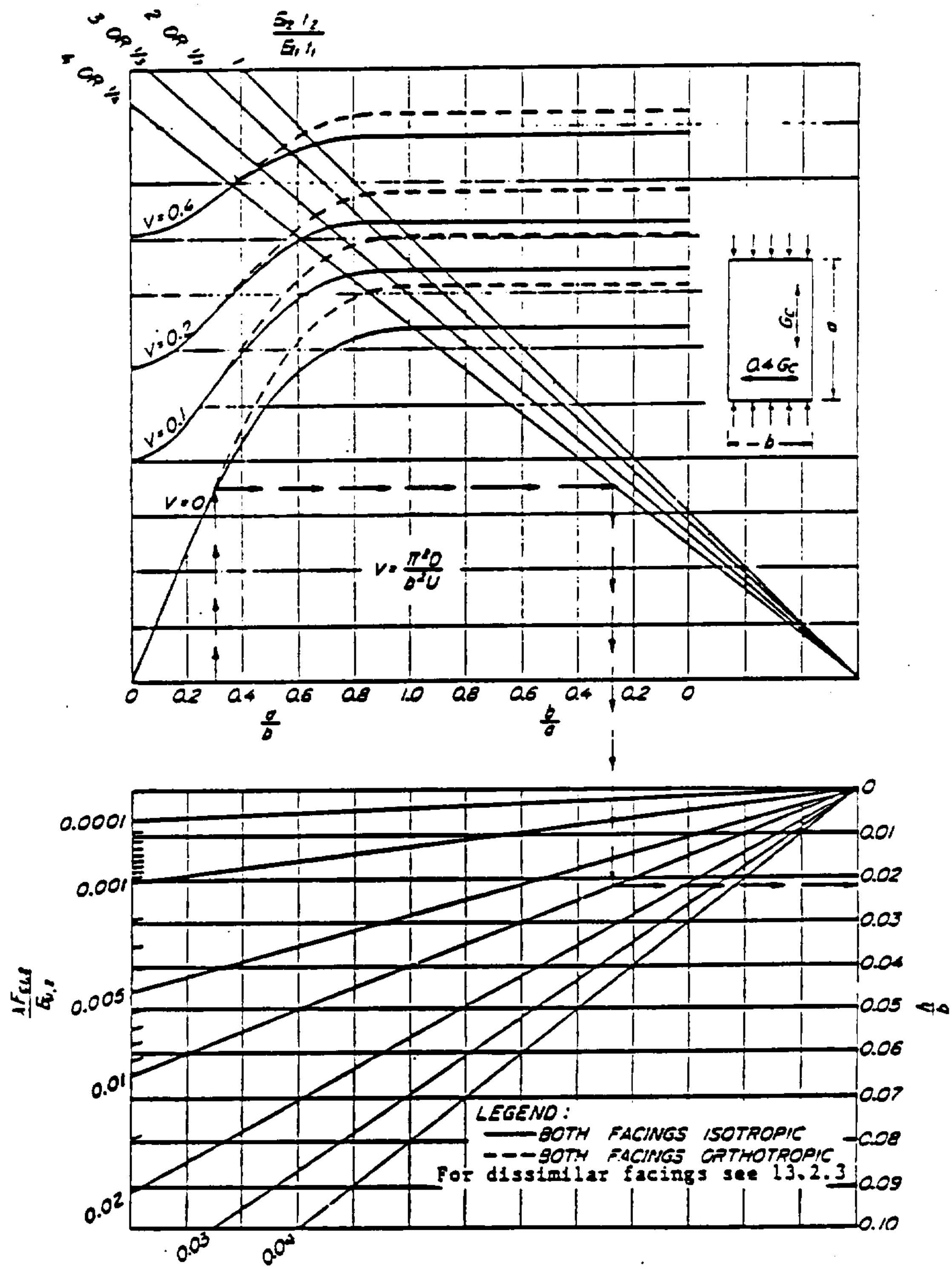

FIGURE 13.13 - CHART FOR DETERMINING h/b RATIO SUCH THAT A SIMPLY SUPPORTED SANDWICH PANEL WITH ORTHOTROPIC CORE (G_{cb} = 0.4 G_{ca}) WILL NOT BUCKLE UNDER EDGEWISE COMPRESSION LOAD.

495

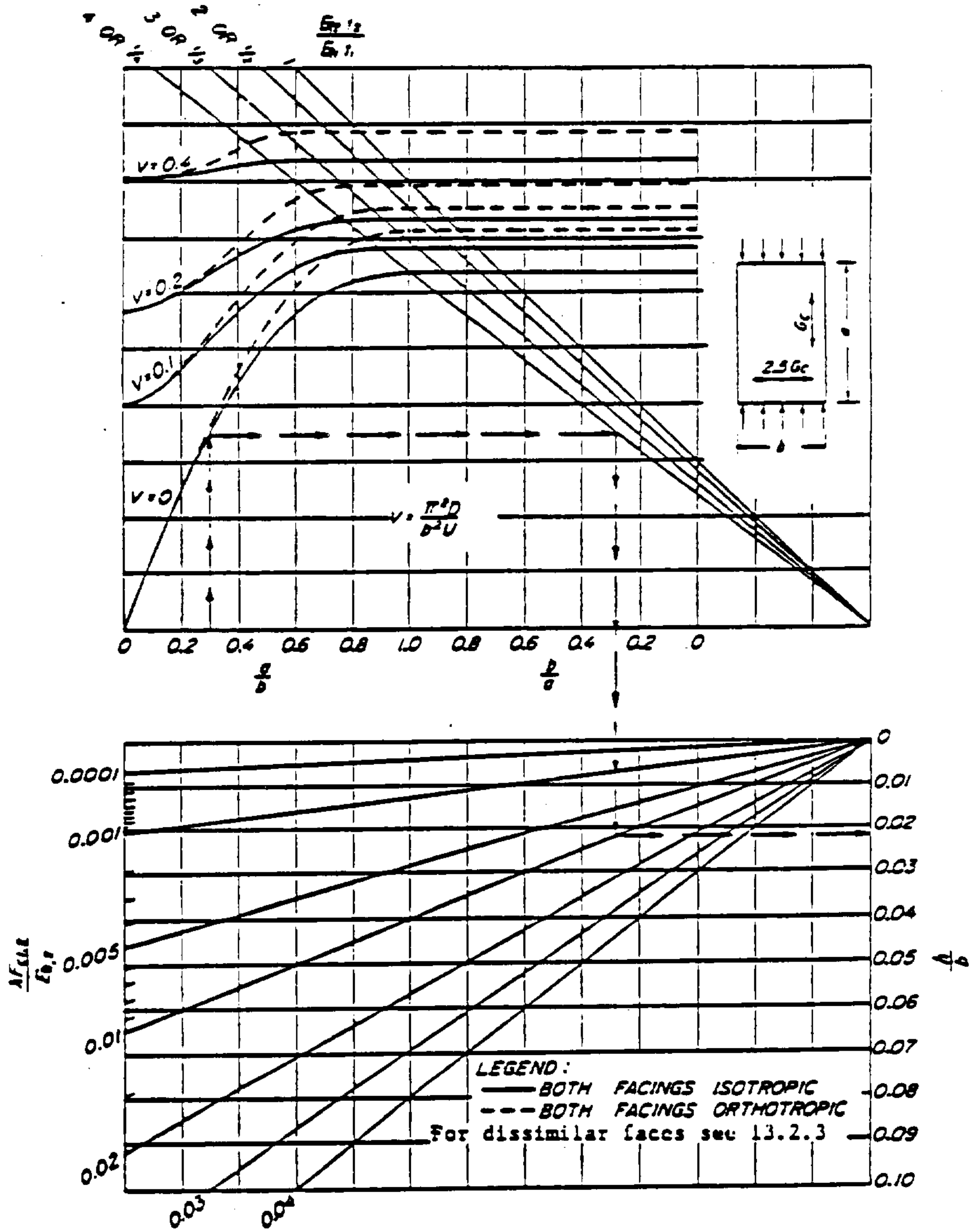

FIGURE 13.14 - CHART FOR DETERMINING h/b RATIO SUCH THAT A SIMPLY SUPPORTED SANDWICH PANEL WITH ORTHOTROPIC CORE (G_{cb} = 2.5 G_{ca}) WILL NOT BUCKLE UNDER EDGEWISE COMPRESSION LOAD.

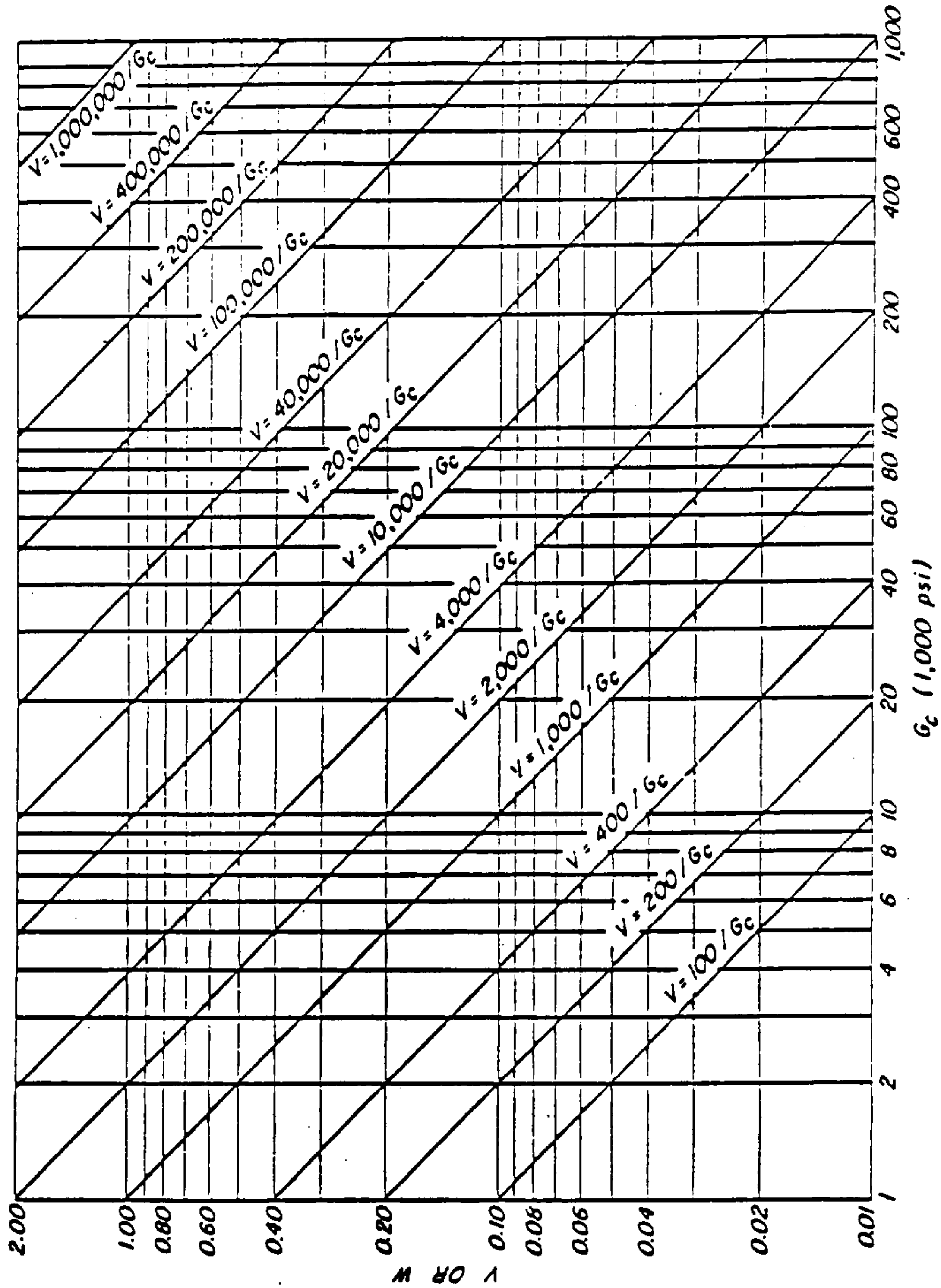

FIGURE 13.15 - CHART FOR DETERMINING V OR W AND G_c FOR SANDWICH IN EDGEWISE COMPRESSION

487

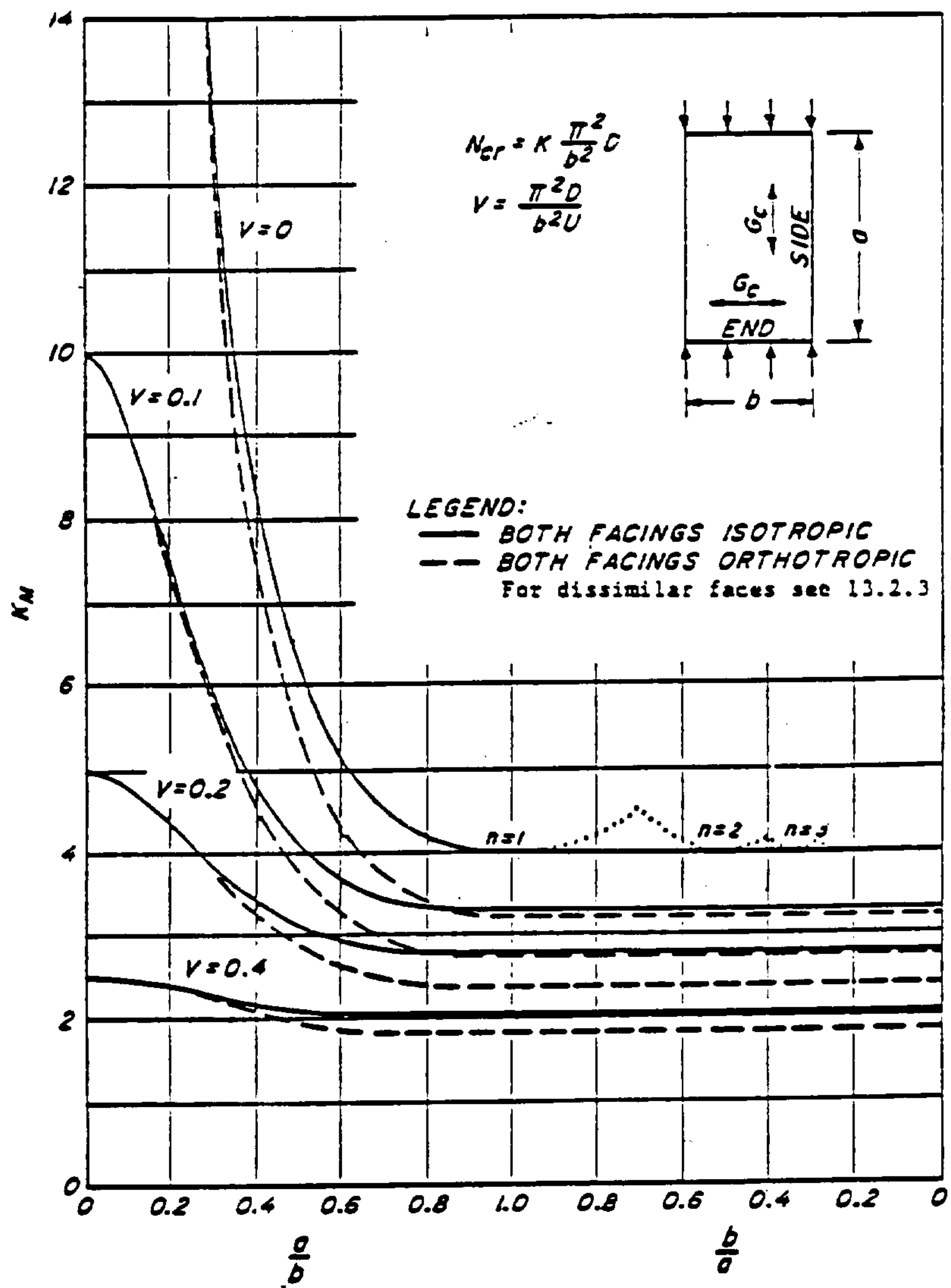

FIGURE 13.16 - K_M FOR SANDWICH PANEL WITH ENDS AND SIDES SIMPLY SUPPORTED AND ISOTROPIC CORE. ($G_{cb} = G_{ca}$).

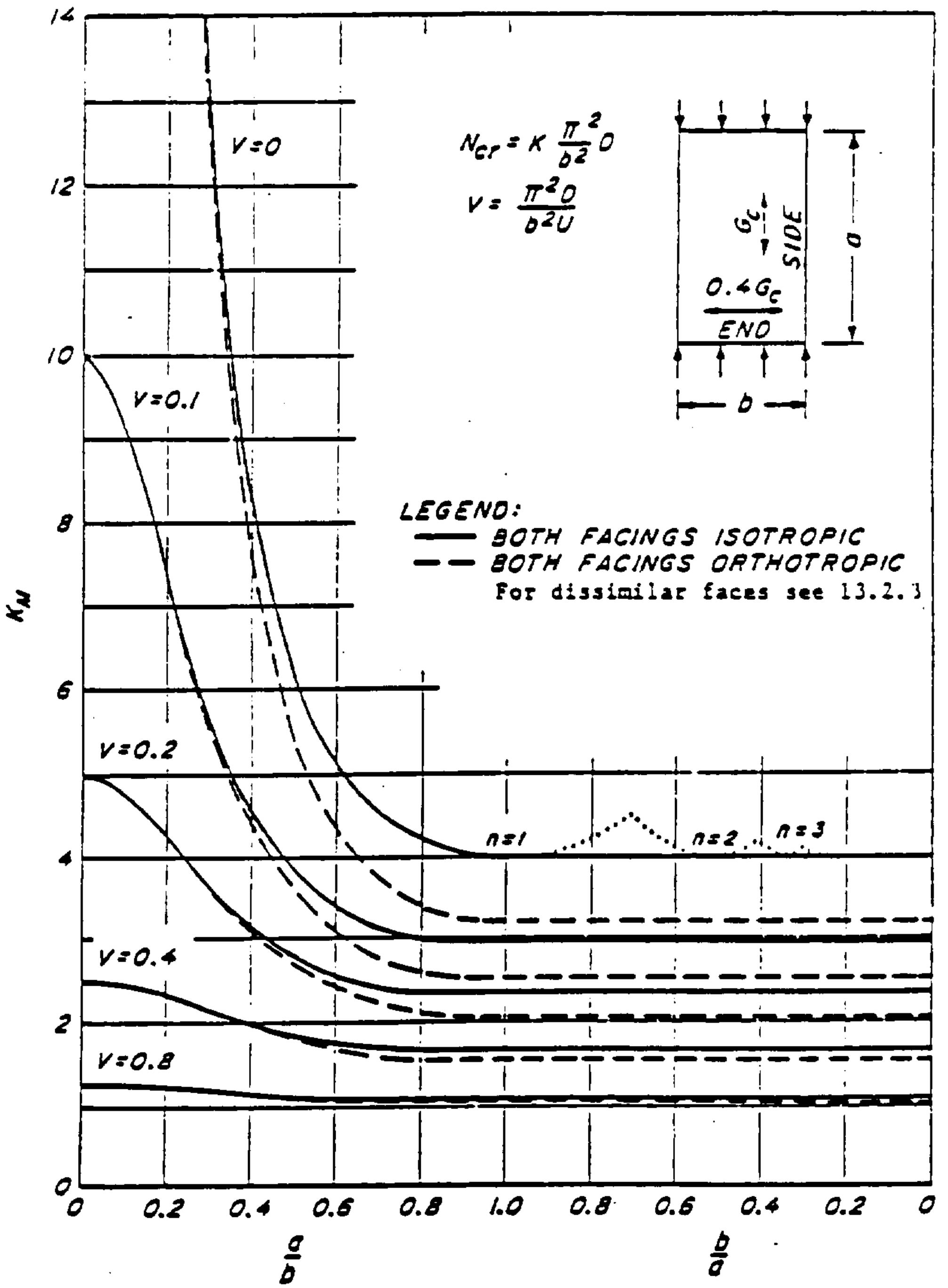

FIGURE 13.17 - K_M FOR SANDWICH PANEL WITH ENDS AND SIDES SIMPLY SUPPORTED AND ORTHOTROPIC CORE. ($G_{cb} = 0.4\ G_{ca}$).

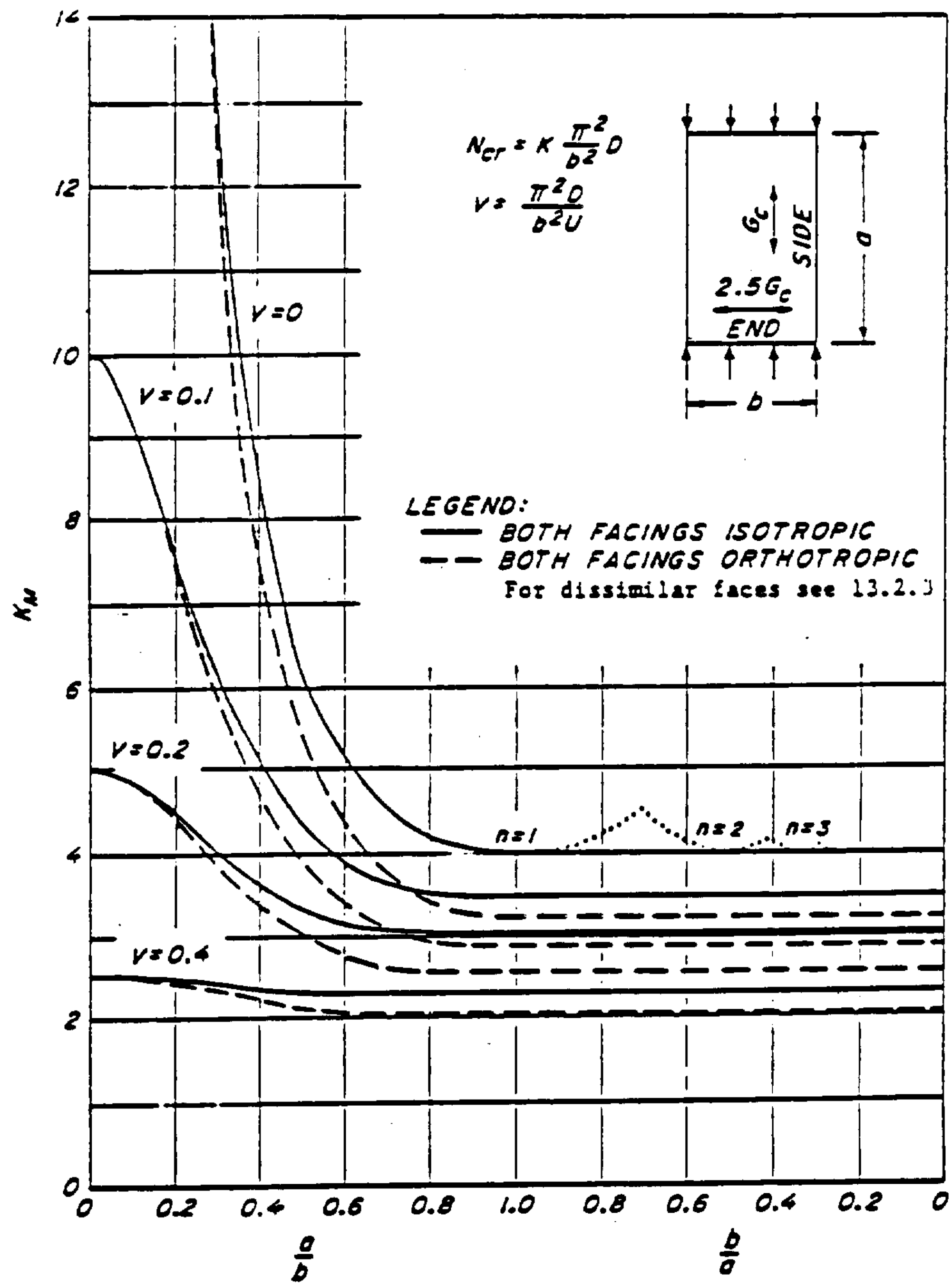

FIGURE 13.18 - K_M FOR SANDWICH PANEL WITH ENDS AND SIDES SIMPLY SUPPORTED AND ORTHOTROPIC CORE ($G_{cb} = 2.5\ G_{ca}$).

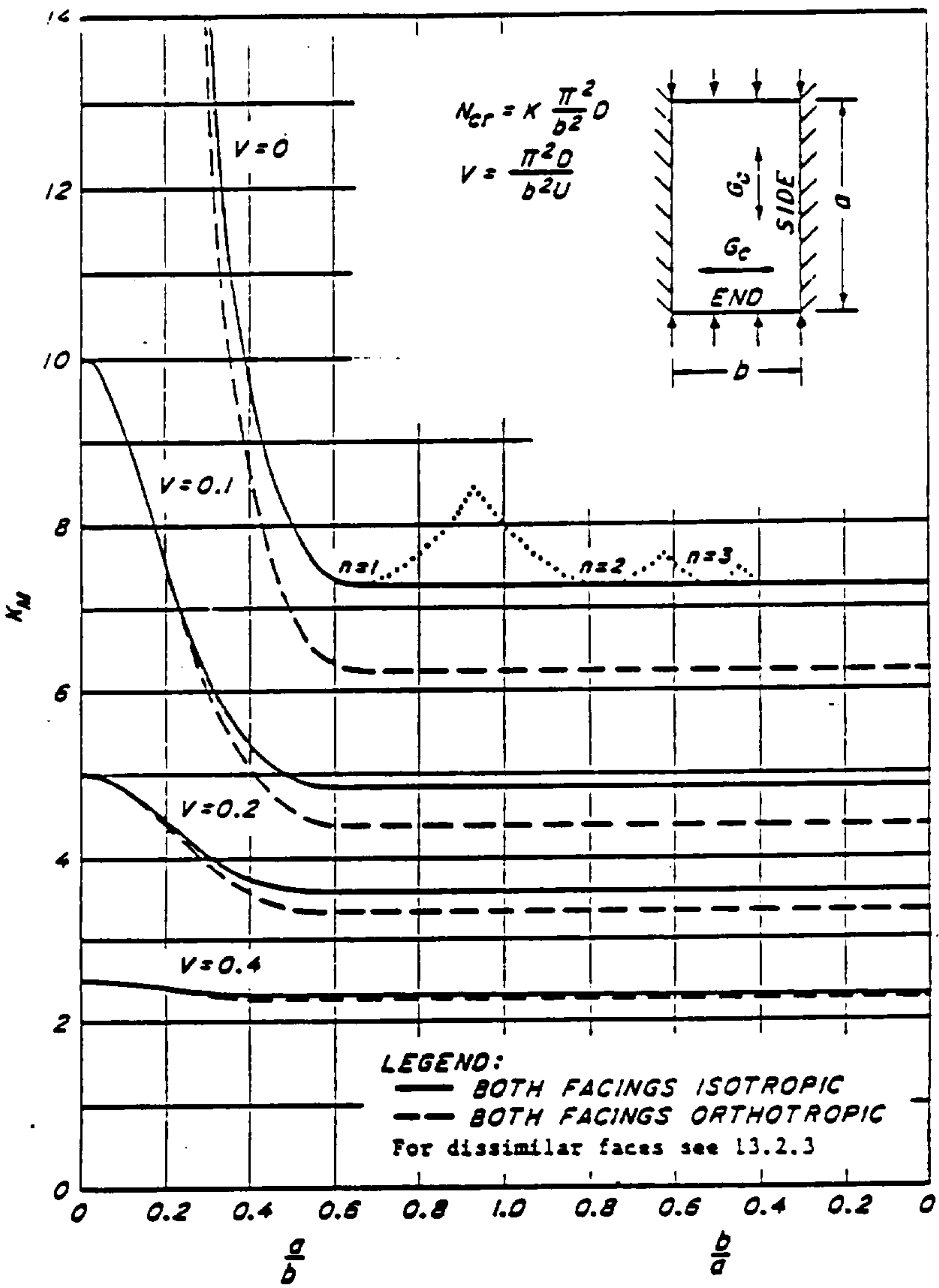

FIGURE 13.19 - K_M FOR SANDWICH PANEL WITH ENDS SIMPLY SUPPORTED AND SIDES CLAMPED AND ISOTROPIC CORE, ($G_{cb}=G_{ca}$).

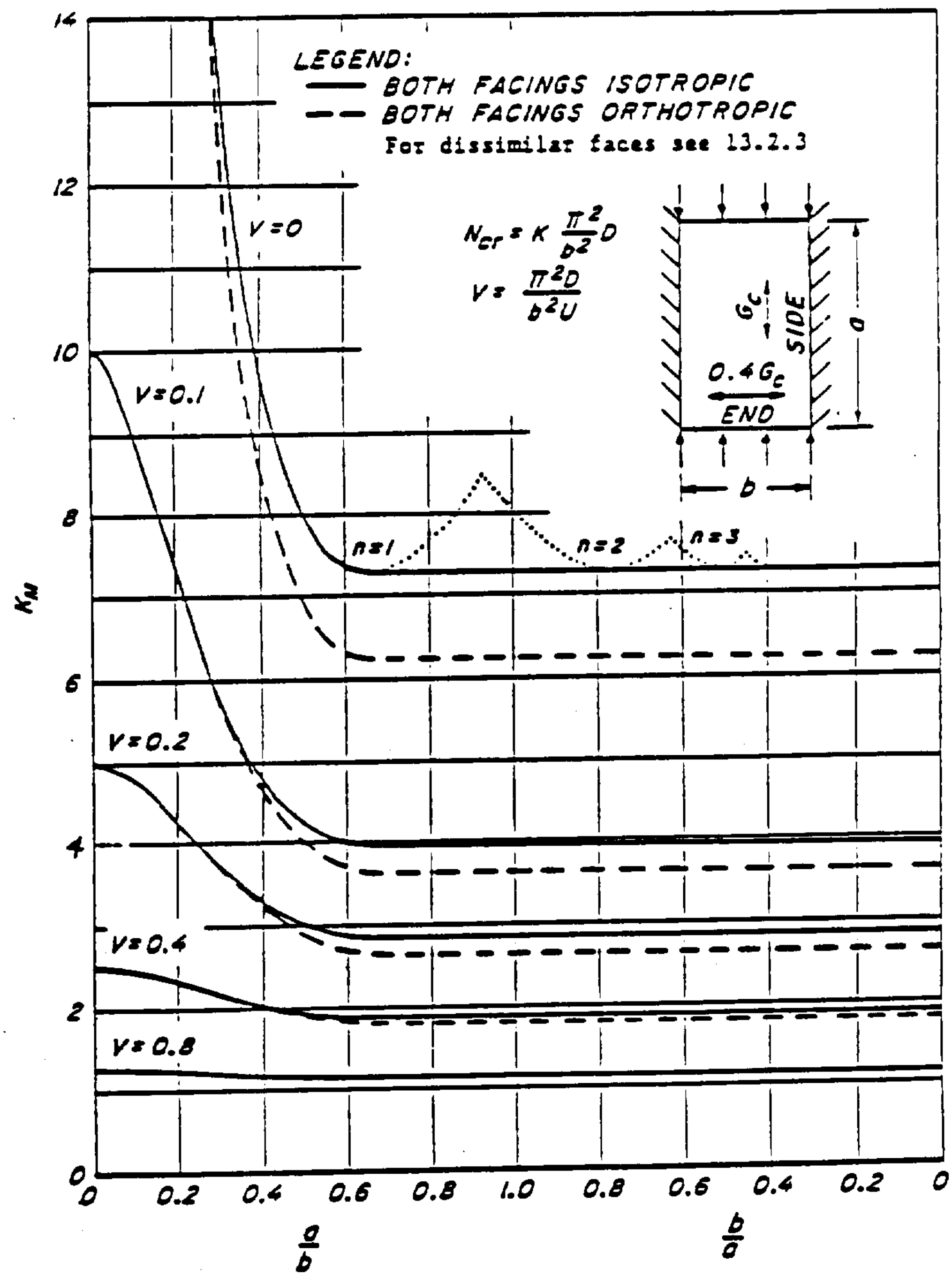

FIGURE 13.20 - K_M FOR SANDWICH PANEL WITH ENDS SIMPLY SUPPORTED AND SIDES CLAMPED AND ORTHOTROPIC CORE (G_{cb}=0.4 G_{ca}).

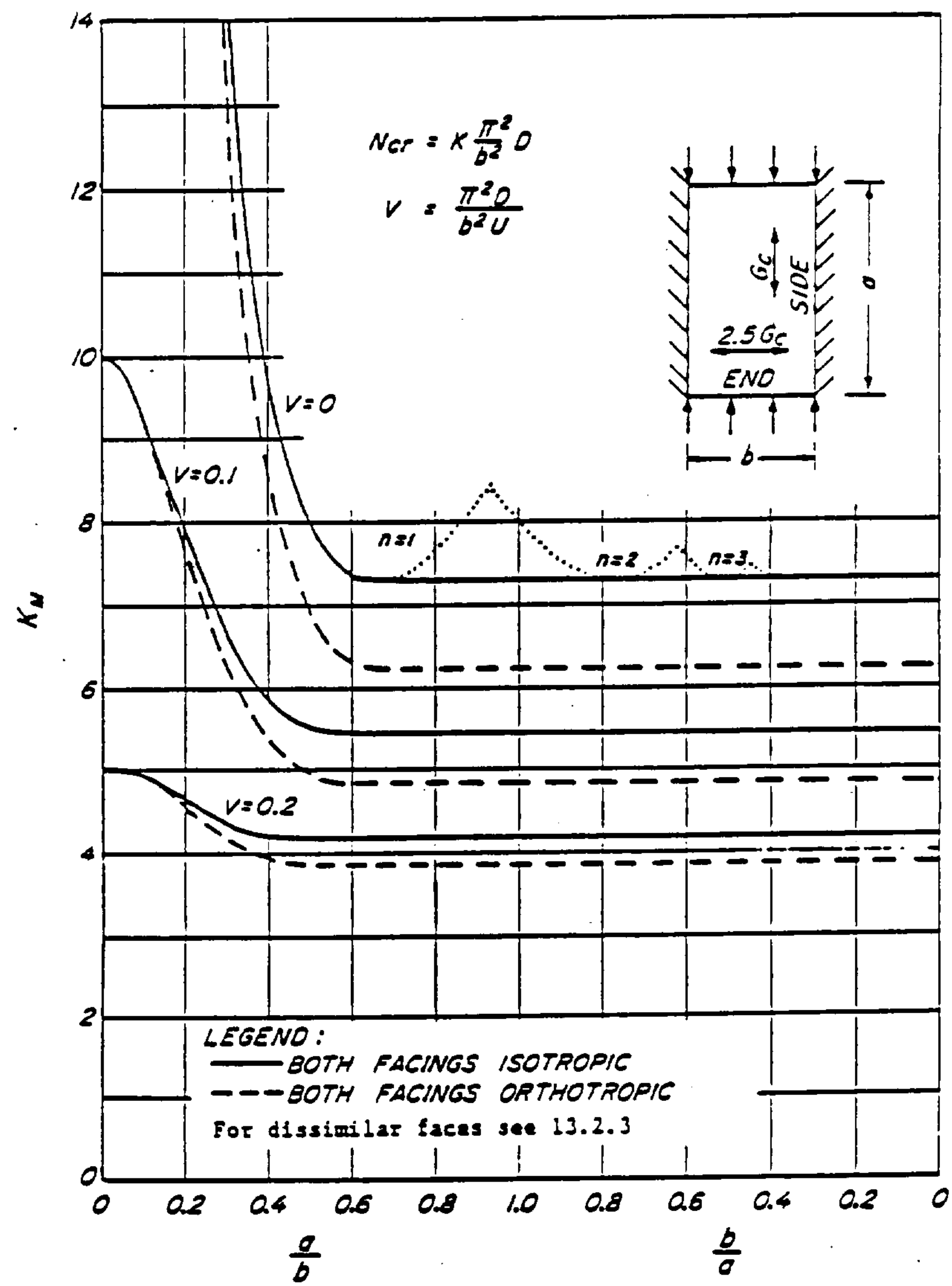

FIGURE 13.21 - K_M FOR SANDWICH PANEL WITH ENDS SIMPLY SUPPORTED AND SIDES CLAMPED AND ORTHOTROPIC CORE (G_{cb}=2.5 G_{ca}).

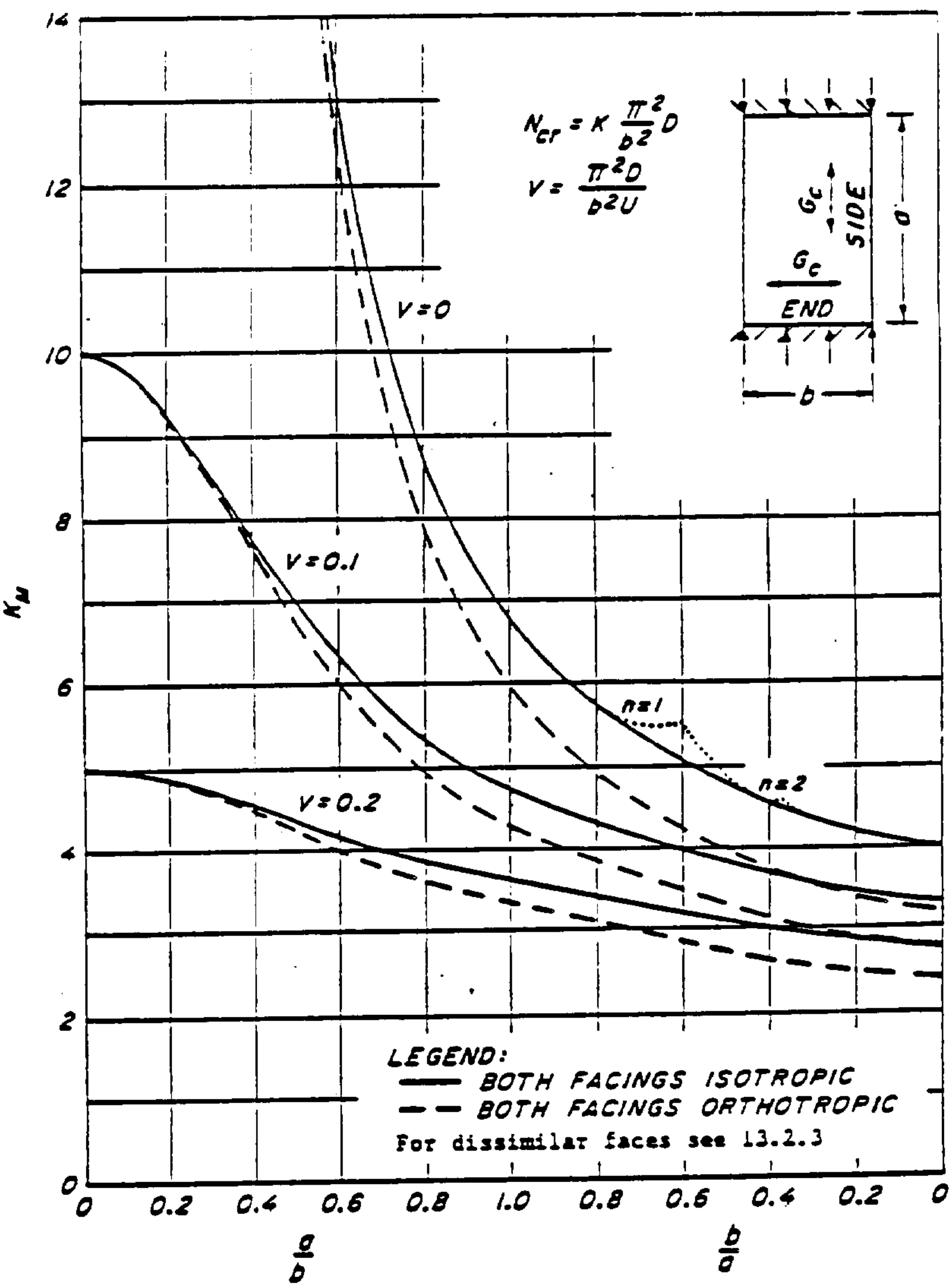

FIGURE 13.22 - K_M FOR SANDWICH PANEL WITH ENDS CLAMPED AND SIDES SIMPLY SUPPORTED AND ISOTROPIC CORE ($G_{cb}=G_{ca}$).

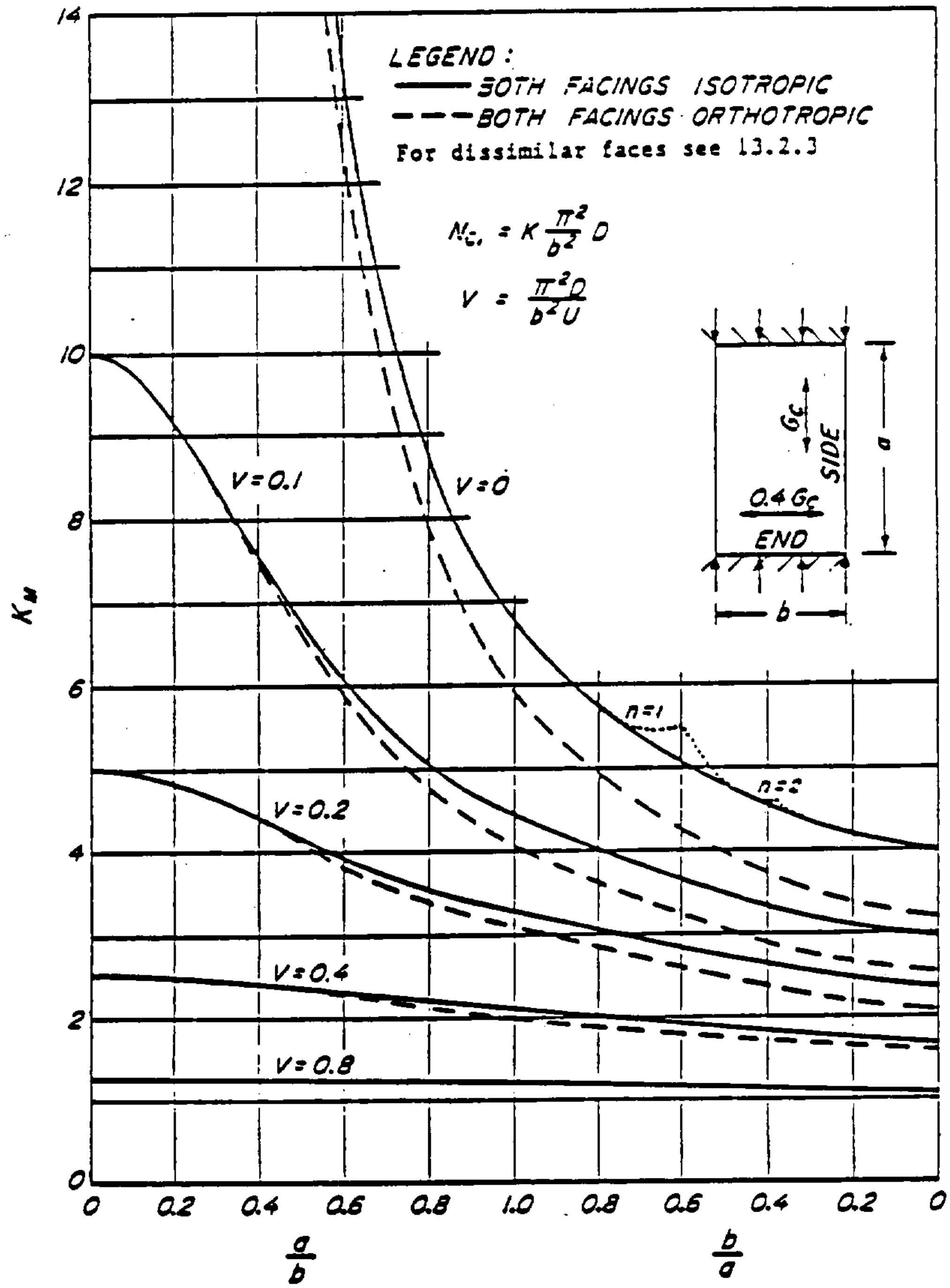

FIGURE 13.23 - K_M FOR SANDWICH PANEL WITH ENDS CLAMPED AND SIDES SIMPLY SUPPORTED AND ORTHOTROPIC CORE ($G_{cb} = 0.4\ G_{ca}$)

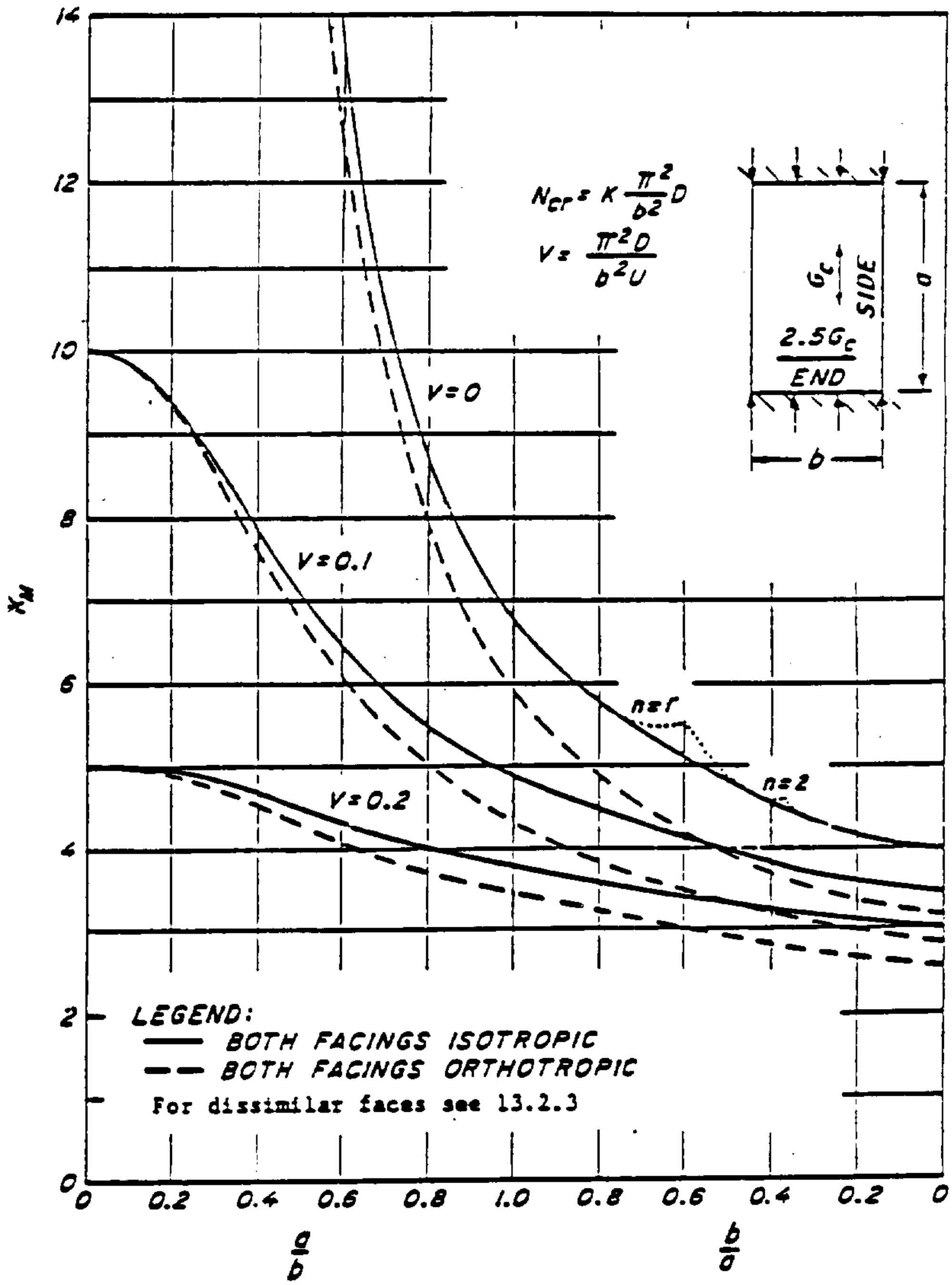

FIGURE 13.24 - K_M FOR SANDWICH PANEL WITH ENDS CLAMPED AND SIDES SIMPLY SUPPORTED AND ORTHOTROPIC CORE (G_{cb}=2.5 G_{ca})

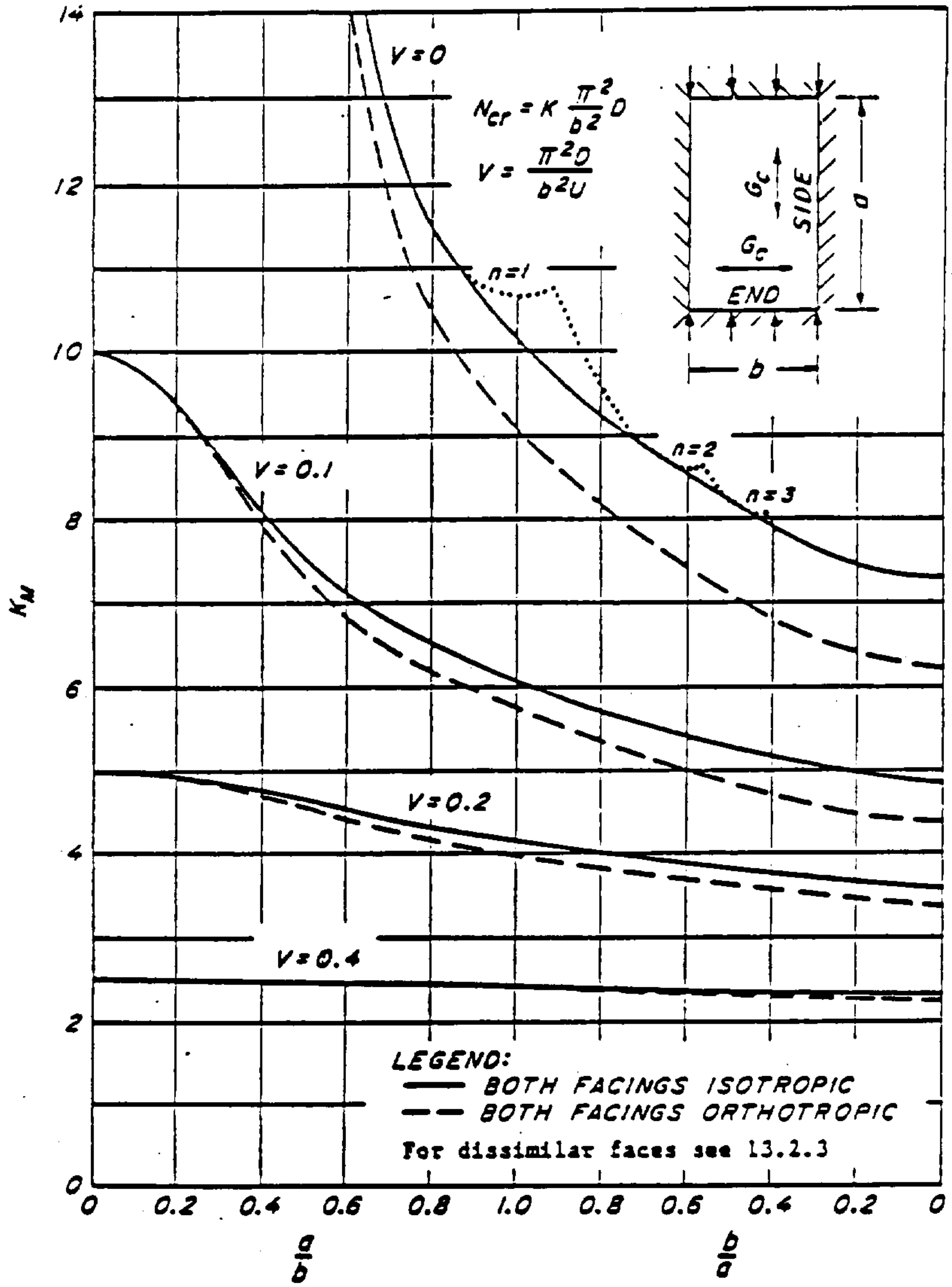

FIGURE 13.25 - K_M FOR SANDWICH PANEL WITH ENDS AND SIDES CLAMPED AND ISOTROPIC CORE ($G_{cb}=G_{ca}$).

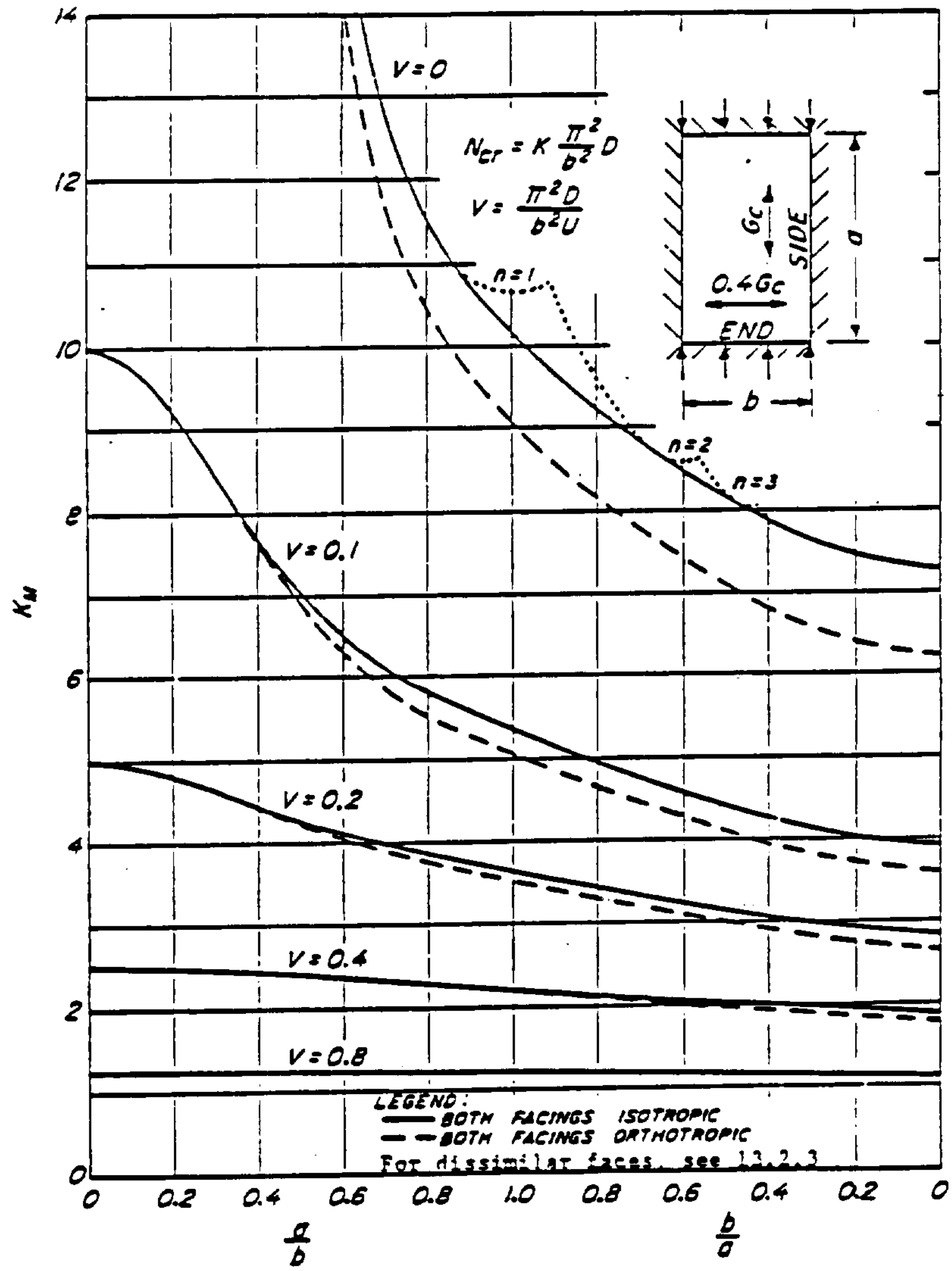

FIGURE 13.26 - K_M FOR SANDWICH PANEL WITH ENDS AND SIDES CLAMPED AND ORTHOTROPIC CORE ($G_{cb} = 0.4\ G_{ca}$)

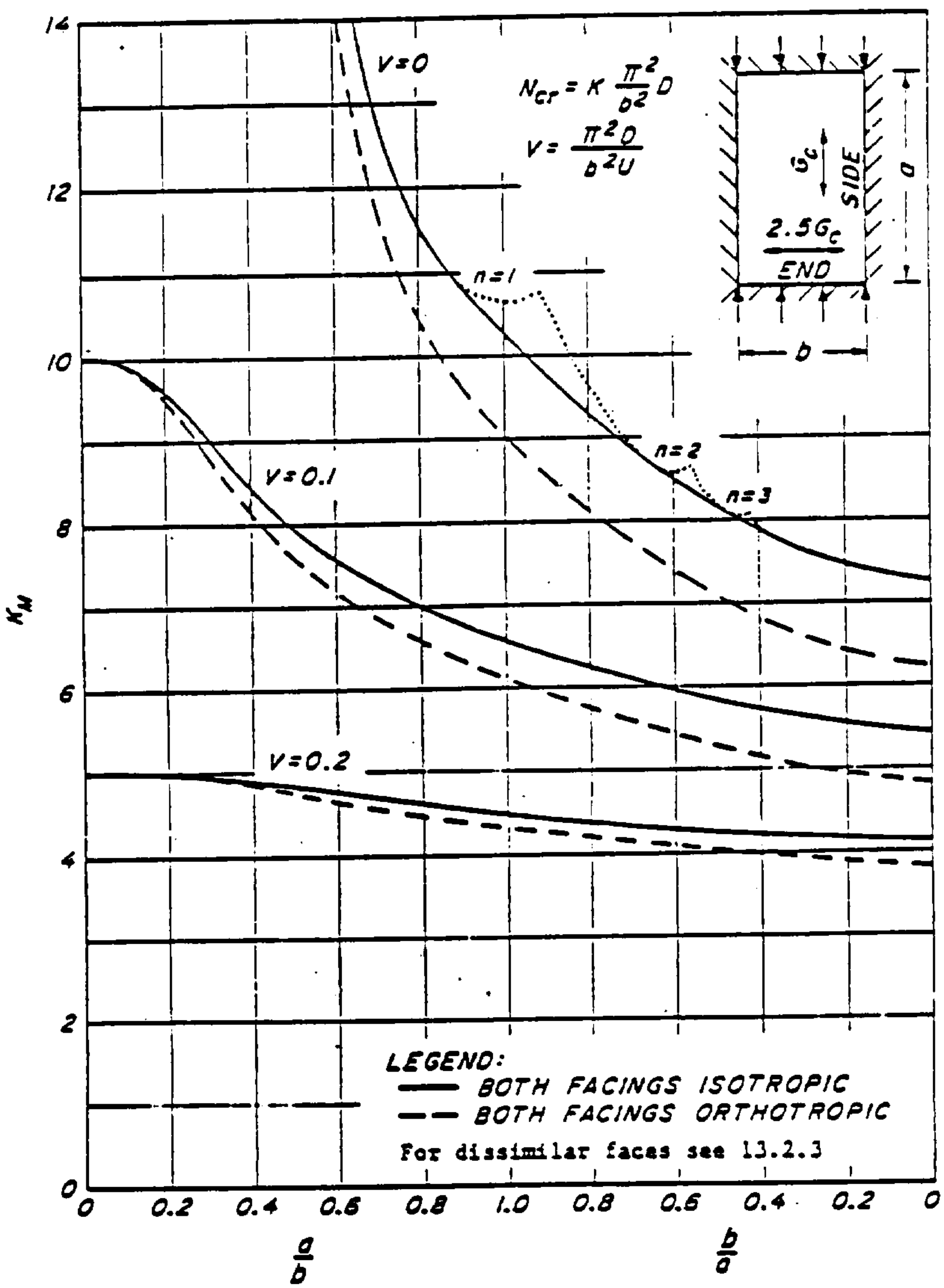

FIGURE 13.27 - K_M FOR SANDWICH PANEL WITH ENDS AND SIDES CLAMPED AND ORTHOTROPIC CORE ($G_{cb} = 2.5\ G_{ca}$)

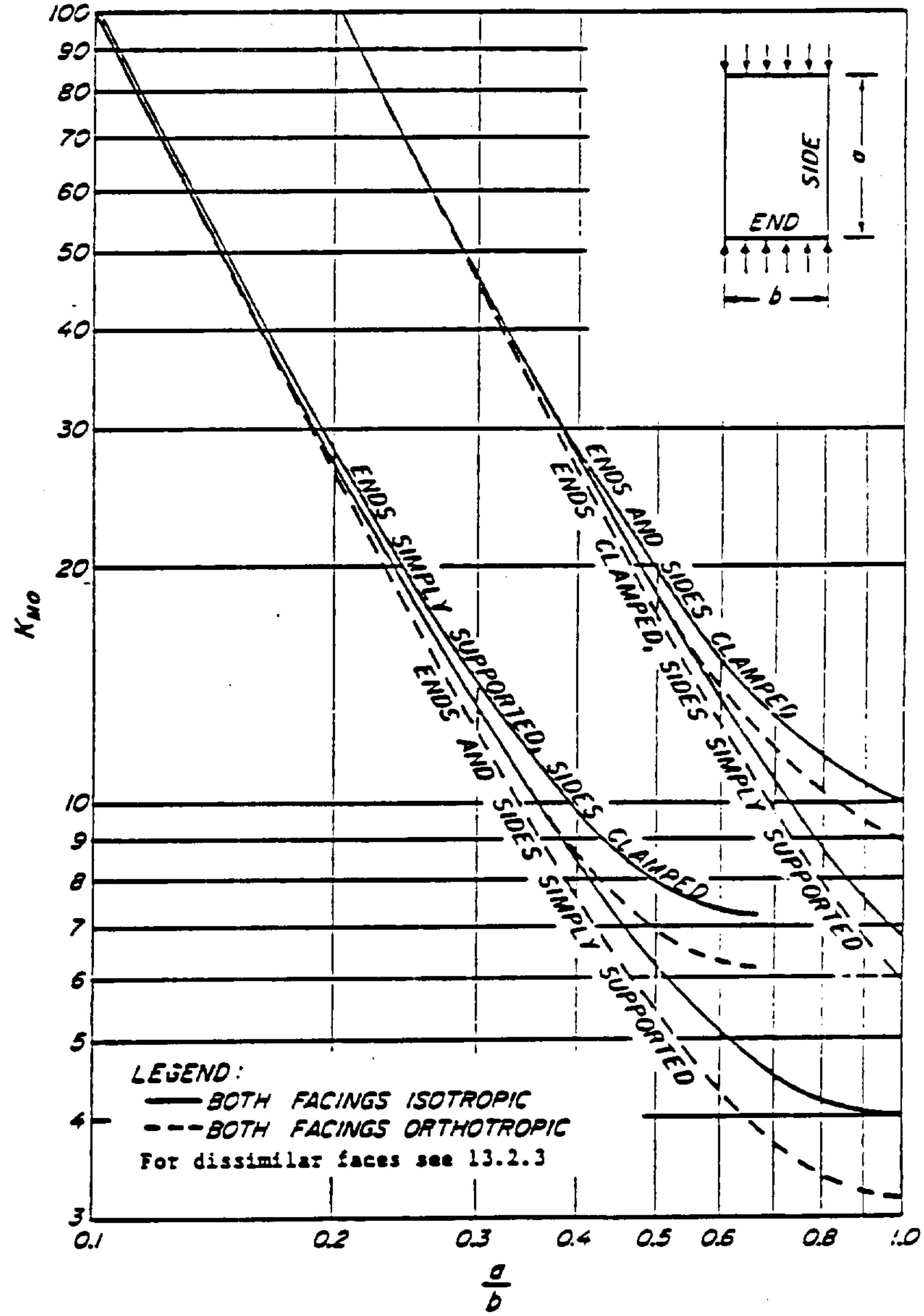

FIGURE 13.28 - VALUES OF K_{MO} FOR SANDWICH PANELS IN EDGEWISE COMPRESSION

(9) Evaluate F_{cr} by using the relationships in step (2). If the applied stress exceeds F_{cr}, repeat steps (3) through (9) for a stronger panel.

(10) Analyze for face wrinkling, Section 13.2.1.

(11) Analyze for intracell buckling, Section 13.2.2.

13.2.4 Flat Rectangular Panels Under Edgewise Shear

The following method is used in the design of flat sandwich shear panels. It is assumed that the shear load is equally and uniformly distributed over the edges of the panel as shown in Figure 13.29.

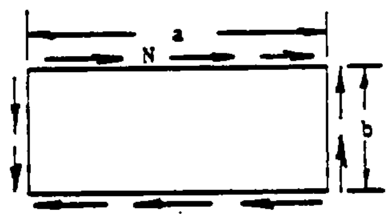

FIGURE 13.29 SHEAR PANELS

Overall buckling of the sandwich or dimpling or wrinkling of the facings cannot occur without possible total collapse of the panel. Detailed procedures follow, giving theoretical formulas and graphs for determining dimensions of the facings and core, as well as necessary core properties. Facing modulus of elasticity, E, shear modulus, G, and stress values, F, shall be values at the conditions of use; for example, if application is at elevated temperature, then facing properties at elevated temperature shall be used in design. The facing shear modulus or modulus of elasticity is the effective value at the facing stress. If this stress is beyond the proportional limit value, an appropriate tangent, reduced or modified value shall be used.

(1) Choose an allowable shear stress (F_{sf}). Determine the facing ~~thickness~~ (t) using

$$t_1 F_{sf1} + t_2 F_{sf2} = N; \text{ unequal faces} \qquad 13.21$$

$$t = N/2F_{sf}; \text{ equal faces} \qquad 13.22$$

When the shear modulus of one face is different from the shear modulus of the other face, the face stresses are balanced by the ratio

$$\frac{F_{sf1}}{G_{s1}} = \frac{F_{sf2}}{G_{s2}} \qquad 13.23$$

The lower of the ratios in equation 13.23 must be used for design, otherwise the face with the lower ratio will be overstressed.

(2) The critical facing stress ($F_{s_{cr}}$) at which panel buckling will occur is given by

$$F_{s_{cr}} = \pi^2 K \frac{E_{f1} t_1 E_{f2} t_2}{(E_{f1} t_1 + E_{f2} t_2)^2} \left(\frac{h}{b}\right)^2 \left(\frac{E_f}{\lambda}\right) \qquad 13.24$$

where E_f and λ are values for the facing with least F_{sf}/G_s ratio as determined from equation 13.23.

If the facings are of equal thickness and of the same material, equation 13.24 becomes

$$F_{s_{cr}} = \frac{\pi^2 K}{4} \left(\frac{h}{b}\right)^2 \left(\frac{E_f}{\lambda}\right) \qquad 13.25$$

In equations 13.24 and 13.25

$$K = K_M + K_F \qquad 13.26$$

(3) Evaluate the following parameters

$$b/a \qquad 13.27$$

$$(E_{f2} t_2)/(E_{f1} t_1) \qquad 13.28$$

$$(\lambda F_{sf})/E_f \qquad 13.29$$

where equation 13.29 uses the values of the facing with the minimum ratio from equation 13.23.

(4) Enter the appropriate chart (Figure 13.30, 13.31 or 13.32) with parameter b/a (13.27) to V = .01. (Choose a low finite value to start since V = 0 gives h as a minimum and G_c as infinite). Move laterally to parameter, equation 13.28, and then downward to equation 13.29. Project laterally and read value of h/b. Determine h.

(5) Evaluate core thickness from

$$t_c = h - \frac{t_1 + t_2}{2} \text{; unequal facings} \qquad 13.30$$

$$t_c = h - t\text{; equal facings} \qquad 13.31$$

(6) Determine the value of K' from

$$K' = \frac{\pi^2 t_c E_{f1} t_1 E_{f2} t_2}{\lambda b^2 (E_{f1} t_1 + E_{f2} t_2)} \text{; unequal facings} \qquad 13.32$$

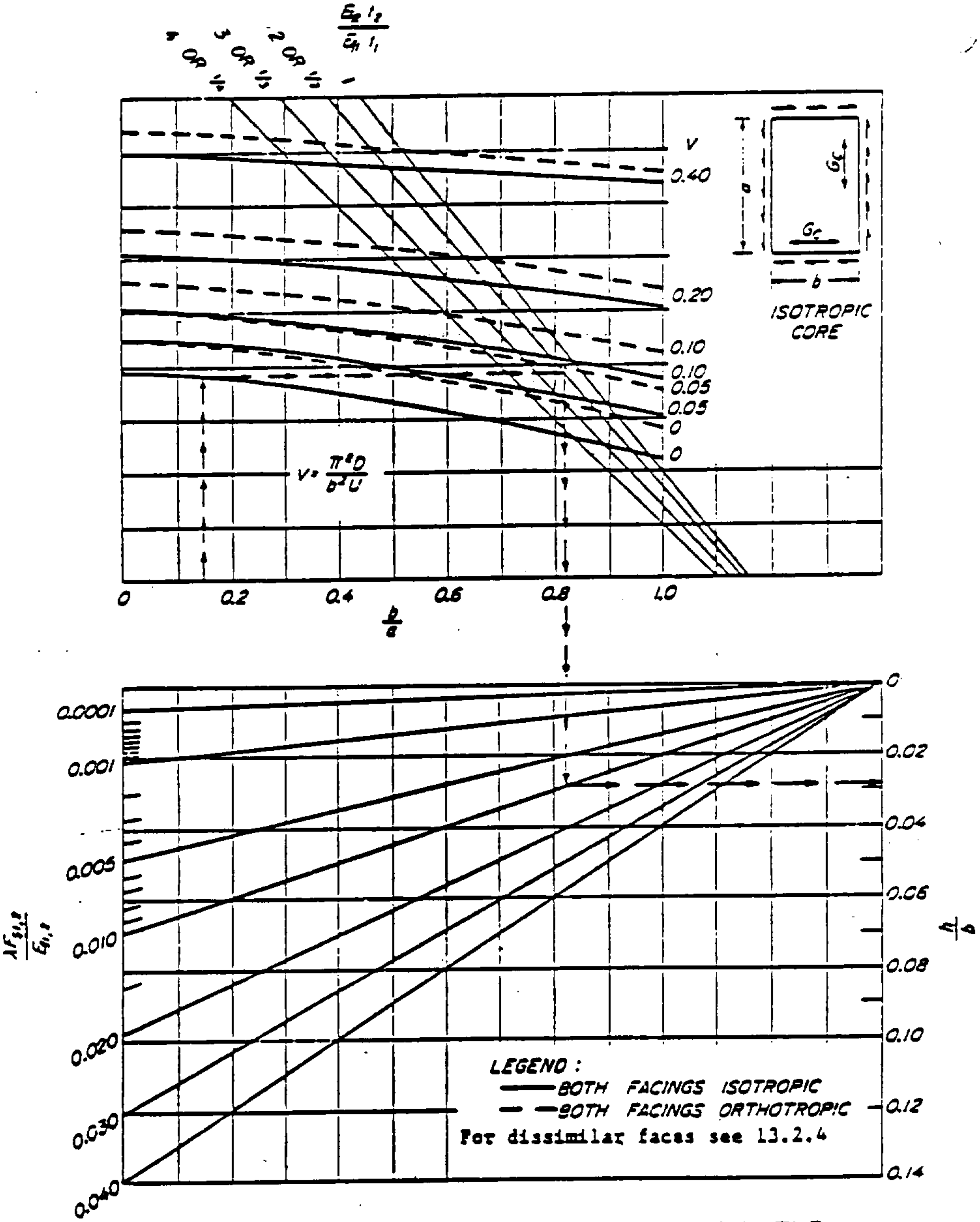

FIGURE 13.30 - CHART FOR DETERMINING h/b RATIO SUCH THAT A SIMPLY SUPPORTED SANDWICH PANEL WITH ISOTROPIC CORE WILL NOT BUCKLE UNDER EDGE-WISE SHEAR LOAD

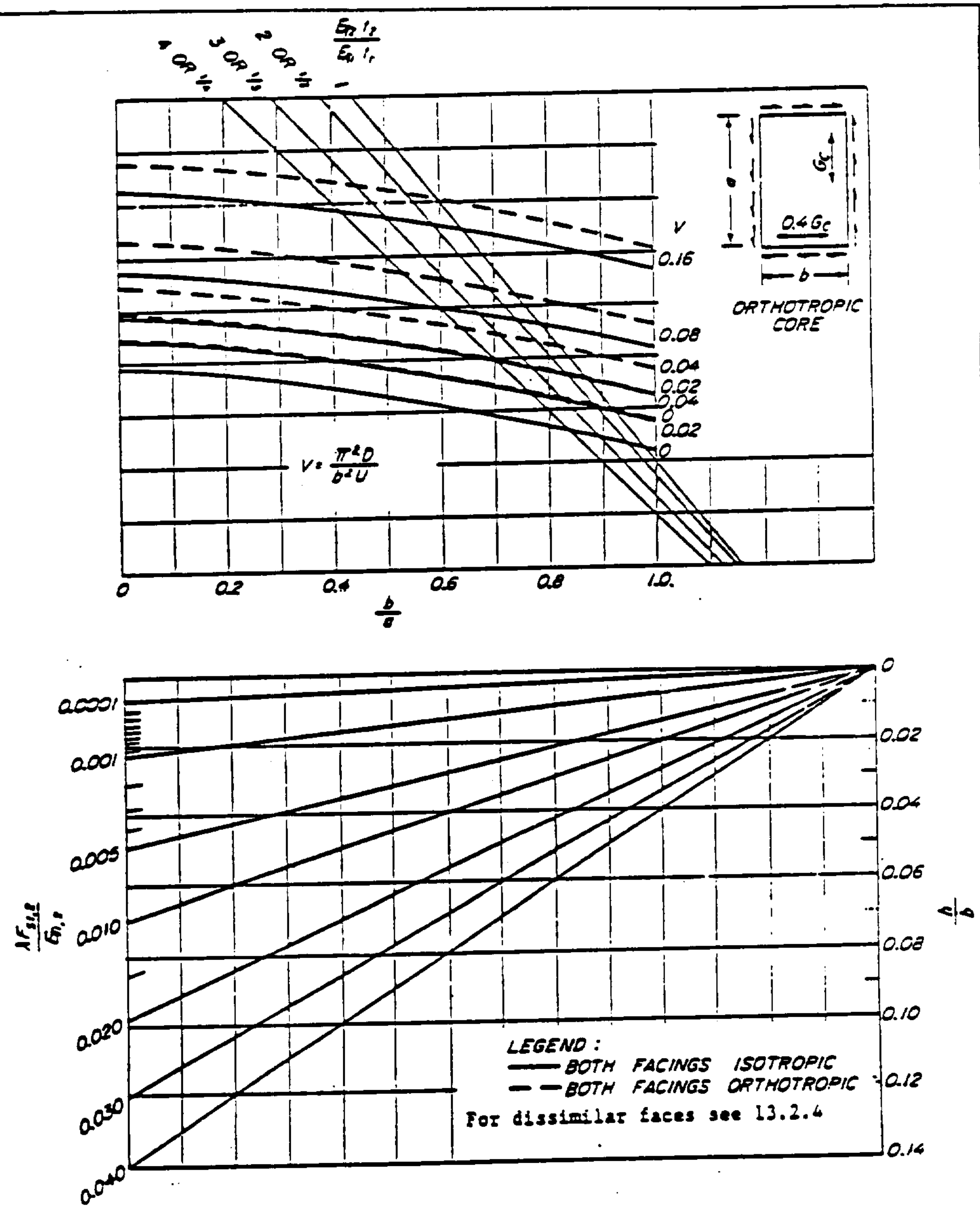

FIGURE 13.31 - CHART FOR DETERMINING h/b RATIO SUCH THAT A SIMPLY SUPPORTED SANDWICH PANEL WITH ORTHOTROPIC CORE WILL NOT BUCKLE UNDER EDGEWISE SHEAR LOAD (G_{cb} = 0.4 G_{ca}).

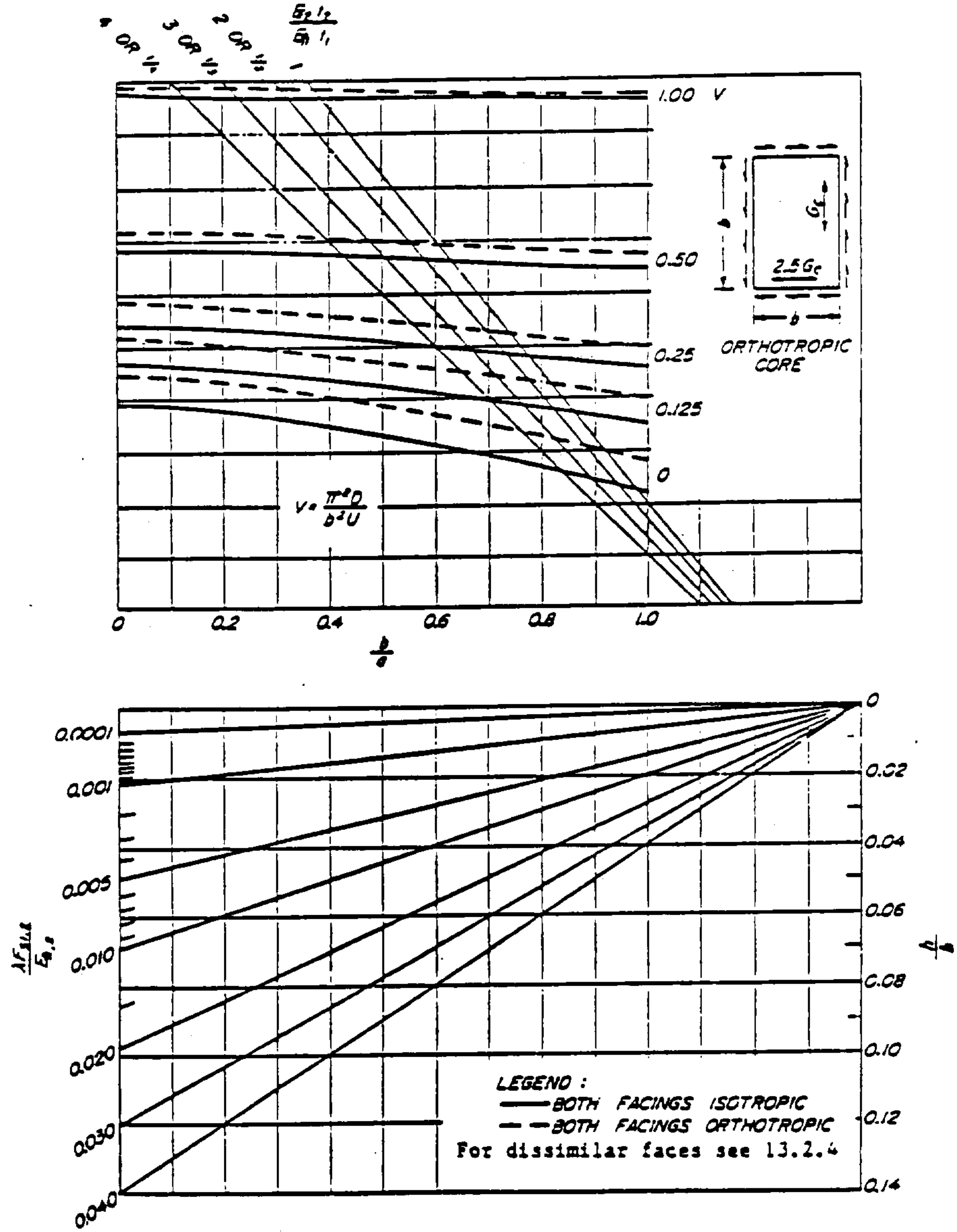

FIGURE 13.32 - CHART FOR DETERMINING h/b RATIO SUCH THAT A SIMPLY SUPPORTED SANDWICH PANEL WITH ORTHOTROPIC CORE WILL NOT BUCKLE UNDER EDGEWISE SHEAR LOAD (G_{cb} = 2.5 G_{ca}).

$$K' = \frac{\pi^2 t_c E_f t}{2\lambda b^2} \text{ ; equal facings} \qquad 13.33$$

(7) Determine tentative core modulus of rigidity (G_c) from 13.34 for V = .01. If this value

$$G_c = K'/V \qquad 13.34$$

of G_c is not within the range available in the desired core material and type, enter chart in Figure 13.33 along line $V = K'/G_c$ until a practical value is reached. For the new value of V repeat steps (4), (5) and (6).

(8) From appropriate charts in Figures 13.34 through 13.39, read directly the values of K_M and K_{Mo}. For determining K_{Mo}, assume V = 0. Evaluate K_F by using

$$K_F = \frac{(E_{f1}t_1{}^3 + E_{f2}t_2{}^3)(E_{f1}t_1 + E_{f2}t_2)}{12E_{f1}t_1E_{f2}t_2h^2} K_{Mo} \qquad 13.35$$

$$K_F = \frac{t^2}{3h^2} K_{Mo}\text{; equal facings} \qquad 13.36$$

Determine the value for K from

$$K = K_M + K_F \qquad 13.37$$

(9) Substitute the value of K into (2) and solve for F_{scr}. This stress must be greater than the allowable stresses F_{sf1} and F_{sf2} determined by step (1).

(10) Check for face wrinkling as outlined in Section 13.2.1.

(11) Check the panel for intercell buckling, Section 13.2.2.

13.2.5 Flat Panels Under Uniformly Distributed Normal Load

This section gives procedures for determining sandwich facing and core thickness and core shear modulus so that design facing stresses and allowable panel deflections will not be exceeded. This procedure is used in the design of a flat sandwich panel with equal facings, simply supported at the four edges and subjected to uniform normal loading. Facings are isotropic; core may be isotropic or orthotropic. In the case of an orthotropic core, G_{ca} is the modulus of rigidity associated with the shear distortion observed in a cross section parallel to side a. Correspondingly, G_{cb} is associated with side b.

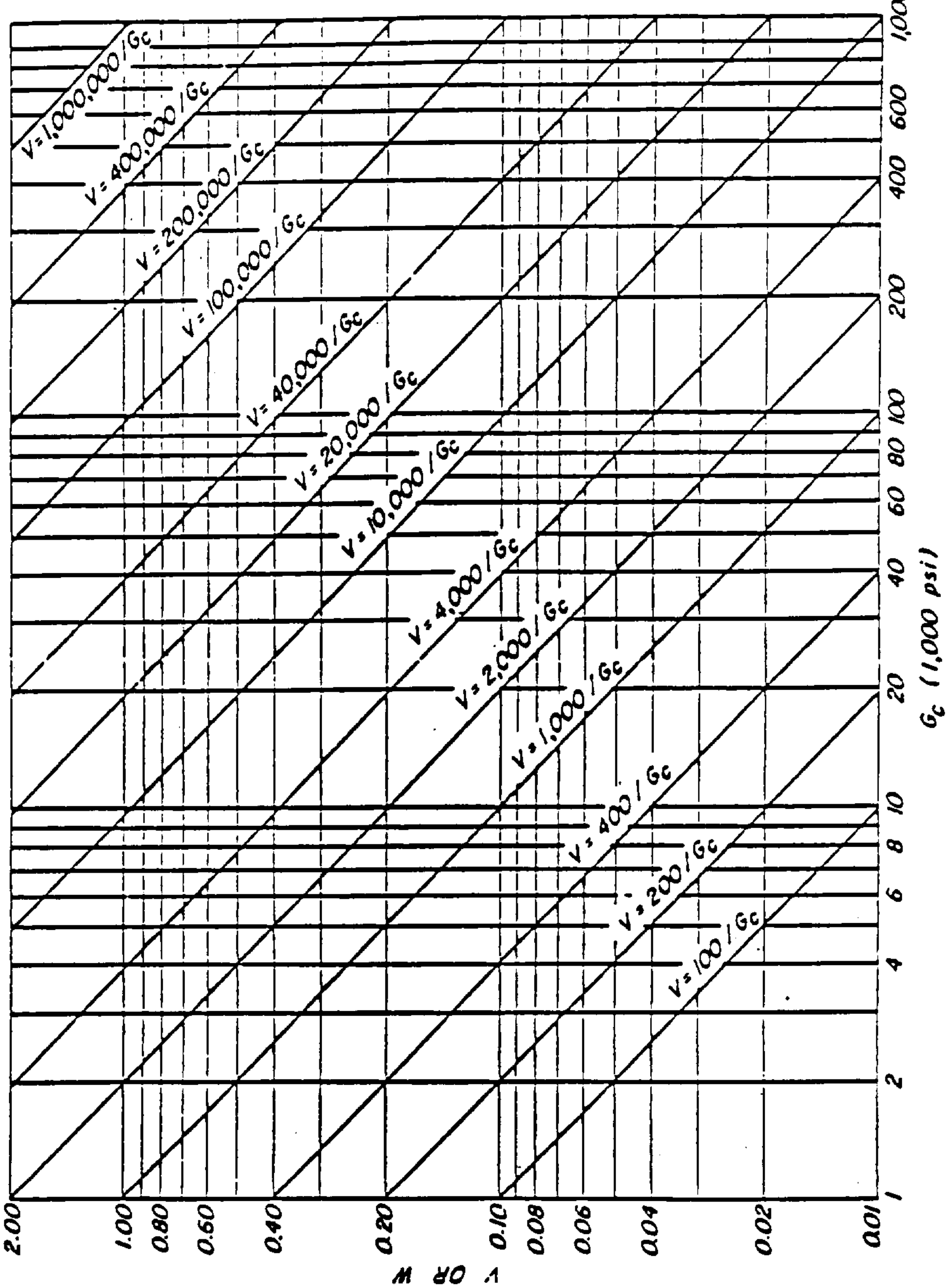

FIGURE 13.33 - CHART FOR DETERMINING V OR W AND G_c FOR SANDWICH IN EDGEWISE SHEAR

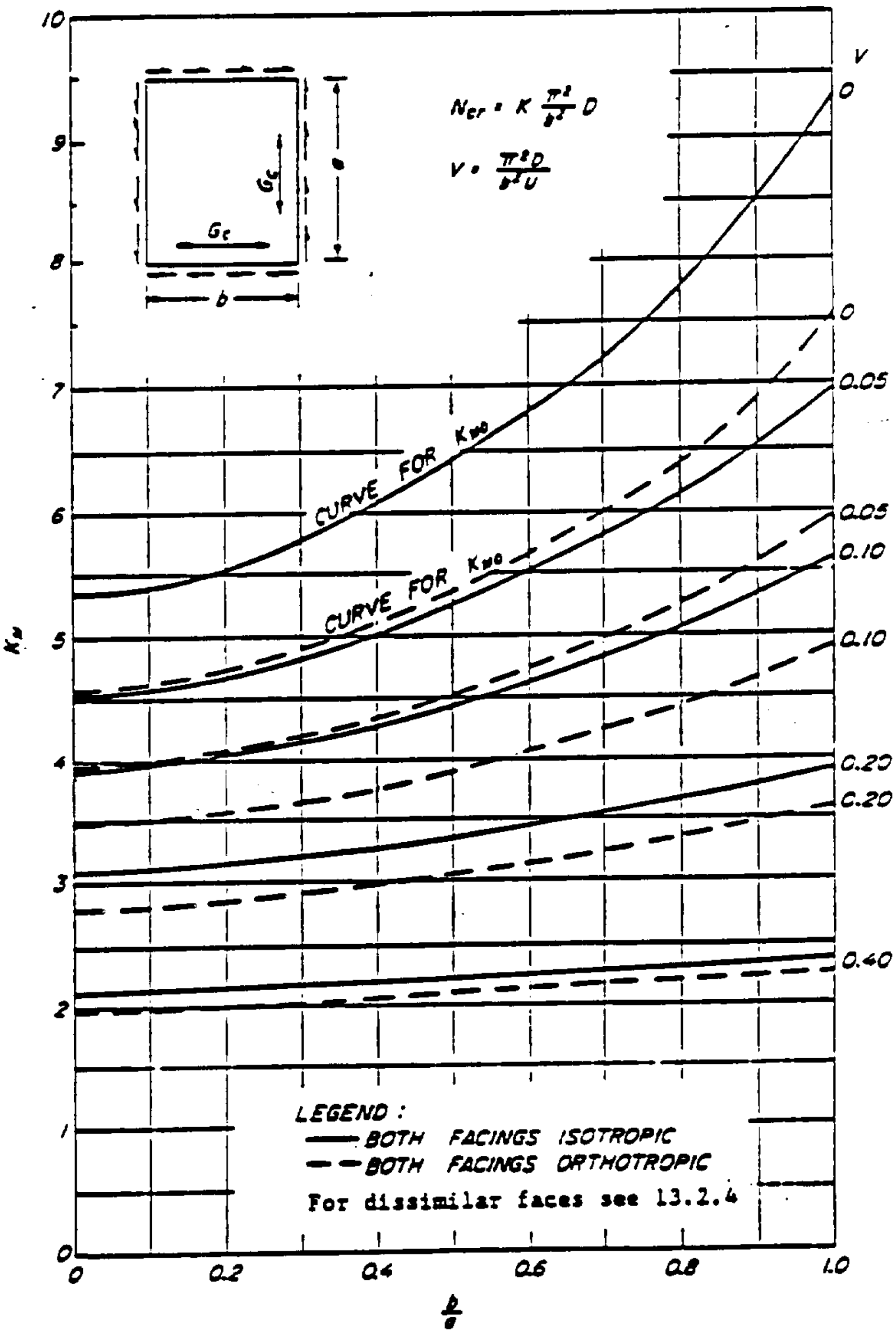

FIGURE 13.34 - K_M FOR SANDWICH PANEL WITH ALL EDGES SIMPLY SUPPORTED, AND ISOTROPIC CORE.

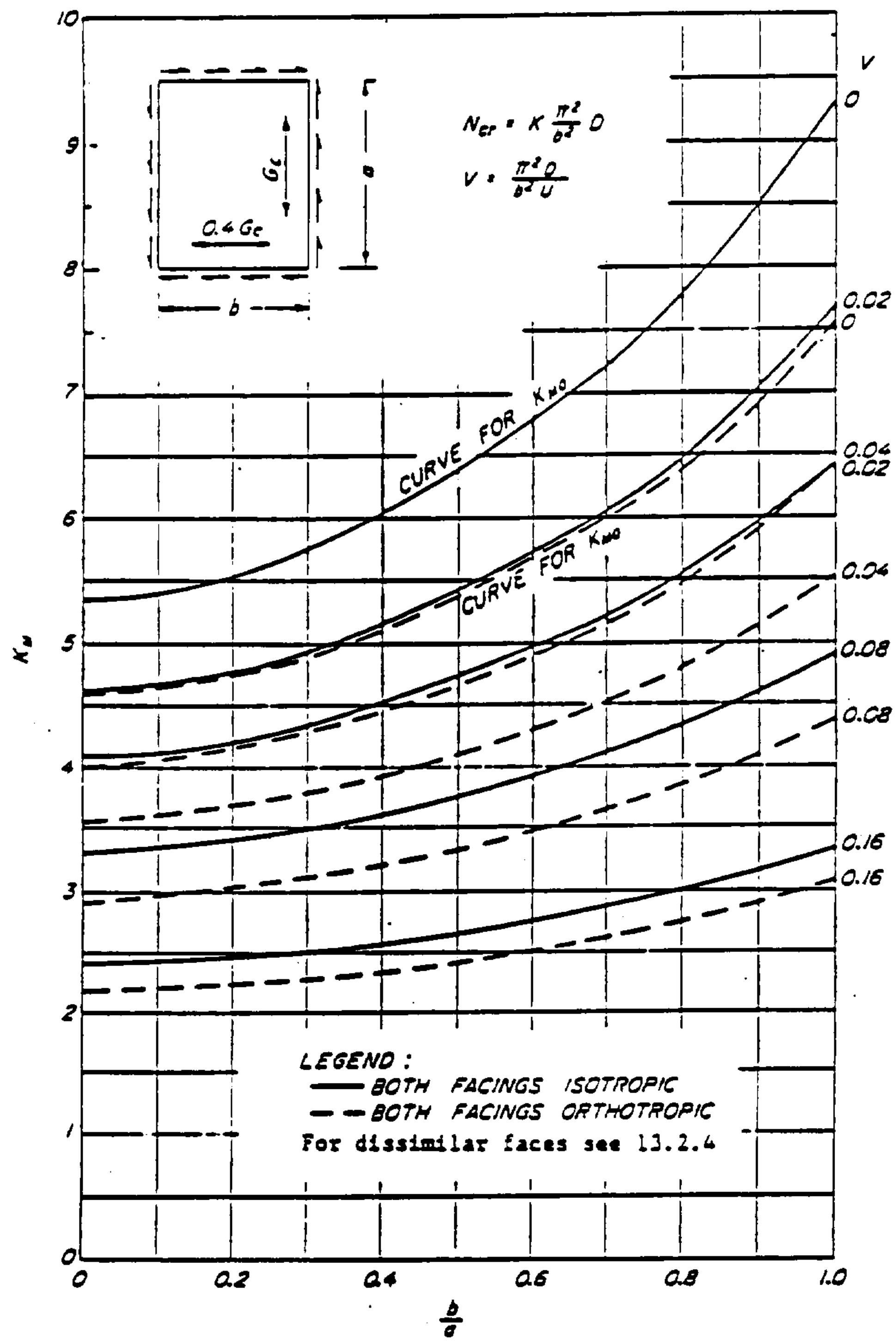

FIGURE 13.35 - K_M FOR SANDWICH PANEL WITH ALL EDGES SIMPLY SUPPORTED, AND ORTHOTROPIC CORE. ($G_{cb} = 0.4\ G_{ca}$).

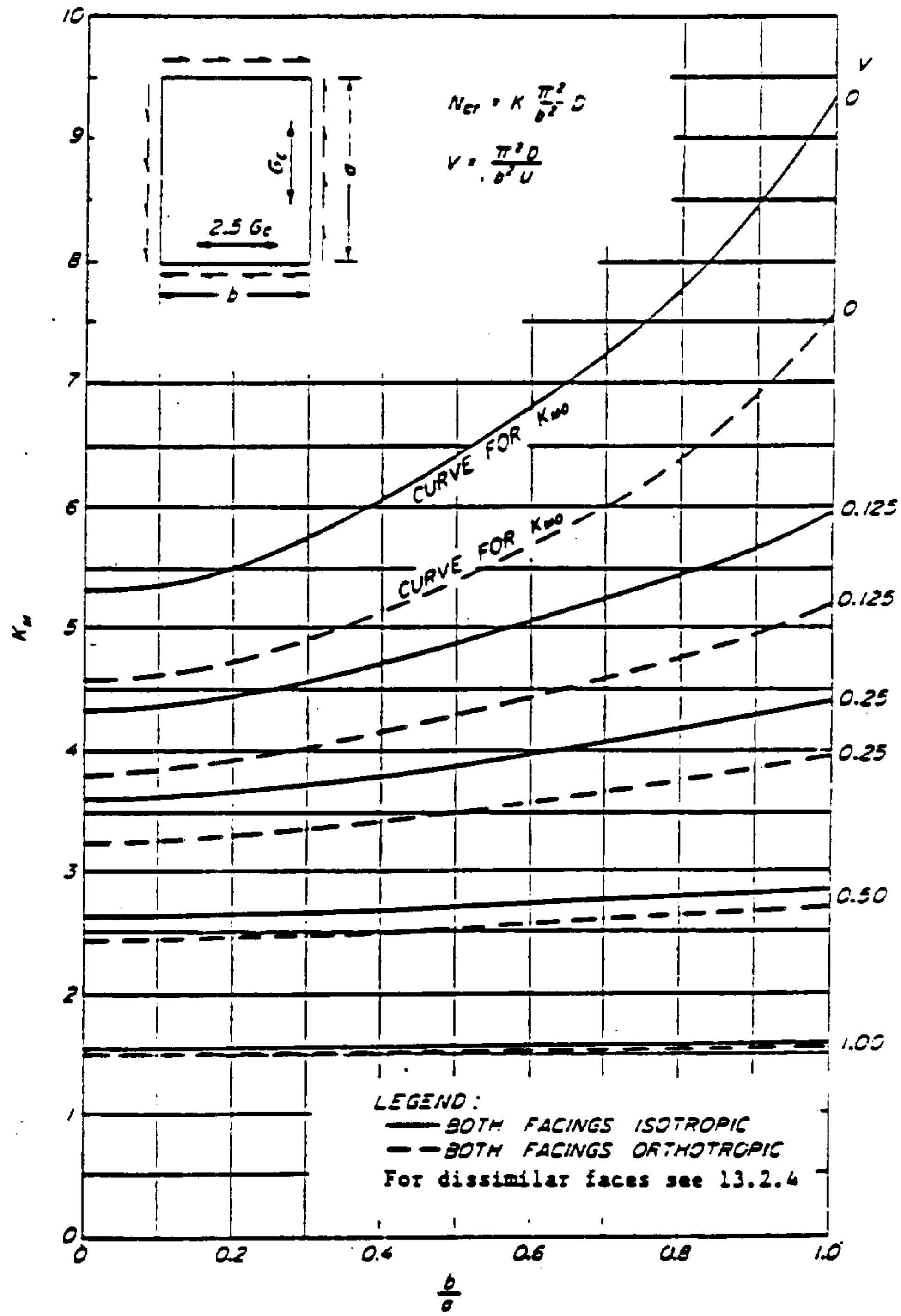

FIGURE 13.36 - K_M FOR SANDWICH PANEL WITH ALL EDGES SIMPLY SUPPORTED, AND ORTHOTROPIC CORE. ($G_{cb} = 2.5\ G_{ca}$).

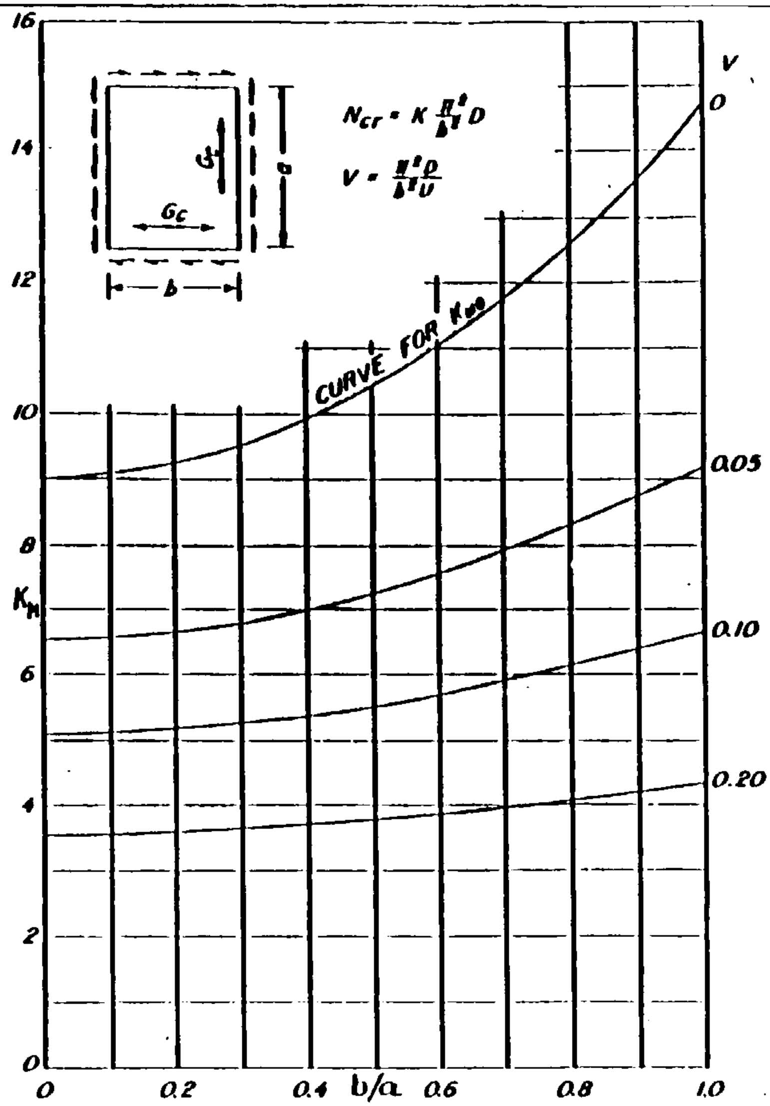

FIGURE 13.37 - K_M FOR SANDWICH PANEL WITH ALL EDGES CLAMPED, ISOTROPIC FACES AND ISOTROPIC CORE

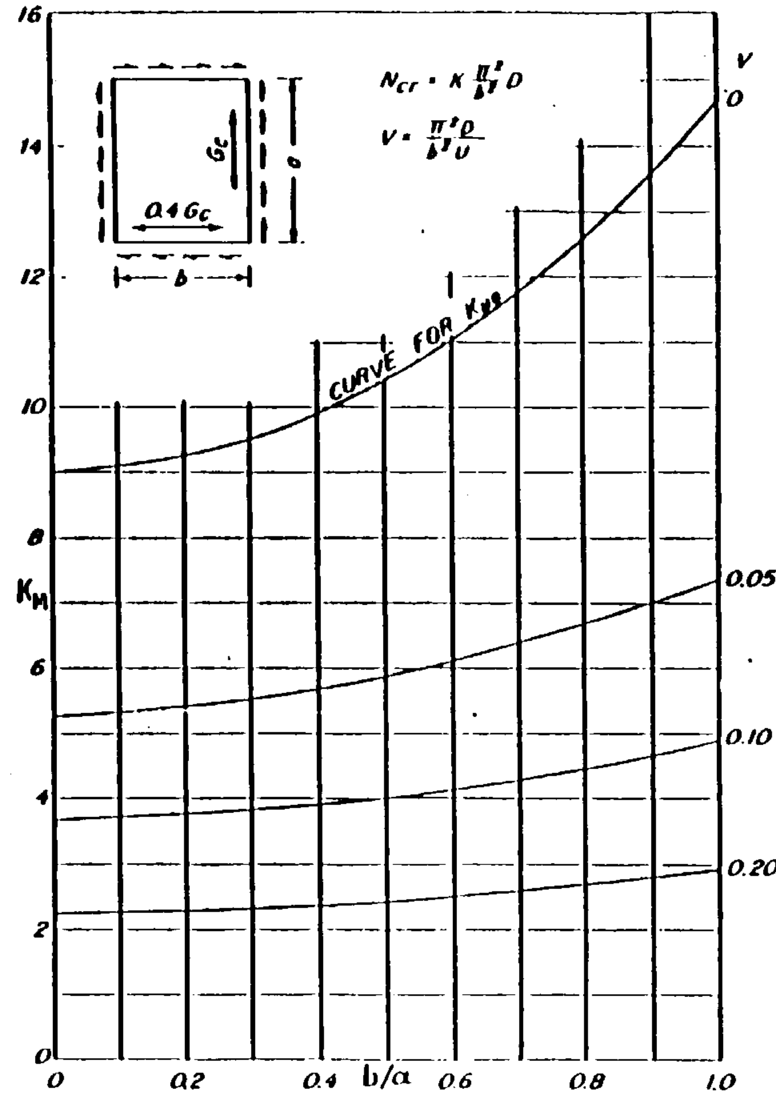

FIGURE 13.38 - K_M FOR SANDWICH PANEL WITH ALL EDGES CLAMPED, ISOTROPIC FACES AND ORTHOTROPIC CORE ($G_{cb} = 0.4\ G_{ca}$)

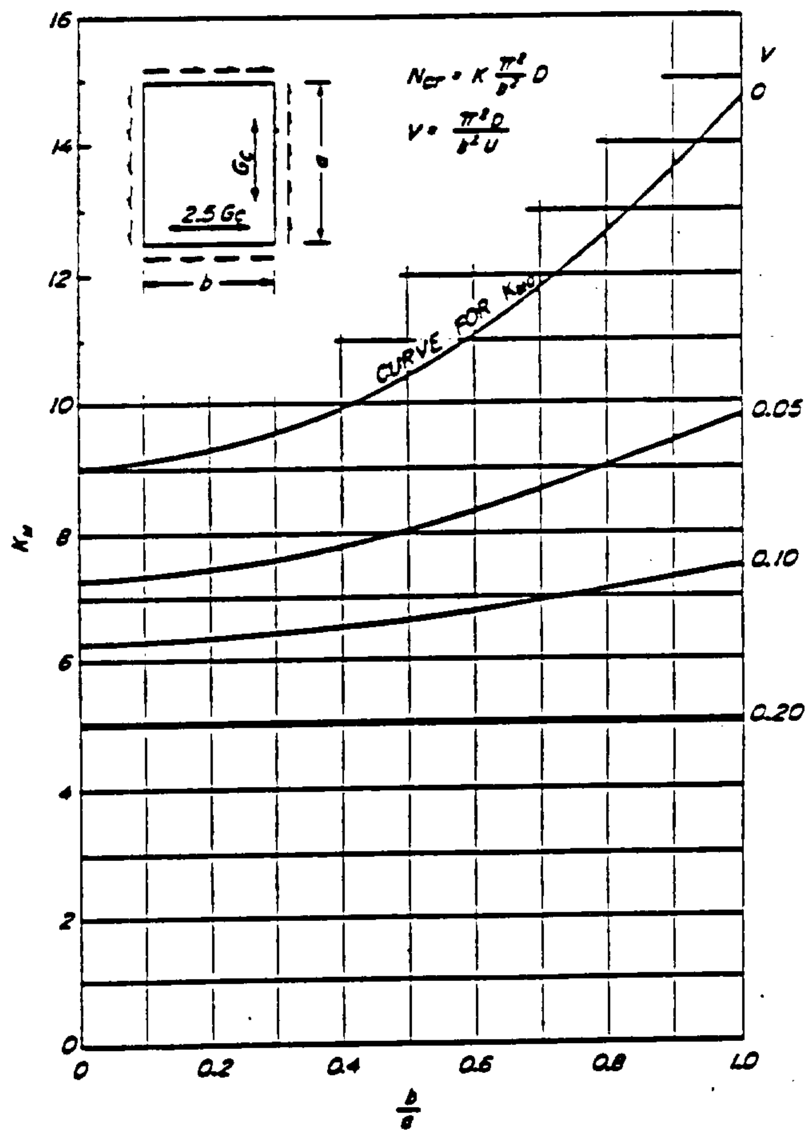

FIGURE 13.39 - K_M FOR SANDWICH PANEL WITH ALL EDGES CLAMPED, ISOTROPIC FACES AND ORTHOTROPIC CORE (G_{cb} = 2.5 G_{ca})

Data Source, Section 1.3 Reference 3

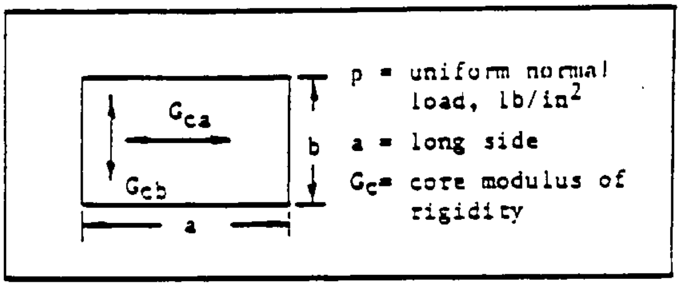

FIGURE 13.40 SIMPLY SUPPORTED FLAT PANEL WITH UNIFORMLY DISTRIBUTED NORMAL LOAD

(1) Evaluate the maximum bending moment per inch using the equation given in Figure 13.41.

(2) Tentatively select panel materials and establish allowable stresses.

(3) Determine facing thickness in the following weight minimizing expression.

$$t = \sqrt{\frac{W_c M}{2W_f F_f}} \qquad 13.38$$

where F_f = allowable facing stress, psi
W_c = density of core, #/in^3
W_f = facing density, #/in^3

Increase t to nearest standard gage.

(4) Determine core thickness (t_c) from

$$t_c = \sqrt{\frac{2W_f M}{W_c F_f}} \qquad 13.39$$

If practical considerations require unequal facings or different t_c, make the necessary changes at this point.

(5) For a panel configuration thus determined, evaluate the parameter V

$$V = \frac{\pi^2 E_{f1} t_1 E_{f2} t_2 t_c}{\lambda(E_{f1} t_1 + E_{f2} t_2) b^2 G_{ca}} \text{ ; unequal faces} \qquad 13.40$$

$$V = \frac{\pi^2 E_f t t_c}{2\lambda b^2 G_{ca}} \text{ ; equal faces} \qquad 13.41$$

Enter the appropriate charts in Figures 13.42 through 13.46 with b/a and V to determine the value for constants C_2 and C_3.

(6) The maximum bending moments occur at the panel center and are determined by the following expression

$$M_a = \frac{16pb^2}{\pi^4}(C_3 + \mu C_2);\ \text{across width} \qquad 13.42$$

$$M_b = \frac{16pb^2}{\pi^4}(C_2 + \mu C_3);\ \text{across length} \qquad 13.43$$

Moments obtained are per unit width and length of panel respectively.

(7) Calculate the resulting facing stress from

$$f_f = \frac{2M_a}{t(d + t_c)} \qquad 13.44$$

$$f_f = \frac{2M_b}{t(d + t_c)} \qquad 13.45$$

The equations 13.44 and 13.45 are based on faces made of the same material and of equal thickness. If materials or thicknesses are different, the stresses must be calculated using Mc/I. If the facing stress is greater than the chosen allowable design stress or if considerably below, iterate the previous procedure to obtain a more nearly optimum design.

(8) The maximum shear loads occur at the mid-length of the panel edges and are determined from

$$S_a = \frac{16pb}{\pi^3} C_4;\ \text{shear on side a} \qquad 13.46$$

$$S_b = \frac{16pb}{\pi^3} C_5;\ \text{shear on side b} \qquad 13.47$$

Enter chart in Figures 13.47 through 13.50 to determine C_4 and C_5.

(9) Evaluate shear stresses

$$f_{sa} = \frac{2S_a}{d + t_c} \qquad 13.48$$

$$f_{sb} = \frac{2S_b}{d + t_c} \qquad 13.49$$

Choose an available core to meet the stress requirement of 13.48 and 13.49.

(10) If panel deflection is limited by the design criteria, it may be determined by

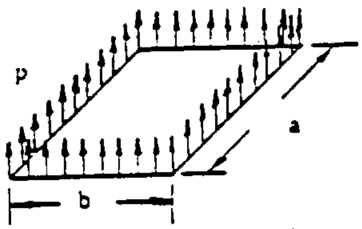

$M_{max} = \beta p b^2$ = moment @ middle of panel

a/b	1	1.2	1.4	1.6	1.8	2	3	4	5	∞
β	.048	.063	.075	.086	.095	.102	.119	.124	.125	.125

FIGURE 13.41 - MOMENT AND DEFLECTION IN THE CENTER OF A RECTANGULAR PANEL WITH UNIFORMLY DISTRIBUTED NORMAL LOAD

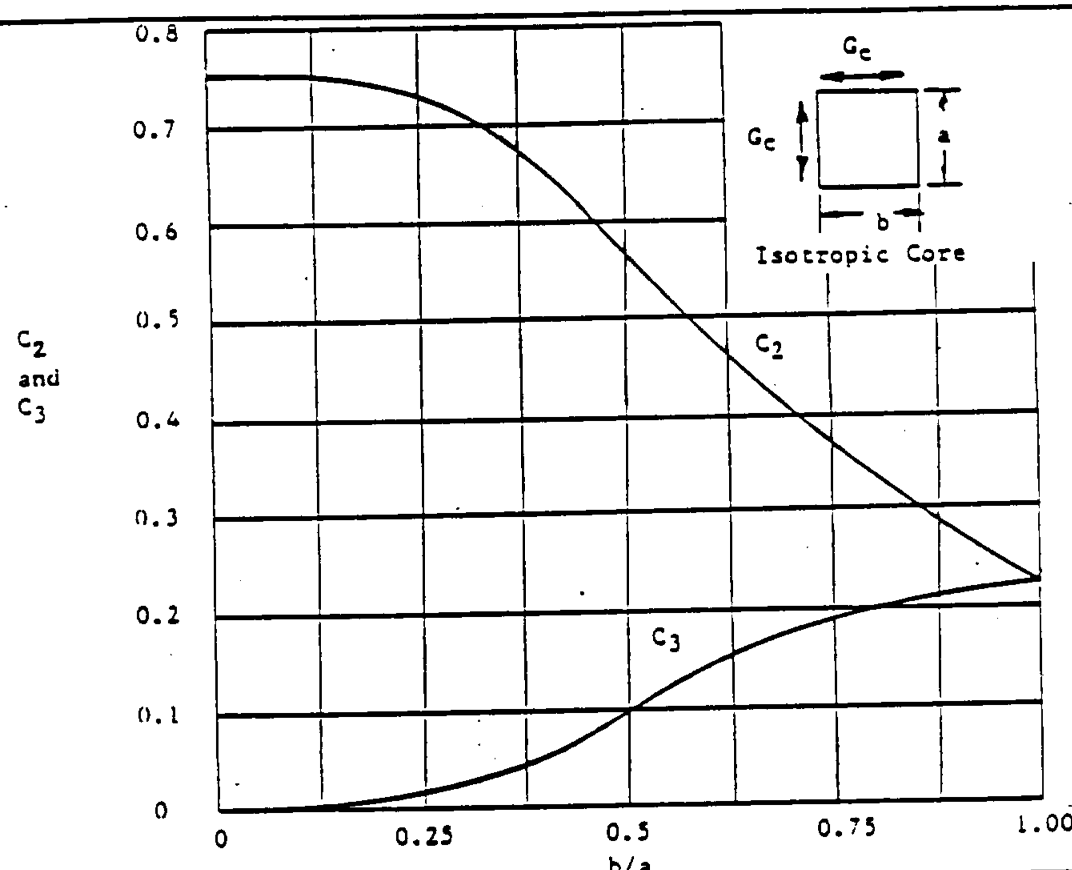

FIGURE 13.42 - MOMENT CONSTANTS FOR FLAT PANEL WITH ISOTROPIC CORE UNDER NORMAL LOAD

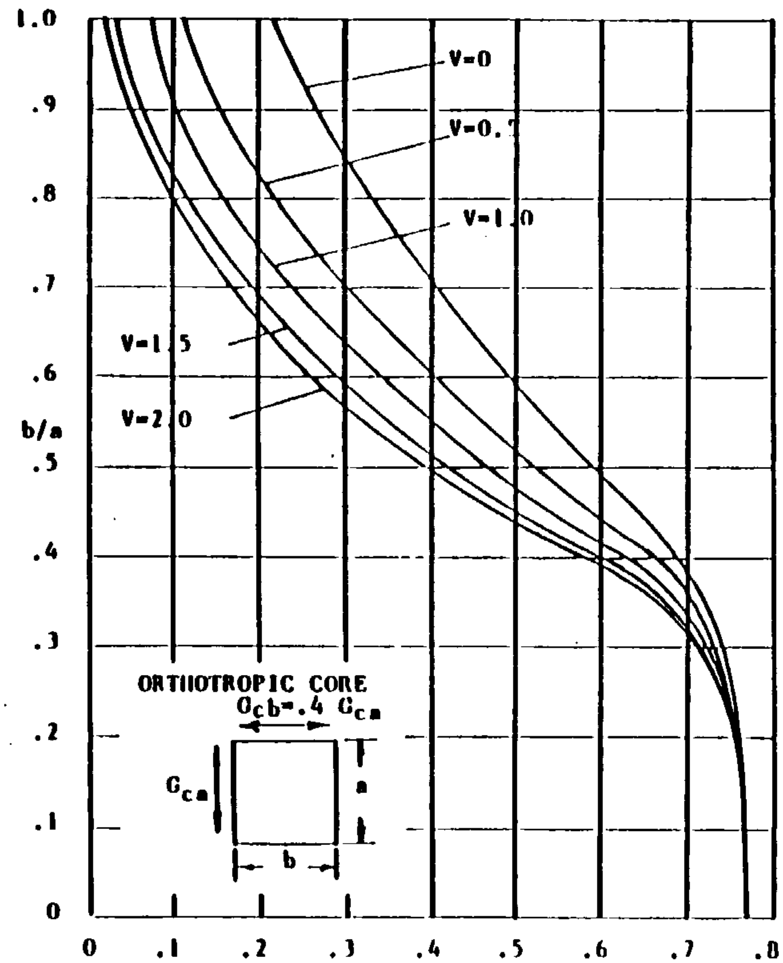

FIGURE 13.43 - MOMENT CONSTANT, C_2, FOR FLAT PANEL WITH ORTHOTROPIC CORE UNDER NORMAL LOAD

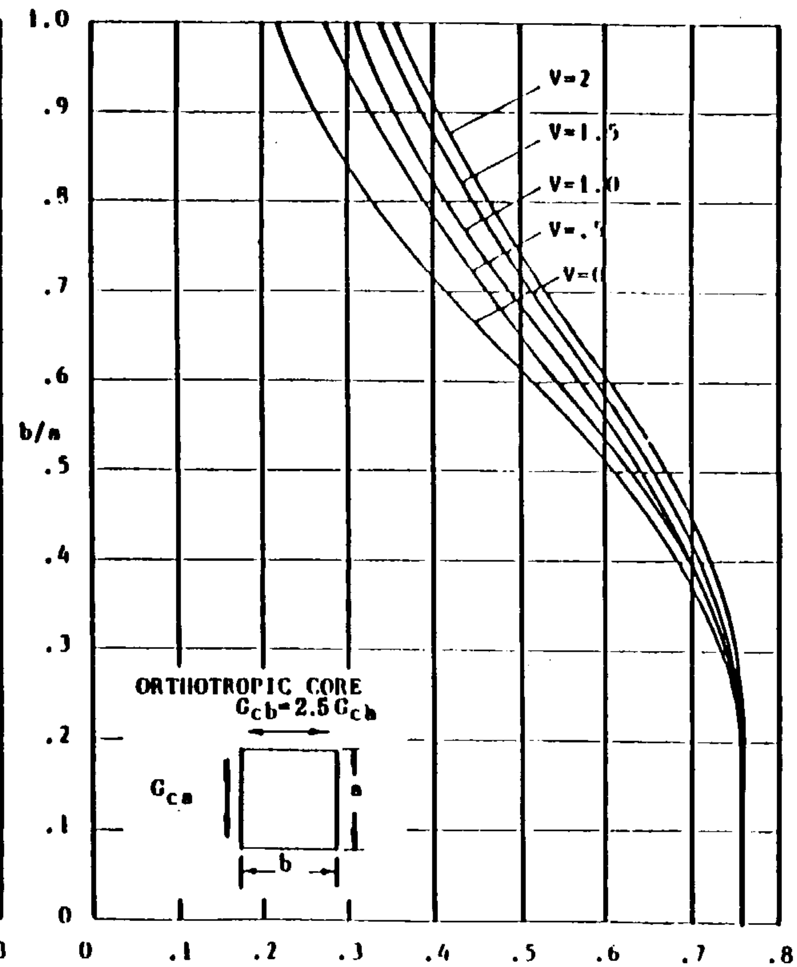

FIGURE 13.44 - MOMENT CONSTANT, C_2, FOR FLAT PANEL WITH ORTHOTROPIC CORE UNDER NORMAL LOAD

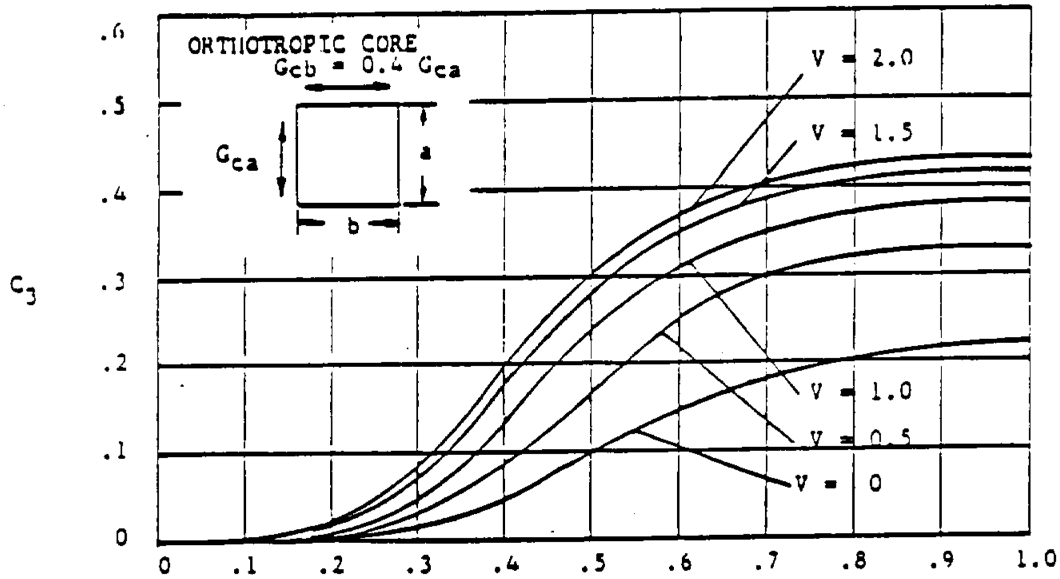

FIGURE 13.45 - MOMENT CONSTANT, C_3, FOR FLAT PANEL WITH ORTHOTROPIC CORE UNDER NORMAL LOAD

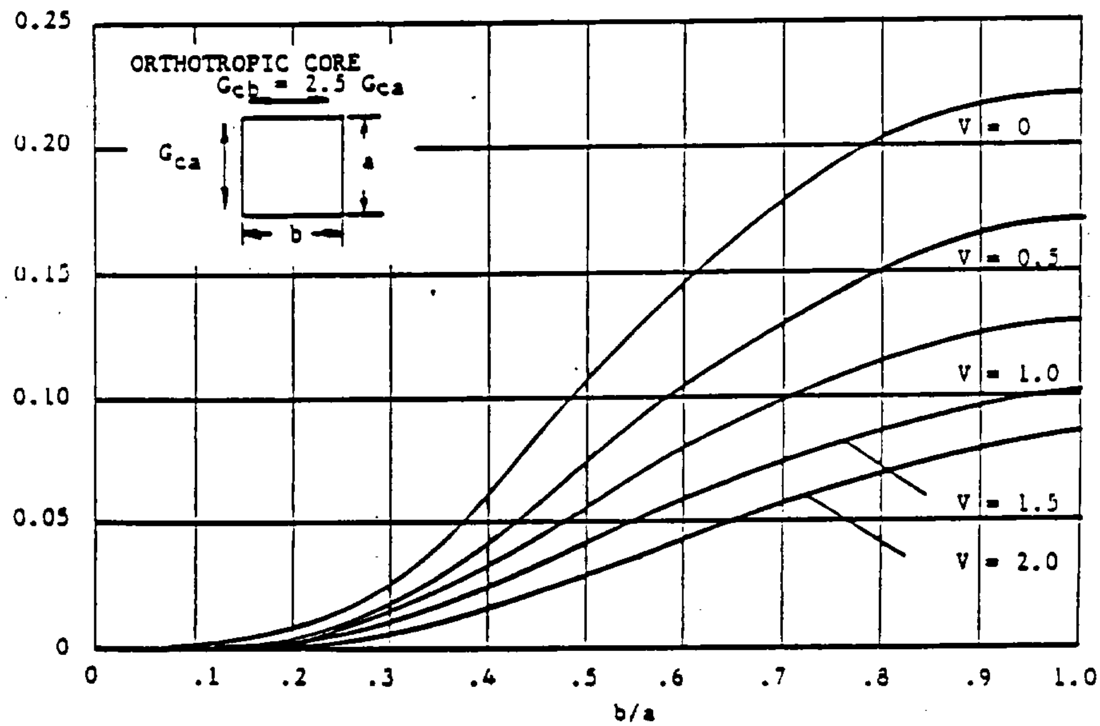

FIGURE 13.46 - MOMENT CONSTANT, C_3, FOR FLAT PANEL WITH ORTHOTROPIC CORE UNDER NORMAL LOAD

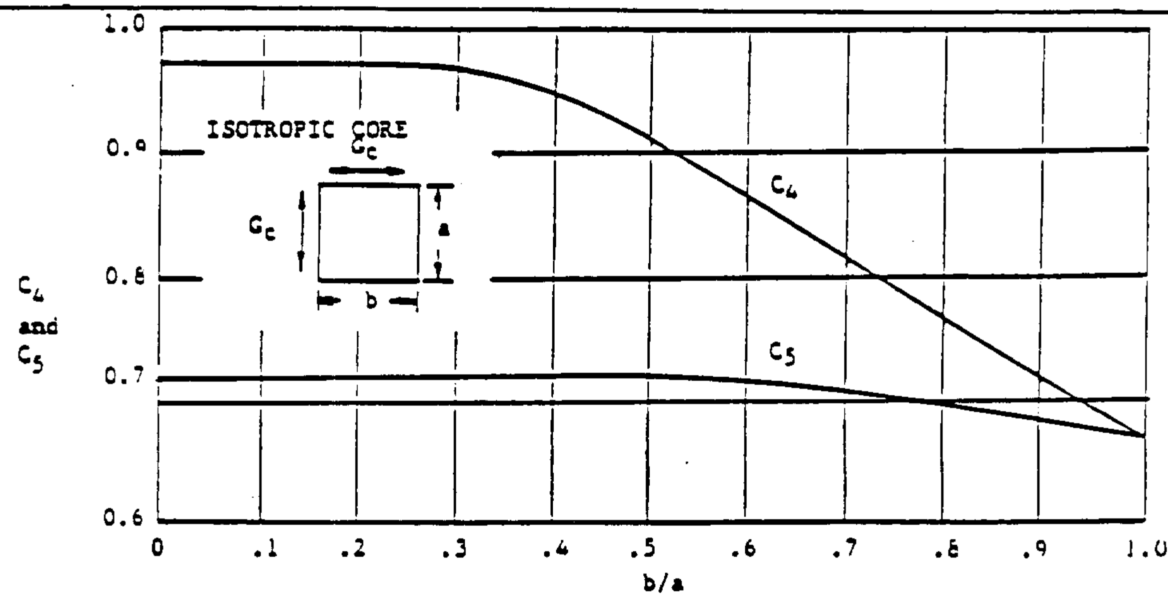

FIGURE 13.47 - SHEAR CONSTANTS, C_4 AND C_5, FOR FLAT PANELS WITH ISOTROPIC CORE AND NORMAL LOAD

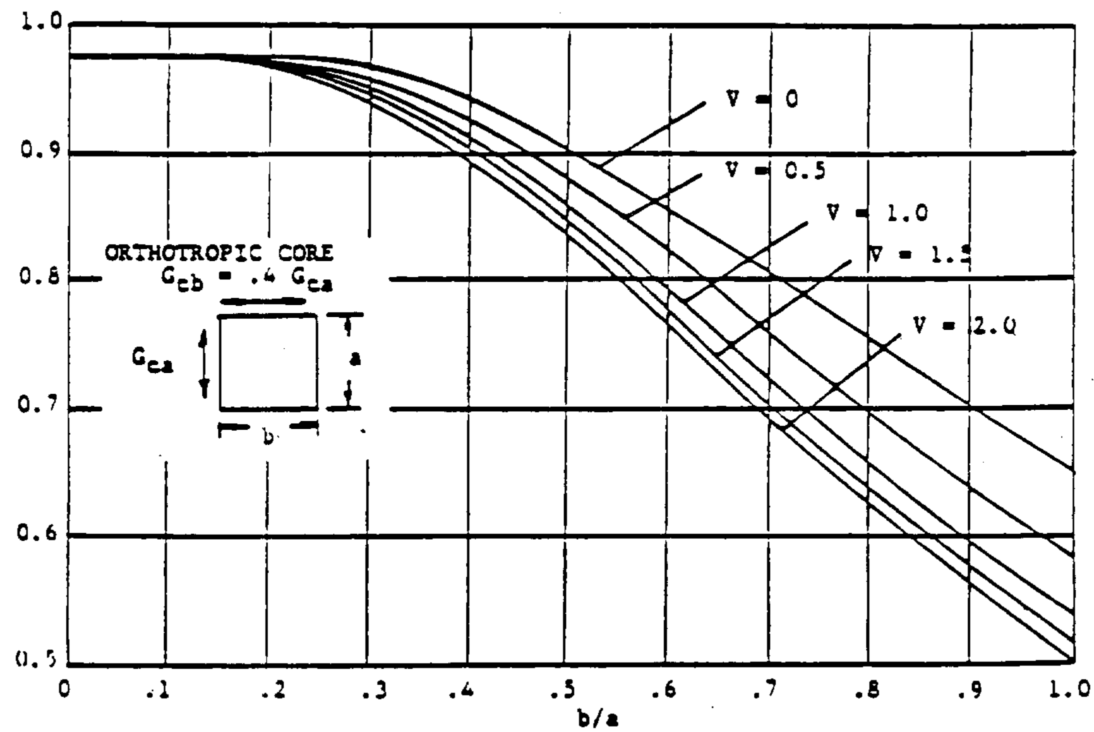

FIGURE 13.48 - SHEAR CONSTANT, C_4, FOR FLAT PANELS WITH ORTHOTROPIC CORE UNDER NORMAL LOAD

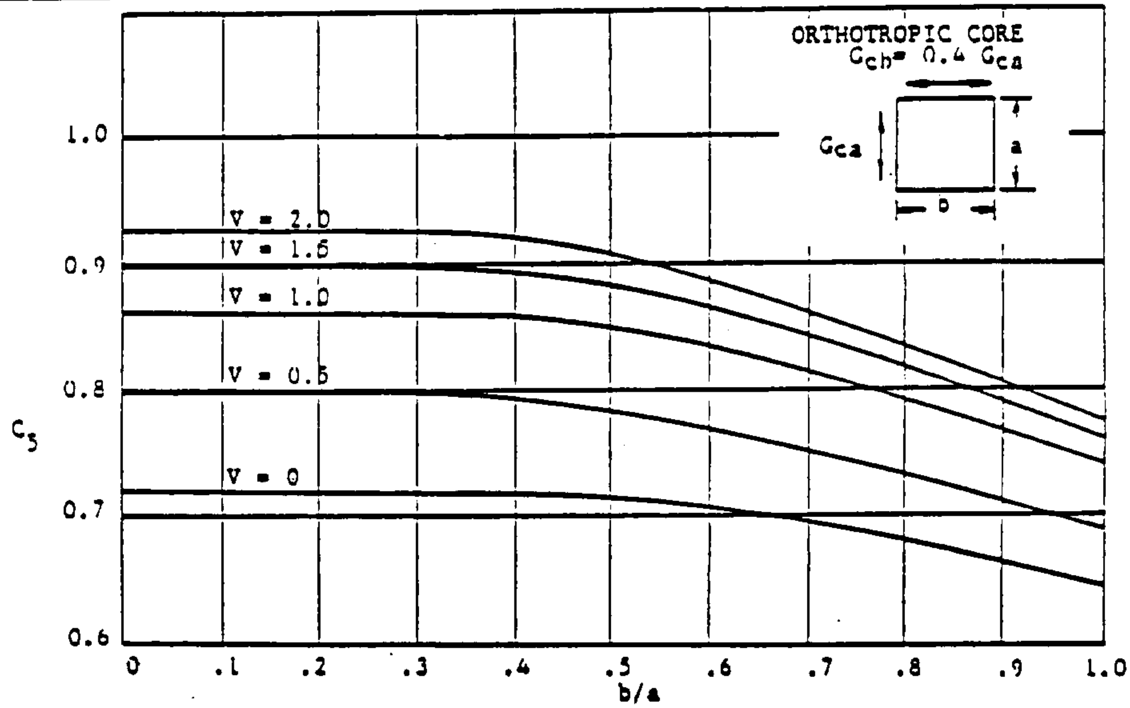

FIGURE 13.49 - SHEAR CONSTANT, C_5, FOR FLAT PANELS WITH ORTHOTROPIC CORE UNDER NORMAL LOAD

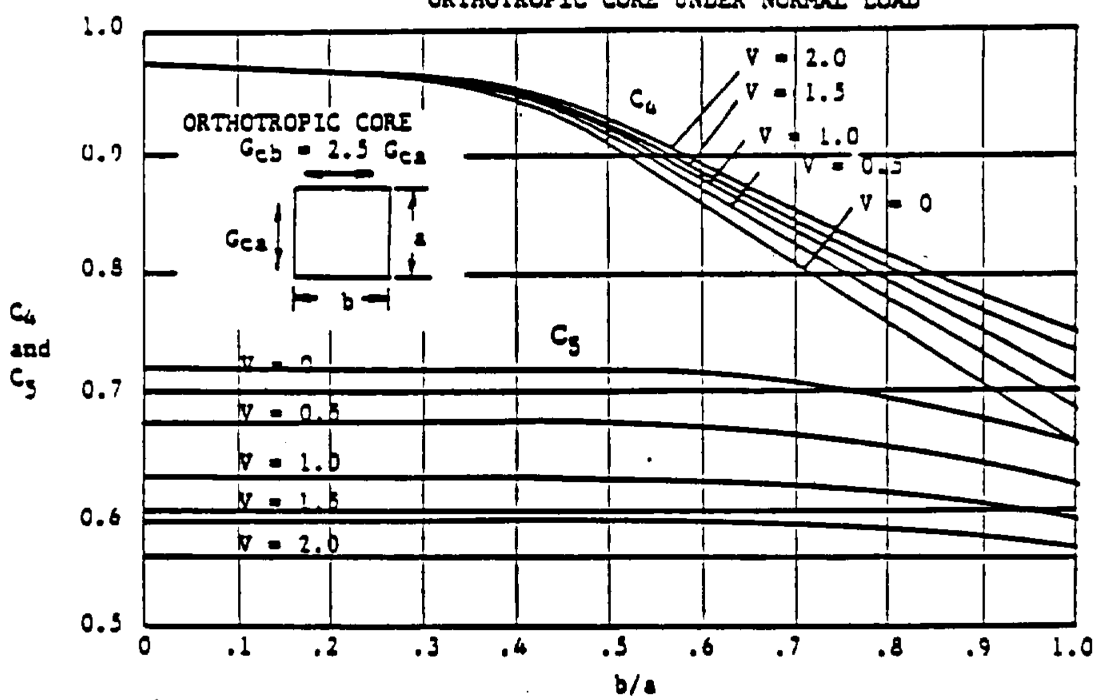

FIGURE 13.50 - SHEAR CONSTANTS, C_4 AND C_5, FOR FLAT PANELS WITH ORTHOTROPIC CORE UNDER NORMAL LOADS

$$\delta = \frac{16pb^4C_1}{\pi^6 D} \qquad 13.50$$

where

$$D = \frac{E_{f1}t_1E_{f2}t_2h^2}{E_{f1}t_1\lambda_2 + E_{f2}t_2\lambda_1} \text{ ; unequal faces} \qquad 13.51$$

$$D = \frac{E_f}{12\lambda}\left[d^3 - tc^3\left(1 - \frac{E_c'}{E_f}\right)\right] \text{ ; equal faces} \qquad 13.52$$

and C_1 is determined from charts in Figures 13.51 through 13.53, interpolating between values when necessary. If δ exceeds the design limit, increase the core thickness, and if necessary, the facing thickness until the deflection is acceptable. Repeat steps (5) through (9) to determine new, lower stresses.

13.2.6 Sandwich Cylinders Under Torsion

This section gives the procedure for determining core thickness and core shear modulus so that overall buckling of the sandwich walls of the cylinder will not occur. Buckling of the sandwich walls, dimpling or wrinkling of the fairings or sidewise buckling of the cylinder cannot occur without possible total collapse of the cylinder. Detailed procedures giving theoretical formulas and graphs for determining dimensions of the facings and core, as well as necessary core properties follow.

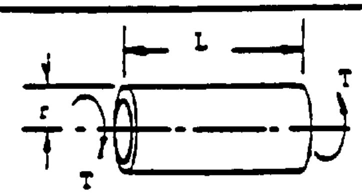

r = radius of outer surface in inches

FIGURE 13.54 CYLINDERS IN TORSION

(1) As a first approximation in determining the required facing thickness assume each face carries half of the shear load. Then

$$t = \frac{1.25T}{4\pi r^2 F_s} \qquad 13.53$$

where T = torque
t = thickness of either face
r = radius of outside surface

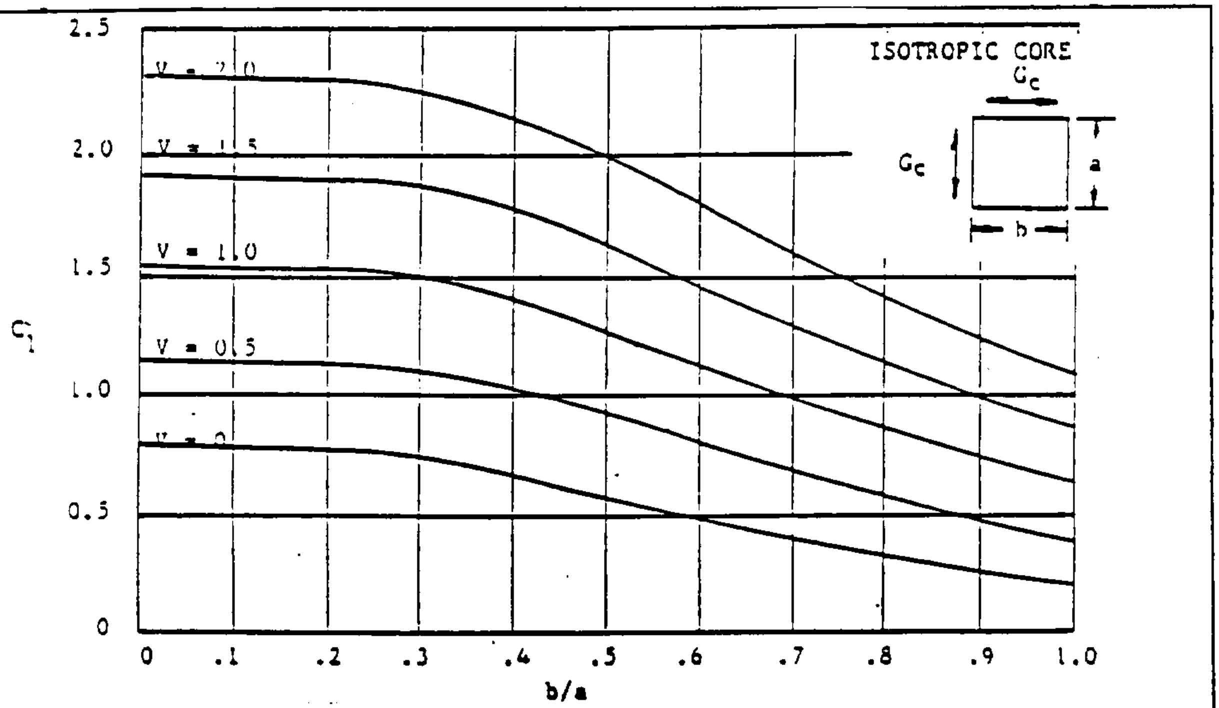

FIGURE 13.51 - DEFLECTION CONSTANT, C_1, FOR FLAT PANELS

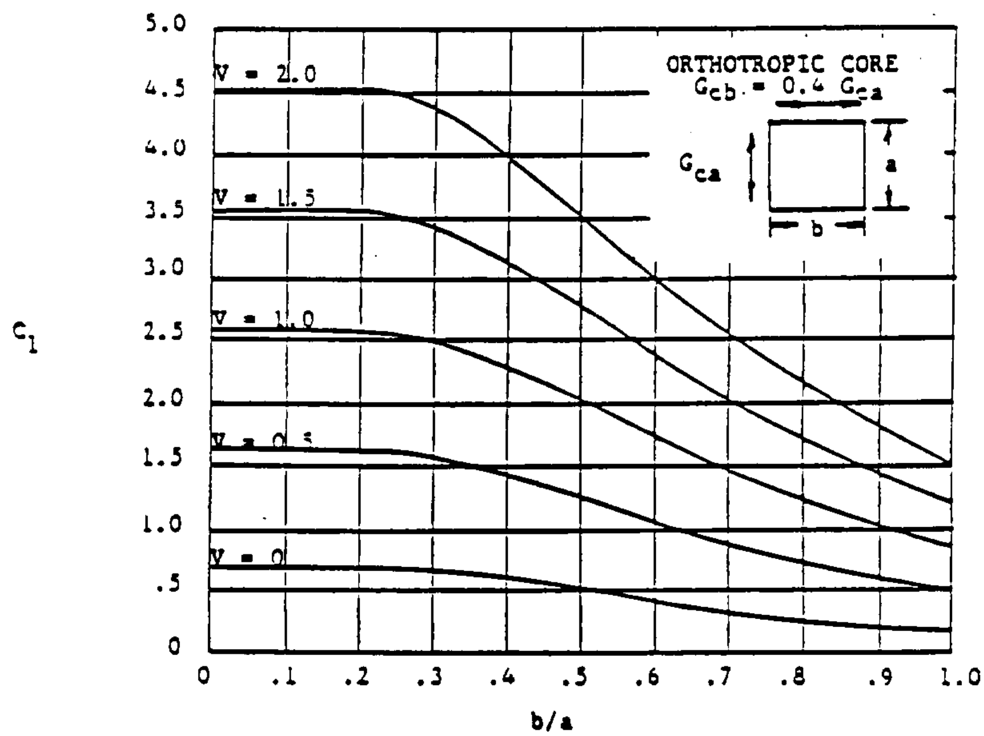

FIGURE 13.52 - DEFLECTION CONSTANT, C_1, FOR FLAT PANELS
WITH ISOTROPIC CORE UNDER NORMAL LOAD

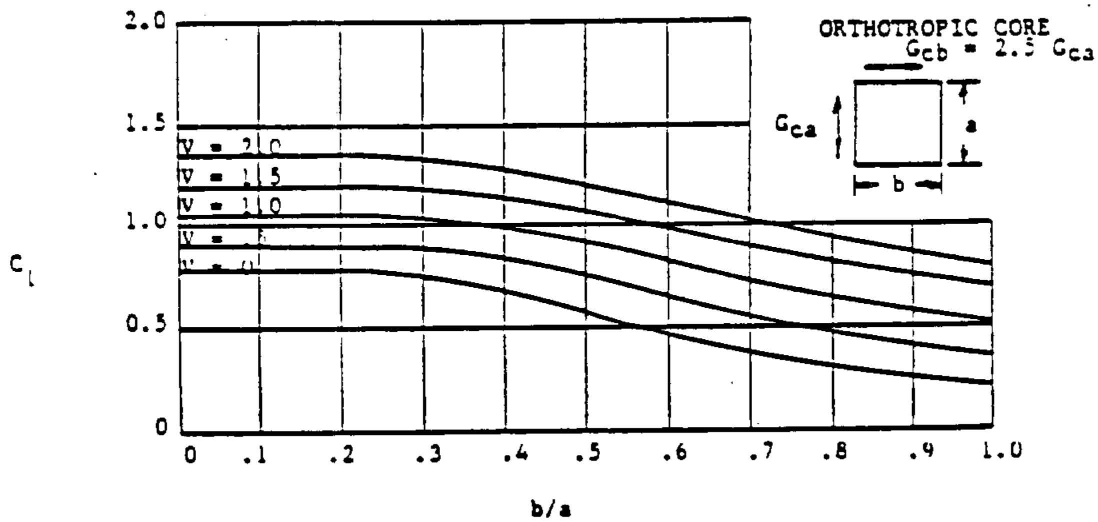

FIGURE 13.53 - DEFLECTION CONSTANT, C_1, FOR FLAT PANELS WITH ORTHOTROPIC CORE UNDER NORMAL LOAD

(2) Choose a practical core depth and density.

(3) For the previous configuration determine the facing stresses by

$$f_{so} = \frac{Tr_o}{J} \text{ ; outer facing} \qquad 13.54$$

$$f_{si} = \frac{Tr_i}{J} \text{ ; inner facing} \qquad 13.55$$

where r_o = radius to midline of outer facing
r_i = radius to midline of inner facing
J = polar moment of inertia of cylinder
$= 2\pi t(r_i^3 + r_o^3)$

(4) Calculate the shear load on the cylinder by

$$q = N_s = \frac{T}{2\pi r_c^2} = \frac{T}{2A} \qquad 13.56$$

where

$$r_c = \frac{r_o + r_i}{2} \qquad 13.57$$

(5) Determine the critical buckling load from

$$N_{cr} = \frac{2KE_f t t_c}{r_c} \qquad 13.58$$

where K is determined by entering the appropriate chart in Figures 13.55, 13.56 or 13.57 with parameters

$$J' = L^2/dr_c \qquad 13.59$$

$$V = \frac{t t_c E_f}{2\lambda r_c d G_c} \qquad 13.60$$

where G_c is the circumferential core shear modulus.

(6) If N_{cr} is smaller than the shear load N_s calculated in step (4), increase the sandwich strength and repeat steps (1) through (6).

(7) Analyze the design for intercell buckling per Section 13.2.2.

13.2.7 Sandwich Cylinders Under Axial Compression

This section gives the procedures for determining core thickness and core shear modulus so that overall buckling of the sandwich walls of the cylinder will not occur.

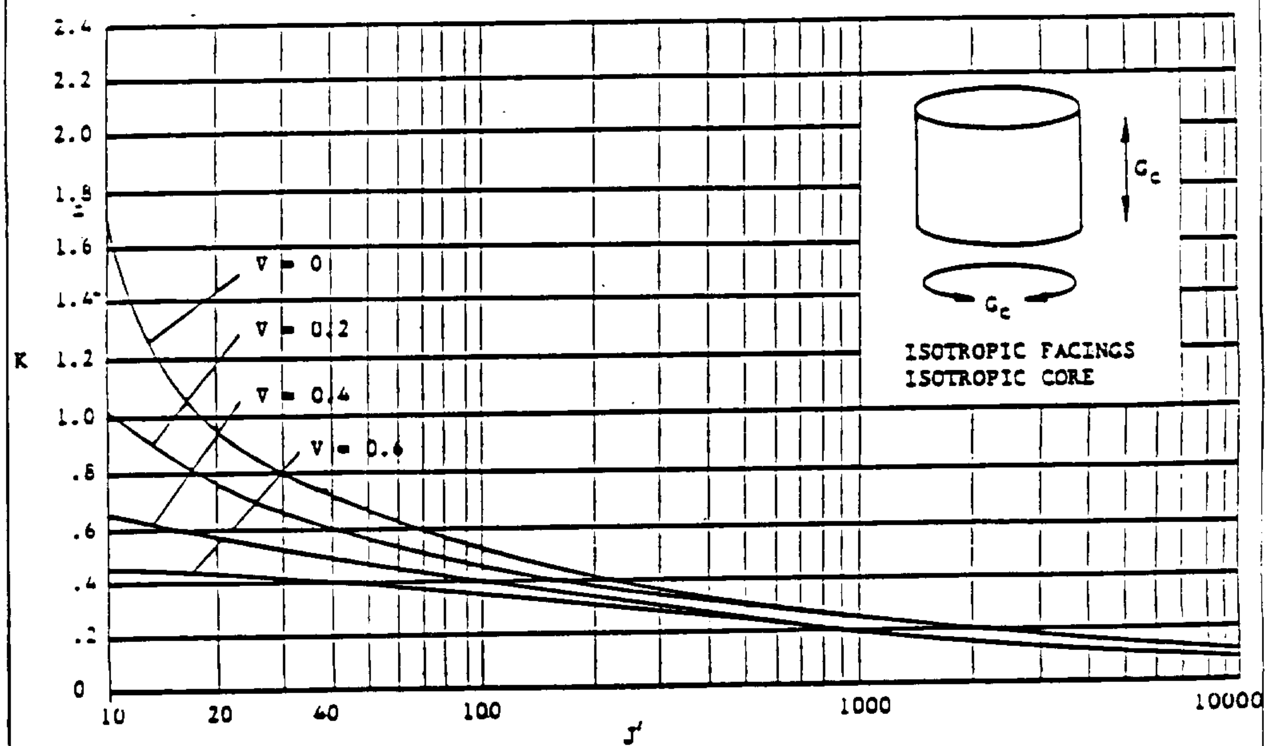

FIGURE 13.55 - BUCKLING CONSTANT, K, FOR CYLINDERS WITH ISOTROPIC FACINGS AND ISOTROPIC CORE AND TORSIONAL LOADING

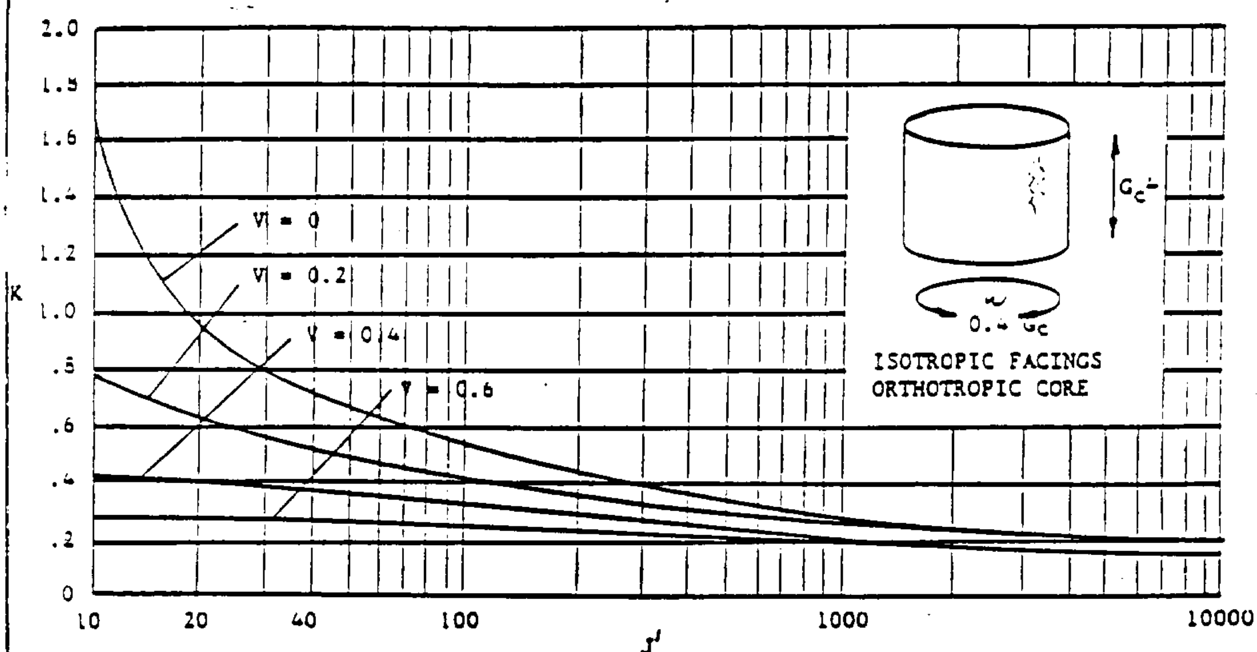

FIGURE 13.56 - BUCKLING CONSTANT, K, FOR CYLINDERS WITH ISOTROPIC FACINGS AND ORTHOTROPIC CORE AND TORSIONAL LOADING

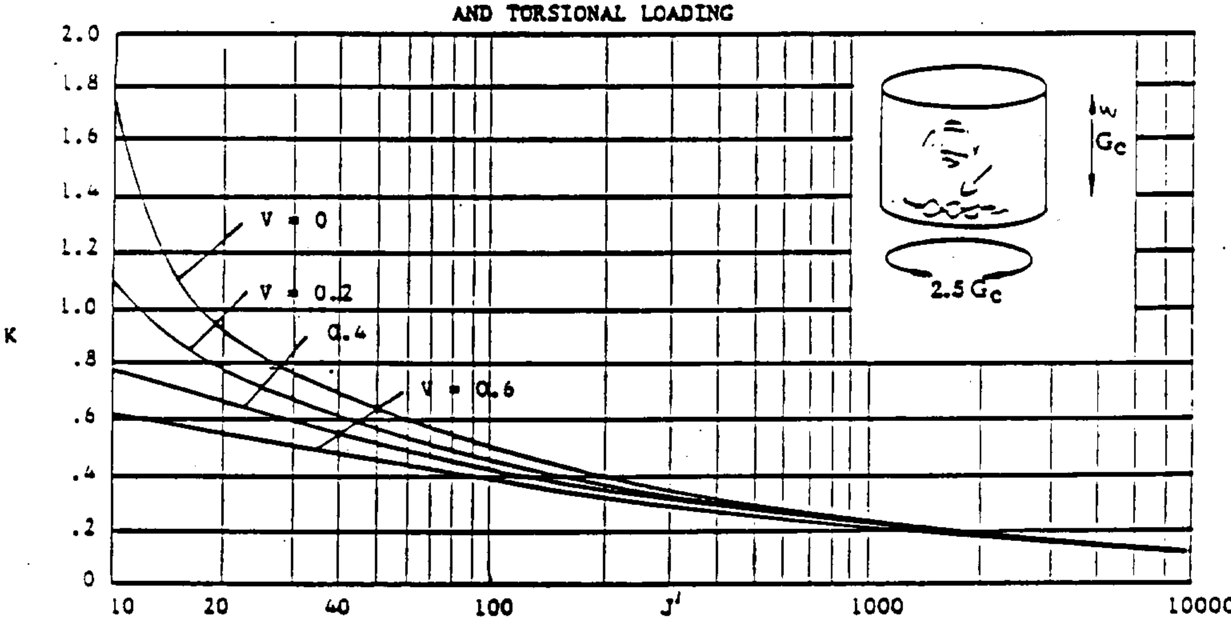

FIGURE 13.57 - BUCKLING CONSTANT, K, FOR CYLINDERS WITH ISOTROPIC FACINGS AND ORTHOGRAPHIC CORE AND TORSIONAL LOADING

Theoretical formulas are based on buckling loads for classical sine-wave buckling. The theory defines the parameters involved rather than determining exact coefficients for computing buckling loads. Large discrepancies exist between theory and tests and, unfortunately, the test values for buckling of thin walled cylinders in axial compression are much lower than expected by theory. Design information based on large deflection theory and diamond shaped buckles give results less than one-half the buckling loads given by classical theory.

Until sufficient test data are available, the two methods of analysis, large deflection, theory, and small deflection or classical theory must be used. The two methods are presented in this section. The designer may take his choice, but this choice should be dictated somewhat by the application of the structure.

A. Large Deflection Theory

The following method is used in the design of a sandwich cylinder subjected to axial compression loading. Assume the load is applied uniformly to both facings. Either the outside or the inside diameter is given. The sandwich has isotropic faces and isotropic or orthotropic core.

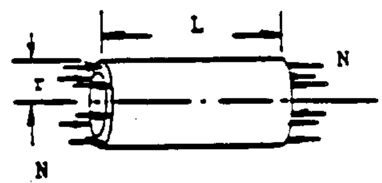

N = uniform axial load in lb/in of circumference

FIGURE 13.58 - CYLINDERS UNDER AXIAL COMPRESSION

(1) Choose an allowable compressive stress (F_f) for the facings and determine the approximate required thicknesses by

$$t_1 F_{f1} + t_2 F_{f2} = N; \text{ unequal faces} \quad 13.61$$

$$t = N/2F_f; \text{ equal faces} \quad 13.62$$

For facings of different materials, maintain the ratio

$$F_{f1}/E_{f1} = F_{f2}/E_{f2} \quad 13.63$$

(2) Determine the following parameters, assigning subscripts in such a manner that equation 13.64 is $\geq$ 1.

$$E_{f2} t_2 / E_{f1} t_1 \quad 13.64$$

$$\frac{F_f \sqrt{\lambda}}{E_f} \quad 13.65$$

(3) Enter chart in Figure 13.59 with $V' = 0.1$. Project vertically upward to parameter determined by equation 13.64. Proceed horizontally to appropriate core shear modulus (G_c) curve, then downward to parameter of equation 13.64 and across to equation 13.65. Project upward to h/r and read the value; use it to determine a tentative sandwich configuration ($r \approx r_o$).

$$h = r\,(h/r) \qquad 13.66$$

Determine core thickness (t_c) from

$$t_c = h - (t_1 + t_2)/2; \text{ unequal faces} \qquad 13.67$$

$$t_c = h - t; \text{ equal faces} \qquad 13.68$$

(4) Estimate the value of r, the radius to the centroid of the cylinder wall, from

$$r = (r_o + r_i)/2 \qquad 13.69$$

This is true for equal facings only but is sufficiently accurate for most practical cases involving unequal faces.

(5) Determine constant K', relating V' to G_c by

$$K' = \frac{2\, E_{f1} t_1 t_c}{3\,\lambda\, rd} \qquad 13.70$$

For unequal facings evaluate K' for each facing; use lower value.

(6) Enter chart in Figure 13.63 with $V' = 0.1$. Project horizontally to approximate $V' = K'/G_c$ diagonal and read the value for G_c. If this value of G_c is impractical, move diagonally to a desired value. Read the new V'. For the new value of V' repeat Steps (3) through (6), iterating until a satisfactory solution is reached.

NOTE: For values of $V' \geq 1.0$ use charts in Figures 13.60, 13.61, and 13.62.

(7) For sandwich buckling analysis, evaluate the parameters

$$V = \frac{2}{3\lambda}\;\frac{E_{f1} t_1 E_{f2} t_2 t_c}{(E_{f1} t_1 + E_{f2} t_2)\, dr\, G_c}\text{; unequal faces} \qquad 13.71$$

$$V = \frac{E_f t t_c}{3\lambda d r G_c}\text{; equal faces} \qquad 13.72$$

$$t_c/d \qquad 13.73$$

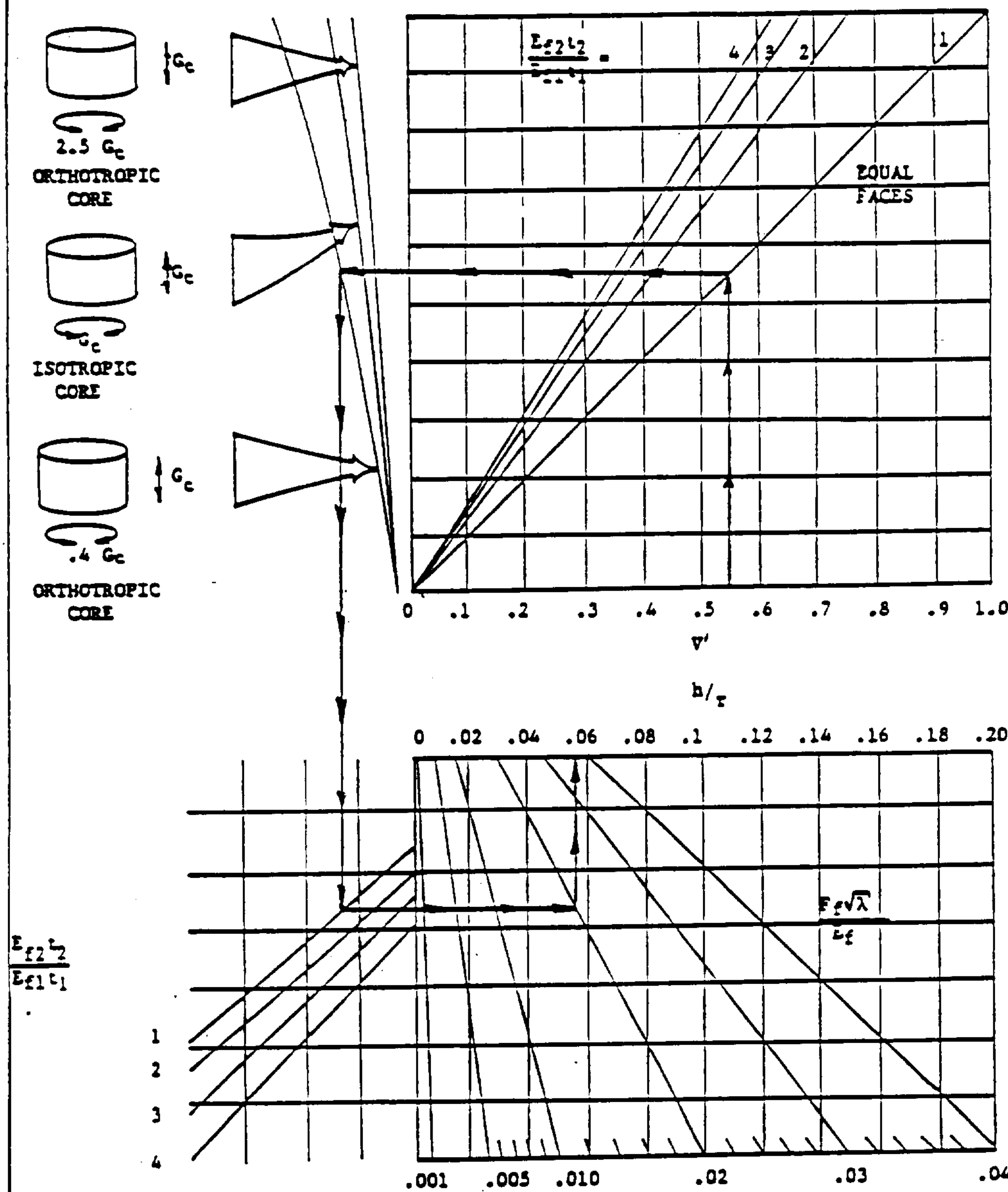

FIGURE 13.59 - APPROXIMATE DESIGN CURVE FOR CYLINDERS UNDER AXIAL COMPRESSION

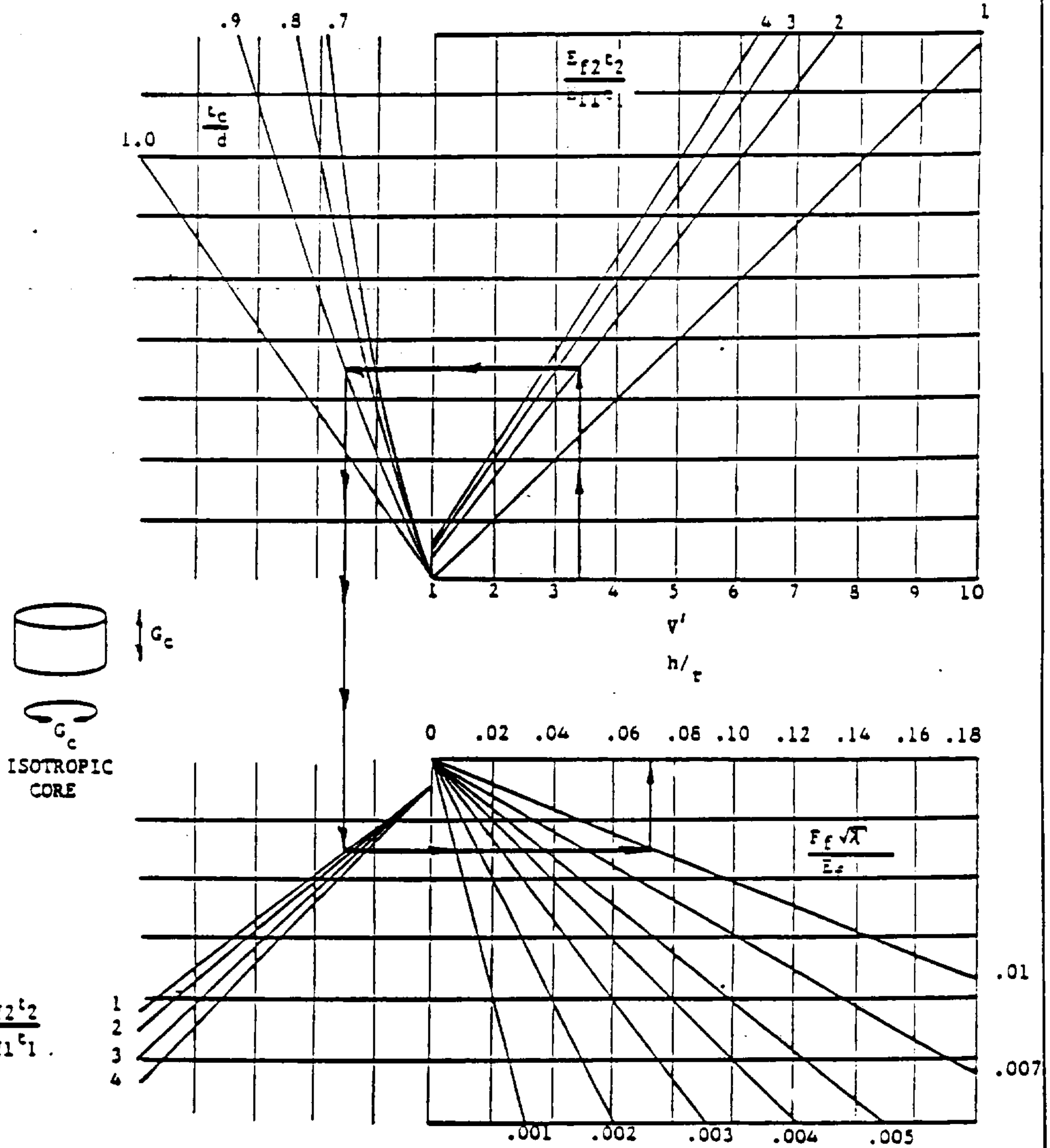

FIGURE 13.60 - DESIGN CURVE FOR CYLINDERS WITH ISOTROPIC CORE UNDER AXIAL COMPRESSION

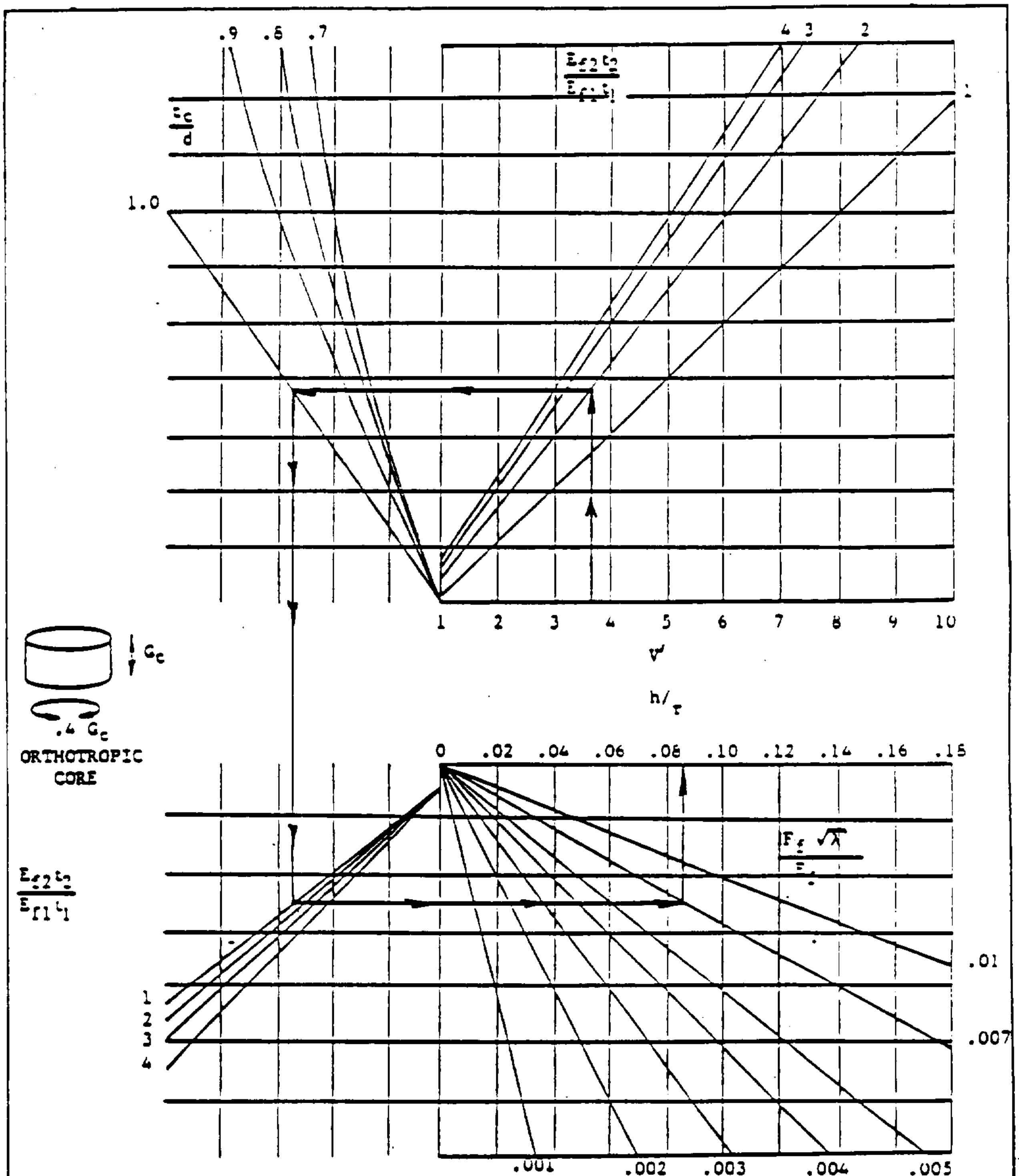

FIGURE 13.61 - DESIGN CURVE FOR CYLINDERS WITH ORTHOTROPIC CORE UNDER AXIAL COMPRESSION

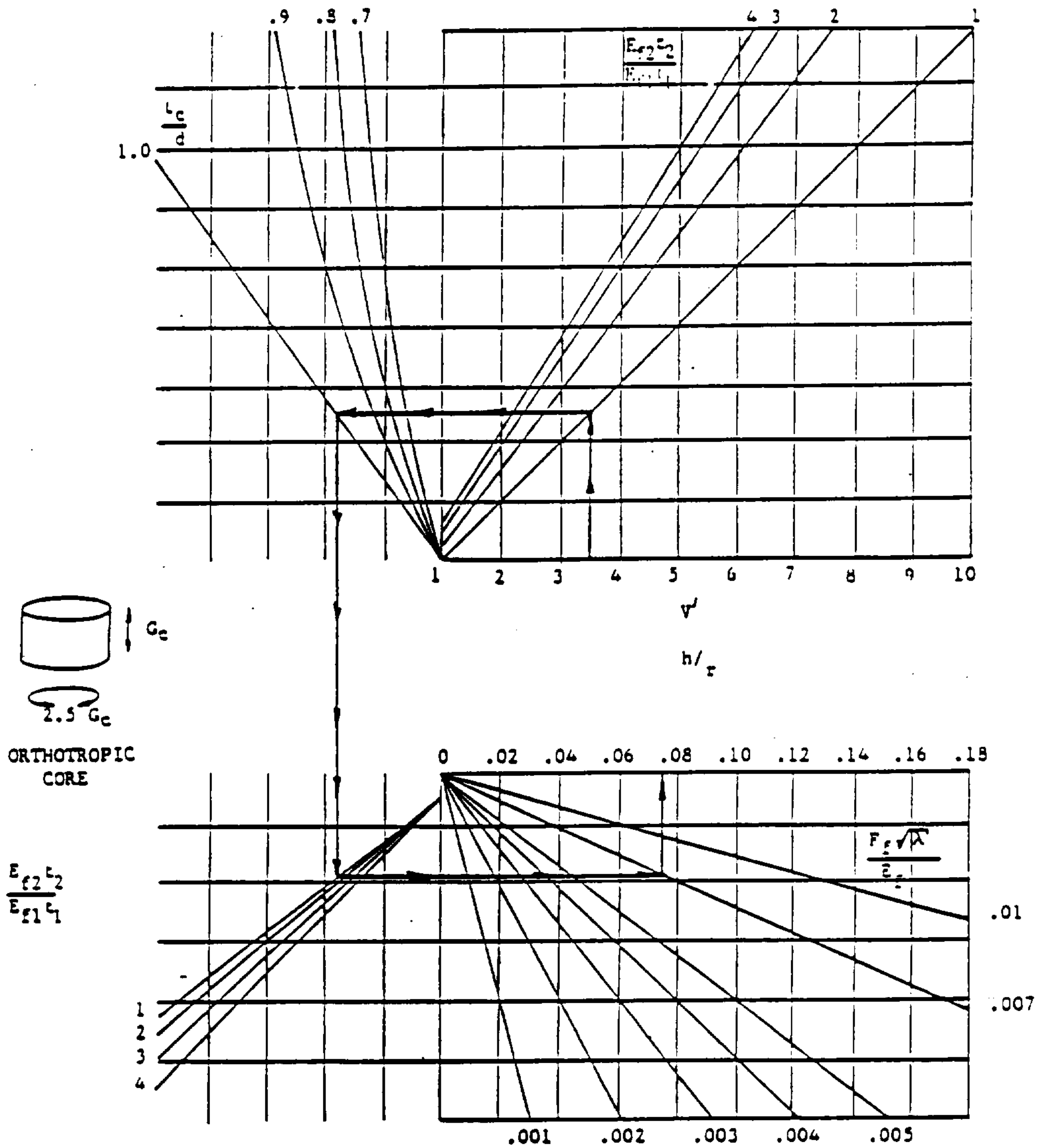

FIGURE 13.62 - DESIGN CURVE FOR CYLINDERS WITH ORTHOTROPIC CORE UNDER AXIAL COMPRESSION

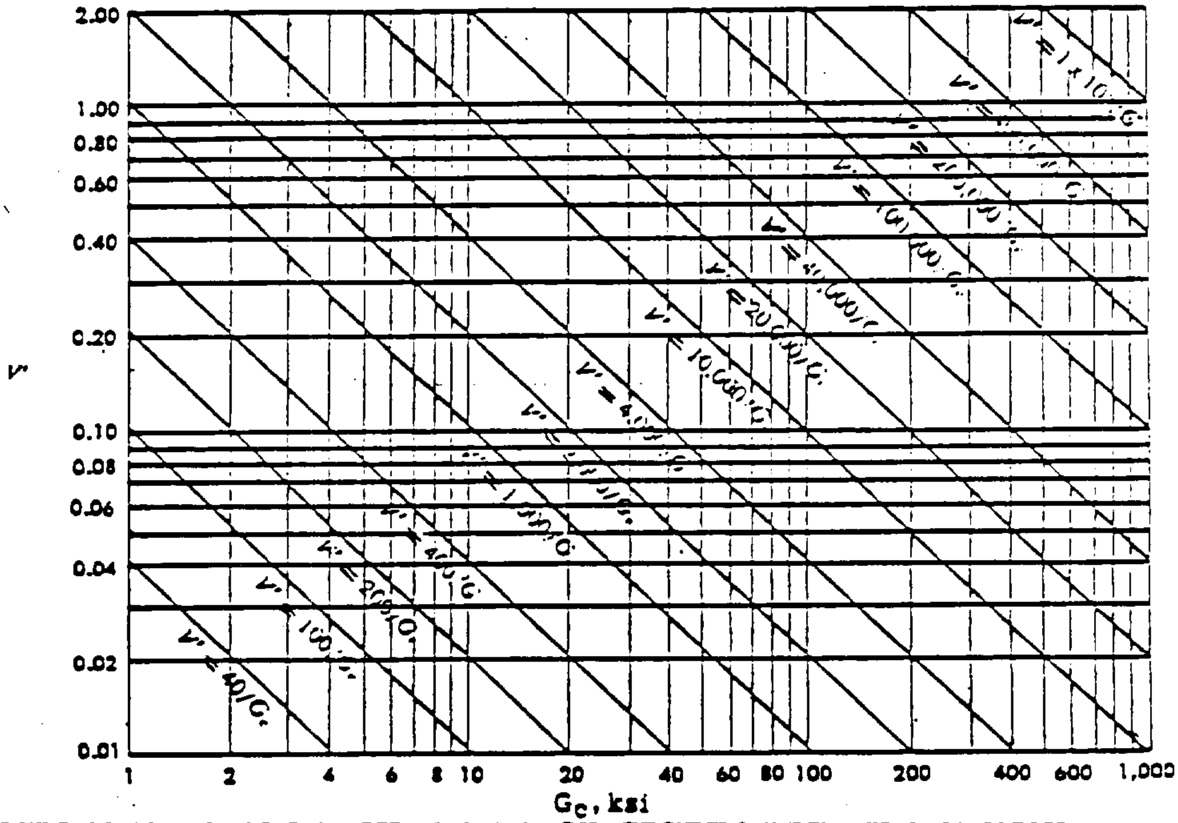

FIGURE 13.63 - CHART FOR DETERMINING G_c FOR CYLINDERS UNDER AXIAL COMPRESSION

FIGURE 13.64 - CHART FOR DETERMINING K FOR CYLINDERS UNDER AXIAL COMPRESSION WITH ISOTROPIC CORE

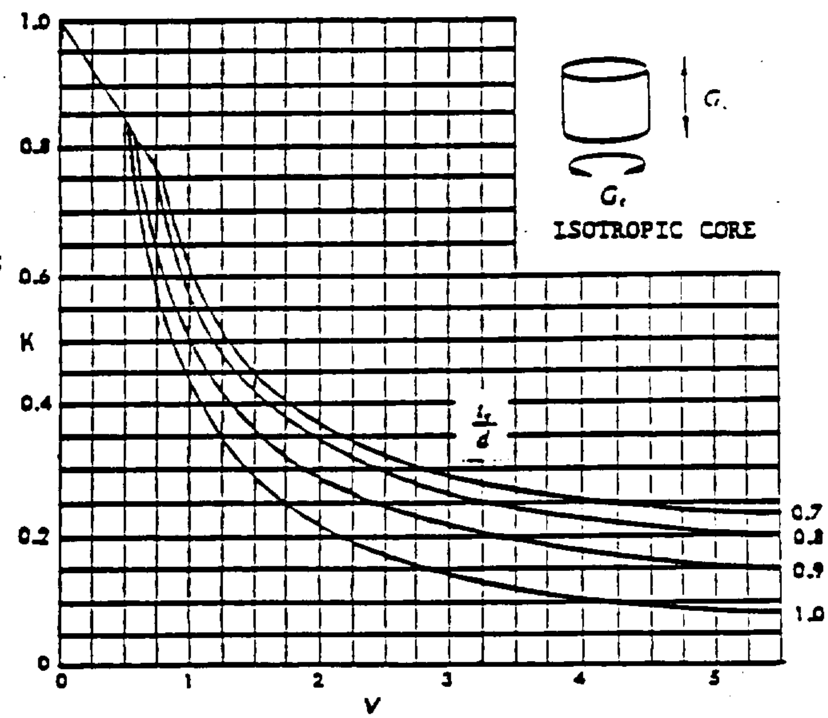

Enter the appropriate chart in Figures 13.64, 13.65, or 13.66. Obtain the value of K.

(8) Determine the ratio of the facing stiffness to the sandwich stiffness

$$R_F = \frac{(E_1 t_1{}^3 + E_2 t_2{}^3)(E_1 t_1 + E_2 t_2)}{12\ E_1 t_1 E_2 t_2 h^2} \quad ; \text{ unequal faces} \qquad 13.74$$

$$R_F = t^2/3h^2 \quad ; \text{ equal faces} \qquad 13.75$$

(9) The value of facing stress (F_{ccr}) at which buckling of sandwich wall will occur is

$$F_{ccr} = \frac{4}{5} K \frac{Eh \sqrt{E_1 t_1 E_2 t_2}}{r\ (E_1 t_1 + E_2 t_2)} \sqrt{\frac{1+R_F}{\lambda}} \quad ; \text{ unequal faces} \qquad 13.76$$

$$F_{ccr} = \frac{2}{5} K \frac{Eh}{r} \sqrt{\frac{1+R_F}{\lambda}} \quad ; \text{ equal faces} \qquad 13.77$$

Unequal faces must both be checked to insure that $F_{ccr} > f_f$.

(10) Check for overall column buckling using

$$N_{ccr} = \frac{\pi^2 r^2\ (E_1 t_1 + E_2 t_2)}{2\ L^2} ; \text{ unequal faces} \qquad 13.78$$

$$N_{ccr} = \frac{\pi^2 r^2 Et}{L^2} \quad ; \text{ equal faces} \qquad 13.79$$

(11) Check the cylinder faces for intracell buckling per Section 13.2.2.

B. Small Deflection or Classical Theory

Proceed through step (6) in the previously described large deflection method. This will give a satisfactory first approximation.

(7) For sandwich buckling analysis evaluate the parameters

$$V = \frac{E_{f1} E_{f2} t_c \sqrt{t_1 t_2}}{(E_{f1} + E_{f2}) \sqrt{\lambda}\, hr\ G_{xz}} \qquad 13.80$$

FIGURE 13.65

CHART FOR DETERMINING K FOR CYLINDERS UNDER AXIAL COMPRESSION WITH ORTHOTROPIC CORE

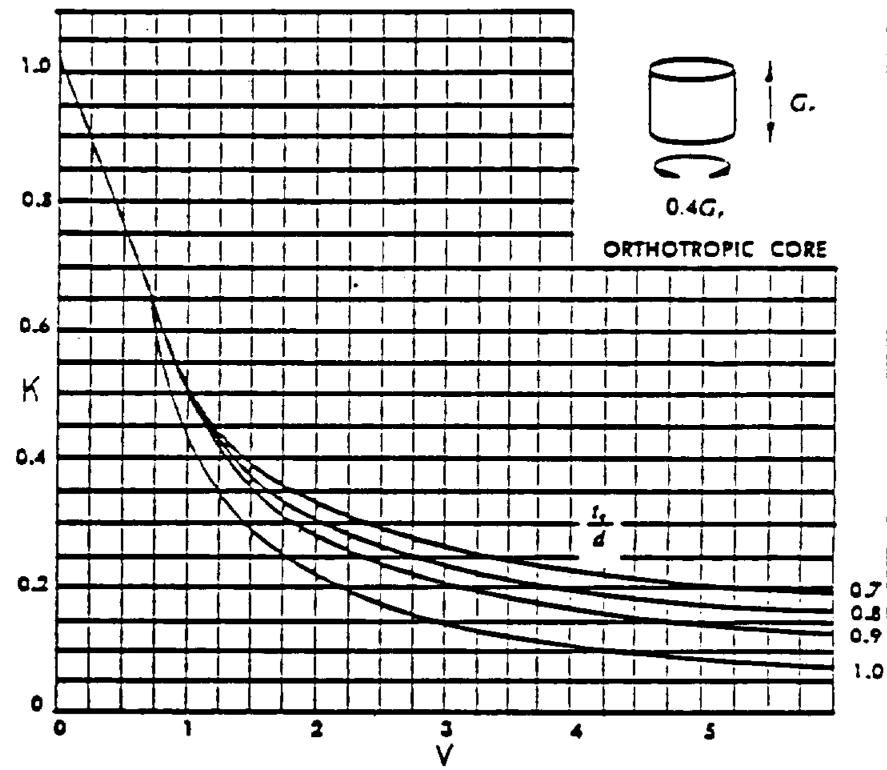

FIGURE 13.66

CHART FOR DETERMINING K FOR CYLINDERS UNDER AXIAL COMPRESSION WITH ORTHOTROPIC CORE

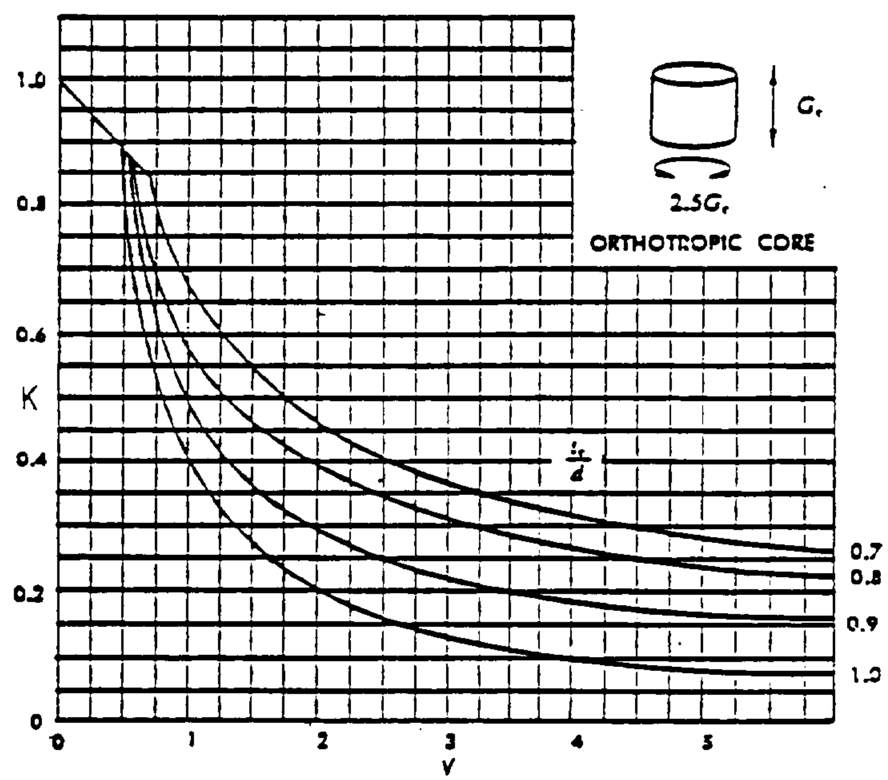

$$V = \frac{E_f t_c t}{2\sqrt{\lambda}\, h r G_{xz}} \text{ ; equal faces} \qquad 13.81$$

(8) Enter chart in Figure 13.67 and obtain a value for K.

(9) The value of F_{cr} at which buckling of the sandwich will occur is

$$F_{cr} = \frac{4KE_{f1}E_{f2}\, h\sqrt{t_1 t_2}}{r\sqrt{\lambda}\,(t_1 t_2)} \text{ ; unequal faces} \qquad 13.82$$

$$F_{cr} = \frac{KE_f h}{r\sqrt{\lambda}} \text{ ; equal faces} \qquad 13.83$$

(10) and (11) Same as steps (10) and (11) for large deflection.

(12) Check for face wrinkling per section 13.2.1.

13.2.8 Cylinders Under Uniform External Pressure

This section presents formulas, theoretical equations, and a design procedure for determining the sandwich facing thickness, core thickness, and core shear modulus such that overall buckling of a sandwich cylinder will not occur at the facing design stresses. The following method is used in the analysis and design of sandwich cylinders subjected to uniform external pressure. The facings are isotropic, but may be of different materials and different thicknesses. The core may be either isotropic or orthotropic. The outside diameter and cylinder length are given as part of the design criteria.

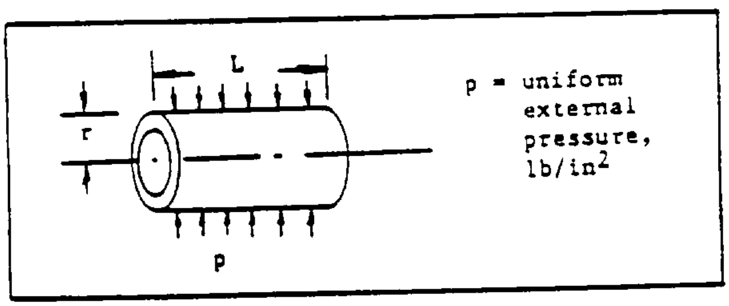

FIGURE 13.68 - CYLINDER UNDER UNIFORM EXTERNAL PRESSURE

(1) Select a tentative sandwich configuration given cylinder length (L), the outside diameter (D_o) and external pressure (p).

Choose:

a. Facing materials and thicknesses.

b. Core material: The flatwise compressive strength of the core, (F_c), must satisfy $F_c \geq 1.5\, p$ 13.84

2

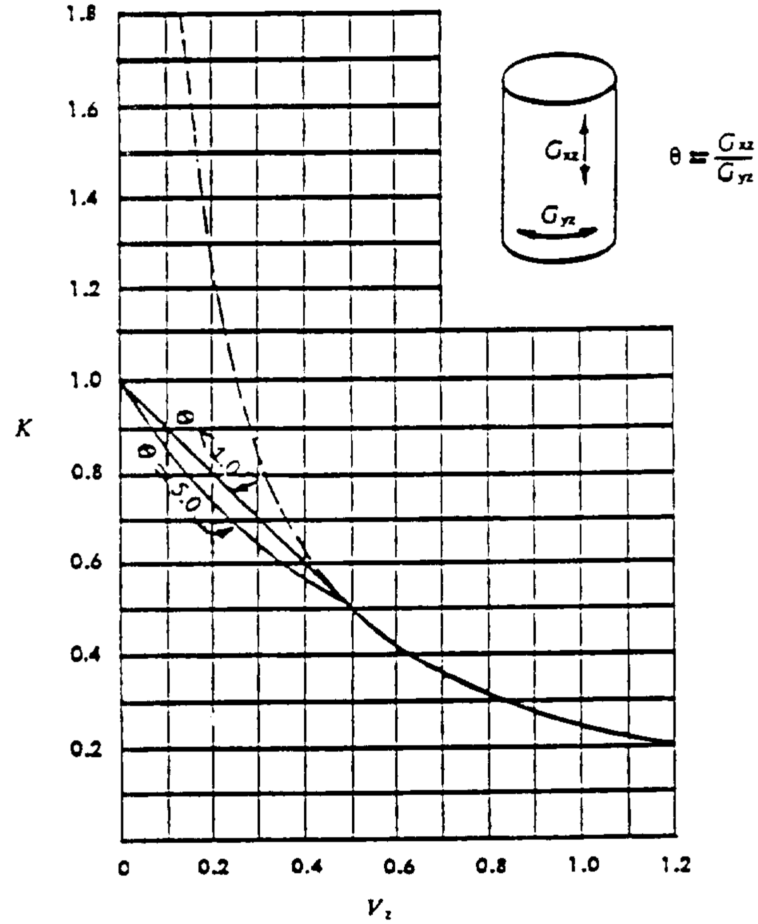

FIGURE 13.67 - CLASSICAL BUCKLING COEFFICIENT - ISOTROPIC FACES AND ORTHOTROPIC CORE

c. A tentative value for the centroidal distance between facings (h).

(2) Calculate the total depth of the sandwich (d) and the mean radius (r_c).

$$d = h + \frac{(t_1 + t_2)}{2} \text{ ; unequal faces} \qquad 13.85$$

$$r_c = \frac{D_o - d}{2} \qquad 13.86$$

$$d = h + t; \text{ equal faces} \qquad 13.87$$

(3) Calculate the parameter (R).

$$R = \frac{E_1 t_1}{E_2 t_2} \text{ ; unequal faces} \qquad 13.88$$

$$R = 1; \text{ equal faces} \qquad 13.89$$

(4) Calculate the parameter (V).

$$V = \frac{2E_1 t_1 E_2 t_2}{3r_c \lambda (E_1 t_1 + E_2 t_2) G_{r\theta}} \text{; unequal faces} \qquad 13.90$$

$$V = \frac{E t}{3r_c \lambda G_{r\theta}} \text{ ; equal faces} \qquad 13.91$$

where $G_{r\theta}$ = Core modulus of rigidity in the radial and tangential direction.

(5) Calculate the parameters (α^2) and (L/r_c).

L/r_c = the ratio of cylinder length to the mean radius 13.92

$$\alpha^2 = \frac{1}{2} (h/r_c)^2 \qquad 13.93$$ 2

h/r_c = the ratio of the centroidial distance between faces to the mean radius, where the mean radius is the distance to the center of the core.

(6) Enter charts in Figures 13.69 through 13.84 with the values of α^2, L/r_c and R. Determine k. If there is no exact chart for the given values, interpolate between adjacent charts.

A simpler but more conservative method based on the assumption of a very long cylinder (L/r_c > 100) may also be used to determine the value for k directly.

$$k = \frac{12R\,\alpha^2}{(R+1)^2\,(1 - 12\,V\alpha)} \text{ ; unequal faces} \qquad 13.94$$

$$k = \frac{3\,\alpha^2}{1 - 12\,V\alpha} \text{ ; equal faces} \qquad 13.95$$

(7) Calculate the critical buckling pressure (q_{cr}).

$$q_{cr} = \left[\frac{E_1 t_1 + E_2 t_2}{r_c\,\lambda}\right] k\text{; unequal faces} \qquad 13.96$$

$$q_{cr} = \frac{2Etk}{r_c \lambda} \text{ ; equal faces} \qquad 13.97$$

(8) If q_{cr} is less than the external pressure, p, select a new sandwich configuration and repeat steps (1) through (7).

13.2.9 Beams

This section contains the procedure for the design of sandwich members used as beams. The load is applied normal to the face of the sandwich and the member has reaction points at the ends. The edge of the beam is assumed to have no support.

(1) Determine the maximum bending moment (M) and maximum beam shear (S) for the design loading and end support conditions. Figure 13.85 shows some commonly used beams with maximum moments and shears.

(2) Choose an allowable design facing stress (F_f) which does not exceed either the tensile or compressive yield stress of the face material.

(3) Calculate the required section modulus per unit width (Z) from

$$Z = \frac{M}{F_f b} \qquad 13.98$$

where b = beam width.

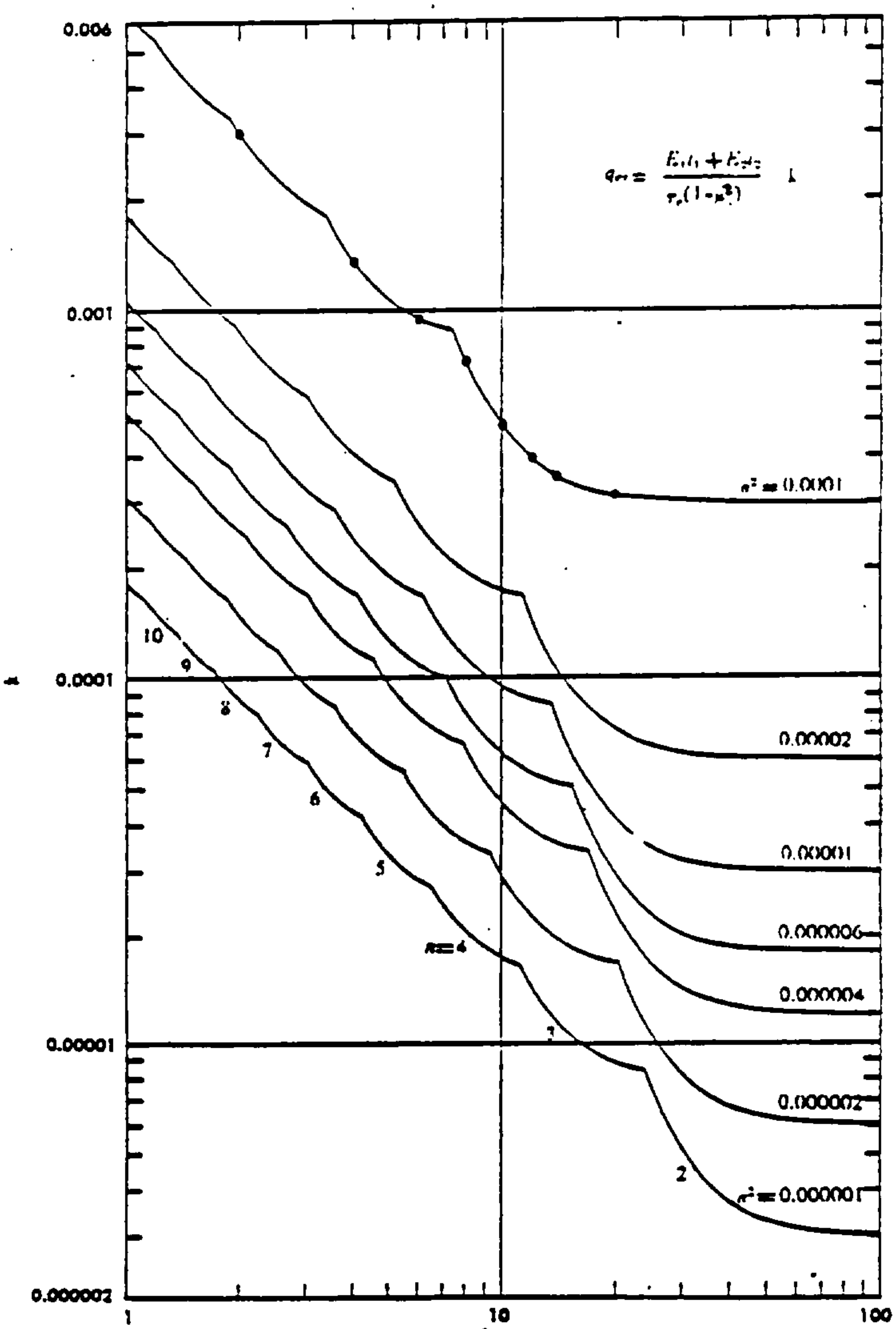

Values of k for $V = 0$, and for $\frac{E_x t_1}{E_y t_2} = 1$.

FIGURE 13.69 - BUCKLING COEFFICIENT FOR CYLINDERS UNDER UNIFORM EXTERNAL PRESSURE

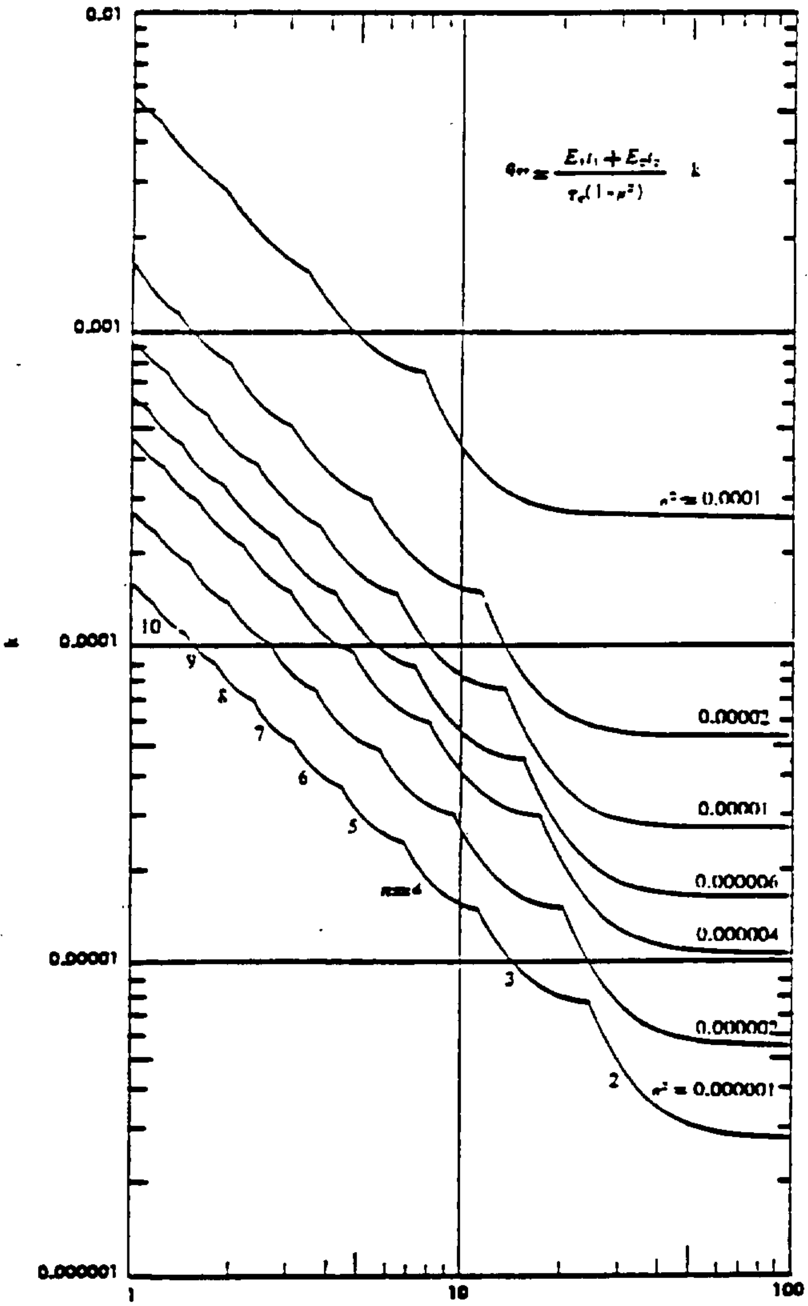

Values of k for $\nu = 0$, and for $\frac{E_1 t_1}{E_2 t_2} = 2$

FIGURE 13.70 - BUCKLING COEFFICIENT FOR CYLINDERS UNDER UNIFORM EXTERNAL PRESSURE

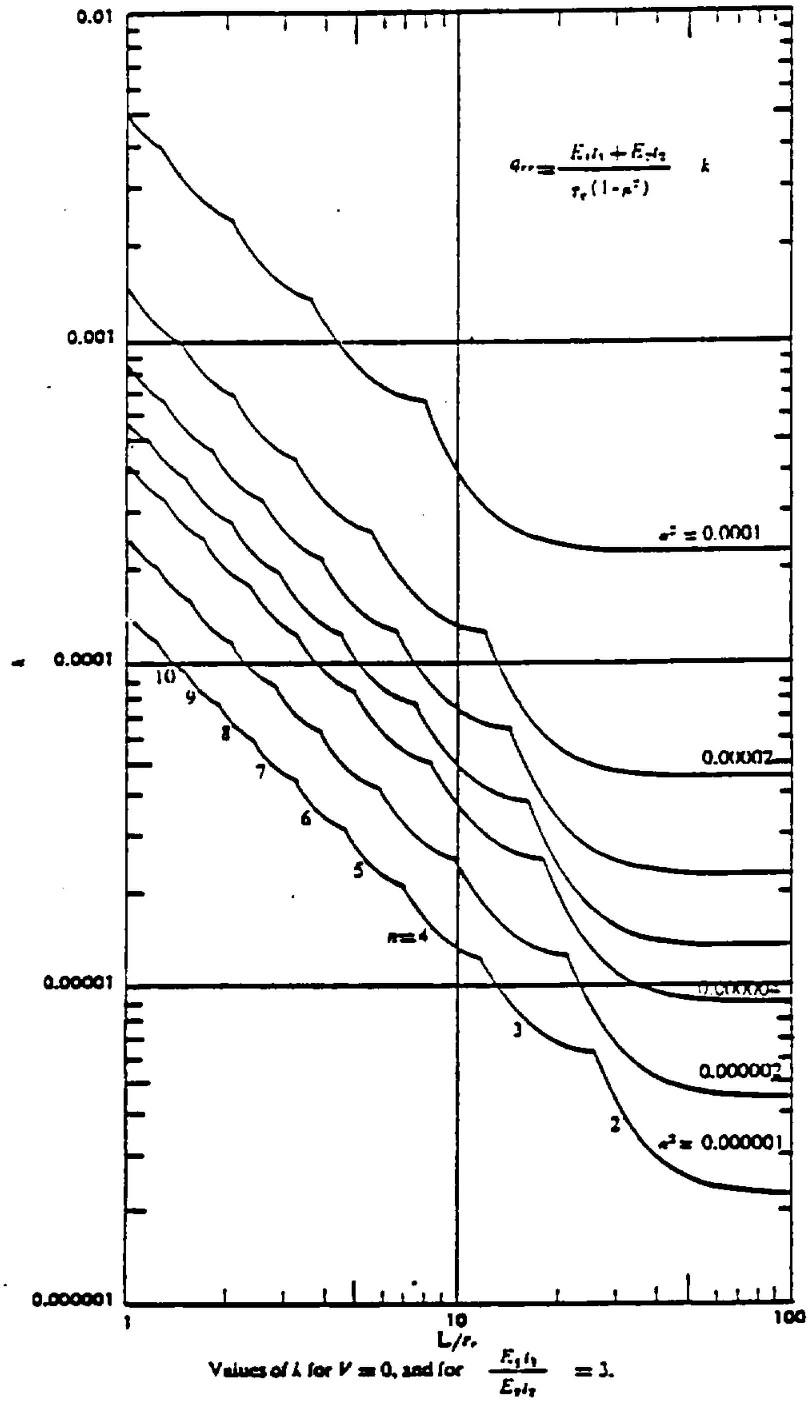

FIGURE 13.71 - BUCKLING COEFFICIENT FOR CYLINDERS UNDER UNIFORM EXTERNAL PRESSURE

541

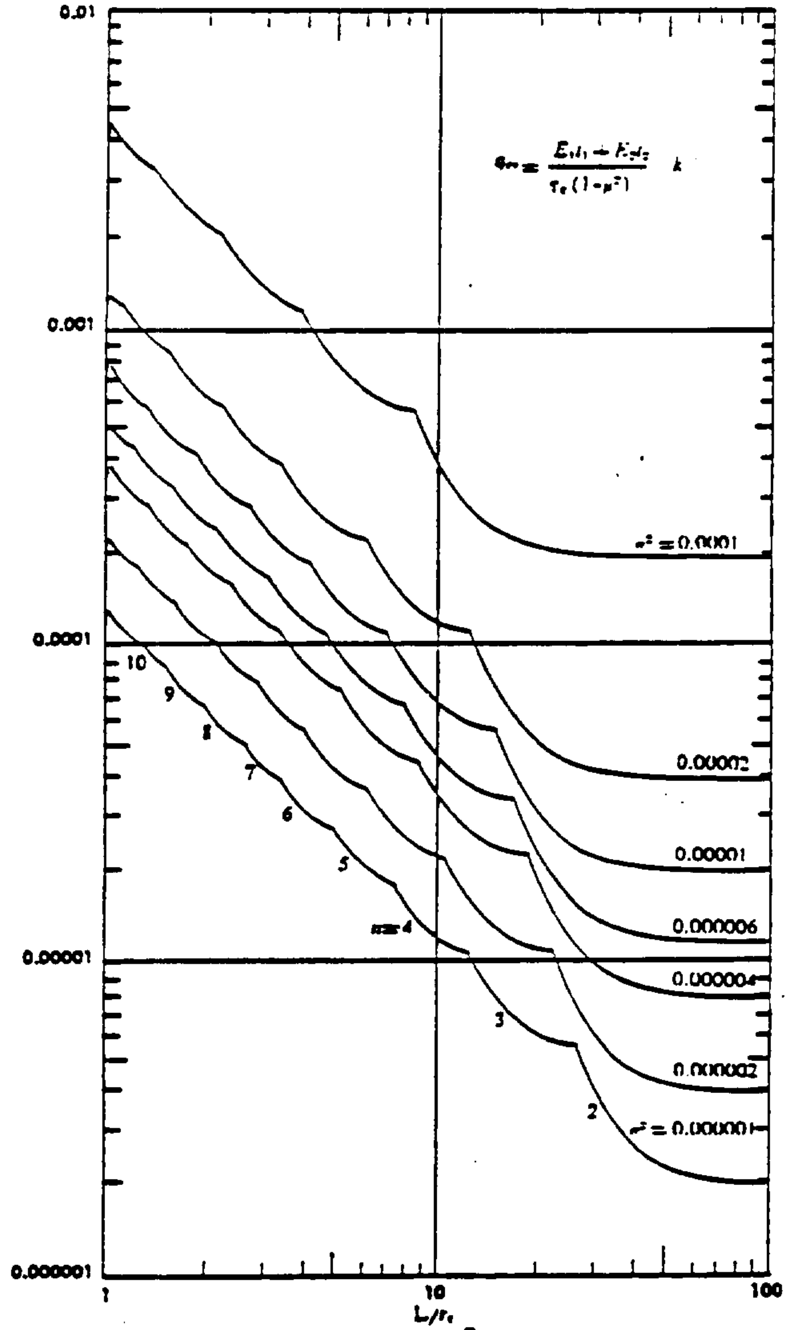

Values of k for ν 0, and for $\frac{E_1 t_1}{E_2 t_2} = 4$.

FIGURE 13.72 - BUCKLING COEFFICIENT FOR CYLINDERS UNDER UNIFORM EXTERNAL PRESSURE

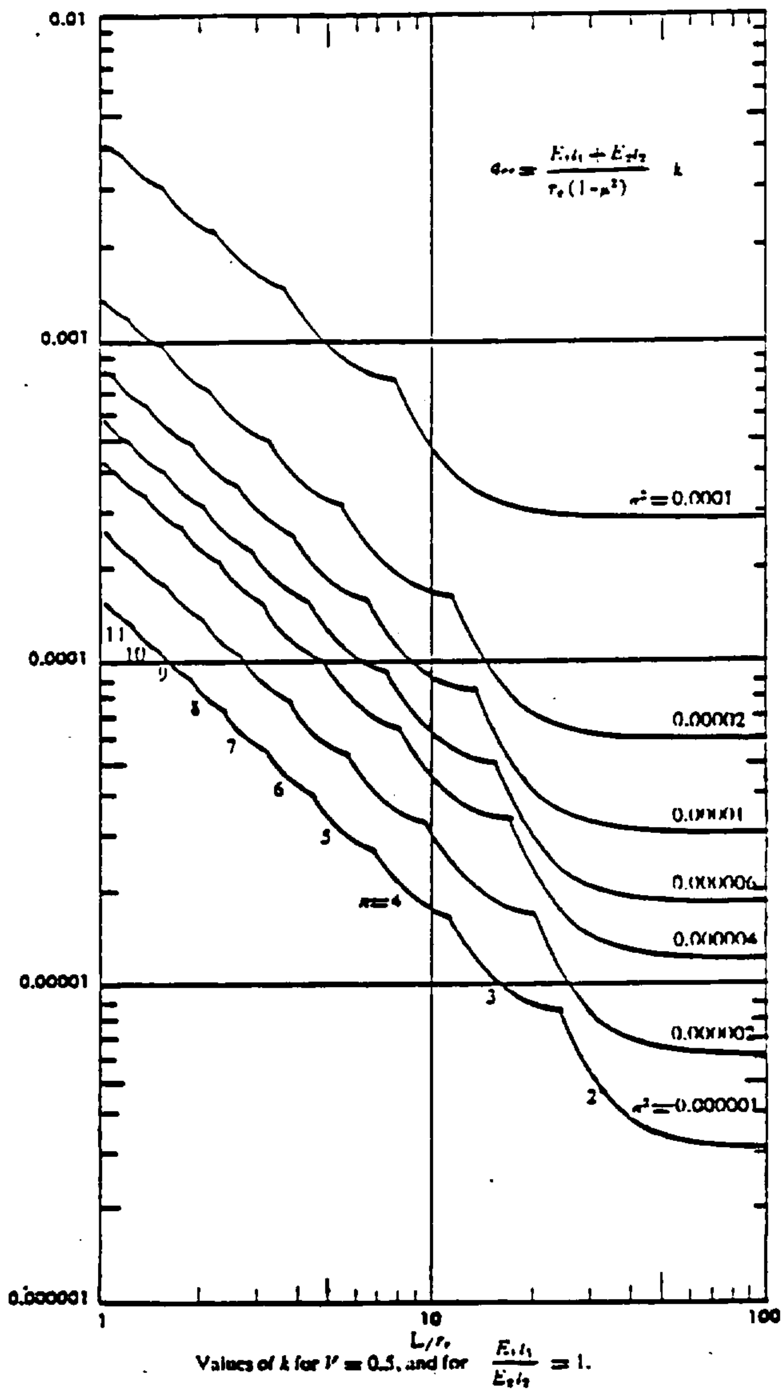

Values of k for $\nu = 0.5$, and for $\frac{E_1 t_1}{E_2 t_2} = 1$.

FIGURE 13.73 - BUCKLING COEFFICIENT FOR CYLINDERS UNDER UNIFORM EXTERNAL PRESSURE

543

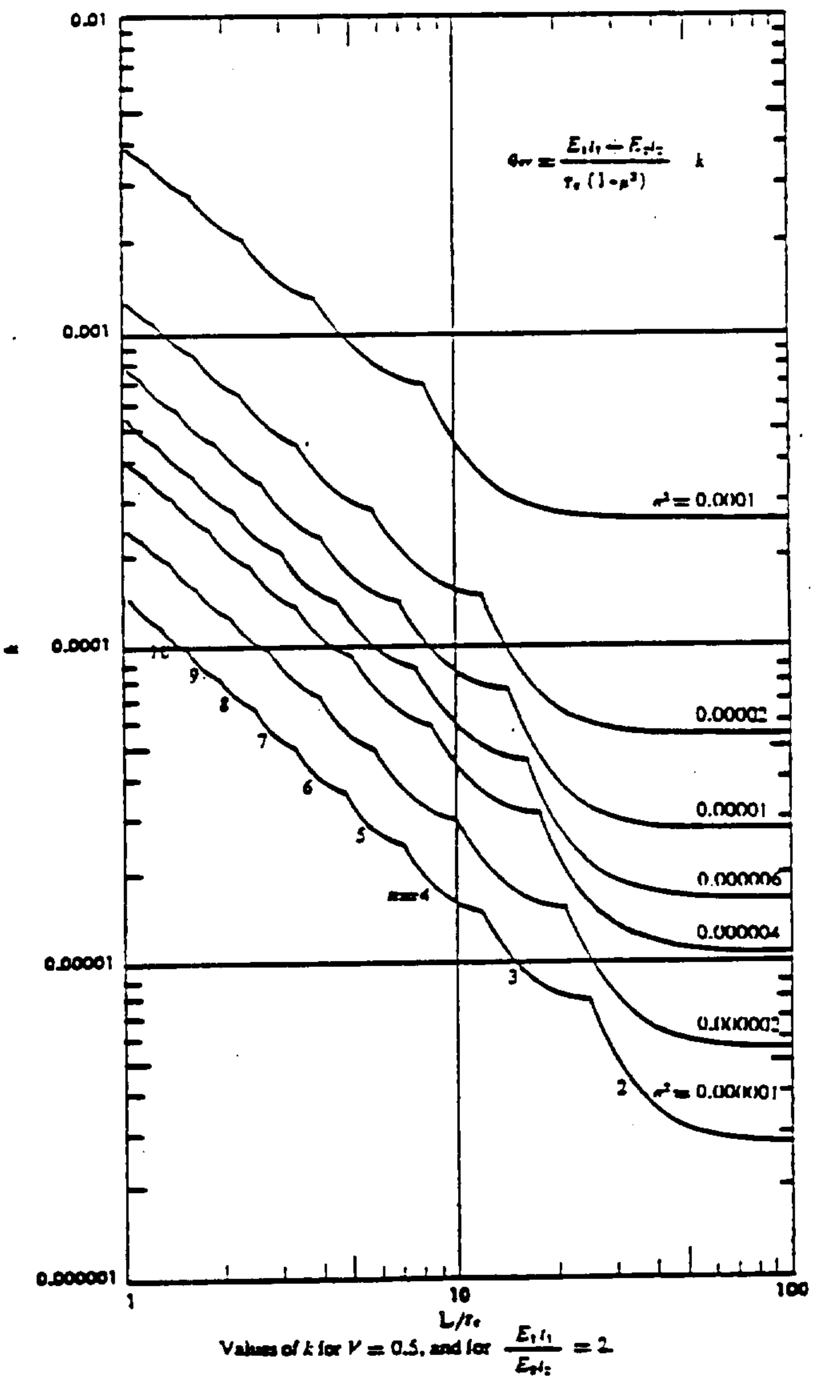

FIGURE 13.74 - BUCKLING COEFFICIENT FOR CYLINDERS UNDER UNIFORM EXTERNAL PRESSURE

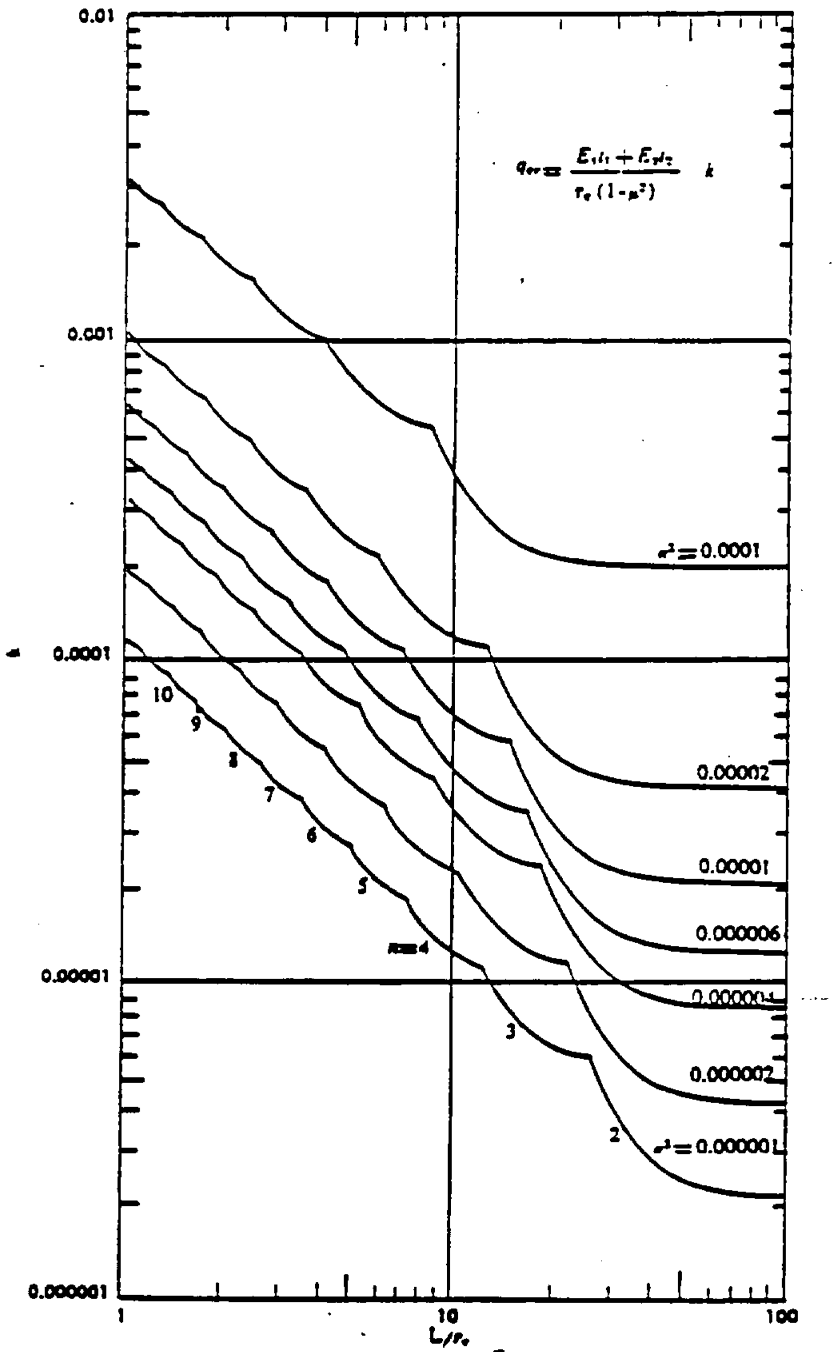

Values of k for $V = 0.5$, and for $\frac{E_x t_1}{E_y t_2} = 3$.

FIGURE 13.75 - BUCKLING COEFFICIENT FOR CYLINDERS UNDER UNIFORM EXTERNAL PRESSURE

545

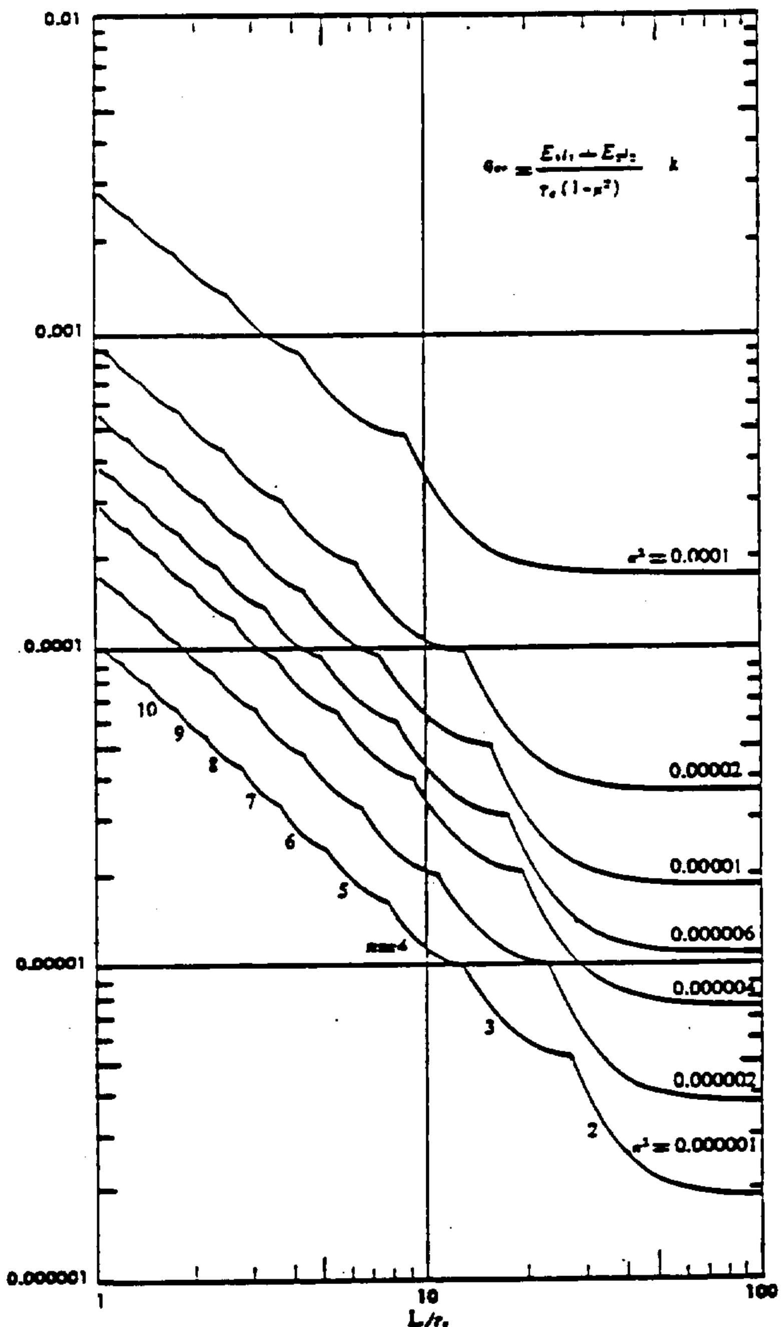

Values of k for $V = 0.5$, and for $\frac{E_1 t_1}{E_\phi t_2} = 4$.

FIGURE 13.76 - BUCKLING COEFFICIENT FOR CYLINDERS UNDER UNIFORM EXTERNAL PRESSURE

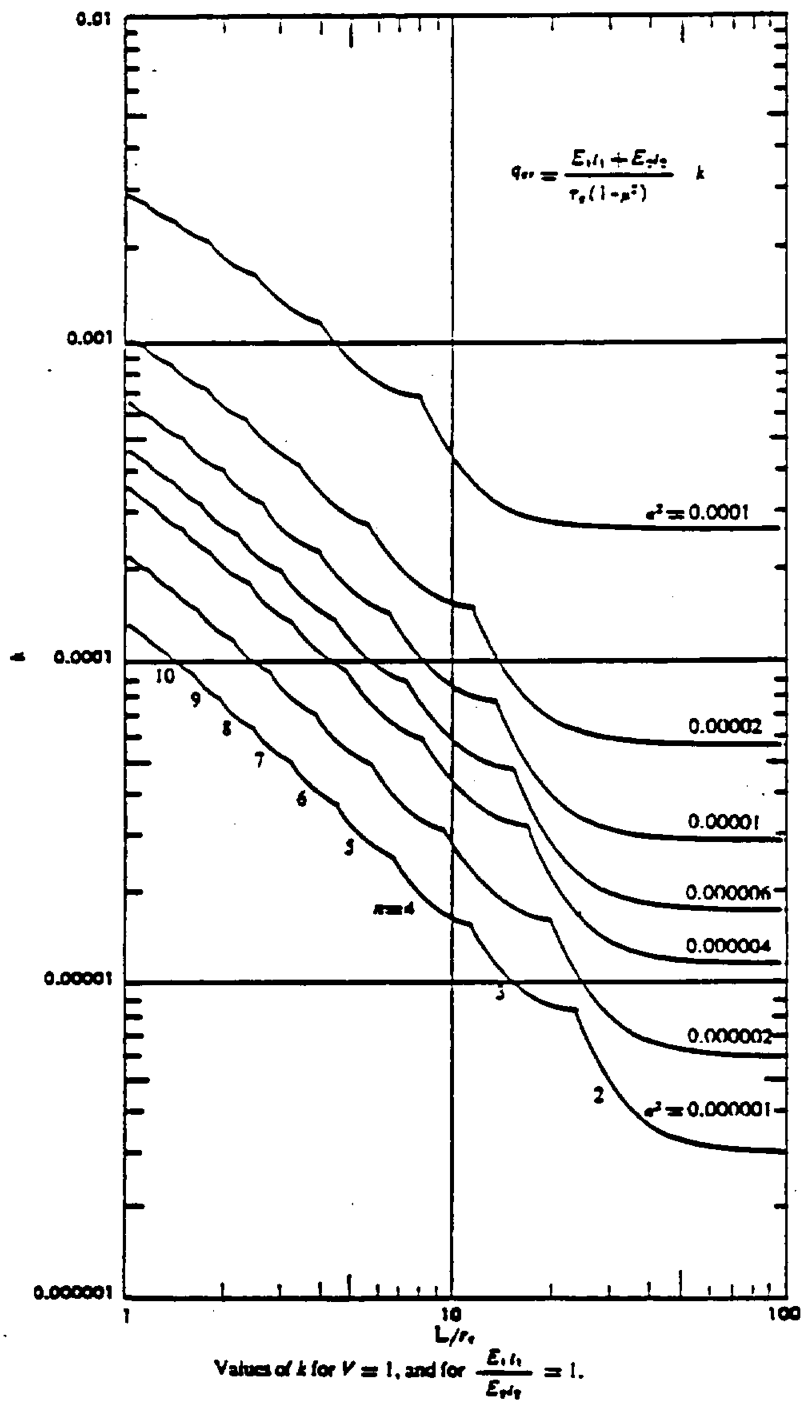

FIGURE 13.77 - BUCKLING COEFFICIENT FOR CYLINDERS UNDER UNIFORM EXTERNAL PRESSURE

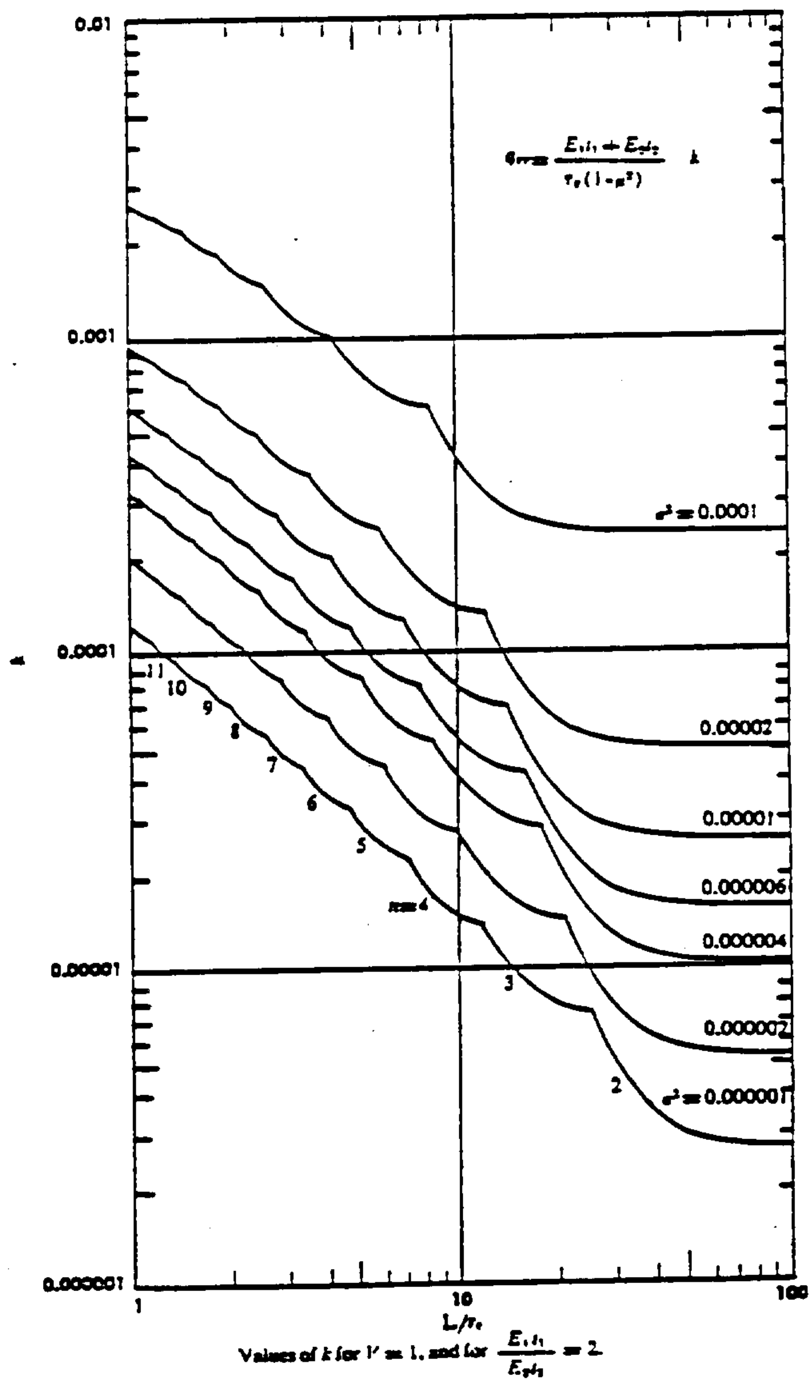

FIGURE 13.78 - BUCKLING COEFFICIENT FOR CYLINDERS UNDER UNIFORM EXTERNAL PRESSURE

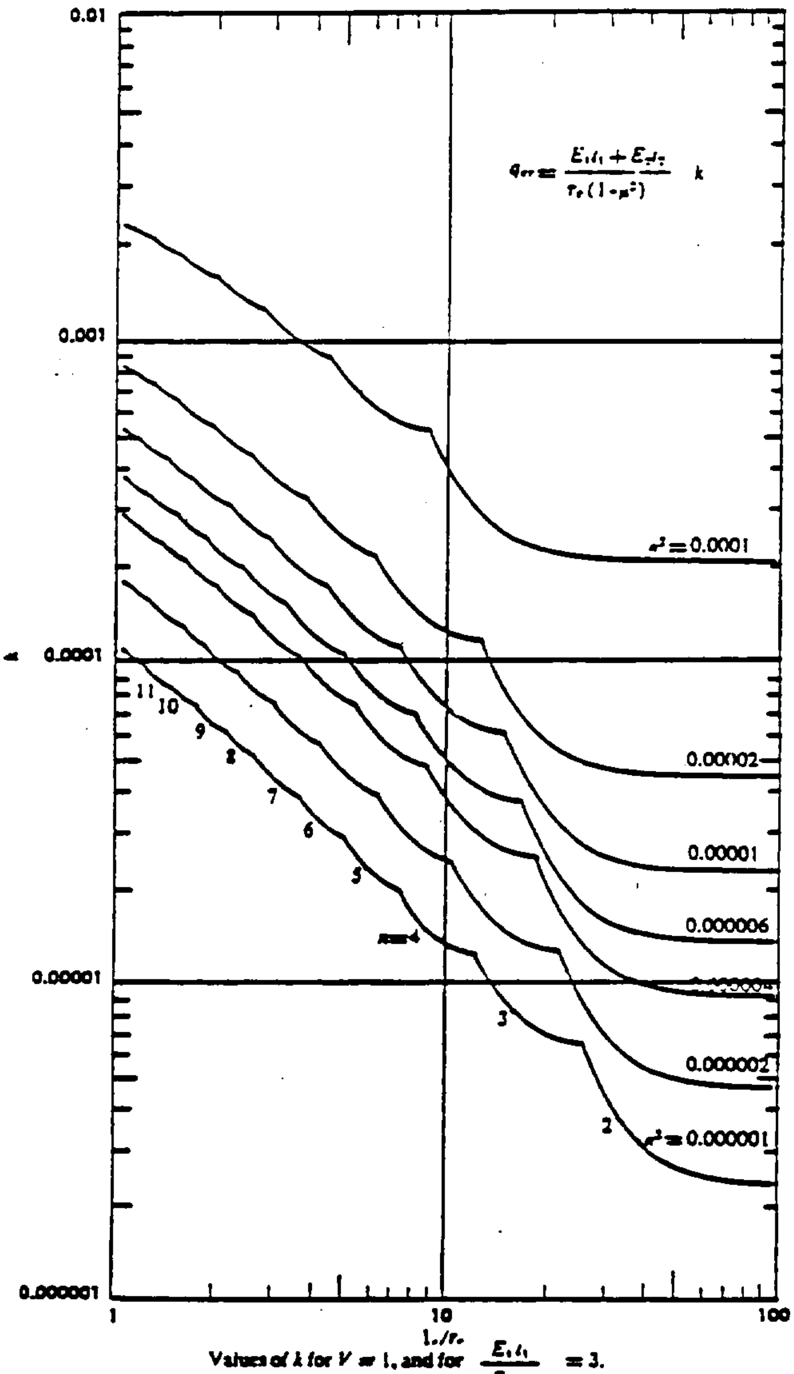

Values of k for $V = 1$, and for $\frac{E_1 t_1}{E_2 t_2} = 3$.

FIGURE 13.79 - BUCKLING COEFFICIENT FOR CYLINDERS UNDER UNIFORM EXTERNAL PRESSURE

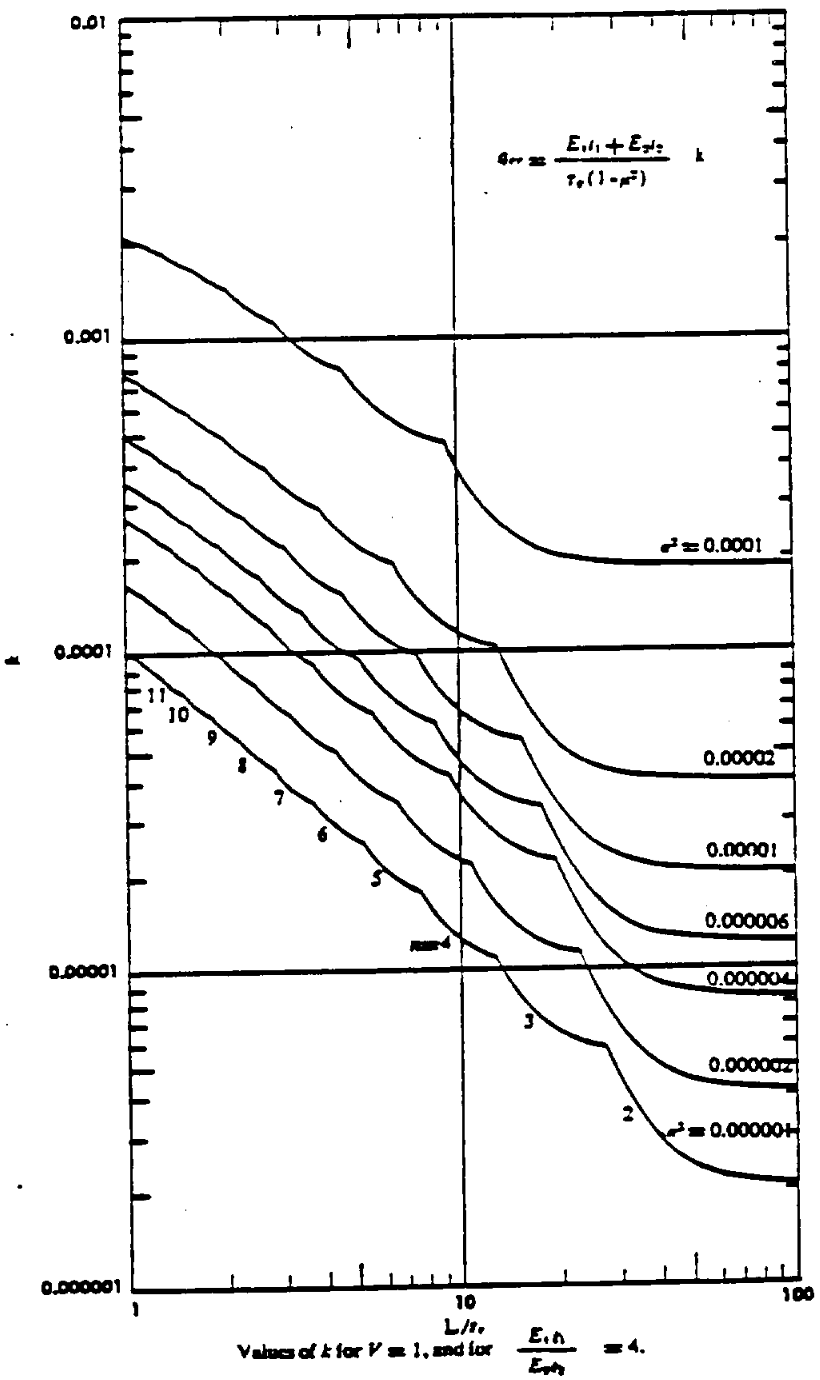

FIGURE 13.80 - BUCKLING COEFFICIENT FOR CYLINDERS UNDER UNIFORM EXTERNAL PRESSURE

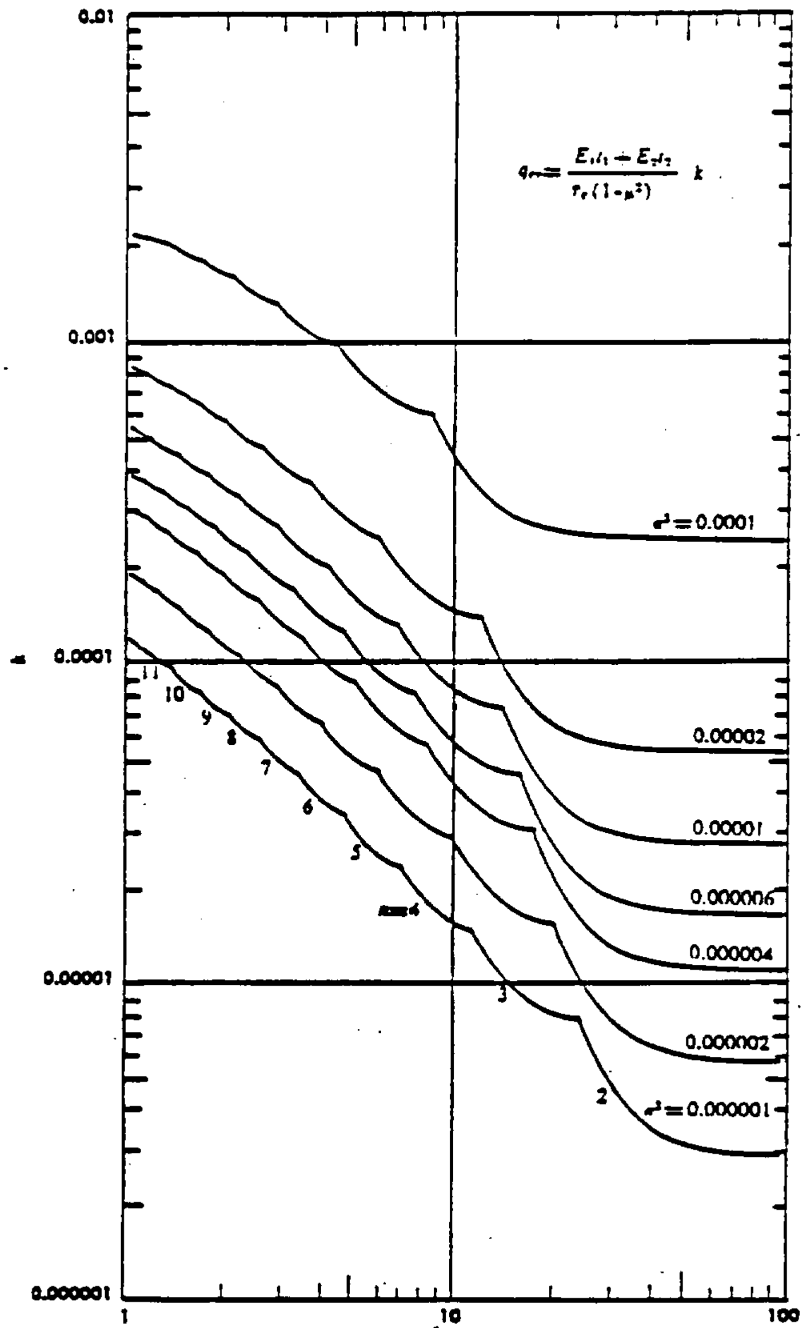

Values of k for $V = 1.5$, and for $\frac{E_1 t_1}{E_2 t_2} = 1$.

FIGURE 13.81 - BUCKLING COEFFICIENT FOR CYLINDERS UNDER UNIFORM EXTERNAL PRESSURE

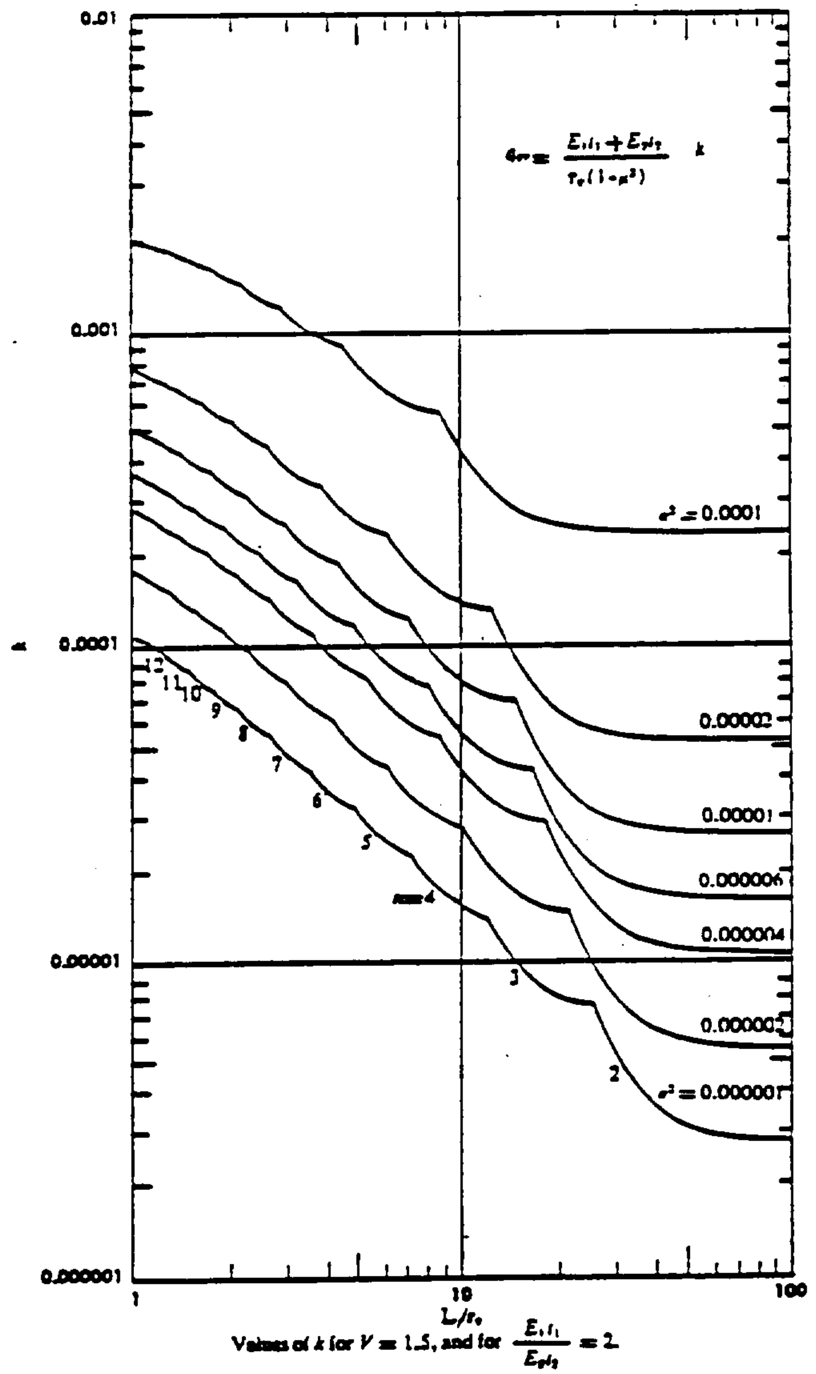

FIGURE 13.82 - BUCKLING COEFFICIENT FOR CYLINDERS UNDER UNIFORM EXTERNAL PRESSURE

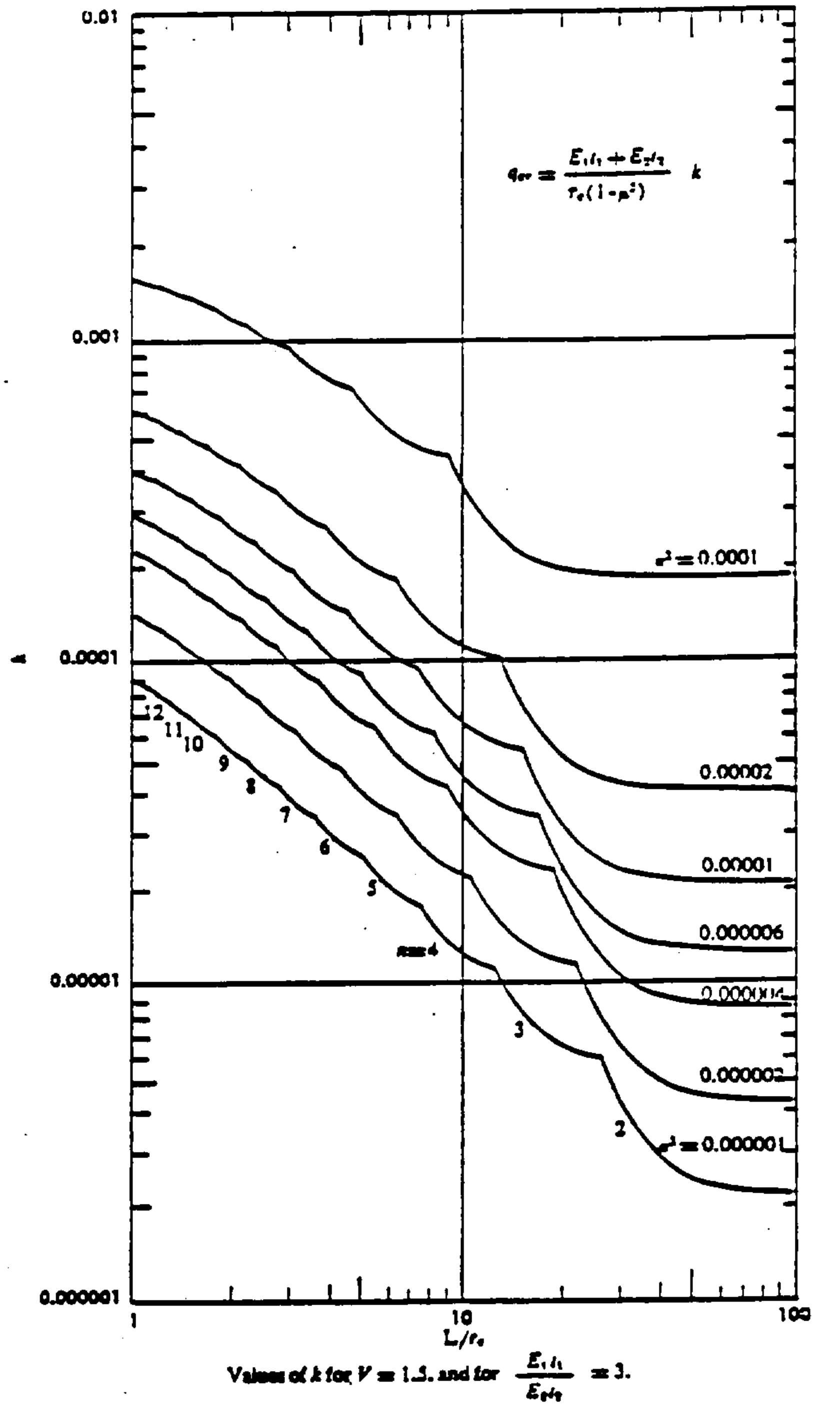

FIGURE 13.83 - BUCKLING COEFFICIENT FOR CYLINDERS UNDER UNIFORM EXTERNAL PRESSURE

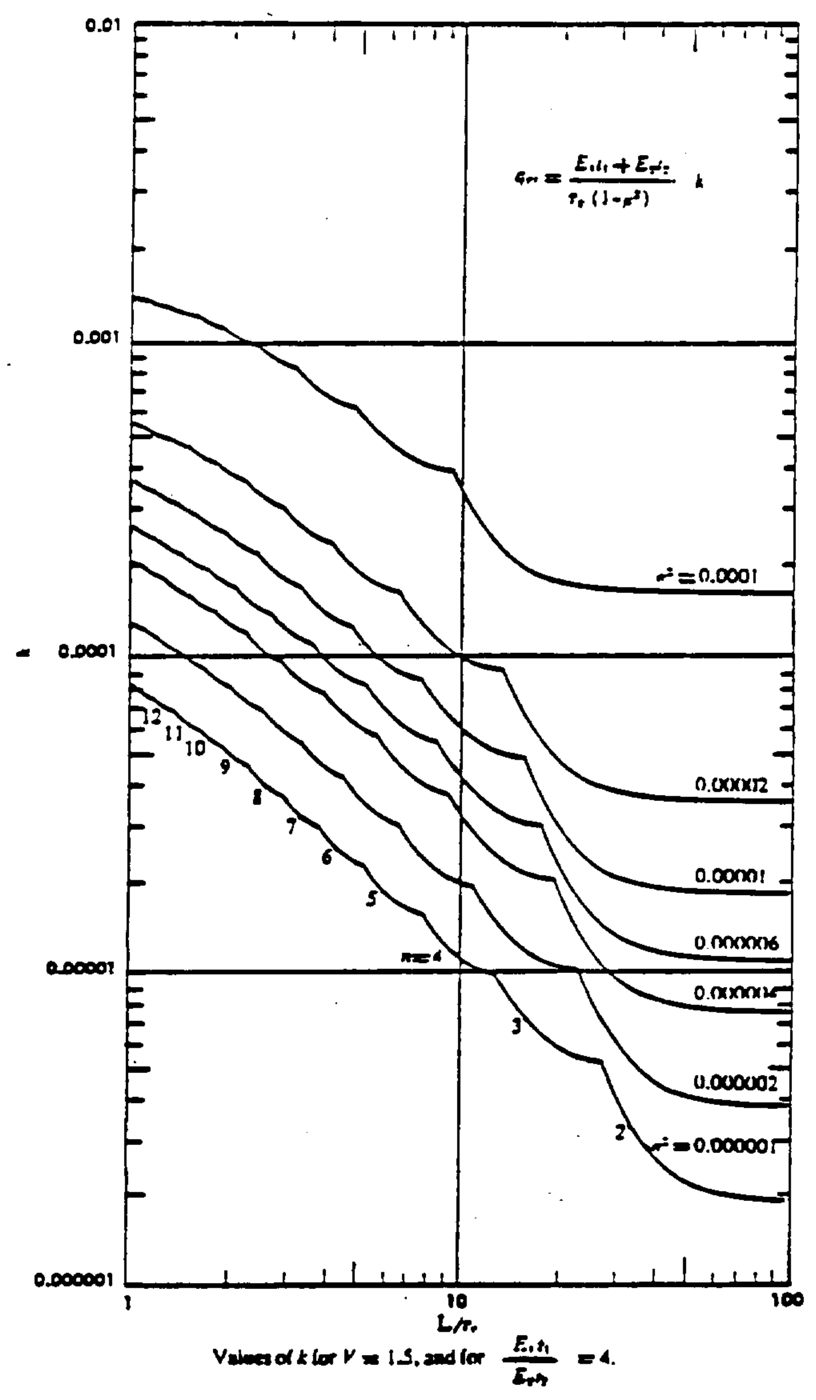

FIGURE 13.84 - BUCKLING COEFFICIENT FOR CYLINDERS UNDER UNIFORM EXTERNAL PRESSURE

TYPE OF LOADING AND END SUPPORTS	POINT OF DEFLECTION	M	V
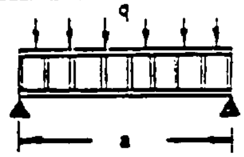 $\frac{P}{a} = q$ UNIFORM LOAD SIMPLY SUPPORTED	MIDSPAN	$\frac{Pa}{8}$	$\frac{P}{2}$
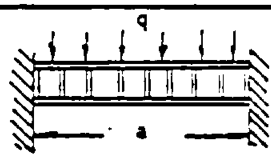 $\frac{P}{a} = q$ UNIFORM LOAD FIXED ENDS	MIDSPAN	$\frac{Pa}{12}$	$\frac{P}{2}$
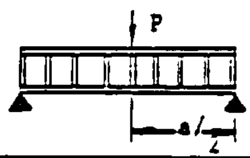 POINT LOAD AT MIDSPAN SIMPLY SUPPORTED	MIDSPAN	$\frac{Pa}{4}$	$\frac{P}{2}$
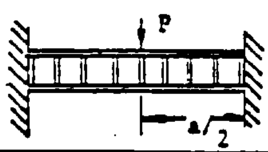 POINT LOAD AT MIDSPAN FIXED ENDS	MIDSPAN	$\frac{Pa}{8}$	$\frac{P}{2}$
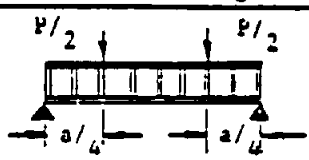 POINT LOADS AT QUARTER SPAN SIMPLY SUPPORTED	MIDSPAN	$\frac{Pa}{8}$	$\frac{P}{2}$
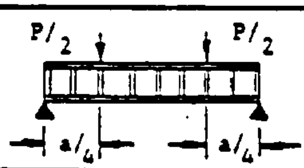 POINT LOADS AT QUARTER SPAN SIMPLY SUPPORTED	LOAD	$\frac{Pa}{8}$	$\frac{P}{2}$
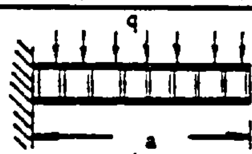 $P/_a = q$ UNIFORM AND CANTILEVER	FREE END	$\frac{Pa}{2}$	P
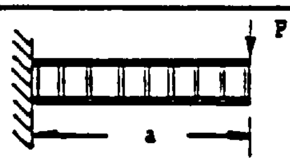 POINT LOAD AT FREE END CANTILEVER	FREE END	Pa	P

FIGURE 13.85(a)- BEAM MOMENTS

TYPE OF LOADING AND END SUPPORTS		POINT OF DEFLECTION	K_B	K_S
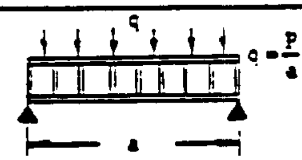	UNIFORM LOAD SIMPLY SUPPORTED	MIDSPAN	$\frac{5}{384}$	$\frac{1}{8}$
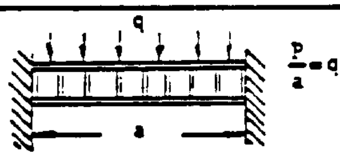	UNIFORM LOAD FIXED ENDS	MIDSPAN	$\frac{1}{384}$	$\frac{1}{8}$
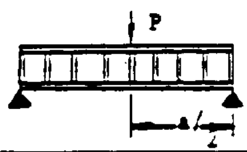	POINT LOAD AT MIDSPAN SIMPLY SUPPORTED	MIDSPAN	$\frac{1}{48}$	$\frac{1}{4}$
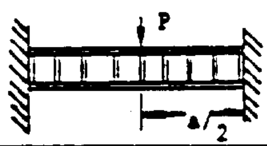	POINT LOAD AT MIDSPAN FIXED ENDS	MIDSPAN	$\frac{1}{192}$	$\frac{1}{4}$
	POINT LOADS AT QUARTER SPAN SIMPLY SUPPORTED	MIDSPAN	$\frac{11}{768}$	$\frac{1}{8}$
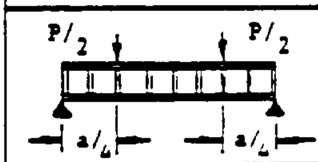	POINT LOADS AT QUARTER SPAN SIMPLY SUPPORTED	LOAD	$\frac{1}{96}$	$\frac{1}{8}$
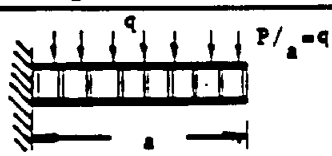	UNIFORM AND CANTILEVER	FREE END	$\frac{1}{8}$	$\frac{1}{2}$
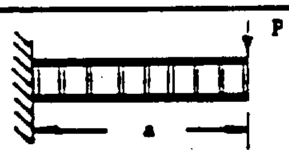	POINT LOAD AT FREE END CANTILEVER	FREE END	$\frac{1}{3}$	1

FIGURE 13.85(b) - DEFLECTION CONSTANTS

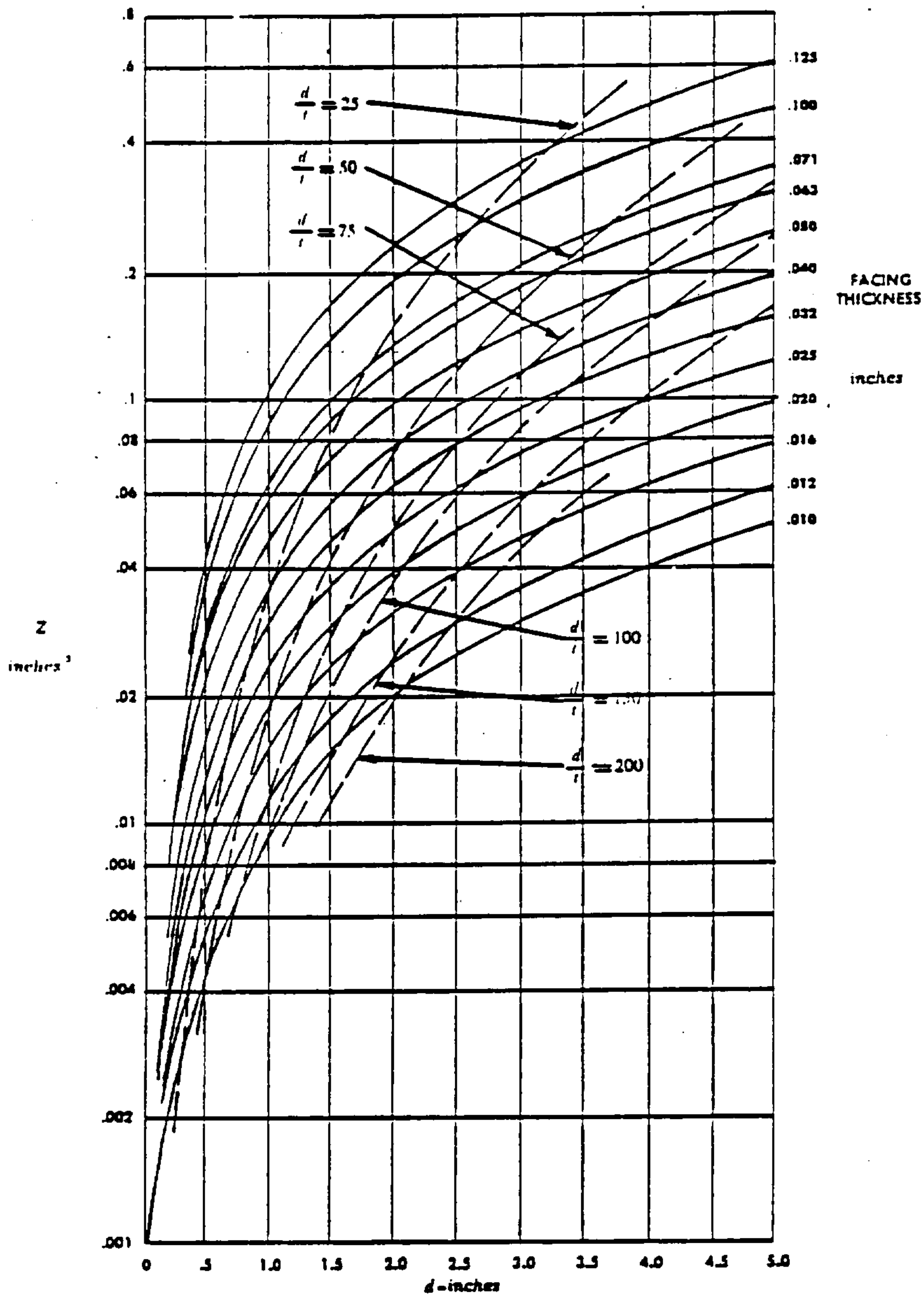

FIGURE 13.86 - DESIGN CHART FOR BEAMS WITH EQUAL THICKNESS FACES

(4) Calculate a starting value of d/t from the weight minimizing relation

$$d/t = 1 + 2\, w_f/w_c \qquad 13.99$$

where w_f and w_c are the densities of chosen facing and core materials respectively.

(5) From Figure 13.86 find the value of d associated with the value of Z determined in step (3), and move horizontally (Z = constant) to the nearest standard sheet gage. Read the corresponding panel thickness d.

(6) With the values of d and t thus determined, check the facing stress,

$$f_f = \frac{M}{bt(d-t)} \qquad 13.100$$

This value of f_f should equal F_f (step (2)).

(7) Determine core thickness

$$t_c = d - 2t \qquad 13.101$$

(8) Solve for core shear stress from

$$f_s = \frac{2S}{b(d + t_c)} \qquad 13.102$$

This value of f_s should not exceed the allowable shear strength of the chosen core.

(9) When stiffness is an important consideration, determine the two stiffness parameters, D and U

$$D = \frac{b E_f}{12\lambda}\left[d^3 - t_c^{\,3}\left(1 - \frac{E'_c}{E_f}\right)\right] \qquad 13.103$$

where E'_c = Elastic modulus of the core in the spanwise direction

E_f = Elastic modulus of face material

$\lambda = 1 - \mu^2$

μ = Poisson's ratio for face material

For beams with cellular cores, E'_c is often very low in comparison to E_f, and the ratio E'_c/E_f is then assumed to be equal zero.

Calculate shear stiffness

$$U = \frac{h^2 G_c b}{t_c} \qquad 13.102$$

where $h = d - t = t_c + t$

G_c = core modulus of ridigity

(10) Compute the deflection (δ) from

$$\delta = \frac{K_B P L^3}{D} + \frac{K_S P L}{U} \qquad 13.103$$

where P = applied load

L = length of beam

The coefficients K_B and K_S are given in Figure 13.85 for various beam loadings and end support conditions. If the computed value of δ is greater than that compatible with the design criteria or good design practices, the beam's stiffness may be increased by increasing core thickness, or by using a core with a higher modulus of rigidity, or both. Any of the above calculations affected by the change should be repeated.

(11) Determine the flexure induced core compressive stress

$$f_c = \frac{2 f_f^2}{E_f (d/t - 1)} \qquad 13.104$$

(12) The core should also be analyzed for local crushing due to concentrated loadings, either applied or at reaction points.

13.3 Attachment Details

All sandwich parts must be attached to the framework of the airframe and often to other similar parts; therefore, means for transferring the concentrated loads imposed at these attachments must be provided. Occasionally, on very lightly loaded parts, unreinforced bolt holes or subsequently inserted reinforcements will suffice, but in most structural applications, local reinforcements must be incorporated during fabrication.

13.3.1 Edge Design

Sandwich parts are normally joined over a framing member. The edge configuration is often dictated by the loads to be transferred, core, smoothness requirement, fasteners, facings, panel usage, etc. Figure 13.87 shows some commonly used edge configurations. Care should be used in selecting the edge design. If the methods of Section 13.2 are used in the design of the panel, both faces are capable of reacting load. Then, in order to fully utilize the sandwich concept, the edges must be designed to be compatible.

Some of the edge configurations have beveled edges, such as a 45° chamfer with fiberglass closure. This is a commonly used configuration at Bell. The load that is introduced into the inner face at the edges is only what can be transferred through the fiberglass edging or shear lagged through the core.

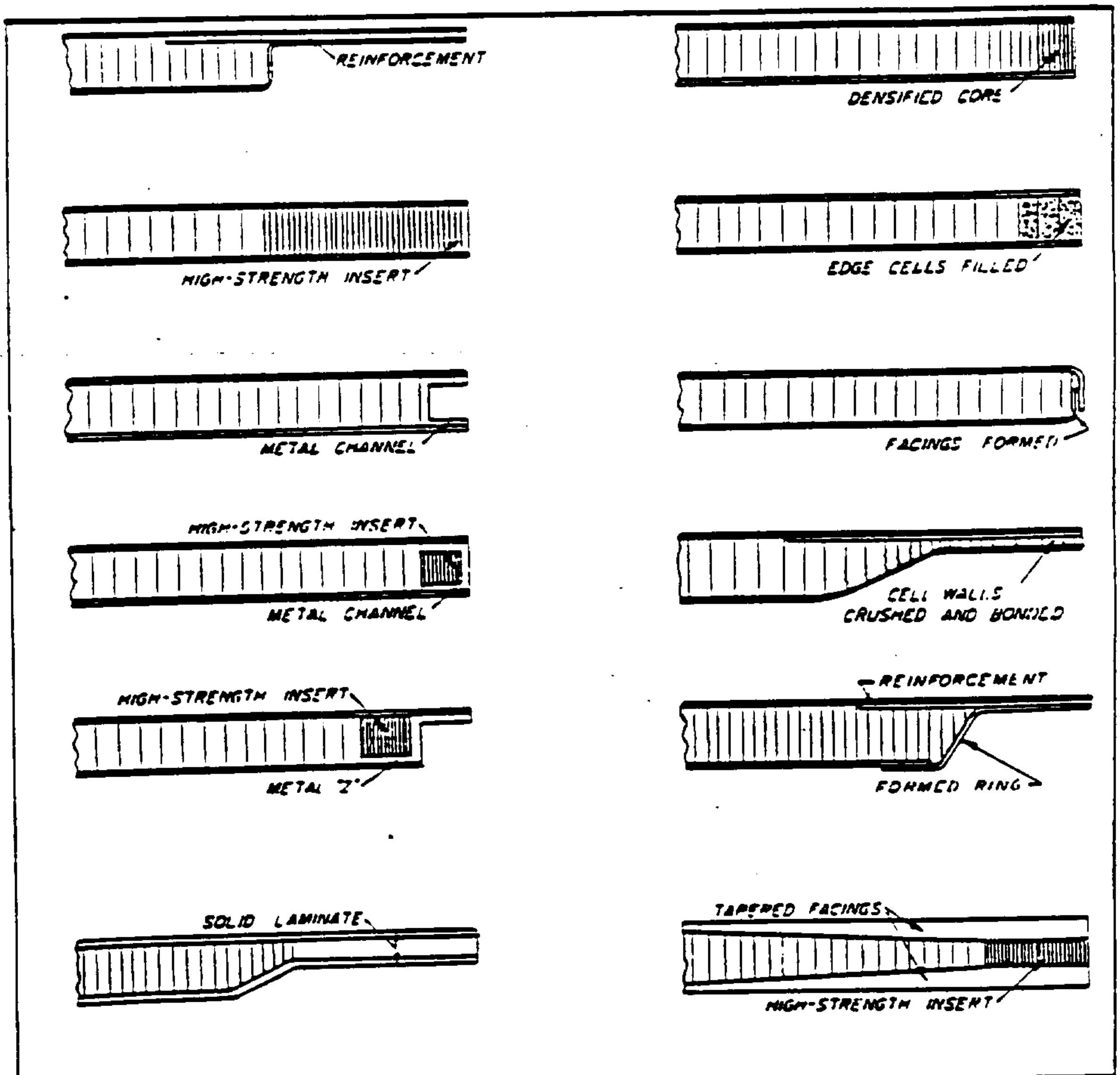

FIGURE 13.87 - SOME TYPICAL EDGE DESIGNS

Regardless of the type of configuration, the edge design should be such as to keep moisture out of the core. This can be accomplished by the use of potting compounds or fiberglass closures.

The facings which have been sized for the type of failure modes discussed in Section 13.2 will not necessarily be thick enough to develop the fasteners. An edge reinforcement must be installed with a thickness sufficient to develop the fasteners. The reinforcement is a doubler, either internally or externally. In some cases, it can be chem-etched integral with one of the faces.

When the loads on a sandwich panel are normal to the panel, the edging doubler may have to react these loads. In this case, it must be thick enough and wide enough to develop the bending moment in the edge.

13.3.2 Doublers and Inserts

The design of a sandwich structure may be such that loads must be transferred to or from individual parts at points other than at their edges. Inserts in the part are required at these attachment points if the loads are of appreciable magnitude. Typical methods of introducing high loads into a sandwich panel are shown in Figure 13.88. These may be in the form of strips (metal, wood, foam), inserted continuously across the panel or as local reinforcements under individual bolt patterns. Shear loads on attachment bolts may require additional reinforcement to provide adequate attachment bearing area. This can be in the form of a doubler which can be installed internally or externally.

One method of densification (increasing the density of the core so that concentrated loads can be introduced) is to cut out an area of the core and insert a piece of denser core. Another method of densification is to compress the core in a local area so that the cell size is smaller than the main body of the core.

13.3.3 Attachment Fittings

Accessories, such as shelves, fittings, mounting brackets, are often fastened to the sandwich panels. Figure 13.89 shows some examples of how fittings can be attached to sandwich panels.

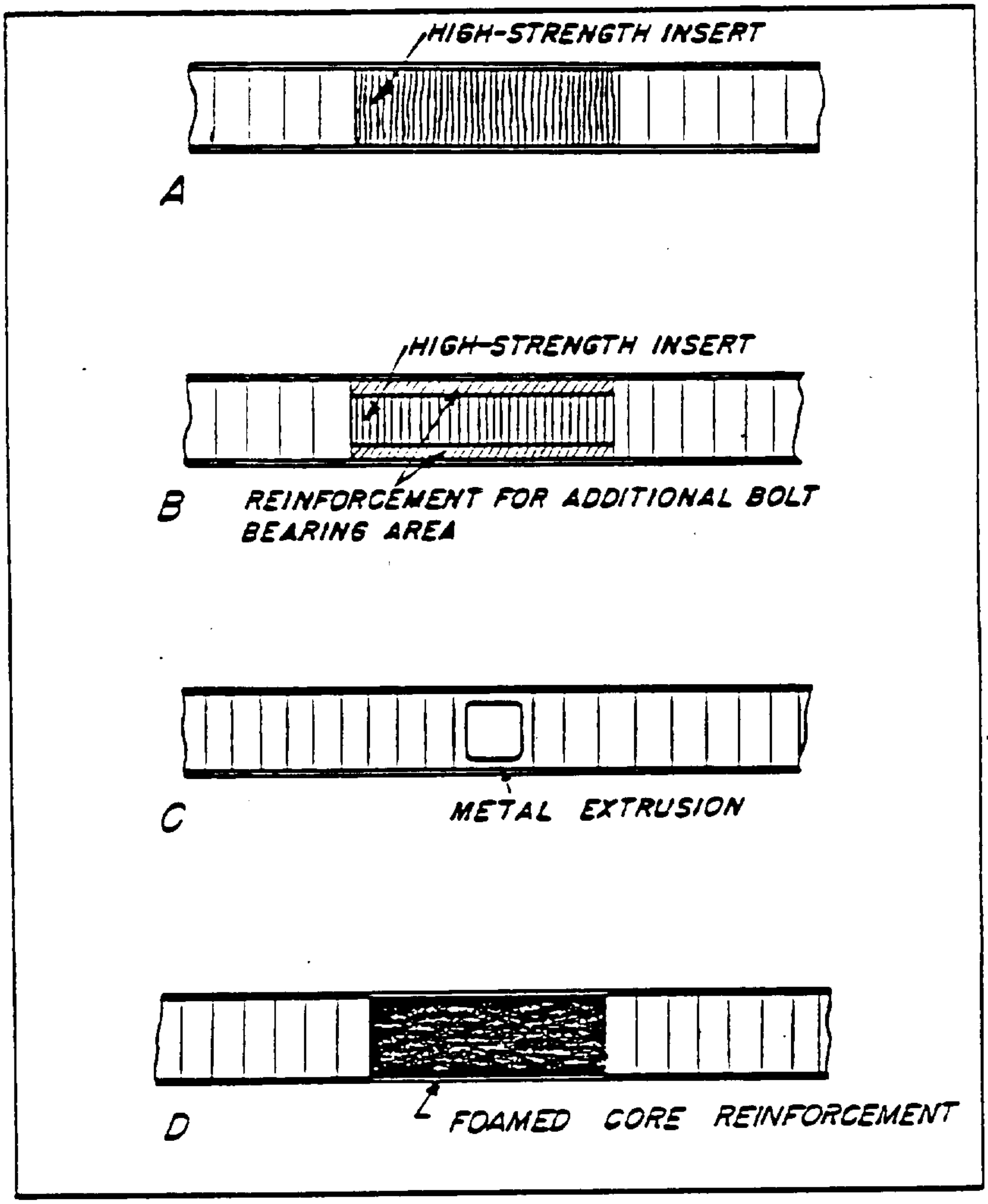

FIGURE 13.88 - SOME TYPICAL HIGH-STRENGTH INSERT DESIGNS

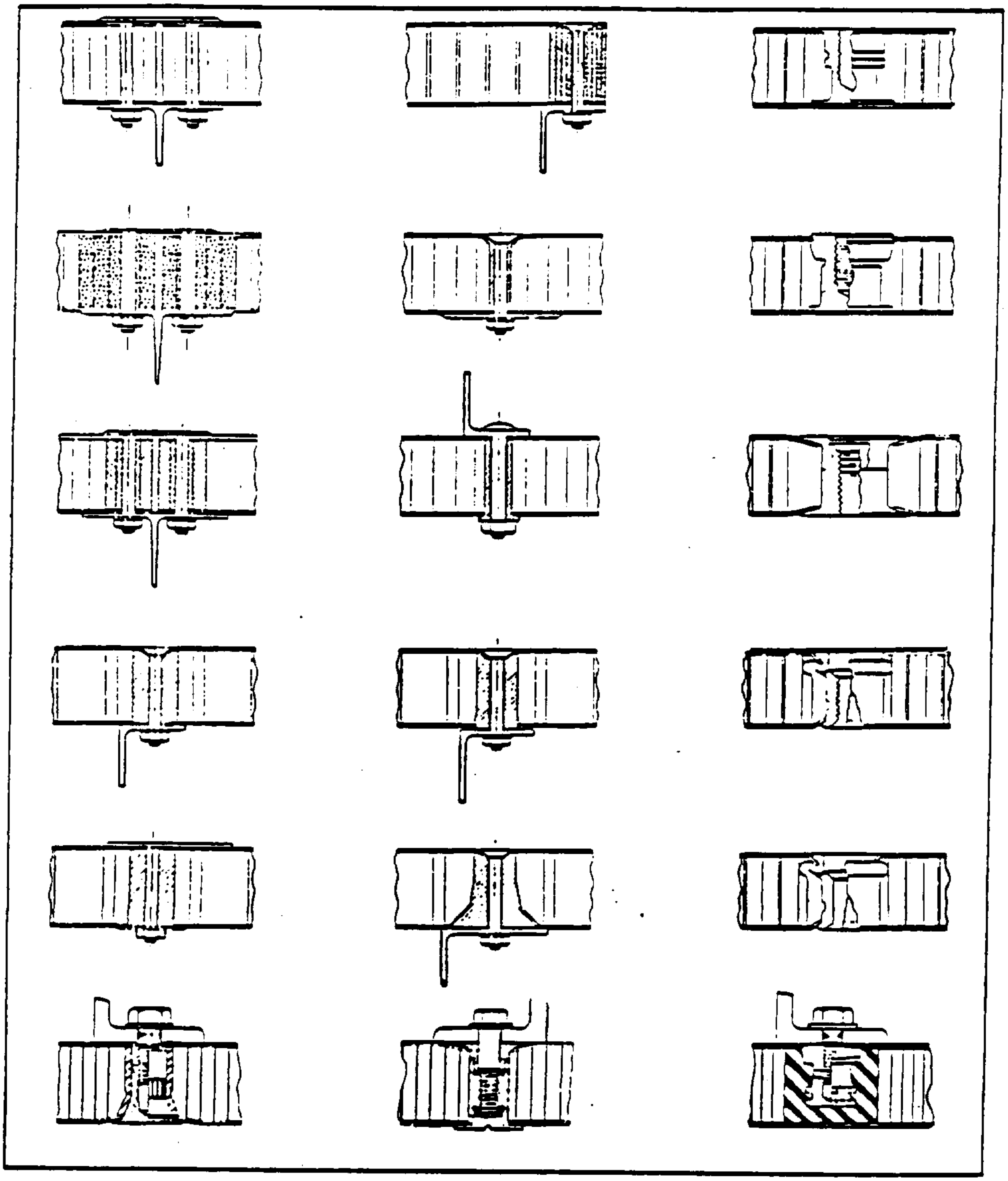

FIGURE 13.89 - SOME TYPICAL ATTACHMENT FITTINGS

SECTION 8.14

SANDWICH CONSTRUCTION-ANALYSIS METHODS

REFERENCES:

NASA CR - 1457 "MANUAL FOR STRUCTURAL STABILITY ANALYSIS OF SANDWICH PLATES AND SHELLS " BY R. T. SULLINS, G . W SMITH, E . E. SPIER. DEC. 1969.

TBS 123 " DESIGN HANDBOOK FOR HONEYCOMB SANDWICH STRUCTURES " HEXEL OCTOBER 1967

ANC - 23 " SANDWICH CONSTRUCTION FOR AIRCRAFT "

CASD - SS0-76-016 " HONEYCOMB SANDWICH PANEL ANALYSIS METHOD. SPACE SHUTTLE ORBITER MID-FUSELAGE " W. S. BUSSEY JR. 22 JULY 1976 (SYNOPSIS INCLUDED IN THIS SECTION OF THE MANUAL).

SYNOPSIS

ANALYSIS OF STRUCTURAL HONEYCOMB SANDWICH PANELS

The structural sandwich is analagous to an I-beam with the sandwich facings and core corresponding to the I-beam flanges and web, respectively. The facings carry axial compression and tension loads, and the core carries transverse shear loads.

Low density cellular (honeycomb) core material is often used in order to achieve light weight designs. As a consequence of employing a light weight core, the design or analysis criteria must allow for the core shearing deformations which result from the low effective core shear modulus. The main difference in the analysis of sandwich structure as compared to analysis of homogenous sheet structure is the inclusion of the effects of core shear deformation on panel strength and deflections.

A thin sandwich facing subjected to edge compression behaves similarly to a column supported on an elastic foundation. Thus, the buckling or wrinkling load depends upon the elasticity and strength of the core. In the design of a sandwich panel, the four conditions summarized below must be satisfied.

1) The sandwich facings must be thick enough to withstand the stresses which result from the design loads.

2) The core must have sufficient thickness, shear rigidity and strength so that general buckling, excessive deflection, or shear failure will not occur under the design loads.

3) The core must have a sufficiently high flatwise modulus of elasticity, flatwise tensile and compressive strength so that wrinkling of either facing will not occur under the design loads.

4) The cell size of a cellular (honeycomb) core must be small enough so that dimpling of either facing into the core cells will not occur under the design loads.

In designing to meet the above conditions, it is assumed that the bond between the facings and core is strong enough to prevent the following under design loads.

1) Face wrinkling caused by either facing pulling loose from the core.

2) Excessive deflection or shear failure at the joint between the facing and core.

Data Source, Section 1.3 Reference 34

SECTION 9.0

PRESSURE VESSELS AND PIPES

DATA SOURCES FOR ANALYSIS OF PRESSURE VESSELS AND PIPES ARE GIVEN, TOGETHER WITH TANK GEOMETRY.

		PAGE
9.1	STRESSES AND DEFLECTIONS	9.1.1
9.2	TANK GEOMETRY	9.2.1
9.3	PIPING SYSTEMS (ELBOWS, BELLOWS, DUCTS)	9.3.1
9.4	DISCONTINUITY ANALYSIS OF SHELLS	9.4.1

SECTION 9.1

STRESSES AND DEFORMATIONS

THESE DATA ARE AVAILABLE IN " FORMULAS FOR STRESS AND STRAIN " R. J. ROARK.

3RD EDITION, SEE CHAPTER 12.

E. F. BRUHN, J. I. ORLANDO, J. F. MEYERS " ANALYSIS AND DESIGN OF MISSILE STRUCTURE " TRI-STATE OFFSET COMPANY, CINICINNATI, OHIO.

SHELL STRESSES

Data Source, Section 1.3 Reference 35

Figure E1.8.2 - Thin Circular Cylinder Under Internal Pressure

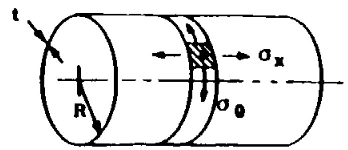

$$\sigma_\theta = +\frac{pR}{t}$$

$$\sigma_x = +\frac{pR}{2t}$$

$$w_R = -\frac{pR^2}{Et}\left(1 - \frac{\nu}{2}\right)$$

Figure E1.8.6 - Thin Conical Shell Under Internal Pressure

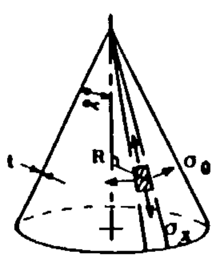

$$\sigma_\theta = +\frac{pR}{t\,\mathrm{Cos}\,\alpha}$$

$$\sigma_x = +\frac{pR}{2t\,\mathrm{Cos}\,\alpha}$$

$$w_R = -\frac{R}{E}(\sigma_\theta - \nu\sigma_x)$$

Increase of α due to p

$$\Delta\alpha = +\frac{2pR\left(1 - \frac{\nu}{2}\right)}{Et}\,\mathrm{Sin}\,\alpha$$

Figure E1.8.3 - Thin Spherical Shell Under Internal Pressure

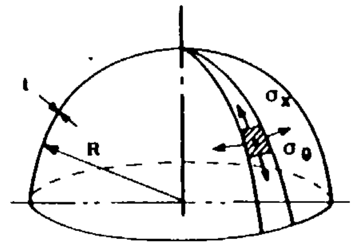

$$\sigma_\theta = \sigma_x = +\frac{pR}{2t}$$

$$w_R = -\frac{pR^2}{2Et}(1 - \nu)$$

Figure E1.8.5 - Any Thin Figure of Revolution Under Internal Pressure

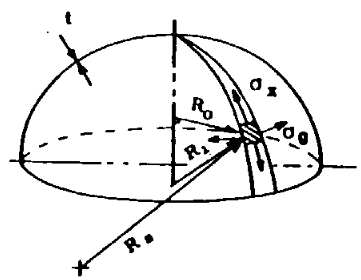

$$\sigma_x = +\frac{pR_1}{2t}$$

$$\sigma_\theta = +\frac{pR_1}{t}\left(1 - \frac{R_1}{2R_2}\right)$$

$$w_R = -\frac{R_0}{E}(\sigma_\theta - \nu\sigma_x)$$

Figure E1.8.4 - Thin Ellipsoidal Shell Under Internal Pressure

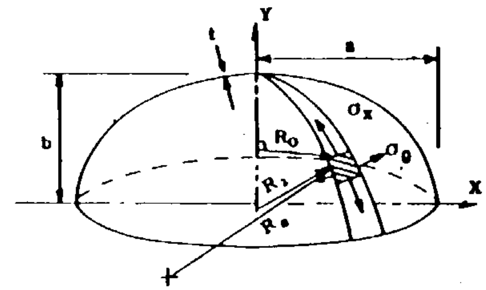

For spheroids defined by ellipse $\frac{x^2}{a^2} + \frac{y^2}{b^2} = 1$

$$R_1 = \frac{\left[a^4Y^2 + b^4X^2\right]^{\frac{1}{2}}}{b^2}$$

$$R_2 = R_1^3\frac{b^2}{a^4}$$

$$\sigma_x = +\frac{pR_1}{2t}$$

$$\sigma_\theta = +\frac{pR_1}{t}\left(1 - \frac{R_1}{2R_2}\right)$$

$$w_R = -\frac{R_0}{E}(\sigma_\theta - \nu\sigma_x)$$

At the equator

$$R_1 = a$$

$$R_2 = \frac{b^2}{a}$$

$$\sigma_x = \frac{pa}{2t}$$

$$\sigma_\theta = +\frac{pa}{t}\left(1 - \frac{a^2}{2b^2}\right)$$

$$w_R = -\frac{pa^2}{2Et}\left[2 - \nu - \frac{a^2}{b^2}\right]$$

At the apex

$$R_1 = R_2 = \frac{a^2}{b}$$

$$\sigma_\theta = \sigma_x = +\frac{pa^2}{2bt}$$

$$w_R = 0$$

SECTION 9.2

TANK GEOMETRY

VOLUME AND SURFACE AREA EQUATIONS FOR VARIOUS TANK GEOMETRIES ARE SHOWN ON THE PAGES FOLLOWING.

E-70

TANK GEOMETRY Data Source, Section 1.3 Reference 14

V_T IS TOTAL VOLUME
S_T IS TOTAL SURFACE AREA

CONE FRUSTUM TANK

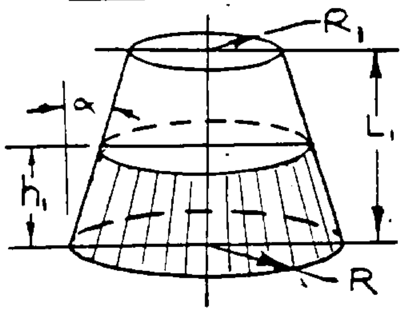

(1) $$V_T = \frac{\pi}{3\,\mathrm{TAN}\,\alpha}\left(R^3 - R_1^3\right)$$

(2) $$S_T = \frac{\pi L_1 (R_1 + R)}{\mathrm{COS}\,\alpha} = \pi (R + R_1)\sqrt{L_1^2 + (R - R_1)^2}$$ *

(3) $$V_{(\mathrm{OF}\ h_1)} = \pi h_1 \left(R^2 - R h_1 \,\mathrm{TAN}\,\alpha + \tfrac{1}{3} h_1^2 \,\mathrm{TAN}^2 \alpha\right)$$

CYLINDRICAL TANK (CLASSIC FORMULAS)

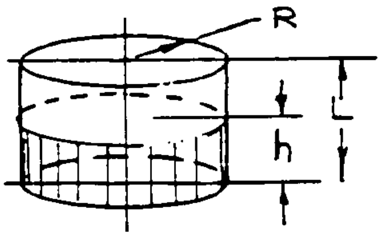

(4) $$V_T = \pi R^2 L$$

(5) $$V_{(\mathrm{OF}\ h)} = \pi R^2 h$$

(6) $$S_T = 2\pi R L$$ *

OGIVE TANK (CIRCULAR)

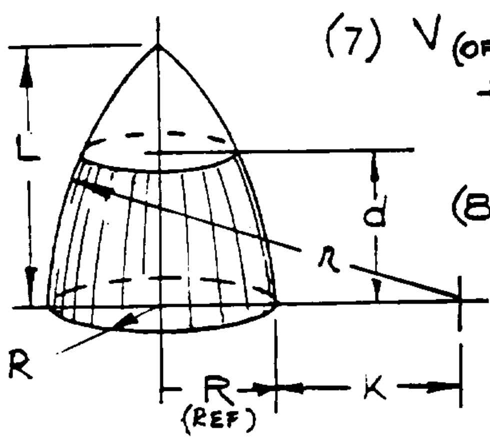

(7) $$V_{(\mathrm{OF}\ d)} = \pi\left[k^2 d - k\left\{d\sqrt{r^2 - d^2} + r^2 \,\mathrm{SIN}^{-1}\left(\frac{d}{r}\right)\right\} + r^2 d - \tfrac{1}{3} d^3\right]$$

(8) $$S_{(\mathrm{OF}\ d)} = 2\pi r\left[d - k\,\mathrm{SIN}^{-1}\left(\frac{d}{r}\right)\right]$$ *

*NOTE - TANK ENDS ARE NOT INCLUDED IN SURF. AREAS.

SPHERICAL BULKHEAD

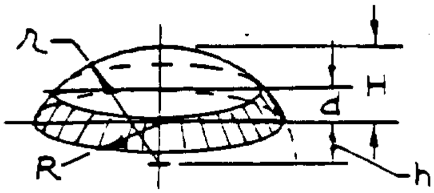

(9) $V_T = \frac{1}{3}\pi H^2 (3\lambda - H)$

(10) $= \frac{1}{6}\pi H (H^2 + 3R^2)$

(11) $\lambda = \frac{H}{2} + \frac{R^2}{2H}$

(12) $S_T = 2\pi\lambda H$ *

(13) $V_{(\text{OF } d)} = \pi d \left[(\lambda^2 - h^2) - d\left(\frac{1}{3}d + h\right) \right]$

$h = \lambda - H$ OR $h = \sqrt{\lambda^2 - R^2}$

ELLIPTICAL BULKHEAD
(IN CYLINDRICAL TANK)

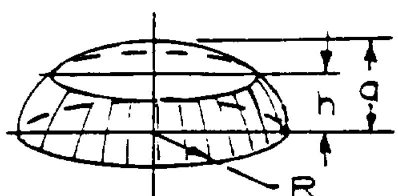

(14) $V_T = \frac{2}{3}\pi R^2 a$

(15) $V_{(\text{OF } h)} = \pi h \left(\frac{R}{a}\right)^2 \left(a^2 - \frac{1}{3}h^2\right)$ *

(16) $S_T = \pi \left\{ a\sqrt{C_1 a^2 + R^2} + \frac{R^2}{\sqrt{C_1}} \left[\text{LOG}\left(a\sqrt{C_1} + \sqrt{C_1 a^2 + R^2}\right) - \text{LOG } R \right] \right\}$

$C_1 = K_1^4 - K_1^2$ WHERE $K_1 = R/a$
LOG IS OF BASE "e"

(17) RADIUS OF CURVATURE (ρ) DIST. X ABOVE BASE PLANE

$$\rho = \frac{\left[R^2 + K_1^2 X^2 (K_1^2 - 1)\right]^{3/2}}{K_1^2 R^2}$$

* NOTE - BULK'D BASE IS NOT INCLUDED IN SURF. AREA

ELLIPTICAL BULKHEAD (IN CONE FRUSTUM TANK)

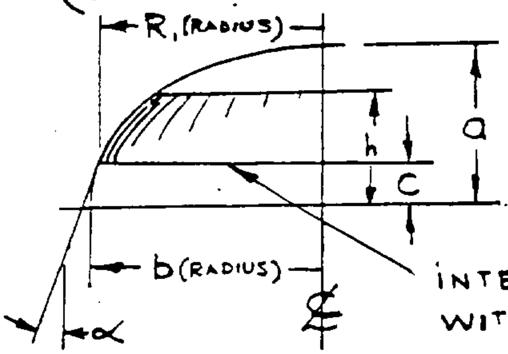

$$C = \frac{R_1 \, TAN \, \alpha}{K_2^2}, \quad K_2 = \frac{b}{a}$$

$$= \frac{a^2 \, TAN \, \alpha}{\sqrt{b^2 + a^2 \, TAN^2 \alpha}}$$

$$R_1 = \frac{b}{a}\sqrt{a^2 - c^2}$$

INTERSECTION LINE OF BULKHEAD WITH TANK (BASE)

α = ANGLE OF CONE FRUSTUM TANK

(18) V_T (TOTAL VOL. OF BULK'D FROM BASE [TANKS INTERSECTION] TO APEX)

$$= \pi\left(\frac{b}{a}\right)^2\left[a^2(a-c) + \frac{1}{3}(c^3 - a^3)\right]$$

(19) V (VOLUME FROM BASE TO h)

$$= \pi\left(\frac{b}{a}\right)^2\left[a^2(h-c) + \frac{1}{3}(c^3 - h^3)\right]$$

(20) S (SURFACE AREA OF BULK'D FROM BASE [TANKS INTERSECTION] TO APEX)

$$S = \pi\left[a\sqrt{C_1 a^2 + b^2} + \frac{b^2}{\sqrt{C_2}} \, LOG\left(a\sqrt{C_2} + \sqrt{C_2 a^2 + b^2}\right) - c\sqrt{C_1 c^2 + b^2} - \frac{b^2}{\sqrt{C_2}} \, LOG\left(c\sqrt{C_2} + \sqrt{C_2 c^2 + b^2}\right)\right]$$

a = BULK'D MINOR SEMI AXIS (HEIGHT)
b = " MAJOR " "
c = DIST. BETWEEN MAJOR AXIS AND BULK'D INTERSECTION WITH TANK $= R_1 \, TAN \, \alpha / K_2^2$
$C_1 = K_2^4 - K_2^2$ WHERE $K_2 = b/a$
LOG IS BASE "e"

TANK GEOMETRY

TORICONICAL BULKHEAD

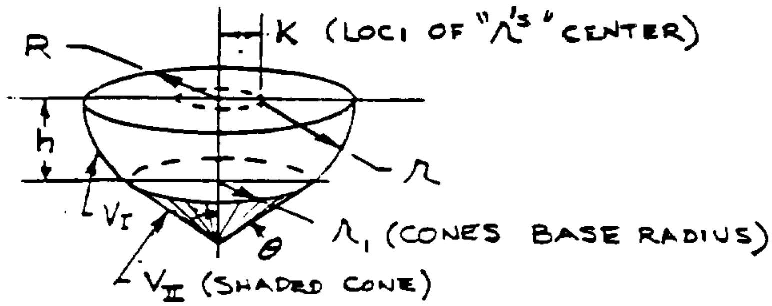

(21) $V_T = V_I + V_{II}$

$$V_I = \pi\left\{h(r^2+K^2)+K\left[h\sqrt{r^2-h^2} + r^2 \sin^{-1}\left(\frac{h}{r}\right)\right]-\frac{h^3}{3}\right\}$$

$$V_{II} = \tfrac{1}{3}\pi r_1^3 \cot\theta$$

(22) $S = S_I + S_{II}$

$$S_I = 2\pi r\left[K \sin^{-1}\left(\frac{h}{r}\right) + h\right]$$

$$S_{II} = \frac{\pi r_1^2}{\sin\theta} \qquad \text{(CONE)}$$

PARABOLIC BULKHEAD

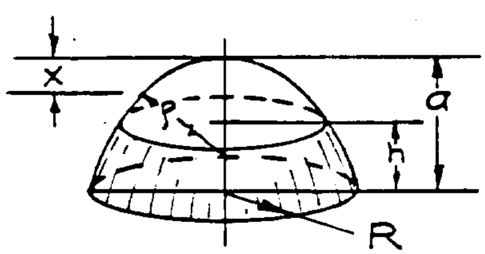

(23) $V_T = \frac{1}{2}\pi R^2 a$

(24) $V_{(\text{of } h)} = \frac{1}{2}\pi R^2 h\left[2 - \frac{h}{a}\right]$

(25) $S_1 = \frac{1}{6}\pi R a\left[\left(4+\frac{R^2}{a^2}\right)^{3/2} - \left(\frac{R}{a}\right)^3\right]$

(27) RADIUS OF CURVATURE (ρ)

$$\rho = \frac{1}{2Ra}\left(4aX + R^2\right)^{3/2}$$

X = VERTICAL DIST FROM VERTEX TO WHERE ρ IS DESIRED (ON THE SURFACE)

TORUS TANK

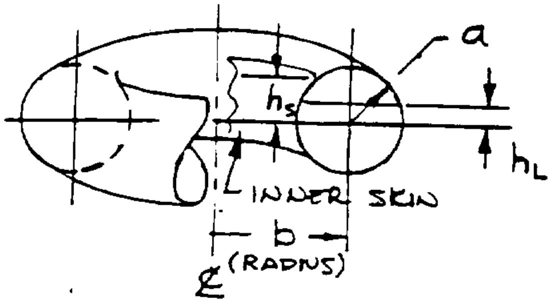

(28) $V_T = 2\pi^2 b a^2 = 19.739\, b a^2$

(29) PARTIALLY FILLED TORUS TO h_L (NOTE h_L MAY BE + OR −) VOL OF LIQUID =

$$V_L = 2\pi a^2 b \left\{ K\sqrt{1-K^2} + \sin^{-1} K + \frac{\pi}{2} \right\}$$

$$K = h_L/a$$

(30) $S_T = 4\pi^2 a b$

(31) OUTER SKIN SURFACE AREA OF $2h_s$ TOTAL WIDTH AND SYMMETRICAL ABOUT THE HORIZONTAL CENTERLINE

$$S_o = 4\pi a \left[b \sin^{-1}\left(\frac{h_s}{a}\right) + h_s \right]$$

(32) INNER SKIN ($2h_s$ WIDE)

$$S_i = 4\pi a \left[b \sin^{-1}\left(\frac{h_s}{a}\right) - h_s \right]$$

SECTION 9.3

PIPING SYSTEMS

ANALYTICAL METHODS FOR ANALYSIS OF PIPING SYSTEMS, INCLUDING ELBOWS, BELLOWS AND DUCTS, ARE PRESENTED IN THIS SECTION.

Data Source, Section 1.3 Reference 4

PIPING SYSTEMS

24.1 INTRODUCTION

Aircraft pressurized systems utilize tubing or ducting to convey fluids or gases. Tubing is thin walled conduit of circular cross-section with outside diameter to wall thickness ratio, $10<D/t<100$. All types of tubing commonly used are relatively malleable and can be bent resulting in a reduced number of joints. Thin walled metal tubing is used extensively in the design of high pressure systems due to its high efficiency in resisting internal pressure loading. Ducting is thin walled conduit of large cross-section, usually circular or rectangular, which is generally used to convey large volume, low pressure fluids or gases.

The classification, piping, although usually associated with large diameter, thick walled conduit is used frequently in this section when referring to thin walled tubular systems. This results from the fact that many of the analysis methods applied to aircraft pressurized systems were developed for complex industrial and marine piping systems.

Examples of aircraft pressurized systems are:

1. Hydraulic system
2. Fuel system
3. Oxygen system
4. Water system
5. Pneumatic system (includes de-icing and airconditioning systems)

The deflection and stress modification factors developed for piping analysis are based on theoretical studies modified empirically by factors determined by test results.

24.2 MATERIALS

Ducting and tubing for aircraft pressurized systems utilize a variety of materials dependent on operational requirements. Material selection is usually governed by two basic considerations of operation which are:

1. System pressure
2. System temperature

Some typical material selections based on operational requirements are shown below:

Application	High Pressure Lines	Low Pressure Lines	High Temp Lines
Material Classification	Corrosion Resistant Steel Titanium	Aluminum Plastics	Nickel Based Alloy
Typical Material	21Cr-6Ni-9Mn 3Al-2.5V	6061-T6 Nylon	Inconel

24.3 PIPING SYSTEM ANALYSIS

Due to the similarity between piping systems and rigid framed structures many of the methods developed for the analysis of framed structures can be applied to piping systems providing the increased flexibility and stresses at the bends are taken into account.

24.3.1 DESIGN CONDITIONS

The pressure lines of aircraft piping systems are subjected to translational and/or rotational displacements due to externally applied forces such as flight induced inertia loads. Stresses generated in the lines due to these external forces must be combined with those resulting from the critical pressure and temperature environment for the system. All systems when fully pressurized must sustain the application of total flight load factors due to maneuvers and gusts.

24.3.2 DESIGN PRESSURES

The design of a pressurized system is based on three pressure conditions:

1. Operating pressure
2. Proof Pressure
3. Burst pressure

The operating pressure is the nominal system pressure with transients such as surge usually limited to a given percentage over nominal. Proof pressure is the operating pressure or in some cases the relief valve setting pressure multiplied by a proof factor. At proof pressure no yielding or permanent deformation is permissible. Burst pressure is an ultimate pressure condition obtained by multiplying the operating pressure by an ultimate factor. No failure shall occur at this pressure.

A burst pressure test is required to qualify a component. A proof pressure test is applied to each component produced to ensure it satisfies strength requirements at that pressure. Functional test pressures are generally lower than component proof pressures and are usually applied to the entire system. Burst, proof and functional pressures are defined in the criteria for the system.

577

24.3.3 DETERMINATION OF PRESSURE STRESSES AND WALL THICKNESS

The stresses due to internal pressure and the determination of the wall thickness are obtained as follows:

For D/t < 100

Based on elastic theory the maximum circumferential tension stress at the inner surface is given by:

$$f_H = p\left(\frac{D^2 + d^2}{D^2 - d^2}\right)$$

where:

p = internal pressure (psi)

D = outside dia (in)

d = inside dia (in)

The associated longitudinal stress is obtained from:

$$f_L = p\left(\frac{d^2}{D^2 - d^2}\right)$$

Required minimum wall thickness is derived by setting $f_H = F_{tu}$ and p = burst pressure, p_b.

$$t_{min} = \frac{D}{2}\left(1 - \sqrt{\frac{F_{tu} - P_b}{F_{tu} + P_b}}\right)$$

For D/t ≥ 100

The circumferential tension stress is assumed to be uniform and given by the expression:

$$f_H = \frac{pD}{2t}$$

The associated longitudinal stress is obtained from:

$$f_L = \frac{pD}{4t}$$

Required minimum wall thickness is based on the circumferential tension stress with $f_H = F_{tu}$ and $p = p_b$.

$$t_{min} = \frac{p_b D}{2F_{tu}}$$

24.3.4 CURVED TUBES UNDER EXTERNAL MOMENTS

A curved tube subjected to bending (See Figures 24.3.4-1) is more flexible and has higher stresses than indicated by the elementary theory of bending. This results from ovalization of the tube cross-section during bending modifying the stress distribution as shown in Figure 24.3.4-2. The increase in flexibility and stress is accounted for by the use of flexibility and stress intensification factors as shown in Sections 24.3.4.1 and 24.3.4.2 respectively.

Notation for Curved Tubes Under External Moments

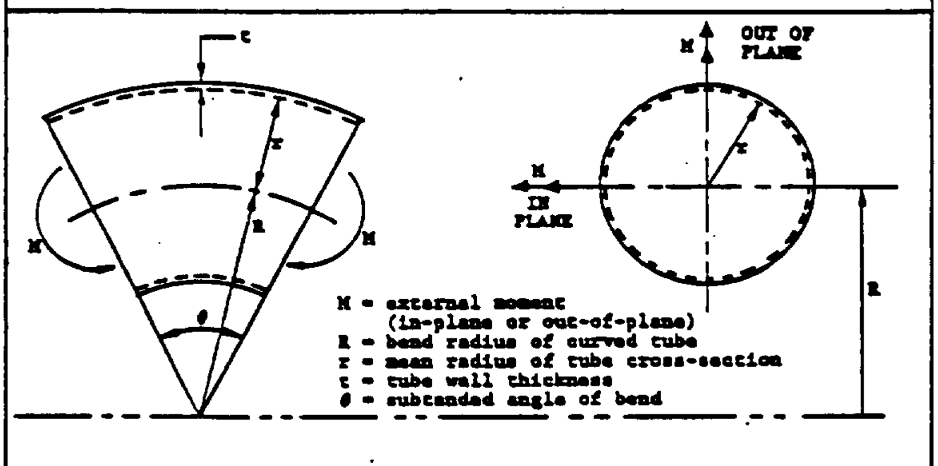

Figure 24.3.4-1

578

24.3.4 CURVED TUBES UNDER EXTERNAL MOMENTS (Continued)

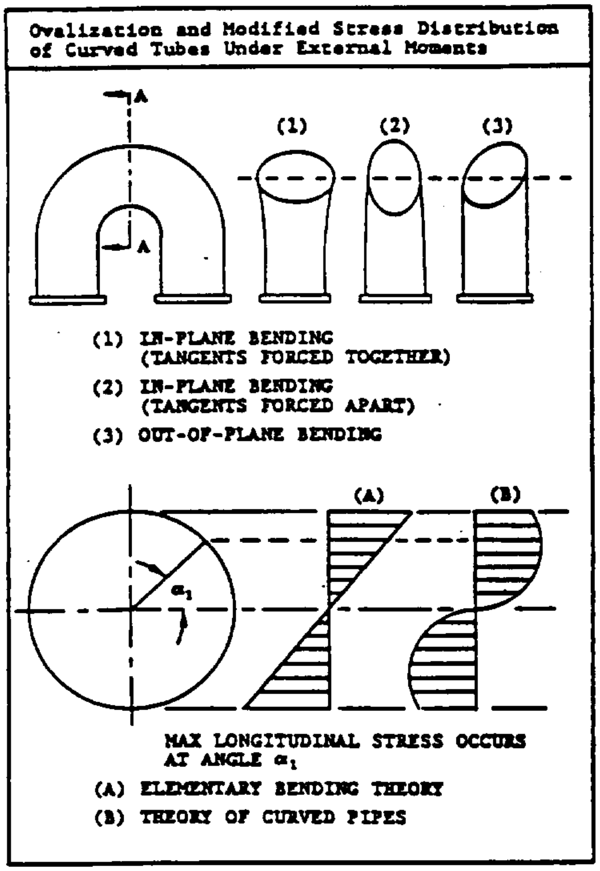

Figure 24.3.4-2

24.3.4.1 FLEXIBILITY FACTOR

The flexibility factor, k, for an unpressurized curved tube subject to in-plane or out-of-plane bending is given by the expression:

$$k = \frac{1.65}{h} \geq 1.0$$

where:

$$h = \frac{tR}{r^2}$$ (See Figure 24.3.4-1 for symbol definition)

NOTE: Thin walled only $10 < D/t < 100$

The increased flexibility is accounted for by dividing the tube rigidity, EI, by k, to give a reduced rigidity, EI/k.

24.3.4.2 STRESS INTENSIFICATION FACTOR

The longitudinal stress intensification factor, β, for an unpressurized curved tube subject to in-plane or out-of-plane bending is given by the expression:

$$\beta = \frac{0.90}{h^{2/3}} \geq 1.0$$

See Section 24.3.4.1 for definition of h.

The intensified longitudinal stress due to bending is given by:

$$f_b = \beta \frac{M}{Z}$$

In addition to the above intensified longitudinal bending stress there is a peak extreme fiber circumferential stress acting at $\alpha = 0°$ (See Figure 24.3.4-2). This peak circumferential stress is approximately equal to twice the longitudinal stress obtained by the above formula.

For static conditions the circumferential stress is usually neglected, as the peak stress is very localized and the high gradient across the tube wall enables a small amount of plastic flow to relieve the high local value. In dynamic loading, the assumption is no longer valid as fatigue becomes a consideration.

24.3.4.3 EFFECT OF INTERNAL PRESSURE ON FLEXIBILITY AND STRESS INTENSIFICATION FACTORS

The formulas for the flexibility factor and stress intensification factors in Sections 23.3.4.1 and 23.3.4.2 are based on theory and tests without internal pressure. The effect of internal pressure on relatively thick walled curved tubes at low stress levels is neglibible but for thin walled curved tubes the effect of internal pressure is significant. The following formulas modify the flexibility factor, k, and stress intensity factor, β, for the effects of internal pressure.

Flexibility factor with internal pressure, k_p, is given by:

$$k_p = \frac{k}{1 + \frac{f_H}{E} X_k} \geq 1.0$$

where:

f_H = hoop stress in straight tube
= pr/t

E = modulus of elasticity of tube material

X_k = function of r/t and R/r

$$= 6 \left(\frac{r}{t}\right)^{4/3} \left(\frac{R}{r}\right)^{1/3}$$

Obtain k from Section 24.3.4.1.

Additional Flexibility factor and Stress Intensification factor data is shown on page 9.3.10

579

24.3.4.3 EFFECT OF INTERNAL PRESSURE ON FLEXIBILITY AND STRESS INTENSIFICATION FACTORS (Continued)

The longitudinal stress intensification factor with internal pressure, β_p, is given by:

$$\beta_p = \frac{\beta}{1 + \frac{f_H}{E} X_1} \geq 1.0$$

where:

X_1 = function of r/t and R/r

$$= 3.25 \left(\frac{r}{t}\right)^{5/2} \left(\frac{R}{r}\right)^{2/3}$$

Obtain β from Section 24.3.4.2.

For a pressurized curved tube subject to in-plane or out-of-plane bending the intensified longitudinal bending stress is given by:

$$f_b = \beta_p \frac{M}{Z}$$

The stress due to internal pressure calculated from Section 24.3.5 must be added to the above bending stresses to obtain the total stress.

24.3.4.4 EFFECT OF FLANGED ENDS ON FLEXIBILITY AND STRESS INTENSIFICATION FACTORS

The curved tube theory is applicable only if end conditions are such that ovalization or flattening of the curved tube is not restricted. Flanges at the end of the bend (tangent point) tend to oppose ovalization and lower the flexibility and stress intensification factors. The smaller the subtended angle of the tube bend the greater the sensitivity of the bend to disturbances due to end restraint. For a 90° bend with flanges at one or both ends the flexibility and stress intensification factors must be multiplied by a correction factor, C_f, given by:

$C_f = h^{1/6}$ (one end flanged)

$C_f = h^{1/3}$ (both ends flanged)

See Section 24.3.4.1 for h. Values of C_f greater than unity should not be used.

24.3.5 STRESSES IN CURVED TUBES SUBJECT TO INTERNAL PRESSURE

In addition to the externally applied forces on curved tubes as discussed in the foregoing sections the tube wall is nearly always loaded by system internal pressure. For a curved tube, D/t>10 subject to an internal pressure, p, the longitudinal and circumferential pressure stresses are as follows: Longitudinal pressure stress, f_{L_B}, is identical to that for a straight tube as shown in Section 24.3.3 ①.

Circumferential pressure stress, f_{H_B}, is given by:

$$f_{H_B} = \frac{2R + r\sin\alpha}{2(R + r\sin\alpha)} f_H \quad ①$$

where f_H is circumferential pressure stress for straight tube as shown in Section 24.3.3, and other symbols in above formula are defined in Figure 24.3.5-1.

Distribution of Circumferential Stresses in Bend Subjected to Internal Pressure

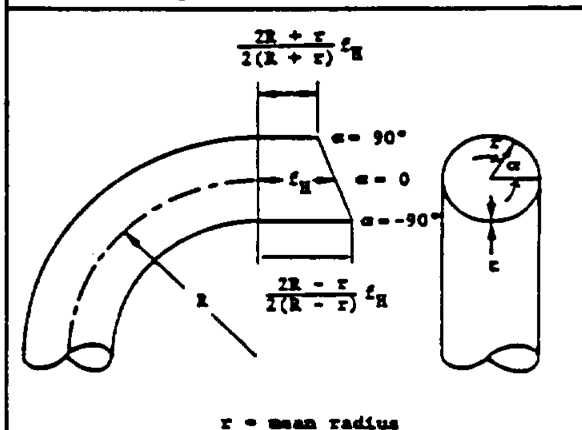

Figure 24.3.5-1

① Safety factors must be applied as indicated in Section 24.3.8.

For curved tubes the redistribution of material, which occurs during fabrication, thinning at the outside and thickening at the inside of the bend is a compensating factor of the same order as the acting circumferential pressure stress.

24.3.6 MOMENTUM CHANGE LOADS AT BENDS

The change in direction of the flow at a tube or duct bend produces a force due to momentum change as shown in Figure 24.3.6–1.

Momentum Change Load At Bend

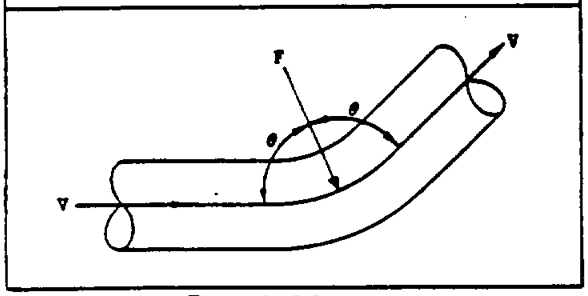

Figure 24.3.6–1

Force, F, in pounds at the bend is given by:

$$F = \frac{2AV^2\rho\cos\theta}{g}$$

where

A = cross–sectional area of tube or duct $(in)^2$.

V = velocity of fluid (in/sec)

ρ = fluid density (lb/in^3)

g = gravitational constant

= 386.4 in/sec^2

24.3.7 PIPING FLEXIBILITY ANALYSIS

The objective of piping flexibility analysis is to ensure that no failure of the piping material or anchor structure occurs due to overstress, no leakage at the joints results from excessive loading and that there is no overstraining of connected equipment.

Piping flexibility analysis is resolved into two parts.

1. The calculation of forces, moments, stresses and displacements in a tubular structural frame due to thermal expansion, support displacement, inertia effects, etc. with the bends analyzed as shown in Section 24.3.4.

2. Comparison of the calculated stresses and displacements with allowable limits to ensure that the stresses in the system are maintained within a range so that direct or fatigue failure is precluded and that displacements do not exceed acceptable limits.

24.3.7.1 GENERAL PROCESS OF SOLUTION

In the flexibility analysis of any system of given line size, configuration and material, with a predetermined amplitude and number of temperature cycles the following steps are involved:

1. The significant physical properties of the material, such as coefficient of thermal expansion, modulus of elasticity, modulus of rigidity and Poisson's ratio must be determined.

2. Assumptions regarding piping dimensions, notably those associated with cross–section, must be made. For simplicity, dimensional tolerances are disregarded and nominal dimensions used throughout.

3. Determine conditions of end restraint for the lines. Normally the ends are assumed fully fixed. In addition to thermally induced expansion and contraction of the lines, equipment expansion and contraction must be considered since these will increase the forces and moments in the system.

4. The significance of intermediate forms of restraint must be assessed. Major restrictions to free movement of the line due to guides, solid hangers, or other supports must be considered in the analysis.

5. Select a method of analysis for the solution from several available for analyzing framed structures. Two analytical methods widely used for piping systems are the energy method known as "Method of Least Work" and the "Elastic Center Method".
   In addition to pressure, thermal and inertia loads, support displacement loads due to airplane structural deflections must be included in the complete analysis.

6. The last step is a comparison of the analysis results with allowables.

24.3.7.2 COMPUTERIZED FLEXIBILITY ANALYSIS

Complex three–dimensional piping systems require prodigious computational effort, which can be facilitated by the use of computer programs. Input data for a typical program is outlined below:

The first step is to calculate the coordinates of all node points.

24.3.7.2 COMPUTERIZED FLEXIBILITY ANALYSIS (Continued)

Once the piping geometry is established the next step is to determine the system operating conditions and properties as listed below:

1. Design conditions of pressure, p, (psi) and temperature, T(°F)
2. Material
3. Modulus of elasticity, E (psi) at temperature
4. Modulus of rigidity, G (psi) at temperature
5. Poisson's ratio, μ
6. Unit thermal expansion of pipe, $\alpha \Delta T$(in/in)
7. Pipe diameter, D(in)
8. Cross sectional area, A(in^2)
9. Moment of inertia about a diameter, I (in^4)
10. Polar moment of inertia, J(in^4)
11. Bend radius of curved pipe, R, (in)
12. Bend flexibility factor, k_p, (See Section 23.3.4.3)
13. Bend stress intensification factor, β, (See Section 23.3.4.3)
14. Effective moments of inertia, I_p and J_p, respectively for the bends. ($I_p = I/k_p$). The torsional flexibility factor is normally assumed to be 1.0 so that $J_p = J$.

The establishment of boundary conditions requires careful attention. Use may be made of the specified deflection options of programs to establish support structure deflections. With the system internal loads obtained from the flexibility analysis, the stresses in the system can be evaluated. Section 24.3.8 discusses the combination of stresses to obtain principal stresses.

24.3.8 STRESSES IN PIPING SYSTEMS

Stresses in piping systems result from:

1. Internal pressure.
2. Thermal expansion and displacement of support structure.
3. Weight of the lines and components fitted into the lines such as flanges, valves, etc. plus inertia effects on the system (system fluid weight may be included if significant)

Internal Pressure:

Internal pressure produces three types of stresses:

A. RADIAL STRESS

For aircraft systems utilizing thin walled tubing these stresses are negligible.

B. HOOP OR CIRCUMFERENTIAL STRESS:

The basic requirement for a pressurized system is that the wall thickness is adequate to withstand all hoop stresses likely to be met in service. Relevant safety factors as defined in the design criteria are applied to the circumferential stress obtained from Section 24.3.3 to obtain a design stress. (1)

C. LONGITUDINAL STRESS:

The same safety factors as discussed in item B. are applied to the longitudinal stress obtained from Section 24.3.3 to obtain a design stress.

(1) This stress is modified for curved tubes as shown in Section 24.3.5.

Thermal Expansion and Support Displacement:

The longitudinal stresses in the lines due to thermal expansion result from the forces and moments, which must be applied to the attachment points of a line to return it to the actual position after a temporary initial freedom for expansion has been assumed.

Thermal effects in an airplane system are due to expansion of the hot lines and contraction or expansion of the airplane structure. Typically, line stream temperatures range between 250° and 900°F, while the airplane structure is subjected to an ambient temperature ranging from −65°F to 160°F.

Thermal stresses in the lines cannot be reduced by increasing wall thickness. If these stresses are too high, expansion joints as discussed in Section 24.4 must be provided.

The lines of the system must be designed to allow for displacement of the supports due to airplane structural deflections based on limit load. Longitudinal and any other stresses induced by support displacement must be included in the resultant stresses.

Weight of Lines and Components

The longitudinal stresses in the lines due to their weight are generally small and are usually neglected in an initial analysis. Components fitted in the line such as valves are considered to act as point loads inducing longitudinal stresses which can be significant.

24.3.8 STRESSES IN PIPING SYSTEMS (Continued)

Maximum Combined Stresses:

These stresses are obtained from combined stress formulas as outlined below and compared with the allowable stresses to obtain the margins of safety. Stresses from all loadings should be included to determine the resultant stresses before insertion in the combined stress formulas.

The resultant principal stresses at the outside fiber are given by:

$$f_1 = 0.5\left[(f_L + f_H) + \sqrt{4f_{St}^2 + (f_L - f_H)^2}\right]$$

$$f_2 = 0.5\left[(f_L + f_H) - \sqrt{4f_{St}^2 + (f_L - f_H)^2}\right]$$

$$f_3 = 0$$

where:

f_L = maximum longitudinal stress due to pressure, weight, and other sustained loading plus expansion/contraction stress, psi ①

f_H = circumferential pressure stress, psi

f_{St} = shear stress due to torsion, psi

= T/2Z

Z = section modulus of tube or duct, in³

T = resultant torsional moment, lb. in.

① For curved tubes or ducts the longitudinal stresses due to bending must include the stress intensification factor, β_p, as discussed in Section 24.3.4.3.

Loadings which cause cyclic stresses are most significant in piping system analysis. These stresses are considered separately from those calculated from the above formulas and compared with allowable stresses obtained from a durability analysis.

24.4 EXPANSION JOINTS AND ABSORPTION DEVICES

Whenever possible piping systems should be designed to absorb expansions by the inherent flexibility of the system. If this is not possible due to excessive expansion, special devices such as expansion joints, bends and loops can be used. Expansion joints can be divided into two categories:

1. Sliding joints
2. Flexible joints

Sliding joints may be further subdivided into slip joints, swivel joints, ball joints, special couplings and screwed joints. Flexible joints may be subdivided into those depending on the flexibility of rubber or other pliable material, bellows joints and metal hose. Use of expansion joints may require additional supports to make the piping system stable for longitudinal loads.

If space is available, coiled tubing or expansion bends and loops represent low cost alternatives to expansion joints. This section gives analysis data for expansion bends and loops and stainless steel bellows joints.

24.4.1 EXPANSION BENDS AND LOOPS

Methods for analyzing several types of commonly used bends and loops are given below. Figure 24.4.1-1 gives formulas which can be used to obtain the reactive forces and moments, P, S and M_o when the horizontal, vertical, and angular displacements, δx, δy and θ due to thermal expansion are known.

The method of obtaining the maximum bending stress in the bend or loop due to thermal expansion is as follows:

1. For known displacements due to thermal expansion δx, δy or θ obtain reactive force or moment, P, S or M_o from formulas given in Figure 24.4.1-1.
2. With the value of reactive force or moment calculate the maximum bending moment, M, on bend or loop.
3. Calculate maximum bending stress due to thermal expansion using bending moment, M, from Step 2 and stress intensification factor, β or β_p from Section 24.3.4.2 or 24.3.4.3 as shown:

$$f_b = \beta\frac{M}{Z} \text{ or } \beta_p\frac{M}{Z}$$

This longitudinal stress due to bending is then combined with the longitudinal stresses due to pressure and inertia effects to obtain a resultant principal stress as shown in Section 24.3.8 and then compared with an allowable stress.

Sign convention for Figure 24.4.1-1 is as shown:

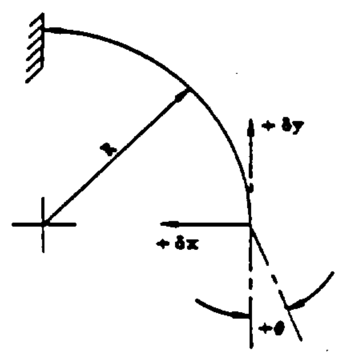

24.4.1 EXPANSION BENDS AND LOOP (Continued)

Bend and Loop Solutions

CASE NO.	DIAGRAM	θ	δ_X	δ_Y	NOTES
1		$-\frac{PR^2}{KEI}$	$0.785\frac{PR^3}{KEI}$	$-\frac{1}{2}\frac{PR^3}{KEI}$	QUARTER-BEND FIXED AT ONE END AND LOADED BY A TRANSVERSE FORCE P.
2	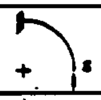	$0.57\frac{SR^2}{KEI}$	$-\frac{1}{2}\frac{SR^3}{KEI}$	$0.356\frac{SR^3}{KEI}$	QUARTER-BEND FIXED AT ONE END AND LOADED BY AN AXIAL FORCE S.
3	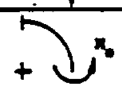	$1.57\frac{M_oR}{KEI}$	$-\frac{M_oR^2}{KEI}$	$0.57\frac{M_oR^2}{KEI}$	QUARTER-BEND FIXED AT ONE END AND ACTED ON BY A BENDING MOMENT M_o AT THE OTHER
4	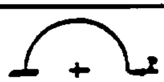	$-\frac{2PR^2}{KEI}$	$1.57\frac{PR^3}{KEI}$	$-2\frac{PR^3}{KEI}$	180-DEG U-BEND FIXED AT ONE END AND LOADED WITH A TRANSVERSE FORCE P.
5		$3.14\frac{SR^2}{KEI}$	$-2\frac{SR^3}{KEI}$	$4.71\frac{SR^3}{KEI}$	180-DEG U-BEND FIXED AT ONE END AND LOADED WITH AN AXIAL FORCE S.
6	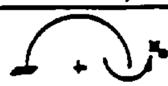	$3.14\frac{M_oR}{KEI}$	$-2\frac{M_oR^2}{KEI}$	$3.14\frac{M_oR^2}{KEI}$	180-DEG U-BEND FIXED AT ONE END AND ACTED ON BY A BENDING MOMENT M_o AT THE OTHER.
7		—	$39.9\frac{PR^3}{KEI}$	—	ENDS HINGED
8		—	$18.7\frac{PR^3}{KEI}$	—	ONE END FIXED. THE OTHER HINGED AND GUIDED IN THE X-DIRECTION.
9		—	$12.3\frac{PR^3}{KEI}$	—	ONE END FIXED. THE OTHER FREE TO MOVE IN THE DIRECTION OF THE X-AXIS BUT NOT FREE TO ROTATE.
10		—	$9.42\frac{PR^3}{KEI}$	—	BOTH ENDS HINGED
11		—	$4.62\frac{PR^3}{KEI}$	—	ONE END FIXED. THE OTHER HINGED AND GUIDED IN THE X-DIRECTION.
12		—	$3.14\frac{PR^3}{KEI}$	—	ONE END FIXED. THE OTHER FREE TO MOVE IN THE DIRECTION OF THE X-AXIS BUT NOT FREE TO ROTATE.

$K = \frac{1}{k}$ or $\frac{1}{k_p}$ (Obtain k and k_p from Sections 24.3.4.1 and 24.3.4.3 respectively)

Figure 24.4.1-1

FLEXIBILITY FACTOR k AND STRESS INTENSIFICATION FACTOR i

Description	Flexibility Factor k	Stress Int. Factor i	Flexibility Characteristic h	Sketch
Welding elbow,[1,2,3] or pipe bend	$\frac{1.65}{h}$	$\frac{0.9}{h^{2/3}}$	$\frac{tR}{r^2}$	
Closely spaced mitre bend,[1,2,3] $s < r(1 + \tan \alpha)$	$\frac{1.52}{h^{5/6}}$	$\frac{0.9}{h^{2/3}}$	$\frac{\cot \alpha}{2} \frac{ts}{r^2}$	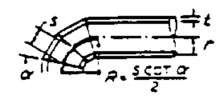
Widely spaced mitre bend,[1,2,4] $s \geq r(1 + \tan \alpha)$	$\frac{1.52}{h^{5/6}}$	$\frac{0.9}{h^{2/3}}$	$\frac{1 + \cot \alpha}{2} \frac{t}{r}$	
Welding tee[1,2] per ASA B16.9	1	$\frac{0.9}{h^{2/3}}$	$4.4 \frac{t}{r}$	
Reinforced fabricated tee,[1,2] with pad or saddle	1	$\frac{0.9}{h^{2/3}}$	$\frac{(t + \frac{1}{2} T)^{5/2}}{t^{3/2} r}$	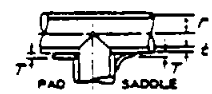
Unreinforced fabricated tee[1,2,4]	1	$\frac{0.9}{h^{2/3}}$	$\frac{t}{r}$	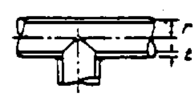

Description	Flexibility Factor k	Stress Int. Factor i
Butt welded joint, reducer, or welding neck flange	1	1.0
Double-welded slip-on or socket weld flange	1	1.2
Fillet welded joint, or single-welded socket weld flange	1	1.3
Lap joint flange (with ASA B16.9 lap joint stub)	1	1.6
Screwed pipe joint, or screwed flange	1	2.3
Corrugated straight pipe, or corrugated or creased bend[5]	5	2.5

[1] The flexibility factors k and stress intensification factors i in the table apply to bending in any plane for fittings of the same nominal weight or schedule as the pipe used in the system and shall in no case be taken less than unity; factors for torsion equal unity. Both factors apply over the effective arc length (shown by heavy center lines in the sketches) for curved and mitre elbows, and to the intersection point for tees.

[2] The value of k and i can be read directly from graph, entering with the characteristic h computed from the formulae given, where:

- R = bend radius of welding elbow or pipe bend
- r = mean radius of matching pipe
- t = wall thickness of matching pipe
- α = one-half angle between adjacent mitre axes
- s = mitre spacing at center line
- T = pad or saddle thickness

[3] Where flanges are attached to one or both ends, the values of k and i in the table shall be corrected by the factors C given below which can be read directly from chart, entering with the computed h:

One end flanged: $h^{1/6}$ Both ends flanged: $h^{1/3}$

[4] Also includes single-mitre joint.

[5] Factors shown apply to bending; flexibility factor for torsion equals 0.9.

Graph for k and i

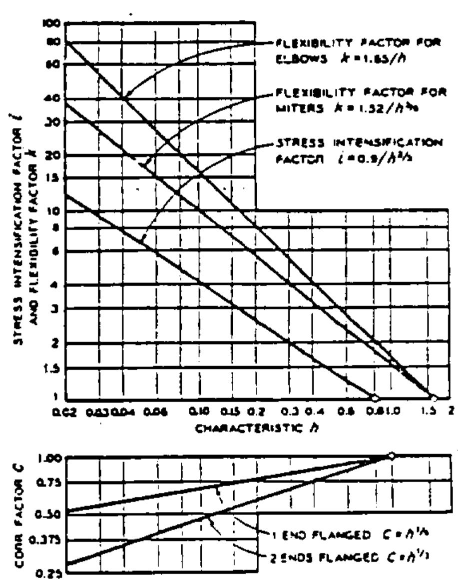

[6] The stress intensification factors i in the table were obtained from tests on full size outlet connections. For less than full size outlets, the full size values should be used until more applicable values are developed.

Reference : GRINNELL — PIPING DESIGN AND ENGINEERING

24.4.2 BELLOWS

This Section gives formulas for estimating the performance of bellows. Configuration and notation are shown in Figure 24.4.2-1.

BELLOWS CONFIGURATION AND NOTATION

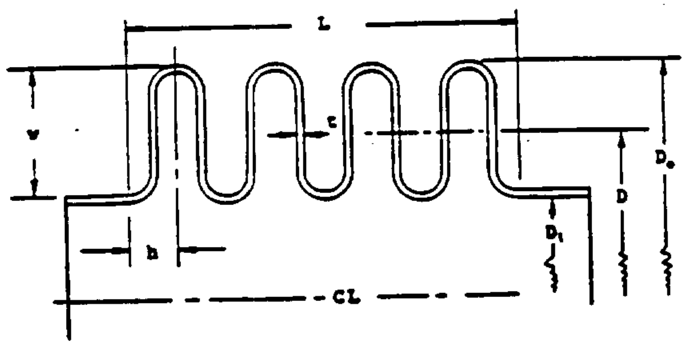

U-Shaped
(4 Convolutions shown)

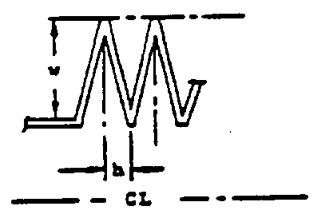

Flat Disc

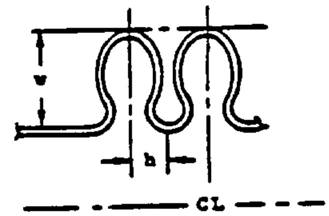

Toroidal

t = bellows thickness (in)
w = convolution or disc height (in)
h = pitch of half-convolution or disc (in)
D = mean bellows diameter (in)
  = $(D_o - D_i)/2$
D_o = outside bellows diameter (in)
D_i = inside bellows diameter (in)
L = overall bellows length (in)
E = modulus of elasticity (psi)
Δ = total axial movement range, extension and compression plus equivalent axial movement as obtained from formulas given in paragraph entitled "Equivalent Axial Movement" (in) (REF pg. 9.3.12)
N_a = number of active bellows discs or half convolutions (in)
p = internal pressure (psi)

Full configuration shown for U-shaped bellows only. Partial configurations shown for flat disc and toroidal bellows to illustrate convolution shape.

Figure 24.4.2-1

24.4.2 BELLOWS (Continued)

Number of cycles to failure is given by the formula:

$$N = \left(\frac{\text{Constant}}{S_R}\right)^e$$

where:

N = number of cycles to failure

S_R = range of alternating stress due to expansion and pressure as obtained from the formulas below (psi).

The constant and exponent are dependent on the material. For AISI Type 321 and 347 Annealled stainless steel the constant is 1,300,000 with an exponent of 3.5 at 70°F. A design service rating for the above material is obtained by using a constant of 650,000 with an exponent of 3.5. To obtain constants and exponents for other materials consult durability group.

For flat disc bellows:

$$S_R = \frac{3Et\Delta}{w^2 N_d} + \frac{pw^2}{2t^2}$$

For U-shaped bellows without equalizing rings

$$S_R = \frac{1.5Et\Delta}{h^{0.5} w^{1.5} N_d} + \frac{pw^2}{2t^2}$$

For U-shaped bellows having equalizing rings which provide support against internal pressure only along inner edge:

$$S_R = \frac{1.5Et\Delta}{h^{0.5} w^{1.5} N_d} + \frac{pw}{t} \quad (1)$$

For modified toroidal bellows having minor axis of ellipse about 0.8 to 0.9w:

$$S_R = \frac{1.5Et\Delta}{w^2 N_d} + \frac{pw}{t}$$

Equivalent Axial Movement:

The equivalent axial movement corresponding to the angular rotation on universal, or hinged type, joints may be determined by:

$$\Delta = D\theta/2$$

where

θ = total angular rotation, radius.

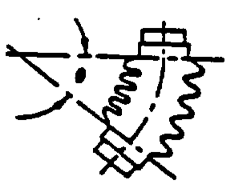

The equivalent axial movement for a single-bellows offset joint, based on the most severely affected convolutions (those at the ends), is found from:

$$\Delta = 3Dh_r/L$$

where

h_r = offset range or total lateral displacement of one end of the joint with respect to the other, in.

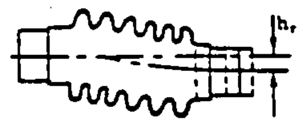

For a joint having a double bellows separated by a spool piece the equivalent axial movement becomes:

$$\Delta = \frac{3Dh_r}{L + \ell\left[(\ell/L) + 1\right]}$$

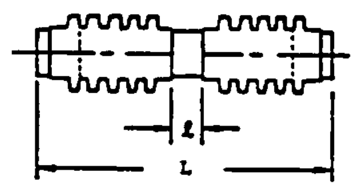

where

L = overall length, end to end, of bellows, including spool piece, in.

ℓ = length of spool piece, in.

Spring Rate:

The force, F, in lbs, necessary to deflect the bellows an amount Δ, can be stated as follows:

For flat disc bellows:

$$F = \frac{\pi E D t^3 \Delta}{w^3 N_d}$$

For U-shaped convolutions:

$$F = \frac{4EDt^3\Delta}{3h^{0.5} w^{2.5} N_d} \quad (1)$$

(1) Limited to $.34\,w \le h \le w$

587

24.5 PIPING SYSTEM SUPPORTS

Aircraft piping system support design must satisfy the following requirements:

A. Supports must be capable of reacting all loadings such as those due to inertia, thermal effects and support structure displacement. The type of support provided should be in agreement with the assumptions of the flexibility analysis.

B. The distance between supports shall be such that resonance of the lines will not occur under the induced vibrational environment.

Maximum allowable support spacings for severe vibrational environments and new system design are usually established from tests.

Local bending stresses in tubing and ducting result from support loads (See figure 24.5–1) which must be checked. Supports should be located to keep these stresses within allowable limits.

Support Loading on Tubing and Ducting

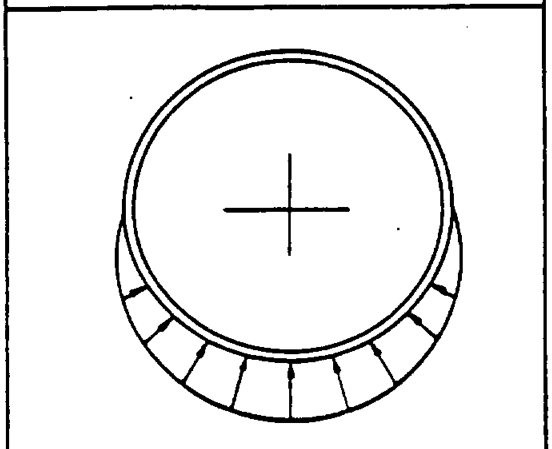

Figure 24.5–1

24.6 RECTANGULAR AND OVAL DUCTS

This section presents methods for the analysis of thin walled ducts of rectangular and oval cross-section used in low pressure applications. The formulas ignore the effect on bending of the direct tension stresses due to P_1 and P_2. (See duct free body diagrams shown below). The effect of the direct stresses is small and tends to reduce the bending stresses in the walls.

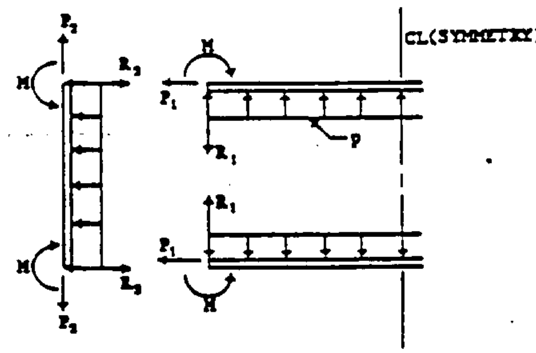

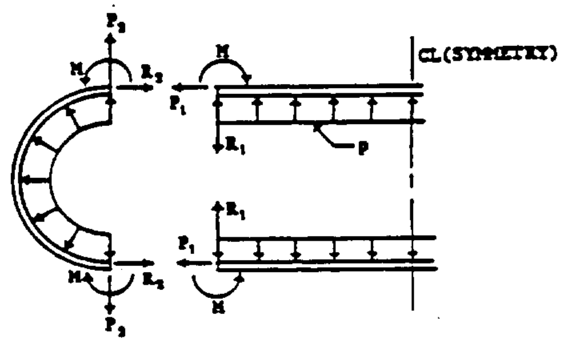

24.6.1 RECTANGULAR DUCTS

The following formulas may be used to obtain the bending moments, stresses and deflections in thin walled ducts of rectangular cross-section.

The bending moment at the duct corner is:

$$M = pb^2 \frac{K^2 - K + 1}{12}$$

or bending moment coefficient $\frac{12M}{pb^2} = K^2 - K + 1$

where:

p = internal duct pressure (psi)

a = long side of duct (in)

b = short side of duct (in)

K = side ratio

= $a/b > 1.0$

The stress derived from the moment at the corner will be modified by the effect of joints, stress concentrations etc.

The bending moment at the center of the long sides is:

$$M = pb^2 \frac{K^2 + 2K - 2}{24}$$

or bending moment coefficient $\frac{12M}{pb^2} = \frac{K^2 + 2K - 2}{2}$

and at the center of the short sides is:

$$M = pb^2 \frac{1 + 2K - 2K^2}{24}$$

or bending moment coefficient $\frac{12M}{pb^2} = \frac{1 + 2K - 2K^2}{2}$

Figure 24.6.1-1 gives values of bending moment coefficients, $12M/pb^2$, for the three locations for various values of K.

The bending stresses are given by $f_b = \frac{6M}{t^2}$

24.6.1 RECTANGULAR DUCTS (Continued)

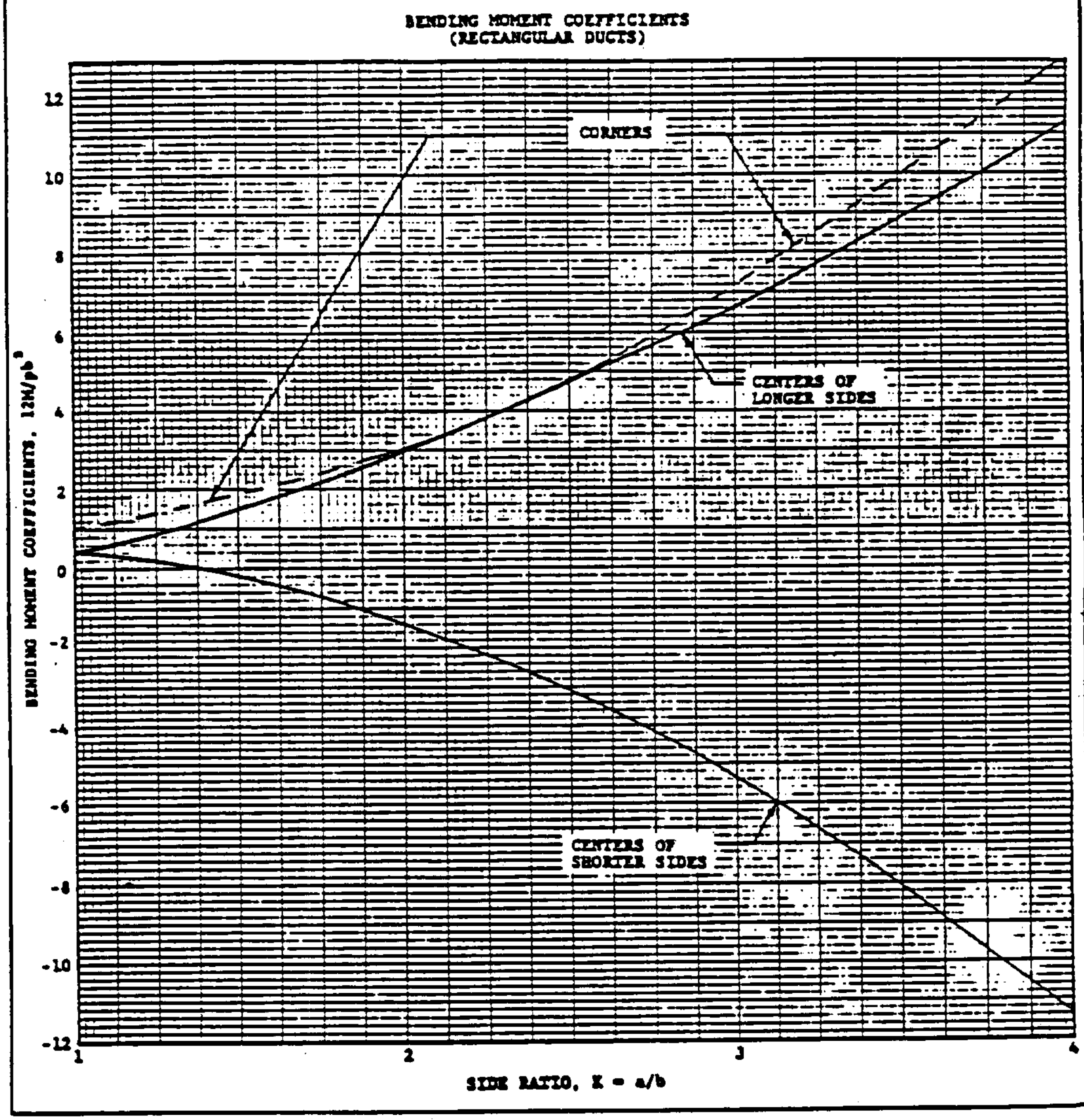

Figure 24.6.1-1

540

24.6.1 RECTANGULAR DUCTS (Continued)

The maximum deflection for a rectangular duct occurs at the center of the long sides and is given by:

$$\delta = \delta_c \frac{K^2 + 4K - 4}{K^2}$$

where δ_c is the deflection at the center of a plate of width a with clamped edges and under pressure p.

$$\delta_c = \frac{pa^4}{384\,D}$$

Plate rigidity, D, is given by $Et^3/12(1-\mu^2)$, Where μ = Poisson's ratio.

Figure 24.6.1-2 gives values of deflection coefficient, δ/δ_c, for various values of K.

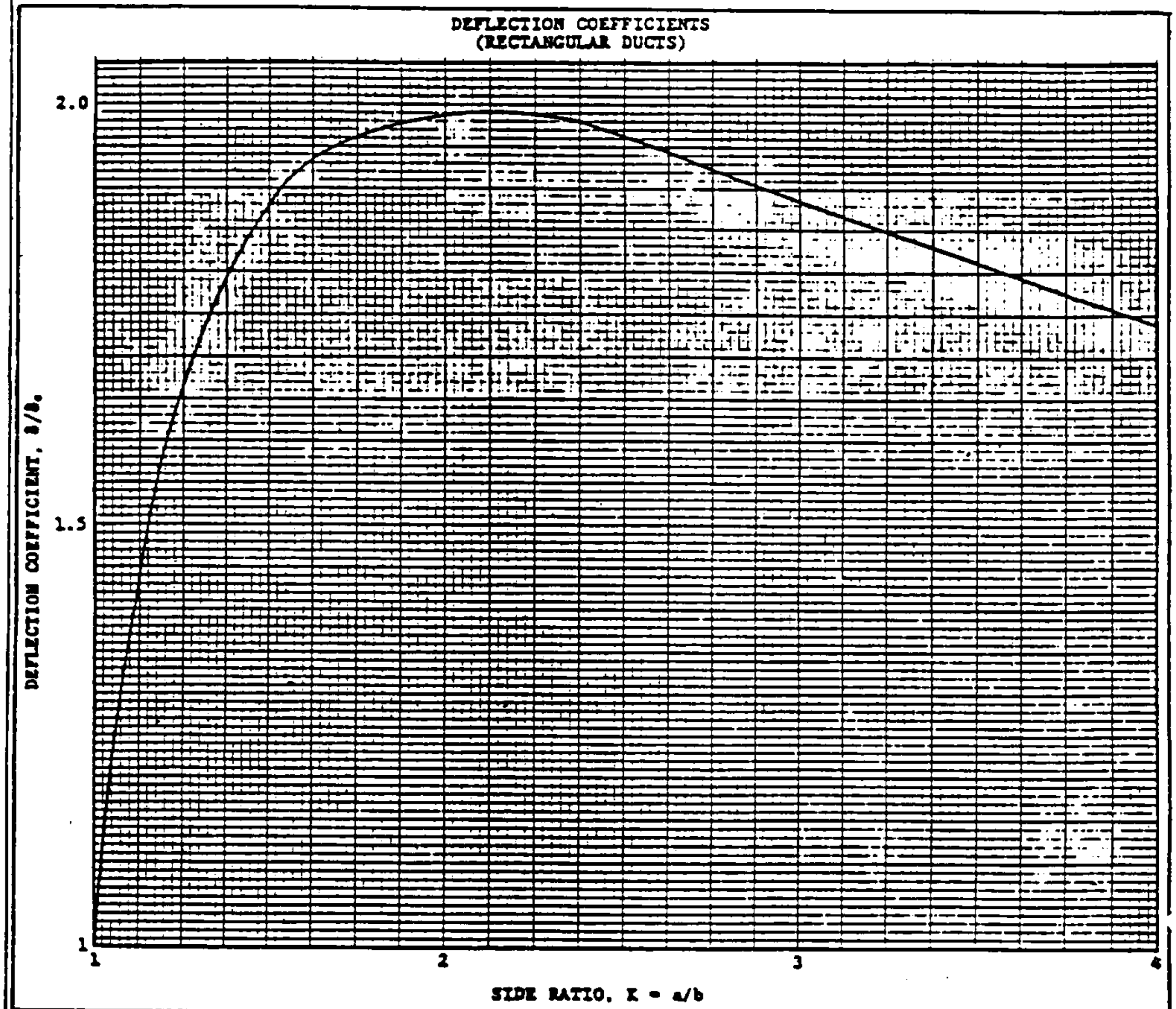

Figure 24.6.1-2

24.6.2 OVAL DUCTS

The following formulas may be used to obtain the bending moments and stresses in thin walled oval ducts as shown in Figure 24.6.2-1. The effect of direct stresses on bending is neglected. The bending moment at the centers of the flat portions, points A, is given by:

$$M = -pb^2\left[\frac{K^3 + 1.5\pi K^2 + 6K}{3\pi + 6K}\right]$$

where K = dimension ratio a/b.

At the junction of the flat and curved portions, points B, the bending moment is given by:

$$M = pb^2\left[\frac{2K^3 - 6K}{3\pi + 6K}\right]$$

The bending moment at the center of the curved portions, points C, is:

$$M = pb^2\left[\frac{2K^3 + 6K^2 - 3K(2-\pi)}{3\pi + 6K}\right]$$

Bending moments are zero for K = 0 when the duct becomes circular in form. Figure 24.6.2-1 gives values of bending moment coefficients, M/pb^2 for points A, B and C for various values of dimension ratio K. The bending stresses in the duct wall are given by:

$$f_b = \frac{6M}{t^2}$$

24.6.2 OVAL DUCTS (Continued)

BENDING MOMENT COEFFICIENTS
(OVAL DUCTS)

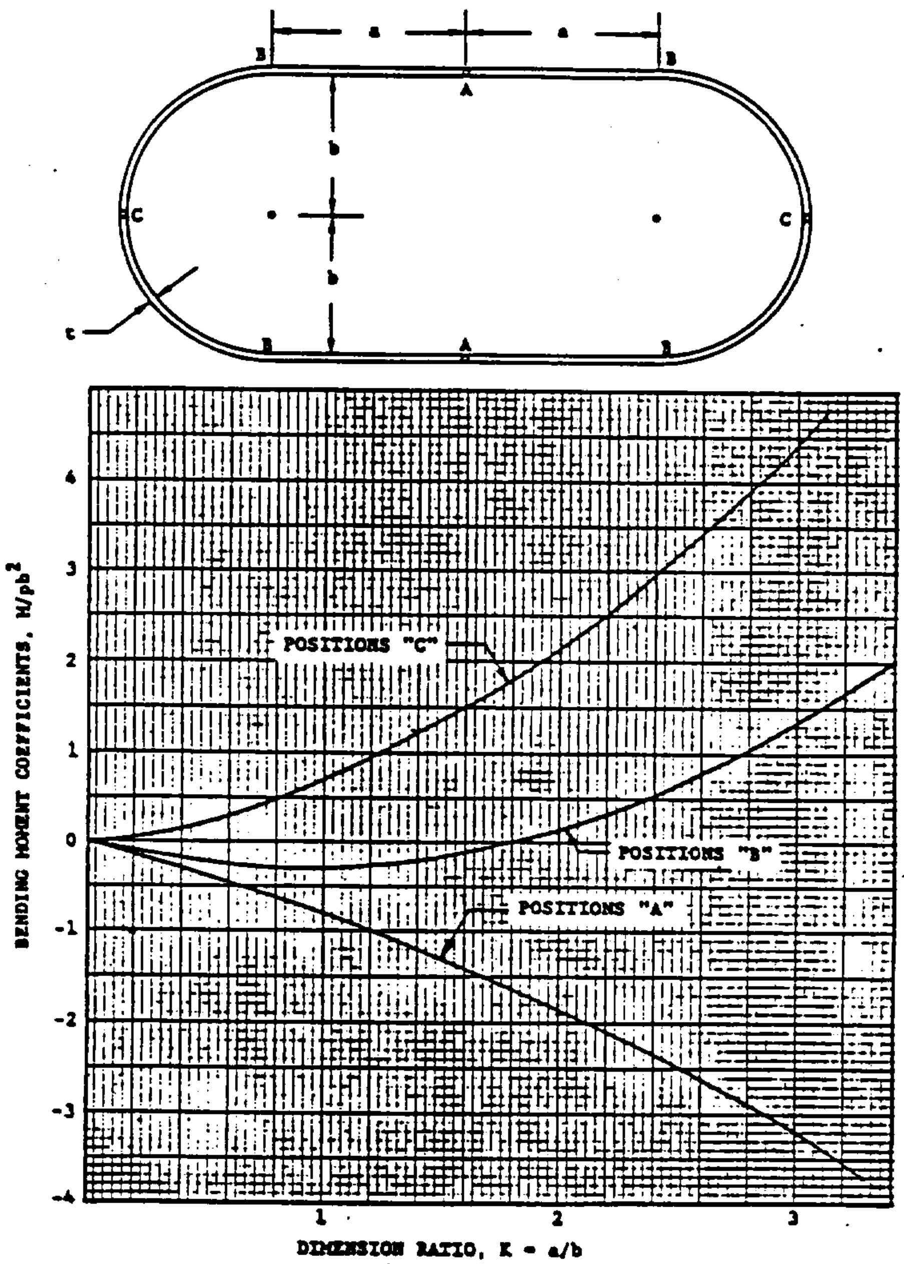

Figure 24.6.2-1

DISCONTINUITY ANALYSIS OF SHELLS

SUMMARY

A method is presented for the analysis of multiple discontinuities in thin-walled pressure vessels. The method accounts for the carry-over effects between neighboring discontinuities where their lengths of separation are sufficiently small to make this a significant factor. The method is based upon the theory for finite beams on an elastic foundation. A program has been prepared to provide rapid solutions on the CYBER data processing machine. The input, output and limitations of this program are presented in Data Source, Section 1.3 Reference 39 and in the updated Convair/Space System Division computer program number P5007.

INTRODUCTION

Much of the stress analysis of a thin-walled pressure vessel can be based upon membrane theory, wherein it is assumed that the skin offers no resistance to bending and transverse shear. By this theory, any loads imposed upon the vessel are reacted by tensile or compressive stresses having a uniform distribution across the wall. In effect the vessel is considered to be a balloon. This results in a statically determinate problem which can be handled by a simple balance of forces on appropriate elements. The membrane stresses are, of course, associated with various deflections of the shell. Where the boundary conditions are such that there is no interference with these deflections, the membrane theory is adequate. However, should the boundary conditions restrict these deformations, the skin is then subjected to local bending moments and transverse shear forces. Such conditions are usually referred to as discontinuities. At these locations, the effects of the local moments and shears must be superimposed upon the membrane stresses. Since the local loads are redundants, it is necessary to make use of the laws of consistant deformation to determine their values.

Aerospace vehicle pressure vessel designs usually include joints of the type shown in Figure 1, where each step in total wall thickness and each change in vessel shape, represent a discontinuity (points 1 thru 7). The program described in this report* was created to perform the task of determining the values for the local shears and moments at such points.

*Data Source, Section 1.3 Reference 39

DISCONTINUITY ANALYSIS OF SHELLS (cont.)

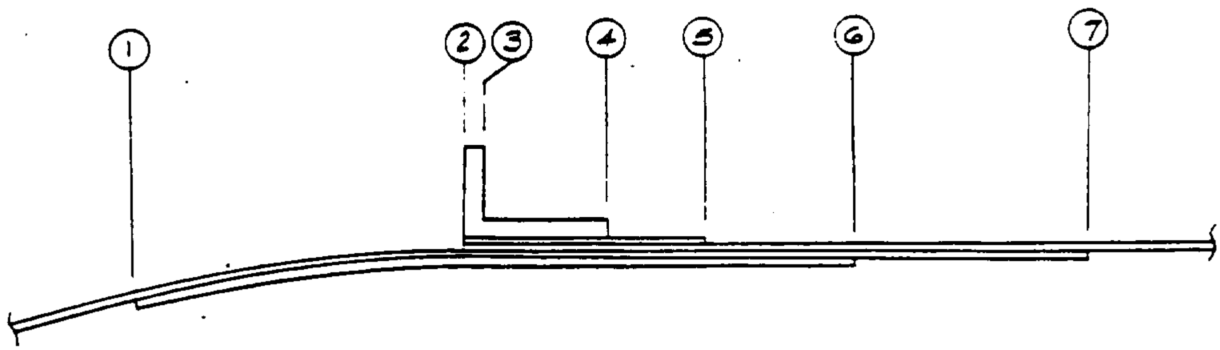

Figure 1

METHODS OF ANALYSIS:

The method of analysis is based upon the theory developed in reference (1) for beams on an elastic foundation. Considering a cylindrical shell under the influence of symmetrically distributed edge loads as shown in Figure 2, Timoshenko (Ref. 2) shows that the equation for the deflection curve of this shell is the same as that for a beam supported by a continuous elastic foundation. A more apparent development of the analogy involved is presented by Hentenyi in Ref. (1).

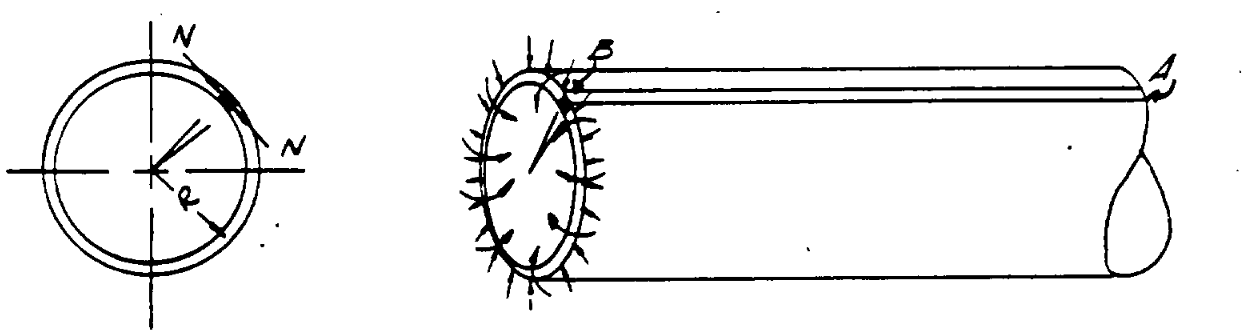

Figure 2

595

10.2.4
Bending

The buckling behavior of a cylinder under bending corresponds to that of axially compressed cylinders in two respects. First, linear theory predicts buckling stresses of the same order in magnitude for both cases. Second, the test data are below the predictions of linear theory by approximately the same amount. Consequently, all of the major investigations have been directed toward the correlation of test data on cylinders in bending in a manner similar to that used for axially compressed cylinders. A comparison shows that reasonably good results can be obtained by multiplying the compressive buckling stress by a factor of 1.3 to obtain the critical bending stress. For best results, a statistical analysis was performed in the same manner as for axial compression in Section 10.2.1. The results are plotted in the form of analysis curves in Figs. 10.2.4.1, 10.2.4.2, and 10.2.4.3. These curves can be used when restricted to the following limitations:

1. Most of the test data upon which these curves are based fall within the range of cylinder dimensions $.25 < L/R < 5$, and $300 < R/t < 1500$.
2. The curves are based on tests of steel, aluminum, and brass cylinders only.

SECTION 10.0

CYLINDER AND SHELL STABILITY

DATA IS PRESENTED FOR PREDICTING THE BUCKLING STRESS OF AXISYMMETRIC VESSELS, TOGETHER WITH ANALYSIS EFFECTS OF LOCAL LOADING.

		PAGE
10.1	UNPRESSURIZED	10.1.1
10.2	INTERNALLY PRESSURIZED	10.2.1
10.3	EXTERNALLY PRESSURIZED	10.3.1
10.4	TRUNCATED CONES	10.4.1
10.5	DOUBLY CURVED SHELLS	10.5.1
10.6	IMPERFECTIONS	10.6.1
10.7	POST-BUCKLING	10.7.1
10.8	LOCAL LOADING ON SHELLS	10.8.1
10.9	LANGLEY SOLUTION	10.9.1

FOR ANALYSIS METHODS OF MAIN PROPELLANT TANK STRUCTURE, SEE SECTION 28.0

Cylinders

This section is devoted to the prediction of the buckling stress of unstiffened circular cylinders, commonly called full monocoque structures. Curves are presented for the prediction of compressive, bending, and torsional buckling loads. Curves are also included to show the effects of internal pressure. These are in the form of best fit curves, 90% probability curves, and 99% probability curves, all at a confidence level of 95%. Interaction equations are also given to account for combined loading effects.

Axial Compression

Many investigations have been made in an attempt to develop methods for predicting the buckling stress of axially compressed circular cylinders. The two major obstacles encountered were:

1. Theoretical Solutions, based on both small and large deflection theories, do not adequately predict the buckling stress.
2. Test data consistently exhibit a large amount of scatter.

The first methods that were "sometimes" successful in predicting the buckling stress were empirical in nature. These methods were normally developed by altering coefficients and/or exponents in theoretically derived expressions so that their plots passed through the "Center of Mass" of test data points. The usefulness of this method is limited since there is so much scatter in the test data. For example, a predicted stress that coincides with the average of the test results will usually be highly unconservative when compared to the lowest test values. The prediction of stresses is further complicated since buckling of an axially compressed circular cylinder occurs suddenly and is catastrophic in nature.

The methods presented in this section are based on the statistical analyses of test data by the method of least squares.

Analyses Curves

The curves in Figs. 10.2.1.1, 10.2.1.2, and 10.2.1.3 can be used when the following restrictions are observed:

1. Most of the test data for these curves fall within the range of cylinder dimensions $L/R < 2$ and $300 < R/t < 1000$.
   Where L is the length of the cylinder
   R is the radius of the cylinder
   t is the wall thickness of the cylinder
   Caution should be taken when curves for $L/R > 2$ are used.
2. The curves are based on tests of steel and aluminum cylinders only. The accuracy of these curves, when used for other materials, has not been substantiated by tests.

The 99% probability curves are recommended as design allowables for structures whose failure would be highly critical. The 90% curves can be used for less critical structures.

Figs. 10.2.1.1, 10.2.1.2, and 10.2.1.3 were constructed with the parameter σ_{cr}/E as the ordinate and R/t as the abscissa. Each figure displays a series of curves for constant L/R's from .125 to 32. It should be remembered that most of the test data were plotted for L/R's < 2 and care should be taken when using curves with an L/R above this limit.

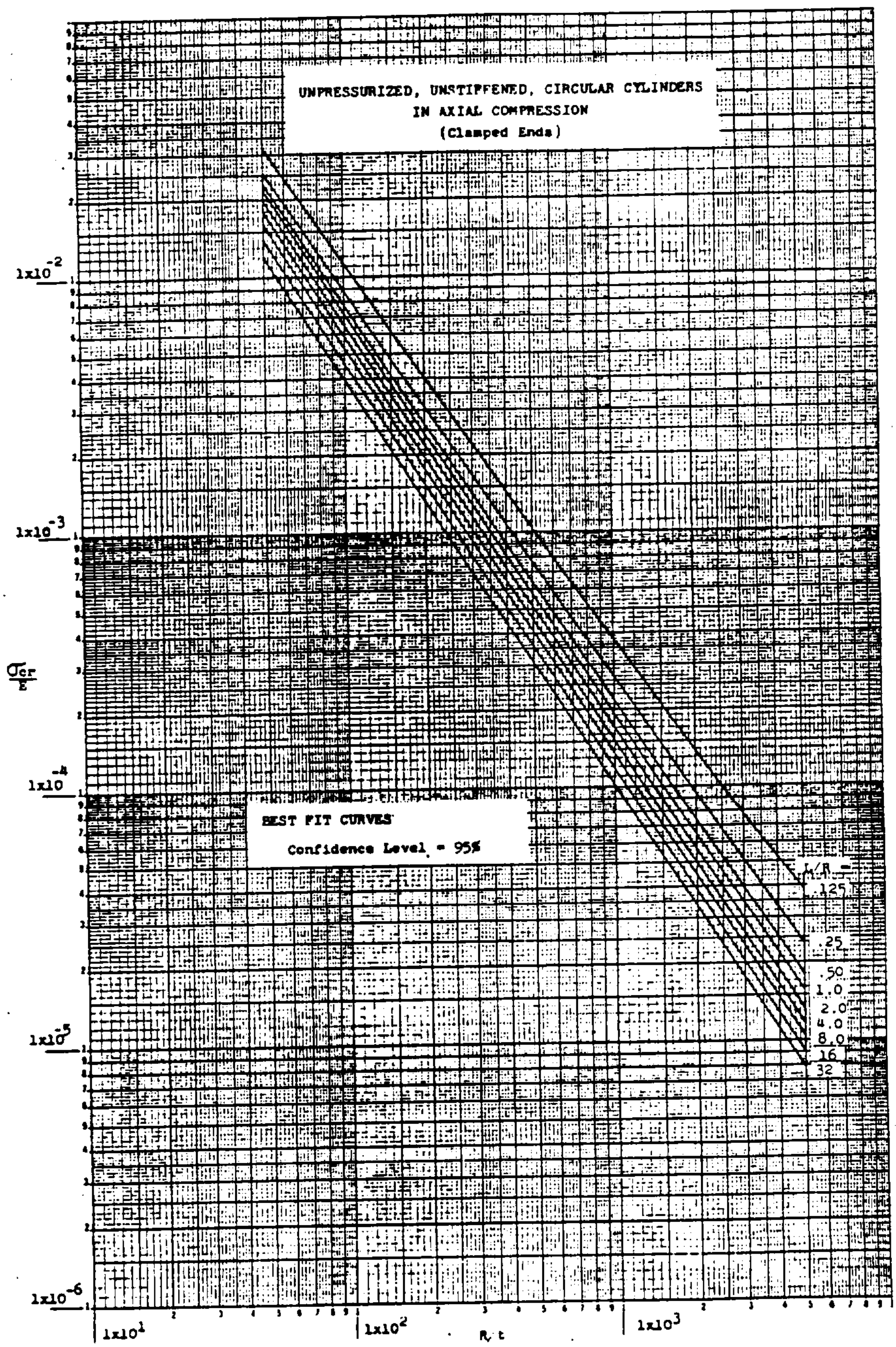
UNPRESSURIZED, UNSTIFFENED, CIRCULAR CYLINDERS
IN AXIAL COMPRESSION
(Clamped Ends)
BEST FIT CURVES
Confidence Level = 95%
L/R =
.125
.25
.50
1.0
2.0
4.0
8.0
16
32
1x10^{-2}
1x10^{-3}
1x10^{-4}
1x10^{-5}
1x10^{-6}
$\frac{\sigma_{cr}}{E}$
1x10^1
1x10^2
1x10^3
R/t

Fig. 10.2.1.1

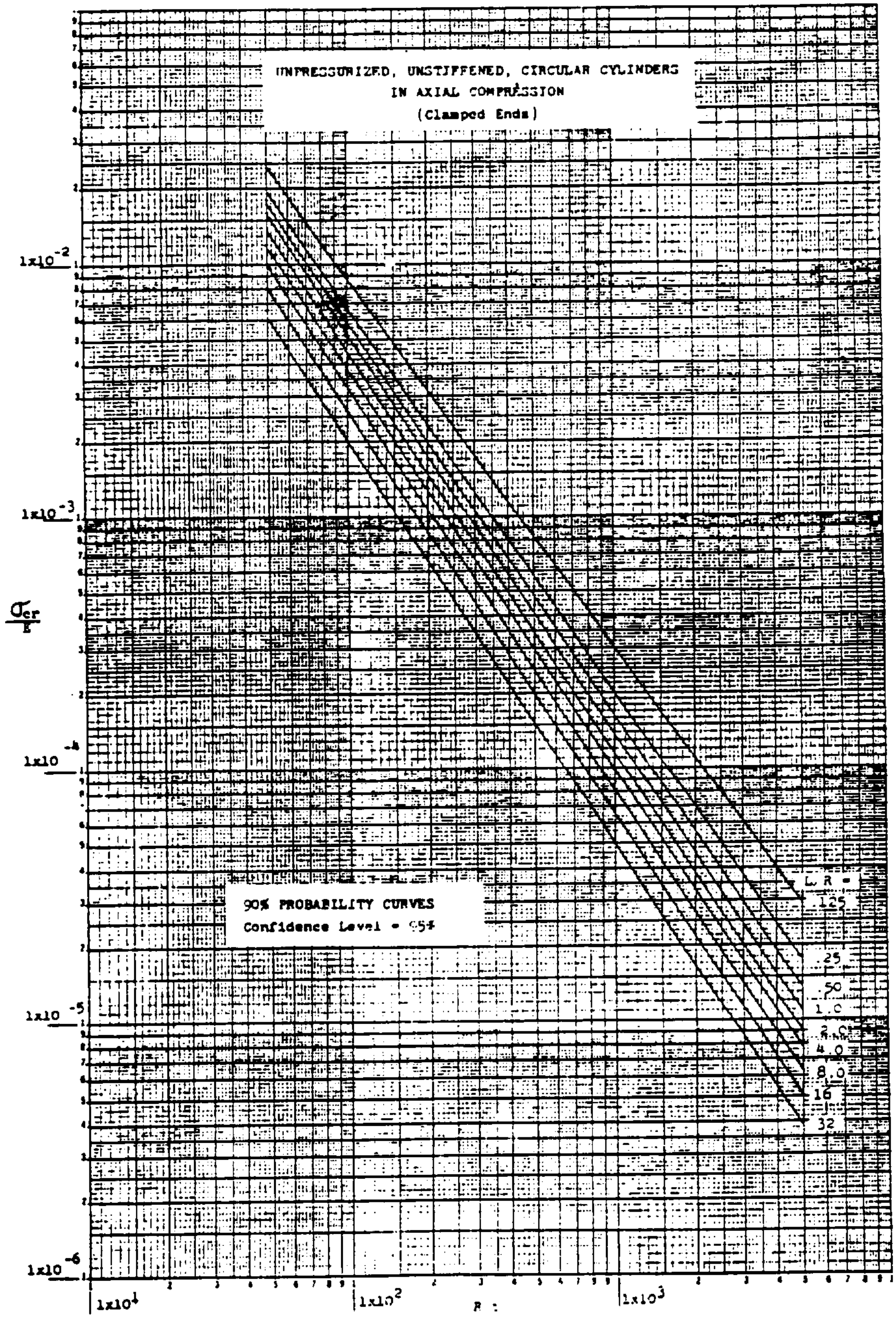
UNPRESSURIZED, UNSTIFFENED, CIRCULAR CYLINDERS
IN AXIAL COMPRESSION
(Clamped Ends)
90% PROBABILITY CURVES
Confidence Level = 95%
L/R =
.125
.25
.50
1.0
2.0
4.0
8.0
16
32
1x10^-2
1x10^-3
1x10^-4
1x10^-5
1x10^-6
σcr/E
1x10^1
1x10^2
1x10^3
R/t

FIG. 10.2.1.2

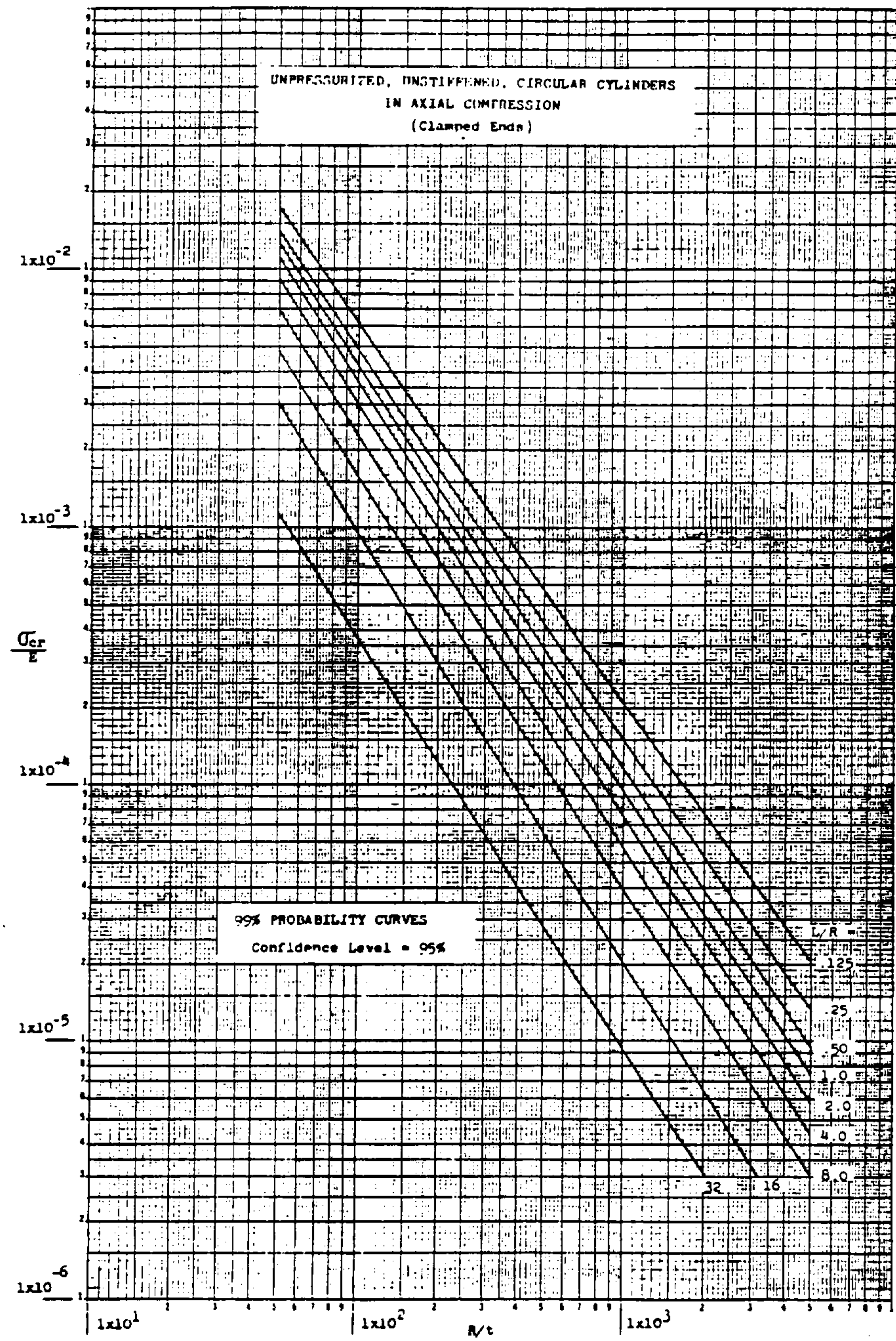
UNPRESSURIZED, UNSTIFFENED, CIRCULAR CYLINDERS
IN AXIAL COMPRESSION
(Clamped Ends)
99% PROBABILITY CURVES
Confidence Level = 95%
L/R =
.125
.25
.50
1.0
2.0
4.0
8.0
16
32
1x10^-2
1x10^-3
1x10^-4
1x10^-5
1x10^-6
σcr/E
1x10^1
1x10^2
1x10^3
R/t

Fig. 10.2.1.3

10.2.2
Effects of Internal Pressure on Axially Compressed Cylinders

Substantial increases in the buckling stress of axially compressed circular cylinders occur as a result of pressurization. The magnitude of this strengthening effect is best predicted by the statistical method of least squares. The curves in Fig. 10.2.2.1 show the increase in buckling stress due to internal pressure. The curves are plotted in terms of the dimensionless parameters

$$\Delta\overline{\sigma}_{cr} = \frac{\Delta\sigma_{cr}}{E}\frac{R}{t}$$

and

$$\overline{p} = \frac{p}{E}\left(\frac{R}{t}\right)^2$$

where p is the internal pressure in pounds per square inch and $\Delta\sigma_{cr}$ is the increase in the buckling stress due to internal pressure based on the unpressurized critical stress given in Section 10.2.1. The curve corresponding to the per cent probability used in determining the unpressurized buckling stress should always be used.

Due to the limited amount of test data available for pressurized cylinders, the curves can be considered reliable only in the ranges:

$1 < L/R \leqslant 6$;

$600 < R/t < 2800$; and

$pR/t \leqslant 0.625\ \sigma_{ty}$

10.2.3
Reduction Factor For Plasticity Effects in Axially Compressed Cylinders

If the buckling stress of the axially compressed cylinder exceeds the yield strength of the material, it must be multiplied by the theoretical plasticity reduction factor, η.

$$\eta = \left(\frac{E_t}{E_s}\right)^{1/2}\left(\frac{E_s}{E}\right)\left[\frac{(1-\mu_e^2)}{(1-\mu^2)}\right]^{1/2}$$

where subscript "e" refers to elastic range.

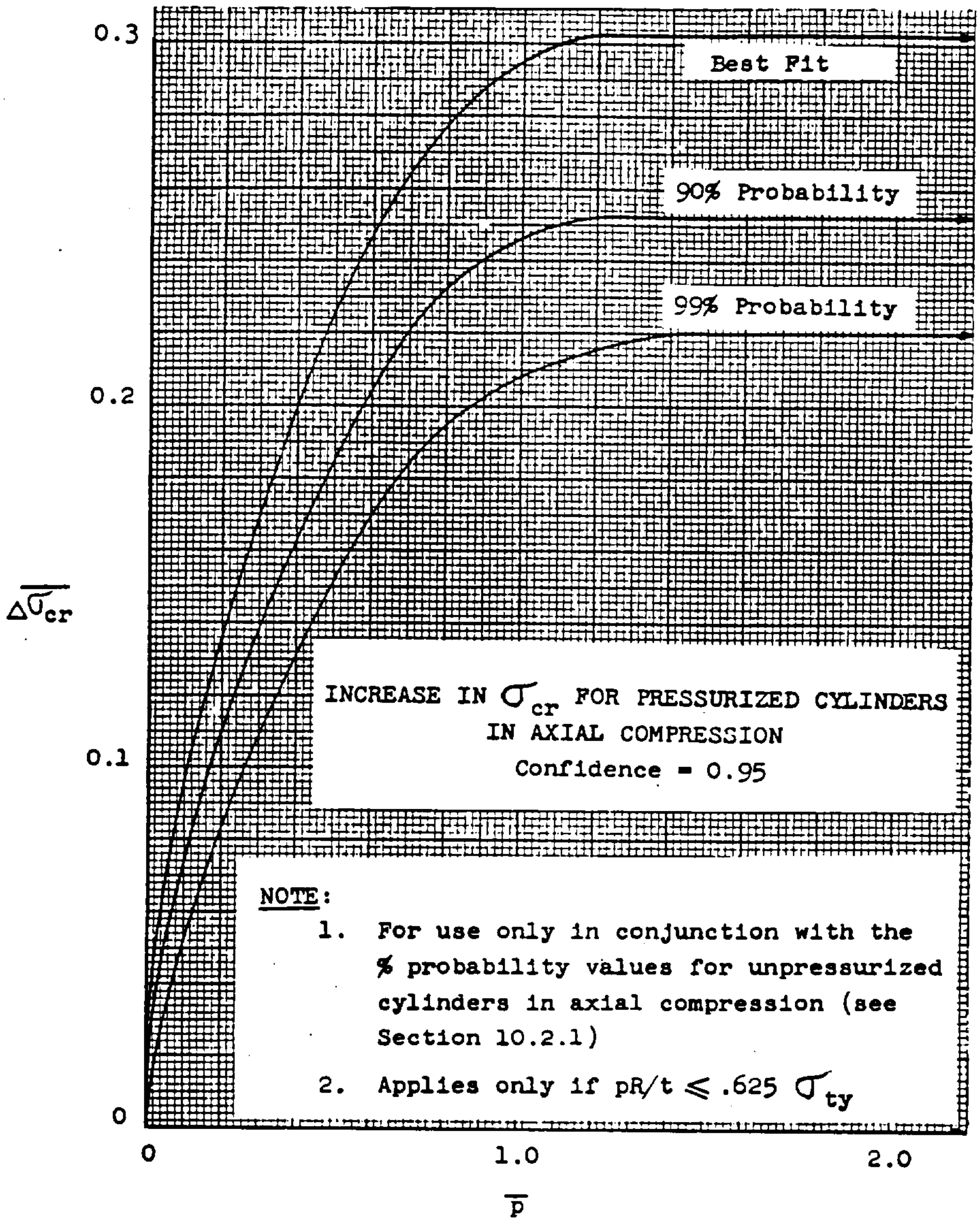
0.3
0.2
0.1
0
$\overline{\Delta\sigma_{cr}}$
0
1.0
2.0
$\overline{p}$
Best Fit
90% Probability
99% Probability
INCREASE IN σ_{cr} FOR PRESSURIZED CYLINDERS
IN AXIAL COMPRESSION
Confidence = 0.95
NOTE:
1. For use only in conjunction with the % probability values for unpressurized cylinders in axial compression (see Section 10.2.1)
2. Applies only if $pR/t \leqslant .625\ \sigma_{ty}$

Fig. 10.2.2.1

10.2.4

Bending

The buckling behavior of a cylinder under bending corresponds to that of axially compressed cylinders in two respects. First, linear theory predicts buckling stresses of the same order in magnitude for both cases. Second, the test data are below the predictions of linear theory by approximately the same amount. Consequently, all of the major investigations have been directed toward the correlation of test data on cylinders in bending in a manner similar to that used for axially compressed cylinders. A comparison shows that reasonably good results can be obtained by multiplying the compressive buckling stress by a factor of 1.3 to obtain the critical bending stress. For best results, a statistical analysis was performed in the same manner as for axial compression in Section 10.2.1. The results are plotted in the form of analysis curves in Figs. 10.2.4.1, 10.2.4.2, and 10.2.4.3. These curves can be used when restricted to the following limitations:

1. Most of the test data upon which these curves are based fall within the range of cylinder dimensions $.25 < L/R < 5$, and $300 < R/t < 1500$.
2. The curves are based on tests of steel, aluminum, and brass cylinders only.

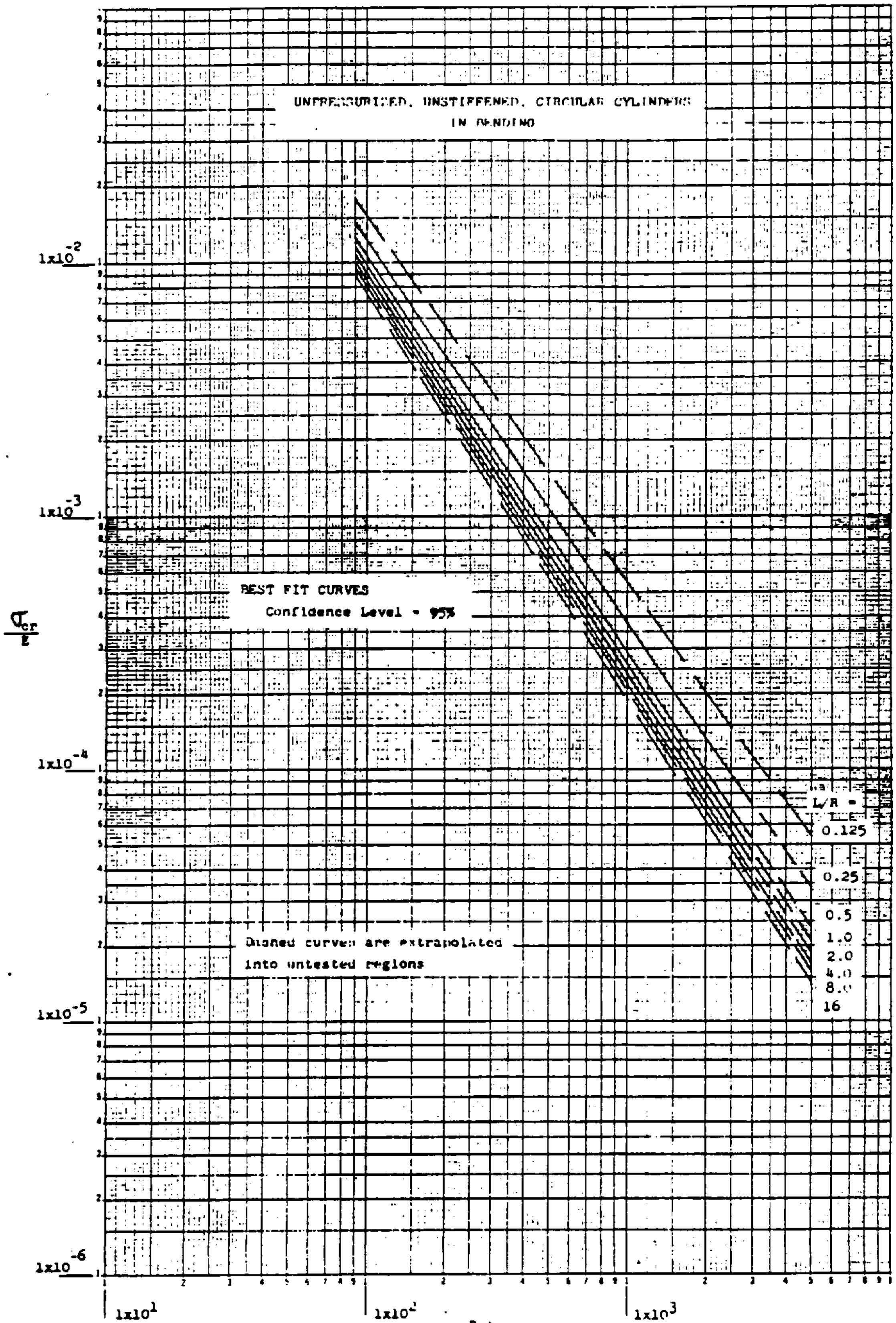
UNPRESSURIZED, UNSTIFFENED, CIRCULAR CYLINDERS
IN BENDING
BEST FIT CURVES
Confidence Level = 95%
Dashed curves are extrapolated
into untested regions
L/R =
0.125
0.25
0.5
1.0
2.0
4.0
8.0
16
1x10^{-2}
1x10^{-3}
1x10^{-4}
1x10^{-5}
1x10^{-6}
$\frac{\sigma_{cr}}{E}$
1x10^{1}
1x10^{2}
1x10^{3}
R/t

Fig. 10.2.4.1

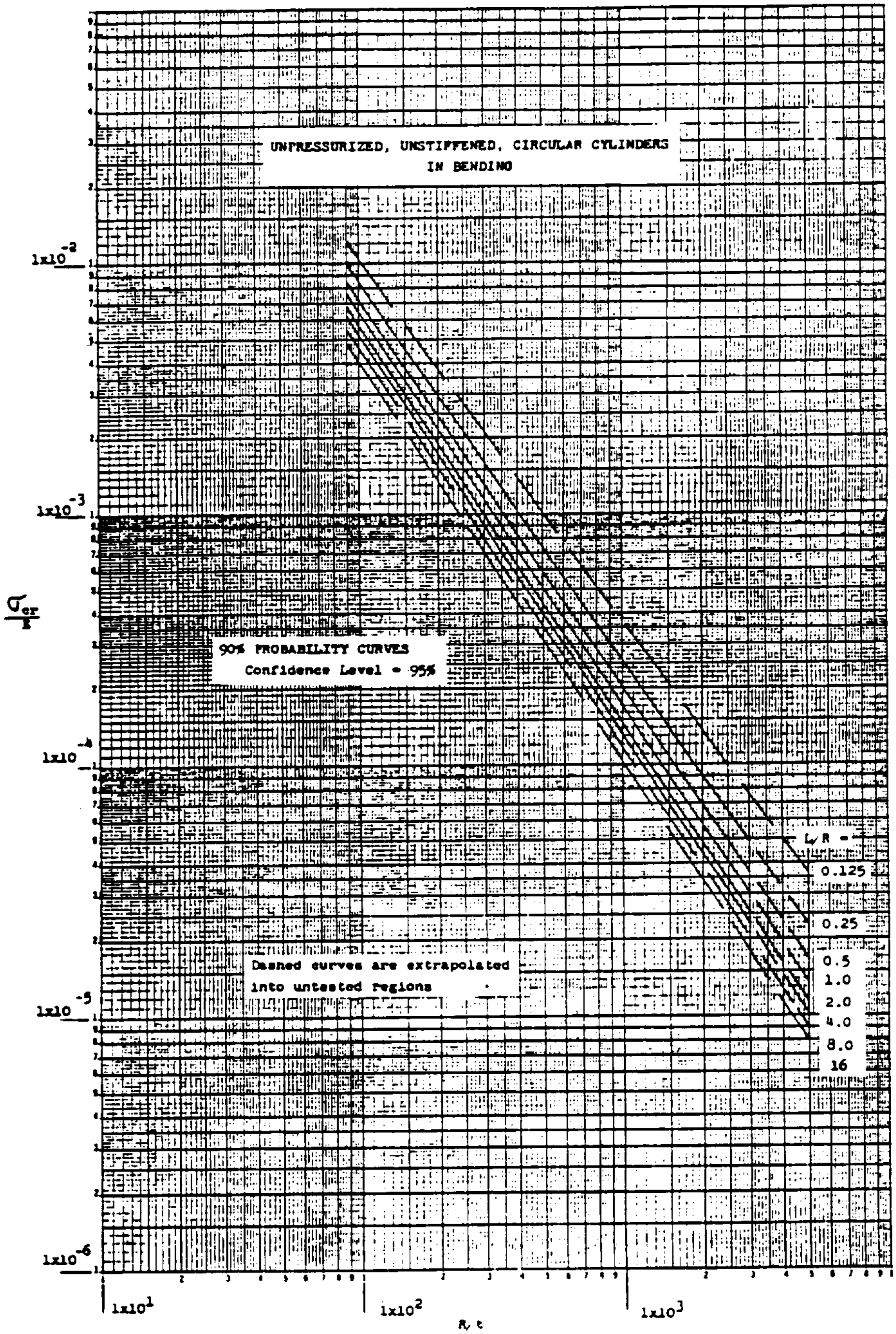
UNPRESSURIZED, UNSTIFFENED, CIRCULAR CYLINDERS IN BENDING
90% PROBABILITY CURVES
Confidence Level = 95%
Dashed curves are extrapolated into untested regions
L/R =
0.125
0.25
0.5
1.0
2.0
4.0
8.0
16
1x10^-2
1x10^-3
1x10^-4
1x10^-5
1x10^-6
σcr/E
1x10^1
1x10^2
1x10^3
R/t

Fig. 10.2.4.2

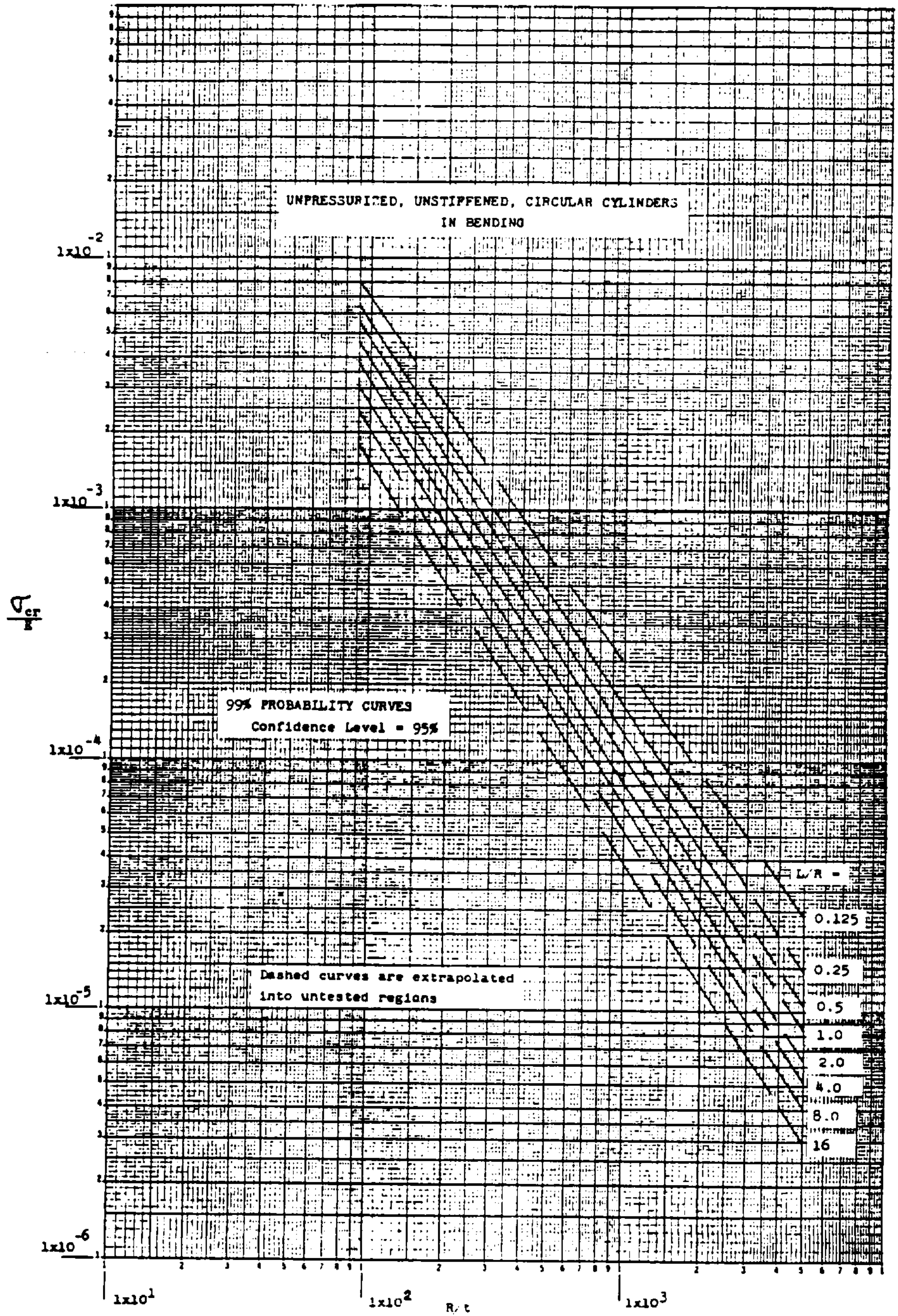
UNPRESSURIZED, UNSTIFFENED, CIRCULAR CYLINDERS IN BENDING
99% PROBABILITY CURVES
Confidence Level = 95%
Dashed curves are extrapolated into untested regions
L/R =
0.125
0.25
0.5
1.0
2.0
4.0
8.0
16
1x10^-2
1x10^-3
1x10^-4
1x10^-5
1x10^-6
σcr/E
1x10^1
1x10^2
1x10^3
R/t

Fig. 10.2.4.3

10.2.7
Torsion

The buckling behavior of a cylinder in torsion differs from cylinders in compression or bending in two respects. First, linear theory more nearly predicts the magnitude of the buckling stress for cylinders in torsion. Second, initial buckling and failure do not occur simultaneously, the former preceding the latter by a small margin. Linear theory, however, is not as accurate as statistical analysis which is again presented in the form of analysis curves. The curves in Figures 10.2.7.1, 10.2.7.2, and 10.2.7.3 can be used for cylinders in torsion when subject to the following limitations:

1. Most of the test data from which these curves are based fall within the range of cylinder dimensions

$$6 < H < 5(R/t)^2$$

where

$$H = \sqrt{1-\mu^2}\ \frac{L^2}{td}$$

2. The curves are based on tests of steel and aluminum cylinders only.

10.2.8
Effects of Internal Pressure on Cylinders in Torsion

Theory and test data indicate that pressurization has a strengthening effect on cylinders in torsion. There is not enough test data available, however, to verify theoretical results or to serve as a basis for a statistical analysis. Further testing will have to be done before design curves can be established.

10.2.9
Reduction Factor For Plasticity Effects in Cylinders in Torsion

If the buckling stress of cylinder in torsion exceeds the yield strength of the material, it must be multiplied by the theoretical plasticity reduction factor, η.

$$\eta = \frac{E_s}{E}\left[\frac{1-\mu_e^2}{1-\mu^2}\right]^{3/4}$$

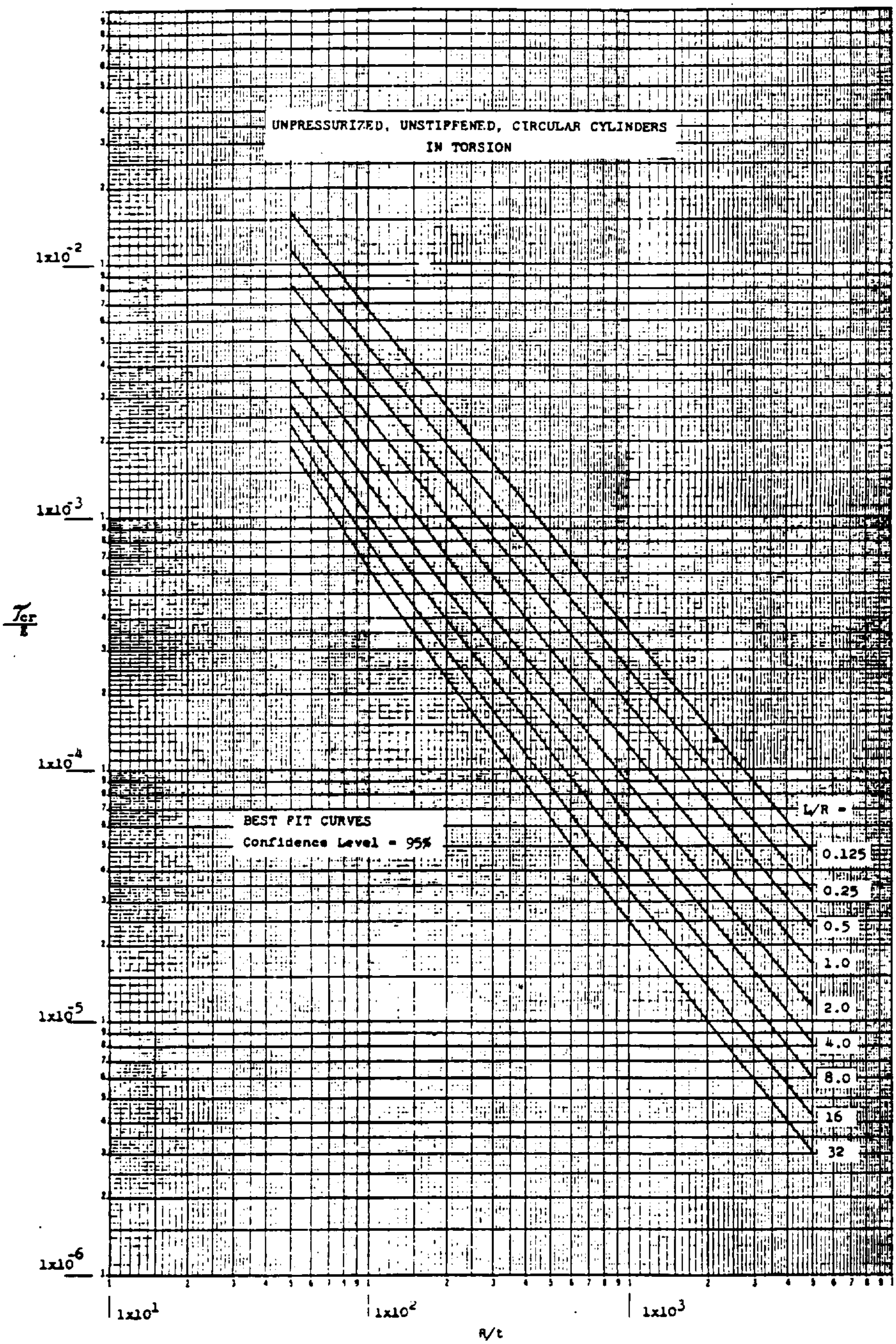
UNPRESSURIZED, UNSTIFFENED, CIRCULAR CYLINDERS
IN TORSION
BEST FIT CURVES
Confidence Level = 95%
L/R =
0.125
0.25
0.5
1.0
2.0
4.0
8.0
16
32
1x10^{-2}
1x10^{-3}
1x10^{-4}
1x10^{-5}
1x10^{-6}
τ_{cr}/E
1x10^{1}
1x10^{2}
1x10^{3}
R/t

Fig. 10.2.7.1

.09

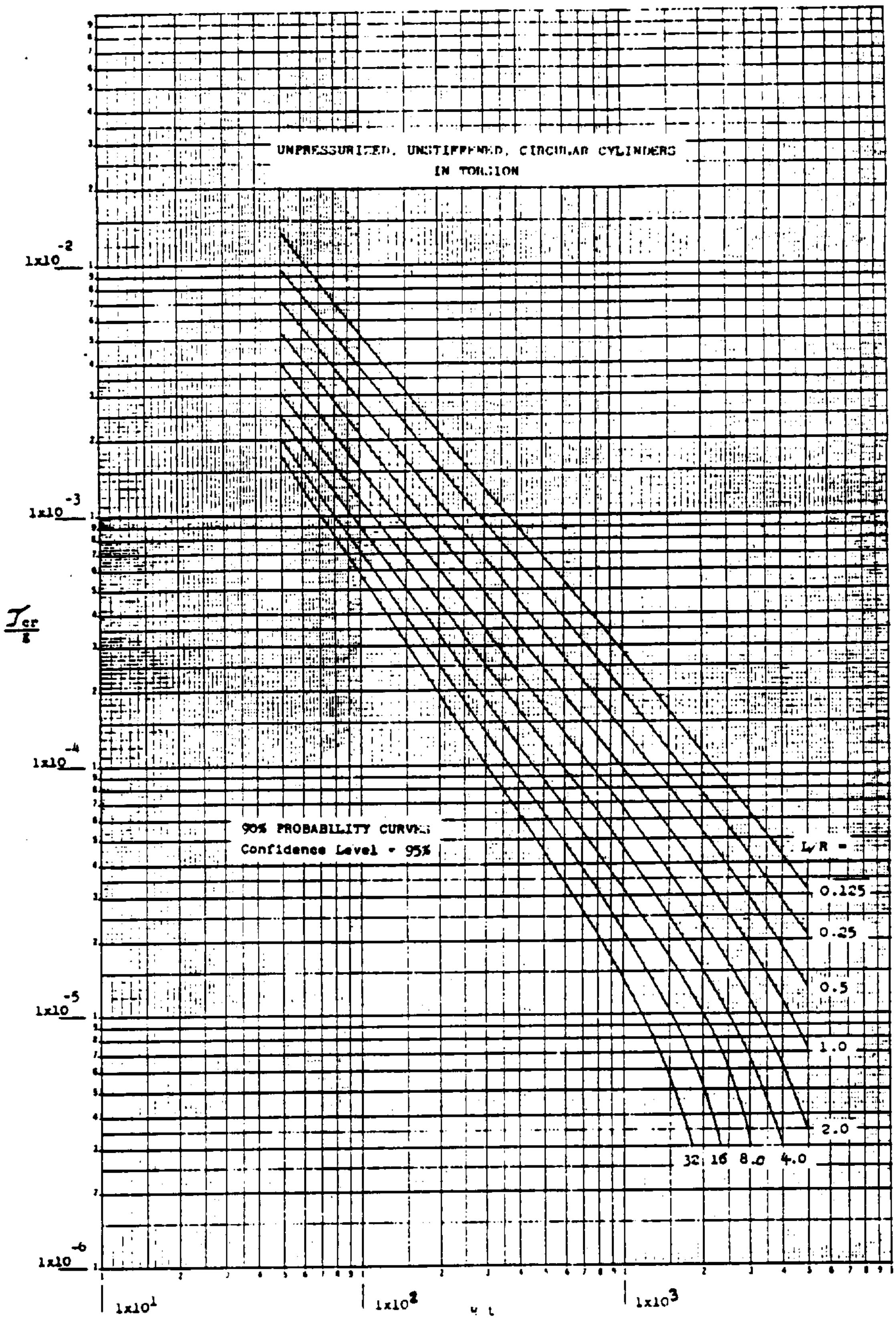
UNPRESSURIZED, UNSTIFFENED, CIRCULAR CYLINDERS
IN TORSION
90% PROBABILITY CURVES
Confidence Level = 95%
L/R =
0.125
0.25
0.5
1.0
2.0
32
16
8.0
4.0
1x10-2
1x10-3
1x10-4
1x10-5
1x10-6
1x10¹
1x10²
1x10³

Fig. 10.2.7.2

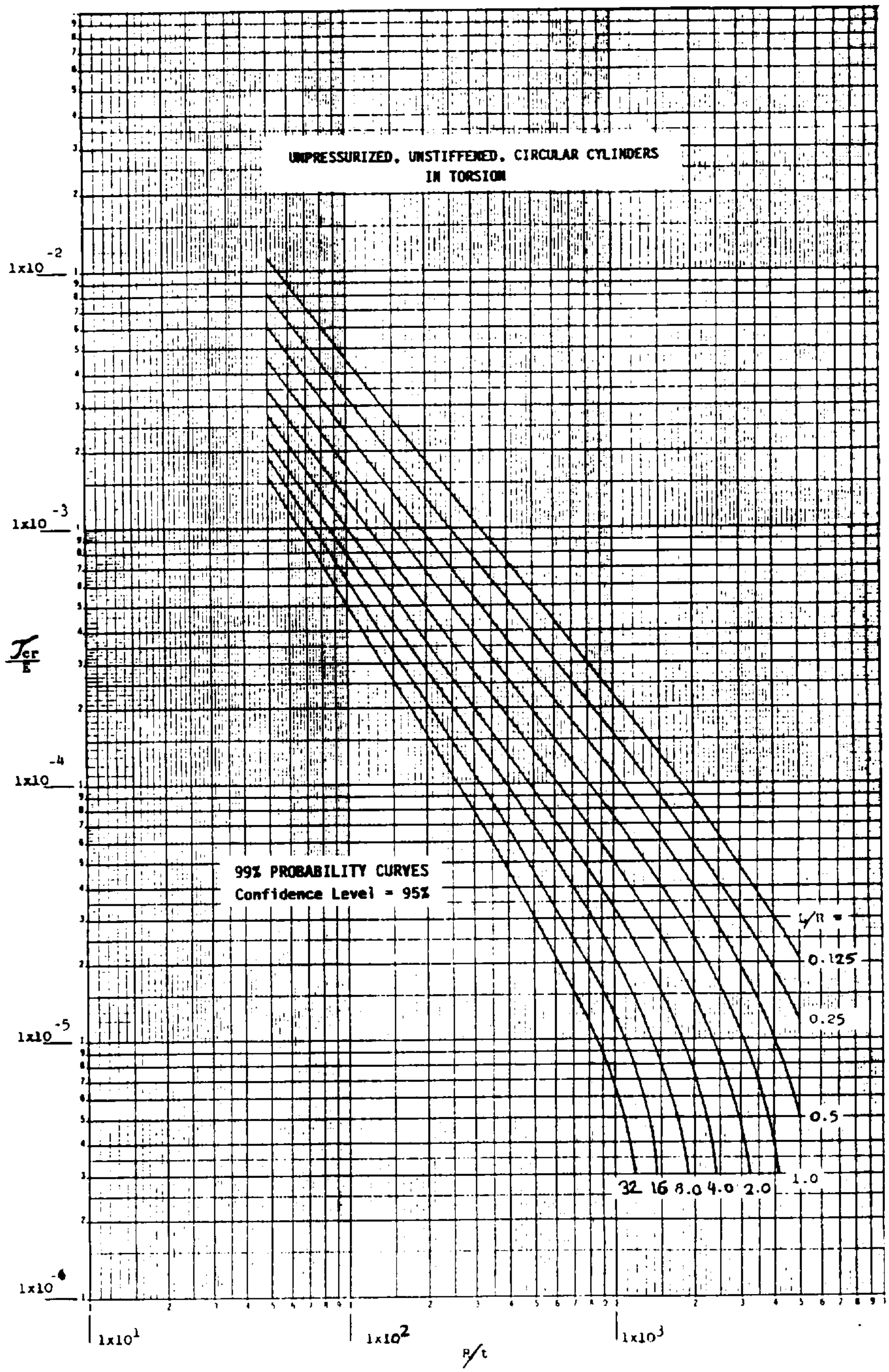
UNPRESSURIZED, UNSTIFFENED, CIRCULAR CYLINDERS
IN TORSION
99% PROBABILITY CURVES
Confidence Level = 95%
L/R =
0.125
0.25
0.5
1.0
32
16
8.0
4.0
2.0
1x10^-2
1x10^-3
1x10^-4
1x10^-5
1x10^-6
τcr/E
1x10^1
1x10^2
1x10^3
R/t

Fig. 10.2.7.3

12

FOR APPLICATIONS, SEE SECTION 28.1

10.2.5
<u>Effects of Internal Pressure on Cylinders in Bending</u>

Test results on cylinders in bending indicate that pressurization has a definite strengthening effect as in the case axial compression; however, no theoretical solutions are available to predict the effect on the buckling strength of cylinders in bending. A statistical analysis, based on a limited amount of test data, has been summarized in the curves in Fig. 10.2.5.1. These curves should be used exactly as those for axial compression when observing the following limitations:

1. The curves have been based on test data from one material (steel) only.

2. Test data has been obtained for only one value of $L/R = 2.46$ and two values of R/t, (1006 and 2734).

10.2.6
<u>Reduction Factor for Plasticity Effects for Cylinders in Bending</u>

The plasticity effects on a cylinder in bending are quite complicated; thus there is no simple equation for the plasticity reduction factor, η. The general trend for the ratio, the rupture modulus to the critical buckling stress in compression, is to decrease in the elasto-plastic range from the elastic value of approximately 1.3 (Ref. Section 10.2.4) to some value between one (1) and 1.3 and to increase to a value of $4/\pi$ in the fully plastic range. A conservative estimate for the buckling stress would be obtained by equating this ratio to unity.

More work must be done on this subject before a definite procedure can be established.

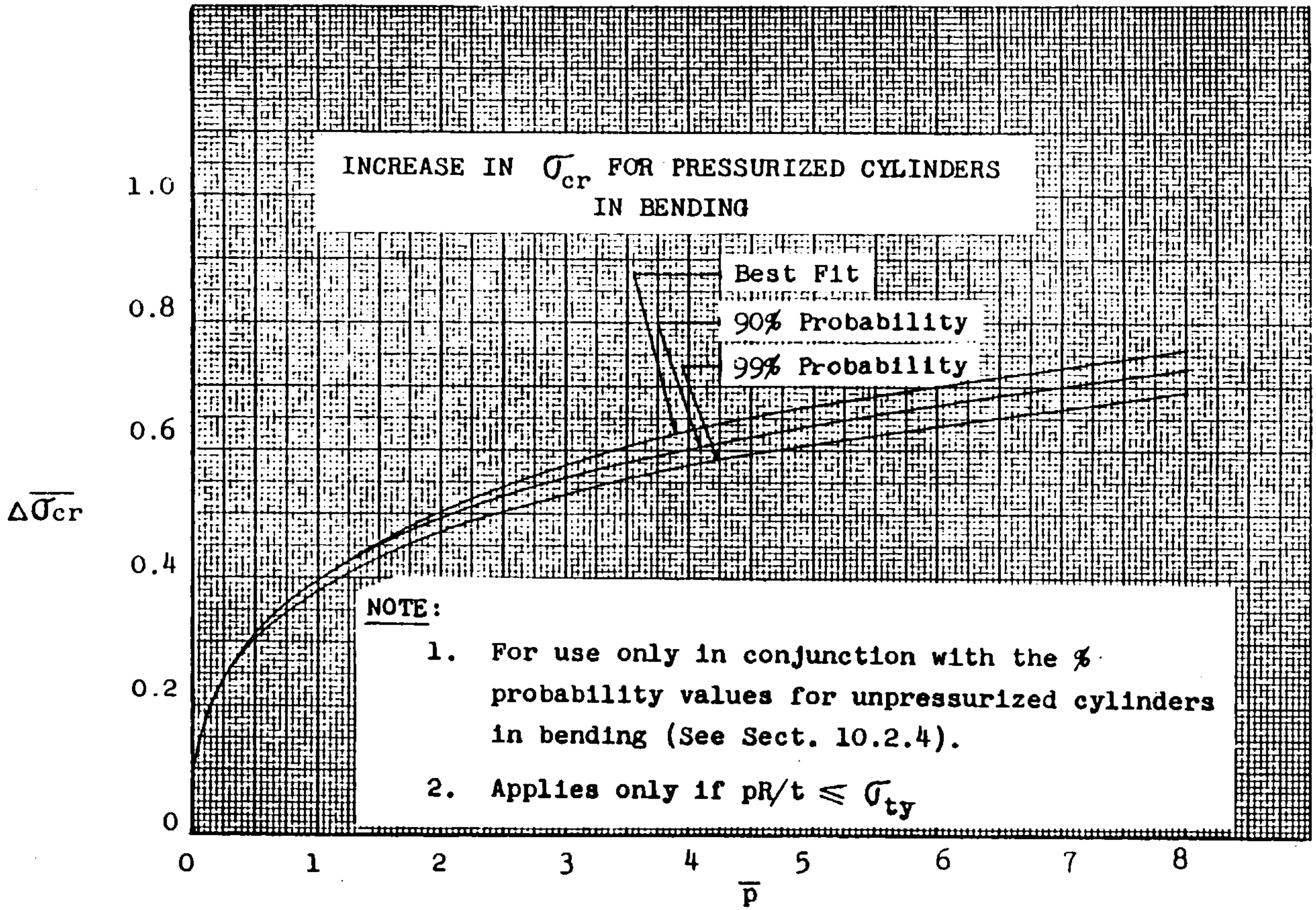
INCREASE IN σ_{cr} FOR PRESSURIZED CYLINDERS IN BENDING
Best Fit
90% Probability
99% Probability
NOTE:
1. For use only in conjunction with the % probability values for unpressurized cylinders in bending (See Sect. 10.2.4).
2. Applies only if $pR/t \leq \sigma_{ty}$
$\Delta\overline{\sigma}_{cr}$
0
0.2
0.4
0.6
0.8
1.0
0
1
2
3
4
5
6
7
8
$\overline{p}$

Fig. 10.2.5.1

10.2.10
Combined Loading

The interaction equations in Table 10.2.10-1 can be used to predict the critical stresses of cylinders under combined loading. The equations are given in terms of the following parameters for use with best fit and 99% probability curves.

$$R_c = \frac{\text{Applied Compressive Load}}{\text{Allowable Compressive Load}}$$

$$R_b = \frac{\text{Applied Bending Moment}}{\text{Allowable Bending Moment}}$$

$$R_t = \frac{\text{Applied Tensile Load}}{\text{Allowable Compressive Load}}$$

$$R_{st} = \frac{\text{Applied Torsional Load}}{\text{Allowable Torsional Load}}$$

Note:

These equations are approximate and should be used with caution.

FIG. 10.2.10-1
COMBINED LOAD INTERACTIONS FOR THE
BUCKLING OF PRESSURIZED AND UNPRESSURIZED CIRCULAR CYLINDERS

COMBINED LOADING CONDITION	INTERACTION EQUATIONS	
	BEST FIT VALUES	99% PROBABILITY VALUES
Axial Compression + Pure Bending	$R_c + R_b = 1.0$	$R_c + R_b = 1.0$
Axial Load + Torsion Comp. + Torsion Tension + Torsion	$R_{st} + R_c = 1.0$ $R_{st} - 0.4R_t = 1.0$	$R_c + (R_{st})^2 = 1.0$ $(R_{st})^3 - R_t = 1.0$ $R_t < 0.8$
Pure Bending + Torsion	$(R_b)^{1.5} + (R_{st})^2 = 1.0$	$(R_b)^{1.5} + (R_{st})^2 = 1.0$
Axial Load (Ten. or Comp.) + Pure Bending + Torsion	$R_c + R_b + (R_{st})^2 = 1.0$	$R_c + R_b + (R_{st})^2 = 1.0$

REFERENCES

10.2.0
Cylinders

Schumacker, J. G., AZS-27-275, Convair, Astronautics, 1959

SECTION 10.3: CYLINDERS EXTERNALLY PRESSURIZED

REFERENCE: NASA SP-8007 "BUCKLING OF THIN-WALLED CIRCULAR CYLINDERS"

The critical lateral pressure is given by:

$$P = \frac{0.855\ E\ (\gamma)^{1/2}}{(1-\mu^2)^{3/4}\ (r/t)^{5/2}\ (l/r)} \qquad \text{PSI}$$

For $\mu = 0.3$, the critical pressure is given by:

$$P^* = \frac{0.926\ E\ (\gamma)^{1/2}}{(r/t)^{5/2}\ (l/r)} \qquad \text{PSI}$$

*For intermediate length cylinders with:

$$\{100 < \gamma Z < 11.8\ (r/t)^2\ (1-\mu^2)\}$$

Where:

μ	=	Poisson's Ratio
E	=	Young's Modulus (PSI)
r	=	Cylinder Radius (IN)
t	=	Cylinder Wall Thickness (IN)
l	=	Cylinder Length (IN)
$(\gamma)^{1/2}$	=	Correlation Factor = 0.75
Z	=	$(l^2/rt)\ (1-\mu^2)^{1/2}$

CYLINDERS, SHELLS AND MEMBRANES

SECTION 10.3: CYLINDERS EXTERNALLY PRESSURIZED (cont.)

REFERENCE: NASA SP-8007 "BUCKLING OF THIN-WALLED CIRCULAR CYLINDERS"

The critical lateral pressure is given by:

$$P^{**} = \frac{\gamma E (t/r)^3}{4(1-\mu^2)} \quad \text{PSI}$$

** For long cylinders, with:

$$\gamma Z > 11.8 (r/t)^2 (1-\mu^2)$$

Where:

μ = Poisson's Ratio

E = Young's Modulus (PSI)

r = Cylinder Radius (IN)

t = Cylinder Wall Thickness (IN)

l = Cylinder Length (IN)

γ = Correlation Factor = 0.90

Z = $(l^2/rt)(1-\mu^2)^{1/2}$

616

SECTION 10.4: TRUNCATED CONES

REFERENCE: NASA SP-8019 "BUCKLING OF THIN-WALLED TRUNCATED CONES"

UNPRESSURIZED ISOTROPIC CONICAL SHELL.

AXIAL COMPRESSION:

The critical load for long conical shells can be expresed as:

$$P_{cr} = \frac{(\gamma\, 2\, \pi\, E\, t^2 \cos^2\alpha)}{\{\, 3\, (1-\mu^2)\, \}^{1/2}}$$

Where: γ = Correlation Factor = 0.33

BENDING:

The buckling moment can be expressed by:

$$M_{cr} = \frac{(\gamma\, \pi\, E\, t^2\, r_1 \cos^2\alpha)}{\{\, 3\, (1-\mu^2)\, \}^{1/2}}$$

Where: γ = Correlation Factor = 0.41

CYLINDERS, SHELLS AND MEMBRANES

SECTION 10.4: TRUNCATED CONES (cont.)

LATERAL PRESSURE:

The critical buckling pressure can be expressed in the approximate form (for $\mu = 0.3$) as:

$$P_{cr} = \frac{0.92\, E\, \gamma}{(L / \bar{\rho})\, (\bar{\rho} / t)^{5/2}}$$

Where: $\gamma = 0.75$

TORSION:

Approximate value for the critical torque of a conical shell is:

$$T_{cr} = 52.8\, \gamma\, D\, (t/l)^{1/2}\, (r/t)^{5/4}$$

Where: $\gamma = 0.67$

and

$$r = r_2 \cos\alpha \, \{1 + [1/2(1 + \{r_2/r_1\})]^{1/2} - [1/2(1 + \{r_2/r_1\})]^{-1/2}\} r_1/r_2$$

The variation of the bracketed function with the cone taper ratio $(1 - \{r_1/r_2\})$ is plotted in figure 1. The theoretical value of γ is unity.

619

CYLINDERS, SHELLS AND MEMBRANES

SECTION 10.4: TRUNCATED CONES (cont.)

SYMBOLS:

P_{cr}	Critical Axial Load on Cone (LB)
E	Young's Modulus (PSI)
t	Skin Thickness (IN)
α	Semi Vertex Angle of Cone (DEG)
μ	Poisson's Ratio
r_1	Radius of Small End of Cone (IN)
r_2	Radius of Large End of Cone (IN)
L	Slant Length of Cone (IN)
$\overline{\rho}$	Average Radius of Curvature of Cone (IN) $(r_1 + r_2)/(2 \cos\alpha)$
l	Axial Length of Cone (IN)

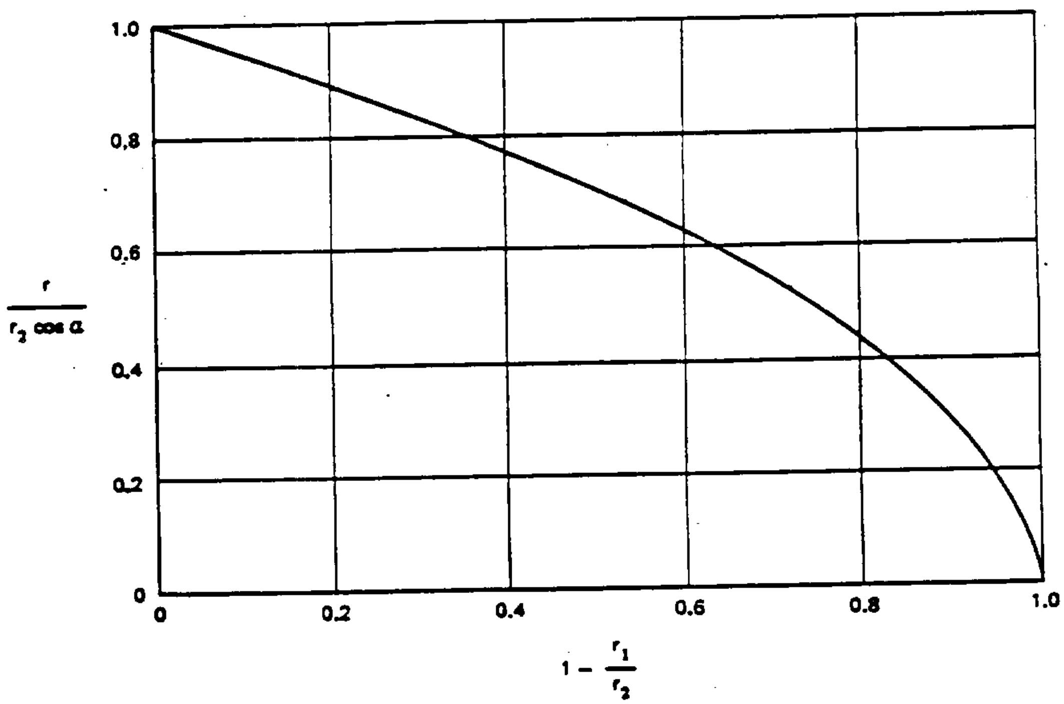

Figure 1
Variation of radius parameter with taper ratio

Data Source, Section 1.3 Reference 17

DOUBLY CURVED SHELLS

SECTION 10.5

REFERENCE NASA SP-8032 "BUCKLING OF THIN-WALLED DOUBLY CURVED SHELLS"

EXTERNAL BUCKLING PRESSURE FOR ELLIPSOIDAL SHELLS IS SHOWN BELOW:

PROLATE SPHEROID, A > B

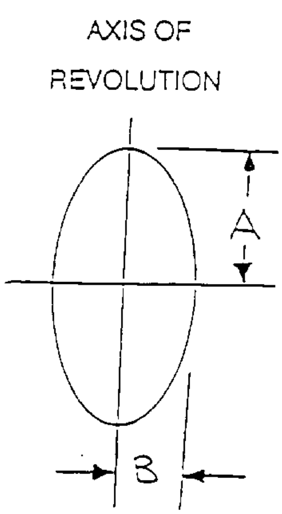

EXTERNAL BUCKLING PRESSURES ARE SHOWN ON FIGURES 6a AND 6b.

FOR A/B $\geq$ 1.5, THE THEORETICAL PRESSURE SHOULD BE MULTIPLIED BY 0.75 TO PROVIDE A LOWER BOUND TO THE DATA.

DOUBLY CURVED SHELLS

OBLATE SPHEROID, B > A

AXIS OF
REVOLUTION

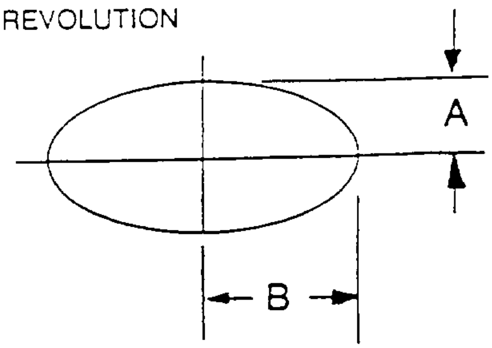

THE EXTERNAL BUCKLING PRESSURE MAY BE APPROXIMATED BY

$$\frac{\sqrt{3\ (1-\mu^2)}}{2} \left(\frac{R_A}{t}\right)^2 \frac{P_{cr}}{E} = 0.14$$ 2

WHERE $R_A = \dfrac{B^2}{A}$

SYMBOLS

t = SHELL THICKNESS, IN

P_{cr} = EXTERNAL BUCKLING PRESSURE, PSI

E = YOUNG'S MODULUS , PSI

μ = POISSON'S RATIO

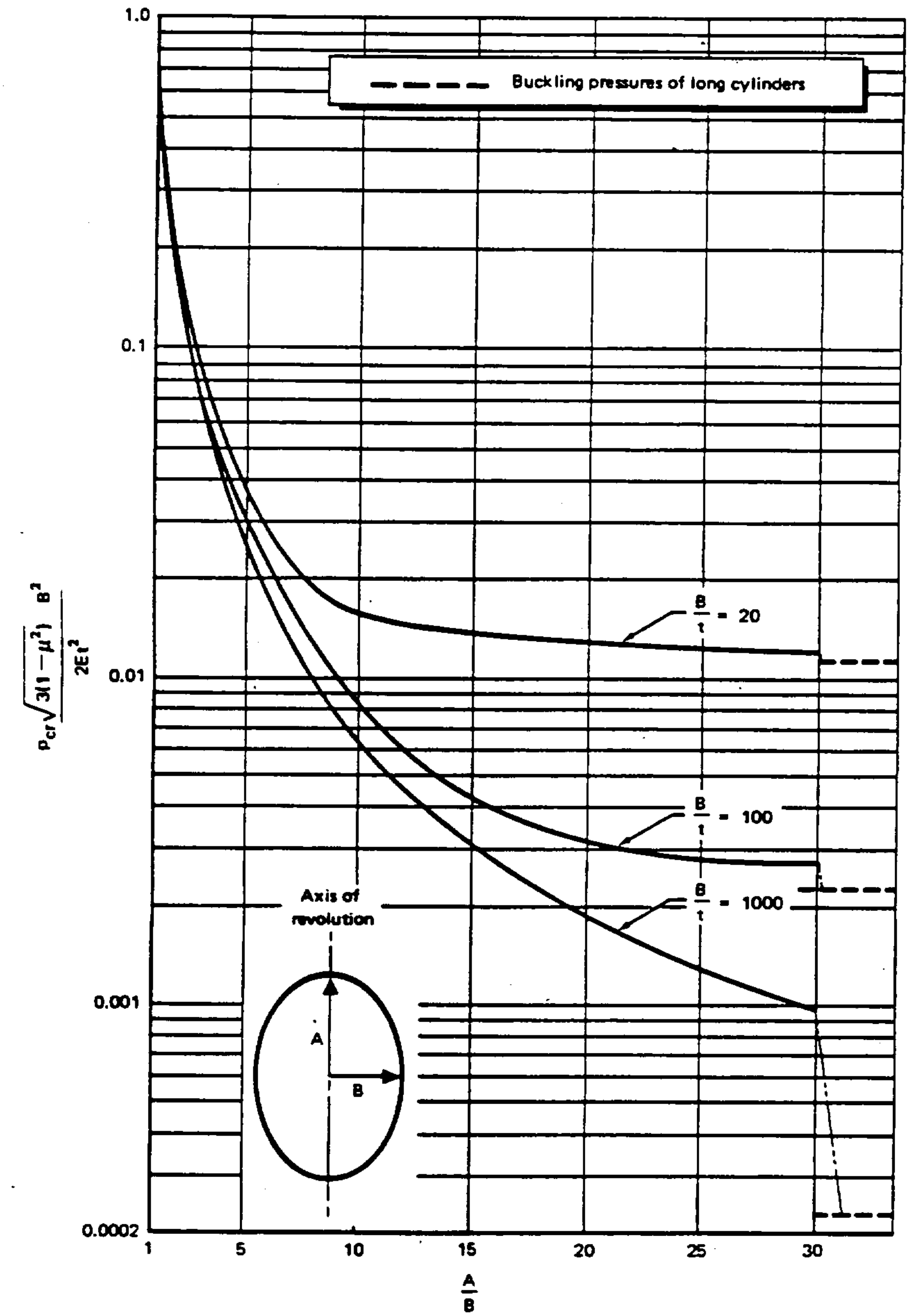

Figure 6a
Theoretical external buckling pressures of prolate spheroids (μ = 0.3)

623

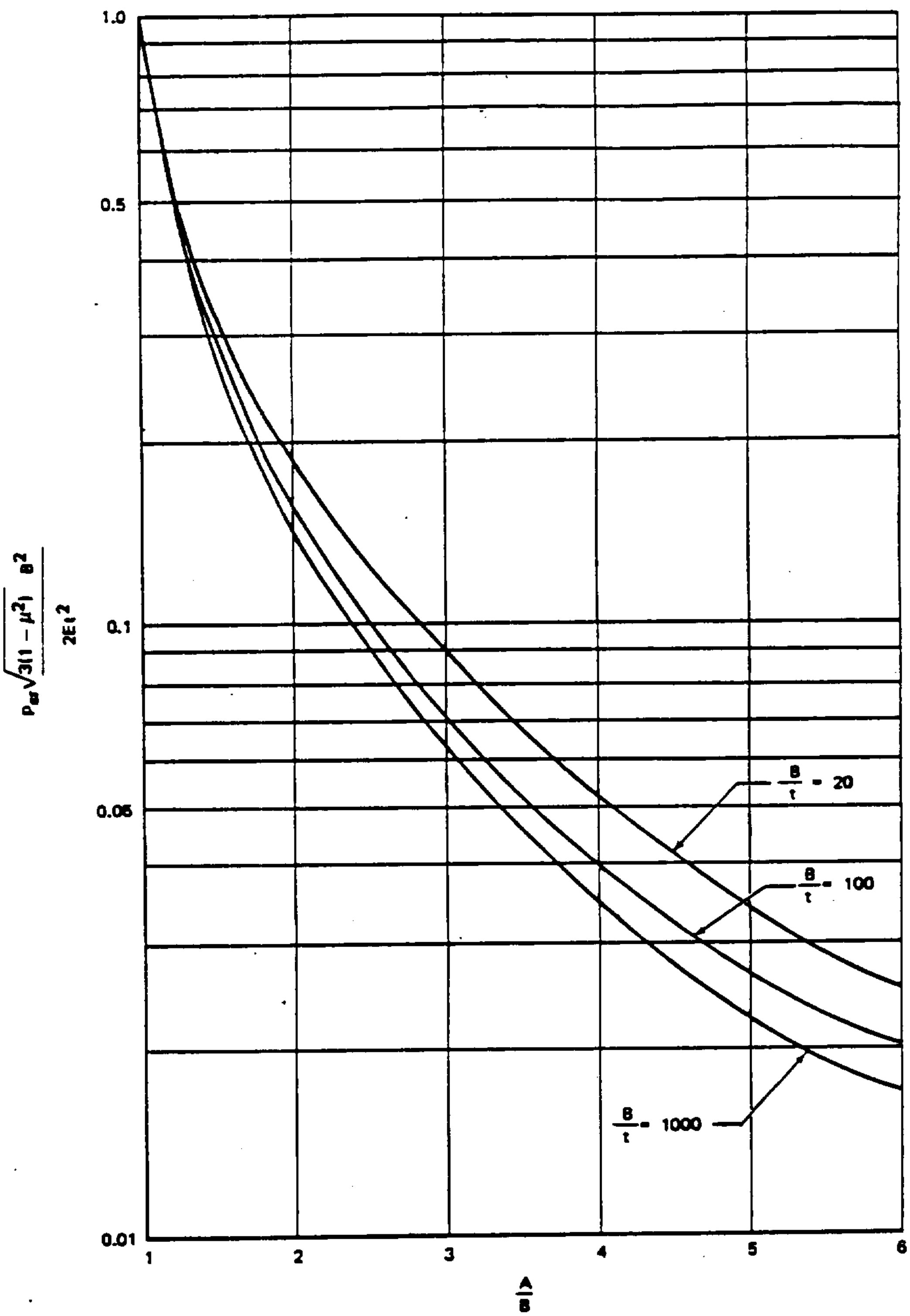

Figure 6b
Theoretical external buckling pressures of prolate spheroids (μ = 0.3)

1024

Data Source, Section 1.3 Reference 18

IMPERFECTIONS

REDUCTION IN THE BUCKLING LOAD OF AN AXIALLY LOADED CYLINDER DUE TO AXISYMMETRIC INITIAL IMPERFECTIONS, IS SHOWN ON THE FIGURE.

REFERENCE: " BUCKLING OF BARS, PLATES, AND SHELLS " D.O. BRUSH AND B. O. ALMROTH.

SYMBOLS:

σ_{CL} = CYLINDER BUCKLING STRESS FOR NO IMPERFECTINS, PSI

= $0.605\ E\ \frac{t}{r}$

σ_{CR} = CYLINDER BUCKLING STRESS WITH INITIAL IMPERFECTIONS, PSI

E = YOUNG'S MODULUS, PSI

t = CYLINDER WALL THICKNESS, IN

r = CYLINDER RADIUS, IN

μ = RATIO OF INITIAL IMPERFECTION TO CYLINDER THICKNESS

= $\frac{e}{t}$

e = DEPTH OF INITIAL IMPERFECTION, IN

25

INFLUENCE OF INITIAL IMPERFECTIONS

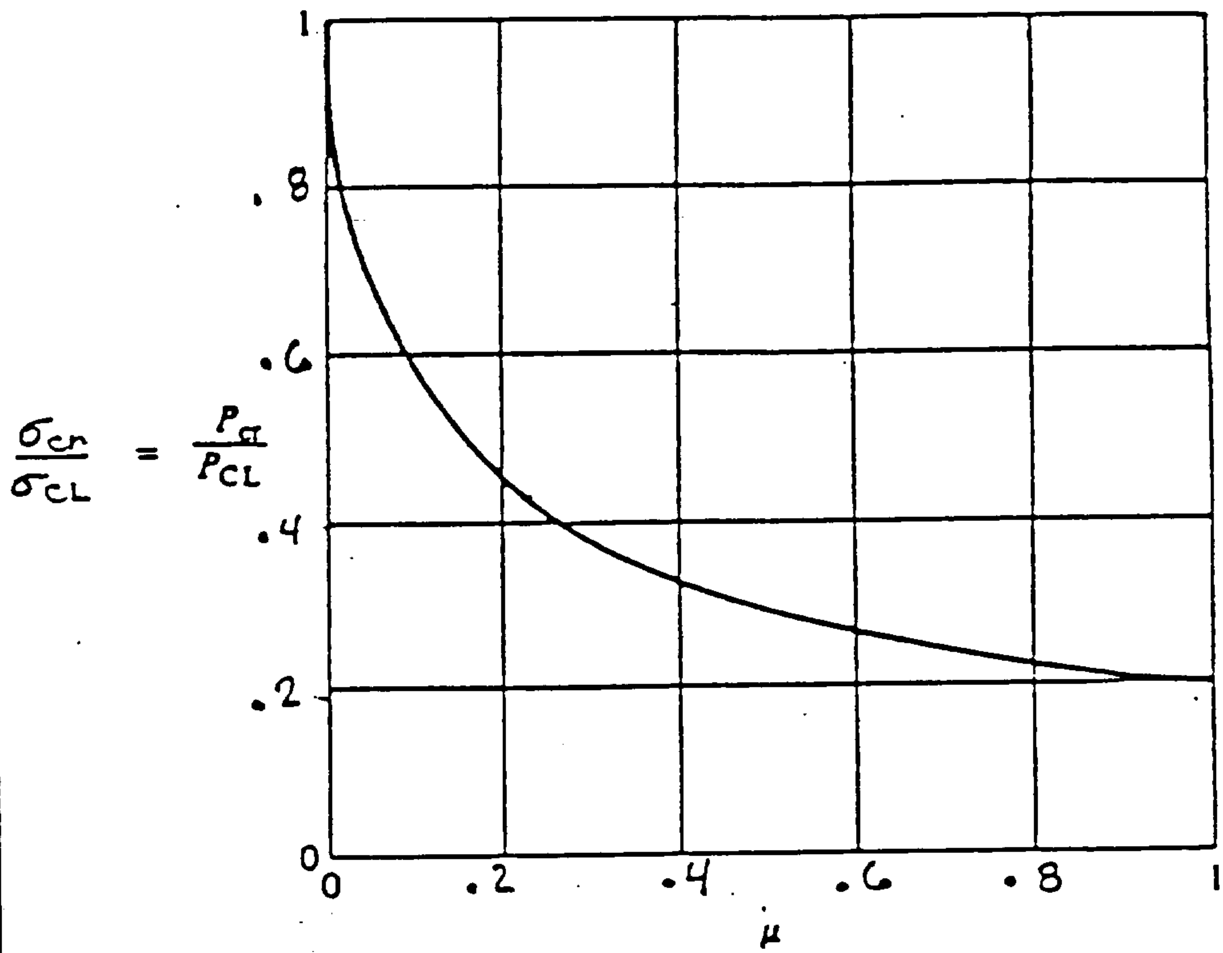

FIGURE 7.3
Influence of imperfection magnitude.

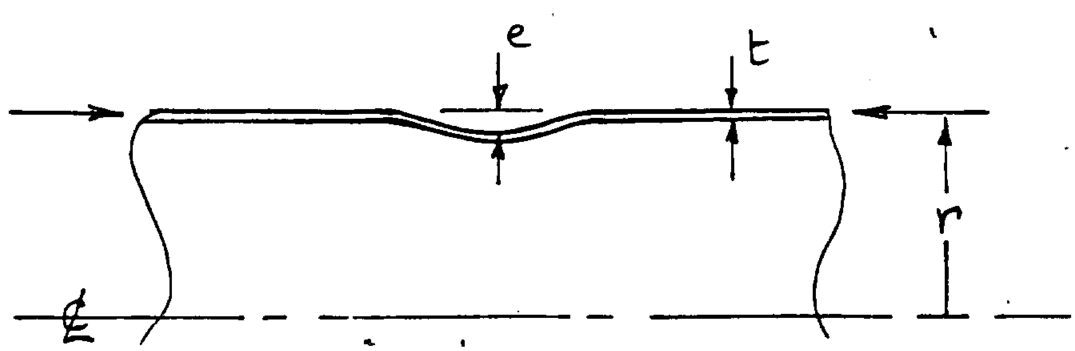

 2

GD
GENERAL DYNAMICS | ASTRONAUTICS

POST-BUCKLING STRENGTH OF A PRESSURIZED CYLINDER

GD/A-DDG 64-024

CONTENTS

	Page
Summary	1
Analysis	1
Numerical Example	2
References	7

ILLUSTRATIONS

No.	Title	Page
1	Loading Conditions	4
2	Stress Distribution	4
3	Bending Strength	5
4	Moment and Tension Stress as Functions of Curvature	6

TABLES

No.	Title	Page
1	Bending Characteristics	3

POST-BUCKLING STRENGTH OF A PRESSURIZED CYLINDER

D. J. Peery

Summary

A simple analysis procedure is presented for a cylinder with axial load and bending moment. The bending stress is assumed linear in the unbuckled region and constant in the buckled region. Further analysis consists of applying the equations of statics. Flexural rigidity is obtained from conventional equations. Charts are presented to simplify numerical calculations.

Analysis

The cylinder of Fig. 1 resists an axial load P_a and an external bending moment M. The assumed stress distribution and notation are shown in Fig. 2. The bending moment is resisted by the load varying from zero at angle θ to a maximum of N per unit length. The pressure, axial load, and uniform load N_c have no moment about the neutral axis. Integrating the values for the triangular distribution, the following results are obtained.

$$P_1 = 2NR \frac{\sin\theta - \theta\cos\theta}{1 - \cos\theta} \tag{1}$$

$$M = NR^2 \frac{\theta - \sin\theta \cos\theta}{1 - \cos\theta} \tag{2}$$

$$\frac{M}{P_1 R} = \frac{\theta - \sin\theta \cos\theta}{2\,(\sin\theta - \theta\cos\theta)} \tag{3}$$

Values of M/P_1R and NR/P_1 are plotted in Fig. 3.

The bending deflection is obtained from the stress distribution of Fig. 2. The stress varies an amount N/t in a distance $R(1-\cos\theta)$. The cylinder bends through an angle ϕ per unit length, obtained as follows.

$$\phi = \frac{N}{EtR\,(1-\cos\theta)} \tag{4}$$

From Equations 1 and 4,

$$P_1 = 2EtR^2\phi\,(\sin\theta - \theta\cos\theta) \qquad (5)$$

From Equations 2 and 4,

$$M = EtR^3\phi\,(\theta - \sin\theta\cos\theta) \qquad (6)$$

It is easier to visualize the characteristics of the cylinder if M is plotted as a function of ϕ, to show a normal type of load-deflection curve. Such a curve is plotted in Fig. 4, which is similar to Fig. 4 of Reference 1. Equations 47 and 48 of Reference 1 correspond to Equations 5 and 6 above, with some change in notation. For N_c=0, the preceding analysis corresponds to the membrane analysis of Reference 1.

Numerical Example

The bending characteristics will be calculated for a cylinder with R = 60", P_a = 40,000 lb, p = 16 psi, t = .014 in, θ = 180°, and N_c = 30 lb/in. The load P_1 is first calculated

$$P_1 = -P_a + \pi R^2 p + 2\pi R N_c$$

$$= -40,000 + 11,300 \times 16 + 377 \times 30 = 152,300 \text{ lb.}$$

From Fig. 3, $M/P_1R = 0.5$, $NR/P_1 = .318$

$$M = 0.5\,P_1R = 0.5 \times 152,300 \times 60 = 4,569,000 \text{ in-lb.}$$

$$N = 0.318\,\frac{P_1}{R} = 0.318 \times 152,300/60 = 807 \text{ lb/in.}$$

$$N_t = N - N_c = 807 - 30 = 777 \text{ lb/in.}$$

$$\sigma_t = N_t/t = 777/.014 = 55,500 \text{ psi}$$

From Fig. 4, $M/(EI\phi) = 1$,

For $E = 33 \times 10^6$, $I = \pi R^3 t = 9.51 \times 10^3$, $EI = 314 \times 10^9$ lb-in^2

For L = 150", $\phi L = ML/EI = 4,569,000 \times 150/314 \times 10^9 = .00218$ rad = .125°

Other values are calculated by the same procedure in Table I. The same cylinder dimensions are used, but various values of θ are considered, and also a pressure increase to 20 psi.

TABLE I

BENDING CHARACTERISTICS

$p = 16$ psi, $P_1 = 152{,}300$ lb.	M	N_t	σ_t	$\phi L = 150\phi$
$\theta = 180°$	4,569,000	777	55,500	.125°
$\theta = 150°$	5,030,000	828	59,100	.141°
$\theta = 120°$	6,010,000	967	69,100	.205°
$\theta = 90°$	7,170,000	1240	88,600	.388°
$p = 20$ psi, $P_1 = 197{,}500$ lb.				
$\theta = 180°$	5,930,000	1018	72,600	.162°
$\theta = 150°$	6,520,000	1083	77,400	.185°
$\theta = 120°$	7,810,000	1265	90,400	.266°
$\theta = 90°$	9,320,000	1618	115,800	.510°

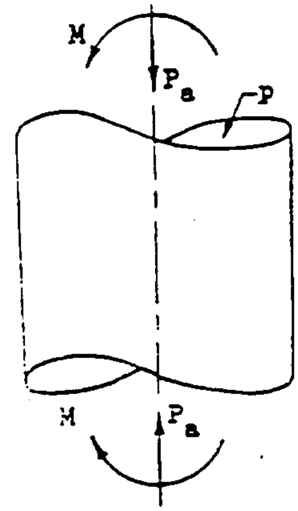

Figure 1 - Loading Conditions

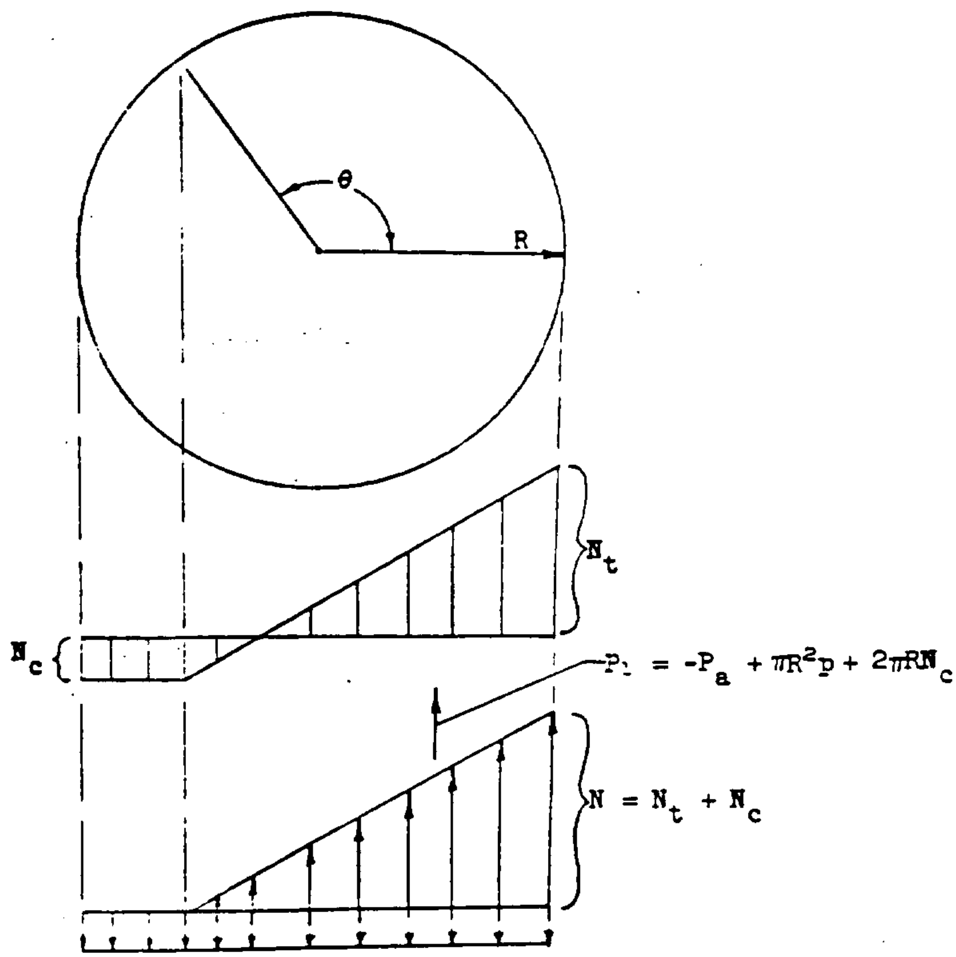

Figure 2 - Stress Distribution

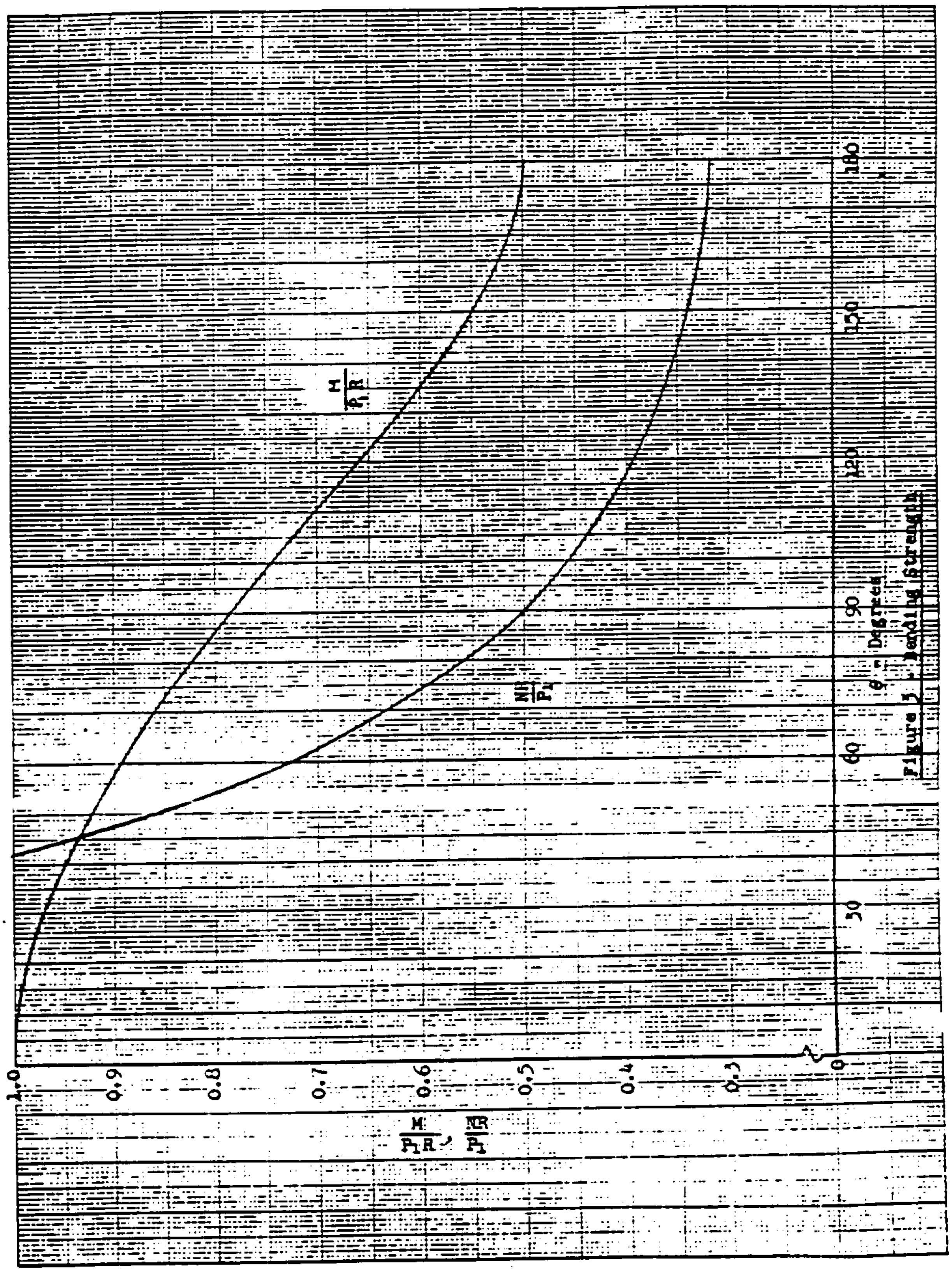

Figure 5 - Bending Strength

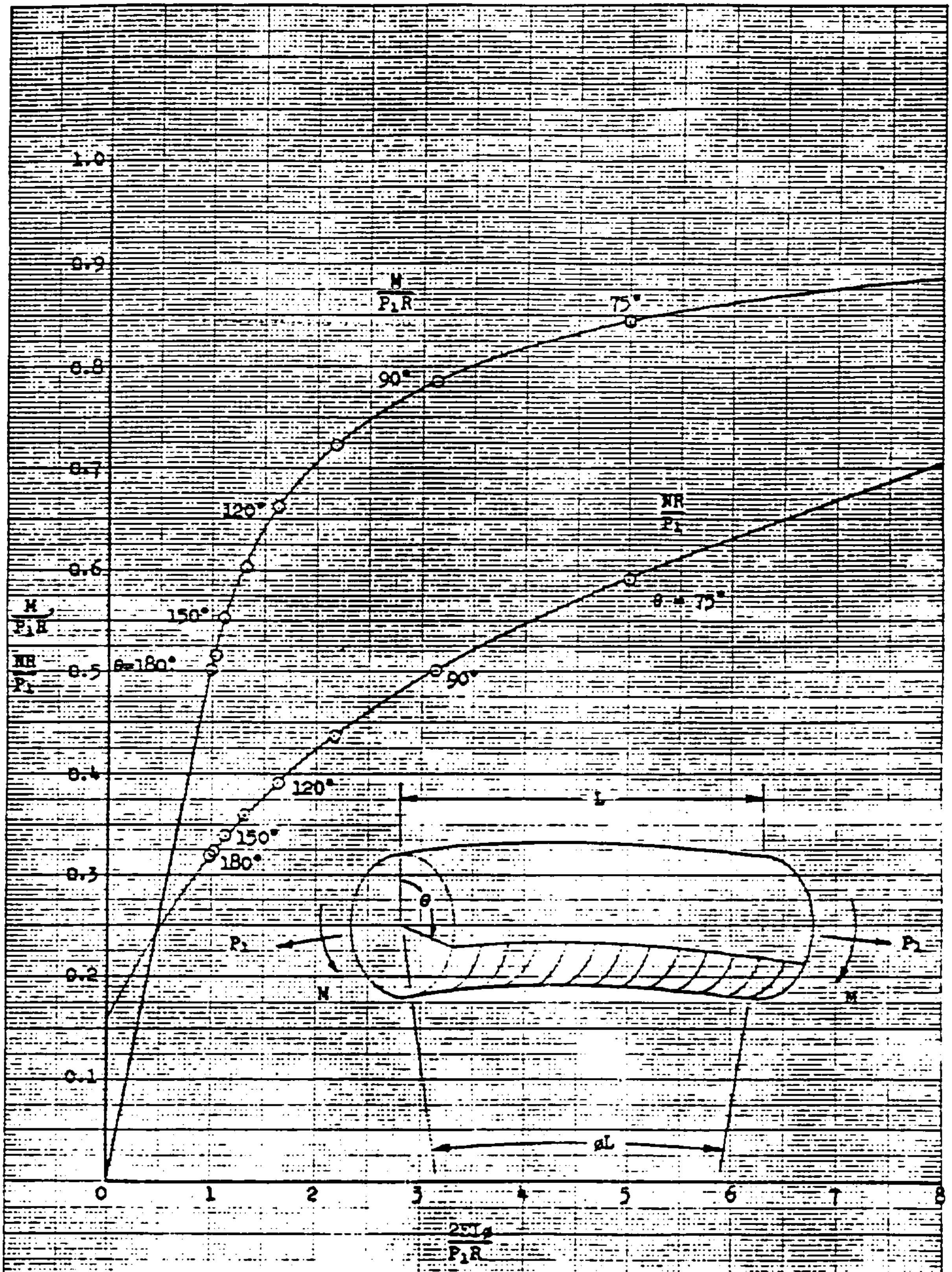

Figure 4 - Moment and Tension Stress as Functions of Curvature

23

GD/A-DDG 64-024

REFERENCES

1. Stein, M., and Hedgepeth, J. M., "Analysis of Partly Wrinkled Membranes," NASA TN D-813, L-1526, July 1961.

Data Source, Section 1.3 Reference 5

TABLE OF CONTENTS

	Page
B7.2.0.0 Local Loads on Thin Shells	10.8.3
7.2.1.0 Local Loads on Spherical Shells	10.8.4
7.2.1.1 General	10.8.5
I Notation	10.8.5
II Sign Convention	10.8.7
III Limitations of Analysis	10.8.10
7.2.1.2 Stresses	10.8.12
I General	10.8.12
II Parameters	10.8.16
III Stresses Resulting from Radial Load	10.8.17
IV Stresses Resulting from Overturning Moment	10.8.19
V Stresses Resulting from Shear Load	10.8.21
VI Stresses Resulting from Twisting Moment	10.8.22
7.2.1.3 Stresses Resulting from Arbitrary Loading	10.8.23
I Calculation of Stresses	10.8.23
II Location and Magnitude of Maximum Stresses	10.8.24
7.2.1.4 Ellipsoidal Shells	10.8.25
7.2.1.5 Nondimensional Stress Resultant Curves	10.8.26
I List of Curves	10.8.26
II Curves	10.8.27
7.2.1.6 Example Problem	10.8.50
7.2.2.0 Local Loads on Cylindrical Shells	10.8.54
7.2.2.1 General	10.8.55
I Notation	10.8.55
II Sign Convention	10.8.57
III Limitations of Analysis	10.8.61

TABLE OF CONTENTS (Concluded)

		Page
7.2.2.2	Stresses	10.8.65
I	General	10.8.65
II	Stresses Resulting from Radial Load	10.8.67
III	Stresses Resulting from Overturning Moment	10.8.69
IV	Stresses Resulting from Shear Load	10.8.71
V	Stresses Resulting from Twisting Moment	10.8.72
7.2.2.3	Stresses Resulting from Arbitrary Loading	10.8.73
I	Calculation of Stresses	10.8.73
II	Location and Magnitude of Maximum Stress	10.8.74
7.2.2.4	Displacements	10.8.75
References		10.8.76

SEE ALSO SECTION 28.3

2

B7.2.0.0 LOCAL LOADS ON THIN SHELLS

The method contained in this section for determining stresses and displacements in thin shells is based on analyses performed by P. P. Bijlaard. These analyses represent the local loads and radial displacement in the form of a double Fourier series. The equations developed using these series and the necessary equilibrium considerations are readily solved by numerical techniques for stresses and displacements.

The stresses and displacements calculated by the methods of this section can be superimposed upon the stresses caused by other loadings if the specified limitations are observed.

The equations for determining stresses in spherical shells caused by local loads have been evaluated within the parametric ranges of space vehicle interest for radial load and overturning moment. The results of this evaluation have been plotted and are contained in this section for use in determining the stresses. A direct method is presented for determining the stresses in spherical shells caused by locally applied shear load or twisting moment. No method is provided to calculate displacements of spherical shells caused by local loads.

The equations for determining stresses and displacements in cylindrical shells caused by local loads have been programmed in Fortran IV for radial load and overturning moment. A direct method is presented for determining the stresses in cylindrical shells caused by a locally applied shear load or twisting moment. No method is provided to calculate displacements of cylindrical shells caused by locally applied shear loads or twisting moments.

B7.2.1.0 LOCAL LOADS ON SPHERICAL SHELLS*

This section presents a method of obtaining spherical shell membrane and bending stresses resulting from loads induced through rigid attachments at the attachment-to-shell juncture. Shell and attachment parameters are used to obtain nondimensional stress resultants from curves for the radial load and overturning moment load condition. The values of the stress resultants are then used to calculate stress components. Shear stresses caused by shearing loads and twisting moment can be calculated directly.

Local load stresses reduce rapidly at points removed from the attachment-to-shell juncture. The shaded areas in Figure B7.2.1.0-1 locate the region where stresses caused by local loads are considered.

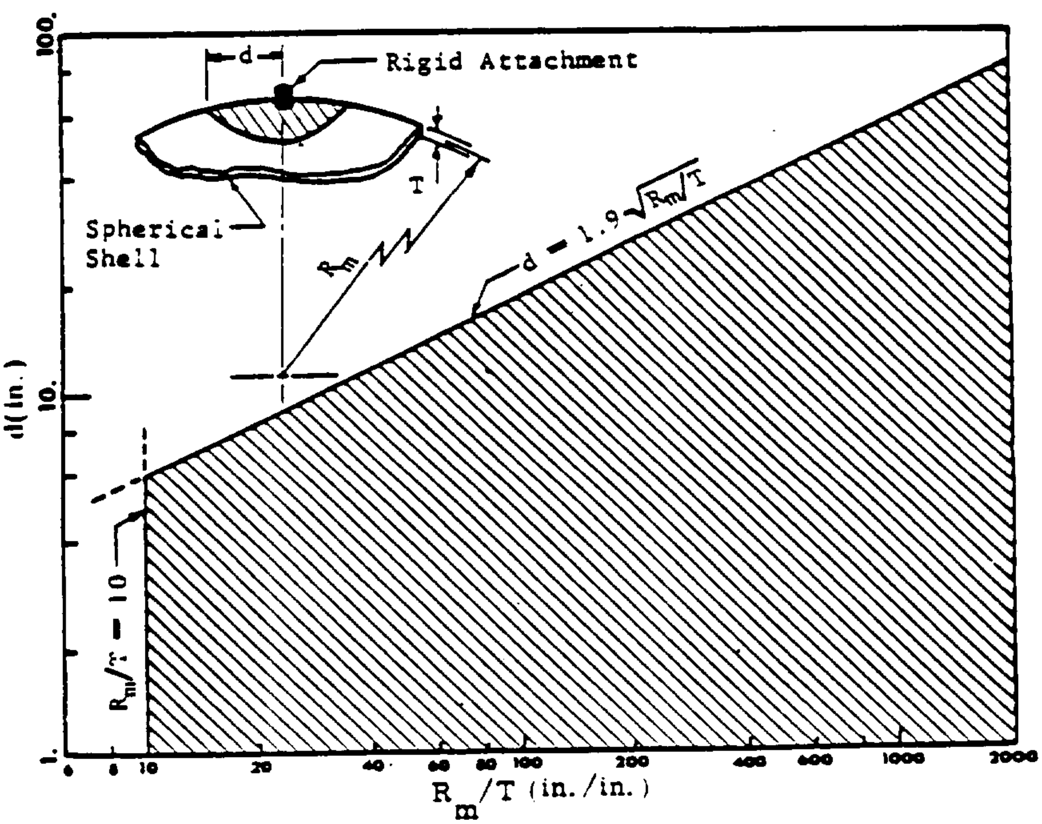

Fig. B7.2.1.0-1 Local Loads Area of Influence

* This section is adapted from the Welding Research Council Bulletin. No. 107, "Local Stresses in Spherical and Cylindrical Shells Due to External Loadings" [5].

638

B7.2.1.1 GENERAL

I NOTATION

- a - fillet radius at attachment-to-shell juncture, in.
- c - half width of square attachment, in.
- d - distance defined by Figure B7.2.1.0-1
- E - modulus of elasticity, psi
- f_x - normal meridional stress, psi
- f_y - normal circumferential stress, psi
- f_{xy} - shear stress, psi
- K_n, K_b - stress concentration parameters for normal stresses and bending stresses, respectively
- M_a - Applied overturning moment, in.-lb.
- M_T - applied twisting moment, in.-lb.
- M_j - internal bending moment stress resultant per unit length of shell, in.-lb/in.
- N_j - internal normal force stress resultant per unit length of shell, lb/in.
- P - applied concentrated radial load, lb.
- R - radius of the shell, in.
- r - radius of the attachment-to-shell, in.
- T - thickness of the shell, in.
- t - thickness of hollow attachment-to-shell, in.
- U - shell parameter, in./in.
- V_a - applied concentrated shear load, lb.
- ρ - hollow attachment-to-shell parameter, in./in.
- θ - circumferential angular coordinate, rad.
- Υ - hollow attachment-to-shell parameter, in./in.
- ϕ - meridional angular coordinate, rad.

B7.2.1.1 GENERAL (Cont'd)

I NOTATION (Cont'd)

Subscripts

a - applied ($a = 1$ or $a = 2$)
b - bending
i - inside
j - internal ($j = x$ or $j = y$)
m - mean (average of outside and inside)
n - normal
o - outside
x - meridional coordinate
y - circumferential coordinate
z - radial coordinate

1 - applied load coordinate
2 - applied load coordinate

B7.2.1.1 GENERAL

II SIGN CONVENTION

Local loads applied at an attachment-to-shell induce a biaxial state of stress on the inside and outside surfaces of the shell. The meridional stress (f_x), circumferential stress (f_y), shear stress (f_{xy}), the positive directions of the applied loads (M_a, M_T, V_a, and P), and the stress resultants (M_j and N_j) are indicated in Figure B7.2.1.1-1.

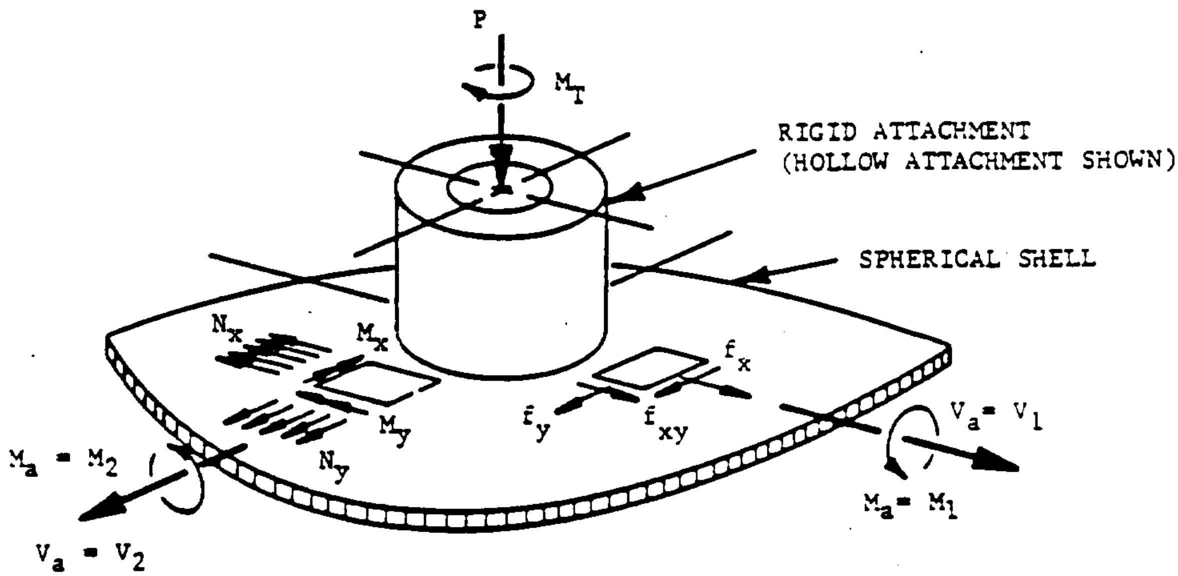

Fig. B7.2.1.1-1 Stresses, Stress Resultants, and Loads

The geometry of the shell and attachment, and the local coordinate system (1-2-3) are indicated in Figure B7.2.1.1-2. It is possible to predict the sign of the induced stresses, tensile (+) or compressive (-), by considering the deflection of the shell resulting from various modes of loading.

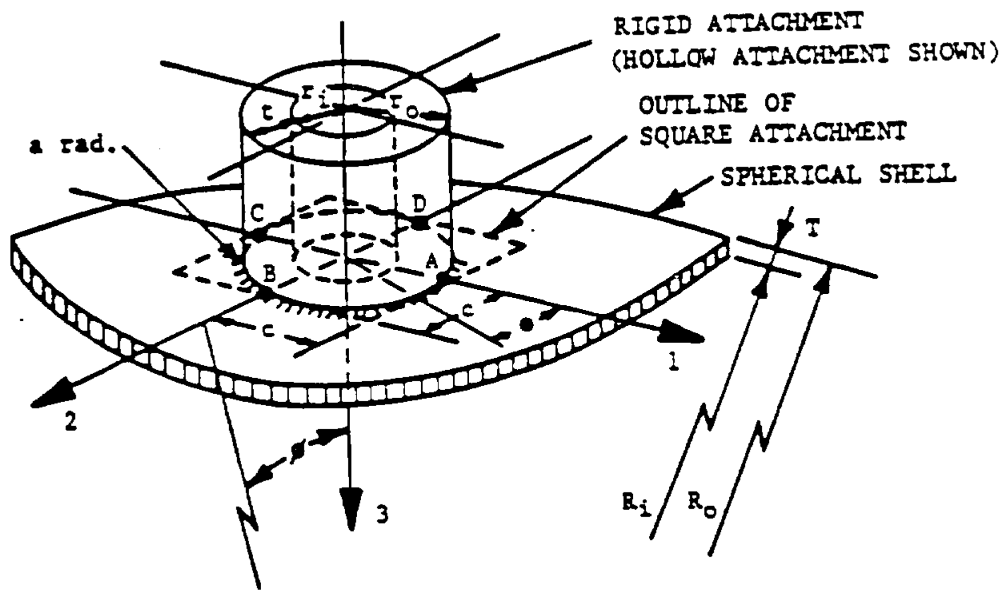

Fig. B7.2.1.1-2 Shell and Attachment Geometry

Mode I, Figure B7.2.1.1-3 shows a positive radial load (P) transmitted to the shell by a rigid attachment. The load (P) causes compressive membrane stresses and local bending stresses adjacent to the attachment. The compressive membrane stresses are similar to the stresses induced by an external pressure. The local bending stresses result in tensile bending stresses on the inside of the shell and compressive bending stresses on the outside of the shell at points C and A.

Mode II, Figure B7.2.1.1-3 shows a negative overturning moment (M_a) transmitted to the shell by a rigid attachment. The overturning moment (M_a) causes compressive and tensile membrane stresses and local bending stresses adjacent to the attachment. Tensile membrane stresses induced in the shell at C are similar to the stresses caused by an internal pressure. Compressive membrane stresses induced in the shell at A are similar to the stresses caused by an external pressure. The local bending stresses cause tensile bending stresses in the shell at C on the outside and A on the inside, and cause compressive bending stresses in the shell at A on the outside and at C on the inside.

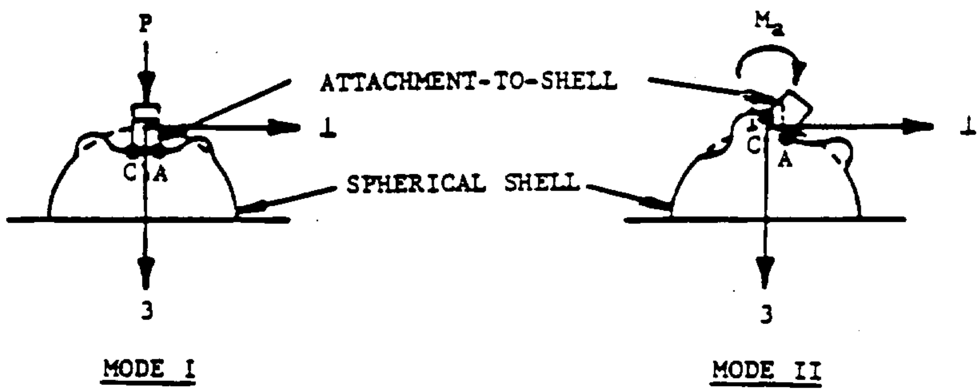

Fig. B7.2.1.1-3 Loading Modes

B7.2.1.1 GENERAL

III LIMITATIONS OF ANALYSIS

Four general areas must be considered for limitations: attachment size and shell thickness, attachment location, shift in maximum stress location, and stresses caused by shear loads.

A. Size of Attachment with Respect to Shell Size

The analysis is applicable to small attachments relative to the shell size and to thin shells. The limitations on these conditions are shown by the shaded area of Figure B7.2.1.1-4.

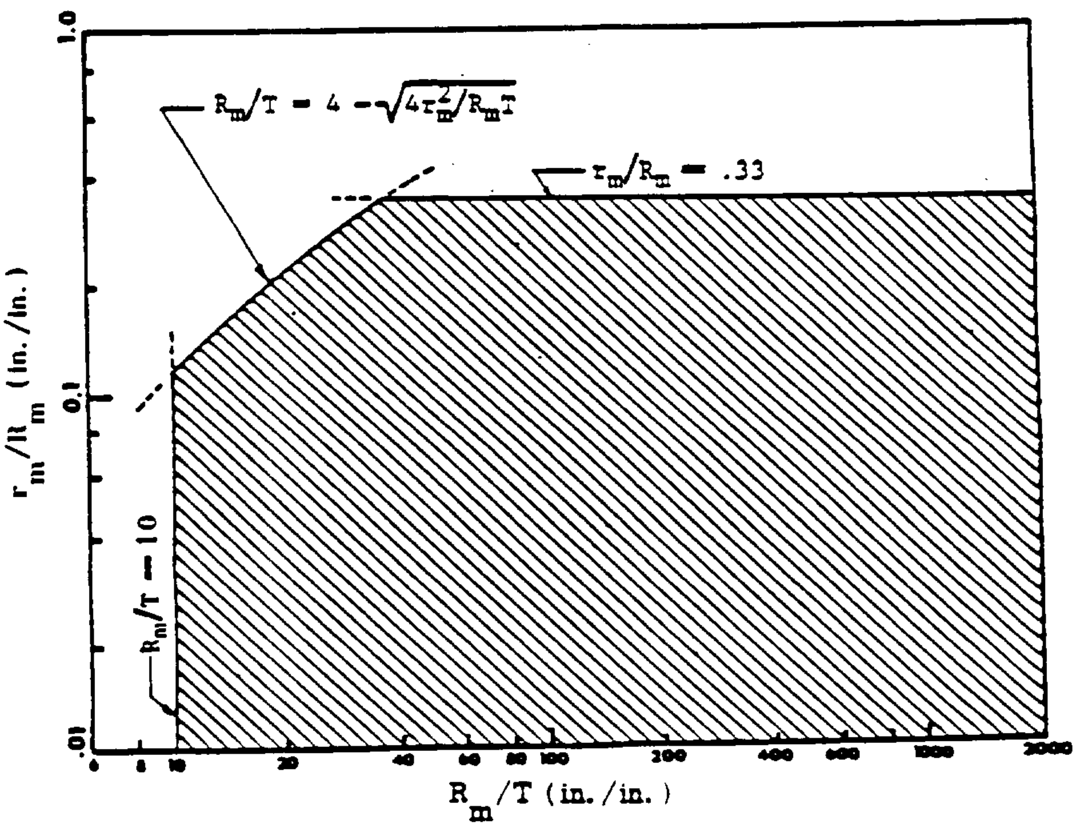

Fig. B7.2.1.1-4

B Location of Attachment with Respect to Boundary Conditions of Shell

The analysis is applicable when any part of the area of influence shown in Figure B7.2.1.0-1 does not contain any stress perturbations. These perturbations may be caused by discontinuity, thermal loading, liquid-level loading, change in section and material change.

C Shift in Maximum Stress Location

Under certain conditions the stresses in the shell may be higher at points removed from the attachment-to-shell juncture than at the juncture. The following conditions should be carefully considered:

1. In some instances, stresses will be higher in the hollow attachment wall than they are in the shell. This is most likely when the attachment opening is not reinforced, when reinforcement is placed on the shell and not on the attachment, and when very thin attachments are used.

2. For some load conditions certain stress resultants peak at points slightly removed from the attachment-to-shell juncture. The maximum value of these stress resultants is determined from the curves in Section B7.2.1.5 and is indicated by dashed lines.

When conditions are encountered that deviate from the limitations of the analysis, Appendix A of Reference 5 should be consulted.

D Stresses Caused by Shear Loads

An accurate stress distribution caused by a shear load (V_a) applied to a spherical shell is not available. The actual stress distribution consists of varying shear and membrane stresses around the rigid attachment. The method [5] presented here assumes that the shell resists the shear load by shear only. If this assumption appears unreasonable, it can be assumed that the shear load is resisted totally by membrane stresses or by some combination of membrane and shear stresses.

B7.2.1.2 STRESSES

I GENERAL

Stress resultants at attachment-to-shell junctures are obtained from the nondimensional stress-resultant curves in section B7.2.1.5. These curves are plots of the shell parameter (U) versus a nondimensional form of the stress resultants (M_j and N_j). Figures B7.2.1.5-1 and B7.2.1.5-2 are used for solid attachments and Figures B7.2.1.5-3 through B7.2.1.5-22 are used for hollow attachments. Additional attachment parameters ($\bar{T}$ and ρ) are required to use Figures B7.2.1.5-3 through B7.2.1.5-22.

The general equation for stresses in a shell at a rigid attachment juncture in terms of the stress resultants is:

$$f_j = K_n(N_j/T) \pm K_b\,(6M_j/T^2)\ .$$

The stress concentration parameters (K_n and K_b) are functions of the ratio of fillet radius to shell thickness (a/T). The value of the stress concentration parameters for $R \gg r$ is equal to unity except in the following cases:

(a) Attachment-to-shell juncture is brittle material;

(b) Fatigue analysis is necessary at attachment-to-shell juncture.

When stress concentration parameters are used they can be determined from Figure B7.2.1.2-1.

The value of the stress resultant at the juncture is indicated by a solid line on the nondimensional stress resultant curves. When the maximum value for a stress resultant does not occur at the attachment-to-shell juncture, it is indicated on the nondimensional stress-resultant curves by dashed lines. An incorrect but conservative analysis would assume this maximum stress to be at the juncture.

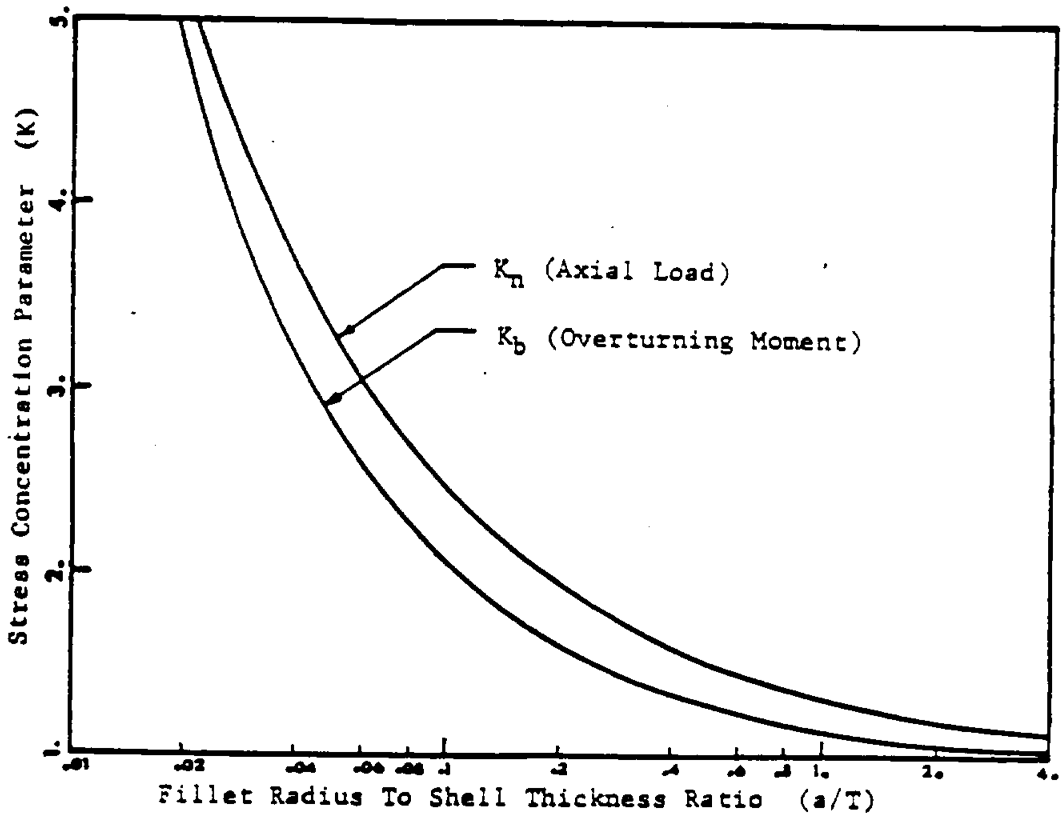

Fig. B7.2.1.2-1 Stress Concentration Parameters for R>>r

The stress calculation sheets (Figs. B7.2.1.2-2 and B7.2.1.2-3) can be used to calculate inside and outside stresses at four points (A, B, C, D on Figure B7.2.1.1-2)around the attachment. The stress calculation sheets also determine the proper sign of the stresses when the applied loads follow the sign convention used in Figure B7.2.1.1-1. The stress calculation sheets provide a place to record applied loads, geometry, parameters and all values calculated or obtained from the step-by-step procedures in paragraphs III-VI below.

STRESS CALCULATION SHEET FOR STRESSES IN SPHERICAL SHELLS CAUSED BY LOCAL LOADS (HOLLOW ATTACHMENT)

APPLIED LOADS	SHELL GEOMETRY	PARAMETERS
P = ______	T = ______	U = ______
V_1 = ______	t = ______	γ = ______
V_2 = ______	R_m = ______	ρ = ______
M_T = ______	r_m = ______	K_n = ______
M_1 = ______	r_o = ______	K_b = ______
M_2 = ______	a = ______	

STRESS	LOAD	NON-DIMENSIONAL STRESS RESULTANT	ADJUSTING FACTOR	STRESS COMPONENT	STRESSES* A_i	A_o	B_i	B_o	C_i	C_o	D_i	D_o
MERIDIONAL STRESS (f_x)	P	$\frac{N_x T}{P}$ =	$\frac{K_n P}{T^2}$ =	$\frac{K_n N_x}{T}$ =	−	−	−	−	−	−	−	−
		$\frac{M_x}{P}$ =	$\frac{6K_b P}{T^2}$ =	$\frac{6K_b M_x}{T^2}$ =	+	−	+	−	+	−	+	−
	M_1	$\frac{N_x T\sqrt{R_m T}}{M_1}$ =	$\frac{K_n M_1}{T^2\sqrt{R_m T}}$ =	$\frac{K_n N_x}{T}$ =			−	−			+	+
		$\frac{M_x\sqrt{R_m T}}{M_1}$ =	$\frac{6K_b M_1}{T^2\sqrt{R_m T}}$ =	$\frac{6K_b M_x}{T^2}$ =			+	−			−	+
	M_2	$\frac{N_x T\sqrt{R_m T}}{M_2}$ =	$\frac{K_n M_2}{T^2\sqrt{R_m T}}$ =	$\frac{K_n N_x}{T}$ =	+	+			−	−		
		$\frac{M_x\sqrt{R_m T}}{M_2}$ =	$\frac{6K_b M_2}{T^2\sqrt{R_m T}}$ =	$\frac{6K_b M_x}{T^2}$ =	−	+			+	−		
	TOTAL MERIDIONAL STRESSES (f_x)											
CIRCUMFERENTIAL STRESS (f_y)	P	$\frac{N_y T}{P}$ =	$\frac{K_n P}{T^2}$ =	$\frac{K_n N_y}{T}$ =	−	−	−	−	−	−	−	−
		$\frac{M_y}{P}$ =	$\frac{6K_b P}{T^2}$ =	$\frac{6K_b M_y}{T^2}$ =	+	−	+	−	+	−	+	−
	M_1	$\frac{N_y T\sqrt{R_m T}}{M_1}$ =	$\frac{K_n M_1}{T^2\sqrt{R_m T}}$ =	$\frac{K_n N_y}{T}$ =			−	−			+	+
		$\frac{M_y\sqrt{R_m T}}{M_1}$ =	$\frac{6K_b M_1}{T^2\sqrt{R_m T}}$ =	$\frac{6K_b M_y}{T^2}$ =			+	−			−	+
	M_2	$\frac{N_y T\sqrt{R_m T}}{M_2}$ =	$\frac{K_n M_2}{T^2\sqrt{R_m T}}$ =	$\frac{K_n N_y}{T}$ =	+	+			−	−		
		$\frac{M_y\sqrt{R_m T}}{M_2}$ =	$\frac{6K_b M_2}{T^2\sqrt{R_m T}}$ =	$\frac{6K_b M_y}{T^2}$ =	−	−			+	−		
	TOTAL CIRCUMFERENTIAL STRESS (f_y)											
SHEAR STRESS (f_{xy})	V_1		$\pi r_o T$ =	$\frac{V_1}{\pi r_o T}$ =			−	−			+	+
	V_2		$\pi r_o T$ =	$\frac{V_2}{\pi r_o T}$ =	−	−			+	+		
	M_T		$2\pi r_o^2 T$ =	$\frac{M_T}{2\pi r_o^2 T}$ =	−	−	+	+	−	−	+	+
	TOTAL SHEAR STRESS (f_{xy})											
PRINCIPAL STRESSES**	f_{max}	$\frac{f_x + f_y}{2} + \sqrt{\frac{(f_x - f_y)^2}{4} + f_{xy}^2}$ ***										
	f_{min}	$\frac{f_x + f_y}{2} - \sqrt{\frac{(f_x - f_y)^2}{4} + f_{xy}^2}$ ***										
	$f_{xy\,max}$	$\pm\sqrt{\frac{(f_x - f_y)^2}{4} + f_{xy}^2}$										

* IF LOAD IS OPPOSITE TO THAT SHOWN IN FIGURE B7.2.1.1-1 THEN REVERSE THE SIGN SHOWN.
** SEE SECTION A3.1.6.
*** CHANGE SIGN OF THE RADICAL IF $(f_x + f_y)$ IS NEGATIVE.

Fig. B7.2.1.2-2 Stress Calculation Sheet (Hollow Attachment)

STRESS CALCULATION SHEET FOR STRESSES IN SPHERICAL SHELLS CAUSED BY LOCAL LOADS
(SOLID ATTACHMENT)

APPLIED LOADS	SHELL GEOMETRY	PARAMETERS
P = ______	T = ______	U = ______
V_1 = ______	R_m = ______	K_n = ______
V_2 = ______	r_o = ______	K_b = ______
MT = ______	a = ______	
M_1 = ______		
M_2 = ______		

STRESS	LOAD	NON-DIMENSIONAL STRESS RESULTANT	ADJUSTING FACTOR	STRESS COMPONENT	STRESSES*							
					A_u	A_L	B_u	B_L	C_u	C_L	D_u	D_L
MERIDIONAL STRESS (f_x)	P	$\frac{N_x T}{P}$ =	$\frac{K_n P}{T^2}$ =	$\frac{K_n N_x}{T}$ =	−	−	−	−	−	−	−	−
		$\frac{M_x}{P}$ =	$\frac{6K_b P}{T^2}$ =	$\frac{6K_b M_x}{T^2}$ =	+	−	+	−	+	−	+	−
	M_1	$\frac{N_x T\sqrt{R_m T}}{M_1}$ =	$\frac{K_n M_1}{T^2\sqrt{R_m T}}$ =	$\frac{K_n N_x}{T}$ =			−	−			+	+
		$\frac{M_x\sqrt{R_m T}}{M_1}$ =	$\frac{6K_b M_1}{T^2\sqrt{R_m T}}$ =	$\frac{6K_b M_x}{T^2}$ =			+	−			−	+
	M_2	$\frac{N_x T\sqrt{R_m T}}{M_2}$ =	$\frac{K_n M_2}{T^2\sqrt{R_m T}}$ =	$\frac{K_n N_x}{T}$ =	+	+			−	−		
		$\frac{M_x\sqrt{R_m T}}{M_2}$ =	$\frac{6K_b M_2}{T^2\sqrt{R_m T}}$ =	$\frac{6K_b M_x}{T^2}$ =	−	+			+	−		
	TOTAL MERIDIONAL STRESSES (f_x)											
CIRCUMFERENTIAL STRESS (f_y)	P	$\frac{N_y T}{P}$	$\frac{K_n P}{T^2}$ =	$\frac{K_n N_y}{T}$ =	−	−	−	−	−	−	−	−
		$\frac{M_y}{P}$	$\frac{6K_b P}{T^2}$ =	$\frac{6K_b M_y}{T^2}$ =	+	−	+	−	+	−	+	−
	M_1	$\frac{N_y T\sqrt{R_m T}}{M_1}$ =	$\frac{K_n M_1}{T^2\sqrt{R_m T}}$ =	$\frac{K_n N_y}{T}$ =			−	−			+	+
		$\frac{M_y\sqrt{R_m T}}{M_1}$ =	$\frac{6K_b M_1}{T^2\sqrt{R_m T}}$ =	$\frac{6K_b M_y}{T^2}$ =			+	−			−	+
	M_2	$\frac{N_y T\sqrt{R_m T}}{M_2}$ =	$\frac{K_n M_2}{T^2\sqrt{R_m T}}$ =	$\frac{K_n N_y}{T}$ =	+	+			−	−		
		$\frac{M_y\sqrt{R_m T}}{M_2}$ =	$\frac{6K_b M_2}{T^2\sqrt{R_m T}}$ =	$\frac{6K_b M_y}{T^2}$ =	−	+			+	−		
	TOTAL CIRCUMFERENTIAL STRESS (f_y)											
SHEAR STRESS (f_{xy})	V_1		$\pi r_o T$ =	$\frac{V_1}{\pi r_o T}$ =			−	−			+	+
	V_2		$\pi r_o T$ =	$\frac{V_2}{\pi r_o T}$ =	−	−			+	+		
	M_T		$2\pi r_o^2 T$ =	$\frac{M_T}{2\pi r_o^2 T}$ =	−	−	+	+	+	−	+	+
	TOTAL SHEAR STRESS (f_{xy})											
PRINCIPAL STRESSES	f_{max}	$\frac{f_x + f_y}{2} + \sqrt{\left(\frac{f_x - f_y}{2}\right)^2 + f_{xy}^2}$ =										
	f_{min}	$\frac{f_x + f_y}{2} - \sqrt{\left(\frac{f_x - f_y}{2}\right)^2 + f_{xy}^2}$ =										
	$f_{s\,max}$	$\pm\sqrt{\left(\frac{f_x - f_y}{2}\right)^2 + f_{xy}^2}$										

* IF LOAD IS OPPOSITE TO THAT SHOWN IN FIGURE B7.2.1.2-1 THEN REVERSE THE SIGN SHOWN.
** SEE SECTION A1.1.0.
*** CHANGE SIGN OF THE RADICAL IF $(f_x - f_y)$ IS NEGATIVE.

Fig. B7.2.1.2-3 Stress Calculation Sheet (Solid Attachment)

B7.2.1.2 STRESSES

II PARAMETERS

The following applicable parameters must be evaluated:

A Geometric Parameters

1. Shell Parameters (U)

a. round attachment

$U = r_0/(R_m T)^{\frac{1}{2}}$

b. square attachment

$U = 1.413c/(R_m T)^{\frac{1}{2}}$

2. Attachment Parameters (T and ρ)

a. hollow round attachment

$T = r_m / t$

$\rho = T/t$

b. hollow square attachment

$T = 1.143c/t$

$\rho = T/t$

B Stress Concentration Parameters

1. Membrane stress-stress concentration parameter $(K_n)^*$

$K_n = 1 + (T/5.6a)^{0.65}$

2. Bending stress-stress concentration parameters $(K_b)^*$

$K_b = 1 + (T/9.4a)^{0.80}$

* K_n and K_b values can be determined from Figure B7.2.1.2-1 with a/T values.

B7.2.1.2 STRESSES

III STRESSES RESULTING FROM RADIAL LOAD

A radial load will cause membrane and bending stress components in both the meridional and circumferential directions.

A Meridional Stresses (f_x)

Step 1. Calculate the applicable geometric parameters as defined in paragraph II above.

Step 2. Using the geometric parameters calculated in step 1, obtain the membrane nondimensional stress resultant ($N_x T/P$) for a solid attachment from Figure B7.2.1.5-1 or for a hollow attachment from Figures B7.2.1.1.5-3 through B7.2.1.5-12.

Step 3. Using P and T values and the membrane nondimensional stress resultant ($N_x T/P$), calculate the membrane stress component N_x/T from:

$N_x/T = (N_x T/P) \cdot (P/T^2)$.

Step 4. Using the geometric parameters calculated in step 1 and the same figures as step 2, obtain the bending nondimensional stress resultant (M_x/P).

Step 5. Using P and T values and the bending nondimensional stress resultant (M_x/P), calculate the bending stress component $6M_x/T^2$ from :

$6M_x/T^2 = (M_x/P) \cdot (6P/T^2)$.

Step 6. Using the criteria in paragraph I, obtain values for the stress concentration parameters (K_n and K_b).

Step 7. Using the stress components calculated in steps 3 and 5 and the the stress concentration parameters calculated in step 6, determine the meridional stress (f_x) from :

$f_x = K_n (N_x/T) \pm K_b (6M_x/T^2)$.

Proper consideration of the sign will give values for the meridional stress on the inside and outside surfaces of the shell.

B Circumferential Stresses (f_y)

The circumferential stress can be determined by following the seven steps outlined above in paragraph A and by using the same curves to obtain the nondimensional stress resultants ($N_y T/P$ and M_y/P) and the following equations to calculate the stress components and circumferential stress:

$$N_y/T = (N_y T/P) \cdot (P/T^2)$$

$$6M_y/ T^2 (M_y/P) \cdot (6P/T^2)$$

$$f_y = K_n(N_y/T) \pm K_b (6 M_y/T^2).$$

15

B7.2.1.2 STRESSES

IV STRESSES RESULTING FROM OVERTURNING MOMENT

An overturning moment will cause membrane and bending stress components in both the meridional and circumferential directions.

A Meridional Stresses (f_x)

Step 1. Calculate the applicable geometric parameters as defined in paragraph II above.

Step 2. Using the geometric parameters calculated in step 1, obtain the membrane nondimensional stress resultant $[N_x T(R_m T)^{\frac{1}{2}}/M_a]$ for a solid attachment from Figure B7.2.1.5-2, or for a hollow attachment from Figures B7.2.1.5-13 through B7.2.2.5-22.

Step 3. Using M_a, R_m and T values and the membrane nondimensional stress resultant $[N_x T(R_m T)^{\frac{1}{2}}/M_a]$, calculate the membrane stress component N_x/T from:

$$N_x/T = [N_x T(R_m T)^{\frac{1}{2}}/M_a]\ [M_a/T^2(R_m T)^{\frac{1}{2}}].$$

Step 4. Using the geometric parameters calculated in step 1 and the same figures as step 2, obtain the bending nondimensional stress resultant $[M_x(R_m T)^{\frac{1}{2}}/M_a]$.

Step 5. Using M_a, R_m and T values and the bending nondimensional stress resultant $[M_x(R_m T)^{\frac{1}{2}}/M_a]$, calculate the bending stress component $6M_x/T^2$ from:

$$6M_x/T^2 = [M_x(R_m T)^{\frac{1}{2}}/M_a]\ [6M_a/T^2(R_m T)^{\frac{1}{2}}].$$

Step 6. Using the criteria in paragraph I, obtain values for the stress concentration parameters (K_n and K_b).

Step 7. Using the stress components calculated in steps 3 and 5 and the stress concentration parameters calculated in step 6, determine the meridional stress (f_x) from:

$$f_x = K_n(N_x/T) \pm K_b(6M_x/T^2)$$

Proper consideration of the sign will give values for the meridional stress on the inside and outside surfaces of the shell.

B Circumferential Stress (f_y)

The circumferential stress can be determined by following the seven steps outlined above in paragraph A and by using the same figures to obtain the nondimensional stress resultants $[N_y T(R_m T)^{\frac{1}{2}}/M_a]$ and the following equations to calculate the stress components and circumferential stress:

$$N_y/T = [N_y T(M_m T)^{\frac{1}{2}}/M_a][M_a/T^2(R_m T)^{\frac{1}{2}}]$$

$$6M_y/T^2 = [M_x(R_m T)^{\frac{1}{2}}/M_a][6M_a/T^2(R_m T)^{\frac{1}{2}}]$$

$$f_y = K_n(N_x/T) \pm K_b(6M_x/T^2).$$

B7.2.1.2 STRESSES

V STRESSES RESULTING FROM SHEAR LOAD

A shear load (V_a) will cause a membrane shear stress (f_{xy}) in the shell at the attachment-to-shell juncture. The shear stress is determined as follows:

A Round Attachment

$$f_{xy} = \frac{V_a}{r_0 T} \sin \Theta \qquad \text{for } V_a = V_1$$

$$\text{or } f_{xy} = \frac{V_a}{r_0 T} \cos \Theta \qquad \text{for } V_a = V_2$$

B Square Attachment

$$\left.\begin{array}{ll} f_{xy} = V_a / 4cT & (\text{at } \Theta = 90° \text{ and } 270°) \\ f_{xy} = 0 & (\text{at } \Theta = 0° \text{ and } 180°) \end{array}\right\} \text{for } V_a = V_1$$

or

$$\left.\begin{array}{ll} f_{xy} = V_a / 4cT & (\text{at } \Theta = 0° \text{ and } 180°) \\ f_{xy} = 0 & (\text{at } \Theta = 90° \text{ and } 270°) \end{array}\right\} \text{for } V_a = V_2$$

B7.2.1.2 STRESSES

VI STRESSES RESULTING FROM TWISTING MOMENT

A Round Attachment

A twisting moment (M_T) applied to a round attachment will cause a shear stress (f_{xy}) in the shell at the attachment-to-shell juncture. The shear stress is pure shear and is constant around the juncture. The shear stress is determined as follows:

$$f_{xy} = M_T / 2\pi \ r_0^2 \ T.$$

B Square Attachment

A twisting moment applied to a square attachment will cause a complex stress field in the shell. No acceptable methods for analyzing this loading are available.

656

B7.2.1.3 STRESSES RESULTING FROM ARBITRARY LOADING

I CALCULATION OF STRESSES

Most loadings that induce local loads on spherical shells are of an arbitrary nature. Stresses are determined by the following procedure:

Step 1. Resolve the applied arbitrary load (forces and/or moments into axial forces, shear forces, overturning moments and twisting moment components. (See paragraph B7.2.1.6, Example Problem.) The positive directions of the components and the point of application of the force components (intersection of centerline of attachment with attachment-shell interface) are indicated in Figure B7.2.1.1-1.

Step 2. Evaluate inside and outside stresses at points A, B, C and D for each component of the applied arbitrary load by the methods in paragraph B7.2.1.2.

Step 3. Obtain the stresses for the arbitrary loading by combining the meridional, circumferential and shear stresses evaluated by step 2 for each of the points A, B, C and D on the inside and outside of the shell. Proper consideration of signs is necessary.

B7.2.1.3 STRESSES RESULTING FROM ARBITRARY LOADING

II LOCATION AND MAGNITUDE OF MAXIMUM STRESSES

The location and magnitude of the maximum stresses caused by an arbitrary load require a consideration of the following:

A The determination of principal stresses (f_{max}, f_{min} and $f_{xy} = 0$ or $f_{xy} = max$) for the calculated stresses (f_x, f_y and f_{xy}) at a specific point.

B The orientation of the coordinate system (1, 2, 3) in Figures B7.2.1.1-1 and B7.2.1.1-2 with respect to an applied arbitrary load may give different values for principal stresses. These different values are caused by a different set of components.

C Whether or not the value for a stress resultant is obtained from the dashed lines or solid lines in Figures B7.2.1.5-3 through B7.2.1.5-22.

B7.2.1.4 ELLIPSOIDAL SHELLS

The analysis presented in this section (B7.2.1.0) can be applied to ellipsoidal shells with attachment at the apex because the radii of curvature are equal. For attachments not located at the apex (points of unequal radii), the analysis is incorrect, and the error increases for attachments at greater distances from the apex.

B7.2.1.5 NONDIMENSIONAL STRESS RESULTANT CURVES

I LIST OF CURVES

A Solid Attachments

1. Nondimensional Stress Resultants for Radial Load (P) B7.2.1.5-1

2. Nondimensional Stress Resultants for Overturning Moment (M_a) B7.2.1.5-2

B Hollow Attachments

1. Nondimensional Stress Resultants for Radial Load (P)

$\Upsilon = 5$	$\rho = 0.25$	B7.2.1.5-3
$\Upsilon = 5$	$\rho = 1.0$	B7.2.1.5-4
$\Upsilon = 5$	$\rho = 2.0$	B7.2.1.5-5
$\Upsilon = 5$	$\rho = 4.0$	B7.2.1.5-6
$\Upsilon = 15$	$\rho = 1.0$	B7.2.1.5-7
$\Upsilon = 15$	$\rho = 2.0$	B7.2.1.5-8
$\Upsilon = 15$	$\rho = 4.0$	B7.2.1.5-9
$\Upsilon = 15$	$\rho = 10.0$	B7.2.1.5-10
$\Upsilon = 50$	$\rho = 4.0$	B7.2.1.5-11
$\Upsilon = 50$	$\rho = 10.0$	B7.2.1.5-12

2. Nondimensional Stress Resultants for Overturning Moment (M_a)

$\Upsilon = 5$	$\rho = 0.25$	B7.2.1.5-13
$\Upsilon = 5$	$\rho = 1.0$	B7.2.1.5-14
$\Upsilon = 5$	$\rho = 2.0$	B7.2.1.5-15
$\Upsilon = 5$	$\rho = 4.0$	B7.2.1.5-16
$\Upsilon = 15$	$\rho = 1.0$	B7.2.1.5-17
$\Upsilon = 15$	$\rho = 2.0$	B7.2.1.5-18
$\Upsilon = 15$	$\rho = 4.0$	B7.2.1.5-19
$\Upsilon = 15$	$\rho = 10.0$	B7.2.1.5-20
$\Upsilon = 50$	$\rho = 4.0$	B7.2.1.5-21
$\Upsilon = 50$	$\rho = 10.0$	B7.2.1.5-22

B7.2.1.5 NONDIMENSIONAL STRESS RESULTANT CURVES

II CURVES

The following curves (Figs. B7.2.1.5-1 — B7.2.1.5-22) are plots of nondimensional stress resultants versus a shell parameter for the axial load and overturning moment loadings and for various attachment parameters.

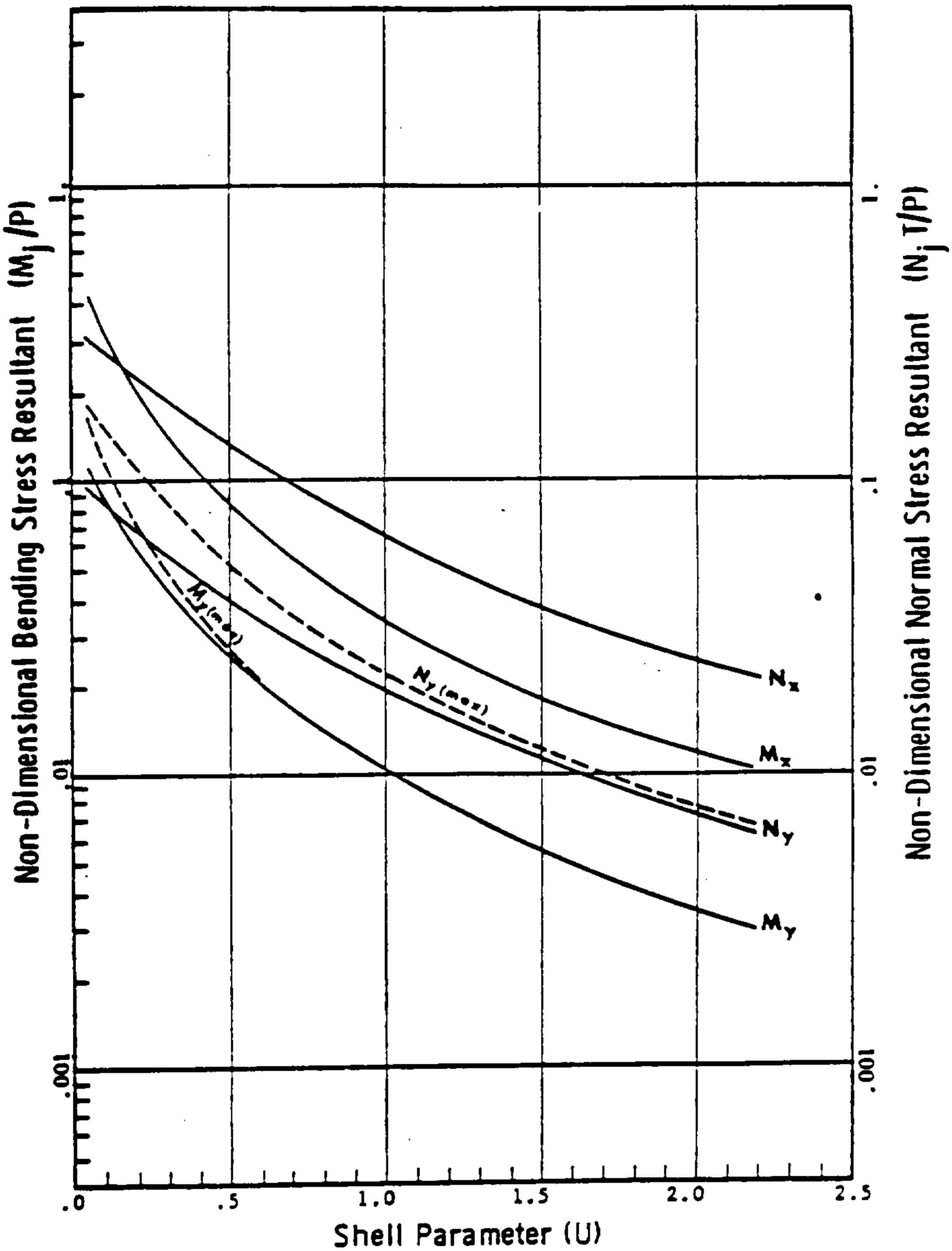

Figure B7.2.1.5-1 Non-Dimensional Stress Resultants for Radial Load (P) Solid Attachment

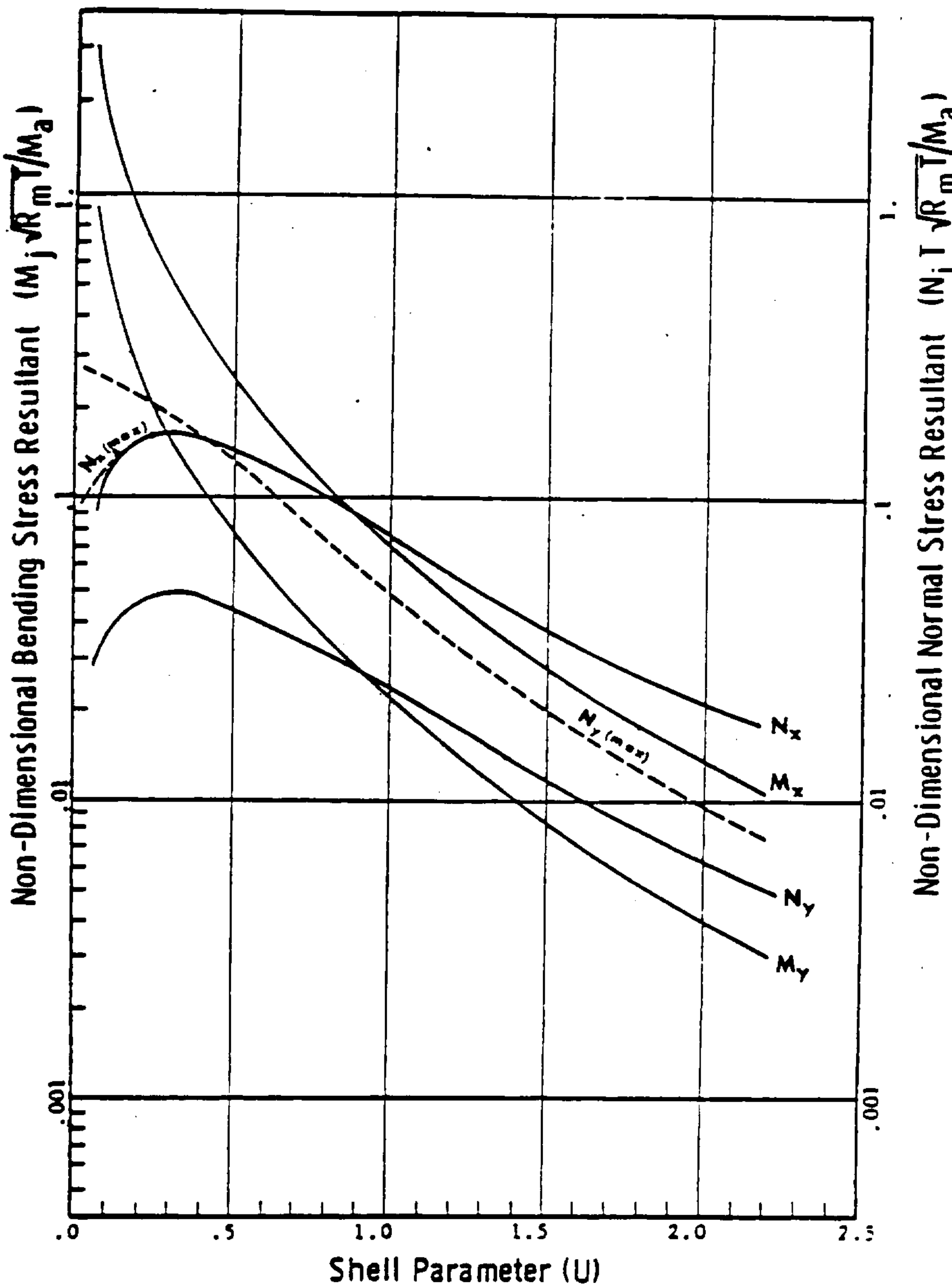

Figure B7.2.1.5-2 Non-Dimensional Stress Resultants for Overturning Moment (M_a) Solid Attachment

63

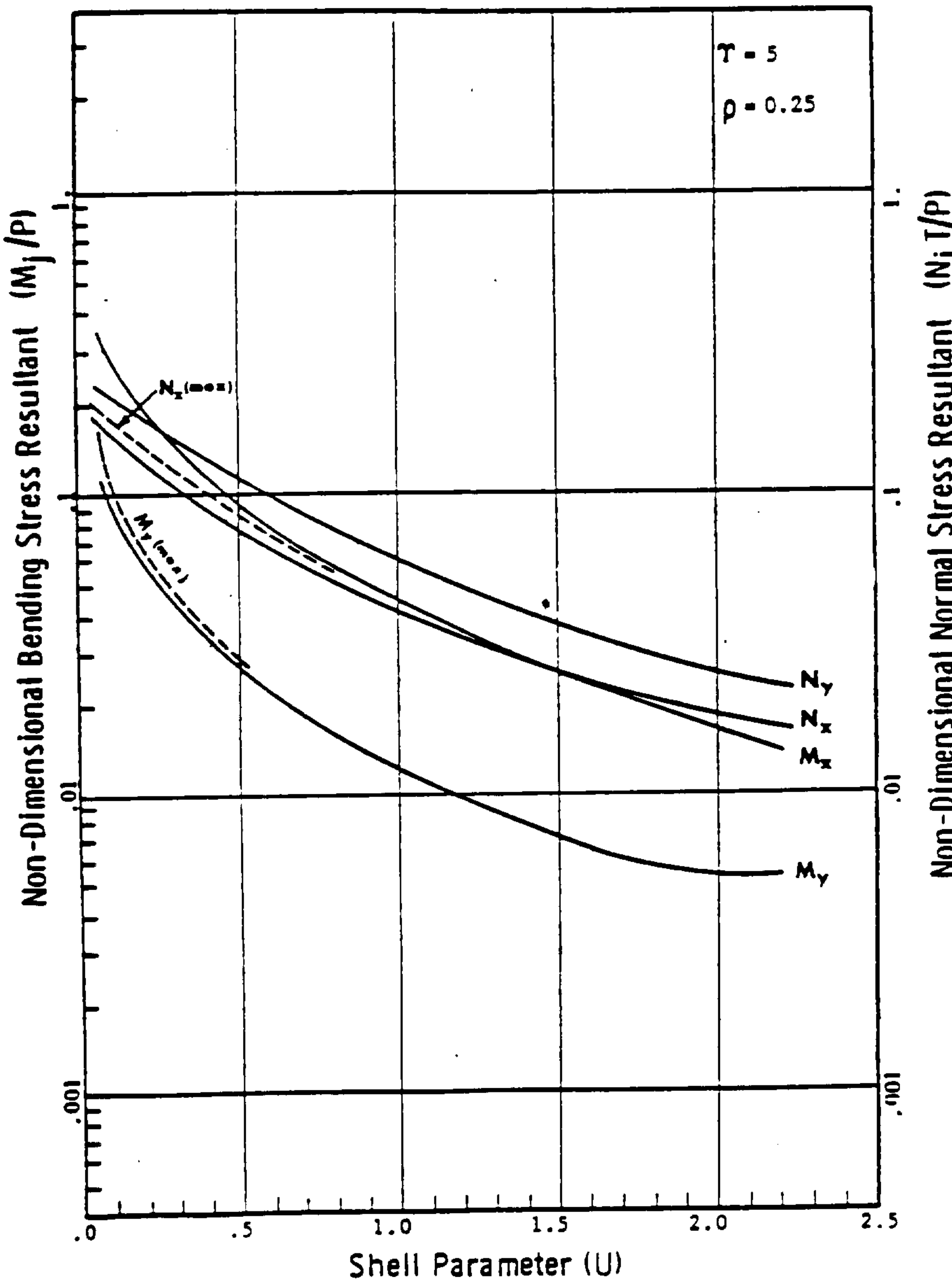

Figure B7.2.1.5-3 Non-Dimensional Stress Resultants for Radial Load (P)
Hollow Attachment T = 5 and ρ = 0.25

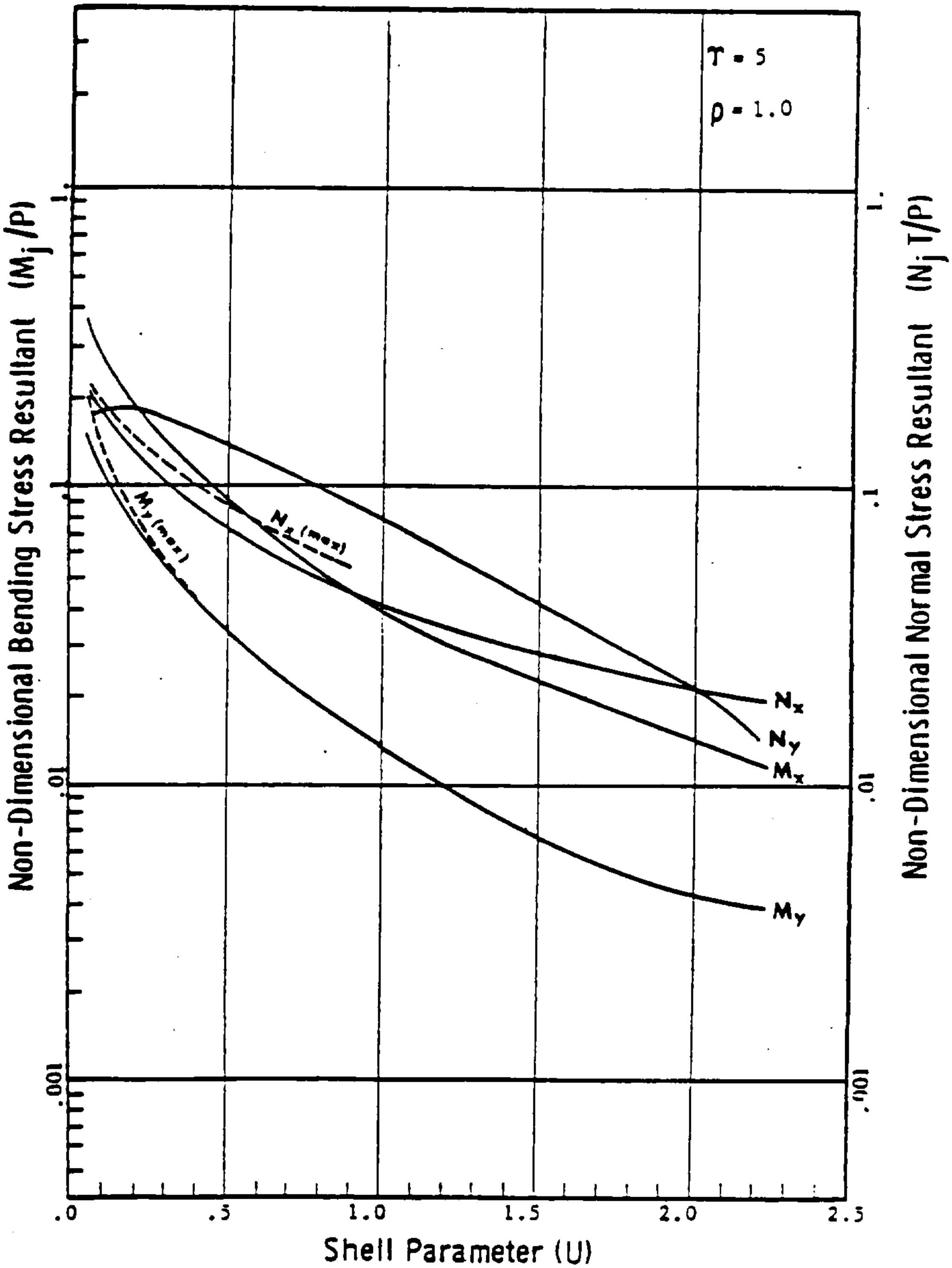

Figure B7.2.1.5-4 Non-Dimensional Stress Resultants for Radial Load (P)
Hollow Attachment $T = 5$ and $\rho = 1.0$

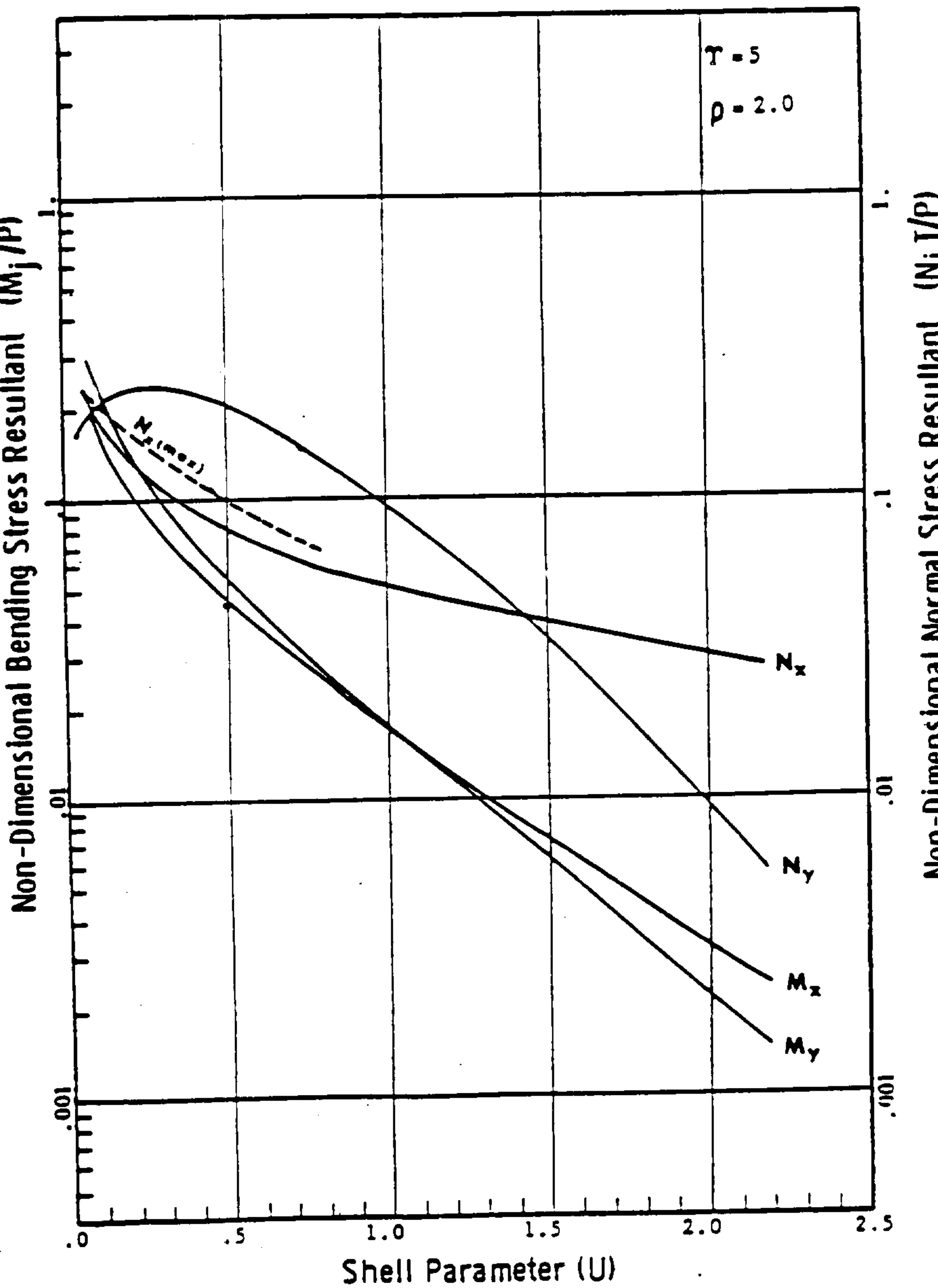

Figure B7.2.1.5-5 Non-Dimensional Stress Resultants for Radial Load (P)
Hollow Attachment T = 5 and ρ = 2.0

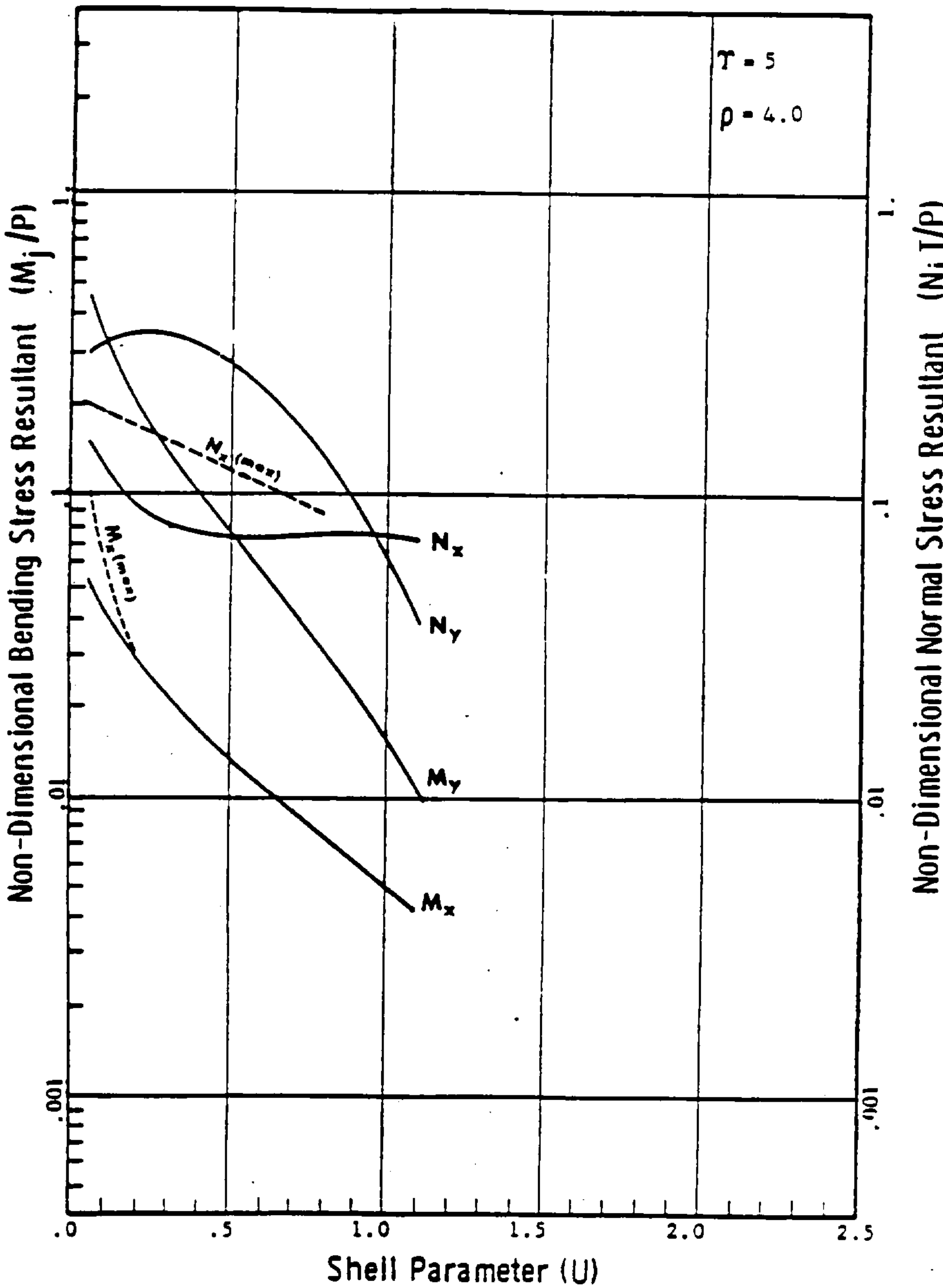

Figure B7.2.1.5-6 Non-Dimensional Stress Resultants for Radial Load (P) Hollow Attachment T = 5 and ρ = 4.0

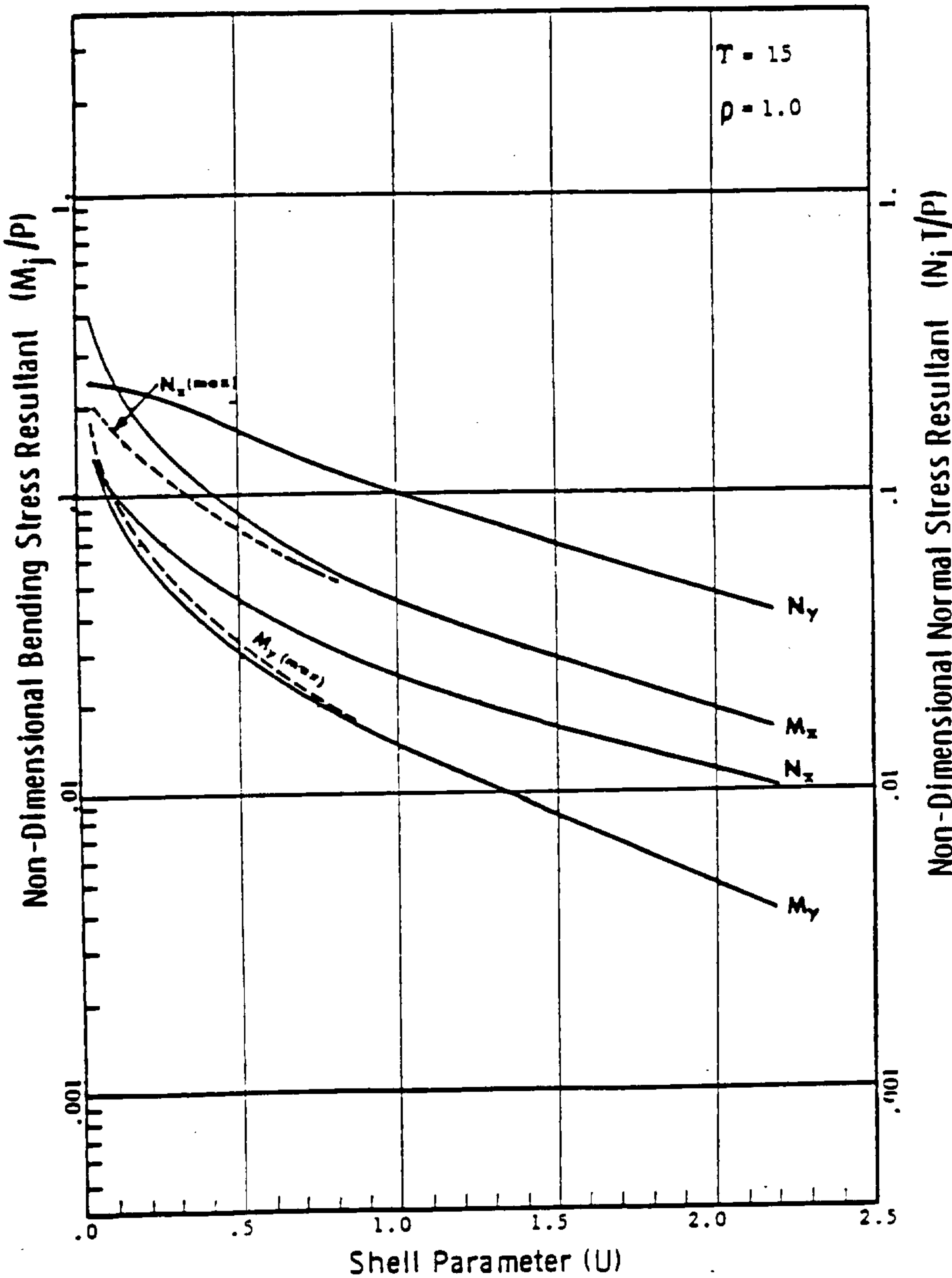

Figure E7.2.1.5-7 Non-Dimensional Stress Resultants for Radial Load (P) Hollow Attachment T = 15 and ρ = 1.0

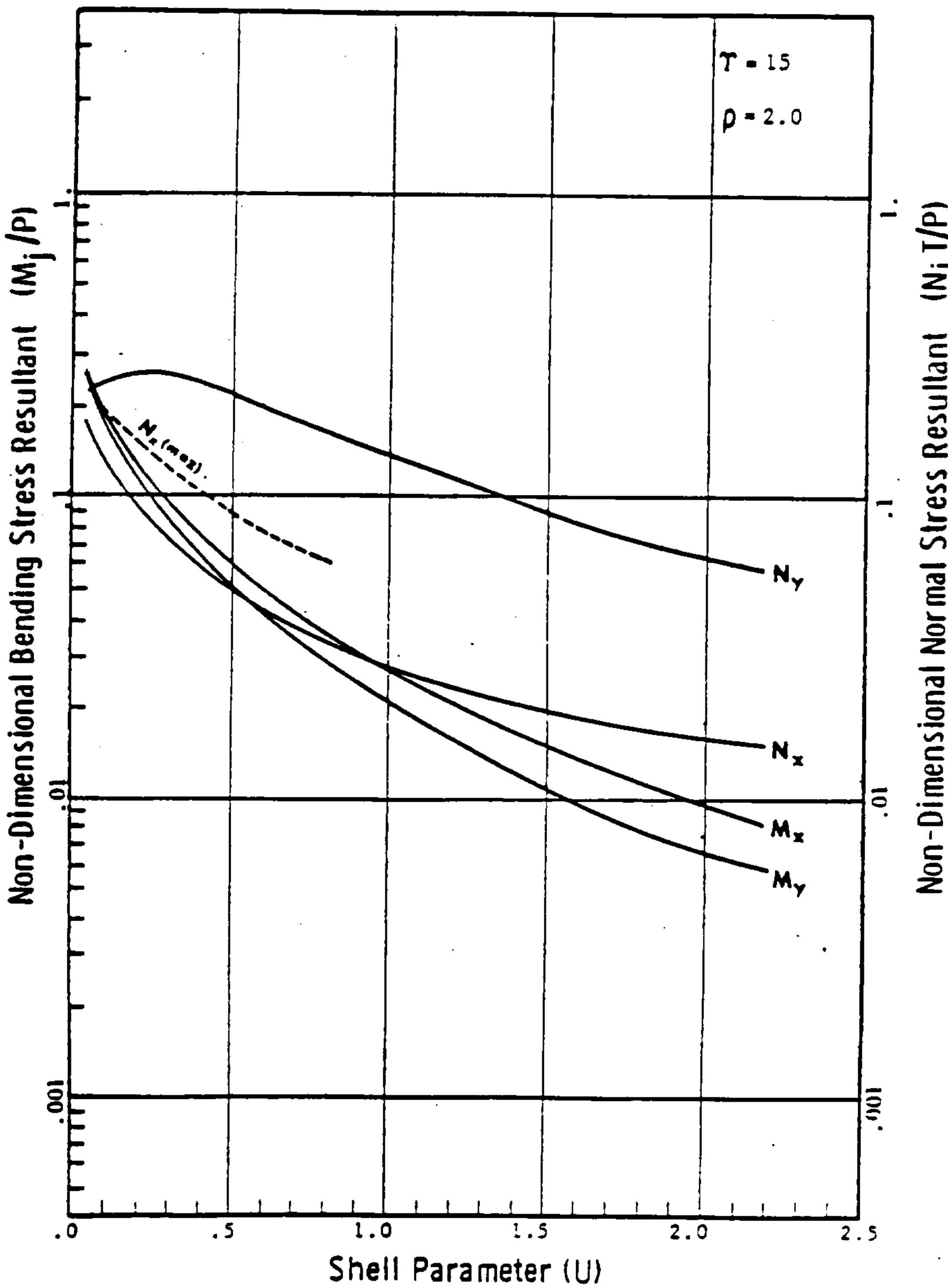

Figure B7.2.1.5-8 Non-Dimensional Stress Resultants for Radial Load (P)
Hollow Attachment T = 15 and ρ = 2.0

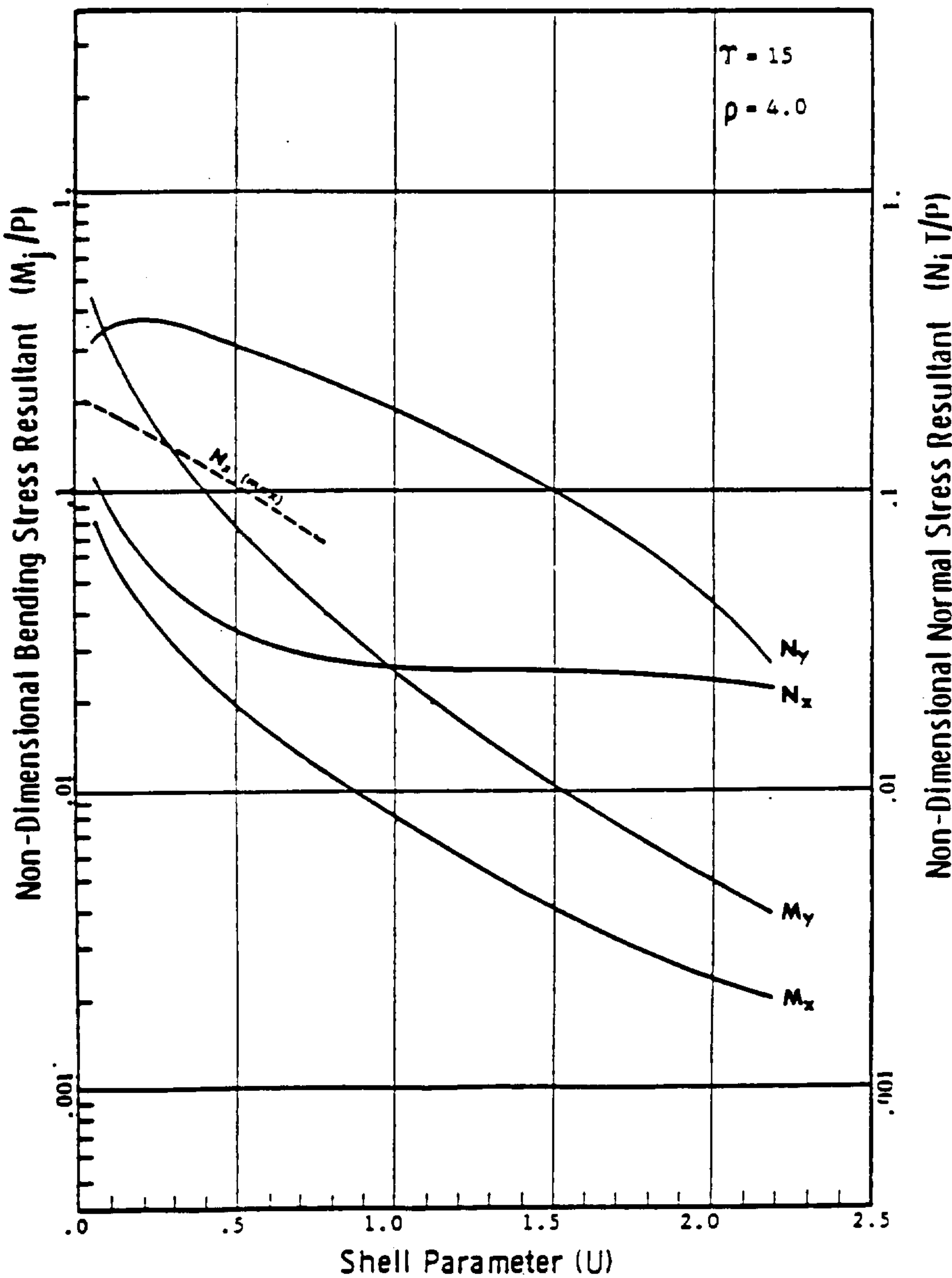

Figure B7.2.1.5-9 Non-Dimensional Stress Resultants for Radial Load (P) Hollow Attachment T = 15 and ρ = 4.0

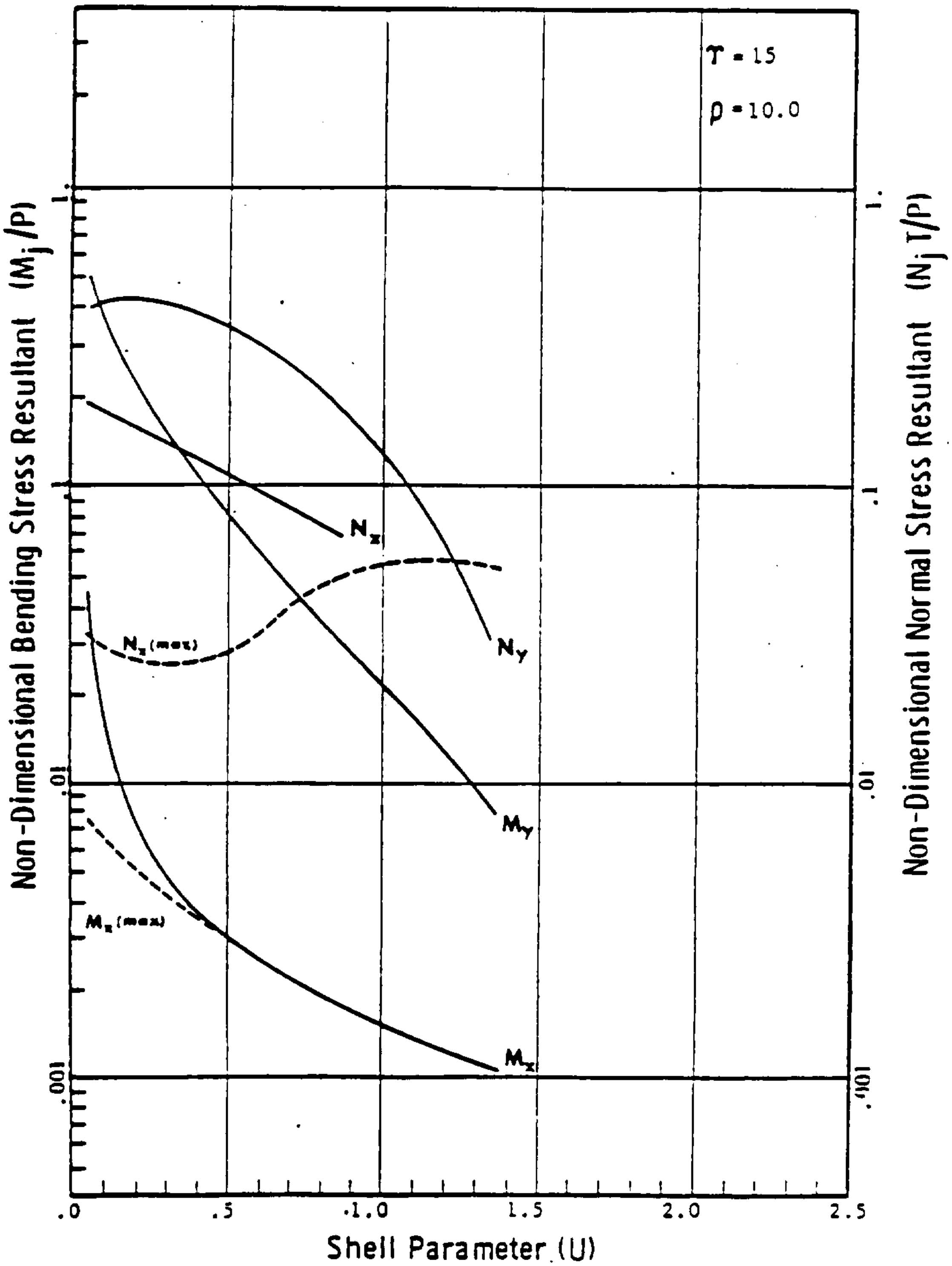

Figure B7.2.1.5-10 Non-Dimensional Stress Resultants for Radial Load (P) Hollow Attachment T = 15 and ρ = 10.0

671

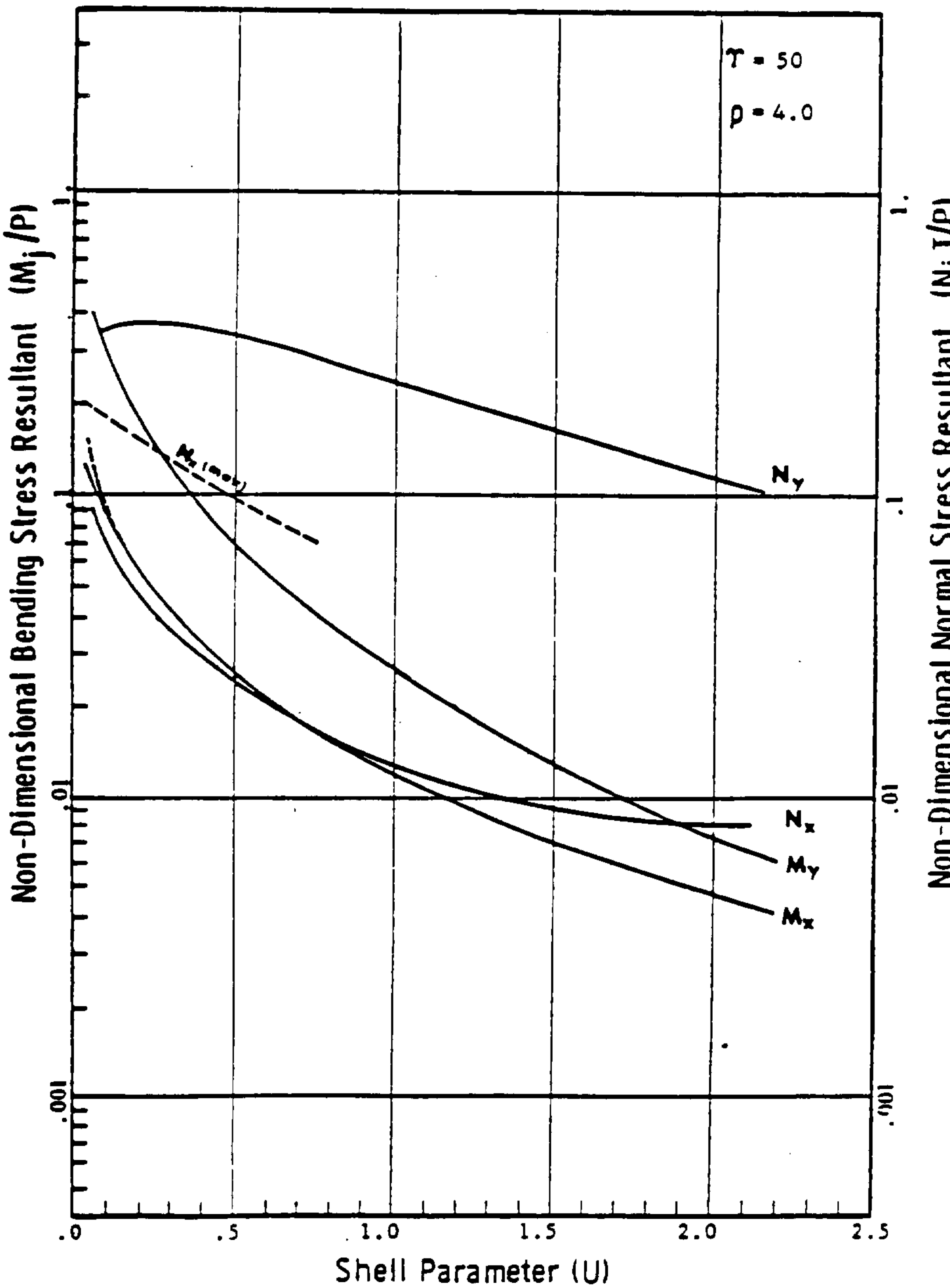

Figure B7.2.1.5-11 Non-Dimensional Stress Resultants for Radial Load (P)
Hollow Attachment τ = 50 and ρ = 4.0

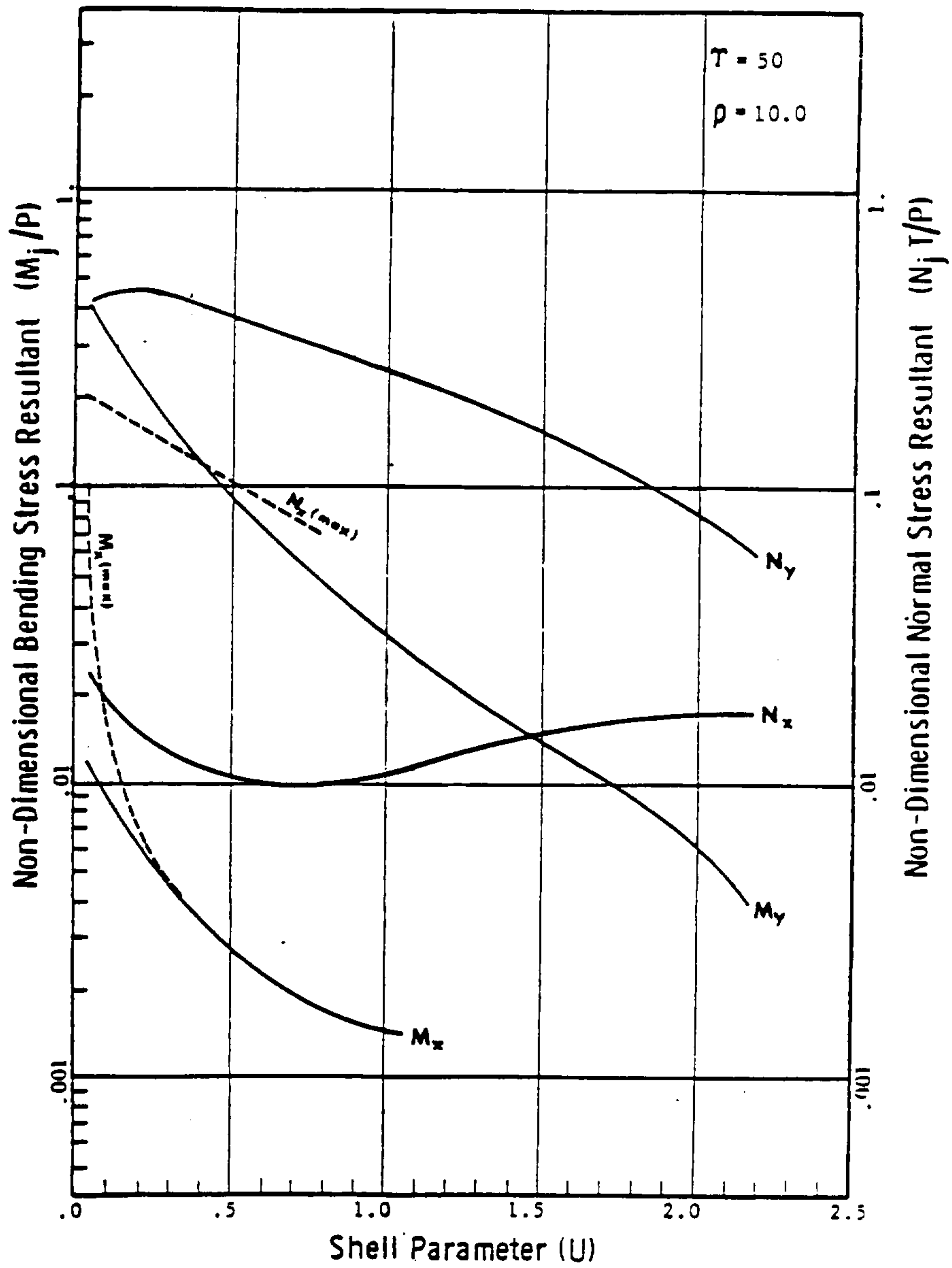

Figure B7.2.1.5-12 Non-Dimensional Stress Resultants for Radial Load (P) Hollow Attachment T = 50 and ρ = 10.0

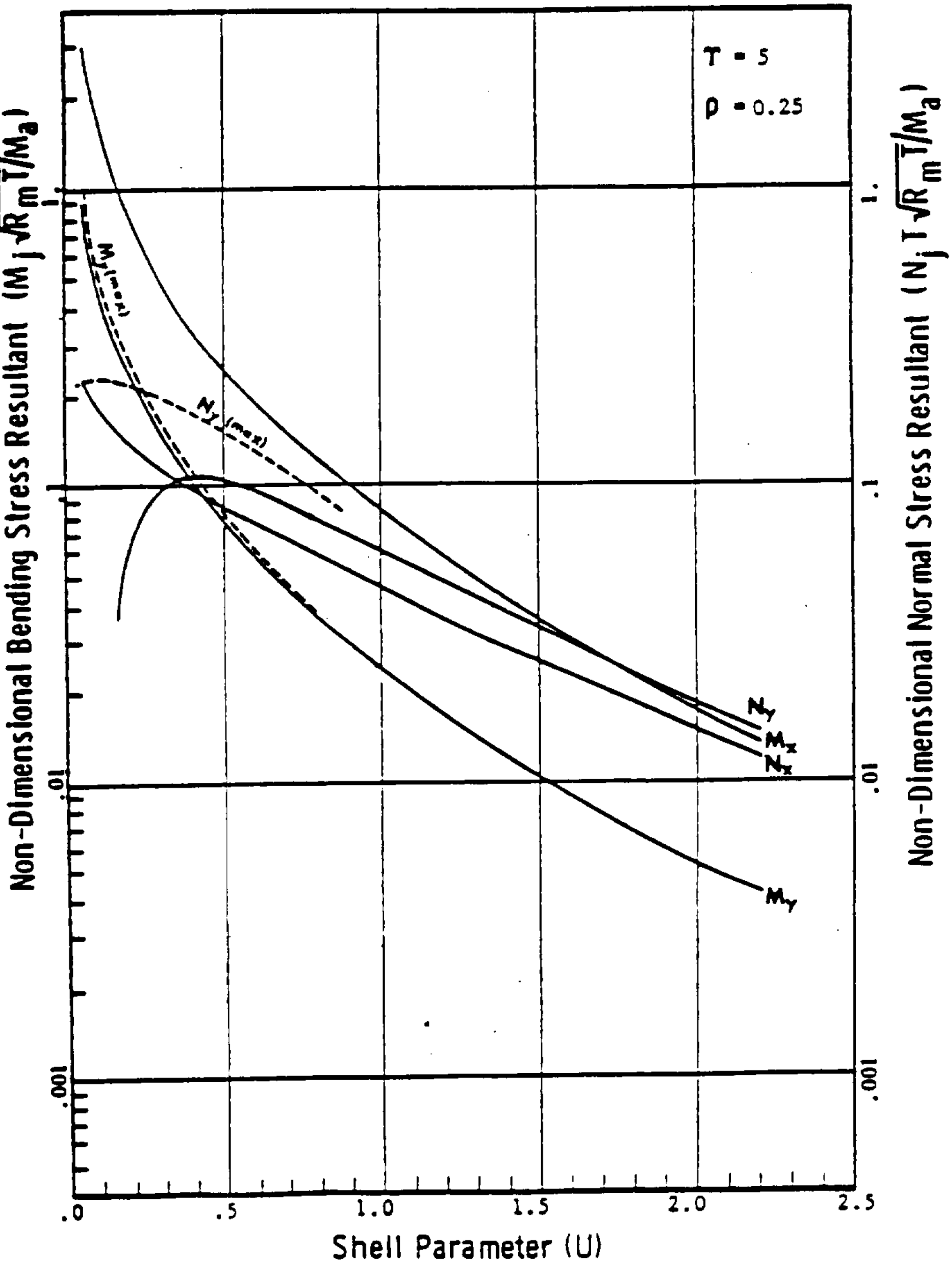

Figure B7.2.1.5-13 Non-Dimensional Stress Resultants for Overturning Moment (M_a) Hollow Attachment T = 5 and ρ = 0.25

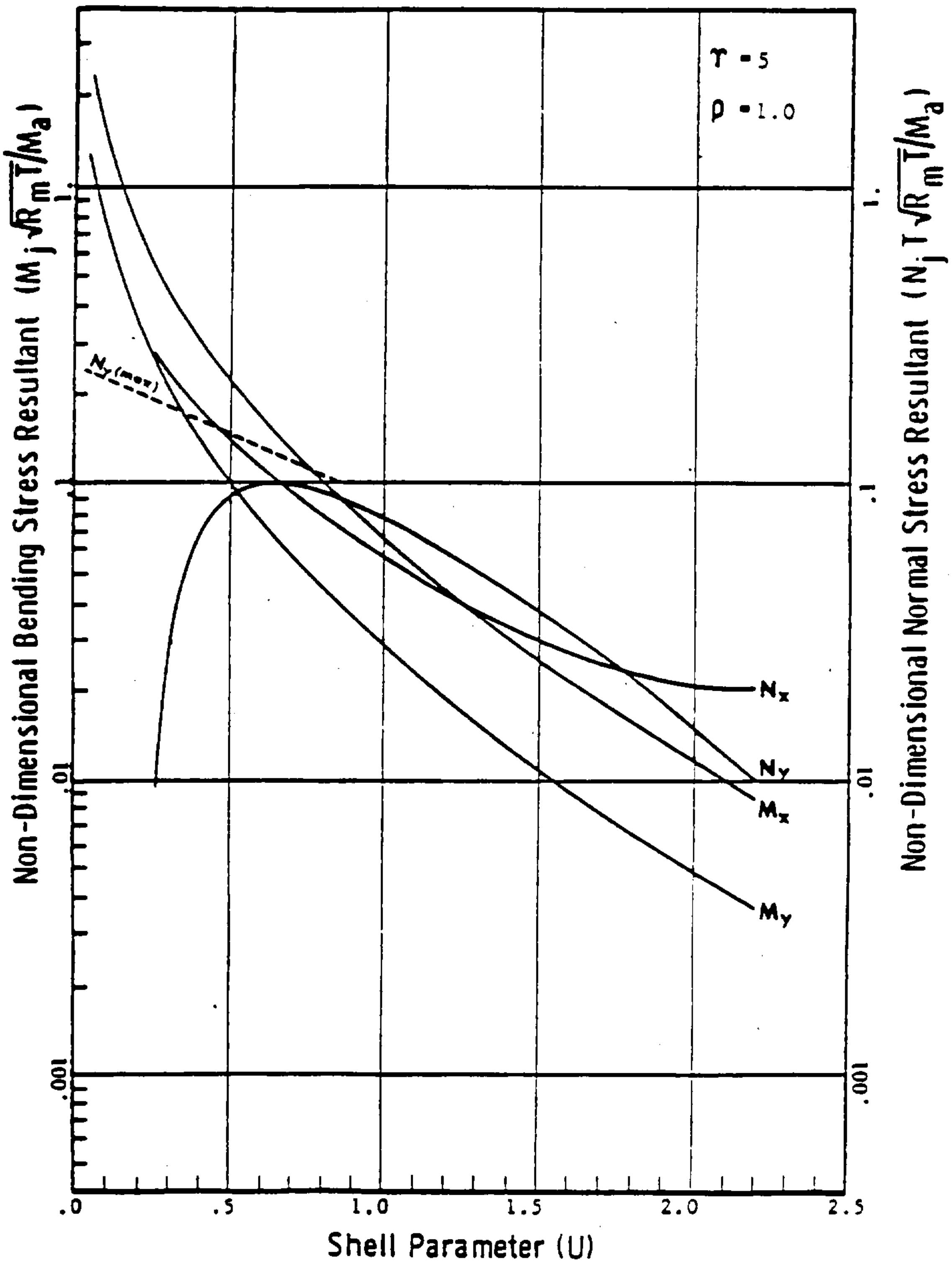

Figure B7.2.1.5-14 Non-Dimensional Stress Resultants for Overturning Moment (M_a) Hollow Attachment T = 5 and ρ = 1.0

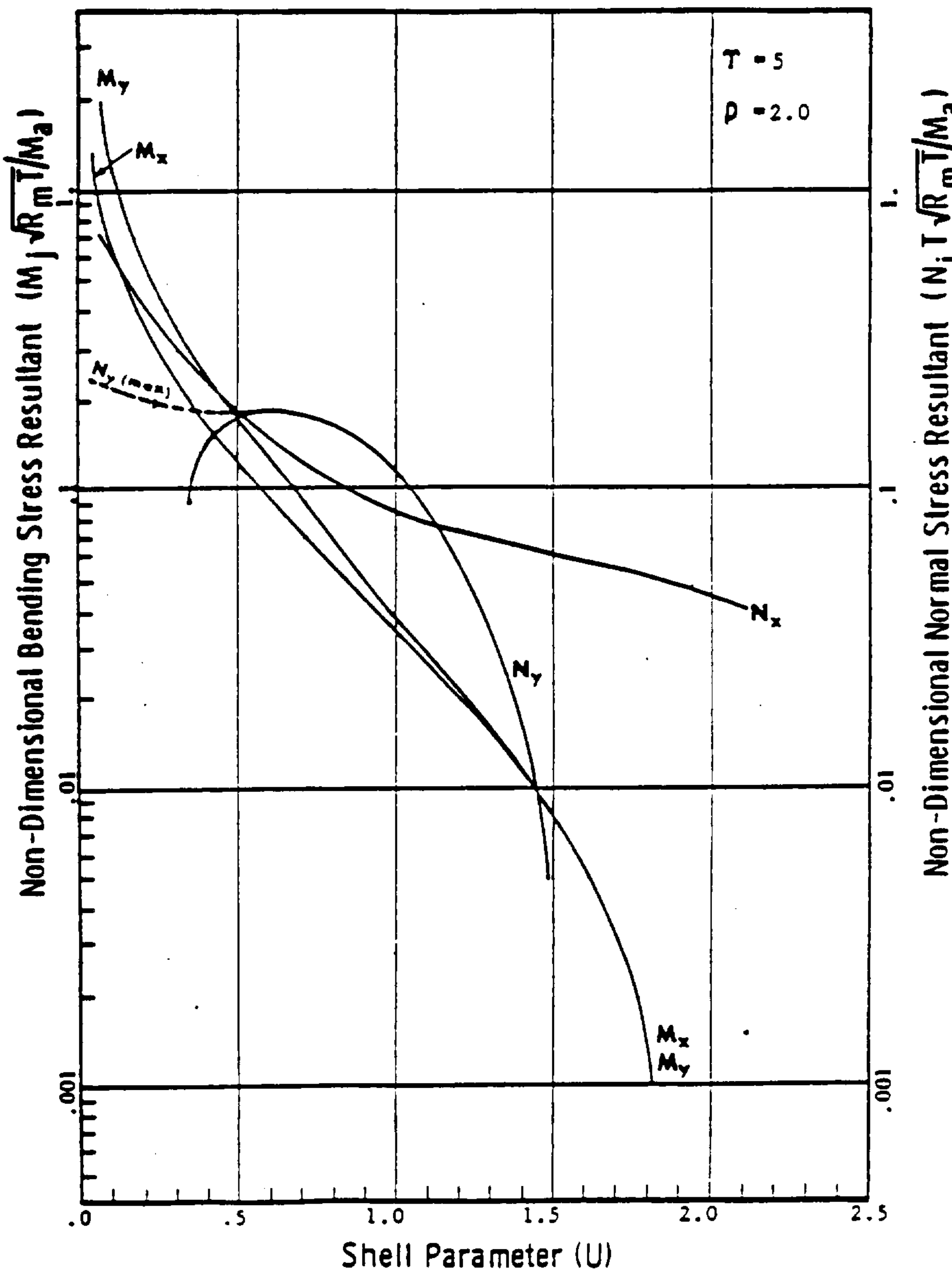

Figure B7.2.1.5-15 Non-Dimensional Stress Resultants for Overturning Moment (M_a) Hollow Attachment T = 5 and ρ = 2.0

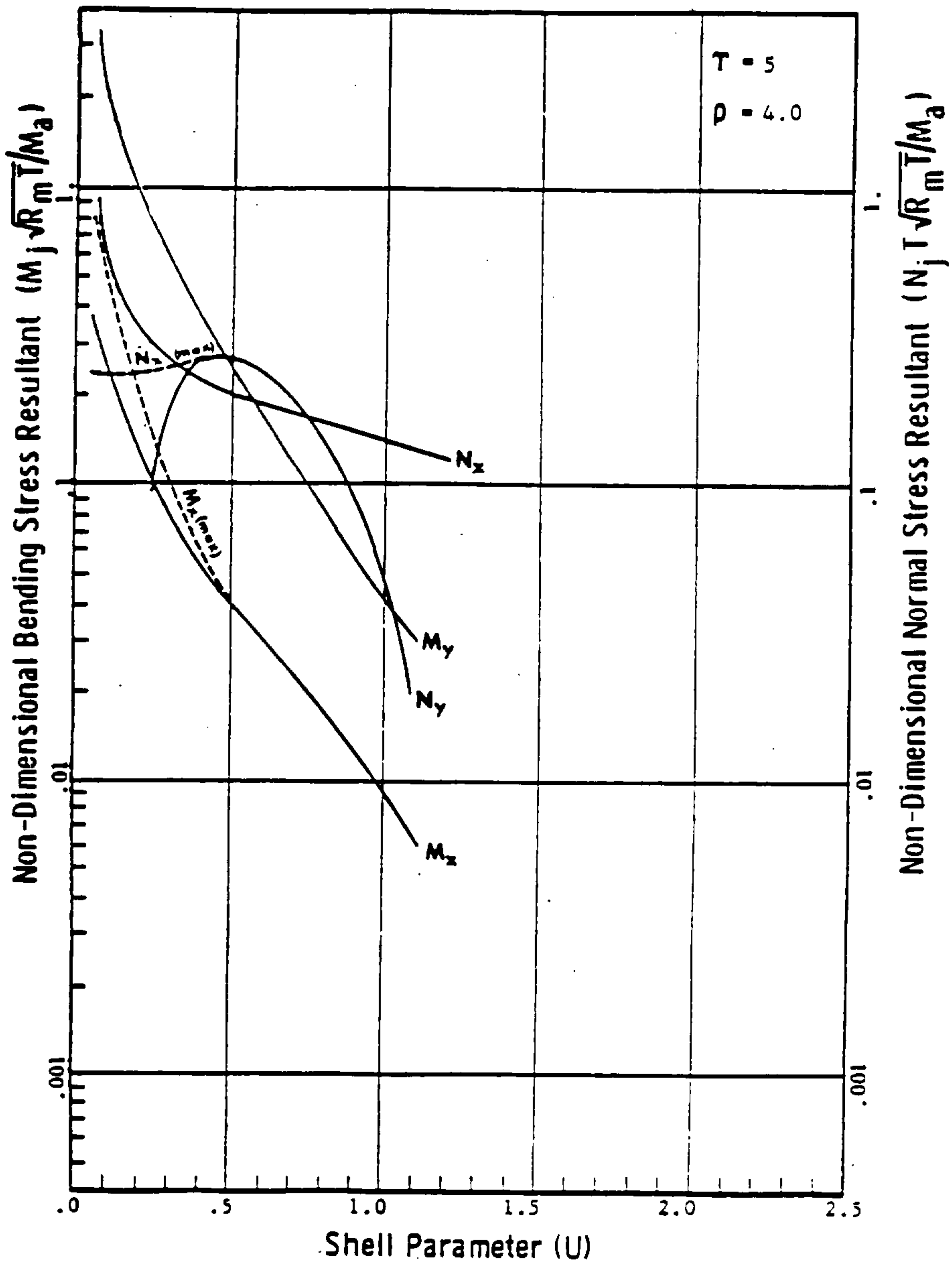

Figure B7.2.1.5-16 Non-Dimensional Stress Resultants for Overturning Moment (M_a) Hollow Attachment Υ = 5 and ρ = 4.0

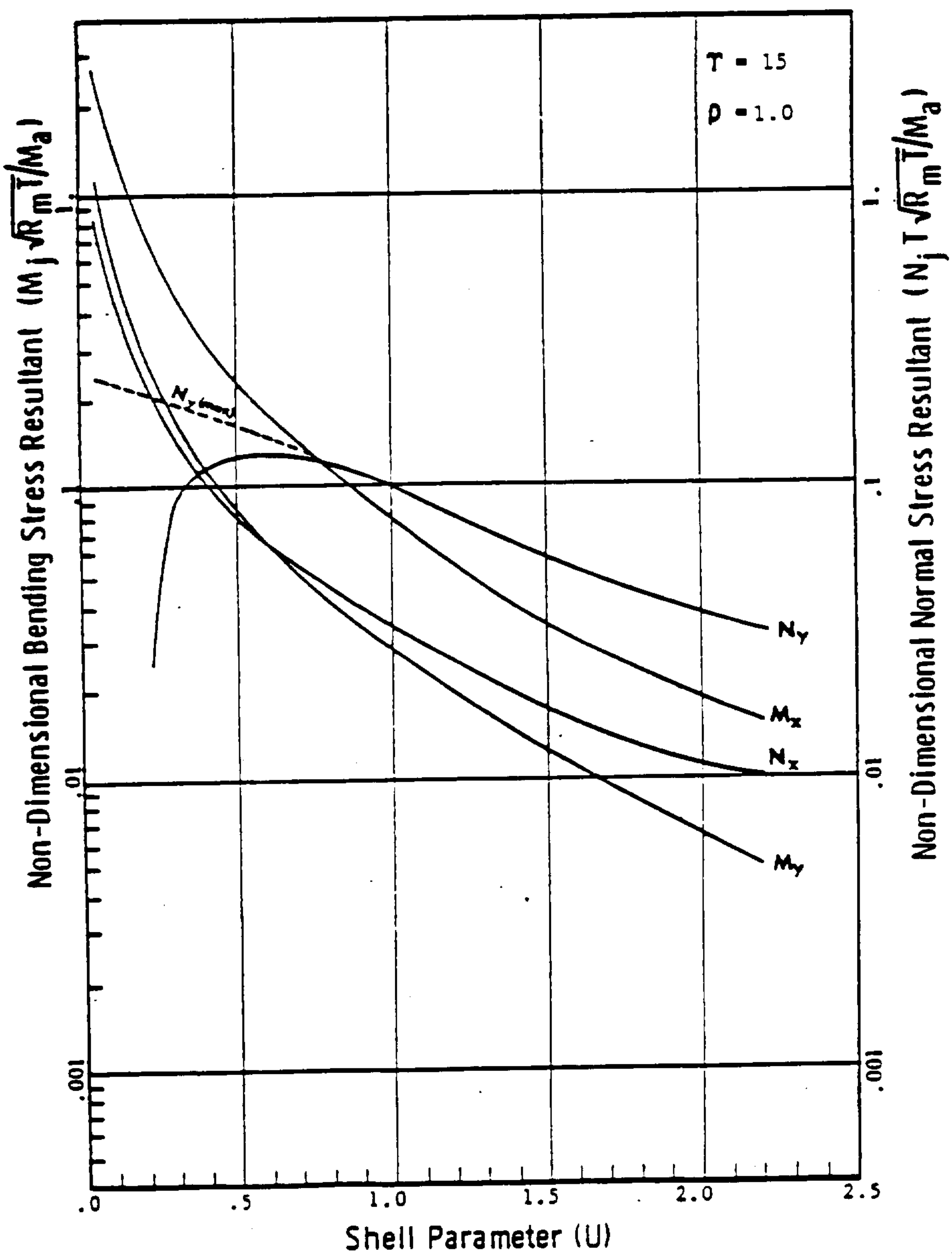

Figure B7.2.1.5-17 Non-Dimensional Stress Resultants for Overturning Moment (M_a) Hollow Attachment T = 15 and ρ = 1.0

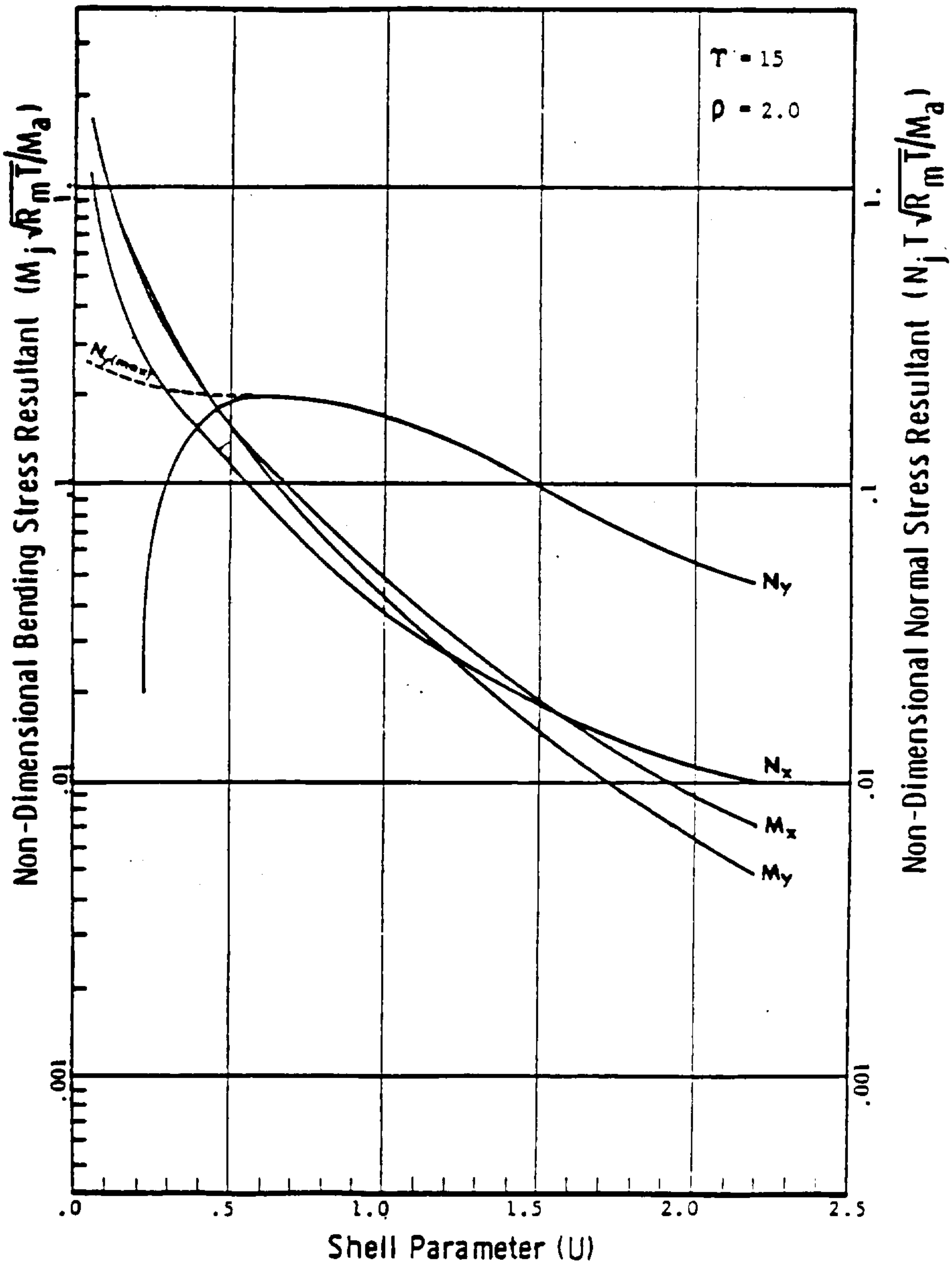

Figure B7.2.1.5-18 Non-Dimensional Stress Resultants for Overturning Moment (M_a) Hollow Attachment T = 15 and ρ = 2.0

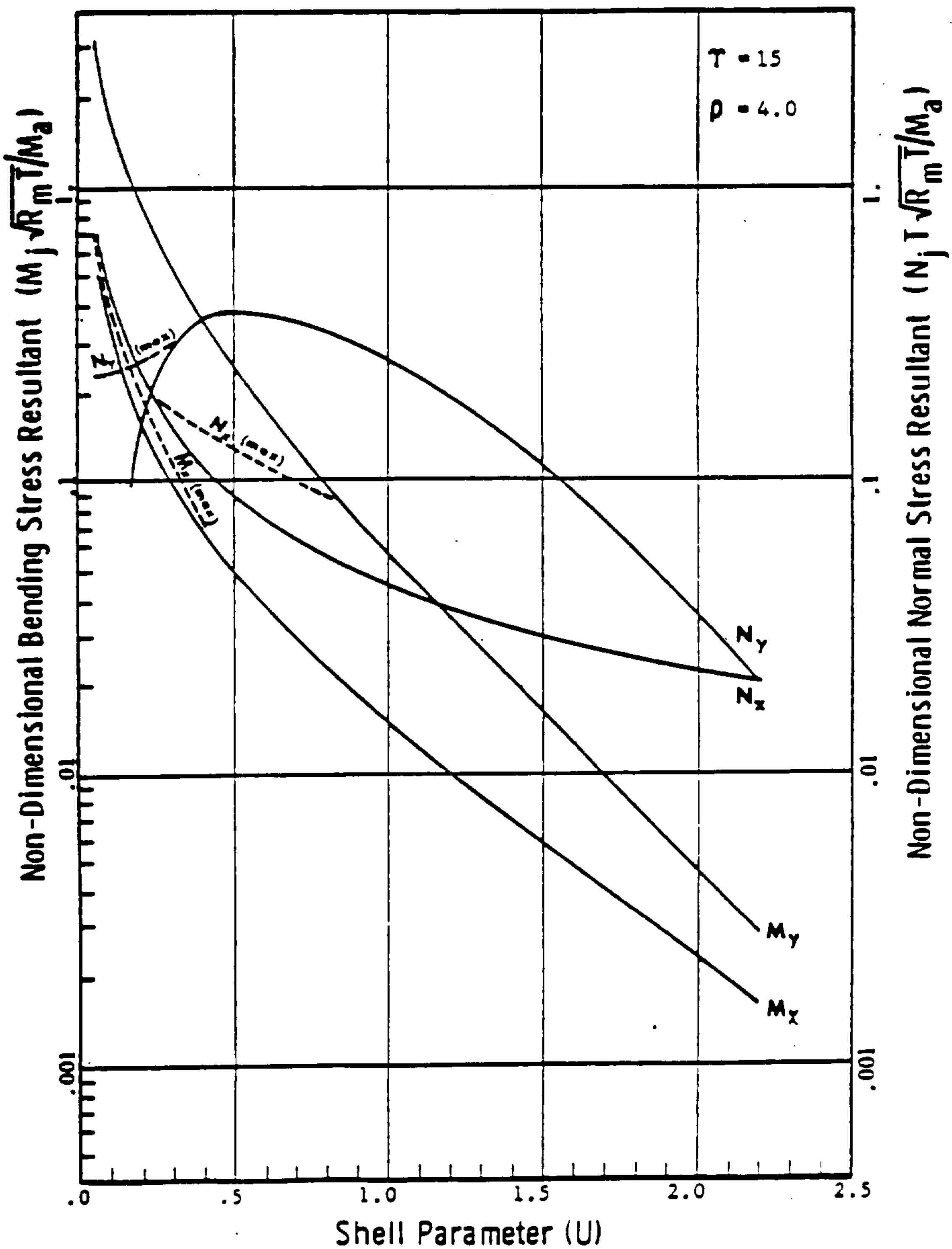

Figure B7.2.1.5-19 Non-Dimensional Stress Resultants for Overturning Moment (M_a) Hollow Attachment T = 15 and ρ = 4.0

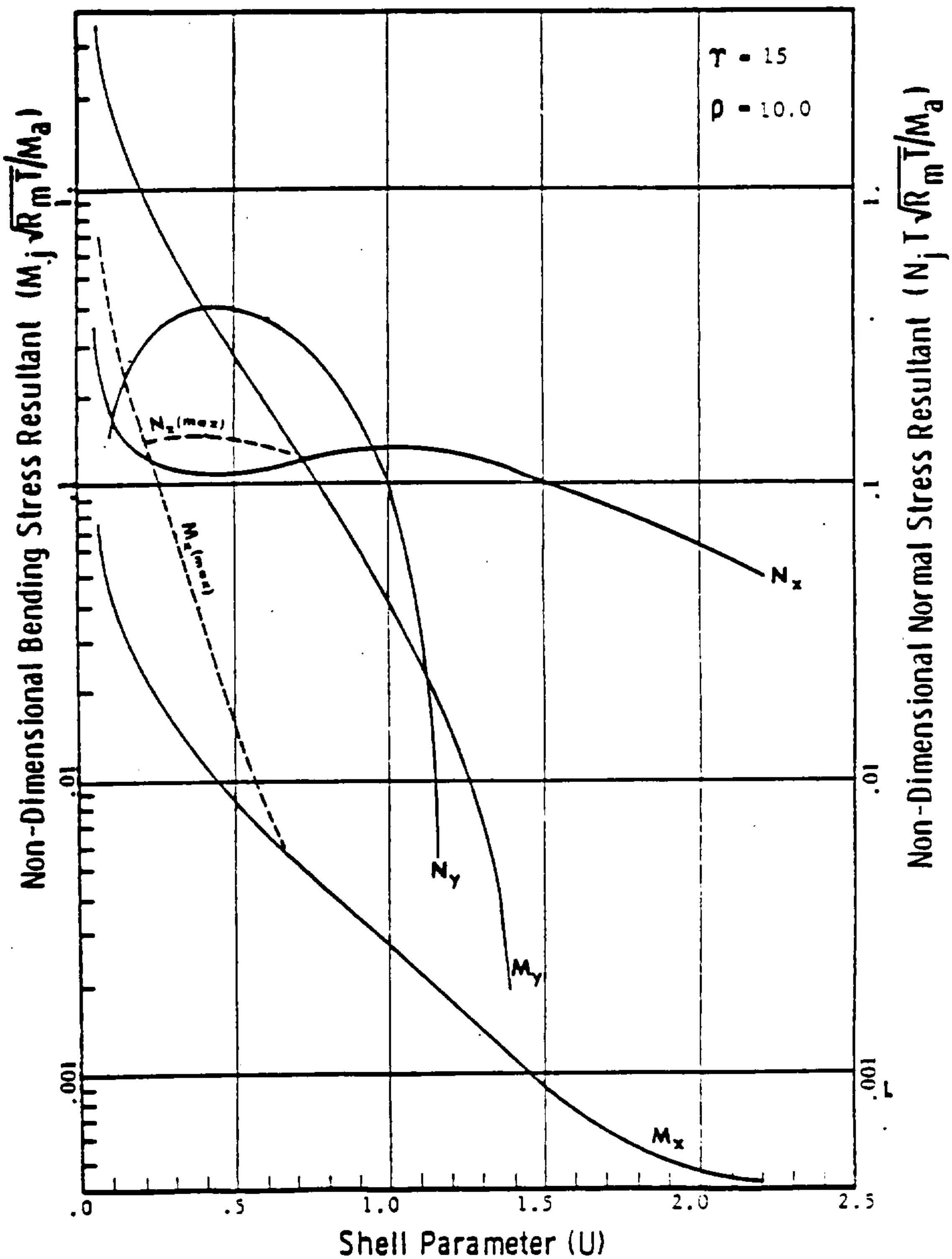

Figure B7.2.1.5-20 Non-Dimensional Stress Resultants for Overturning Moment (M_a) Hollow Attachment τ = 15 and ρ = 10.0

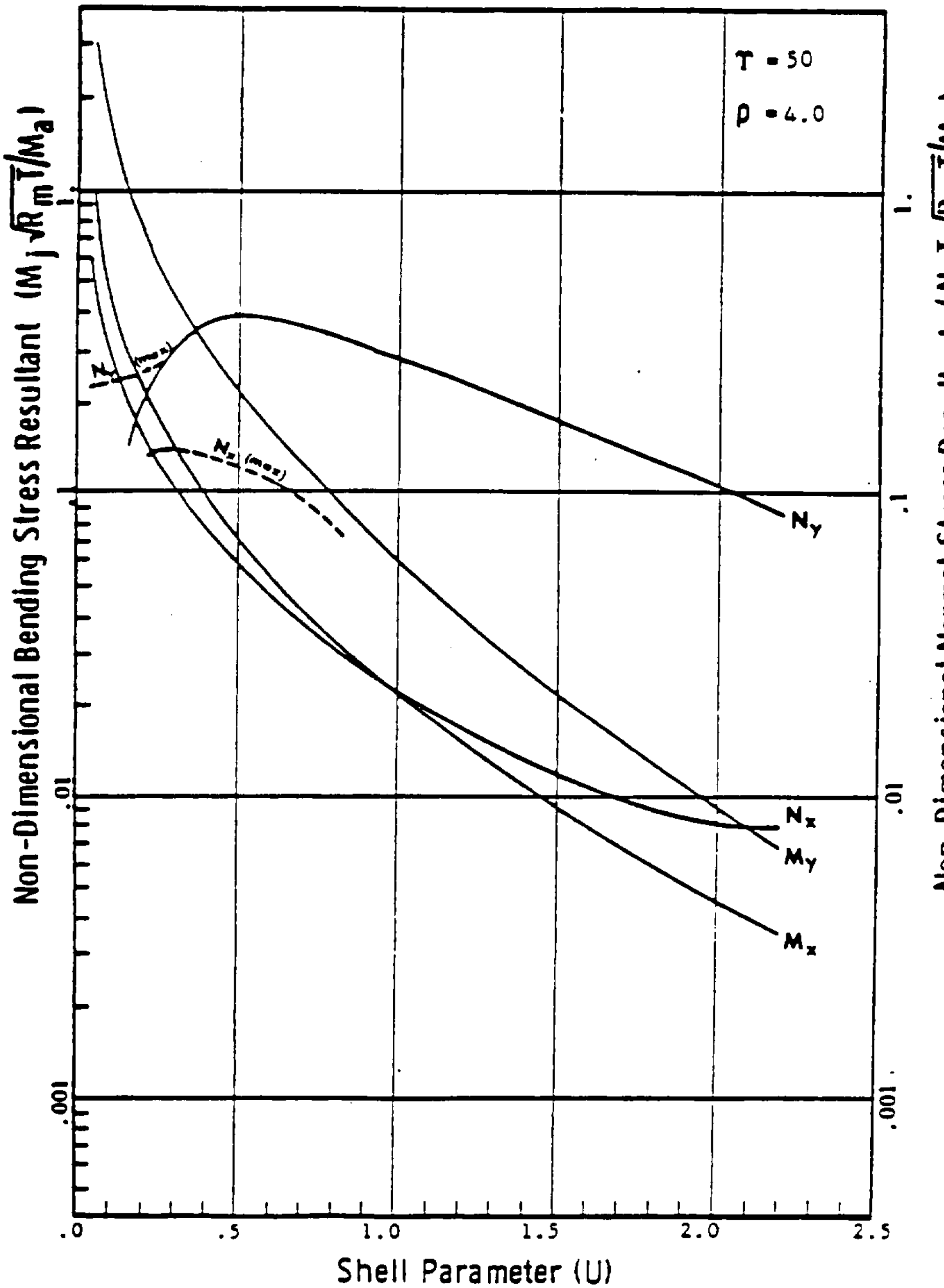

Figure B7.2.1.5-21 Non-Dimensional Stress Resultants for Overturning Moment (M_a) Hollow Attachment γ = 50 and ρ = 4.0

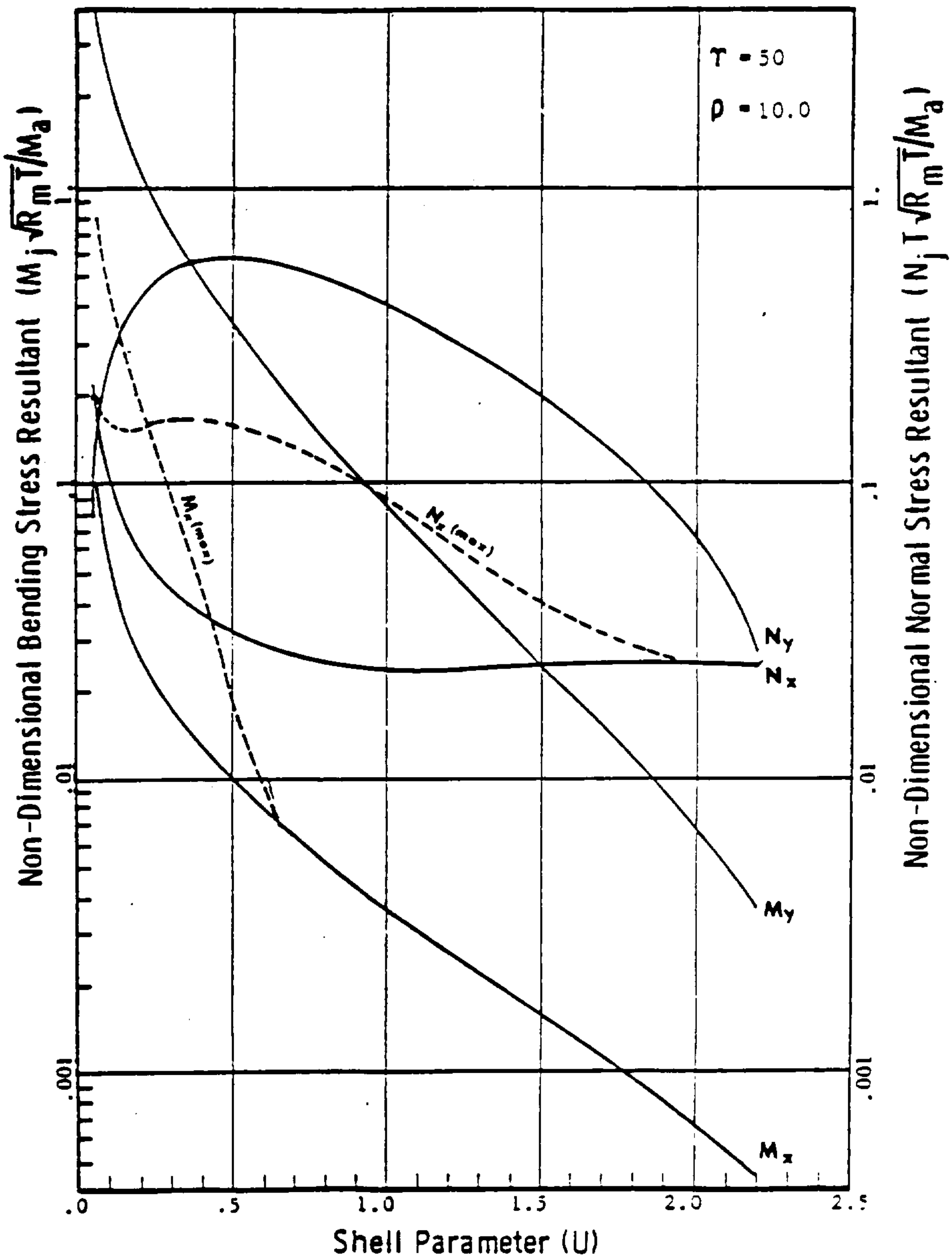

Figure B7.2.1.5-22 Non-Dimensional Stress Resultants for Overturning Moment (M_a) Hollow Attachment T = 50 and ρ = 10.0

B7.2.1.6 EXAMPLE PROBLEM

A spherical bulkhead with a welded hollow attachment is subjected to the force and moments shown in Figure B7.2.1.6-1. Shell and attachment geometry are shown in Figures B7.2.1.6-1 and B7.2.1.6-2.

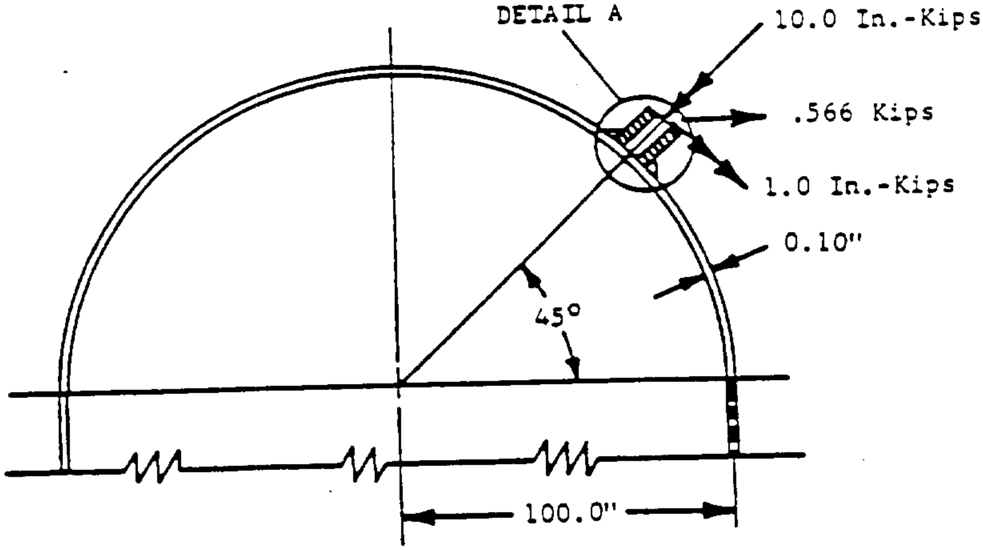

Fig. B7.2.1.6-1 Spherical Bulkhead

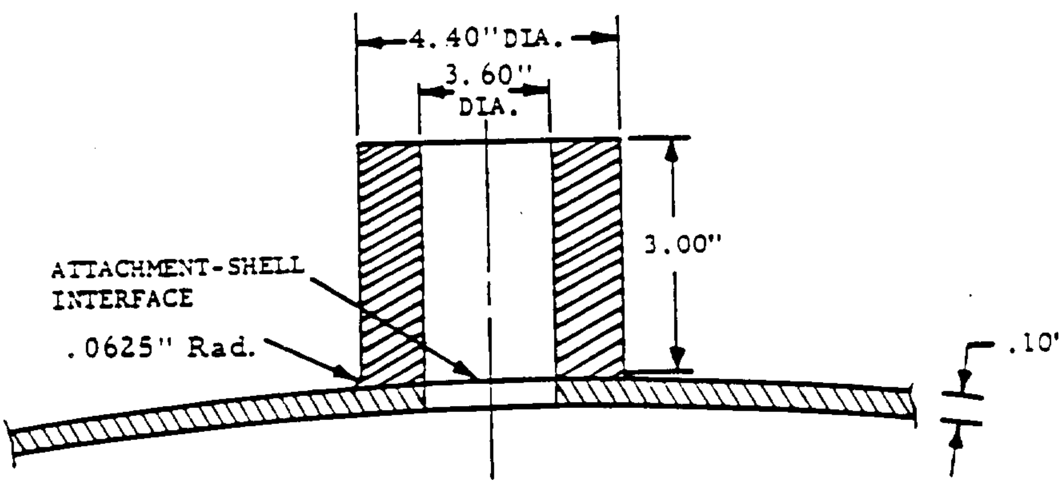

Fig. B7.2.1.6-2 Welded Hollow Attachment (Detail A)

1. Establish a local coordinate system (Figs. B7.2.1.1-1 and B7.2.1.6-3) on the center line of the attachment at the attachment-shell interface, so that the loading in Figure B7.2.1.6-1 is in the 2-3 plane.

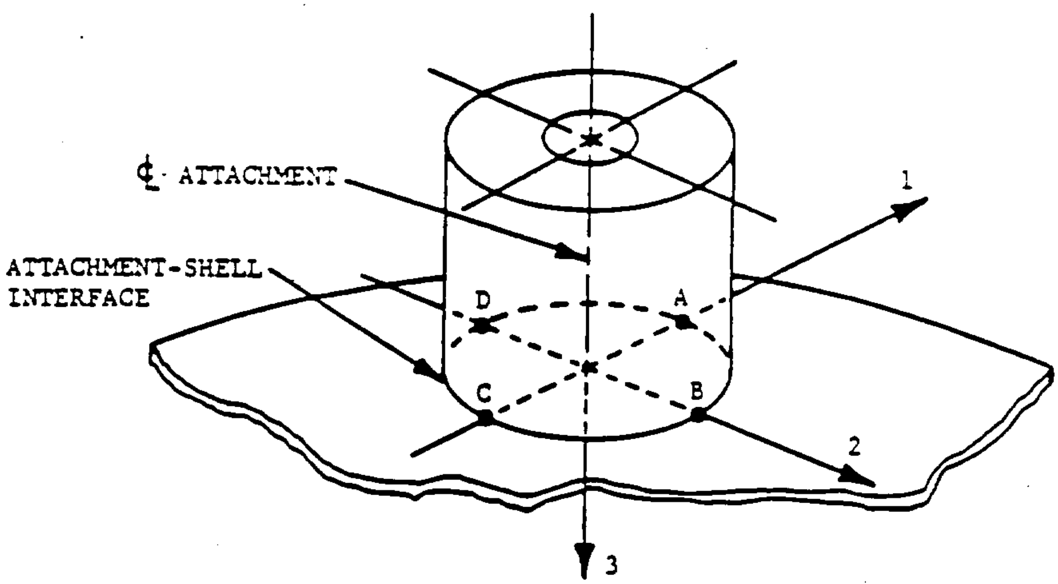

Fig. B7.2.1.6-3 Local Coordinate System

2. Resolve the load system into components (Figs. B7.2.1.1-1 and B7.2.1.6-4) and enter results on the appropriate stress calculation sheet (Figs. B7.2.1.2-2 for hollow attachments and B7.2.1.2-3 for solid attachments). Figure B7.2.1.6-5 shows the stress calculation sheet for the example problem.

3. Establish the appropriate shell geometric properties (Figure B7.2.1.1-2) and enter results on the stress calculation sheet. All dimensions are in inches.

$R_m = 100.0$

$T = 0.10$

$r_0 = 2.20$

$r_m = 2.00$

$t = 0.40$

$a = 0.0625$

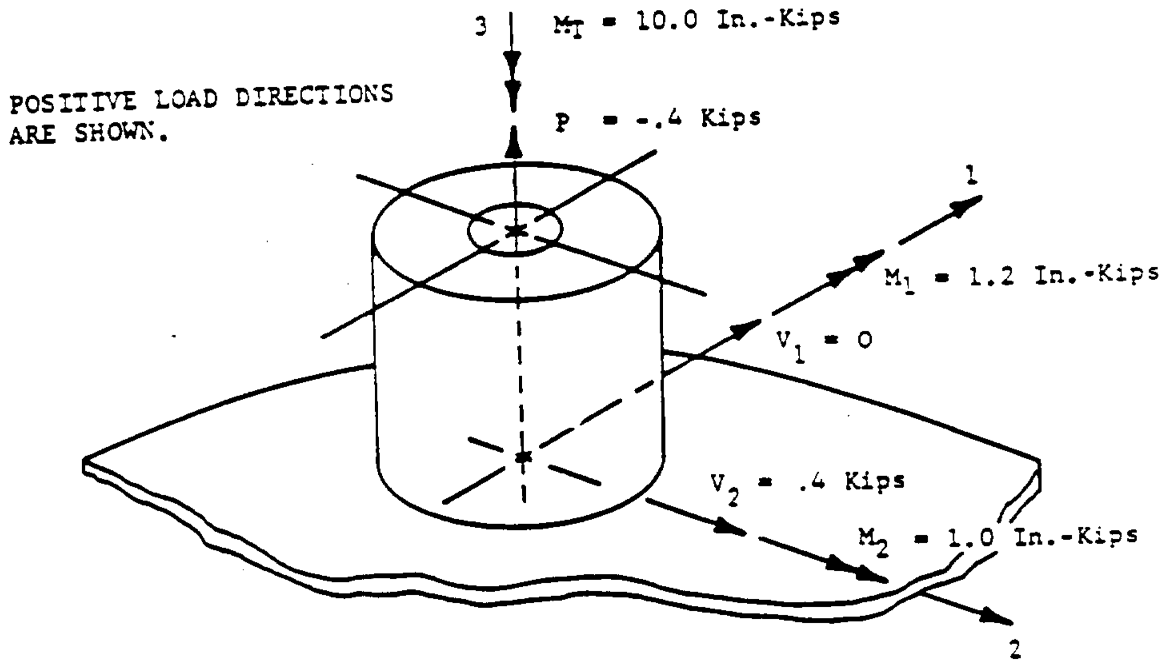

Fig. B7.2.1.6-4 Arbitrary Load System Components

4. Determine the appropriate parameters according to paragraph B7.2.1.2-II, and enter results on the stress calculation sheet.

$$U = r_0/(R_m T)^{\frac{1}{2}} = 2.20/(100 \times 0.1)^{\frac{1}{2}} = 0.695$$

For hollow attachment:

$$\Upsilon = r_m/t = 2.00/0.40 = 5.0$$

$$\rho = T/t = 0.10/0.40 = 0.25$$

For a brittle material (weld) at the attachment-to-shell juncture:

$$K_n = 1 + (T/5.6\,a)^{0.65} = 1 + (0.1/5.6 \times .0625)^{0.65} = 1.44$$

$$K_b = 1 + (T/9.4\,a)^{0.80} = 1 + (0.1/9.4 \times .0625)^{0.80} = 1.70$$

5. Determine the stresses according to paragraph B7.2.1.2-III through VI and enter results on the stress calculation sheet. The nondimensional stress resultants are obtained from Figure B7.2.1.5-3 (Hollow Attachment- Υ = 5 and ρ = 0.25) for the radial load and from Figure B7.2.1.5-13 (Hollow Attachment - Υ = 5 and ρ = 0.25) for the overturning moments.

STRESS CALCULATION SHEET FOR STRESSES IN SPHERICAL SHELLS CAUSED BY LOCAL LOADS (HOLLOW ATTACHMENT)

APPLIED LOADS	SHELL GEOMETRY	PARAMETERS
P = -.4 kips	T = .10	U = .695
V_1 = 0 "	t = .40	τ = 5.0
V_2 = .4 "	R_m = 100.	ρ = .25
M_T = 10.0 in-kips	r_m = 2.00	K_n = 1.44
M_1 = 1.2 "	r_o = 2.20	K_b = 1.70
M_2 = 1.0 "	s = .0625	

STRESS	LOAD	NON-DIMENSIONAL STRESS RESULTANT	ADJUSTING FACTOR	STRESS COMPONENT	STRESSES* A_1	A_o	B_1	B_o	C_1	C_o	D_1	D_o
MERIDIONAL STRESS (f_x)	P	$\frac{N_xT}{P}$ (.064) .066	$\frac{K_nP}{T^2}$ -57.6	$\frac{K_nN_x}{T}$ =	(+3.5) ∓8.2	(+3.6) ∓8.2	(+3.6) ∓8.2	(+3.6) ∓8.2	(+3.6) ∓8.2	(+3.6) ∓8.2	(+3.0) ∓8.2	(+3.6) ∓8.2
		$\frac{M_x}{P}$ .064	$\frac{6K_bP}{T^2}$ -408	$\frac{6K_bM_x}{T^2}$ =	-26.1	+26.1	-26.1	+26.1	-26.1	+26.1	-26.1	+26.1
	M_1	$\frac{N_xT\sqrt{R_mT}}{M_1}$ .067	$\frac{K_nM_1}{T^2\sqrt{R_mT}}$ 54.7	$\frac{K_nN_x}{T}$ =			-3.7	-3.7			+3.7	-3.7
		$\frac{M_x\sqrt{R_mT}}{M_1}$ .15	$\frac{6K_bM_1}{T^2\sqrt{R_mT}}$ 387.3	$\frac{6K_bM_x}{T^2}$ =			+58.1	-58.1			-58.1	+58.1
	M_2	$\frac{N_xT\sqrt{R_mT}}{M_2}$ .067	$\frac{K_nM_2}{T^2\sqrt{R_mT}}$ 46.6	$\frac{K_nN_x}{T}$ =	+3.1	+3.1			-3.1	-3.1		
		$\frac{M_x\sqrt{R_mT}}{M_2}$ .15	$\frac{6K_bM_2}{T^2\sqrt{R_mT}}$ 322.8	$\frac{6K_bM_x}{T^2}$ =	-48.4	+48.4			+48.4	-48.4		
	TOTAL MERIDIONAL STRESSES (f_x)				-68.2	81.1	31.8	-32.5	22.7	-22.2	-77.3	91.4
CIRCUMFERENTIAL STRESS (f_y)	P	$\frac{N_yT}{P}$ .087	$\frac{K_nP}{T^2}$ -57.6	$\frac{K_nN_y}{T}$ =	±5.0	±5.0	±5.0	±5.0	±5.0	±5.0	±5.0	±5.0
		$\frac{M_y}{P}$ .019	$\frac{6K_bP}{T^2}$ -408	$\frac{6K_bM_y}{T^2}$ =	-7.8	+7.8	-7.8	+7.8	-7.8	+7.8	-7.8	+7.8
	M_1	$\frac{N_yT\sqrt{R_mT}}{M_1}$ (.11) .087	$\frac{K_nM_1}{T^2\sqrt{R_mT}}$ 54.7	$\frac{K_nN_y}{T}$ =			(6.0) -4.8	(6.0) -4.8			(6.0) +4.8	(6.0) +4.8
		$\frac{M_y\sqrt{R_mT}}{M_1}$ (.048) .045	$\frac{6K_bM_1}{T^2\sqrt{R_mT}}$ 387.3	$\frac{6K_bM_y}{T^2}$ =			(18.6) +17.4	(18.6) -17.4			(18.6) -17.4	(18.6) +17.4
	M_2	$\frac{N_yT\sqrt{R_mT}}{M_2}$ (.11) .087	$\frac{K_nM_2}{T^2\sqrt{R_mT}}$ 46.6	$\frac{K_nN_y}{T}$ =	(5.0) +4.0	(5.0) +4.0			(5.0) -4.0	(5.0) -4.0		
		$\frac{M_y\sqrt{R_mT}}{M_2}$ (.048) .045	$\frac{6K_bM_2}{T^2\sqrt{R_mT}}$ 322.8	$\frac{6K_bM_y}{T^2}$ =	(15.5) -14.5	(15.5) +14.5			(15.5) +14.5	(15.5) -14.5		
	TOTAL CIRCUMFERENTIAL STRESS (f_y)				-14.3	33.3	11.0	-11.8	8.7	-7.7	-16.6	37.4
SHEAR STRESS (f_{xy})	V_1	0	πr_oT .69	$\frac{V_1}{\pi r_oT}$ = 0			-0	-0			+0	+0
	V_2	.40	πr_oT .69	$\frac{V_2}{\pi r_oT}$ = .6	-.6	-.6			+.6	+.6		
	M_T	10.0	$2\pi r_o^2T$ 3.04	$\frac{M_T}{2\pi r_o^2T}$ = 3.3	-3.3	-3.3	+3.3	+3.3	-3.3	-3.3	+3.3	+3.3
	TOTAL SHEAR STRESS (f_{xy})				-3.9	-3.9	3.3	3.3	-2.7	-2.7	3.3	3.3
PRINCIPAL STRESSES**	f_{max}	$\frac{f_x+f_y}{2}+\sqrt{\frac{(f_x-f_y)^2}{4}+f_{xy}^2}$ ***			-68.5	81.4	32.3	-33.0	23.2	-22.9	-77.5	91.6
	f_{min}	$\frac{f_x+f_y}{2}-\sqrt{\frac{(f_x-f_y)^2}{4}+f_{xy}^2}$ ***			-14.0	33.0	10.5	-11.3	8.2	-7.0	-16.4	37.2
	$f_{xy\,max}$	$\pm\sqrt{\frac{(f_x-f_y)^2}{4}+f_{xy}^2}$			27.2	24.2	10.9	10.9	7.5	8.0	30.5	27.2

* IF LOAD IS OPPOSITE TO THAT SHOWN IN FIGURE B7.2.1.1-1 THEN REVERSE THE SIGN SHOWN.
** SEE SECTION A1.1.6.
*** CHANGE SIGN OF THE RADICAL IF $(f_x + f_y)$ IS NEGATIVE.

Figure B7.2.1.6-5 Stress Calculation Sheet (Example Problem)

.87

B7.2.2.0 LOCAL LOADS ON CYLINDRICAL SHELLS

This section presents a method to obtain cylindrical shell membrane and bending stresses at an attachment-to-shell juncture resulting from arbitrary loads induced through rigid attachments on pressurized or unpressurized shells. Shell geometry and loading conditions are used to obtain normal and bending stress resultants and deflections from a computer program for radial-type loads (P and M_a). Membrane shear stresses caused by shearing loads (V_a) and twisting moments (M_T) can be calculated directly without the computer program. Deflections are not calculated for shearing loads and twisting moments.

Local load stresses reduce rapidly at points removed from the attachment-to-shell juncture. Boundaries of that region of the shell influenced by the local loads can be determined for those load cases calculated with the computer program by investigation of the stresses and deflections at points removed from the attachment.

The additional stiffness of the shell caused by internal pressure (pressure coupling) is taken into account by the computer program for determination of local load stress resultants and deflections. The stress resultants induced in the shell by the internal pressure are not included in the computer program results and must be superimposed upon the local load stress resultants calculated by the method contained in this section.

B7.2.2.1 GENERAL

I NOTATION

The notations presented in this section are not applicable to the computer program. The computer program variables are defined in Paragraph B7.2.2.5-II.

a	-	fillet radius at attachment-to-shell juncture or longitudinal half diameter of elliptical load pad, in.
b	-	x-coordinate distance to center of attachment (b = L/2) or circumferential half diameter of elliptical load pad, in.
c	-	half length of square attachment, in.
c_1	-	longitudinal half length of rectangular attachment, in.
c_2	-	circumferential half length of rectangular attachment, in.
E	-	modulus of elasticity, psi
f_x	-	normal longitudinal stress, psi
f_y	-	normal circumferential stress, psi
f_{xy}	-	shear stress, psi
K_n, K_b	-	stress concentration parameters for normal stresses and bending stresses, respectively
L	-	length of cylinder
M_a	-	applied overturning moment, in.-lb.
M_T	-	applied twisting moment, in.-lb.
M_j	-	internal bending moment stress resultant per unit length of shell, in.-lb/in.
n	-	number of equally spaced attachments in the circumferential direction
N_j	-	internal normal force stress resultant per unit length of shell, lb/in.
p	-	uniform load intensity, psi
P	-	radial load or total distributed radial load, lb.
q	-	internal pressure, psi

B7.2.2.1 GENERAL (Concluded)

I NOTATION (Concluded)

r - radius of circular attachment, in.

R - radius of cylindrical shell, in.

s - circumferential arc length, in.

T - thickness of cylindrical shell, in.

u - longitudinal displacement, in.

v - circumferential displacement, in.

V_a - applied concentrated shear load or total distributed shear load, lb.

w - radial displacement, in.

x - longitudinal coordinate, in.

y - circumferential coordinate, in.

z - radial coordinate, in.

θ - polar coordinate

ν - Poisson's ratio

ϕ - circumferential cylindrical coordinate

Subscripts

a - applied ($a = 1$ or $a = 2$)
b - bending
i - inside
j - internal ($j = x$ or $j = y$)
m - mean (average of outside and inside)
n - normal
o - outside
x - longitudinal
y - circumferential
z - radial

1 - longitudinally directed applied load vector or longitudinal direction

2 - circumferentially directed applied load vector or circumferential direction

B7.2.2.1 GENERAL

II SIGN CONVENTION

Local loads applied at an attachment-to-shell induce a biaxial state of stress on the inside and outside surfaces of the shell. The longitudinal stress (f_x), circumferential stress (f_y), shear stress (f_{xy}), the positive directions of the applied loads (M_a*, M_T, P, q, and V_a), the stress resultants (M_j and N_j), and the positive directions of the displacements (u, v, and w) are indicated in Figure B7.2.2.1-1.

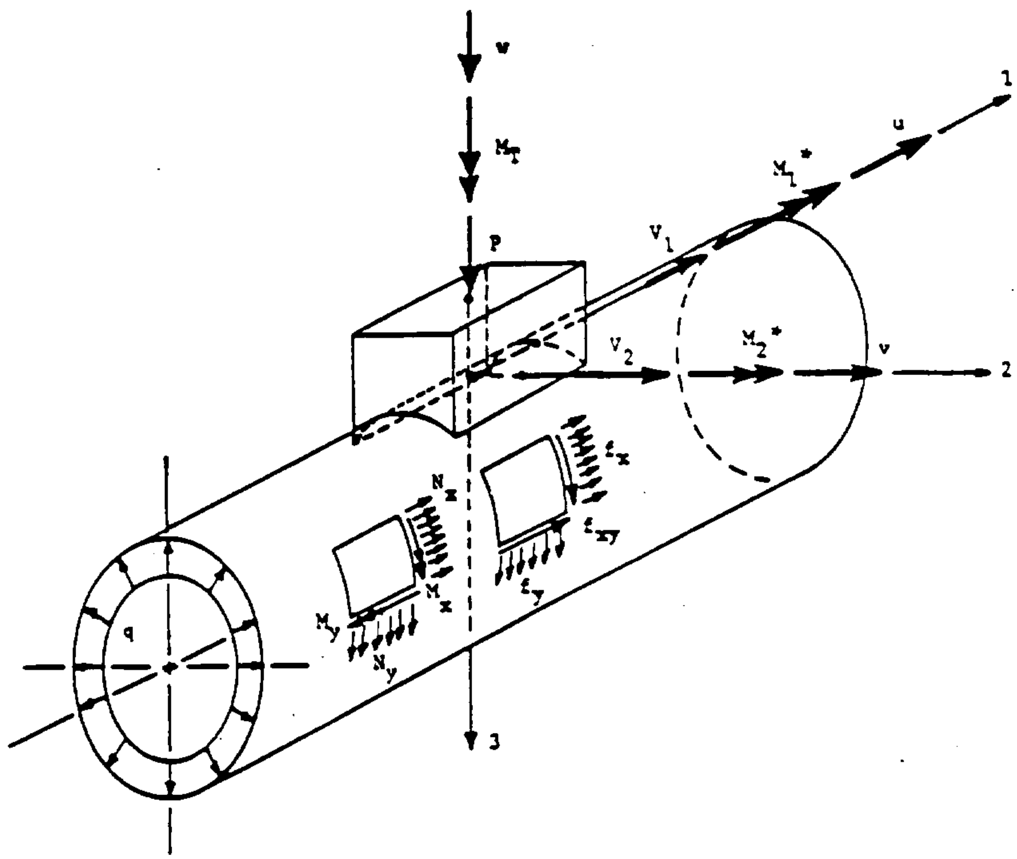

Fig. B7.2.2.1-1 Stresses, Stress Resultants, Loads, and Displacements

* The applied overturning moment M_1 (M_2) is represented by a longitudinally (circumferentially) directed vector but is defined as an applied circumferential (longitudinal) overturning moment since its effect is in the circumferential (longitudinal) direction.

The geometry of the shell and attachment, the local coordinate system at the attachment, and the coordinate system of the shell are indicated in Figure B7.2.2.1-2.

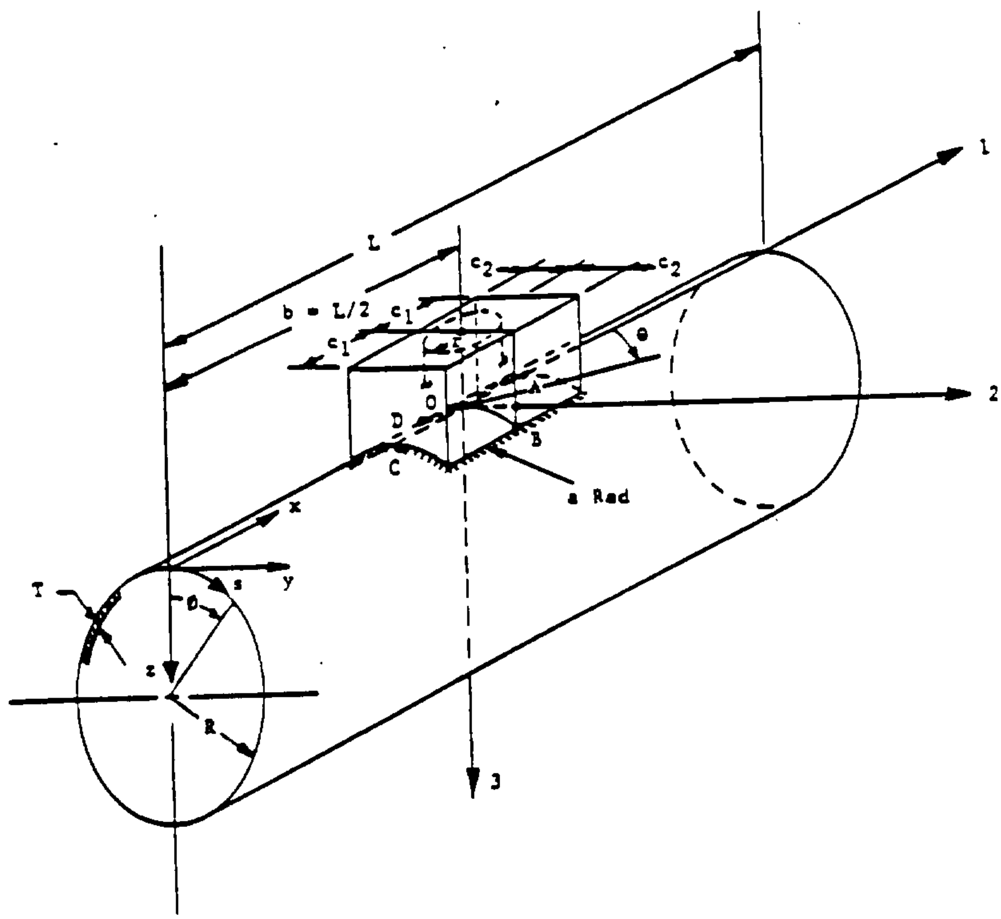

Fig. B7.2.2.1-2 Shell and Attachment Geometry

It is possible to predict the sign of the induced stress, tensile (+) or compressive (-), by considering the deflections of the shell resulting from various loading modes.

Mode I (radial load), Figure B7.2.2.1-3, shows a positive radial load (P) transmitted to the shell by a rigid attachment. The load (P) causes compressive membrane stresses and local bending stresses adjacent to the

attachment. The compressive membrane stresses are similar to the stresses induced by an external pressure. The local bending stresses result in tensile bending stresses on the inside of the shell and compressive bending stresses on the outside of the shell at points A, B, C and D.

Modes II (circumferential moment) and III (longitudinal moment), Figure B7.2.2.1-3, show negative overturning moments (M_a) transmitted to the shell by rigid attachments. The overturning moments (M_a) cause compressive and tensile membrane stresses and local bending stresses adjacent to the attachment. Tensile membrane stresses are induced in the shell at B or C, similar to the stresses caused by an internal pressure. Compressive membrane stresses are induced in the shell at D or A, similar to the stresses caused by an external pressure. The local bending stresses cause tensile bending stresses in the shell at B or C on the outside and at D or A on the inside, and cause compressive bending stresses in the shell at B or C on the inside and at D or A on the outside.

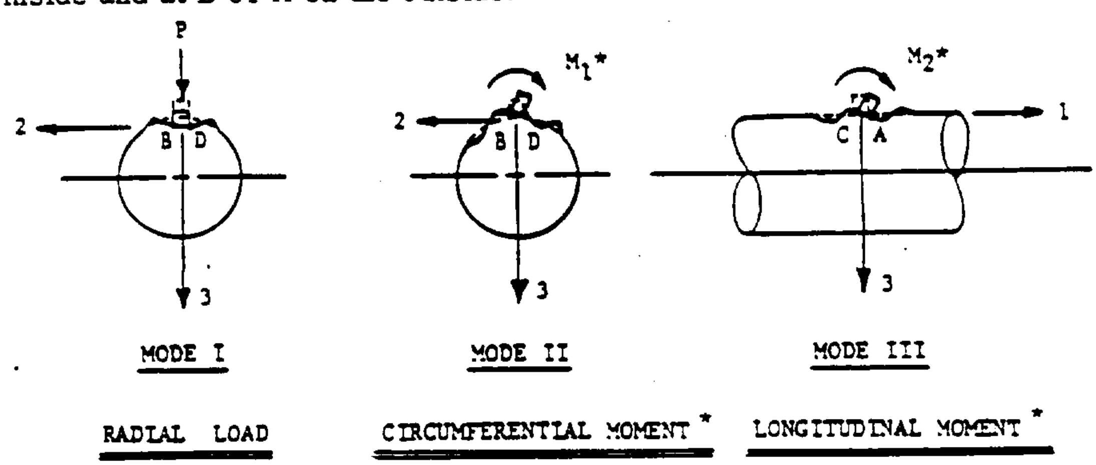

Fig. B7.2.2.1-3 Loading Modes

* The applied overturning moment M_1 (M_2) is represented by a longitudinally (circumferentially) directed vector but is defined as an applied circumferential (longitudinal) overturning moment since its effect is in the circumferential (longitudinal) direction.

The signs of the stresses induced in the shell adjacent to the attachment by positive applied loads for rigid attachments are shown in Figure B7.2.2.2-1 "Stress Calculation Sheet". The figure or parts thereof can be reproduced and used as calculation sheets.

B7.2.2.1 GENERAL

III LIMITATIONS OF ANALYSIS

Considerable judgment must be used in the interpretation of the results of this section and in the establishment of the geometry and loadings used in the analysis.

Six general areas must be considered for limitations: attachment and shell size, attachment location, shift in maximum stress location, stresses caused by shear loads, geometry and loading.

A Size of Attachment with Respect to Shell Size

The analysis is applicable to small attachments relative to the shell size and to thin shells. The limitations on these conditions are shown by the shaded area of Figure B7.2.2.1-4.

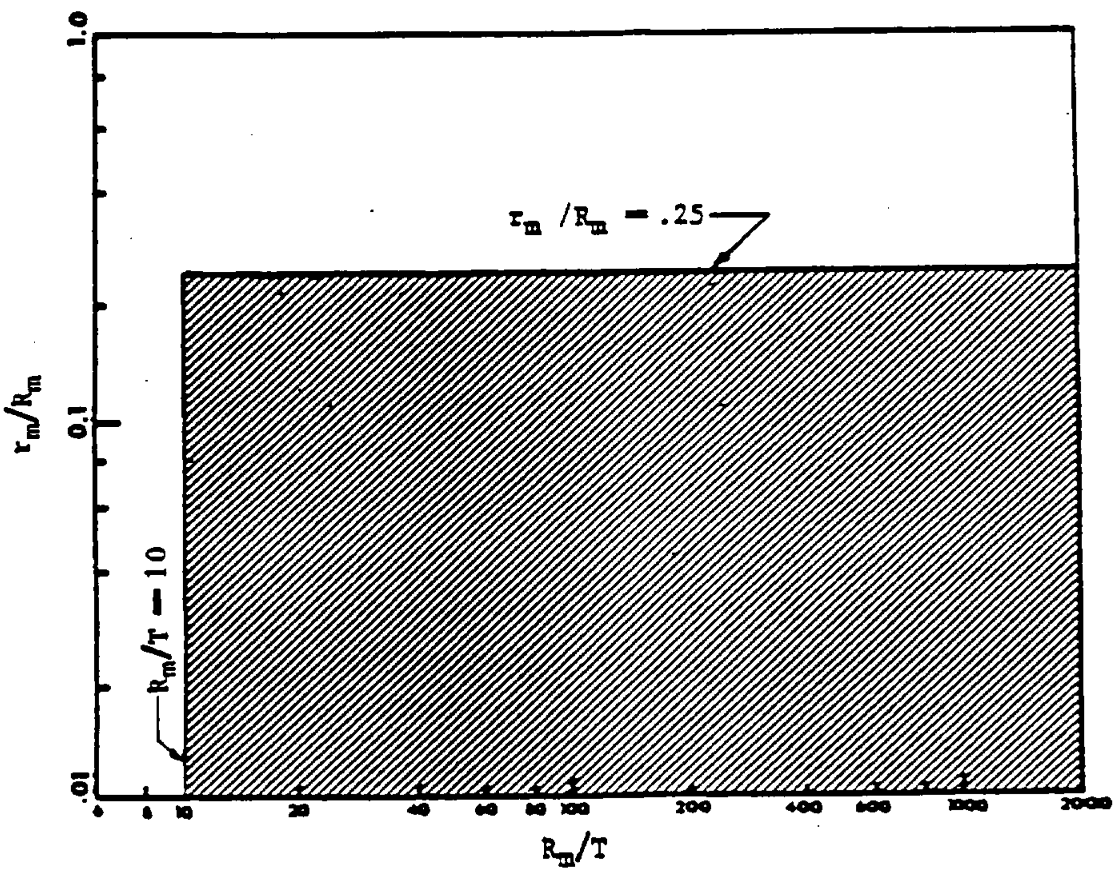

Fig. B7.2.2.1-4

95

B Location of Attachment with Respect to Boundary Conditions to Shell

The analysis is applicable when there are no stress perturbations caused by other loadings in the area influenced by the local loads. These perturbations can be caused by discontinuity, thermal loading, liquid level loading, change in section and material change. The area influenced by the local loading can be determined by an investigation of the stresses and deflections at points removed from the attachment.

C Shift in Maximum Stress Locations

Under certain conditions the stresses in the shell may be higher at points removed from the attachment-to-shell juncture than at the juncture. The following conditions should be carefully considered:

1. Stresses can be higher in the attachment than in the shell. This is most likely when the attachment is not reinforced, when reinforcement is placed on the shell and not on the attachment, and when very thin attachments are used.

2. For some load conditions certain stress resultants peak at points slightly removed from the attachment-to-shell juncture. The load conditions that cause this peaking are in most cases the same load cases that cause peaking for local loads on spherical shells. The extent of the peaking can be evaluated by an investigation of the stresses and deflections at points slightly removed from the attachment.

3. Comparison of analytical and experimental results [2] for membrane stresses shows that membrane stress resultants can be calculated at the point where stresses are desired. Comparison of analytical and experimental results [2, 5] for bending stress resultants at loaded attachments shows that the bending stress resultants must be calculated at the center of the attachment and

then shifted to the edge for the determination of stresses at the edge of the attachment. The determination of bending stresses at other points requires that the bending stress resultants be calculated at a distance $C_{1/2}$ or $C_{2/2}$ closer to the attachment.

D Stresses Caused by Shear Loads

An accurate stress distribution caused by a shear load (V_a) applied to a cylindrical shell is not available. The actual stress distribution consists of varying shear and membrane stresses around the rigid attachment. The method [5] presented here assumes that the shell resists the shear load by shear only. If this assumption appears unreasonable, it can be assumed that the shear load is resisted totally by membrane stresses or by some combination of membrane and shear stresses.

E Shell and Attachment Geometry

The analysis assumes that the cylindrical shell has simply supported end conditions or is of sufficient length that simply supported end conditions can be assumed.

The computer program requires that circular and elliptical attachments be converted to equivalent square and rectangular attachments, respectively. The equivalent attachment must have an area equal to the area of the actual attachment for a radially applied force. The equivalent attachment must have a moment of inertia about the bending axis equal to the moment of inertia about the bending axis of the actual attachment for bending loads. In both cases the aspect ratios (a/b and c_1/c_2) of the attachments (actual and equivalent, respectively) must be equal. If the attachment is welded, the weld size must be added to the attachment when determining equivalent attachments.

L/R_m is a secondary parameter and has little effect on the solution of $1.0 \leq L/R_m \leq 5.0$. The attachment coordinate system, defined by Figure B7.2.2.1-2, must be located at $x = L/2$.

F <u>Shell Loading</u>

The computer program accounts for pressure coupling (that is, the increase in shell stiffness caused by internal pressure). The internal pressure (q) must be positive or a positive differential. The stresses caused by the internal pressure must be calculated separately and superimposed upon the local loads stresses calculated by the method presented here.

The shell deflections must be small, approximately equal to the cylindrical shell thickness, for the analysis to be valid and to allow superposition of stresses.

B7.2.2.2 STRESSES

I GENERAL

Stress resultants and displacements caused by radial load (P) and overturning moment (M_a) are obtained from the computer program described in Ref. 5, B7.2.2.5. Stresses caused by shear load (V_a) and twisting moment (M_T) are calculated directly from attachment geometry and loading.

The stress resultants (M_j and N_j) and displacements (u, v, and w) determined by the computer program are for a specific location. The location is specified by x and ϕ input values determined according to the coordinate system (x, ϕ, z) defined in Figure B7.2.2.1-2.

The computer program will calculate stress resultants and displacements for configurations (see Figure B7.2.2.5-1):

Case 1 - One Uniformly Distributed Radial Load

Case 2 - "n" Equally Spaced Uniformly Distributed Radial Loads

Case 3 - One Concentrated Radial Load

Case 4 - "n" Equally Spaced Concentrated Radial Loads

Case 5 - Longitudinal Overturning Moment

Case 6 - Circumferential Overturning Moment

The general equation for stresses in a shell at a rigid attachment juncture in terms of the stress resultants is of the form:

$$f_j = K_n (N_j/T) \pm K_b (6M_j/T^2)$$

The stress concentration parameters (K_n and K_b) are defined and can be evaluated from Paragraph B7.2.1.2, Sections I and IIB.

Figure B7.2.2.2-1 "Stress Calculation Sheet" can be used for the calculation of all stresses caused by an arbitrary local loading. The sheet automatically accounts for signs.

STRESS CALCULATION SHEET FOR STRESSES IN CYLINDRICAL SHELLS CAUSED BY LOCAL LOADS

APPLIED LOADS	SHELL GEOMETRY	CO-ORDINATES			PARAMETERS
			x	θ	
p = ______	T = ______	O =	______	______	K_a = ______
P = ______	R_m = ______	A =	______	______	K_b = ______
V_1 = ______	L = ______	B =	______	______	
V_2 = ______	c_1 = ______	C =	______	______	
M_T = ______	c_2 = ______	D =	______	______	
M_1 = ______	a = ______		______	______	
M_2 = ______	r_o = ______		______	______	

STRESS	LOAD	STRESS RESULT.	ADJUST. FACTOR	CALC. STRESS	STRESSES* A_i	A_o	C_i	C_o	STRESS RESULT.	ADJUST. FACTOR	CALC. STRESS	STRESSES* B_i	B_o	D_i	D_o
LONGITUDINAL STRESS (f_x)	P case I	N_x (A)=**	$\frac{K_a}{T}$ =		+	+	+	+	N_x (B)=**	$\frac{K_a}{T}$ =		+	+	+	+
	P case IV	M_x (O)=	$\frac{6K_b}{T^2}$ =		+	−	+	−	M_x (O)=	$\frac{6K_b}{T^2}$ =		+	−	+	−
	M_1 case VI	N_x (A)=	$\frac{K_a}{T}$ =						N_x (B)=	$\frac{K_a}{T}$ =		+	+	−	−
		M_x (A)=	$\frac{6K_b}{T^2}$ =						M_x (B)=	$\frac{6K_b}{T^2}$ =		−	−	+	−
	M_2 case V	N_x (A)=	$\frac{K_a}{T}$ =		−	−	+	+	N_x (B)=	$\frac{K_a}{T}$ =					
		M_x (A)=	$\frac{6K_b}{T^2}$ =		−	+	+	−	M_x (B)=	$\frac{6K_b}{T^2}$ =					
	TOTAL LONGITUDINAL STRESSES (f_x)														
CIRCUMFERENTIAL STRESS (f_y)	P	N_y (A)=**	$\frac{K_a}{T}$ =		+	+	+	+	N_y (B)=**	$\frac{K_a}{T}$ =		+	+	+	+
		M_y (O)=	$\frac{6K_b}{T^2}$ =		+	−	+	−	M_y (O)=	$\frac{6K_b}{T^2}$		+	−	+	−
	M_1	N_y (A)=	$\frac{K_a}{T}$ =						N_y (B)=	$\frac{K_a}{T}$ =		+	+	−	−
		M_y (A)=	$\frac{6K_b}{T^2}$ =						M_y (B)=	$\frac{6K_b}{T^2}$ =		+	−	+	−
	M_2	N_y (A)=	$\frac{K_a}{T}$ =		−	−	+	+	N_y (B)=	$\frac{K_a}{T}$ =					
		M_y (A)=	$\frac{6K_b}{T^2}$ =		−	+	+	−	M_y (B)=	$\frac{6K_b}{T^2}$ =					
	TOTAL CIRCUMFERENTIAL STRESSES (f_y)														
SHEAR STRESS (f_{xy})	V_1	V_1 =	$\frac{1}{\pi r_o T}$ =									−	−	+	+
	V_2	V_2 =	$\frac{1}{\pi r_o T}$ =		−	−	+	+							
	M_T	M_T =	$\frac{1}{2\pi r_o^2 T}$ =		−	−	−	−				+	+	+	+
	TOTAL SHEAR STRESS (f_{xy})														
PRINCIPAL STRESSES	f_{max}	$\frac{f_x+f_y}{2} + \sqrt{\frac{(f_x-f_y)^2}{4} + f_{xy}^2}$ ***													
	f_{min}	$\frac{f_x+f_y}{2} - \sqrt{\frac{(f_x-f_y)^2}{4} + f_{xy}^2}$ ***													
	$f_{xy\,max}$	$\pm\sqrt{\frac{(f_x-f_y)^2}{4} + f_{xy}^2}$													

* CHANGE SIGN OF CALCULATED STRESS WHERE NEGATIVE SIGNS ARE INDICATED.

** LETTER IN PARENTHESIS DESIGNATES THE POINT (A, B, OR O) AT WHICH THE STRESS RESULTANTS SHOULD BE COMPUTED BY THE COMPUTER PROGRAM. THE STRESSES FOR POINTS (A, B, C, AND D) CAN BE OBTAINED FROM THESE STRESS RESULTANTS USING THE SIGNS INDICATED.

*** CHANGE SIGN OF THE RADICAL IF $(f_x + f_y)$ IS NEGATIVE.

Fig. B7.2.2.2-1 Stress Calculation Sheet

B7.2.2.2 STRESSES

II STRESSES RESULTING FROM A RADIAL LOAD

Radial load configuration Cases I and II (see Figure B7.2.2.5-1) will cause membrane and bending stress components in both the longitudinal and circumferential directions.

A Longitudinal Stress (f_x)

Step 1. Determine the required load and geometric load input for the computer program.

Step 2. Determine the bending stress resultant (M_x) at point O and the normal stress resultant (N_x) at points A and B with the computer program. See Figure B7.2.2.1-2 for the location of points A, B and O.

Step 3. Using the criteria in Paragraph B7.2.1.2, Section I, obtain values for the stress concentration parameters (K_n and K_b).

Step 4. Using the bending stress resultant (M_x) at point O and the normal stress resultant (N_x) at point A as determined in Step 2, and the stress concentration parameters as determined in Step 3, determine the longitudinal stresses (f_x) at point A using the following equation:

$$f_x = K_n(N_x/T) \pm K_b(6M_x/T^2)$$

Proper consideration of the sign will give the values for the longitudinal stress at the inside and outside surfaces of the shell.

Step 5. Repeat Step 4, but use the normal stress resultant (N_x) as determined for point B and the bending stress resultant (M_x) as determined for point O to determine the longitudinal stresses (f_x) at point B.

B Circumferential Stresses (f_y)

The circumferential stresses (f_y) can be determined by following the five steps outlined in Paragraph A, above, except for determining M_y and N_y instead of M_x and N_x in Step 2 and using the following stress equation in Step 4.

$$f_y = K_n(N_y/T) = K_b(6M_y/T^2)$$

C Concentrated Load Stresses

Points A, B, C and D in Figure B7.2.2.1-2 do not exist for Load Cases III and IV. Longitudinal and circumferential membrane and bending stress caused by concentrated loads (Cases III and IV) is determined from stress resultants calculated at point O. The stresses are calculated using Paragraph A, above, after applying proper modifications to the equations.

B7.2.2.2 STRESSES

III STRESSES RESULTING FROM AN OVERTURNING MOMENT

Overturning moment load configurations, Cases V and VI (see Figure B7.2.2.5-1), will cause membrane and bending stress components in both the longitudinal and circumferential directions.

A Longitudinal Stress (f_x)

Step 1. Determine load and geometric input for the computer program.

Step 2. Determine the bending stress resultant (M_x) and normal stress resultant (N_x) at points A for Load Case V and B for Load Case VI with the computer program.

Step 3. Using the criteria in Paragraph B7.2.1.2, Section I, obtain the values for the stress concentration parameters (K_n and K_b).

Step 4. Using the bending stress resultant (M_x) and the normal stress resultant (N_x) at point A as determined in Step 2 and the stress concentration parameters as determined in Step 3, determine the longitudinal stress (f_x) at point A using the following equation:

$$f_x = K_n(N_x/T) \pm K_b(6M_x/T^2)$$

Proper consideration of the sign will give the values for longitudinal stresses at the inside and outside surfaces of the shell.

Step 5. Repeat Step 4, but use stress resultants as determined for point B to determine the longitudinal stresses at point B.

B Circumferential Stress (f_y)

The circumferential stresses (f_y) can be determined by following the five steps outlined in Paragraph A, above, except for determining M_y and N_y instead of M_x and N_x in Step 2, and using the following stress equation in Step 4:

$$f_y = K_n (N_y/T) \pm K_b (6M_y/T^2)$$

B7.2.2.2 STRESSES

IV STRESSES RESULTING FROM A SHEAR LOAD

A shear load (V_a) will cause a shear stress (f_{xy}) in the shell at the attachment-to-shell juncture. The shear stress is determined as follows:

A Round Attachment

$$f_{xy} = \frac{V_a}{\pi r_0 T} \sin\theta \qquad \text{for } V_a = V_1$$

$$f_{xy} = \frac{V_a}{\pi r_0 T} \cos\theta \qquad \text{for } V_a = V_2$$

B Rectangular Attachment

$$f_{xy} = \frac{V_a}{4c_1 T} \qquad \text{for } V_a = V_1$$

$$f_{xy} = \frac{V_a}{4c_2 T} \qquad \text{for } V_a = V_2$$

B7.2.2.2 STRESSES

V STRESSES RESULTING FROM A TWISTING MOMENT

A Round Attachment

A twisting moment (M_T) applied to a round attachment will cause a shear stress (f_{xy}) in the shell at the attachment-to-shell juncture. The shear stress is pure shear and is constant around the juncture. The shear stress is determined as follows:

$$f_{xy} = M_T / 2\pi r_0 T$$

B Square Attachment

A twisting moment applied to a square attachment will cause a complex stress field in the shell. No acceptable methods for analyzing the loading are available.

B7.2.2.3 STRESS RESULTING FROM ARBITRARY LOADING

I CALCULATION OF STRESSES

Most loadings that induce loads on cylindrical shells are of an arbitrary nature. Stresses are determined by the following procedure:

Step 1. Resolve the arbitrary applied load (forces and/or moments) into axial force, shear forces, overturning moments and twisting moment components. See Paragraph B7.2.1.6 Example Problem. The positive directions of the components and the point of application of the load components (intersection of centerline of attachment with attachment-shell interface) are indicated in Figure B7.2.2.1-1.

Step 2. Evaluate inside and outside stresses at desired points (such as A, B, C and D) around the attachment for each component of the arbitrary applied loading by the methods in Paragraph B7.2.2.2.

Step 3. Obtain the stresses for the arbitrary loading by combining the longitudinal, circumferential and shear stresses evaluated by Step 2 for each of the points selected on the inside and outside of the shell. Proper consideration of signs is necessary.

B7.2.2.3 STRESSES RESULTING FROM ARBITRARY LOADING

II LOCATION AND MAGNITUDE OF MAXIMUM STRESS

The location and magnitude of the maximum stresses caused by an arbitrary load require a consideration of the following:

A. The determination of principal stresses (f_{max}, f_{min}, $f_{xy} = 0$, or $f_{xy} = max$) for the determined stresses (f_x, f_y, and f_{xy}) at a specific point.

B. The proper selection of points for determining the stresses.

B7.2.2.4 DISPLACEMENTS

Shell displacements caused by radial load configurations and overturning moments are obtained from the computer program described in Paragraph B7.2.2.5. Shell displacements caused by twisting moment and shear loads are not determined.

Comparison of experimental and theoretical deflections indicate that deflections are sensitive to the detailed conditions of the attachment. In general, however, the experimental and theoretical values are of the same order of magnitude.

REFERENCES:

1. Bijlaard, P. P., "Stresses From Local Loadings in Cylindrical Pressure Vessels," Transactions ASME, Vol. 77, 1955, PP. 805-816.

2. Lowry, J. K., "Stresses and Deflections in Pressurized Cylindrical Shells, Due to the Application of Asymmetric Local Loadings," General Dynamics/Astronautics, San Diego, California, Report No. GD/A-DDG64-019, September 1, 1964.

3. Timoshenko, S., Woinowsky-Krieger, S., "Theory of Plates and Shells," McGraw-Hill Book Co., Inc., Second Ed., New York, N.Y., 1959.

4. Lowry, J. K., "Computer Program, Parameter Study, and Experimental Comparison for Stresses and Deflections in Pressurized Cylindrical Shells Due to Asymmetric Local Loads," General Dynamics/Astronautics, San Diego, California, Report No. GD/C-DDG65-008, June 14, 1965.

5. Wichman, K. R.; Hopper, A. G.; and Mershon, J. L., "Local Stresses in Spherical and Cylindrical Shells due to External Loadings," Welding Research Council Bulletin, Bulletin No. 107, August 1965.

SECTION 10.9

CYLINDERS AND SHELLS: LANGLEY SOLUTION.

SYNOPSIS

REFERENCE REPORT NO GDC DDG 67-006 VOL. VI " THE STABILITY OF ECCENTRICALLY STIFFENED CIRCULAR CYLINDERS. "

THIS PROGRAM PROVIDES A SOLUTION TO THE NASA - LANGLEY EQUATION FOR THE BUCKLING OF STIFFENED ORTHOTROPIC CYLINDERS SUBJECTED TO AXIAL COMPRESSION. THIS IS A SMALL DEFLECTION SOLUTION WHICH INCLUDES THE EFFECTS OF ECCENTRICITIES OF THE STIFFENING ELEMENTS WITH RESPECT TO THE SKIN MIDDLE SURFACE. SELECTED NUMBERS OF AXIAL HALF WAVE LENGTHS AND CIRCUMFERENTIAL FULL WAVE LENGTHS ARE SCREENED FOR A MIMIMUM BUCKLING LOAD. THIS CRITICAL VALUE IS PRINTED OUT ALONG WITH THE LOADS ASSOCIATED WITH NEIGHBORING NON-CRITICAL DEFLECTION PATTERNS.

SECTION 11.0

TORSION

ANALYSIS METHODS FOR SOLID AND THIN WALLED SECTIONS SUBJECTED TO TORSION ARE PRESENTED

		PAGE
11.1	TORSION OF SOLID SECTIONS	11.1.1
11.2	TORSION OF THIN-WALLED CLOSED SECTIONS	11.2.1
11.3	TORSION OF THIN-WALLED OPEN SECTIONS	11.3.1
11.4	MULTICELL CLOSED BEAMS IN TORSION	11.4.1
11.5	PLASTIC TORSION	11.5.1
11.6	ALLOWABLE STRESSES	11.6.1
11.7	RESTRAINED TORSION	11.7.1

TORSION

8.0 GENERAL

This section presents the analysis methods and allowables for members torsionally loaded. Members subjected to torsion are categorized according to their cross sections for analysis purposes, i.e. (1) solid sections, (2) thin walled closed sections and (3) thin walled open sections.

8.1 Torsion of Solid Sections

The torsional stress (f_s) and resulting angle of twist (ϕ) for an applied twisting moment can be determined when the material and section properties of the bar are known.

The torsional shear stress (f_s) distribution on any cross section of a circular bar will vary linearly along any radial line emanating from the geometric centroid and will have the same distribution on all radial lines. The longitudinal shear stress (f_x) which is equal to the torsional shear stress (f_s) produces no warping of the cross section when the stress distribution is the same on adjacent radial lines. For non-circular sections the torsional shear stress distribution is nonlinear (except along lines of symmetry where the cross section contour is normal to the radial line) and will be different on adjacent radial lines. When the torsional and longitudinal shear stresses are different on adjacent radial lines, warping of the cross section will occur.

When the warping deformation induced by longitudinal shear stresses is restrained, normal stress (σ) are induced to maintain equilibrium. These normal stresses are neglected in the torsional analysis of solid sections since they are small, attenuate rapidly and have little effect on the angle of twist. Restraints to the warping deformation occur at fixed ends and at points where there is an abrupt change in the applied twisting moment.

The torsional analysis of solid cross sections is subject to the following limitations:

1) The material is homogeneous and isotropic.
2) The shear stress does not exceed the shearing proportional limit and is proportional to the shear strain (elastic analysis).
3) The stresses calculated at points of constraint and at abrupt changes of applied twisting moment are not exact.
4) The applied twisting moment cannot be an impact load.
5) If the bar has an abrupt change in cross section, stress concentrations must be used.

The basic equation for determining the torsional shear stress at some arbitrary point on an arbitrary cross section is

$$f_s = T_{(x)}/Q_{(x)} \qquad 8.1$$

where $T_{(x)}$ is the applied torque at some distance x along the beam and Q is the torsional section modulus at the same place.

The basic equation for determining the angle of twist between two points x distance apart is

$$\phi = 1/G \int_{x_1}^{x_2} T_{(x)}/K_{(x)} \; dx \qquad 8.2$$

where $K_{(x)}$ is the torsional constant. The area-moment technique can be used to determine the angle of twist between any two sections by plotting $T_{(x)}/GK_{(x)}$ for the beam.

Table 8.1 shows equations for calculating stress and angle of twist for some commonly used cross sections. The equations are for points of maximum torsional shear stress. Some cross sections have torsional stress equations shown for more than one section. The angle of twist equations are for a bar of length L and constant cross section.

When a circular beam of nonuniform cross section is twisted, the radii of a cross section becomes curved. Since the radii of a cross section were assumed to remain straight in the derivation of the equations for stress in uniform circular beams, these equations no longer hold if a beam is nonuniform. However, the stress at any section of a nonuniform circular beam is given with sufficient accuracy by the equations for uniform bars if the diameter changes gradually. If the change in section is abrupt, as at a shoulder with a small fillet, a stress concentration must be applied.

In nonuniform circular beams having gradual diameter changes, the angle of twist can be determined using equation 8.2. This equation is used to determine the equations for ϕ in Table 8.2 for various beams of uniform taper.

8.2 Torsion of Thin-Walled Closed Sections

A closed section is any section where the center line of the wall forms a closed curve. The torsional shear stress distribution varies along any radial line emanating from the geometric centroid of the thin-walled closed section. Since the thickness of the thin walled section is small compared to the radius, the stress varies very little through the thickness of the cross section and is assumed to be constant through the thickness at that point.

The angle of twist of a thin-walled closed beam of length, L, due to an applied torque, T, is given by

$$\phi = \frac{TL}{4A^2G} \int \frac{du}{t} \qquad 8.3$$

$\phi = \frac{TL}{KG}$	T = Applied Torque(in-lb)	G = Modulus of Rigidity(psi)
$f_s = \frac{T}{Q}$	L = Length of Beam(in)	ϕ = Angle of Twist(rad)
	K = Torsional Constant(in^4)	f_s = Shear Stress(psi)
	Q = Section Modulus(in^3)	

SECTION	K	Q	MAX STRESS
①  SOLID CIRCLE	$\frac{\pi r^4}{2}$	$\frac{\pi r^3}{2}$	at r_{max}
② 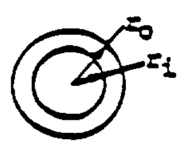 HOLLOW CIRCLE	$\frac{\pi}{2}(r_o^4 - r_i^4)$	$\frac{\pi}{2}(r_o^3 - r_i^3)$	at r_o
③ 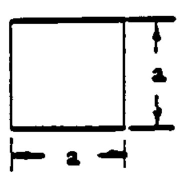 SOLID SQUARE	$0.1406\,a^4$	$0.208\,a^3$	at midpoint of each side
④ 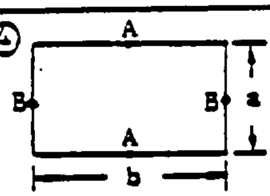 SOLID RECTANGLE	$\beta b a^3$ $\beta = \left[.333 - \frac{.21}{(b/a)}\left(1 - \frac{0.0833}{(b/a)^4}\right)\right]$	$\alpha b a^2$ $\alpha = \frac{1}{\left[3 + \frac{1.8}{(b/a)}\right]}$	@A: $f_s = \frac{T}{Q}$ @B: $f_s = \frac{Ta}{Qb}$
⑤ 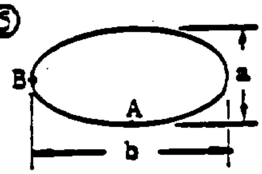 SOLID ELLIPSE	$\frac{\pi b^3 a^3}{16(b^2 + a^2)}$	$\frac{\pi b a^2}{16}$	@A: $f_s = \frac{T}{Q}$ @B: $f_s = \frac{Ta}{Qb}$

TABLE 8.1 - EQUATIONS FOR STRESS AND DEFORMATION IN SOLID SECTIONS LOADED IN TORSION

SECTION	K	Q	MAX STRESS
(6) 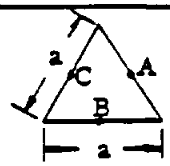 SOLID EQUILATERAL TRIANGLE	$\frac{a^4\sqrt{3}}{80}$	$\frac{a^3}{20}$	at A, B & C
(7)  SOLID HEXAGON	$0.1045\,d^4$	$0.1704\,d^3$	at midpoint of each side
(8)  SOLID OCTAGON	$0.1021\,d^4$	$0.1751\,d^3$	at midpoint of each side
(9) 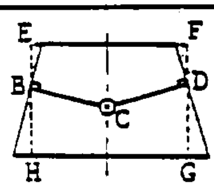 SOLID ISOSCELES TRAPEZOID	Form equivalent rectangle through points B and D. Then use equations for rectangle to determine stress and twist. To locate B and D, construct perpendiculars from centroid (c) to each side (B and D).		
(10) 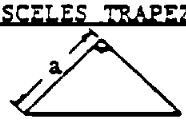 SOLID RIGHT ISOSCELES TRIANGLE	$0.0261\,a^4$	$0.0554\,a^3$	at center of long side
(11) 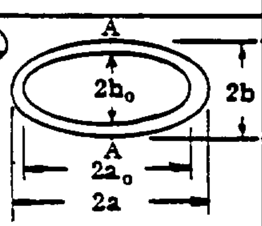 HOLLOW ELLIPSE	$\frac{\pi a^3 b^3 (1-q^4)}{a^2+b^2}$ $q=\frac{a_o}{a}=\frac{b_o}{b}$	$\frac{\pi a b^2 (1-q^4)}{2}$	at A

TABLE 8.1 (CONT'D) - EQUATIONS FOR STRESS AND DEFORMATION IN SOLID SECTIONS LOADED IN TORSION

SECTION	K	Q	MAX STRESS
(12) 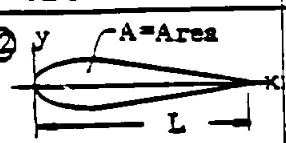	$\dfrac{4I_x}{\left(1+\dfrac{16I_x}{AL^2}\right)}$	For cases 12 through 18, f_{max} occurs at or very near one of the points where the largest inscribed circle touches the boundary unless there is a sharp re-entrant at some other point on the boundary causing high local stresses. Of the points where the largest inscribed circle touches the boundary, f_{max} occurs at the one where the boundary curvature is algebraically least. Convexity represents positive, concavity negative, curvature of the boundary. At a point where the curvature is positive (boundary of section straight or convex) the maximum stress is given approximately by: $f_{s_{max}} = G\theta C/L$ or $f_{s_{max}} = TC/K$ $C = \dfrac{D}{1+\dfrac{\pi^2D^4}{16A^2}}\left[1+0.15\left(\dfrac{\pi^2D^4}{16A^2}-\dfrac{D}{2r}\right)\right]$ D = dia. of largest inscribed circle r = radius of curvature of boundary at the point (convex). A = area of section At a point where the curvature is negative (boundary of section concave or reentrant) the maximum stress is given approximately by: $f_{s_{max}} = G\theta C/L$ or $f_{s_{max}} = TC/K$ $C = \dfrac{D}{1+\dfrac{\pi^2D^4}{16A^2}}\left[1+\left\{0.118\ln\left(1-\dfrac{D}{2r}\right)-0.238\dfrac{D}{r}\right\}\tanh\dfrac{2\theta}{\pi}\right]$	
(13)  dL = element length along median	$\dfrac{.333F}{1+\dfrac{4F}{3AL^2}}$ $F=\int_0^L t^3\,dL$		
(14) 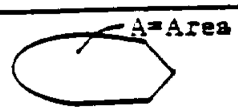 SOLID FAIRLY COMPACT SECTION WITHOUT REENTRANT ANGLES	$\dfrac{A^4}{40J}$ J = Polar Moment of Inertia		
(15) 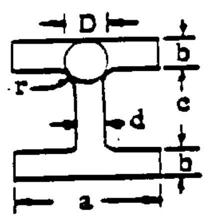 D = dia. inscribed cir t = b if b < d t = d if d < b t_1 = b if b > d t_1 = d if d > b	$2K_1+K_2+2\alpha D^4$ $K_1=ab^3\left[\dfrac{1}{3}-\dfrac{0.21b}{a}\left(1-\dfrac{b^4}{12a^4}\right)\right]$ $K_2=\dfrac{cd^3}{3}$ $\alpha=\dfrac{t}{t_1}\left(0.15+0.1\dfrac{r}{b}\right)$		
(16) 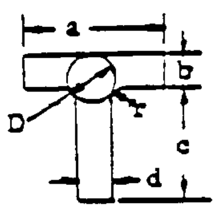 r, D, t, t_1 same as case (15)	$K_1+K_2-\alpha D^4$ $K_1=ab^3\left[\dfrac{1}{3}-\dfrac{0.21b}{a}\left(1-\dfrac{b^4}{12a^4}\right)\right]$ $K_2=cd^3\left[\dfrac{1}{3}-\dfrac{0.105d}{c}\left(1-\dfrac{d^4}{192c^4}\right)\right]$ $\alpha=\dfrac{t}{t_1}\left(0.15+0.1\dfrac{r}{b}\right)$		

TABLE 8.1 (CONT'D) - EQUATIONS FOR STRESS AND DEFORMATION IN SOLID SECTIONS LOADED IN TORSION

<table>
<tr><th>SECTION</th><th>K</th><th>Q</th><th>MAX STRESS</th></tr>
<tr><td>17 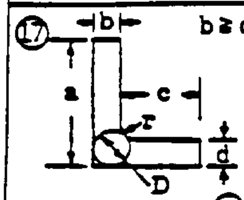
b ≥ d
r & D same as 15</td><td>$K = K_1 + K_2 + \alpha D^4$
K_1 & K_2 per 16
$\alpha = \frac{d}{b}\left(0.07 + 0.076\frac{r}{b}\right)$</td><td colspan="2" rowspan="2">The angle Ø is the angle through which a tangent to the boundary rotates in turning or traveling around the reentrant portion, measured in radians.</td></tr>
<tr><td>18 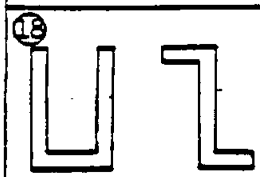</td><td>Sum of K's of constituent 'L' sections computed per 17</td></tr>
<tr><td>19 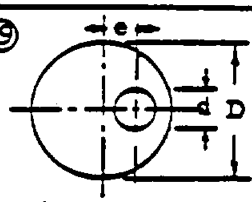
$e/d = \lambda$
$d/D = n$</td><td>$\pi(D^4 - d^4)/32Q$
$Q = 1 + \left[\frac{16n^2}{(1-n^2)(1-n^4)}\right]\lambda^2 + \left[\frac{384n^4}{(1-n^2)^2(1-n^4)^4}\right]\lambda^4$</td><td colspan="2">$f_{s_{max}} = 16TDF/\pi(D^4 - d^4)$
$F = 1 + \left[\frac{4n^2}{1-n^2}\right]\lambda + \left[\frac{32n^2}{(1-n^2)(1-n^4)}\right]\lambda^2 + \left[\frac{48n^2(1+2n^2+3n^4+2n^6)}{(1-n^2)(1-n^4)(1-n^6)}\right]\lambda^3 + \left[\frac{64n^2(2+12n^2+19n^4+28n^6+18n^8+14n^{10}+3n^{12})}{(1-n^2)(1-n^4)(1-n^6)(1-n^8)}\right]\lambda^4$</td></tr>
<tr><td>20 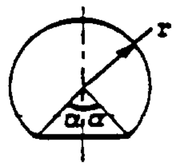</td><td>Cr^4<table><tr><td>α</td><td>0</td><td>30°</td><td>60°</td><td>80°</td><td>90°</td></tr><tr><td>C</td><td>1.57</td><td>1.47</td><td>.91</td><td>.48</td><td>.296</td></tr></table></td><td colspan="2">$f_{s_{max}} = T/Q$; $Q = Cr^3$<table><tr><td>α</td><td>0</td><td>30°</td><td>60°</td><td>80°</td><td>90°</td></tr><tr><td>C</td><td>1.57</td><td>1.25</td><td>.80</td><td>.49</td><td>.35</td></tr></table></td></tr>
<tr><td>21 </td><td>Cr^4<table><tr><td>α</td><td>45°</td><td>60°</td><td>90°</td><td>120°</td></tr><tr><td>C</td><td>.0181</td><td>.0349</td><td>.0825</td><td>.148</td></tr><tr><td>α</td><td>180°</td><td>270°</td><td>300°</td><td>360°</td></tr><tr><td>C</td><td>.296</td><td>.528</td><td>.686</td><td>.878</td></tr></table></td><td colspan="2">$f_{s_{max}} = T/Q$; $Q = Cr^3$<table><tr><td>α</td><td>60°</td><td>120°</td><td>180°</td></tr><tr><td>C</td><td>.0712</td><td>.227</td><td>.35</td></tr></table></td></tr>
</table>

TABLE 8.1 (CONT'D) - EQUATIONS FOR STRESS AND DEFORMATION IN SOLID SECTIONS LOADED IN TORSION

TYPE OF BEAM	ANGLE OF TWIST
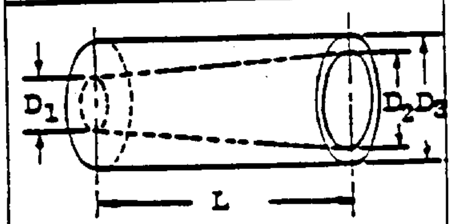 INSIDE TAPERED, OUTSIDE CONSTANT	$\Theta = \frac{8TL}{\pi G(D_2 - D_1)D_3^3}\left\{2\arctan\left(\frac{D_2}{D_3}\right) - 2\arctan\left(\frac{D_1}{D_3}\right) + \mathrm{Ln}\left[\left(\frac{D_3+D_2}{D_3-D_2}\right)\left(\frac{D_3-D_1}{D_3+D_1}\right)\right]\right\}$
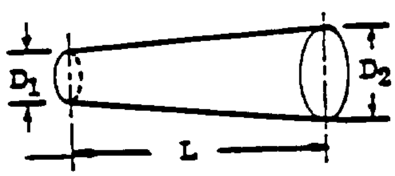 SOLID BEAM, OUTSIDE TAPERED	$\Theta = \frac{32TL}{3\pi G D_1 D_2}\left(\frac{1}{D_1^2} + \frac{1}{D_1 D_2} + \frac{1}{D_2^2}\right)$
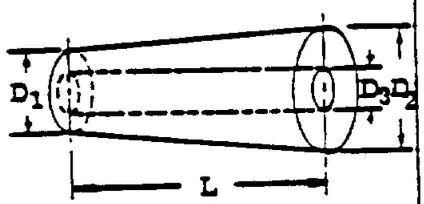 INSIDE UNIFORM OUTSIDE TAPERED	$\Theta = \frac{8TL}{\pi G(D_2\ D_1)D_3^3}\left\{2\arctan\left(\frac{D_2}{D_3}\right) - 2\arctan\left(\frac{D_1}{D_3}\right) + \mathrm{Ln}\left[\left(\frac{D_3+D_2}{D_3-D_2}\right)\left(\frac{D_3-D_1}{D_3+D_1}\right)\right]\right\}$
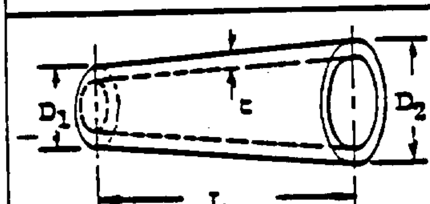 THIN TAPERED TUBE WITH CONSTANT WALL THICKNESS	$\Theta = \frac{2TL(D_1+D_2)}{\pi G t D_1^2 D_2^2}$

TABLE 8.2 - EQUATIONS FOR ANGLE OF TWIST FOR NONUNIFORM CIRCULAR BEAMS IN TORSION

Data Source, Section 1.3 Reference 3

where A is the area enclosed by the median line of the thickness, t, and u is the length along the median. The shear flow is constant around the tube and is

$$q = \frac{T}{2A} \qquad 8.4$$

The shear stress is assumed to be constant through the thickness and is

$$f_s = q/t = T/2At \qquad 8.5$$

If the cross section is of nonuniform thickness, the shear stress will be maximum where the thickness is minimum.

Table 8.3 shows the angle of twist and shear stress for thin-walled closed sections subject to an applied twist, T.

8.3 Torsion of Thin-Walled Open Sections

An open section is one in which the centerline of the wall does not form a closed curve. Channels, angles, I-beams, Tees and wide flanges are among structural shapes characterized by a combination of thin-walled rectangular shapes. Additionally many thin-walled open sections are curved. This section presents the means to calculate the stress and twisting angle for these sections.

For a bar of rectangular cross section of width b and thickness t the equations for maximum shearing stress and the angle of twist are

$$f_{s_{max}} = T/\alpha bt^2 \qquad 8.6$$

$$\phi = TL/\beta bt^3G \qquad 8.7$$

where α and β are defined in Table 8.1, Case 4 . When the ratio b/t becomes very large, α and β become 0.333. Equations 8.6 and 8.7 become

$$f_{s_{max}} = 3T/bt^2 \qquad 8.8$$

$$\phi = 3TL/bt^3G \qquad 8.9$$

These equations, 8.8 and 8.9, are applicable for narrow rectangles. They also apply to an approximate analysis of shapes made up of thin rectangular members such as those shown in Figure 8.1

SECTION	K	Q	MAX STRESS
① 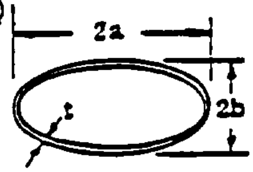	$\frac{4\pi^2 t\,[(a-.5t)^2(b-.5t)^2]}{U}$ U = length of median $U=\pi(a+b-t)\left[1+\frac{.27(a-b)^2}{(a+b)^2}\right]$	$2\pi t(a-.5t)(b-.5t)$	constant if t is small
② 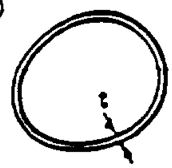	$\frac{4A^2t}{U}$ U = length of median A = mean of areas enclosed by two boundaries	$2tA$	constant if t is small
③ 	$\frac{4A^2}{\int \frac{dU}{t}}$ U & A same as ②	$2tA$	at t_{min}
④ 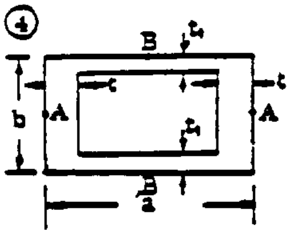	$\frac{2tt_1(a-t)^2(b-t_1)^2}{at+bt_1-t^2-t_1^2}$	@A: $2t(a-t)(b-t_1)$ @B: $2t_1(a-t)(b-t_1)$	There will be higher stresses at inner corners unless fillets of fairly large radius are used

Equations for twist and stress are shown in Table 8.1

TABLE 8.3 - EQUATIONS FOR STRESS AND DEFORMATION IN HOLLOW CLOSED SECTIONS LOADED IN TORSION

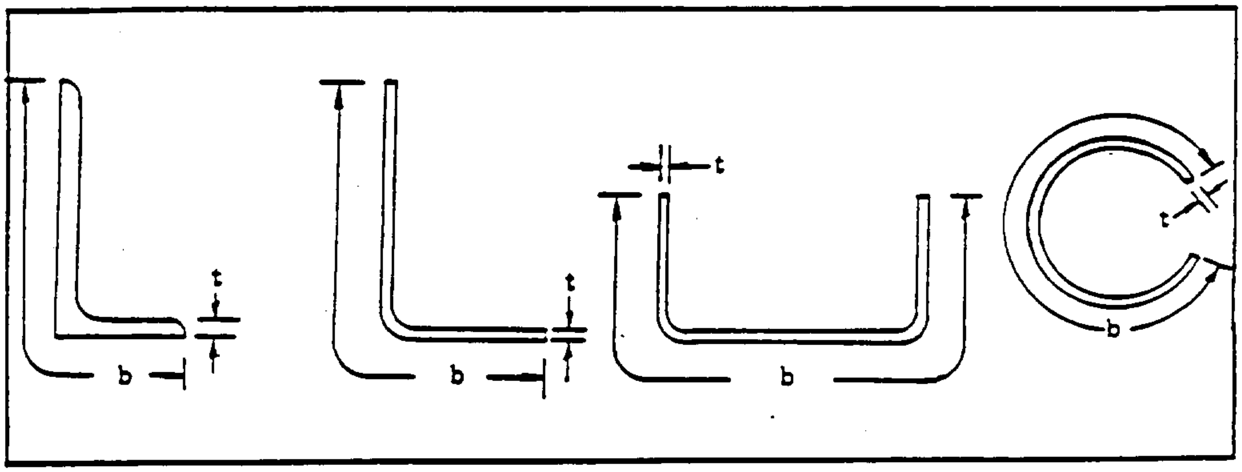

FIGURE 8.1 - BEAMS WITH THIN RECTANGULAR MEMBERS
WITH CONTINUOUS CENTERLINES

For the members shown in Figure 8.1, b can be taken as the continuous centerline of the member and equations 8.8 and 8.9 used to determine stress and angle of twist.

Shapes with a member of thin rectangular members such as T and H sections shown in Figure 8.2

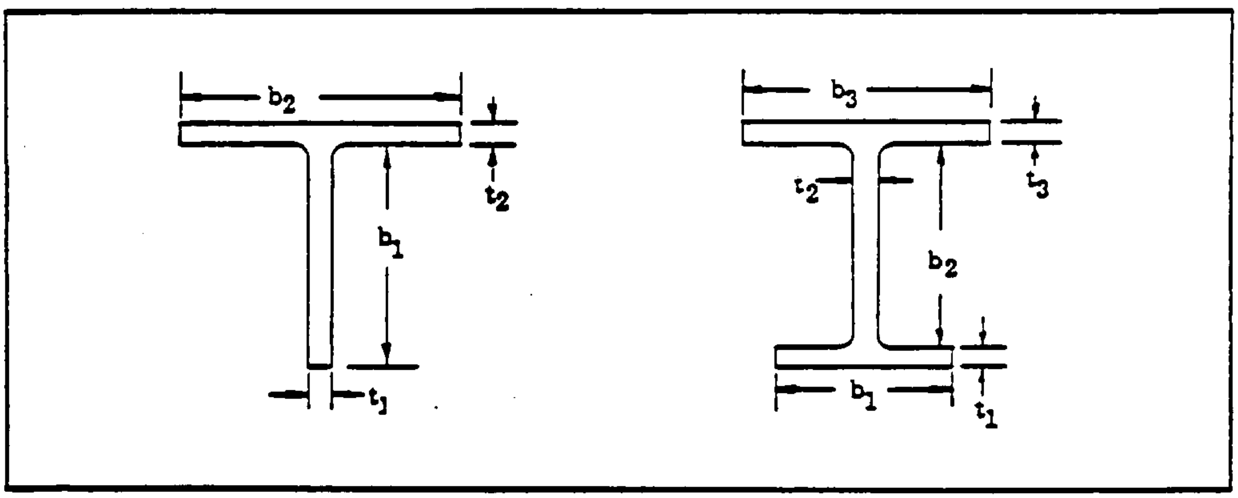

FIGURE 8.2 - BEAMS WITH THIN RECTANGULAR
MEMBERS OF COMPOSITE SHAPES

can be analyzed using equations 8.10 and 8.11

$$f_{s_{max_n}} = 3Tt_n / \Sigma bt^3 \quad 8.10$$

$$\phi = 3TL/G\,\Sigma bt^3 \quad 8.11$$

For the T section in Figure 8.2 the angle of twist is

$$\phi = 3TL/G(b_1 t_1^3 + b_2 t_2^3) \quad 8.12$$

and the shear stress is

$$f_{s_1} = 3Tt_1/(b_1 t_1^3 + b_2 t_2^3) \quad 8.13$$

$$f_{s_2} = 3Tt_2/(b_1 t_1^3 + b_2 t_2^3) \quad 8.14$$

The same procedure is applicable for any type of shape; however, the accuracy is considerably improved when sharp corners are avoided by the use of liberal radii.

8.4 Multicell Closed Beams in Torsion

Figure 8.3 shows a multicell tube with an externally applied torsion. The torsion is reacted in the tube by internal shear flows acting around each cell.

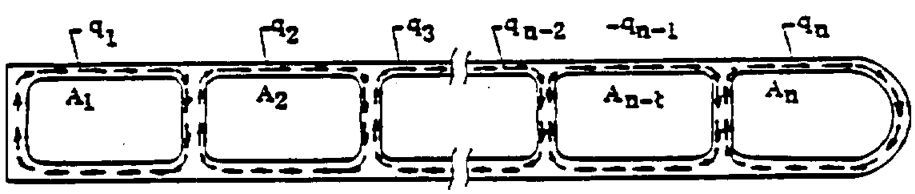

FIGURE 8.3 - MULTICELL TUBE IN TORSION

The tube has n cells with a pure torsion, T, applied. The torsion applied externally must be reacted internally. This is expressed by

$$T = 2q_1A_1 = 2q_2A_2 + \dots + 2q_nA_n \qquad 8.15$$

where A_1 through A_n are the areas enclosed by the median lines of cells 1 through n. q_1 through q_n are the reaction shear flows acting on cells 1 through n.

For elastic continuity, the twist of each cell must be equal, or

$$\phi_1 = \phi_2 = \dots = \phi_n \qquad 8.16$$

The angular twist of a cell is

$$\phi = q/2AG \oint ds/t \qquad 8.17$$

or

$$2G\phi = q/A \oint ds/t \qquad 8.18$$

Thus for each cell of multicell structure an expression for $q/A \oint ds/t$ can be written and equated to $2G\phi$. The line integral $\oint ds/t$ is represented by a. Then a_{KL} is the value of the integral along the wall between cells K and L where the area outside the tube is designated as cell 0. The shear flows acting in a clockwise direction are assumed to be positive. Using this rotation, equation 8.13 can be applied to each cell resulting in the following:

$$\text{cell (1): } 1/A_1[q_1a_{10} + (q_1 - q_2)a_{12}] = 2G\phi \qquad 8.19$$

$$\text{cell (2): } 1/A_2[(q_2 - q_1)a_{12} + q_2a_{20} + (q_2 - q_3)a_{23}] = 2G\phi \qquad 8.20$$

$$\text{cell (3): } 1/A_3[(q_3 - q_2)a_{23} + q_3a_{30} + (q_3 - q_4)a_{34}] = 2G\phi \qquad 8.21$$

$$\text{cell(n-1): } 1/A_{n-1}[(q_{n-1} - q_{n-2})a_{n-2,n-1} + q_{n-1} + q_{n-1}a_{n-1,0}$$
$$+ (q_{n-1} - q_n)a_{n-1,n}] = 2G\phi \qquad 8.22$$

$$\text{cell (n): } 1/A_n\ [(q_n - q_{n-1})a_{n-1,n} + q_na_{no}] = 2G\phi \qquad 8.23$$

The shear flows, q_1 through q_n, may be found by solving equations 8.15 and 8.19 through 8.23 simultaneously. From these shear flows, the shear stresses may be found using $f_s = q/t$.

As an example, consider the multicell beam shown in Figure 8.4.

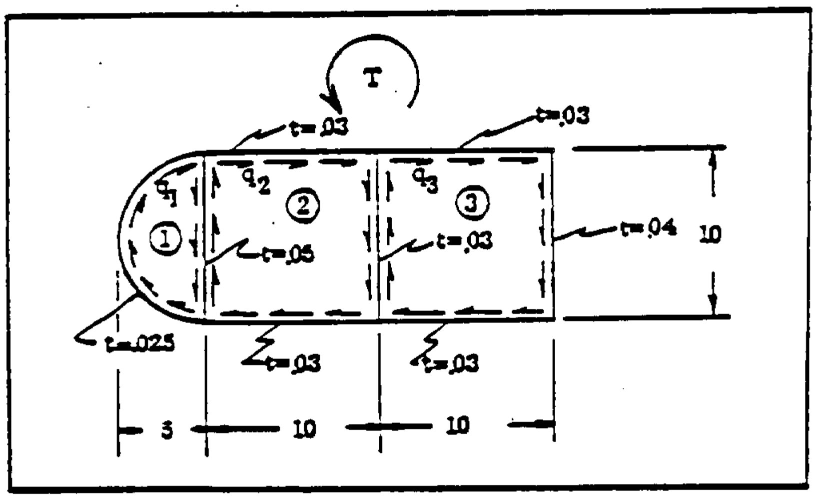

FIGURE 8.4 - EXAMPLE OF MULTICELL BEAM IN TORSION

Cell Areas:

$A_1 = 39.3 \qquad A_2 = 100 \qquad A_3 = 100$

Line integrals for each cell:

$a_{10} = 1/2(\pi)(10)/.025 = 628$

$a_{12} = 10/.05 = 200$

$a_{20} = 2(10)/.03 = 667$

$a_{23} = 10/.03 = 333$

$a_{30} = 2(10)/.03 + 10/.04 = 917$

Equate external torque to internal reactions:

$T = 2q_1A_1 + 2q_2A_2 + 2q_3A_3$, Equation 8.15

$100000 = 2(39.3)q_1 + 2(100)q_2 + 2(100)q_3$

$100000 = 78.6q_1 + 200q_2 + 200q_3$

Write the expression for angular twist of each cell:

Cell (1): $1/39.3\ [628q_1 + 200(q_1 - q_2)] = 2G\theta = 21.07q_1 - 5.09q_2$

Cell (2): $1/100\ [200(q_2 - q_1) + 667q_2 + 333(q_2 - q_3)] = 2G\theta = -2q_1 + 12q_2 - 3.33q_3$

Cell (3): $1/100\ [333(q_3 - q_2) + 917q_3] = 2G\theta = -3.33q_2 + 12.5q_3$

Solving the equations simultaneously:

q_1 = 144 #/in, q_2 = 234 #/in, q_3 = 209 #/in, $\emptyset$ = .0002288 rad

8.5 Plastic Torsion

The previous methods of analysis are based on stress levels in the elastic range. These stress levels are based on limit loads. For ultimate loads, it is often desirable to allow the section to operate in the plastic region. All types of cross sections not subject to local crippling can be analyzed for allowable torsion by use of the plastic torsion theory at ultimate load. The method of analysis is called the "sand heap" analogy.

If the maximum amount of dry sand is heaped on a level platform having the same shape as the cross section of the beam in torsion, the slope of the heap represents the shear stress. The shear stress for this condition has the same magnitude over the entire cross section. The torsional moment, T, is related to the volume of the heap, V, by

$$T = 2VF_{su} \qquad 8.24$$

where F_{su} is the ultimate allowable shear stress. The difficulty of the sand heap analogy is determining the volume of the heap. This is simplified somewhat by constructing contour lines. A contour line defines the contour of the heap at some constant elevation. It is a plane passed through the heap parallel to the torsional section. Also, it is assumed that the maximum possible slope of the heap is achieved, i.e. slope is equal unity.

It is easy to construct a contour map of the sand heap surface. Contour lines intersect normals through the section boundary at right angles and at a distance from the boundary equal to the elevation of the contour line.

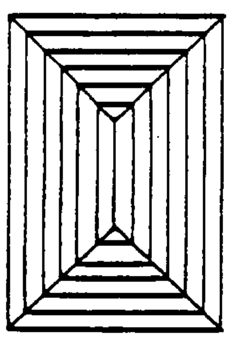

RECTANGLE

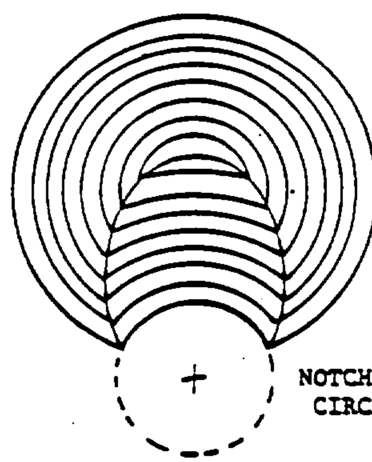

NOTCHED CIRCLE

It is possible to determine the volume of the sand heap for any cross section by integration. Figure 8.5 shows equations for sand heap volumes with various bases.

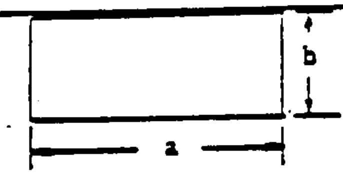

$$V = \frac{b^2(3a-b)}{12} \qquad a \geq b$$

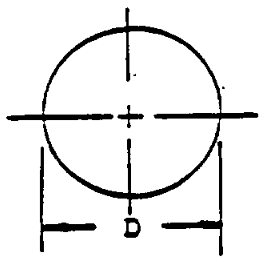

$$V = \frac{\pi D^3}{24}$$

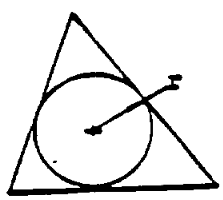

$$V = \frac{Ar}{3}$$

A = Area of triangle

FIGURE 8.5 - SAND HEAP VOLUMES

8.6 Allowable Stresses

For limit load conditions, the applied stresses should be kept below the ultimate shear stress, F_{su}. These are defined for various materials in MIL-HDBK-5.

The torsional failure of tubes may be due to plastic failure of the material, instability of the walls, or an intermediate condition. Pure shear failure will not usually occur within the range of wall thicknesses commonly used for aircraft tubing. Torsional allowable stresses are shown in Figure 8.6 through 8.22. These curves take into account the parameter L/D and are in good agreement with experimental results.

Data Source, Section 1.3 Reference 5

B8.1.0 GENERAL

* Section B8.1 presents the notation and sign convention for local co-ordinate systems, applied twisting moments, internal resisting moments, stresses, deformations, and derivations of angle of twist. These conventions will be followed in * Sections B8.4.

Restrained torsion and unrestrained torsion are considered for the thin-walled open and thin-walled closed cross sections, and unrestrained torsion is considered for the solid cross section. Restrained torsion requires that no relative longitudinal displacement shall occur between two similar points on any two similar cross sections. Warping is restrained.

Restrained torsion of solid cross sections is not considered because it is a localized stress condition and attenuates rapidly. The stresses and deformations determined by the methods contained in this section can be superimposed upon stresses and deformations caused by other types of loading if the deformations are small and the maximum combined stress does not exceed the yield stress of the material.

* Data Source, Section 1.3 Reference 5

B5.1.1 NOTATION

All general terms used in this section are defined herein. Special terms are defined in the text as they occur.

a	Width of rectangular section, in.
A	Enclosed area of mean periphery of thin-walled closed section, $in.^2$
b	Length of element, width of flange, in.
b'	Width of flange minus thickness of web, in.
C	Length of wall centerline (circumference), in.
d	Total section depth, in.
D	Diameter of circular bar, in.
E	Young's modulus, $lb/in.^2$
G	Shear modulus of elasticity, $lb/in.^2$
h	Distance between flange centerlines, in.
I	Moment of inertia, $in.^4$
J	Polar moment of inertia, $in.^4$
K	Torsional constant, $in.^4$
L	Length of bar, in.
L_x	Arbitrary distance along x-axis from origin, in.
m_t	Applied uniform twisting moment or maximum value of varying applied twisting moment, in.-lb/in.
M_i	Internal twisting moment, in.-lb.
M_t	Applied concentrated twisting moment, in.-lb.
$M_{(x)}$	Internal twisting moment at point x along bar, written as function of x
p	Pressure, $lb/in.^2$

P	Arbitrary point on cross section
q	Shear flow, lb/in.
r	Radius of circular cross section, in.
R	Radius of circular fillet, in.
s	Distance measured along thin-walled section from origin, in.
S_t	Torsional modulus, in.^{3}
$S_w(s)$	Warping statical moment, in.^{4}
t	Thickness of element, in.
t_w	Thickness of web, in.
T	Tensile force per unit length, lb/in.^{2}
u	Displacement in the x direction, in.
v	Displacement in the y direction, in.
w	Displacement in the z direction, in.
$W_n(s)$	Normalized warping function, in.^{2}
V	Volume, in.^{3}
α	Defined in Section B8.4.1-IV
β	Defined in Section B8.4.1-IV
Γ	Warping constant, in.^{6}
γ	Shear strain
θ	Unit twist, rad/in. ($\theta = d\phi/dx = \phi'$)
μ	Poisson's ratio
ρ	Radial distance from the centroid of the cross section to arbitrary point P, in.
ρ_o	Radial distance to tangent line of arbitrary point P from shear center, in.

σ_x	Longitudinal normal stress, lb/in.^{2}
τ	Total shear stress, lb/in.^{2}
τ_t	Torsional shear stress, lb/in.^{2}
τ_l	Longitudinal shear stress, lb/in.^{2}
τ_w	Warping shear stress, lb/in.^{2}
φ	Angle of twist, rad ($\varphi = \int_0^{L_x} \theta dx$)
$\varphi', \varphi'', \varphi'''$	First, second, and third derivatives of angle of twist with respect to x, respectively
Φ	Saint-Venant stress function

Subscripts:

i	inside
l	longitudinal
n	normal
o	outside
s	point s
t	torsional or transverse
w	warping
x	longitudinal direction

B8.4.3 RESTRAINED TORSION

I. ANGLE OF TWIST AND DERIVATIVES

It was shown that for unrestrained torsion, the torsional moment resisted by the section is $M_1 = GK\phi'$ (Section B8.4.2-I)*.

Longitudinal bending occurs when a section is restrained from free warping. This bending is accompanied by shear stresses in the plane of the cross section, and these stresses resist the external applied torsional moment according to the following relationship:

$$M_2 = -E\Gamma\phi'''$$

where

M_2 = resisting moment caused by restrained warping of the cross section, in.-lb

E = modulus of elasticity, psi

Γ = warping constant for the cross section (Section B8.4.1-IVB)*, in.[6]

ϕ''' = third derivative of the angle of rotation with respect to x.

Therefore, the total torsional moment resisted by the section is the sum of M_1 and M_2. The first of these is always present; the second depends on the resistance to warping. Denoting the total torsional resisting moment by M, the following expression is obtained.

$$M = M_1 + M_2 = GK\phi' - E\Gamma\phi'''$$

or

$$\frac{1}{a^2}\phi' - \phi''' = \frac{M}{E\Gamma}$$

* Data Source, Section 1.3 Reference 5. (SEE pg. 11.7.10 AND pg 11.7.14 REF 8)

where

$$a^2 = \frac{E\Gamma}{GK}$$

The solution of this equation depends upon the distribution of applied torque (M) and the boundary or end restraints of the member. Numerical evaluation of this equation for ϕ, ϕ', ϕ'', and ϕ''' is obtained from the computer program in Ref.* B8.4.3-IV for many loading and end conditions.

It is necessary to evaluate the foregoing expressions for the angle of twist and its derivatives before a complete picture of stress distribution and warping can be defined.

* Data Source, Section 1.3 Reference 5 AND pg. 11.7.14 REF. 7 & 9.

B8.4.3 RESTRAINED TORSION

II. STRESSES

A. Pure Torsional Shear Stress

The equation for torsional shear stress is the same as given in *Section B8.4.2-II; however, now the angle of twist varies along the member and must be determined from the previous section.

Neglecting stress concentrations at reentrant corners, the pure torsional shear stress equation is

$$\tau_t = Gt\,\phi' .$$

This stress will be largest in the thickest element of the cross section. For distribution of this stress for common sections, see Figures* B8.4.1-3, B8.4.1-4, and B8.4.1-5. This stress can be calculated by the computer program in Ref. * B8.4.3-IV for many loading and end conditions.

B. Warping Shear Stress

When the cross section is restrained from warping freely along the entire length of the member, warping shear stresses are induced. These stresses are essentially uniform over the thickness (t), but the magnitude varies at different locations of the cross section (Figs.* B8.4.1-3, B8.4.1-4, and B8.4.1-5). These stresses are determined from the equation:

$$\tau_{ws} = -\frac{ES_{ws}}{t}\,\phi'''$$

* Data Source, Section 1.3 Reference 5

134

where

τ_{ws} = warping shear stress at point s, psi

E = modulus of elasticity, psi

S_{ws} = warping statical moment at point s (Section *B8.4.1-IVD), in.^{4}

t = thickness of the element, in.

ϕ''' = third derivative of the angle of twist with respect to x, distance measured along the length of the member.

This stress can be calculated by the computer program in Section *B8.4.3-IV for many loading and end conditions.

C. Warping Normal Stress

Warping normal stresses are caused when the cross section is restrained from warping freely along the entire length of the member. These stresses act perpendicular to the surface of the cross section and are constant across the thickness of an element but vary in magnitude along the length of the element. The magnitude of these stresses is determined by the equation:

$$\sigma_{ws} = E\, W_{ns}\, \phi''$$

where

σ_{ws} = warping normal stress at point s, psi

E = modulus of elasticity, psi

W_{ns} = normalized warping function at point s (Section *B8.4.1-IVC), in.^{2}

ϕ'' = record derivative of the angle of twist with respect to x, distance measured along the length of the member.

This stress can be calculated by the computer program in Section *B8.4.3-IV for many loading and end conditions.

* Data Source, Section 1.3 Reference 5

B8.4.3 RESTRAINED TORSION

III. WARPING DEFORMATIONS

Warping deformations can be calculated by using the same equation that was given in Section* B8.4.2-III, except that now the expression for ϕ' will vary along the length of the member. The expression for ϕ' can be obtained from Section* B8.4.3-I or from the computer program in * B8.4.3-IV. It should be noted that the warping normal stresses are proportional to corresponding warping displacements; hence, by knowing the warping displacements, a picture of distribution of the warping stresses is evident.

* Data Source, Section 1.3 Reference 5

Warping Constant (Γ)

The torsional coefficient (Γ) is called the warping constant. Its value depends only on the geometry of the cross section. For the generalized section shown in Figure B8.4.1-8, the following equation is used for calculating Γ:

$$\Gamma = \int_0^b W_n(s)\, t^2 ds .$$

The value of $W_n(s)$ is determined from page 11.7.12 Some values for frequently used sections are:

1. For symmetrical wide flange and I shapes (Fig. B8.4.1-9A):

$$\Gamma = \frac{h^2 b^3 t}{24} = \frac{I_y h^2}{4}$$

2. For channel sections (Fig. B8.4.1-9B):

$$\Gamma = 1/6\ (b'3E_o)\, h^2 (b')\ t + F_o^2\ I_x .$$

3. For zee sections:

$$\Gamma = \frac{(b')^3 t h^2}{12}\ \frac{b't + 2ht_w}{ht_w + 2b't}$$

where h, b, t, t_w, b', and E_o are defined on page 11.7.2, I_x = the moment of inertia of the entire section about the xx axis, and I_y = the moment of inertia of the entire section about the yy axis.

Normalized Warping Function (W_n)

The torsional coefficient (W_n) is called the normalized warping function. Its value depends upon the geometry of the cross section and upon specific points on the cross section.

For the generalized section shown in Figure B8.4.1-8, the following equation is used for calculating $W_n(s)$ at any point (s) on the section:

$$W_n(s) = \frac{1}{A} \int_0^b W_{os}\, t\, ds - w_{os}$$

where

$$A = \int_0^b t\, ds$$

$$W_{os} = \int_0^s \rho_o\, ds.$$

Some W_n values for frequently used sections include:

1. For symmetrical wide flange and I shapes (Fig. B8.4.1-9A):

$$W_{no} = \frac{bh}{4} .$$

2. For channel sections (Fig. B8.4.1-9B):

$$W_{no} = \frac{uh}{2}$$

$$W_{n2} = \frac{E_o h}{2}$$

ρ Perpendicular distance to tangent line from centroid
ρ_o Perpendicular distance to tangent line from shear center
cg Centroid of cross section
sc Shear center of cross section
z,y Coordinates referred to the principal centroidal axes
ϕ Angle of twist

[All directions are shown positive. ρ and ρ_o are positive if they are on the left side of an observer at P (z,y) facing the positive direction of s.]

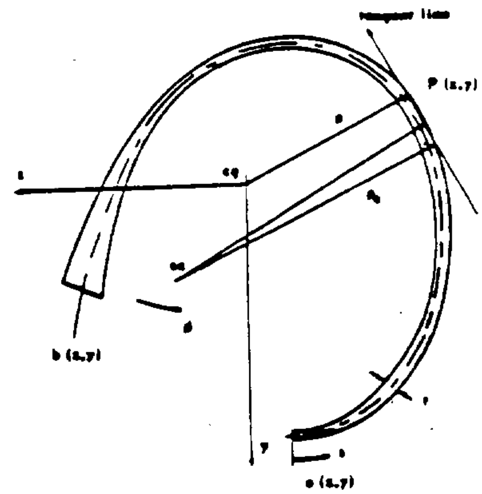

Figure B8.4.1-8. General Thin-Walled Open Cross Section

where

$$E_o = \frac{(b')^2 t}{2b't + h\, t_w/3}$$

and

$$u = b' - E_o$$

3. For zee sections (Fig. B8.4.1-9C):

$$W_{no} = \frac{uh}{2}$$

$$W_{n2} = \frac{u'h}{2}$$

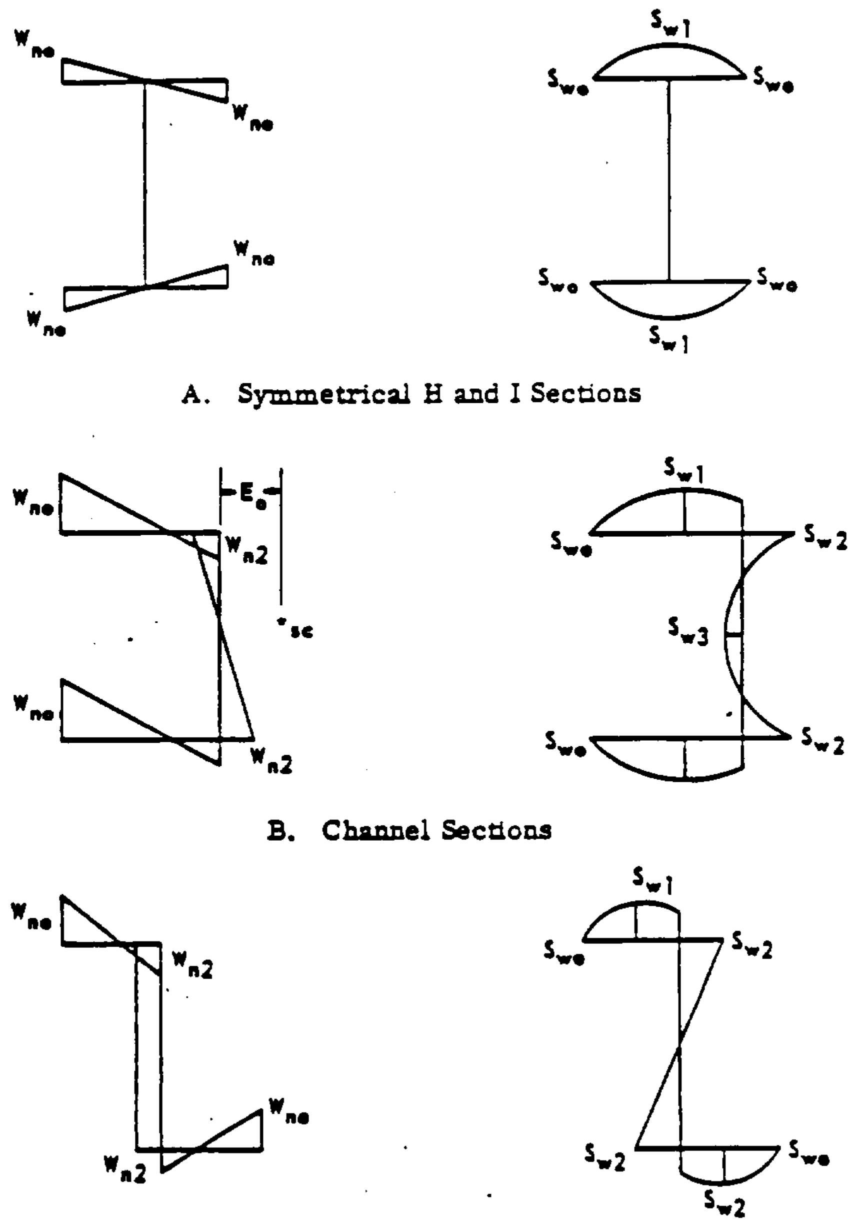

A. Symmetrical H and I Sections

B. Channel Sections

C. Zee Sections

Figure B8.4.1-9. Distribution of W_n and S_w for Standard Sections

B8.4 TORSION

REFERENCES

1. Files, J. H.: Computer Program for Restrained Torsion of Thin-Walled Open Sections. IN-P&VE-S-67-2, June 20, 1967.

2. Files, J. H.: Restrained Torsion of Thin-Walled Open Sections. IN-P&VE-S-67-1, August 20, 1967.

3. Heins, C. P., Jr. and Seaburg, D. A.: Torsion Analysis of Rolled Steel Design File/Design Data. Bethlehem Steel AIA File No-13-A-1.

4. Oden, J. T.: Mechanics of Elastic Structures. McGraw-Hill Book Co., Inc., 1967.

5. Flügge, W.: Handbook of Engineering Mechanics. McGraw-Hill Book Co., Inc., 1962.

6. Lyse, I. and Johnston, B. G.: Structural Beams in Torsion. ASCE Transactions, vol. 101, 1946.

7. AISC, "Torsional Analysis of Steel Members", Chicago, Illinois, 1983.

8. Galambes, T. V., "Structural Members and Frames", Saint Louis, Missouri, 1978.

9. Barsoum, R. S. and Gallagher, R. H., "Finite Element Analysis of Torsional and Torsional-Flexural Stability Problems", Institute of the Journal of Numerical Methods in Engineering, Volume 2, 1970.

SECTION 12.0

SPRINGS

DESIGN AND ANALYSIS OF THE MORE COMMON SPRINGS IS PRESENTED IN THIS SECTION.

		PAGE
12.1	COMPRESSION SPRINGS	12.1.1
12.2	EXTENSION SPRINGS	12.2.1
12.3	TORSION SPRINGS	12.3.1
12.4	CONSTANT FORCE SPRINGS	12.4.1
12.5	FLAT SPRINGS	12.5.1
12.6	CONED DISC (BELLEVILLE) SPRINGS	12.6.1
12.7	WORKING STRESSES	12.7.1

20. SPRING DESIGN

20.1 GENERAL. The proper design of springs requires an understanding of 1 — spring materials, 2 — design formulas and stress analysis and 3 — manufacture. Various aids to designers are available including special spring slide rules, tables of constants, curves, charts and nomographs. All are helpful, but an understanding of the basic fundamental formulas and experience in their use is essential to good design. Except for a few sizes of valve and die springs, there are very few springs manufactured for stock because of the infinite variety of characteristics involved. Utmost care in their design and manufacture and thorough analysis of service conditions are required for satisfactory performance.

20.1.1 Purpose. The purpose of this section is to describe the design methods used for each type of spring commonly used.

20.1.2 Scope. The data in this appendix are sufficient for general design purposes, and is not intended to include information for unusual designs or seldom used types of springs.

201.3 Abbreviations and Symbols. The following abbreviations and symbols are used throughout the appendix, unless otherwise noted:

A	= constant, for rectangular wire.
B	= constant, for rectangular wire.
b	= breadth or width, in.
C	= Spring index = D/d.
CL	= compressed length, in.
D	= mean coil diameter, in.
d	= diameter of wire or side of square, in.
E	= modulus of elasticity in tension, psi
F	= deflection, for N coils with load P, in.
F°	= deflection, for N coils, rotary, deg.
FL	= free length, unloaded spring, in.
f	= deflection, for one active coil, in., at load P.
G	= modulus of elasticity in torsion, psi.
ID	= inside diameter, in.
in.	= inch.
K	= curvature stress-correction factor
L	= active length subject to deflection, in.
l	= length, in.
lb	= pound
M	= bending moment ,in. lb.
N	= total active coils
n′	= vibration per minute.
OD	= outside diameter, in.
P	= load, lb.
P_1	= applied load, lb (also P_2, etc.).
p	= pitch, in.
psi	= pounds per square inch.
R	= distance from load to central axis, in.

r	= spring rate, load per inch, lb/in.
r_t	= spring rate, inch lbs per deg. (Torsion springs).
S_b	= stress, bending, psi.
S_t	= stress, torsional psi.
S_{it}	= stress, torsional, due to initial tension, psi.
SG	= squared and ground.
SH	= solid height, in. (or SL = solid length).
s	= height, load is dropped, in.
T	= torque = P x R, lb. in.
TC	= total coils.
t	= thickness, in.
U	= number of revolutions = $F^\circ \div 360^\circ$.
W	= weight, lb (also applied dynamic load).
x	= multiplied by
Y	= constant, for coned disc (Belleville) springs.
Z_1	= constant, for coned disc (Belleville) springs.
Z_2	= constant, for coned disc (Belleville) springs.
α	= alpha, angle of movement, deg.
π	= pi, 3.1416, in.
σ	= sigma, Poissons Ratio, 0.3 for steel.

21. COMPRESSION SPRINGS

21.1 DESIGN FORMULAS. The design formulas in Table II are used in the design of helical compression and extention springs. Note that the same formulas apply to both types of springs. The formulas in Table III are for determining compression spring dimensions only.

21.2 Compression Spring Ends. Figure 3 illustrates the types of ends on compression springs. Their characteristics follow:

(a) **Open Ends Not Ground;** also called Plain Ends, has the largest eccentricity of loading. These are used only when accuracy of loads is not important. This type is seldom used because such springs tangle severely during shipping.

(b) **Closed Ends Not Ground;** also called squared ends, cost approximately the same as open end type and have less eccentricity. This type is often used on light wire springs under 1/32 in. dia wire and for heavier wire where the index exceeds 13.

(c) **Open Ends Ground;** also called Plain Ends Ground, are seldom used as they cost about the same as the closed ends ground, but have high eccentricity of loading and tangle during shipping. They are sometimes used where the solid height is very limited and it is necessary to have as many active coils as possible in the least space.

(d) **Closed Ends Ground;** also called Squared and Ground, is the most popular type as it provides a level seat and reduces the tendency to buckle. This is the most expensive type and should be avoided for springs made from very light wire. Each end coil is ground for 270° plus or minus 30°.

21.3 DIAMETER CHANGES IN COMPRESSION SPRINGS. When a helical compression spring is compressed an increase in the outside diameter occurs because the angularity of the coils changes so that it is nearly at a right angle to the axis. The outside diameter, when the spring is compressed solid, can be obtained from the following formula:

$$OD_c = \sqrt{D^2 + \frac{p^2 - d^2}{\pi^2}} + d$$

In which:

OD_c = outside diameter at solid length

TABLE II. *Formulas for compression springs and extension springs without initial tension*

Property	Round wire	Square wire	Rectangular wire *
Torsional stress, psi S_t	$\frac{P D}{0.393\ d^3}$	$\frac{P D}{0.416\ d^3}$	$\frac{P D}{B\ b\ t^2}$
	$\frac{G\ d\ F}{\pi N\ D^2}$	$\frac{G\ d\ F}{2.32\ N\ D^2}$	$\frac{A\ G\ t\ F}{N\ D^2}$
Deflection, in. F	$\frac{8\ P\ N\ D^3}{G\ d^4}$	$\frac{5.58\ P\ N\ D^3}{G\ d^4}$	$\frac{S_t\ N\ D^2}{A\ G\ t}$
	$\frac{\pi S_t\ N\ D^2}{G\ d}$	$\frac{2.32\ S_t\ N\ D^2}{G\ d}$	....
Change in load lb $P_2 - P_1$ Extension springs only	$\frac{L_1 - L_2}{\frac{F}{P}}$	$\frac{L_1 - L_2}{\frac{F}{P}}$	$\frac{L_1 - L_2}{\frac{F}{P}}$
Change in load lb $P_2 - P_1$ Extension springs only	$\frac{L_2 - L_1}{\frac{F}{P}}$	$\frac{L_2 - L_1}{\frac{F}{P}}$	$\frac{L_2 - L_1}{\frac{F}{P}}$
Stress due to initial tension, psi S_{it}	$\frac{S_t}{P} \times IT$	$\frac{S_t}{P} \times IT$	$\frac{S_t}{P} \times IT$
Rate lb/in. r	$\frac{P}{F}$	$\frac{P}{F}$	$\frac{P}{F}$

* See figure 24.

TABLE III. *Compression spring formulas for dimensional characteristics*

Dimensional characteristics	Type of ends: Open or plain (not ground)	Open or plain with ends ground	Square or closed (not ground)	Closed and ground
Pitch (p)	$\frac{FL - d}{N}$	$\frac{FL}{TC}$	$\frac{FL - 3d}{N}$	$\frac{FL - 2d}{N}$
Solid Height (SH)	$(TC + 1)\ d$	$TC \times d$	$(TC + 1)\ d$	$TC \times d$
Active Coils (N)	$N = TC$ or $\frac{FL - d}{p}$	$N = TC - 1$ or $\frac{FL}{p} - 1$	$N = TC - 2$ or $\frac{FL - 3d}{p}$	$N = TC - 2$ or $\frac{FL - 2d}{p}$
Total Coils (TC)	$\frac{FL - d}{p}$	$\frac{FL}{p}$	$\frac{FL - 3d}{p} + 2$	$\frac{FL - 2d}{p} + 2$
Free Length (FL)	$(p \times TC) + d$	$p \times TC$	$(p \times N) + 3d$	$(p \times N) + 2d$

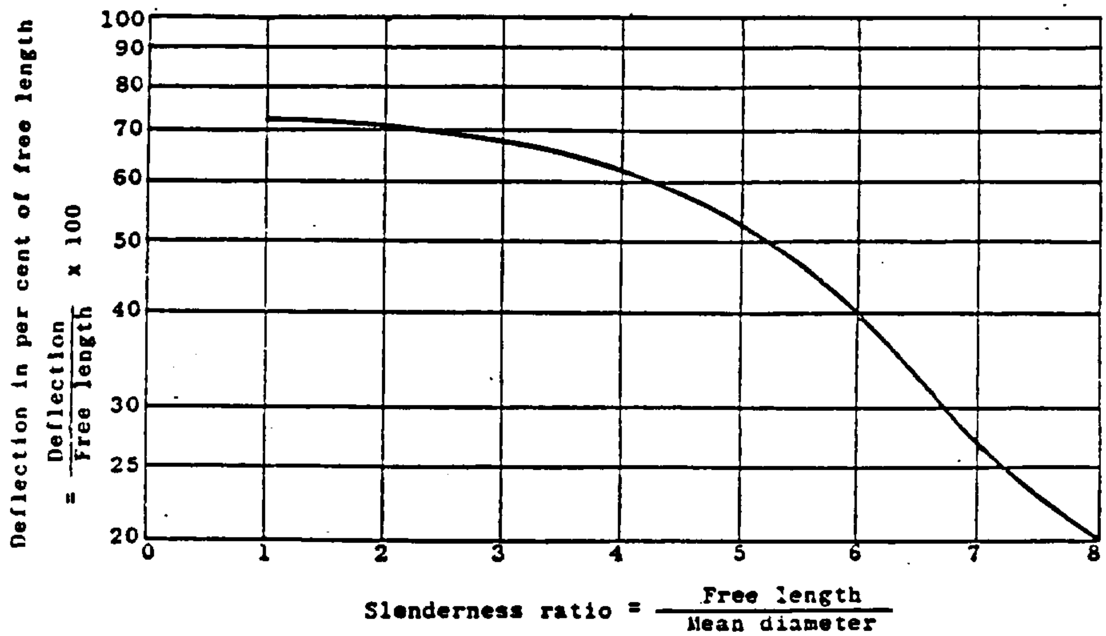

FIGURE 31

p = pitch, at free length

D = mean coil diameter at free length

d = wire diameter

21.4 BUCKLING. Compression springs having a free length greater than four (4) times their mean diameter become critical in lateral stability. When deflected beyond a certain percentage of the free length a spring will buckle. Figure 31 shows the maximum deflection which may be expected without buckling if the ends of the spring are closed and ground. Buckling can be reduced, space permitting, by a redesign using a heavier size wire and increasing the diameter of the coil. Buckling causes an undesirable reduction of the load and may cause early spring failure. If properly guided in a cylinder or over a rod, buckling can be reduced, although friction against the guiding member will affect the load and shorten the spring life.

21.5 DIRECTION OF HELIX. Unless functional requirements dictate a definite direction, the helix of compression and extension springs should be specified as optional. To prevent intermeshing of coils when springs operate one inside the other (see Figure 33), the helixes should be specified as opposite hand. For the same reason, springs which operate to slide freely over screw threads should have the helix specified opposite to that of the screw threads, but when a spring screws onto the threads of a screw or bolt, it should have the same helix as that of the screw or bolt.

21.6 NATURAL FREQUENCY, VIBRATION AND SURGE. The use of springs for loads which are applied dynamically, i.e., with impact or rapidly repeated will be in error if the spring is designed on the basis of static or slow loading. The load, stress, deflection, etc., will have been calculated for applications where the load is applied and held, or the rate of load application is below the natural frequency of the spring. Because of the inertia effect of the coils in instances where the load is suddenly applied, the load on the spring does not have time to distribute it-

self uniformly throughout the mass of the spring. This non-uniform loading causes deflection or a surge wave (see Figure 32) in a few coils of the spring which results in a high stress in this area and a lower stress in the remainder of the spring. In applications of high rate of repeated loading, non-uniform load distribution occurs in the same manner as suddenly applied loads and the natural frequency of vibration of the spring may be excited. The excitation of the natural frequency of vibration, in some instances, may be of such magnitude as to cause the spring coils to clash causing the spring to destroy its constraint on the mechanism. This is known as spring surge.

The following methods may be employed to prevent spring surging:

1. Stiffen spring
   (a) Increase diameter of wire
   (b) Decrease mean diameter of spring
   (c) Decrease number of coils
   (d) Use square or rectangular wire
2. Use spring nests
3. Use conical spring
4. Reduce or vary the pitch of the coils near the end of the spring
5. Use stranded wire springs

Formulas for natural frequency of steel springs follow:

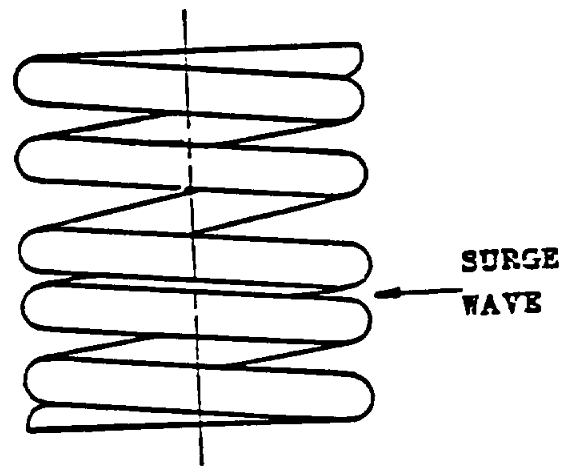

FIGURE 32

UNLOADED SPRING

$$n' = \frac{761{,}500\ d}{N\ D^2}$$

LOADED SPRING

$$n' = 187.6\sqrt{\frac{1}{F}}$$

(Neglecting spring weight)

If the frequency of the spring and its harmonics are too low, the spring will surge causing the coils to clash. In general, if the natural frequency of the spring is at least thirteen times that of the maximum frequency of the applied load, the design should be satisfactory.

21.7 IMPACT

21.8 SPRING NESTS. The nesting (one in-

TABLE IV. *Formulas for load deflections of compression and extension springs*

Slowly applied load	Suddenly applied load
$F = \frac{W}{r}$	$F = \frac{2W}{r}$
Applied load dropped vertically (spring initially compressed)*	Applied load with striking velocity of V in/sec. (spring in horizontal plane)
$F = \frac{W - P_1 + \sqrt{(W - P_1)^2 + 2Wrs}}{r}$	$F = \frac{-P_1 + \sqrt{P_1^2 + \frac{W r V^2}{386}}}{r}$

* If spring is not initially compressed, disregard P_1

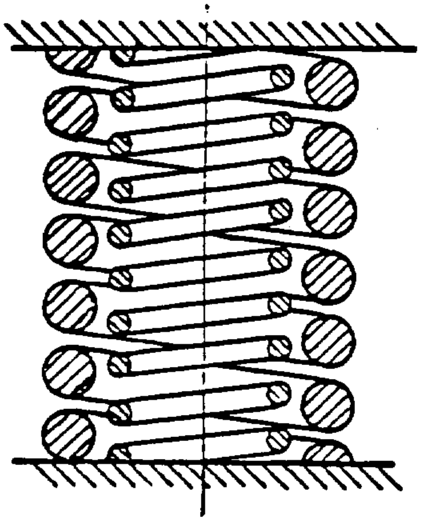

FIGURE 33

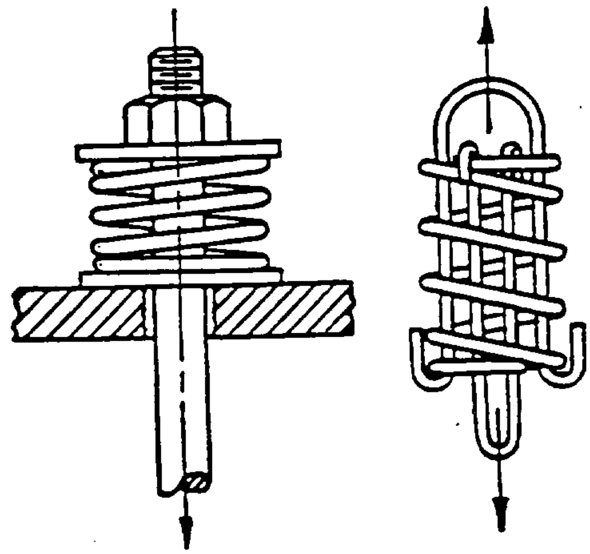

FIGURE 35

side the other) of helical compression springs (see Figure 33) is a method of obtaining maximum energy storage in a limited space. It is desirable to design the springs for equal life with 60 to 70 percent of the load on the outer spring. Maximum energy storage is obtained in a spring nest when the value of the spring indexes are between 5 and 7, when solid lengths of all the springs are approximately the same and when the working stroke $(L_2 - L_1)$ is of constant magnitude. The percentage of stress reduction obtained with nested springs is directly proportional to the spring index of the single spring when considering a constant working stroke. Not only is a reduction in the final stress obtained, but the use of nested springs effects a similar reduction in the stress range. Figure 34 shows the variation of the percentage reduction in the final stress and stress range with respect to the spring index of the single spring. The graph is based on the conditions that the nested springs and the single spring have the same values for:

(a) Active solid height H_s
(b) Load-deflection rate R
(c) Final Load P_2
(d) Modulus of torsion G
(e) OD D_o

The OD of single spring equals the OD of outer spring in nested design.

21.9 COMPRESSION SPRING USED AS AN EXTENSION SPRING. Occassionally certain applications require the action of an extension spring; but the use thereof would produce excessive deflection. This deflection would result in serious distortion, or set,

TABLE V. *Curvature stress correction factors (K) for compression and extension springs*

Spring index D/d	K	Spring index D/d	K	Spring index D/d	K	Spring index D/d	K
3.0	1.580	4.2	1.381	5.8	1.262	7.8	1.189
3.2	1.533	4.4	1.360	6.0	1.252	8.0	1.185
3.4	1.493	4.6	1.342	6.4	1.235	9.0	1.162
3.6	1.459	4.8	1.325	6.8	1.220	10.0	1.145
3.8	1.430	5.0	1.310	7.0	1.213	11.0	1.131
4.0	1.404	5.4	1.284	7.4	1.200	12.0	1.119

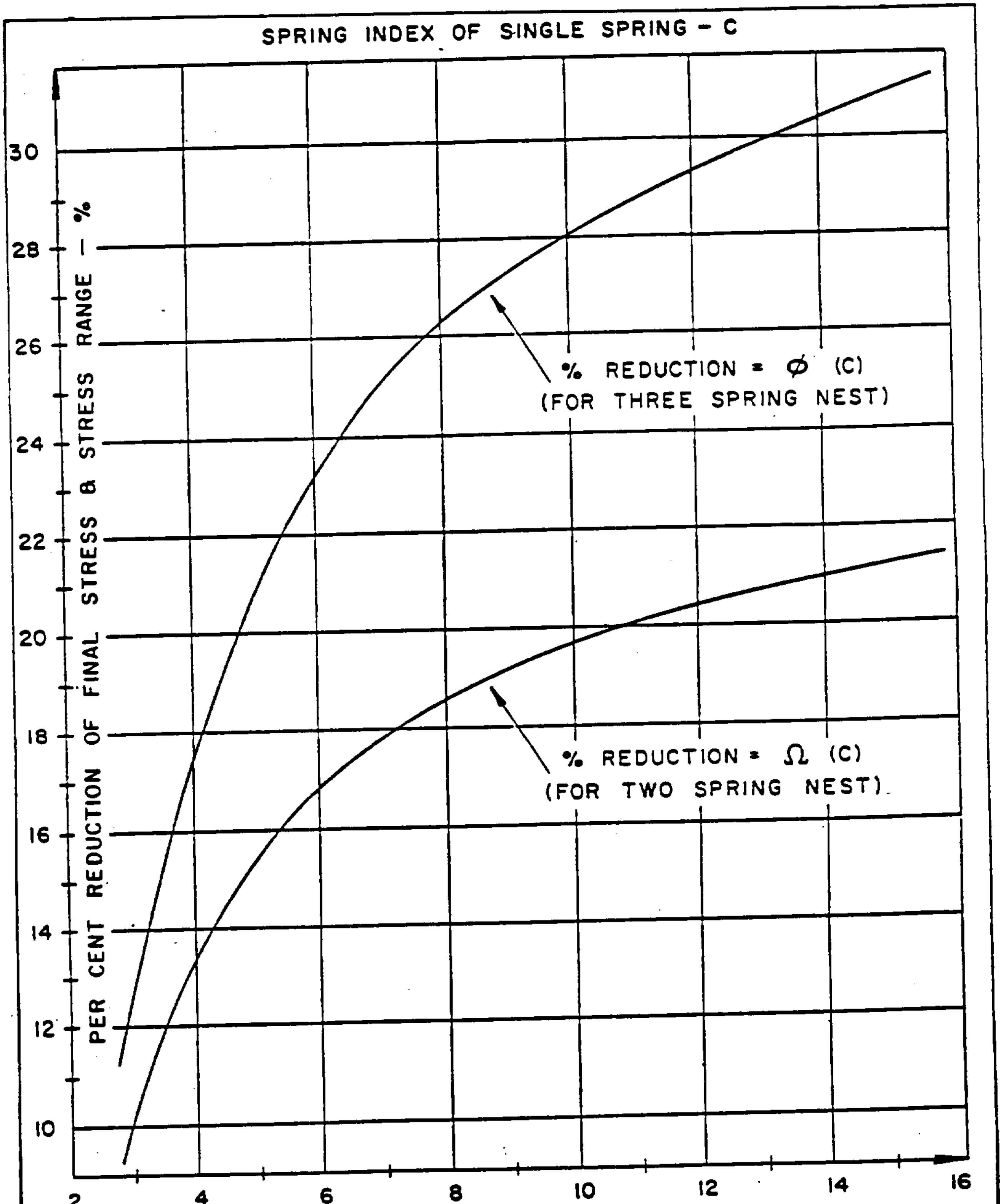

FIGURE 34. *Stress Reduction in spring nests*

of the extension spring and impairment of its fastenings (hooks). Under such circumstances, a compression spring can be used to produce the same action (See Figure 35). Such a device as a through bolt and washer, or a yoke-like drawbar can be utilized, resulting in a spring mount that has the carrying capacity and safety (by virtue of its definite solid length) of a compression spring.

21.10 SPRING INDEX (D/d). The spring index is the ratio of the mean coil diameter of a spring to the wire diameter (D/d). This ratio is one of the most important considerations in spring design inasmuch as the deflection, stress, number of coils, and selection of either annealed or tempered material depends to a considerable extent upon this ratio. The best proportioned springs have an index of 7 to 9. Ratios of 4 to 7 and 9 to 16 are often used. Springs with values larger than 16 require more than standard tolerances for manufacturing; those with values less than 5 are difficult to coil on automatic coiling machines.

21.11 CURVATURE STRESS-CORRECTION FACTORS.

(a) For helical compression and extension springs the curvature stress-correction factor (K) is determined from the following formula:

$$K = \frac{4C - 1}{4C - 4} + \frac{.615}{C}$$

The total stress,
$S_{MAX} = S_t \times K$

(b) For helical torsion springs the curvature stress-correction factor, (K_1), is determined from the following formula:

$$K_1 = \frac{4C^2 - C - 1}{4C\,(C - 1)}$$

The total stress,
$S_{MAX} = S_b \times K_1$

Values of (K) are obtained from Table V and Figure 39. Values of (K_1) are obtained from Figure 51.

EXAMPLE. If a spring with an index of 7.4 has a torsional stress S_t of 80,000 psi, what is the total stress in the spring? From the table it will be found that K equals 1.200; therefore, the total stress equals 80,000 times 1.200 = 96,000 psi. This is the stress that should be compared with allowable stresses to determine whether or no tthe spring is safely designed, and is the sole use made of such data.

In designing a spring it should be borne in mind that the total stress, as determined by this method, should not be used in calculating the deflection or number of coils. The torsional stress $S_t = PD/0.393\,d^3$ or $S_t = G\,d\,F/\pi\,N\,D^2$ should be utilized for such purposes.

21.12 KEYSTONE EFFECT. When square wire and rectangular wire are coiled into springs, a change in shape occurs. This change takes place because some of the material on the outside diameter is drawn into the spring and the material on the inside diameter upsets, thereby changing the wire into a trapezoidal section. The original thickness of the wire is maintained at or near the mean diameter of the coil. It is necessary to take into account this upsetting of the material in determining the solid height of the spring. This dimensional change depends upon the spring index and the thickness of the material and may be determined by the following formula:

$$t' = 0.48t\left(\frac{OD}{D} + 1\right)$$

t' = new thickness of inner edge after coiling

t = thickness before coiling
This formula may be used for both square and rectangular wire.

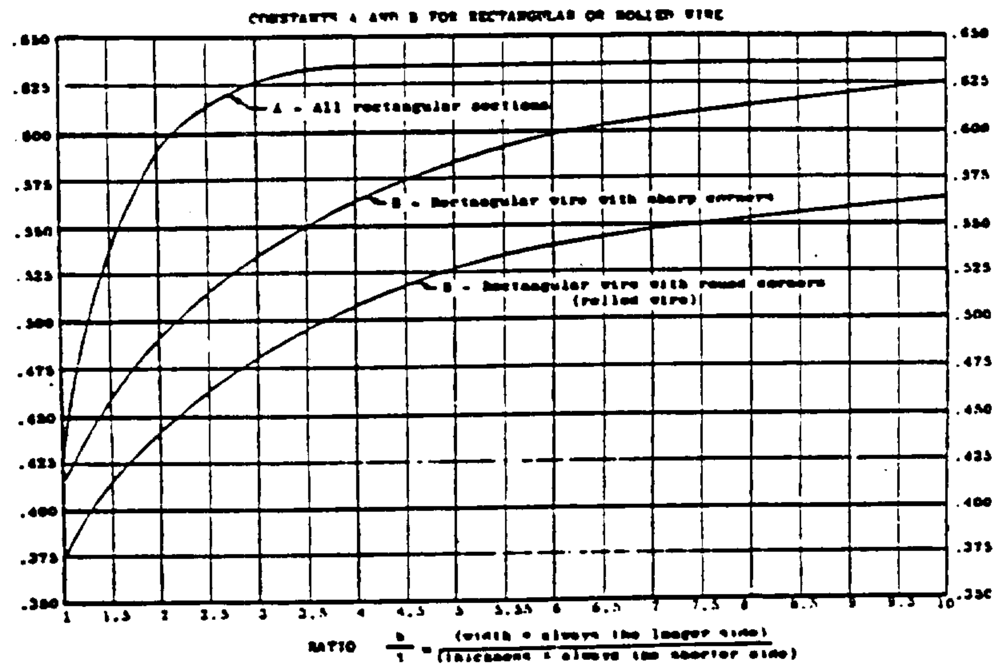

FIGURE 36

21.13 CONSTANTS FOR RECTANGULAR WIRE. The constants A and B in the formulas in Table II for compression and extension springs made from rectangular sections having either sharp or rounded edges are shown in Figure 36.

21.14 PRECAUTIONS AND SUGGESTIONS FOR EFFECTIVE DESIGN OF COMPRESSION SPRINGS.

(a) Compression springs ordinarily should not be permitted to go solid; exceptions occur when they are used as bumpers.

(b) Whenever practicable, springs should be designed so that if they were compressed to the solid length the corrected stress still would not exceed the minimum elastic limit.

(c) The length of a compression spring at maximum working deflection must not be too close to the solid length. As a minimum, a clearance of 10% of the wire diameter should exist between the coils.

(d) The selection of springs for continuous cycling should be made so that the stress range $\dfrac{(\text{MAX STRESS} - \text{MIN STRESS})}{\text{MAX STRESS}}$ will be as small as possible consistent with other design requirements.

(e) The outside diameter of a compression spring when compressed solid must be less than the minimum hole diameter, if the spring operates in a hole. When operating over a guide the minimum inside diameter must be larger than the maximum diameter of the guide.

(f) The possibility of buckling should be investigated and guides used if necessary.

(g) Use compression springs in preference to other types as they are easier to produce, less expensive and have a deflection limiting feature in the solid length.

(h) The best proportioned springs from the standpoint of manufacture and design have a spring index between 7 and 9, although indexes of 5 to 16 are commonly used.

(i) For indexes less than 5 in the larger

diameter wires, it may be necessary to use annealed material and harden after forming.

(j) Specify baking immediately after plating to relieve hydrogen embrittlement.

(k) Three compression springs of identical characteristics standing side by side (in parallel) will have a spring rate and a solid load three times that of one spring.

(l) Three compression springs of identical characteristics placed one on top of another (in series) will have a spring rate only one-third that of one spring and the solid load will be the same as for one spring.

21.15 TABLES OF SPRING CHARACTERISTICS FOR COMPRESSION AND EXTENSION SPRINGS. Table VI, in 5 parts, may be used in the design of helical compression and extension springs made from round wire. The data in Table VI also may be used for square wire by multiplying the deflection per coil f by .707 and the load P by 1.2. In these tables, the upper figure in each box is the deflection f in inches of one coil under a load P in pounds, which is the lower figure in the box. Both terms are based on a torsional modulus G of 11,200,000 psi and on an uncorrected torsional stress of 100,000 psi, which simplifies changing to other stress values.

21.15.1 Example. If a helical compression spring has an OD of 13/16 in. and is made of .041 in. dia wire, the tables shows that at a torsional stress of 100,000 psi such a spring would exert a load of 3.51 lbs and each coil would deflect .407 in. If the spring had 5 active coils, the load would be the same, but the deflection would equal 5 × .407 = 2.035 in.

If the allowable stress were only 60,000 psi, both values 3.51 and .407 should be multiplied by .60.

21.16 DESIGN NOMOGRAPHS FOR COMPRESSION AND EXTENSION SPRINGS. As an alternative to Table VI, the nomographs, Figures 37 to 42 may be used in the design of compression and extension springs made from round wire. Note, however, that the values of the torsional modulus G used in Table VI is 11,200,000 psi and the value used in the nomographs is 11,500,000 psi. The design conditions will indicate the type of material required for the application. It will be noted from the formulas for deflection (F) in Table II that the deflection varies inversely as the first power of G. Therefore, for materials having values of G differing from 11.2×10^6 or 11.5×10^6 the value of F (or f) determined from the use of either Table VI or the nomographs must be corrected by multiplying by the ratio of 11.2×10^6 (or 11.5×10^6) to the proper value of G for the material.

21.16.1 Example. Design a spring to develop a load (P_2) at final assembled length (L_2), the OD of the spring being limited to a maximum permissible value and the initial assembled length (L_1) also being known. Thus the approximate mean spring diameter (D) is known. Assume a stress valve somewhat lower than the recommended maximum working stress for the selected spring material and the intended service (deflection cycles). On the nomograph of Figure 37 or 38, connect with a straight line the value of P_2 on the (P) scale with the value of the mean spring diameter on the (D) scale. Through the intersection of this line with the transfer axis AB, draw a line from the assumed value of the stress on the (S) scale to the (d) scale and read the wire diameter (d). On the left portion of the nomograph of Figure 39, draw a line through the values of wire diameter and mean spring diameter on the (d) and (D) scales, respectively, and read the curvature stress correction factor (K) on the (K) scale. Determine the corrected stress by multiplying K by the assumed stress used in the above derivation of wire diameter (d). If the corrected stress is greater than the recommended maximum working stress, the pring must be recalculated using a lower assumed stress in the determination of wire diameter. Also, as stated in para-

graph 21.14(b), it is desirable to leave an additional margin whenever practicable so that if the spring were compressed to solid length the corrected stress still would not exceed the allowable working stress. On the nomograph of Figure 40 or 41, connect with a straight line the value of final assembled load (P_2) on the (P) scale with the value of mean spring diameter on the (D) scale. Through the intersection of this line with the transfer axis AB, draw a line from the wire diameter (d) to the (f) scale and read the deflection per coil (f). Values of total number of coils (TC), active coils (N), free length (FL), solid height (SH), and corrected stress at solid height (if pertinent) may be determined in a manner similar to that described in paragraph 21.17.

21.17 EXAMPLE OF COMPRESSION SPRING CALCULATION. A compression spring is required to have the following characteristics:

- Work in a $^{13}/_{16}$ inch diameter bore
- Final Assembled Length, $L_2 = 1\frac{1}{8}$ in
- Initial Assembled Length, $L_1 = 1\frac{5}{8}$ in
- Load at $L_2 = P_2 = 25$ lb
- Desired Load at $L_1 = P_1 = 20$ lb (tentative)
- Frequency of Deflections = 2000 cycles per hr max.
- Total Deflections = 500,000 cycles
- Ends closed and ground

These additional drawing requirements must be determined:

- Material specification
- Free length
- Diameter of wire
- Total coils, REF only

Proceed with the calculation as follows:

Select music wire for the material.

Utilizing Table VI in this calculation, an OD slightly smaller than $^{13}/_{16}$ and a load greater than 25 lb should be selected.

Thus from Table VI, select

OD = .750 in.

Load = 30 lb.

Deflection at 30 lb = .1574 in. per coil

Dia wire = d = .080 in.

Above values are for a stress of 100,000 psi

$D = OD - d = .75 - .08 = .67$ in.

The clearance between each coil when spring is at final assembled length should be a minimum of 10% of the wire diameter.

Using 10%, d + clearance = 1.1d

$$\text{Total coils} = TC = L_2/1.1d = \frac{1.125}{1.1 \times .08} = 12.8$$

Use TC = 12

Active coils = N = 12 − 2 = 10

Defl/coil/lb = .1574/30 = .00525 in.

Defl/10 coils/lb = .0525 in.

$$\text{Change in Load} = \frac{L_1 - L_2}{.0525} = \frac{1.625 - 1.125}{.0525} = 9.5 \text{ lb}$$

$P_1 = P_2 - 9.5 = 25 - 9.5 = 155$ lb

This is smaller than the desired load of 20 lb at initial assembled length. If the 15.5 lb ± 1.5 lb load is acceptable, proceed with the computation. If not acceptable, a more flexible spring must be designed. This will require one or more of the following changes:

(a) An increase in the final compressed length, and the same increase in the initial compressed length to allow for additional coils.

(b) An increase in D, possibly accompanied by an increase in d in order to maintain a safe stress.

Assuming in this case that a P_1 of 15.5 lb is satisfactory, proceed as follows:

$$\text{Free length} = FL = 1.125 + (25 \times .0525) = 1.125 + 1.31 = 2.435$$

Solid height = SH = 12 × .080 = .96

Total Deflection = 2.437 — .96 = 1.477

Load at Solid Height = $\frac{1.477}{.0525}$ = 28 lb

Stress at 28 lb = 100,000 × 28/30

= 93,500 psi

Stress at 25 lb = 100,000 × 25/30

= 83,500 psi

Spring Index = $\frac{D}{d} = \frac{.61}{.08} = 8.37$

From Figure 39, Correction Factor K = 1.16

Corrected Stress at 28 lb (Solid Height) = 93,500 × 1.16 = 108,000 psi

Since this spring is not designed to deflect to solid height in normal operation, the frequency of such a deflection should not approach the magnitude of even light service. The minimum elastic curve provides the limit for the maximum allowable solid stress.

From Figure 62, the recommended maximum solid stress for .080 music wire is 140,000 psi.

755

Loads and deflections of helical compression and extension springs

OD of spring			W & M wire size														19	18	17	16	15	14	13	12
			Decimal wire size																					
In.	Dec.		.010	.012	.014	.016	.018	.020	.022	.024	.026	.028	.030	.032	.034	.038	.041	.0475	.054	.0625	.072	.080	.0915	.1055
3/32	.0938	f	.01970	.01564	.01276	.01061	.00895	.00764	.00657	.00570	.00496													
		P	.469	.830	1.351	2.07	3.02	4.26	5.83	7.78	10.18													
7/64	.1094	f	.0277	.0222	.01824	.01529	.01302	.01121	.00974	.00853	.00751	.00664	.00589											
		P	.395	.697	1.130	1.722	2.51	3.52	4.79	6.36	8.28	10.59	13.35											
1/8	.125	f	.0371	.0299	.0247	.0208	.01784	.01546	.01353	.01192	.01057	.00943	.00844	.00758	.00683									
		P	.342	.600	.971	1.475	2.14	2.99	4.06	5.37	6.97	8.89	11.16	13.83	16.95									
9/64	.1406	f	.0478	.0387	.0321	.0272	.0234	.0204	.01793	.01590	.01417	.01271	.01144	.01034	.00937	.00777								
		P	.301	.528	.852	1.291	1.869	2.61	3.53	4.65	6.02	7.66	9.59	11.84	14.47	21.0								
5/32	.1563	f	.0600	.0487	.0406	.0345	.0298	.0261	.0230	.0205	.01832	.01649	.01491	.01354	.01234	.01033	.00909							
		P	.268	.470	.758	1.146	1.658	2.31	3.11	4.10	5.30	6.72	8.39	10.35	12.62	18.22	23.5							
11/64	.1719	f	.0735	.0598	.0500	.0426	.0369	.0324	.0287	.0256	.0230	.0208	.01883	.01716	.01569	.01321	.01172	.00914						
		P	.243	.424	.683	1.031	1.488	2.07	2.79	3.67	4.73	5.99	7.47	9.19	11.19	16.09	20.7	33.8						
3/16	.1875	f	.0884	.0720	.0603	.0516	.0448	.0394	.0349	.0312	.0281	.0255	.0232	.0212	.01944	.01650	.01468	.01157	.00926					
		P	.221	.387	.621	.938	1.351	1.876	2.53	3.32	4.27	5.40	6.73	8.27	10.05	14.41	18.47	30.07	46.3					
13/64	.2031	f	.1046	.0854	.0716	.0614	.0534	.0470	.0418	.0375	.0338	.0307	.0280	.0257	.0236	.0201	.01798	.01430	.01155					
		P	.203	.355	.570	.859	1.237	1.716	2.31	3.03	3.90	4.92	6.12	7.52	9.13	13.05	16.69	27.1	41.5					
7/32	.2188	f		.1000	.0840	.0721	.0628	.0555	.0494	.0444	.0401	.0365	.0333	.0306	.0282	.0241	.0216	.01733	.01411	.01096				
		P		.328	.525	.793	1.140	1.580	2.13	2.79	3.58	4.52	5.61	6.88	8.35	11.93	15.23	24.6	37.6	61.3				
1/4	.250	f			.1116	.0960	.0839	.0742	.0663	.0597	.0541	.0494	.0453	.0417	.0385	.0332	.0299	.0242	.01996	.01578	.01234			
		P			.457	.687	.987	1.366	1.834	2.40	3.08	3.88	4.82	5.90	7.14	10.17	12.95	20.8	31.6	51.1	82.4			
9/32	.2813	f			.1432	.1234	.1080	.0958	.0857	.0774	.0703	.0643	.0591	.0545	.0505	.0437	.0395	.0323	.0268	.0215	.01707	.01421		
		P			.403	.606	.870	1.202	1.613	2.11	2.70	3.40	4.22	5.16	6.24	8.86	11.26	18.01	27.2	43.8	70.0	99.9		
5/16	.3125	f				.1541	.1351	.1200	.1076	.0973	.0886	.0811	.0746	.0690	.0640	.0556	.0504	.0415	.0347	.0281	.0225	.01895		
		P				.542	.778	1.074	1.440	1.881	2.41	3.03	3.75	4.59	5.54	7.85	9.97	15.89	23.9	38.4	61.0	86.5		
11/32	.3438	f					.1653	.1470	.1321	.1195	.1090	.0999	.0921	.0853	.0792	.0690	.0627	.0518	.0436	.0355	.0288	.0244	.01952	
		P					.703	.970	1.300	1.697	2.17	2.73	3.38	4.13	4.98	7.05	8.94	14.21	21.3	34.1	53.8	76.2	119.2	
3/8	.375	f						.1769	.1589	.1440	.1314	.1206	.1113	.1031	.0960	.0839	.0764	.0634	.0535	.0438	.0358	.0305	.0247	.01931
		P						.885	1.185	1.546	1.978	2.48	3.07	3.75	4.53	6.40	8.10	12.85	19.27	30.7	48.4	68.2	106.1	171.1

NOTE: For steel wire, f is the deflection of each active coil caused by a load P. Both terms are based on a torsional stress of 100,000 psi and a torsional modulus of 11,200,000 psi.

TABLE VI

Loads and deflections of helical compression and extension springs

OD of spring			W & M wire size																					
									19	18	17	16	15	14	13	12	11	3/16	10	9	8	7	6	5
			Decimal wire size																					
In.	Dec.		.022	.024	.028	.030	.034	.038	.041	.0475	.054	.0625	.072	.080	.0915	.1055	.1205	.125	.135	.1483	.162	.177	.192	.207
25/64	.3906	f p	.1733 1.135	.1571 1.480	.1434 1.893	.1216 2.94	.1049 4.33	.0918 6.11	.0838 7.74	.0695 12.37	.0589 15.37	.0483 29.2	.0395 46.0	.0338 66.8	.0275 100.5	.0218 161.7								
13/32	.4063	f p	.1883 1.088	.1708 1.420	.1560 1.815	.1324 2.82	.1143 4.16	.1001 5.85	.0913 7.41	.0760 11.73	.0615 17.56	.0531 27.9	.0436 43.9	.0373 61.6	.0301 95.6	.0241 153.3								
27/64	.4219	f p	.2039 1.046	.1851 1.364	.1691 1.744	.1436 2.71	.1242 3.98	.1084 5.61	.0993 7.10	.0828 11.24	.0703 16.81	.0590 26.7	.0477 41.9	.0410 58.8	.0335 91.0	.0264 145.7	.0212 223.							
7/16	.4375	f p	.220 1.604	.1990 1.312	.1827 1.670	.1553 2.60	.1343 3.82	.1178 5.39	.1075 6.32	.0899 10.79	.0744 16.13	.0631 25.6	.0521 40.1	.0448 56.3	.0367 86.9	.0293 136.9	.0234 217.	.0219 215.						
29/64	.4531	f p	.237 .870	.215 1.285	.1968 1.616	.1674 2.61	.1449 3.68	.1272 5.19	.1162 6.57	.0971 10.38	.0827 15.30	.0685 21.5	.0566 38.5	.0483 53.9	.0401 83.2	.0321 132.6	.0258 207.	.0242 231.						
15/32	.4688	f p		.231 1.220	.212 1.550	.1800 2.42	.1560 3.55	.1370 5.00	.1252 6.33	.1048 9.99	.0894 14.91	.0741 23.6	.0614 37.0	.0530 51.7	.0437 79.7	.0351 124.9	.0282 197.3	.0265 221	.0272 289.					
31/64	.4844	f p		.240 1.179	.227 1.506	.1931 2.33	.1674 3.43	.1471 4.63	.1345 6.10	.1127 8.81	.0962 14.37	.0799 22.7	.0663 35.6	.0573 49.7	.0473 76.6	.0382 121.7	.0308 189.6	.0290 213.	.0259 277.					
1/2	.500	f p			.343 1.456	.207 2.26	.1792 3.31	.1575 4.67	.1441 5.90	.1209 8.30	.1033 13.67	.0859 21.9	.0711 34.3	.0619 47.9	.0512 73.6	.0414 116.9	.0335 181.1	.0316 205.	.0277 265.					
17/32	.5313	f p			.276 1.366	.235 2.12	.204 3.10	.1798 4.37	.1645 5.52	.1383 8.70	.1183 12.96	.0987 20.5	.0823 31.9	.0714 44.6	.0593 68.4	.0452 108.3	.0393 167.3	.0371 165.8	.0327 244.	.0377 335.				
9/16	.5625	f p				.265 1.991	.230 2.92	.203 4.11	.1861 5.19	.1566 8.18	.1343 12.16	.1122 18.17	.0937 29.9	.0816 41.7	.0680 63.9	.0555 100.9	.0435 155.5	.0430 175.3	.0380 226.	.0325 309.	.0278 417.			
5/8	.625	f p				.331 1.782	.288 2.61	.254 3.67	.233 4.63	.1969 7.29	.1693 10.83	.1420 17.04	.1191 26.5	.1041 36.9	.0873 56.4	.0718 88.7	.0593 138.2	.0561 153.4	.0499 197.1	.0430 269.	.0371 360	.0318 438.		
11/16	.6875	f p					.352 2.38	.311 3.32	.286 4.19	.242 6.58	.208 9.76	.1753 15.34	.1476 23.8	.1294 33.1	.1069 50.5	.0901 79.2	.0748 121.2	.0710 138.3	.0634 174.0	.0550 218.	.0479 317.	.0413 426	.0359 561.	
3/4	.750	f p						.374 2.03	.344 2.82	.291 5.99	.252 8.80	.212 13.94	.1791 21.6	.1574 30.0	.1329 45.7	.1105 71.3	.0923 109.2	.0577 139.7	.0760 157.1	.0685 213.	.0598 283.	.0520 380.	.0455 498	[illegible] 641.
13/16	.8125	f p							.407 3.51	.316 5.50	.299 8.15	.253 12.78	.214 19.60	.1881 27.5	.1694 41.7	.1329 65.3	.1115 90.3	.1061 111.5	.0954 143.6	.0834 192.9	.0733 256	.0640 343	.0563 448.	.0497 575

TABLE VI.—(*Continued*)

Loads and deflections of helical compression and extension springs

OD of spring			W & M wire size																					
			17	16	15	14	13	12	11	1/8	10	9	5/32	8	7	3/16	6	5	7/32	1/4	9/32	5/16	11/32	3/8
			Decimal wire size																					
In.	Dec.		.054	.0625	.072	.080	.0915	.1055	.1205	.125	.135	.1483	.1563	.162	.177	.1875	.192	.207	.2188	.250	.2813	.3125	.3438	.375
7/8	.875	f	.350	.295	.251	.222	.1882	.1574	.1325	.1262	.1138	.0999	.0938	.0890	.0773	.0707	.0652	.0605	.0552					
		P	7.53	11.00	16.20	25.3	39.4	60.0	91.1	102.3	130.5	170.3	209.	231.	313.	377.	407.	521.	626.					
29/32	.9063	f	.377	.320	.271	.239	.204	.1705	.1435	.1370	.1236	.1087	.1018	.0950	.0843	.0773	.0746	.0663	.0606					
		P	7.26	11.36	17.57	24.3	36.9	57.0	87.8	95.2	125.2	160.0	199.0	221.	299.	360.	359.	495.	598.					
15/16	.9375	f	.405	.344	.292	.258	.219	.1841	.1556	.1479	.1339	.1175	.1098	.1011	.0917	.0842	.0812	.0723	.0662	.0530				
		P	7.00	10.96	16.94	23.5	35.6	55.4	84.1	96.4	120.6	162.3	191.0	215.	290.	345.	373.	477.	673.	893.				
31/32	.9688	f	.435	.369	.313	.277	.236	.1992	.1675	.1598	.1445	.1273	.1183	.1127	.0994	.0913	.0882	.0780	.0721	.0590				
		P	6.76	10.59	16.35	22.6	34.3	53.4	81.0	90.0	115.0	156.1	184.5	207.	278.	332.	358.	457.	648.	854.				
1	1.000	f	.465	.395	.336	.297	.253	.213	.1801	.1719	.1555	.1372	.1278	.1216	.1074	.0996	.0954	.0852	.0783	.0631	.0515			
		P	6.54	10.23	15.80	21.9	33.1	51.6	78.1	87.6	111.7	150.6	177.0	198.8	264.	310.	344.	439.	526.	818.	1216.			
1 1/32	1.031	f	.498	.421	.359	.317	.271	.228	.1931	.1843	.1669	.1474	.1374	.1308	.1157	.1065	.1029	.0921	.0845	.0655	.0561			
		P	6.33	9.90	15.29	21.1	32.0	49.8	75.5	84.8	107.0	145.1	171.3	181.6	255.	307.	331.	423.	506.	786.	1165.			
1 1/16	1.063	f	.520	.449	.382	.338	.289	.244	.207	.1972	.1788	.1580	.1474	.1406	.1243	.1145	.1107	.0993	.0913	.0740	.0609			
		P	6.13	9.59	14.90	20.5	31.0	48.3	73.0	81.8	104.3	140.1	165.4	185.0	218.	296.	319.	407.	487.	765.	1119.			
1 3/32	1.094	f		.477	.417	.380	.308	.260	.221	.211	.1910	.1691	.1578	.1503	.1332	.1229	.1188	.1066	.0982	.0799	.0657	.0540		
		P		9.30	14.34	19.83	30.0	46.7	70.0	78.2	100.6	135.5	159.0	178.8	238.	286.	308.	393.	470.	727.	1076.	1333.		
1 1/8	1.125	f		.507	.432	.383	.328	.277	.235	.224	.204	.1804	.1685	.1604	.1424	.1315	.1273	.1142	.1053	.0950	.0710	.0592		
		P		9.02	13.92	19.24	29.1	45.3	68.6	76.7	97.8	131.2	154.7	173.0	230.	276.	298.	370.	454.	705.	1036.	1474.		
1 3/16	1.188	f		.568	.485	.431	.368	.311	.265	.254	.231	.204	.1900	.1812	.1620	.1498	.1448	.1303	.1203	.0986	.0819	.0687	.0581	
		P		8.53	13.14	18.15	27.5	42.6	64.4	72.1	91.7	123.3	145.4	162.4	218.	259.	279.	355.	424.	655.	965.	1369.	1891.	
1 1/4	1.250	f		.623	.541	.480	.412	.348	.297	.284	.258	.230	.215	.205	.1824	.1690	.1635	.1474	.1363	.1173	.0936	.0780	.0670	
		P		8.07	12.44	17.19	26.0	40.3	60.8	68.2	86.8	116.2	137.0	153.1	203.	241.	263.	334.	399.	614.	902.	1278.	1761.	
1 5/16	1.313	f			.600	.533	.457	.387	.331	.317	.288	.256	.240	.229	.205	.1894	.1834	.1657	.1535	.1288	.1052	.0890	.0768	.0457
		P			11.81	16.31	24.8	38.2	57.7	64.6	82.0	110.1	129.7	111.7	191.0	230.	248.	318.	378.	577.	858.	1198.	1647.	2249.
1 3/8	1.375	f			.662	.588	.506	.429	.367	.351	.320	.285	.267	.255	.227	.211	.204	.1848	.1713	.1420	.1184	.1014	.0847	.0718
		P			11.25	15.53	23.4	36.3	54.8	61.4	77.9	104.4	123.0	137.3	181.7	210.	235.	298.	358.	546.	799.	1127.	1540.	2071.
1 7/16	1.438	f			.727	.647	.556	.472	.404	.387	.353	.314	.295	.282	.252	.234	.227	.205	.1905	.1583	.1332	.1136	.0977	.0815
		P			10.73	14.81	22.3	34.6	52.2	58.6	74.1	99.4	117.8	130.0	172.0	207.	223.	283.	337.	517.	758.	1045.	1439.	1940.

TABLE VI.—(*Continued*)

Loads and deflections of helical compression and extension springs

OD of spring			W & M wire size																					
			3/32	12	11	1/8	10	9	5/32	8	7	3/16	6	5	7/32	4	1/4	9/32	5/16	11/32	3/8	13/32	7/16	1/2
			Decimal wire size																					
In.	Dec.		.0938	.1055	.1205	.125	.135	.1483	.1563	.162	.177	.1875	.192	.207	.2188	.2253	.250	.2813	.3125	.3438	.375	.4063	.4375	.500
1 13/32	1.406	f	.565	.494	.423	.405	.370	.329	.310	.296	.265	.250	.238	.218	.200	.1924	.1667	.1407	.1199	.1033	.0895	.0780		
		p	23.6	33.6	41.0	47.1	72.4	97.1	114.2	127.6	168.6	202.	218.	276.	329.	361.	504.	.736	1036.	1419.	1893.	2478.		
1 1/2	1.500	f	.591	.517	.443	.424	.387	.350	.324	.310	.277	.258	.250	.227	.210	.202	.1764	.1482	.1267	.1050	.0947	.0828	.0724	
		p	23.1	33.1	49.6	55.0	70.0	94.6	111.6	124.5	164.0	197.1	213.	260.	321.	352.	491.	717.	1005.	1381.	1841.	2400.	3093.	
1 9/16	1.563	f	.645	.565	.484	.464	.424	.378	.355	.340	.305	.283	.275	.249	.232	.223	.1934	.1636	.1402	.1212	.1055	.0922	.0812	
		p	23.1	31.7	47.7	53.3	67.7	90.6	106.6	118.9	157.1	188.3	203.	257.	306.	336.	468.	682.	958	1309.	1743.	2279.	2923.	
1 5/8	1.625	f	.701	.614	.527	.505	.461	.413	.387	.370	.332	.309	.300	.273	.254	.244	.212	.1801	.1547	.1339	.1169	.1028	.0905	
		p	21.3	30.2	45.7	51.1	64.6	86.7	102.0	113.9	150.3	180.0	193.9	246.	292.	321.	446.	650.	912.	1246.	1657.	2161.	2768.	
1 11/16	1.688	f	.760	.666	.572	.548	.501	.448	.421	.403	.362	.337	.327	.297	.277	.268	.232	.1971	.1697	.1474	.1290	.1133	.1002	
		p	20.3	29.1	43.0	49.1	62.2	83.2	97.0	108.3	144.1	172.6	185.8	235.	280.	307.	427.	622.	871.	1188.	1577.	2056.	2631.	
1 3/4	1.750	f	.820	.720	.619	.593	.542	.485	.456	.437	.392	.366	.355	.323	.301	.290	.253	.216	.1856	.1613	.1414	.1247	.1105	.0977
		p	19.68	28.0	42.2	47.2	59.9	80.0	94.0	104.9	138.5	165.6	178.4	228.	269	295.	409.	595.	833.	1135.	1506.	1959.	2504.	3927.
1 13/16	1.813	f	.884	.775	.667	.639	.585	.526	.492	.472	.424	.395	.384	.350	.326	.314	.274	.234	.202	.1761	.1547	.1365	.1212	.0967
		p	18.66	27.0	40.6	45.4	57.6	77.0	90.5	100.8	133.1	159.3	171.4	217.	255.	283.	393.	571.	799.	1086.	1440.	1876.	2391.	3739.
1 7/8	1.875	f	.948	.833	.71.	.687	.629	.564	.530	.508	.457	.426	.414	.377	.351	.339	.298	.253	.219	.1912	.1683	.1490	.1326	.1061
		p	18.20	26.1	39.2	43.6	55.5	74.2	87.2	97.3	129.2	153.4	165.1	209.	246.	273.	378.	548.	767.	1042.	1381.	1793.	2287.	3570.
1 15/16	1.938	f		.892	.769	.735	.676	.605	.569	.546	.492	.455	.446	.405	.379	.365	.320	.273	.237	.207	.1827	.1618	.1442	.1160
		p		25.2	37.6	42.3	53.6	71.6	84.2	93.8	123.6	147.9	159.2	201.	239.	262.	364.	528.	737.	1001.	1325.	1720.	2192.	3414.
2	2.000	f		.956	.823	.789	.723	.649	.610	.585	.527	.492	.478	.435	.407	.392	.344	.295	.256	.224	.1975	.1754	.1560	.1262
		p		24.3	36.0	40.9	51.6	69.2	81.3	90.6	119.4	142.8	153.7	194.3	231.	253.	351.	509.	710.	964.	1274.	1653.	2101.	3273.
2 1/8	2.125	f			.936	.898	.823	.730	.698	.667	.602	.562	.546	.499	.466	.449	.395	.339	.295	.259	.228	.204	.1826	.1182
		p			34.3	38.3	48.6	64.6	76.1	84.9	111.6	133.6	143.6	181.6	216.	230.	327.	471.	681.	896.	1183.	1532.	1918.	3021.
2 1/4	2.250	f			1.054	1.013	.930	.835	.787	.735	.661	.637	.619	.566	.529	.511	.449	.387	.337	.296	.263	.235	.211	.1718
		p			32.3	36.1	45.7	60.9	71.6	79.6	106.7	125.6	135.0	170.6	203.	222.	307.	444.	618	837.	1105.	1428.	1814.	2205.
2 3/8	2.375	f			1.184	1.136	1.043	.938	.884	.818	.763	.716	.696	.637	.596	.576	.507	.437	.393	.337	.298	.268	.241	.1972
		p			30.5	34.1	43.1	57.6	67.6	75.3	99.1	116.3	127.3	160.7	190.7	209.	289.	417.	581.	785.	1036.	1338.	1697.	2613.
2 1/2	2.500	f				1.366	1.163	1.046	.986	.948	.855	.800	.776	.712	.667	.644	.568	.491	.430	.379	.338	.303	.273	.224
		p				32.2	40.9	54.5	64.0	71.2	93.7	111.6	120.4	151.6	180.2	197.5	273.	394.	548.	741.	975	1259.	1594.	2155

TABLE VI.—(*Continued*)

Loads and deflections of helical compression and extension springs

OD of spring In.	Dec.		W & M wire size: 9	5/32	8	7	3/16	6	5	7/32	4	3
			Decimal wire size: .1483	.1563	.162	.177	.1875	.192	.207	.2188	.2253	.2437
2 3/4	2.750	f	1.290	1.208	1.180	1.049	.983	.956	.876	.821	.794	.723
		P	60.3	57.8	64.6	84.6	101.0	106.6	137.0	162.4	177.9	227.
2 7/8	2.875	f	1.408	1.327	1.274	1.154	1.091	1.052	.985	.904	.874	.787
		P	47.0	65.1	61.7	80.7	96.8	103.6	130.5	151.8	169.5	216.
3	3.000	f		1.452	1.394	1.263	1.194	1.152	1.057	.992	.959	.874
		P		62.7	60.7	77.1	92.0	99.0	121.7	147.8	161.0	200.
3 1/8	3.125	f			1.520	1.370	1.291	1.257	1.154	1.083	1.017	.955
		P			66.3	73.9	88.1	91.0	119.4	141.5	151.9	197.2
3 1/4	3.250	f				1.497	1.404	1.368	1.255	1.178	1.139	1.040
		P				70.9	84.6	90.9	114.5	135.6	140.8	169.0
3 3/8	3.375	f				1.621	1.520	1.480	1.360	1.277	1.235	1.128
		P				68.1	81.3	87.3	109.8	130.3	142.6	161.5
3 1/2	3.500	f					1.613	1.589	1.460	1.379	1.330	1.220
		P					78.1	84.0	105.0	125.3	137.2	174.5
3 5/8	3.625	f					1.768	1.723	1.553	1.487	1.439	1.310
		P					75.3	81.0	101.9	120.7	132.1	168.1
3 3/4	3.750	f						1.850	1.701	1.599	1.518	1.415
		P						78.1	98.3	116.4	127.4	162.1
4	4.000	f							1.950	1.833	1.774	1.624
		P							91.8	108.7	119.0	151.3
4 1/2	4.500	f									2.28	2.08
		P									105.1	133.5
5	5.000	f										
		P										
5 1/2	5.500	f										
		P										
6	6.000	f										
		P										

OD of spring In.	Dec.		W & M wire size: 1/4	2	9/32	0	5/16	2-0	11/32	3/8	13/32	7/16	1/2	9/16
			Decimal wire size: .250	.2625	.2813	.3065	.3125	.331	.3438	.375	.4063	.4375	.500	.5625
2 3/4	2.750	f	.701	.682	.608	.547	.534	.498	.472	.422	.370	.343	.281	.219
		P	246.	260.	334.	463.	491.	659.	663.	872.	1120.	1432.	2182	3195.
2 7/8	2.875	f	.773	.730	.671	.604	.590	.519	.523	.469	.421	.391	.317	.247
		P	234.	272.	337.	410.	447.	560.	631.	828.	1067.	1349.	2067.	3022.
3	3.000	f	.849	.801	.737	.664	.649	.604	.576	.515	.465	.421	.351	.298
		P	223.	260.	322.	420.	416.	634.	601.	789.	1015.	1253.	1961.	2867
3 1/8	3.125	f	.927	.876	.807	.727	.710	.662	.631	.566	.510	.463	.387	.325
		P	214.	210.	307.	401.	426.	510.	574.	753.	969.	1223.	1870.	2727.
3 1/4	3.250	f	1.010	.954	.879	.793	.775	.722	.689	.618	.558	.507	.431	.370
		P	205.	239.	291.	384.	408.	488.	549.	720.	920.	1169.	1795	2630.
3 3/8	3.375	f	1.094	1.036	.955	.862	.842	.785	.750	.673	.609	.553	.461	.395
		P	198.4	220.	283.	369.	30.1	466.	527.	690.	857.	1119.	1708	2485.
3 1/2	3.500	f	1.185	1.120	1.033	.933	.912	.851	.813	.731	.661	.602	.505	.431
		P	188.9	219.	272.	354.	376.	410.	506.	663.	851.	1073.	1636	2379.
3 5/8	3.625	f	1.278	1.209	1.115	1.009	.986	.919	.878	.790	.715	.651	.548	.466
		P	181.9	211.	261.	341.	36.2	432.	486.	637.	818.	1031.	1571.	2282.
3 3/4	3.750	f	1.374	1.301	1.200	1.085	1.061	.991	.946	.852	.772	.701	.592	.507
		P	175.4	204.	253.	328.	340.	417.	468.	614.	788.	993.	1511.	2193.
4	4.000	f	1.578	1.493	1.379	1.248	1.221	1.141	1.091	.983	.892	.814	.687	.590
		P	163.7	190.0	235.	306.	325.	358.	437.	571.	733.	923.	1403.	2033.
4 1/2	4.500	f	2.03	1.970	1.775	1.616	1.574	1.473	1.409	1.273	1.157	1.058	.898	.774
		P	144.4	167.6	207.	270.	288.	342.	384.	502.	643.	809.	1227.	1775.
5	5.000	f	2.53	2.40	2.22	2.02	1.973	1.817	1.769	1.600	1.457	1.335	1.136	.982
		P	129.2	149.8	185.2	241.	256.	305.	343.	448.	573.	721.	1091.	1575.
5 1/2	5.500	f			2.72	2.47	2.43	2.28	2.17	1.965	1.792	1.640	1.403	1.218
		P			167.5	218.	231.	278.	310.	404.	517.	649.	982	1416.
6	6.000	f					2.90	2.72	2.61	2.35	2.16	1.986	1.697	1.474
		P					211.	251.	282.	368	471.	591.	893	1283.

TABLE VI.—(*Continued*)

Hence, the corrected stress at solid height is less than the recommended minimum elastic limit and is satisfactory.

Corrected stress at 25 lb=83,500 × 1.16 =97,000 psi

From paragraph 28, Average Service would cover 500,000 cycles at a frequency not exceeding 2000 cycles per hour.

From Figure 62, the recommended maximum working stress for .080 music wire under average service is 112,000 psi. Therefore the design is satisfactory for the corrected design stress of 97,000 psi

From Table III, $p = \dfrac{FL - 2d}{N}$

$$= \frac{2.437 - 2 \times .08}{10}$$

$$= .228$$

From paragraph 21.3:

$$OD_c = \sqrt{D^2 + \frac{p^2 - d^2}{\pi^2}} + d$$

$$= \sqrt{.67^2 + \frac{.228^2 - .08^2}{\pi^2}} + .08$$

$$= .753$$

From Table XVI, tolerance on OD= ± .015

Hence, Max OD=.753 + .015=.768, which is satisfactory in an .812 dia bore.

The requirements have been met by a spring having the following characteristics:

OD = .75 d = .08, N = 10, TC = 12, FL = 2.437 (P_1 load at initial assembled length having been changed to 15.5).

21.17.1 Necessity for Several Calculations. Frequently the first set of calculations does not result in a satisfactory design for the conditions involved. It is usually necessary to make several sets of calculations before determining the final design. This often is caused by a stress that is too high, a difficult index for manufacture, or a length that would buckle and require support in a tube or over a rod.

21.18 STRANDED WIRE HELICAL COMPRESSION SPRINGS.

21.18.1 General. Helical compression springs made from standard wire have an inherent tendency about twice as high as round wire springs to dampen high velocity displacement of their coils under shock loading. Under such conditions of loading, they have withstood 3 to 4 times as many deflections as round wire springs having the same load-deflection and stress conditions, before failure. For this reason, they have been used for machine guns. They do not have longer life than round wire springs under normal types of load applications. Good results have been obtained by using three strands of music wire twisted so that the ratio of length of lay to the strand diameter is between 5 and 5½. The length of lay is the distance parallel to the strand axis in which a single wire makes one turn. Preforming the wire by twisting it slightly just prior to the actual stranding operation helps to keep the strands tightly together. Corrosion resisting steel wire also could be used, Springs with an index D/d of 13 can be coiled on automatic spring coilers, but springs with a smaller index usually require coiling over an arbor. Shot peening is not recommended as the small shot lodges tightly between the strands and is difficult to detect and remove.

21.18.2 Stress. High stresses are used in design. The following stresses have been used at solid length; for music wire .030 in. dia 170,000 to 195,000 and for music wire .070 in. dia 150,000 to 170,000 psi.

21.18.3 Formulas for 3 Stranded Wire Spring Design Follow: The S_t and d values are for each strand of wire, and P is the actual load on the spring.

$$P = \frac{G\, d^4\, F}{2.54\, D^3\, N}$$

$$S_t = \frac{G\,d\,F}{\pi\,N\,D^2}$$

$$N = \frac{G\,d^4\,F}{2.54\,P\,D^3}$$

$$r = \frac{P}{F}$$

The design procedure is the same as for other types of compression springs except that each strand carries its proportionate share of the load.

22. EXTENSION SPRINGS

22.1 DEFLECTION OF EXTENSION SPRING ENDS. Loading an extension spring having hook (loop) ends causes the hooks to deflect. The amount of this deflection depends on the type of hook used. For a half hook the deflection per hook is equivalent to .1 of a full coil and the total number of active coils for design purposes will be N + .2. When a full hook is turned up from a full coil, the deflection per hook is equivalent to .5 of a full coil and the total number of active coils for design purposes will be N + 1.

22.2 STRESSES IN HOOKS OF EXTENSION SPRINGS. The hooks at the ends of extension springs are subjected to both tension (bending) and torsional stresses. See Figure 43. These combined stresses are frequently the limiting factor which determines the characteristics of the spring. These stresses occur at the base of the hooks and their magnitude is higher than the stress in the body. Therefore this is the weakest point in an extension spring and the stresses shoud be calculated. The allowable working stresses should not exceed those shown in the curves, Figure 62, Section II of this Appendix, if long life is required.

FIBER STRESS (Not Corrected for Curvature) vs. LOAD
Helical Extension and Compression Springs

Low Range {Mean Diameter: .1" to 3"; Wire Diameter: .015" to .5"}

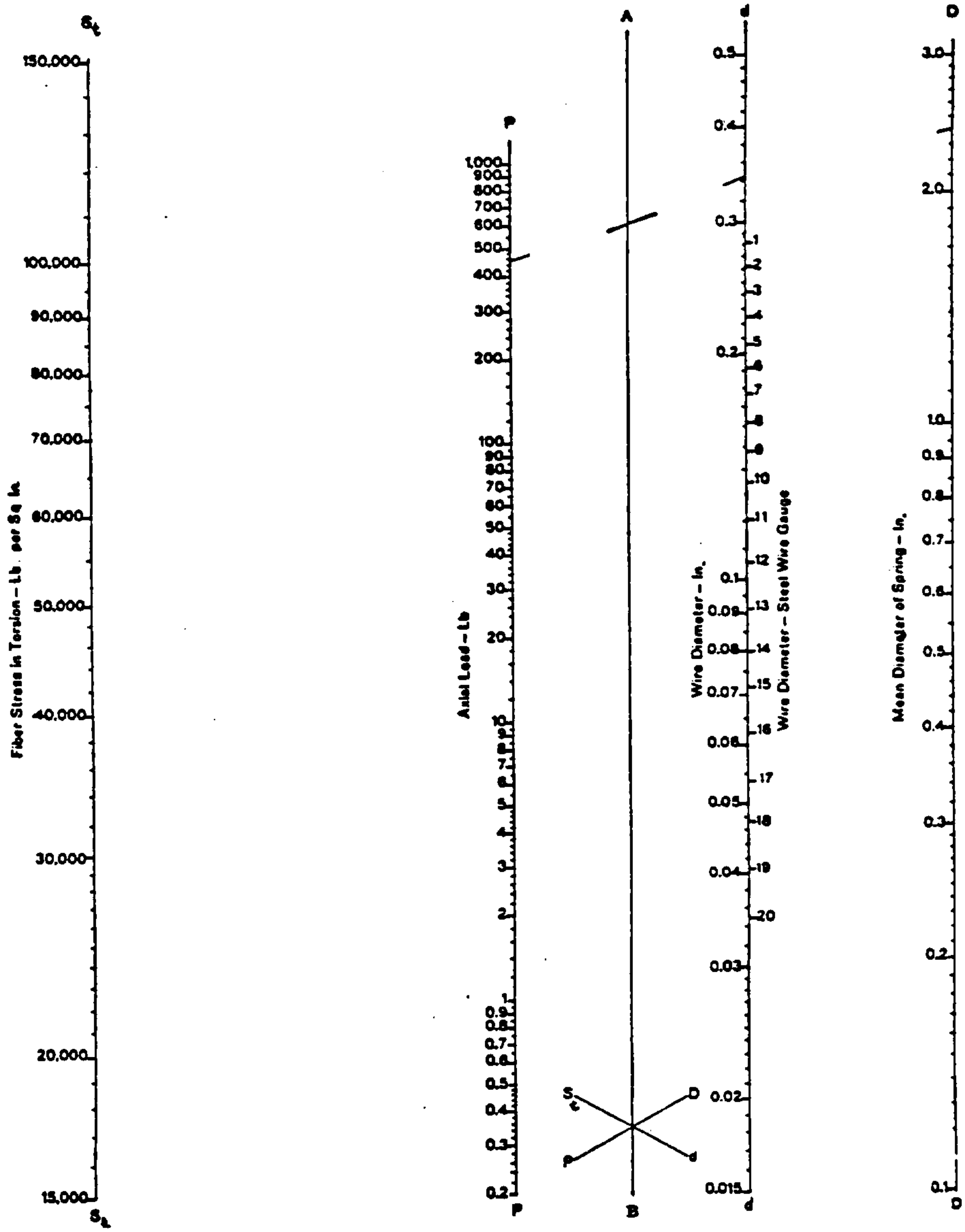

FIGURE 37

763

FIBER STRESS (Not Corrected for Curvature) vs. LOAD
Helical Extension and Compression Springs

High Range {Mean Diameter: 1" to 10"; Wire Diameter: .15" to 2.5"}

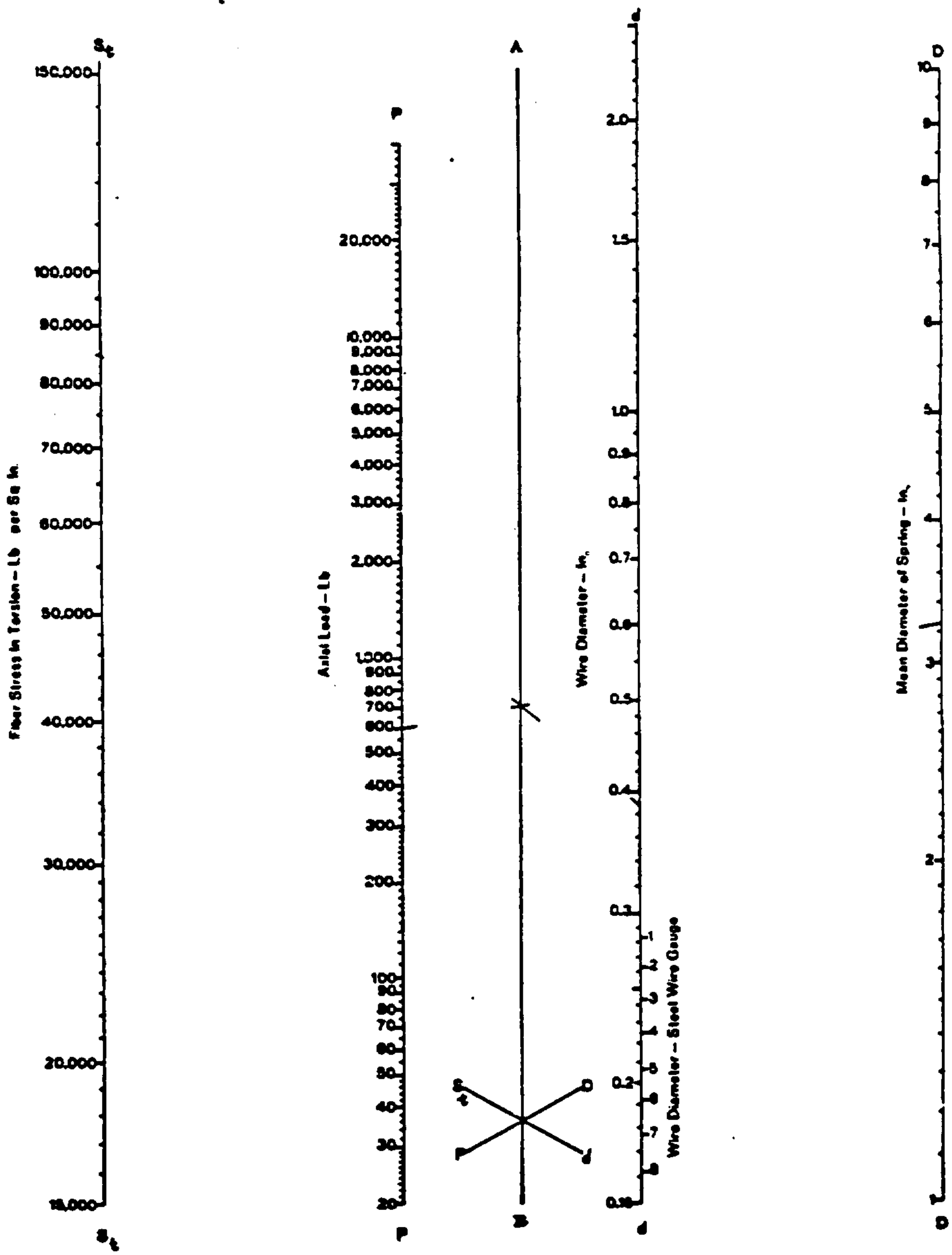

FIGURE 38

FIBER STRESS CORRECTION FOR CURVATURE

Helical Extension and Compression Springs

Find Correction Factor From Spring Index

Using Correction Factor Found on Left Half of Chart — Determine True Fiber Stress

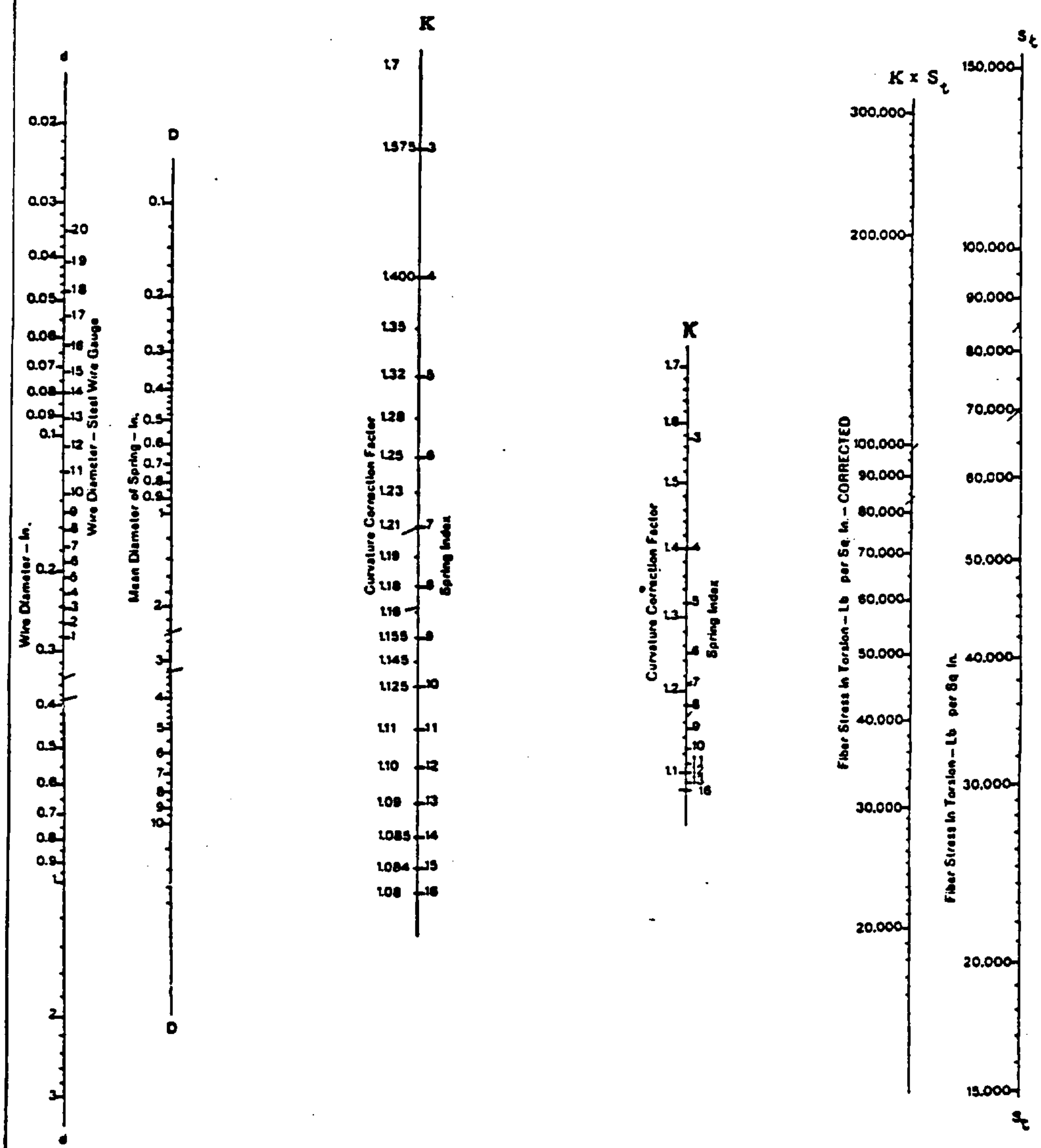

FIGURE 39

DEFLECTION PER COIL vs. LOAD
Helical Extension and Compression Springs

Low Range {Mean Diameter: .1" to 3"; Wire Diameter: .015" to .5"}

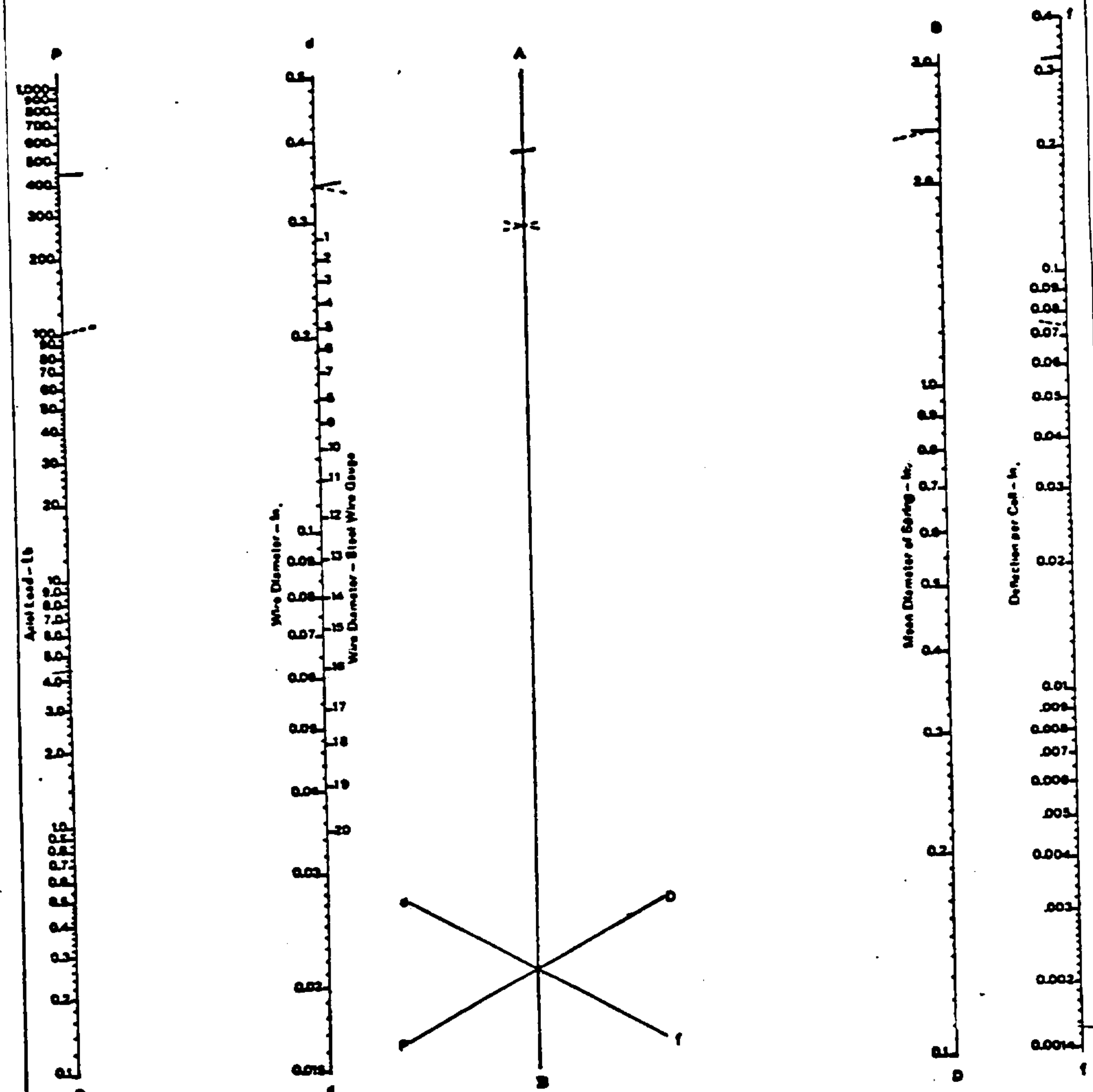

Figure 40

DEFLECTION PER COIL vs. LOAD
Helical Extension and Compression Springs

High Range {Mean Diameter: 1" to 10"; Wire Diameter: .15" to 2"}

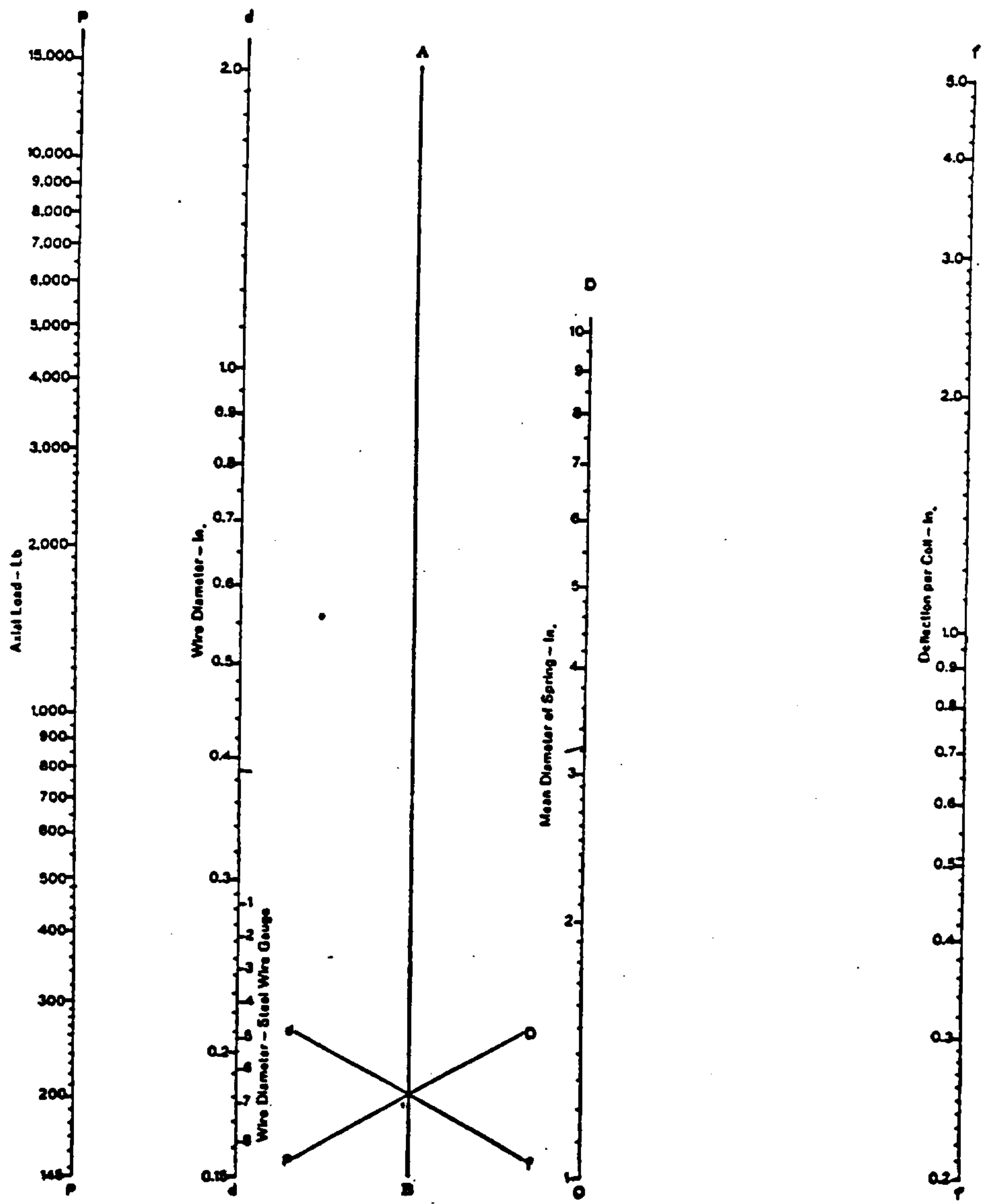

FIGURE 41

767

DEFLECTION PER COIL

Modulus (G) Other Than 11.5 × 10⁶

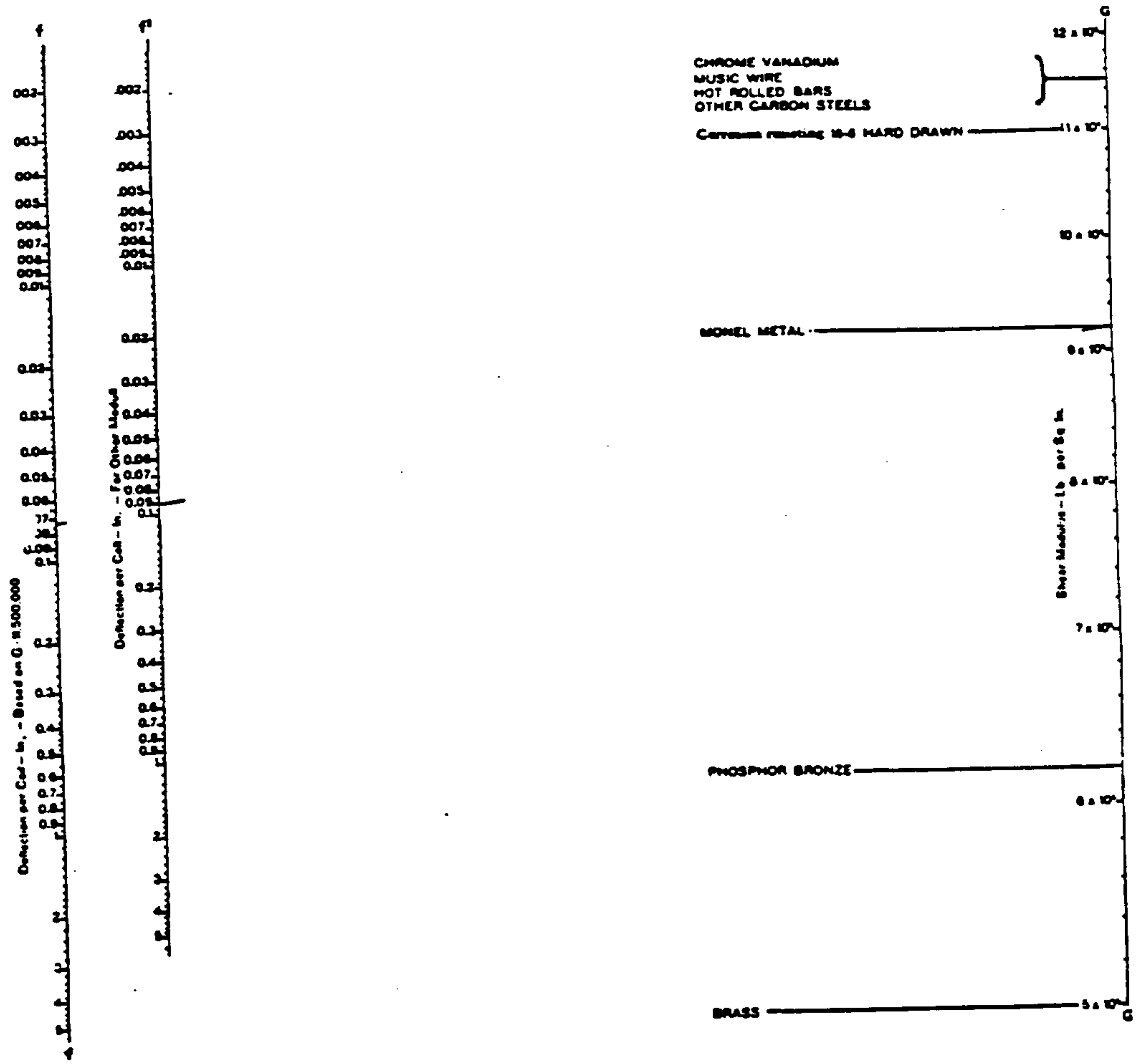

FIGURE 42

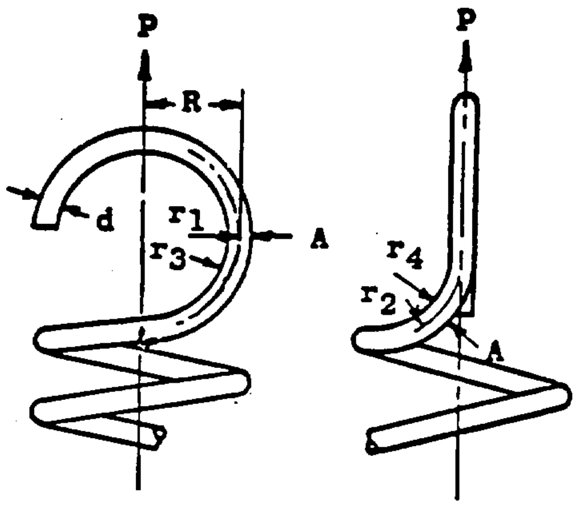

FIGURE 43

Bending Stress at Section A

$$S_b = \frac{PR}{.098\, d^3} \times \frac{r_1}{r_3}$$

Torsional Stress at Section A'

$$S_t = \frac{16\, P\, R}{\pi\, d^3} \times \frac{r_2}{r_4}$$

Where:

r_1 = Mean Radius of Hook, in.
r_2 = Mean Radius of Bend, in.
r_3 = Inside Radius of Hook, in.
r_4 = Inside Radius of Bend, in.

For best results the inside radius should be at least twice the wire diameter. Special ends can be used when high stresses occur in the hooks. By using a smaller diameter for the last few coils, see Figure 44, before the loop, the magnitude of PR is reduced. Thus the stress is reduced in direct proportion to the decrease in the magnitude of PR. By using as large radii for r_3 and r_4 as the design will permit the stress value is further reduced. The values of r_3 and r_4 can be determined by layout.

In extension springs with hooks bent off the body (see Figure 6, Off-set hook at side) the moment arm of the load on which the maximum torsion stress in the spring depends is about twice what it would be if the load were applied axially. This means doubling the stress for a given load.

22.3 INITIAL TENSION. Initial tension is a load in pounds which opposes the opening of the coils by an external force. It is wound into the springs during the coiling operation. Extension springs will have a uniform rate after the applied load overcomes the load due

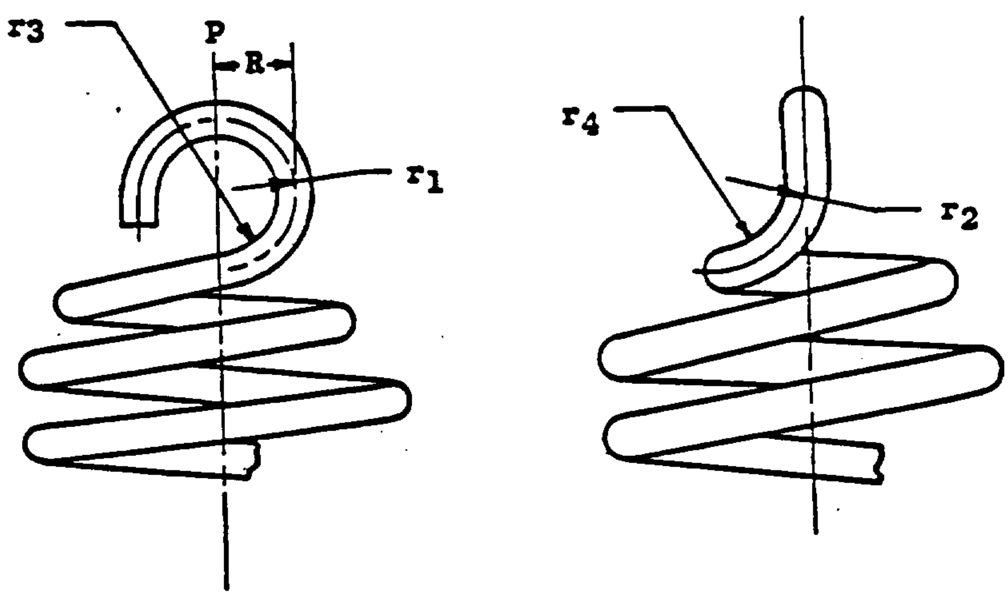

FIGURE 44

769

to initial tension. The number of coils do not affect the amount of initial tension except when the weight of the coils is heavier than the initial tension. The amount of initial tension is dependent on the spring index (D/d); the smaller the index the larger the initial tension. Initial tension does not increase the ultimate load or capacity of the spring but causes a larger portion thereof to be exerted during the initial deflection. For example, if the initial tension is 4 lbs and the spring rate is 9 lb then, at 1 inch deflection the load is

$(1 \times 9) \div 4 = 13$ lb

3-inches deflection the load is

$(3 \times 9) \div 4 = 31$ lb

In computing the total torsional stress add the torsional stress caused by initial tension to the torsional stress caused by deflection. Figure 45 shows the amount of initial tension in terms of torsional stress (without application of curvature stress correction factor) which can be coiled into extension springs made of music wire, oil tempered, corrosion resisting steel and hard drawn spring steels. Reduce these values 20 percent for springs made from nickel-base alloys such as Monel and Inconel. Hot rolled springs and those made of annealed materials cannot be wound with initial tension. Springs which require stress relieving will lose 25 to 50 percent of their initial tension. This loss can be compensated for during the coiling operation by winding more initial tension into the spring and thus obtain the required initial tension after stress relieving.

22.4 EXAMPLE OF EXTENSION SPRING CALCULATION. An extension spring is required to exert a force (load) of 27 lb at 2 in. deflection and be deflected an additional 3 in. (5 in. total) and then exert a total load of 55 lb. It must operate within a 1.812 in. minimum diameter bore.

Select a suitable oil tempered wire diameter and determine the number of coils, length over coils, free length inside ends, maximum extended length inside ends without set, stresses at all loads, etc., stressed for light service (see Figure 62)

From Table VI it will be found that a spring with an OD of 1¾ in., and made from 5/32 in. (0.156 in.) diameter wire, will exert a force (load) of 94.0 lb at a stress of 100,000 psi and have a deflection per coil of 0.456 in. at that load.

$$\text{Stress at 55 lb} = \frac{55}{94} \times 100{,}000$$

$$= 58{,}500 \text{ psi}$$

$$\text{Rate or load per inch, } \frac{55\text{-}27}{3} = 9.33 \text{ lb/in,}$$

Load due to deflection of 2 in., $2 \times 9.33 = 18.66$ lb

Load required is 27 lb; therefore the initial tension is $27 - 18.66 = 8.34$ lb

Load at 5 in. deflection $= (5 \times 9.33) \div 8.34 = 46.65 + 8.34 = 54.99$ (say 55 lb)

Stress at 5 in. deflection (due to 46.65 lb load) =

$$\frac{46.65}{94} \times 100{,}000 = 49{,}650 \text{ psi}$$

Stress due to initial tension,

$$\frac{8.34}{94} \times 100{,}000 = 8{,}880 \text{ psi}$$

$$\text{Deflection per coil, } \frac{49{,}650}{100{,}000} \times 0.456 = 0.226 \text{ in.}$$

Number of active coils for 5 in. deflection.

$$\frac{5}{.226} = 22.1 \text{ (say 22)}$$

Length over coils, $(22 \div 1) \times 0.156 = 3.58$ (say 3-9/16 in.)

Length of hook (assuming 80 per cent of ID), $0.80 \times 1.437 = 1.15$ (say, 1 5/32 in.)

Free length, inside ends (hooks), 3 9/16 + (2 × 1 5/32 in.) = 5⅞ in.

The formulas for solving the example follow:

Stress due to 46.65 lb load.

$$S_t = \frac{PD}{0.393d^3} = \frac{46.65 \times 1.594}{0.393 \times 0.156^3}$$

49,650 psi

$$N = \frac{GDF}{3.14S_tD^2}$$

$$= \frac{11{,}200{,}000 \times 0.156 \times 5}{3.14 \times 49{,}650 \times 1.594^2} = 22.1$$

Stress due to initial tension, =

$$S_{it} = \frac{S_t}{P} \times IT = \frac{49{,}650}{46.65} \times 8.34$$

$= 8{,}870$ psi

Final stress, $49{,}650 \pm 8{,}870$

$= 58{,}520$ psi

Spring Index$= \frac{1.594}{.156} = 10.2$ From

Figure 39, Correction Factor

$= 1.12$

Corrected torsion stress in coils at 55 lb load

$= 58{,}520 \times 1.12 = 65{,}200$ psi

Since the allowable stress from Figure 62= $92{,}000 \times .85 = 78{,}200$ psi, design is satisfactory so far.

Torsional stress in hooks at 55 lb load=

$$\frac{16PR}{\pi d^3} \times \frac{r_2}{r_4} = \frac{16(55)\ .797}{\pi(.00380)}$$

$$\times \frac{.797}{.719} = \frac{700}{.01196} \times 1.11 = 65{,}000 \text{ psi}$$

Bending stress in hooks at 55 lb load

$$= \frac{PR}{.098d^3} \times \frac{r_1}{r_3} = \frac{55 \times .797}{.098 \times .156^3}$$

$$\times \frac{.797}{.719} = 130{,}000 \text{ psi}$$

Since the allowabe stress from Figure 62= $92{,}000 \times 1.5 = 138{,}000$ psi, the present hook configuration is satisfactory.

To determine the maxium extended length inside ends without permanent set we determine (Figure 62) the minimum elastic limit for .156 dia oil tempered wire to be 100,000 $\times$ .85 = 85,000 psi.

Allowing for curvature stress correction factor of 1.12, the allowable stress =

$$\frac{85{,}000}{1.12} = 75{,}800$$

From Table VI, we know that a load of 94 lb will produce a stress of 100,000 psi. Therefore, the load producing 75,800 psi is as follows:

$$\frac{X}{94} = \frac{75{,}800}{100{,}000};\ X = \frac{94(75{,}800)}{100{,}000} = 71 \text{ lb}$$

Since load at 5 in. = 55 lb and rate = 9.33 lb/in., a 71 lb load would occur at

$$\frac{71-55}{9.33} + 5 \text{ in.} = \frac{16}{9.33} + 5 = 1.715 + 5 =$$

6.715 in. (say 6⅝ in.) This length is tentative, depending on the following stress checks.

Checking the torsion stress in the hooks at maximum extended length (load=71 lb):

$$S_t = \frac{16PR}{\pi d^3} \times \frac{r_2}{r_4} = \frac{16 \times 71 \times .797}{\pi(.00380)}$$

$$\times \frac{.797}{.719} = 84{,}000 \text{ psi}$$

Since the allowable torsional stress from Figure 62 = $100{,}000 \times .85 = 85{,}000$ psi, the hooks torsional stress is satisfactory.

Checking the bending stress in the hooks at maximum extended length (load = 71 lb)

$$S_b = \frac{PR}{.098d^3} \times \frac{r_1}{r_3}$$

$$= \frac{71 \times .797}{.098 \times .156^3} \times \frac{.797}{.719}$$

$= 168{,}000$ psi

Since the allowable bending stress at maximum extended length = 102,000 × 1.50 = 153,000 psi; the hook is overstressed and the maximum extended length must be decreased. Therefore, we calculate the maximum load without set.

$$\frac{153{,}000}{168{,}000} = \frac{X}{71}; \; X = \frac{71(153{,}000)}{168{,}000}$$

$= 64.7$ lb

Since 55 lb 5 in., with rate of 9.33 lb/in., a 64.7 lb load would occur at

$$\frac{64.7-55}{9.33} + 5 \text{ in.} = \frac{9.7}{9.33} + 5 = 1.04 + 5 =$$

6.04 in.

The maximum extended length inside ends without permanent set is: 6.04 + 5.875 = 11.915, say 11.90.

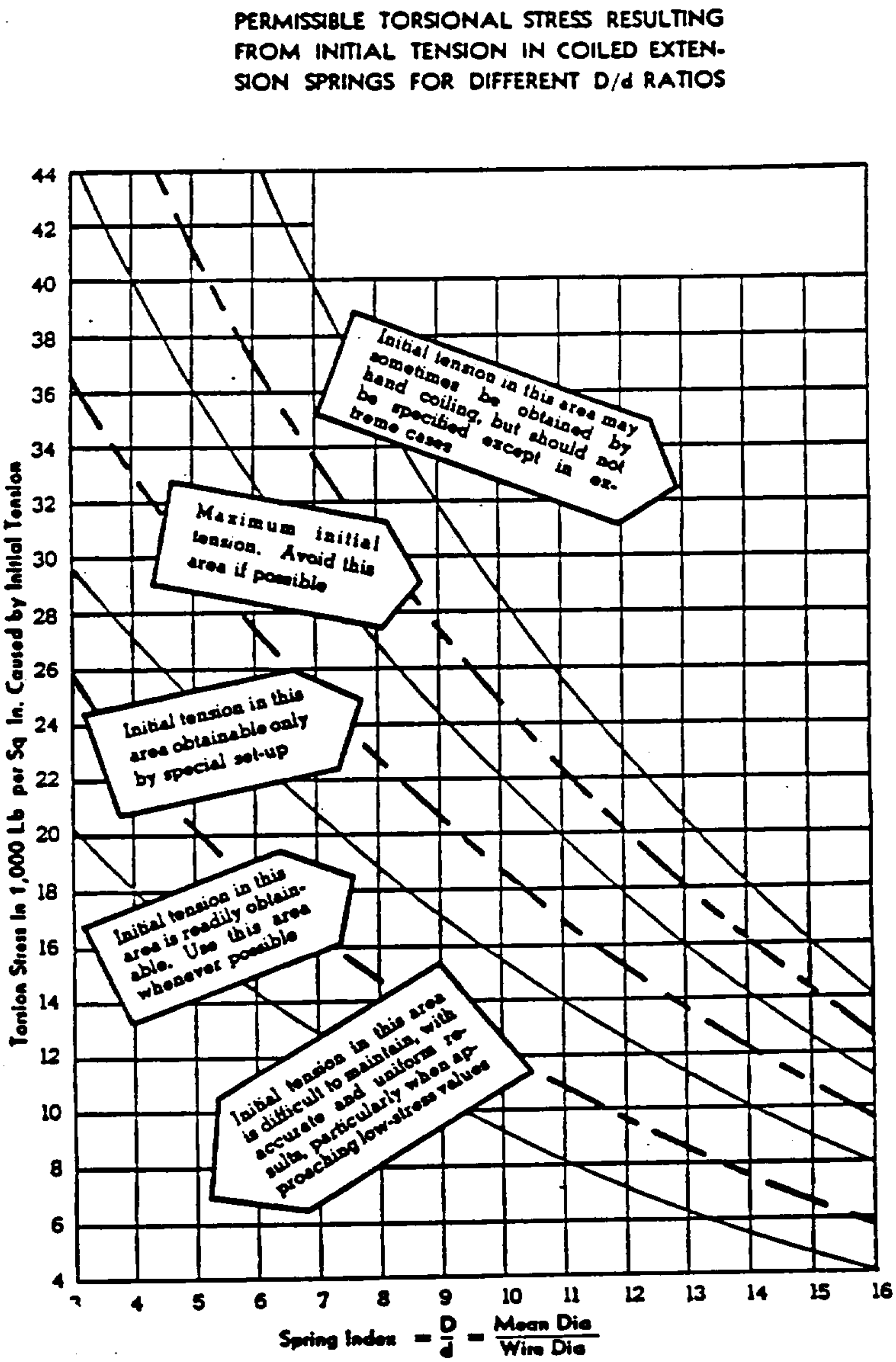
PERMISSIBLE TORSIONAL STRESS RESULTING FROM INITIAL TENSION IN COILED EXTENSION SPRINGS FOR DIFFERENT D/d RATIOS
Initial tension in this area may sometimes be obtained by hand coiling, but should not be specified except in extreme cases
Maximum initial tension. Avoid this area if possible
Initial tension in this area obtainable only by special set-up
Initial tension in this area is readily obtainable. Use this area whenever possible
Initial tension in this area is difficult to maintain, with accurate and uniform results, particularly when approaching low-stress values
Torsion Stress in 1,000 Lb per Sq In. Caused by Initial Tension
44
42
40
38
36
34
32
30
28
26
24
22
20
18
16
14
12
10
8
6
4
3
4
5
6
7
8
9
10
11
12
13
14
15
16
Spring Index $= \frac{D}{d} = \frac{\text{Mean Dia}}{\text{Wire Dia}}$

FIGURE 45

22.5 PRECAUTIONS AND SUGGESTIONS FOR EFFECTIVE DESIGN OF EXTENSION SPRINGS.

(a) Avoid using enlarged, extended, or specially shaped hooks or loops; they may double the cost of the spring and have high stress concentrations.

(b) If a plug must screw into the end of a spring, the spring should be coiled right hand.

(c) Nearly all extension springs are wound with enough initial tension to keep the spring together. Always figure on at least 5 to 10 per cent of the final load as initial tension, unless otherwise specified.

(d) Electroplating does not deposit a good coating on the inside of, or between, the coils of extension springs.

(e) Hooks on extension springs deflect under a load. Each half hook, made by bending one-half of a coil, deflects an amount equivalent to 0.1 of an active coil. Each full hook is equivalent to 0.5 of an active coil. Allowance for this deflection should be considered in design.

(f) If the relative position of the ends is not important note this fact on the drawing.

(g) For standard hooks keep the OD of the hook the same as the OD of the spring, and the distance from the end of the body, or from the last coil, to the inside of the hook about 75 to 85 per cent of the ID of the spring.

(h) The body length or closed portion of an extension spring equals the number of coils in the body plus one, multiplied by the wire diameter.

(i) When deflected $1\frac{1}{4}$ times the maximum deflection as assembled, the total stress should be less than the Minimum Elastic Limit shown by the curves in Figure 62, as modified by their multiplying constants.

22.6 GARTER SPRINGS

22.6.1 General. Close coiled extension springs used in the form of rings by connecting the ends are often used as driving belts, for oil seals and as retainers. The ends may have half or full loops and then be hooked together or one end may be reduced in diameter for three to six coils and screwed into the other end. Connecting the ends with a separate short section, called a connector, is occasionally done.

22.6.2 Formulas. The following formulas for design purposes may be used:

$$\text{Deflection, } F = \pi\,(\text{Shaft Diameter} + \text{OD of spring}) - (\text{FL})$$

$$\text{Rate} = r = \frac{G\,d^4}{8\,N\,D^3}$$

Pressure per inch of circumference on shaft for spring with initial tension, equals

$$2\,\pi r - \frac{2\,\pi\,(\text{ID of Connected Ring})\,r}{\text{Shaft dia}} + \frac{2\,(\text{IT})}{\text{Shaft dia}}$$

(Wherein ID of Connected Ring equals π (FL—OD)

Pressure of each coil on the shaft equals the pressure per inch of circumference on shaft divided by the number of active coils per inch of spring.

22.6.3 Example. A close wound extension spring made from 0.050 in. dia wire, with .40 in. OD, 232 active coils, 3.4 in. inside dia of ring, 25 lb IT, with half hooks joined to form a ring is expanded over a 6 in. dia shaft. What is the pressure per inch of circumference on the shaft?

$$\text{FL} = \pi(3.4 + .40) = 11.95 \text{ in.}$$

$$\text{FL also} = d(\text{TC} + 1) + 2\,(\text{ID}/2)$$

$$= .050\,(232 + 1) + 2\,(.300/2)$$

$$= 11.65 + .30 = 11.95 \text{ in.}$$

$$F = \pi(6 + .40) - 11.95$$

$= 20.10 - 11.95 = 8.15$ in.

$$\text{Rate} = r = \frac{G\ d^4}{8\ N\ D^3} = \frac{11.2 \times 10^6 \times .050^4}{8 \times 232.2 \times .350^3}$$

$= .877$ lb/in.

(.2 coil allowed for deflection of 2 half hooks)

Pressure per inch of circumference on shaft,

$$\text{equals } 2\pi(.877) - \frac{2\pi 3.4 \times .877}{6} + \frac{2 \times 2.5}{6}$$

$= 5.52 - 3.13 + .83 = 3.22$ lb.

23. TORSION SPRINGS

23.1 DESIGN FORMULAS. The stress in helical torsion springs is a bending or tensile stress. The stress caused by a load should be compared with the elastic limit in tension of the material to determine the allowable stress. Comparison should also be made with the curves of allowable stresses (corrected for torsion springs) as shown in Figure 62, Section II, of this Appendix. In Table VII for helical torsion springs two formulas are listed for each property. Either may be used; one is based on load P, the other on deflection F°, and the results should be the same.

23.2 STRESSES IN TORSION SPRING ENDS. Frequently the limiting stress value in helical torsion springs is the stress value in the ends. When a helical torsion spring has an eye as in Figure 46, or bent off the coil as in Figure 47 the stress at the inside of the bend is a tensile stress. The sharp curvature causes the neutral axis to move inward toward the center of the curve and the

TABLE VII. *Formulas for helical torsion springs*

Property	Round wire	Square wire	Rectangular wire *
Torque, lb in. T (also, PR)	$\frac{E\,d^4\,F°}{4{,}000\,N\,D}$	$\frac{E\,d^4\,F°}{2{,}375\,N\,D}$	$\frac{E\,b\,t^3\,F°}{2{,}375\,N\,D}$
	$\frac{S_b\,d^3}{10.2}$	$\frac{S_b\,d^3}{6}$	$\frac{S_b\,b\,t^2}{6}$
Bending stress, psi S_b	$\frac{10.2\,P\,R}{d^3}$	$\frac{6\,P\,R}{d^3}$	$\frac{6\,P\,R}{b\,t^2}$
	$\frac{E\,d\,F°}{392\,N\,D}$	$\frac{E\,d\,F°}{392\,N\,D}$	$\frac{E\,t\,F°}{392\,N\,D}$
Deflection, F°	$\frac{4{,}000\,P\,R\,N\,D}{E\,d^4}$	$\frac{2{,}375\,P\,R\,N\,D}{E\,d^4}$	$\frac{2{,}375\,P\,R\,N\,D}{E\,b\,t^3}$
	$\frac{392\,S_b\,N\,D}{E\,d}$	$\frac{392\,S_b\,N\,D}{E\,d}$	$\frac{392\,S_b\,N\,D}{E\,t}$
Change in moment $T_2 - T_1$	$\frac{F°_2 - F°_1}{\frac{F°}{T}}$	$\frac{F°_2 - F°_1}{\frac{F°}{T}}$	$\frac{F°_2 - F°_1}{\frac{F°}{T}}$
ID after deflection in. ID_1	$\frac{N\,(ID\ free)}{N + \frac{F°}{360}}$	$\frac{N\,(ID\ free)}{N + \frac{F°}{360}}$	$\frac{N\,(ID\ free)}{N + \frac{F°}{360}}$
Rate r_t lb. in./Deg	$\frac{T}{F°}$	$\frac{T}{F°}$	$\frac{T}{F°}$

When a spring has (makes) several complete revolutions, F° = 360° multiplied by the number of revolutions.

* Rectangular wire may be coiled on edge or on flat, but b is always parallel to the axis of the spring and t is always perpendicular to the axis.

ms

tensile stress becomes that of a cantilever loading multiplied by a constant (K). The formula for determining the stress in the bend of the eye in Figure 46 follows:

$$S_b = \frac{32\ P\ R\ K}{\pi\ d^3}$$

Where: K = Curvature Stress Correction Factor Figure 51

R = Mean Radius of Eye in.

$$= \frac{\text{ID of eye} + d}{2}$$

$$= \frac{\text{OD of eye} - d}{2}$$

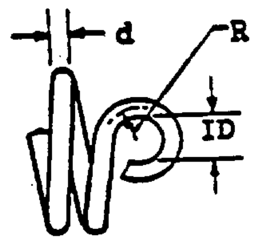

FIGURE 46

For bends off the coil as in Figure 47 the stress value in the bend is:

$$S_b = \frac{32\ P\ l_1\ K}{\pi\ d^3}$$

Where l_1=distance from center of bend to load

K=stress correction factor Figure 51.

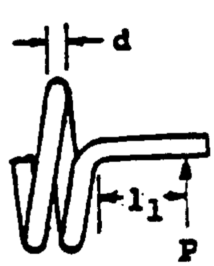

FIGURE 47

For the determination of K from Figure 51 in this instance D = 2 times the inside radius of the bend.

23.3 DEFLECTION OF TORSION SPRING ENDS. When the length of the material in the arms of a helical torsion spring approaches the length of material in one coil, the deflection of the arms will cause the deflection under applied loads to be in error (See Figure 48.) Such ends deflect as a cantilever and may be calculated as such or the formula for spring rate including arms may be used.

The formula for spring rate when the deflection of the arms should be included is:

$$r_t = \frac{Ed^4}{1170\left(L + \frac{l_1}{3} + \frac{l_2}{3}\right)}$$

l_1=Length of arms from the center of the coil to the point of load, in.

l_2=Length of arm from the center of the coil to the point of load, in.

r_t=Spring rate, lb in./degree.

L=Active length of material equals $\pi D N$

In springs with a large number of coils and short arms the deflection of thearms is neglected. However, short arms should be avoided as this causes difficulty in coiling and forming.

23.4 CHANGE IN DIAMETER AND LENGTH. When a helical torsion spring is deflected a reduction in diameter and an increase in length occurs. In order to prevent binding or scuffing, which reduces spring life, sufficient space must be provided when operating over a rod or in a cylinder. The new inside diameter ID_1 in a helical torsion spring due to deflection is obtained by the formula shown in Tabie VII. The shaft diameter should be slightly less than the calculated diameter to prevent binding and distortion in service. The change in length is due to the increase in the number of coils at the deflected position. If a helical torsion

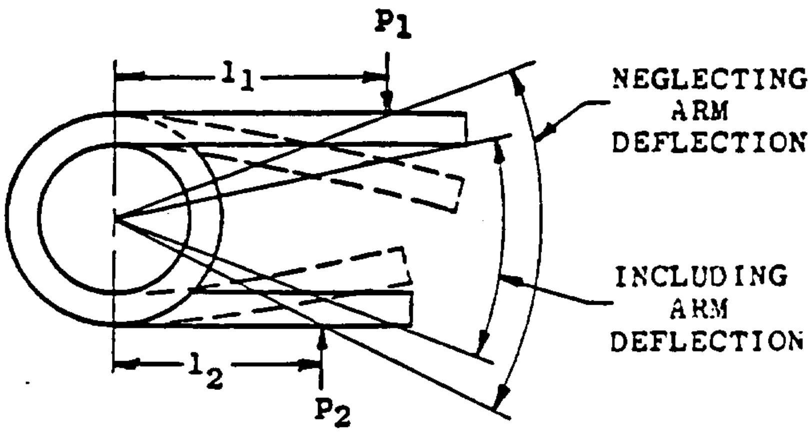

FIGURE 48

spring makes one complete revolution the increase in length is equal to one thickness of wire, plus an allowance for the space between coils, if any.

23.5 HELIX OF TORSION SPRINGS. The hand or direction of coiling (helix) should always be specified for torsion springs. A torsion spring should be so designed that the applied load tends to wind up the spring and increase its length. In springs operating under high stress it is desirable to design the springs with open coils. A slight space of about 1/64 inch or 20 to 25 per cent of the wire diameter will eliminate friction between coils and reduce stress concentration which will lengthen the spring life. When long helical torsion springs are used there exists the possibility of buckling. Since buckling will cause abrasion between coils, erratic loads and early spring failure, it should be avoided. Buckling may be reduced in varying amounts by providing some means of lateral support such as:

1. Mounting the spring over a rod or guide.
2. Mounting the spring in a tube.
3. Clamping the ends.
4. Winding the spring with a small amount of initial tension.

23.6 DESIGN NOMOGRAPHS FOR HELICAL TORSION SPRINGS. The nomographs in Figures 49 through 54 are for general guidance. They are based on a modulus E of 30,000,000 and can be used to reduce the time required to design a helical torsion spring. All results should be checked by the formulas in Table VII.

23.7 MOMENT VS. WIRE SIZE CHART. Table VIII is an aid to quickly determine the torque. (T or PR) that can be applied to a wire diameter at the suggested basic stress listed. For example, what wire diameter is required to support a torque of 10.5 in. lbs? From the table it will be observed that .090 in. diameter music wire or corrosion resisting steel; 0915 in diameter carbon or alloy steel and .125 in. diameter copper and nickel alloys (phosphor-bronze or monel) could be considered. The final determination should be arrived at by formula and evaluation of allowable stresses depending upon type of service. The basic stress indicated is a bending stress S_b caused by a torque T or PR, corrected for curvature.

FIBER STRESS (Not Corrected for Curvature) vs. MOMENT
Torsion Springs

Low Range — Wire Diameter .015" to .150"

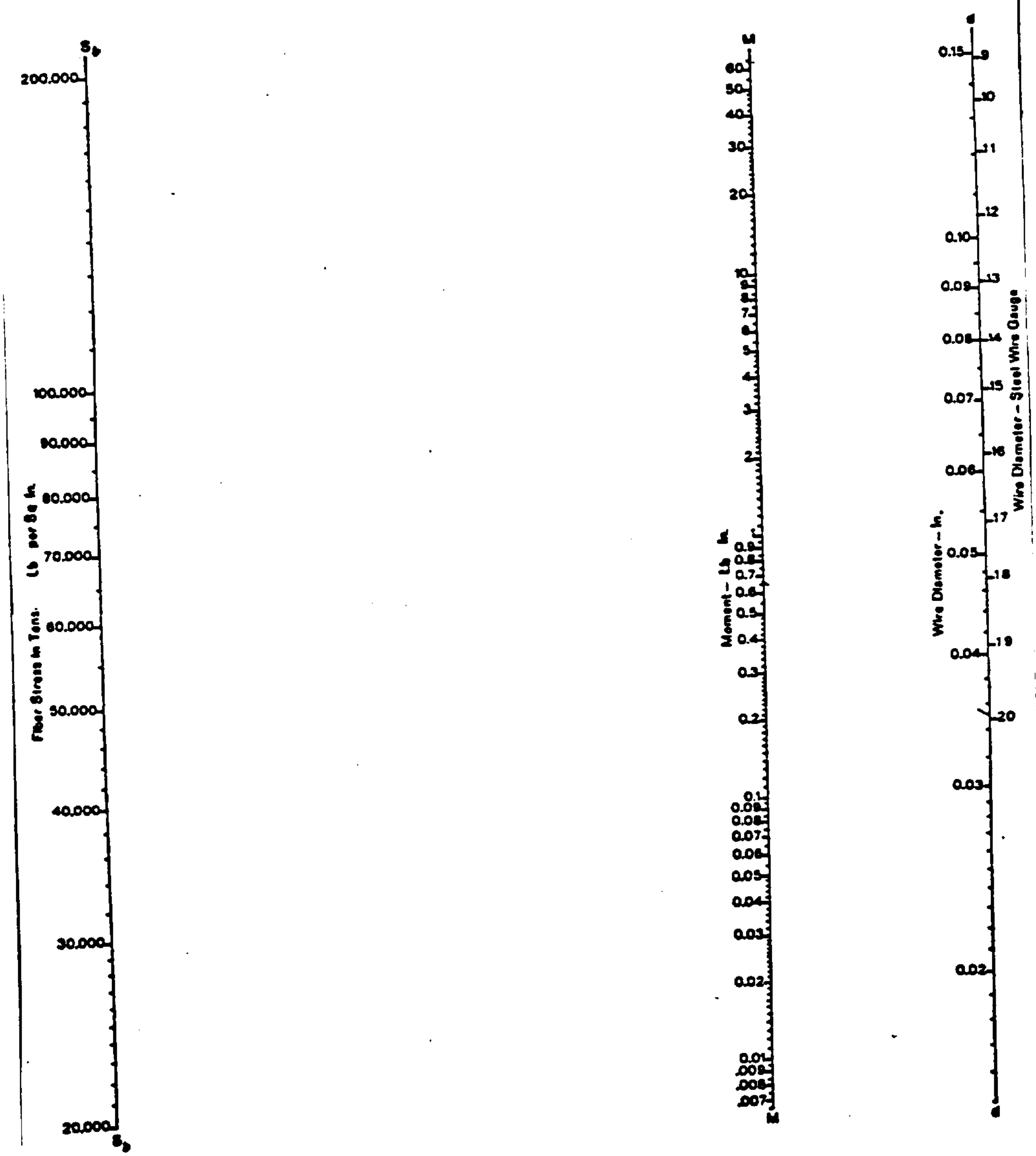

FIGURE 49

FIBER STRESS (Not Corrected for Curvature) vs. MOMENT
Torsion Springs

High Range — Wire Diameter .1" to 1"

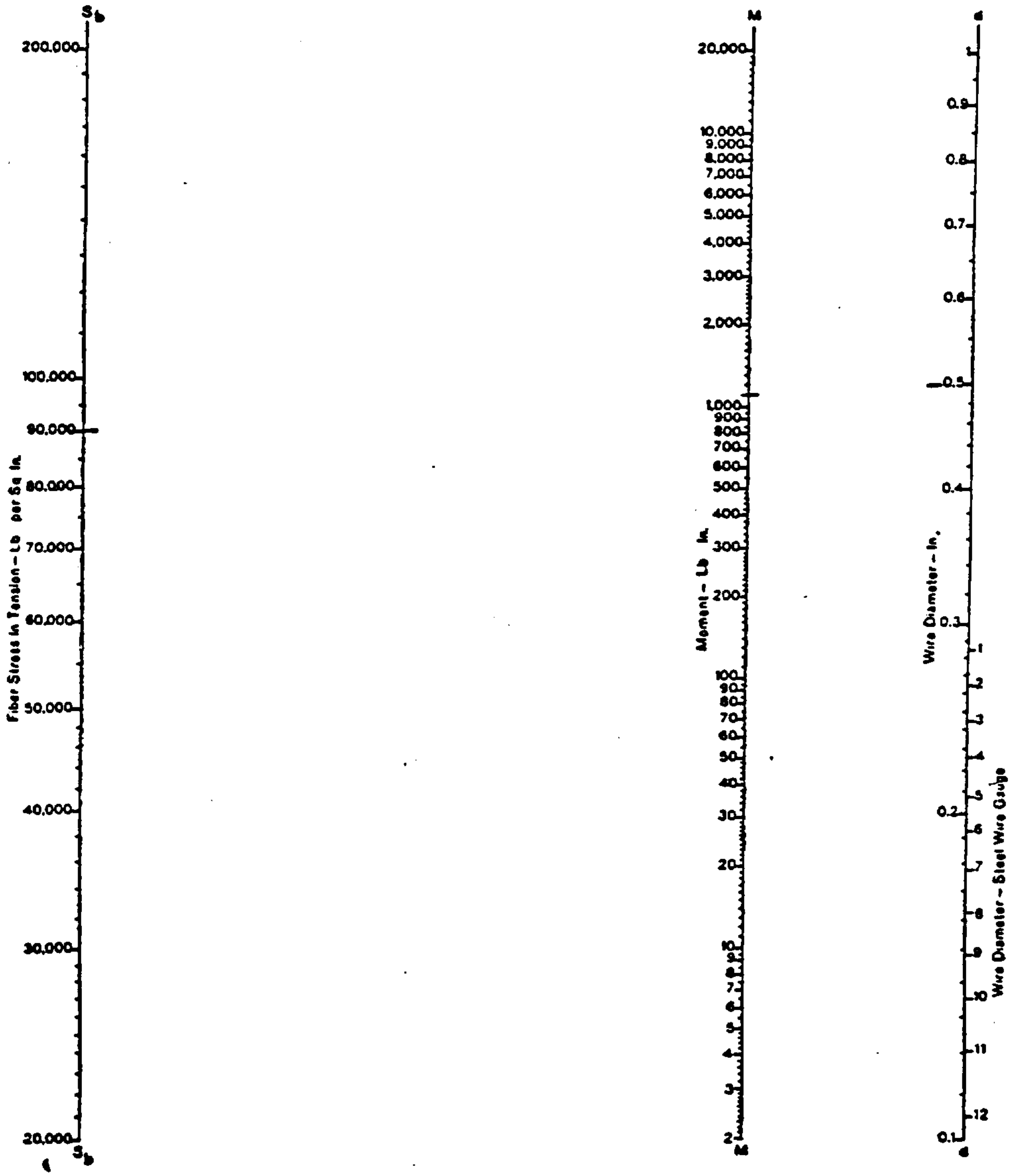

FIGURE 50

FIBER STRESS CORRECTION FOR CURVATURE

Torsion Springs

Find Correction Factor — Using Correction Factor Found on Left Half of Chart — Determine True Fiber Stress

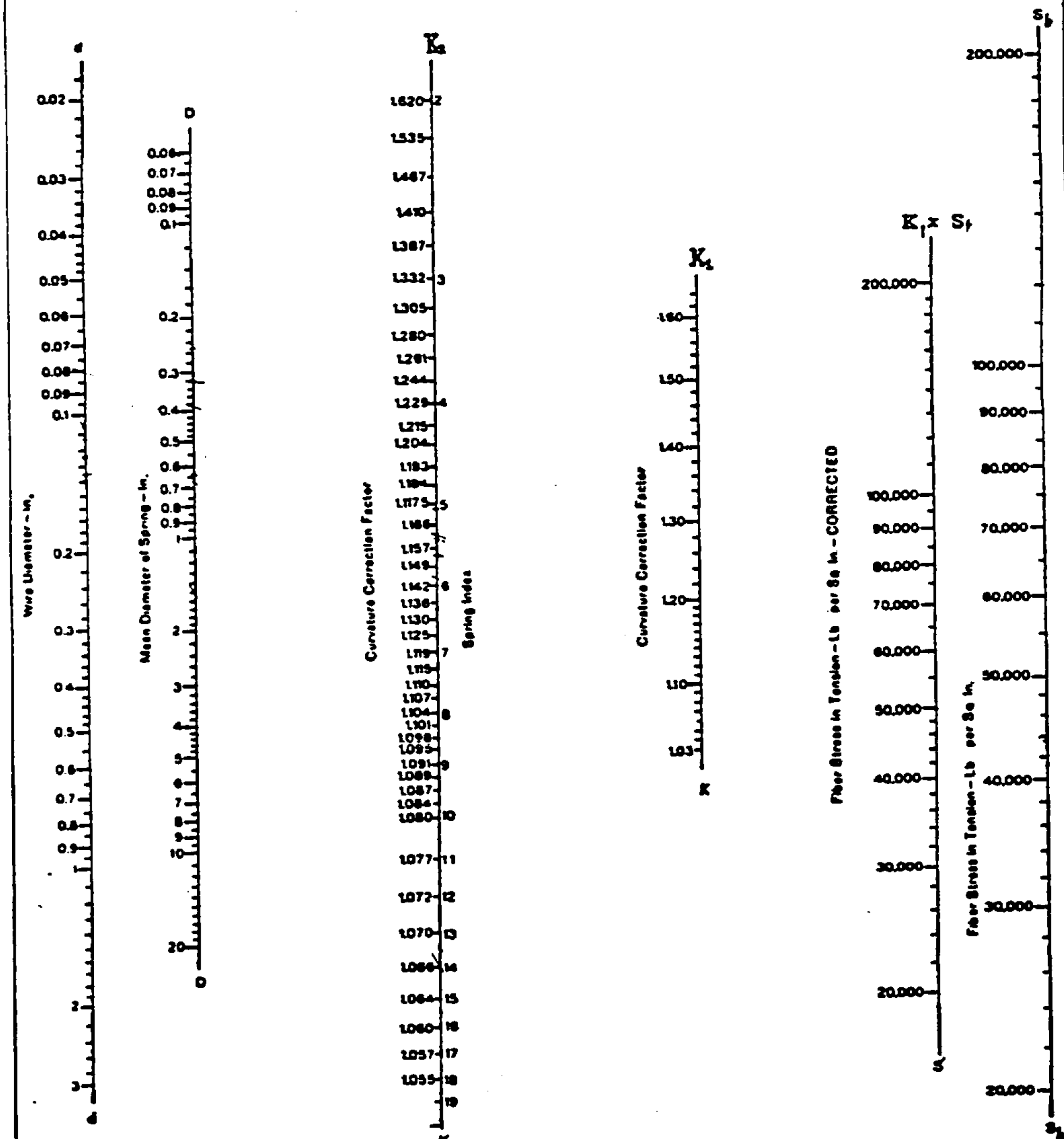

FIGURE 51

TURNS SPRING WILL GIVE PER COIL vs. MOMENT
Torsion Springs

Low Range {Mean Diameter: .1" to 3"
Wire Diameter: .015" to .150"

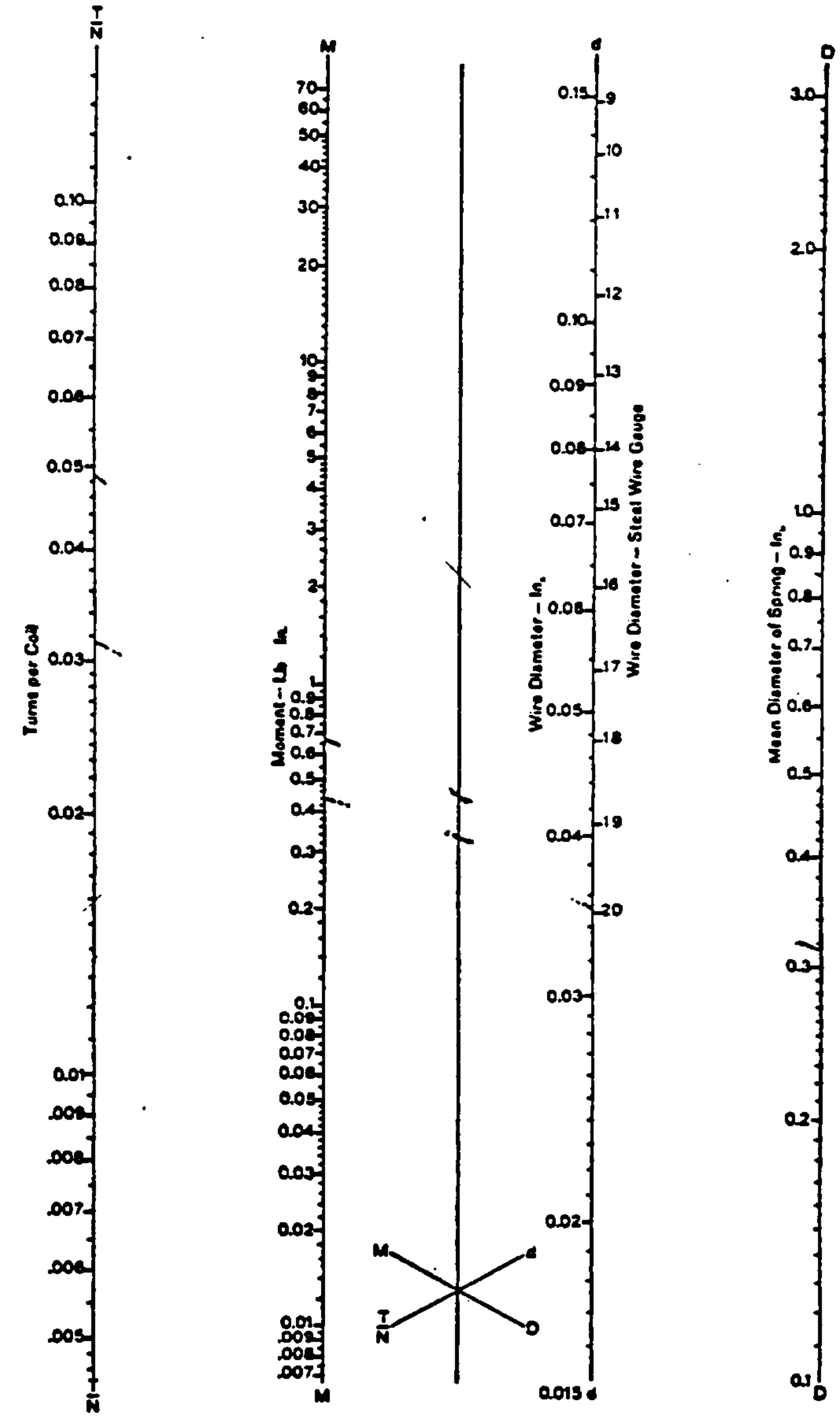

FIGURE 52

TURNS SPRING WILL GIVE PER COIL vs. MOMENT
Torsion Springs

High Range { Mean Diameter: 1" to 10"; Wire Diameter: .1" to 1" }

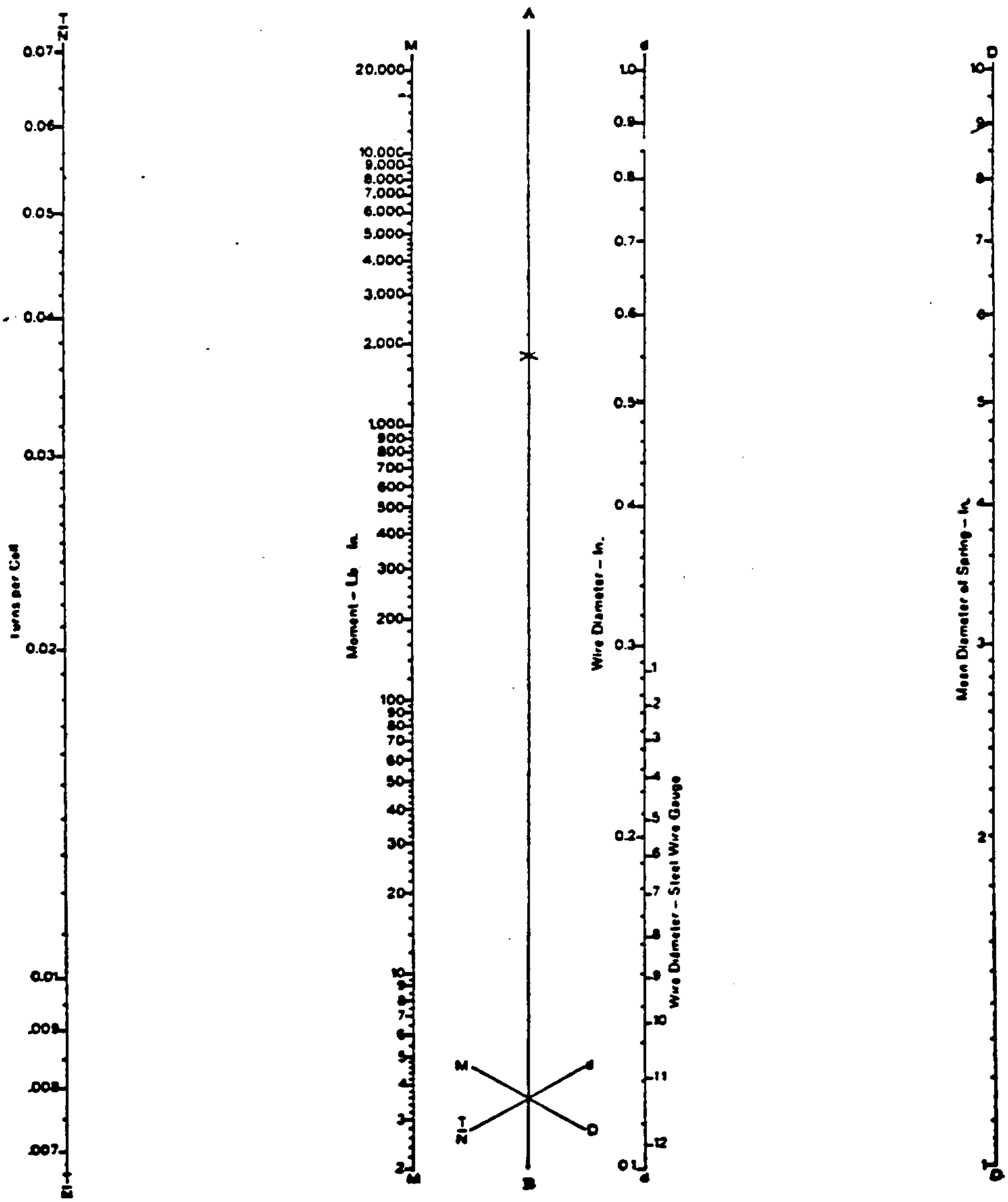

FIGURE 58

TURNS SPRING WILL GIVE PER COIL

Modulus (E) Other Than 30 × 10⁶

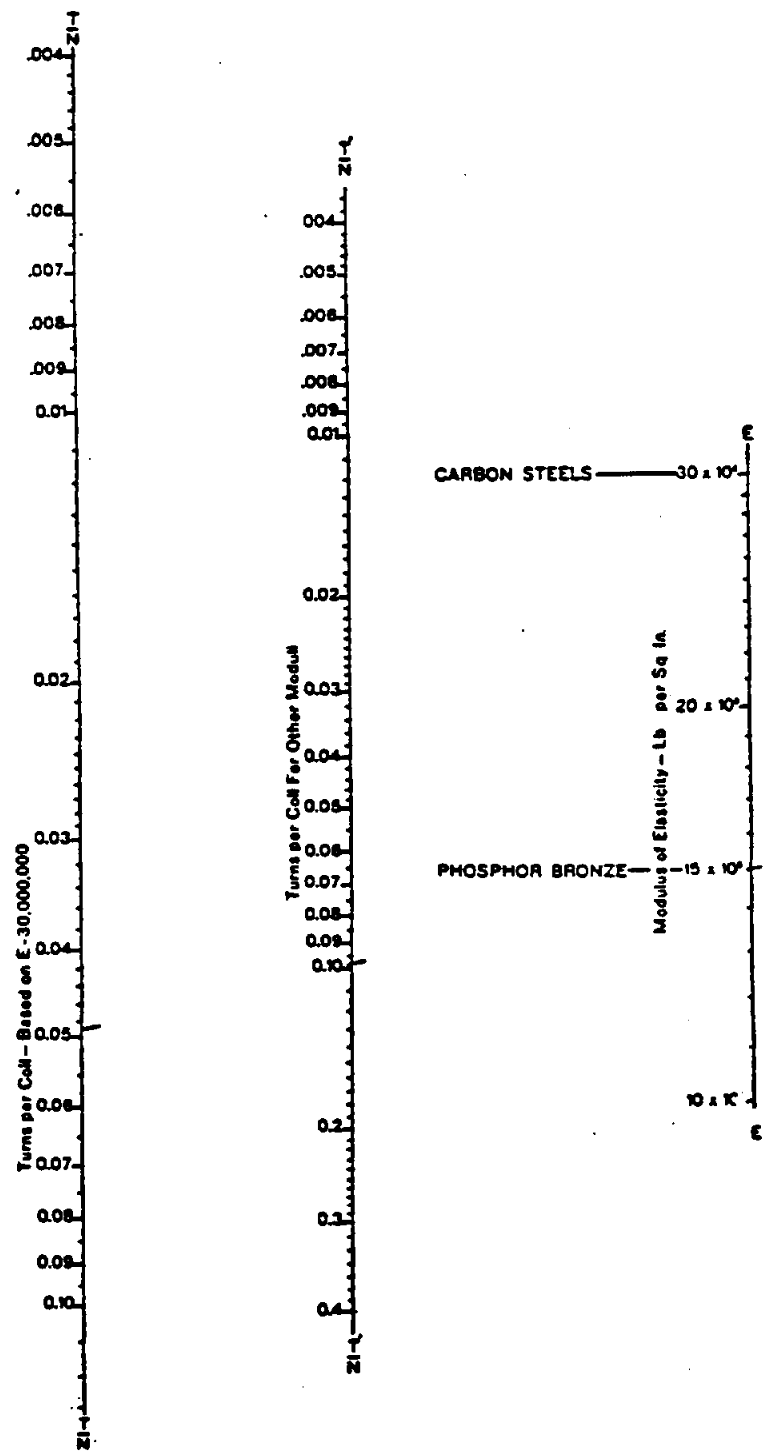

FIGURE 54

TABLE VIII. *Moment vs. wire size chart*

MUSIC WIRE			CARBON & ALLOY STEELS			COPPER & NICKEL ALLOYS		
Corrected Moment lb.-in.	Wire Diam. in.	Basic Stress psi	Corrected Moment lb.-in.	Wire Diam. in.	Basic Stress psi	Corrected Moment lb.-in.	Wire Diam. in.	Basic Stress psi
.0101	.008	201,000	1.013	.041	149,500	.00358	.008	71,200
.0143	.009	200,000	1.555	.0475	148,000	.00509	.009	71,000
.0196	.010	199,500	2.27	.054	146,700	.00694	.010	70,800
.0259	.011	198,500	3.47	.0625	145,000	.00925	.011	70,600
.0337	.012	198,000	5.24	.072	143,000	.0152	.013	70,500
.0425	.013	196,800	7.12	.080	141,500	.0189	.014	70,200
.0527	.014	195,500	10.49	.0915	139,800	.0281	.016	69,800
.0780	.016	194,000	11.21	.0937	139,000	.0398	.018	69,500
.1103	.018	193,000	15.72	.1055	136,600	.0546	.020	69,300
.1505	.020	192,000	23.05	.1205	134,000	.0827	.023	69,100
.199	.022	190,000	25.5	.125	133,000	.1056	.025	69,000
.256	.024	189,000	31.8	.135	131,700	.1635	.029	68,200
.323	.026	187,500	41.4	.1483	129,200	.219	.032	67,900
.443	.029	185,000	48.0	.1562	128,100	.310	.036	67,700
.533	.031	182,000	53.1	.162	127,100	.422	.040	67,200
.638	.033	181,000	68.0	.177	124,800	.598	.045	66,900
.735	.035	179,500	79.8	.1875	123,100	.866	.051	66,500
.886	.037	178,000	85.0	.192	122,400	1.194	.057	65,600
1.030	.039	177,000	104.6	.207	120,200	1.664	.064	64,600
1.185	.041	175,500	116.5	.2187	118,400	2.35	.072	64,100
1.350	.043	173,000	131.0	.2253	117,000	3.17	.080	63,200
1.535	.045	171,500	163	.2437	115,000	4.61	.091	62,300
1.73	.047	170,000	175	.250	114,000	6.43	.102	61,600
1.95	.049	169,000	199	.2625	112,200	8.82	.114	60,600
2.18	.051	167,500	239	.2812	109,600	11.5	.125	59,800
2.70	.055	165,000	301	.3065	106,400	12.2	.128	59,500
3.26	.059	162,000	315	.3125	105,300	17.2	.144	58,500
3.95	.063	161,000	367	.331	103,000	23.9	.162	57,200
4.70	.067	159,300	405	.3437	101,700	33.4	.182	56,200
5.80	.071	157,000	464	.3625	99,000	45.9	.204	55,100
6.29	.075	154,000	506	.375	97,800	63.5	.229	53,800
7.68	.080	153,000	575	.3938	95,800	88.7	.258	52,600
9.04	.085	150,000	623	.4062	94,600	122	.289	51,300
10.56	.090	147,500	753	.4375	91,800	169	.325	50,100
12.30	.095	146,500	898	.4687	88,800	234	.365	48,800
14.35	.100	146,000	1060	.500	86,500	320	.410	47,300
16.98	.106	145,000	1445	.5625	82,700	441	.460	46,200
19.80	.112	143,600	1910	.625	79,800			

NOTE: The values for Music Wire may also be used for Corrosion Resisting Steels.

23.8 HELICAL TORSION SPRING CALCULATION. The stress in a helical torsion spring is normally a bending stress (tension) and, for this reason E is used in the formulas. Tables and nomographs of characteristics for helical torsion springs aid in design. The wire diameter also can be obtained by solving an equation as in the following example.

23.8.1 Example. A torsion spring made of corrosion resisting steel Type FS 302 is required to exert a load of 9 lb at the end of a 2 in. arm of the spring (measuring from the center line of the spring to the point of contact) at 100 degrees of deflection; the ID being 1¼ in. Select a suitable wire diameter for average service and determine the number of coils, body length, etc. (assuming that the stress for average service from Figure 62 for torsion springs may be equal to 120,000 psi max)

Theoretical wire diameter d,

$$d = \sqrt[3]{\frac{10.2\ PR}{S_b}}$$

$$= \sqrt[3]{\frac{10.2 \times 9 \times 2}{120{,}000}}$$

$$= \sqrt[3]{0.0015} = 0.116 \text{ in.}$$

From Table I, select .120 inch diameter wire. Stress at the 9 lb load,

$$S_b = \frac{10.2\ PR}{d^3} = \frac{10.2 \times 9 \times 2}{.120^3}$$

$$= 106{,}300 \text{ psi}$$

From Figure 51, $K_1 = 1.075$ S max.

$$= 106{,}300 \times 1.075 = 114{,}300 \text{ max. psi}$$

Since Figure 62 allows maximum working stress of 123,000 psi (82,000 × 1.5), wire diameter selected is satisfactory.

To determine a safe maximum deflection without permanent set beyond the final position, first find the maximum safe load.

From above we know that 9 lb will stress the material to 114,300 psi

From Figure 62, the minimum elastic limit for compression springs = 102,000 psi. Multiplying this by 1.5 = 153,000 psi, the stress for a safe maximum deflection without permanent set. The load to produce this stress is

$$\frac{9}{X} = \frac{114{,}300}{153{,}000};\ X = \frac{9 \times 153{,}000}{114{,}300}$$

$$= 12.04 \text{ lb (say 12 lb)}$$

$$\text{Since spring rate} = \frac{T}{F^\circ} = \frac{9 \times 2}{100^\circ}$$

..18 lb in./Deg, the additional deflection to produce a load of

$$12 \text{ lb is } \frac{12-9}{.18} = \frac{3.0}{.18}$$

$$= 16.7^\circ$$

Number of active coils,

$$N = \frac{Ed^4 F^\circ}{4{,}000\ PRD}$$

$$= \frac{28{,}000{,}000 \times 0.120^4 \times 100}{4{,}000 \times 9 \times 2 \times 1.370}$$

$$= 5.88 \text{ (say, 6 coils)}$$

Free length over coils,

$$(6 + 1) \times 0.120 = 0.840 \text{ in.}$$

It is usually desirable to coil torsion springs with a slight space between the coils equal to about 20 to 25 per cent of the wire diameter. Assuming 20 per cent, the space equals 0.20 × 0.120 = 0.024 in. Six coils would have 6 spaces and equals 6 × 0.024 = 0.144 in.

The free length over coils would equal 0.840 + 0.144 = 0.984 in. (say, 1.0 in.)

The ID of the spring reduces slightly due to deflection. After maximum deflection without permanent set has taken place,

$$ID_1 = \frac{N\,(\text{ID free})}{N + \dfrac{F^\circ}{360}} = \frac{6 \times 1.25}{6 + 115/360}$$

$$= \frac{7.50}{6 + 0.32} = 1.18 \text{ in.}$$

The shaft over which such a spring is fitted should, therefore, be less than 1.18 in. A shaft $1\frac{5}{32}$ in. diameter would be satisfactory.

The letters P (lb load) and R (moment arm) may be replaced by T where T equals the torque in inch pounds. In this example, T would equal 9 × 2 + 18 in. lb.

Specifying loads in inch-pounds torque (T) or as pounds times the lever arm P×R gives the same results; either method may be used.

23.9 PRECAUTIONS AND SUGGESTIONS FOR EFFECTIVE DESIGN OF HELICAL TORSION SPRINGS.

(a) Always try to support a torsion spring by a rod running through the center of the spring. Torsion springs unsupported or held by clamps or lugs alone are unsteady, will buckle, and cause additional stresses in the wire.

(b) Torsion springs should be designed and installed so that the deflection increases the number of coils. This increase should be allowed for in the design of space requirements.

(c) The inside diameter reduces during deflection and should be computed to determine the clearance over the supporting rod.

(d) Use as few bends in the ends as possible. They are often formed in separate operations, are expensive, and cause concentrations of stress and frequent breakage.

(e) Consider tolerances on diameters when determining clearances over rods.

(f) Always specify the direction of coiling as either right-hand or left-hand on drawings. Right-hand coiling follows the same direction as standard bolt and screw threads.

(g) Springs may be closely or loosely wound, but they should not be wound tightly except when frictional resistance between the coils is desired.

(h) Avoid using double-torsion springs. Two single-torsion springs, one coiled left-hand and the other right-hand, usually can perform the same action as a double-torsion spring, at less than half the cost.

(i) When deflected $1\frac{1}{4}$ times the maximum deflection as assembled, the total stress should be less than the Minimum Elastic Limit shown by the curves in Figure 62, as modified by their multiplying constants.

24. SPIRAL TORSION SPRINGS

24.1 GENERAL. A spiral torsion spring delivers torque at its inner end to the shaft on which it is mounted and to the part on which its outer end is fastened.

24.2 STRESS. The stress is in bending and should be compared with the elastic limit in tension of the material to determine the allowable stress. The recommended allowable stress for thickness under .060 inch is 175,000 psi and for heavier sizes 150,000 psi for commercial spring steels. Lower stresses will increase fatigue life.

TABLE IX. *Formulas for spiral torsion springs of rectangular section*

Property	Formula
Bending Stress, psi S_b	$S_b = \frac{6PR}{bt^2}$
	$S_b = \frac{EtF^\circ}{114.6L}$
Torque, in. lb T	$T = P \times R$
	$T = \frac{S_b b t^2}{6}$
Active Length, in. L	$L = \frac{EtF^\circ}{114.6 S_b}$
	$L = \frac{\pi E U t}{S_b}$
Deflection F°	$F^\circ = \frac{114.6 S_b L}{Et}$
Rate r_t in. lbs/Deg	$\frac{T}{F^\circ}$

TABLE X. *Torque for 1 in. wide spiral torsion springs stressed at 100,000 psi (Other widths directly by proportion)*

t in.	T in. lbs	t in.	T in. lbs	t in.	T in. lbs	t in.	T in. lbs
.008	1.07	.025	10.4	.063	66.2	.105	182
.010	1.66	.032	17.1	.072	86.5	.125	260
.015	3.75	.041	28.1	.080	107.0	.156	410
.020	6.68	.054	48.7	.092	141.0	.188	538

24.3 ENDS. A variety of end shapes can be used. Inner ends usually are bent to fit in a slot. Outer ends usually are formed to fit over a bolt or pin.

25. CONSTANT FORCE SPRINGS

25.1 GENERAL. These springs have an appearance similar to clock or motor springs but are wound so that a constant force P causes a continuous unwinding of the coils. The springs are made from a strip of flat spring material which has been given a curvature by continuous heavy forming so that in its relaxed condition it is in the form of a tightly wound spiral. In Figure 56 the outer end has been extended by a constant force P and each incremental part of the straightened portion L has been deflected from its natural curvature in passing through the working zone X. The force P at any extension is determined only by the work required to straighten the material in zone X from its natural curvature in its coiled condition. The constant force giving a zero rate or gradient can be changed during manufacture to make springs with a slightly altered rate; thereby producing springs with a small negative, positive or changing rate if desired, but the zero rate has the broadest practical application possibilities. Such springs should have widths equal to 5 to 200 times (250 max) their thickness to have good stability, (100 times thickness is often used). They are not generally used in elevated temperatures over 140°F. Most applications are for the extension type, but these springs also may be used as motor springs to turn rollers at a constant torque.

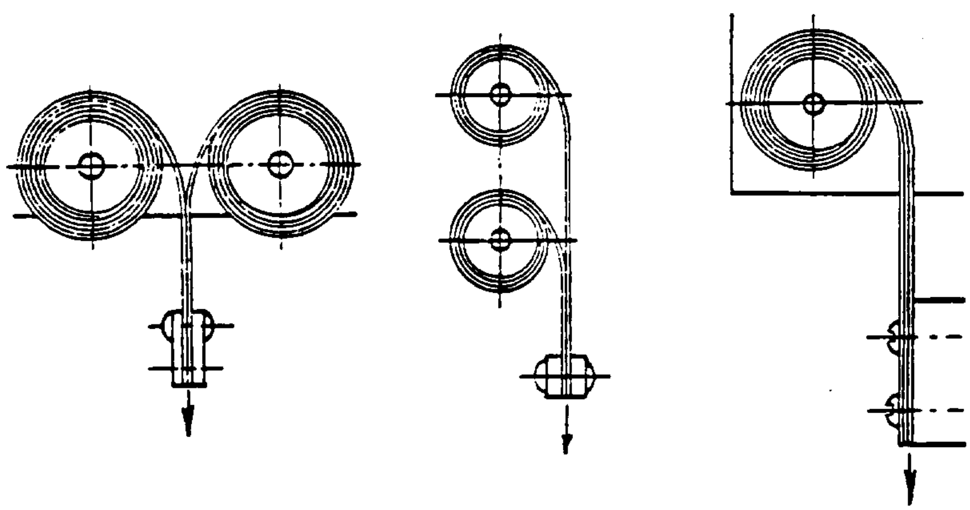

BACK TO BACK MOUNTING　　TANDEM MOUNTING　　LAMINAR MOUNTING

FIGURE 55

25.2 MATERIALS. The two most generally used spring materials and method of specifying them on drawings follow: STEEL, SPRING, TEMPERED, BLUE, SAE 1095, NO. 1 EDGE, HARDNESS RANGE Rc 48 to 51 and STEEL, CORROSION RESISTING AISI 302 ¾ HARD. Other materials are used if essential to design requirements. In specifying the length any additional material for forming special loops or straight portions should be added to the length determined by the formulas. If in a formula for thickness t, the result derived is an odd size such as .0096 inch, the next standard larger thickness such as .010 inch should be used.

25.3 INNER ENDS. Normally the inner end of a constant force extension spring is held to the roller by its natural gripping action, when about 1½ turns of material remain on the roller at full deflection. No other fastening is required, except where there is some tendency for the material to be wound onto the roller in improper alignment or if danger of overtravel exists. In such cases the inner end may be bent and inserted into a slot in the roller, or retained by a small upset hook, or held by a small screw. Inner ends held by screws should be recessed and applied in a manner to prevent the screw head from deforming the natural curvature of the spring. Flanges on rollers also aid in guiding the flow of the material onto the rollers.

25.4 OUTER ENDS. Outer ends usually have round or pear shaped holes to fit over a screw. These ends may be left square, rounded or trimmed to suit. The ends also may be annealed and bent to form a loop and then riveted, for mounting over pins. The outer ends normally follow the regular curvature of the spring diameter, but they may, if desired, be manufactured with a preformed straight end to facilitate attachment.

25.5 MULTIPLE MOUNTING. Two springs

TABLE XI. *Stress factor S_f for varying fatigue life*

Material	Fatigue life					
	Up to 5,000	10,000	13,000	20,000	25,000	100,000 to 1,000,000
High carbon steel SAE 1095	.020	.0155	.014	.012	.010	.009
Corrosion resisting steels	.024	.019	.017	.015	.012	.009

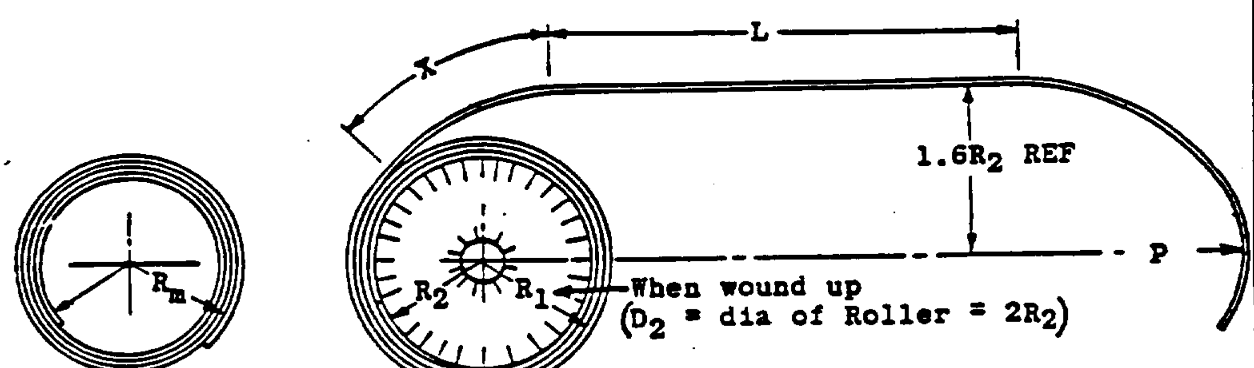

FREE POSITION
UNMOUNTED

OPERATING POSITION
MOUNTED ON ROLLER

FIGURE 56

may be mounted back to back, each on its own roller, and thus double the load. Two springs also may be mounted in tandem, one above the other, to double the load. Two or more springs can also be mounted on the same roller (laminar mounting) to obtain multiple loads, see Figure 55.

25.6 STRESS FACTOR. When designing constant force springs, a stress factor, S_f, based on fatigue life, endurance limit, and actual tests, is used in place of the customary stress formulas because of the combination of stresses occurring in this type of spring. Values of S_f, determined for certain materials and fatigue life are given in Table XI. Intermediate values may be interpolated.

25.7 EXTENSION TYPE. The most commonly used is the extension type and the spring is supplied in a coil. It must then be rewound onto a roller which should be about 20 per cent larger in diameter than the inside diameter of the spring. An extension spring of this type is shown in Figure 56.

25.8 FORMULAS. The following formulas may be used to compute approximate proportions of the spring:

$$bt = \frac{26.4\ p}{E\ S_f^2}$$

10 Revolutions or Less

$$R_n = \sqrt{\frac{E\ b\ t^3}{26.4\ p}}$$

$$R_2 = 1.20\ R_n$$

Over 10 Revolutions

$$R_m = \sqrt{\frac{E\ b\ t^3}{26.4\ p}}$$

$$R_n = \frac{R_m}{1.20}$$

$$R_2 = 1.20\ R_m$$

$$L = F + 10\ R_2 \quad \text{or} \quad L = F + 5\ D_2$$

The following formula may be used to compute the adjusted load P which the spring will exert based on the proportions established by the formulas above:

$$P = \frac{E\ b\ t^3}{26.4}\left[\frac{1}{R_n^2} - \left(\frac{1}{R_n} - \frac{1}{R_1}\right)^2\right]$$

The abbreviations in 20.1.3 are used plus the following:

R_n = natural radius of curvature in inches (minimum) in the free position = ID/2.

R_m = natural radius of curvature in inches (minimum) in the free position = ½ (OD — 2t).

R_1 = radius of outer coil in inches when mounted. It is the expanded radius of curvature due to material build up = ½ (OD — 2t) where OD equals the roller diameter plus allowance for the number of coils used.

R_2 = radius of roller over which spring is mounted.

D_2 = Diameter of roller = 2 R_2.

25.9 SIMPLIFIED DESIGN. The design of extension type constant force springs can be simplified by replacing the modulus of elasticity E, and other terms by a varying factor Q. The values of Q have been worked out for springs having 10 coils or less and the simplified formula for load P follows:

$$P = Q\ b\ t$$

TABLE XII. *Factor Q for varying fatigue life*

Material	Fatigue life								
	2,500	4,000	5,000	10,000	15,000	20,000	25,000	100,000	1,000,000
High carbon steel SAE 1095	----	521	417.5	270.5	----	169	123	101.2	81.3
Corrosion resisting steels	660	----	502	----	316	233	151	86.9	69.4

CONSTANT FORCE SPRING DESIGN CHART HIGH CARBON STEELS

CHART A — FATIGUE LIFE 4,000 CYCLES MINIMUM

Q=521

t	2R	D_o	1/8	3/16	1/4	5/16	3/8	1/2	5/8	3/4	1	1 1/4	1 1/2	2	2 1/2	3	4
		b →	LOAD P														
.002	.174	.201	.130	.195	.260	.325	.390										
.003	.261	.313	.195	.292	.390	.487	.585	.780	.975								
.004	.348	.418		.390	.520	.650	.780	1.04	1.30	1.56	2.08						
.005	.435	.523			.650	.813	.975	1.30	1.63	1.95	2.60						
.006	.522	.627			.780	.975	1.17	1.56	1.95	2.34	3.12	3.90					
.007	.609	.730				1.14	1.36	1.82	2.28	2.73	3.64	4.55	5.46				
.008	.696	.835					1.56	2.08	2.60	3.12	4.16	5.20	6.24				
.010	.870	1.04					1.95	2.60	3.25	3.90	5.20	6.50	7.80	10.4			
.012	1.04	1.25						3.12	3.90	4.68	6.24	7.80	9.36	12.5			
.014	1.22	1.46							4.55	5.46	7.28	9.10	10.9	14.6	18.2		
.015	1.31	1.57								5.85	7.80	9.75	11.7	15.6	19.5	23.4	
.016	1.39	1.67									8.32	10.4	12.5	16.6	20.8	25.0	
.018	1.57	1.88									9.36	11.7	14.0	18.7	23.4	28.1	
.020	1.74	2.09									10.4	13.0	15.6	20.8	26.0	31.2	41.6
.022	1.91	2.29										14.3	17.2	22.9	28.6	34.3	45.8
.025	2.18	2.62											19.5	26.0	32.5	39.0	52.0
.028	2.43	2.92											21.8	29.1	36.4	43.7	58.2
.032	2.78	3.34												33.3	41.6	49.9	66.5

CHART B — FATIGUE LIFE 5,000 CYCLES MINIMUM

Q=417.5

t	2R	D_o	1/8	3/16	1/4	5/16	3/8	1/2	5/8	3/4	1	1 1/4	1 1/2	2	2 1/2	3	4
		b →	LOAD P														
.002	.200	.240	.104	.156	.208	.260	.312										
.003	.300	.360	.156	.234	.312	.390	.469	.625	.782								
.004	.400	.480		.312	.415	.520	.623	.830	1.04	1.25	1.66						
.005	.500	.600			.520	.650	.780	1.04	1.30	1.56	2.08						
.006	.600	.720			.623	.780	.935	1.25	1.56	1.87	2.50	3.12					
.007	.700	.840				.910	1.09	1.46	1.82	2.18	2.91	3.64	4.37				
.008	.800	.960					1.25	1.67	2.08	2.50	3.33	4.16	5.00				
.010	1.00	1.20					1.56	2.08	2.60	3.12	4.16	5.20	6.24	8.32			
.012	1.20	1.44						2.50	3.12	3.74	5.00	6.24	7.49	9.99			
.014	1.40	1.68							3.64	4.36	5.82	7.28	8.72	11.6	14.5		
.015	1.50	1.80								4.68	6.24	7.80	9.35	12.5	15.6	18.7	
.016	1.60	1.92									6.66	8.32	9.99	13.3	16.6	20.0	
.018	1.80	2.16									7.50	9.36	11.2	15.0	18.7	22.4	
.020	2.00	2.40									8.32	10.4	12.5	16.6	20.8	24.9	33.3
.022	2.20	2.64										11.4	13.7	18.3	22.9	27.4	36.6
.025	2.50	3.00											15.6	20.8	26.0	31.2	41.6
.028	2.80	3.36											17.5	23.3	29.0	34.8	46.4
.032	3.20	3.84												26.6	33.2	39.7	53.2

CHART C — FATIGUE LIFE 10,000 CYCLES MINIMUM

Q=270.5

t	2R	D_o	1/8	3/16	1/4	5/16	3/8	1/2	5/8	3/4	1	1 1/4	1 1/2	2	2 1/2	3	4
		b →	LOAD P														
.002	.260	.312	.0675	.101	.135	.169	.202										
.003	.390	.468	.101	.152	.202	.253	.304	.405	.506								
.004	.520	.625		.202	.270	.337	.405	.539	.675	.809	1.08						
.005	.649	.779			.337	.422	.506	.675	.843	1.01	1.35						
.006	.779	.935			.405	.506	.607	.809	1.01	1.21	1.62	2.02					
.007	.910	1.09				.592	.708	.945	1.17	1.42	1.89	2.36	2.84				
.008	1.04	1.25					.810	1.08	1.35	1.62	2.16	2.70	3.24				
.010	1.30	1.56					1.01	1.35	1.69	2.02	2.70	3.37	4.05	5.40			
.012	1.56	1.87						1.62	2.02	2.43	3.24	4.05	4.85	6.48			
.014	1.82	2.19							2.37	2.84	3.78	4.73	5.67	7.56	9.45		
.015	1.95	2.34								3.04	4.05	5.05	6.06	8.10	10.1	12.1	
.016	2.08	2.50									4.32	5.39	6.48	8.64	10.8	12.9	
.018	2.34	2.81									4.86	6.06	7.28	9.70	12.1	14.5	
.020	2.60	3.12									5.40	6.75	8.10	10.8	13.5	16.2	21.6
.022	2.85	3.42										7.40	8.93	11.9	14.8	17.8	23.7
.025	3.25	3.90											10.1	13.5	16.9	20.2	27.0
.028	3.64	4.36											11.3	15.1	18.9	22.7	30.2
.032	4.15	4.98												17.3	22.2	26.7	35.6

CHART D — FATIGUE LIFE 20,000 CYCLES MINIMUM

Q=169

t	2R	D_o	1/8	3/16	1/4	5/16	3/8	1/2	5/8	3/4	1	1 1/4	1 1/2	2	2 1/2	3	4
		b →	LOAD P														
.002	.336	.403	.0420	.0630	.0840	.105	.126										
.003	.504	.605	.0630	.0945	.126	.158	.189	.252	.315								
.004	.672	.805		.126	.168	.211	.252	.336	.420	.504	.672						
.005	.840	1.01			.211	.264	.316	.420	.525	.630	.840						
.006	1.01	1.21			.252	.316	.378	.504	.630	.756	1.01	1.26					
.007	1.18	1.42				.367	.441	.589	.735	.883	1.18	1.47	1.76				
.008	1.34	1.61					.504	.673	.840	1.01	1.34	1.68	2.02				
.010	1.68	2.01					.631	.841	1.05	1.26	1.68	2.10	2.52	3.36			
.012	2.02	2.42						1.01	1.26	1.51	2.02	2.52	3.02	4.03			
.014	2.35	2.82							1.47	1.76	2.35	2.94	3.53	4.70	5.88		
.015	2.52	3.02								1.89	2.52	3.15	3.78	5.04	6.30	7.56	
.016	2.69	3.23									2.69	3.36	4.03	5.37	6.72	8.06	
.018	3.02	3.62									3.02	3.78	4.54	6.05	7.56	9.07	
.020	3.36	3.97									3.36	4.20	5.04	6.72	8.40	10.1	13.4
.022	3.70	4.44										4.62	5.54	7.39	9.24	11.1	14.8
.025	4.20	5.04											6.30	8.40	10.5	12.6	16.8
.028	4.71	5.64											7.05	9.41	11.8	14.1	18.8
.032	5.37	6.44												10.8	13.4	16.1	21.5

FIGURE 57

CONSTANT FORCE SPRING DESIGN CHART HIGH CARBON STEELS

CHART E — FATIGUE LIFE 35,000 CYCLES MINIMUM (Q=123)

t	2Rn	Dn \ b→	1/8	3/16	1/4	5/16	3/8	1/2	5/8	3/4	1	1 1/4	1 1/2	2	2 1/2	3	4
			LOAD P														
.002	.400	.480	.0308	.0462	.0614	.0769	.0923										
.003	.600	.720	.0462	.0693	.0923	.115	.138	.185	.231								
.004	.800	.960		.0924	.123	.154	.185	.246	.307	.369	.493						
.005	1.00	1.20			.154	.192	.231	.308	.384	.461	.616						
.006	1.20	1.44			.184	.231	.277	.369	.461	.554	.738	.923					
.007	1.40	1.68				.269	.323	.431	.538	.646	.862	1.07	1.29				
.008	1.60	1.92					.369	.492	.615	.738	.984	1.23	1.48				
.010	2.00	2.40					.461	.615	.769	.923	1.23	1.54	1.85	2.46			
.012	2.40	2.88						.739	.923	1.11	1.48	1.84	2.21	2.95			
.014	2.80	3.36							1.07	1.29	1.72	2.15	2.58	3.44	4.31		
.015	3.00	3.60								1.38	1.85	2.31	2.77	3.69	4.61	5.54	
.016	3.20	3.84									1.97	2.46	2.95	3.94	4.92	5.90	
.018	3.60	4.32									2.22	2.77	3.32	4.43	5.54	6.64	
.020	4.00	4.80									2.46	3.08	3.69	4.92	6.15	7.38	9.84
.022	4.40	5.28										3.38	4.06	5.41	6.77	8.12	10.8
.025	5.00	6.00											4.61	6.15	7.69	9.23	12.3
.028	5.60	6.72											5.19	6.89	8.61	10.3	13.8
.032	6.40	7.68												7.38	9.84	11.8	15.7

CHART F — FATIGUE LIFE 100,000 CYCLES MINIMUM (Q=101.2)

t	2Rn	Dn \ b→	1/8	3/16	1/4	5/16	3/8	1/2	5/8	3/4	1	1 1/4	1 1/2	2	2 1/2	3	4
			LOAD P														
.002	.444	.533	.0253	.0379	.0505	.0632	.0758										
.003	.667	.800	.0379	.0568	.0758	.0947	.114	.152	.189								
.004	.889	1.07		.0758	.101	.126	.152	.202	.253	.303	.404						
.005	1.11	1.33			.126	.158	.189	.253	.316	.379	.505						
.006	1.33	1.60			.152	.189	.227	.303	.379	.455	.606	.758					
.007	1.56	1.87				.221	.265	.354	.442	.530	.707	.884	1.06				
.008	1.78	2.14					.303	.404	.505	.606	.808	1.01	1.21				
.010	2.22	2.66					.379	.505	.631	.758	1.01	1.26	1.52	2.02			
.012	2.67	3.20						.606	.758	.909	1.21	1.52	1.82	2.42			
.014	3.11	3.73							.884	1.06	1.41	1.77	2.12	2.83	3.54		
.015	3.33	4.00								1.14	1.51	1.89	2.27	3.03	3.79	4.55	
.016	3.56	4.27									1.62	2.02	2.42	3.23	4.04	4.85	
.018	4.00	4.80									1.82	2.27	2.73	3.64	4.55	5.45	
.020	4.44	5.33									2.02	2.53	3.03	4.04	5.05	6.07	8.06
.022	4.89	5.87										2.78	3.33	4.44	5.56	6.67	8.89
.025	5.56	6.67											3.79	5.05	6.31	7.58	10.1
.028	6.22	7.46											4.24	5.73	7.07	8.48	11.3
.032	7.11	8.53												6.54	8.08	9.70	12.9

CHART G — FATIGUE LIFE 1,000,000 CYCLES MINIMUM (Q=81.3)

t	2Rn	Dn \ b→	1/8	3/16	1/4	5/16	3/8	1/2	5/8	3/4	1	1 1/4	1 1/2	2	2 1/2	3	4
			LOAD P														
.002	.500	.600	.0203	.0305	.0407	.0508	.0610										
.003	.750	.900	.0305	.0457	.0610	.0762	.0914	.122	.152								
.004	1.00	1.20		.0610	.0815	.102	.122	.163	.203	.244	.326						
.005	1.25	1.50			.102	.127	.152	.203	.254	.305	.407						
.006	1.50	1.80			.122	.152	.183	.244	.305	.366	.488	.609					
.007	1.75	2.10				.178	.213	.285	.356	.427	.569	.711	.854				
.008	2.00	2.40					.244	.325	.406	.488	.650	.812	.975				
.010	2.50	3.00					.305	.407	.508	.610	.813	1.02	1.22	1.63			
.012	3.00	3.60						.488	.610	.732	.976	1.22	1.46	1.95			
.014	3.50	4.20							.711	.854	1.14	1.42	1.71	2.28	2.84		
.015	3.75	4.50								.915	1.22	1.52	1.83	2.43	3.04	3.65	
.016	4.00	4.80									1.30	1.63	1.95	2.60	3.25	3.90	
.018	4.50	5.40									1.46	1.83	2.19	2.93	3.65	4.39	
.020	5.00	6.00									1.63	2.03	2.44	3.25	4.06	4.88	6.50
.022	5.50	6.60										2.24	2.68	3.58	4.47	5.37	7.15
.025	6.25	7.50											3.05	4.07	5.08	6.10	8.13
.028	7.00	8.40											3.41	4.55	5.68	6.83	9.11
.032	8.00	9.60												5.20	6.50	7.80	10.4

FIGURE 58

CONSTANT FORCE SPRING
DESIGN CHART
CORROSION RESISTANT STEEL

CHART H — FATIGUE LIFE 2,500 CYCLES MINIMUM

LOAD P (b →)

t	2Rn	Dn	1/8	3/16	1/4	5/16	3/8	1/2	5/8	3/4	1	1 1/4	1 1/2	2	2 1/2	3	4
.002	.145	.121	.164	.246	.329	.411	.492										
.003	.218	.261	.247	.370	.494	.616	.740	.900	1.32								
.004	.291	.349		.493	.650	.822	.986	1.33	1.66	1.97	2.62						
.005	.363	.436			.821	1.03	1.23	1.64	2.05	2.46	3.28						
.006	.436	.523			.986	1.23	1.48	1.97	2.47	2.96	3.95	4.94					
.008	.581	.697					1.97	2.63	3.29	3.95	5.26	6.58	7.90				
.010	.727	.873					2.46	3.30	4.12	4.95	6.60	8.25	9.90	13.2			
.012	.873	1.05						3.96	4.95	5.94	7.92	9.90	11.9	15.8			
.014	1.02	1.22							5.77	6.93	9.24	11.5	13.9	18.5	23.1		
.016	1.16	1.40							6.60	7.92	10.6	13.2	15.8	21.1	26.4	31.7	
.018	1.31	1.57							7.44	8.89	11.9	14.9	17.8	23.8	29.7	35.6	
.020	1.46	1.75							8.25	9.90	13.2	16.5	19.8	26.4	33.0	39.6	52.8
.022																	
.025	1.82	2.18									16.5	20.6	24.8	33.0	41.2	49.5	66.0
.028																	
.031	2.26	2.71												40.9	51.1	61.3	81.0

Q=660

CHART J — FATIGUE LIFE 5,000 CYCLES MINIMUM

t	2Rn	Dn	1/8	3/16	1/4	5/16	3/8	1/2	5/8	3/4	1	1 1/4	1 1/2	2	2 1/2	3	4
.002	.171	.205	.126	.189	.253	.315	.379										
.003	.257	.308	.189	.283	.377	.473	.567	.757	.946								
.004	.343	.411		.379	.505	.630	.757	1.01	1.26	1.51	2.01						
.005	.428	.513			.632	.791	.941	1.26	1.57	1.88	2.52						
.006	.514	.617			.757	.945	1.13	1.51	1.89	2.27	3.02	3.78					
.008	.684	.821					1.51	2.01	2.51	3.02	4.02	5.04	6.04				
.010	.855	1.03					1.89	2.51	3.14	3.77	5.02	6.28	7.53	10.0			
.012	1.03	1.23						3.01	3.77	4.52	6.03	7.53	9.04	12.1			
.014	1.20	1.44							4.39	5.27	7.03	8.79	10.5	14.1	17.6		
.016	1.37	1.64							5.01	6.03	8.04	10.0	12.1	16.1	20.1	24.1	
.018	1.54	1.85							5.65	6.80	9.04	11.3	13.6	18.1	22.6	27.1	
.020	1.71	2.05							6.28	7.53	10.0	12.6	15.1	20.1	25.1	30.1	40.2
.022																	
.025	2.14	2.56									12.6	15.7	18.8	25.1	31.4	37.7	50.2
.028																	
.031	2.65	3.18												31.1	38.9	46.7	62.4

Q=502

CHART K — FATIGUE LIFE 13,000 CYCLES MINIMUM

t	2Rn	Dn	1/8	3/16	1/4	5/16	3/8	1/2	5/8	3/4	1	1 1/4	1 1/2	2	2 1/2	3	4
.002	.222	.267	.079	.119	.158	.198	.237										
.003	.333	.400	.119	.178	.237	.296	.356	.474	.593								
.004	.444	.533		.236	.316	.395	.474	.632	.790	.948	1.26						
.005	.555	.665			.395	.494	.592	.790	.988	1.19	1.58						
.006	.666	.798			.474	.593	.711	.948	1.19	1.42	1.90	2.37					
.008	.888	1.06					.948	1.26	1.58	1.90	2.53	3.16	3.79				
.010	1.11	1.33					1.19	1.58	1.98	2.37	3.16	3.95	4.74	6.33			
.012	1.33	1.59						1.90	2.37	2.84	3.79	4.74	5.69	7.58	9.48		
.015	1.66	1.99								3.56	4.74	5.93	7.11	9.48	11.7	14.2	
.018	2.00	2.40									5.69	7.11	8.53	11.4	14.2	17.1	
.020	2.22	2.65									6.32	7.90	9.48	12.6	15.8	19.0	25.3
.022	2.42	2.91										8.69	10.4	13.9	17.4	20.9	27.8
.025	2.78	3.33											11.9	15.8	19.8	23.7	31.6
.028	3.11	3.73												17.7	22.1	26.5	35.4
.031	3.44	4.12												19.6	24.5	29.4	39.2

Q=316

CHART L — FATIGUE LIFE 20,000 CYCLES MINIMUM

LOAD P (b →)

t	2Rn	Dn	1/8	3/16	1/4	5/16	3/8	1/2	5/8	3/4	1	1 1/4	1 1/2	2	2 1/2	3	4
.002	.263	.316	.0585	.0874	.117	.145	.174										
.003	.395	.474	.0874	.131	.175	.218	.262	.350	.437								
.004	.526	.631		.175	.233	.291	.350	.466	.582	.699	.932						
.005	.658	.787			.291	.364	.437	.583	.728	.874	1.17						
.006	.789	.947			.350	.437	.524	.699	.874	1.05	1.40	1.75					
.008	1.05	1.26					.699	.932	1.16	1.40	1.86	2.33	2.80				
.010	1.32	1.58					.874	1.17	1.46	1.75	2.33	2.91	3.50	4.66			
.012	1.58	1.90						1.40	1.75	2.10	2.80	3.50	4.19	5.59	6.99		
.015	1.98	2.37								2.62	3.50	4.37	5.24	6.99	8.74	10.5	
.018	2.37	2.84									4.19	5.33	6.29	8.39	10.5	12.6	
.020	2.63	3.16									4.66	5.83	6.99	9.32	11.7	14.0	18.6
.022	2.89	3.47										6.41	7.69	10.3	12.8	15.4	20.5
.025	3.30	3.96											8.74	11.7	14.6	17.5	23.3
.028	3.68	4.42												13.0	16.3	19.6	26.1
.031	4.08	4.89												14.4	18.1	21.7	28.9

Q=233

FIGURE 59

CONSTANT FORCE SPRING DESIGN CHART
CORROSION RESISTANT STEEL

CHART M — FATIGUE LIFE 35,000 CYCLES MINIMUM

t	$2R_n$	D_o \ b →	1/8	3/16	1/4	5/16	3/8	1/2	5/8	3/4	1	1¼	1½	2	2½	3	4
			LOAD P														
.002	.331	.397	.0380	.0570	.0760	.0950	.114										
.003	.496	.595	.0570	.0855	.114	.143	.171	.228	.285								
.004	.662	.794		.114	.152	.190	.228	.304	.380	.456	.608						
.005	.827	.992			.190	.238	.285	.380	.475	.570	.760						
.006	.993	1.19			.228	.285	.342	.456	.570	.684	.912	1.14					
.008	1.32	1.58					.456	.608	.760	.912	1.22	1.52	1.82				
.010	1.65	1.98					.570	.760	.950	1.14	1.52	1.90	2.28	3.04			
.012	1.98	2.38						.912	1.14	1.37	1.82	2.28	2.74	3.65	4.56		
.015	2.48	2.98								1.71	2.28	2.85	3.42	4.56	5.70	6.84	
.018	2.98	3.58									2.74	3.42	4.10	5.47	6.84	8.21	
.020	3.31	3.97									3.04	3.80	4.56	6.08	7.60	9.12	12.2
.022	3.64	4.37										4.18	5.02	6.69	8.36	10.0	13.4
.025	4.14	4.97											5.70	7.60	9.50	11.4	15.2
.028	4.63	5.56												8.51	10.6	12.8	17.0
.031	5.03	6.04												9.42	11.8	14.1	18.9

Q=151

CHART N — FATIGUE LIFE 100,000 CYCLES MINIMUM

t	$2R_n$	D_o \ b →	1/8	3/16	1/4	5/16	3/8	1/2	5/8	3/4	1	1¼	1½	2	2½	3	4
			LOAD P														
.002	.445	.534	.0217	.0326	.0435	.0543	.0652										
.003	.666	.800	.0326	.0489	.0652	.0815	.0978	.130	.163								
.004	.890	1.07		.0652	.0869	.109	.130	.174	.217	.261	.348						
.005	1.11	1.33			.109	.136	.163	.217	.272	.326	.435						
.006	1.33	1.57			.130	.163	.196	.261	.326	.391	.521	.652					
.008	1.78	2.14					.261	.348	.434	.521	.695	.869	1.04				
.010	2.22	2.66					.326	.435	.543	.652	.869	1.09	1.30	1.74			
.012	2.67	3.20						.522	.652	.782	1.04	1.30	1.56	2.09	2.61		
.015	3.33	4.00								.978	1.30	1.63	1.96	2.61	3.26	3.91	
.018	4.00	4.80									1.56	1.95	2.35	3.13	3.91	4.69	
.020	4.44	5.33									1.74	2.17	2.61	3.48	4.35	5.21	6.95
.022	4.89	5.87										2.39	2.87	3.82	4.78	5.74	7.65
.025	5.55	6.66											3.26	4.35	5.43	6.52	8.69
.028	6.23	7.46												4.87	6.08	7.30	9.73
.031	6.90	8.28												5.39	6.74	8.08	10.8

Q=86.9

CHART P — FATIGUE LIFE 1,000,000 CYCLES MINIMUM

t	$2R_n$	D_o \ b →	1/8	3/16	1/4	5/16	3/8	1/2	5/8	3/4	1	1¼	1½	2	2½	3	4
			LOAD P														
.002	.500	.600	.0174	.0260	.0347	.0434	.0521										
.003	.750	.900	.0260	.0390	.0521	.0651	.0781	.104	.130								
.004	1.00	1.20		.0520	.0694	.0868	.104	.139	.174	.208	.278						
.005	1.25	1.50			.0868	.108	.130	.174	.217	.260	.347						
.006	1.50	1.80			.104	.130	.156	.208	.260	.312	.416	.52					
.008	2.00	2.40					.208	.278	.347	.416	.555	.694	.833				
.010	2.50	3.00					.260	.347	.434	.521	.694	.868	1.04	1.39			
.012	3.00	3.60						.416	.521	.625	.833	1.04	1.25	1.67	2.08		
.015	3.75	4.50								.781	1.04	1.30	1.56	2.08	2.60	3.12	
.018	4.50	5.40									1.25	1.56	1.87	2.50	3.12	3.75	
.020	5.00	6.00									1.39	1.74	2.08	2.78	3.47	4.16	5.55
.022	5.50	6.60										1.91	2.29	3.05	3.81	4.58	6.11
.025	6.25	7.50											2.60	3.47	4.34	5.21	6.94
.028	7.00	8.40												3.89	4.86	5.83	7.77
.031	7.75	9.30												4.30	5.38	6.45	8.61

Q=69.4

FIGURE 60

In using the simplified formula, b and t ratios can be estimated. For length L the regular formulas apply. See Figures 57 to 60 as these values apply and were determined from the simplified formula with values of Q as shown in Table XII.

25.10 TABLES OF SPRING CHARACTERISTICS (DESIGN CHARTS) FOR EXTENSION TYPE CONSTANT FORCE SPRINGS. As as aid to the selection of constant force springs, combinations of width b, thickness t, natural radius of curvature R_n, roller diameter D_2 (20 per cent larger than ID of spring). for high carbon spring steel SAE 1095 and corrosion resisting steels are shown in Figuers 57 to 60. Lengths should be determined by the regular formula $L = F + 10\ R_2$ or $L = F + 5\ D_2$.

25.11 EXAMPLE. If a high carbon steel extension type constant force spring is required to deflect 24 inches, have a fatigue life of 4000 cycles and exert a load P of 10.4 pounds, it could be made, as shown in Figure 57 Chart A, with a width b of 1 inch, thickness t of .020 inch, provided that the roller diameter D_2 equals 2.09 inches and the inside diameter

FORMULAS FOR FLAT SPRINGS
(Based upon standard beam formulas where the deflection is small)

TABLE XIII

PROPERTY	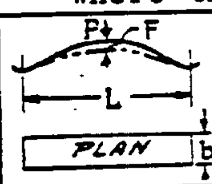	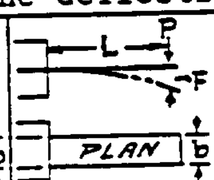	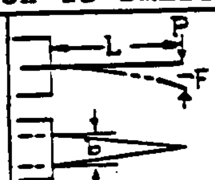	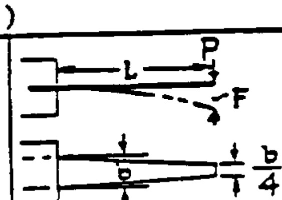
Deflection F Inches	$\frac{P\ L^3}{4\ E\ b\ t^3}$	$\frac{4\ P\ L^3}{E\ b\ t^3}$	$\frac{6\ P\ L^3}{E\ b\ t^3}$	$\frac{5.22\ P\ L^3}{E\ b\ t^3}$
	$\frac{S_b\ L^2}{6\ E\ t}$	$\frac{2\ S_b\ L^2}{3\ E\ t}$	$\frac{S_b\ L^2}{E\ t}$	$\frac{.87\ S_b\ L^2}{E\ t}$
Load P Pounds	$\frac{2\ S_b\ b\ t^2}{3\ L}$	$\frac{S_b\ b\ t^2}{6\ L}$	$\frac{S_b\ b\ t^2}{6\ L}$	$\frac{S_b\ b\ t^2}{6\ L}$
	$\frac{4\ E\ b\ t^3\ F}{L^3}$	$\frac{E\ b\ t^3\ F}{4\ L^3}$	$\frac{E\ b\ t^3\ F}{6\ L^3}$	$\frac{E\ b\ t^3\ F}{5.22\ L^3}$
Stress S_b Bending psi	$\frac{3\ P\ L}{2\ b\ t^2}$	$\frac{6\ P\ L}{b\ t^2}$	$\frac{6\ P\ L}{b\ t^2}$.	$\frac{6\ P\ L}{b\ t^2}$
	$\frac{6\ E\ t\ F}{L^2}$	$\frac{3\ E\ t\ F}{2\ L^2}$	$\frac{E\ t\ F}{L^2}$	$\frac{E\ t\ F}{.87\ L^2}$
Thickness t Inches	$\frac{S_b\ L^2}{6\ E\ F}$	$\frac{2\ S_b\ L^2}{3\ E\ F}$	$\frac{S_b\ L^2}{E\ F}$	$\frac{.87\ S_b\ L^2}{E\ F}$
	$\sqrt[3]{\frac{P\ L^3}{4\ E\ b\ F}}$	$\sqrt[3]{\frac{4\ P\ L^3}{E\ b\ F}}$	$\sqrt[3]{\frac{6\ P\ L^3}{E\ b\ F}}$	$\sqrt[3]{\frac{5.22\ P\ L^3}{E\ b\ F}}$

of the spring in the free position equals 1.74 inches.

The length L required for 24 inches of deflection F. is obtained from the formula $L = F + 5 D_2$ and equals: 24 + 5 (2.09) = 34.45 inches (say 34½ in.).

To adjust an available load P in the charts to some other desired load P^1, select from the chart a value of P just greater than P^1 and determine R_n^1 by the following formula: (holding b and t constant).

$$R_n^1 = R_n \sqrt{\frac{P}{P^1}}$$

26. FLAT SPRINGS

26.1 GENERAL. Load requirements are intimately connected with spring dimensioning and the space available for the spring. The point of load application, deflection, length, width, and thickness should be clearly specified. Formulas in the following table may be used to determine various flat spring characteristics.

26.2 STRESS. The stress is in bending and should be compared with the elastic limit in tension of the material to determine the allowable stress. The recommended allowable stress for thickness under .060 inch is 175,000 psi and for heavier sizes 150.000 psi for commercial spring steels. Lower stresses will increase fatigue life.

27. CONED DISC (BELLEVILLE) SPRINGS

27.1 GENERAL. The coned disc (Belleville) spring or washer is a plain dished washer of a particular diameter, sectional profile, and height suited for an intended purpose. It is used in a variety of applications, all having

STRESS AND DEFLECTION CONSTANTS FOR BELLEVILLE WASHERS OF UNIFORM THICKNESS

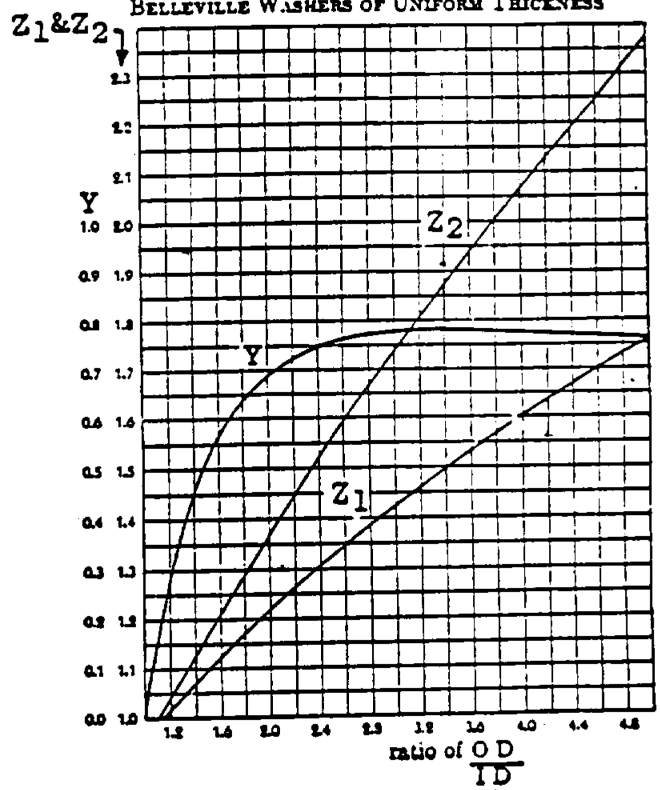

FIGURE 61

the common characteristic of necessity for short range of motion and attendant high loads.

The primary disk parameters are identified in the cross-section shown below.

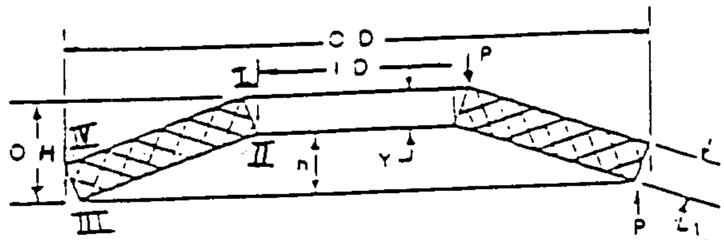

Fig. 1

Nomenclature

O.D. = Maximum outside dia. (upper surface)
I.D = Minimum inside dia. (bottom surface)
h = Conical disc height (cone height)
O.H. = Overall height = Y + h ≅ t + h
t = Actual thickness of disc
t^1 = Reduced thickness of disk associated with Load Bearing Flats
μ = poisson's ratio (.3 for steel)
E = Young's modulus (30,000000 for steel)
F = Deflection of disc
a = Ratio of diameters (O.D./I.D.)
P = Load in lbs. at a given deflection
P_f = Load in Lbs. at Flat Deflection

S_b = Design bending stress ($S_b = -S_I$), (always compressive)

S_I = Stress at cotner I
S_{II} = Stress at corner II
S_{III} = Stress at corner III
S_{IV} = Stress at corner IV

27.1.1

Load Deflection Characteristics.

The load deflection characteristics of a belleville disk can be tailored from nearly linear to strongly degressive. This is accomplished by varying the disk parameter h/t. The resulting load deflection characteristics are shown in figure-2

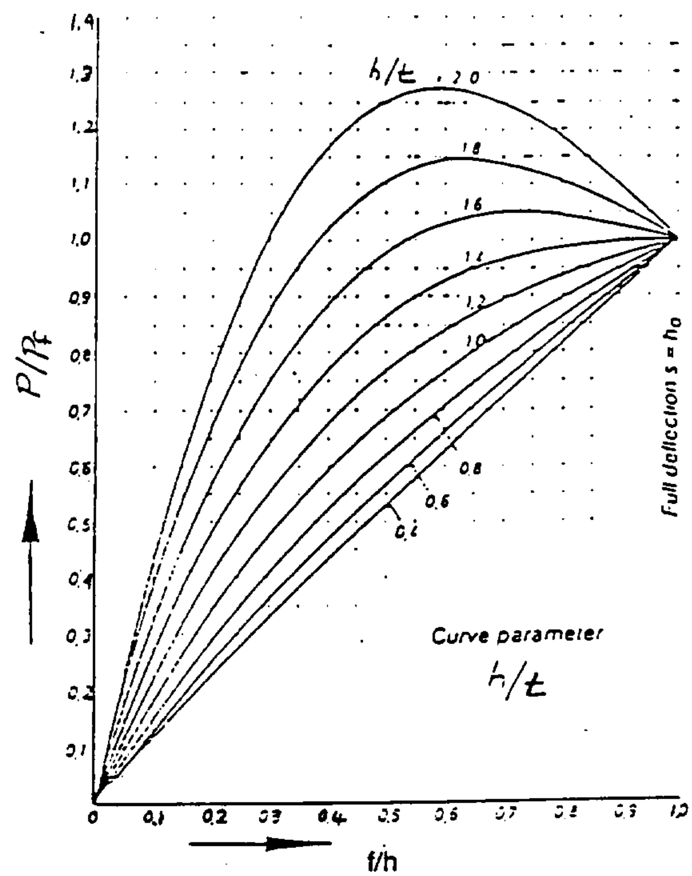

Figure-2

27.1.2

Design Formulas

By obtaining the value for constant (Y) from the proper curve, the following formula can be used to calculate the load-deflection characteristics:

$$P = \frac{Ef}{(1-\mu^2)\ Y\ a^2}\left[\left(h-\frac{f}{2}\right)(h-f)\,t + t^3\right]$$

where a = one half the outside diameter, in
h = free height minus thickness, in
f = deflected position, in

By obtaining the values for constants Z_1 and Z_2 from the proper curves, the following formula can be used to calculate stress

$$S_b = \frac{Ef}{(1-\mu^2)\ Y\ a^2}\left[Z_1\left(h-\frac{f}{2}\right) + Z_2 t\right]$$

It is possible for the term (h-f/2) to become negative if f is large. When this occurs, the terms inside the bracket should be changed to read Z_1 (h-f/2)-Z_2t. This means, in this instance, the maximum stress is a tensile stress. For a spring life of less than one-half million (500,000) cycles, a stress of 200,000 psi can be substituted for S_b, even though this limit might be slightly beyond the elastic limit of the steel. This is because the stress is calculated at the point of greatest intensity, which is on an extremely small part of the disc. Immediately surrounding this area is a much lower stressed portion which so supports the higher stressed point that very little yielding results at atmospheric temperatures. For higher than a atmospheric temperatures and long spring life, lower stresses must be employed.

Stresses at the 4 individual corners can be calculated using the following formulas. (Ref. figure 1)

$$S_I = -S_B$$

$$S_{II} = \frac{Ef}{(1-\mu^2)\ Y\ a^2}\left[-Z_1\left(h-\frac{f}{2}\right) + Z_2 t\right]$$

$$S_{III} = \frac{ID}{OD}\,\frac{Ef}{(1-\mu^2)\ Y\ a^2}\left[(2Z_2 - Z_1)\left(h-\frac{f}{2}\right) + Z_2 t\right]$$

$$S_{IV} = \frac{I.D.}{O.D.}\,\frac{Ef}{(1-\mu^2)\ Y\ a^2}\left[(2Z_2 - Z_1)\left(h-\frac{f}{2}\right) - Z_2 t\right]$$

27.1.3

Load Bearing Surfaces

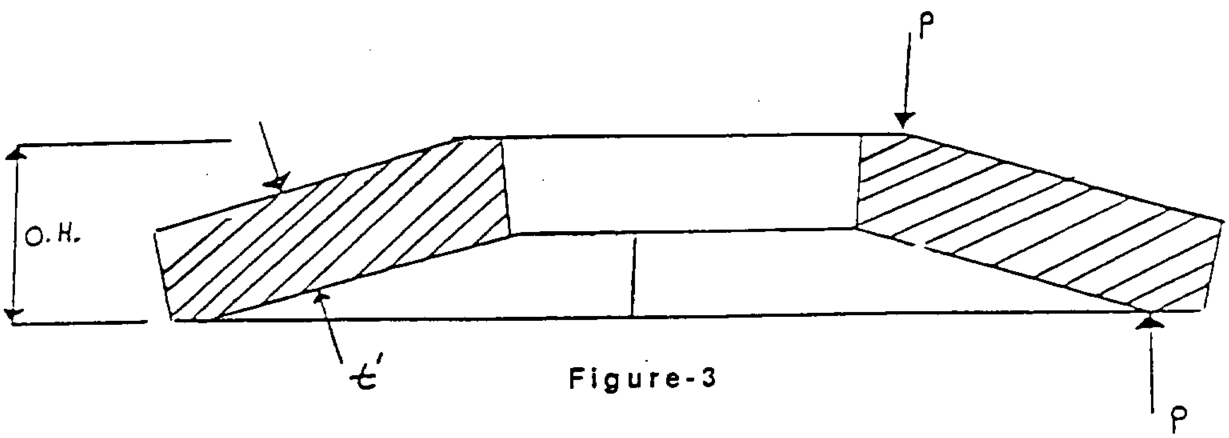

Figure-3

The use of load surfaces causes the load bearing points to displace toward each other. This displacement results in an increase force at equal displacement. In order to generate an equivilent load deflection curve as a disk without bearing surfaces, the thickness of the disk must be reduced to (t'). A resonable load bearing width occurs when the reduced material thickness (t') is about 0.94t.

The standard load and stress equations must be modified by the introduction of a coefficient (ε). The transpositions required are as follows.

P is replaced by $\frac{P}{\varepsilon}$

t is replaced by t'

f is replaced by f

h is replaced by $h' \cdot \varepsilon$ with $h' = O.H. - t'$

The coefficient (ε) is chosen so that the force for both forms of construction are equal at a deflection of $f = 0.75\ (O.H. - t)$.

27.1.4

Prestressed Discs

Prestressed discs are generaly preferred to Belleville washers. The primary advantage to prestressed disks is that they provide dimensional stability and exact repeatability of load deflection curves.

Belleville washer design formulas can be used as a design guide to prestressed discs. Final dimensions, load capability, load-deflection characteristics and fatigue life should be provided by the spring manufacture.

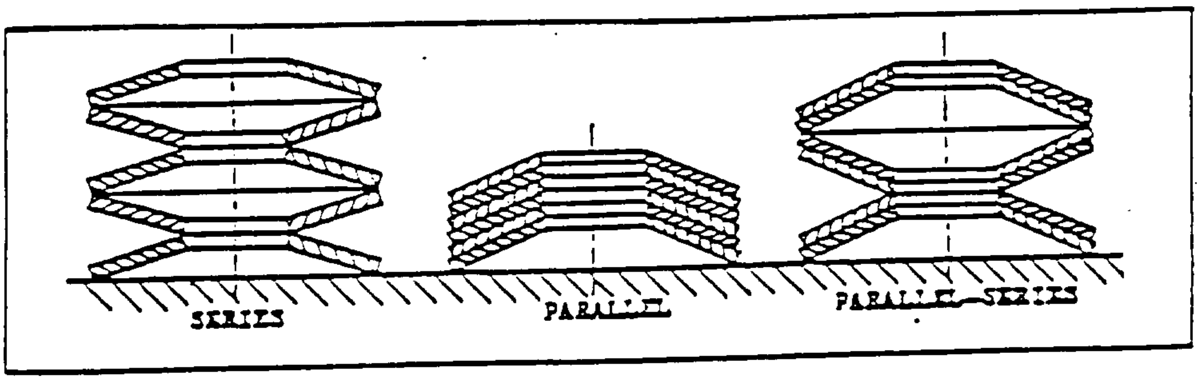

FIGURE-4 METHODS OF STACKING CONED DISC (BELLEVILLE) SPRINGS

Data Source, Section 1.3 Reference 21

28. RECOMMENDED MAXIMUM WORKING STRESSES

28.1 FATIGUE STRENGTH CURVES. The fatigue strength curves Figure 62 are for the most popular spring materials. These are for compression springs, based on the minimum torsional elastic limit of each material. The values may be increased 25 per cent for springs that are properly stress relieved, cold set and shotpeened.

TABLE XIV
CRITICAL STRESS DATA
(For use in association with Figure 62.)*

COMPRESSION SPRING	EXTENSION SPRING	TORSION SPRING
1. TORSION STRESS—Compare calculated stress in coils with *service* curve of Fig. 62. 2. SOLID STRESS — Compare torsion stress in coils when compressed solid with *minimum elastic limit* curve.	1. TORSION STRESS (COILS) — Compare calculated design stress in coils with *service* curve of Fig. 62 multiplied by .85. 2. TORSION STRESS (HOOKS)— Compare calculated design stress in hooks with *service* curve multiplied by .85. 3. BENDING STRESS (HOOKS)— Compare calculated design stress in hooks with *service* curve multiplied by 1.5. 4. TORSION STRESS (COILS) AT MAX EXTENDED LENGTH— Compare calculated stress at this length with *min elastic limit* curve multiplied by 8.5. 5. TORSION STRESS (HOOKS) AT MAX EXTENDED LENGTH—Compare calculated stress at this length with *min elastic limit curve* multiplied by .85. 6. BENDING STRESS (HOOKS) AT MAX EXTENDED LENGTH—Compare calculated stress at this length with *min elastic limit* curve multiplied by 1.5.	1. BENDING STRESS (COILS) —Compare calculated design stress in coils with *service* curve of Fig. 62 multiplied by 1.5. 2. BENDING STRESS (ENDS) —Compare calculated design stress in ends with *service* curve multiplied by 1.5. 3. BENDING STRESS IN COILS AT MAXIMUM DEFLECTION — Compare calculated stress in coils at this deflection with *min elastic limit* of Fig. 62 multiplied by 1.5. 4. BENDING STRESS IN ENDS AT MAXIMUM DEFLECTION — Compare calculated stress in ends at this deflection with *min elastic limit* of Fig. 62 multiplied by 1.5.

* Note 1: After tentative spring configuration has been determined, use data in above table in association with Figure 62, to ascertain that allowable stresses are not exceeded.

Note 2: The above referenced "calculated design stresses" are TOTAL STRESSES. They include curvature stress-correction factors of Figures 39 and 51 (see para 21.11), except for extension spring hook stresses which include correction factor in basic formulas.

28.1.1 Light Service. This includes springs subjected to static loads or small deflections and seldom used springs such as those in bomb fuzes, projectiles, and safety devices. This service is for 1000 to 10,000 deflections.

28.1.2 Average Service. This includes springs in general use in machine tools, mechanical products and electrical components. Normal frequency of deflections not exceeding 3600 per hour permit such springs to withstand 100,000 to 1,000,000 deflections.

28.1.3 Severe Service. This includes springs subjected to rapid deflections over long periods of time and to shock loading such as in pneumatic hammers, hydraulic controls and valves. This service is for 1,000,000 deflections and above. Lowering the values 10 per cent permits 10,000,000 deflections.

28.1.4 Other Materials. For materials not shown on the curves in Figure 62, the following multiplying constants may be used.

(a) For Beryllium Copper, multiply the values of the Phosphor Bronze curves by 1.20.

(b) For Spring Brass, multiply the values

Recommended maximum working stresses for compression springs
(Fatigue Strength Curves)

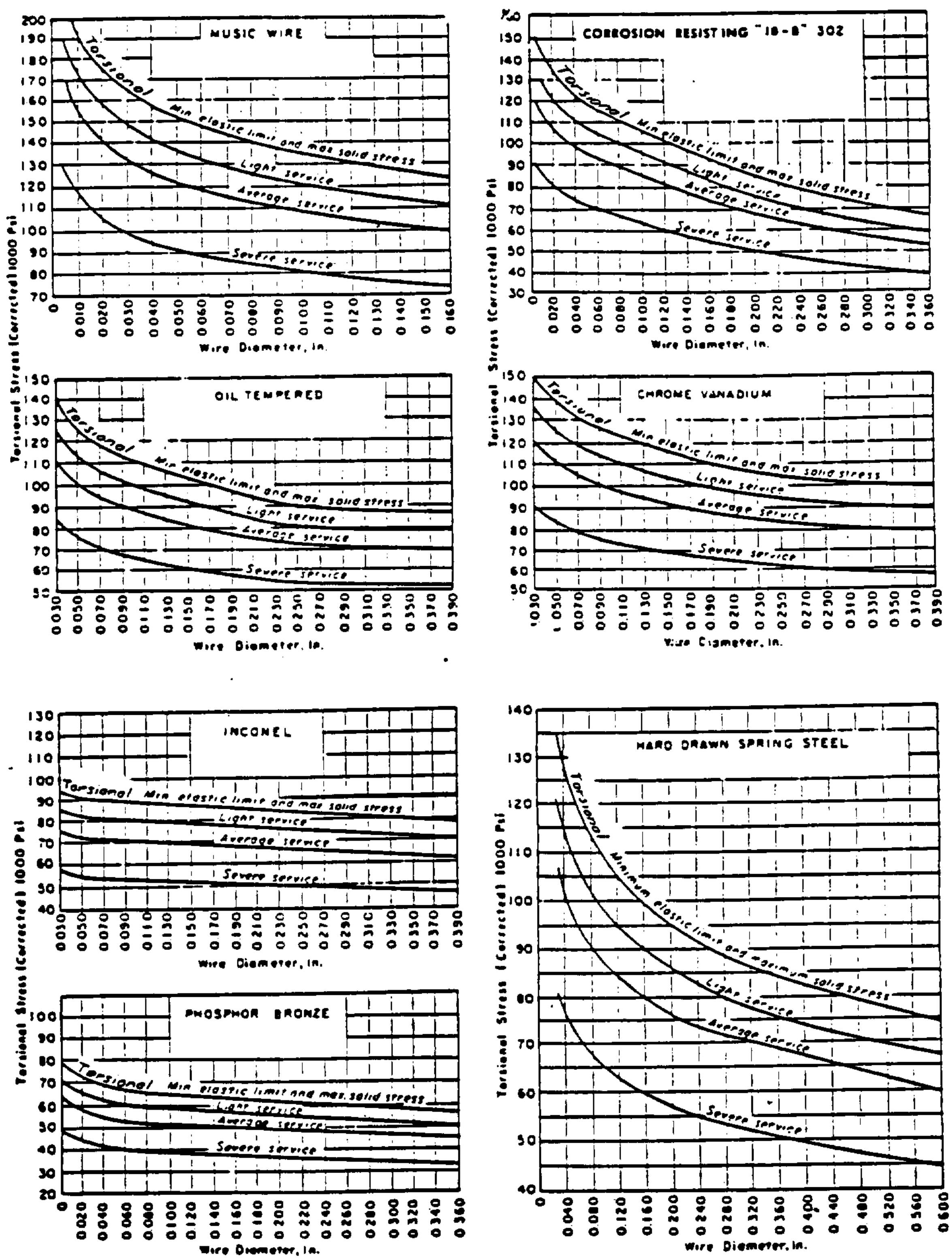

Figure 62
(Use with Table XIV)

of the Phosphor Bronze curves by .75.

(c) **For Monel,** multiply the values of the Inconel curves by .82.

(d) **For K-Monel,** multiply the values of the Inconel curves by .90.

(e) **For Duranickel,** use the same values as for Inconel.

(f) **For Inconel X,** (drawn to spring temper and precipitation hardened) multiply the values of the Inconel curves by 1.25.

(g) **For Silico-Manganese,** multiply the values of the Chrome-Vanadium curves by .90.

(h) **For Chrome-Silicon,** multiply the values of the Chrome-Vanadium curves by 1.20.

(i) **For Valve Spring Quality Wire,** use the same values as for Chrome-Vanadium.

(j) **For Corrosion Resisting Steels type FS304 and FS420,** multiply the values of the Corrosion Resisting Steel curves by .95.

(k) **For Corrosion Resisting Steel type FS316,** multiply the values of the Corrosion Resisting Steel curves by .90.

(l) **For Corrosion Resisting Steels type AISI 431 and 17-7 PH,** multiply the values of the Music Wire curves by .90.

28.2 PERMISSIBLE ELEVATED TEMPERATURES. Springs used at high temperatures exert less load and have larger deflections under load than at room temperature. Compression and extension springs subjected to the temperatures and stresses shown in the following table will have a loss of load of 5 per cent or less, (or if the load remains constant, they will deflect an additional 5 per cent), in 48 hours. Elastic limits and modulus values are also reduced, thus necessitating thse lower allowable working stresses.

TABLE XV. *Permissible elevated temperatures for compression and extension springs. Loss of load at these temperatures is less than 5 percent in 48 hours.*

Spring material	Permissible elevated temperature F deg	Maximum recommended working stress St PSI
Brass Spring Wire	150	30,000
Phosphor Bronze	225	35,000
Music Wire	250	75,000
Beryllium-Copper	300	40,000
Hard Drawn Steel Wire	325	50,000
Carbon Spring Steels	375	55,000
Alloy Spring Steels	400	65,000
Monel	425	40,000
K-Monel	450	45,000
Duranickel	500	50,000
Corrosion Resisting FS-302	550	55,000
Corrosion Resisting AISI 431	600	50,000
Inconel	700	50,000
High Speed Steel	775	70,000
Cobenium, Elgiloy	800	75,000
Inconel X	850	55,000
Chrome-Moly-Vanadium	900	55,000